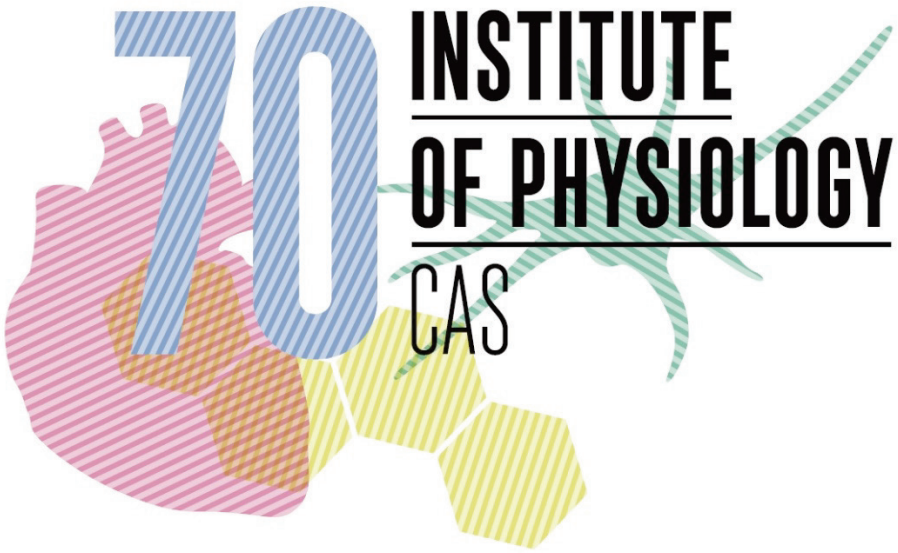

70 years

Institute of Physiology Czech Academy of Sciences

Editor
Josef Zicha

Prague, 2024

Contents

The 70th Anniversary of the Foundation of the Institute of Physiology, Czech Academy of Sciences, Prague

Physiol. Res. 73 (Suppl. 1): i, 2024

Seventy Years of Systematic Biomedical Research at the Institute of Physiology of the Czech(oslovak) Academy of Sciences

This special issue of the *Physiological Research* journal is intended for the celebration of seventy years since the founding of the Institute of Physiology (IPHYS) of the Czech (former Czechoslovak) Academy of Sciences (CAS). True to its name, IPHYS has been systematically dedicated to the research in the field of normal and pathological physiology, with a special focus on biomedical research. Three main closely interconnected research directions gradually crystallized, which IPHYS continues to pursue today: research in the fields of neuroscience, metabolism, and cardiovascular physiology. Over the seven decades, our society has grown considerably older and fatter, while obesity rates have tripled. Modern medicine is thus facing new challenges in the form of an increased onslaught of so-called lifestyle (or civilization) diseases. The cost of their treatment represents a major burden on health care systems worldwide. The main current goal of IPHYS is to characterize the causes of these non-communicable diseases associated with obesity and ageing.

The origin of the current research at IPHYS is traced back to 1950 when two outstanding personalities, Prof. Zdeněk Servít (1913-1986) and Prof. Arnošt Gutmann (1910-1977), met at the Department of Neurophysiology within the Central Biological Institutes. In 1952, the Czechoslovak Academy of Sciences was founded. Servít´s laboratory (epileptology) and Gutmann´s laboratory (neuromuscular function) joined a group interested in critical periods of ontogenetic development headed by Prof. Jiří Křeček (1923-2014) to form a section of the new Biological Institute. On the basis of successful research and acceptance at home as well as abroad, IPHYS was officially founded on January 1, 1954 and consisted of these three laboratories. In 1956, a fourth group led by Prof. Otakar Poupa (1916-1999), who studied the adaptation of the organism to its environment, joined the Institute. The outstanding contribution of these scientists in the fields of neurophysiology, muscle regeneration, heart adaptation to hypoxia and late effects of early interventions was subsequently enriched by their students and follower scientists at IPHYS.

In this introductory article it is not possible to mention all the important bits that make up the seventy-year history of IPHYS. The information about important personalities and key results can be found in previous two anniversary issues of *Physiological Research* (53 (suppl. 1) 2004 and 63 (suppl. 1) 2014) and on the Institute's website (https://www.fgu.cas.cz/en/about). The fates of prominent scientists, who worked at IPHYS and who emigrated abroad after 1968, are described in a dedicated book (Štrbáňová & Kostlán: Sto českých vědců v exilu. Academia, Prague, 2011). Most recently, in 2024, this information was presented concisely, including a list of the most important publications in various research fields, in the *Presentation Institute´s brochure* (which can be downloaded from the website above). Six articles in this special issue are dedicated to the history of research in the key areas of interest, written by the most respectable scientists in their respective fields, namely by Helena Illnerová, Bohuslav Ošťádal, Jaroslav Kuneš, Zdeněk Drahota, Pavel Mareš and František Vyskočil.

In addition to the six articles devoted to the history of research conducted at IPHYS over the last 70 years, most of the articles in this special issue review specific topics that reflect the scientific interests and expertise of the scientists who represent the main drivers of contemporary research at IPHYS. I believe that you will learn important and interesting information while reading these articles. I thank all my colleagues who were involved in their writing.

Jan Kopecký
Director
Institute of Physiology of the Czech Academy of Sciences, Prague

From the Pineal Gland to the Central Clock in the Brain: Beginning of Studies of the Mammalian Biological Rhythms in the Institute of Physiology of the Czech Academy of Sciences

Helena ILLNEROVÁ[1]

[1]Laboratory of Biological Rhythms, Institute of Physiology of the Czech Academy of Sciences, Prague, Czech Republic

Received April 8, 2024
Accepted April 22, 2024

Summary

The Institute of Physiology of the Czech Academy of Sciences (CAS) has been involved in the field of chronobiology, i.e., in research on temporal regulation of physiological processes, since 1970. The review describes the first 35 years of the research mostly on the effect of light and daylength, i.e., photoperiod, on entrainment or resetting of the pineal rhythm in melatonin production and of intrinsic rhythms in the central biological clock. This clock controls pineal and other circadian rhythms and is located in the suprachiasmatic nuclei (SCN) of the hypothalamus. During the early chronobiological research, many original findings have been reported, e.g. on mechanisms of resetting of the pineal rhythm in melatonin production by short light pulses or by long exposures of animals to light at night, on modulation of the nocturnal melatonin production by the photoperiod or on the presence of high affinity melatonin binding sites in the SCN. The first evidence was given that the photoperiod modulates functional properties of the SCN and hence the SCN not only controls the daily programme of the organism but it may serve also as a calendar measuring the time of a year. During all the years, the chronobiological community has started to talk about "the Czech school of chronobiology". At present, the today´s Laboratory of Biological Rhythms of the Institute of Physiology CAS continues in the chronobiological research and the studies have been extended to the entire circadian timekeeping system in mammals with focus on its ontogenesis, entrainment mechanisms and circadian regulation of physiological functions.

Key words

Pineal • Melatonin • AA-NAT rhythm • Light entrainment • Photoperiod • SCN clock

Corresponding author

Helena Illnerová, Laboratory of Biological Rhythms, Institute of Physiology of the Czech Academy of Sciences, Vídeňská 1083, 142 00 Prague 4, Czech Republic. E-mail: illnerova@kav.cas.cz

Effect of light on the melatonin metabolism in the pineal gland

After I had defended my CSc. (PhD) thesis (*Urea formation in rats during postnatal development*) in 1966, my then boss Professor Jiří Křeček, Head of the Department of Developmental Physiology and Pathophysiology of the Institute of Physiology of the then Czechoslovak Academy of Sciences, brought to my attention a paper of Fiske *et al.* [1] on the effect of light on the weight of the pineal in the rat. I became interested in the pineal gland as I knew that newborn rats opened their eyes only at the age of 14 days after birth and I was curious to learn whether the opening of their eyes and thus perception of light might affect their pineals.

At the end of sixties it has been already clear that the mammalian pineal is a secretory organ [2]. In 1958, Lerner *et al.* [3] isolated a factor from bovine pineal glands that lightened amphibian melanophores and named it melatonin. In 1959, Lerner *et al.* [4] described the melatonin structure as N-acetyl 5-methoxytryptamine. It is said that on reading of the isolation and characterization of melatonin, Julius Axelrod, the later Nobel Prize winner for his work on the release, reuptake and metabolism of catecholamines, considered that the enzyme machinery requested for such a synthesis within the body did not exist [5]. However, between 1960-1968

he and his coworkers then proceeded to demonstrate the existence of all elements of the pathway within the pineal gland, summarized in a review in *Science* in 1974 [6]. According to the review, the amino acid tryptophan is hydroxylated by tryptophan-5-hydroxylase to 5-hydroxy-tryptophan which is then decarboxylated by aromatic L-amino acid decarboxylase to 5-hydroxy-tryptamine, i.e., serotonin. Serotonin is acetylated by N-acetyl-transferase (NAT), nowadays characterized as arylalkylamine N-acetyltransferase (AA-NAT) [7], to N-acetylserotonin which is then methylated by hydroxyl-indole-O-methyltransferase (HIOMT) to melatonin [5]. In 1963, Quay [8] described the daily rhythm in the melatonin precursor serotonin in the rat pineal, with high levels during the day and low levels at night. In 1970, Klein and Weller [9] found a robust daily rhythm in the N-acetyltransferase (NAT) activity in the rat pineal, with the nighttime values 100 fold higher than the daytime ones. The end of the pathway leading to melatonin synthesis is shown on Fig. 1A [5] and the daily rhythm in N-acetyltransferase activity on Fig. 1B [10].

During my first studies on the effect of light on the pineal gland I found that following exposure of rats to a sudden light at night, the pineal serotonin content increased within 13 min from low nighttime to high daytime levels and stayed high at light (Fig. 2) [11]. The rapid serotonin increase on light at night suggested that the pineal melatonin metabolism might respond to the sudden light at night almost instantaneously. I was quite surprised by these results as at that time I did not know anything about the biological clock and how an environmental light might affect and reset it. The concept of the biological clock was mostly introduced at the symposium "The Biological Clock" organized in Cold Spring Harbor in 1960. At that symposium it has been accepted that daily rhythms are endogenous and not just a passive response to environmental cycles of light and darkness and hence that they must be driven by an endogenous clock or pacemaker [12, 13]. Our paper on the rapid serotonin rise on light was published in 1971 and one year later, in 1972, Klein and Weller [14] and independently Deguchi and Axelrod [15] reported that a sudden light at night induced an almost instantaneous decline of the pineal N-acetyltransferase (NAT) activity. Both groups cited our previous work on the serotonin rise on light [11]. Apparently, when the NAT activity declined on light, serotonin as its substrate might increase.

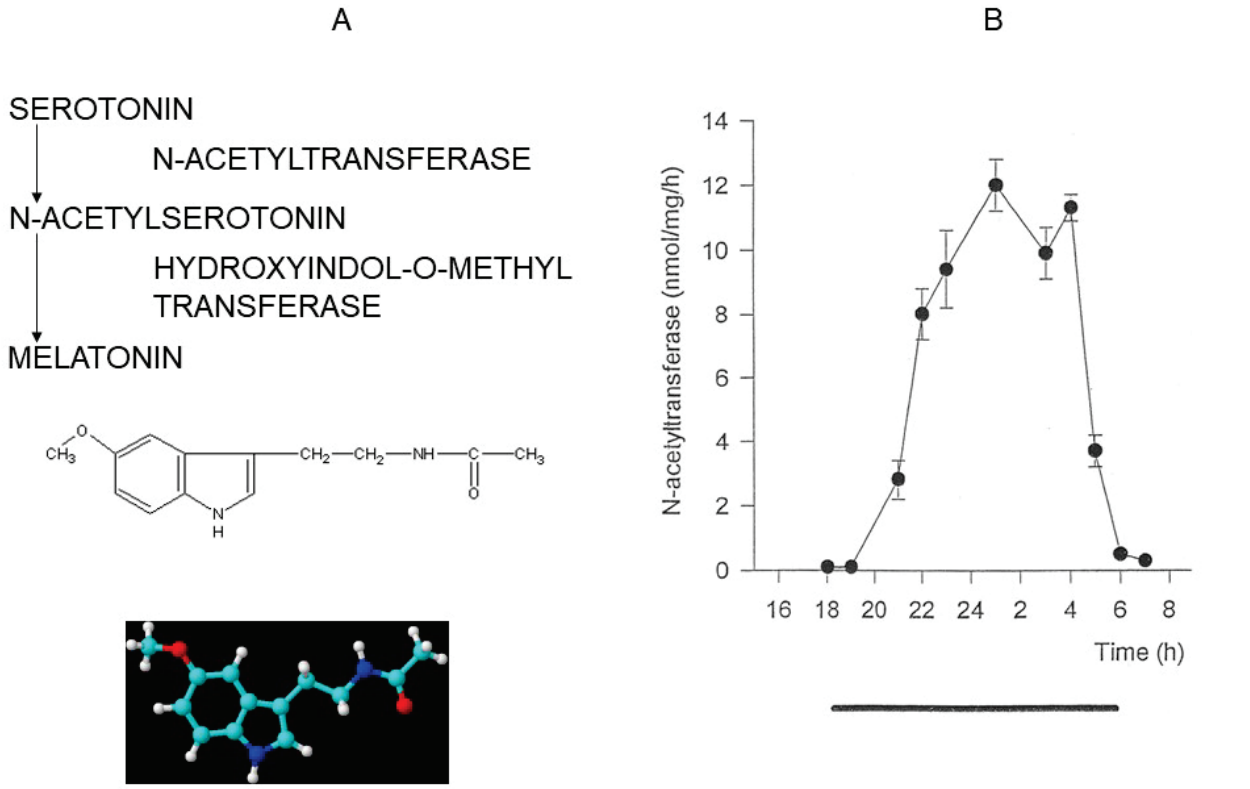

Fig. 1. A: End of the pathway leading to melatonin synthesis in the pineal gland [5]. **B**: The circadian rhythm in N-acetyltransferase activity in the rat pineal gland. The black bar under the abcissa indicates the duration of the dark period. Data were taken from [10].

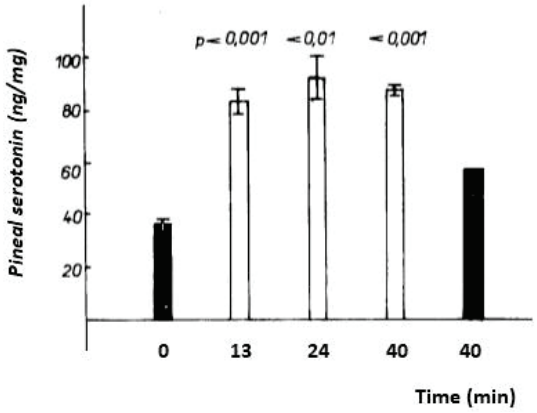

Fig. 2. The effect of a sudden light at night on the pineal serotonin content. Rats maintained in LD 12:12 were exposed to light at night after 4 h in darkness and killed after 13, 24 and 40 min on light (open columns). Some of the rats were left all the time in darkness and killed at the beginning or at the end of the experiment (dark columns). Numbers under the abcissa denote time in min since the start of the experiment. Data were taken from [11].

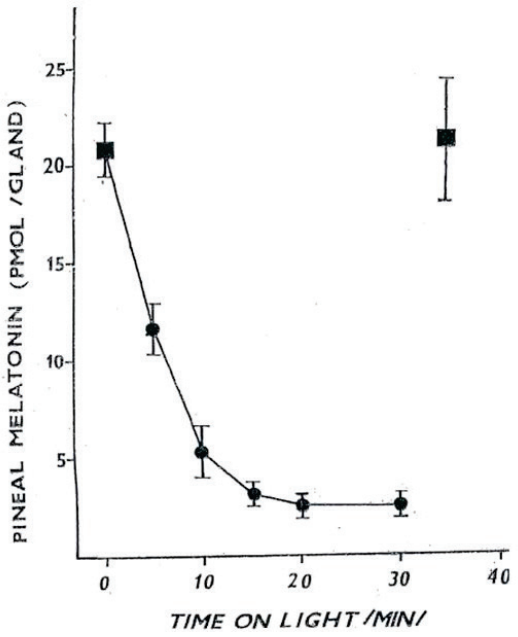

Fig. 3. The effect of a sudden light at night on the pineal melatonin content. Rats maintained in LD 12:12 were exposed to light at night after 5 h in darkness and killed at different times on light (circles). Some of the rats were left in darkness and killed at the beginning and end of the experiment in darkness (squares). Data were taken from [17].

Later, radioimmunoassays (RIAs) for melatonin were developed. In 1978, using a modified Arendt´s RIA [16], we showed with Lennart Wetterberg and his coworkers for the first time the rapid decline of the pineal melatonin content (Fig. 3) and of the serum melatonin concentration following exposure of rats to a sudden light at night [17, 18]. The pineal melatonin decreased rapidly on light with a half- time around 5 min and reached the lowest level already after 20 min. The melatonin concentration in serum fell precipitously on light as well, in a manner almost identical to the drop in the pineal melatonin, only with a 5 min time lag [17]. The half-time for the pineal melatonin decline correlated well with the half-time of 3-5 min reported for the decline in the pineal NAT activity after exposure of rats to light at night [14]. It thus seems that the rapid changes in the pineal melatonin content are due to changes in the pineal NAT activity. Indeed, the evening rise and the morning decline in the pineal NAT activity and in the pineal melatonin content occur at the same time, be it in pineals of rats or Djungarian hamsters [19]. Hence, the NAT rhythm in the pineal drives the rhythm in the melatonin synthesis at least in the two above mentioned species.

The above mentioned finding showed that the pineal NAT activity [14] as well as the pineal melatonin content [17] declined very rapidly when rats were exposed to light for the whole time interval before killing. Such a precipitous drop suggested that even a very brief exposure of rats to light at night, such as for 1 min, after which rats would continue to be in darkness, could trigger a decrease in NAT activity and in melatonin content to low levels. This was indeed the case. Only a 1 min exposure to light 5 hours after the evening onset of darkness caused a rapid decline in NAT activity and in melatonin content with a half-life less than 5 min, the same as in rats exposed to light 5 hours after the evening onset of darkness and then left on light [20].

We then explored, together with Jiří Vaněček, effect of 1 min light pulses applied at night on the pineal rhythm in NAT activity as the indicator of the nocturnal melatonin production. Importantly, the NAT rhythm in the rat pineal has two well-defined phase markers, namely the time of the evening NAT rise (E) and the time of the morning NAT decline (M) (see Fig. 1B). Rats maintained under a 12 h of light and 12 h of darkness regime (LD 12:12) were either left unpulsed or they were exposed to a 1 min light pulse at different night times before or after midnight and then they were released into darkness (Fig. 4). After the 1 min light pulse before midnight the NAT activity, after an initial decline, increased anew; after the pulse applied after midnight, the activity also rapidly declined, but it stayed low for at least another 8 hours in darkness [21-25]. We were fascinated by the sharp boundary between the effect of light pulses before and past midnight. I must admit that I am fascinated by the boundary even now and I wonder whether we have a good explanation for it.

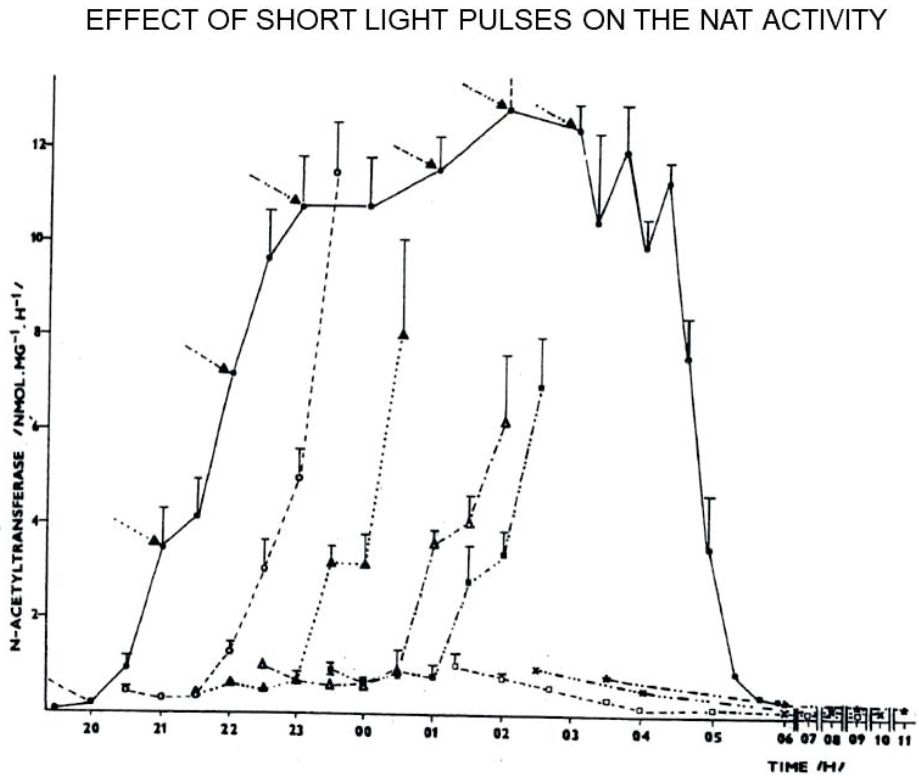

Fig. 4. The N-acetyltransferase (NAT) rhythm in the course of the night when 1 min light pulses were presented. Rats maintained in LD 12:12, with lights on from 06 to 18 h, were either unpulsed (filled circles) or exposed to a 1 min light pulse at 20 h (open circles), or at 21 h (filled triangles), or at 22 h (open triangles), or at 23 h (filled squares), or at 01 h (open squares), or at 02 h (crosses), or at 03 h (asterisks) and from that time on they were kept in darkness until they were killed. Arrows indicate times of the pulse presentation and point to the NAT activity in darkness at the moment of the light pulse. Data were taken from [21,22] and the picture was modulated from that in [23].

Entrainment or resetting of the rhythm in melatonin production by light

In non-periodic environment, e.g. in constant darkness, circadian rhythms free run with a period close, but not identical with 24 h. With the 24 h day, they are synchronized or entrained by an environmental light-dark cycle. Light experienced during the subjective night may reset circadian rhythms to another endogenous time [12, 13]. We thus wanted to find out whether a 1 min light pulse might entrain or reset the NAT rhythm. First, we looked on the effect of the 1 min light pulse administered before midnight on the NAT rhythm on day 0, when rats were pulsed, or on day 1 and 4 after the pulse. Following the pulse, the rats were released into constant darkness (Fig. 5). The pulse at 21 h delayed the evening NAT rise (E) the same night while the morning NAT decline (M) was phase-delayed just slightly. However, after 1 and 4 days, the evening rise and the morning decline were phase-delayed almost to the same extent (Fig. 5A). Fig. 5B shows phase delays of the evening NAT rise (E) and of the morning decline (M) read from the Fig. 5A and other similar figures and plotted as a function of time when pulses were applied [10, 22]. The picture reveals that phase delays of E on day 0 might be quite large while those of M were only small. However, on day 1 and 4, phase delays of M were almost the same as those of E. It appears that at the beginning the pulse in the first half of the night phase delays primarily the evening NAT rise (E), however, within one day E and M are phase-delayed almost to the same extent. Hence, the whole NAT rhythm may be phase-delayed within one day [10, 22, 23, 26, 27].

We got a very different picture when we looked on the effect of the 1 min light pulse administered after midnight (Fig. 6). Following the 1 min light pulse administered at 03 h, the NAT activity immediately declined as if the morning decrease were phase-advanced. On day 1 after the pulse, only the morning decline (M) was phase-advanced, but not yet the evening rise (E). Only after 4 days, E started to be phase-advanced as well, though still to a lesser extent than M (Fig. 6A). Fig. 6B shows phase shifts of the evening NAT rise (E) and of the morning decline (M) read from the Fig. 6A and other similar figures and plotted as a function of time when 1 min light pulses were applied. The picture reveals that on day 1 after administration of the 1 min light pulse, only the morning NAT decline (M) was phase-advanced but not yet the evening NAT rise (E). Four days after the pulse presentation, there were also phase advances of E, but still substantially smaller than those of M [10, 22, 23, 26, 27].

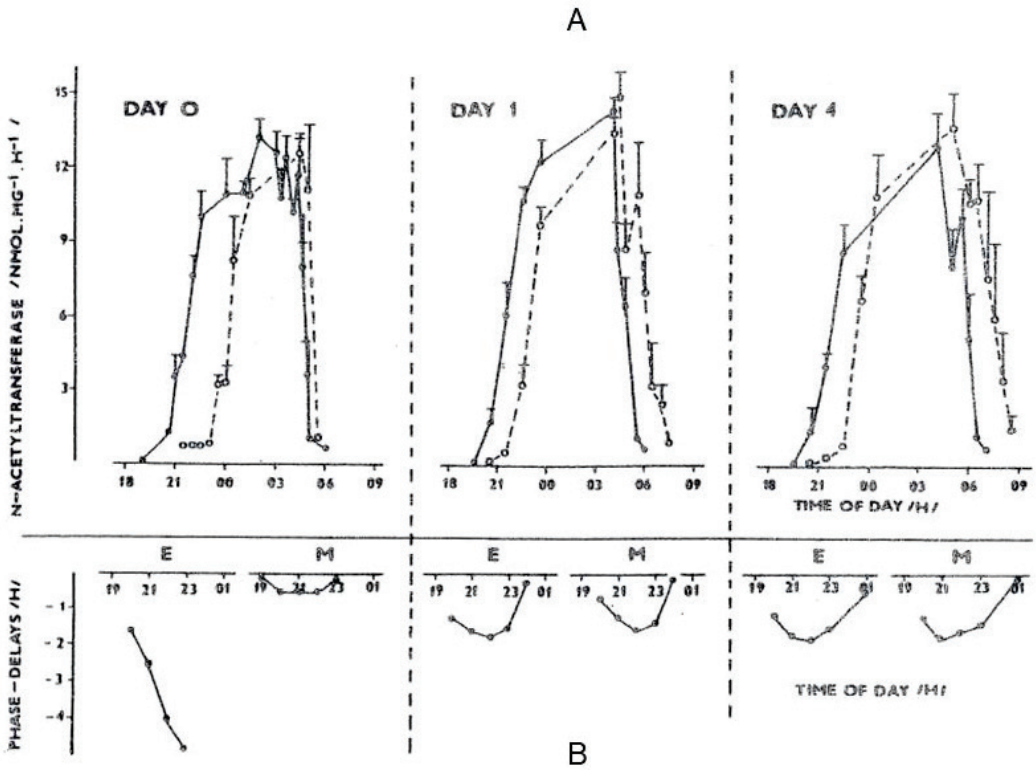

Fig. 5. Phase delays of the N-acetyltransferase (NAT) rhythm after 1 min light pulses applied before midnight. **A**: The NAT rhythm after presentation of a 1 min light pulse at 21 h. Rats maintained in LD 12:12 with lights on from 06 h to 18 h, were either exposed to a 1 min light pulse (open circles, broken line) or left unpulsed (filled circles, full line). Thereafter, they were released into constant darkness and killed during the night when they were pulsed (day 0), or 1 (day 1), or 4 days (day 4) after the pulse presentation. **B**: Phase delays of the evening NAT rise (E) and of the morning NAT decline (M) during the night when rats were pulsed and after 1 and 4 days. Phase shifts were determined at the level of 3 nmol/mg.h of the NAT activity from Fig. 5 A and other similar figures and they were plotted as a function of time when the pulses were presented. Phase delays were plotted with the sign -. The abcissa denotes time of the pulse administration. Data were taken from [10, 22, 23].

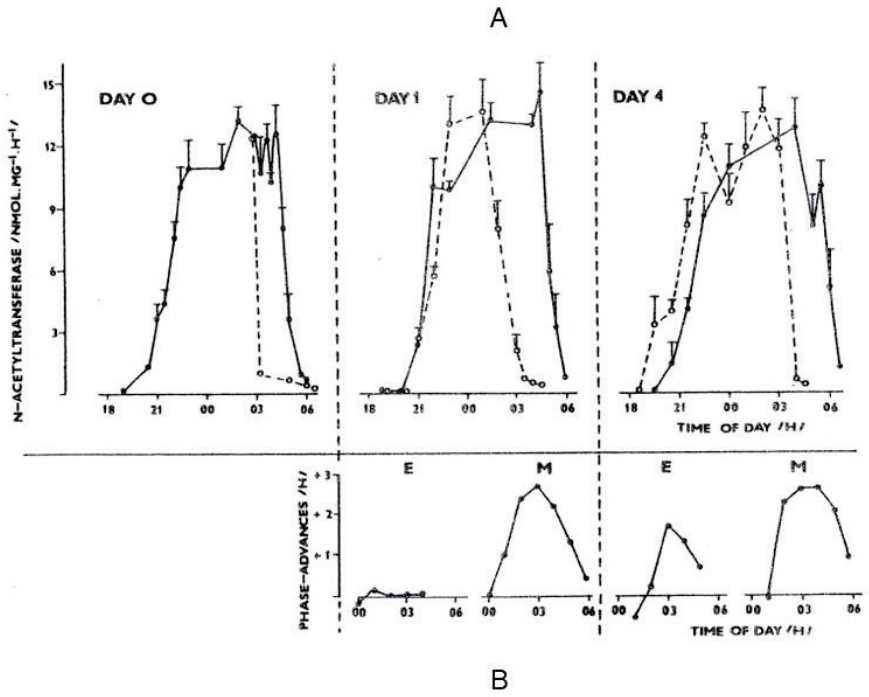

Fig. 6. Phase advances of the N-acetyltransferase (NAT) rhythm after 1 min light pulses applied after midnight. **A**: The NAT rhythm after presentation of a I min light pulse at 03 h. Rats maintained in LD 12:12, with lights on from 06 to 18 h, were either exposed to the 1 min light pulse (open circles, broken line) or left unpulsed (filled circles, full line). Thereafter, they were released into constant darkness and killed during the night when they were pulsed (day 0), or 1 day (day 1), or 4 days (day 4) after the pulse presentation. **B**: Phase shifts of the of the evening NAT rise (E) and of the morning NAT decline (M) during days 1 and 4 were determined at the level of 3 nmol/mg.h of the NAT activity from Fig. 6A and other similar figures and they were plotted as a function of time when the pulses were applied. Phase advances were plotted with the sign +, phase delays with the sign -. The abcissa denotes time of the pulse presentation. The data are taken from [10, 22].

Experiments with light pulses at night showed for the first time that such short light pulses as was the 1 min light pulse might entrain the pineal rhythm in melatonin production. Before, a longer exposure to light at night had been used to entrain or reset mammalian circadian rhythms. The fact that the 1 min light pulse may phase shift mammals into a different endogenous time seems to me still as science fiction. Another important piece of knowledge is that delays of the evening NAT rise (E) and of the morning NAT decline (M) are accomplished almost within one cycle and hence the NAT rhythm as a whole is phase-delayed within one cycle. Advances of the morning NAT decline are accomplished also within one cycle, in contrast to the then dogma that several transients cycles are necessary before phase advances are accomplished. Transient cycles are, however, necessary for the complete phase advancing of E.

From the above mentioned facts it is possible to deduce that rats might better adapt to delaying of the light-dark cycle, i.e. to a simulated westward time-zones transition, than to advancing of the light-dark cycle, i.e. to a simulated eastward time-zones transition. And it is indeed so. After an 8 h delay of a light -dark (LD) 12:12 cycle by lengthening of one light period by 8 h, the pineal N-acetyltransferase rhythm adjusted to the delay shift almost within one cycle. In contrast, after an 8 h advance of the LD cycle accomplished by shortening of one dark period by 8 h, the NAT rhythm adjusted to the advance shift within 5 cycles only; during the first 2-3 cycles the rhythm was abolished [28]. However, when the 8 h advance of the LD cycle was accomplished by twice delaying the LD cycle during two consecutive nights by 8 h, the NAT rhythm persisted and attained its original waveform by 2 days earlier than under the former advance of the LD cycle [29]. Finally, non-parallel phase shifts of E and M point to a possibility of a complex pacemaker driving the pineal NAT rhythm [22, 24], such as was proposed by Pittendrigh and Daan [30] for the circadian pacemaker driving the rhythm in the locomotor activity.

With 1 min light pulses, we could phase shift the NAT rhythm by 2-3 h at most. A question arose whether a longer light exposure at night might phase shift mammalian circadian rhythms by more than 3 h. Rats maintained in LD 12:12 experienced a prolongation of the light period into the evening and night hours and thereafter they were released into darkness (Fig. 7). Fig.7A shows that on day 0, the prolonged light till 22 h and 02 h, respectively, phase delayed primarily the evening NAT rise (E), but not so much the morning decline (M). After prolongation of the light period till 02 h, the phase delay of E was about 8 hours. On day 1, both the rise and decline were phase-delayed almost to the same extent, i.e., by about 6 hours at most (Fig. 7B) [31]. Thus, it is possible to phase delay the whole NAT rhythm by prolongation of the light period into the night by as much as by 6 hours within one cycle [23, 26, 27, 31]. Next we studied response of the NAT rhythm to an earlier light onset in the morning. Rats maintained in LD 12:12 experienced either the usual morning lights-on at 06 h or an advance of the morning lights-on to 01 h or to 23 h. After the advance of the morning light onset, the NAT activity immediately declined (day 0).

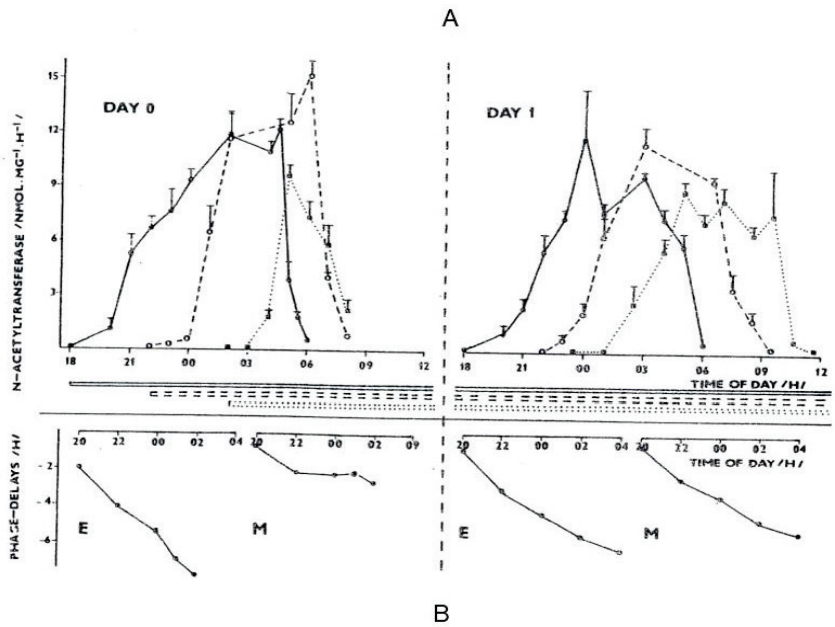

Fig. 7. Phase delays of the N-acetyl-transferase (NAT) rhythm after delays of the evening lights off. **A**: The NAT rhythm during the night when the lights-off was delayed (day 0) and during the next night (day 1). Rats maintained in LD 12:12, with lights on from 06 h to 18 h, were subjected either to the expected lights-off (filled circles, full line), or to a delay of the lights-off till 22 h (open circles, broken line) or till 02 h (filled squares, dotted line), respectively. Thereafter, they were released into darkness. Lines under the abcissa indicate dark periods. **B**: Phase delays of the evening NAT rise (E) and of the morning NAT decline (M) of the experimental animals relative to the control ones determined at the level of 3 nmol/mg.h of the NAT activity from Fig. 7A and other similar figures. The abcissa denotes time of the onset of darkness on day 0. Data were taken from [31].

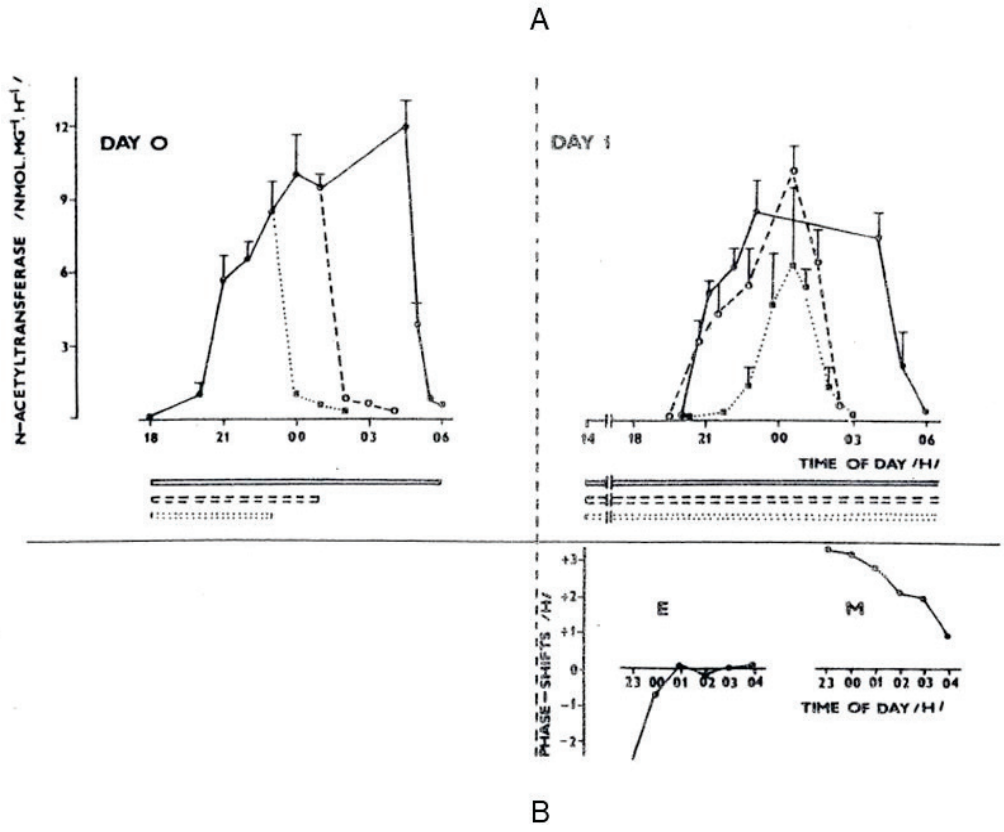

Fig. 8. Phase shifts of the N-acetyltransferase (NAT) rhythm after bringing forward the morning lights-on. **A**: The NAT rhythm during the night when the lights-on was brought forward (day 0) and during the next night (day 1). Rats maintained in LD 12:12, with lights on from 06 h to 18 h, were subjected to the usual lights-off at 18 h and later that night either to the usual morning lights-on at 06 h (filled circles, full line), or to an advance of the lights-on to 01 h (open circles, broken line), or to 23 h (filled squares, dotted line), respectively (day 0). Thereafter, light was turned off at 14 h and the NAT rhythm was followed during the subsequent night (day 1). Lines under the abcissa indicate dark periods. **B**: Phase shifts of the evening NAT rise (**E**) and of the morning NAT decline (**M**) the next night after bringing forward the morning lights-on, determined at the level of 3 nmol/mg.h of the NAT activity from Fig. 8A and other similar figures. Phase advances are expressed with the sign +, phase delays with the sign -. The abcissa denotes time of the light onset on day 0. Data were taken from [31].

Thereafter, the rats were released into darkness at 14 h and the NAT rhythm was followed in the subsequent night (Day 1, Fig. 8A) [31]. All phase shifts of the morning NAT decline (M) and of the evening NAT rise (E) on day 1 after bringing forward the morning light onset on day 0 are shown in Fig. 8B [31]. After the advance of the morning light onset, only the morning NAT declines (M) were phase-advanced by 3 h at most, but not the evening NAT rises (E) [23, 27, 31]. When the morning light onset was brought forward to before midnight, the evening NAT rise (E) was even phase-delayed and the NAT rhythm waveform and amplitude might change dramatically [31]

Effect of the photoperiod on the rhythm in melatonin production

If the evening light phase delays primarily the evening NAT rise (E) and the morning light phase advances primarily the morning NAT decline (M), we may expect that on long summer days the duration of the elevated melatonin production might be compressed due to the phase delaying effect of the evening light intruding into the late evening hours on E and to the phase advancing effect of the morning light intruding into the early morning hours on M, and on short winter days the duration might be decompressed. And it was indeed the case (Fig. 9B) [32]. On long summer days in June, the duration of the elevated NAT activity and hence of the high melatonin production was by more than 4 hours shorter than the duration on short winter days in December. Similarly, under an artificial LD 16:8 regime, the duration of the elevated NAT activity was shorter than that under the LD 8:16 regime (Fig. 9A) [32]. Hence the phase relationship between the evening NAT rise (E) and the morning NAT decline (M), determining the duration of the nocturnal melatonin production, might transduce the information on a changing daylength, i.e.

on the photoperiod, onto mammals [24, 32]. In 1979, we sent the manuscript on the pineal NAT rhythm in rats under different artificial photoperiods and in natural daylight in the course of a year to the *Journal of Endocrinology*, but it was rejected with an explanation that the difference in the duration of the nocturnal melatonin production between long and short days was not enough dramatic for showing that the melatonin signal duration might be the sought photoperiodic message. But the difference was dramatic – it was more than 4 hours! In 1980, the manuscript was published in *Neuroendocrinology* [32]. At about the same time, an article on Syrian hamsters appeared, in which a difference in the melatonin signal duration between a short and a long photoperiod was visible, but the authors did not yet recognized the importance of this observation [33]. In 1981, the difference in melatonin signal duration in animals maintained under long days and those maintained under short days was already reported for ewes [34], Djungarian hamsters [35] and white-footed mice [36].

When rats were exposed to six different photoperiods, the NAT rise (E) depended on the photoperiod [23, 37, 38]. The time interval between the onset of darkness and the evening NAT rise (E) increased with the increasing duration of the dark period to more than 6 hours in LD 6:18. In contrast, the time interval between the morning NAT decline (M) and the onset of light was almost constant under all photoperiods, i.e., between 1-2 hours [23, 38]. The NAT rhythm is therefore locked to the morning lights-on rather than to the evening lights-off. It appears that the morning light may entrain the NAT rhythm to the 24 h day and the evening light may serve rather as a photoperiodic signal.

Decompression of the phase relationship between the evening NAT and melatonin rise (E) and the morning decline (M) after a change from a long to a short photoperiod is a gradual process. After a change from LD 16:8 to LD 8:16 accomplished by a symmetrical prolongation of the dark period around midnight, extension of the pattern of the NAT rhythm proceeded mainly into the morning hours and was thus achieved more by phase delays of the morning NAT decline (M) than by phase advances of the evening NAT rise (E) [39]. Extension of the period of the elevated nocturnal NAT activity proceeded more rapidly when the change from LD 16:8 to LD 8:16 was accomplished asymmetrically by prolongation of the dark period into the morning and daytime hours than when the dark period was extended into the evening and late day hours [38, 39]. Whereas the extension of the phase relationship between the evening NAT rise (E) and the morning decline (M) may be a gradual and slow process, compression of the duration by long days may proceed rapidly [18, 32].

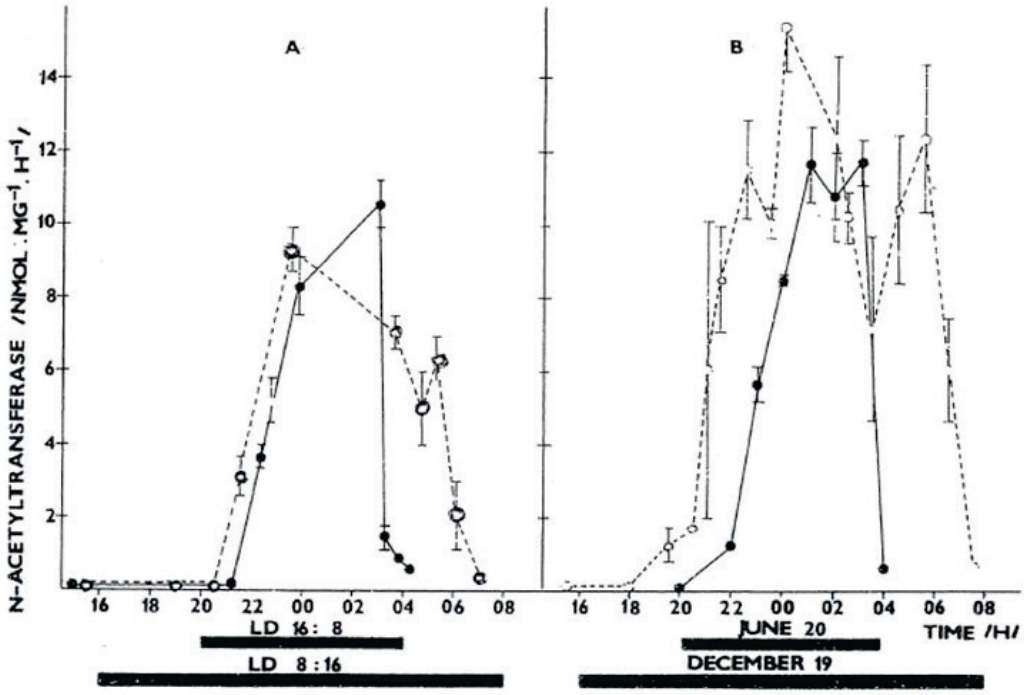

Fig. 9. The N-acetyltransferase rhythm in rats maintained under artificial light-dark regimes (**A**) or in natural daylight (**B**). Filled circles represent rats kept for 5 weeks in LD 16:8 (A) or rats kept in natural daylight and killed on June 20 (B). Open circles represent rats maintained for 5 weeks in LD 8:16 (A) or rats maintained in natural daylight and killed on December 19 (B). Data were taken from [32].

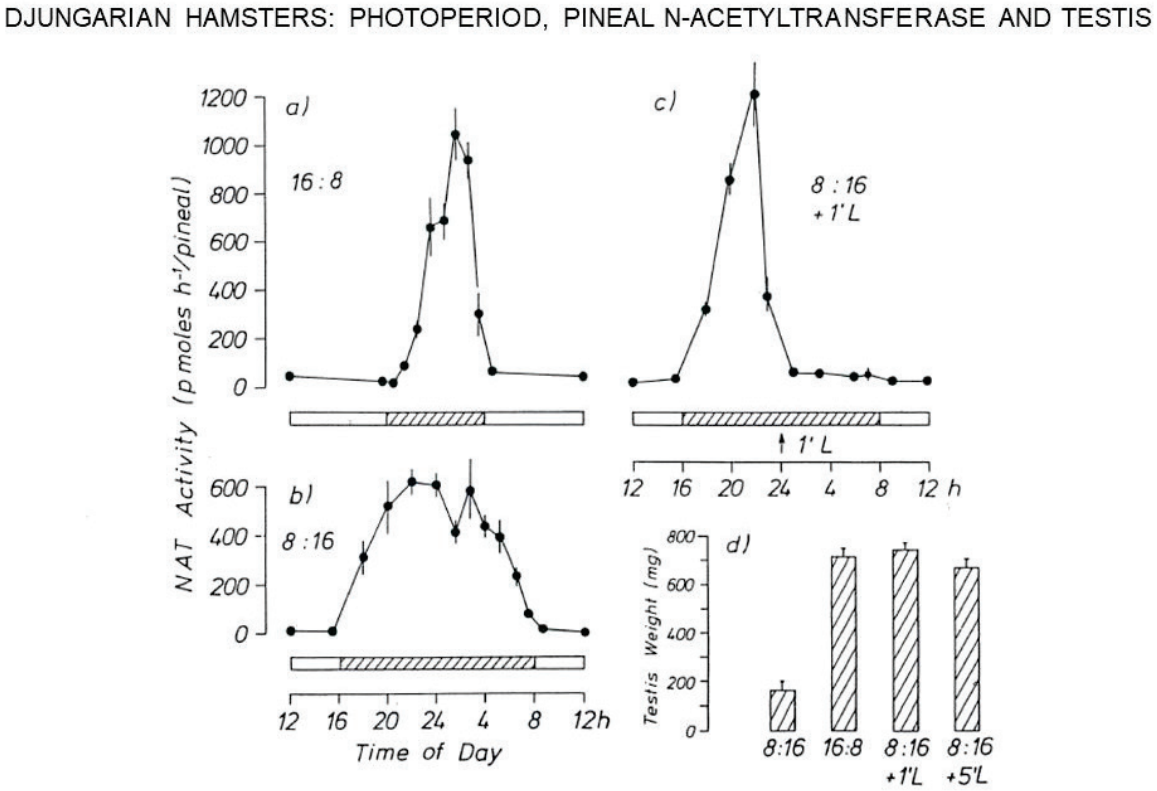

Fig. 10. Diurnal rhythm of N-acetyltransferase (NAT) activity in pineals of Djungarian hamsters under different photoperiods (**a-c**) and effects of such photoperiods on testicular recrudescence (**d**). NAT activity profile **a**) in long photoperiods (LD 16:8); **b**) in short photoperiods (LD 8:16); **c**) in short photoperiods in which the dark period was interrupted by 1 min of light each night. **d**) Testis weight after 45 days in the photoperiods indicated. Open horizonal bars in (a-c) represent light, hatched bars darkness. Note similarity of patterns in (a) and (c) and similarity of effect of LD 16:8, LD 8:16 + 1 min light and LD 8:16 + 5 min light in 3(d). Data were taken from [35].

In all mammals so far studied the melatonin signal duration changes according to a season of the year. However, in humans the melatonin signal duration appears to depend just slightly on the ambient photoperiod and only at higher latitudes, e.g., at 60 °N in Sweden [40] and at 68 °S in Antarctica [41]. In the temperate zone 50 °N, we found no difference in the duration of elevated nocturnal melatonin concentration between summer and winter in plasma of healthy urbanized people [18, 42]. Only in winter the melatonin rhythms were phase-delayed by about 1.5 hours as compared with summer patterns. However, at 50 °N in summer, exposure of human subjects to a natural 16 h bright light photoperiod phase-advanced the morning salivary melatonin decline and shortened thus the nocturnal melatonin signal by 2 hours relative to the winter patterns of the same subjects followed under a combined artificial and natural light 16 h photoperiod [43]. The data suggest that natural summer days experienced from sunrise till sunset and not winter days with a combined artificial and natural light photoperiod evoke a true long days response of the human circadian system.

Duration of the nocturnal melatonin production as the photoperiodic signal?

We have mostly used the rat as a model animal. However, rats are only marginally photoperiodic under normal conditions, that means that they do not respond to a change in daylength, i.e., in the photoperiod, by a change in gonadal size, body weight or pelage color. To find out whether the melatonin signal duration might be indeed the sought photoperiodic signal, we joined our forces with Klaus Hoffmann from the Max Planck Institute in Andechs who was an expert on photoperiodism and had as model animals the photoperiodic Djungarian hamsters. In these hamsters short photoperiods induce regression of testes and accessory glands [44] and the nocturnal melatonin synthesis is also driven by the pineal NAT activity as in rats [19]. When Djungarian hamsters were maintained in

short, LD 8:16 days, the duration of the nocturnal elevated NAT activity and hence of the high nocturnal melatonin production was long and the testis weight was low (Fig. 10) [35]. When Djungarian hamsters were maintained either in a long, LD 16:8 photoperiod or in a short, LD 8:16 photoperiod with the dark period interrupted by 1 min of light in the middle of night, the duration of the nocturnal NAT activity was short and the testis weight was high. Apparently under short days, with a 1 min light pulse in the middle of the dark period, the Djungarian hamsters perceived the pulse already as a dawn. Results of our study indicated that duration of the nocturnal melatonin formation might be indeed the photoperiodic signal [35].

Our next study brought similar conclusions [45]. Djungarian hamsters maintained on a regime of 16 h of light and 8 h of darkness per day (LD 16:8) were transferred to a LD 8:16 regime either by extending the dark period into the morning hours till noon (A) or by bringing forward the evening dark onset to the afternoon hours till noon (B). Under the schedule A, extension of the compressed state of the nocturnal melatonin signal proceeded more rapidly and regression of testes and accessory glands proceeded with a higher velocity than under the schedule B [45]. The different rate of gonadal regression after different ways of transition into the same short photoperiod might be due to the different rate of decompression of the melatonin pattern.

Two years after our first study on photoperiodism in Djungarian hamsters had been published [35], Carter and Goldman brought a direct proof that duration of the nocturnal melatonin signal was indeed the proper photoperiodic message [46, 47]. They found that melatonin infusion to young pinealectomized Djungarian hamsters for 8 or more hours per day induced a gonadal regression similar to that induced by short days whereas the infusion for 4-6 hours per day stimulated a gonadal growth similar to that induced by long days. When Bruce Goldman sent reprints of these two papers to Klaus Hoffmann, he wrote there: “You had it all the time right, Klaus”.

However, when considering the importance of the melatonin signal duration in conveying the photoperiodic message, a question arises whether an absolute value of the duration is important or whether rather a change in the duration is important. To solve this question, we maintained Djungarian hamsters under a long, LD 16:8 photoperiod and we transferred them to another long, but a shorter LD 14:10 photoperiod. We also maintained Djungarian hamsters under a short, LD 8:16 photoperiod, and we transferred them to a long, LD14:10 photoperiod [18, 48]. Finally, both groups were under the same, LD 14:10 photoperiod (Fig. 11). Melatonin profiles of both groups under LD 14:10 were the same and consequently the melatonin signal duration was the same as well, regardless of whether the animals came from the long or from the short photoperiod. However, the reproductive organs of Djungarian hamsters responded to the same signal duration in a different way depending on whether they came from the long or from the short photoperiod (Fig. 12). When the male Djungarian hamsters came to the LD14:10 photoperiod from the LD 16:8 photoperiod, they responded to shortening of the photoperiod and hence to lengthening of the original melatonin signal duration by a decrease in reproductive organs weight, whereas when they came to the LD 14:10 photoperiod from the LD 8:16 photoperiod, they responded to the lengthening of the photoperiod and hence to shortening of the melatonin signal duration by a dramatic increase in reproductive organs weight. This finding showed for the first time that mammals might read rather a change in the melatonin signal duration than the absolute value of the duration [18, 48].

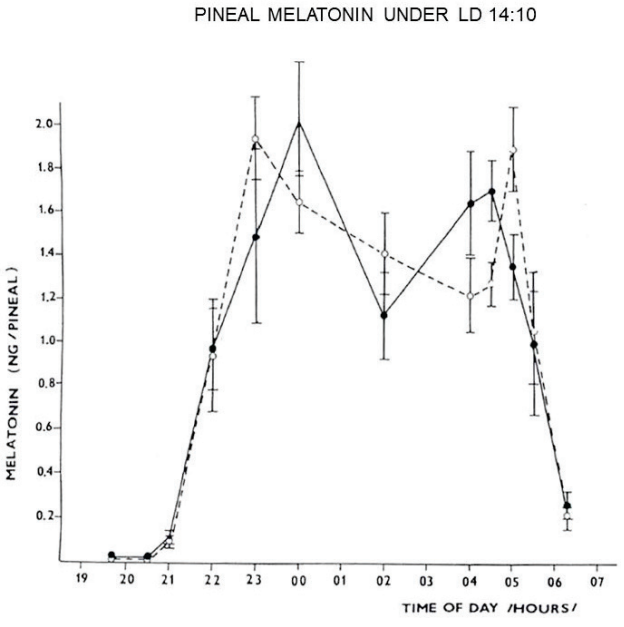

Fig. 11. Profiles of the rhythm in pineal melatonin concentration in Djungarian hamsters under LD 14:10. Djungarian hamsters maintained under LD 16:8 (closed circles) or under LD 8:16 (open circles) were transferred to LD 14:10 and killed 10 weeks later. Data were taken from [48].

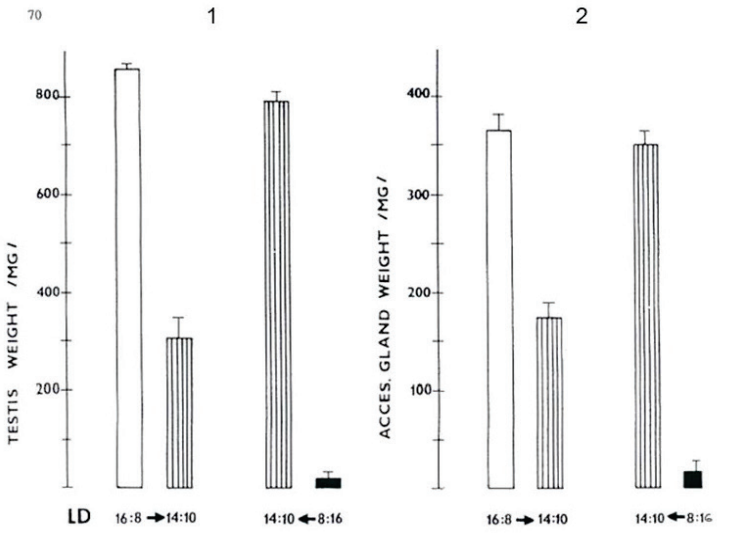

Fig. 12. Testis (**1**) and accessory gland (seminal vesicles, coagulating glands and ampullary glands) (**2**) weight in Djungarian hamsters under LD 14:10. Djungarian hamsters maintained in LD 16:8 (open bars) or in LD 8:16 (closed bars) were transferred to LD 14:10 and killed 10 weeks later (stripped bars). Data were taken from [48].

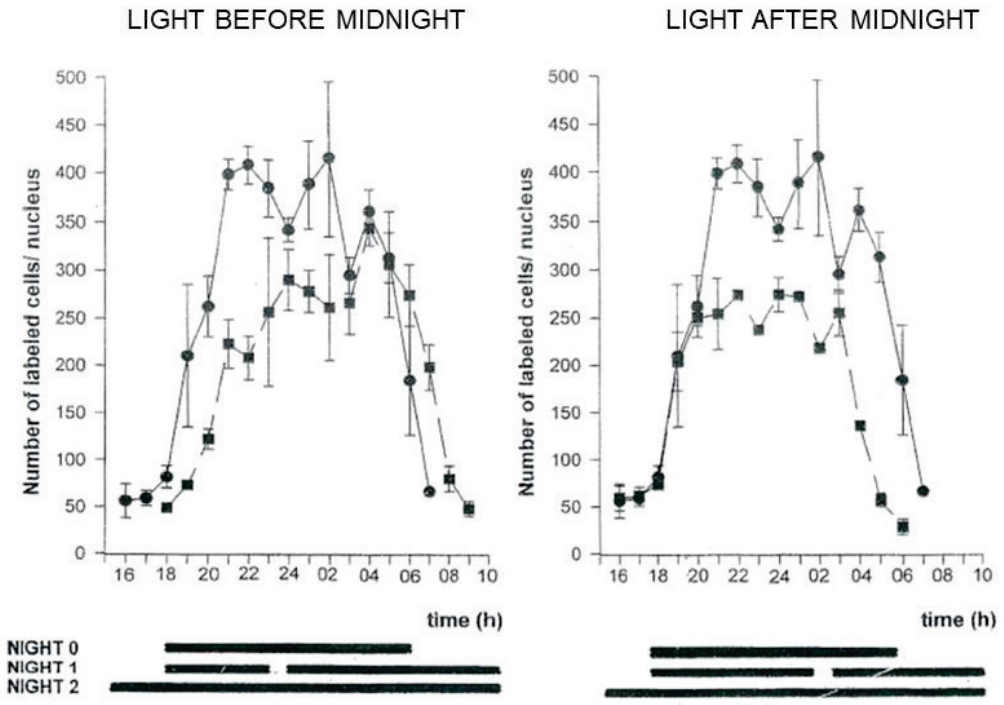

Fig. 13. Resetting of the suprachiasmatic nucleus (SCN) rhythm in light induced c-Fos immune-reactivity. Rats maintained in LD 12:12 (night 0) were either untreated (circles) or exposed to a 1 h of light (squares) from 23 to 24 h before midnight (left) or from 02 to 03 h after midnight (right) (night 1) and then they were released into darkness. The next night (night 2), they were exposed to a single 30 min light pulse at different nighttimes, returned to darkness and killed 30 min later for c-Fos immunoreactivity determi-nation. Filled bars under the abcissa indicate dark periods. Data were taken from [58].

Possible effect of the photoperiod on the circadian pacemaker in the suprachiasmatic nuclei (SCN)

Under longer days, the discrete entrainment of the NAT rhythm is accomplished by smaller phase shifts than under shorter days [18, 49]. Rats maintained under a long, LD 18:6 photoperiod or under a short, LD 6:18 photoperiod were exposed to a 1 min light pulse at different times of night, then they were released into darkness and the next night phase shifts of the evening NAT rise (E) and of the morning NAT decline (M) were determined. In rats maintained under the long, LD 18:6 photoperiod, E was phase-delayed by at most 0.5 h, while in those maintained under the short, LD 6:18 photoperiod, E was phase-delayed by as much as by 2.8 h. Similarly, M was phase-advanced by at most 1.9 h under LD 18:6, but by as much as by 3.5 h under LD 6:18 [49]. Smaller phase shifts under the long than under the short photoperiod point to a possibility that the compressed E-M phase relationship under long days does not allow greater phase shifts [18, 49]. Difference in the magnitude of phase shifts between long and short days might indicate that a state of the pacemaker controlling

the NAT rhythm depends on the photoperiod. Hence, we decided to study the effect of the photoperiod on the circadian pacemaker itself.

The circadian pacemaker or the central biological clock controlling the pineal N-acetyltransferase rhythm [50] as well as other circadian rhythms, e.g., the locomotor activity rhythm or the rhythm in corticosterone formation in the adrenals is located in two suprachiasmatic nuclei (SCN) of the anterior hypothalamus [51, 52]. The SCN consists of two subdivisions, which are morphologically and functionally distinct, namely of the ventrolateral (vl) part called the core and of the dorsomedial (dm) part called the shell [53, 54]. Cells of the ventrolateral SCN receive direct photic signals from the retina and at night respond to them by expression of immediate early genes (IEGs) [55,56]. Cells of the dorsomedial SCN exhibit spontaneous rhythms and their resetting requires communication with the light sensitive cells of the ventrolateral SCN [54].

Effect of light and photoperiod on the ventrolateral SCN

Together with Alena Sumová we tried to find out how photic resetting of the SCN intrinsic rhythmicity proceeds *in vivo* [58]. As a marker of the SCN intrinsic rhythmicity, we used the circadian rhythm in photic induction of IEGs, namely of c-fos [55, 56, 57]. Rats maintained in LD 12:12 were either left untreated or experienced a 1 hour light exposure either before or after midnight (Fig. 13). Then they were released into darkness and the next night they were exposed to a 30 min light pulse at different night times in order to get a profile of the SCN rhythm in the light-induced c-Fos immunoreactivity [58]. Following the 1 hour light exposure before midnight, the next night both the evening rise (E) and the morning decline (M) of c-Fos immunoreactivity were phase-delayed, however, E was delayed slightly more than M. After the 1 hour light exposure after midnight, only the morning decline in c-Fos immunoreactivity was phase-advanced the next night, but not the evening rise (E) [58]. It appears that the light exposure in the first half of the night might phase delay primarily the evening rise in c-fos photoinduction (E), while the light exposure in the second part of the night phase-advanced primarily the morning decline (M), as it was the case with the pineal NAT rhythm [23, 26, 31].

Consequently, the duration of the interval enabling c-Fos photoinduction at night in the rat SCN might be compressed on long "summer" days with light intruding into the late evening and early morning hours and decompressed on short "winter" days. In collaboration with Bill Schwartz from the university of Massachusetts Medical School we proved that this was actually the case (Fig. 14) [56]. The duration of the interval between the evening rise (E) in c-fos mRNA and the morning decline (M) under long days with only 8 hours of darkness was by about 5-6 hours shorter than that under short days with 16 hours of darkness. We got a similar picture when we used c-Fos immunoreactivity instead of c-fos mRNA as a marker of the rhythm in c-fos photoinduction [56]. The duration represents again the phase relationship between the evening (E) and the morning (M) marker of the circadian rhythm, but this time in the SCN rhythm itself and not in a rhythm controlled by the SCN. Under the short photoperiod, there was a robust correlation between c-fos photoindu-

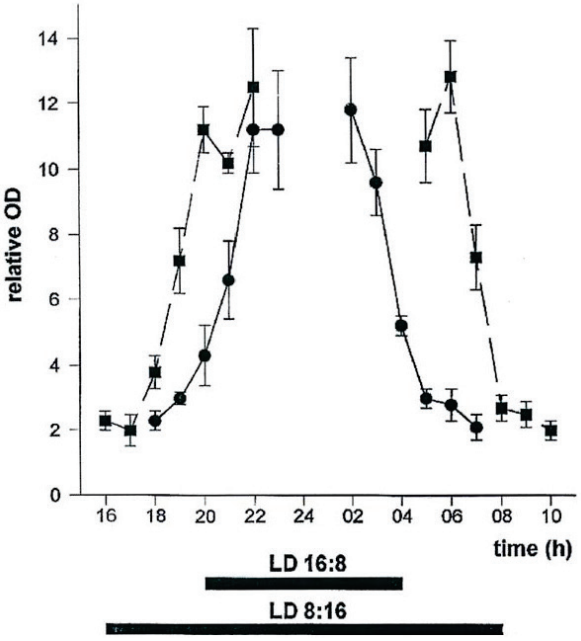

Fig. 14. Light induced c-fos gene expression in the SCN under long and short photoperiods. Rats were maintained under a long, LD 16:8 photoperiod, with lights on from 04 till 20 h, or under a short, LD 8:16 photoperiod, with lights on from 08 to 16 h. On the day of the experiment, the evening onset of darkness was advanced to 12 h or the morning onset of light was delayed to 12 h, respectively, and the rats were exposed to a single 30 min light pulse at different times in darkness. At the end of the pulse, they were killed and phase-dependent photic induction of c-fos mRNA was assayed by *in situ* hybridization in the SCN of rats maintained previously under the long (circles) or under the short (squares) photoperiod. Bars under the abcissa represent original periods of darkness under the long or under the short photoperiod. Data were taken from [56].

ction and the magnitude of phase shifts of the pineal NAT rhythm [59]. Under the long photoperiod, there was also a good correlation between c-fos photoinduction and the magnitude of phase shifts of the intrinsic ventrolateral SCN rhythmicity [60]. Under a very long LD 18:6 photoperiod, even a 5 min light pulse applied around midnight phase delayed the evening NAT rise (E) and phase-advanced the morning decline (M) and at the same time lowered the amplitude of the rhythm in c-fos photoinduction [58]. Apparently, under such a long photoperiod, the E-M phase relationship in the SCN might be so compressed that even only the 5 min light pulse might hit both E and M at the same time. The fact that the photoperiod affects the intrinsic rhythm in c-fos photoinduction in the rat SCN brings the first evidence that the photoperiod modulates the central circadian pacemaker [56]. Hence, the pacemaker may not serve only as a daily program, but also as a calendar, as it was suggested by Pittendrigh and Daan [30]. Importantly, the effect of the photoperiod is not altered by pinealectomy which indicates that the daylength affects the functional state of the SCN circadian pacemaking system directly and not via the pineal melatonin signal [61].

Complex pacemaker in the ventrolateral SCN

The Pittendrigh´s and Daan´s model [30] based on modeling the locomotor activity rhythm in nocturnal rodents anticipates the complex circadian pacemaker consisting of two oscillators or clusters of oscillators, the evening one, E, and the morning one, M, where E controls the evening onset of the activity and is coupled to sunset, while M controls the morning offset of the activity and is coupled to sunrise. Both oscillators interact with each other and their interaction may be affected by the photoperiod [30]. At the time when the model was suggested, the idea of a complex pacemaker underlying circadian rhythms was ingenious as then a prevailing opinion was that the SCN clock in the brain was just a unified single clock, a homogenous population of cells that produced a synchronous daily oscillatory signal. Though the idea of Pittendigh and Daan was ingenious, the two oscillator model was based on splitting of the locomotor activity of hamsters into two activity peaks 180° apart. But this splitting was based just on the existence of the left and right SCN and these „split“ oscillators are not likely to represent E and M because they appear to be functionally equivalent [62].

We thus proposed a similar two-oscilator model, but based on the pineal NAT rhythm [22] and on the SCN rhythm in c-fos photoinduction [56,58]. Non-parallel phase shifts of the E and M phase markers of the pineal NAT rhythm [22] as well as of the rhythm in c-fos photoinduction in the SCN [58] indicate a possibility that the central pacemaker consists of at least two clusters of oscillators, E and M, which interact. The E-M phase relationship is photoperiod-dependent and it determines the subjective night, namely the duration of the nocturnal melatonin signal, the SCN gate for sensitivity to light and the SCN gate for phase shifting circadian rhythms by light. M, coupled to dawn, may entrain the pineal and the ventrolateral SCN rhythms to the 24 h day, while E may serve rather as a photoperiodic signal [56, 62, 63, 64].

More studies support the E-M model. For example, in SCN slices from Syrian hamsters, the circadian rhythm of SCN multiunit neural activity exhibits distinct morning and evening peaks when the slices are cut in the horizontal plane [65]. The morning peak follows the projected dawn, while the evening peak occurs around the projected dusk. The two peaks are differently affected by changes in the antecedent photoperiod. Also in Drosophila, morning and evening oscillators were reported [66,67] as well as in mice [68] and in humans [69,70]. Assuming that E and M oscillators indeed exist, it is not clear whether they are a property of individual SCN cells or instead emerge from an intercellular network interaction. However, as the rhythm in c-fos photoinduction exists only in the ventrolateral, but not in the dorsomedial SCN [71], the assumed E and M oscillators might also exist only in the ventrolateral SCN.

The effect of photoperiod on the intrinsic rhythmicity in the dorsomedial SCN

A question arises whether the circadian rhythmicity of the dorsomedial SCN is also modulated by the photoperiod. Two circadian rhythms are typical for the dorsomedial SCN, the rhythm of arginine vasopressin (AVP) mRNA expression and AVP peptide formation [72] and the spontaneous rhythm in c-Fos immuno-reactivity [53]. The circadian rhythm of AVP mRNA levels in the SCN of rats maintained under a short LD 8:16 photoperiod differed from that of rats maintained under a long LD 16:8 photoperiod. Under the short photoperiod, the morning AVP mRNA rise occurred by about 4 hours later than that under the long one (Fig. 15)

[72]. Similarly, in rats maintained under the short, LD 8:16 photoperiod or under a natural photoperiod in December, the morning rise in c-Fos immunoreactivity in the dorsomedial SCN occurred by about 4 hours later than that in rats maintained under the long, LD 16:8 photoperiod or under a natural photoperiod in June [71,73]. Apparently, the dorsomedial SCN rhythmicity is also affected by the photoperiod and hence the whole SCN state is photoperiod-dependent.

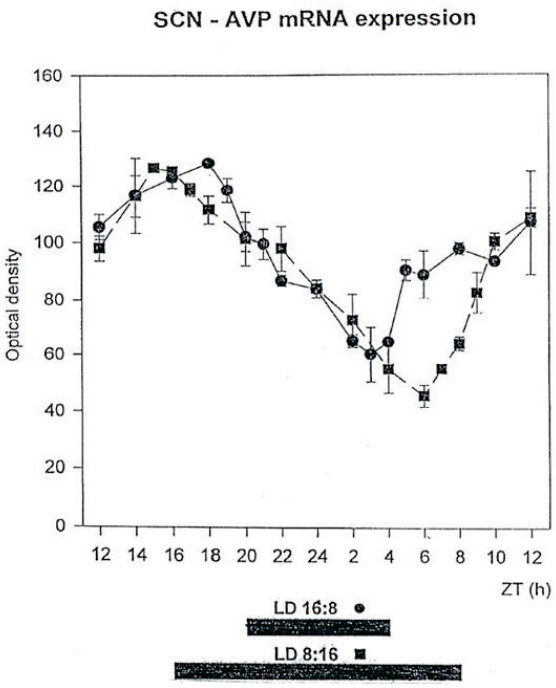

Fig. 15. Daily profiles of arginine vasopressin (AVP) mRNA levels in the SCN of rats maintained either under a long, LD 16:8 (circles) or under a short, LD 8:16 (squares) photoperiod. Bars under the abcissa represent dark periods. Data were taken from [72].

By then, the molecular clockwork in the mammalian SCN has been described, mostly by the groups of Takahashi [74] and Reppert [75]. Eight cloned clock genes are thought to be involved in interacting transcriptional-translational feedback loops that compose the molecular clockwork. We studied the expression of some of the clock genes in the rat SCN under various photoperiods in order to find out whether even the rat molecular clockwork is modulated by the photoperiod. First, we studied the rhythm of a clock gene Per 1 product, PER 1 protein, with the maximum level late in the subjective day and early night and the minimum level in the morning [76]. Under a long, LD 16:8 artificial photoperiod, the interval of elevated PER 1 immunoreactivity was at least by 4 hours longer than that under a short, LD 8:16 photoperiod, due mainly to an earlier PER 1 daytime rise under the long photoperiod [76]. Under a natural photoperiod, profiles of the PER 1 rhythm in summer and in winter resembled those under corresponding artificial photoperiods. Importantly, under all photoperiods, when PER 1 immunoreactivity was elevated, immunopositive cells were localized in the dorsomedial rather than in the ventrolateral SCN [76]. When daily profiles of mRNA of four clock genes, namely of *Per 1*, *Cry 1*, *Bmal 1* and *Clock* were studied under different photoperiods, the photoperiod affected phase, waveform and amplitude of the rhythmic gene expression as well as a phase relationship between their profiles. Under a long photoperiod, the high daytime *Per 1* mRNA expression was lengthened and the high nighttime *Bmal 1* mRNA expression was shortened as compared with the expression under a short photoperiod [77, 78]. Altogether, the whole complex molecular clockwork in the rat SCN appears to be photoperiod dependent and hence it may differ according to the season of the year [77, 78].

A functional divergence among subpopulations of SCN cells may exist not only along the ventrodorsal, but also along the rostro-caudal axis of the SCN [68, 79]. In mice maintained under a long LD 18:6 photoperiod, daily profiles of two clock genes, namely of Per 1 and of Per 2 expression in the rostral and caudal SCN were desynchronized and the peak of expression in the caudal SCN preceded that in the rostral SCN [80]. Following transition of the mice from the long photoperiod to a short LD 6:18 photoperiod, the Per 1 and Per 2 profiles in the rostral SCN became gradually synchronized with those in the caudal SCN; simultaneously, waveform of the rhythms changed as well [81].

Before leaving the fascinating and complex world of the SCN with its gate for photic sensitivity, which, according to my opinion, has not been sufficiently explained, let´s consider shortly another way of entrainment of the SCN, this time not by light, but by the pineal hormone melatonin.

Entrainment of the rhythm in the pineal melatonin production and of the SCN rhythm in the light-induced c-Fos immunoreactivity by melatonin

In 1987, Jiří Vaněček from our laboratory described for the first time the presence of high affinity melatonin binding sites in the SCN of the rat hypothalamus [82]. The presence of melatonin receptors

in the mammalian circadian pacemaker correlated well with the proposed role of melatonin in entrainment of the SCN controlled rhythms such as are the rhythm in the locomotor activity or in the pineal melatonin production. Melatonin injected at 24 h intervals into free running rats maintained in constant darkness entrained them to the 24 h day [83]. Melatonin given to human volunteers in the late afternoon phase-advanced the onset of their own nocturnal melatonin production [84]. When exogenous melatonin was administered to humans at various times with respect to the time of their own melatonin production and the evening onset of melatonin secretion in dim light was used as a phase marker, maximum phase advances of the marker were found when melatonin was administered in the late afternoon; sporadically, some phase delays also occurred when melatonin was administered in the morning hours [85].

In rats maintained on a regime with 10 hours of light and 14 hours of darkness per day, after a single melatonin injection before the dark onset or after administration of melatonin for 5 successive days or after a 4 day treatment with melatonin and a 1 day withdrawal, the evening NAT rise was phase-advanced relative to that in rats treated with vehicle only; the phase shift was larger after a repeated than after a single melatonin injection [86]. Under all the above mentioned paradigms, the evening NAT rise was phase-advanced significantly, while the morning decline was almost not phase shifted. Melatonin administration for 5 consecutive days phase-advanced the evening NAT rise only in rats maintained under a LD 10:14 or a LD 8:16 photoperiods, but not in those maintained under a LD 12:12 photoperiod [87]. Under the longer photoperiod, the end of the light period exhibited a phase delaying effect on the NAT rise and overrode the phase advancing effect of melatonin. Apparently, light is a stronger entraining agent than melatonin.

Melatonin might act by modulating directly the pacemaking system *via* highly sensitive melatonin receptors in the SCN [82]. The *in vitro* exposure of the rat brain hypothalamic slices to melatonin for 1 hour in the late subjective day phase-advanced the SCN circadian rhythm of neuronal firing rate the next day [88]. However, nothing was known about resetting of a SCN circadian oscillation by melatonin *in vivo*. To fill this gap, i.e., to find out whether melatonin applied *in vivo* resets an intrinsic circadian rhythm in the SCN and how rapidly the resetting is accomplished, we chose as a marker of the SCN intrinsic rhythmicity the rhythm in c-Fos photoinduction [55, 56]. Rats were maintained either under a short, LD 8:16 photoperiod, with the dark period starting at 16 h, or under a long LD16:8 photoperiod, with the dark period starting at 20 h. On the day of the experiment, the dark period started as usually at 16 h in short days, whereas in long days the dark onset was advanced to 16 h as well in order to avoid the masking effect of the evening light [87]. Melatonin and vehicle were administered in the late subjective day and thereafter the rats were exposed to a single light pulse at various times (Fig. 16) [89]. In rats maintained under short days, the evening rise in the light-induced c-Fos immunoreactivity in the melatonin-treated rats was phase-advanced by about 1.4 h relative to the rise in the vehicle-treated animals and by about 1.7 h relative to the rise in the intact animals. In rats maintained under long days, the evening rise in the light-induced c-Fos immunoreactivity in the melatonin-treated rats was phase-advanced by 1.5 h relative to the rise in the vehicle-treated animals and by about 1.2 h relative to the rise in the intact animals [89]. Hence, a single melatonin administration to rats during the late day may advance the evening rise in c-Fos photoinduction be it under short or long days when the masking effect of the evening light is avoided. The data indicate that melatonin administration *in vivo* may instantaneously reset the intrinsic SCN rhythmicity. As the rise in the evening c-Fos photoinduction in the SCN is phase-advanced after melatonin administration, the gate for the SCN sensitivity to light and at the same time the SCN gate for phase shifting of circadian rhythms by light might widen. Extension of the gate might partly explain why melatonin administration accelerated reentrainment of the pineal NAT rhythm after an 8 h advance of the light-dark 12:12 cycle [90].

Towards the circadian timekeeping system in mammals

Apart from the central circadian pacemaker within the SCN, the circadian system may consist of numerous peripheral clocks [91]. It appears that biological clocks are most probably present in all organs, tissues and cells. However, the central clock in the SCN is the only one which is entrained directly by environmental light *via* its connections with the retina. Peripheral clocks are entrained to the outside world mostly *via* yet not fully identified neuronal and humoral pathways from the SCN [92]. Altogether, the central

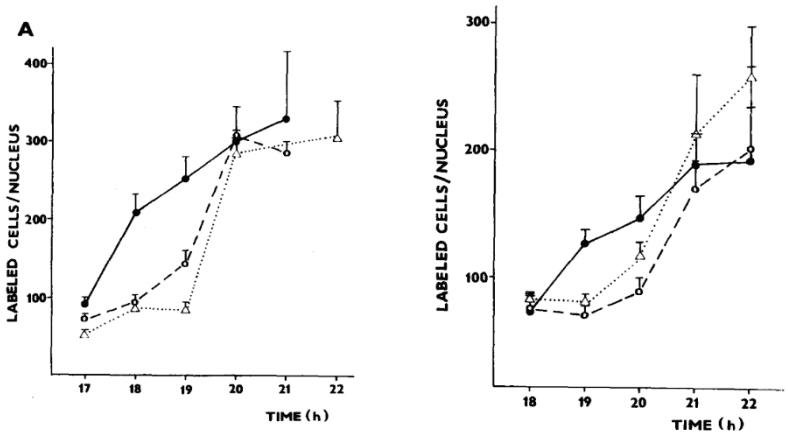

Fig. 16. The effect of melatonin on the evening rise in the light-induced c-Fos immunoreactivity in the suprachiasmatic nucleus of rats maintained originally under a short, LD 8:16 (left) or under a long, LD16:8 (right) photoperiod. On the day of the experiment, the dark period started at 16 h. Rats were either left intact (open triangles, dotted line) or injected with vehicle (open circles, broken line) or with melatonin (closed circles, full line) in the late subjective day, i.e., between 16.30 h and 17.00 h (left) and between 17:30 and 18.00 h (right), respectively. Thereafter, they were exposed to a single 30 min light pulse at various times, returned to darkness and 30 min later they were killed for c-Fos immunoreactivity determination. Data were taken from [89].

SCN clock together with all other clocks and interconnections form a circadian timekeeping system. It is the most integrative system in the body as it integrates all parts to one time, i.e., it keeps all constituent oscillators appropriately phased to each other. Our former Laboratory of Neurohumoral Regulations and nowadays the Laboratory of Biological Rhythms under the guidance of Alena Sumová does not concentrate its attention anymore only to the SCN controlled rhythms in one organ and to the SCN itself, as we had done previously. Instead, it focuses on the circadian system as a whole, namely on central and peripheral clocks and their entrainment by external environment including the mechanism of photic, photoperiodic and non-photic entrainment; on ontogenesis of the circadian system and the mechanisms of how maternal and environmental factors affect the development of the system in mammals; on circadian regulation of physiological function with attention to the circadian regulation of the gastrointestinal tract, the pancreas, the choroid plexus and the hippocampus; on circadian system in humans in health and diseases, mostly on the relationship between the circadian system and neuropsychiatric diseases.

Circadian biology is a marvelous field for research. It teaches us how to live in harmony with the outside day and world. When studying it, you may feel all the time like Alice in Wonderland.

Conflict of Interest

There is no conflict of interest.

Acknowledgement

At the end, I would like to thank my closest collaborators, namely Jiří Vaněček, Alena Sumová and the late Klaus Hoffmann, as well as other collaborators, e.g., Lennart Wetterberg, William J. Schwartz, Martin Sládek, Ivan Hájek, the late Petr Zvolský and Milena Burešová and my students Ludmila Samková, Zdeňka Trávníčková-Bendová, Martin Jáč, Dana Vondrašová-Jelínková and the late Martina Humlová.

I thank also the then European Pineal Study Group, nowadays the European Biological Rhythms Society, for their support in the time of the cold war and for organizing symposia in Poland or Hungary where I was allowed to go.

I thank cordially also David Klein from the National Institute of Health, U.S.A., the best expert on the pineal biochemistry, and the late Jo Arendt from the University of Surrey, Great Britain, the best expert on the pineal physiology, for their generous gifts of isotopes and antibodies to melatonin, respectively.

My thanks go also to the late Jürgen Aschoff from the Max Planck Institute in Andechs, one of the founders of chronobiology from the European side, who invited me to his symposium in the castle Ringberg and introduced me to the then chronobiological community.

And last but not least, I thank the late Colin S. Pittendrigh called Pitt from the Stanford and Princeton University, one of the founders of chronobiology from the American side, for his wonderful papers which showed me the beauty of the circadian biology. Pitt was not only an outstanding scientist but also a great human being. He once sent me an epitaph he had found on a tomb in an English cemetery. In remembrance of Pitt, I would like to share the epitaph for its joy of life with all potential readers.

The wonder of the world,
the beauty and the power,
the shapes of things,
their colors, light and shades.
These I saw.
Look ye also while life lasts.

References

1. Fiske V M, Bryant G K, Putnam J. Effect of light on the weight of the pineal in the rat. Endocrinology 1960; 66: 489-491. https://doi.org/10.1210/endo-66-3-489
2. Quay W B. Pineal Chemistry In Cellular and Physiological Mechanisms. Charles C Thomas, Springfield, Illinois, 1974; pp 1-430.
3. Lerner A B, Case J D, Takahashi Y, Lee T H, Mori W. Isolation of melatonin, the pineal gland factor that lightens melanocytes. J Am Chem Soc 1958; 80: 2587-2591. https://doi.org/10.1021/ja01543a060
4. Lerner A B, Case J D, Heinzelman R V. Structure of melatonin. J Am Chem Soc 1959; 81: 6084-6088. https://doi.org/10.1021/ja01531a060
5. Arendt J. Melatonin and the Mammalian Pineal Gland. Chapman C Hall, London, 1995, pp 1-321.
6. Axelrod J. The pineal gland: a neurochemical transducer. Science 1974; 184:1341-1348. https://doi.org/10.1126/science.184.4144.1341
7. Klein D C. Serotonin N-acetylltransferase. A personal historical perspective. In: Melatonin after Four Decades. J OLCESE (ed). Kluwer Academic, Plenum Publishers, New York 2000, pp 5-16. https://doi.org/10.1007/0-306-46814-X_2
8. Quay W B. Circadian rhythm in the rat pineal serotonin and its modification by estrous cycle and photoperiod. Gen Comp Endocrinol 1963; 31: 473-479. https://doi.org/10.1016/0016-6480(63)90079-0
9. Klein D C, Weller J L. Indole metabolism in the pineal gland. A circadian rhythm in N-acetyltransferase activity. Science 1970; 169: 1093-1095. https://doi.org/10.1126/science.169.3950.1093
10. Illnerová H, Vaněček J. Dynamics of discrete entrainment of the circadian rhythm in the rat pineal N-acetyltransferase activity during transient cycles. J Biol Rhythms 1987; 2: 85-108. https://doi.org/10.1177/074873048700200202
11. Illnerová H. Effect of light on the serotonin content of the pineal gland. Life Sci 1971; 10, Part I: 956-960. https://doi.org/10.1016/0024-3205(71)90360-2
12. Pittendrigh C S. Circadian rhythms and the circadian organization in living systems. In: Cold Spring Harbor Symposia on Quantitative Biology 1960; 25:159-184. https://doi.org/10.1101/SQB.1960.025.01.015
13. Aschoff J. Exogenous and endogenous components in circadian rhythms. In: Cold Spring Harbor Symposia on Quantitative Biolology 1960; 25: 11-28. https://doi.org/10.1101/SQB.1960.025.01.004
14. Klein D C, Weller J L. Rapid light induced decrease in pineal serotonin N-acetyltransferase. Science 1972; 177: 532-533. https://doi.org/10.1126/science.177.4048.532
15. Deguchi T, Axelrod J. Control of circadian change in serotonin N-acetyltransferase in the pineal organ by the beta-adrenergic receptor. Proc Natl Acad Sci U.S.A. 1972; 69: 2547-2550. https://doi.org/10.1073/pnas.69.9.2547
16. Arendt J, Paunier L, Sizonenko P D. Melatonin radioimmunoassay. J Clin Endocr Metab 1975; 40: 347-350. https://doi.org/10.1210/jcem-40-2-347
17. Illnerová H, Backström M, Sääf J, Wetterberg L, Vangbo B. Melatonin in the rat pineal and serum: rapid parallel decline after light exposure at night. Neurosci Lett 1978; 9: 189-193. https://doi.org/10.1016/0304-3940(78)90070-8
18. Illnerová H. Circadian Rhythms in the Mammalian Pineal Gland. Rozpravy Československé akademie věd 1986; 96 (1): pp 1-105.
19. Illnerová H, Vaněček J, Hoffmann K. Regulation of the pineal melatonin concentration in the rat (RATTUS NORVEGICUS) and in the Djungarian hamster (PHODOPUS SUNGORUS). Comp Biochem Physiol 1983; 74 A: 155-159. https://doi.org/10.1016/0300-9629(83)90727-2
20. Illnerová H, Vaněček J, Křeček J, Wetterberg L, Sääf J. Effect of one minute exposure to light at night on rat pineal serotonin N-acetyltransferase and melatonin. J Neurochem 1979; 32: 673-675. https://doi.org/10.1111/j.1471-4159.1979.tb00407.x
21. Illnerová H, Vaněček J. Response of the rat pineal serotonin N-acetyltransferase to one min light pulse at different night times. Brain Res 1979; 167:431-434. https://doi.org/10.1016/0006-8993(79)90841-2

22. Illnerová H, Vaněček J. Two oscillator structure of the pacemaker controlling the circadian rhythm of N-acetyltransferase in the rat pineal gland. J Comp Physiol 1982; 145: 539-548. https://doi.org/10.1007/BF00612819
23. Illnerová H. Entrainment of Mammalian Circadian Rhythms in Melatonin Production by Light. Pineal Research Reviews 1988; 6:173-217.
24. Illnerová H, Vaněček J. Complex contol of the circadian rhythm in N-acetyltransferase activity in the rat pineal gland. In: Vertebrate Circadian Systems. J ASCHOFF, S DAAN, G GROSS (eds). Springer Verlag, Berlin, Heidelberg, 1982; pp 285-291. https://doi.org/10.1007/978-3-642-68651-1_32
25. Illnerová H. Vaněček J. Complex control of the circadian rhythm in pineal melatonin production. In: The Pineal. Current State of Pineal Research. B MESS, Cs RÚZSÁS, L TIMA, P PÉVET (eds). Akadémiai Kiadó, Budapest and Elsevier, Amsterdam 1985; pp 137-153.
26. Illnerová H, Vaněček J. Entrainment of the rat pineal rhythm in melatonin production by light. Reprod Nutr Develop 1988; 28: 515-526. https://doi.org/10.1051/rnd:19880315
27. Illnerová H, Vaněček J, Hoffmann K. Different mechanisms of phase delays and phase advances of the circadian rhythm in the rat pineal N-acetyltransferase activity. J Biol Rhythms 1989; 4: 187-200. https://doi.org/10.1177/074873048900400207
28. Illnerová H, Vaněček J, Hoffmann K. Adjustment of the rat pineal N-acetyltransferase rhythm to eight hour shifts of the light-dark cycle: advance of the cycle disturbs the rhythm more than delay. Brain Res 1987; 417: 167-171. https://doi.org/10.1016/0006-8993(87)90194-6
29. Humlová M, Illnerová H. Rate of re-entrainment of circadian rhythms to advances of light-dark cycles may depend on ways of shifting the cycles. Brain Res 1990; 531: 304-306. https://doi.org/10.1016/0006-8993(90)90790-I
30. Pittendrigh C S, Daan S. A functional analysis of circadian pacemakers in nocturnal rodents. V. Pacemaker structure: A clock for all seasons. J Comp Physiol 1976; 103: 333-355. https://doi.org/10.1007/BF01417860
31. Illnerová H, Vaněček J. Entrainment of the circadian rhythm in the rat pineal N-acetyltransferase activity by prolonged periods of light. J Comp Physiol A 1987;165: 495-510. https://doi.org/10.1007/BF00603974
32. Illnerová H, Vaněček J. Pineal rhythm in N-acetyltransferase activity in rats under different artificial photoperiods and in natural daylight in the course of a year. Neuroendocrinology 1980; 31: 321-326. https://doi.org/10.1159/000123095
33. Rollag M D, Panke E S, Reiter R J. Pineal melatonin content in male hamsters throughout the seasonal reproductive cycle. Proc Soc Exp Biol and Med 1980; 165: 330-334. https://doi.org/10.3181/00379727-165-40981
34. Arendt J, Symons A M, Laud C. Pineal function in the sheep: evidence for possible mechanism mediating seasonal reproductive activity. Experientia 1981; 37: 584-586. https://doi.org/10.1007/BF01990063
35. Hoffmann K, Illnerová H, Vaněček J. Effect of photoperiod and of one minute light at night-time on the pineal rhythm in N-acetyltransferase activity in the Djungarian hamster Phodopus sungorus. Biol Reprod 1981; 24: 551-556. https://doi.org/10.1095/biolreprod24.3.551
36. Petterborg L, Richardson B A, Reiter R J. Effect of long and short photoperiod on pineal melatonin content in the white-footed mouse , Peromyscus leucopus. Life Sci 1981; 29: 1623-1627. https://doi.org/10.1016/0024-3205(81)90063-1
37. Illnerová H, Vaněček J. The evening rise in the rat pineal N-acetyltransferase activity under various photoperiods. Neurosci Lett 1983; 36: 279-284. https://doi.org/10.1016/0304-3940(83)90013-7
38. Illnerová H. The suprachiasmatic nucleus and rhythmic pineal melatonin production. In: *Suprachiasmatic Nucleus. The Mind's Clock*. DC Klein, RY Moore, SM Reppert (eds). Oxford University Press, New York, Oxford 1991; pp 197-216.
39. Illnerová H, Hoffmann K, Vaněček J. Adjustment of the rat pineal N-acetyltransferase rhythm to a change from long to short photoperiod depends on the direction of the extension of the dark period. Brain Res 1985; 362: 403-408. https://doi.org/10.1016/0006-8993(86)90473-7
40. Beck-Fries D, Van Rosen D, Kjelmann, B F, Ljungren J G, Wetterberg L. Melatonin in relation to body measures, sex, age, season and the use of drugs in patients with major affective disorders and healthy subjects. Psychoneuroendocrinology 1985;10: 173-183.

41. Makkison J, Arendt J. Melatonin secretion in humans on two different arctic bases (68° and 75°S). J Interdisc Cycle Res 1991; 22:149-150.
42. Illnerová H, Zvolský P, Vaněček J. The circadian rhythm in plasma melatonin concentration of the urbanized man: the effect of summer and winter time. Brain Res 1985; 328: 186-189. https://doi.org/10.1016/0006-8993(85)91342-3
43. Vondrašova D, Hájek I, Illnerová H. Exposure to long summer days affects the human melatonin and cortisol rhythms. Brain Res 1997; 759: 166-170. https://doi.org/10.1016/S0006-8993(97)00358-2
44. Illnerová H, Hoffmann K, Vaněček J. Adjustment of pineal melatonin and N-acetyltransferase rhythms to change from long to short photoperiod in the Djungarian hamster Phodopus sungorus. Neuroendocrinology 1984; 38: 226-231. https://doi.org/10.1159/000123895
45. Hoffmann K, Illnerová H. Photoperiodic effects in the Djungarian hamster. Rate of testicular regression and extension of pineal melatonin pattern depends on the way of change from long to short photoperiod. Neuroendocrinology 1986; 43: 317-321. https://doi.org/10.1159/000124562
46. Carter D S, Goldman B D. Antigonadal effects of timed melatonin infusion in pinealectomized male Djungarian hamsters Phodopus sungorus: duration is the critical parameter. Endocrinology 1983;113: 1261-1267. https://doi.org/10.1210/endo-113-4-1261
47. Carter D S, Goldman B D., Progonadal role of the pineal in the Djungarian hamster (Phodopus sungorus): mediation by melatonin. Endocrinology 1983; 113: 1268-1273. https://doi.org/10.1210/endo-113-4-1268
48. Hoffmann K, Illnerová H, Vaněček J. Change in duration of the nighttime melatonin peak may be a signal driving photoperiodic responses in the Djungarian hamsters (Phodopus sungorus). Neurosci Lett 1986; 67: 68-72. https://doi.org/10.1016/0304-3940(86)90210-7
49. Illnerová H, Vaněček J. Entrainment of the circadian rhythm in rat pineal N-acetyltransferase under extremely long and short photoperiods. J Pineal Res 1985; 2: 67-78. https://doi.org/10.1111/j.1600-079X.1985.tb00628.x
50. Klein D C, Moore R J. Pineal N-acetyltransferase and hydroxyindole- O-methyltransferase : control by the retinal hypothalamic tract and the suprachiasmatic nucleus. Brain Res 1979; 174: 245-262. https://doi.org/10.1016/0006-8993(79)90848-5
51. Moore R Y, Eichler V B. Loss of a circadian adrenal corticosteron rhythm following suprachiasmatic lesions in the rat. Brain Res 1972; 42: 201-206. https://doi.org/10.1016/0006-8993(72)90054-6
52. Stephan F K, Zucker J. Circadian rhythms in drinking, behavior and locomotor activity of rats are eliminated by hypothalamic lesions. Proc Natl Acad Sci U.S.A. 1972; 69:1583-1586. https://doi.org/10.1073/pnas.69.6.1583
53. Sumová A, Trávníčková Z, Mikkelsen J D, Illnerová H. Spontaneous rhythm in c-Fos immunoreactivity in the dorsomedial part of the rat suprachiasmatic nucleus. Brain Res 1998; 801: 254-258. https://doi.org/10.1016/S0006-8993(98)00619-2
54. Moore R Y, Speh J C, Leak R K. Suprachiasmatic nucleus organization. Cell Tissue Res 2002; 309: 89-98. https://doi.org/10.1007/s00441-002-0575-2
55. Schwartz W J, Aronin N, Takeuchi J, Bennet MR, Peters R J. Towards a molecular biology of the suprachiasmatic nucleus: photic and temporal regulation of c-fos gene expression. Semin Neurosci 1995; 7: 53-60. https://doi.org/10.1016/1044-5765(95)90017-9
56. Sumová A, Trávníčková Z, Peters R, Schwartz W J, Illnerová H. The rat suprachiasmatic nucleus is a clock for all seasons. Proc Natl Acad Sci U.S.A. 1995; 92: 7754-7758. https://doi.org/10.1073/pnas.92.17.7754
57. Kornhauser J M, Mayo K M, Takahashi J S. Immediate-early genes expression in a mammalian circadian pacemaker, the suprachiasmatic nucleus. In: *Molecular Genetics of Biological Rhythms*. MW Young (ed), Dekker, New York, 1993; pp 271-307.
58. Sumová A, Illnerová H. Photic resetting of intrinsic rhythmicity of the rat suprachiasmatic nucleus under various photoperiods. Am J Physiol 1998; 274 (Regulatory Integrative Comp Physiol 43): R 857-R 863. https://doi.org/10.1152/ajpregu.1998.274.3.R857
59. Trávníčková Z, Sumová A, Peters R, Schwartz W J, Illnerová H. Photoperiod-dependent correlation between light-induced SCN c-fos expression and resetting of circadian phase. Am J Physiol 1996; 271 (Regulatory Integrative Comp Physiol 40): R 825-R 831. https://doi.org/10.1152/ajpregu.1996.271.4.R825

60. Jelínková D, Illnerová H, Sumová A. Gate for photic resetting of intrinsic rhythmicity of the rat suprachiasmatic nucleus under a long photoperiod. Neurosci Lett 2000; 280: 143-146. https://doi.org/10.1016/S0304-3940(00)00773-4
61. Sumová A, Illnerová H. Endogenous melatonin signal does not mediate the effect of photoperiod on the rat suprachiasmatic nucleus. Brain Res 1996; 725: 281-283. https://doi.org/10.1016/0006-8993(96)00408-8
62. Schwartz W J, de la Iglesia H O, Zlomanczuk P, Illnerová H. Encoding Le Quatro Stagioni within the Mammalian Brain: Photoperiodic Orchestration through the Suprachiasmatic Nucleus. J Biol Rhythms 2001; 16: 302-311. https://doi.org/10.1177/074873001129002024
63. Illnerova H, Sumová A. Photic entrainment of the mammalian rhythm in melatonin production. J Biol Rhythms 1997; 12: 547-555. https://doi.org/10.1177/074873049701200609
64. Illnerová H, Sumová A, Trávníčková Z, Jáč M, Jelínková D. Hormones, subjective night and season of the year. Physiol Res 2000; 49 (Suppl 1): S1-S10.
65. Jagota A, de la Iglesia H O, Schwartz W J. Morning and evening circadian oscillations in the suprachiasmatic nucleus in vitro. Nature Neurosci 2000; 3: 372-376. https://doi.org/10.1038/73943
66. Stoleru D, Peng Y, Agosto J, Rosbasch M. Coupled oscillators control morning and evening locomotor behaviour in Drosophila. Nature 2004; 431: 862-866. https://doi.org/10.1038/nature02926
67. Lamba P, Bilodeau Wentworth D, Emery P, Zhang Y. Morning and evening oscillators cooperate to reset circadian behaviour in response to light input. Cell Reports 2014; 7: 601-606. https://doi.org/10.1016/j.celrep.2014.03.044
68. Inagaki N, Honma S, Ono D, Tanahashi Y, Honma K. Proc Natl Acad Sci U.S.A, 2007; 104: 7664-7669. https://doi.org/10.1073/pnas.0607713104
69. Hashimoto S, Endo T, Honma S, Yamanaka Y, Honma K. Differential responses to artificial photoperiods of the raising and falling phases of human melatonin rhythm are consistent with a dual oscillator hypothesis. Am J Physiol Regul Integr Comp Physiol 2023; 325: R619-R628. https://doi.org/10.1152/ajpregu.00095.2023
70. Hashimoto S, Endo T, Honma S, Yamanaka Y, Honma K. Two oscillator components detected by forced splitting of the sleep-wake cycle in humans. Am J Physiol Regul Integr Comp Physiol 2024; 326: R19-R28. https://doi.org/10.1152/ajpregu.00094.2023
71. Jáč M, Sumová A, Illnerová H. c Fos rhythm in subdivisions of the rat suprachiasmatic nucleus under artificial and natural photoperiods. Am J Physiol Regul Integr Comp Physiol 2000; 279: R2270-R2276. https://doi.org/10.1152/ajpregu.2000.279.6.R2270
72. Jáč M, Kiss A, Sumová A, Illnerová H, Ježová D. Daily profiles of arginin vasopressin mRNA in the suprachiasmatic, supraoptic and paraventricular nuclei of the rat hypothalamus under various photoperiods. Brain Res 2000; 887: 472-476. https://doi.org/10.1016/S0006-8993(00)03050-X
73. Sumová A, Trávníčková Z, Illnerová H. Spontaneous c-Fos rhythm in the rat suprachiasmatic nucleus: location and effect of photoperiod. Am J Physiol Regul Integr Comp Physiol 2000; 279: R2262-R2269. https://doi.org/10.1152/ajpregu.2000.279.6.R2262
74. King D P, Takahashi J S. Molecular genetics of circadian rhythms in mammals. Annu Rev Neurosci 2000; 23: 713-742. https://doi.org/10.1146/annurev.neuro.23.1.713
75. Reppert S M, Weaver D R. Molecular analysis of mammalian circadian rhythms. Annu Rev Physiol 2001; 63: 647-676. https://doi.org/10.1146/annurev.physiol.63.1.647
76. Sumová A, Sládek M, Jáč M, Illnerová H. The circadian rhythm of Per 1 gene product in the rat suprachiasmatic nucleus and its modulation by seasonal changes in daylength. Brain Res 2002; 947: 260-270. https://doi.org/10.1016/S0006-8993(02)02933-5
77. Sumová A, Jáč M, Sládek M, Šauman I, Illnerová H. Clock gene daily profiles and their phase relationship in the rat suprachiasmatic nucleus are affected by photoperiod. J Biol Rhythms 2003; 18: 134-144. https://doi.org/10.1177/0748730403251801
78. Sumová A, Bendová Z, Sládek M, Kovačíková Z, Illnerová H. Seasonal molecular timekeeping within the rat circadian clock. Physiol Res 2004; 53 (Suppl 1): S167-S176. https://doi.org/10.33549/physiolres.930000.53.S167
79. Hazlerigg D G, Ebling F J. Johnston J D. Photoperiod differentially regulates gene expression rhythms in the rostral and caudal SCN. Curr Biol 2005; 15: R449-R450. https://doi.org/10.1016/j.cub.2005.06.010

80. Sosniyenko S, Hut R A, Daan S, Sumová A. Influence of photoperiod duration and light-dark transition on entrainment of Per 1 and Per 2 gene and protein expression in subdivisions of the mouse suprachiasmatic nucleus. Eur J Neurosci 2009; 30: 1802-1814. https://doi.org/10.1111/j.1460-9568.2009.06945.x
81. Sosniyenko S, Parkanová D, Illnerová H, Sládek M, Sumová A. Different mechanisms of adjustment to a change of the photoperiod in the suprachiasmatic and liver circadian clocks. Am J Physiol Regul Integr Comp Physiol 2010; 298: R959-R971. https://doi.org/10.1152/ajpregu.00561.2009
82. Vaněček J. Pavlík A, Illnerová H. Hypothalamic melatonin receptor sites revealed by autoradiography. Brain Res 1987; 435: 359-362. https://doi.org/10.1016/0006-8993(87)91625-8
83. Redman J, Armstrontg S, Ng K T. Free running activity rhythms in the rat: entrainment by melatonin. Science 1983; 219: 1089-1091. https://doi.org/10.1126/science.6823571
84. Arendt J, Bojkowski C, Folkard S, Franey C, Marks V, Minors D, Waterhouse J, Wever R A, Wildgruber C, Wright J. Some effects of melatonin and the control of its secretion in humans. In: *Ciba Foundation Symposium 117, Photoperiodism, Melatonin and the Pineal*. D Evered, S Clark (eds), Pitman, London 1985; pp 266-283. https://doi.org/10.1002/9780470720981.ch16
85. Lewy A J, Saeeduddin A, Latham-Jackson J M et al. Melatonin shifts human circadian rhythms according to a phase response curve. Chronobiology International 1992; 9: 380-392. https://doi.org/10.3109/07420529209064550
86. Humlová M, Illnerová H. Melatonin entrains the circadian rhythm in the rat pineal N-acetyltransferase activity. Neuroendocrinology 1990; 52: 196-199. https://doi.org/10.1159/000125573
87. Humlová M, Illnerová H. Entrainment of the rat pineal N-acetyltransferase activity by melatonin is photoperiod dependent. J Pineal Res 1992; 13:151-157. https://doi.org/10.1111/j.1600-079X.1992.tb00070.x
88. Mc Arthur A J, Gillette M U, Prosser R A. Melatonin directlyt resets the rat suprachiasmatic clock in vitro. Brain Res 1991; 565: 158-161. https://doi.org/10.1016/0006-8993(91)91748-P
89. Sumová A, Illnerová H. Melatonin instantaneously resets intrinsic circadian rhythmicity in the rat suprachiasmatic nucleus. Neurosci Lett 1996; 218: 181-184. https://doi.org/10.1016/S0304-3940(96)13159-1
90. Illnerová H, Trentini G P, Maslova L. Melatonin accelerates reentrainment of the circadian rhythm of its own production after an 8-h advance of the light dark cycle. J Comp Physiol A 1989; 166: 97-102. https://doi.org/10.1007/BF00190214
91. Balsalobre A, Damiola F, Schibler U. A serum shock induces circadian gene expression ín mammalian tissue culture cells. Cell 1998; 93: 929-937. https://doi.org/10.1016/S0092-8674(00)81199-X
92. Kalsbeek A, Palm I F, La Fleur S E, Scheer S A, Perreau-Lenz S, Reiter M, Kreier F, Cailotto C, Buijs R M. SCN outputs and the hypothalamic balance of life. J Biol Rhythms 2006; 21: 458-469. https://doi.org/10.1177/0748730406293854

REVIEW

Czech Footprints in the Bioenergetics Research

Zdeněk DRAHOTA[1], Josef HOUŠTĚK[1], Alena PECINOVÁ[1]

[1]Laboratory of Bioenergetics, Institute of Physiology, Prague, Czech Republic

Received May 5, 2024
Accepted May 13, 2024

Summary

Life manifests as growth, movement or heat production that occurs thanks to the energy accepted from the outside environment. The basis of energy transduction attracted the Czech researchers since the beginning of the 20th century. It further accelerated after World War II, when the new Institute of Physiology was established in 1954. When it was found that energy is stored in the form of adenosine triphosphate (ATP) that can be used by numerous reactions as energy source and is produced in the process called oxidative phosphorylation localized in mitochondria, the investigation focused on this cellular organelle. Although the Czech scientists had to overcome various obstacles including Communist party leadership, driven by curiosity, boldness, and enthusiasm, they characterized broad spectrum of mitochondrial properties in different tissues in (patho)physiological conditions in collaboration with many world-known laboratories. The current review summarizes the contribution of the Czech scientists to the bioenergetic and mitochondrial research in the global context.

Keywords

Mitochondria • Bioenergetics • Chemiosmotic coupling

Corresponding author

Alena Pecinová, Institute of Physiology, the Czech Academy of Sciences, Vídeňská 1083, Prague, Czech Republic. E-mail: alena.pecinova@fgu.cas.cz

Mitochondria

Bioenergetics is a study of the transformation of energy in living organisms that is tightly connected with the cellular organelles - mitochondria. Research on these organelles began in the middle of the 19th century when their structure was recognized [1]. In 1890, Richard Altmann named these organelles "bioblasts" and concluded that they are elementary organisms inside the cells [2]. Later, Carl Benda started to call them mitochondria (from the Greek "mitos" – thread and "chondros" - granule) because of their tendency to form long chains [3]. However, many important findings were reported before the relationship of these particles to mitochondria was known [1].

In 1913, Otto Warburg linked cellular respiration to particles isolated from guinea pig liver, which he called "grana" [4]. During the late 1930s, significant advancements were made in the elucidation of the reaction pathways and energetics of aerobic metabolism. In 1937, Hans Krebs, Otto Warburg's student formulated the citric acid cycle (CAC) [5] and the first indications of aerobic phosphorylation have been published [6-8]. In the following years, it was found that these particles contain all the enzyme equipment needed for aerobic oxidation of the metabolites from CAC and that it relates to the synthesis of ATP molecule [9,10] and Albert L. Lehninger and colleagues linked oxidative phosphorylation to mitochondria [11]. With the development of thin-sectioning techniques, the first high-resolution images of mitochondria were published (Fig. 1) showing that the mitochondrion possesses cristae (infoldings) created by the inner membrane that are surrounded by the outer membrane [12].

Nevertheless, it took a long time to begin to understand how the energy released by oxido-reduction enzymes is coupled to ADP phosphorylation. The answer to this question was published in 1961 by Peter Mitchell, who proposed a chemiosmotic hypothesis of oxidative phosphorylation [13]. He hypothesized that energy

released in the oxido-reduction chain is stored in the form of a proton gradient across the coupling membrane and that the membrane contains a proton-translocating reversible ATP synthase, which can utilize the proton gradient to synthesize ATP from ADP and P_i. In 1978 he won the Nobel Prize for the chemiosmotic theory (Fig. 2).

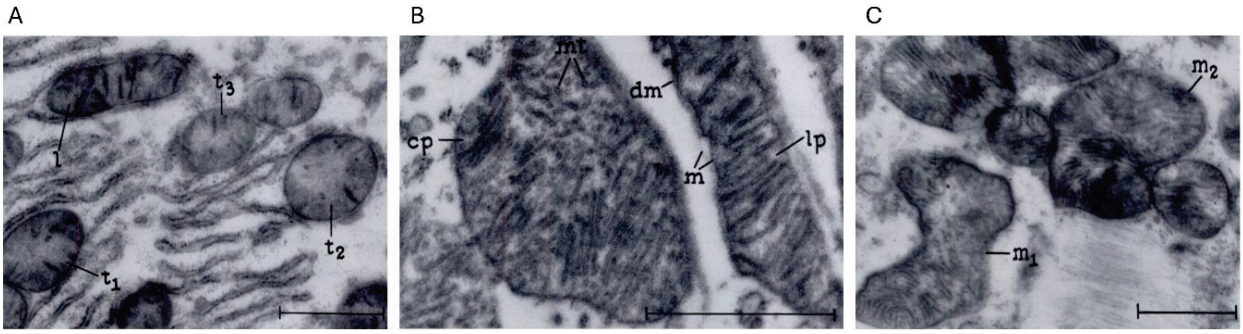

Fig. 1. Electron micrographs of mitochondria from the liver (**A**, magnification: 31,300x), kidney (**B**, magnification: 50,000x), and muscle (**C**, magnification: 30,700x) published by Palade et al., 1953 [12].

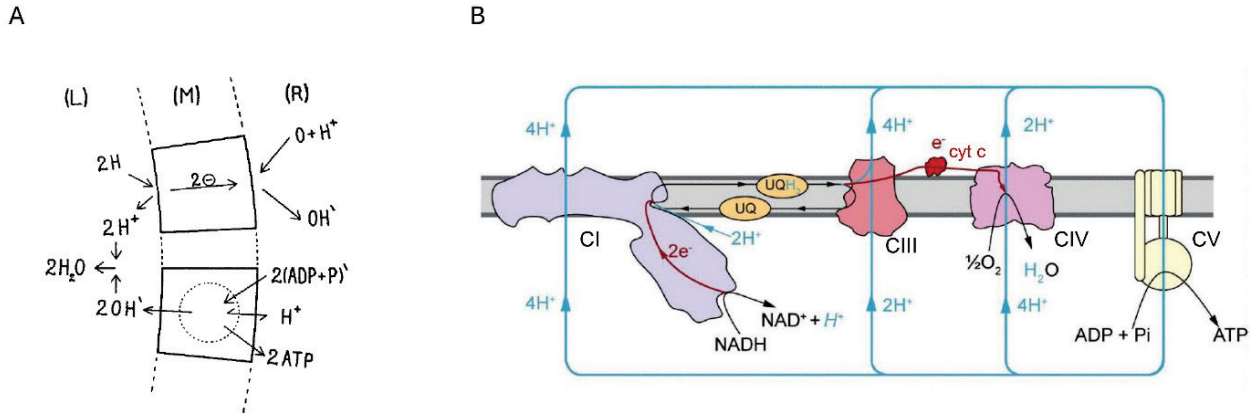

Fig. 2. (**A**) Electron transport system (above) and reversible "ATPase" system (below) chemiosmotically coupled in charge impermeable membrane (M) enclosing aqueous phase (L) in aqueous phase (R) [13]. (**B**) Simplified scheme of the mitochondrial oxidative phosphorylation apparatus consisting of 3 H^+-translocating complexes (CI, III, IV) that transfer electrons from NADH-linked substrates, ubiquinone pool, cytochrome *c* and ATP synthase (CV, complex V) that utilizes energy stored as H^+ gradient across the inner mitochondrial membrane. CI – $4H^+/2e^-$, CIII – $4H^+/2e^-$, CIV – $2H^+/2e^-$, UQ – ubiquinone, UQH_2 – ubiquinol (adapted from [14]).

The Czech bioenergetics beginnings

The beginnings of bioenergetic research in our country date to 1917, when Prof. Edward Babák (1873 – 1926) wrote the book "On the transformation of energies in the living bodies" [15]. In 1933, his student and collaborator Prof. Vilém Laufberger (1890 – 1986), while breaking up hepatocytes [16] isolated small grains, later known as mitochondria. During WWII, an enthusiastic student Arnošt Kleinzeller (1914 – 1997) fled to England from the Nazi regime and studied for many years in the laboratory of Hans Krebs at the University of Sheffield. When he returned to Prague after the war, he established the Cell Metabolism Laboratory and became a lecturer in Biochemistry at the Faculty of Sciences of Charles University. Besides his knowledge, he brought to Prague laboratory equipment including a Warburg respirometer that allowed to measure cellular respiration. He chose five students of Biochemistry – Ladislav Kováč, Arnošt Kotyk, Jiří Čerkasov, Radovan Žák, and Zdeněk Drahota.

"Nature" coincidences

After graduation, Radovan Žák and Zdeněk Drahota started to work at the newly established Institute of Physiology of the Czechoslovak Academy of Sciences (CSAS) under the supervision of Ernest Gutmann. They started to isolate mitochondria from muscle on a Janetzki centrifuge in a cold room and with the limited methods they had at hand, they studied amino acid degradation and with youthful virtue sent their work to *Nature journal*. Due to Gutmann's perfect Oxford English (to the

surprise of the reviewers), the paper was accepted for print [17]. However, the two young men were aware that it was probably pure coincidence. Browsing the *Nature journal*, their attention was caught by an article about the swelling of mitochondria by Samuel V. Perry [18]. They wrote a bold letter to Perry, as his colleagues from Nature, and asked him if he would be so kind to come to Prague for a few days and show them how mitochondria are isolated in Oxford.

No one assumed that Prof. Perry would dare to go behind the Iron Curtain. He came not only to teach the two Prague students to isolate mitochondria, but above all to find a place called "Mährisch Trübau in Böhmen" (Moravská Třebová in the Czech Republic), where he was deported from Africa as a prisoner during the WWII after being captured during the Western Desert Campaign. With the help of an English professor and a homemade refrigerated centrifuge, the mitochondria in Prague were isolated for the first time in the same way as in practices in Oxford. At the same time, the barracks in Moravská Třebová, a former POW camp, were successfully identified, and Prof. Perry exchanged greetings with the mayor and signed the memorial book with great fame. Perry's stay behind the Iron Curtain was successful and the Institute of Physiology obtained a precious friend who returned to Prague with pleasure for the Symposium held in Liblice and, on the other hand, a bed & breakfast was always prepared for the guests from the institute in England.

"Italian "coincidence

Based on these experiences, the mitochondrial research in Prague successfully continued. Since two are better than one and Warsaw is close to Prague, the joint works of the Institute of Physiology CSAS and the Institute of Biology of the Polish Academy of Sciences about the fatty acids oxidation in liver mitochondria soon appeared in *Biochimica et Biophysica Acta* [19]. Luckily, the first author of the publication, Lech Wojtzak, and his wife Anna performed the research at Johns Hopkins Medical School in Baltimore in the laboratory of Albert L. Lehninger, and thus Zdeněk Drahota also got the chance to do the research in this famous lab. He continued with the research on liver mitochondria and discovered that sodium and potassium do not influence calcium-activated respiration and calcium retention capacity [20].

In Baltimore, a third happy accident occurred. During his "sabbatical" in Italy, Prof. Lehninger wrote the famous Biochemistry textbook [21] and his laboratory in Baltimore was always full of Italian students and researchers. The joint Czech-Italian-American publication in the *Journal of Biological Chemistry* [22], which studied in detail the calcium accumulation by mitochondria, represented the first result of a long-lasting collaboration. Thus, Zdeněk Drahota appeared at the first of the series of international Symposia on mitochondria in Italy. These symposia were organized by Ernesto Quagliariello, the rector of the University of Bari, with the support of the committee for the development of tourism in southern Italy. At that time, nobody knew how important this coincidence would be for the development of bioenergetic research at the Institute of Physiology. Prof. Quagliariello soon became the president of the Italian Academy of Sciences (CNR) and he made sure that every bilateral agreement on cooperation between CSAS and CNR, would contain the stay for the bioenergetic researchers in Italy. Then Prof. Quagliariello, in the letter addressed to the president of the CSAS, extended the stay for a few months, claiming that extra costs, of course, would be covered by the Italian side. That is how Ernesto Quagliariello became the first patron of the Czech researchers who have always been very grateful to him for his support.

"Swedish" coincidence

The fourth lucky coincidence gave the bioenergetics research at CSAS new energy and another patron. It started when Jiří Křeček's Department of Developmental Physiology started to sprout. One of his students, Petr Hahn, founded a Laboratory of the Development of Metabolic Functions. The group was interested in lipid metabolism and mitochondria, and in collaboration with the Institute for Mother and Child Care studied the regulation of lipid metabolism in newborns. Their results were utilized during the development of the new infant formula enriched with lipids [23]. At that time, a new physiological-bioenergetic function was demonstrated - the thermogenic function of brown adipose tissue [24]. From there, it was only a step to the idea to see what substrate brown fat mitochondria utilize to generate heat. Therefore, Zdeněk Drahota and Eva Honová isolated mitochondria from brown fat, and after a series of experiments they demonstrated high oxidation of carnitine esters of fatty acids. Together with Marie Schutzová they prepared the graphs and Petr Hahn, while lying on the divan, dictated the first version of the manuscript to his wife Nada, and in a few days the text

was on its way to Switzerland to the *Experientia journal* [25]. As soon as the article was published, a letter arrived from Olov Lindberg, the director of the Wenner-Gren Institute of the University in Stockholm and a world-known scientist in brown adipose tissue research [26]. Due to his high moral qualities and the character of a calm Northerner, he was not upset that this "short communication" was published a few months earlier than his "full paper" and generously invited members of Hahn's group to cooperate. As he later stated, another reason for his friendly help was that he felt personal responsibility for the damage caused by the Swedish army by the end of the Thirty Years' War at Prague Castle.

Similarly to the first Italian patron and Prof. Lindberg, a member of the Royal Swedish Academy, made sure that the bilateral cooperation agreement between the Royal Swedish Academy and CSAS always included the topic of "Thermogenetic function of brown adipose tissue", and he also extended the stays of the Czech partners in Stockholm from weeks to months. In exchange, the members of the Swedish laboratory used to come for discussion on the mechanisms of thermogenesis organized by Zdeněk Drahota's students and collaborators: Josef Houštěk, Petr Svoboda, and Jan Kopecký. The scientific discussions were accompanied by hiking and the consumption of incredibly good and cheap beer in the mountain huts. It was the beginning of long-lasting cooperation.

1968

When the year 1968 was approaching, the 5th meeting of the Federation of European Biochemical Societies (FEBS) was being prepared in Prague. One of the topical subjects was "Mitochondrial Structure and Function" which was proposed by Dr. Drahota from the Institute of Physiology CSAS during the first discussions, which symposia would be included in the program. Just after the committee's meeting, Lars Ernster, a mitochondrial physiologist, who mentored many foreign students, received a phone request to organize this symposium. He immediately accepted. The very next day, the requests for symposia from other institutes appeared. However, to cancel the symposium organized by this distinguished biochemist, Olov Lindberg's student, director of the Institute of Biochemistry of the Royal Swedish Academy, and a member of the Nobel Committee for Chemistry was no longer feasible. Thus, the mitochondrial symposium survived.

The meeting preparations culminated during the "Prague Spring". An incredible number of people poured into Prague for the symposium on mitochondria, not only because of the mitochondria, but because they also wanted to know what was happening in Prague.

When the mitochondrial researchers arrived in Prague in July, they were surprised at how little excited the organizers about the current situation were. When saying goodbye at the end of the congress, the Italian patrons assured the organizers from the Institute of Physiology that they could always count on Italian friends. The Swedish patron heartily shook both hands and even without words, everything was clear. Nobody realized that some weeks later the "Prague Spring" would end abruptly in an unbelievable disaster during the shocking and sad days of August 1968 and how important would be the support of the patrons for the bioenergetic research at the Institute of Physiology CSAS to survive the next 20 years.

Normalization

A few weeks after the entrance of the troops of Warsaw Pact countries into Czechoslovakia, the researchers interested in mitochondria Petr Hahn and Josef Houštěk were already in England, and Zdeněk Drahota in Italy. When Zdeněk Drahota and Josef Houštěk met in the half-empty institute in 1969, mitochondrial research started to wake up only slowly. The normalization policy of the Communist Party led to the emigration of many researchers, others could not attend international meetings or proceed with their research at all. Nevertheless, new young colleagues appeared and the patrons in Italy and Sweden kept the doors open.

At the beginning of the 1970s, the collaboration with Stockholm University focused on the function of the brown adipose tissue started to take shape. First, the uncoupling mechanism via uncoupling protein 1 (UCP1) and its regulation was studied [27]. Later, also other complexes specific to the brown adipose tissue and involved in mitochondrial metabolism were investigated. Together with Barbara Cannon and Olov Lindberg, Josef Houštěk found that mitochondrial glycerol-3-phosphate dehydrogenase activity is high in this tissue compared to other tissues [28]. When possible, international congresses, symposia, and courses were organized. In particular, the 4th European Bioenergetics Conference

organized in Prague in 1986 further stimulated mitochondrial research and attracted young talented students (Fig. 3). It certainly contributed to the development of the independent research programs of the laboratory members and building of several new scientific laboratories within the institute, including Department of Bioenergetics with Josef Houštěk as the head. Two other departments also focused their research on mitochondria – Petr Ježek's group investigated the role of uncoupling proteins and oxidative stress, and Jan Kopecký's department further explored thermogenesis in the fat and muscle tissue and obesity in general.

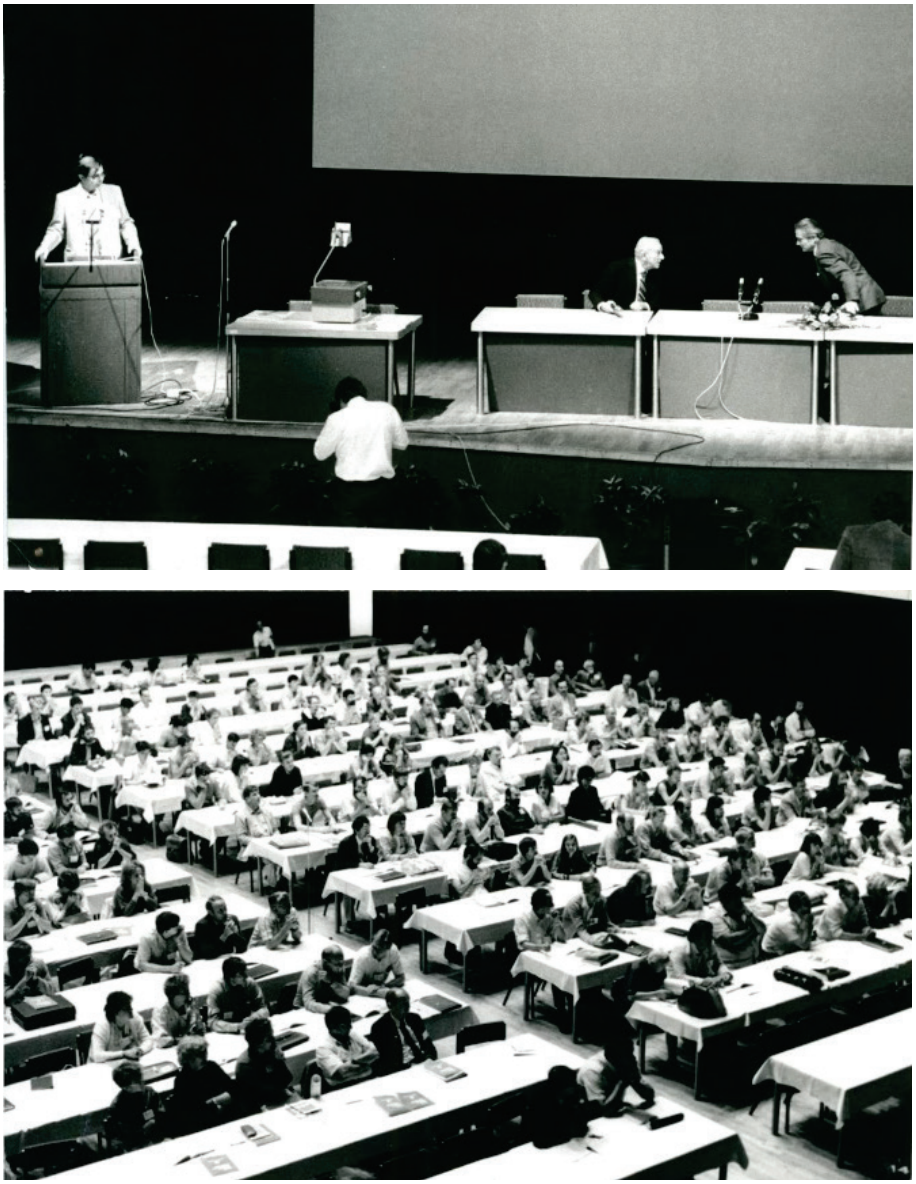

Fig. 3. 4th European Bioenergetics Conference (EBEC) in 1986 in Prague, Czechoslovakia. Left (from left to right): Josef Houštěk, Lars Ernster, and Zdeněk Drahota.

Collaboration with the Italian scientists was focused on the mitochondrial ATP synthase and with the groups from Bari they investigated ATP synthase inhibitor - DCCD (dicyclohexylcarbodiimide) [29]. They found that, besides inhibiting proton-pumping enzymes, e.g. ATP synthase, it also binds to another 33 kDa mitochondrial transport protein [30]. Later, in collaboration with the group of Štefan Kužela from Bratislava, they proposed that DCCD also binds to UCP1 protein in brown adipose tissue [31]. With the group of Giorgio Lenaz from Bologna, they identified two distinct, temperature-dependent states of the F_1 domain of ATP synthase (hydrophilic part) [32].

August 1968, the Soviet occupation of our country and the following communist persecutions slowed down the scientific career of many researchers,

Fig. 4. 36th International Conference on Bioenergetics in 2023.

among them also Štefan Kužela from the Institute of Experimental Oncology CSAS. Despite the persecution, he remained active and further promoted unique mitochondrial genetics studies in Bratislava. Illegal seminars in his office also initiated the unofficial winter Czechoslovak conferences on Bioenergetics, which continue to these days (Fig. 4).

1989

The change of the regime after the Velvet Revolution in November 1989, allowed to travel and collaborate freely even with people who emigrated after 1968. The research in Prague on brown adipose tissue continued in cooperation with the groups from Stockholm. It focused on the low capacity of mitochondrial ATP synthase in brown adipose tissue compared to other tissues. It was published that the abundant pool of mRNA of the β subunit is not fully translatable and thus it may account for the decreased content of mitochondrial ATP synthase [33,34]. Further, high levels of transcripts of other subunits were detected, except for the subunit *c*. It suggested that the expression of subunit *c* and its synthesis critically controls the biosynthesis of the whole ATP synthase [35]. The joint studies on UCP1 and its function in brown adipose tissue were focused on hormonal regulation of UCP1 expression [36] adrenergic receptors [37,38], or the role of interleukins [39,40]. A recent study also showed that UCP1 is involved in the control of reactive oxygen species generation [41].

During the 1990s increasing attention was paid to mitochondrial disorders causing human disease. The first publications arose from the collaborations with the laboratory of Coby van den Bogert at The Academic Medical Center in Amsterdam and long-lasting cooperation with Jiří Zeman from the Department of Pediatrics (First Faculty of Medicine, Charles University). In patients with atypical NARP/LS syndrome and impaired ATP synthase [42,43] they observed mtDNA defects caused by *ATP6* mutations in subunit *a* [44,45]. In 1999, the case of the first patient with ATP synthase defect of nuclear origin was published [46]. The ATP synthase complex was selectively reduced, and the newly synthesized enzyme had the same subunit composition as control, implying the altered biosynthesis

of the enzyme. Nine years later, in cooperation with the groups of Wolfgang Sperl from Salzburg and Stanislav Kmoch from the Institute of Inherited Metabolic Disorders in Prague, the *TMEM70* gene was identified as the disease-causing gene, which also uncovered TMEM70 protein as novel specific biogenetics factor of mammalian ATP synthase [47-49]. Within this cooperation, also the first patient with somatic mutation in ATP synthase subunit ε was described [50]. In collaboration with Catherine Godinot's group from Lyon, the functional alterations of patients with disordered cytochrome *c* oxidase assembly factor SURF1 were described [51]. This collaboration further continued and a series of papers studying the role of oxidative phosphorylation in cancer was published [52,53]. All these efforts stimulated further the interest in elucidation of the molecular basis of various inherited mitochondrial disorders and led to numerous joint international research projects in successive years.

With the expansion of the laboratory, the research interests and collaboration also expanded. Thus, the ability of glycerol-3-phosphate dehydrogenase to produce reactive oxygen species [54-56] and its interaction with the coenzyme Q pool [57] were investigated together with the group of Giorgio Lenaz. Within the Czech Republic, cooperation with the laboratory of Zuzana Červinková from the Faculty of Medicine in Hradec Králové developed during the 1990s. Their research focused on the effect of triiodothyronine on regenerating liver [58-60], the role of oxidative stress [61-63] and mitochondrial membrane permeability [64-67]. Also, the ambiguous effect of biguanides (the most common treatment of type II diabetes) on oxidative phosphorylation was studied [68,69].

Since 1917, when Edward Babák described living organisms as energy convertors [15], bioenergetics research in the Czech Republic has advanced greatly with significant input from studies originating from and/or performed at the Institute of Physiology, Czech Academy of Sciences. It would not have been possible without the enthusiastic scientists and the scientists would not be enthusiastic without the initial ignition by their teachers.

"*Scientists are not so much born as made by those who teach them research*" Sir Hans Krebs

Acknowledgements

This work was supported by the project National Institute for Research of Metabolic and Cardiovascular Diseases (Programme EXCELES, ID Project No. LX22NPO5104) - Funded by the European Union - Next Generation EU.

Conflict of Interest

There is no conflict of interest.

References

1. Ernster L, Schatz G. Mitochondria: a historical review. J Cell Biol 1981;91:227s-255s. https://doi.org/10.1083/jcb.91.3.227s
2. Altman R. Die Elementarorganismen und ihre Beziehungen zu den Zellen (The cellular organelles and their relations to cells). Leipzig, Germany: Veit & Co.; 1890. p. 1.
3. Benda C. Weitere Mitteilungen über die Mitochondria. Verh Dtsch Physiol Ges 1898:376-383.
4. Warburg O. Uber sauerstoffatmende Kornchen aus Leberzellen und uber Sauerstoffatmung in Berkefeld-Filtraten wassriger Leberextrakte. Pfluger's Arch ges Physiol 1913;154:599-617. https://doi.org/10.1007/BF01681207
5. Krebs HA, Johnson WA. Metabolism of ketonic acids in animal tissues. Biochem J 1937;31:645-660. https://doi.org/10.1042/bj0310645
6. Belitser VATET. The mechanism of phosphorylation associated with respiration. Biokhimiya 1939;4:516-535.
7. Engelhardt WA. [Ortho- and pyrophosphate in aerobic and anaerobic metabolism of erythrocytes (Biochem. Zeitschrift, 227, 16-38, 1930)]. Mol Biol (Mosk) 1930;28:1210-1217.
8. Kalckar H. Phosphorylation in kidney tissues. Enzymologia 1937;2:47-52. https://doi.org/10.1103/PhysRev.52.273
9. Lehninger AL. On the activation of fatty acid oxidation. J Biol Chem 1945;161:437-451. https://doi.org/10.1016/S0021-9258(17)41479-7, https://doi.org/10.1016/S0021-9258(17)41557-2
10. Ochoa S. Efficiency of aerobic phosphorylation in cell-free heart extracts. J Biol Chem 1943;151:493-505. https://doi.org/10.1016/S0021-9258(18)44922-8
11. Kennedy EP, Lehninger AL. Oxidation of fatty acids and tricarboxylic acid cycle intermediates by isolated rat liver mitochondria. J Biol Chem 1949;179:957-972. https://doi.org/10.1016/S0021-9258(19)51289-3

12. Palade GE. An electron microscope study of the mitochondrial structure. J Histochem Cytochem 1953;1:188-211. https://doi.org/10.1177/1.4.188
13. Mitchell P. Coupling of phosphorylation to electron and hydrogen transfer by a chemi-osmotic type of mechanism. Nature 1961;191:144-148. https://doi.org/10.1038/191144a0
14. Nicholls DG, Ferguson SJ. Bioenergetics. Fourth edition / ed. Amsterdam: Academic Press, Elsevier; 2013.
15. Babák E. On the transformation of energies in the living bodies (in Czech). Prague: Jos. R. Vilímek; 1917.
16. Laufberger V. Désintégration de la cellule. (in Czech) Brno: Spisy Lék. fak. Masarykovy univ v Brně; 1933.
17. Zak R, Drahota Z. Release of methionine labelled with sulphur-35 from muscle tissue and mitochondria. Nature 1960;186:973-974. https://doi.org/10.1038/186973a0
18. Chappell JB, Perry SV. Biochemical and osmotic properties of skeletal muscle mitochondria. Nature 1954;173:1094-1095. https://doi.org/10.1038/1731094a0
19. Wojtczak L, Zaluska H, Drahota Z. Evidence for the activation of fatty acids in liver mitochondria by high-energy intermediates for oxidative phosphorylation. Biochim Biophys Acta 1965;98:8-18. https://doi.org/10.1016/0005-2760(65)90003-2
20. Drahota Z, Lehninger AL. Movements of H^+, K^+, and Na^+ during energy-dependent uptake and retention of Ca^{++} in Rat Live Mitochondria. Biochem Biophys Res Commun 1965;19:351-356. https://doi.org/10.1016/0006-291X(65)90467-5
21. Lehninger AL. *Principles of Biochemistry*. First edition ed: Worth Publishers; 1990.
22. Drahota Z, Carafoli E, Rossi CS, Gamble RL, Lehninger AL. The Steady State Maintenance of Accumulated Ca++ in Rat Liver Mitochondria. J Biol Chem 1965;240:2712-2720. https://doi.org/10.1016/S0021-9258(18)97385-0
23. Melichar V, Drahota Z, Hahn P. Ketone bodies in the blood of full term newborns, premature and dysmature infants and infants of diabetic mothers. Biol Neonat 1967;11:23-28. https://doi.org/10.1159/000240051
24. Smith RE. Thermogenic activity of the hibernating gland in the cold-acclimated rat. Physiologist 1961;4:113.
25. Drahota Z, Honova E, Hahn P. The effect of ATP and carnitine on the endogenous respiration of mitochondria from brown adipose tissue. Experientia 1968;24:431-432. https://doi.org/10.1007/BF02144369
26. Lindberg O. *Brown Adipose Tissue*. American Elsevier Pub. Co; 1970.
27. Bulychev A, Kramar R, Drahota Z, Lindberg O. Role of a specific endogenous fatty acid fraction in the coupling-uncoupling mechanism of oxidative phosphorylation of brown adipose tissue. Exp Cell Res 1972;72:169-187. https://doi.org/10.1016/0014-4827(72)90579-4
28. Houstek J, Cannon B, Lindberg O. Gylcerol-3-phosphate shuttle and its function in intermediary metabolism of hamster brown-adipose tissue. Eur J Biochem 1975;54:11-18. https://doi.org/10.1111/j.1432-1033.1975.tb04107.x
29. Kopecky J, Guerrieri F, Papa S. Interaction of dicyclohexylcarbodiimide with the proton-conducting pathway of mitochondrial H+-ATPase. Eur J Biochem 1983;131:17-24. https://doi.org/10.1111/j.1432-1033.1983.tb07226.x
30. Houstek J, Pavelka S, Kopecky J, Drahota Z, Palmieri F. Is the mitochondrial dicyclohexylcarbodiimide-reactive protein of Mr 33 000 identical with the phosphate transport protein? FEBS Lett 1981;130:137-140. https://doi.org/10.1016/0014-5793(81)80682-5
31. Kolarov J, Houstek J, Kopecky J, Kuzela S. The binding of dicyclohexylcarbodiimide to uncoupling protein in brown adipose tissue mitochondria. FEBS Lett 1982;144:6-10. https://doi.org/10.1016/0014-5793(82)80557-7
32. Baracca A, Amler E, Solaini G, Parenti Castelli G, Lenaz G, Houstek J. Temperature-induced states of isolated F1-ATPase affect catalysis, enzyme conformation and high-affinity nucleotide binding sites. Biochim Biophys Acta 1989;976:77-84. https://doi.org/10.1016/S0005-2728(89)80191-4
33. Houstek J, Tvrdik P, Pavelka S, Baudysova M. Low content of mitochondrial ATPase in brown adipose tissue is the result of post-transcriptional regulation. FEBS Lett 1991;294:191-194. https://doi.org/10.1016/0014-5793(91)80666-Q
34. Tvrdik P, Kuzela S, Houstek J. Low translational efficiency of the F1-ATPase beta-subunit mRNA largely accounts for the decreased ATPase content in brown adipose tissue mitochondria. FEBS Lett 1992;313:23-26. https://doi.org/10.1016/0014-5793(92)81175-L
35. Houstek J, Andersson U, Tvrdik P, Nedergaard J, Cannon B. The expression of subunit c correlates with and thus may limit the biosynthesis of the mitochondrial F0F1-ATPase in brown adipose tissue. J Biol Chem 1995;270:7689-7694. https://doi.org/10.1074/jbc.270.13.7689

36. Rehnmark S, Kopecky J, Jacobsson A, Nechad M, Herron D, Nelson BD, Obregon MJ, Nedergaard J, Cannon B. Brown adipocytes differentiated in vitro can express the gene for the uncoupling protein thermogenin: effects of hypothyroidism and norepinephrine. Exp Cell Res 1989;182:75-83. https://doi.org/10.1016/0014-4827(89)90280-2
37. Svartengren J, Svoboda P, Cannon B. Desensitisation of beta-adrenergic responsiveness in vivo. Decreased coupling between receptors and adenylate cyclase in isolated brown-fat cells. Eur J Biochem 1982;128:481-488. https://doi.org/10.1111/j.1432-1033.1982.tb06990.x
38. Svoboda P, Svartengren J, Snochowski M, Houstek J, Cannon B. High number of high-affinity binding sites for (-)-[3H]dihydroalprenolol on isolated hamster brown-fat cells. A study of the beta-adrenergic receptors. Eur J Biochem 1979;102:203-210. https://doi.org/10.1111/j.1432-1033.1979.tb06281.x
39. Cannon B, Houstek J, Nedergaard J. Brown adipose tissue. More than an effector of thermogenesis? Ann N Y Acad Sci 1998;856:171-187. https://doi.org/10.1111/j.1749-6632.1998.tb08325.x
40. Mracek T, Cannon B, Houstek J. IL-1 and LPS but not IL-6 inhibit differentiation and downregulate PPAR gamma in brown adipocytes. Cytokine 2004;26:9-15. https://doi.org/10.1016/j.cyto.2003.12.001
41. Shabalina IG, Vrbacky M, Pecinova A, Kalinovich AV, Drahota Z, Houstek J, Mracek T, Cannon B, Nedergaard J. ROS production in brown adipose tissue mitochondria: the question of UCP1-dependence. Biochim Biophys Acta 2014;1837:2017-2030. https://doi.org/10.1016/j.bbabio.2014.04.005
42. Klement P, Nijtmans LG, Van den Bogert C, Houstek J. Analysis of oxidative phosphorylation complexes in cultured human fibroblasts and amniocytes by blue-native-electrophoresis using mitoplasts isolated with the help of digitonin. Anal Biochem 1995;231:218-224. https://doi.org/10.1006/abio.1995.1523
43. Nijtmans LG, Klement P, Houstek J, van den Bogert C. Assembly of mitochondrial ATP synthase in cultured human cells: implications for mitochondrial diseases. Biochim Biophys Acta 1995;1272:190-198. https://doi.org/10.1016/0925-4439(95)00087-9
44. Houstek J, Klement P, Hermanska J, Houstkova H, Hansikova H, Van den Bogert C, Zeman J. Altered properties of mitochondrial ATP-synthase in patients with a T-->G mutation in the ATPase 6 (subunit a) gene at position 8993 of mtDNA. Biochim Biophys Acta 1995;1271:349-357. https://doi.org/10.1016/0925-4439(95)00063-A
45. Jesina P, Tesarova M, Fornuskova D, Vojtiskova A, Pecina P, Kaplanova V, Hansikova H, Zeman J, Houstek J. Diminished synthesis of subunit a (ATP6) and altered function of ATP synthase and cytochrome c oxidase due to the mtDNA 2 bp microdeletion of TA at positions 9205 and 9206. Biochem J 2004;383:561-571. https://doi.org/10.1042/BJ20040407
46. Houstek J, Klement P, Floryk D, Antonicka H, Hermanska J, Kalous M, Hansikova H, Houstkova H, Chowdhury SK, Rosipal T, Kmoch S, Stratilova L, Zeman J. A novel deficiency of mitochondrial ATPase of nuclear origin. Hum Mol Genet 1999;8:1967-1974. https://doi.org/10.1093/hmg/8.11.1967
47. Cizkova A, Stranecky V, Mayr JA, Tesarova M, Havlickova V, Paul J, Ivanek R, Kuss AW, Hansikova H, Kaplanova V, Vrbacky M, Hartmannova H, Noskova L, Honzik T, Drahota Z, Magner M, Hejzlarova K, Sperl W, Zeman J, Houstek J, Kmoch S. TMEM70 mutations cause isolated ATP synthase deficiency and neonatal mitochondrial encephalocardiomyopathy. Nat Genet 2008;40:1288-1290. https://doi.org/10.1038/ng.246
48. Honzik T, Tesarova M, Mayr JA, Hansikova H, Jesina P, Bodamer O, Koch J, Magner M, Freisinger P, Huemer M, Kostkova O, van Coster R, Kmoch S, Houstek J, Sperl W, Zeman J. Mitochondrial encephalocardio-myopathy with early neonatal onset due to TMEM70 mutation. Arch Dis Child 2010;95:296-301. https://doi.org/10.1136/adc.2009.168096
49. Kovalcikova J, Vrbacky M, Pecina P, Tauchmannova K, Nuskova H, Kaplanova V, Brazdova A, Alan L, Elias J, Cunatova K, Korinek V, Sedlacek R, Mracek T, Houstek J. TMEM70 facilitates biogenesis of mammalian ATP synthase by promoting subunit c incorporation into the rotor structure of the enzyme. FASEB J 2019;33:14103-14117. https://doi.org/10.1096/fj.201900685RR
50. Mayr JA, Havlickova V, Zimmermann F, Magler I, Kaplanova V, Jesina P, Pecinova A, Nuskova H, Koch J, Sperl W, Houstek J. Mitochondrial ATP synthase deficiency due to a mutation in the ATP5E gene for the F1 epsilon subunit. Hum Mol Genet 2010;19:3430-3439. https://doi.org/10.1093/hmg/ddq254
51. Pecina P, Capkova M, Chowdhury SK, Drahota Z, Dubot A, Vojtiskova A, Hansikova H, Houstkova H, Zeman J, Godinot C, Houstek J. Functional alteration of cytochrome c oxidase by SURF1 mutations in Leigh syndrome. Biochim Biophys Acta 2003;1639:53-63. https://doi.org/10.1016/S0925-4439(03)00127-3

52. Hervouet E, Cizkova A, Demont J, Vojtiskova A, Pecina P, Franssen-van Hal NL, Keijer J, Simonnet H, Ivanek R, Kmoch S, Godinot C, Houstek J. HIF and reactive oxygen species regulate oxidative phosphorylation in cancer. Carcinogenesis 2008;29:1528-1537. https://doi.org/10.1093/carcin/bgn125
53. Hervouet E, Demont J, Pecina P, Vojtiskova A, Houstek J, Simonnet H, Godinot C. A new role for the von Hippel-Lindau tumor suppressor protein: stimulation of mitochondrial oxidative phosphorylation complex biogenesis. Carcinogenesis 2005;26:531-539. https://doi.org/10.1093/carcin/bgi001
54. Drahota Z, Chowdhury SK, Floryk D, Mracek T, Wilhelm J, Rauchova H, Lenaz G, Houstek J. Glycerophosphate-dependent hydrogen peroxide production by brown adipose tissue mitochondria and its activation by ferricyanide. J Bioenerg Biomembr 2002;34:105-113. https://doi.org/10.1023/A:1015123908918
55. Mracek T, Drahota Z, Houstek J. The function and the role of the mitochondrial glycerol-3-phosphate dehydrogenase in mammalian tissues. Biochim Biophys Acta 2013;1827:401-410. https://doi.org/10.1016/j.bbabio.2012.11.014
56. Mracek T, Pecinova A, Vrbacky M, Drahota Z, Houstek J. High efficiency of ROS production by glycerophosphate dehydrogenase in mammalian mitochondria. Arch Biochem Biophys 2009;481:30-36. https://doi.org/10.1016/j.abb.2008.10.011
57. Rauchova H, Battino M, Fato R, Lenaz G, Drahota Z. Coenzyme Q-pool function in glycerol-3-phosphate oxidation in hamster brown adipose tissue mitochondria. J Bioenerg Biomembr 1992;24:235-241. https://doi.org/10.1007/BF00762682
58. Drahota Z, Rauchova H, Sedlak V, Koci J, Cervinkova Z. The effect of triiodothyronine on changes of membrane fluidity in regenerating rat liver. Physiol Res 1999;48:167-170.
59. Mracek T, Jesina P, Krivakova P, Bolehovska R, Cervinkova Z, Drahota Z, Houstek J. Time-course of hormonal induction of mitochondrial glycerophosphate dehydrogenase biogenesis in rat liver. Biochim Biophys Acta 2005;1726:217-223. https://doi.org/10.1016/j.bbagen.2005.06.011
60. Svatkova R, Cervinkova Z, Kalous M, Rauchova H, Drahota Z. The effect of triiodothyronine on cell oxidative capacity in regenerating rat liver. Physiol Res 1997;46:237-240.
61. Drahota Z, Krivakova P, Cervinkova Z, Kmonickova E, Lotkova H, Kucera O, Houstek J. Tert-butyl hydroperoxide selectively inhibits mitochondrial respiratory-chain enzymes in isolated rat hepatocytes. Physiol Res 2005;54:67-72. https://doi.org/10.33549/physiolres.930578
62. Kmonickova E, Drahota Z, Kamenikova L, Cervinkova Z, Masek K, Farghali H. Modulatory effect of cyclosporin A on tert-butyl hydroperoxide-induced oxidative damage in hepatocytes. Immunopharmacol Immunotoxicol 2001;23:43-54. https://doi.org/10.1081/IPH-100102566
63. Krivakova P, Labajova A, Cervinkova Z, Drahota Z. Inhibitory effect of t-butyl hydroperoxide on mitochondrial oxidative phosphorylation in isolated rat hepatocytes. Physiol Res 2007;56:137-140. https://doi.org/10.33549/physiolres.931006
64. Drahota Z, Endlicher R, Stankova P, Rychtrmoc D, Milerova M, Cervinkova Z. Characterization of calcium, phosphate and peroxide interactions in activation of mitochondrial swelling using derivative of the swelling curves. J Bioenerg Biomembr 2012;44:309-315. https://doi.org/10.1007/s10863-012-9443-2
65. Endlicher R, Drahota Z, Kucera O, Cervinkova Z. Age-dependent changes in the function of mitochondrial membrane permeability transition pore in rat liver mitochondria. Physiol Res 2021;70:905-911. https://doi.org/10.33549//physiolres.934734, https://doi.org/10.33549/physiolres.934734
66. Endlicher R, Drahota Z, Stefkova K, Cervinkova Z, Kucera O. The mitochondrial permeability transition pore-current knowledge of its structure, function, and regulation, and optimized methods for evaluating its functional state. Cells 2023;12:1273. https://doi.org/10.3390/cells12091273
67. Labajova A, Kofranek J, Krivakova P, Cervinkova Z, Drahota Z. Tetraphenylphosphonium-selective electrode as a tool for evaluating mitochondrial permeability transition pore function in isolated rat hepatocytes. Gen Physiol Biophys 2006;25:325-331.
68. Drahota Z, Palenickova E, Endlicher R, Milerova M, Brejchova J, Vosahlikova M, Svoboda P, Kazdova L, Kalous M, Cervinkova Z, Cahova M. Biguanides inhibit complex I, II and IV of rat liver mitochondria and modify their functional properties. Physiol Res 2014;63:1-11. https://doi.org/10.33549/physiolres.932600

69. Pecinova A, Drahota Z, Kovalcikova J, Kovarova N, Pecina P, Alan L, Zima M, Houstek J, Mracek T. Pleiotropic effects of biguanides on mitochondrial reactive oxygen species production. Oxid Med Cell Longev 2017;2017:7038603. https://doi.org/10.1155/2017/7038603

Physiol. Res. 73 (Suppl. 1): S35-S48, 2024 *https://doi.org/10.33549/physiolres.935337*

REVIEW

Sixty Years of Heart Research in the Institute of Physiology of the Czech Academy of Sciences

Bohuslav OŠŤÁDAL[1], František KOLÁŘ[1]

[1]Institute of Physiology of the Czech Academy of Sciences, Prague, Czech Republic

Received February 10, 2024
Accepted February 23, 2024

Summary

In 2023 six decades have elapsed since the first experimental work on the heart muscle was published, in which a member of the Institute of Physiology of the Czech Academy of Sciences participated as an author; Professor Otakar Poupa was the founder and protagonist of this research domain. Sixty years – more than half of the century – is certainly significant enough anniversary that is worth looking back and reflecting on what was achieved during sometimes very complicated periods of life. It represents the history of an entire generation of experimental cardiologists; it is possible to learn from its successes and mistakes. The objective of this review is to succinctly illuminate the scientific trajectory of an experimental cardiological department over a 60-year span, from its inaugural publication to the present. The old truth – *historia magistra vitae* – is still valid.

Key words

Heart • Adaptation • Development • Hypoxia • Protection

Corresponding author

B. Ostadal, Laboratory of Developmental Cardiology, Institute of Physiology of the Czech Academy of Sciences, Videnska 1083, 14200 Prague 4, Czech Republic. E-mail: ostadal@biomed.cas.cz

Fig. 1. Participants of the Symposium on Scientific Basis for the Practice of Cardiology", organized by Department of Developmental Cardiology in Prague, 2010.

Introduction

Cardiovascular diseases represent the most serious health disorders in the contemporary era, accounting for over 50 % of total mortality in the developed countries. A singular illness, ischemic heart disease, is responsible for half of this grim statistic. It is, therefore, understandable that the interest of both experimental and clinical cardiologists is driven by the effort to positively influence this unfavourable situation. Moreover, clinical-epidemiological studies have clearly shown that the risk factors of serious cardiovascular diseases manifest already during the early phases of ontogenetic development. Hence, ischemic heart disease and atherosclerosis are thus no longer diseases of the fifth and higher decades of life, necessitating a shift in experimental studies on the pathogenetic mechanisms of these disturbances to the early phases of ontogenetic development. Moreover, sex differences in the sensitivity to ischemia-reperfusion injury are so obvious that they should be taken into consideration in both experimental and clinical cardiology. The importance of the developmental and sex approach for experimental and clinical cardiology is thus indisputable. And, finally, cardiology is the scientific discipline where the close cooperation between the theoretical and clinical cardiologists has the longstanding tradition, spanning from the molecular level to the patient´s bed.

The aim of the present survey is to demonstrate briefly the real scientific life of one experimental cardiological department over the 60-year period, from its inaugural experimental work to the present time. It is necessary to emphasize that the program of the cardiovascular research in the Institute of Physiology of the Czech Academy of Sciences was based on all the above presumptions.

Establishment of the Prague school of experimental cardiology

In 2023, six decades have elapsed since the first experimental work on the heart muscle was published, in which a member of the Institute of Physiology participated as an author; he was the founder and protagonist of this research domain, professor Otakar Poupa [1]. This luminary scientist, possessing charisma and renaissance qualities, came with his “Laboratory for Physiology and Pathophysiology of Metabolism” to the Institute of Physiology from the then Institute for Nutrition Research. In a short time, within the newly established department, he founded a cardiological laboratory, which worked closely with the Institute of Pathological Physiology of the Faculty of Pediatrics (today the 2nd Faculty of Medicine of the Charles University), of which he concurrently assumed external leadership. Shortly, he managed to create very unique example of cooperation between the Academy of Sciences and the Faculty of Medicine, both in the field of experimental research and in teaching the medical students. He developed broad-based research on the phylogenetic and ontogenetic development of the heart muscle, with special attention to the needs of clinical cardiology, particularly pediatric cardiology. This orientation attracted a large number of young adepts of science and became the basis of the Prague School of Adaptive and Developmental Cardiology, successfully continuing the Czech tradition in evolutionary medicine, pioneered by Eduard Babák. There were published numerous still cited original results about the development of cardiac muscle during phylogeny and ontogeny [2-8], the cardioprotective effect of adaptation to chronic hypoxia [9,10] and factors influencing the extent of experimental cardiac necrosis, induced by high doses of isoproterenol [11-13]. Studies on increasing cardiac tolerance to oxygen deprivation in animals adapted to chronic hypoxia were the first published experimental results in this field. Poupa´s group closely cooperated with the excellent cardioembryologist Zdeněk Rychter, author of the first work on experimental heart defects [14], one of the founders of Czech experimental embryology. In this connection it is necessary to mention, that even a modern cardioprotective phenomenon – preconditioning – has its roots in Poupa´s department. Already in 1966, twenty years before the originally recognized discovery of this phenomenon, Poupa and his colleagues published a paper in which they showed that repeated administration of small doses of isoprenaline significantly reduced the extent of heart muscle damage, induced by subsequent high dose of this catecholamine [15]. Unfortunately, this work was published in the local journal, and the described effect was not given a commercially successful name. However, persisting interest of world cardiologists in this originally forgotten publication remains a source of pride for Czech cardiologists. The successes of Poupa´s Prague school soon crossed the borders of the country. By the late 1960s, Poupa in collaboration with US scientists Bing and Bajusz conceived the idea to create an international

scientific society that would bring together experimental cardiologists from all over the world. This was indeed successful, and the International Society for Heart Research (ISHR), as it is now called, represents the only world society of its kind. Naturally, Poupa became a member of the editorial board of the official journal of this society, the Journal of Molecular and Cellular Cardiology, which is still one of the prestigious world-renowned periodicals. The fruitful years culminated in the time of the Prague Spring during which Poupa´s merits were recognized with a state prize.

Development after 1968

The Soviet occupation in August 1968, which started the so-called normalization era, adversely affected the development of the entire Czech science including experimental cardiology for many years. Poupa, as one of the authors of the memorable manifesto "Two Thousands Words", chose emigration in September 1968, setting in motion the gradual departure of other Prague school members. The significant limitation of foreign contacts gradually led to the interruption of promising development, to professional isolation and a substantial lag behind global scientific advancements.

Experimental cardiologists in the Institute of Physiology (Faltova, Ostadal, Pelouch, Prochazka, later Kolar, Ostadalova, Papousek and Rychter) perpetuated Poupa´s legacy, establishing the Department of Developmental Cardiology (further Department). Their main task became the study of the structural, functional and metabolic properties of the developing cardiac muscle, crucial for understanding the ontogenetic changes of cardiac resistance to oxygen deprivation [16-19]. Interestingly, it was observed that fetal spongious musculature persists in children with congenital heart disease [20]. Special attention was paid to the possibilities of protective influence on the myocardium, especially by the adaptation to chronic hypoxia [21-25]. Moreover, for the first time sex difference in cardiac sensitivity to hypoxia was described [26]. This orientation led to the establishment of very effective cooperation both with other laboratories in the Institute of Physiology as well as with cardiologists addressing cardiopulmonary diseases (Institute for Clinical and Experimental Medicine - IKEM Prague, led by Jiří Widimský) [27-32] and clinical department of pediatric cardiology (Children´s Cardiac Center Prague-Motol, under the leadership of Milan Samanek) [33-39]. Simultaneously, at the Institute of Physiology, Krecek´s department continued the research activities in the field of ontogenesis: developmental aspects of the pathogenesis of hypertension were very successfully addressed by Jelinek, Kunes and Zicha [40,41]. However, the history of this research would deserve a separate treatise.

Period after November 1989

Only a greatest optimist could assume that the possibility of verifying dreams and reality in the open field of world science is not a utopia. The events of November 1989 ushered in a transformative era, offering Czech science the invaluable gift of global reintegration. First came the altruistic invitations from foreign colleagues but at the same time become clear that excuses for past unhappy years would not be enough. Of course, all of this also applies to experimental cardiology. Where possible, old contacts were established, long-standing literary acquaintances were personified, and seminal results timidly found their way to scientific meetings and prestigious journals. The explosion of foreign sojourns of young researchers began to bear fruit, and the intellectual and methodological background gradually improved. In this context, it should be stressed that molecular cardiology, without which we can no longer imagine current experimental research, began to be developed with great delay. The grant system established a competitive approach to financial resources and undoubtedly contributed to the improvement of the scientific quality.

The advantage of our experimental cardiology was that it entered the last 30 years organizationally prepared. The Committee of Experimental Cardiology (KEK), with the foundation of which (1973 by Braveny and Ostadal) the cardiologists from the Institute of Physiology are intrinsically connected, represented a unique national scientific society, even on a world scale, with its philosophy, organization and scientific activity. This strategic advantage prompted ISHR to entrust KEK with organizing the 1995 World Congress in Prague. The president was Pavel Braveny from Brno, the secretary general Ostadal and the entire team of the Department participated in the organization. With the passage of time, it can be emphasized that the first meeting of ISHR organized east of Alps, with more than 1200 participants, became a real culmination of the KEK´s activities to date. It was also possible to present

adequately the traditional issues of the Institute of Physiology, i.e. cardiac development and adaptation.

The scientific research of the Department during this period was concentrated on the question, how to increase cardiac tolerance to oxygen deficiency. Focused investigation probed the molecular and cellular mechanisms involved in the protection of the ischemic myocardium [42-56] and the analyses of the cardiac resistance during early phases of ontogenetic development [57-62]. Other studies have investigated e.g. the effect of increased pressure on neonatal heart growth [63-65] or right ventricular function in hypoxic pulmonary hypertension [43, 66-68]. The Department seized opportunities offered both for substantional improvements of methodical equipment as well as for significant expansion of contacts with the top foreign laboratories. Very fruitful was the intensive cooperation with the groups at University of Manitoba, Winnipeg [69-71], University of Ottawa [72-78], Max-Planck Institute in Bad Nauheim [79], Free University Berlin [80-82], Catholic University of Louvain in Brussels [83-85], University of Strathclyde, Glasgow [86], INSERM Paris [87,88], Institute for Heart Research, Bratislava [89,90], and others. The representatives of the Department became members of the committees of the international scientific societies, such as ISHR and the International Academy of Cardiovascular Sciences. International activities of the Department continued in the organization of several scientific meetings, such *as Czech-French-Slovak Symposium on Basic Cardiology* (1994), *The Developing Heart* (2000), *Mendel symposium I on Genes and the Heart* (2003), *Mendel Symposium II* (2008) and *Symposium on Scientific Basis for the Practice of Cardiology* (2010). The interest of many pre- and post-graduate students, both from the Faculty of Science and from the Faculty of Medicine was gratifying. Intensive cooperation has developed with domestic experimental laboratories of the Faculty of Science or the 2nd Faculty of Medicine and continued successful collaboration with the clinical institutions such as Children´s Cardiac Center and IKEM.

Research Center for Cardiovascular Diseases

In 1999, the first representative research centers were established as part of a project of the Ministry of Education, Youth and Sports. An informal group of cardiology-oriented, internationally experienced and freely cooperating laboratories of the Institute of Physiology of the Czech Academy of Sciences (Department of Developmental Cardiology, Department of Hypertension), of the 2nd Faculty of Medicine (Departments of Physiology and Pathophysiology) and Center for Experimental Medicine of IKEM, seemed to be a suitable model for this purpose. “Center for Cardiovascular Research” was acknowledged among the first, with Ostadal as the responsible researcher. The research concept of this Center aligned with cardiovascular research priorities in the European Union. The aim of the research activity was to clarify some of the molecular and cellular mechanisms involved in the development of ischemic heart disease and main risk factors, such as atherosclerosis and high blood pressure. The orientation on developmental approach in cardiovascular diseases was based on long-standing traditions of Czech cardiac research. At the end of the five-year period the evaluating council stated that the Center represents a research base that has no parallels in our country, leading to a resounding endorsement for another seven years. New competition rules included the close cooperation with clinical research facilities, Children´s Cardiac Center in Prague-Motol and Departments of Cardiology and Cardiac Surgery of IKEM. The theoretical part was further significantly strengthened by a group from the Faculty of Science and two further departments of the Institute of Physiology, the newly established Department of Cardiac Morphogenesis and the Department of Biomaterials and Tissue Engineering. The Center gradually ceased to be a formal grouping of individual workplaces but became a virtual institute. New laboratories were created and methodical approaches and technical equipment increased significantly. The main output of the Center´s activities were high-quality original results published in renowned journals. The Center was very successful in attracting young researchers: a number of future cardiologists and cardiac surgeons completed their scientific training in the experimental and clinical research. The number of full-time researchers was in average 109, 30 of them were under 35 years of age. During existence of the Center, 25 postgraduate students defended their PhD thesis. Regrettably, the dissolution of this long-established team of experimental and clinical researchers interrupted the well-started and effective cooperation; the successful system of scientific centers officially terminated in 2012.

Cardiovascular research in the last decade

Although the cessation of the Centre's activities led to the end of joint funding, the scientific cooperation

of the Department with several partners, in particular the Faculty of Science, continued and developed further on a bilateral basis. In the framework of this collaboration, a number of studies have recently been published that have further characterized the differences in cardioprotective mechanisms induced by various regimens of continuous and intermittent chronic hypoxia [91-97]. Together with the Center for Experimental Medicine of IKEM, we have also addressed questions concerning the influence of comorbidities, especially various forms of systemic hypertension, on myocardial ischemic tolerance and new possibilities of therapeutic pharmacological interventions [98-102]. The merger with the Department of Cardiac Morphogenesis has led to the expansion of the studied topics to include the development of the structure and function of the cardiac conduction system and to the enrichment of the methodological tools [103-106]. Special attention was paid to the developmental and sex differences in cardiac tolerance to ischemia/reperfusion injury and the possible role of mitochondria in this process [107-116]. A newly established international collaboration with the Medical College of Wisconsin, Milwaukee, has yielded new findings with translational potential on the beneficial effects of eicosanoids on cardiac injury by ischemia and on the development of post-ischemic heart failure [117-120]. The traditional focus of the Department's research programme on the cardiovascular effects of chronic hypoxia has prompted joint projects with the Laboratory of Molecular Pathogenetics, Institute of Biotechnology, investigating the role of the transcription factor HIF-1α in the mechanism of ischemic tolerance and in the pathogenesis of diabetic cardiomyopathy and heart failure [121-124]. Last but not least, we are involved with colleagues from Comenius University in Bratislava in research on mechanisms of new forms of cell death in myocardial infarction and heart failure [125-127]. Recently, the Department (newly Laboratory) has also shown promising developments in advanced molecular biology methods and their use in the study of epigenetic RNA regulatory mechanisms involved in the ontogenetic development of the heart and in the pathogenesis of heart disease [128-131]. Number of young enthusiastic researchers, modern methodologies and attractive scientific programme represent promising perspectives for future.

The scientific contribution of experimental cardiologists from the Institute of Physiology

To evaluate the contribution of scientific work is always tricky; it depends on many points of view. On the first place is of course the originality of the published results, but it is also necessary to asses to whom the results will help, what are the perspectives of their further use and how they have been accepted by the world scientific community, i.e. how often they were cited. The harshest critic is time, which will test the results and show “evergreen” ones. For the sake of completeness, we would like to summarize at least some of them.

- studies on the normal phylogenetic and ontogenetic development of the cardiac muscle, myocardial blood supply and conduction system;
- persistence of the fetal avascular spongious myocardium, supplied by diffusion from the ventricular cavity in patients with pulmonary stenosis;
- cardiac adaptation to pressure overload during early postnatal development;
- the first observation in experimental cardiology, demonstrating that the female heart is more tolerant to hypoxia than the male heart;
- developmental and sex differences in cardiac tolerance to oxygen deprivation; the role of mitochondria, and protective strategies for the immature myocardium;
- metabolic adaptation to chronic hypoxia in children with congenital heart disease;
- intermittent chronic hypoxia–induced right ventricular hypertrophy and pulmonary hypertension; possibilities of pharmacological interventions;
- studies on the effect of perinatal hypoxia on the sex-dependent hypoxic tolerance of the adult myocardium;
- molecular mechanisms of the long-lasting cardioprotective effect of adaptation to chronic hypoxia, regular exercise and other adaptive interventions;
- altered cardiac ischemic tolerance associated with various forms of systemic hypertension; possibilities of genetic and pharmacological interventions;
- pathogenetic mechanisms of diabetic cardiomyopathy; ischemic tolerance of diabetic heart;

- progression of post-ischemic heart failure in hypertensive animals; novel experimental therapy;
- role of epitranscriptomic regulatory mechanisms in heart physiology and pathophysiology.

Conclusion

60 years – more than half of the century – is certainly significant enough anniversary that it is worth looking back and reflecting on what has been achieved. It represents the history of an entire generation of experimental cardiologists; it is possible to learn from its successes and mistakes; and that was the main purpose of this historical reflection. Indeed, the old truth – *historia magister vitae* – is still valid.

Conflict of Interest

There is no conflict of interest.

Acknowledgements

This study was supported by the project National Institute for Research of Metabolic and Cardiovascular Diseases (Program EXCELLES, Project No. LX22NPO5104) - Funded by the European Union - Next Generation EU.

Fig. 2. Participants of the "Mendel symposium II: Genes and the Heart", organized by Department of Developmental Cardiology in Liblice, 2008.

References

1. Rakusan K, Poupa O. Changes in the diffusion distance in the rat heart muscle during development. Physiol Bohemoslov 1963;12:220-227.
2. Rakusan K, Poupa O. Development postnatal des vaisseaux terminaux et des fibres musculaires dans le coeur du rat. J Physiol Paris 1964;56:636.
3. Rakusan K, Jelinek J, Korecky B, Soukupova M, Poupa O. Postnatal development of muscle fibres and capillaries in the rat heart. Physiol Bohemoslov 1965;14:32-37.

4. Rakusan K, Poupa O. Developmental changes in the protein composition of heart muscle in the rat. Physiol Bohemoslov 1966;15:132-136.
5. Dbaly J, Ostadal B, Rychter Z. Development of the coronary arteries in rat embryos. Acta anat (Basel) 1968;71:209-222. https://doi.org/10.1159/000143186
6. Poupa O, Ostadal B. Experimental cardiomegalies and cardiomegalies"- in free-living animals. Ann NY Acad Sci 1969;156:445-468. https://doi.org/10.1111/j.1749-6632.1969.tb16744.x
7. Poupa O, Rakusan K, Ostadal B: The effect of physical activity upon the heart of vertebrates. In: Medicine and Sport. Physical Activity and Aging. D BRUNNER, E JOKL (eds). Karger, New York, Basel, 1970, pp 202-233. https://doi.org/10.1159/000387290
8. Ostadal B, Rychter Z, Poupa O. Comparative aspects of the development of the terminal vascular bed in the myocardium. Physiol Bohemoslov 1970;19:1-7.
9. Poupa O, Rakusan K, Prochazka J, Krofta K. Resistance of the myocardium to hypoxia induced by anaemia of different types. Physiol Bohemoslov 1965;14:452-455.
10. Poupa O, Turek Z, Kalus M, Krofta K. Acute cardiac infarct like necrosis in high altitude adaptes rats. Physiol Bohemoslov 1965;14:542-545.
11. Poupa O, Turek Z, Pelouch V, Prochazka J, Krofta K. Increased resistance of the myocardium to anoxia in vitro after repeated application of isoprenalin. Physiol Bohemoslov 1965;14:536-541.
12. Poupa O, Prochazka J, Pelouch V. Effect of catecholamines on resistance of the myocardium to anoxia and on the heart glycogen concentration. Physiol Bohemoslov 1968;17:36-42.
13. Ostadal B, Rychterova V, Poupa O. Isoproterenol-induced acute experimental cardiac necrosis in the turtle (Testudo Horsfieldi). Amer Heart J 1968;76:645-649. https://doi.org/10.1016/0002-8703(68)90163-4
14. Rychter Z. Experimental morphology of the aortic arches and the heart loop in chick embryos. In: *Advances in morphogenesis.* Academic Press, New York/London, 1962, pp 333-371. https://doi.org/10.1016/B978-1-4831-9949-8.50012-2
15. Turek Z, Kalus M, Poupa O. The effect of isoprenaline pretreatment on the size of acute myocardial necrosis induced by the same drug. Physiol Bohemoslov 1966;15:353-356.
16. Ostadal B, Schiebler TH. Kapillarentwicklung in Rattenherzen. Elektronenmikroskopische Untersuchungen. Z Anat Entwickl-Gesch 1971;133:288-304. https://doi.org/10.1007/BF00519304
17. Bass A, Ostadal B, Pelouch V, Vitek V. Differences in weight parameters, myosin ATPase activity and the enzyme pattern of energy supplying metabolism between the compact and spongious cardiac musculature of carp (Cyprinus carpio) and turtle (Testudo Horsfieldi). Pflügers Arch 1973;343:65-77. https://doi.org/10.1007/BF00586575
18. Ostadal B, Schiebler TH, Rychter Z: Relations between development of the capillary wall and myoarchitecture of the rat heart. In: Cell Impairment in Aging and Development. VJ CRISTOFALO, E HOLECKOVA (eds). Adv Exp Med Biol 1975;53:375-388. https://doi.org/10.1007/978-1-4757-0731-1_33
19. Ostadal B, Rychter Z, Rychterova V. The action of isoproterenol on the chick embryo heart. J Mol Cell Cardiol 1976;8:533-544. https://doi.org/10.1016/0022-2828(76)90054-7
20. Dusek J, Ostadal B, Duskova M. Postnatal persistence of spongy myocardium with embryonic blood supply. Arch Path 1975; 99:312-317.
21. McGrath J, Prochazka J, Pelouch V, Ostadal B. Physiological responses of rats to intermittent high-altitude stress: effects of age. J Appl Physiol 1973;34:289-293. https://doi.org/10.1152/jappl.1973.34.3.289
22. McGrath J, Ostadal B, Prochazka J, Wachtlova M, Rychterova V. Experimental cardiac necrosis in hypobaric and anemic hypoxia. J Appl Physiol 1975;39:205-208. https://doi.org/10.1152/jappl.1975.39.2.205
23. Wachtlova M, Mares V, Ostadal B. DNA synthesis in the ventricular myocardium of young rats exposed to intermittent high altitude (IHA) hypoxia. An autoradiographic study. Virchows Arch B Cell Path 1977;24:335-342. https://doi.org/10.1007/BF02889289
24. Ostadal B, Mirejovska E, Hurych J, Pelouch V, Procházka J. Effect of intermittent high altitude hypoxia on the synthesis of collagenous and non-collagenous proteins of the right and left ventricular myocardium. Cardiovasc Res 1978;12:303-308. https://doi.org/10.1093/cvr/12.5.303

25. Jarkovska D, Ostadal B. Intermittent high altitude hypoxia-induced structural changes of the pulmonary myocardium in young mice. Virchows Arch (Cell Pathol) 1983;43:327-336. https://doi.org/10.1007/BF02932965
26. Ostadal B, Prochazka J, Pelouch V, Urbanova D, Widimsky J. Comparison of cardiopulmonary responses of male and female rats to intermittent high altitude hypoxia. Physiol Bohemoslov 1984;33:129-138.
27. Widimsky J, Urbanova D, Ressl J, Ostadal B, Pelouch V, Prochazka J. The effect of intermittent altitude hypoxia on the myocardium and lesser circulation in rat. Cardiovasc Res 1973;7:798-808. https://doi.org/10.1093/cvr/7.6.798
28. Widimsky J, Urbanova D, Ressl J, Ostadal B, Pelouch V, Prochazka J: Chronic pulmonary hypertension induced by intermittent high altitude exposure. In: Pulmonary Circulation. J WIDIMSKY, S KARGER (eds), Prog Resp Res, Basel, New York, 1975;9:121-125.
29. Widimsky J, Ostadal B, Urbanova D, Ressl J, Prochazka J, Pelouch V. Intermittent high altitude hypoxia. Chest 1980;77:383-389. https://doi.org/10.1378/chest.77.3.383
30. Pelouch V, Ostadal B, Urbanova D, Prochazka J, Ressl J, Widimsky J. The effect of intermittent high altitude hypoxia on the structure and enzymatic activity of cardiac myosin. Physiol bohemoslov 1980;29:313-322.
31. Pelouch V, Ostadal B, Prochazka J, Urbanova D, Widimsky J. Effect of high altitude hypoxia on the protein composition on the right ventricular myocardium. Progr Resp Res 1985;20:41-48. https://doi.org/10.1159/000410421
32. Kolar F, Ostadal B, Prochazka J, Pelouch V, Widimsky J. Comparison of cardiopulmonary response to intermittent high-altitude hypoxia in young and adult rats. Respiration 1989;56:57-62. https://doi.org/10.1159/000195778
33. Skovranek J, Ostadal B, Pelouch V, Prochazka J. Ontogenetic differences in cardiac sensitivity to verapamil in rats. Pediatr Cardiol 1986;7:25-29. https://doi.org/10.1007/BF02315478
34. Bass A, Samanek M, Ostadal B, Hucin B, Stejskalova M, Pelouch V. Differences between atrial and ventricular energy supplying enzymes in children. J Appl Cardiol 1988;3:397-405.
35. Samanek M, Bass A, Ostadal B, Hucin B, Stejskalova M. Effect of hypoxaemia on enzymes supplying myocardial energy in children with congenital heart disease. Int J Cardiol 1989;25:265-270. https://doi.org/10.1016/0167-5273(89)90216-7
36. Samanek M, Bass A, Ostadal B, Hucin B: The importance of the energy-supplying metabolism of the heart in pre- and postoperative care of patiens with tetralogy of Fallot. In: *Perspectives in Paediatric Cardiology.* GK SRUPI, L PARENZANI, RH ANDERSON (eds), Future Publ Comp, Inc, Mount Kisco, New York, 1989, pp 152-154.
37. Jarkovska D, Janatova T, Hruda J, Ostadal B, Samanek M. The physiological closure of ductus arteriosus in the rat. An ultrastructural study. Anat Embryol 1989;180:497-504. https://doi.org/10.1007/BF00305125
38. Janatova T, Jarkovska D, Hruda J, Samanek M, Ostadal B. Effect of the administration of prostaglandins (PGE2) in the early postnatal period on closure of the ductus arteriosus in the laboratory rat. Physiol Bohemoslov 1989;38:201-206.
39. Pelouch V, Milerova M, Ostadal B, Hucin B, Samanek M. Differences between atrial and ventricular protein profiling in children with congenital heart disease. Mol Cell Biochem 1995;147:43-49. https://doi.org/10.1007/BF00944782
40. Zicha J, Kunes J, Jelinek J. Experimental hypertension in young and adult animals. Hypertension 1986;8:1096-1104. https://doi.org/10.1161/01.HYP.8.12.1096
41. Zicha J, Kunes J. Ontogenetic aspects of hypertension development: analysis in the rat. Physiol Rev 1999;79:1227-1282. https://doi.org/10.1152/physrev.1999.79.4.1227
42. Kolar F, Cole WC, Ostadal B, Dhalla NS. Transient inotropic effects of low extracellular sodium in perfused rat heart. Am J Physiol Heart Circ Physiol 1990;259:H712-H719. https://doi.org/10.1152/ajpheart.1990.259.3.H712
43. Kolar F, Ostadal B. Right ventricular function in rats with hypoxic pulmonary hypertension. Pflügers Arch 1991;419:121-126. https://doi.org/10.1007/BF00372996
44. Asemu G, Papousek F, Ostadal B, Kolar F. Adaptation to high altitude hypoxia protects the rat heart against ischemia-induced arrhythmias. Involvement of mitochondrial KATP channel. J Mol Cell Cardiol 1999;31:1821-1831. https://doi.org/10.1006/jmcc.1999.1013

45. Szarszoi O, Asemu G, Vanecek J, Ostadal B, Kolar F. Effects of melatonin on ischemia and reperfusion injury of the rat heart. Cardiovasc Drugs Ther 2001;15:251-257. https://doi.org/10.1023/A:1011920407691
46. Neckar J, Papousek F, Novakova O, Ostadal B, Kolar F. Cardioprotective effects of chronic hypoxia and ischaemic preconditioning are not additive. Basic Res Cardiol 2002; 97:161-167. https://doi.org/10.1007/s003950200007
47. Neckar J, Szarszoi O, Koten L, Papousek F, Ostadal B, Grover GJ, Kolar F. Effects of mitochondrial KATP modulators on cardioprotection induced by chronic high altitude hypoxia in rats. Cardiovasc Res 2002;55:567-575. https://doi.org/10.1016/S0008-6363(02)00456-X
48. Kolar F, Ostadal B. Molecular mechanisms of cardiac protection by adaptation to chronic hypoxia. Physiol Res 2004;53:S3-S13. https://doi.org/10.33549/physiolres.930000.53.S3
49. Neckar J, Markova I, Novak F, Novakova O, Szarszoi O, Ostadal B, Kolar F. Increased expression and altered subcellular distribution of PKC-delta in chronically hypoxic rat myocardium: involvement in cardioprotection. Am J Physiol Heart Circ Physiol 2005;288:H1566-H1572. https://doi.org/10.1152/ajpheart.00586.2004
50. Kolar F, Neckar J, Ostadal B. MCC-134, a blocker of mitochondrial and opener of sarcolemmal ATP-sensitive K+ channels, abrogates cardioprotective effects of chronic hypoxia. Physiol Res 2005;54:467-471. https://doi.org/10.33549/physiolres.930000.54.467
51. Fitzpatrick CM, Shi Y, Hutchins WC, Su j, Gross GJ, Ostadal B, Tweddell JS, Baker JE. Cardioprotection in chronically hypoxic rabbits persists upon exposure to normoxia: Role of nitric oxide synthase and KATP channels. Am J Physiol Heart Circ Physiol 2005;288:H62-H68. https://doi.org/10.1152/ajpheart.00701.2004
52. Kolar F, Jezkova J, Balkova P, Breh J, Neckar J, Novak F, Novakova O, Tomasova H, Srbova M, Ostadal B, Wilhelm J, Herget J. Role of oxidative stress in PKC-δ upregulation and cardioprotection induced by chronic intermittent hypoxia. Am J Physiol Heart Circ Physiol 2007;292:H224-H230. https://doi.org/10.1152/ajpheart.00689.2006
53. Hlavackova M, Neckar J, Jezkova J, Balkova P, Stankova B, Novakova O, Kolar F, Novak F. Dietary polyunsaturated fatty acids alter myocardial protein kinase C expression and affect cardioprotection induced by chronic hypoxia. Exp Biol Med 2007;232:823-832.
54. Hlavackova M, Kozichova K, Neckar J, Kolar F, Musters RJP, Novak F, Novakova O. Up-regulation and redistribution of protein kinase C-δ in chronically hypoxic heart. Mol Cell Biochem 2010;345:271-282. https://doi.org/10.1007/s11010-010-0581-8
55. Borchert GH, Yang C-T, Kolar F. Mitochondrial BKCa channels contribute to protection of cardiomyocytes isolated from chronically hypoxic rats. Am J Physiol Heart Circ Physiol 2011; 300:H507-H513. https://doi.org/10.1152/ajpheart.00594.2010
56. Snorek M, Hodyc D, Sedivy V, Durisova J, Skoumalova A, Wilhelm J, Neckar J, Kolar F, Herget J. Short-term fasting reduces the extent of myocardial infarction and incidence of reperfusion arrhythmias in rats. Physiol Res 2012;61:567-574. https://doi.org/10.33549/physiolres.932338
57. Kolar F, Seppet EK, Vetter R, Prochazka J, Grünermel J, Zilmer K, Ostadal B. Thyroid control of contractile function and calcium handling in neonatal rat heart. Pflügers Arch 1992;421:26-31. https://doi.org/10.1007/BF00374729
58. Ostadalova I, Kolar F, Ostadal B, Rohlicek V, Rohlicek J, Prochazka J. Early postnatal development of contractile performance and responsiveness to Ca2+, verapamil and ryanodine in the isolated rat heart. J Mol Cell Cardiol 1993;25:733-740. https://doi.org/10.1006/jmcc.1993.1085
59. Ostadalova I, Kolar F, Ostadal B. Inotropic effect of low extracellular sodium on perfused perinatal rat heart. Can J Physiol Pharmacol 1995;73:50-54. https://doi.org/10.1139/y95-007
60. Kolar F, Papousek F, Pelouch V, Ostadal B, Rakusan K. Pressure overload induced in newborn rats: effects on left ventricular growth, morphology, and function. Pediatr Res 1998;43:521-526. https://doi.org/10.1203/00006450-199804000-00014
61. Ostadalova I, Ostadal B, Jarkovska D, Kolar F. Ischemic preconditioning in chronically hypoxic neonatal rat heart. Pediatr Res 2002;52:561-567. https://doi.org/10.1203/00006450-200210000-00016

62. Rakusan K, Chvojkova Z, Oliviero P, Ostadalova I, Kolar F, Chassagne C, Samuel J-L, Ostadal B. ANG II type 1 receptor antagonist irbesartan inhibits coronary angiogenesis stimulated by chronic intermittent hypoxia in neonatal rats. Am J Physiol Heart Circ Physiol 2007;292:H1237-H1244. https://doi.org/10.1152/ajpheart.00965.2006
63. Kolar F, Papousek F, Pelouch V, Ostadal B, Rakusan K. Pressure overload induced in newborn rats: Effects on left ventricular growth, morphology, and function. Pediatr Res 1998;43:521-526. https://doi.org/10.1203/00006450-199804000-00014
64. Sedmera D, Thompson RP, Kolar F. Effect of increased pressure loading on heart growth in neonatal rats. J Mol Cell Cardiol 2003;35:301-309. https://doi.org/10.1016/S0022-2828(03)00011-7
65. Novotny J, Hrbasova M, Kolar F, Svoboda P. Cardiomegaly induced by pressure overload in newborn rats is accompanied by altered expression of the long isoform of Gsα protein and deranged signaling of adenylyl cyclase. Mol Cell Biochem 2003;245:157-166. https://doi.org/10.1023/A:1022828430565
66. Cihak R, Kolar F, Pelouch V, Prochazka J, Ostadal B, Widimsky J. Functional changes in the right and left ventricle during development of cardiac hypertrophy and after its regression. Cardiovasc Res 1992;26:845-850. https://doi.org/10.1093/cvr/26.9.845
67. Pelouch V, Kolar F, Ostadal B, Milerova M, Cihak R, Widimsky J. Regression of chronic hypoxia-induced pulmonary hypertension, right ventricular hypertrophy and fibrosis: Effect of enalapril. Cardiovasc Drugs Ther 1997;11:177-185. https://doi.org/10.1023/A:1007788915732
68. Rivolta I, Lucchini V, Rocchetti M, Kolar F, Palazzo F, Zaza A, Miserocchi G. Interstitial pressure and lung oedema in chronic hypoxia. Eur Respir J 2011;37:943-949. https://doi.org/10.1183/09031936.00066710
69. Dhalla NS, Yates JC, Naimark B, Dhala KS, Beamish RE, Ostadal B: Cardiotoxicity of catecholamines and related agents. In: Cardiovascular Toxicology. D ACOSTA (ed), Raven Press, New York, 1992, pp 239-282.
70. Lee S L, Ostadalova I, Kolar F, Dhalla NS. Alterations in Ca2+-channels during the development of diabetic cardiomyopathy. Mol Cell Biochem 1992;109:173-179. https://doi.org/10.1007/BF00229773
71. Ostadal B, Ostadalova I, Dhalla NS. Development of cardiac sensitivity to oxygen deficiency: comparative and ontogenetic aspects. Physiol Rev 1999;79:635-659. https://doi.org/10.1152/physrev.1999.79.3.635
72. Kolar F, MacNaughton C, Papousek F, Korecky B. Systolic mechanical performance of heterotopically transplanted hearts in rats treated with cyclosporin. Cardiovasc Res 1993;27:1244-1247. https://doi.org/10.1093/cvr/27.7.1244
73. Kolar F, MacNaughton C, Papousek F, Korecky B, Rakusan K. Changes in calcium handling in atrophic heterotopically isotransplanted rat hearts. Basic Res Cardiol 1995;90:475-481. https://doi.org/10.1007/BF00788540
74. Kolar F, Papousek F, MacNaughton C, Pelouch V, Milerova M, Korecky B. Myocardial fibrosis and right ventricular function of heterotopically transplanted hearts in rats treated with cyclosporin. Mol Cell Biochem 1996;163/164:253-260. https://doi.org/10.1007/BF00408666
75. Sladek T, Sladkova J, Kolar F, Papousek F, Cicutti N, Korecky B, Rakusan K. The effect of AT1 receptor antagonist on chronic cardiac response to coronary artery ligation in rats. Cardiovasc Res 1996;31:568-576. https://doi.org/10.1016/0008-6363(95)00244-8
76. Heron MI, Kolar F, Papousek F, Rakusan K. Early and late effect of neonatal hypo- and hyperthyroidism on coronary capillary geometry and long-term heart function in rat. Cardiovasc Res 1997; 33:230-240. https://doi.org/10.1016/S0008-6363(96)00198-8
77. Rakusan K, Cicutti N, Kolar F. Effect of anemia on cardiac function, microvascular structure, and capillary hematocrit in rat hearts. Am J Physiol Heart Circ Physiol 2001; 280:H1407-H1414. https://doi.org/10.1152/ajpheart.2001.280.3.H1407
78. Rakusan K, Cicutti N, Kolar F. Cardiac function, microvascular structure and capillary hematocrit in hearts of polycythemic rats. Am J Physiol Heart Circ Physiol 2001; 281:H2425-H2431. https://doi.org/10.1152/ajpheart.2001.281.6.H2425
79. Deindl E, Kolar F, Neubauer E, Vogel S, Schaper W, Ostadal B. Effect of intermittent high altitude hypoxia on gene expression in rat heart and lung. Physiol Res 2003;52:147-157. https://doi.org/10.33549/physiolres.930295

80. Kolar F, Seppet E K, Vetter R, Prochazka J, Grünermel J, Zilmer K, Ostadal B. Thyroid control of contractile function and calcium handling in neonatal rat heart. Pflügers Arch 1992;421:26-31. https://doi.org/10.1007/BF00374729
81. Vetter R, Studer R, Reinecke H, Kolar F, Ostadalova I, Drexler H. Reciprocal changes in the postnatal expression of the sarcolemmal Na+-Ca2+-exchanger and SERCA2 in rat heart. J Mol Cell Cardiol 1995;27:1689-1701. https://doi.org/10.1016/S0022-2828(95)90788-2
82. Cernohorsky J, Kolar F, Pelouch V, Korecky B, Vetter R. Thyroid control of sarcolemmal Na^{+}-Ca^{2+} exchanger and SR Ca2+-ATPase in developing rat heart. Am J Physiol Heart Circ Physiol 1998;275:H264-H273. https://doi.org/10.1152/ajpheart.1998.275.1.H264
83. Wibo M, Kolar F, Zheng L, Godfraind T. Influence of thyroid status on postnatal maturation of calcium channels, beta-adrenoceptors and cation transport ATPases in rat ventricular tissue. J Mol Cell Cardiol 1995;27:1731-1743. https://doi.org/10.1016/S0022-2828(95)90887-0
84. Zheng L, Wibo M, Kolar F, Godfraind T. Calcium channels and cation transport ATPases in cardiac hypertrophy induced by aortic constriction in newborn rats. Mol Cell Biochem 1996;163/164:23-29. https://doi.org/10.1007/BF00408637
85. Wibo M, Feron O, Zheng L, Maleki M, Kolar F, Godfraind T. Thyroid status and postnatal changes in subsarcolemmal distribution and isoform expression of rat cardiac dihydropyridine receptors. Cardiovasc Res 1998;37:151-159. https://doi.org/10.1016/S0008-6363(97)00228-9
86. Ostadalova I, Ostadal B, Kolar F, Parratt JR, Wilson S. Tolerance to ischaemia and ischaemic preconditioning in neonatal rat heart. J Mol Cell Cardiol 1998;30:857-865. https://doi.org/10.1006/jmcc.1998.0653
87. Oliviero P, Chassagne C, Kolar F, Adamy C, Marotte F, Samuel J-L, Rappaport L, Ostadal B. Effect of pressure overload on angiotensin receptor expression in the rat heart during early postnatal life. J Mol Cell Cardiol 2000;32:1631-1645. https://doi.org/10.1006/jmcc.2000.1198
88. Ratajczak P, Oliviero P, Marotte F, Kolar F, Ostadal B, Samuel J-L. Expression and localization of caveolins during postnatal development in rat heart: implication of thyroid hormone. J Appl Physiol 2005;99:244-251. https://doi.org/10.1152/japplphysiol.01292.2004
89. Ravingerova T, Neckar J, Kolar F, Stetka R, Volkovova K, Ziegelhöffer A, Styk J. Ventricular arrhythmias following coronary artery occlusion in rats: is the diabetic heart less or more sensitive to ischaemia? Basic Res Cardiol 2001;96:160-168. https://doi.org/10.1007/s003950170066
90. Ravingerova T, Neckar J, Kolar F. Ischemic tolerance of rat hearts in acute and chronic phases of experimental diabetes. Mol Cell Biochem 2003;249:167-174. https://doi.org/10.1023/A:1024751109196
91. Hrbasova M, Novotny J, Hejnova L, Kolar F, Neckar J, Svoboda P. Altered myocardial Gs protein and adenylyl cyclase signaling in rats exposed to chronic hypoxia and normoxic recovery. J Appl Physiol 2003;94:2423-2432. https://doi.org/10.1152/japplphysiol.00958.2002
92. Neckar J, Borchert GH, Hlouskova P, Micova P, Novakova O, Novak F, Hroch M, Papousek F, Ostadal B, Kolar F. Brief daily episode of normoxia inhibits cardioprotection conferred by chronic continuous hypoxia. Role of oxidative stress and BKCa channels. Curr Pharm Des 2013;19:6880-6889. https://doi.org/10.2174/13816128193931127115154
93. Waskova-Arnostova P, Kasparova D, Elsnicova B, Novotny J, Neckar J, Kolar F, Zurmanova J. Chronic hypoxia enhances expression and activity of mitochondrial creatine kinase and hexokinase in the rat ventricular myocardium. Cell Physiol Biochem 2014;33:310-320. https://doi.org/10.1159/000356671
94. Chytilova A, Borchert GH, Mandikova-Alanova P, Hlavackova M, Kopkan L, Hye Khan A, Imig JD, Kolar F, Neckar J. Tumour necrosis factor α contributes to improved cardiac ischaemic tolerance in rats adapted to chronic continuous hypoxia. Acta Physiol 2015;214:97-108. https://doi.org/10.1111/apha.12489
95. Waskova-Arnostova P, Elsnicova B, Kasparova D, Hornikova D, Kolar F, Novotny J, Zurmanova J. Cardioprotective adaptation of rats to intermittent hypobaric hypoxia is accompanied by the increased association of hexokinase with mitochondria. J Appl Physiol 2015;119:1487-1493. https://doi.org/10.1152/japplphysiol.01035.2014

96. Alanova P, Chytilova A, Neckar J, Hrdlicka J, Micova P, Holzerova K, Hlavackova M, Machackova K, Papousek F, Vasinova J, Benak D, Novaková O, Kolar F. Myocardial ischemic tolerance in rats subjected to endurance exercise training during adaptation to chronic hypoxia. J Appl Physiol 2017;122:1452-1461. https://doi.org/10.1152/japplphysiol.00671.2016
97. Kohutova J, Elsnicova B, Holzerova K, Neckar J, Sebesta O, Jezkova J, Vecka M, Vebr P, Hornikova D, Szeiffova-Bacova B, Egan Benova T, Hlavackova M, Tribulova T, Kolar F, Novakova O, Zurmanova JM. Anti-arrhythmic cardiac phenotype elicited by chronic intermittent hypoxia is associated with alterations in connexin-43 expression, phosphorylation and distribution. Front Endocrinol 2019;9:789. https://doi.org/10.3389/fendo.2018.00789
98. Neckar J, Kopkan L, Huskova Z, Kolar F, Papousek F, Kramer HJ, Hwang SH, Hammock BD, Imig JD, Maly J, Netuka I, Ostadal B, Cervenka L. Inhibition of soluble epoxide hydrolase by cis-4-[4-(3-adamantan-1-yl-ureido)cyclohexyl-oxy]benzoic acid exhibits antihypertensive and cardioprotective actions in transgenic rats with angiotensin II-dependent hypertension. Clin Sci 2012;122:513-525. https://doi.org/10.1042/CS20110622
99. Neckar J, Svatonova A, Weissova R, Drahota Z, Zajickova P, Brabcova I, Kolar D, Alanova P, Vasinova J, Silhavy J, Hlavackova M, Tauchmannova K, Milerova M., Ostadal B, Cervenka L, Zurmanova J, Kalous M, Novakova O, Novotny J, Pravenec M, Kolar F. Selective replacement of mitochondrial DNA increases the cardioprotective effect of chronic continuous hypoxia in spontaneously hypertensive rats. Clin Sci 2017;131:865-881. https://doi.org/10.1042/CS20170083
100. Neckar J, Alanova P, Olejnickova V, Papousek F, Hejnova L, Silhavy J, Behuliak M, Bencze M, Hrdlicka J, Vecka M, Jarkovska D, Sviglerova J, Mistrova E, Stengl M, Novotny J, Ostadal B, Pravenec M, Kolar F. Excess ischemic tachyarrhythmias trigger protection against myocardial infarction in hypertensive rats. Clin Sci 2021;135:2143-2163. https://doi.org/10.1042/CS20210648
101. Nedvedova I, Kolar D, Elsnicova B, Hornikova D, Novotny J, Kalous M, Pravenec M, Neckar J, Kolar F, Zurmanova J. Mitochondrial genome modulates myocardial Akt/GLUT/HK salvage pathway in spontaneously hypertensive rats adapted to chronic hypoxia. Physiol Genomics 2018;50:532-541. https://doi.org/10.1152/physiolgenomics.00040.2017
102. Nedvedova I, Kolar D, Neckar J, Kalous M, Pravenec M, Silhavy J, Korenkova V, Kolar F, Zurmanova JM. Cardioprotective regimen of adaptation to chronic hypoxia diversely alters myocardial gene expression in SHR and SHR-mtBN conplastic rat strains. Front Endocrinol 2019;9:809. https://doi.org/10.3389/fendo.2018.00809
103. Kolesova H, Bartos M, Hsieh WC, Olejnickova V, Sedmera D. Novel approaches to study coronary vasculature development in mice. Dev Dyn 2018;247:1018-1027. https://doi.org/10.1002/dvdy.24637
104. Kvasilova A, Olejnickova V, Jensen B, Christoffels VM, Kolesova H, Sedmera D, Gregorovicova M. The formation of the atrioventricular conduction axis is linked in development to ventricular septation. J Exp Biol 2020;223:jeb229278. https://doi.org/10.1242/jeb.229278
105. Olejnickova V, Kocka M, Kvasilova A, Kolesova H, Dziacky A, Gidor T, Gidor L, Sankova B, Gregorovicova M, Gourdie RG, Sedmera D. Gap junctional communication via connexin43 between Purkinje fibers and working myocytes explains the epicardial activation pattern in the postnatal mouse left ventrikle. Int J Mol Sci 2021;22:2475. https://doi.org/10.3390/ijms22052475
106. Neffeova K, Olejnickova V, Nanka O, Kolesova H. Development and diseases of the coronary microvasculature and its communication with the myocardium. WIREs Mech Dis 2022;e1560. https://doi.org/10.1002/wsbm.1560
107. Skarka L, Bardova K, Brauner P, Flachs P, Jarkovska D, Kopecky J, Ostadal B. Expression of mitochondrial uncoupling protein 3 and adenine nucleotide translocase 1 genes in developing rat heart: putative involvement in control of mitochondrial membrane potential. J Mol Cell Cardiol 2003;35:321-330. https://doi.org/10.1016/S0022-2828(03)00016-6
108. Netuka I, Szarszoi O, Maly J, Besik J, Neckar J, Kolar F, Ostadalova I, Pirk J, Ostadal B. Effect of perinatal hypoxia on cardiac tolerance to acute ischaemia in adult male and female rats. Clin Exp Pharmacol Physiol 2006;33:714-719. https://doi.org/10.1111/j.1440-1681.2006.04423.x
109. Ostadal B, Netuka I, Maly J, Besik J, Ostadalova I. Gender differences in cardiac ischemic injury and protection-experimental aspects. Exp Biol Med 2009;234:1011-1019. https://doi.org/10.3181/0812-MR-362

110. Netuka I, Szarszoi O, Maly J, Riha H, Turek D, Ostadalova I, Ostadal B. Late effect of early hypoxic disturbance in the rat heart: Gender differences. Physiol Res 2010;59:127- 31. https://doi.org/10.33549/physiolres.931833
111. Milerova M, Charvatova Z, Skarka L, Ostadalova I, Drahota Z, Fialova M, Ostadal B. Neonatal cardiac mitochondria and ischemia/reperfusion injury. Mol Cell Biochem 2010;335:147-153. https://doi.org/10.1007/s11010-009-0251-x
112. Ostadal B, Ostadal P. Sex-based differences in cardiac ischaemic injury and protection: therapeutic implications. Br J Pharmacol 2014;171:541-554. https://doi.org/10.1111/bph.12270
113. Ostadal P, Ostadal B. Women and the management of acute coronary syndrome. Can J Physiol Pharmacol 2012;90:1151-1159. https://doi.org/10.1139/y2012-033
114. Milerova M, Drahota Z, Chytilova A, Tauchmannova K, Houstek J, Ostadal B. Sex difference in the sensitivity of cardiac mitochondrial permeability transition pore to calcium load. Mol Cell Biochem 2016;412:147-154. https://doi.org/10.1007/s11010-015-2619-4
115. Ostadal B, Drahota Z, Houstek J, Milerova M, Ostadalova I, Hlavackova M, Kolar F. Developmental and sex differences in cardiac tolerance to ischemia-reperfusion injury: the role of mitochondria. Can J Physiol Pharmacol 2019;97:808-814. https://doi.org/10.1139/cjpp-2019-0060
116. Ostadal B, Ostadalova I, Szarszoi O, Netuka I, Olejnickova V, Hlavackova M. Sex-dependent effect of perinatal hypoxia on cardiac tolerance to oxygen deprivation in adults. Can J Physiol Pharmacol 2021;99:1-8. https://doi.org/10.1139/cjpp-2020-0310
117. Alanova P, Huskova Z, Kopkan L, Sporkova A, Jichova S, Neckar J, Imig JD, Klevstig M, Kolar F, Reddy NR, Falck JR, Sadowski J, Nishiyama A, Kramer HJ, Melenovsky V, Cervenkova L, Kujal P, Vernerova Z, Cervenka L. Orally active epoxyeicosatrienoic acid analog does not exhibit antihypertensive and reno- or cardioprotective actions in two-kidney, one-clip Goldblatt hypertensive rats. Vasc Pharmacol 2015;73:45-56. https://doi.org/10.1016/j.vph.2015.08.013
118. Neckar J, Hsu A, Md Hye Khan A, Gross G, Nithipatikom K, Cyprova M, Benak D, Hlavackova M, Sotaova-Kasparova D, Falck J, Sedmera D, Kolar F, Imig J. Infarct size-limiting effect of epoxyeicosatrienoic acid analog EET-B is mediated by hypoxia inducible factor-1α via down regulation of prolyl hydroxylase 3. Am J Physiol Heart Circ Physiol 2018;315:H1148-H1158. https://doi.org/10.1152/ajpheart.00726.2017
119. Neckar J, Md Hye Khan A, Gross GJ, Cyprova M, Hrdlicka J, Kvasilova A, Falck JR, Campbell WB, Sedlakova L, Skutova S, Olejnickova V, Gregorovicova M, Sedmera D, Kolar F, Imig JD. Epoxyeicosatrienoic acid analog EET-B attenuates post-myocardial infarction remodeling in spontaneously hypertensive rats. Clin Sci 2019;133:936-951. https://doi.org/10.1042/CS20180728
120. Hrdlicka J, Neckar J, Papousek F, Huskova Z, Kikerlova S, Vanourkova Z, Vernerova Z, Akat F, Vasinova J, Hammock BD, Hwang SH, Imig JD, Falck JR, Cervenka L, Kolar F. Epoxyeicosatrienoic acid-based therapy attenuates the progression of postischemic heart failure in normotensive Sprague-Dawley but not in hypertensive Ren-2 transgenic rats. Front Pharmacol 2019;10:159. https://doi.org/10.3389/fphar.2019.00159
121. Bohuslavova R, Kolar F, Kuthanova L, Neckar J, Tichopad A, Pavlinkova G. Gene expression profiling of sex differences in HIF1-dependent adaptive cardiac responses to chronic hypoxia. J Appl Physiol 2010;109:1195-1202. https://doi.org/10.1152/japplphysiol.00366.2010
122. Cerychova R, Bohuslavova R, Papousek F, Sedmera D, Abaffy P, Benes V, Kolar F, Pavlinkova G. Adverse effects of Hif1a mutation and maternal diabetes on the offspring heart. Cardiovasc Diabetol 2018;17:68. https://doi.org/10.1186/s12933-018-0713-0
123. Bohuslavova R, Cerychova R, Papousek F, Olejnickova V, Bartos M, Gorlach A, Kolar F, Sedmera D, Semenza GL, Pavlinkova G. HIF-1 α is required for development of the sympathetic nervous system. Proc Natl Acad Sci USA 2019;116:13414-13423. https://doi.org/10.1073/pnas.1903510116
124. Hrabalova P, Bohuslavova R, Matejkova K, Papousek F, Sedmera D, Abaffy P, Kolar F, Pavlinkova G. Dysregulation of hypoxia-inducible factor 1α in the sympathetic nervous system accelerates diabetic cardiomyopathy. Cardiovasc Diabetol 2023;22:88. https://doi.org/10.1186/s12933-023-01824-5
125. Adameova A, Hrdlicka J, Szobi A, Farkasova V, Kopaskova K, Murarikova M, Neckar J, Kolar F, Ravingerova T, Dhalla NS. Evidence of necroptosis in hearts subjected to various forms of ischemic insults. Can J Physiol Pharmacol 2017;95:1163-1169. https://doi.org/10.1139/cjpp-2016-0609

126. Lichy M, Szobi A, Hrdlicka J, Horvath C, Kormanova V, Rajtik T, Neckar J, Kolar F, Adameova A. Different signaling in infarcted and non-infarcted areas of rat failing hearts: a role of necroptosis and inflammation. J Cell Mol Med 2019;23:6429-6441. https://doi.org/10.1111/jcmm.14536
127. Lichy M, Szobi A, Hrdlicka J, Neckar J, Kolar F, Adameova A. Programmed cell death in the left and right ventricle of the late phase of post-infarction heart failure. Int J Mol Sci 2020;21:7782. https://doi.org/10.3390/ijms21207782
128. Semenovykh D, Benak D, Holzerova K, Cerna B, Telensky P, Vavrikova T, Kolar F, Neckar J, Hlavackova M. Myocardial m6A regulators in postnatal development: effect of sex. Physiol Res 2022;71:877-882. https://doi.org/10.33549/physiolres.934970
129. Benak D, Kolar F, Zhang L, Devaux Y, Hlavackova M. RNA modification m6Am: the role in cardiac biology. Epigenetics 2023;18:2218771. https://doi.org/10.1080/15592294.2023.2218771
130. Benak D, Benakova S, Plecita-Hlavata L, Hlavackova M. The role of m6A and m6Am RNA modifications in the pathogenesis of diabetes mellitus. Front Endocrinol 2023;14:1223583. https://doi.org/10.3389/fendo.2023.1223583
131. Benak D, Holzerova K, Hrdlicka J, Kolar F, Olsen M, Karelson M, Hlavackova M. Epitranscriptomic regulation in fasting hearts: implications for cardiac health. RNA Biol 2024;21:1-14. https://doi.org/10.1080/15476286.2024.2307732

Physiol. Res. 73 (Suppl. 1): S49-S66, 2024 *https://doi.org/10.33549/physiolres.935425*

REVIEW

Research on Experimental Hypertension in Prague (1966-2009)

Jaroslav KUNEŠ[1], Josef ZICHA[1]

[1]Laboratory of Experimental Hypertension, Institute of Physiology, Czech Academy of Sciences, Prague, Czech Republic

Received June 6, 2024
Accepted June 14, 2024

Summary
The study of ontogenetic aspects of water and electrolyte metabolism performed in the Institute of Physiology (Czechoslovak Academy of Sciences) led to the research on the increased susceptibility of immature rats to salt-dependent forms of hypertension since 1966. Hemodynamic studies in developing rats paved the way to the evaluation of hemodynamic mechanisms during the development of genetic hypertension in SHR. A particular attention was focused on altered renal function and kidney damage in both salt and genetic hypertension with a special respect to renin-angiotensin system. Renal damage associated with hypertension progression was in the center of interest of several research groups in Prague. The alterations in ion transport, cell calcium handling and membrane structure as well as their relationship to abnormal lipid metabolism were studied in a close cooperation with laboratories in Munich, Glasgow, Montreal and Paris. The role of NO and oxidative stress in various forms of hypertension was a subject of a joint research with our Slovak colleagues focused mainly on NO-deficient hypertension elicited by chronic L-NAME administration. Finally, we adopted a method enabling us to evaluate the balance of vasoconstrictor and vasodilator mechanisms in BP maintenance. Using this method we demonstrated sympathetic hyperactivity and relative NO deficiency in rats with either salt-dependent or genetic hypertension. At the end of the first decennium of this century we were ready to modify our traditional approach towards modern trends in the research of experimental hypertension.

Keywords: Salt-dependent hypertension • Genetic hypertension • Body fluids • Hemodynamics • Ion transport • Cell membrane structure and function • Renal function • Renin-angiotensin systems

Corresponding author
Josef Zicha, Institute of Physiology, Czech Academy of Sciences, Vídeňská 1083, 142 00 Prague 4, Czech Republic. E-mail: Josef.Zicha@fgu.cas.cz

Our teachers

Physiological changes occurring during the ontogenesis belong to the historical research topics in the Institute of Physiology (Czechoslovak Academy of Sciences) (IPHYS). Water and electrolyte metabolism, body fluid distribution, renal function and vasopressin action were studied in developing rats since 1954 [1,2]. Dr. Jiří Jelínek focused his attention to the characteristic changes of water, sodium, potassium and chloride content in the body and body fluids of laboratory rats in particular developmental periods (suckling, weaning, prepuberty) [3,4]. Later he was inspired by the paper of Guillebeau and Skelton [5] who reported that immature rats are more susceptible to the induction of salt hypertension elicited by adrenal regeneration after its enucleation. In 1966 he published two papers indicating that not only adrenal-regeneration hypertension but also deoxycorticosterone (DOCA)-salt hypertension are more severe and self-sustaining in young than in adult animals [6-8]. Jelínek´s research group paid a special attention to the study of changes in body fluids, renal function and structure with a special attention to renin-angiotensin system (RAS) [9-15]. They also performed fundamental studies on salt hypertension in monkeys (*Papio hamadrys*), indicating a greater blood pressure elevation (BP) in primates exposed to high salt intake from birth as compared to those exposed to this hypertensinogenic factor during sexual maturation. On the other hand, in adult salt hypertensive primates there was enhanced pulse pressure and reduced plasma volume as compared to control animals. They also demonstrated that blood pressure was inversely related to plasma volume in salt hypertensive monkeys [16,17].

In parallel, Prof. Jiří Křeček, who investigated the antidiuretic action of vasopressin in suckling and weanling rats [2,18,19], also started to study developmental aspects of salt hypertension using a peculiar model of uninephrectomized vasopressin-deficient Brattleboro rats drinking 0.6 % saline [20]. His experiments indicated that the age-dependent salt hypertension can be elicited even in the absence of vasopressin [21] and that prepuberty seems to be a critical period for the induction of more pronounced form of salt hypertension [22]. Subsequent hemodynamic studies, which used a dye dilution technique for the estimation of cardiac output in conscious animals [23], confirmed a significant BP elevation due to the increase in peripheral resistance and a major reduction of arterial compliance in young but not in adult animals with the above form of salt hypertension [24].

Newly formed research group

In 1983 two young investigators from the above research groups – Dr. Jaroslav Kuneš and Dr. Josef Zicha – formed an independent research team and combined their methodical experience on body fluids and hemodynamic measurements in order to study further aspects of age-dependent salt hypertension. Using homozygous and heterozygous Brattleboro rats we demonstrated that sodium retention, which is not accompanied by sufficient water retention, did not induce of DOCA-salt hypertension. Thus, antidiuretic rather than vasopressor effects of vasopressin are important for the development of DOCA-salt hypertension [25-27]. Another important topic of our study was the age-dependent role of digoxin-like factor (DLF) in BP maintenance in young and adult rats with DOCA-salt hypertension. Using the approach of Kojima *et al.* [28] based upon the acute administration of antidigoxin antibody, we found that endogenous DLF is important for BP maintenance especially in young DOCA-salt hypertensive rats [29,30], while this was not true for adult BP-matched rats with either DOCA-salt or spontaneous hypertension [31]. These findings were esteemed by Demuth Prize (Young Investigator Award of International Society of Hypertension, Interlaken 1984). Our subsequent review in *Hypertension* [32] suggested that prepuberty might be a critical period for enhanced salt-induced DLF production (Fig. 1). The third interesting field of our research was the role of sodium and chloride in the development of DOCA-salt hypertension. At that time there was an idea that chloride might be more important than sodium in the pathogenesis of salt-dependent forms of hypertension [32-36]. Our hemodynamic studies [37-39] revealed the delayed induction of hypertension and the absence of decreased arterial compliance in DOCA-treated rats, in which the dietary NaCl was replaced by $NaHCO_3$ to avoid the excess chloride intake.

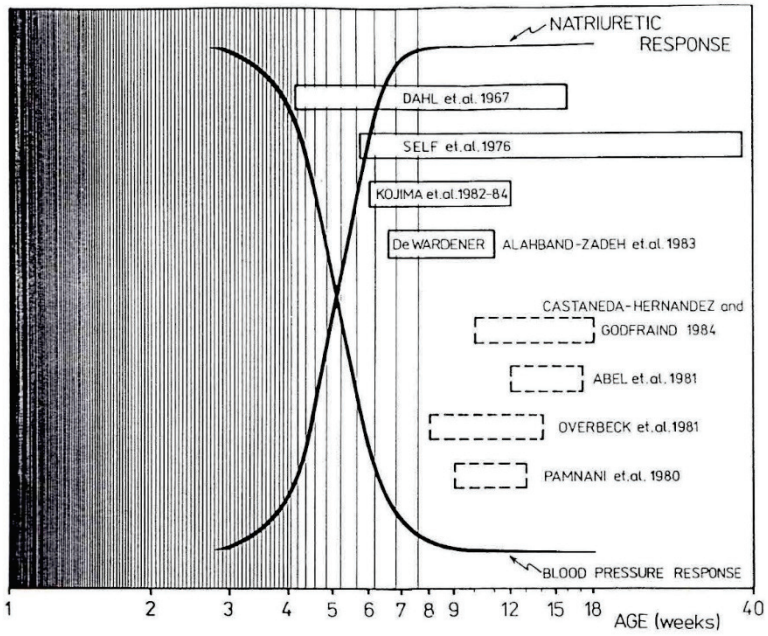

Fig. 1. The inverse relationship of natriuretic response to plasma volume expansion [176] and blood pressure response to high salt intake during prepuberty and puberty [21,177]. Full horizontal bars indicate the onset and duration of high salt intake in the studies revealing a positive evidence for digoxin-like natriuretic factor [178-181], whereas negative studies are depicted as broken bars [182-185]. The density of vertical lines reflects the intensity of maturation processes. Modified from our review [32].

The research of genetic hypertension at the IPHYS in Prague was started by Dr. Ivan Albrecht who received first breeding pairs of spontaneously hypertensive rats (SHR) from Prof. Yukio Yamori in 1972. His measurements of cardiac output revealed that the prepuberty is a hyperkinetic phase of hypertension development in SHR [40,41]. Furthermore, on the basis of his original pharmacological interventions he proposed the prepuberty as a critical period for the development of genetic hypertension in this rat strain [42]. In 1981 Dr. Kuneš joined the laboratory of Dr. Pavel Hamet in Montreal and they started a long-term cooperation on the research of several important aspects of genetic hypertension. At the beginning they were interested in cardiac and renal hyperplasia of newborn SHR [43-46]. Ontogenetic aspects of hypertension development in the rat were later reviewed in *Physiological Reviews* in 1999 [47].

Jiří Heller and Prague hypertensive rats

In the late 80ties Dr. Jiří Heller (Institute of Clinical and Experimental Medicine, Prague) developed a new model of genetic hypertension based upon Wistar rats – Prague hypertensive (PHR) and normotensive (PNR) rats [48]. This form of hypertension had many features similar to SHR but the main advantage of this model was that PHR and PNR had no histocompatibility problems so that kidneys could be transplanted between both lines without any signs of rejection [49,50]. The cross-transplantation of PNR kidney to bilaterally nephrectomized PHR animal lowered its blood pressure, while the transplantation of PHR kidney to PNR always induced hypertension development. This was true even if the transplanted kidney originated from PHR animals treated with antihypertensive drugs (captopril or nifedipine) since weaning [49]. A later study [50] indicated that the transplanted PHR kidney is important for the development but not for the maintenance of this Prague form of genetic hypertension. Using isolated kidneys from this model, Vaněčková *et al.* [51] reported the impairment of renal sodium excretion in adult PHR animals. Renal endothelin system was considered to be a possible candidate for a "hypertensinogenic" substance produced by PHR kidney [52].

Blood pressure and proteinuria were lowered in both PHR and PNR by chronic administration of AT_1 receptor inhibitor losartan, which also prevented later development of renal damage in PHR animals [53]. One of the most fascinating findings in this rat strain was the demonstration of long-term blood pressure effects elicited by a brief treatment of young PHR with antihypertensive drugs inhibiting renin-angiotensin system. The beneficial BP effects were observed in 30-week-old PHR treated with losartan or perindopril at the age 5-9 weeks. Blood pressure reduction was even enhanced if this antihypertensive intervention was repeated at the age of 15-19 weeks. In addition, this long-term BP reduction was accompanied by a substantial antiproteinuric effect [54]. Blood pressure effects of early RAS blockade in PHR were considerably greater than those that we observed in similarly treated SHR [55].

Recombinant inbred strains as a research tool in the research of genetic hypertension

A major stimulus for further research of the genetics in SHR was the establishment of recombinant inbred (RI) strains derived from SHR and normotensive BN.lx rats by Prof. Vladimír Křen and Dr. Michal Pravenec [56,57]. Blood pressure in this set of RI strains was initially determined by Dr. Kuneš using a direct carotid puncture [56]. Later he verified it by radiotelemetry measurement [58].The initial papers started a very productive international cooperations (Theodore W. Kurtz, Tim J. Aitman, Pavel Hamet) leading to numerous highly cited papers [59-64] in prestigious journals including *Nature Genetics* [64-70]. A part of the results on the role of RI strains in the progress of genetics in SHR was summarized by Pravenec *et al.* [71,72]. However, the history of this extraordinary successful international research would deserve a separate review.

Red cell ion transport in experimental hypertension

At the same time Dr. Zicha received the breeding pairs of inbred salt-sensitive (SS/Jr) and salt-resistant (SR/Jr) Dahl rats [73] from Prof. John P. Rapp (Toledo, OH). In these rats we studied red cell ion transport, effect of dietary calcium on blood pressure, alterations in arterial baroreflex function, changes in particular compartments of body fluids, adrenergic vascular innervation etc. [74-78]. In 1987-1988 Dr. Zicha studied the kinetics of ouabain-sensitive Na^+ and K^+ transport in erythrocytes of young and old Dahl rats in

the laboratory of Prof. Jochen Duhm in Munich. The data obtained in Munich [79] confirmed our earlier study done in Prague [74], which disclosed the enhanced ouabain-sensitive ion transport in red blood cells but a reduced activity of Na^+-K^+-ATPase in young salt hypertensive SS/Jr rats. The explanation of these experimental findings was simple but shocking. Salt hypertension in Dahl rats was associated with two major kinetic abnormalities of Na^+-K^+ pump – the combination of increased affinity for internal sodium and decreased maximal transport rate. The former alteration is responsible for the enhanced ouabain-sensitive Na^+ and K^+ transport (studied under low physiological concentrations of internal sodium), while the latter kinetic change caused the decreased Na^+-K^+-ATPase activity (determined under saturating Na^+ concentrations) [74,79]. Our further studies on membrane ion transport in Dahl rats indicated that the altered function of Na^+-K^+ pump was related to abnormalities in cholesterol metabolism rather than to a mutation in *Atp1a1* gene [80-82].

In the early 90´s Dr. Hasan Karama Bin Talib from Yemen made his PhD Thesis in our lab. He was trained in the study of red cell ion transport at Prof. Alan R. Chipperfield (Dundee, UK). Thanks to his dedication to experimental work we were able to extend our ion transport studies to further hypertensive models such as DOCA-salt treated rats [83,84], hereditary hypertriglyceridemic rats [85] or SHR and RI strains [86]. Our papers indicated that enhanced inward sodium leak and/or augmented Na^+-K^+-cotransport are responsible for the increased red cell Na^+ content, which is compensated by the acceleration of ouabain-sensitive Na^+ extrusion by the Na^+-K^+ pump. This was in line with our cooperative study with Dr. Sergei N. Orlov [87] which revealed a higher Na^+-K^+-ATPase activity and enhanced passive K^+ permeability in erythrocytes of SHR compared to WKY or BN.lx rats. The findings on the red cell Na^+ and K^+ transport in experimental hypertension were later summarized in our reviews [88,89].

New cooperations, new possibilities, new challenges

After the Velvet revolution the close cooperation of Dr. Zicha and Dr. Kuneš continued not only in traditional but also in newly added fields. They became to be the Editors of the journal *Physiological Research* (formerly *Physiologia bohemoslovaca*) published by IPHYS since 1954. Dr. Kuneš returned from his second stay in Montreal where the attention was focused on numerous genetic determinants of high BP in SHR - HSP70 [90-92], HSP27 [93], stress genes [94], major histocompatibility complex [95] etc. In 1993 Dr. Kuneš accepted a surprising idea of Dr. Hamet to apply for the organization of the congress of the International Society of Hypertension in Prague 2002. Thus, we spent further 10 years not only with scientific research but also with the preparation of this major event which brought to Prague almost 8000 participants of the first Joint ISH/ESH Meeting (Fig. 2).

Fig. 2. Dr. Kuneš and Dr. Zicha with the President of ISH Prof. Kikuo Arakawa.

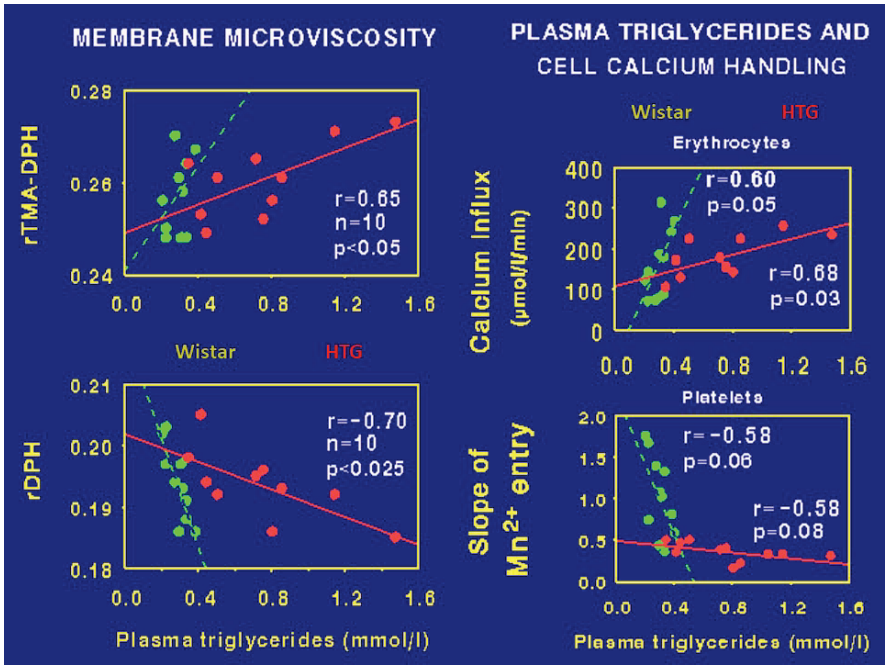

Fig. 3. The relationship of plasma triglycerides to membrane microviscosity (left panels) and cell calcium handling (right panels) in platelets of Wistar rats (green symbols) and HTG rats (red symbols). The data were published in our papers [110, 111].

A new model of Prague hereditary hypertriglyceridemic (HTG) rats was developed by Vrána and Kazdová [96] and a moderate hypertension was disclosed in these animals by our lab [97]. HTG rats were utilized to evaluate the relationship of abnormalities in BP, lipid and glucose metabolism or ion transport [85,97,98] with particular genetic determinants [99-101]. Further studies evaluated the role of *Cd36* and *Igf2* genes in this model of hypertension [102,103]. The findings obtained in HTG rats were summarized in two review papers [104,105].

In 1991 we established a long-term cooperation with Dr. Marie-Aude Devynck (Hospital Necker, Paris) on the analysis of alterations in membrane structure and function, cell calcium handling, intracellular pH regulation and platelet aggregation in several hypertensive models such as Sabra, Dahl, Lyon and HTG rats. Our first joint study, which was focused on the effects of sodium on membrane fluidity in platelets of Wistar rats, indicated that the changes of intracellular rather than extracellular sodium are responsible for the alterations of platelet membrane microviscosity in the membrane outer leaflet (TMA-DPH anisotropy) but not in the membrane lipid core (DPH anisotropy). Sodium depletion increased TMA-DPH anisotropy and sodium repletion lowered it [106]. The next study in Lyon hypertensive (LH) rats demonstrated a positive correlation of TMA-DPH anisotropy with the intracellular calcium (Ca^{2+}_i) in both platelets and erythrocytes, while DPH anisotropy correlated negatively with blood pressure and Ca^{2+}_i [107]. DPH anisotropy but not TMA-DPH anisotropy was reduced in erythrocytes of Sabra and Dahl rats prone to develop salt hypertension in which DPH anisotropy also correlated negatively with blood pressure [108]. Platelets of LH rats were characterized by substantially elevated basal Ca^{2+}_i values, higher Ca^{2+}_i levels after thrombin stimulation, and enhanced initial rate of thrombin-induced Mn^{2+} entry through the receptor-operated Ca^{2+} channels. Plasma triglycerides but not cholesterol seemed to be related to platelet calcium handling [109].

Platelet or erythrocyte Ca^{2+}_i values were similar in HTG and Wistar rats, the same was true for Ca^{2+} influx into erythrocytes. On the other hand, Ca^{2+}_i response to thrombin stimulation and Mn^{2+} entry through the receptor-operated Ca^{2+} channels were reduced in platelets of HTG rats [110]. Plasma triglycerides correlated positively with platelet TMA-DPH anisotropy and negatively with DPH anisotropy. These relationships were present in both HTG and Wistar rats but the slopes of these relationships were considerably smaller in HTG than in Wistar rats (Fig. 3). In addition, platelet Ca^{2+}_i correlated positively with TMA-DPH anisotropy and negatively with DPH anisotropy, but the slopes of these relationships were almost identical in both rat strains [111,112]. HTG rats were also characterized by platelet hypoaggregability. The initial rate of platelet aggregation

was dependent on plasma triglycerides and the slope of this relationship was smaller in HTG than in normotensive control rats [113]. Furthermore, we tried to increase circulating triglycerides by drinking of fructose solution or to lower them by gemfibrozil treatment. Chronic reduction of plasma triglycerides was associated with increased DPH anisotropy, while chronic increase of plasma triglycerides was accompanied by decreased DPH anisotropy [114].

Our experiments also revealed different platelet calcium handling in rats with salt-dependent hypertension (Sabra and Dahl rats) and those with genetic hypertension (Lyon rats). In the former rat strains there was a highly significant correlation of platelet Ca^{2+}_i with pulse pressure but not with diastolic blood pressure, whereas platelet Ca^{2+}_i in Lyon rats correlated with diastolic blood pressure but not with pulse pressure [115,116]. Finally, we also paid attention to the cytosolic pH (pH_i) and Ca^{2+}_i in platelets of Dahl and Sabra rats susceptible to salt hypertension development. Although there were no strain or salt-dependent differences in platelet Ca^{2+}_i, both strains had lower cytosolic pH_i [116,117]. Basal platelet pH_i of Dahl rats correlated positively with plasma triglycerides and plasma cholesterol and the changes in microviscosity of the outer membrane leaflet might be involved in pH_i regulation [117,118]. The above findings were summarized in a review on the abnormalities of membrane function and lipid metabolism in hypertension, which was published in *American Journal of Hypertension* in 1999 [112].

Center for Cardiovascular Research

In 1999 the *Center for Cardiovascular Research* was established to combine the effort and expertise of leading Czech cardiovascular investigators. On this platform we have met an excellent newly formed research team of Dr. Luděk Červenka (Institute of Clinical and Experimental Medicine, Prague). He started his study in experimental nephrology and hypertension under the supervision of Dr. Jiří Heller [119,120]. In 1998 Dr. Červenka joined the laboratory of Dr. L. Gabriel Navar in New Orleans. There he studied the participation of renin-angiotensin system in the pathogenesis of two-kidney, one-clip Goldblatt hypertension with a special focus on renal functions [121-124]. He also paid the attention to the salt-sensitive hypertensive mice, in which bradykinin B_2 receptor was inactivated, showing that high-salt diet and angiotensin II infusion induces the increase in blood pressure [125,126]. Moreover, genetic inactivation of B_2 receptor led to the worsening of 2K-1C Glodblatt hypertension [127] (Červenka 2003). After the return to Prague, Dr. Červenka succeeded to establish a breeding colony of Ren-2 transgenic rats (harboring mouse renin gene), the breeding pairs being provided by Prof. Detlev Ganten and Dr. Michael Bader (Berlin). Thanks to a long-term fruitful cooperation with Prof. Herbert J. Kramer (Bonn) the experimental research performed in Ren-2 transgenic rats covered not only the contribution of particular RAS components such as angiotensin II receptor subtype AT_{1A} [128,129] or angiotensin 1-7 [130,131] but also the role of neuronal NO synthase [132,133] and oxidative stress [134-136] as well as the influence of salt intake [137,138] or anesthesia [139]. Importantly, they demonstrated substantial differences in plasma and renal angiotensin II concentrations depending on whether the animals were anesthetized or conscious. A considerable attention was paid to endothelin system. They demonstrated that non-selective ET receptor blockade reduced proteinuria and attenuated cardiac hypertrophy in homozygous TGR [140]. Later, they focused on selective ET_A receptor blockade both in heterozygous and homozygous TGR [141-143]. Another important topic of his research were CYP-450-dependent oxygenase products – epoxyeicosatrienoic acids (EETs) and 20-hydroxyeicosatetraenoic acid (20-HETE). They found higher urinary 20-HETE and lower EETs excretion in TGR as compared with normotensive HanSD, suggesting that the imbalance between pro-hypertensive and anti-hypertensive CYP-450 products contribute to hypertension in TGR [144]. The inhibition of 20-HETE formation and EETs degradation led to BP decrease [145,146]. Dr. Červenka also acquired CYP1a1-Ren-2 transgenic rats in which hypertension is inducible by xenobiotic indole-3-carbinole. Severe hypertension develops already two days following its administration and is accompanied by substantial body weight loss and cardiac hypertrophy [147]. Moreover, impaired renal autoregulation precedes the development of hypertension in this experimental model [148].

Since hypertension is largely caused by the enhanced constriction of small resistance arteries together with the attenuation of vasodilator mechanisms, we directed our research to both *in vitro* and *in vivo* abnormalities of vascular tone in various form of experimental hypertension. We also paid our attention to the accelerated growth of vascular smooth muscle cells (VSMC) isolated from SHR aorta and to the respective

sex differences in this strain. We demonstrated a shorter doubling time in VSMC from male SHR compared to those from female animals [149,150]. VSMC isolated from the aorta of male SHR proliferate more rapidly than those obtained from female SHR. Angiotensin II stimulation of VSMC growth was more pronounced in cells isolated from the aorta of male SHR compared to cells from female SHR [151]. Furthermore, we observed that the augmented $[Ca^{2+}]_i$ response to angiotensin II in male compared to female aortic VSMC was dependent on Ca^{2+} influx [152].

The balance of vasoconstrictor and vasodilator mechanisms

In 1987 we started to evaluate the contribution of various pressor systems to BP maintenance in DOCA-salt hypertensive rats [153]. Simultaneously, we were inspired by the papers of Dr. Haralambos Gavras and Dr. Bernard Waeber [154-157] who performed the acute blockade of particular vasoactive systems in conscious rats. Therefore, we adapted the experimental protocol described by Minami *et al.* [158] for the estimation of the contribution of three principal vasoactive systems (renin-angiotensin, sympathetic and nitric oxide) to BP maintenance. A sequential blockade of these three systems in conscious cannulated animals was used for this purpose. This gave us the opportunity to study the role of sympathetic nervous system (SNS) which seemed to be enhanced in various salt-dependent forms of hypertension [76,159,160]. Our first studies, which were performed in Dahl and HTG rats, indicated the sympathetic hyperactivity and relative NO deficiency in both forms of hypertension [161,162]. A comparison of BP response to the acute administration of tempol (superoxide dismutase mimetic) in young and adult Dahl rats suggested a greater involvement of reactive oxygen species in young salt hypertensive animals [163].

At that time Dr. Kuneš became a director of IPHYS and we established a valuable cooperation with Dr. Olga Pecháňová from the Institute of Normal and Pathological Physiology (Slovak Academy of Sciences, Bratislava). She introduced to us a model of NO-deficient hypertension elicited by chronic administration of non-specific NO synthase inhibitor L-NAME [164-166] and we started to examine this model using our techniques. One of our first joint papers [167] revealed the importance of sympathetic hyperactivity in this form of hypertension. We also reported that a considerable part of vasodilation persisting in L-NAME-treated rats can be abolished by the acute administration of the inhibitors of inducible NO synthase. Our further studies indicated a similarity of L-NAME-induced hypertension in immature and adult rats [169] and a possibility to attenuate the development of this NO-deficient form of hypertension by chronic N-acetylcysteine (NAC) administration [170]. Furthermore, we demonstrated that chronic NAC treatment augmented NO-dependent vasodilatation, whereas chronic captopril treatment reduced sympathetic vasoconstriction in rats with L-NAME-induced hypertension [171]. The importance of sympathetic hyperactivity in this form of hypertension was confirmed in our further study indicating the attenuated development of L-NAME-induced hypertension in rats pretreated with pertussis toxin inactivating Gi protein [172].

Within the frame of this cooperation we also studied the effects of chronic NAC administration on the development of genetic hypertension in young SHR (preventive study) [173] and on the maintenance of hypertension in adult SHR with established hypertension (therapeutic study) [174]. Finally, Dr. Kuneš upgraded the original concept that hypertension is a result of the interaction between genetic and environmental factors [175] by considering the significant role of epigenetic inheritance [176] (Fig. 4).

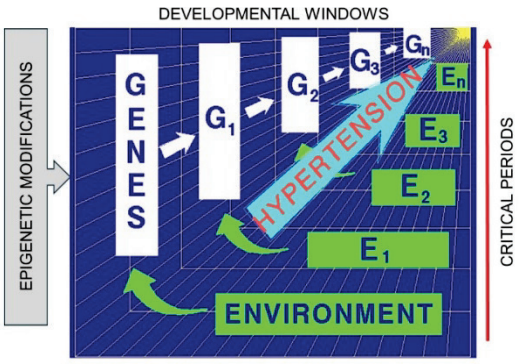

Fig. 4. Epigenetic and gene interactions with environmental factors during blood pressure ontogeny and hypertension development. E_1 - E_n represent environmental stimuli affecting expression of genetic information (G_1 - G_n) occurring in particular critical periods (developmental windows). Modified from our review [47].

Future perspectives

Another major profit from the collaboration with Dr. Pecháňová was the facilitation of the long-term work of several young Slovak colleagues in our lab – Drs Ludovít Paulis, Silvia Líšková, Mária Pintérová, Michal Behuliak and Michal Bencze. Together with the return of Dr. Ivana Vaněčková from the Institute of Clinical and Experimental Medicine (Prague) in 2010, this team was prepared for a further development of the Laboratory of Experimental Hypertension in IPHYS. The original direction of our research was modified towards new hypertensive models (Ren-2 transgenic rats) and new mechanisms in blood pressure control and hypertension development (role of endothelin, interaction of RAS and SNS, central and peripheral effects of angiotensin II, mechanisms of sympathetic hyperactivity, contribution of Ca^{2+} influx and Ca^{2+} sensitization, wire myography for the examination of conduit and resistance arteries). Thus, we were ready for a new chapter in the history of the Laboratory of Experimental Hypertension in IPHYS.

Conflict of Interest

There is no conflict of interest.

Acknowledgements

This study was supported by institutional support from the Institute of Physiology, Czech Academy of Sciences, the grant Nr. RVO 67985823 and by the project National Institute for Research of Metabolic and Cardiovascular Diseases (Programme EXCELES, ID Project No. LX22NPO5104) – Funded by the European Union – Next Generation EU.

References

1. Čapek K, Jelínek J. The development of the control of water metabolism. I. The excretion of urine in young rats. Physiol Bohemoslov 1956;5:91-96.
2. Křeček J, Křečková J. The development of the regulation of water metabolism. III. The relation between water and milk intake in infant rats. Physiol Bohemoslov 1957;6: 26-34.
3. Jelínek J. The development of the regulation of water metabolism .5. Changes in content of water, potassium, sodium and chloride in body and body fluids of the rat during development. Physiol Bohemoslov 1961;10: 249-258.
4. Jelínek J. The development of the regulation of water metabolism .6. Changes in the volume of cellular and extracellular fluid in the body of rats during development. Physiol Bohemoslov 1961;10: 259-266.
5. Guillebeau J, Skelton FR. The influence of age on the development of adrenal-regeneration hypertension. Endocrinology 1956;59:201-212. https://doi.org/10.1210/endo-59-2-201
6. Jelínek J, Albrecht I, Musilová H. The age factor in experimental hypertension: hypertension due to adrenal regeneration. Physiol Bohemoslov 1966;15:424-433.
7. Jelínek J. Salt intake and sexual differences in sensitivity of rats to adrenal-regeneration hypertension. Physiol Bohemoslov 1967;16:389-399.
8. Musilová H, Jelínek J, Albrecht I. The age of factor in experimental hypertension of the DCA type in rats. Physiol Bohemoslov 1966;15:525-531.
9. Jelínek J. Blood volume in rats with DOCA-hypertension elicited at different ages. Physiol Bohemoslov 1972;21:581-588.
10. Karen P, Deyl Z, Jelínek J. Influence of age and treatment with sodium chloride and desoxycorticosterone acetate on collagenous stroma of compensatory growing kidneys in the rat. Mech Ageing Dev 1974;3:157-163. https://doi.org/10.1016/0047-6374(74)90012-8
11. Kuneš J, Karen P, Čapek K, Jelínek J. The influence of salt intake on glomerular count in compensatory kidney hypertrophy in rats of different ages. Experientia 1976;32:887-888. https://doi.org/10.1007/BF02003748
12. Pohlová I, Kuneš J, Jelínek J. The influence of age on the activity of the renin-angiotensin system in rats with adrenal-regeneration hypertension. Physiol Bohemoslov 1983;32:438-448.
13. Kuneš J, Jelínek J. Influence of age on saline hypertension in subtotal nephrectomized rats. Physiol Bohemoslov 1984;33:123-128.
14. Hausmann J, Jelínek J, Deyl Z. Changes in glomerular basement membrane collagen caused by DOCA-NaCl treatment in rats. Nephron 1985;39:250-254. https://doi.org/10.1159/000183380

15. Vaněčková I, Kuneš J, Jelínek J. Function of the isolated perfused kidneys from young or adult rats with post-DOCA-salt hypertension. Clin Exp Hypertens 1999;21:407-421. https://doi.org/10.3109/10641969909068673
16. Cherchovich GM, Čapek K, Jefremova Z, Pohlová I, Jelínek J. High salt intake and blood pressure in lower primates (Papio hamadryas). J Appl Physiol 1976;40:601-604. https://doi.org/10.1152/jappl.1976.40.4.601
17. Kuneš J, Čapek K, Jelínek J, Cherkovich GM. Extracellular fluid distribution in salt-hypertensive monkeys. Experientia 1978;34:753-754. https://doi.org/10.1007/BF01947304
18. Dlouhá H, Křeček J, Krečková J. Water diuresis and the effect of vasopressin in infant rats. Physiol Bohemoslov 1963;12:443-452.
19. Dlouhá H, Kraus M, Křeček J, Pliška V. Sensitivity of rats to vasopressin in the weaning period. Physiol Bohemoslov 1965;14:217-224.
20. Hall CE, Ayachi S, Hall O. Spontaneous hypertension in rats with hereditary hypothalamic diabetes insipidus (Brattleboro strain). Tex Rep Biol Med 1973;31:471-487.
21. Dlouhá H, Křeček J, Zicha J. Hypertension in rats with hereditary diabetes insipidus. The role of age. Pflugers Arch. 1977;369:177-182. https://doi.org/10.1007/BF00591574
22. Dlouhá H, Křeček J, Zicha J. Effect of age on hypertensive stimuli and the development of hypertension in Brattleboro rats. Clin Sci (Lond) 1979;57:273-275. https://doi.org/10.1042/cs0570273
23. Albrecht I, Hallbäck M, Julius S, Lundgren Y, Stage L, Weiss L, Folkow B. Arterial pressure, cardiac output and systemic resistance before and after pithing in normotensive and spontaneously hypertensive rats. Acta Physiol Scand. 1975;94:378-385. https://doi.org/10.1111/j.1748-1716.1975.tb05897.x
24. Zicha J, Křeček J, Dlouhá H. Age-dependent salt hypertension in Brattleboro rats: a hemodynamic analysis. Ann N Y Acad Sci 1982;394:330-342. https://doi.org/10.1111/j.1749-6632.1982.tb37444.x
25. Zicha J, Kuneš J, Jelínek J. Age-dependent DOCA-salt hypertension in Brattleboro rats: the role of vasopressin. Physiol Bohemoslov 1987;36:33-42.
26. Kuneš J, Nedvídek J, Zicha J. Vasopressin and water distribution in rats with DOCA-salt hypertension. J Hypertens 1989;7 (Suppl 6):S204-S205. https://doi.org/10.1097/00004872-198900076-00098
27. Zicha J, Kuneš J, Lébl M, Pohlová I, Slaninová J, Jelínek J. Antidiuretic and pressor actions of vasopressin in age-dependent DOCA-salt hypertension. Am J Physiol 1989;256:R138-R145. https://doi.org/10.1152/ajpregu.1989.256.1.R138
28. Kojima I, Yoshihara S, Ogata E. Involvement of endogenous digitalis-like substance in genesis of deoxycorticosterone-salt hypertension. Life Sci 1982 May 24;30:1775-1781. https://doi.org/10.1016/0024-3205(82)90313-7
29. Zicha J, Štolba P, Pohlová I, Kunes J, Jelínek J. A different role of digoxin-like factor in the maintenance of elevated blood pressure in rats treated with DOCA and saline in youth or only in adulthood. J Hypertens Suppl. 1984;2 (Suppl 3):S481-S483.
30. Zicha J, Kuneš J, Štolba P. Endogenous digoxin-like factor contributes to the elevation of systemic resistance in rats exposed to high salt intake from prepuberty. J Hypertens 1985;3 (Suppl 3):S17-S19.
31. Kuneš J, Štolba P, Pohlová I, Jelínek J, Zicha J. The importance of endogenous digoxin-like factors in rats with various forms of experimental hypertension. Clin Exp Hypertens A 1985;7(5-6):707-720. https://doi.org/10.3109/10641968509077222
32. Zicha J, Kuneš J, Jelínek J. Experimental hypertension in young and adult animals. Hypertension 1986;8:1096-1104. https://doi.org/10.1161/01.HYP.8.12.1096
33. Kurtz TW, Morris RC Jr. Dietary chloride as a determinant of "sodium-dependent" hypertension. Science 1983;222:1139-1141. https://doi.org/10.1126/science.6648527
34. Kurtz TW, Morris RC Jr. Hypertension in the recently weaned Dahl salt-sensitive rat despite a diet deficient in sodium chloride. Science 1985;230:808-810. https://doi.org/10.1126/science.4059913
35. Whitescarver SA, Ott CE, Jackson BA, Guthrie GP Jr, Kotchen TA. Salt-sensitive hypertension: contribution of chloride. Science 1984;223:1430-1432. https://doi.org/10.1126/science.6322303
36. Whitescarver SA, Holtzclaw BJ, Downs JH, Ott CE, Sowers JR, Kotchen TA. Effect of dietary chloride on salt-sensitive and renin-dependent hypertension. Hypertension 1986;8:56-61. https://doi.org/10.1161/01.HYP.8.6.552, https://doi.org/10.1161/01.HYP.8.1.56

37. Zicha J, Kuneš J, Jelínek J, Leont'eva GR, Govyrin VA. The importance of sodium and chloride ions for the development of DOCA-NaCl hypertension: a haemodynamic study. Physiol Bohemoslov 1986;35:308-312.
38. Zicha J, Kuneš J. Haemodynamic changes induced by short- and long-term sodium chloride or sodium bicarbonate intake in deoxycorticosterone-treated rats. Acta Physiol Scand 1994;151:217-223. https://doi.org/10.1111/j.1748-1716.1994.tb09740.x
39. Kuneš J, Zicha J, Jelínek J. The role of chloride in deoxycorticosterone hypertension: selective sodium loading by diet or drinking fluid. Physiol Res 2004;53:149-154. https://doi.org/10.33549/physiolres.930000.53.149
40. Albrecht I. The hemodynamics of early stages of spontaneous hypertension in rats. Part I: Male study. Jpn Circ J 1974;38):985-990. https://doi.org/10.1253/jcj.38.985
41. Albrecht I. The hemodynamics of early stages of spontaneous hypertension in rats. Part II: Female study. Jpn Circ J 1974;38:991-996. https://doi.org/10.1253/jcj.38.991
42. Albrecht I. Critical period for the development of spontaneous hypertension in rats. Mech Ageing Dev 1974;3:75-79. https://doi.org/10.1016/0047-6374(74)90007-4
43. Pang SC, Long C, Poirier M, Tremblay J, Kuneš J, Vincent M, Sassard J, Duzzi L, Bianchi G, Ledingham J, et al. Cardiac and renal hyperplasia in newborn genetically hypertensive rats. J Hypertens 1986;4 (Suppl 3):S119-S122.
44. Kuneš J, Pang SC, Cantin M, Genest J, Hamet P. Cardiac and renal hyperplasia in newborn spontaneously hypertensive rats. Clin Sci (Lond) 1987;72:271-275. https://doi.org/10.1042/cs0720271
45. Dobešová Z, Zicha J, Kuneš J. Newborn organ weight and spontaneous hypertension: recombinant inbred strain study. Clin Exp Hypertens 1997;19:403-415. https://doi.org/10.3109/10641969709084504
46. Hamet P, Pausova Z, Dumas P, Sun YL, Tremblay J, Pravenec M, Kuneš J, Křenová D, Křen V. Newborn and adult recombinant inbred strains: a tool to search for genetic determinants of target organ damage in hypertension. Kidney Int 1998;53:1488-1492. https://doi.org/10.1046/j.1523-1755.1998.00938.x
47. Zicha J, Kuneš J. Ontogenetic aspects of hypertension development: analysis in the rat. Physiol Rev 1999;79:1227-1282. https://doi.org/10.1152/physrev.1999.79.4.1227
48. Heller J, Hellerová S, Dobešová Z, Kuneš J, Zicha J. The Prague Hypertensive Rat: a new model of genetic hypertension. Clin Exp Hypertens 1993;15:807-818. https://doi.org/10.3109/10641969309041643
49. Heller J, Schubert G, Havlíčková J, Thurau K. The role of the kidney in the development of hypertension: a transplantation study in the Prague hypertensive rat. Pflugers Arch 1993;425:208-212. https://doi.org/10.1007/BF00374168
50. Heller J, Havlíčková J, Hellerová S, Schubert G, Thurau K. A transient role of the kidney in the maintenance of hypertension. Kidney Int 1996; Suppl 55:S163-S165.
51. Vaněčková I, Heller J, Thurau K. Possible contribution of impaired sodium excretion to the development and maintenance of hypertension: a study of the isolated kidneys of the Prague hypertensive rat. Pflugers Arch 1997;434:587-591. https://doi.org/10.1007/s004240050440
52. Vogel V, Bäcker A, Heller J, Kramer HJ. The renal endothelin system in the Prague hypertensive rat, a new model of spontaneous hypertension. Clin Sci (Lond) 1999;97:919-918. https://doi.org/10.1042/cs0970091
53. Heller J, Kramer HJ, Červenka L, Hellerová S. Losartan protects the rat kidney from ischemic injury. Kidney Int 1996; Suppl 55:S113-S114.
54. Heller J, Hellerová S. Long-term effect on blood pressure of early brief treatment by different antihypertensive agents: a study in the Prague hypertensive rat. Kidney Blood Press Res 1998;21:445-451. https://doi.org/10.1159/000025898
55. Zicha J, Dobešová Z, Kuneš J. Late blood pressure reduction in SHR subjected to transient captopril treatment in youth: possible mechanisms. Physiol Res 2008;57:495-498. https://doi.org/10.33549/physiolres.931615
56. Pravenec M, Klír P, Křen V, Zicha J, Kuneš J. An analysis of spontaneous hypertension in spontaneously hypertensive rats by means of new recombinant inbred strains. J Hypertens 1989;7:217-221. https://doi.org/10.1097/00004872-198903000-00008
57. Kuneš J, Křen V, Klír P, Zicha J, Pravenec M. Genetic determination of heart and kidney weights studied using a set of recombinant inbred strains: the relationship to blood pressure. J Hypertens 1990;8:1091-1095. https://doi.org/10.1097/00004872-199012000-00004

58. Kuneš J, Dobešová Z, Musilová A, Zídek V, Vorlíček J, Pravenec M, Křen V, Zicha J. Hemodynamic characterization of recombinant inbred strains: twenty years later. Hypertens Res 2008;31:1659-1668. https://doi.org/10.1291/hypres.31.1659
59. Pravenec M, Křen V, Kuneš J, Scicli AG, Carretero OA, Simonet L, Kurtz TW. Cosegregation of blood pressure with a kallikrein gene family polymorphism. Hypertension 1991;17:242-246. https://doi.org/10.1161/01.HYP.17.2.242
60. Pravenec M, Simonet L, Křen V, Kuneš J, Levan G, Szpirer J, Szpirer C, Kurtz T. The rat renin gene: assignment to chromosome 13 and linkage to the regulation of blood pressure. Genomics 1991;9:466-472. https://doi.org/10.1016/0888-7543(91)90412-8
61. Pravenec M, Gauguier D, Schott JJ, Buard J, Křen V, Bílá V, Szpirer C, Szpirer J, Wang JM, Huang H, et al. Mapping of quantitative trait loci for blood pressure and cardiac mass in the rat by genome scanning of recombinant inbred strains. J Clin Invest 1995;96:1973-1978. https://doi.org/10.1172/JCI118244
62. Bottger A, van Lith HA, Křen V, Křenová D, Bílá V, Vorlíček J, Zídek V, Musilová A, Zdobinská M, Wang JM, van Zutphen BF, Kurtz TW, Pravenec M. Quantitative trait loci influencing cholesterol and phospholipid phenotypes map to chromosomes that contain genes regulating blood pressure in the spontaneously hypertensive rat. J Clin Invest 1996;98:856-862. https://doi.org/10.1172/JCI118858
63. Pravenec M, Gauguier D, Schott JJ, Buard J, Křen V, Bílá V, Szpirer C, Szpirer J, Wang JM, Huang H, St Lezin E, Spence MA, Flodman P, Printz M, Lathrop GM, Vergnaud G, Kurtz TW. A genetic linkage map of the rat derived from recombinant inbred strains. Mamm Genome 1996;7:117-127. https://doi.org/10.1007/s003359900031
64. Křen V, Pravenec M, Lu S, Křenová D, Wang JM, Wang N, Merriouns T, Wong A, St Lezin E, Lau D, Szpirer C, Szpirer J, Kurtz TW. Genetic isolation of a region of chromosome 8 that exerts major effects on blood pressure and cardiac mass in the spontaneously hypertensive rat. J Clin Invest 1997;99:577-581. https://doi.org/10.1172/JCI119198
65. Aitman TJ, Gotoda T, Evans AL, Imrie H, Heath KE, Trembling PM, Truman H, Wallace CA, Rahman A, Doré C, Flint J, Křen V, Zídek V, Kurtz TW, Pravenec M, Scott J. Quantitative trait loci for cellular defects in glucose and fatty acid metabolism in hypertensive rats. Nat Genet 1997;16:197-201. https://doi.org/10.1038/ng0697-197
66. Aitman TJ, Glazier AM, Wallace CA, Cooper LD, Norsworthy PJ, Wahid FN, Al-Majali KM, Trembling PM, Mann CJ, Shoulders CC, Graf D, St Lezin E, Kurtz TW, Křen V, Pravenec M, Ibrahimi A, Abumrad NA, Stanton LW, Scott J. Identification of Cd36 (Fat) as an insulin-resistance gene causing defective fatty acid and glucose metabolism in hypertensive rats. Nat Genet 1999;21:76-83. https://doi.org/10.1038/5013
67. Pravenec M, Landa V, Zídek V, Musilová A, Křen V, Kazdová L, Aitman TJ, Glazier AM, Ibrahimi A, Abumrad NA, Qi N, Wang JM, St Lezin EM, Kurtz TW. Transgenic rescue of defective Cd36 ameliorates insulin resistance in spontaneously hypertensive rats. Nat Genet 2001;27:156-158. https://doi.org/10.1038/84777
68. Hübner N, Wallace CA, Zimdahl H, Petretto E, Schulz H, Maciver F, Mueller M, Hummel O, Monti J, Zidek V, Musilová A, Křen V, Causton H, Game L, Born G, Schmidt S, Müller A, Cook SA, Kurtz TW, Whittaker J,
69. Pravenec M, Aitman TJ. Integrated transcriptional profiling and linkage analysis for identification of genes underlying disease. Nat Genet 2005;37:243-253. https://doi.org/10.1038/ng1522
70. Guryev V, Saar K, Adamovic T, Verheul M, van Heesch SA, Cook S, Pravenec M, Aitman T, Jacob H, Shull JD, Hubner N, Cuppen E. Distribution and functional impact of DNA copy number variation in the rat. Nat Genet 2008;40:538-545. https//doi.org/10.1038/ng.141
71. Pravenec M, Churchill PC, Churchill MC, Viklický O, Kazdová L, Aitman TJ, Petretto E, Hubner N, Wallace CA, Zimdahl H, Zídek V, Landa V, Dunbar J, Bidani A, Griffin K, Qi N, Maxová M, Křen V, Mlejnek P, Wang J, Kurtz TW. Identification of renal Cd36 as a determinant of blood pressure and risk for hypertension. Nat Genet 2008;40:952-954. https://doi.org/10.1038/ng.164
72. Pravenec M, Zídek V, Landa V, Šimáková M, Mlejnek P, Kazdová L, Bílá V, Křenová D, Křen V. Genetic analysis of "metabolic syndrome" in the spontaneously hypertensive rat. Physiol Res 2004;53 (Suppl 1):S15-S22. https://doi.org/10.33549/physiolres.930000.53.S15

73. Pravenec M, Křen V, Landa V, Mlejnek P, Musilová A, Šilhavý J, Šimáková M, Zídek V. Recent progress in the genetics of spontaneously hypertensive rats. Physiol Res 2014;63 (Suppl 1):S1-S8. https://doi.org/10.33549/physiolres.932622
74. Rapp JP, Dene H. Development and characteristics of inbred strains of Dahl salt-sensitive and salt-resistant rats. Hypertension 1985;7:340-349. https://doi.org/10.1161/01.HYP.7.3_Pt_1.340, https://doi.org/10.1161/01.HYP.7.3.340
75. Zicha J, Byšková E, Kuneš J, Pohlová I, Jelínek J. Sodium pump activity in young and adult salt hypertensive Dahl rats. Klin Wochenschr. 1987;65 (Suppl 8):76-81.
76. Kuneš J, Zicha J, Hamet P. Effects of dietary calcium on the development of salt hypertension in young and adult Dahl rats. J Hypertens 1988;6 (Suppl 4):S225-S227. https://doi.org/10.1097/00004872-198812040-00067
77. Kuneš J, Leontjeva GR, Byšková E, Pohlová I, Govyrin VA, Zicha J. Adrenergic innervation of blood vessels in Dahl rats with salt hypertension. Clin Exp Hypertens A 1991;13:1343-1355. https://doi.org/10.3109/10641969109048797
78. Dobešová Z, Kuneš J, Zicha J. Body fluid alterations and organ hypertrophy in age-dependent salt hypertension of Dahl rats. Physiol Res 1995;44:377-387.
79. Nedvídek J, Zicha J. Baroreflex control of heart rate in young and adult salt hypertensive inbred Dahl rats. Physiol Res 2000;49:323-330.
80. Zicha J, Duhm J. Kinetics of Na+ and K+ transport in red blood cells of Dahl rats. Effects of age and salt. Hypertension 1990;15:612-627. https://doi.org/10.1161/01.HYP.15.6.612
81. Zicha J, Negrin CD, Dobešová Z, Carr F, Vokurková M, McBride MW, Kuneš J, Dominiczak AF. Altered Na+-K+ pump activity and plasma lipids in salt-hypertensive Dahl rats: relationship to Atp1a1 gene. Physiol Genomics 2001;6:99-104. https://doi.org/10.1152/physiolgenomics.2001.6.2.99
82. Vokurková M, Dobešová Z, Kuneš J, Zicha J. Membrane ion transport in erythrocytes of salt hypertensive Dahl rats and their F2 hybrids: the importance of cholesterol. Hypertens Res 2003;26:397-404. https://doi.org/10.1291/hypres.26.397
83. Vokurková M, Nováková O, Dobešová Z, Kuneš J, Zicha J. Relationships between membrane lipids and ion transport in red blood cells of Dahl rats. Life Sci 2005;77:1452-1464. https://doi.org/10.1016/j.lfs.2005.03.014
84. Bin Talib HK, Zicha J. Red cell sodium in DOCA-salt hypertension: a Brattleboro study. Life Sci 1992;50:1021-1030. https://doi.org/10.1016/0024-3205(92)90097-9
85. Bin Talib HK, Kuneš J, Zicha J. Complete dissociation of DOCA-salt hypertension and red cell ion transport alterations. Life Sci 1992;51:PL243-PL248. https://doi.org/10.1016/0024-3205(92)90044-P
86. Kuneš J, Bin Talib HK, Dobešová Z, Vrána A, Zicha J. Erythrocyte ion transport alterations in hypertriglyceridaemic rats. Clin Sci (Lond) 1994;86:11-13. https://doi.org/10.1042/cs0860011
87. Bin Talib HK, Dobešová Z, Klír P, Křen V, Kuneš J, Pravenec M, Zicha J. Association of red blood cell sodium leak with blood pressure in recombinant inbred strains. Hypertension 1992;20:575-582. https://doi.org/10.1161/01.HYP.20.4.575
88. Orlov SN, Petrunyaka VV, Pokudin NI, Kotelevtsev YV, Postnov YV, Kunes J, Zicha J. Cation transport and adenosine triphosphatase activity in rat erythrocytes: a comparison of spontaneously hypertensive rats with the normotensive Brown-Norway strain. J Hypertens 1991;9:977-982. https://doi.org/10.1097/00004872-199110000-00012
89. Zicha J. Red cell ion transport abnormalities in experimental hypertension. Fundam Clin Pharmacol. 1993;7(3-4):129-41. https://doi.org/10.1111/j.1472-8206.1993.tb00227.x
90. Zicha J, Kuneš J. Membrane defects and the development of hypertension. In: *Handbook of Hypertension*, Vol. 19, Development of Hypertensive Phenotype: Basic and Clinical Studies, R. McCarty, D.A. Blizard, R.L. Chevalier (eds), Elsevier, Amsterdam, 1999, pp 213-251.
91. Hamet P, Tremblay J, Malo D, Kuneš J, Hashimoto T. Genetic hypertension is characterized by the abnormal expression of a gene localized in major histocompatibility complex HSP70. Transplant Proc 1990;22:2566-2567.
92. Hamet P, Kong D, Pravenec M, Kuneš J, Křen V, Klir P, Sun YL, Tremblay J. Restriction fragment length polymorphism of hsp70 gene, localized in the RT1 complex, is associated with hypertension in spontaneously hypertensive rats. Hypertension 1992;19:611-614. https://doi.org/10.1161/01.HYP.19.6.611.a

93. Kuneš J, Poirier M, Tremblay J, Hamet P. Expression of hsp70 gene in lymphocytes from normotensive and hypertensive humans. Acta Physiol Scand 1992;146:307-311. https://doi.org/10.1111/j.1748-1716.1992.tb09424.x
94. Hamet P, Kaiser MA, Sun Y, Pagé V, Vincent M, Křen V, Pravenec M, Kuneš J, Tremblay J, Samani NJ. HSP27 locus cosegregates with left ventricular mass independently of blood pressure. Hypertension 1996;28:1112-1117.
95. Hamet P, Sun YL, Malo D, Kong D, Křen V, Pravenec M, Kuneš J, Dumas P, Richard L, Gagnon F, et al. Genes of stress in experimental hypertension. Clin Exp Pharmacol Physiol. 1994;21:907-911. https://doi.org/10.1111/j.1440-1681.1994.tb02464.x
96. Kuneš J, Zicha J. Association of salt sensitivity in rats with genes of the major histocompatibility complex. Hypertension 1994;24:645-647. https://doi.org/10.1161/01.HYP.24.6.645
97. Vrána A, Kazdová L. The hereditary hypertriglyceridemic nonobese rat: an experimental model of human hypertriglyceridemia. Transplant Proc 1990;22:2579.
98. Štolba P, Dobešová Z, Hušek P, Opltová H, Zicha J, Vrána A, Kuneš J. The hypertriglyceridemic rat as a genetic model of hypertension and diabetes. Life Sci 1992;51:733-740. https://doi.org/10.1016/0024-3205(92)90482-5
99. Zicha J, Dobešová Z, Kuneš J. Plasma triglycerides and red cell ion transport alterations in genetically hypertensive rats. Hypertension 1997;30:636-640. https://doi.org/10.1161/01.HYP.30.3.636
100. Ueno T, Tremblay J, Kuneš J, Zicha J, Dobešova Z, Pausova Z, Deng AY, Sun YL, Jacob HJ, Hamet P. Resolving the composite trait of hypertension into its pharmacogenetic determinants by acute pharmacological modulation of blood pressure regulatory systems. J Mol Med (Berl) 2003;81:51-60. https://doi.org/10.1007/s00109-002-0394-7
101. Ueno T, Tremblay J, Kuneš J, Zicha J, Dobešová Z, Pausova Z, Deng AY, Sun Y, Jacob HJ, Hamet P. Gender-specific genetic determinants of blood pressure and organ weight: pharmacogenetic approach. Physiol Res 2003;52:689-700. https://doi.org/10.33549/physiolres.930000.52.689
102. Ueno T, Tremblay J, Kuneš J, Zicha J, Dobešová Z, Pausova Z, Deng AY, Sun YL, Jacob HJ, Hamet P. Rat model of familial combined hyperlipidemia as a result of comparative mapping. Physiol Genomics 2004;17:38-47. https://doi.org/10.1152/physiolgenomics.00043.2003
103. Kadlecová M, Čejka J, Zicha J, Kuneš J. Does Cd36 gene play a key role in disturbed glucose and fatty acid metabolism in Prague hypertensive hypertriglyceridemic rats? Physiol Res 2004;53:265-271. https://doi.org/10.33549/physiolres.930000.53.265
104. Kadlecová M, Dobešová Z, Zicha J, Kuneš J. Abnormal Igf2 gene in Prague hereditary hypertriglyceridemic rats: its relation to blood pressure and plasma lipids. Mol Cell Biochem 2008;314:37-43. https://doi.org/10.1007/s11010-008-9762-0
105. Klimeš I, Vrána A, Kuneš J, Šeböková E, Dobešová Z, Štolba P, Zicha J. Hereditary hypertriglyceridemic rat: a new animal model of metabolic alterations in hypertension. Blood Press 1995;4:137-142. https://doi.org/10.3109/08037059509077585
106. Zicha J, Pecháňová O, Čačányiová S, Cebová M, Kristek F, Török J, Šimko F, Dobešová Z, Kuneš J. Hereditary hypertriglyceridemic rat: a suitable model of cardiovascular disease and metabolic syndrome? Physiol Res 2006;55 (Suppl 1):S49-S63. https://doi.org/10.33549/physiolres.930000.55.S1.49
107. Zicha J, Kuneš J, Le Quan Sang KH, Devynck MA. Regulation of the dynamic properties of platelet plasma membrane by intracellular sodium ions. Life Sci 1993;521559-1565. https://doi.org/10.1016/0024-3205(93)90056-9
108. Le Quan Sang KH, Kuneš J, Zicha J, Vincent M, Sassard J, Devynck MA. Platelet and erythrocyte membrane microviscosity in Lyon hypertensive rats. Am J Hypertens 1994;7:276-281. https://doi.org/10.1093/ajh/7.3.276
109. Kuneš J, Zicha J, Devynck MA. Erythrocyte membrane microviscosity and blood pressure in rats with salt-induced and spontaneous hypertension. J Hypertens 1994;12:229-234. https://doi.org/10.1097/00004872-199403000-00002
110. Zicha J, Pernollet MG, Kuneš J, Lacour B, Vincent M, Sassard J, Devynck MA. Alterations of cytosolic calcium in platelets and erythrocytes of Lyon hypertensive rats. Am J Hypertens 1995;8:842-849. https://doi.org/10.1016/0895-7061(95)00121-5
111. Zicha J, Kuneš J, David-Dufilho M, Pernollet MG, Devynck MA. Cell calcium handling and intracellular pH regulation in hereditary hypertriglyceridemic rats: reduced platelet response to thrombin stimulation. Life Sci 1996;59:803-813. https://doi.org/10.1016/0024-3205(96)00371-2

112. Devynck MA, Kuneš J, Le Quan Sang KH, Zicha J. Membrane microviscosity and plasma triacylglycerols in the rat. Clin Sci (Lond) 1998;94:79-85. https://doi.org/10.1042/cs0940079
113. Zicha J, Kuneš J, Devynck MA. Abnormalities of membrane function and lipid metabolism in hypertension: a review. Am J Hypertens 1999;12:315-331. https://doi.org/10.1016/S0895-7061(98)00178-2
114. Kuneš J, Mazeaud MM, Devynck MA, Zicha J. Platelet hypoaggregability in hereditary hypertriglyceridemic rats: relation to plasma triglycerides. Thromb Res 1997;88:347-353. https://doi.org/10.1016/S0049-3848(97)00264-8
115. Kuneš J, Devynck MA, Zicha J. Chronic changes in plasma triglyceride levels do modify platelet membrane microviscosity in rats. Life Sci 2000;67:959-967. https://doi.org/10.1016/S0024-3205(00)00691-3
116. Zicha J, Kuneš J, Devynck MA. Platelet calcium handling is different in rats with salt-dependent and spontaneous forms of genetic hypertension. Am J Hypertens 1996;9:812-818. https://doi.org/10.1016/0895-7061(96)00101-X
117. Zicha J, Kuneš J, Ben-Ishay D, Devynck MA. Abnormal regulation of cytosolic calcium and pH in platelets of Sabra rats in early phases of salt hypertension development. Can J Physiol Pharmacol 1996;74:1222-1228. https://doi.org/10.1139/y96-134
118. Zicha J, David-Dufilho M, Kuneš J, Pernollet MG, Devynck MA. Cytosolic pH and calcium in Dahl salt-sensitive and salt-resistant rats: the relationship to plasma lipids. J Hypertens 1997;15:1715-1721. https://doi.org/10.1097/00004872-199715120-00078
119. Zicha J, Sang KH, Kuneš J, Devynck MA. Membrane microviscosity, blood pressure and cytosolic pH in Dahl rats: the influence of plasma lipids. J Hypertens 1999;17:785-792. https://doi.org/10.1097/00004872-199917060-00010
120. Červenka L, Heller J. A comparison of the effect of feeding a low-protein diet and of pharmacological intervention on the course of ablation nephropathy in the rat. Ren Fail 1995;17:27-35. https://doi.org/10.3109/08860229509036372
121. Červenka L, Heller J. Comparison of the effects of a low-protein diet with the effects of a converting enzyme inhibitor on the progression of renal insufficiency in hypertensive rats. Ren Fail 1996;18:173-180. https://doi.org/10.3109/08860229609052787
122. Červenka L, Wang CT, Navar LG. Effects of acute AT1 receptor blockade by candesartan on arterial pressure and renal function in rats. Am J Physiol 1998;274:F940-F945. https://doi.org/10.1152/ajprenal.1998.274.5.F940
123. Červenka L, Wang CT, Mitchell KD, Navar LG. Proximal tubular angiotensin II levels and renal functional responses to AT1 receptor blockade in nonclipped kidneys of Goldblatt hypertensive rats. Hypertension 1999;33:102-107. https://doi.org/10.1161/01.HYP.33.1.102
124. Červenka L, Navar LG. Renal responses of the nonclipped kidney of two-kidney/one-clip Goldblatt hypertensive rats to type 1 angiotensin II receptor blockade with candesartan. J Am Soc Nephrol 1999;10 (Suppl 11):S197-S201.
125. Červenka L, Horáček V, Vaněčková I, Hubáček JA, Oliverio MI, Coffman TM, Navar LG. Essential role of AT1A receptor in the development of 2K1C hypertension. Hypertension 2002;40:735-741. https://doi.org/10.1161/01.HYP.0000036452.28493.74
126. Červenka L, Harrison-Bernard LM, Dipp S, Primrose G, Imig JD, El-Dahr SS. Early onset salt-sensitive hypertension in bradykinin B2 receptor null mice. Hypertension 1999;34:176-180. https://doi.org/10.1161/01.HYP.34.2.176
127. Červenka L, Malý J, Karasová L, Šímová M, Vítko Š, Hellerová S, Heller J, El-Dahr SS. Angiotensin II-induced hypertension in bradykinin B2 receptor knockout mice. Hypertension 2001;37:967-973. https://doi.org/10.1161/01.HYP.37.3.967
128. Červenka L, Vaněčková I, Malý J, Horáček V, El-Dahr SS. Genetic inactivation of the B2 receptor in mice worsens two-kidney, one-clip hypertension: role of NO and the AT2 receptor. J Hypertens 2003;21:1531-1538. https://doi.org/10.1097/00004872-200308000-00018
129. Kopkan L, Kramer HJ, Husková Z, Vaňourková Z, Bäcker A, Bader M, Ganten D, Červenka L. Plasma and kidney angiotensin II levels and renal functional responses to AT1 receptor blockade in hypertensive Ren-2 transgenic rats. J Hypertens 2004;22:819-825. https://doi.org/10.1097/00004872-200404000-00026

130. Červenka L, Vaněčková I, Husková Z, Vaňourková Z, Erbanová M, Thumová M, Škaroupková P, Opočenský M, Malý J, Čertíková Chábová V, Tesař V, Bürgelová M, Viklický O, Teplan V, Želízko M, Kramer HJ, Navar LG. Pivotal role of angiotensin II receptor subtype 1A in the development of two-kidney, one-clip hypertension: study in angiotensin II receptor subtype 1A knockout mice. J Hypertens. 2008 Jul;26(7):1379-89. https://doi.org/10.1097/HJH.0b013e3282fe6eaa
131. Bürgelová M, Kramer HJ, Teplan V, Thumová M, Červenka L. Effects of angiotensin-(1-7) blockade on renal function in rats with enhanced intrarenal Ang II activity. Kidney Int 2005;67:1453-1461. https://doi.org/10.1111/j.1523-1755.2005.00222.x
132. Bürgelová M, Vaňourková Z, Thumová M, Dvořák P, Opočenský M, Kramer HJ, Želízko M, Malý J, Bader M, Červenka L. Impairment of the angiotensin-converting enzyme 2-angiotensin-(1-7)-Mas axis contributes to the acceleration of two-kidney, one-clip Goldblatt hypertension. J Hypertens 2009;27:1988-2000. https://doi.org/10.1097/HJH.0b013e32832f0d06
133. Červenka L, Kramer HJ, Malý J, Heller J. Role of nNOS in regulation of renal function in angiotensin II-induced hypertension. Hypertension 2001;38:280-285. https://doi.org/10.1161/01.HYP.38.2.280
134. Červenka L, Kramer HJ, Malý J, Vaněčková I, Bäcker A, Bokemeyer D, Bader M, Ganten D, Mitchell KD. Role of nNOS in regulation of renal function in hypertensive Ren-2 transgenic rats. Physiol Res 2002;51:571-580. https://doi.org/10.33549/physiolres.930316
135. Vaněčková I, Kramer HJ, Novotná J, Kazdová L, Opočenský M, Bader M, Ganten D, Červenka L. Roles of nitric oxide and oxidative stress in the regulation of blood pressure and renal function in prehypertensive Ren-2 transgenic rats. Kidney Blood Press Res 2005;28:117-126. https://doi.org/10.1159/000084649
136. Kopkan L, Husková Z, Vaňourková Z, Thumová M, Škaroupková P, Červenka L, Majid DS. Superoxide and its interaction with nitric oxide modulates renal function in prehypertensive Ren-2 transgenic rats. J Hypertens 2007;25:2257-2265. https://doi.org/10.1097/HJH.0b013e3282efb195
137. Kopkan L, Červenka L. Renal interactions of renin-angiotensin system, nitric oxide and superoxide anion: implications in the pathophysiology of salt-sensitivity and hypertension. Physiol Res 2009;58 (Suppl 2):S55-S68. https://doi.org/10.33549/physiolres.931917
138. Husková Z, Kramer HJ, Vaňourková Z, Červenka L. Effects of changes in sodium balance on plasma and kidney angiotensin II levels in anesthetized and conscious Ren-2 transgenic rats. J Hypertens 2006;24:517-527. https://doi.org/10.1097/01.hjh.0000209988.51606.c7
139. Husková Z, Kramer H, Vaňourková Z, Thumová M, Malý J, Opočenský M, Škaroupková P, Kolský A, Vernerová Z, Červenka L. Effects of dietary salt load and salt depletion on the course of hypertension and angiotensin II levels in male and female heterozygous Ren-2 transgenic rats. Kidney Blood Press Res 2007;30:45-55. https://doi.org/10.1159/000099028
140. Husková Z, Kramer HJ, Thumová M, Vaňourková Z, Bürgelová M, Teplan V, Malý J, Červenka L. Effects of anesthesia on plasma and kidney ANG II levels in normotensive and ANG II-dependent hypertensive rats. Kidney Blood Press Res 2006;29:74-83. https://doi.org/10.1159/000092981
141. Dvořák P, Kramer HJ, Bäcker A, Malý J, Kopkan L, Vaněčková I, Vernerová Z, Opočenský M, Tesař V, Bader M, Ganten D, Janda J, Červenka L. Blockade of endothelin receptors attenuates end-organ damage in homozygous hypertensive ren-2 transgenic rats. Kidney Blood Press Res 2004;27:248-258. https://doi.org/10.1159/000080052
142. Vaněčková I, Kramer HJ, Bäcker A, Vernerová Z, Opočenský M, Červenka L. Early endothelin-A receptor blockade decreases blood pressure and ameliorates end-organ damage in homozygous Ren-2 rats. Hypertension 2005;46:969-974. https://doi.org/10.1161/01.HYP.0000173426.06832.b5
143. Opočenský M, Kramer HJ, Bäcker A, Vernerová Z, Eis V, Červenka L, Čertíková Chábová V, Tesař V, Vaněčková I. Late-onset endothelin-A receptor blockade reduces podocyte injury in homozygous Ren-2 rats despite severe hypertension. Hypertension 2006;48:965-971. https://doi.org/10.1161/01.HYP.0000245117.57524.d6
144. Vernerová Z, Kramer HJ, Bäcker A, Červenka L, Opočenský M, Husková Z, Vaňourková Z, Eis V, Chábová VC, Tesař V, Malý J, Vaněčková I. Late-onset endothelin receptor blockade in hypertensive heterozygous REN-2 transgenic rats. Vascul Pharmacol 2008;48:165-173. https://doi.org/10.1016/j.vph.2008.01.009

145. Čertíková Chábová V, Kramer HJ, Vaněčková I, Thumová M, Škaroupková P, Tesař V, Falck JR, Imig JD, Červenka L. The roles of intrarenal 20-hydroxyeicosatetraenoic and epoxyeicosatrienoic acids in the regulation of renal function in hypertensive Ren-2 transgenic rats. Kidney Blood Press Res 2007;30:335-346. https://doi.org/10.1159/000107710
146. Čertíková Chábová V, Kramer HJ, Vaněčková I, Vernerová Z, Eis V, Tesař V, Škaroupková P, Thumová M, Schejbalová S, Husková Z, Vaňourková Z, Kolský A, Imig JD, Červenka L. Effects of chronic cytochrome P-450 inhibition on the course of hypertension and end-organ damage in Ren-2 transgenic rats. Vascul Pharmacol 2007;47:145-159. https://doi.org/10.1016/j.vph.2007.05.005
147. Čertíková Chábová V, Walkowska A, Kompanowska-Jezierska E, Sadowski J, Kujal P, Vernerová Z, Vaňourková Z, Kopkan L, Kramer HJ, Falck JR, Imig JD, Hammock BD, Vaněčková I, Červenka L. Combined inhibition of 20-hydroxyeicosatetraenoic acid formation and of epoxyeicosatrienoic acids degradation attenuates hypertension and hypertension-induced end-organ damage in Ren-2 transgenic rats. Clin Sci (Lond) 2010;118:617-632. https://doi.org/10.1042/CS20090459
148. Vaňourková Z, Kramer HJ, Husková Z, Vaněčková I, Opočenský M, Čertíková Chábová V, Tesař V, Škaroupková P, Thumová M, Dohnalová M, Mullins JJ, Červenka L. AT1 receptor blockade is superior to conventional triple therapy in protecting against end-organ damage in Cyp1a1-Ren-2 transgenic rats with inducible hypertension. J Hypertens 2006;24:2465-2472. https://doi.org/10.1097/01.hjh.0000251909.00923.22
149. Erbanová M, Thumová M, Husková Z, Vaněčková I, Vaňourková Z, Mullins JJ, Kramer HJ, Bürgelová M, Rakušan D, Červenka L. Impairment of the autoregulation of renal hemodynamics and of the pressure-natriuresis relationship precedes the development of hypertension in Cyp1a1-Ren-2 transgenic rats. J Hypertens 2009;27:575-586. https://doi.org/10.1097/HJH.0b013e32831cbd5a
150. Bačáková L, Kuneš J. Sex-dependent differences in growth of vascular smooth muscles cells from spontaneously hypertensive rats. Physiol Res 1995;44:127-130.
151. Bačáková L, Kuneš J. Gender differences in growth of vascular smooth muscle cells isolated from hypertensive and normotensive rats. Clin Exp Hypertens. 2000 Jan;22(1):33-44. https://doi.org/10.1081/CEH-100100060
152. Loukotová J, Bačáková L, Zicha J, Kuneš J. The influence of angiotensin II on sex-dependent proliferation of aortic VSMC isolated from SHR. Physiol Res 1998;47:501-505.
153. Loukotová J, Kuneš J, Zicha J. Gender-dependent difference in cell calcium handling in VSMC isolated from SHR: the effect of angiotensin II. J Hypertens 2002;20:2213-2219. https://doi.org/10.1097/00004872-200211000-00021
154. Zicha J, Kuneš J, Lébl M, Pohlová I, Jelínek J. Haemodynamics and the participation of pressor systems in young and adult rats with age-dependent DOCA-salt hypertension. Physiol Bohemoslov 1987;36:89-92.
155. Hatzinikolaou P, Gavras H, Brunner HR, Gavras I. Role of vasopressin, catecholamines, and plasma volume in hypertonic saline-induced hypertension. Am J Physiol 1981 Jun;240:H827-H831. https://doi.org/10.1152/ajpheart.1981.240.6.H827
156. Gavras H, Hatzinikolaou P, North WG, Bresnahan M, Gavras I. Interaction of the sympathetic nervous system with vasopressin and renin in the maintenance of blood pressure. Hypertension 1982;4:400-405. https://doi.org/10.1161/01.HYP.4.3.400
157. Burnier M, Biollaz J, Brunner DB, Gavras H, Brunner HR. Alpha and beta adrenoceptor blockade in normotensive and deoxycorticosterone (DOC)-hypertensive rats; plasma vasopressin and vasopressin pressor effect. J Pharmacol Exp Ther 1983;224:222-227.
158. Waeber B, Nussberger J, Brunner HR. Alpha 1-adrenoceptor blockade in renal hypertensive rats with low and high renin levels. Am J Physiol 1984;246:H573-H578. https://doi.org/10.1152/ajpheart.1984.246.4.H573
159. Minami N, Imai Y, Hashimoto J, Abe K. Contribution of vascular nitric oxide to basal blood pressure in conscious spontaneously hypertensive rats and normotensive Wistar Kyoto rats. Clin Sci (Lond) 1995;89:177-182. https://doi.org/10.1042/cs0890177
160. Kazda S, Pohlová I, Bíbr B, Kočková J. Norepinephrine content of tissues in Doca-hypertensive rats. Am J Physiol 1969;216:1472-1475. https://doi.org/10.1152/ajplegacy.1969.216.6.1472

161. Křeček J, Doležel S, Dlouhá H, Zicha J. Sympathetic nervous system and age-dependent salt hypertension in Brattleboro rats. Clin Exp Hypertens A 1987;9:2075-2093. https://doi.org/10.1080/07300077.1987.11978716, https://doi.org/10.3109/10641968709159076
162. Zicha J, Dobešová Z, Kuneš J. Relative deficiency of nitric oxide-dependent vasodilation in salt-hypertensive Dahl rats: the possible role of superoxide anions. J Hypertens 2001;19:247-254. https://doi.org/10.1097/00004872-200102000-00011
163. Kuneš J, Dobešová Z, Zicha J. Altered balance of main vasopressor and vasodepressor systems in rats with genetic hypertension and hypertriglyceridaemia. Clin Sci (Lond) 2002;102:269-277. https://doi.org/10.1042/cs1020269
164. Dobešová Z, Kuneš J, Zicha J. The altered balance between sympathetic nervous system and nitric oxide in salt hypertensive Dahl rats: ontogenetic and F2 hybrid studies. J Hypertens 2002;20:945-955. https://doi.org/10.1097/00004872-200205000-00030
165. Pecháňová O, Bernátová I, Pelouch V, Šimko F. Protein remodelling of the heart in NO-deficient hypertension: the effect of captopril. J Mol Cell Cardiol 1997;29:3365-3374. https://doi.org/10.1006/jmcc.1997.0566
166. Bernátová I, Pecháňová O, Pelouch V, Šimko F. Regression of chronic L -NAME-treatment-induced left ventricular hypertrophy: effect of captopril. J Mol Cell Cardiol 2000;32:177-185. https://doi.org/10.1006/jmcc.1999.1071
167. Bernátová I, Pecháňová O, Babál P, Kyselá S, Štvrtina S, Andriantsitohaina R. Wine polyphenols improve cardiovascular remodeling and vascular function in NO-deficient hypertension. Am J Physiol Heart Circ Physiol. 2002;282:H942-H948. https://doi.org/10.1152/ajpheart.00724.2001
168. Pecháňová O, Dobešová Z, Čejka J, Kuneš J, Zicha J. Vasoactive systems in L-NAME hypertension: the role of inducible nitric oxide synthase. J Hypertens 2004;22:167-173. https://doi.org/10.1097/00004872-200401000-00026
169. Zicha J, Pecháňová O, Dobešová Z, Kuneš J. Hypertensive response to chronic NG-nitro-L-arginine methyl ester (L-NAME) treatment is similar in immature and adult Wistar rats. Clin Sci (Lond) 2003;105:483-489. https://doi.org/10.1042/CS20030078
170. Rauchová H, Pecháňová O, Kuneš J, Vokurková M, Dobešová Z, Zicha J. Chronic N-acetylcysteine administration prevents development of hypertension in Nω-nitro-L-arginine methyl ester-treated rats: the role of reactive oxygen species. Hypertens Res 2005;28:475-482. https://doi.org/10.1291/hypres.28.475
171. Zicha J, Dobešová Z, Kuneš J. Antihypertensive mechanisms of chronic captopril or N-acetylcysteine treatment in L-NAME hypertensive rats. Hypertens Res 2006;29:1021-1027. https://doi.org/10.1291/hypres.29.1021
172. Zicha J, Kuneš J, Vranková S, Jendeková L, Dobešová Z, Pintérová M, Pecháňová O. Influence of pertussis toxin pretreatment on the development of L-NAME-induced hypertension. Physiol Res 2009;58:751-755. https://doi.org/10.33549/physiolres.931898
173. Pecháňová O, Zicha J, Kojšová S, Dobešová Z, Jendeková L, Kuneš J. Effect of chronic N-acetylcysteine treatment on the development of spontaneous hypertension. Clin Sci (Lond). 2006;110:235-242. https://doi.org/10.1042/CS20050227
174. Pecháňová O, Zicha J, Paulis L, Zenebe W, Dobešová Z, Kojšová S, Jendeková L, Sládková M, Dovinová I, Simko F, Kuneš J. The effect of N-acetylcysteine and melatonin in adult spontaneously hypertensive rats with established hypertension. Eur J Pharmacol. 2007;561:129-136. https://doi.org/10.1016/j.ejphar.2007.01.035
175. Kuneš J, Zicha J. Developmental windows and environment as important factors in the expression of genetic information: a cardiovascular physiologist's view. Clin Sci (Lond) 2006;111:295-305. https://doi.org/10.1042/CS20050271
176. Kuneš J, Zicha J. The interaction of genetic and environmental factors in the etiology of hypertension. Physiol Res 2009;58 (Suppl 2):S33-S42. https://doi.org/10.33549/physiolres.931913
177. Bengele HH, Solomon S. Development of renal response to blood volume expansion in the rat. Am J Physiol 1974;227:364-368. https://doi.org/10.1152/ajplegacy.1974.227.2.364
178. Brownie AC, Bernardis LL, Niwa T, Kamura S, Skelton FR. The influence of age and sex on the development of adrenal regeneration hypertension. Lab Invest 1966;15:1342-1356.

179. Dahl LK, Knudsen KD, Heine M, Leitl G. Effects of chronic excess salt ingestion. Genetic influence on the development of salt hypertension in parabiotic rats: evidence for a humoral factor. J Exp Med 1967;126:687-699. https://doi.org/10.1084/jem.126.4.687
180. Self LE, Battarbee HD, Gaar KA Jr, Meneely GR. A vasopressor potentiator for norepinephrine in hypertensive rats. Proc Soc Exp Biol Med 1976;153:7-12. https://doi.org/10.3181/00379727-153-39470
181. Kojima I. Circulating digitalis-like substance is increased in DOCA-salt hypertension. Biochem Biophys Res Commun 1984;122:129-136. https://doi.org/10.1016/0006-291X(84)90449-2
182. Alaghband-Zadeh J, Fenton S, Hancock K, Millett J, de Wardener HE. Evidence that the hypothalamus may be a source of a circulating Na+-K+-ATPase inhibitor. J Endocrinol 1983;98:221-226. https://doi.org/10.1677/joe.0.0980221
183. Castaneda-Hernandez G, Godfraind T. Effect of high sodium intake on tissue distribution of endogenous digitalis-like material in the rat. Clin Sci (Lond) 1984;66:225-228. https://doi.org/10.1042/cs0660225
184. Abel PW, Trapani A, Matsuki N, Ingram MJ, Ingram FD, Hermsmeyer K. Unaltered membrane properties of arterial muscle in Dahl strain genetic hypertension. Am J Physiol 1981;241:H224-H227. https://doi.org/10.1152/ajpheart.1981.241.2.H224
185. Overbeck HW, Ku DD, Rapp JP. Sodium pump activity in arteries of Dahl salt-sensitive rats. Hypertension 1981;3:306-312. https://doi.org/10.1161/01.HYP.3.3.306
186. Pamnani MB, Clough DL, Huot SJ, Haddy FJ. Vascular Na^+-K^+ pump activity in Dahl S and R rats. Proc Soc Exp Biol Med 1980;165:440-444. https://doi.org/10.3181/00379727-165-41001

REVIEW

Epilepsy Research in the Institute of Physiology of the Czech Academy of Sciences in Prague

Pavel MAREŠ[1]

[1]Laboratory of Developmental Epileptology, Institute of Physiology of the Czech Academy of Sciences, Prague, Czech Republic

Received April 23, 2024
Accepted April 23, 2024

Summary

Starting from simple clinical statistics, the spectrum of methods used in epilepsy research in the Institute of Physiology of the Czechoslovak (now Czech) Academy of Sciences progressively increased. Professor Servít used electrophysiological methods for study of brain activity in lower vertebrates, neuropathology was focused on electronmicroscopic study of cortical epileptic focus and ion-sensitive microelectrodes were used for studies of cortical direct current potentials. Developmental studies used electrophysiological methods (activity and projection of cortical epileptic foci, EEG under the influence of convulsant drugs, hippocampal, thalamic and cortical electrical stimulation for induction of epileptic afterdischarges and postictal period). Extensive pharmacological studies used seizures elicited by convulsant drugs (at first pentylenetetrazol but also other GABA antagonists as well as agonists of glutamate receptors). Motor performance and behavior were also studied during brain maturation. The last but not least molecular biology was included into the spectrum of methods. Many original data were published making a background of position of our laboratory in the first line of laboratories interested in brain development.

Key words

Epileptic foci • Epileptic seizures • Phylogenesis • Ontogenesis • Rat

Corresponding author

P. Mareš, Laboratory of Developmental Epileptology, Institute of Physiology of the Czech Academy of Sciences, Vídeňská 1083, Prague, Czech Republic, 14200. E-mail: pavel.mares@fgu.cas.cz

Epilepsy research in Prague started before the Institute of Physiology (Czechoslovak Academy of Sciences) was founded. Young associate professor of neurology Zdeněk Servít formed a group of medical students interested in neuroscience. In this group were among others Jan Bureš, Olga Burešová, Jozef Zachar and Darja Zacharová. When the original Institute of Biology of the Czechoslovak Academy of Sciences was divided into three independent institutes, Zdeněk Servít became the director of the Institute of Physiology. The group continued its action for some time [1,2], then Zachars left for the newly established Slovak Academy of Sciences in Bratislava. Jan Bureš formed his own group and prof. Servít continued with new collaborators (e.g. Jiří Machek, Jaroslav Šterc, Alena Štercová, Libuše Chocholová, Věra Nováková, Zdeněk Lodin and others). The official names of the laboratories corresponded to the political situation – Department of Central Excitation (epilepsy research) and Department of Central Inhibition (Bureš´ lab studying spreading depression). One of the models frequently used in the laboratory were audiogenic seizures [3-8].

The new people in the Servít´s laboratory – outstanding neurophysiologist Josef Holubář and neuropathologist Jindřich Fischer – extended the spectrum of methods [9-10] and started to study cortical epileptic focus elicited by cobalt implanted into cerebral cortex of rats [11-17]. Unfortunately, Josef Holubář died in a car accident in autumn 1967. Professor Servít studied epileptic phenomena during phylogenesis [18-20]. In this research were involved Alexandra Strejčková (originally technical assistant, later successful absolvent of Faculty of Natural Sciences of the Charles University) and for some time also Dan Volanschi from Romania [21-31].

Zdeněk Servít, who became full time professor at the Faculty of Pediatrics (Charles University), was also active in the Czechoslovak Academy of Sciences and was promoted from the corresponding member to the regular Member of Academy. He never left clinical epileptology and on the background of his older experimental data [32] he published an important paper in collaboration with a clinical neurologist assoc. prof. František Musil [33]. This paper provoked U.S. epileptologists to make a big study in soldiers with head injuries from the war in Vietnam. This extensive study made a conclusion that prophylactic treatment is important in people with serious brain injuries but it is not necessary in patients with simple brain contusion. Professor Servít continued his clinical studies in collaboration with an experienced neurologist Miroslav Krištof and their topic was the activation of epileptic phenomena by nasal hyperventilation [34-37].

I entered Servít´s laboratory in September 1967 and Professor Servít wanted to involve me in phylogenetic studies. At the entrance presentation I showed my results from ontogenetic studies of visual and somatosensory evoked potentials in rats and immediately after this presentation prof. Servít decided that we will study phylogenetic and ontogenetic development in parallel. My developmental orientation was thus approved and I could continue in the research, which started during my student years at medical school.

Further development was affected by political events. After hopes of Prague Spring came September 1968. Professor Servít refused to annulate his signature under the manifest „*Two thousand words*“ qualified by the new government and by the leadership of Czechoslovak Academy of Sciences as an anticommunist manifest. He was progressively withdrawn from his positions and finished as a regular scientist. His employment was prolonged always only for one month. This was contrary to the existing law according to which the employee with time-restricted contract must be informed three months before the end of the contract whether it will or will not be prolonged. The employment of prof. Servít in the Institute of Physiology was preserved thanks to his medical practice – some of his patients were in “good” positions in the communist party. After a certain (not short) time his employment was prolonged for six months and then repeatedly for one year. The only Servít´s position preserved was the Member of Academy because this title might be withdrawn only if the scientist was participating in a criminal action. However, at that time the emigration to West was qualified as a crime for which several Members of Academy were stripped of their title.

Professor Servít was also withdrawn from the leadership of the laboratory and it was necessary to have a new head of the laboratory. We proposed Jindřich Fischer to Ladislav Vyklický (at that time a temporary head of the institute) and he accepted this proposal.

Studies of epileptic seizures continued in the laboratory but individual scientists had their own topics and only occasionally collaborated. Professor Servít with Dr. Strejčková continued in the studies of epileptic foci in amphibia and reptiles and published their results mostly in *Experimental Neurology*, which was one of the leading neuroscience journals at that time. Professor Servít also continued his clinical activity not only by seeing patients but also by performing some clinical research [34-37]. Jiří Machek studied the role of potassium ions in direct current potentials of cerebral cortex [38-41], Libuše Chocholová was interested in cobalt foci [42,43] and pharmacology of hippocampal and cortical epileptic afterdischarges in rats with chronically implanted electrodes [44-46]. Jindřich Fischer continued in electron microscopic studies of semichronic cortical epileptic foci elicited by the implantation of aluminium hydroxide into cerebral cortex. He demonstrated important changes in neurons and astroglial cells [47-54]. Original findings were published with the model of cortical stimulation in collaboration with Jan Mareš [55-58]. Later he changed the model for epileptic foci elicited by local application of penicillin on cerebral cortex and in this method we met and published a common paper [59]. His excellent morphological results were published in good journals but the impact of these results was much smaller than they deserved.

Jindřich Fischer died unexpectedly during Christmas 1980. Professor Radil tried to include our laboratory into his department, but he did not succeed and I was established as the head of the laboratory. I started in the Institute of Physiology with studies of the ontogeny of cortical penicillin foci, especially of projection into the contralateral hemisphere including synchronization of symmetrical penicillin foci [60-62]. The research of this topic continued in collaboration with my student Jan Mareš (later associated professor at the Department of Physiology of the Faculty of General Medicine) and we used also cortical stimulation to elicit transcallosal responses and cortical

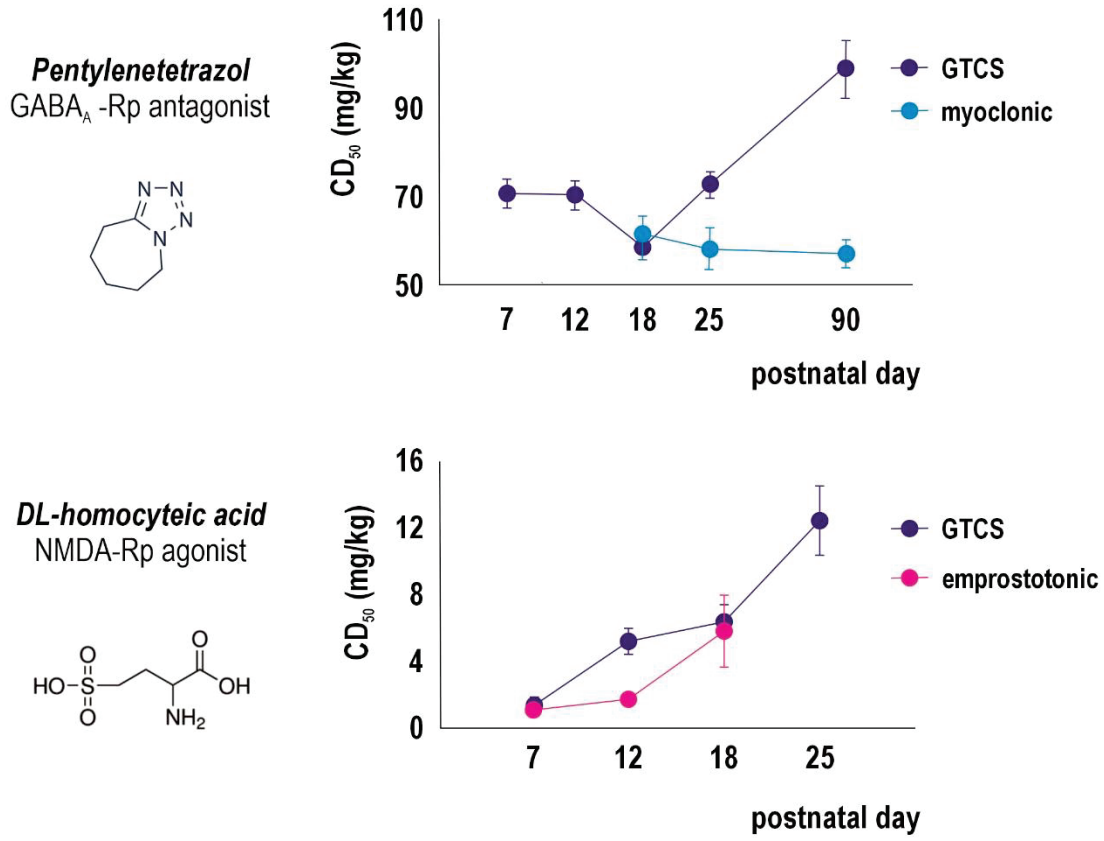

Fig. 1. Fifty-percent convulsant doses of pentylenetetrazol (upper part) and homocysteic acid (lower part). There are two types of seizures in either graph: generalized tonic-clonic (GTCS) and minimal clonic (myoclonic) seizures in pentylenetetrazol graph and GTCS and emprosthotonic (flexion) seizures in homocysteic acid graph. For both graphs: x-axis – age in days; y-axis – doses in mg/kg.

epileptic afterdischarges [63-65]. Model of cortical epileptic afterdischarges is used in our laboratory up to now mostly in pharmacological experiments. Spectrum of epileptic seizures studied was extended by chemically elicited seizures, mostly by subcutaneous administration of pentylenetetrazol [66-69] (Fig. 1). This model is generally accepted in the pharmacology of antiseizure medications.

Personal composition of the laboratory changed after the death of Dr. Fischer. Jiří Machek left the institute and Marie Kolínová, who started after finishing the medical school to work with me and Libuše Chocholová, decided to go into neurological practice. PhD student of the late Jindřich Fischer, Miloš Langmeier, finished his PhD study under my formal tutorship and continued morphological studies of consequences of epileptic seizures [70,71]. After a short time he was attracted by academic career and left us for the Department of Physiology of the First Medical Faculty, where he successfully defended dissertation to become associate professor and later he was promoted to the full professor. Collaboration with this Department of Physiology (Jan Mareš, Dana Staudacherová-Marešová, René Schickerová) continued and all these three students finished and defended PhD Thesis under my informal tutorship. René Schickerová then decided for clinical neurology and left basic research. There were many pregraduate students in our laboratory, their results were published and all of them continued their career in neurology or psychiatry – they were imprinted with neuroscience.

In 1988 I started an extra part time job as a head of Department of Pathophysiology of the Third Medical Faculty. I spent there seven years and two of my assistant professors (Klára Bernášková and Iveta Matějovská defended their PhD Thesis under my tutorship. My pregraduate student Michal Pohl finished the Faculty of General Medicine and started PhD study under my tutorship. Among other features of epileptic seizures he studied a possible role of thalamus in generation and spread of epileptic seizures using spreading depression as a tool [72-74]. Another pregraduate student Libor Velíšek also decided to stay in basic research. He entered the pharmacological program with a focus on the antagonists of glutamate receptors [75-80]. We published a possibility to elicit flexion convulsions by

N-methyl-D-aspartate [81]. This model was later used as a background for studies of severe epileptic encephalopathies of early age. In 1990 after defending her PhD thesis at Faculty of Pharmacy of Charles University Hana Kubová came to the laboratory and she worked in the field of developmental pharmacology [82-91]. In collaboration with Professor Rastislav Druga from the Second Medical Faculty she also studied morphological consequences of status epilepticus induced in immature brain [92,93].

Future of the laboratory seemed to be optimistic with three young collaborators (Pohl, Kubová, Velíšek). In a short time the situation was completely changed: Michal Pohl left to a pharmaceutical company, Libor Velíšek started his postdoc stay in the Laboratory of Developmental Epilepsy at Albert Einstein College of Medicine in New York (prof. Solomon L. Moshé) and Hana Kubová went to the same laboratory two years later. There were also some positive changes, because Nina Mikulecká from the Laboratory of Ethology came into our laboratory. She started behavioral studies and modified many tests for immature rats [94-103] (Fig. 2). From the canceled laboratory of František Šťastný came Jaroslava Folbergrová and Renata Haugvicová. Jarka Folbergrová was an experienced biochemists with her own experience in the field of epilepsy and continued in her research on the role of glutamate receptors in epileptic seizures [104-110]. Renata joined the pharmacological developmental program and participated in many studies [111-118].

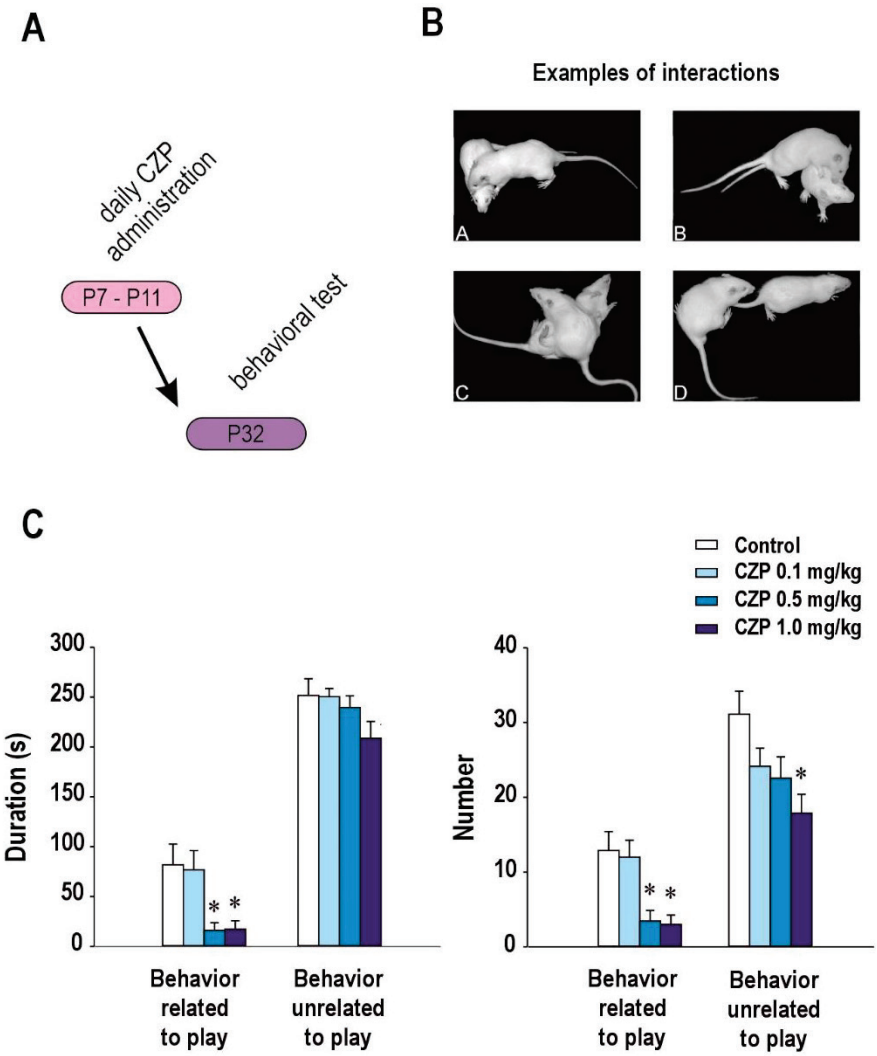

Fig. 2. The repeated administration of benzodiazepine clonazepam (CZP) to immature rats results to long-term alterations of the social interaction including the play behavior in pubescent rats. CZP was administered daily starting at postnatal day (P) 7 till P11 and animals were tested at puberty onset (P32) (scheme of experiment is shown at panel A). Play behavior was suppressed in CZP-exposed animals by dose-dependent manner (panel C). Examples of social interaction are demonstrated at panel B (**A**) pouncing, (**B**) wrestling, (**C**) pinning, (**D**) following. Modified from Mikulecká *et al.* [100].

From 1994 I served as a deputy director of the Institute of Physiology. In 1995 the Director of the Institute Professor Ošťádal abdicated due to his serious health problems. I was established as a temporary head of the Institute and after two months I was regularly elected to be a director. I did not want to have two relatively high positions and therefore I finished my activity at the Third Medical Faculty. I recommended Libor Velíšek, who came back from USA to replace me in the Department of Pathophysiology. He stayed there for more than one year and then he came back to USA because his wife Jana with children refused to return to Prague. We thus lost a possibility of collaboration and friendly competition in the field of developmental epilepsy. Before the second Libor's leaving to USA Hana Kubová came back and continued in the collaboration with Professor Druga [119,120] and started a collaboration with Professor Asla Pitkanen from Kuopio. This collaboration lasted more than 10 years and led to a number of outstanding publications mostly on the consequences of status epilepticus elicited in immature rats [121-123]. One of their common papers demonstrated for the first time that status epilepticus elicited in rats less than two weeks old resulted in neuronal degeneration in thalamus (Fig. 3). This collaboration ended when Asla Pitkanen focused her research on posttraumatic epilepsy, while our laboratory continued to study status epilepticus elicited by pilocarpine. Among postgraduate students Pavel Kršek defended PhD Thesis on nonconvulsive status epilepticus [124,125] and then left for the Department of Child Neurology at the Second Medical Faculty. Today he is the head of this department and continues to study childhood epilepsies in clinics. Lucie Suchomelová (postgraduate student of Hana Kubová), who defended her PhD Thesis little later, left for postdoc to the laboratory of Professor Claude Wasterlain in University of California in Los Angeles. It was a start of a collaboration (mostly Hana's) with Claude who was also involved in experimental studies of epilepsy in immature brain [126,127]. This collaboration lasted up to 2023 when Prof. Wasterlain was retired.

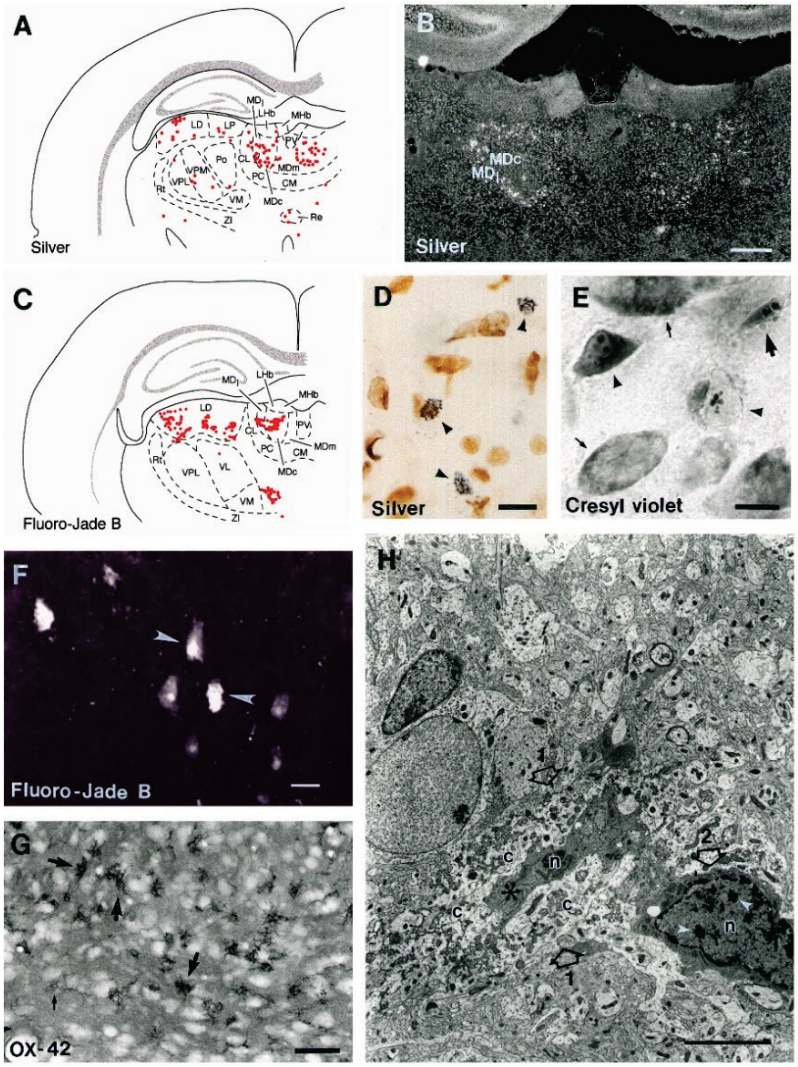

Fig. 3. Early life status epilepticus-induced neurodegeneration in the mediodorsal thalamus. Status epilepticus (SE) was induced chemically in P12 rats. The distribution of degenerating neurons is demonstrated in the computer-generated plots (**A** and **C**). Degenerating neurons were detected using silver staining (**B** and **D**), Fluoro Jade B staining (**F**) and cresyl violet staining (**E**) 48 h after SE. Panel (**G**) illustrated activated microglia surrounding degenerating neurons. The presence of irreversibly damaged neurons was confirmed by electron microscopy (**H**). Modified from Kubová *et al.* [121].

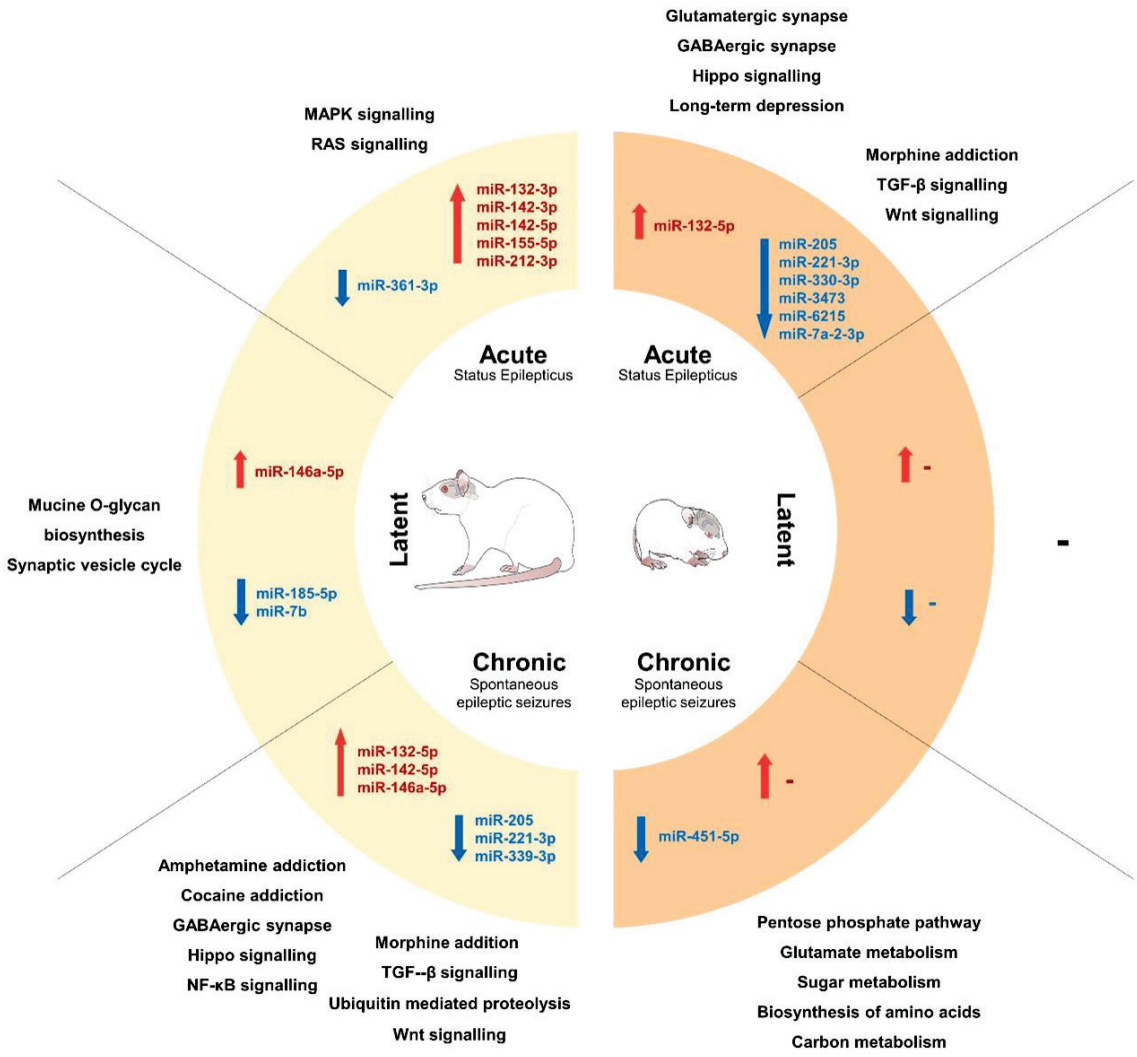

Fig. 4. The overview of dysregulated miRNAs after status epilepticus (SE) induced in adult (adult rat) and infant (rat pup) rats. The inner parts specify the stage of epileptogenesis with a short description of seizure occurrence. The middle parts contain the lists of dysregulated miRNAs in the respective stages. Upregulated miRNAs are displayed in red, while downregulated miRNA after SE are shown in blue. The outer parts list the predicted pathways affected by dysregulated miRNAs in the given stage. Modified from Bencurova *et al.* [176].

Přemysl Jiruška, a postgraduate student of Professor Brožek, asked me to be his tutor after Brožek´s death. He finished his PhD Thesis and after the successfull defense he left for United Kingdom (Department of Physiology in University of Birmigham led by Professor John Jefferys). There he spent four years and published some very good papers mostly on fast EEG frequencies and their role in epileptic seizures and epileptogenesis [128-131]. He came back after a drastic reduction of money for universities in the United Kingdom and continued in our laboratory with the analysis of EEG [132-135]. In 2021 he left the Institute of Physiology and became head of Department of Physiology in Second Medical Faculty of Charles University where he continues in epilepsy research. In 2001 Jakub Otáhal entered our laboratory and became fully involved in the study of epileptic seizures and their consequences utilizing his experience with brain hypoxia [136-143]. His collaboration with Jaroslava Folbergrová resulted in a series of excellent papers [144-148]. He also had four PhD students, two of them finished and defended their PhD Thesis (Carol Brožíčková and Tufi Brima) [149,150].

Two girls started their PhD studies under my (Denisa Lojková) and Hana´s (Adéla Máteffyová) tutorships and successfully finished their PhD studies [151-155]. A little later Grigoryi Tsenov came from Ukraine, absolved PhD studies [156-158] and stayed for some time in the laboratory before he went to Italy to make his postdoc in Verona. After coming back to Prague he took a position in National Institute of Mental Health and till now he has a small collaboration

with our laboratory.

In the meantime I started to lecture basic neurophysiology for physiotherapeuts and nearly each year at least one student prepared bachelor or magister thesis on motor development of rats and possibilities to affect this development by antiseizure medication or by treatment with agonist or antagonist of various mediator systems [102,159]. The result of collaboration with Professor Jana Tchekalarova from Sofia was a series of papers on possible effects of caffeine postnatal administration [160-168]. It was in accordance with our program because one of the topics in the laboratory was the role of adenosine in epileptic seizures [169]. PhD student Petr Fábera prepared his PhD Thesis in this field [170,171]. In relation to the role of adenosine in the arrest of epileptic seizures we started to study changes of excitability after epileptic seizures [172-175].

Hana Kubová started collaboration with CEITEC and Masaryk University in Brno (prof. Milan Brázdil) on microRNA and their regulatory role in epilepsies [176,177] (Fig. 4). We also began collaboration with neurosteroid group of Eva Kudová (Institute of Organic Chemistry and Biochemistry of the Czech Academy of Sciences) and with Karel Valeš from National Institute of Mental Health in the field of neuroactive steroids. This collaboration up till now resulted in three common publications [178-180] and a patent. In this collaboration we are using not only pentylenetetrazol-induced seizures but also a new model of temporal epileptic seizures – seizures elicited by transcorneal 6 Hz stimulation. In this field we started collaboration with Department of Pharmacology, University of Utah, Salt Lake City (Cameron S. Metcalf) and the first common publication is submitted.

Present situation in the Department of Developmental Epileptology is not optimistic. The department is old but still producing good publications. On the other hand, many our former PhD students continue in epilepsy research at their new leading positions. Another positive fact is that Czech experimental as well as clinical epileptologists publish their results in high quality international journals.

Conflict of Interest

There is no conflict of interest.

Acknowledgements

This research was supported by the project National Institute for Neurology Research (Programme EXCELES, ID Project No. LX22NPO5107) – Funded by the European Union-Next Generation EU.

References

1. Servít Z, Bureš J. Effect of electrotonus on readiness for convulsions in various stages of phylogenic development. (Article in Russian) Chekh Fiziol 1952;1:301-311.
2. Servít Z, Bureš J. Cerebral water metabolism and convulsion threshold in frogs. (Article in Czech) Cesk Fysiol 1952;1:88-92.
3. Nováková V, Lodin Z, Servít Z, Chocholová L. Relation of experimental neuroses to audiogernic epilepsy. (Article in Czech). Cesk Fyziol 1957;6:389-396.
4. Chocholová L. The role of cerebral cortex in audiogenic seizures in the rat. Physiol Bohemoslov 1962;11:452-457.
5. Chocholová L. The effect of epileptogenic acoustic stimulation and seizures on the retention of a memory trace in the rat. Physiol Bohemoslov 1965;14:523-529.
6. Servít Z, Šterc J. Audiogenic epileptic seizures evoked in rats by artificial epileptogenic foci. Nature 1958;181:1475-1476. https://doi.org/10.1038/1811475b0
7. Servít Z. Prophylactic treatment of post-traumatic audiogenic epilepsy. Nature 1960;188:669-670. https://doi.org/10.1038/188669a0
8. Machek J, Horák F. Studies on function of the cerebral cortex in the mechanism determining the course and initial motor deviations in audiogenic epileptic seizures in laboratory rats. (Article in Czech) Cesk Fysiol 1958;7:196-197.
9. Holubář J, Hanke B, Malík V. Intracellular recording from cortical pyramids and small interneurons as identified by subsequent staining with the recording microelectrode. Exp Neurol 1967;19:257-264. https://doi.org/10.1016/0014-4886(67)90024-6
10. Fischer J, Holubář J, Malík V. A new method of producing chronic epileptogenic cortical foci in rats. Physiol Bohemoslov 1967;16:272-277.

11. Holubář J, Fischer J. Electrophysiological properties of the epileptogenic cortical foci produced by a new cobalt-gelatine method in rats an attempt to correlate the electrophysiological, histological and histochemical data. Physiol Bohemoslov 1967;16:278-284.
12. Fischer J, Holubář J, Malík V. Dehydrogenase patterns of the experimental epileptogenic cortical focus in the rat. A correlation of histochemical and electrophysiological findings. Acta Histochem 1968;31:296-304.
13. Fischer J, Holubář J, Malík V. Neurohistological study of the development of experimental epileptogenic cortical cobalt-gelatine foci in rats and their correlation with the onset of epileptic electrical activity. Acta Neuropathol 1968;11:45-54. https://doi.org/10.1007/BF00692794
14. Fischer J. Electron microscopic changes in the perikarya and in the processes of ganglion cells in the cobalt gelatine epileptogenic focus (their correlation with electrophysiological data). Physiol Bohemoslov 1969;18:387-394.
15. Fischer J. Electron microscopic alterations in the vicinity of epileptogenic cobalt-gelatine necrosis in the cerebral cortex of the rat. A contribution to the ultrastructure of "plasmatic infiltration" of the central nervous system. Acta Neuropathol 1969;14:201-214. https://doi.org/10.1007/BF00685300
16. Fischer J. Electron microscopy findings with respect to epileptogenic cobalt necrosis in the rat brain. (Article in German) Experientia 1968;24:162. https://doi.org/10.1007/BF02146961
17. Fischer J. Attempt at an ultrastructural analysis of blood-brain barrier damage in the epileptogenic zone round experimental cobalt-gelatine necrosis in the rat. Physiol Bohemoslov 1972;21:171-176.
18. Servít Z. Phylogenesis and ontogenesis of the epileptic seizure. A comparative study. World Neurol 1962;3:259-274.
19. Servít Z. Comparative pathophysiology of the epileptic seizure. (Article in French). Actual Neurophysiol (Paris) 1964;5:163-179.
20. Servít Z, Machek J, Fischer J. Electrical activity of the frog brain during electrically induced seizures. A comparative study of the spike and wave complex. Electroenceph Clin Neurophysiol 1965;19:162-171. https://doi.org/10.1016/0013-4694(65)90226-9
21. Servít Z, Strejčková A. Comparative pathophysiology of the paroxysmal electroencephalogram. Paroxysmal electroencephalogram (spike and wave activity) in the lizard (Lacerta agilis). Physiol Bohemoslov 1966;15:117-121.
22. Servít Z, Strejčková A, Fischer J. Effects of strychnine and gamma-aminobutyric acid on spike and wave activity in the frog telencephalon. Exp Neurol 1967;17:389-402. https://doi.org/10.1016/0014-4886(67)90115-X
23. Servít Z, Strejčková A, Volanschi D. An epileptogenic focus in the frog telencephalon. Pathways of propagation of focal activity. Exp Neurol 1968;21:383-396. https://doi.org/10.1016/0014-4886(68)90060-5
24. Volanschi D, Servít Z. Epileptic focus in the forebrain of the turtle. Exp Neurol 1969;24:137-146. https://doi.org/10.1016/0014-4886(69)90011-9
25. Servít Z. Focal epileptic activity and its spread in the brain of lower vertebrates. A comparative electrophysiological study. Epilepsia 1970;11:227-240. https://doi.org/10.1111/j.1528-1157.1970.tb03887.x
26. Servít Z, Strejčková A. An electrographic epileptic focus in the fish forebrain. Conditions and pathways of propagation of focal and paroxysmal activity. Brain Res 1970;17:103-113. https://doi.org/10.1016/0006-8993(70)90310-0
27. Servít Z, Strejčková A. Epileptic focus in the frog forebrain. Triggering of the focal discharge with sensory stimuli. Exp Neurol 1970;28:371-383. https://doi.org/10.1016/0014-4886(70)90174-3
28. Servít Z, Strejčková A, Volanschi D. Epileptic focus in the forebrain of the turtle (Testudo graeca). Triggering of focal discharges with different sensory stimuli. Physiol Bohemoslov 1971;20:221-228.
29. Servít Z, Strejčková A. Thalamocortical relations and the genesis of epileptic electrographic phenomena in the forebrain of the turtle. Exp Neurol 1972;35:50-60. https://doi.org/10.1016/0014-4886(72)90059-3
30. Servít Z, Strejcková A. Experimental thalamic focus and thalamocortical epileptogenic mechanisms in the brain of turtle. Epilepsia 1973;14:437-445. https://doi.org/10.1111/j.1528-1157.1973.tb03984.x
31. Servít Z, Strejčková A. Thalamocortical relations in the brain of the frog, Their role in the genesis of epileptic electrographic phenomena. Physiol Bohemoslov 1975;24:315-324.
32. Servít Z. Pathophysiological principles of prevention of post-traumatic epilepsy. (Article in Czech) Cas Lek Cesk 1969;108:129-133.
33. Servít Z, Musil F. Prophylactic treatment of posttraumatic epilepsy: results of a long-term follow-up in Czechoslovakia. Epilepsia 1981;22:315-320. https://doi.org/10.1111/j.1528-1157.1981.tb04115.x

34. Servít Z, Krištof M, Kolínová M. Activation of epileptic electrographic phenomena in the human EEG by nasal air flow. Physiol Bohemoslov 1977;26:499-506.
35. Krištof M, Servít Z, Manas K. Activating effect of nasal air flow on epileptic electrographic abnormalities in the human EEG. Evidence for the reflect origin of the phenomenon. Physiol Bohemoslov 1981;30:73-77.
36. Servít Z, Krištof M, Strejčková A. Activating effect of nasal and oral hyperventilation on epileptic electrographic phenomena: reflex mechanisms of nasal origin. Epilepsia 1981;22:321-329. https://doi.org/10.1111/j.1528-1157.1981.tb04116.x
37. Krištof M, Preiss J, Servít Z. Physiological asymmetry of brain functions--its influence on the lateralization, symptomatology and course of the epileptic process. Physiol Bohemoslov 1986;35:447-455.
38. Machek J, Ujec E, Pavlík V. Cortical extracellular potassium concentration during the development of the interhemispheric response into the selfsustained afterdischarge. Physiol Bohemoslov 1975;24:41-44.
39. Machek J, Ujec E, Pavlík V. Extracellular potassium concentration and focal electrical potentials elicited in the cerebral cortex of rat by interhemispheric stimulation. Neurosci Lett 1976;2:147-152. https://doi.org/10.1016/0304-3940(76)90006-9
40. Machek J, Ujec E, Pavlík V, Horák F. Interhemispheric field potentials, spreading depression and kindling. Neurosci Lett 1977;4:337-341. https://doi.org/10.1016/0304-3940(77)90180-X
41. Machek J, Ujec E, Pavlík V. Slow potential changes in experimental neocortical propagated foci. Neurosci Lett 1981;25:327-332. https://doi.org/10.1016/0304-3940(81)90413-4
42. Roldán E, Radil-Weiss T, Chocholová L. Influence of chlordiazepoxide on paroxysmal EEG activity induced by hippocampal and-or thalamic cobalt foci. Psychopharmacologia 1971;19:266-272. https://doi.org/10.1007/BF00401943
43. Roldán E, Radil-Weiss T, Chocholová L. Epileptic electroencephalographic activity induced by cobalt foci in the dorsal hippocampus and-or thalamus. Int J Neurosci 1971;2:293-300. https://doi.org/10.3109/00207457109147012
44. Chocholová L, Kolínová M, Fischer J. Stimulation of the thalamus and its effect on electrographic manifestations of the brain in unrestrained rats. Physiol Bohemoslov 1977;26:507-515.
45. Kolínová M, Chocholová L. Stimulation of the hippocampus and its effect on electrographic manifestations of the brain in unrestrained rats. Physiol Bohemoslov 1977;26:517-224.
46. Kolínová M, Chocholová L. The relationship between vigilance and cortical EEG manifestations after electrical stimulation of the thalamus and hippocampus in unrestrained rats. Physiol Bohemoslov 1978;27:321-328.
47. Fischer J. Electron microscopy findings with respect to epileptogenic cobalt necrosis in the rat brain. (Article in German) Experientia 1968;24:162. https://doi.org/10.1007/BF02146961
48. Fischer J. Electron microscopic alterations in the vicinity of epileptogenic cobalt-gelatine necrosis in the cerebral cortex of the rat. A contribution to the ultrastructure of "plasmatic infiltration" of the central nervous system. Acta Neuropathol 1969;14:201-214. https://doi.org/10.1007/BF00685300
49. Fischer J. Attempt at an ultrastructural analysis of blood-brain barrier damage in the epileptogenic zone round experimental cobalt-gelatine necrosis in the rat. Physiol Bohemoslov 1972;21:171-176.
50. Fischer J. Change in the number of vesicles in synapses of a projected epileptic cortical focus in rats. Physiol Bohemoslov 1973;22:537-42
51. Fischer J. Electron microscopic changes in the active zone of the synapses in an acute projected epileptic cortical focus in the rat. Physiol Bohemoslov 1977;26:189-192.
52. Nagy Z, Fischer J. Development of perifocal edema in experimental epilepsy nduced by cobalt-gelatin. Acta Neuropathol 1978;41:191-195. https://doi.org/10.1007/BF00690434
53. Langmeier M, Fischer J. The thinning of synaptic and glial membranes in an acute projected epileptic cortical focus in the rat. An electronmicroscopical, morphometrical study. Physiol Bohemoslov 1979;28:381-384.
54. Fischer J, Langmeier M. Changes in the number, size, and shape of synaptic vesicles in an experimental, projected cortical epileptic focus in the rat. Epilepsia 1980;21:571-585. https://doi.org/10.1111/j.1528-1157.1980.tb04311.x
55. Langmeier M, Fischer J, Mareš J. Number of synaptic vesicles in the rat somatosensory cortex after repetitive electrical stimulation prolonging self-sustained after-discharges. Epilepsia 1980;21:255-260. https://doi.org/10.1111/j.1528-1157.1980.tb04071.x
56. Langmeier M, Fischer J, Mareš J. Ultrastructural changes in cortical synapses shortly after termination of a seizure during kindling. Physiol Bohemoslov 1982;31:213-216.

57. Havel J, Langmeier M, Fischer J, Mareš J. Changes in the size and shape of synaptic vesicles in the sensorimotor cortex of the rat brain after repeated epileptic seizures. Physiol Bohemoslov 1982;31:91-94.
58. Langmeier M, Mareš J, Fischer J. Number of synaptic vesicles in rat cortex immediately after cessation of the self-sustained afterdischarge during kindling. Epilepsia 1983;24:616-627. https://doi.org/10.1111/j.1528-1157.1983.tb03427.x
59. Fischer J, Mareš P, Kostka J, Malík V, Filip J. Na-G-penicillin penetration into rat cerebral cortex and formation of an epileptic focus. Physiol Bohemoslov 1978;27:171-177.
60. Mareš P. Bioelectrical activity of an epileptogenic focus in rat neocortex. Brain Res 1973;56:203-213. https://doi.org/10.1016/0006-8993(73)90335-1
61. Mareš P. Ontogenetic development of bioelectrical activity of the epileptogenic focus in rat neocortex. Neuropadiatrie 1973;4:434-445. https://doi.org/10.1055/s-0028-1091759
62. Mareš P. Symmetrical epileptogenic foci in immature rat cerebral cortex. Epilepsia 1973;14:427-435. https://doi.org/10.1111/j.1528-1157.1973.tb03983.x
63. Mareš J, Mareš P. Triggering of discharges from an epileptogenic focus in the rat by stimulation of the contralateral hemisphere. An ontogenetic study. Physiol Bohemoslov 1978;27:15-22.
64. Mareš P, Filip J, Mareš J. The role of the corpus callosum in the interhemispheric transmission of epileptic interictal activity. Physiol Bohemoslov 1978;27:23-29.
65. Mareš J, Mareš P, Trojan S. The ontogenesis of cortical self-sustained after-discharges in rats. Epilepsia 1980;21:111-121. https://doi.org/10.1111/j.1528-1157.1980.tb04051.x
66. Mareš P, Schickerová R. Seizures elicited by subcutaneous injection of metrazol during ontogenesis in rats. Activ Nerv Super 1980;22:264-248.
67. Mareš P, Marešová D, Schickerová R. Effect of antiepileptic drugs on metrazol convulsions during ontogenesis in the rat. Physiol Bohemoslov 1981;30:113-121.
68. Pohl M, Mareš P. Flunarizine influences metrazol-induced seizures in developing rats. Epilepsy Res 1987;1:302-305. https://doi.org/10.1016/0920-1211(87)90006-4
69. Kubová H, Mareš P. Time course of the anticonvulsant action of clonazepam in the developing rats. Arch Int Pharmacodyn 1989;298:15-24.
70. Langmeier M, Fischer J, Mareš J. Ultrastructural changes in cortical synapses shortly after termination of a seizure during kindling. Physiol Bohemoslov 1982;31:213-236.
71. Langmeier M, Mareš J, Fischer J. Number of synaptic vesicles in rat cortex immediately after cessation of the self-sustained afterdischarge during kindling. Epilepsia 1983;24:616-627. https://doi.org/10.1111/j.1528-1157.1983.tb03427.x
72. Pohl M, Mareš P. Flunarizine influences metrazol-induced seizures in developing rats. Epilepsy Res 1987;1:302-305. https://doi.org/10.1016/0920-1211(87)90006-4
73. Pohl M, Mareš P. Localisation of the origin of self-sustained afterdischarges (SSADs) in the rat: the serrated wave (SerW) type of SSAD. Physiol Bohemoslov 1990;39:335-342.
74. Pohl M, Mareš P, Langmeier M. Localization of the origin of self-sustained after-discharges (SSADs) in the rat. I. The spike-and-wave (S+W) type of SSAD. Epilepsia 1986;27:516-522. https://doi.org/10.1111/j.1528-1157.1986.tb03577.x
75. Velíšková J, Velíšek L, Mareš P. Epileptic phenomena produced by kainic acid in laboratory rats during ontogenesis. Physiol Bohemoslov 1988;37:395-405.
76. Velíšek L, Kusá R, Kulovaná M, Mareš P. Excitatory amino acid antagonists and pentylenetetrazol-induced seizures during ontogenesis: 1. The effects of 2-amino-7-phosphonoheptanoate. Life Sci 1990;46:1349-1357. https://doi.org/10.1016/0024-3205(90)90334-N
77. Velíšek L, Verešová S, Pobišová H, Mareš P. Excitatory amino acid antagonists and pentylenetetrazol-induced seizures during ontogenesis. 2. The effects of MK-801. Psychopharmacology 1991;14:510-514. https://doi.org/10.1007/BF02245658
78. Velíšek L, Kubová H, Mareš P, Vachová D. Kainate/AMPA receptor antagonists are anticonvulsant against the tonic hindlimb component of pentylenetetrazol-induced seizures in developing rats. Pharmacol Biochem Behav 1995;51:153-158. https://doi.org/10.1016/0091-3057(94)00329-H

79. Velíšek L, Roztočilová L, Kusá R, Mareš P. Excitatory amino-acid antagonists and pentylenetetrazol-induced seizures during ontogenesis: III. The action of kynuretic acid and glutamic acid diethylester. Brain Res Bull 1995;38:525-529. https://doi.org/10.1016/0361-9230(95)02019-3
80. Velíšek L, Vachová D, Mareš P. Excitatory amino acid antagonists and pentylenetetrazol-induced seizures during ontogenesis. IV. Effect of CGP 39551. Pharmacol Biochem Behav 1997;56:493-498. https://doi.org/10.1016/S0091-3057(96)00245-6
81. Mareš P, Velíšek L. N-Methyl-D aspartate (NMDA)-induced seizures in developing rats. Dev Brain Res 1992;65:185-189. https://doi.org/10.1016/0165-3806(92)90178-Y
82. Kubová H, Mareš P. Anticonvulsant effects of phenobarbital and primidone during ontogenesis in rats. Epilepsy Res 1991;10:148-155. https://doi.org/10.1016/0920-1211(91)90007-3
83. Kubová H, Mareš P. The effect of ontogenetic development on the anticonvulsant activity of midazolam. Life Sci 1992;50:1665-1672. https://doi.org/10.1016/0024-3205(92)90421-K
84. Kubová H, Mareš P. Anticonvulsant action of oxcarbazepine, hydroxycarbamazepine and carbamazepine against metrazol-induced motor seizures in developing rats. Epilepsia 1993;34:188-192. https://doi.org/10.1111/j.1528-1157.1993.tb02397.x
85. Kubová H, Rathouská J, Mareš P. Anticonvulsant effects of bretazenil (Ro 16-6028) during ontogenesis. Epilepsia 1993;34:1130-1134. https://doi.org/10.1111/j.1528-1157.1993.tb02145.x
86. Kubová H, Mareš P. Effects of MK-801 (Dizocilpine) and ketamine on strychnine-induced convulsions in rats: Comparison with benzodiazepines and standard anticonvulsants. Physiol Res 1994;43:313-320.
87. Kubová H, Folbergrová J, Mareš P. Seizures induced by homocysteine in rats during ontogenesis. Epilepsia 1995;36:750-756. https://doi.org/10.1111/j.1528-1157.1995.tb01611.x
88. Kubová H, Lanštiaková M, Mocková M, Mareš P, Vorlíček J. Pharmacology of cortical epileptic afterdischarges in rats. Epilepsia 1996;37:336-341. https://doi.org/10.1111/j.1528-1157.1996.tb00569.x
89. Kubová H, Világi I, Mikulecká A, Mareš P. NonNMDA antagonist GYKI 52466 suppresses cortical afterdischarges in immature rats. Eur J Pharmacol 1997;333:17-26. https://doi.org/10.1016/S0014-2999(97)01119-9
90. Kubová H, Haugvicová R, Mareš P. Effects of NNC 711, a GABA uptake inhibitor, on pentylenetetrazol-induced seizures in developing and adult rats. Naunyn Schmiedebergs Arch Pharmacol 1998;358:334-341. https://doi.org/10.1007/PL00005262
91. Kubová H, Mikulecká A, Haugvicová R, Mareš P. The benzodiazepine receptor partial agonist Ro 19-8022 suppresses generalized seizures without impairing motor functions in developing rats. Naunyn Schmiedebergs Arch Pharmacol 1999;360:565-574. https://doi.org/10.1007/s002109900126
92. Druga R, Kubová H, Mareš P. Degenerative neuronal changes in the rat thalamus induced by status epilepticus at different developmental stages. Epilepsy Res 2005;63:43-65. https://doi.org/10.1016/j.eplepsyres.2004.11.001
93. Druga R, Mareš P, Kubová H. Time course of neuronal damage in the hippocampus following lithium-pilocarpine status epilepticus in 12-day-old rats. Brain Res 2010;1355:174-179. https://doi.org/10.1016/j.brainres.2010.07.072
94. Mikulecká A, Mareš P. NMDA receptor antagonists impair motor performance in immature rats. Psychopharmacology 2002;162:364-372. https://doi.org/10.1007/s00213-002-1122-2
95. Mikulecká A, Kubová H, Mareš P. Lamotrigine does not impair motor performance and spontaneous behavior in developing rats. Epilepsy Behav 2004;5:464-471. https://doi.org/10.1016/j.yebeh.2004.04.013
96. Mareš P, Mikulecká A. MPEP, an antagonist of metabotropic glutamate receptors, exhibits anticonvulsant action in immature rats without a serious impairment of motor performance. Epilepsy Res 2004;60:17-26. https://doi.org/10.1016/j.eplepsyres.2004.04.008
97. Mikulecká A, Mareš P. Postictal behavior after two types of cortical epileptic afterdischarges in rats. Epilepsy Behav 2007;10:213-218. https://doi.org/10.1016/j.yebeh.2006.11.015
98. Mareš P, Mikulecká A. Different effects of two NMDA receptor antagonists on seizures, spontaneous behavior and motor performance in immature rats. Epilepsy Behav 2009;14:32-39. https://doi.org/10.1016/j.yebeh.2008.08.013
99. Mikulecká A, Mareš P, Kubová H. Rebound increase of seizure susceptibility but not isolation calls after single administration of clonazepam and Ro 19-8022 in infant rats. Epilepsy Behav 2011;20:12-19. https://doi.org/10.1016/j.yebeh.2010.10.021

100. Mikulecká A, Šubrt M, Pařízková M, Mareš P, Kubová H: Consequences of early postnatal benzodiazepines exposure in rats. II. Social behavior. Frontiers Behav Sci 2014;8:169. https://doi.org/10.3389/fnbeh.2014.00169
101. Mikulecká A, Druga R, Stuchlík A, Mareš P, Kubová H. Comorbidities of early-onset temporal epilepsy: Cognitive, social, emotional, and morphologic dimensions. Exp Neurol 2019;320:113005. https://doi.org/10.1016/j.expneurol.2019.113005
102. Mareš P, Kozlová L, Mikulecká A, Kubová H. The GluN2B-selective antagonist Ro 25-6981 is effective against PTZ-induced seizures and safe for further development in infantile rats. Pharmaceutics 2021;13:1482. https://doi.org/10.3390/pharmaceutics13091482
103. Kubová H, Mikulecká A, Mareš P. The outcome of early life status epilepticus - lessons from laboratory animals. Epilepsia Open 2023;8(Suppl 1):S90-S109. https://doi.org/10.1002/epi4.12664
104. Folbergrová J. Cerebral energy state of neonatal rats during seizures induced by homocysteine. Physiol Res 1993;42:155-160.
105. Folbergrová J, He QP, Li PA, Smith ML, Siesjö BK. The effect of alpha-phenyl-N-tert-butyl nitrone on bioenergetic state in substantia nigra following flurothyl-induced status epilepticus in rats. Neurosci Lett 1999;266:121-124. https://doi.org/10.1016/S0304-3940(99)00279-7
106. Folbergrová J, Ješina P, Drahota Z, Lisý V, Haugvicová R, Vojtíšková A, Houštěk J. Mitochondrial complex I inhibition in cerebral cortex of immature rats following homocysteic acid-induced seizures. Exp Neurol 2007;204:597-609. https://doi.org/10.1016/j.expneurol.2006.12.010
107. Folbergrová J, Ješina P, Haugvicová R, Lisý V, Houštěk J. Sustained deficiency of mitochondrial complex I activity during long periods of survival after seizures induced in immature rats by homocysteic acid. Neurochem Int 2010;56:394-403. https://doi.org/10.1016/j.neuint.2009.11.011
108. Folbergrová J, Kunz WS. Mitochondrial dysfunction in epilepsy. Mitochondrion 2012;12:35-40. https://doi.org/10.1016/j.mito.2011.04.004
109. Folbergrová J, Ješina P, Nůsková H, Houštěk J. Antioxidant enzymes in cerebral cortex of immature rats following experimentally-induced seizures: upregulation of mitochondrial MnSOD (SOD2). Int J Dev Neurosci 2013;31:123-130. https://doi.org/10.1016/j.ijdevneu.2012.11.011
110. Mareš P, Folbergrová J, Haugvicová R, Kubová H. Do stereoisomers of homocysteic acid exhibit different convulsant action in immature rats? Physiol Res 2019;63(Suppl 3):S361-S366. https://doi.org/10.33549/physiolres.934347
111. Mareš P, Folbergrová J, Langmeier M, Haugvicová R, Kubová, H. Convulsant action of D,L-homocysteic acid and its stereoisomers in immature rats. Epilepsia 1997;38:767-776. https://doi.org/10.1111/j.1528-1157.1997.tb01463.x
112. Mareš P, Haugvicová R. Anticonvulsant action of gabapentin during postnatal development in rats. Epilepsia 1997;38:893-896. https://doi.org/10.1111/j.1528-1157.1997.tb01254.x
113. Haugvicová R, Kubová H, Mareš P. Qualitative changes of anticonvulsant action of felbamate during development in rats. Brain Dev 1998;20:222-226. https://doi.org/10.1016/S0387-7604(98)00030-8
114. Haugvicová R, Kubová H, Mareš P. Antipentylenetetrazol action of clobazam in developing rats. Physiol Res 1999;48:501-507.
115. Haugvicová R, Škutová M, Kubová H, Suchomelová L, Mareš P. Two different anticonvulsant actions of tiagabine in developing rats. Epilepsia 2000;41:1375-1381. https://doi.org/10.1111/j.1528-1157.2000.tb00112.x
116. Mareš P, Haugvicová R, Kubová H. Unequal development of thresholds for various phenomena induced by cortical stimulation in rats. Epilepsy Res 2002;49:35-43. https://doi.org/10.1016/S0920-1211(02)00009-8
117. Haugvicová R, Bílková E, Kubová H, Mareš P. Effects of classical antiepileptics on thresholds for phenomena induced by cortical stimulation in rats. J Pharm Pharmacol 2002;54:1011-1015. https://doi.org/10.1211/002235702760089153
118. Mareš P, Mikulecká A, Haugvicová R, Kasal A. Anticonvulsant action of allopregnanolone in immature rats. Epilepsy Res 2006;70:110-117. https://doi.org/10.1016/j.eplepsyres.2006.03.009
119. Druga R, Salaj M, Barinka F, Edelstein L, Kubová H. Calretinin immunoreactivity in the claustrum of the rat. Front Neuroanat 2015;8:160. https://doi.org/10.3389/fnana.2014.00160
120. Salaj M, Barinka F, Kubová H, Druga R. Differences in expression of calcium binding proteins in the perirhinal and retrosplenial cortex of the rat. Physiol Res 2021;70:273-285. https://doi.org/10.33549/physiolres.934548

121. Kubová H, Druga R, Lukasiuk K, Suchomelová L, Haugvicová R, Jirmanová I, Pitkänen A. Status epilepticus causes necrotic damage in the mediodorsal nucleus of the thalamus in immature rats. J Neurosci 2001;21:3593-3599. https://doi.org/10.1523/JNEUROSCI.21-10-03593.2001
122. Kubová H, Druga R, Haugvicová R, Suchomelová L, Pitkänen A. Dynamic changes of status epilepticus-induced neuronal degeneration in the mediodorsal nucleus of the thalamus during postnatal development of the rat. Epilepsia 2002;43(Suppl 5):54-60. https://doi.org/10.1046/j.1528-1157.43.s.5.36.x
123. Nairismägi J, Pitkänen A, Kettunen MI, Kauppinen RA, Kubova H. Status epilepticus in 12-day-old rats leads to temporal lobe neurodegeneration and volume reduction: a histologic and MRI study. Epilepsia 2006;47:479-488. https://doi.org/10.1111/j.1528-1167.2006.00455.x
124. Kršek P, Mikulecká A, Druga R, Hliňák Z, Kubová H, Mareš P. An animal model of nonconvulsive status epilepticus: a contribution to clinical controversies. Epilepsia 2001;42:171-180. https://doi.org/10.1046/j.1528-1157.2001.35799.x
125. Kršek P, Mikulecká A, Druga R, Kubová H, Hliňák Z, Suchomelová, L, Mareš P. Long-term behavioral and morphological consequences of nonconvulsive status epilepticus in rats. Epilepsy Behav 2004;5:180-191. https://doi.org/10.1016/j.yebeh.2003.11.032
126. Suchomelova L, Baldwin RA, Kubova H, Thompson KW, Sankar R, Wasterlain CG. Treatment of experimental status epilepticus in immature rats: dissociation between anticonvulsant and antiepileptogenic effects. Pediatr Res 2006;59:237-243. https://doi.org/10.1203/01.pdr.0000196333.16608.30
127. Suchomelova L, Lopez-Meraz ML, Niquet J, Kubova H, Wasterlain CG. Hyperthermia aggravates status epilepticus-induced epileptogenesis and neuronal loss in immature rats. Neuroscience 2015;305:209-224. https://doi.org/10.1016/j.neuroscience.2015.08.006
128. Jefferys JGR, Jiruska P, de Curtis M, Avoli M. Limbic network synchronization and temporal lobe epilepsy. In: *Jasper's Basic Mechanisms of the Epilepsies [Internet]*. Noebels JL, Avoli M, Rogawski MA, Olsen RW, Delgado-Escueta AV (eds), 4th edition. Bethesda (MD), National Center for Biotechnology Information (US), 2012. https://doi.org/10.1093/med/9780199746545.003.0014
129. Jiruska P, de Curtis M, Jefferys JG, Schevon CA, Schiff SJ, Schindler K. Synchronization and desynchronization in epilepsy: controversies and hypotheses. J Physiol 2013;591:787-797. https://doi.org/10.1113/jphysiol.2012.239590
130. Zijlmans M, Jiruska P, Zelmann R, Leijten FS, Jefferys JG, Gotman J. High-frequency oscillations as a new biomarker in epilepsy. Ann Neurol 2012;71:169-178. https://doi.org/10.1002/ana.22548
131. Jiruska P, de Curtis M, Jefferys JG, Schevon CA, Schiff SJ, Schindler K. Synchronization and desynchronization in epilepsy: controversies and hypotheses. J Physiol 2013;591:787-797. https://doi.org/10.1113/jphysiol.2012.239590
132. Janca R, Krsek P, Jezdik P, Cmejla R, Tomasek M, Komarek V, Marusic P, Jiruska P. the sub-regional functional organization of neocortical irritative epileptic networks in pediatric epilepsy. Front Neurol 2018;9:184. https://doi.org/10.3389/fneur.2018.00184
133. Chang WC, Kudlacek J, Hlinka J, Chvojka J, Hadrava M, Kumpost V, Powell AD, ET AL. Loss of neuronal network resilience precedes seizures and determines the ictogenic nature of interictal synaptic perturbations. Nat Neurosci 2018;21:1742-1752. https://doi.org/10.1038/s41593-018-0278-y
134. Dulla CG, Janigro D, Jiruska P, Raimondo JV, Ikeda A, Lin CK, Goodkin HP, ET AL. How do we use in vitro models to understand epileptiform and ictal activity? A report of the TASK1-WG4 group of the ILAE/AES Joint Translational Task Force. Epilepsia Open 2018;3:460-473. https://doi.org/10.1002/epi4.12277
135. Janca R, Krsek P, Jezdik P, Cmejla R, Tomasek M, Komarek V, Marusic P, Jiruska P. Corrigendum: The sub-regional functional organization of neocortical irritative epileptic networks in pediatric epilepsy. Front Neurol 2019;10:631. https://doi.org/10.3389/fneur.2019.00631
136. Kann O, Kovács R, Njunting M, Behrens CJ, Otáhal J, Lehmann TN, Gabriel S, Heinemann U. Changes in cytochrome oxidase in the piriform cortex after status epilepticus in adult rats. Metabolic dysfunction during neuronal activation in the ex vivo hippocampus from chronic epileptic rats and humans. Brain 2005;128:2396-2407. https://doi.org/10.1093/brain/awh568
138. Dugladze T, Vida I, Tort AB, Gross A, Otahal J, Heinemann U, Kopell NJ, Gloveli T. Impaired hippocampal rhythmogenesis in a mouse model of mesial temporal lobe epilepsy. Proc Natl Acad Sci U S A 2007;104:17530-17535. https://doi.org/10.1073/pnas.0708301104

139. Tolner EA, Hochman DW, Hassinen P, Otáhal J, Gaily E, Haglund MM, Kubová H, ET AL. Five percent CO_2 is a potent, fast-acting inhalation anticonvulsant. Epilepsia 2011;52:104-114. https://doi.org/10.1111/j.1528-1167.2010.02731.x
140. Beamer E, Otahal J, Sills GJ, Thippeswamy T. N(w)-propyl-L-arginine (L-NPA) reduces status epilepticus and early epileptogenic events in a mouse model of epilepsy: behavioural, EEG and immunohistochemical analyses. Eur J Neurosci 2012;36:3194-3203. https://doi.org/10.1111/j.1460-9568.2012.08234.x
141. Kudlacek J, Chvojka J, Posusta A, Kovacova L, Hong SB, Weiss S, Volna K, ET AL. Lacosamide and levetiracetam have no effect on sharp-wave ripple rate. Front Neurol 2017;8:687. https://doi.org/10.3389/fneur.2017.00687
142. Kudlacek J, Chvojka J, Kumpost V, Hermanovska B, Posusta A, Jefferys JGR, Maturana MI, ET AL. Long-term seizure dynamics are determined by the nature of seizures and the mutual interactions between them. Neurobiol Dis 2021;154:105347. https://doi.org/10.1016/j.nbd.2021.105347
143. Daněk J, Danačíková Š, Kala D, Svoboda J, Kapoor S, Pošusta A, Folbergrová J, ET AL. Sulforaphane ameliorates metabolic changes associated with status epilepticus in immature rats. Front Cell Neurosci 2022;16:855161. https://doi.org/10.3389/fncel.2022.855161
144. Folbergrová J, Otáhal J, Druga R. Brain superoxide anion formation in immature rats during seizures: protection by selected compounds. Exp Neurol 2012;233:421-429. https://doi.org/10.1016/j.expneurol.2011.11.009
145. Otáhal J, Folbergrová J, Kovacs R, Kunz WS, Maggio N. Epileptic focus and alteration of metabolism. Int Rev Neurobiol 2014;114:209-243. https://doi.org/10.1016/B978-0-12-418693-4.00009-1
146. Folbergrová J, Ješina P, Kubová H, Otáhal J. Effect of resveratrol on oxidative stress and mitochondrial dysfunction in immature brain during epileptogenesis. Mol Neurobiol 2018;55:7512-7522. https://doi.org/10.1007/s12035-018-0924-0
147. Folbergrová J, Ješina P, Otáhal J. Treatment With resveratrol ameliorates mitochondrial dysfunction during the acute phase of status epilepticus in immature rats. Front Neurosci 2021;15:634378. https://doi.org/10.3389/fnins.2021.634378
148. Folbergrová J, Ješina P, Otáhal J. Protective effect of sulforaphane on oxidative stress and mitochondrial dysfunction associated with status epilepticus in immature rats. Mol Neurobiol 2023;60:2024-2035. https://doi.org/10.1007/s12035-022-03201-x
149. Brožíčková C, Mikulecká A, Otáhal J. Effect of 7-nitroindazole, a neuronal nitric oxide synthase inhibitor, on behavioral and physiological parameters. Physiol Res 2014;63:637-648. https://doi.org/10.33549/physiolres.932781
150. Brima T, Otáhal J, Mareš P. Increased susceptibility to pentetrazol-induced seizures in developing rats after cortical photothrombotic ischemic stroke at P7. Brain Res 2013;1507:146-153. https://doi.org/10.1016/j.brainres.2013.02.037
151. Lojková D, Mareš P. Anticonvulsant action of an antagonist of metabotropic glutamate receptors mGluR5 MPEP in immature rats. Neuropharmacology 2005;49:219-229. https://doi.org/10.1016/j.neuropharm.2005.04.020
152. Lojková D, Živanovič D, Mareš P. Different effects of nonNMDA and NMDA receptor antagonists (NBQX and dizocilpine) on cortical epileptic afterdischarges in rats. Brain Res 2006;1124:167-175. https://doi.org/10.1016/j.brainres.2006.09.072
153. Lojková-Janečková D, Ng J, Mareš P. Antagonists of group I metabotropic glutamate receptors and cortical afterdischarges in immature rats. Epilepsia 2009;50:2123-2129. https://doi.org/10.1111/j.1528-1167.2009.02091.x
154. Mátéffyová A, Otáhal J, Tsenov G, Mareš P, Kubová H. Intrahippocampal injection of endothelin-1 in immature rats results in neuronal death, development of epilepsy, and behavioral abnormalities later in life. Eur J Neurosci 2006;24:351-360. https://doi.org/10.1111/j.1460-9568.2006.04910.x
155. Tsenov G, Mátéffyová A, Mareš P, Otáhal J, Kubová H. Intrahippocampal injection of endothelin-1, a new model of ischemia-induced seizures in immature rats. Epilepsia 2007;48(Suppl 5):7-13. https://doi.org/10.1111/j.1528-1167.2007.01282.x
156. Tsenov G, Kubová H, Mareš P. Changes of cortical epileptic afterdischarges after status epilepticus in immature rats. Epilepsy Res 2008;78:178-185. https://doi.org/10.1016/j.eplepsyres.2007.11.008
157. Tsenov G, Redkozubova O, Kubová H, Mareš P. Effects of lamotrigine on cortically-elicited phenomena in adult rats: differences between acute application and late consequences of early postnatal administration. Brain Res 2009;1258:65-70. https://doi.org/10.1016/j.brainres.2008.12.054
158. Tsenov G, Kubová H, Mareš P. Which component of treatment is important for changes of cortical epileptic afterdischarges after status epilepticus in immature rats? Neurosci Lett 2017;644:1-4. https://doi.org/10.1016/j.neulet.2017.02.043

159. Mareš P, Stehlíková M. Anticonvulsant doses of ganaxolone do not compromise motor performance in immature rats. Neurosci Lett 2010;469:396-399. https://doi.org/10.1016/j.neulet.2009.12.037
160. Tchekalarova J, Kubová H, Mareš P. Postnatal caffeine exposure: effects on motor skills and locomotor activity during ontogenesis. Behav Brain Res 2005;160:99-106. https://doi.org/10.1016/j.bbr.2004.11.018
161. Tchekalarova J, Kubová H, Mareš P. Biphasic effect of chronic postnatal caffeine treatment on cortical epileptic afterdischarges during ontogeny in rats. Brain Res 2006;1082:43-49. https://doi.org/10.1016/j.brainres.2006.01.067
162. Tchekalarova J, Kubová H, Mareš P. Effects of postnatal caffeine exposure on seizure susceptibility in developing rats. Brain Res 2007;1150:32-39. https://doi.org/10.1016/j.brainres.2006.10.035
163. Tchekalarova J, Kubová H, Mareš P. Postnatal caffeine treatment affects differently two pentylenetetrazol seizure models in rats. Seizure 2009;18:463-469. https://doi.org/10.1016/j.seizure.2009.04.002
164. Tchekalarova J, Kubová H, Mareš P. Effects of early postnatal caffeine exposure on seizure susceptibility of rats are age- and model-dependent. Epilepsy Res 2010;88:231-238. https://doi.org/10.1016/j.eplepsyres.2009.11.015
165. Tchekalarova J, Kubová H, Mareš P. Postnatal period of caffeine treatment and time of testing modulate the effect of acute caffeine on cortical epileptic afterdischarges in rats. Brain Res 2010;1356:121-129. https://doi.org/10.1016/j.brainres.2010.07.107
166. Tchekalarova J, Kubová H, Mareš P. Transient changes of cortical interhemispheric responses after repeated caffeine administration in immature rats. Physiol Res 2011;60:961-969. https://doi.org/10.33549/physiolres.932147
167. Tchekalarova J, Kubová H, Mareš P. Different effects of postnatal caffeine treatment on two pentylentetrazol-induced seizure models persist into adulthood. Pharmacol Rep 2013;65:847-853. https://doi.org/10.1016/S1734-1140(13)71065-X
168. Tchekalarova J, Kubová H, Mareš P. Early caffeine exposure: transient and long-term consequences on brain excitability. Brain Res Bull 2014;104:27-35. https://doi.org/10.1016/j.brainresbull.2014.04.001
169. Mareš P. A1 not A2A adenosine receptors play a role in cortical epileptic afterdischarges in immature rats. J Neural Transm 2014;121:1329-1336. https://doi.org/10.1007/s00702-014-1234-y
170. Fábera P, Pařizková M, Uttl L, Vondráková K, Kubová H, Tsenov G, Mareš P. Adenosine A1 receptor agonist 2-chloro-N6-cyclopentyladenosine and hippocampal excitability during brain development in rats. Front Pharmacol 2019;10:656. https://doi.org/10.3389/fphar.2019.00656
171. Fábera P, Uttl L, Kubová H, Tsenov G, Mareš P. Adenosine kinase regulates hippocampal excitability after LiCl-pilocarpine SE in immature rats. Int J Mol Sci 2022;23:2510. https://doi.org/10.3390/ijms23052510
172. Mareš P, Kubová H. GABA-B, not GABA-A receptors play a role in cortical postictal refractoriness. Neuropharmacology 2015;88:99-102. https://doi.org/10.1016/j.neuropharm.2014.09.007
173. Mareš P, Kubová H. Developmental patterns of postictal refractoriness and potentiation akin to cortical stimulation. Epilepsia 2015;56:e10-e14. https://doi.org/10.1111/epi.12870
174. Mareš P, Kubová H. Does status epilepticus induced at early postnatal period change excitability after cortical epileptic afterdischarges? Epilepsia 2016;57:e183-e186. https://doi.org/10.1111/epi.13438
175. Mareš P. Participation of GABAB receptors in cortical postictal excitability in immature rats. Eur J Pharmacol 2018;818:26-29. https://doi.org/10.1016/j.ejphar.2017.10.022
176. Bencurova P, Baloun J, Hynst J, Oppelt J, Kubova H, Pospisilova S, Brazdil M. Dynamic miRNA changes during the process of epileptogenesis in an infantile and adult-onset model. Sci Rep 2021;11:9649. https://doi.org/10.1038/s41598-021-89084-9
177. Bencurova P, Laakso H, Salo RA, Paasonen E, Manninen E, Paasonen J, Michaeli S, ET AL. Infantile status epilepticus disrupts myelin development. Neurobiol Dis 2022;162:105566. https://doi.org/10.1016/j.nbd.2021.105566
178. Mareš P, Kudová E, Valeš K, Kubová H. Three neurosteroids as well as GABAergic drugs do not convert immediate postictal potentiation to depression in immature rats. Pharmacol Rep 2020;72:1573-1578. https://doi.org/10.1007/s43440-020-00113-2
179. Kudová E, Mareš P, Hill M, Vondráková K, Tsenov G, Chodounská H, Kubová H, Valeš K. The neuroactive steroid pregnanolone glutamate: Anticonvulsant effect, metabolites and its effect on neurosteroid levels in developing rat brains. Pharmaceuticals (Basel) 2021;15:49. https://doi.org/10.3390/ph15010049

180. Chvíla S, Kubová H, Mareš P, Kudová E, Štěpánek F. A zuranolone nanocrystal formulation enables solubility-independent in vivo study of pentylenetetrazol-induced seizures in a rat model. RSC Pharm 2024;1:37-46. https://doi.org/10.1039/d3pm00043e

Physiol. Res. 73 (Suppl. 1): S83-S103, 2024 *https://doi.org/10.33549/physiolres.935414*

REVIEW

From Frog Muscle to Brain Neurons: Joys and Sorrows in Neuroscience

František VYSKOČIL[1]

[1]Laboratory of Cellular Neurophysiology, Institute of Physiology of the Czech Academy of Sciences, Prague, Czech Republic

Received May 14, 2024
Accepted June 7, 2024

Summary

One element, potassium, can be identified as the connecting link in the research of Czech neurophysiologist Prof. František Vyskočil. It accompanied him from the first student experiments on the frog muscle (Solandt effect) *via* sodium-potassium pump and quantum and non-quantum release of neurotransmitters (e.g. acetylcholine) to the most appreciated work on the reversible leakage of K^+ from brain neurons during the Leao´s spreading cortical depression, often preceding migraine. He used a wide range of methods at the systemic, cellular and genetic levels. The electrophysiology and biochemistry of nerve-muscle contacts and synapses in the muscles and brain led to a range of interesting findings and discoveries on normal, denervated and hibernating laboratory mammals and in tissue cultures. Among others, he co-discovered the facilitating effects of catecholamines (adrenaline in particular) by end-plate synchronization of individual evoked quanta. This helps to understand the general effectiveness of nerve-muscle performance during actual stress. After the transition of the Czech Republic to capitalism, together with Dr. Josef Zicha from our Institute, he was an avid promoter of scientometry as an objective system of estimating a scientist´s success in basic research (journal *Vesmír*, 69: 644-645, 1990 in Czech).

Key words

Skeletal muscle • Neuromuscular end-plate • Neuropharmacology • Excitable membrane • Acetylcholine release • Ion sensitive microelectrodes • Synaptic delay • Brain potassium • Na^+, K^+-ATPase

Corresponding author

F. Vyskočil, Institute of Physiology of the Czech Academy of Sciences, Videnska 1083, Prague, Czech Republic. E-mail: kinacka@seznam.cz

Early times

My first research project in the high school was about alopecia. To this day, I can move the subcutaneous muscles and thus improve blood circulation and nutrition in the hair follicles, so at the age of 82 years, I have a lush, minimally gray mane. I used to stop people on the street, bald and hairy alike, asking if they could also move their hair. It turned out that 80 % of bald individuals could not. However, I truly discovered real science at the Department of Physiology of the Faculty of Science, Charles University in Prague. During the summer holidays between the third and fourth semester of my pregradual studies, on the recommendation of my supervisor, Dr. Ivan Novotný (1931-2021), I started experimenting with a Fenn micromanometer made by a skillful Faculty glassblower. It measured oxygen consumption in an isolated frog muscle. A supposed weak depolarization by application of 10 mM K^+ increased oxygen consumption up to 10 times without any muscle contraction. We demonstrated that this "Solandt effect" could be inhibited by several substances affecting the internal concentration of Ca^{2+} ions. Years later, I asked Ivan why he believed unconditionally my measurements. Answer was "I secretly asked the lab technician Jane to measure it again after you for extra money in the evenings". The work was published a few months later in the journal Nature [1]. However, how much the muscle fibers were depolarized without contracting was an important question. Dr. Novotný had a friend at the Institute of Physiology of the Czechoslovak Academy of Sciences (IPHYS), Dr. Radan

Beránek, who was experimenting to introduce a method of measuring the transmembrane potential of cells using glass ultramicroelectrodes. I began to visit the institute, and together with Drs R. Beránek and L. Vyklický Sr. we implemented this method [2,3]. Stimulators and high-resistance input amplifiers were manufactured directly in the laboratory by Ing. Evžen Ujec, using high-quality microtransistors smuggled into Czechoslovakia in the pockets of random institutional travelers with Communist Party credentials. We directly measured the depolarization of muscle fibers by impaling microelectrodes into muscle fibers and found that the depolarization by potassium remained unchanged despite the blockade by physostigmine, ouabain, and caffeine [2-5].

At the student research competition in 1961, I won a second position nationally behind a team of radiophysiologists from Hradec Králové, Czech Republic. In 1963, after graduating with honors, I began my postgraduate studies when Dr. Beránek returned from a year-long stay with Nobel Prize laureate Prof. Bernard Katz at University College London. For my dissertation, I was tasked to measure dose-response curves of curare and atropine inhibition – antagonists of acetylcholine receptors (nAChR). Using microelectrodes this was done on standard end-plate potentials of innervated rat diaphragm muscle after stimulation of the phrenic nerve and then after a week of denervation when new acetylcholine receptors are formed along the entire length of the sarcolemma. An iontophoretic dose of acetyl-choline (ACh) replaced the nerve. I was deeply engrossed in this work; we were a generation hungry for new information. Thus, I often slept in the lab, conducting experiments and also helping with the institute's relocation from Dejvice to the new campus in Prague's Krč district.

When I compared the effect of curare on native and denervated nAChRs, I found no difference. However, I noticed that the lab assistant, Mrs. Petrtýlová, had prepared a stock solution of curare for experiments on denervated nAChRs that exhibited peculiar opalescence. Upon inquiry, it turned out that the concentration of curare was by mistake 10 times higher than for innervated rat fibers. Nearly missing this discovery, I corrected the concentration error and found that denervated nAChRs receptors (similar to those in embryonic muscles) had 10 times lower sensitivity to this drug and likely had a different composition. This was confirmed by molecular biology methods. One of the first findings of two different subtypes of the same receptor was thus made. After my first publication in *Nature*, Radan Beránek and I wrote two articles together, which were virtually unchanged when published in the iconic *Journal of Physiology London*, focusing on this surprising discovery [6,7].

The second paper described how atropine reduces and shortens synaptic end-plate potentials. This was the basis for the use of atropine in anticholinesterase poisoning (sarin, soman, etc.) (Fig. 1) and soldiers carry it with them at all times in case of chemical attack.

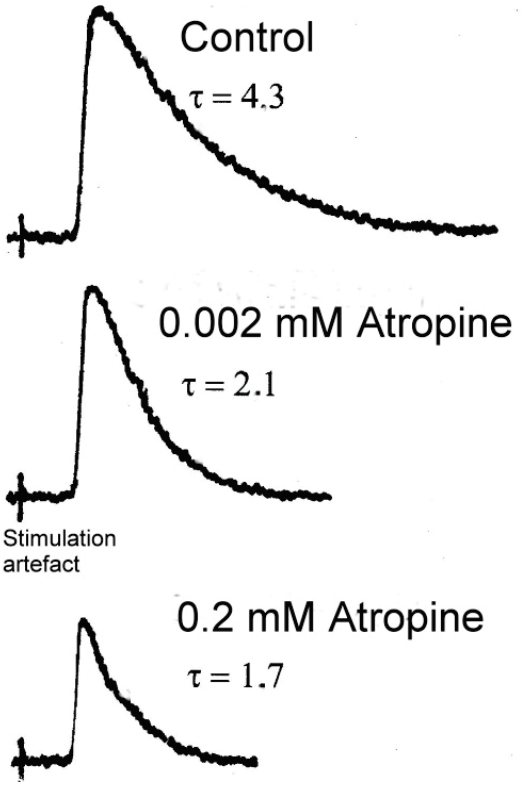

Fig. 1. Atropine reduces the amplitude and shortens the exponential time course (see values of T) of intracellularly recorded end-plate potentials (F. Vyskočil, unpublished).

At that time, we were relatively isolated from the rest of the world except for Russia. It was recommended to maintain contacts there, so Dr. Beránek sent me to Kyiv Ukraine, for a conference. In 1967, I presented our results on adult and embryonic receptor types. I traveled to Kyiv by train, with some time to explore the beaches along the Dnipro and the ancient Ukrainian city with its grand boulevard, Khreshchatyk. One afternoon, before the conference, I was sunbathing on the Dnipro's shore when two young men asked me for a cigarette. They turned out to be thieves and stole my new shoes. The next morning, before the conference, my colleagues took me to a store where I bought some unsightly replacement shoes.

On the conference I met an interesting and smart man from St. Petersburg named Lev G. Magazanik. We spent the entire night discussing neuromuscular junctions, science, and we clicked instantly. When I returned to Prague, we attended a stage performance of Gogol's play "*The Government Inspector*" in a small theatre. When famous Czech actor (Mr. Jiří Kodet) appeared as Chlestakov, the impostor posing as the inspector, wearing exactly the same shoes I had acquired in Kyiv, I could not contain myself and loudly whispered from the second row, "Those are my shoes!" The actor glanced at me somewhat curiously, wondering what it meant. The costume director had gone to great lengths to ensure authenticity, even procuring genuine Russian ugly army shoes.

After completing my postgraduate studies, I was supposed to go to the USA for a research internship at Prof. Del Castillo's laboratory and then to Prof. Kuffler, both renowned neurophysiologists. However, there was an incident typical of the communistic time. In the Institute of Physiology, like everywhere else, there was a local Communist Party organization. Its chairman, Dr. Hrůza, left for the West and wrote to the Academy's president Prof. Šorm, that he would not return, intending to emigrate and denounce the socialist regime. Punishment fell not on the guilty but on the innocents. Despite being a good organic chemist, Prof. Šorm issued a ban on travel to Western countries for Institute of Physiology staff. Thus, my trip to the USA was cancelled. Then, suddenly, a call came from St. Petersburg. Dr. Lev Magazanik had received a special six-month stipend for a foreign guest and remembered me. We could conduct experiments together, just as we had discussed in Kyiv. Frustrated by my thwarted trip to America, I accepted his invitation, and my wife and I traveled to St. Petersburg. I found that we had to either make many technical setups in the laboratory ourselves or somehow modify other devices. For example, we converted a camera from a captured wartime German aircraft into an oscilloscopic camera, which we used to record cell potentials and currents. In this Russian intellectual environment, there were personalities like the biophysicist Sergei Kovalyov, a well-known Russian dissident who vehemently protested after the 1968 invasion of troops to Prague. He was imprisoned, and went through the Gulag. When we met years later at President Havel's Forum 2000, we reminisced about those years that were essentially taken from us by communist regimes, preventing us from realizing ourselves in life as we might have imagined.

Together with my colleague Lev Magazanik, we made several significant discoveries about nAChRs desensitization, the effects of toxins on neuromuscular synapses, and the influence of ethanol on glutamatergic fly synapses (Fig. 2) [8-19]. One of them [10] was cited about 170 times in literature today, the other [15] about 70 times. At that time, we were nominated for a joint Award by the Academy of the Soviet Union and the Czechoslovak Academy of Sciences. The problem was that I had a career halt status because I was involved in the all-academic Committee against the Russian invasion in 1968. However, a directive came from Moscow that we should receive the award regardless of how inconvenient or uncomfortable Dr. Vyskočil might be. This demonstrates that good scientific results can be appreciated independently of the political system.

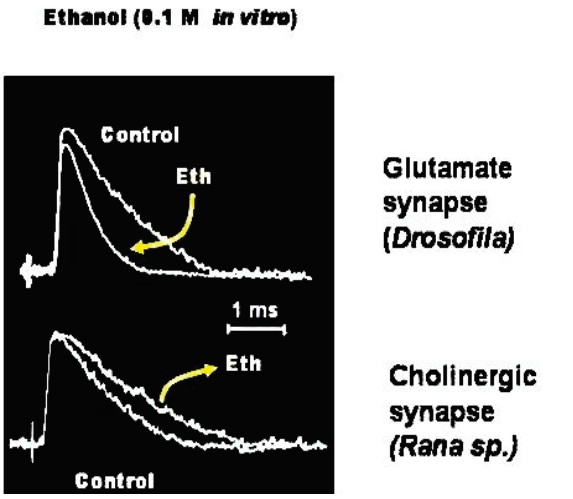

Fig. 2. Ethanol shortens excitatory postsynaptic potentials to the glutamatergic synapse (where glutamate is the neurotransmitter, mediator), but prolongs cholinergic EPSP, the mediator is acetylcholine and the receptors are nicotine-type. The resulting confusion contributes to drunkenness (after Magazanik and Vyskočil, unpublished).

After 1968 and the sudden death of Dr. Radan Beránek, our cellular neurophysiology laboratory underwent little personnel change. I remained alone to study intracellular nerve-muscle electrophysiology. I enjoyed collaboration with colleagues from the Faculty of Science, Charles University in Prague, notably Prof. Ladislav Janský and Dr. Jan Moravec in hibernation neurophysiology [20-22]. Of course, many collaborators were from the IPHYS and its electrophysiological laboratory. It was Dr. Pavel Hník working on physiology of the musculoskeletal system using long-term implanted electrodes. Pavel was also the

English editor of our local journal *Physiologia bohemoslovaca*, now *Physiological Research*. Furthermore, I made a couple of experiments with Dr. Ladislav Vyklický Sr., otherwise studying pain pathways [23], and electrical engineer Evžen Ujec, who constructed amplifiers, stimulators and studied biophysics and morphology of glass microelectrodes [24]. A useful cooperation was also with physical chemist Norbert Kříž and with excellent biochemists ing. Jan Teisinger and Dr. Petr Svoboda, as well as with some other members of the *Spinal Cord Physiology and Neuromuscular System Department*. I have collaborated with histological and electron microscopy laboratory led by Dr. Jiřina Zelená [25] biochemical laboratory of Dr. Ivo Syrový, who studied slow and fast muscle myosin [26,27], neurochemist Dr. Stanislav Tuček [25] and some other specialists and Institute colleagues. Another fruitful interdisciplinary works emerged from my contact with the lead scientist that time and founder of the concept of trophic influence of nerves on muscles, Prof. Ernest Gutmann. We studied together the aging neuromuscular junction and hormonal effects on skeletal muscle and muscle drafts continuously until his death in 1978 [28-35].

Numerous studies were performed – as indicated later –, while visitors came to our laboratory from USA (Prof. Charles Edwards, University of Tampa, Florida), Hungary (Prof. Peter Illes and the president of the Hungarian Academy of Sciences Prof. Sylvester Vizi), Italian and Swedish neurophysiologists Dr. Alfredo Gorio and Prof. Stephen Thesleff, Algerian specialist Dr. Nasira Tabti, and – after 1989 – Prof. Gerta Vrbová (London), Dr. Martin Ward (Newcastle upon Tyne), and Dr. Rosemary Jones (Cambridge) [36]. I was also host and visitor of many Russian colleagues, primarily from Kazan University and the Academy of Sciences under the leadership of Prof. Eugeny Nikolsky (Republic of Tatarstan, joint State Prize in 1994). Those were the only off-line professional relationships when my Western personal contacts were denied for political reasons. One example of such a successful study across the Iron Curtain is an article from the Prague laboratory on non-quantum release of a mediator on the motor end-plate by Prof. C. Edwards (USA), E. Nikolsky (Kazan, SU) and me from 1983, cited 110 times [37].

As reasons for the ban on trips to the West, the directors (first L. Vyklický Sr. and then Z. Drahota) recommended me to write to the inviters that I am seriously ill or that my grandfather would have a funeral at the time of the conference. Occasionally, however, I managed to go out for a short period of time, when the secretaries of the local Communist Party in our Prague district were changing and chaos reigned in their centers. This happened, for example, in 1985, when we have conducted a study for *Journal of Physiology (London)* in the laboratory of Prof. Thesleff in Lund, Sweden, within a few weeks [38,39] or a leak to an Italian laboratory in Abano Terme studying gangliosides [40,41]. On the way to Lund, Sweden, I arrived in Malmö from Copenhagen as the only passenger on board Boeing 747, as I didn't possess some 12 Swedish crowns to cross the Öresund Strait on a boat like other travelers. Alone at the small airport in Malmö, I was looking for some kind of custom or other declaration sheet to fill out, as educated by "socialist" airports. Sure enough, there was a small table with a form in the corner. I started to fill in the fields: Name, nationality, birth, where I am going, what I came from, by what type of airplane (Boeing 747, I wrote, I saw it through the window), what fuel it flies on... That struck me, such Swedish thoroughness! There was an attendant leaning against the doorposts. So I asked him why I should mention it, as I didn't know any type of aviation fuel. With a kind smile, he said, "We need to know what fuel to fill on your personal plane". When I laughingly said that this Boeing is not my personal possession because I am from the East country, where no one had such personal aircraft, he asked me "Well, why not? Why can't you have your private large-capacity plane right in Prague?"

Ion-selective glass microelectrodes

In 1972, we introduced as a second laboratory a new technique called ion-selective glass micro-electrodes for direct measurement of concentrations of K^+, Na^+, Ca^{2+} and Cl^- ions in the cellular environment. Liquid ion-exchanger "membranes" in the tiny tip of glass microelectrode were developed by J. L. Walker for chloride and potassium in 1971 [42]. These liquid ion exchangers were smuggled by Dr. Pavel Hník from Walker´s laboratory in Salt Lake City to Prague that year. Norbert Kříž and me, having already mastered the production of the microelectrodes, put together the necessary equipment and developed many modifications of the technique for recording intra- and extracellular ion concentrations [43]. We decided to use the potassium-specific microelectrodes for testing the hypothesis that potassium is released from cells in working animal and human muscles to their veins [44-48] and also during

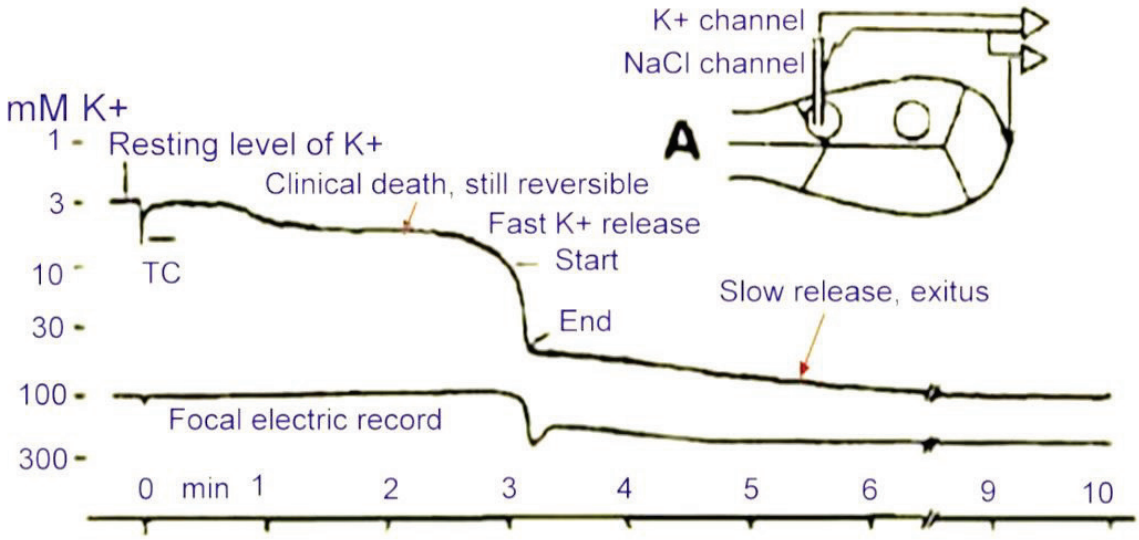

Fig. 3. Terminal anoxia. Failure of the sodium/potassium pump in the cerebral cortex of a narcotized rat is evidently due to deficiency of ATP during anoxia. (**A**) Diagram of a rat skull with holes for scanning $[K^+]_e$ in mM using double-barrel microelectrode. A second channel filled with 100 mM NaCl was used for simultaneous recording of the electrical focal potential at the measuring point of the cerebral cortex. For the first 3 min after down-stopped breathing by tubocurarine injection (TC), the potassium is still mostly in the cell, the pump is more or less working and animal can be resuscitated. After a sudden fast K^+ release, (downward drop), this clinical death turns into exitus (after Vyskočil *et al.* [49]).

self-propagating wave of Leao´s spreading depression of rat brain EEC activity due depolarized neurons probably by extracellular potassium $[K^+]_e$ [49]. This was studied in the cooperation with Dr. Jan Bureš from *Memory Department* of our institute. Such high $[K^+]_e$ has already been expected, but its absolute magnitude remained unknown. The actual experiments on rat cortex were performed in my small, crowded laboratory during two weeks of intensive work in the late summer of 1972. Already the first results confirmed our expectations: intercortical $[K^+]_e$ rose in a few seconds from the resting level of 3 mM to over 60 mM during spreading depression and up to 100 mM during terminal anoxia (downward drop in Fig. 3). The wave of propagating depression was accompanied by a 30-fold increase in the extracellular concentration of potassium, which flows from the depolarized cells. After a few minutes, K^+ was pumped back into the cells and the depression moved further. Spreading depression is therefore a reversible process, ATP for potassium reuptake by the ATPase is plentiful.

We were fascinated by the reproducibility of results and by the power of the method, which offered definitive answers to speculation about brain microenvironment. It was also surprising that the normal $[K^+]_e$ concentration in rat brain was not the same as in blood plasma (5 mM), but significantly lower (3 mM). Anoxic total release of K^+ led to irreversible brain death within 2-3 min [50] (Fig. 3).

Undoubtedly, other groups were hot on the same trail. The feeling that we were participating in a race contributed to the exhilarating atmosphere of those days as well as to the decision to expedite publication by submitting the results in the short-communication format [49]. Indeed, results of similar research in Munich, 400 kilometers from Prague, were published only a year later, and publications from six other laboratories followed in 1974-1975. Our paper thus became the first of a series marking a wave of renewed interest in the mechanism of spreading depression, which was recognized as a dramatic example of the failure of ionic homeostasis in the central nervous system. It was used in numerous later studies employing ion-selective microelectrodes to demonstrate transmembrane shifts not only of K^+, but also of Cl^-, Na^+, H^+ and Ca^{2+} during various physiological and pathophysiological states. This wave crested in the early 1980s, when anoxic depolarization started to be used for testing the role of excitotoxic amino acids and their antagonists in ischemic brain damage.

The high impact of this paper [49] was already obvious in the late 1970s as it won the contest for the most-cited week paper in *Current Content* published by the Institute of Scientific information (ISI) in Philadelphia. Besides ISI, this study did not receive any

particular recognition from the national or international academic establishment. Spreading depression has recently been linked with the onset of migraine, which predominantly affects women. Using a potassium-selective microelectrode technique, we confirmed in the next paper [50] that the threshold $[K^+]_e$ concentration for the initiation of spreading depression in the extracellular space of the cerebral cortex in the female rat brain is lower more than half compared to the male one.

Non-quantal release of acetylcholine at the neuromuscular junction

In the next part of this article, I will describe a number of other activities in the research of neuromuscular junction and its physiology, pharmacology and biochemistry in *Cellular Neurophysiology Department* of IPHYS and adjacent laboratories. With the exception of non-quantal release of neurotransmitters, especially of acetylcholine (ACh), other aspects will be mentioned only in shortened form. There are two principal mechanisms of ACh release from the resting motor nerve terminal: quantal (miniature and stimulation evoked end-plate potentials, QR) and non-quantal (NQR); the former being only a small fraction of the total, at least at rest [51]. The first demonstrations of non-quantal transmitter release on mouse and rat diaphragm and analysis of the mechanism release, action mechanism and physiological significance were obtained in 1977 [52,53]. In the series of original articles we then described basic research about the NQR which we quantified at end-plate zone as hyperpolarization due to a removal of the slight depolarization by NQR in anticholinesterase-treated skeletal muscles by curare. In mammals, it exceeded ten times the similar effect found in frog muscle [cf. 52]. Possible mechanisms of the non-quantal release were suggested and proved by the inhibition of NQR using vesicular ACh-transporter inhibitors, mostly vesamicol [37,54,55]. QR means that vesicular ACh-transporter (transferring normally Ach into vesicles during their intracellular refilling) is incorporated into the presynaptic membrane in the moment of the release of quanta, when the vesicular membrane spline with the membrane of the nerve endings (Fig. 4). This creates an outward directed pathway for the non-quantal escape of ACh into the synaptic cleft [56].

Another candidate can be a choline transporter, the inhibition of which also does suppress the NQR. But this may be an indirect consequence of choline deficiency for ACh production in the nerve terminal [57]. In general, the permanent NQR release and hydrolysis of ACh in the cleft, together with the quick uptake of the newly produced choline, could keep the synthetic machinery within the terminal ready for prompt fulfillment of different physiological demands when quantal release is augmented for example during exhaustive physical work [58] and ionic changes around the synapse [58-61].

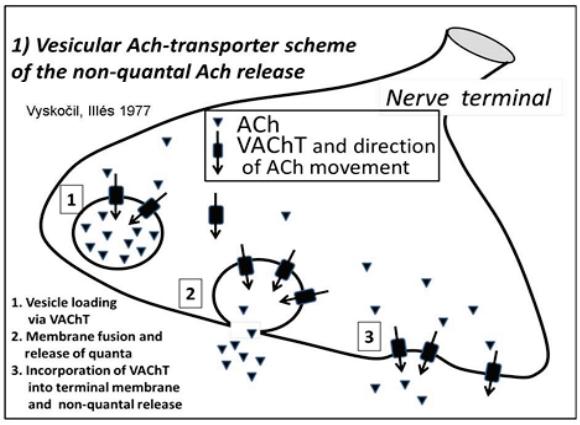

Fig. 4. Scheme of possible mechanism of non-quantal Ach release. Follow numbers from 1 to 3. ACh molecules are schematized as the full triangles. VAChT – Ach transporter, arrows show the direction of Ach movement (F. Vyskočil, unpublished).

We found further that NQR is undoubtedly an important trophic factor in adult neuromuscular contacts [62-64] and during end-plate development. It helps to eliminate the polyneural innervation of developing muscles, supports higher excitability of the end-plate subsynaptic membrane by surplus polarization and protects the resting membrane potential from postdenervation depolarization. NQR might shorten the end-plate potentials by promoting postsynaptic receptor desensitization when acetylcholine esterase (AChE) is inhibited during anti-AChE poisoning [65,66]. It ensures higher excitability of the adult subsynaptic membrane by surplus polarization and protects the resting membrane potential from depolarization by regulating the NO cascade and chloride transport [69]. In adult synapses, it can also activate the electrogenic Na^+/K^+-pump, change the degree of synchronization of quanta released by the nerve stimulation and affects the contractility of skeletal muscles *via* purinergic effects [52,62-71].

Apparently NQR is not restricted to the cholinergic neuromuscular junction only, since massive non-quantal release was shown also at the glutamatergic neuromuscular junction of the blowfly larvae and in calyx-bearing fibers of the turtle ampula posterior crista.

Similar transmitter release ("tonic" release) mediated by a transporter was also described in certain brain GABAergic synapses playing the role in perinatal changes of $GABA_A$ receptors from excitatory to inhibitory mode [cf. 67].

In adult vertebrates, some of the ACh released from the nerve terminal might escape hydrolysis by AChE if it is released perisynaptically, and might then act as a "local hormone" on more remote parts of muscle fibers, for example, activating the electrogenic Na^+/K^+ pump. It can also change the degree of synchronization of quanta released by the nerve stimulation [68]. Non-quantal ACh release can also alter the ovalbumin-induced functional properties of postjunctional ACh receptors and contribute to the disturbance of carbachol-induced contractility of skeletal muscles as reported by Teplov *et al.* [70a].

Other molecular mechanisms of interaction between excitable cells

Over the past decades, we have been interested in several molecular mechanisms of chemical interaction between excitable cells and factors determining the excitability of nerve cells and regeneration, including NO pathway. For this purpose, we used tissue cultures of dissociated nerve cells, spinal cord of the rat, mouse and frog synapses and, of course, neuromuscular junctions. Explored techniques were mostly glass microelectrodes, ion-sensitive microelectrodes, voltage and current clamp including patch clamp and systems for rapid application of drugs to particular cell area. Besides open-channel blockade**,** desensitization of nicotinic ACh receptors is a classical model of functional fatigue of ion channels. We proved as the first that nAChR desensitization is dependent on postsynaptic fiber voltage, temperature and Ca^{2+} ions as well as on some otherwise biologically inactive substances [10,15,17]. Role of negatively charged amino acids in beta 4 F-loop in activation and desensitization of alpha 3 beta 4 rat neuronal nicotinic receptors was demonstrated together with our students and coworkers [69-76]. Occasionally, synaptic events were mathematically modeled in respect to NO effect on denervated muscle resting potential, ionic changes and space conditions in the nerve ending possessing also glutamatergic auto-receptors of NMDA-type calcium channels [77-83]. We found that muscle NMDA receptors regulate the resting membrane potential through NO synthase [79]. The structural and functional similarity between imidazole derivatives and the known NO synthase inhibitor, 7-nitro-indazole suggests that imidazole, carnosine and anserine might act by inhibiting NO production which is stimulated by glutamate and carbachol [84]. Interestingly, an early postdenervation depolarization develops faster at end-plates of hibernating golden hamsters where spontaneous quantal and non-quantal acetylcholine release is very small [85]. On the other hand, acetylcholine and carbachol prevent muscle depolarization in denervated rat diaphragm [86]. This coincides nicely with immunocytochemical demonstration of M_1 muscarinic acetylcholine receptors at the presynaptic and postsynaptic membranes of rat diaphragm end-plates [87,88].

Synchronization over time of evoked quantal release

Another mechanism for regulating synaptic transmission is the time delay between the presynaptic nerve spike and the release of individual quanta, which accumulate over time to form the final postsynaptic potential. Improved synchronization of individual delays is one of the ways to make synaptic signal transmission much more efficient without any extra energy requirements. Extracellular miniature and nerve-evoked end-plate currents were measured in the studies of synaptic delays between nervous stimulation and the outpouring of quanta. It is worth of noting, given the long-term non-quantal release of ACh into the end-plate cleft, that the long release latencies are even increased by acetylcholine [87]. This desynchronization is in contrast with synchronizing positive effect of catecholamines, adrenaline in particular, on neuromuscular latencies. First demonstration and subsequent explanation of the beta-adrenergic receptor mediated action on synchronization and thus better time synchronization of the quantal release was done during my visits in Kazan in 1998 and 1999 in the laboratory of Prof. E. E. Nikolsky [89-92]. Better synchronization increased the amplitude of end-plate potentials by up to 20 %. These findings were further elaborated and the somewhat complicated relation-ships between the sensitivity of different types of skeletal muscles to catecholamines were gradually specified. The truth remains, that adrenaline increases the number of spontaneous and nerve-evoked quanta and improves synchronization on the mammalian neuromuscular end-plate of the skeletal muscles by up to 40 % [93].

Patch-clamp studies on nerve and muscle cells

The patch clamp method is a powerful technique used in electrophysiology to measure the electrical currents through individual ion channels in cell membranes. A fine heat polished glass micropipette (tip diameter about 2 μm) is filled with an electrolyte solution and brought into contact with the cell membrane under microscopic control. The glass microhole has an incredible affinity for membrane phospholipids. Gentle suction by experimentator´s mouth through plastic capillary is applied to the micropipette to form a tight seal (gigaohm seal, controlled by microohm-meter on the PC screen) between the pipette and the cell membrane, isolating a small patch of membrane. The patch clamp can be configured in different modes. Cell-attached, whole-cell mode, inside-out and outside-out patch and even perforated patch, preventing the outflow of cell plasma into the attached micropipette.

The electrical currents of the nano- to pico-amperes flowing through the ion channels in the patch of membrane provide insights into the channel's conductance, ion selectivity, and gating mechanisms. It is invaluable since the 80's and was soon introduced in our laboratory [94] on a home-made apparatus by Ladislav Vyklický Sr. and Ladislav Vyklický Jr. with the help of other collaborators, namely Dr. Jan Krůšek and Dr. Viktorie Vlachová, who are still combining mathematical modeling with transfection of artificially mutated receptors for pain and other channels. Patch clamp microphysiology and micropharmacology is based on locally focused one-cell targeted and very fast multiple drug application, which was developed by Ing. Ivan Dittert in our laboratory.

We were able to provide first demonstration of K^+ channel subtypes during myotube formation [95], presence of Cl^- channels in neuroblastoma cells [96,97] and evidence that excitatory amino-acids not only activate the receptor channel complex but also lead to use-dependent block [98,99]. Several other joint papers have pointed to the GABAergic effect of cerebrolysin (used to treat vascular dementia), inhibition of glutamate transmission by cobalt, etc. [98-104]. Also interesting was the finding of the inhibitory effect of the standard selective serotonin reuptake inhibitor citalopram on Ca^{2+} currents in cardiomyocytes [105]. With substantial help of Dr. Jan Krůšek I was happy to confirm – using molecular biology and patch-clamp records – previous findings about muscle nicotinic receptors [6], different degree of cooperativity in adult, embryonic and mutated mouse nAChR in particular [106]. The new data provided the basis for mathematical modeling of the course of end-plate currents and prediction of further research directions in this synaptic connection [107-111].

Sodium-potassium membrane pump

Starting with the connection between the non-quantum outpouring of acetylcholine and the membrane Na^+/K^+ pump [52], the functional correlation between Na^+, K^+-ATPase in membrane fractions and electrogenic sodium pump in intact muscle cells was also in the center of our experimental interests. We discovered the direct effect of acetylcholine on the Na^+, K^+-ATPase and surplus postsynaptic hyperpolarization of muscle fibers that can be inhibited by AChR inhibitors such as alpha-bungarotoxin, curare and atropine [112]. A discrepancy has been found between the inhibitory effects of vanadate on the membrane Na^+, K^+-ATPase (reportedly responsible as a pollutant for mental depressions in the industrial areas in England) and the Na^+/K^+ pump of the skeletal muscle. Vanadate in concentrations, which are necessary to block the enzyme Na^+, K^+-ATPase activity of membrane fractions, failed to inhibit the electrogenic Na^+/K^+ pump in intact muscle cells [113], probably due to non-enzymatic reduction of vanadate to the less efficient vanadyl ion [113-115]. We also studied the effects of high calcium and calcium-channel blockers on Na^+/K^+ pump [116] and internal calcium measured electrophysiologically and by the fluorescent indicator [117]. It could be stressed that increase of Ca^{2+} concentration up to 10 mM in bath medium induced in diaphragm muscle tissue an elevation of intracellular $[Ca^{2+}]_i$ accompanied by a depression of sodium pump electrogenic activity and a depression of energy metabolism [118]. These changes may be involved in pathology of muscle tissue during the Ca^{2+} overload. The K^+-induced hyperpolarization of Na^+-loaded mouse diaphragm muscle, enzymatic activity of Na^+, K^+-ATPase and ^{3}H-ouabain binding to rat brain microsomes were also affected by K^+ channel blockers – tetraethylammonium (TEA), tetrabutylammonium (TBA) and apamin. TBA, and to a lesser extent TEA in millimolar concentrations, inhibited the electrogenic effect of the Na^+/K^+ pump, Na^+, K^+-ATPase activity, and ^{3}H-ouabain binding. The site of action of apamin on Na^+, K^+-ATPase is different from that of tetralkylammonium compounds; it apparently decreases the turnover rate of the enzyme [119]. Arachidonate (polyunsaturated fatty acid participating in the

regulation of membrane fluidity, axonal growth, development, memory, and inflammatory responses) was also tested on both electrogenicity and ATPase activity [120,121]. When applied to Na^+-loaded muscles without potassium, arachidonate induced an ouabain-sensitive hyperpolarization of the muscle fibers. The arachidonate also increased the rate of hyperpolarization induced in Na^+-loaded mouse diaphragm fibers by 5 mM K^+. The activity of rat brain microsomal Na^+, K^+-ATPase was stimulated by arachidonate in reaction media with reduced amounts of ATP or K^+ and after short-lasting sonication of the samples. It was concluded that, under particular conditions, arachidonate might serve as a Na^+, K^+-ATPase activator or inhibitor regulating its ion transport and electrogenicity [120,121]. We also found that Na^+, K^+-ATPase of brown adipose tissue and brain responds similarly to higher doses of isoprenaline, norepinephrine and epinephrine. But this stimulation of brown fat Na^+, K^+-ATPase by catecholamines does not have much relevance to the norepinephrine-stimulated thermogenesis in this tissue [122].

We remotely touched on cosmic muscle physiology when we measured some muscle during modeling of hypogravity. Antiorthostatic hindlimb suspension (unloading) of rats decreased the resting membrane potential (RMP) of skeletal muscle fibers in both fast extensor digitorum longus and slow soleus muscle of the rat by about 10 % within 7 days and more [123]. We compared these changes with kinetics of neurotransmitter release in neuromuscular synapses of newborn and adult rats [124].

Traveling with older and more recent attractions

After the Velvet Revolution in 1989, I was able to travel and work at several Western universities. I received an invitation to England, for example, where I spent several months at University College London in 1991. Together with Prof. Gerta Vrbová, an emigrant from 1958, we showed how important this non-quantum Ach release is in the formation of synapses during the development of an organism [65, cf.124]. At that time, I was invited to lecture at a number of universities in the UK. At Trinity College, Cambridge, four Nobel laureates were present at one of my lectures. During my speech, some seemed to be falling asleep. But then during the discussion, it turned out that this was only my illusion. They asked precisely targeted and even slightly uncomfortable questions. First of all, there were present Sir Alan Hodgkin and Sir Andrew Huxley, who was already in a wheelchair at that time. Both friends joined the faculty at Cambridge after conducting radar research for the British Air Ministry (1939-1945). They remembered that to disguise their success in aerial combat against Nazi Luftwaffe with a radar lead, the English propagandists claimed that their pilots ate a lot of carrots and had better eyesight than Germans. At Trinity College, Hodgkin and Huxley showed experimentally that the electrical potential of a nerve fiber behaves similarly to submarine electric cables. The third Nobel participant on my session was Sir Bernard Katz, a neuromuscular superstar, and finally Sir John C. Eccels. Interesting, though somewhat sad, was that Sir John was divorced after he was awarded the Nobel Prize in 1963 for synaptic inhibition in the brain. In 1966 he left his wife, four daughters and four sons and married my colleague from the Institute of Physiology, Dr. Helena Táboříková. She was experimentally rather inept, but she cared devotedly for Sir John until his passing at the age of 94.

Despite sharp and relatively long discussion on my topics [125-129] Sir Andrew invited me to Trinity College dinner (I admired his sincere prayer in a medieval cloak for her Excellence Queen Mother) and then to spend the weekend at his house. We discussed the history of the neuroscience and with his grand-daughter we played joyfully her violin. This sweet girl was very proud that in about five minutes she was able to “teach” me how to play the violin, even the virtuoso encore “Canary” by M. B. Polyakin (Figs 5,6).

Fig. 5. A weekend at Sir Andrew Huxley's (right).

Fig. 6. Sir Andrew with his wife Jocelyn in Prague (circa 1997), tasting imported wine from Moravia.

The violin has accompanied me practically all my life. After graduating from high school, I played Beethoven's Romance in F major at a local music school competition, and the present professor Moravec at the Janáček Academy of Music and Performing Arts in Brno told me: "If you don't do well in Prague at Charles University, study violin, you have a talent test with me." In the end, I was left with violin (as a hobby) and my wife, (who liked my Beethoven) to this day. For me, she did her modern gymnastics and love.

The violin often got me out of a precarious situation. There is a little incident here from the 90's, when my colleague dr. Evžen Amler and I were traveling by car (Pontiac) from the University of Geneva to Prague. There was a car breakdown, we had to call the yellow angel. But we had no money at that time, only 100 DM for gasoline in Germany. Before the repairman arrived, I played cheerfuly melodies on my violin by the parked car, when suddenly a local TV station reporters from Bern arrived and filmed us waiting in peace. I said them: before the yellow angel helps us, Mozart does it: Ta ta, Ta ta, this tata ta... The repairman came, changed the injection fuse for two marks but asked for exactly 100 DM for the trip. But how do we get home? It occurred to me to ask the TV reporters for a fee for half an hour of violin play. And they actually paid in the blink of an eye. I signed the bill with my address and we got to Prague with a full tank. About a month later, I received a cassette from Bern with the recording. I still have it digitized. TV played it to the drivers on Sundays so that they would not be surprised by problems when returning from the weekend in the country and solve any difficulties with a smile as our Czech friends did.

When my travel ban was lifted, I was also invited to give lectures at three Indian universities, Bombay, New Delhi and Bangalore. I have presented a number of our published as well as still unpublished observations on nerve and muscle contacts, from earthworm to rats [130-142]. I had quite uncompromising discussions with a respected muscular physiologist, Prof. Manik Sahani about action potentials of skeletal muscle fibers and their sensitivity to tetrodotoxin during postnatal-development and old age. Our findings documented the gradual exchange of at least two types of sodium channels throughout life [142]. This sodium-channel family eventually expanded to other important subtypes affecting for example the pain sensation.

In Bangalore, in the south of the India peninsula, they have a beautiful university campus. The local students were at one of my lectures, which I ended with some musical interlude – a piece of Bach sonata – and the students at that time won the opportunity to have one more seminar with me, which they held in the large student hall. I said to myself, "That's great, how interested they are in my science, they want even more knowledge". When I got there, it turned out that most of the students had guitars and other musical instruments such as chikara with them, and they did not want me to tell nothing more about quantum and non-quantum synaptic releases or something like that. They said, "Play us some European melodies again, please". In the pre-internet era, I played a number of genres on the violin, such as the tango Jalousie, Mozart´s Little Night Music, Dvořák's Humoresque, Monti's Czardas and so on. They liked it very much. So in the evenings I taught several local guitarists to play Monti's Czardas note by note until my departure. Indians love the violin, but they play it along with the zither in a completely different way, usually sitting on the ground, resting it on the instep. In Bangalore, they even have a large concert hall in the shape of a violin and celebrate their famous violinists.

It is worth mentioning at least one work from our group in collaboration with Kazan scientists (Fig. 7) [141]. New cholinesterase inhibitors were synthesized, based on 1,3-bis[5-(o-nitrobenzylethylammonium) pentyl]-6-methyluracilic unit with selectivity towards mammalian AChE vs. butyryl cholinesterase E8,9,10,11. These inhibitors were found to be efficacious on skeletal muscles with the exception of respiratory muscles such as the diaphragm. The most selective compound, 6-methyluracil derivative, C547, was pharmacologically profiled on human AChE and BChE. It can be used for

specific treatment of pathological muscle weakness syndromes in humans of the myasthenia gravis or Alzheimer's disease without any sighs of respiratory muscle failure.

Fig. 7. Prof. Eugeny E. Nikolsky and Dr. Ellya Bukcharaeva receive the Purkyně Prize of the Czech Academy of Sciences from the hands of the President, Prof. Helena Illnerová (left) in 1999.

I also obtained a stipendium from Fogarty's extramural program, which provide funding to perform research and to train researchers in a variety of global biomedical areas. I spent nine months in the laboratory of Prof. Zach W. Hall (University of California in San Francisco). He created an interdepartmental neuroscience program, which acted as a model for stimulating cross-disciplinary research. There I learned some molecular neurobiology and biochemistry, DNA sequencing and targeted mutagenesis. Zach was known for biochemistry of the adult, embryonic and brain nAChRs. In the 1970s he came to see me in Prague, „to meet the man who gave direction to my research" as he wrote to me back then [6, cf. 142,143]. We still keep in touch after his retirement from the post of Director of the National Institute of Neurological Disorders and Stroke, an institution that had been in the forefront of brain research since 1950.

Later, I taught at The University of North Carolina at Charlotte, where I informed students, faculty members and former collaborators (Dr. A. Urazaev) about a number of other aspects of cellular excitability that have interested me throughout my career [144-175]. These include, for example, the unexpected membrane anticonvulsive action of diazepam and prostaglandin E_1 [147], calcium-dependent inhibition by prostaglandin-E_1 of spontaneous acetylcholine release from frog motor-nerve [148], dual effect of cortisol on the excitability of the rat muscle fiber membrane and neuromuscular-transmission [149]. On the basis of functional properties of muscle autografts substituted for the rat levator ani muscle [150] a surgical procedure was developed and used for many human patients with anal incontinence. Some results had to be defended in writing due to the ban on travel to Western conferences [151,152].

Our interest in hibernation led to an important observation that within the temperature range between 10 °C and 5 °C the activity of Na^+,K^+-ATPase of hamster preparations was about 2.4 times higher than in the case of the never-hibernating mouse. It demonstrates an adaptation for low-temperature hibernation [153-155] preventing hamsters from cold depolarization and death.

From the experiments on organ level we can also mention primary afferent depolarization and changes in extracellular potassium concentration induced by L-glutamate and presumed antagonist L-proline. It was measured in the isolated spinal cord of the frog in cooperation with Dr. Ladislav Vyklicky Sr. Our results showed that L-glutamate and the hopeful compound L-proline act on different receptors [156]. Post-denervation decrease of intracellular potassium and increase of sodium were estimated first time directly, by ion-selective microelectrodes, in rat soleus and extensor digitorum longus muscle fibers. This explains the decrease of resting potential and the onset of post-denervation fibrillation due to "giant" miniature potentials of degenerating nerve-ending origin [157, cf. 38]. The history of vanadate-vanadyl effectiveness has been further supplemented by the knowledge that vanadyl (VO_2^+) and vanadate (VO_3^-) ions inhibit the brain microsomal Na^+,K^+-ATPase with similar affinities and showed protective abilities of the transferrin and noradrenaline [158-162].

The effects of the replacement of K^+ by Tl^+, Rb^+, and NH_4^+ on the muscle membrane potential confirmed the degree of selectivity of the voltage-dependent K^+ channel (delayed rectifier) in frog nerve and muscle. This similarity suggests that the resting membrane potential is controlled mainly by this channel [163]. This fact should always be taken into account when studying hyperpolarization and depolarization effects, e.g. N-methyl D-aspartate (NMDA), anion-transport inhibitors, catecholamines or venoms and toxins [164-169].

My interest in the physiology of the heart was manifested by measuring the activities of $[K^+]_e$ and $[Ca^{2+}]_e$ during cardiac contraction using suction ion-sensitive electrode. The application of negative pressure of -40 kPa (-300 mm Hg) for 10 min under

a suction electrode placed on the surface of the spontaneously beating frog ventricle showed changes the $[K^+]_e$ activity in three phases: a phase of rapidly rising, then a slowly decaying phase and a phase of slowly rising $[K^+]_e$ [170].

In frog muscle we unexpectedly found nAChR desensitization during repetitive end-plate activity with high number of released ACh quanta [171]. But it's not just synaptic activity that's important. The condition of skeletal muscle composed from either red or white fibers might also depend on whether they are stretched or contracted at rest. Therefore wet mass, resting membrane potential, frequency of miniature end-plate potentials and the concentration of [^{3}H]ouabain-binding sites were studied after 7 days of immobilization of the rat soleus (slow) and extensor digitorum longus (fast) muscles in the shortened or stretched position and after 3 and 7 days of remobilization. We observed that the loss of muscle mass by 37 % in the rat soleus immobilized for 7 days in the shortened position is accompanied by a membrane depolarization of about 5 mV, a decrease in frequency of miniature end-plate potentials by 60 % and a decrease of [^{3}H]ouabain binding by 25 %. Only minor changes were found in stretched soleus as well as in shortened and stretched extensor digitorum longus [172]. But it is possible that it is a combination of external synaptic and contractile systems within the muscle fiber, which determines overall muscle plasticity [173].

The last two publications presented here are the culmination of my collaboration with specialists in binding studies, biochemistry of membrane enzymes and molecular changes in the structure of proteins and masters of the path clamp records. Papers concern chemical modifications of melatonin receptors in chicken brain, ouabain binding, ATP hydrolysis, and Na^+, K^+-ATPase after chemical modification of these ATPases [174,175].

In the United States of America, I was invited several times to join bluegrass musicians. I admired the interesting neuromuscular style, which consists of a rhythmic sequence of solo individuals on a given, often popular, theme and melody. What was nice was that there were no drums in the band, the rhythm is held by a wooden or electric bass. Once I was asked to play a Czech classic. I chose Dvořák's Humoresque, which is the second most famous melody in the world after Beethoven's “for Elise”. They soon joined me and we all had a good time with variations of the melody in their style. I started playing as a violinist and ended up as a bluegrass fiddler with the whole band. In a sense, this also applies to my scientific career, as this article attests.

Conflict of Interest

There is no conflict of interest.

References

1. Novotný I, Vyskočil F. Inhibition by physostigmine of the increase of oxygen consumption induced by potassium in muscle. Nature 1961;191:916-917. https://doi.org/10.1038/191916a0
2. Novotný I, Vyskočil F, Vyklický L, Berárdfnek R. Potassium and caffeine induced increase of oxygen consumption in frog muscle and its inhibition by drugs. Physiol Bohemoslov 1962;11:277-284.
3. Novotný I, Vyskočil F, Vyklický L. Effect of drugs on calcium influx in frog sartorius muscle. Biochem Pharmacol 1963;12:266-268.
4. Novotný I, Vyskočil F. Der Einfluss von membranstabilisierenden Stoffen aufden Ca45-Einstrom in den Froschmuskel. Pflugers Arch 1963;278:8. https://doi.org/10.1007/BF00672490
5. Novotný I, Vyskočil F. Possible role of Ca ions in the resting metabolism of frog sartorius muscle during potassium depolarization. J Cell Physiol 1966;67:159-168. https://doi.org/10.1002/jcp.1040670118
6. Beránek R, Vyskočil F. The action of tubocurarine and atropine on the normal and denervated rat diaphragm. J Physiol 1967;188:53-66. https://doi.org/10.1113/jphysiol.1967.sp008123
7. Beránek R, Vyskočil F. The effect of atropine on the frog sartorius neuromuscular junction. J Physiol 1968;195:493-503. https://doi.org/10.1113/jphysiol.1968.sp008470
8. Magazanik LG, Vyskočil F. On the possible existence of muscarinic cholinoreceptors on the postsynaptic membrane of the frog muscle. Experientia 1969;25:606-607. https://doi.org/10.1007/BF01896540
9. Magazanik LG, Vyskočil F. Different action of atropine and some analogues on the end-plate potentials and induced acetylcholine potentials. Experientia 1969;25:618-619. https://doi.org/10.1007/BF01896548

10. Magazanik LG, Vyskočil F. Dependence of acetylcholine desensitization on the membrane potential of frog muscle fibre and on the ionic changes in the medium. J Physiol 1970;210:507-518. https://doi.org/10.1113/jphysiol.1970.sp009223
11. Vyskočil F, Magazanik LG. The desensitization of postjunctional muscle membrane after intracellular application of membrane stabilizers and snake venom polypeptides. Brain Res 1972;48:417-419. https://doi.org/10.1016/0006-8993(72)90202-8
12. Magazanik LG, Vyskočil F. The loci of α-bungarotoxin action on the muscle postjunctional membrane. Brain Res 1972;48:420-423. https://doi.org/10.1016/0006-8993(72)90203-X
13. Magazanik LG, Vyskočil F. Spontaneous junctional currents in Drosophila muscle-fibers. Physiol Bohemoslov 1979;28:259-260.
14. Vyskočil F, Magazanik LG. Temperature dependence of naja toxin blocking effect in Rana temporaria. Experientia 1973;29:158-160. https://doi.org/10.1007/BF01945447
15. Magazanik LG, Vyskočil F. The effect of temperature on desensitization kinetics at the post-synaptic membrane of the frog muscle fibre. J Physiol 1975;249:285-300. https://doi.org/10.1113/jphysiol.1975.sp011016
16. Vyskočil F, Magazanik LG. Dual end-plate potentials at the single neuromuscular junction of the adult frog. Pflugers Arch 1977;368:271-273. https://doi.org/10.1007/BF00585207
17. Magazanik LG, Nikolsky E, Vyskočil F. Effect of the desensitization-potentiating agent SKF-525a on frog end-plate currents. Eur J Pharmacol 1982;80:115-119. https://doi.org/10.1016/0014-2999(82)90185-6
18. Magazanik LG, Vyskočil F. Spontaneous junctional currents in Drosophila muscle fibres: effects of temperature, membrane potential and ethanol. Experientia 1979;35:213-214. https://doi.org/10.1007/BF01920623
19. Magazanik LG, Vyskočil F. Some characteristics of end-plate potentials after partial blockade by α-bungarotoxin in Rana temporaria. Experientia 1973;29:157-158. https://doi.org/10.1007/BF01945446
20. Vyskočil F, Moravec J, Janský L. Resting state of the myoneural junction in a hibernator. Brain Res 1971;34:381-384. https://doi.org/10.1016/0006-8993(71)90291-5
21. Moravec J, Melichar I, Janský L, Vyskočil F. Effect of hibernation and noradrenaline on the resting state of neuromuscular junction of golden hamster (Mesocricetus auratus). Pflugers Arch 1973;345:93-106. https://doi.org/10.1007/BF00585833
22. Melichar I, Brožek G, Janský L, Vyskočil F. Effect of hibernation and noradrenaline on acetylcholine release and action at neuromuscular junction of the golden hamster (Mesocricetus auratus). Pflugers Arch 1973;345:107-122. https://doi.org/10.1007/BF00585834
23. Vyskočil F, Vyklický L, Huston R. Quantum content at the neuromuscular junction of fast muscle after cross-union with the nerve of slow muscle in the chick. Brain Res 1971;26:443-445. https://doi.org/10.1016/0006-8993(71)90237-X
24. Ujec E, Vít Z, Vyskočil F, Králík O. Analysis of geometrical and electrical parameters of the tips of glass microelectrodes. Physiol Bohemoslov 1973;22:329-336.
25. Tuček S, Zelená J, Ge I, Vyskočil F. Choline acetyltransferase in transected nerves, denervated muscles and Schwann cells of the frog: correlation of biochemical electron microscopical and electrophysiological observations. Neuroscience 1978;3:709-724. https://doi.org/10.1016/0306-4522(78)90067-2
26. Vyskočil F, Syrový I, Prusík Z. Induction of extrajunctional acetylcholine sensitivity of rat EDL muscle by peptidic component of peripheral nerve. Pflugers Arch 1981;390:265-269. https://doi.org/10.1007/BF00658274
27. Vyskočil F, Syrový I. Do peripheral nerves contain a factor inducing acetylcholine sensitivity in skeletal muscle? Experientia 1979;35:218-219. https://doi.org/10.1007/BF01920626
28. Vyskočil F, Gutmann E. Spontaneous transmitter release from motor nerve endings in muscle fibres of castrated and old animals. Experientia 1969;25:945-946. https://doi.org/10.1007/BF01898080
29. Gutmann E, Hanzlíková V, Vyskočil F. Age changes in cross striated muscle of the rat. J Physiol 1971;216:331-343. https://doi.org/10.1113/jphysiol.1971.sp009528
30. Vyskočil F, Gutmann E. Electrophysiological and contractile properties of the levator ani muscle after castration and testosterone administration. Pflugers Arch 1977;368:105-109. https://doi.org/10.1007/BF01063461
31. Vyskočil F, Gutmann E. Spontaneous transmitter release from nerve endings and contractile properties in the soleus and diaphragm muscles of senile rats. Experientia 1972;28:280-281. https://doi.org/10.1007/BF01928688

32. Vyskočil F, Gutmann E. Anabolic effect of testosterone on the levator ani muscle of the rat. Pflugers Arch 1977;371:3-8. https://doi.org/10.1007/BF00580765
33. Vyskočil F, Gutmann E. Control of ACh sensitivity in temporarily unconnected ("decentralized") segments of diaphragm-muscle fibres of the rat. Pflugers Arch 1976;367:43-47. https://doi.org/10.1007/BF00583655
34. Vyskočil F, Gutmann E. Contractile and histochemical properties of skeletal-muscles in hibernating and awake golden-hamsters. J Comp Physiol 1977;122:385-390. https://doi.org/10.1007/BF00692523
35. Vyskočil F, Carlson B, Gutmann E. Changes in resting membrane potential and contractility of innervated and denervated skeletal muscle free grafts in the rat. Pflugers Arch 1973;344:181-186. https://doi.org/10.1007/BF00586551
36. Jones R, Vyskočil F. An electrophysiological examination of the changes in skeletal muscle fibres in response to degenerating nerve tissue. Brain Res 1975;88:309-317. https://doi.org/10.1016/0006-8993(75)90392-3
37. Vyskočil F, Nikolsky E, Edwards C. An analysis of the mechanisms underlying the non-quantal release of acetylcholine at the mouse neuromuscular junction. Neuroscience 1983;9:429-435. https://doi.org/10.1016/0306-4522(83)90305-6
38. Lupa MT, Tabti N, Thesleff S, Vyskočil F, Yu SP. The nature and origin of calcium-insensitive miniature end-plate potentials at rodent neuromuscular junctions. J Physiol 1986;381:607-618. https://doi.org/10.1113/jphysiol.1986.sp016346
39. Thesleff S, Vyskočil F, Ward MR. The action potential in end-plate and extrajunctional regions of rat skeletal muscle. Acta Physiol Scand 1974;91:196-202. https://doi.org/10.1111/j.1748-1716.1974.tb05676.x
40. Janigro D, Di Gregorio F, Vyskočil F, Gorio A. Gangliosides' dual mode of action: a working hypothesis. J Neurosci Res 1984;12:499-509. https://doi.org/10.1002/jnr.490120233
41. Vyskočil F, Di Gregorio F, Gorio A. The facilitating effect of gangliosides on the electrogenic (Na^+/K^+) pump and on the resistance of the membrane potential to hypoxia in neuromuscular preparation. Pflugers Arch 1985;403:1-6. https://doi.org/10.1007/BF00583273
42. Walker JL Jr: ion specific liquid ion exchanger microelectrodes. Analyt Chem 1971;43:90-93. https://doi.org/10.1021/ac60298a780
43. Vyskočil F, Kříž N. Modifications of single and double-barrel potassium specific microelectrodes for physiological experiments. Pflugers Arch 1972;337:365-376. https://doi.org/10.1007/BF00586850
44. Hnik P, Vyskočil F, Kříž N, Holas M. Work-induced increase of extracellular potassium concentration in muscle measured by ion-specific electrodes. Brain Res 1972;40:559-562. https://doi.org/10.1016/0006-8993(72)90162-X
45. Hník P, Kříž N, Vyskočil F, Smieško V, Mejsnar J, Ujec E, Holas M. Work-induced potassium changes in muscle venous effluent blood measured by ion-specific electrodes. Pflugers Arch 1973;338:177-181. https://doi.org/10.1007/BF00592752
46. Hník P, Holas M, Krekule I, Kříž N, Mejsnar J, Smieško V, Ujec E, Vyskočil F. Work-induced potassium changes in skeletal muscle and effluent venous blood assessed by liquid ion-exchanger microelectrodes. Pflugers Arch 1976;362:85-94. https://doi.org/10.1007/BF00588685
47. Hník P, Kříž N, Vyskočil F, Smieško V, Mejsnar J, Ujec E, Holas M. Work-induced increase of potassium in venous effluent blood measured by ion-specific electrodes. Physiol Bohemoslov 1973;22:67-68 https://doi.org/10.1007/BF00592752
48. Vyskočil F, Hník P, Rehfeldt H, Vejsada R, Ujec E. The measurement of K^+_e concentration changes in human muscles during volitional contractions. Pflugers Arch 1983;399:235-237. https://doi.org/10.1007/BF00656721
49. Vyskočil F, Kříž N, Bureš J. Potassium-selective microelectrodes used for measuring the extracellular brain potassium during spreading depression and anoxic depolarization in rats. Brain Res 1972;39:255-259. https://doi.org/10.1016/0006-8993(72)90802-5
50. Adámek S, Vyskočil F. Potassium-selective microelectrode revealed difference in threshold potassium concentration for cortical spreading depression in female and male rat brain. Brain Res 2011;1370:215-219. https://doi.org/10.1016/j.brainres.2010.11.018
51. Vizi ES, Vyskočil F. Changes in total and quantal release of acetylcholine in the mouse diaphragm during activation and inhibition of membrane ATPase. J Physiol 1979;286:1-14. https://doi.org/10.1113/jphysiol.1979.sp012603

52. Vyskočil F, Illés P. Non-quantal release of transmitter at mouse neuromuscular junction and its dependence on the activity of Na^+-K^+ ATP-ase. Pflugers Arch 1977;370:295-297. https://doi.org/10.1007/BF00585542
53. Vyskočil F, Illés P. Electrophysiological examination of transmitter release in non-quantal form in the mouse diaphragm and the activity of membrane ATP-ase. Physiol Bohemoslov 1978;27:449-455.
54. Edwards C, Doležal V, Tuček S, Zemková H, Vyskočil F. Is an acetylcholine transport system responsible for nonquantal release of acetylcholine at the rodent myoneural junction? Proc Natl Acad Sci U S A 1985;82:3514-3518. https://doi.org/10.1073/pnas.82.10.3514
55. Vyskočil F. Inhibition of non-quantal acetylcholine leakage by 2(4-phenylpiperidine)cyclohexanol in the mouse diaphragm. Neurosci Lett 1985;59:277-280. https://doi.org/10.1016/0304-3940(85)90144-2
56. Zemková H, Vyskočil F, Edwards C. The effects of nerve terminal activity on non-quantal release of acetylcholine at the mouse neuromuscular junction. J Physiol 1990;423:631-640. https://doi.org/10.1113/jphysiol.1990.sp018044
57. Nikolsky EE, Voronin VA, Oranska TI, Vyskočil F. The dependence of non-quantal acetylcholine release on the choline-uptake system in the mouse diaphragm. Pflügers Arch 1991;418:74-78. https://doi.org/10.1007/BF00370454
58. Zemková H, Vyskočil F, Edwards C. A study on early post-denervation changes of non-quantal and quantal acetylcholine release in the rat diaphragm. Pflugers Arch 1987;409:540-546. https://doi.org/10.1007/BF00583813
59. Zemková H, Vyskočil F. Effect of Mg^{2+} on non-quantal acetylcholine release at the mouse neuromuscular junction. Neurosci Lett 1989;103:293-297. https://doi.org/10.1016/0304-3940(89)90115-8
60. Nikolsky EE, Voronin VA, Vyskočil F. Kinetic differences in the effect of calcium on quantal and non-quantal acetylcholine release at the murine diaphragm. Neurosci Lett 1991;123:192-194. https://doi.org/10.1016/0304-3940(91)90928-M
61. Nikolsky EE, Oranska TI, Vyskočil F. Non-quantal acetylcholine release after cholinesterase inhibition in vivo. Physiol Res 1992;41:333-334.
62. Giniatullin RA, Khazipov RN, Oranska TI, Nikolsky EE, Voronin VA, Vyskočil F. The effect of non-quantal acetylcholine release on quantal miniature currents at mouse diaphragm. J Physiol 1993;466:105-114. https://doi.org/10.1113/jphysiol.1993.sp019711
63. Giniatullin RA, Khazipov RN, Vyskočil F. A correlation between quantal content and decay time of endplate currents in frog muscles with intact cholinesterase. J Physiol 1993;466:95-103. https://doi.org/10.1113/jphysiol.1993.sp019710
64. Nikolsky EE, Zemková H, Voronin VA, Vyskočil F. Role of non-quantal acetylcholine release in surplus polarization of mouse diaphragm fibres at the endplate zone. J Physiol 1994;477:497-502. https://doi.org/10.1113/jphysiol.1994.sp020210
65. Vyskočil F, Vrbová G. Non-quantal release of acetylcholine affects polyneuronal innervation on developing rat muscle fibres. Eur J Neurosci 1993;5:1677-1683. https://doi.org/10.1111/j.1460-9568.1993.tb00235.x
66. Shakiryanova DM, Zefirov AL, Nikolsky EE, Vyskočil F. The effect of acetylcholine and related drugs on currents at the frog motor nerve terminal. Eur J Pharmacol 1994;263:107-114. https://doi.org/10.1016/0014-2999(94)90530-4
67. Vyskočil F, Malomouzh AI, Nikolsky EE. Non-quantal acetylcholine release at the neuromuscular junction. Physiol Res 2009;58:763-784. https://doi.org/10.33549/physiolres.931865
68. Nikolsky EE, Oranska TI, Vyskočil F. Non-quantal acetylcholine release in the mouse diaphragm after phrenic nerve crush and during recovery. Exp Physiol 1996;81:341-348. https://doi.org/10.1113/expphysiol.1996.sp003938
69. Mukhtarov MR, Urazaev AK, Nikolsky EE, Vyskočil F. Effect of nitric oxide and NO synthase inhibition on nonquantal acetylcholine release in the rat diaphragm. Eur J Neurosci 2000;12:980-986. https://doi.org/10.1046/j.1460-9568.2000.00992.x
70. Galkin AV, Giniatullin RA, Mukhtarov MR, Svandová I, Grishin SN, Vyskočil F. ATP but not adenosine inhibits nonquantal acetylcholine release at the mouse neuromuscular junction. Eur J Neurosci 2001;13:2047-2053. https://doi.org/10.1046/j.0953-816x.2001.01582.x

70a. Teplov AY, Grishin SN, Mukhamedyarov MA, Ziganshin AU, Zefirov AL, Palotás A: Ovalbumin- induced sensitization affects non-quantal acetylcholine release from motor nerve terminals and alters contractility of skeletal muscles in mice. Exp Physiol 2009;94:264-268. https://doi.org/10.1113/expphysiol.2008.045740

71. Malomouzh AI, Nikolsky EE, Vyskočil F. Purine P2Y receptors in ATP-mediated regulation of non-quantal acetylcholine release from motor nerve endings of rat diaphragm. Neurosci Res 2011;71:219-225. https://doi.org/10.1016/j.neures.2011.07.1829
72. Giniatullin RA, Talantova M, Vyskočil F. Desensitization shortens the high-quantal-content endplate current time course in frog muscle with intact cholinesterase. J Physiol 1997;502:641-648. https://doi.org/10.1111/j.1469-7793.1997.641bj.x
73. Lindovský J, Kaniaková M, Svobodová L, Vyskočil F, Krůšek J. Role of negatively charged amino acids in beta 4 F-loop in activation and desensitization of alpha 3 beta 4 rat neuronal nicotinic receptors. Biochim Biophys Acta 2008;1778:864-871. https://doi.org/10.1016/j.bbamem.2008.01.010
74. Kaniaková M, Lindovský J, Krůšek J, Adámek S, Vyskočil F. Dual effect of lobeline on α4β2 rat neuronal nicotinic receptors. Eur J Pharmacol 2011;658:108-113. https://doi.org/10.1016/j.ejphar.2011.02.012
75. Lindovský J, Petrov K, Krůšek J, Reznik VS, Nikolsky EE, Vyskočil F. Effect of tissue-specific acetylcholinesterase inhibitor C-547 on α3β4 and αβεδ acetylcholine receptors in COS cells. Eur J Pharmacol 2012;688:22-26. https://doi.org/10.1016/j.ejphar.2012.05.010
76. Skorinkin AI, Shaihutdinova AR, Vyskočil F. Model of concentration changes across the synaptic cleft during a single quantum release. Gen Physiol Biophys 2008;27:19-24.
77. Gilmanov IR, Samigullin DV, Vyskočil F, Nikolsky EE, Bukharaeva EA. Modeling of quantal neurotransmitter release kinetics in the presence of fixed and mobile calcium buffers. J Comput Neurosci 2008;25:296-307. https://doi.org/10.1007/s10827-008-0079-5
78. Adámek S, Shakirzyanova AV, Malomouzh AI, Naumenko NV, Vyskočil F. Interaction of glutamate- and adenosine-induced decrease of acetylcholine quantal release at frog neuromuscular junction. Physiol Res 2010;59:803-810. https://doi.org/10.33549/physiolres.932024
79. Urazaev AK, Magsumov ST, Poletayev GI, Nikolsky EE, Vyskočil F. Muscle NMDA receptors regulate the resting membrane potential through NO-synthase. Physiol Res 1995;44:205-208.
80. Mukhtarov MR, Vyskočil F, Urazaev AK, Nikolsky EE. Non-quantal acetylcholine release is increased after nitric oxide synthase inhibition. Physiol Res 1999;48:315-317.
81. Urazaev A, Nikolsky E, Vyskočil F. Muscarinic M-1-receptors are involved in neural regulation of membrane potential in rat muscles. J Neurochem 1998;71(Suppl 1):S22.
82. Urazaev AKh, Naumenko NV, Poletayev GI, Nikolsky EE, Vyskočil F. The effect of glutamate and inhibitors of NMDA receptors on postdenervation decrease of membrane potential in rat diaphragm. Mol Chem Neuropathol 1998;33:163-174. https://doi.org/10.1007/BF02815179
83. Urazaev AKh, Naumenko NV, Poletayev GI, Nikolsky EE, Vyskočil F. Nitroprusside decreases the early post-denervation depolarization of diaphragm muscle fibres of the rat. Eur J Pharmacol 1996;316:219-222. https://doi.org/10.1016/S0014-2999(96)00817-5
84. Urazaev AKh, Naumenko NV, Nikolsky EE, Vyskočil F. Carnosine and other imidazole-containing compounds enhance the postdenervation depolarization of the rat diaphragm fibres. Physiol Res 1998;47:291-295.
85. Moravec J, Vyskočil F. Early postdenervation depolarization develops faster at endplates of hibernating golden hamsters where spontaneous quantal and non-quantal acetylcholine release is very small. Neurosci Res 2005;51:25-29. https://doi.org/10.1016/j.neures.2004.09.003
86. Urazaev AK, Naumenko NV, Poletayev GI, Nikolsky EE, Vyskočil F. Acetylcholine and carbachol prevent muscle depolarization in denervated rat diaphragm. Neuroreport 1997;8:403-406. https://doi.org/10.1097/00001756-199701200-00004
87. Urazaev AK, Naumenko NV, Nikolsky EE, Vyskočil F. The glutamate and carbachol effects on the early post-denervation depolarization in rat diaphragm are directed towards furosemide-sensitive chloride transport. Neurosci Res 1999;33:81-86. https://doi.org/10.1016/S0168-0102(98)00117-5
88. Malomouzh AI, Arkhipova SS, Nikolsky EE, Vyskočil F. Immunocytochemical demonstration of M(1) muscarinic acetylcholine receptors at the presynaptic and postsynaptic membranes of rat diaphragm endplates. Physiol Res 2011;60:185-188. https://doi.org/10.33549/physiolres.932131
89. Samigullin D, Bukharaeva EA, Nikolsky E, Adámek S, Vyskočil F. Long release latencies are increased by acetylcholine at frog endplate. Physiol Res 2003;52:475-480. https://doi.org/10.33549/physiolres.930407

90. Bukcharaeva EA, Kim KC, Moravec J, Nikolsky EE, Vyskočil F. Noradrenaline synchronizes evoked quantal release at frog neuromuscular junctions. J Physiol 1999;517:879-888. https://doi.org/10.1111/j.1469-7793.1999.0879s.x
91. Bukharaeva E, Nikolsky E, Kim K, Gainulov R, Vyskočil F. Catecholamines change the time course of the evoked quanta mediator release via beta(1)-adrenoreceptors . J Neurochem 1998;71(Suppl 1):S49.
92. Bukharaeva EA, Samigullin D, Nikolsky E, Vyskočil F. Protein kinase A cascade regulates quantal release dispersion at frog muscle endplate. J Physiol 2002;538:837-848. https://doi.org/10.1113/jphysiol.2001.012752
93. Khuzakhmetova V, Bukharaeva E. Adrenaline facilitates synaptic transmission by synchronizing release of acetylcholine quanta from motor nerve endings. Cell Mol Neurobiol 2021;41:395-401. https://doi.org/10.1007/s10571-020-00840-3
94. Ujec E, Vyklický L Jr, Vyskočil F, Vyklický L Sr. A simple version of the patch clamp technique for measuring currents in single ionic channels of biological-membranes. Physiol Bohemoslov 1984;33:570-571.
95. Zemková H, Vyskočil F, Tolar M, Vlachová V, Ujec E. Single K^+ currents during differentiation of embryonic muscle cells in vitro. Biochim Biophys Acta 1989;986:146-150. https://doi.org/10.1016/0005-2736(89)90284-8
96. Bolotina V, Borecký J, Vlachová V, Baudyšová M, Vyskočil F. Voltage-dependent chloride channels with several substates in excised patches from mouse neuroblastoma cells. Neurosci Lett 1987;77:298-302. https://doi.org/10.1016/0304-3940(87)90516-7
97. Vyklický L Jr, Michl J, Vlachová V, Vyklický L, Vyskočil F. Ionic currents in neuroblastoma clone E-7 cells. Neurosci Lett 1985;55:197-201. https://doi.org/10.1016/0304-3940(85)90019-9
98. Krůšek J, Dittert I, Hendrych T, Hník P, Horák M, Petrovic M, Sedláček M, Sušánková K, Svobodová L, Toušová K, Ujec E, Vlachová V, Vyklický L, Vyskočil F, Vyklický L Jr. Activation and modulation of ligand-gated ion channels. Physiol Res 2004;53(Suppl 1):S103-S113. https://doi.org/10.33549/physiolres.930000.53.S103
99. Vlachová V, Vyklický L, Vyklický L Jr, Vyskočil F. The action of excitatory amino acids on chick spinal cord neurones in culture. J Physiol 1987;386:425-438. https://doi.org/10.1113/jphysiol.1987.sp016542
100. Vyklický L, Vyklický L Jr, Vyskočil F, Vlachová V, Ujec E, Michl J. Evidence that excitatory amino acids not only activate the receptor channel complex but also lead to use-dependent block. Brain Res 1986;363:148-151. https://doi.org/10.1016/0006-8993(86)90668-2
101. Zemková H, Krůšek J, Vyskočil F. Potentiation of GABAA receptor in cultured mouse hippocampal cells by brain-derived peptide mixture cerebrolysin. Physiol Res 1995;44:151-155.
102. Vyklický L, Vyklický L Jr, Vlachová V, Michl J, Vyskočil F. Cobalt ions block L-glutamate and L-aspartate-induced currents in cultured neurons from embryonic chick spinal cord. Neurosci Lett 1985;61:345-350. https://doi.org/10.1016/0304-3940(85)90488-4
103. Vyskočil F, Vyklický L, Vlachová V, Ujec E. Miniature endplate currents at the neuromuscular-junction of the larva of the fly (Sarcophaga bullata). Mol Physiol 1985;7:143-154.
104. Vyklický L, Vyklický L, Vlachová V, Vyskočil F, Michl J. Action of L-glutamate and L-aspartate on spinal cord neurons in cell culture. Physiol Bohemoslov 1986;35:375.
105. Hamplová-Peichlová J, Krůšek J, Paclt I, Slavíček J, Lisá V, Vyskočil F. Citalopram inhibits L-type calcium channel current in rat cardiomyocytes in culture. Physiol Res 2002;51:317-321. https://doi.org/10.33549/physiolres.930216
106. Krůšek J, Vyskočil F. Different degree of cooperativity in adult, embryonic and mutated mouse muscle nicotinic receptors. Biochim Biophys Acta 2003;1646:119-130. https://doi.org/10.1016/S1570-9639(02)00552-6
107. Giniatullin RA, Kheeroug LS, Vyskočil F. Modelling endplate currents: dependence on quantum secretion probability and decay of miniature current. Eur Biophys J 1995;23:443-446. https://doi.org/10.1007/BF00196832
108. Shaihutdinova AR, Nikolsky EE, Vyskočil F, Skorinkin AI. Mechanisms of the inhibition of endplate acetylcholine receptors by antiseptic chlorhexidine (experiments and models). Naunyn Schmiedebergs Arch Pharmacol 2009;380:551-560. https://doi.org/10.1007/s00210-009-0458-0
109. Giniatullin RA, Talantova MV, Vyskočil F. The role of desensitisation in decay time of miniature endplate currents in frogs Rana ridibunda and Rana temporaria. Neurosci Res 2001;39:287-292. https://doi.org/10.1016/S0168-0102(00)00225-X

110. Strunsky EG, Borisover MD, Nikolsky EE, Vyskočil F. Temperature effect on carbachol-induced depression of spontaneous quantal transmitter release in frog neuromuscular junction. Neurochem Res 2001;26:891-897. https://doi.org/10.1023/A:1012372115058
111. Kovyazina IV, Nikolsky EE, Giniatullin RA, Adámek S, Vyskočil F. Dependence of miniature endplate current on kinetic parameters of acetylcholine receptors activation: a model study. Neurochem Res 2003;28:443-448. https://doi.org/10.1023/A:1022896601271
112. Dlouhá H, Teisinger J, Vyskočil F. Activation of membrane Na^+/K^+-ATPase of mouse skeletal muscle by acetylcholine and its inhibition by alpha-bungarotoxin, curare and atropine. Pflugers Arch 1979;380:101-104. https://doi.org/10.1007/BF00582620
113. Dlouhá H, Teisinger J, Vyskočil F. The effect of vanadate on the electrogenic Na^+/K^+ pump, intracellular Na^+ concentration and electrophysiological characteristics of mouse skeletal muscle fibre. Physiol Bohemoslov 1981;30:1-10.
114. Vyskočil F, Teisinger J, Dlouhá H. A specific enzyme is not necessary for vanadate-induced oxidation of NADH. Nature 1980;286:516-517. https://doi.org/10.1038/286516a0
115. Amler E, Teisinger J, Svobodová J, Vyskočil F. Vanadyl ions increase the order parameter of plasma membranes without changing the rotational relaxation time. Biochim Biophys Acta 1986;863:18-22. https://doi.org/10.1016/0005-2736(86)90382-2
116. Stankovičová T, Zemková H, Breier A, Amler E, Burkhard M, Vyskočil F. The effects of calcium and calcium channel blockers on sodium pump. Pflugers Arch 1995;429:716-721. https://doi.org/10.1007/BF00373994
117. Amler E, Teisinger J, Svoboda P, Vyskočil F. The changes in conformation of (Na^+ K^+)-ATPase from rat brain membranes are accompanied by changes of protein segment movements in the nanosecond range. Physiol Bohemoslov 1988;37:145-148.
118. Sulová Z, Vyskočil F, Stankovičová T, Breier A. Ca^{2+}-induced inhibition of sodium pump: effects on energetic metabolism of mouse diaphragm tissue. Gen Physiol Biophys 1998;17:271-283.
119. Zemková H, Teisinger J, Vyskočil F. Inhibition of the electrogenic Na,K pump and Na,K-ATPase activity by tetraethylammonium, tetrabutylammonium, and apamin. J Neurosci Res 1988;19:497-503. https://doi.org/10.1002/jnr.490190414
120. Vyskočil P, Zemková H, Teisinger J, Vyskočil F. Arachidonate has a positive effect on the electrogenic sodium-potassium pump in the mouse diaphragm. Physiol Bohemoslov 1987;36:167-169.
121. Vyskočil F, Zemková H, Teisinger J, Svoboda P. Arachidonate activates muscle electrogenic sodium pump and brain microsome Na^+,K^+-ATPase under suboptimal conditions. Brain Res 1987;436:85-91. https://doi.org/10.1016/0006-8993(87)91559-9
122. Svoboda P, Teisinger J, Vyskočil F. Effect of catecholamines and metal chelating agents on the brain and brown adipose tissue Na,K-ATPase. Comp Biochem Physiol C Comp Pharmacol 1986;84:283-290. https://doi.org/10.1016/0742-8413(86)90095-2
123. Tyapkina O, Volkov E, Nurullin L, Shenkman B, Kozlovskaya I, Nikolsky E, Vyskočil F. Resting membrane potential and Na^+,K^+-ATPase of rat fast and slow muscles during modeling of hypogravity. Physiol Res 2009;58:599-603. https://doi.org/10.33549/physiolres.931810
124. Khuzakhmetova V, Samigullin D, Nurullin L, Vyskočil F, Nikolsky E, Bukharaeva E. Kinetics of neurotransmitter release in neuromuscular synapses of newborn and adult rats. Int J Dev Neurosci 2014;34:9-18. https://doi.org/10.1016/j.ijdevneu.2013.12.010
125. Bukharaeva E, Ipatova T, Nikolsky EE, Vyskočil F. The effect of carbachol and alpha-bungarotoxin on the frequency of miniature endplate potentials at the frog neuromuscular junction. Exp Physiol 2000;85:125-131. https://doi.org/10.1017/S0958067000019497
126. Doležal V, Vyskočil F, Tuček S. Decrease of the spontaneous non-quantal release of acetylcholine from the phrenic nerve in botulinum-poisoned rat diaphragm. Pflugers Arch 1983;397:319-322. https://doi.org/10.1007/BF00580268
127. Samigullin D, Bukharaeva E, Nikolsky E, Vyskočil F. Temperature effect on proximal to distal gradient of quantal release of acetylcholine at frog endplate. Neurochem Res 2003;28:507-514. https://doi.org/10.1023/A:1022817205814
128. Vyskočil F. Early postdenervation depolarization is controlled by acetylcholine and glutamate via nitric oxide regulation of the chloride transporter. Neurochem Res 2003;28:575-585. https://doi.org/10.1023/A:1022833709448

129. Malomouzh AI, Mukhtarov MR, Nikolsky EE, Vyskočil F, Lieberman EM, Urazaev AK. Glutamate regulation of non-quantal release of acetylcholine in the rat neuromuscular junction. J Neurochem 2003;85:206-213. https://doi.org/10.1046/j.1471-4159.2003.01660.x
130. Volkov EM, Nurullin LF, Nikolsky E, Krůšek J, Vyskočil F. Chloride cotransport in the membrane of earthworm body wall muscles. Physiol Res 2003;52:587-592. https://doi.org/10.33549/physiolres.930182
131. Nikolsky EE, Vyskočil F, Bukharaeva EA, Samigullin D, Magazanik LG. Cholinergic regulation of the evoked quantal release at frog neuromuscular junction. J Physiol 2004;560:77-88. https://doi.org/10.1113/jphysiol.2004.065805
132. Svobodová L, Krůšek J, Hendrych T, Vyskočil F. Allosteric modulation of nicotinic acetylcholine receptor by physostigmine. Biophysics from Molecules to Brain: In Memory of Radoslav K. Andjus 2005;1048:251-255.
133. Bukharaeva EA, Salakhutdinov RI, Vyskočil F, Nikolsky EE. Spontaneous quantal and non-quantal release of acetylcholine at mouse endplate during onset of hypoxia. Physiol Res 2005;54:251-255. https://doi.org/10.33549/physiolres.930718
134. Samigullin D, Bukharaeva EA, Vyskočil F, Nikolsky EE. Calcium dependence of uni-quantal release latencies and quantal content at mouse neuromuscular junction. Physiol Res 2005;54:129-132. https://doi.org/10.33549/physiolres.930712
135. Petrov KA, Kovyazina LV, Zobov VV, Bukharaeva EA, Nikolsky EE, Vyskočil F. Different sensitivity of miniature endplate currents of the rat extensor digitorum longus, soleus and diaphragm muscles to a novel acetylcholinesterase inhibitor C-547. Physiol Res 2006;55:585-589. https://doi.org/10.33549/physiolres.930980
136. Svobodová L, Krůšek J, Hendrych T, Vyskočil F. Physostigmine modulation of acetylcholine currents in COS cells transfected with mouse muscle nicotinic receptor. Neurosci Lett 2006;401:20-24. https://doi.org/10.1016/j.neulet.2006.02.065
137. Malomouzh AI, Mukhtarov MR, Nikolsky EE, Vyskočil F. Muscarinic M1 acetylcholine receptors regulate the non-quantal release of acetylcholine in the rat neuromuscular junction via NO-dependent mechanism. J Neurochem 2007;102:2110-2117. https://doi.org/10.1111/j.1471-4159.2007.04696.x
138. Volkov EM, Nurullin LF, Nikolsky E, Vyskočil F. Miniature excitatory synaptic ion currents in the earthworm Lumbricus terrestris body wall muscles. Physiol Res 2007;56:655-658. https://doi.org/10.33549/physiolres.931269
139. Volkov EM, Nurullin LF, Volkov ME, Nikolsky EE, Vyskočil F. Mechanisms of carbacholine and GABA action on resting membrane potential and Na^+/K^+-ATPase of Lumbricus terrestris body wall muscles. Comp Biochem Physiol A Mol Integr Physiol 2011;158:520-524. https://doi.org/10.1016/j.cbpa.2010.12.016
140. Nurullin LF, Mukhitov AR, Tsentsevytsky AN, Petrova NV, Samigullin DV, Malomouzh AI, Bukharaeva EA, Vyskočil F, Nikolsky EE. Voltage-dependent P/Q-type calcium channels at the frog neuromuscular junction. Physiol Res 2011;60:815-823. https://doi.org/10.33549/physiolres.932219
141. Petrov KA, Yagodina LO, Valeeva GR, Lannik NI, Nikitashina AD, Rizvanov AA, Zobov VV, Bukharaeva EA, Reznik VS, Nikolsky EE, Vyskočil F. Different sensitivities of rat skeletal muscles and brain to novel anti-cholinesterase agents, alkylammonium derivatives of 6-methyluracil (ADEMS). Br J Pharmacol 2011;163:732-744. https://doi.org/10.1111/j.1476-5381.2011.01211.x
142. Vyskočil F. Action potentials of the rat diaphragm and their sensitivity to tetrodotoxin during postnatal development and old age. Pflugers Arch 1974;352:155-163. https://doi.org/10.1007/BF00587514
143. Kaniakova M, Skrenkova K, Adamek S, Vyskocil F, Krusek J. Different effects of lobeline on neuronal and muscle nicotinic receptors. Eur J Pharmacol 2014;738:352-359. https://doi.org/10.1016/j.ejphar.2014.05.057
144. Vyskočil F. Recovery of sensitivity to acetylcholine following desensitization in muscles of different vertebrate species. Pflugers Arch 1975;361:83-87. https://doi.org/10.1007/BF00587345
145. Vyskočil F. Miniature end-plate potentials and sensitivity to acetylcholine in the fast and slow limb muscles of hibernating golden hamsters. Pflugers Arch 1976;361:165-167. https://doi.org/10.1007/BF00583461
146. Vyskočil F. Diazepam blockade of repetitive action potentials in skeletal muscle fibres. A model of its membrane action. Brain Res 1977;133:315-328. https://doi.org/10.1016/0006-8993(77)90767-3
147. Vyskočil F. Effect of diazepam on the frog neuromuscular junction. Eur J Pharmacol 1978;48:117-124. https://doi.org/10.1016/0014-2999(78)90049-3
148. Illés P, Vyskočil F. Calcium-dependent inhibition by prostaglandin E1 of spontaneous acetylcholine release from frog motor nerve. Eur J Pharmacol 1978;48:455-457. https://doi.org/10.1016/0014-2999(78)90175-9

149. Dlouhá H, Vyskočil F. The effect of cortisol on the excitability of the rat muscle fibre membrane and neuromuscular transmission. Physiol Bohemoslov 1979;28:485-494.
150. Vejsada R, Hník P, Dittertová-Vlasáková L, Smetana K Jr, Haninec P, Grim M, Vyskočil F. Functional properties of muscle autografts substituted for the rat levator ani muscle. Physiol Bohemoslov 1981;30:515-524.
151. Vyskočil F, Teisinger J, Dlouhá H. Importance of cardiac cell membranes in vanadate-induced NADH oxidation - Reply. Nature 1981;294:288. https://doi.org/10.1038/294288b0
152. Vyskočil F, Teisinger J, Dlouhá H. The disparity between effects of vanadate (V) and vanadyl (IV) ions on (Na^+-K^+)-ATPase and K^+-phosphatase in skeletal muscle. Biochem Biophys Res Commun 1981;100:982-987. https://doi.org/10.1016/0006-291X(81)91920-3
153. Teisinger J, Vyskočil F, Dlouhá H. The activation of membrane ATPase by ouabain in several tissues of the golden hamster (Mesocricetus auratus) in the absence of potassium. Experientia 1981;37:383-384. https://doi.org/10.1007/BF01959875
154. Vyskočil F, Donselaar Y, Teisinger J, Dlouhá H. Temperature dependence of membrane Na^+-K^+-ATPase and effect of ouabain in golden hamster and mouse diaphragm. Cryobiology 1981;18:100-101. https://doi.org/10.1016/0011-2240(81)90057-2
155. Dlouhá H, Donselaar Y, Teisinger J, Vyskočil F. Effect of temperature and ouabain on the Na^+-K^+ activated membrane ATPase and electrogenic ionic pump of the golden hamster and mouse diaphragm. Physiol Bohemoslov 1980;29:543-552.
156. Vyklický L, Vyskočil F, Kolaj M, Jastreboff P. Primary afferent depolarization and changes in extracellular potassium concentration induced by L-glutamate and L-proline in the isolated spinal cord of the frog. Neurosci Lett 1982;32:159-164. https://doi.org/10.1016/0304-3940(82)90267-1
157. Shabunova I, Vyskočil F. Postdenervation changes of intracellular potassium and sodium measured by ion selective microelectrodes in rat soleus and extensor digitorum longus muscle fibres. Pflugers Arch 1982;394:161-164. https://doi.org/10.1007/BF00582919
158. Zemková H, Teisinger J, Vyskočil F. The comparison of vanadyl (IV) and insulin-induced hyperpolarization of the mammalian muscle cell. Biochim Biophys Acta 1982;720:405-410. https://doi.org/10.1016/0167-4889(82)90119-7
159. Vyskočil F, Pilař J, Zemková H, Teisinger J. Reduction of vanadate to vanadyl by methylene-blue, imipramine, and chlorpromazine in absence of NADH. Lancet 1982;1:1078-1079. https://doi.org/10.1016/S0140-6736(82)92141-9
160. Vyskočil F, Pilař J, Zemková H, Svoboda P, Vítek V, Teisinger J. Bleomycin stimulates both membrane (Na^+-K^+) ATPase and electrogenic (Na^+-K^+) pump and partially removes the inhibition by vanadium ions. Biochem Biophys Res Commun 1983;116:783-790. https://doi.org/10.1016/0006-291X(83)90593-4
161. Svoboda P, Teisinger J, Pilař J, Vyskočil F. Vanadyl (VO_2^+) and vanadate (VO_3^-) ions inhibit the brain microsomal Na,K-ATPase with similar affinities. Protection by transferrin and noradrenaline. Biochem Pharmacol 1984;33:2485-2891. https://doi.org/10.1016/0006-2952(84)90722-6
162. Svoboda P, Teisinger J, Vyskočil F. Vanadyl (VO_2^+) induced lipoperoxidation in the brain microsomal fraction is not related to VO_2^+ inhibition of Na,K-ATPase. Biochem Pharmacol 1984;33:2493-2497. https://doi.org/10.1016/0006-2952(84)90723-8
163. Edwards C, Vyskočil F. The effects of the replacement of K^+ by Tl^+, Rb^+, and NH_4^+ on the muscle membrane potential. Gen Physiol Biophys 1984;3:259-264.
164. Zemková H, Teisinger J, Vyskočil F. Hyperpolarization of mouse skeletal muscle plasma membrane induced by extracellular NADH. Biochim Biophys Acta 1984;775:64-70. https://doi.org/10.1016/0005-2736(84)90235-9
165. Teisinger J, Zemková H, Vyskočil F. The effect of anion channel blockers on enzymatic activity of Na^+/K^+-ATPase and the electrogenic Na^+/K^+ pump. FEBS Lett 1984;175:275-278. https://doi.org/10.1016/0014-5793(84)80750-4
166. Teisinger J, Zemková H, Vyskočil F. The effect of anion transport inhibitors on enzymatic Na^+/K^+-ATPase and electrogenic Na^+/K^+ pump aktivity. Physiol Bohemoslov 1985;34:282.
167. Zemková H, Svoboda P, Teisinger J, Vyskočil F. On the mechanism of catecholamine-induced hyperpolarization of skeletal muscle cells. Naunyn Schmiedebergs Arch Pharmacol 1985;329:18-23. https://doi.org/10.1007/BF00695186
168. Vyskočil F, Vyklický L, Jirmanová I, Ujec E. Neuromuscular junction in the larva of the fly (Sarcophaga bullata). Mol Physiol 1985;7:127-142.

169. Vyklický L Jr, Krůšek J, Vyklický L, Vyskočil F. Spider venom of Araneus opens and desensitizes glutamate channels in chick spinal cord neurones. Neurosci Lett 1986;68:227-231. https://doi.org/10.1016/0304-3940(86)90147-3
170. Slavíček J, Vyskočil F. Extracellular K^+ and Ca^{2+} activities measured during the action of negative pressure under a suction electrode placed on the surface of frog heart ventricle. Physiol Bohemoslov 1985;34:201-207.
171. Giniatullin RA, Khamitov G, Khazipov R, Magazanik LG, Nikolsky EE, Snetkov VA, Vyskočil F. Development of desensitization during repetitive end-plate activity and single end-plate currents in frog muscle. J Physiol 1989;412:113-122. https://doi.org/10.1113/jphysiol.1989.sp017606
172. Zemková H, Teisinger J, Almon RR, Vejsada R, Hník P, Vyskočil F. Immobilization atrophy and membrane properties in rat skeletal muscle fibres. Pflugers Arch 1990;416:126-129. https://doi.org/10.1007/BF00370233
173. Nikolsky EE, Bukharaeva EA, Strunsky EG, Vyskočil F. Depression of miniature endplate potential frequency by acetylcholine and its analogues in frog. Br J Pharmacol 1991;104:1024-1032. https://doi.org/10.1111/j.1476-5381.1991.tb12544.x
174. Kosař E, Teisinger J, Vyskočil F, Vaněček J. Chemical modifications of melatonin receptors in chicken brain. J Neurochem 1994;63:662-670. https://doi.org/10.1046/j.1471-4159.1994.63020662.x
175. Teisinger J, Zemková H, Svoboda P, Amler E, Vyskočil F. Ouabain binding, ATP hydrolysis, and Na^+,K^+-pump activity during chemical modification of brain and muscle Na^+,K^+-ATPase. J Neurochem 1992;58:1066-1072. https://doi.org/10.1111/j.1471-4159.1992.tb09363.x

Research Topics studied in the Institute of Physiology (Czech Academy of Sciences) 1954 - 2024

For the detailed description of particular research topics and their representative papers see

https://www.biomed.cas.cz/physiolres/pdf/2024/73_S105.pdf

or

IPHYS Brochure

https://www.fgu.cas.cz/en/about

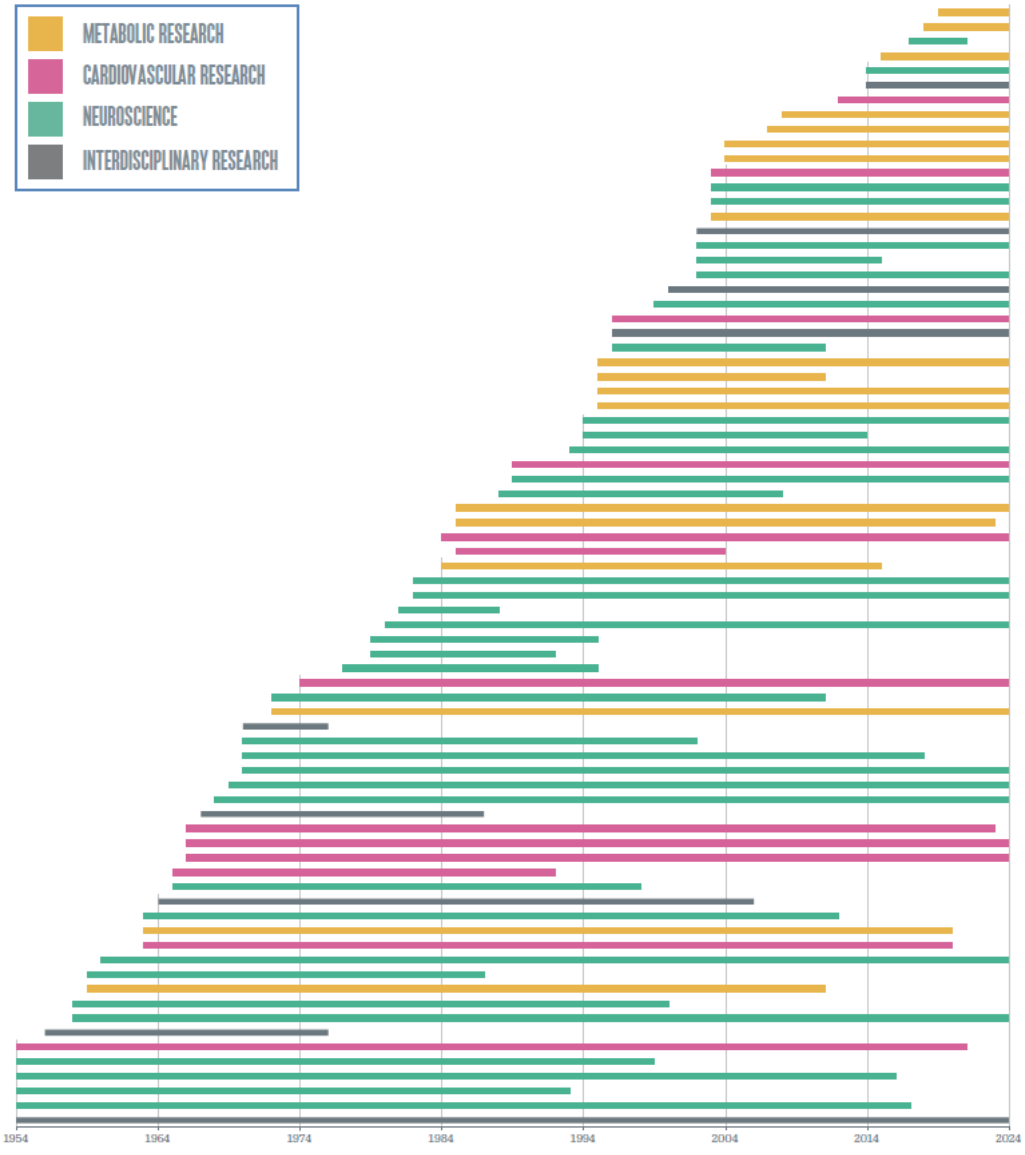

PHYSIOLOGICAL RESEARCH • ISSN 1802-9973 (online) - an open access article under the CC BY license

Fax +420 241 062 164, e-mail: physres@fgu.cas.cz, www.biomed.cas.cz/physiolres

REVIEW

Nutrition and Bone Marrow Adiposity in Relation to Bone Health

Martina DZUBANOVA[1,2], Andrea BENOVA[1,2], Michaela FERENCAKOVA[1], Roman COUPEAU[1], Michaela TENCEROVA[1]

[1]Laboratory of Molecular Physiology of Bone, Institute of Physiology of the Czech Academy of Sciences, Prague, Czech Republic, [2]Faculty of Science, Charles University, Prague, Czech Republic

Received December 2, 2023
Accepted April 29, 2024

Summary

Bone remodeling is energetically demanding process. Energy coming from nutrients present in the diet contributes to function of different cell type including osteoblasts, osteocytes and osteoclasts in bone marrow participating in bone homeostasis. With aging, obesity and osteoporosis the function of key building blocks, bone marrow stromal cells (BMSCs), changes towards higher accumulation of bone marrow adipose tissue (BMAT) and decreased bone mass, which is affected by diet and sex dimorphism. Men and women have unique nutritional needs based on physiological and hormonal changes across the life span. However, the exact molecular mechanisms behind these pathophysiological conditions in bone are not well-known. In this review, we focus on bone and BMAT physiology in men and women and how this approach has been taken by animal studies. Furthermore, we discuss the different diet interventions and impact on bone and BMAT in respect to sex differences. We also discuss the future perspective on precision nutrition with a consideration of sex-based differences which could bring better understanding of the diet intervention in bone health and weight management.

Key words

Nutrition • Diet composition • Bone • Bone marrow adiposity • Sex differences

Corresponding author

M. Tencerova, Laboratory of Molecular Physiology of Bone, Institute of Physiology of the Czech Academy of Sciences, Videnska 1083, Prague 4, 142 00, Czech Republic. E-mail: michaela.tencerova@fgu.cas.cz

Introduction

Bone is a complex, continually changing tissue that provides mechanical support for ligaments, tendons and joints, protects vital organs from damage, and serves as a reservoir for phosphate and calcium in maintaining regular mineral homeostasis [1,2]. Bone matrix contains several types of collagens including type I collagen [1] as well as non-collagenous proteins and growth factors, which are unique to bone tissue and important for mineralization.

The bone tissue consists of two main parts: dense cortical bone, forming a solid outer layer, and porous trabecular (spongy) bone, mainly found at bone ends and inner parts. Cortical bone makes up 80 % of the skeleton, providing structure, while trabecular bone has a larger surface area and is less dense and more susceptible to rapid loss during increased bone turnover [2]. The composition and structure of these bones support the skeleton's mechanical functions [1].

Under hard core of bone, there is bone marrow (BM) which consists of various cell types, including: i) hematopoietic stem cells (HSCs) and progenitor HSCs, which can differentiate into different types of blood cells, such as red blood cells (erythrocytes), white blood cells (leukocytes), myeloid precursors for osteoclast formation (bone resorptive cells) and platelets (thrombocytes); ii) bone marrow stromal cells (BMSCs) which can differentiate towards adipocytes or bone forming cells – osteoblasts and chondrocytes; iii)) fibroblasts that produce connective tissue and support the structure of the BM; iv) endothelial cells, and v) nerve cells [3,4].

Another compartment of BM is bone marrow adipose tissue (BMAT) arising from BMSCs. BMAT makes up to 10 % of whole-body fat mass in lean and healthy adults [5]. This overlooked fat depot has been considered as an inert filler of the bone cavity for a long time. However, increased scientific interest in last decades brought new findings on BMAT to be characterized as a secretory and metabolically active organ that responds to nutritional challenges and secretes cytokines that indirectly influence bone and energy metabolism [3,5-7].

In this review we present the overview of the literature in animal and human studies investigating bone and BMAT physiology in respect to sex differences. Furthermore, we discuss the impact of diet interventions and the contribution of different nutrients to bone health and BMAT accumulation. As most of the studies has been performed in males, it raises a question for the precise nutrition how different dietary demands can be applied in both sexes with consideration on healthy aging and longer life expectancy.

Bone structure and bone marrow composition in males and females

It has been well-documented that genetic and non-genetic (diet, exercise, age, and sex) factors influence bone strength and quality [8]. Notably, sex differences in bone morphology, mechanical properties and response to mechanical loading have been reported in various mouse models [9,10]. Yao *et al*. [10a] observed significant sex differences in trabecular and cortical bone geometry and morphology of 4-month-old C57BL/6J mice, where male mice had inherently more bone compared to female mice, with significantly higher cortical and trabecular bone volume and thickness [11]. Considering sex difference in humans, the study comparing 18-year-old male and female participants indicated that despite comparable body size, males have greater bone mineral content (BMC) and bone mineral density (BMD) at the hip and distal tibia and greater tibial cortical thickness which may confer greater skeletal integrity in males [11]. In humans, the sexual dimorphism is expressed in bone length, BMD and geometry, providing men with a potential advantage in bone mechanical resistance compared to women [12]. Importantly, the study using high-resolution peripheral quantitative computer tomography [13] showed larger total bone area in distal radius and tibia in young men compared to women. Moreover, this study showed, that in young men trabecular number and thickness were 7-20 % higher than in women in both sites and cortical porosity was 31-44 % decreased in young women than in young men. The distal radius cortex of young women carried 14 % more load compared to young men. However, bone strength was 34-47 % greater in young men compared to women [13]. More studies have analyzed the difference of cortical and trabecular parameters of lumbar vertebra [14]. Single-energy quantitative computed tomography (CT) of lumbar vertebrae in subjects of both sexes younger than 40 years versus group older than 65 years showed no difference in cortical bone of younger subject, but there was significant decrease of cortical volume in women compared to males caused by aging [15]. However, trabecular volume was significantly decreased in adult females compared to males with no significant age difference. On the other hand, trabecular BMD was significantly lower in old female group compared to old males. Another study showed age- and sex-related changes of lumbar bone microstructure, e.g. decreased cortical and trabecular BMD in females leading to increased fracture load of analyzed L1-L3 vertebrae compared to men in 6-year follow-up study (patients were over 50 years old with no previous lumbar fractures) [14].

Bone matrix composition and the total collagen content might not significantly differ between males and females, however, there could be differences in the composition or structure of collagen between sexes [16]. On the other hand, in mature individuals, the male skeleton contains roughly 1400 g of calcium, while the female skeleton contains about 1200 g [17]. However, there are no specific data on sex-specific content of phosphorus in bones. Therefore, further investigation might be necessary to better understand physiological differences between males and females on the BMC and mineralization process.

In terms of BM cellular composition, several studies have identified differences between male and female hematopoietic systems [18]. Nakada *et al.* [19] found that males and females have similar basal numbers of HSCs and their multipotent progenitor cells. However, female HSCs undergo more frequent self-renewing divisions without depletion of the stem cell pool driven by estrogen receptor alpha (ERα) signaling. Another animal study showed that increased estrogen levels decrease B lymphopoiesis [20]. Singer *et al.* [21] reported that obese males have increased myelopoiesis and

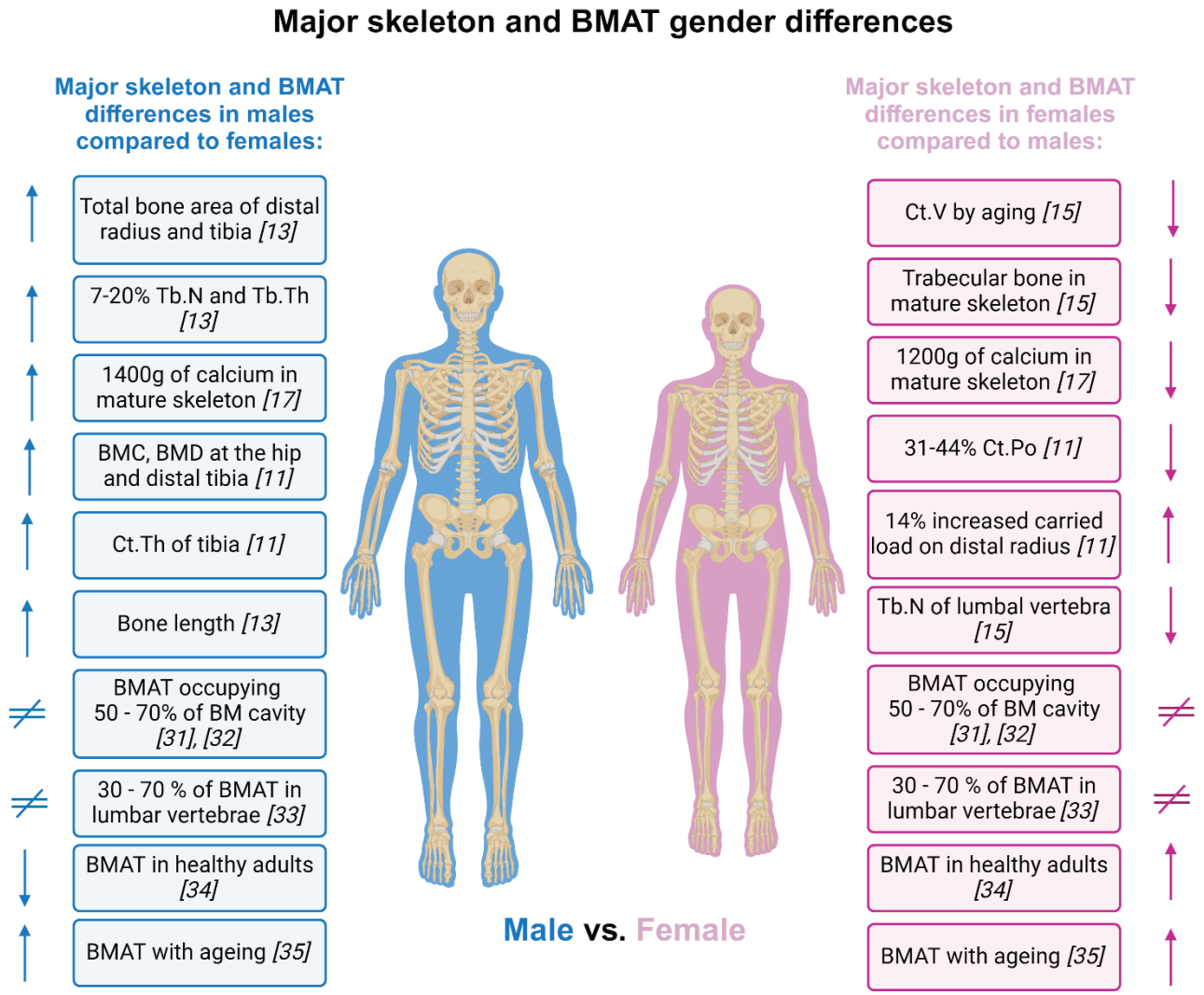

Fig. 1. Major skeleton and BMAT sex differences in adult and elder humans (Created with Biorender.com).

increased pro-inflammatory response of macrophages compared to age-matched females. However, more studies using single cell RNA sequencing are needed to dissect sex dimorphism in BM composition, especially on BMSC heterogeneity under physiological conditions and how it is affected with aging, osteoporotic or metabolic challenges in relation to bone homeostasis. Main differences in BM composition between sexes have been reported in context of BM adiposity, which is discussed later in this review. The major differences in skeleton between males and females are depicted in Figure 1.

During the lifetime, bone undergoes remodeling (coupling of bone formation and bone resorption) which is the process of changing size or shape of bones in response to physiological or mechanical stimuli [1]. An imbalance of these two processes leads to bone impairment and bone loss [22]. Several studies documented the role of growth hormone and sex steroids as key regulators of bone development and growth [23,24]. It suggests that sex differences in long bone structure may arise from the different hormonal environments in female and male BM as BMSCs express ERα affecting BMSC differentiation potential and expansion in BM [25]. Additionally, the impact of sex steroids on the response of bone cells to mechanical loading is emphasized, as demonstrated by studies on sex steroid receptor knock-out mice [26].

Another key factor contributing to the impact on bone remodeling in respect to sex differences is aging [27]. In perimenopausal and early postmenopausal women the remodeling is increased, slowing down with further aging but remaining faster than in premenopausal women [28]. Remodeling is also slightly increased in aging men [27] but there is still a lack of studies directly comparing bone remodeling processes in men and women.

Clinical study including adults with a mean age of 50 years, found that female participants have lower trabecular parameters compared to men [29]. Khosla *et al.* [30] demonstrated the same results in the cohort of 90-year-old participants. This discrepancy in bone parameter characteristics suggests potential differences in skeletal integrity between males and females, serving as a critical point for this review.

BMAT development and physiology in males and females

BMAT, derived from BMSCs, represents important part of BM cavity and its presence changes with age, sex and skeletal site. At the birth red BM is mostly filled with HSCs, which is substituted during adulthood (around the age of 25 years) with yellow BM filled with BMAT occupying around 70 % of the BM volume, mostly in distal bones [31]. In the literature, two types of BMAT have been described: constitutive BMAT (cBMAT), which is located within the yellow BM of the distal skeleton, where hematopoiesis is nearly absent, and regulated BMAT (rBMAT), which is localized in the proximal skeleton, where bone remodeling and hematopoiesis are active. rBMAT can be modulated by different factors such as nutrition, aging and endocrine status, while cBMAT is much more inert [32]. rBMAT changes in response to ovariectomy (OVX), obesity, caloric restriction (CR) and irradiation, are typically accompanied by hematopoietic abnormalities and/or bone loss [33]. Therefore, the changes in BMAT volume are important to be measured in relation to bone health and also in respect to sex differences.

BMAT volume changes through lifetime and its distribution and composition are also affected by sex [34]. In humans, the expansion of BMAT in long bones occurs from distal to proximal sites and is more prevalent at distal sites after birth. BMAT is easily detected in distal epiphyses of long bones by age of 6-7 years and in the midshaft around 12-14 years of age in both sexes [35]. Then, in adults aged about 25 years, BMAT is occupying approximately 50-70 % of the total BM cavity, with at least some bone marrow adipocytes (BMAds) also present in sternum, ribs, pelvis and vertebrae [35,36]. In lumbar vertebrae, BMAT expands varying from 30 % to 70 % in both sexes between 8 and 57 years of age, respectively [37]. Healthy adult women tend to have higher levels of BMAT compared to healthy adult men, this difference is particularly evident in the hips and femur. In women, BMAT is often distributed in the lower extremities, including the hips and thighs, whereas in men is more concentrated in the trunk and abdomen [38,39]. Notably, the accumulation of BMAT with age is also influenced by sex. Females younger than 55 years have approximately 5-10 % lower level of BMAT than age-matched males [40]. Moreover, the significant increase of BMAT in postmenopausal women causes about 10 % higher BMAT content than in males at the age over 60 years [41]. With aging, both men and women experience an increase in BMAT [38,41]. However, the rate and extent of this increase may vary between sexes influenced by age and pathophysiological and metabolic status. In postmenopausal women, there is a significant increase in BMAT due to hormonal changes [42]. Estrogens play a crucial role in BMAT regulation. Reduction in estrogen levels, particularly during menopause in women, is associated with an increase in BMAT [43,44]. Androgen levels in men may also influence BMAT, low endogenous testosterone is associated with high BMAT in older men [42]. These changes are summarized in Figure 1.

In contrast, mice have lower BM adiposity than humans, but the sequence and timing in bone marrow adipocyte development are very similar. In mice, BMAT is present in caudal vertebrae as early as one week after birth. BMAT may also be found in sacrum and lower lumbar vertebral bodies in adults, but it is rare to see BMAT in cervical and thoracic vertebrae. BMAT in distal tibias are readily detectable at four weeks and continue to accumulate until the cavity is filled at around eight weeks of age (adults) [45]. BMAT in proximal tibia and femur appears later than in distal tibia and caudal vertebrae. Male mice usually develop BMAT later and less extensively in proximal tibia than age-matched females [5,45], which is a little bit different compared to humans. Importantly, the different expansion of BMAT in males and females during lifetime may differently contribute to the bone homeostasis and by secretion of bioactive molecules to the regulation of bone remodeling and energy metabolism [5,46]. Moreover, since BMAT is derived from BMSCs, sex differences in BMAT expansion may be caused by different differentiation capacity of BMSCs in males and females [4]. However, more studies are needed to understand the molecular mechanism behind these changes.

Moreover, the understanding of potential ethnic and sex differences in the relationship between BMD and BMAT is important for future studies focused on

developing of the prevention and treatment strategies for bone loss and fracture risk. Shen *et al.* [47] showed that healthy men and premenopausal women had higher total body BMD levels than postmenopausal women for the same amount of BMAT. The increased BMAT in postmenopausal women is linked to osteoporosis and impaired bone quality [48]. Understanding these sex differences in BMAT is essential for investigating its role in bone health, metabolic disorders, and for designing targeted interventions in various conditions affecting bone and metabolism. However, up to now, prospective studies examining BMAT variations with age, sex and skeletal sites are still lacking.

Dietary factors affecting bone and BMAT

Besides micronutrients (minerals, vitamins), there are also macronutrients like carbohydrates, proteins, fat and fiber that are important parts of diet composition affecting bone homeostasis. All of these components play a critical role in maintenance of bone health and it is necessary to keep them in a healthy balance. They can have positive or negative impact on bone and fat metabolism. Therefore, we will provide an overview of animal and clinical studies using different dietary interventions in the context of bone health and fracture risk in relation to sex differences (summarized in Tables 1 and 2).

Diets enriched in carbohydrates and their effect on bone and BMAT

Carbohydrates, especially glucose, are usually considered as main sources of energy for cellular metabolism in many cell types [49,50]. However, chronic exposure to high glucose levels in the body represents a pathological condition impairing glucose metabolism and leading to insulin resistance, diabetes and bone loss [51,52]. Several *in vitro* studies using osteoblastic cell lines (MC3T3-E1) documented a negative impact of high glucose (22-30.5 mM) on osteoblast differentiation [51-53] inducing higher reactive oxygen species production, decreased proliferation and cellular mineralization. Negative effect of high-sucrose diet on bones in rodents of both sexes has been known for a long time [54,55]. More recent studies are adding further information about the effect of different saccharides on bones. Yarrow *et al.* [56] reported a negative effect of diet enriched with 40 % fructose in 8-week-old Sprague-Dawley male rats on bone homeostasis compared to control diet. After 12 weeks of treatment bone marrow adipocyte density measured in histology slides was increased, while bone volume and trabecular number of proximal tibia measured by micro-CT (μCT) were decreased by high-fructose diet compared to control diet (more details in Table 1). On the other hand, drinking of 10 % fructose during 28 days in adult male Sprague-Dawley rats had a deleterious effect on osteocyte density, while no difference on BMAT was observed in femur compared to control diet [57]. Moreover, differentiation analysis of primary BMSCs showed decreased osteoblast and increased adipocyte differentiation supporting *in vivo* bone phenotype.

Testing the effect of different sweetener in drinking water (glucose, fructose, sucrose etc.) on bone properties of 35-day-old female Sprague-Dawley rats during 8 weeks [58] showed no significant changes in terms of bone mass and bone strength between the groups. However, the increased consumption of glucose altered mineral homeostasis which led to decreased phosphorus and calcium intake and increased calcium excretion compared to fructose beverage suggesting that glucose exerts more detrimental effect on bones than fructose in female rats, but this study did not investigate BMAT in treated rats.

Negative effects on bone quality were observed in 9-week-old C57BL/6 female mice which were treated for 10 weeks with high-fat/high-sucrose diet [59]. μCT analysis of tibias showed decreased bone mass along with lower mechanical properties in high-fat/high sucrose diet compared to control diet. Osteoclastogenesis expressed as Receptor activator of NFκB ligand/osteoprotegerin ratio was not affected, but the expression of cyclooxygenase-2 was increased suggesting increased inflammation. On the other hand, Minematsu *et al.* [60] reported a positive effect of 24-week feeding of high-fat/high-sucrose diet on bone quality in aging model of over one-year-old Wistar male rats measured by μCT analysis of trabecular and cortical bone volume and biochemical analysis of Tartrate-resistant acid phosphatase (TRAP) and calcium levels, while BMAT was not measured.

In humans, the most pronounced effect of higher intake of sugar on bones has been observed in teenagers who consume excess refined carbohydrates and sugars, by increased fracture risk associated with drinking of sweetened beverages [61,62]. Moreover, hyperglycemia commonly driven by high-saccharide diet is strongly associated with increased osteoporotic fracture risk in

older patients [63]. However, there is still a lack of studies directly comparing the effect of high-saccharide diet on bone homeostasis in adult men and women. Previous studies were mostly focused on the effect of different dietary conditions (including diet enriched with saccharides) on fracture risk or BMD in elderly population showing a negative association of higher glycemic index with increased prevalence of fractures in both sexes [64,65]. The different results in animal and clinical studies just point out the lack of comprehensive studies comparing effect of increased saccharide intake in both males and females with a more focus on measurement of BMAT in the context of bone health and fracture risk.

Calorie-restricted diet vs diet enriched in fatty acids and their impact on bone and BMAT

BMAT is unique in its origin and its response to dietary changes. It is known that both caloric restriction (CR) and high-fat diet (HFD) may increase BMAT in rodents and humans [66-70] (see listed in Tables 1 and 2). Many studies have considered BMAT composition and quantity in the context of bone health and metabolic risk. In mice models, both nutrient challenges (CR and HFD) cause enhanced BM adiposity, whereas the extramedullary responses are quite distinct [6,71].

Moreover, expansion of BMAT with CR (10 kcal% fat) has been consistently observed across sex, age and durations from 6 to 19 weeks, but the reduction of bone mass is not uniformly observed in all mouse models. CR of male mice causes bone loss during their active growth (three weeks to about three months of age) [70,72]. On the other hand, female mice have much slighter bone changes despite the significant changes in BMAT after CR. Although CR causes bone loss in very young actively growing female mice, the effects on bone gradually diminish with age [69,73]. It is possible that estrogen contributes to differences between sexes. Moreover, estrogen deficiency drives BM adiposity in mice and can act as an interactive component associated with dietary changes [74,75]. Devlin *et al.* [70] studied the effect of 9-week CR in 3-week-old male mice and they reported significant elevation in BMAT volume which was associated with decreased cortical bone mass in the femur. Interestingly, another study of 12-week CR in 6-month-old female Sprague Dawley rats reported decreased body weight but an increase in bone marrow adipocytes in proximal femur and tibia, and decreased BMD of the proximal tibia [76].

The effects of CR on BMAT in human studies are not clear, with some reports showing an increase in BMAT [68,77,78], whereas others demonstrating no change or less BMAT [79,80]. However, discrepancies between these studies may be affected by different age, sex, treatment protocols or the method of BMAT evaluation (Table 2). Interestingly, CR is considered to have health benefits including reduced adiposity, improved metabolism and increased lifespan; however, a downside includes effects on bone and BMAT. Fazeli *et al.* [66] revealed in an acute 10-day high-calorie feeding protocol followed by a 10-day fasting protocol in healthy men that BMAT elevated in response to both interventions, but the pathophysiology and cues for these changes may differ. Furthermore, 18 months of randomized dietary interventional study with 138 participants (including men and women, mean age 47.8±9.1 years) showed that physiological weight loss can transiently reduce BMAT (MRI quantification) in adults with a more prominent effect in younger adults of both sexes [81]. Another study determined by proton magnetic resonance spectroscopy that women with anorexia nervosa have elevated BMAT content in the lumbar spine as well as in the femoral diaphysis and metaphysis compared with normal weight control group [67]. Taken together, preclinical models of CR and various nutritional status can differently affect BMAT volume and composition in animal models and humans with different response in respect to sex, age, strain, site-specificity and treatment protocol. Thus, it seems that the mechanisms underlying these changes are different between men and women. Giving the evidence of BMAT accumulation under different metabolic conditions, future strategies are needed to define causal mechanism and better reveal the age and sex contribution.

The diets with different content of saturated and unsaturated fatty acids (FA) can have detrimental or beneficial effect on bone, fat metabolism and homeostasis. The role of saturated and unsaturated FA in bone and fat homeostasis can exhibit sex-specific differences. In general, females tend to have higher levels of essential body fat mass for reproductive and hormonal reasons [11,82]. However, dietary patterns play a key role in how saturated and unsaturated fats affect bone metabolism [83]. Consuming an excessive number of calories or maintaining an unbalanced diet, typically characterized by the presence of saturated and trans-unsaturated FA, is associated with an elevated body mass index, obesity and complications that impact both bone

and fat metabolism [84]. HFD enriched in saturated FA induces increased inflammation and oxidative stress, and thus affecting bone density and increasing fracture risk [6,85,86]. Studies using HFD in rodents aimed to induce metabolic changes leading to increased BMAT and bone impairment. The impact appears to depend on factors like the duration of the HFD and the percentage of fat content. Prolonged exposure to a HFD (4 kcal%) may initially increase bone mass, but over time, it seems to lead to decreased bone formation and turnover, potentially associated with metabolic impairment in male mice [87] and ovariectomized 6-month-old female rats [88]. Diets with higher fat content (60 kcal%) are generally associated with more detrimental effects by increasing BMAT and bone loss [6], decreasing cortical and trabecular thickness and increasing bone porosity more in males than females [89,90]. On the contrary, lower fat content diets (42 kcal%) may have an anabolic effect on bone, at least over a more extended period, in mice of both sexes [91]. Our previous study and others [6,89] using 8-week-old male C57BL/6J mice showed that 12-week treatment with 60 kcal% HFD decreased bone volume and increased trabecular separation and cortical porosity of proximal tibia. Moreover, bone formation rate was decreased in tibia as well as in vertebrae compared to control diet. Furthermore, BMAT analysis using hematoxylin-eosin staining and osmium-tetroxide staining showed increased adiposity in proximal tibia after HFD diet, which was accompanied by increased adipocyte differentiation of primary mouse BMSCs. According to these studies, the higher is saturated fat content, the more damage is delivered to a bone. Findings from other studies focused on the effects of obesity on BMAT changes are well summarized in our previous review [7].

Conversely, it is considered that the incorporation of unsaturated FA, particularly omega-3 polyunsaturated FA (omega-3 PUFAs), have a more favorable impact on BMAT and overall bone and fat homeostasis in both males and females. Furthermore, unsaturated FA play a role in fat homeostasis by positive influence on overall body fat composition. Docosahexaenoic acid (DHA; 22:6n-3) and eicosatetraenoic acid (EPA; 20:5n-3) as main representatives of omega-3 PUFAs help to reduce the accumulation of excess fat and improve glucose metabolism in metabolic complications [92,93].

Animal studies employing HFD supplemented with omega-3 PUFAs in osteoporotic models demonstrated a reduced negative impact on bone loss and BMAT [94,95]. Our recent study using omega-3 PUFAs supplementation in C57BL/6N male mice for two months [96] or other study using 6-month dietary intervention [97] decreased BMAT and prevented bone impairment. Human study focused on different types of omega-3 PUFAs and hip fracture risk, involving men and postmenopausal women, found that higher alpha-linolenic acid consumption was linked to a decreased risk of hip fractures in women but not in men. Interestingly, there was no correlation between intake of EPA+DHA and the risk of hip fractures [98], which was confirmed by other study focused on male and female participants aged 65 years or older [99]. Senile osteoporotic women treated with combination of PUFAs and calcium maintained lumbar and increased femoral neck BMD compared to control group [100]. While current evidence in humans does not strongly support a positive relationship between omega-3 PUFAs and human osteoporosis prevention or treatment, it suggests potential benefits when incorporating omega-3 PUFAs into the diet rich in calcium, vitamins, and minerals or concentrated oil mixtures with other PUFAs. To comprehensively explore the effect of omega-3 PUFAs on fracture risk, further large-scale investigations are needed, particularly focusing on the treatment with different types of omega-3 PUFAs on bone quality. The intake of EPA, DHA and EPA+DHA has been found to be significantly higher in males than females in several age categories [101]. While there may be some sex-specific differences in bone health and susceptibility to conditions like osteoporosis, the effects of saturated and unsaturated FA on bone and BMAT are generally similar for both sexes. More details are summarized in Table 2. A diet rich in unsaturated fats and low in saturated fats is recommended to promote healthier bone and fat homeostasis in both males and females.

Protein-enriched diet and its effect on bone and BMAT

The optimal dietary protein intake has been studied for decades, as non-pharmacological approach how to maintain skeletal health in adults. It is also becoming clear that protein and their individual amino acids (AA) can have different effects on cell function and impact on bone formation. However, it is still unclear whether dietary protein exerts a positive or negative effect on bone health. Protein undernutrition is a known factor in the pathogenesis of osteoporotic fracture in the elderly, but the mechanisms of bone loss

resulting from this deficiency are still poorly understood. The details of these studies are summarized in Tables 1 and 2. On the cellular level, it has been shown that protein malnutrition induced increased adipocyte differentiation of BMSCs isolated from 2-month-old male Balb/c mice fed for 3 weeks with 2 % low-protein diet compared to 12 % control protein diet. This protein malnutrition led to impaired hematopoietic microenvironment and inducing the BM failure [102]. Similar results were observed in another study using C57BL/6N male mice with the same protein supplementation on impaired HSC differentiation towards lymphoid, granulocytic and megakaryocytic-erythroid lineage [103]. In animal models, both low and high dietary protein intakes have shown to suppress the acquisition of bone mass and the increase in bone strength during growth in comparison to moderate protein intake [104-108]. Takeda *et al.* [104] showed the effect of different levels of protein diet in growing 5-week-old male rats after 2 months of dietary intervention. Measurement of BMD and bone strength by dual-energy X-ray absorptiometry (DXA) and three-point bending test revealed suppressed acquisition of bone mass and increased bone strength with low protein diet compared to medium and high protein diets. Furthermore, Dubois-Ferrière *et al.* [105] reported that mechanical properties measured by three-point bending test and bone microstructure were decreased in 6-month-old Sprague-Dawley female rats fed with low-protein diet for 10 weeks. Another study [106] using a selective isocaloric protein-restricted diet in adult female rats showed similar detrimental effect on both cortical and trabecular parameters, through the impact on the insulin-like growth factor 1 (IGF-1) and sex hormone regulation. Prevention design of the study using casein or soy protein supplementation in CR-induced bone loss in 8-month-old Sprague-Dawley male rats did show a beneficial effect on bone mass [109]. Moreover, Wright *et al.* [108] investigated the effect of 12-week feeding of four CR diets varying in predominate protein source (beef, milk, soy, casein) and protein quantity (control diet 15 % vs. high-protein diet 35 %) on bone and body composition outcomes in 32-week-old female rat model of postmenopausal obesity. Overall, CR had a negative impact on bone parameters with different extent depending on the protein source. Thus, these results suggest that specific protein source recommendations may be needed to attenuate the adverse alterations in bone quality following a high-protein CR diet in a model of postmenopausal obesity. Other animal studies supporting these results are summarized in Table 1. However, none of these studies measured BMAT in the context of bone health.

The effects of protein diet in humans have been studied in various conditions. However, it is not well-known whether this dietary intervention can modulate the BMAT volume. Trudel *et al.* [110] investigated the effect of high-protein diet and bed rest interventions (two bed rest campaigns consisted of 7 days of baseline data collection, 21 days of head-down tilt and 6 days of recovery) in healthy men on the lumbar BMAT volume showing no change of lumbar bone marrow fat fraction measured by MRI. In a different study combining bed rest and a high-protein, leucine-supplemented diet, 8 healthy women aged 25-40 years, showed no change in lumbar fat fraction [111]. Even 18 months of protein supplementation in diet did not improve lumbar spine BMD measured by DXA in 208 older women (70.5±6.4 years) [112]. Cao *et al.* [113] demonstrated that short-term consumption of high-protein diets (31 days) during CR did not disrupt calcium homeostasis and it was not accompanied by any changes of BMC and BMD in young adult men and women aged 20-21 years. Arjmandi *et al.* [114] found that one-year supplementation with soy protein positively modulated markers of bone formation in postmenopausal women (≤ 65 years), but on the other hand this amount of protein was unable to prevent lumbar and whole-body bone loss. Contrary, Holm *et al.* [115] showed that whey protein supplementation resulted in superior improvements in femoral neck BMD and bone formation during 24 weeks of strength training in postmenopausal women (55±1 years). The observed differences following such a short intervention emphasize the significance of post-exercise nutrient supply on musculoskeletal maintenance. All published studies of protein enriched diet and its effect on bone and BMAT are summarized in Table 2.

Taken together, animal and clinical studies regarding the impact of protein intake on bone health and BMAT are not very conclusive as the studies differ in the design, targeted group of subjects and methods of bone and BMAT evaluation. Further studies are needed to study the impact of low or high protein intake on bone and BMAT parameters in relation to prevention strategies to decrease fracture risk.

The diet with essential branched chain amino acids (BCAAs) and its effect on bone and BMAT

Several studies suggest that further attention is warranted to the impact of specific AA on skeletal health, rather than just considering protein content as a whole. BCAAs, which include valine, leucine, and isoleucine, account for upwards of 40 % of the preformed AA. These are essential AA that must be acquired by dietary intake [116]. However, there is a lack of studies on the effects of BCAAs on skeletal health and BMAT. In animal studies, *in vitro* BCAAs supplementation increased metabolic activity and proliferation of BMSCs and enhanced the immunomodulatory capacity of BMSCs by decreasing the p-NFκB/NFκB ratio and increasing synthesis of the anti-inflammatory mediators TGF-β and PGE_2 [117]. Furthermore, Mu *et al.* [118] reported that BCAA supplementation in 4-month-old male C57BL/6J mice increased body weight, lean mass, and fat mass with increased adipose tissue inflammation and worsen insulin sensitivity compared to mice fed with low-protein diet. These data suggest that dietary protein levels and BCAAs play a role in modulating whole-body metabolism. However, in this study they did not measure impact on bone and BMAT. More animal and human studies investigating the effect of BCAAs on BMAT and bone formation are needed in respect to sex differences.

Amino acids enriched diet and its effect on bone and BMAT

Another AA supplementation in diet showed that N-acetylcysteine in HFD diet in male C57BL/6 mice fed for 17 weeks showed protection from HFD-induced bone impairment measured in distal femur, which was accompanied by decreased bone resorption but the measurement of BMAT parameters was missing [119]. Cysteine is linked to the methionine metabolism. Animal study using a 12-week feeding of methionine-enriched diet induced increased bone fragility and reduced bone quality in Wistar rats, especially in the cancellous bone [120] without BMAT measurement. However, the feeding of methionine-restricted diet for 5-12 weeks, which was aimed to improve glucose metabolism in young male and female mice as well as in aged male mice (C57BL/6J), caused similar negative impact on bone lengths and trabecular parameters accompanied by decreased osteoblast differentiation, while preserving the bone strength compared to control group [121-123].

Selenium in the form of selenocysteine is critical for bone remodeling. Recent study by Kim *et al.* [124] defined a negative effect of selenoprotein W on bone mass by stimulating osteoclastogenesis in bone as selenoprotein W-deficient mice exhibit high bone mass phenotype. Selenoprotein is usually made from selenocysteine. In rats, femoral BMD was increased by 77 % together with improved bone growth andn development with supplementation of L-Se-methylselenocysteine in selenium-deficient rats [125].

Even, a combination of different AAs could have a positive effect on bone health as showed in the study of Ding *et al.* [126] using 8-week-old male C57BL/6J mice treated for 2 months with low-protein diet supplemented with either a triad of serine, valine and threonine or a triad of phenylalanine, tyrosine and tryptophan. This AA-supplemented diet had a positive effect on BMSC proliferation and osteoblast differentiation.

In humans, the presence of specific AA in the diet has been linked to various aspects of bone health. Studies have indicated that a diet enriched with vitamin D, calcium, and leucine can potentially increase BMD in sarcopenic older adults [127]. Furthermore, post-menopausal women with high BMD levels were found to have higher concentrations of certain AA, including leucine, valine, and tyrosine, suggesting potential associations between these AA and BMD [128]. Conversely, lower intake of phenylalanine in patients of both sexes (8-16 years) has been linked to reduced BMD values [129]. Additionally, studies have demonstrated that tryptophan supplementation can stimulate BMSC proliferation and differentiation, potentially through the upregulation of the RUNX2 expression factor [130,131]. Despite a positive association between high tryptophan intake and hip BMD in individuals aged over 45 years, it was concluded that excessive tryptophan consumption may not play a critical role in bone health [132].

Glutamine-enriched diet

Glutamine represents a non-essential AA, which plays important role in regulation of oxidoreductase activity and inflammation [133]. Glutamine enrichment of the diet has been shown to have a positive effect on bone metabolism [134]. Glutamine metabolism plays a pivotal role in regulating BMSC proliferation, lineage allocation and osteoblast differentiation [134,135]. Recent study using knock-out of key enzyme of glutamine metabolism, glutaminase, reported negative effect on bone formation manifested by reduced osteoblast numbers and increased adipocyte

differentiation, highlighting the critical involvement of glutamine metabolism in BMSC function and bone health in mice [134].

Furthermore, Blais *et al.* [135] showed that monosodium glutamate supplementation of low-protein diet in 8-week-old Balb/C female mice increased glutamine plasma levels, increased BMD, trabecular and cortical bone microarchitecture, osteoblast differentiation and improved bone quality compared to mice under protein restriction. However, supplementation did not restore these parameters to the levels obtained in animals fed with control diet [135].

In addition, glutamine contributes to proline production, an important AA for collagen synthesis and connective tissue formation. This cascade of effects underscores the positive impact of glutamine on bone tissue, reinforcing its significance in bone health [136]. Hanaa *et al.* [137] reported the potential beneficial effect of oral administration of glutamine in ovariectomized female Sprague Dawley rats (starting 3 months after OVX and lasting for further 3 months) documented by increased $1,25(OH)_2D_3$, IGF-1 and TGF-β levels, along with improved BMC and BMD. Notably, glutamine supplementation fosters the production of glutathione, a potent calcium enhancer through calcium sensing receptor activation. However, more studies are needed to investigate the effect of glutamine supplementation on bone health and BMAT formation in different animal models and human studies.

Conclusions and future perspectives

The importance of healthy and well-balanced diet is crucial, as shown by several animal and clinical studies of different ages and metabolic conditions. It helps to counteract the negative effects of obesity, osteoporosis and aging on bone health, reducing the risk of fractures. Presence of BMAT in different stages of life span may differ between sexes. However, its impact on bone mass in males and females are still not well-known (Fig. 2). Even though there are some mild differences in nutrient levels among sexes, the impact of dietary intervention and nutrient supplementation on bone health is similar and the major determinant of bone health. There are differences between men and women in steroid hormone levels, which could primarily drive the heterogeneity of BMSC and HSC populations in BM affected by ERα signaling in response to hormonal or nutritional stimuli participating in bone formation.

Fig. 2. The effect of different diet interventions on bone and BMAT in humans and mice with respect to sex differences. ↑ increased, ↓ decreased, N/A – not available (Created with Biorender.com).

However, more detailed and well-controlled clinical studies are needed to determine the best nutrient-enriched diet designed for each subject individually as their metabolism can differ and much of what is known about bone health and BMAT analysis is based on the research conducted in male mice. We move into the era of precision nutrition, understanding these sex-based differences may help to optimize recommendations and interventions chosen to support bone health and weight management.

Conflict of Interest

There is no conflict of interest.

Acknowledgements

This work was supported by START UP Research program by the Institute of Physiology of the Czech Academy of Sciences and the Czech Science Foundation GACR 20-03586S, GACR 22-12243S (MT), EFSD/NovoNordisk foundation Future leaders award (NNF20SA0066174), National Institute for Research of Metabolic and Cardiovascular Diseases (Program EXCELES, ID Project No. LX22NPO5104) – Funded by the European Union – Next Generation EU, Grant Agency of Charles University GAUK 339821 (AB), the Ministry of Health of the Czech Republic (NU23-01-00125), and 52310168 Intra-Visegrad Scholarship) (MD).

Abbreviations

AA, Amino acids; AAD, Average American diet; AD, Adipocyte; ALA, Alpha-linolenic acid; ALP, Alkaline phosphatase; AN, Anorexia nervosa; ArA, Arachidonic acid; BCAA, Branched chain amino acids; BM, Bone marrow; BMAds, Bone marrow adipocytes; BMAT, Bone marrow adipose tissue; BMC, Bone mineral content; BMD, Bone mineral density; BMSCs, Bone marrow stromal cells; BMI, Body mass index; BO, Borage oil; BV, Bone volume; BV/TV, Bone volume fraction; cBMAT, Constitutive BMAT; CO, Corn oil; CR, Caloric restriction, CT, Computed tomography; µCT, Micro-computed tomography; Ct.Po, Cortical porosity; Ct.Th, Cortical thickness; DHA, Docosahexaenoic acid; DXA, Dual-energy X-ray absorptiometry; ED, energy deficit; ELISA, Enzyme-linked immunosorbent assay; EPA, Eicosatetraenoic acid; ERα, Estrogen receptor alpha; F, Female; FA, Fatty acids; FO, Fish oil; GLA, Gamma-linolenic acid; HFCS-5, High-fructose corn syrup; HFD, High-fat diet; HFDD, HFD deficient in D3 and calcium; HFD+FO, High-fat diet supplemented with fish oil; HFD/F, High-fat diet supplemented with fructose; HFD/HSD, High-fat/high-sucrose diet; HP, High-protein; HSD, High-sucrose diet; ^{1}H-MRS, Proton magnetic resonance spectroscopy; HSCs, Hematopoietic stem cells; IGF-1, Insulin-like growth factor 1; LA, Linoleic acid; LP, Low-protein; M, Male; MR, Methionine restriction; MRI, Magnetic resonance imaging; MSG, Monosodium glutamate; MUFAs, Monounsaturated fatty acids; N/A, Not available; NP, Normal protein; OA, Oleic acid; OB, Osteoblast; OVX, Ovariectomy; PGE_2, Prostaglandin E_2; p-NFκB/NFκB, ratio of phosphorylated to total Nuclear Factor κB; pQCT, peripheral quantitative computed tomography; PTT, triad of phenylalanine, tyrosine and tryptophan; PUFAs, Polyunsaturated fatty acids; RANKL/OPG, Receptor activator of NFκB ligand/osteoprotegerin ratio; rBMAT, Regulated BMAT; RSG, Rosiglitazone; RUNX2, Runt-related transcription factor 2; SFAs, Saturated fatty acids; SFO, Sunflower oil; SO, Safflower oil; SVT, triad of serine, valine and threonine; Tb.N, Trabecular number; Tb.Sp, Trabecular separation; Tb.Th, Trabecular thickness; Tb.V, Trabecular volume; TGF-β, transforming growth factor β; TRAP, Tartrate-resistant acid phosphatase

Table 1. Dietary factors affecting bone and BMAT in animal models.

Metabolic condition	Animal model	Age	Sex	Duration of the diet	Composition of the diet	Methods	Effect on bone	Effect on BMAT	Reference
Diet enriched in carbohydrates									
High-saccharide diet	Sprague-Dawley rats	60 days	M	12 weeks	high-fructose (40% fructose, 10% glucose) or high-glucose diet (50% glucose)	histology histomorphometry 3-point bending test µCT	High fructose diet vs. high glucose diet: ↑ bone volume of distal femur; ↑ Tb.V of tibia; ↑ bone mechanical properties	N/A	Bass *et al.* 2013 [138]
HFD enriched with fructose (HFD/F)	Sprague-Dawley rats	8 weeks	M	12 weeks	30% (sugar-free) control HFD; 30% HFD+ 40% fructose	µCT; bone mechanical testing; histology; plasma analysis	HFD and HFD/F vs. control diet: ↑ BV/TV and Tb.N of proximal tibia; ↓ cancellous BMD, BV/TV, Tb.N, osteoblast surface and circulating osteocalcin levels; ≠ between HFD and HFD/F	↑ BMAT	Yarrow *et al.* 2016 [56]
High fructose intake	Sprague-Dawley rats	Adult	M	28 days	Control (H_2O); 10% fructose solution	Bone histomorphometry measurement of reossification area; primary BMSC analysis of OB and AD differentiation	↓ osteocyte and osteoclast density; ≠BMAT; ↓ bone regeneration; ↓ OB differentiation, ↓ *Runx2* expression; ↑ AD differentiation, ↑ Peroxisome proliferator-activated receptor gamma expression	≠ BMAT	Felice *et al.* 2014 [57]
High sugar beverages	Sprague-Dawley rats	35 days	F	8 weeks	Control (H_2O); 13% fructose/glucose/sucrose/ HFCS-5	Bone morphometry; bone turnover markers; DXA; three-point bending test	With high-glucose: ≠ bone mass; ≠ bone strength; ↓ calcium and phosphate intake; ↑ calcium excretion	N/A	Tsanzi *et al.* 2008 [58]
HFD/HSD	C57BL/6 mice	9 weeks	F	10 weeks	Low-fat diet (68% complex carbohydrates; 0% sucrose; 6% fat, 26% protein), HFD/HSD (0% complex carbohydrates, 39.5% sucrose, 39.5% fat, 21% protein)	µCT; three-point bending test; gene expression analysis	With HFD/HSD: ↓ tibia mass, length and Ct.Th; ↓ maximal load; ≠ RANKL/OPG ratio; ↑ cyclooxygenase 2 expression	N/A	Lorincz *et al.* 2010 [59]

HFD/HSD	Wistar rats	12 months	M	24 weeks	Control diet (4.7% crude fat); HFD/HSD (13.8% crude fat, 25% sucrose)	µCT; plasma analysis	With HFD/HSD: ↑ BV/TV, Tb.N, Tb.Th, Ct.Th, cortical volume fraction, medullary volume of tibia and femur; ↑ TRACP and calcium levels	N/A	Minematsu *et al.* 2018 [60]
HFD	C57BL/6J mice	6 weeks	M	12-20 weeks	Control diet (13.5% calories from fat); 60% HFD; weight loss group (HFD for 12 weeks followed by control diet for 8 weeks)	Body weight; µCT; mechanical testing of femurs; osmium staining of BMAT	With HFD: ↑ body weight; ↓ Tb.V, BMC and Tb.N, ↓ fracture resistance	↑ BMAT in HFD vs. control diet; ↓ BMAT in weight loss vs. HFD	Scheller *et al.* 2016 [89]
Caloric restriction (CR)									
CR	C57BL/6J mice	5 weeks	F	5 weeks	Control diet (10% kcal/fat) or a 30% CR diet + leptin (1-2 mg/kg/day)	DXA; µCT; histology, histomorphometry analysis; osmium tetroxide staining	With leptin treatment: ≠ trabecular or cortical microarchitecture	With leptin treatment: ↓ BMAT expansion	Devlin *et al.* 2016 [69]
CR	C57BL/6J mice	3 weeks	M	3-9 weeks on the diet	Control phytoestrogen-free diet (10% kcal fat); 30% CR	DXA; µCT; histology; histomorphometry analysis; three-point bending test	CR vs. control group: ↓ trabecular bone volume, number and thickness and ↓ bone strength with inhibited bone formation and bone resorption	↑ BMAT	Devlin *et al.* 2010 [70]
CR	mice	14 weeks	M	10 weeks	10% restriction at 14 weeks of age, increased to 25% restriction at 15 weeks, increased to 40% restriction at 16 weeks and maintained until 24 weeks of age	DXA; pQCT; histomorphometry analysis; radiography	With CR: ↓ femur BMC, BMD, cortical thickness, and fracture strength and ↑ spine BMC, BMD, and trabecular bone volume fraction	↑ BMAT	Hamrick *et al.* 2008 [72]
CR	Sprague-Dawley rats	4 months	F	12 weeks	Control diet Control diet with β-blocker 40% CR diet 40% CR diet with β-blocker	DXA; pQCT; histomorphometry analysis; immunohistochemistry	With β-adrenergic blockade: ↓ metaphyseal bone loss	↑ BMAT	Baek *et al.* 2012 [76]
CR	C57BL/6J mice C3H/HeJ mice Ocn-Wnt10b mice	9 weeks	M	6 weeks	control group; 30% CR group	µCT; osmium staining	N/A	↑ BMAT	Cawthorn *et al.* 2014 [5]

CR	C57BL/6 mice	11 weeks	F	6 weeks	Control group; 30% CR group	MRI; histomorphometry; qRT-PCR	With CR: ↓ Femoral BV; ↓ Tb.Th and Ct.Th	↑ BMAT	McGrath *et al.* 2020 [73]
Diet enriched in fatty acids									
HFD	C57BL/6J mice	8 weeks	M	12 or 20 weeks	60 kcal% HFD (35% fat, 26% protein, 26% carbohydrate, 8.8% sucrose) and control diet (6% fat, 30% protein, 63% carbohydrate, 7.7% sucrose)	µCT; histomorphometry analysis	HFD compared to control diet: ↓ trabecular bone mass and ↓ Ct. Th	↑ BMAT	Tencerova *et al.* 2018 [6]
HFD	C57BL/6J mice	3 weeks	M	12 weeks	HFD diet (60% fat); control diet (10% fat);	µCT; DXA; histomorphometry	HFD vs. control diet: ≠ bone mass	HFD vs. control diet: ↑ BMAT	Doucette *et al.* 2015 [71]
HFD	C57BL/6 mice	12 weeks	M	11 weeks	HFD diet (45 kcal%/fat); Control diet (12 kcal%/fat)	µCT; bone histomorphometry	HFD vs. control diet: ↑ bone mass but over time ↓ bone mass	HFD vs. control diet: ↑ BMAT	Leczka-Cernik *et al.* 2015 [87]
HFD and HFD deficient in D3 and calcium (HFDD)	Sprague-Dawley rats OVX	6 months	F	N/A	control diet; HFD; HFDD; OVX with HFD (OVX-HFD); OVX with HFDD (OVX-HFDD)	Glucose tolerance test; serum analysis; Masson-Goldner trichrome staining; histomorphometry; immunohistochemistry	With HFD: ↑ bone calcium content and bone strength of OVX rats; With HFDD: ↓ BMC, ↓ BMD; ↓ bone calcium content; ↓ bone strength	N/A	Wang *et al.* 2017 [88]
HFD	C57BL6/J mice	6 weeks	M	12, 16 or 20 weeks	Control diet or 60% HFD diet	µCT; osmium staining	HFD vs. control diet: ↓ Tb.Th and Ct.Th; ↑ bone loss in tibia	HFD vs. control diet: ↑ BMAT	Scheller *et al.* 2016 [89]
HFD	C57BL/6 mice	4 weeks	M F	10 weeks	control diet or 60 % HFD diet	µCT; AD and OB differentiation of BMSC	HFD vs. control diet: ↑ bone loss; ≠ cortical bone parameters and strength	N/A	Gautam *et al.* 2014 [90]
HFD	LG/J and SM/J mice	5 months	M F	N/A	control diet relatively high in fat (42% calories from fat); low fat diet (15% calories from fat)	µCT; three-point bending test	Low fat diet vs. control HFD diet: ↑ mechanical properties of the bones	N/A	Silva *et al.* 2019 [91]

HFD	C57BL/6J mice OVX	8 weeks	F	12 weeks	HFD (60%fat) or control diet (10% fat);	Glucose tolerance test; µCT; qRT-PCR; Western blot; RNA sequencing	HFD vs. control diet: ↑ cellular senescence; ↓ bone mass	↑ BMAT at estrogen deficiency	Ali *et al.* 2022 [75]
HFD and HFD + FO	C57BL/6 N mice	12 weeks	M	8 weeks	Control diet (3.4% w/w lipid content); HFD (35% w/w lipid content, primary corn oil); HFD+FO (46% w/w DHA, 14% EPA)	µCT; histology; three-point bending test; *in vitro* analysis; plasma analysis	HFD + FO vs. HFD: ↑ Tb.BV/TV and Tb.N of proximal tibia; ↓ Ct.Po., ↑ Ct.Th., ↑ bone strength; ↑ N-terminal propeptide of type I procollagen/TRAP ratio; ↑ osteoblastogenesis and ↓ adipogenic and osteoclastic differentiation	HFD+ FO vs. HFD: ↓ BMAds number, volume and diameter	Benova *et al.* 2023 [96]
n-3 and n-6 PUFA enriched diet	F344 x BNF1 rats	12 months	M	20 weeks	N6+N3 diet (n-6/n-3 PUFA ratio 10); N6 diet (n-6/n-3 PUFA ratio 242); N3 diet (n-6/n-3 PUFA ratio 0.16)	serum analysis, DXA	N6 diet vs. N6+N3 group: ≠ ALP activity, ↓ BMC and ≠ BMD; N3 vs. N6+N3 diet: ↑ ALP activity, ↑ BMC and BMD	N/A	Shen *et al.* 2006 [94]
n-3 and n-6 PUFA enriched diet	SAMP8 mice	4 weeks	F	10 months	Control diet n-6/n-3 PUFA ratio (9.13); SFO (enriched diet in favor of ω6; n-6/n-3 PUFA ratio 18.35); BO (enriched in GLA; n-6/n-3 PUFA ratio 20.67); FO (enriched by EPA and DHA; n-6/n-3 PUFA ratio 3.52)	µCT	FO vs. other groups: ↑ bone volume; SFO and BO vs. control diet: ↑ bone volume	FO vs. other groups ↓ BMAT % SFO, BO vs. control diet: ↓ BMAT %	Bani Hassan *et al.* 2019 [95]
HFD and HFD + FO	C57BL/6 mice	6 weeks	M	6 months	Control diet (10% energy as fat) HFD (45% energy as fat) containing either 0%, 3%, or 9% energy as FO (0FO, 3FO, and 9FO, respectively)	µCT ; serum analysis	3FO vs. 9FO: ↑ BV, BV/TV, Tb.N, and ↓ Tb.Sp in femur; 3FO vs. 0FO: ↑ BV/TV 3FO vs. 9FO: ↑ BV/TV and ≠ cortical parameters; FO ↓ concentrations of serum TRAP	N/A	Cao *et al.* 2020 [97]
HFD and HFD + FO	C57BL/6 mice	13 months	F	5 months	Control diet (10% energy as fat); HFD (45% energy as fat) containing either 0%, 3%, or 9% energy as FO (0FO, 3FO, and 9FO, respectively)	DXA	FO+RSG vs. FO: ↓ BMD and induced bone loss	N/A	Cugno *et al.* 2021 [139]

HFD + FO	Balb/c mice OVX	8 weeks	F	24 weeks	CO (5%; low in n-3 fatty acids) FO (5% FO + 0.5% CO; high in n-3 fatty acids)	DXA, histology, *in vitro* analysis	FO-OVX and CO-OVX vs. sham: ↓ BMD in distal femur; CO-OVX vs. FO-OVX: ↑ bone loss; n-3 FA vs. n-6 FA: ↓ osteoclast maturation	N/A	Sun *et al.* 2003 [140]
n-3 PUFA enriched diet	B6.C3H-6T (6T) mice and C57BL/6J (B6J) mice	12 weeks	F	12 months	SO (22%) FO (22%)	DXA, *in vivo* μCT; histology; three-point bending test	B6J-FO vs. B6J-SO:↑ BMD, ↓ osteoclast number, ≠ mechanical properties; 6T-FO vs. 6T-SO: ≠ osteoclast number and surfaces; ↓ ultimate force and plastic energy, associated with ↓ Ct.Th	6T-FO mice had ↑BMAT vs.B6J mice on FO diet	Bonnet *et al.* 2014 [141]
HFD and HFD + FO	C57BL/6J mice	8 months	F	8 weeks	Control diet (15% protein, 75% carbohydrate, 10% fat, 0.6% Ca) HFD (45%, either enriched with MUFAs (15% protein, 39% carbohydrate, 46% fat, 0.7% Ca) SFAs (19% protein, 37% carbohydrate, 44% fat, 0.7% Ca)	DXA; μCT analysis	≠ effect on final calcium balance, secretion or excretion in all groups; SFAs vs. control diet: ↓ total body and femur BMD and BMC; SFAs vs. HFD diet: ≠ effects on BMC or BMD	N/A	Wang *et al.* 2016 [142]
SO enriched diet	C57BL/6 × C3H fat-1 mice	3 weeks	M F	9 weeks	modified AIN-93G diet (containing 10% SO, high in LA)	DXA, three-point bending test, femur neck fracture test	M vs. F: ↑ femur weight, length, toughness and stiffness at femur midpoint; ↑ BMC and BMD with ↑ percentage composition of total n-3 PUFA (EPA, DHA) and n-6 PUFAs (arachidonic acid)	N/A	Lau *et al.* 2009 [143]
Protein-enriched diet									
Low-protein diet containing 2% protein;	Balb/c mice	2 months	M	3 weeks	Protein source - casein (>85% protein) Control diet contained 12 % casein; the low-protein diet contained 2% casein	Histology; Western blot; ELISA BMSC AD differentiation	low-protein diet vs. control diet: ↑ adipogenesis of BMSC and BM failure	N/A	Cunha *et al.* 2013 [102]

Normoproteic diet 12%, Hypoproteic diet 2%	C57BL/6 NTaq mice	2 months	M	35-40 days	protein source casein (>85% protein) control normoproteic diet contained 12% casein hypoproteic diet contained 2% casein	Flow cytometry; qRT-PCR; BMSC differentiation and proliferation measurement	hypoproteic diet vs. normoproteic diet: ↓ differentiation potential of BMSC; altered the regulatory function of BMSCs and promotes proliferation	N/A	Hastreiter *et al.* 2021 [103]
Isocaloric low-protein diet	Sprague Dawley rats	6 months	F	10 weeks	control (15% casein) and isocaloric low-protein (2.5% casein) diet	µCT; three-point bending test	low protein diet vs. control diet: ↓ bone material level properties ; ↓ bone area, total area, and maximum second moment of inertia	N/A	Dubois-Ferrière *et al.* 2014 [105]
Isocaloric synthetic diets containing varying amounts of casein	Sprague-Dawley rats OVX	Adult	F	16 weeks	Isocaloric synthetic diets with 15, 7.5, 5, and 2.5% casein, + daily dose of vitamin D dissolved in peanut oil	DXA; histomorphometry analysis; three-point bending test	2.5% casein diet vs. other diets: ↓ bone mineral mass and strength	N/A	Ammann *et al.* 2000 [106]
Casein or soy enriched diet	Sprague-Dawley rats	8 months	M	24 weeks on protein diet after 2 weeks of CR	control diet containing 20% casein or soy	Serum biochemistry; Immunohistochemistry; Immunofluorescence	with protein diet after CR-induced bone loss: ≠ bone parameters	N/A	Duque *et al.* 2020 [109]
Casein-containing diet	Sprague-Dawley rats	1 month	F	10 weeks	10% casein, 7.5% casein, or 5% casein with normal or low level of Ca/P	DXA; µCT; qRT-PCR; biochemistry analysis	low-Ca-P diet with reduced protein intakes: ↓ of bone mass and ↓ bone strength	N/A	Fournier *et al.* 2014 [107]
Casein/soy/CR diet	Sprague-Dawley rats	2 months	F	10 weeks	casein diet; soy diet; 40% CR+ casein diet; 40% CR + soy diet	three-point bending test; DXA; µCT; serum biochemistry	Soy diet without CR:↑ BMD and BMC; ≠ effect on bone strength soy diet with CR ↓ BMD and BMC	N/A	Kioka *et al.* 2022 [144]
HFD with caloric restriction based on protein supplementation	Sprague-Dawley OVX rats	7 months	F	12 weeks	12 weeks of obesity-inducing diet (HFD/HSD + 15% protein) followed by 12 weeks of CR diet with different levels and source of proteins (normal protein 15%; high protein (HP)-milk 35%; high protein (HP)-beef 35%; high protein (HP)-soy 35%)	DXA; µCT; histology; three-point bending test	With CR: ↓ bone quantity and microarchitecture, ↓ body composition parameters. With HP-beef diet: ↑ trabecular separation and ↑ endocortical bone formation rates, ↓ bone retention and trabecular BMC compared to HP-soy With HP-milk diet: ≠ weight loss induced bone loss	N/A	Wright *et al.* 2022 [108]

Protein enriched diet combined with exercise	Wistar rats	5 weeks	F	2 months	10%, 20% and 40% protein diet groups + Exercise group rats were trained 6 days per week on a treadmill (25-30 m/min, 60 min) or no-exercise group	DXA; three-point bending test	With 10% protein diet: ↓ bone mass and bone strength	N/A	Takeda *et al.* 2012 [104]
Amino acids enriched diet									
Cysteine supplementation	C57BL/6 mice	6 weeks	M	17 weeks	HFD (45% energy from fat) enriched with N-acetylcysteine (1 g/kg)	Osteoclast culture; qRT-PCR in osteoclast; µCT	With HFD + cysteine: ↑ BV, BV/TV, Tb.Th and BMD in distal femur. ↓ osteoclast number; ↓ osteoclast differentiation from BM cells; ↓ bone resorption	N/A	Cao and Picklo 2014 [119]
Glutamine supplementation of low-protein diet	Balb/C mice	10 weeks	F	12 weeks	Monosodium glutamate (MSG) supplementation in low-protein (LP) diet (6% energy from soy protein)	µCT; determination of the femur protein fraction; determination of free amino acids in plasma	With LP diet + glutamine supplementation: ↑ glutamine plasma concentration LP diet: ↓ BMD gain; With higher concentrations of MSG (0.5/1/2%): ↑ BMD gain, ↑ the trabecular and cortical bone microarchitecture; ↑osteoblast activity; ↑ bone quality	N/A	Blais *et al.* 2019 [135]
Glutamine supplementation	Sprague Dawley OVX rats	N/A	F	3 months	Control diet combined with orally administered L-glutamine dissolved in 10% lactose in a dose of 3.2 g/kg/day	DXA; histology	With control diet + glutamine: ↑ BMD and BMC in femur	N/A	Hanna *et al.* 2009 [137]
Diet restricted in methionine	C57BL/6J mice	3 weeks	M	5 weeks	Control diet with 0.86% methionine or methionine-restricted diet (0.12%, MR)	µCT analysis, four-point bending test, qRT-PCR, osmium tetroxide staining; BMAT evaluation	With HFD restricted in MR: ↓ bone length, ↓ mechanical properties, ↓ Runx 2 mRNA, ↓ OB differentiation	With HFD restricted in methionine: ↑ BMAT in femur	Plummer *et al.* 2016 [123]

HFD restricted in methionine	C57BL/6J mice	8 weeks and 9 months	M F	12 weeks	Control HFD with methionine (0.84% w/w) or HFD restricted in methionine (0.12% w/w)	Whole body and femur length; µCT	With HFD restricted in methionine: ↓ body length; ↓ femur length in young M+F mice and aged M mice; ↓ Cortical BMD in M mice and aged F mice; ↓ trabecular BMD in young mice and aged F; ↓ cortical BMC in all MR mice while trabecular BMC ↓ in young mice No sex differences	N/A	Ouattara *et al.* 2016 [121]
Diet enriched in methionine	Wistar rats	10-12 weeks	F	12 weeks	2.4% methionine-enriched diet	Histomorphometry, Bone turnover markers t	With HFD enriched in MR: ↑ bone fragility, ↓ bone quality; ↑ bone loss in the cancellous bone	N/A	Herrmann *et al.* 2007 [120]
Amino acid supplemented low-protein diet	C57BL/6J mice	18 months	N/A	2 months	Low-protein diet and low-protein diet with AA supplementation: triad of serine, valine and threonine (SVT) and triad of phenylalanine, tyrosine and tryptophan (PTT)	three-point bending test, DXA, µCT, primary BMSC differentiation	With low-protein diet with AA: ↑ OB proliferation and differentiation. SVT ↓ bone mass but PTT revert effects of low-protein diet in terms of femoral and spinal BMD and BV/TV	N/A	Ding *et al.* 2018 [126]

↑- increased; ↓- decreased; ≠ not changed.

Table 2. Dietary factors affecting bone and BMAT in humans.

Clinical study	Age	Sex	Duration of the diet	Composition of the diet	Methods	Effect on bone	Effect on BMAT	Reference
Diet enriched in carbohydrates								
Carbonated beverages	14.3±1.8 years girls 14.6±1.6 years boys	M F	N/A	Various carbonated beverages consumption	Food intake; bone fracture risk analysis	↑ strong association between drinking cola beverage and bone fracture in girls; total caloric intake inversely associated with fracture risk in boys	N/A	Wyshak *et al.* 1994 [61]
Carbonated beverages	9-16 years	M F	N/A	Soft drinks and milk consumption	DXA; metacarpal morphometry	Positive association between cola drinking and increased fracture rate of wrist and forearm; ≠ between different beverages in BMD	N/A	Ma and Jones 2004 [62]
Mediterranean diet in patients with high glycemic index	F 60-80 years M 55-80 years	M F	7 years	Mediterranean diet (MedDiet; supplemented with extra-virgin olive oil (50 ml/day)); MedDiet supplemented with mixed nuts (30 g/day)	Bone fracture assessment; dietary assessment	Patients with ↑ glycemic index and glycemic load had significantly ↑ risk of osteoporotic fractures	N/A	Garcia-Gavilan *et al.* 2018 [64]
Carbohydrate quality index in postmenopausal women	45-65 years	F	N/A	Low carbohydrate diet and diet with higher glycemic index	DXA; dietary assessment; carbohydrate quality index analysis	Diets with ↑ glycemic index had ↑ fracture risk; low-carbohydrate diet score and carbohydrate quality index ↓ fracture risk of osteopenia in osteoporotic subjects	N/A	Nouri *et al.* 2023 [65]
Calorie-restricted diet								
CR (anorexia nervosa (AN))	29-42 years	F	N/A	AN group and control group	^{1}H-MRS; MRI; DXA	BMAT correlates inversely with BMD	AN patients ↑ BMAT compared to control group	Bredella *et al.* 2009 [67]
CR	47.8 ± 9.1 years	M F	6-18 months	low-fat diet or low-carbohydrate diet	MRI	N/A	Transiently ↓ BMAT	Ofir *et al.* 2023 [81]
CR + HFD	22-44 years	M F	10 days on HFD, then 10 days on CR	HFD diet (30-40% fat, 45-55% carbohydrates, ≥25% protein); CR diet (drink water *ad libitum*)	DXA; MRI	N/A	HFD: ↑ BMAT CR: ↑ BMAT	Fazeli *et al.* 2021 [66]

Obesity								
Cross-sectional study in lean and obese subjects	≥ 18 years	F	N/A	Obese and lean group (according to composition of visceral adipose tissue)	CT; ^{1}H-MRS	BMAT correlates inversely with BMD	↑ VAT is accompanied with ↑ BMAT	Bredella *et al.* 2011 [77]
Cross-sectional study in obese subjects in respect to sex	13.6 ± 1.4 years	M F	N/A	Boys and girls with obesity (BMI percentile 98.5 ± 1.2%)	MRI	N/A	↑ thoracic and lumbar BMAT in men compared to women	Vander Wyst *et al.* 2021 [78]
Cross-sectional study in obese subjects in respect to sex	33.7 ± 6.8 years	M F	N/A	Men and women obese groups (BMI 33.1 ± 7.1 kg/m^2; range 18.1-48.8 kg/m^2)	^{1}H-MRS	N/A	↑ ectopic and serum lipid levels associated with ↑ BMAT	Bredella et al. 2013 [68]
Longitudinal study	± 16.7 years	M	Study after 6 years; follow up after 8 years	No dietary intervention	DXA	n-3 FA (especially DHA) positively associated with peak BMD and negatively correlated with oleic acid and MUFAs in young men	N/A	Högström *et al.* 2007 [145]
Diet enriched in fatty acids								
Longitudinal study	25-40 years premenopausal 50-65 years postmenopausal	F	12 months	Control groups (1.0 g calcium) treatment group (1.0 g calcium, 4.0 g primrose oil and 440 mg marine FO)	DXA	BMD ↑ in both groups; ≠ between premenopausal and postmenopausal females; Postmenopausal vs. premenopausal F: ↓ total body BMD, ↑ bone turnover markers	N/A	Bassey *et al.* 2000 [146]
Flaxseed dietary supplementation	45-65 years	F	12 months	40 g flaxseed/day or placebo (wheat germ)	Serum analysis, DXA	Flaxseed vs. placebo: ≠ BMD	N/A	Dodin *et al.* 2005 [147]
Senile osteoporosis	±79.5 years	F	18 months	Treatment group: 6 g of a mixture of evening primrose oil and FO (60% LA, 8% GLA, 4% EPA, 3% DHA) + 600 mg/day calcium Control group: 6 g of coconut oil as placebo (97% saturated fat; 0.2% LA) + 600 mg/day calcium	Serum and urine analysis; FA analysis; bone densitometry – Lunar DPX-L	Treatment vs. control group: FA + Calcium maintain lumbar and ↑ femoral neck BMD	N/A	Kruger *et al.* 1998 [100]

Short-term n-3 PUFA supplementation	18-67 years	F M	12 weeks	1.48 g/day n-3 PUFAs (0.63 g EPA, 0.85 g DHA) or placebo – olive oil	Serum analysis	n-3 PUFAs vs. placebo: ≠ on bone resorption	N/A	Appleton *et al.* 2011 [148]
Long-term n-3 PUFA supplementation (Rheumatoid arthritis patients)	47-69 years	F M	12 weeks of diet and 8 weeks of washout	Treated group: n-3 fortified dairy (1.1 g ALA, 0.7 g EPA, 0.4 g DHA) Control group: standard dairy	Lipid extraction and FA analysis; blood and urinary analysis	Treated group vs. control group: ↓ urinary marker of bone resorption	N/A	Dawczynski *et al.* 2009 [149]
Hyperlipidemic adults	48.6 ± 1.6 years	F M	6 weeks of diet and 3 weeks of washout	Treated groups: LA diet (n-6/n-3 ratio 3.5); ALA diet (n-6/n-3 ratio 1.6) Control group: Average American diet (AAD, n-6/n-3 ratio 9)	Serum analysis	ALA diet: ↓ N-terminal telopeptide- marker of bone resorption compared to AAD	N/A	Griel *et al.* 2007 [150]
n-6 PUFA supplementation	65 years and older	F M	10 years	Dietary EPA and DHA intakes calculated from questionnaire responses	Statistical analysis; DXA	≠ between intake of EPA/DHA combined and the risk of hip fractures	N/A	Virtanen *et al.* 2010 [99]
Protein-enriched diet								
Head-down-tilt-bed-rest + protein supplementation	20-45 years	M	3 weeks	high protein intake (1.2 g/kg body weight/d) + whey protein with alkaline salts; control group – 1.2 g/kg body weight/day of protein	MRI	N/A	≠ in lumbar vertebral fat fraction	Trudel *et al.* 2019 [110]
Soy protein diet	≤ 65 years	F	12 months	Soy containing diet (25 g protein and 60 mg isoflavones)	DXA; Immunoassay analysis of serum and urine	≠ hip BMD and BMC; ↑ bone formation markers in both group	N/A	Arjmandi *et al.* 2005 [114]
Protein diet	20 ± 1 years	F M	1 month	Protein at 0.8; 1.6; 2.4 g/kg/day. Ten days of weight maintenance preceded 21 days of energy deficit (ED), during which total daily ED was 40%, achieved by reduced dietary energy intake (w30%) and increased physical activity (w10%)	DXA; ELISA	≠ BMC, BMD ↑ bone turnover markers in serum	N/A	Cao *et al.* 2014 [113]

Strength training with nutrient supplementation	55 ± 1 years	F	24 weeks	Nutrient group: - 730 kJ, composed of 10 g of protein (whey protein), 31 g of carbohydrate, 1 g of fat, 5.0 µg of vitamin D, and 250 mg of calcium; the placebo (control) group received 102 kJ as 6 g of carbohydrate and 12 mg of calcium	DXA; MRI	↑ femoral neck BMD; ↑ bone formation	N/A	Holm *et al.* 2008 [115]
Bed rest and a high protein diet	25-40 years	F	2 years	Bedrest + exercise group; bed rest + nutrition group or bed rest only (control group)	MRI	N/A	≠ in lumbar vertebral fat fraction	Trudel *et al.* 2009 [111]
Protein supplementation	70.5 ± 6.4 years	F M	18 months	Protein supplementation (160 kcal/45 g powder)	DXA	≠ lumbar spine BMD	N/A	Kerstetter *et al.* 2015 [112]

↑- increased; ↓- decreased; ≠ not changed.

References

1. Buckwalter JA, Cooper RR. Bone structure and function. Instr Course Lect 1987;36:27-48.
2. Ralston SH. Bone structure and metabolism. Medicine 2021;49:567-571. https://doi.org/10.1016/j.mpmed.2021.06.009
3. Benova A, Tencerova M. Obesity-induced changes in bone marrow homeostasis. Front Endocrinol (Lausanne) 2020;11:294. https://doi.org/10.3389/fendo.2020.00294
4. Tencerova M, Kassem M. The bone marrow-derived stromal cells: Commitment and regulation of adipogenesis. Front Endocrinol (Lausanne) 2016;7:127. https://doi.org/10.3389/fendo.2016.00127
5. Cawthorn WP, Scheller EL, Learman BS, Parlee SD, Simon BR, Mori H, Ning X, ET AL. Bone marrow adipose tissue is an endocrine organ that contributes to increased circulating adiponectin during caloric restriction. Cell Metab 2014;20:368-375. https://doi.org/10.1016/j.cmet.2014.06.003
6. Tencerova M, Figeac F, Ditzel N, Taipaleenmaki H, Nielsen TK, Kassem M. High-fat diet-induced obesity promotes expansion of bone marrow adipose tissue and impairs skeletal stem cell functions in mice. J Bone Miner Res 2018;33:1154-1165. https://doi.org/10.1002/jbmr.3408
7. Tencerova M, Ferencakova M, Kassem M. Bone marrow adipose tissue: Role in bone remodeling and energy metabolism. Best Pract Res Clin Endocrinol Metab 2021;35:101545. https://doi.org/10.1016/j.beem.2021.101545
8. Carleton SM, Whitford GM, Phillips CL. Dietary fluoride restriction does not alter femoral biomechanical strength in col1a2-deficient (oim) mice with type I collagen glomerulopathy. J Nutr 2010;140:1752-1756. https://doi.org/10.3945/jn.109.120261
9. Lindberg MK, Alatalo SL, Halleen JM, Mohan S, Gustafsson JA, Ohlsson C. Estrogen receptor specificity in the regulation of the skeleton in female mice. J Endocrinol 2001;171:229-236. https://doi.org/10.1677/joe.0.1710229
10. Wallace JM, Rajachar RM, Chen XD, Shi S, Allen MR, Bloomfield SA, Les CM, Robey PG, Young MF, Kohn DH. The mechanical phenotype of biglycan-deficient mice is bone- and gender-specific. Bone 2006;39:106-116. https://doi.org/10.1016/j.bone.2005.12.081

10a. Yao X, Carleton SM, Kettle AD, Melander J, Phillips CL, Wang Y. Gender-dependence of bone structure and properties in adult osteogenesis imperfecta murine model. Ann Biomed Eng 2013;41:1139-1149. https://doi.org/10.1007/s10439-013-0793-7

11. Nieves JW, Formica C, Ruffing J, Zion M, Garrett P, Lindsay R, Cosman F. Males have larger skeletal size and bone mass than females, despite comparable body size. J Bone Miner Res 2005;20:529-535. https://doi.org/10.1359/JBMR.041005
12. Laurent M, Antonio L, Sinnesael M, Dubois V, Gielen E, Classens F, Vanderschueren D. Androgens and estrogens in skeletal sexual dimorphism. Asian J Androl 2014;16:213-222. https://doi.org/10.4103/1008-682X.122356
13. Gabel L, Macdonald HM, McKay HA. Sex differences and growth-related adaptations in bone microarchitecture, geometry, density, and strength from childhood to early adulthood: A mixed longitudinal HR-pQCT study. J Bone Miner Res 2017;32:250-263. https://doi.org/10.1002/jbmr.2982
14. Oppenheimer-Velez ML, Giambini H, Rezaei A, Camp JJ, Khosla S, Lu L. The trabecular effect: A population-based longitudinal study on age and sex differences in bone mineral density and vertebral load bearing capacity. Clin Biomech (Bristol, Avon) 2018;55:73-78. https://doi.org/10.1016/j.clinbiomech.2018.03.022
15. Tanno M, Horiuchi T, Nakajima I, Maeda S, Igarashi M, Yamada H. Age-related changes in cortical and trabecular bone mineral status. A quantitative CT study in lumbar vertebrae. Acta Radiol 2001;42:15-19. https://doi.org/10.1080/028418501127346396
16. Nieuwoudt MK, Shahlori R, Naot D, Patel R, Holtkamp H, Aguergaray C, Watson M, ET AL. Raman spectroscopy reveals age- and sex-related differences in cortical bone from people with osteoarthritis. Sci Rep 2020;10:19443. https://doi.org/10.1038/s41598-020-76337-2
17. Anderson JJ. Calcium requirements during adolescence to maximize bone health. J Am Coll Nutr 2001;20(2 Suppl):186S-191S. https://doi.org/10.1080/07315724.2001.10719030
18. Heo HR, Chen L, An B, Kim KS, Ji J, Hong SH. Hormonal regulation of hematopoietic stem cells and their niche: a focus on estrogen. Int J Stem Cells 2015;8:18-23. https://doi.org/10.15283/ijsc.2015.8.1.18

19. Nakada D, Oguro H, Levi BP, Ryan N, Kitano A, Saitoh Y, Takeichi M, Wendt GR, Morrison SJ. Oestrogen increases haematopoietic stem-cell self-renewal in females and during pregnancy. Nature 2014;505:555-558. https://doi.org/10.1038/nature12932
20. Smithson G, Couse JF, Lubahn DB, Korach KS, Kincade PW. The role of estrogen receptors and androgen receptors in sex steroid regulation of B lymphopoiesis. J Immunol 1998;161:27-34. https://doi.org/10.4049/jimmunol.161.1.27
21. Singer K, Maley N, Mergian T, DelProposto J, Cho KW, Zamarron BF, Martinez-Santibanez G, ET AL. Differences in hematopoietic stem cells contribute to sexually dimorphic inflammatory responses to high fat diet-induced obesity. J Biol Chem 2015;290:13250-13262. https://doi.org/10.1074/jbc.M114.634568
22. Feng X, McDonald JM. Disorders of bone remodeling. Annu Rev Pathol 2011;6:121-145. https://doi.org/10.1146/annurev-pathol-011110-130203
23. Connelly KJ, Larson EA, Marks DL, Klein RF. Neonatal estrogen exposure results in biphasic age-dependent effects on the skeletal development of male mice. Endocrinology 2015;156:193-202. https://doi.org/10.1210/en.2014-1324
24. Dunsworth HM. Expanding the evolutionary explanations for sex differences in the human skeleton. Evol Anthropol 2020;29:108-116. https://doi.org/10.1002/evan.21834
25. Eriksen EF, Colvard DS, Berg NJ, Graham ML, Mann KG, Spelsberg TC, Riggs BL. Evidence of estrogen receptors in normal human osteoblast-like cells. Science 1988;241:84-86. https://doi.org/10.1126/science.3388021
26. Saxon LK, Galea G, Meakin L, Price J, Lanyon LE. Estrogen receptors alpha and beta have different gender-dependent effects on the adaptive responses to load bearing in cancellous and cortical bone. Endocrinology 2012;153:2254-2266. https://doi.org/10.1210/en.2011-1977
27. Demontiero O, Vidal C, Duque G. Aging and bone loss: new insights for the clinician. Ther Adv Musculoskelet Dis 2012;4:61-76. https://doi.org/10.1177/1759720X11430858
28. Lo JC, Burnett-Bowie SA, Finkelstein JS. Bone and the perimenopause. Obstet Gynecol Clin North Am 2011;38:503-517. https://doi.org/10.1016/j.ogc.2011.07.001
29. Dalzell N, Kaptoge S, Morris N, Berthier A, Koller B, Braak L, van Rietbergen B, Reeve J. Bone micro-architecture and determinants of strength in the radius and tibia: age-related changes in a population-based study of normal adults measured with high-resolution pQCT. Osteoporos Int 2009;20:1683-1694. https://doi.org/10.1007/s00198-008-0833-6
30. Khosla S, Riggs BL, Atkinson EJ, Oberg AL, McDaniel LJ, Holets M, Peterson JM, Melton LJ 3rd. Effects of sex and age on bone microstructure at the ultradistal radius: a population-based noninvasive in vivo assessment. J Bone Miner Res 2006;21:124-131. https://doi.org/10.1359/JBMR.050916
31. Fazeli PK, Horowitz MC, MacDougald OA, Scheller EL, Rodeheffer MS, Rosen CJ, Klibanski A. Marrow fat and bone - new perspectives. J Clin Endocrinol Metab 2013;98:935-945. https://doi.org/10.1210/jc.2012-3634
32. Li Z, Hardij J, Bagchi DP, Scheller EL, MacDougald OA. Development, regulation, metabolism and function of bone marrow adipose tissues. Bone 2018;110:134-140. https://doi.org/10.1016/j.bone.2018.01.008
33. Li Y, Meng Y, Yu X. The unique metabolic characteristics of bone marrow adipose tissue. Front Endocrinol (Lausanne) 2019;10:69. https://doi.org/10.3389/fendo.2019.00069
34. Lecka-Czernik B, Stechschulte LA, Czernik PJ, Sherman SB, Huang S, Krings A. Marrow adipose tissue: Skeletal location, sexual dimorphism, and response to sex steroid deficiency. Front Endocrinol (Lausanne) 2017;8:188. https://doi.org/10.3389/fendo.2017.00188
35. Kricun ME. Red-yellow marrow conversion: its effect on the location of some solitary bone lesions. Skeletal Radiol 1985;14:10-19. https://doi.org/10.1007/BF00361188
36. Scheller EL, Troiano N, Vanhoutan JN, Bouxsein MA, Fretz JA, Xi Y, Nelson T, ET AL. Use of osmium tetroxide staining with microcomputerized tomography to visualize and quantify bone marrow adipose tissue in vivo. Methods Enzymol 2014;537:123-139. https://doi.org/10.1016/B978-0-12-411619-1.00007-0
37. Liney GP, Bernard CP, Manton DJ, Turnbull LW, Langton CM. Age, gender, and skeletal variation in bone marrow composition: a preliminary study at 3.0 Tesla. J Magn Reson Imaging 2007;26:787-793. https://doi.org/10.1002/jmri.21072

38. Beekman KM, Regenboog M, Nederveen AJ, Bravenboer N, den Heijer M, Bisschop PH, Hollak CE, Akkerman EM, Maas M. Gender- and age-associated differences in bone marrow adipose tissue and bone marrow fat unsaturation throughout the skeleton, quantified using chemical shift encoding-based water-fat MRI. Front Endocrinol (Lausanne) 2022;13:815835. https://doi.org/10.3389/fendo.2022.815835
39. Baum T, Rohrmeier A, Syvari J, Diefenbach MN, Franz D, Dieckmeyer M, Scharr A, ET AL. Anatomical variation of age-related changes in vertebral bone marrow composition using chemical shift encoding-based water-fat magnetic resonance imaging. Front Endocrinol (Lausanne) 2018;9:141. https://doi.org/10.3389/fendo.2018.00141
40. Kugel H, Jung C, Schulte O, Heindel W. Age- and sex-specific differences in the 1H-spectrum of vertebral bone marrow. J Magn Reson Imaging 2001;13:263-268. https://doi.org/10.1002/1522-2586(200102)13:2<263::AID-JMRI1038>3.0.CO;2-M
41. Griffith JF, Yeung DK, Ma HT, Leung JC, Kwok TC, Leung PC. Bone marrow fat content in the elderly: a reversal of sex difference seen in younger subjects. J Magn Reson Imaging 2012;36:225-230. https://doi.org/10.1002/jmri.23619
42. Mistry SD, Woods GN, Sigurdsson S, Ewing SK, Hue TF, Eiriksdottir G, Xu K, Hilton JF, Kado DM, Gudnason V, Harris TB, Rosen CJ, Lang TF, Li X, Schwartz AV. Sex hormones are negatively associated with vertebral bone marrow fat. Bone 2018;108:20-24. https://doi.org/10.1016/j.bone.2017.12.009
43. Syed FA, Oursler MJ, Hefferanm TE, Peterson JM, Riggs BL, Khosla S. Effects of estrogen therapy on bone marrow adipocytes in postmenopausal osteoporotic women. Osteoporos Int 2008;19:1323-1330. https://doi.org/10.1007/s00198-008-0574-6
44. Limonard EJ, Veldhuis-Vlug AG, van Dussen L, Runge JH, Tanck MW, Endert E, Heijboer AC, ET AL. Short-term effect of estrogen on human bone marrow fat. J Bone Miner Res 2015;30:2058-2066. https://doi.org/10.1002/jbmr.2557
45. Scheller EL, Doucette CR, Learman BS, Cawthorn WP, Khandaker S, Schell B, Wu B, ET AL. Region-specific variation in the properties of skeletal adipocytes reveals regulated and constitutive marrow adipose tissues. Nat Commun 2015;6:7808. https://doi.org/10.1038/ncomms8808
46. Mosialou I, Shikhel S, Luo N, Petropoulou PI, Panitsas K, Bisikirska B, Rothman NJ, ET AL. Lipocalin-2 counteracts metabolic dysregulation in obesity and diabetes. J Exp Med 2020;217:e20191261. https://doi.org/10.1084/jem.20191261
47. Shen W, Chen J, Gantz M, Punyanitya M, Heymsfield SB, Gallagher D, Albu J, ET AL. Ethnic and sex differences in bone marrow adipose tissue and bone mineral density relationship. Osteoporos Int 2012;23:2293-2301. https://doi.org/10.1007/s00198-011-1873-x
48. Beekman KM, Duque G, Corsi A, Tencerova M, Bisschop PH, Paccou J. Osteoporosis and bone marrow adipose tissue. Curr Osteoporos Rep 2023;21:45-55. https://doi.org/10.1007/s11914-022-00768-1
49. Karner CM, Long F. Glucose metabolism in bone. Bone 2018;115:2-7. https://doi.org/10.1016/j.bone.2017.08.008
50. Zhu M, Fan Z. The role of the Wnt signalling pathway in the energy metabolism of bone remodelling. Cell Prolif 2022;55:e13309. https://doi.org/10.1111/cpr.13309
51. Dong K, Hao P, Xu S, Liu S, Zhou W, Yue X, Rausch-Fan X, Liu Z. Alpha-lipoic acid alleviates high-glucose suppressed osteogenic differentiation of MC3T3-E1 cells via antioxidant effect and PI3K/Akt signaling pathway. Cell Physiol Biochem 2017;42:1897-1906. https://doi.org/10.1159/000479605
52. Ogawa N, Yamaguchi T, Yano S, Yamauchi M, Yamamoto M, Sugimoto T. The combination of high glucose and advanced glycation end-products (AGEs) inhibits the mineralization of osteoblastic MC3T3-E1 cells through glucose-induced increase in the receptor for AGEs. Horm Metab Res 2007;39:871-875. https://doi.org/10.1055/s-2007-991157
53. Medeiros C, Wallace JM. High glucose-induced inhibition of osteoblast like MC3T3-E1 differentiation promotes mitochondrial perturbations. PLoS One 2022;17:e0270001. https://doi.org/10.1371/journal.pone.0270001
54. Tjaderhane L, Larmas M. A high sucrose diet decreases the mechanical strength of bones in growing rats. J Nutr 1998;128:1807-1810. https://doi.org/10.1093/jn/128.10.1807
55. Li KC, Zernicke RF, Barnard RJ, Li AF. Effects of a high fat-sucrose diet on cortical bone morphology and biomechanics. Calcif Tissue Int 1990;47:308-313. https://doi.org/10.1007/BF02555914

56. Yarrow JF, Toklu HZ, Balaez A, Phillips EG, Otzel DM, Chen C, Wronski TJ, Aguirre JI, Sakarya Y, Tumer N, Scarpace PJ. Fructose consumption does not worsen bone deficits resulting from high-fat feeding in young male rats. Bone 2016;85:99-106. https://doi.org/10.1016/j.bone.2016.02.004
57. Felice JI, Gangoiti MV, Molinuevo MS, McCarthy AD, Cortizo AM. Effects of a metabolic syndrome induced by a fructose-rich diet on bone metabolism in rats. Metabolism 2014;63:296-305. https://doi.org/10.1016/j.metabol.2013.11.002
58. Tsanzi E, Light HR, Tou JC. The effect of feeding different sugar-sweetened beverages to growing female Sprague-Dawley rats on bone mass and strength. Bone 2008;42:960-968. https://doi.org/10.1016/j.bone.2008.01.020
59. Lorincz C, Reimer RA, Boyd SK, Zernicke RF. High-fat, sucrose diet impairs geometrical and mechanical properties of cortical bone in mice. Br J Nutr 2010;103:1302-1308. https://doi.org/10.1017/S0007114509993084
60. Minematsu A, Nishii Y, Sakata S. High-fat/high-sucrose diet results in higher bone mass in aged rats. Bone Rep 2018;8:18-24. https://doi.org/10.1016/j.bonr.2018.01.001
61. Wyshak G, Frisch RE. Carbonated beverages, dietary calcium, the dietary calcium/phosphorus ratio, and bone fractures in girls and boys. J Adolesc Health 1994;15:210-215. https://doi.org/10.1016/1054-139X(94)90506-1
62. Ma D, Jones G. Soft drink and milk consumption, physical activity, bone mass, and upper limb fractures in children: a population-based case-control study. Calcif Tissue Int 2004;75:286-291. https://doi.org/10.1007/s00223-004-0274-y
63. Montagnani A, Gonnelli S, Alessandri M, Nuti R. Osteoporosis and risk of fracture in patients with diabetes: an update. Aging Clin Exp Res 2011;23:84-90. https://doi.org/10.1007/BF03351073
64. Garcia-Gavilan JF, Bullo M, Camacho-Barcia L, Rosique-Esteban N, Hernandez-Alonso P, Basora J, Martinez-Gonzalez MA, ET AL. Higher dietary glycemic index and glycemic load values increase the risk of osteoporotic fracture in the PREvencion con DIeta MEDiterranea (PREDIMED)-Reus trial. Am J Clin Nutr 2018;107:1035-1042. https://doi.org/10.1093/ajcn/nqy043
65. Nouri M, Mahmoodi M, Shateri Z, Ghadiri M, Rajabzadeh-Dehkordi M, Vali M, Gargari BP. How do carbohydrate quality indices influence on bone mass density in postmenopausal women? A case-control study. BMC Womens Health 2023;23:42. https://doi.org/10.1186/s12905-023-02188-4
66. Fazeli PK, Bredella MA, Pachon-Pena G, Zhao W, Zhang X, Faje AT, Resulaj M, ET AL. The dynamics of human bone marrow adipose tissue in response to feeding and fasting. JCI Insight 2021;6:e138636. https://doi.org/10.1172/jci.insight.138636
67. Bredella MA, Fazeli PK, Miller KK, Misra M, Torriani M, Thomas BJ, Ghomi RH, Rosen CJ, Klibanski A. Increased bone marrow fat in anorexia nervosa. J Clin Endocrinol Metab 2009;94:2129-2136. https://doi.org/10.1210/jc.2008-2532
68. Bredella MA, Gill CM, Gerweck AV, Landa MG, Kumar V, Daley SM, Torriani M, Miller KK. Ectopic and serum lipid levels are positively associated with bone marrow fat in obesity. Radiology 2013;269:534-541. https://doi.org/10.1148/radiol.13130375
69. Devlin MJ, Brooks DJ, Conlon C, Vliet M, Louis L, Rosen CJ, Bouxsein ML. Daily leptin blunts marrow fat but does not impact bone mass in calorie-restricted mice. J Endocrinol 2016;229:295-306. https://doi.org/10.1530/JOE-15-0473
70. Devlin MJ, Cloutier AM, Thomas NA, Panus DA, Lotinun S, Pinz I, Baron R, Rosen CJ, Bouxsein ML. Caloric restriction leads to high marrow adiposity and low bone mass in growing mice. J Bone Miner Res 2010;25:2078-2088. https://doi.org/10.1002/jbmr.82
71. Doucette CR, Horowitz MC, Berry R, MacDougald OA, Anunciado-Koza R, Koza RA, Rosen CJ. A high fat diet increases bone marrow adipose tissue (MAT) but does not alter trabecular or cortical bone mass in C57BL/6J mice. J Cell Physiol 2015;230:2032-2037. https://doi.org/10.1002/jcp.24954
72. Hamrick MW, Ding KH, Ponnala S, Ferrari SL, Isales CM. Caloric restriction decreases cortical bone mass but spares trabecular bone in the mouse skeleton: implications for the regulation of bone mass by body weight. J Bone Miner Res 2008;23:870-878. https://doi.org/10.1359/jbmr.080213
73. McGrath C, Sankaran JS, Misaghian-Xanthos N, Sen B, Xie Z, Styner MA, Zong X, Rubin J, Styner M. Exercise degrades bone in caloric restriction, despite suppression of marrow adipose tissue (MAT). J Bone Miner Res 2020;35:106-115. https://doi.org/10.1002/jbmr.3872

74. Bermudez B, Ishii T, Wu YH, Carpenter RD, Sherk VD. Energy Balance and bone health: a nutrient availability perspective. Curr Osteoporos Rep 2023;21:77-84. https://doi.org/10.1007/s11914-022-00765-4
75. Ali D, Figeac F, Caci A, Ditzel N, Schmal C, Kerckhofs G, Havelund J, ET AL. High-fat diet-induced obesity augments the deleterious effects of estrogen deficiency on bone: Evidence from ovariectomized mice. Aging Cell 2022;21:e13726. https://doi.org/10.1111/acel.13726
76. Baek K, Bloomfield SA. Blocking beta-adrenergic signaling attenuates reductions in circulating leptin, cancellous bone mass, and marrow adiposity seen with dietary energy restriction. J Appl Physiol 2012;113:1792-1801. https://doi.org/10.1152/japplphysiol.00187.2012
77. Bredella MA, Torriani M, Ghomi RH, Thomas BJ, Brick DJ, Gerweck AV, Rosen CJ, Klibanski A, Miller KK. Vertebral bone marrow fat is positively associated with visceral fat and inversely associated with IGF-1 in obese women. Obesity (Silver Spring) 2011;19:49-53. https://doi.org/10.1038/oby.2010.106
78. Vander Wyst KB, Hu HH, Pena A, Olson ML, Bailey SS, Shaibi GQ. Bone marrow adipose tissue content in Latino adolescents with prediabetes and obesity. Obesity (Silver Spring) 2021;29:2100-2107. https://doi.org/10.1002/oby.23279
79. Devlin MJ. Why does starvation make bones fat? Am J Hum Biol 2011;23:577-585. https://doi.org/10.1002/ajhb.21202
80. Dimitri P, Bishop N, Walsh JS, Eastell R. Obesity is a risk factor for fracture in children but is protective against fracture in adults: a paradox. Bone 2012;50:457-466. https://doi.org/10.1016/j.bone.2011.05.011
81. Ofir N, Mizrakli Y, Greenshpan Y, Gepner Y, Sharabi O, Tsaban G, Zelicha H, ET AL. Vertebrae but not femur marrow fat transiently decreases in response to body weight loss in an 18-month randomized control trial. Bone 2023;171:116727. https://doi.org/10.1016/j.bone.2023.116727
82. Karastergiou K, Smith SR, Greenberg AS, Fried SK. Sex differences in human adipose tissues - the biology of pear shape. Biol Sex Differ 2012;3:13. https://doi.org/10.1186/2042-6410-3-13
83. Liu AG, Ford NA, Hu FB, Zelman KM, Mozaffarian D, Kris-Etherton PM. A healthy approach to dietary fats: understanding the science and taking action to reduce consumer confusion. Nutr J 2017;16:53. https://doi.org/10.1186/s12937-017-0271-4
84. Swinburn BA, Caterson I, Seidell JC, James WP. Diet, nutrition and the prevention of excess weight gain and obesity. Public Health Nutr 2004;7:123-146. https://doi.org/10.1079/PHN2003585
85. Kruger MC, Coetzee M, Haag M, Weiler H. Long-chain polyunsaturated fatty acids: selected mechanisms of action on bone. Prog Lipid Res 2010;49:438-449. https://doi.org/10.1016/j.plipres.2010.06.002
86. Wang D, Haile A, Jones LC. Dexamethasone-induced lipolysis increases the adverse effect of adipocytes on osteoblasts using cells derived from human mesenchymal stem cells. Bone 2013;53:520-530. https://doi.org/10.1016/j.bone.2013.01.009
87. Lecka-Czernik B, Stechschulte LA, Czernik PJ, Dowling AR. High bone mass in adult mice with diet-induced obesity results from a combination of initial increase in bone mass followed by attenuation in bone formation; implications for high bone mass and decreased bone quality in obesity. Mol Cell Endocrinol 2015;410:35-41. https://doi.org/10.1016/j.mce.2015.01.001
88. Wang T, Zhu X, Dai F, Li C, Huang D, Fang Z, Zhang Q, Lu Y. Effects of a standard high-fat diet with or without multiple deficiencies on bone parameters in ovariectomized mature rat. PLoS One 2017;12:e0184983. https://doi.org/10.1371/journal.pone.0184983
89. Scheller EL, Khoury B, Moller KL, Wee NK, Khandaker S, Kozloff KM, Abrishami SH, Zamarron BF, Singer K. Changes in skeletal integrity and marrow adiposity during high-fat diet and after weight loss. Front Endocrinol (Lausanne) 2016;7:102. https://doi.org/10.3389/fendo.2016.00102
90. Gautam J, Choudhary D, Khedgikar V, Kushwaha P, Singh RS, Singh D, Tiwari S, Trivedi R. Micro-architectural changes in cancellous bone differ in female and male C57BL/6 mice with high-fat diet-induced low bone mineral density. Br J Nutr 2014;111:1811-1821. https://doi.org/10.1017/S0007114514000051
91. Silva MJ, Eekhoff JD, Patel T, Kenney-Hunt JP, Brodt MD, Steger-May K, Scheller EL, Cheverud JM. Effects of high-fat diet and body mass on bone morphology and mechanical properties in 1100 advanced intercross mice. J Bone Miner Res 2019;34:711-725. https://doi.org/10.1002/jbmr.3648

92. Sistilli G, Kalendova V, Cajka T, Irodenko I, Bardova K, Oseeva M, Zacek P, Kroupova P, Horakova O, Lackner K, Gastaldelli A, Kuda O, Kopecky J, Rossmeisl M. Krill oil supplementation reduces exacerbated hepatic steatosis induced by thermoneutral housing in mice with diet-induced obesity. Nutrients 2021;13:437. https://doi.org/10.3390/nu13020437
93. van Schothorst EM, Flachs P, Franssen-van Hal NL, Kuda O, Bunschoten A, Molthoff J, Vink C, ET AL. Induction of lipid oxidation by polyunsaturated fatty acids of marine origin in small intestine of mice fed a high-fat diet. BMC Genomics 2009;10:110. https://doi.org/10.1186/1471-2164-10-110
94. Shen CL, Yeh JK, Rasty J, Li Y, Watkins BA. Protective effect of dietary long-chain n-3 polyunsaturated fatty acids on bone loss in gonad-intact middle-aged male rats. Br J Nutr 2006;95:462-468. https://doi.org/10.1079/BJN20051664
95. Bani Hassan E, Alderghaffar M, Wauquier F, Coxam V, Demontiero O, Vogrin S, Wittrant Y, Duque G. The effects of dietary fatty acids on bone, hematopoietic marrow and marrow adipose tissue in a murine model of senile osteoporosis. Aging (Albany NY) 2019;11:7938-7947. https://doi.org/10.18632/aging.102299
96. Benova A, Ferencakova M, Bardova K, Funda J, Prochazka J, Spoutil F, Cajka T, ET AL. Omega-3 PUFAs prevent bone impairment and bone marrow adiposity in mouse model of obesity. Commun Biol 2023;6:1043. https://doi.org/10.1038/s42003-023-05407-8
97. Cao JJ, Gregoire BR, Michelsen KG, Picklo MJ. Increasing dietary fish oil reduces adiposity and mitigates bone deterioration in growing C57BL/6 mice fed a high-fat diet. J Nutr 2020;150:99-107. https://doi.org/10.1093/jn/nxz215
98. Farina EK, Kiel DP, Roubenoff R, Schaefer EJ, Cupples LA, Tucker KL. Dietary intakes of arachidonic acid and alpha-linolenic acid are associated with reduced risk of hip fracture in older adults. J Nutr 2011;141:1146-1153. https://doi.org/10.3945/jn.110.133728
99. Virtanen JK, Mozaffarian D, Cauley JA, Mukamal KJ, Robbins J, Siscovick DS. Fish consumption, bone mineral density, and risk of hip fracture among older adults: the cardiovascular health study. J Bone Miner Res 2010;25:1972-1979. https://doi.org/10.1002/jbmr.87
100. Kruger MC, Coetzer H, de Winter R, Gericke G, van Papendorp DH. Calcium, gamma-linolenic acid and eicosapentaenoic acid supplementation in senile osteoporosis. Aging (Milano) 1998;10:385-394. https://doi.org/10.1007/BF03339885
101. Thompson M, Hein N, Hanson C, Smith LM, Anderson-Berry A, Richter CK, Stessy Bisselou K, ET AL. Omega-3 fatty acid intake by age, gender, and pregnancy status in the United States: National Health and Nutrition Examination Survey 2003-2014. Nutrients 2019;11:177. https://doi.org/10.3390/nu11010177
102. Cunha MC, Lima Fda S, Vinolo MA, Hastreiter A, Curi R, Borelli P, Fock RA. Protein malnutrition induces bone marrow mesenchymal stem cells commitment to adipogenic differentiation leading to hematopoietic failure. PLoS One 2013;8:e58872. https://doi.org/10.1371/journal.pone.0058872
103. Hastreiter AA, Dos Santos GG, Makiyama EN, Santos EWC, Borelli P, Fock RA. Effects of protein malnutrition on hematopoietic regulatory activity of bone marrow mesenchymal stem cells. J Nutr Biochem 2021;93:108626. https://doi.org/10.1016/j.jnutbio.2021.108626
104. Takeda S, Kobayashi Y, Park JH, Ezawa I, Omi N. Effect of different intake levels of dietary protein and physical exercise on bone mineral density and bone strength in growing male rats. J Nutr Sci Vitaminol (Tokyo) 2012;58:240-246. https://doi.org/10.3177/jnsv.58.240
105. Dubois-Ferriere V, Rizzoli R, Ammann P. A low protein diet alters bone material level properties and the response to in vitro repeated mechanical loading. Biomed Res Int 2014;2014:185075. https://doi.org/10.1155/2014/185075
106. Ammann P, Bourrin S, Bonjour JP, Meyer JM, Rizzoli R. Protein undernutrition-induced bone loss is associated with decreased IGF-I levels and estrogen deficiency. J Bone Miner Res 2000;15:683-690. https://doi.org/10.1359/jbmr.2000.15.4.683
107. Fournier C, Rizzoli R, Ammann P. Low calcium-phosphate intakes modulate the low-protein diet-related effect on peak bone mass acquisition: a hormonal and bone strength determinants study in female growing rats. Endocrinology 2014;155:4305-4315. https://doi.org/10.1210/en.2014-1308
108. Wright CS, Hill ER, Reyes Fernandez PC, Thompson WR, Gallant MA, Campbell WW, Main RP. Effects of dietary protein source and quantity on bone morphology and body composition following a high-protein weight-loss diet in a rat model for postmenopausal obesity. Nutrients 2022;14:2262. https://doi.org/10.3390/nu14112262

109. Duque G, Al Saedi A, Rivas D, Miard S, Ferland G, Picard F, Gaudreau P. Differential effects of long-term caloric restriction and dietary protein source on bone and marrow fat of the aging rat. J Gerontol A Biol Sci Med Sci 2020;75:2031-2036. https://doi.org/10.1093/gerona/glaa093
110. Trudel G, Melkus G, Sheikh A, Ramsay T, Laneuville O. Marrow adipose tissue gradient is preserved through high protein diet and bed rest. A randomized crossover study. Bone Rep 2019;11:100229. https://doi.org/10.1016/j.bonr.2019.100229
111. Trudel G, Payne M, Madler B, Ramachandran N, Lecompte M, Wade C, Biolo G, ET AL. Bone marrow fat accumulation after 60 days of bed rest persisted 1 year after activities were resumed along with hemopoietic stimulation: the Women International Space Simulation for Exploration study. J Appl Physiol 2009;107:540-548. https://doi.org/10.1152/japplphysiol.91530.2008
112. Kerstetter JE, Bihuniak JD, Brindisi J, Sullivan RR, Mangano KM, Larocque S, Kotler BM, ET AL. The effect of a whey protein supplement on bone mass in older caucasian adults. J Clin Endocrinol Metab 2015;100:2214-2222. https://doi.org/10.1210/jc.2014-3792
113. Cao JJ, Pasiakos SM, Margolis LM, Sauter ER, Whigham LD, McClung JP, Young AJ, Combs GF Jr. Calcium homeostasis and bone metabolic responses to high-protein diets during energy deficit in healthy young adults: a randomized controlled trial. Am J Clin Nutr 2014;99:400-407. https://doi.org/10.3945/ajcn.113.073809
114. Arjmandi BH, Lucas EA, Khalil DA, Devareddy L, Smith BJ, McDonald J, Arquitt AB, Payton ME, Mason C. One year soy protein supplementation has positive effects on bone formation markers but not bone density in postmenopausal women. Nutr J 2005;4:8. https://doi.org/10.1186/1475-2891-4-8
115. Holm L, Olesen JL, Matsumoto K, Doi T, Mizuno M, Alsted TJ, Mackey AL, Schwarz P, Kjaer M. Protein-containing nutrient supplementation following strength training enhances the effect on muscle mass, strength, and bone formation in postmenopausal women. J Appl Physiol 2008;105:274-281. https://doi.org/10.1152/japplphysiol.00935.2007
116. Le Couteur DG, Solon-Biet SM, Cogger VC, Ribeiro R, de Cabo R, Raubenheimer D, Cooney GJ, Simpson SJ. Branched chain amino acids, aging and age-related health. Ageing Res Rev 2020;64:101198. https://doi.org/10.1016/j.arr.2020.101198
117. Sartori T, Santos ACA, Oliveira da Silva R, Kodja G, Rogero MM, Borelli P, Fock RA. Branched chain amino acids improve mesenchymal stem cell proliferation, reducing nuclear factor kappa B expression and modulating some inflammatory properties. Nutrition 2020;78:110935. https://doi.org/10.1016/j.nut.2020.110935
118. Mu WC, VanHoosier E, Elks CM, Grant RW. Long-term effects of dietary protein and branched-chain amino acids on metabolism and inflammation in mice. Nutrients 2018;10:918. https://doi.org/10.3390/nu10070918
119. Cao JJ, Picklo MJ. N-acetylcysteine supplementation decreases osteoclast differentiation and increases bone mass in mice fed a high-fat diet. J Nutr 2014;144:289-296. https://doi.org/10.3945/jn.113.185397
120. Herrmann M, Wildemann B, Claes L, Klohs S, Ohnmacht M, Taban-Shomal O, Hubner U, Pexa A, Umanskaya N, Herrmann W. Experimental hyperhomocysteinemia reduces bone quality in rats. Clin Chem 2007;53:1455-1461. https://doi.org/10.1373/clinchem.2007.086272
121. Ouattara A, Cooke D, Gopalakrishnan R, Huang TH, Ables GP. Methionine restriction alters bone morphology and affects osteoblast differentiation. Bone Rep 2016;5:33-42. https://doi.org/10.1016/j.bonr.2016.02.002
122. Ables GP, Johnson JE. Pleiotropic responses to methionine restriction. Exp Gerontol 2017;94:83-88. https://doi.org/10.1016/j.exger.2017.01.012
123. Plummer J, Park M, Perodin F, Horowitz MC, Hens JR. Methionine-restricted diet increases miRNAs that can target RUNX2 expression and alters bone structure in young mice. J Cell Biochem 2017;118:31-42. https://doi.org/10.1002/jcb.25604
124. Kim H, Lee K, Kim JM, Kim MY, Kim JR, Lee HW, Chung YW, ET AL. Selenoprotein W ensures physiological bone remodeling by preventing hyperactivity of osteoclasts. Nat Commun 2021;12:2258. https://doi.org/10.1038/s41467-021-22565-7
125. Lai J, Zhou J, Yin S. Effect of selenium and zinc level in diet on bone development in rats exposed to lead. (Article in Chinese) Wei Sheng Yan Jiu 2004;33:584-586.
126. Ding KH, Cain M, Davis M, Bergson C, McGee-Lawrence M, Perkins C, Hardigan T, ET AL. Amino acids as signaling molecules modulating bone turnover. Bone 2018;115:15-24. https://doi.org/10.1016/j.bone.2018.02.028

127. Hill TR, Verlaan S, Biesheuvel E, Eastell R, Bauer JM, Bautmans I, Brandt K, ET AL. A vitamin D, calcium and leucine-enriched whey protein nutritional supplement improves measures of bone health in sarcopenic non-malnourished older adults: The PROVIDE Study. Calcif Tissue Int 2019;105:383-391. https://doi.org/10.1007/s00223-019-00581-6
128. Palacios-Gonzalez B, Ramirez-Salazar EG, Rivera-Paredez B, Quiterio M, Flores YN, Macias-Kauffer L, Moran-Ramos S, ET AL. A multi-omic analysis for low bone mineral density in postmenopausal women suggests a relationship between diet, metabolites, and microbiota. Microorganisms 2020;8:1630. https://doi.org/10.3390/microorganisms8111630
129. Mendes AB, Martins FF, Cruz WM, da Silva LE, Abadesso CB, Boaventura GT. Bone development in children and adolescents with PKU. J Inherit Metab Dis 2012;35:425-430. https://doi.org/10.1007/s10545-011-9412-7
130. Michalowska M, Znorko B, Kaminski T, Oksztulska-Kolanek E, Pawlak D. New insights into tryptophan and its metabolites in the regulation of bone metabolism. J Physiol Pharmacol 2015;66:779-791.
131. Lv Z, Shi W, Zhang Q. Role of essential amino acids in age-induced bone loss. Int J Mol Sci 2022;23:11281. https://doi.org/10.3390/ijms231911281
132. Cleminson JR, Stuart AL, Pasco JA, Hodge JM, Berk M, Samarasinghe RM, Williams LJ. Dietary tryptophan and bone health: a cross-sectional, population-based study. Arch Osteoporos 2020;15:167. https://doi.org/10.1007/s11657-020-00838-w
133. Cruzat VF, Rogero MM, Tirapegui J. Effects of supplementation with free glutamine and the dipeptide alanyl-glutamine on parameters of muscle damage and inflammation in rats submitted to prolonged exercise. Cell Biochem Funct 2010;28:24-30. https://doi.org/10.1002/cbf.1611
134. Yu Y, Newman H, Shen L, Sharma D, Hu G, Mirando AJ, Zhang H, Knudsen E, Zhang GF, Hilton MJ, Karner CM. Glutamine metabolism regulates proliferation and lineage allocation in skeletal stem cells. Cell Metab 2019;29:966-978e964. https://doi.org/10.1016/j.cmet.2019.01.016
135. Blais A, Rochefort GY, Moreau M, Calvez J, Wu X, Matsumoto H, Blachier F. Monosodium glutamate supplementation improves bone status in mice under moderate protein restriction. JBMR Plus 2019;3:e10224. https://doi.org/10.1002/jbm4.10224
136. Tapiero H, Mathe G, Couvreur P, Tew KD. II. Glutamine and glutamate. Biomed Pharmacother 2002;56:446-457. https://doi.org/10.1016/S0753-3322(02)00285-8
137. Ahmed HH, Hamza AH. Potential role of arginine, glutamine and taurine in ameliorating osteoporotic biomarkers in ovariectomized rats. Rep Opin 2009;1:24-35.
138. Bass EF, Baile CA, Lewis RD, Giraudo SQ. Bone quality and strength are greater in growing male rats fed fructose compared with glucose. Nutr Res 2013;33:1063-1071. https://doi.org/10.1016/j.nutres.2013.08.006
139. Cugno C, Kizhakayil D, Calzone R, Rahman SM, Halade GV, Rahman MM. Omega-3 fatty acid-rich fish oil supplementation prevents rosiglitazone-induced osteopenia in aging C57BL/6 mice and in vitro studies. Sci Rep 2021;11:10364. https://doi.org/10.1038/s41598-021-89827-8
140. Sun D, Krishnan A, Zaman K, Lawrence R, Bhattacharya A, Fernandes G. Dietary n-3 fatty acids decrease osteoclastogenesis and loss of bone mass in ovariectomized mice. J Bone Miner Res 2003;18:1206-1216. https://doi.org/10.1359/jbmr.2003.18.7.1206
141. Bonnet N, Somm E, Rosen CJ. Diet and gene interactions influence the skeletal response to polyunsaturated fatty acids. Bone 2014;68:100-107. https://doi.org/10.1016/j.bone.2014.07.024
142. Wang Y, Dellatore P, Douard V, Qin L, Watford M, Ferraris RP, Lin T, Shapses SA. High fat diet enriched with saturated, but not monounsaturated fatty acids adversely affects femur, and both diets increase calcium absorption in older female mice. Nutr Res 2016;36:742-750. https://doi.org/10.1016/j.nutres.2016.03.002
143. Lau BY, Ward WE, Kang JX, Ma DW. Femur EPA and DHA are correlated with femur biomechanical strength in young fat-1 mice. J Nutr Biochem 2009;20:453-461. https://doi.org/10.1016/j.jnutbio.2008.05.004
144. Kioka K, Aikawa Y, Wakasugi Y, Narukawa T, Fukuyasu T, Ohtsuki M, Yamashita T, Sasai N, Omi N. Soy protein intake increased bone mineral density under nonenergy-deficiency conditions but decreased it under energy-deficiency conditions in young female rats. Nutr Res 2022;106:1-11. https://doi.org/10.1016/j.nutres.2022.08.001

145. Hogstrom M, Nordstrom P, Nordstrom A. n-3 Fatty acids are positively associated with peak bone mineral density and bone accrual in healthy men: the NO2 Study. Am J Clin Nutr 2007;85:803-807. https://doi.org/10.1093/ajcn/85.3.803
146. Bassey EJ, Littlewood JJ, Rothwell MC, Pye DW. Lack of effect of supplementation with essential fatty acids on bone mineral density in healthy pre- and postmenopausal women: two randomized controlled trials of Efacal v. calcium alone. Br J Nutr 2000;83:629-635. https://doi.org/10.1017/S0007114500000805
147. Dodin S, Lemay A, Jacques H, Legare F, Forest JC, Masse B. The effects of flaxseed dietary supplement on lipid profile, bone mineral density, and symptoms in menopausal women: a randomized, double-blind, wheat germ placebo-controlled clinical trial. J Clin Endocrinol Metab 2005;90:1390-1397. https://doi.org/10.1210/jc.2004-1148
148. Appleton KM, Fraser WD, Rogers PJ, Ness AR, Tobias JH. Supplementation with a low-moderate dose of n-3 long-chain PUFA has no short-term effect on bone resorption in human adults. Br J Nutr 2011;105:1145-1149. https://doi.org/10.1017/S0007114510004861
149. Dawczynski C, Schubert R, Hein G, Muller A, Eidner T, Vogelsang H, Basu S, Jahreis G. Long-term moderate intervention with n-3 long-chain PUFA-supplemented dairy products: effects on pathophysiological biomarkers in patients with rheumatoid arthritis. Br J Nutr 2009;101:1517-1526. https://doi.org/10.1017/S0007114508076216
150. Griel AE, Kris-Etherton PM, Hilpert KF, Zhao G, West SG, Corwin RL. An increase in dietary n-3 fatty acids decreases a marker of bone resorption in humans. Nutr J 2007;6:2. https://doi.org/10.1186/1475-2891-6-2

Physiol. Res. 73 (Suppl. 1): S139-S152, 2024 *https://doi.org/10.33549/physiolres.935259*

REVIEW

Redox Status as a Key Driver of Healthy Pancreatic β-Cells

Blanka HOLENDOVÁ[1], Štěpánka BENÁKOVÁ[1,2], Monika KŘIVONOSKOVÁ[1,3], Lydie PLECITÁ-HLAVATÁ[1]

[1]Laboratory of Pancreatic Islet Research, Institute of Physiology of the Czech Academy of Sciences, Prague, Czech Republic, [2]First Faculty of Medicine, Charles University, Prague, Czech Republic, [3]Faculty of Science, Charles University, Prague, Czech Republic

Received October 17, 2023
Accepted April 2, 2024

Summary

Redox status plays a multifaceted role in the intricate physiology and pathology of pancreatic β-cells, the pivotal regulators of glucose homeostasis through insulin secretion. They are highly responsive to changes in metabolic cues where reactive oxygen species are part of it, all arising from nutritional intake. These molecules not only serve as crucial signaling intermediates for insulin secretion but also participate in the nuanced heterogeneity observed within the β-cell population. A central aspect of β-cell redox biology revolves around the localized production of hydrogen peroxide and the activity of NADPH oxidases which are tightly regulated and serve diverse physiological functions. Pancreatic β-cells possess a remarkable array of antioxidant defense mechanisms although considered relatively modest compared to other cell types, are efficient in preserving redox balance within the cellular milieu. This intrinsic antioxidant machinery operates in concert with redox-sensitive signaling pathways, forming an elaborate redox relay system essential for β-cell function and adaptation to changing metabolic demands. Perturbations in redox homeostasis can lead to oxidative stress exacerbating insulin secretion defect being a hallmark of type 2 diabetes. Understanding the interplay between redox signaling, oxidative stress, and β-cell dysfunction is paramount for developing effective therapeutic strategies aimed at preserving β-cell health and function in individuals with type 2 diabetes. Thus, unraveling the intricate complexities of β-cell redox biology presents exciting avenues for advancing our understanding and treatment of metabolic disorders.

Key words

Redox homeostasis • Pancreatic β-cells • NOX • Heterogeneity

Corresponding author

L. Plecitá-Hlavatá, Laboratory of Pancreatic Islet Research, Czech Academy of Sciences, Videnska 1083, 142 20 Prague 4, Czech Republic. E-mail: lydie.plecita@fgu.cas.cz

Introduction to redox milieu in β-cells with emphasis on pro-oxidative sources

There is no doubt that redox homeostasis is a critical feature of cellular signaling in a variety of cells. A transient increase in cellular reactive oxygen species (ROS) has been identified as an essential second messenger, while permanently increased production leads to oxidative stress, which has been linked to many diseases, including diabetes [1,2]. Many have shown that pancreatic β-cells, as the major glucose sensor in the body, are sensitive to perturbations in redox homeostasis and that long-term disruption of redox homeostasis leads to deterioration of β-cells and thus insulin secretion and glucose balance in the body, the prominent feature of diabetes (more in [3-7]).

It has been suggested that glucose-induced metabolism in β-cells can produce ROS *via* many pathways [8]. However, due to significant limitations in the methods used to detect ROS *in situ* (in terms of their species and cellular localization), the exact site of ROS production and oxygen species remained undetermined until recently [9,10]. By using redox probes targeting organelles that are also more ROS species-specific, we observed the increased production of ROS, particularly hydrogen peroxide (H_2O_2), under condition

of glucose stimulation in the cytoplasm by NADPH oxidase, isoform 4, NOX 4 [11] (Fig. 1). Interestingly, the production of ROS (especially superoxide) in the mitochondrial matrix was decreased upon glucose induction due to the decreasing $NADH/NAD^+$ ratio in the mitochondrial matrix [12]. This does not necessarily refute the role of mitochondria as a source of ROS during glucose induction, as the complex III of the respiratory chain is able to produce superoxide outside the mitochondria and is therefore undetectable with probes in the mitochondrial matrix (Fig. 1). Increased glucose-stimulated metabolism can also lead to increased autooxidation of glyceraldehyde, producing H_2O_2 and ketoaldehydes in diabetes [13]. Glycolysis produces dihydroxyacetone, which undergoes the reduction to glycerol-3-phosphate and acylation, producing diacylglycerol, which activates protein kinase C (PKC) [14-17]. PKC can phosphorylate NOX isoforms leading to the induction of their activity and thus increase in cytosolic ROS production. Metabolism of sorbitol, hexosamine, or methylglyoxal derived from glucose catabolism can also stimulate ROS production in diabetic conditions [8,18]. However, mitochondrial ROS production in β-cells has been documented mainly under conditions of the increased flux of fatty acids and amino acids as substrates, the conditions associated with diabetic pathology [11,19-24] (Fig. 1). Superoxide produced along the electron transport chain (complex I/III) is rapidly converted by superoxide dismutase, SOD2 isoform, to H_2O_2, being able to diffuse out of mitochondria [19,24-29] This production has been found to be controlled by the uncoupling activity of UCP2 in β-cells [30-32].

Be that as it may, H_2O_2 has been identified as a critical molecule for signal transduction in pancreatic β-cells. Its low concentration (nanomolar) is involved in signal transduction by cysteine oxidation of participating proteins, known as redox relay [33,34] (Fig. 1), whereas increased production in the micromolar concentration range causes oxidative stress because β-cells are unable to adequately increase antioxidant protection especially in long-term horizon [35] (Fig. 2). H_2O_2 is a small electroneutral molecule that can cross lipid membranes either alone or through peroxiporins, members of the aquaporin family (more in [36]). Its toxicity is tracked by the production of hydroxyl radicals (OH^-), which are generated when it encounters free iron or copper, rather than interacting with protective high-affinity thiols [37]. Hydroxyl radicals have a high oxidation potential, and their small radius and uncharged state provide great mobility so that chemical reactions can proceed at high rates [37]. Therefore, H_2O_2 is also a crucial mediator of toxicity under conditions of chronic oxidative stress.

The specific properties of H_2O_2 in terms of its reactivity allow it to specifically target reactive thiols of cysteine residues within protein structures. However, only some thiols are predetermined to undergo the oxidation reaction. This is given by the vicinity of the surrounding amino acids (local electrostatic environment) and pH. Thus, cysteines in proteins must display low pKa, to enhance the thiolate fraction, as a prerequisite for fast and efficient oxidation by peroxides, although its nucleophilicity (to attack the H_2O_2 electrophile) and its capacity to stabilize both the transition state with the reactant, H_2O_2, and the leaving group (which occurs after the rupture of the peroxidic bond) also must be preserved [38]. The reactive thiols then react with H_2O_2 to form sulfenic acid (reversible oxidation). The oxidized thiols are regenerated by reaction with other thiols groups on i) diverse proteins giving rise to the so-called redox relay system by which the redox signal is transferred or ii) proteins of the antioxidant defense system serving as the ROS scavengers [33,39].

The specific redox situation prevails in the endoplasmic reticulum (ER) of β-cells since ROS are involved in oxidation during insulin folding in β-cells (Fig. 1). Each proinsulin molecule folded at ER generates 3 molecules of H_2O_2 [40]. This is generated during protein disulfide isomerase oxidoreductase (PDI) reoxidation by ER oxidoreductin 1 (ERO1), which are involved in insulin folding. High amounts of H_2O_2 with limited efflux from ER and a low ratio of reduced to oxidized glutathione (GSH/GSSG) create a strong oxidative milieu in the ER of β-cells [41]. In the case of chronic nutrient excess, e.g., obesity, when β-cells struggle to maintain glucose homeostasis in the body by overproduction of insulin (hyperinsulinemia), ER stress develops [42]. This is associated with an imbalance in redox status in ER and leads to β-cell exhaustion over time.

The inappropriate composition of nutrition and especially its chronic overload leads not only to an increase in blood glucose levels but also to an increase in fatty acid levels circulating in the bloodstream, being sensed by β-cells. Under conditions of increased circulation of fatty acids in the blood, long-chain and medium-chain fatty acids can produce H_2O_2 during their β-oxidation in peroxisomes and mitochondria, where little catalase is present [41] (Fig. 1). The β-oxidation in

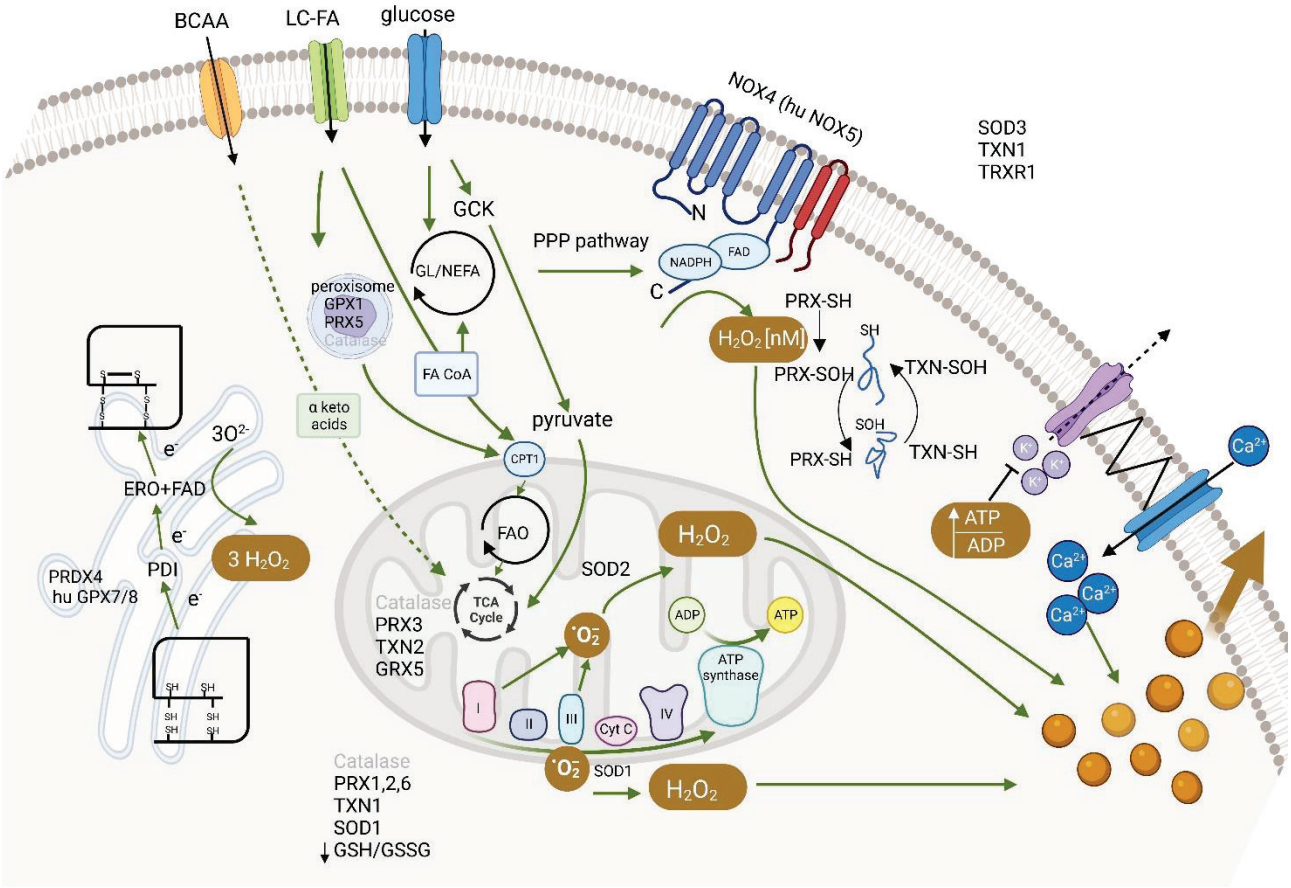

Fig. 1. Physiological amplification of insulin secretion by redox signaling in pancreatic β-cells. Glucose, the major trigger of insulin secretion, initiates glycolysis while being phosphorylated by glucokinase (GCK). As it proceeds, the metabolites also enter the pentose phosphate cycle (PPP), which generates NADPH in the cytosol, the substrate for NADPH oxidase 4 or human isoform 5 (NOX4, hu NOX5). Pyruvate, the product of glycolysis, enters the mitochondria to generate ATP and possibly superoxide ($^{\bullet}O_2$-) on Complex III directed out of the mitochondria. Glycerol-3-phosphate derived from glycolysis is involved in lipogenesis in β-cells. Stimulation by glucose leads to increased activity of NOX4/hu NOX5, generating H_2O_2, which at nM concentration is involved in redox relay signaling to target proteins involving peroxiredoxins (PRX) and thioredoxins (TXN). Redox signaling, H_2O_2 directly, and together with increased ATP lead to inhibition of the K_{ATP} channel, causing plasma membrane depolarization, calcium influx, and insulin granule release. Stimulation by glucose also increases endoplasmic reticulum (ER) activity, where folding of proinsulin requires a pro-oxidant environment, i.e., 3 molecules of H_2O_2 per 1 proinsulin. The presence of long-chain fatty acids (LC-FA) allows their accumulation in lipid droplets or, at low glucose, fatty acid oxidation (FAO) in mitochondria or peroxisomes, potentially generating ROS. Branched chain amino acids (BCAA) exhibit insulinotropic effects through α-keto acid metabolism, TCA cycling in mitochondria with the potential for ROS production. Pancreatic β-cells show low expression of catalase and glutathione peroxidases but express various forms of thioredoxins (TXN), peroxiredoxin (PRX), and superoxide dismutases (SOD) compartmentalized intracellularly. Created with Biorender.com.

peroxisomes produces H_2O_2 and shortens the length of the fatty acid chain before it is passed to mitochondria for complete oxidation, another site of ROS production [42]. Thus, mitochondria are functionally linked to peroxisomes in fatty acid processing. Chronically elevated concentrations of free fatty acids termed lipotoxicity together with hyperglycemia (often associated with diabetes) cause the impairment of insulin secretion and β-cell death. Another insulinotropic potentiator of β-cell is selected amino acids. The state of elevated dietary branched-chain amino acids (BCAAs) such as leucine, isoleucine, and valine, plays a critical role in stimulating insulin secretion by serving as both metabolic fuel and allosteric activator of glutamate dehydrogenase [43,44] (Fig. 1). Its acute action stimulates insulin secretion *via* direct inhibition of K_{ATP} channel currents in β-cells [45], where ROS may be part of the signaling action originating from mitochondria or NADPH oxidases [23,46].

Thus, it is clear that redox status reflects the nutritional conditions to which β-cells are subjected. The major signaling molecule is H_2O_2. Its involvement in redox signaling is required for efficient insulin secretion and function while its long-term increase leads to development of oxidative stress accompanying the development of diabetes.

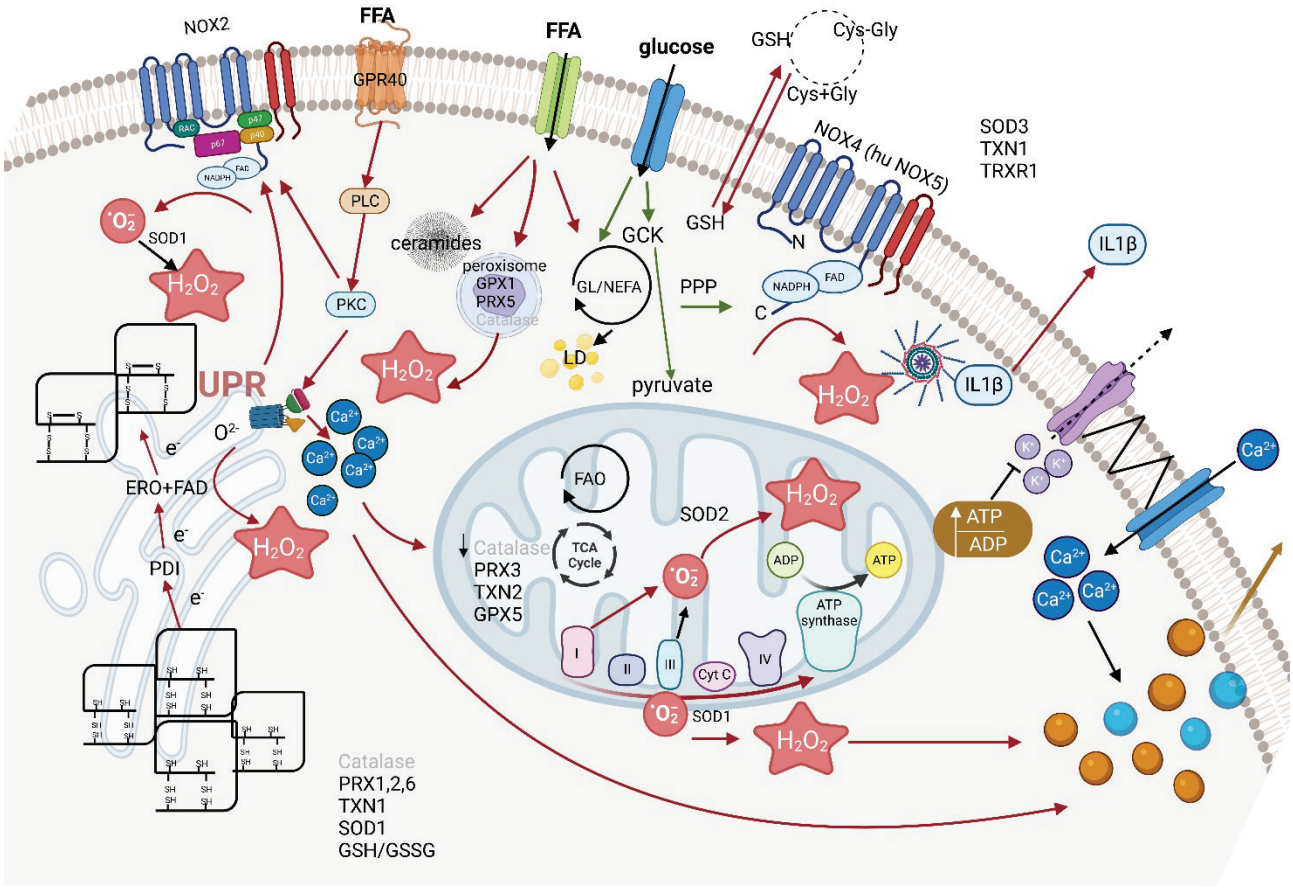

Fig. 2. Detrimental prooxidative intracellular environment upon chronic nutrient overload in pancreatic β-cells. Chronic hyperglycemia activates NADPH oxidase 4, which leads to increased assembly of inflammasome and maturation of IL1β, initiating local inflammation. Increased requirement for insulin secretion and enhanced pro-oxidative milieu in cytoplasm establish unfolded protein response (UPR), which is accompanied by oxidative stress in endoplasmic reticulum (ER). Increased amount of proinsulin is secreted (blue circles). Increased amount of free fatty acids (FFA) in plasma induces ceramide accumulation with the potential to induce apoptosis. FFA also signal through the GPR40 receptor to induce the activity of phospholipase C (PLC), protein kinase C (PKC) to regulate NADPH oxidase 2 (NOX2) to produce ROS and contribute to calcium release from ER for insulin granule release. FFA also enter peroxisomes for FAO, generating enhanced ROS because of the low expression of catalase. Prooxidative intracellular environment induces the degradation of glutathione outside of the cells to produce components for its synthesis inside the cells. Created with Biorender.com.

NOXs are good and evil in the redox homeostasis of pancreatic β-cells

There is an increasing number of reports showing that NOXs are significantly involved in β-cells physiology and pathology. They are essential regulators of physiological insulin secretion and promote superoxide/H_2O_2 for efficient signaling of insulin secretion. At the same time, they can have deleterious effects when chronically overactivated. There is ample evidence for the specific expression of isoforms of NOX1, NOX2, NOX4, and p22phox and their cytosolic regulators in rodent and human β-cells [43,44]. NOX5 is expressed only in human β-cells and no homolog was found in rats and mice [45]. Regarding its role and activity in β-cells, it was revealed that knocking down p47phox, the subunit of the originally phagocytic NOX2 isoform, significantly reduced glucose-induced H_2O_2 production and insulin secretion (GSIS) [46]. However, direct ablation of NOX2 in mice showed no impairment of GSIS. Until recently, many studies using nonspecific inhibitors also failed to shed light on the function of NOXs in β-cells [44,47]. Recently, we found that the NOX4 isoform, which is constitutively expressed and lacks many regulatory subunits present in other isoforms, is metabolically stimulated to activity, resulting in H_2O_2 production that supports GSIS [11] (Fig. 1). This was previously demonstrated with the nonspecific NOX4 inhibitor GLX351322 [48]. Its activity depends on the amount of NADPH normally derived from glucose metabolism in the vicinity of the enzyme. Unfortunately, the exact intracellular location in β-cells has not yet been defined due to a lack of reliable antibodies. However, NOXs are transmembrane proteins that transport electrons across biological membranes and reduce oxygen to superoxide or directly produce H_2O_2 (more in

[49]). Inhibition of NOX4 either by silencing of cultured β-cells or its ablation, specifically in mouse pancreatic β-cells, significantly increased the probability of K_{ATP} channel opening, thereby reducing the first phase of GSIS in particular [11]. Interestingly, β-cell specific *Nox4* knockout animals show suppressed insulin secretion upon glucose stimulation and constantly secrete low levels of insulin, prolonging the time needed to establish normoglycemia. This affects the feeding habits of these knock-out mice, as they consume less food to maintain the physiological glucose concentration [50]. NOX4 is thus an important redox molecule in the physiology of pancreatic β-cells. Recently, human NOX5 was also found to be important for proper GSIS [45].

However, NOXs may also contribute to β-cell dysfunction in chronic hyperglycemia in animals and humans with type 2 diabetes (T2D) (Fig. 2). Chronic overeating activates NOXs to produce superoxide/H_2O_2, leading to long-term oxidative stress and consequent β-cell damage and apoptosis [4,51]. Proinflammatory, hyperglycemic, and lipotoxic conditions have been shown to activate NOXs [11,52-55]. Gene expression profiling of islets from patients with T2D also showed increased expression of *NOX2/4/5* compared with nondiabetic individuals (Geoprofiles GDS3382). Proinflammatory cytokines upregulate the expression of 12-lipoxygenase, which can activate NOX1 in β-cells, leading to their failure [56,57]. Lipotoxicity, particularly from saturated free fatty acids, induces NOX2 activity, leading to impaired insulin secretion, calcium homeostasis, and viability [54]. It has been shown that GPR40, the free fatty acid receptor, can also activate NOX2 in β-cells [58]. Thus excess palmitate activates NOX2 triggering transient receptor potential melastatin 2 (TRPM2) channels. This can lead to an increase in mitochondrial zinc ions, resulting in a loss of membrane potential and mitochondrial fission, affecting energy metabolism and thus β-cell viability [53]. Upregulation of NOX5 has been shown to worsen insulin secretion under hyperglycemic/diabetogenic (palmitate-induced) conditions by increasing the depletion of cAMP, a critical enhancer component of insulin secretion [45]. We have observed that chronic overnutrition induced either by high-fat diet *in vivo* or by hyperglycemia *in vitro*, causes chronic activation of NOX4 and establishes an intracellular pro-oxidant status [50]. This leads to the assembly and activation of the inflammasome and further maturation of the proinflammatory interleukin 1β (IL1β). The release of IL1β from β-cells can then activate macrophages toward proinflammation, causing local inflammation (Fig. 2). Thus, chronic overproduction of ROS by NOXs in β-cells leads to their pathology and eventual loss of viability. Recent reports have shown that islets from *Nox2* knockout mice improved islet transplantation outcome. *Nox2*$^{-/-}$ islets showed decreased superoxide production, higher GSIS, and enhanced antioxidant defense by increased expression of Nrf2, and Sod1, improved Ho1 expression causing early revascularization. This leads to restoration of normoglycemia in diabetic transplanted mice [59].

New inhibitors of specific NOX isoforms have been developed and are being investigated in the treatment of diabetes (more in [60]). Many diabetic complications such as diabetic nephropathy, retinopathy, neuropathy, and cardiopathy, collectively termed diabetic vasculopathy, have been associated with chronic NOX activity. NOXs, especially NOX2 and 4, have been associated with endothelial dysfunction and are the target of the studies. However, the role of NOX overactivation and prooxidant signaling in pancreatic β-cells under conditions of chronic overeating require the development of antioxidants or inhibitors that target β-cells only. Their short-term treatment could be useful in restoring β-cell signaling and viability during the development of diabetes.

Pancreatic β-cells antioxidant defense system: Are β-cells so vulnerable towards oxidative stress?

Cellular antioxidant defense comprises enzymatic machinery and glutathione (GSH), which can buffer excessive reactive (oxygen, nitrogen, and sulfur) species produced by cellular metabolism. Cellular compartments differ in their pH, redox potential, and concentrations of reactive metabolites allowing redox signaling events or direct usage of these reactive compounds for metabolic reactions (e.g. protein folding in ER) in a specifically compartmentalized manner [61,62]. Consequently, the antioxidant enzymes are also strictly compartmentalized, with specific isoforms of the enzymes in these compartments. Also, the content of glutathione redox couple i.e., GSH/GSSG (reduced/oxidized glutathione) and its redox potential, differs throughout the compartments [63,64]. The difference is given not only by the diverse NADPH concentration and availability, ROS production, and expression of antioxidant enzymes but also because GSH is only synthesized in cytosol and can be only transported through the membranes in its reduced form [65]. Notably, the compartment-specific redox state of GSH affects not only the direct redox GSH partners but

also the specialized function given by the respective organelle [66]. GSH is synthesized by a two-step enzymatic reaction involving γ-glutamylcysteine synthetase (γ-GCS) and GSH synthetases (GSHS) in sequence. γ-GCS catalyzes the formation of the dipeptide γ-glutamylcysteine (γ-Glu-Cys), and GSHS catalyzes the binding of glycine to γ-Glu-Cys to form GSH [67]. The rate-limiting step of the synthesis is the presence of cysteine, which is mainly derived from the trans-sulfuration pathway of methionine and/or the reduction of cystine, which is transported from the extracellular space [67]. Except for these traditional pathways, a study done by Fu *et. al.* revealed that 25 % of carbon derived from glucose in human islets is directed to GSH synthesis *via* pyruvate carboxylase pathway and probably glutamate [68]. The degradation of GSH occurs in extracellular space, where it is converted to cysteinylglycine (CysGly) and then to Cys at tissue sites rich in the ectoenzymes γ-glutamyltranspeptidase (γ-GT) and dipeptidases (mainly kidney and lung) by the sequential action of these two enzymes [69] (Fig. 2). The amino acids can be taken by the cells again and used for GSH *de novo* biosynthesis. Interestingly pancreatic β-cells express significantly higher amounts of GSH degradation enzymes than those of the synthesis pathway, and as a result, rely on glutathione transferred from the liver [70].

From the historical perspective, β-cells were considered to contain low amounts of the main antioxidant enzymes [71,72] (Fig. 1). Still, this feature has always been compared with the liver and kidney, specialized organs for detoxification, which naturally contain high amounts of antioxidant enzymes [71]. An explanation for the low expression profile is nowadays interpreted by the fact that redox signaling, which is tightly associated with glucose sensing and its metabolism in pancreatic β-cells, is a required coupling factor for insulin secretion [11].

Superoxide dismutase (SOD) is considered one of the most important antioxidant enzymes. The enzyme accelerates the otherwise spontaneous dismutation of superoxide anion O^{2-} to less reactive H_2O_2 up to 10^4 [73]. SOD exists in three isoforms, whose activity is optimized according to the compartment-specific conditions. *Cu/Zn-SOD1* is expressed in the cytosol, the mitochondrial intermembrane space, the peroxisomes, and the nucleus. *Mn-SOD2* is expressed in the mitochondrial matrix, and Cu/Zn-SOD3 is targeted to extracellular space, but its expression in β-cells has only been detected on the mRNA level [74]. In addition to SODs other H_2O_2 degrading enzymes are expressed in β-cells. Interestingly, catalase is expressed at a very low level and is even considered one of the disallowed genes in β-cells [75]. Glutathione peroxidase 1 (*GPX1*) is expressed in cytosol and peroxisomes, *GPX7/8* and *PRDX4* in ER, and *PRDX3* exclusively in mitochondria [40]. However, the expression profile also depends on species, as *GPX1* and catalase were shown to have protective effects in human pancreatic islets but not in rodents [76]. In recent years the opinion of oxidative damage vulnerable β-cells is shifting as β-cells were shown to express thioredoxin (*TXN*) and thioredoxin reductase (*TXNRD*) isoforms, glutathione reductases (*GSR*), glutaredoxins (*GRX*), and peroxiredoxins (*PRDX*) [34,77-82].

Interestingly it has also been shown that cells are able to secrete oxidoreductases to extracellular milieu [83]. This phenomenon has been first observed for immune cells, but secretion of cytoplasmic isoforms of TXN1 and TXNRD1 by murine and porcine β-cells has been revealed under hypoxic and inflammatory conditions [84]. Extracellular TXN1 seems to cause autocrine or paracrine regulation of β-cells, overall having beneficial effect by improving cell viability and blood glucose control, preventing apoptosis, and preserving insulin secretion [84,85].

The β-cells therefore possess delicate redox balance in which a rich antioxidant system is involved. This enables effective redox signaling. Nevertheless, β-cells do not have such a robust antioxidant system and are therefore unable to withstand prolonged oxidative stress, leading to a deterioration in their function and ultimately contributing to the onset of diabetes.

Redox status in other endocrine cells of pancreatic islets

β-cells are the most studied and represented cell type of the pancreatic islets. However, there are other important endocrine cell types that are required for proper islet function. These are glucagon-producing α-cells, somatostatin-producing δ-cells, ghrelin-producing ε-cells, and pancreatic polypeptide-producing PP cells. There is little knowledge about these endocrine cells in terms of their redox status and signal transduction. However, their synchronized paracrine function with the β-cells is critical for proper islet activity. Cell lines of individual type of endocrine cells are scarce (this does not apply to α-cells, for which a cell line already exists), and individual cell types are difficult to isolate from islets, which probably explains the lack of knowledge [86]. Moreover, redox status setting of cell lines might differ from primary endocrine cells as the cell lines are adapted to cultivation conditions which significantly vary in terms of oxygen pressure, glucose levels etc.

As α-cells are the second best studied cell type after β-cells, pertinent information exists about their antioxidant capacity. Human α-cells are capable producers of antioxidant enzymes such as catalase and GPX. Interestingly, human α-cells express more of these enzymes than human β-cells. β-cells showed increased oxidative damage to DNA and decreased viability when exposed to H_2O_2 and NO donors, whereas α-cells showed no change in viability [87]. Expression of antioxidant enzymes is clearly associated with enhanced protection of α-cells from oxidative stress. In addition, the pancreas of T2D patients exhibited increased numbers of apoptotic β-cells but not α-cells [88]. However, both endocrine cell types showed increased volume density of ER [89]. Moreover, the better survival of α-cells in T1D was explained by differences in the expression of SOD2 compared to β-cells, in addition to the specificity of the immune response [90]. On the other hand, mouse cell cultures of α- and β-cells showed increased expression of mitochondrial *SOD* and catalase in β-cells under hyperglycemic conditions. In α-cells, these enzymes are decreased [91]. The question here is whether the difference in expression of these enzymes is due to species or to the different effects and timing of the various oxidants. Inhibition of phosphoinositide 3-kinases (PI3K) signaling in α-cells does reduce mitochondrial *SOD* expression under hyperglycemic conditions, suggesting that this pathway is involved in mitochondrial *SOD* expression [91].

Thus, we lack the knowledge about the paracrine redox signaling and involvement of redox status within individual endocrine cell types in synchronized action of insulin and other endocrine hormones secretion by pancreatic islet.

Heterogeneity of β-cells and the role of redox status

Pancreatic β-cells exhibit considerable heterogeneity, contributing to the complexity of islets [92]. Distinct subpopulations differ at the molecular, morphological, and functional levels [93,94]. Most importantly, individual β-cells have diverse sensitivity to glucose, which subsequently affects their ability to synthesize and secrete insulin [95,96]. Thus, the heterogeneity of β-cells and β-cell intercommunication within subpopulations is critical for the regulation of insulin secretion [94,97]. Changes in β-cell heterogeneity as well as altered redox homeostasis have been associated with T2D, however, their interconnection is far from being understood [98,99].

The origins of β-cell heterogeneity research go far back in history. Already in the 1940s, it was found that β-cell size differs between large and small pancreatic islets [100]. Later, regional differences in the nuclear size and the position of the nucleoli within the nuclei of various β-cells were identified [101]. Also, morphological differences in response to glucose stimulation were described with regards to β-cell localization. Hyperglycemia decreased the volume density of β-cell secretory granules and increased the size of the endoplasmic reticulum and Golgi apparatus earlier in β-cells within the core of the islets compared to the peripheral β-cells [102]. The distinct insulin secretory patterns broadly divided β-cells into two types – responsive and unresponsive [103]. The differences in insulin secretory response were also associated with altered gene expression of important enzymes, such as glucokinase [104]. Recently, it has been described that insulin secretion responses were orchestrated by two populations of cells: hub cells with pacemaker properties dictating the insulin secretion dynamics and follower cells controlled by the hubs through calcium waves [105]. The development of molecular methods has enabled the identification of many markers specific to distinct β-cell populations, including E-cadherin (CDH1) [106]; polysialylated-neural cell adhesion molecule (PSA-NCAM) [107]; Flattop (FLTP) [108]; CD9 molecule (CD9) [109,110]; ST8 alpha-N-acetyl-neuraminide alpha-2,8-sialyltransferase1 (ST8SIA1) [110]; Dickkopf WNT signaling pathway inhibitor 3 (DKK3) [111]; solute carrier family 18 member (A2SLC18A2/VMAT2) [112].

For instance, β-cells can be divided into two sub-populations with different glucose responsiveness according to the level of surface PSA-NCAM, a prominent marker of functional β-cells [107]. Low PSA-NCAM-labeled β-cell population (β^{low}-cells) exhibited altered gene expression profile (e.g. downregulation of *Neurod1, Pdx1, Nkx6.1, Pax6*, i.e. β-cell identity genes; and upregulation of *Ldha, Hk1m*, i.e. β-cell forbidden genes) which suggested that these cells were composed of immature and/or non-functional cells in contrast to high PSA-NCAM-labeled population (β^{high}-cells). Moreover, these two populations also differed in the expression of antioxidant enzymes. For example, *Gpx1* was upregulated, while *Sod2* and *Trx2* were significantly downregulated in β^{low}-cells. Besides antioxidant enzymes, the expression of nitric oxide synthase 1 (*Nos1*) was also decreased [107]. These results indicate extensive dysregulation of the redox state in the poorly glucose-responsive β-cells. Importantly, the distribution of β^{high} and β^{low}-cells was completely inversed in ZDF rats (a genetic model of T2D) as the

β^{low}-cells became the predominant population in these animals [107]. In ST8SIA1+ β-cells, which are also less responsive to glucose compared to ST8SIA1-β-cells, *Gpx3* was significantly enriched. Representation of these cells was found to be abnormally high in T2D islets [110].

Although subpopulations of β-cells have been shown to differ in redox homeostasis in response to altered metabolism, redox regulations independent of β-cell heterogeneity have also been reported. Inhibition of NOX4 protected human islets from glucolipotoxicity regardless of their size, activity, and reactivity to glucose. These results suggested that NOX4-induced β-cell death occurs in all types of islets and may involve a mechanism that acts independently of the insulin-releasing activity of the islet [113].

Since redox homeostasis is a key factor determining β-cell fate, identification of differences in redox regulations in distinct populations of β-cells is required to unravel the role of β-cell heterogeneity in the physiology and pathology of pancreatic islets. Our laboratory focuses on this topic. This knowledge could potentially lead to novel therapeutic approaches to restoring β-cell function and mass.

Interestingly, α-cells were reported also in several distinct subpopulations based on proglucagon-derived peptides [114]. It was suggested to be reflected by the α-cell maturity state. However, no link to the redox state was reported.

Conclusions

There is no doubt that redox status is a critical determinant of pancreatic β-cell function. Their fragile redox homeostasis is a key part of nutrition-induced insulin signaling. However, long-term chronic nutritional overload leading to metabolic dysregulation impairs insulin secretion, induce inflammation, and consequently glucose homeostasis in the body. This leads to the development of T2D. It is important to decipher the mechanisms of balanced homeostasis and its disruption leading to oxidative stress and subsequent dysregulation of signaling in pancreatic β-cells. It is known that to maintain glycemic control and reduce oxidative stress and inflammation, restrained caloric intake and physical activity show the strongest beneficial effects. Chronic physical activity reduces ROS production, increases antioxidant potential, and improves insulin sensitivity. However, we must also define how to act in the prediabetic phase, when the first glucose imbalance occurs. To do this, we need to determine the right targets and timing for ROS production in pancreatic β-cells. NOXs in pancreatic β-cells in prediabetic conditions could be one of them for pharmacotherapy.

Conflict of Interest

There is no conflict of interest.

Acknowledgements

This work was supported by the Grant Agency of the Czech Republic, grant No. 22-11439S to L.P.-H. and by the project National Institute for Research of Metabolic and Cardiovascular Diseases (Programme EXCELES, ID Project No. LX22NPO5104) – Funded by the European Union Next Generation EU to the Institute of Physiology. All figures were created in Biorender.com, thus we kindly acknowledge the software.

References

1. Jonas JC, Bensellam M, Duprez J, Elouil H, Guiot Y, Pascal SM. Glucose regulation of islet stress responses and beta-cell failure in type 2 diabetes. Diabetes Obes Metab 2009;11(Suppl 4):65-81. https://doi.org/10.1111/j.1463-1326.2009.01112.x
2. Benáková Š, Holendová B, Plecitá-Hlavatá L. Redox Homeostasis in Pancreatic β-Cells: From Development to Failure. Antioxidants (Basel) 2021;10:526. https://doi.org/10.3390/antiox10040526
3. Nishikawa T, Araki E. Impact of mitochondrial ROS production in the pathogenesis of diabetes mellitus and its complications. Antioxid Redox Signal 2007;9:343-353. https://doi.org/10.1089/ars.2006.1458
4. Newsholme P, Morgan D, Rebelato E, Oliveira-Emilio HC, Procopio J, Curi R, Carpinelli A. Insights into the critical role of NADPH oxidase(s) in the normal and dysregulated pancreatic beta cell. Diabetologia 2009;52:2489-2498. https://doi.org/10.1007/s00125-009-1536-z
5. Roma LP, Jonas JC. Nutrient Metabolism, Subcellular Redox State, and Oxidative Stress in Pancreatic Islets and beta-Cells. J Mol Biol 2020;432:1461-1493. https://doi.org/10.1016/j.jmb.2019.10.012
6. Pi J, Bai Y, Zhang Q, Wong V, Floering LM, Daniel K, Reece JM, Deeney JT, Andersen ME, Corkey BE, Collins S. Reactive Oxygen Species as a Signal in Glucose-Stimulated Insulin Secretion. Diabetes 2007;56:1783-1791. https://doi.org/10.2337/db06-1601

7. Plecita-Hlavata L, Engstova H, Jezek J, Holendova B, Tauber J, Petraskova L, Kren V, Jezek P. Potential of Mitochondria-Targeted Antioxidants to Prevent Oxidative Stress in Pancreatic beta-cells. Oxid Med Cell Longev 2019;2019:1826303. https://doi.org/10.1155/2019/1826303
8. Robertson RP. Chronic oxidative stress as a central mechanism for glucose toxicity in pancreatic islet beta cells in diabetes. J Biol Chem 2004;279:42351-42354. https://doi.org/10.1074/jbc.R400019200
9. Ihara Y, Toyokuni S, Uchida K, Odaka H, Tanaka T, Ikeda H, Hiai H, Seino Y, Yamada Y. Hyperglycemia causes oxidative stress in pancreatic beta-cells of GK rats, a model of type 2 diabetes. Diabetes 1999;48:927-932. https://doi.org/10.2337/diabetes.48.4.927
10. Bindokas VP, Kuznetsov A, Sreenan S, Polonsky KS, Roe MW, Philipson LH. Visualizing Superoxide Production in Normal and Diabetic Rat Islets of Langerhans. J Biol Chem 2003;278:9796-9801. https://doi.org/10.1074/jbc.M206913200
11. Plecita-Hlavata L, Jaburek M, Holendova B, Tauber J, Pavluch V, Berkova Z, Cahova M, Schroeder K, Brandes RP, Siemen D, Jezek P. Glucose-Stimulated Insulin Secretion Fundamentally Requires H2O2 Signaling by NADPH Oxidase 4. Diabetes 2020;69:1341-1354. https://doi.org/10.2337/db19-1130
12. Plecitá-Hlavatá L, Engstová H, Holendová B, Tauber J, Špaček T, Petrásková L, Křen V, Špačková J, Gotvaldová K, Ježek J, Dlasková A, Smolková K, Ježek P. Mitochondrial Superoxide Production Decreases on Glucose-Stimulated Insulin Secretion in Pancreatic β Cells Due to Decreasing Mitochondrial Matrix NADH/NAD(+) Ratio. Antioxid Redox Signal 2020;33:789-815. https://doi.org/10.1089/ars.2019.7800
13. Wolff SP, Dean RT. Glucose autoxidation and protein modification. The potential role of 'autoxidative glycosylation' in diabetes. Biochem J 1987;245:243-250. https://doi.org/10.1042/bj2450243
14. Koya D, King GL. Protein kinase C activation and the development of diabetic complications. Diabetes 1998;47:859-866. https://doi.org/10.2337/diabetes.47.6.859
15. Lee TS, Saltsman KA, Ohashi H, King GL. Activation of protein kinase C by elevation of glucose concentration: proposal for a mechanism in the development of diabetic vascular complications. Proc Natl Acad Sci U S A 1989;86:5141-5145. https://doi.org/10.1073/pnas.86.13.5141
16. Inoguchi T, Battan R, Handler E, Sportsman JR, Heath W, King GL. Preferential elevation of protein kinase C isoform beta II and diacylglycerol levels in the aorta and heart of diabetic rats: differential reversibility to glycemic control by islet cell transplantation. Proc Natl Acad Sci U S A 1992;89:11059-11063. https://doi.org/10.1073/pnas.89.22.11059
17. Ishii H, Jirousek MR, Koya D, Takagi C, Xia P, Clermont A, Bursell SE, Kern TS, Ballas LM, Heath WF, Stramm LE, Feener EP, King GL. Amelioration of vascular dysfunctions in diabetic rats by an oral PKC beta inhibitor. Science 1996;272:728-731. https://doi.org/10.1126/science.272.5262.728
18. Brownlee M. Biochemistry and molecular cell biology of diabetic complications. Nature 2001;414:813-820. https://doi.org/10.1038/414813a
19. Ly LD, Xu S, Choi SK, Ha CM, Thoudam T, Cha SK, Wiederkehr A, Wollheim CB, Lee IK, Park KS. Oxidative stress and calcium dysregulation by palmitate in type 2 diabetes. Exp Mol Med 2017;49:e291. https://doi.org/10.1038/emm.2016.157
20. Lin N, Chen H, Zhang H, Wan X, Su Q. Mitochondrial reactive oxygen species (ROS) inhibition ameliorates palmitate-induced INS-1 beta cell death. Endocrine 2012;42:107-117. https://doi.org/10.1007/s12020-012-9633-z
21. Graciano MFR, Valle MMR, Kowluru A, Curi R, Carpinelli AR. Regulation of insulin secretion and reactive oxygen species production by free fatty acids in pancreatic islets. Islets 2011;3:213-223. https://doi.org/10.4161/isl.3.5.15935
22. Gehrmann W, Elsner M, Lenzen S. Role of metabolically generated reactive oxygen species for lipotoxicity in pancreatic β-cells. Diabetes, Obesity and Metabolism 2010;12:149-158. https://doi.org/10.1111/j.1463-1326.2010.01265.x
23. Li N, Frigerio F, Maechler P. The sensitivity of pancreatic beta-cells to mitochondrial injuries triggered by lipotoxicity and oxidative stress. Biochem Soc Trans 2008;36:930-934. https://doi.org/10.1042/BST0360930
24. Ježek P, Holendová B, Jabůrek M, Dlasková A, Plecitá-Hlavatá L. Contribution of Mitochondria to Insulin Secretion by Various Secretagogues. Antioxid Redox Signal 2022;36:920-952. https://doi.org/10.1089/ars.2021.0113

25. Lortz S, Gurgul-Convey E, Lenzen S, Tiedge M. Importance of mitochondrial superoxide dismutase expression in insulin-producing cells for the toxicity of reactive oxygen species and proinflammatory cytokines. Diabetologia 2005;48:1541-1548. https://doi.org/10.1007/s00125-005-1822-3
26. Escribano-Lopez I, Bañuls C, Diaz-Morales N, Iannantuoni F, Rovira-Llopis S, Gomis R, Rocha M, Hernandez-Mijares A, Murphy MP, Victor VM. The Mitochondria-Targeted Antioxidant MitoQ Modulates Mitochondrial Function and Endoplasmic Reticulum Stress in Pancreatic β Cells Exposed to Hyperglycaemia. Cell Physiol Biochem 2019;52:186-197. https://doi.org/10.33594/000000013
27. Edalat A, Schulte-Mecklenbeck P, Bauer C, Undank S, Krippeit-Drews P, Drews G, Düfer M. Mitochondrial succinate dehydrogenase is involved in stimulus-secretion coupling and endogenous ROS formation in murine beta cells. Diabetologia 2015;58:1532-1541. https://doi.org/10.1007/s00125-015-3577-9
28. Barlow J, Affourtit C. Novel insights into pancreatic β-cell glucolipotoxicity from real-time functional analysis of mitochondrial energy metabolism in INS-1E insulinoma cells. Biochem J 2013;456:417-426. https://doi.org/10.1042/BJ20131002
29. Sarre A, Gabrielli J, Vial G, Leverve XM, Assimacopoulos-Jeannet F. Reactive oxygen species are produced at low glucose and contribute to the activation of AMPK in insulin-secreting cells. Free Radic Biol Med 2012;52:142-150. https://doi.org/10.1016/j.freeradbiomed.2011.10.437
30. Barlow J, Hirschberg Jensen V, Affourtit C. Uncoupling protein-2 attenuates palmitoleate protection against the cytotoxic production of mitochondrial reactive oxygen species in INS-1E insulinoma cells. Redox Biol 2015;4:14-22. https://doi.org/10.1016/j.redox.2014.11.009
31. Mailloux RJ, Fu A, Robson-Doucette C, Allister EM, Wheeler MB, Screaton R, Harper M-E. Glutathionylation State of Uncoupling Protein-2 and the Control of Glucose-stimulated Insulin Secretion. J Biol Chem 2012;287:39673-39685. https://doi.org/10.1074/jbc.M112.393538
32. Pi J, Collins S. Reactive oxygen species and uncoupling protein 2 in pancreatic β-cell function. Diabetes Obes Metab 2010;12(Suppl 2):141-148. https://doi.org/10.1111/j.1463-1326.2010.01269.x
33. Holendova B, Plecita-Hlavata L. Cysteine residues in signal transduction and its relevance in pancreatic beta cells. Front Endocrinol (Lausanne) 2023;14:1221520. https://doi.org/10.3389/fendo.2023.1221520
34. Stancill JS, Corbett JA. The Role of Thioredoxin/Peroxiredoxin in the β-Cell Defense Against Oxidative Damage. Front Endocrinol (Lausanne) 2021;12:718235. https://doi.org/10.3389/fendo.2021.718235
35. Ransy C, Vaz C, Lombès A, Bouillaud F. Use of H(2)O(2) to Cause Oxidative Stress, the Catalase Issue. Int J Mol Sci 2020;21. https://doi.org/10.3390/ijms21239149
36. Bienert GP, Chaumont F. Aquaporin-facilitated transmembrane diffusion of hydrogen peroxide. Biochim Biophys Acta 2014;1840:1596-1604. https://doi.org/10.1016/j.bbagen.2013.09.017
37. Lenzen S, Lushchak VI, Scholz F. The pro-radical hydrogen peroxide as a stable hydroxyl radical distributor: lessons from pancreatic beta cells. Arch Toxicol 2022;96:1915-1920. https://doi.org/10.1007/s00204-022-03282-6
38. Poole LB. The basics of thiols and cysteines in redox biology and chemistry. Free Radic Biol Med 2015;80:148-157. https://doi.org/10.1016/j.freeradbiomed.2014.11.013
39. Winterbourn CC, Hampton MB. Thiol chemistry and specificity in redox signaling. Free Radic Biol Med 2008;45:549-561. https://doi.org/10.1016/j.freeradbiomed.2008.05.004
40. Lenzen S. Chemistry and biology of reactive species with special reference to the antioxidative defence status in pancreatic β-cells. Biochim Biophys Acta Gen Subj 2017;1861:1929-1942. https://doi.org/10.1016/j.bbagen.2017.05.013
41. Konno T, Pinho Melo E, Lopes C, Mehmeti I, Lenzen S, Ron D, Avezov E. ERO1-independent production of H2O2 within the endoplasmic reticulum fuels Prdx4-mediated oxidative protein folding. J Cell Biol 2015;211:253-259. https://doi.org/10.1083/jcb.201506123
42. Cnop M, Ladrière L, Igoillo-Esteve M, Moura RF, Cunha DA. Causes and cures for endoplasmic reticulum stress in lipotoxic β-cell dysfunction. Diabetes Obes Metab 2010;12(Suppl 2):76-82. https://doi.org/10.1111/j.1463-1326.2010.01279.x
43. Oliveira HR, Verlengia R, Carvalho CR, Britto LR, Curi R, Carpinelli AR. Pancreatic beta-cells express phagocyte-like NAD(P)H oxidase. Diabetes 2003;52:1457-1463. https://doi.org/10.2337/diabetes.52.6.1457

44. Uchizono Y, Takeya R, Iwase M, Sasaki N, Oku M, Imoto H, Iida M, Sumimoto H. Expression of isoforms of NADPH oxidase components in rat pancreatic islets. Life Sci 2006;80:133-139. https://doi.org/10.1016/j.lfs.2006.08.031
45. Bouzakri K, Veyrat-Durebex C, Holterman C, Arous C, Barbieux C, Bosco D, Altirriba J, Alibashe M, Tournier BB, Gunton JE, Mouche S, Bietiger W, Forterre A, Berney T, Pinget M, Christofori G, Kennedy C, Szanto I. Beta-Cell-Specific Expression of Nicotinamide Adenine Dinucleotide Phosphate Oxidase 5 Aggravates High-Fat Diet-Induced Impairment of Islet Insulin Secretion in Mice. Antioxid Redox Signal 2020;32:618-635. https://doi.org/10.1089/ars.2018.7579
46. Morgan D, Rebelato E, Abdulkader F, Graciano MFR, Oliveira-Emilio HR, Hirata AE, Rocha MS, Bordin S, Curi R, Carpinelli AR. Association of NAD(P)H Oxidase with Glucose-Induced Insulin Secretion by Pancreatic β-Cells. Endocrinology 2009;150:2197-2201. https://doi.org/10.1210/en.2008-1149
47. Imoto H, Sasaki N, Iwase M, Nakamura U, Oku M, Sonoki K, Uchizono Y, Iida M. Impaired Insulin Secretion by Diphenyleneiodium Associated with Perturbation of Cytosolic Ca ²⁺ Dynamics in Pancreatic β-Cells. Endocrinology 2008;149:5391-5400. https://doi.org/10.1210/en.2008-0186
48. Anvari E, Wikström P, Walum E, Welsh N. The novel NADPH oxidase 4 inhibitor GLX351322 counteracts glucose intolerance in high-fat diet-treated C57BL/6 mice. Free Radic Res 2015;49:1308-1318. https://doi.org/10.3109/10715762.2015.1067697
49. Bedard K, Krause K-H. The NOX Family of ROS-Generating NADPH Oxidases: Physiology and Pathophysiology. Physiol Rev 2007;87:245-313. https://doi.org/10.1152/physrev.00044.2005
50. Holendova B, Benakova S, Krivonoskova M, Pavluch V, Tauber J, Gabrielova E, Jezek P, Plecita-Hlavata L. NADPH oxidase 4 in mouse beta cells participates in inflammation on chronic nutrient overload. Obesity (Silver Spring) 2024;32:339-351. https://doi.org/10.1002/oby.23956
51. Syed I, Kyathanahalli CN, Jayaram B, Govind S, Rhodes CJ, Kowluru RA, Kowluru A. Increased phagocyte-like NADPH oxidase and ROS generation in type 2 diabetic ZDF rat and human islets: role of Rac1-JNK1/2 signaling pathway in mitochondrial dysregulation in the diabetic islet. Diabetes 2011;60:2843-2852. https://doi.org/10.2337/db11-0809
52. Weaver JR, Grzesik W, Taylor-Fishwick DA. Inhibition of NADPH oxidase-1 preserves beta cell function. Diabetologia 2015;58:113-121. https://doi.org/10.1007/s00125-014-3398-2
53. Li F, Munsey TS, Sivaprasadarao A. TRPM2-mediated rise in mitochondrial Zn(2+) promotes palmitate-induced mitochondrial fission and pancreatic β-cell death in rodents. Cell Death Differ 2017;24:1999-2012. https://doi.org/10.1038/cdd.2017.118
54. Vilas-Boas EA, Nalbach L, Ampofo E, Lucena CF, Naudet L, Ortis F, Carpinelli AR, Morgan B, Roma LP. Transient NADPH oxidase 2-dependent H(2)O(2) production drives early palmitate-induced lipotoxicity in pancreatic islets. Free Radic Biol Med 2021;162:1-13. https://doi.org/10.1016/j.freeradbiomed.2020.11.023
55. Sato Y, Fujimoto S, Mukai E, Sato H, Tahara Y, Ogura K, Yamano G, Ogura M, Nagashima K, Inagaki N. Palmitate induces reactive oxygen species production and β-cell dysfunction by activating nicotinamide adenine dinucleotide phosphate oxidase through Src signaling. J Diabetes Investig 2014;5:19-26. https://doi.org/10.1111/jdi.12124
56. Weaver J, Taylor-Fishwick DA. Relationship of NADPH Oxidase-1 expression to beta cell dysfunction induced by inflammatory cytokines. Biochem Biophys Res Commun 2017;485:290-294. https://doi.org/10.1016/j.bbrc.2017.02.089
57. Weaver JR, Holman TR, Imai Y, Jadhav A, Kenyon V, Maloney DJ, Nadler JL, Rai G, Simeonov A, Taylor-Fishwick DA. Integration of pro-inflammatory cytokines, 12-lipoxygenase and NOX-1 in pancreatic islet beta cell dysfunction. Mol Cell Endocrinol 2012;358:88-95. https://doi.org/10.1016/j.mce.2012.03.004
58. Nunes Marsiglio-Librais G, Aparecida Vilas-Boas E, Carlein C, Hoffmann MDA, Roma LP, Carpinelli AR. Evidence for NADPH oxidase activation by GPR40 in pancreatic β-cells. Redox Rep 2020;25:41-50. https://doi.org/10.1080/13510002.2020.1757877
59. Wrublewsky S, Glas J, Carlein C, Nalbach L, Hoffmann MDA, Pack M, Vilas-Boas EA, Ribot N, Kappl R, Menger MD, Laschke MW, Ampofo E, Roma LP. The loss of pancreatic islet NADPH oxidase (NOX)2 improves islet transplantation. Redox Biol 2022;55:102419. https://doi.org/10.1016/j.redox.2022.102419

60. Laddha AP, Kulkarni YA. NADPH oxidase: A membrane-bound enzyme and its inhibitors in diabetic complications. Eur J Pharmacol 2020;881:173206. https://doi.org/10.1016/j.ejphar.2020.173206
61. Casey JR, Grinstein S, Orlowski J. Sensors and regulators of intracellular pH. Nat Rev Mol Cell Biol 2010;11:50-61. https://doi.org/10.1038/nrm2820
62. Jones DP, Go YM. Redox compartmentalization and cellular stress. Diabetes Obes Metab 2010;12(Suppl 2):116-125. https://doi.org/10.1111/j.1463-1326.2010.01266.x
63. Kemp M, Go YM, Jones DP. Nonequilibrium thermodynamics of thiol/disulfide redox systems: a perspective on redox systems biology. Free Radic Biol Med 2008;44:921-937. https://doi.org/10.1016/j.freeradbiomed.2007.11.008
64. Kirlin WG, Cai J, Thompson SA, Diaz D, Kavanagh TJ, Jones DP. Glutathione redox potential in response to differentiation and enzyme inducers. Free Radic Biol Med 1999;27:1208-1218. https://doi.org/10.1016/S0891-5849(99)00145-8
65. Vázquez-Meza H, Vilchis-Landeros MM, Vázquez-Carrada M, Uribe-Ramírez D, Matuz-Mares D. Cellular Compartmentalization, Glutathione Transport and Its Relevance in Some Pathologies. Antioxidants (Basel) 2023;12:834. https://doi.org/10.3390/antiox12040834
66. Deponte M. Glutathione catalysis and the reaction mechanisms of glutathione-dependent enzymes. Biochim Biophys Acta 2013;1830:3217-3266. https://doi.org/10.1016/j.bbagen.2012.09.018
67. Giustarini D, Milzani A, Dalle-Donne I, Rossi R. How to Increase Cellular Glutathione. Antioxidants (Basel) 2023;12:1094. https://doi.org/10.3390/antiox12051094
68. Fu A, van Rooyen L, Evans L, Armstrong N, Avizonis D, Kin T, Bird GH, Reddy A, Chouchani ET, Liesa-Roig M, Walensky LD, Shapiro AMJ, Danial NN. Glucose metabolism and pyruvate carboxylase enhance glutathione synthesis and restrict oxidative stress in pancreatic islets. Cell Rep 2021;37:110037. https://doi.org/10.1016/j.celrep.2021.110037
69. Meister A. Glutathione metabolism. Methods Enzymol 1995;251:3-7. https://doi.org/10.1016/0076-6879(95)51106-7
70. Azarova I, Polonikov A, Klyosova E. Molecular Genetics of Abnormal Redox Homeostasis in Type 2 Diabetes Mellitus. Int J Mol Sci 2023;24:4738. https://doi.org/10.3390/ijms24054738
71. Lenzen S, Drinkgern J, Tiedge M. Low antioxidant enzyme gene expression in pancreatic islets compared with various other mouse tissues. Free Radic Biol Med 1996;20:463-466. https://doi.org/10.1016/0891-5849(96)02051-5
72. Tiedge M, Lortz S, Drinkgern J, Lenzen S. Relation between antioxidant enzyme gene expression and antioxidative defense status of insulin-producing cells. Diabetes 1997;46:1733-1742. https://doi.org/10.2337/diab.46.11.1733
73. Buettner GR. Superoxide dismutase in redox biology: the roles of superoxide and hydrogen peroxide. Anticancer agents Med Chem 2011;11:341-346. https://doi.org/10.2174/187152011795677544
74. Bogdani M, Henschel AM, Kansra S, Fuller JM, Geoffrey R, Jia S, Kaldunski ML, Pavletich S, Prosser S, Chen YG, Lernmark A, Hessner MJ. Biobreeding rat islets exhibit reduced antioxidative defense and N-acetyl cysteine treatment delays type 1 diabetes. J Endocrinol 2013;216:111-123. https://doi.org/10.1530/JOE-12-0385
75. Schuit F, Van Lommel L, Granvik M, Goyvaerts L, de Faudeur G, Schraenen A, Lemaire K. beta-cell-specific gene repression: a mechanism to protect against inappropriate or maladjusted insulin secretion? Diabetes 2012;61:969-975. https://doi.org/10.2337/db11-1564
76. Welsh N, Margulis B, Borg LA, Wiklund HJ, Saldeen J, Flodström M, Mello MA, Andersson A, Pipeleers DG, Hellerström C. Differences in the expression of heat-shock proteins and antioxidant enzymes between human and rodent pancreatic islets: implications for the pathogenesis of insulin-dependent diabetes mellitus. Mol Med 1995;1:806-820. https://doi.org/10.1007/BF03401895
77. Bensellam M, Van Lommel L, Overbergh L, Schuit FC, Jonas JC. Cluster analysis of rat pancreatic islet gene mRNA levels after culture in low-, intermediate- and high-glucose concentrations. Diabetologia 2009;52:463-476. https://doi.org/10.1007/s00125-008-1245-z
78. Godoy JR, Funke M, Ackermann W, Haunhorst P, Oesteritz S, Capani F, Elsässer HP, Lillig CH. Redox atlas of the mouse. Immunohistochemical detection of glutaredoxin-, peroxiredoxin-, and thioredoxin-family proteins in various tissues of the laboratory mouse. Biochim Biophys Acta 2011;1810:2-92. https://doi.org/10.1016/j.bbagen.2010.05.006

79. Stancill JS, Broniowska KA, Oleson BJ, Naatz A, Corbett JA. Pancreatic beta-cells detoxify H2O2 through the peroxiredoxin/thioredoxin antioxidant system. J Biol Chem 2019;294:4843-4853. https://doi.org/10.1074/jbc.RA118.006219
80. Jin MH, Shen GN, Jin YH, Sun HN, Zhen X, Zhang YQ, Lee DS, Cui YD, Yu LY, Kim JS, Kwon T, Han YH. Peroxiredoxin I deficiency increases pancreatic β-cell apoptosis after streptozotocin stimulation via the AKT/GSK3β signaling pathway. Mol Med Rep 2020;22:1831-1838. https://doi.org/10.3892/mmr.2020.11279
81. Pacifici F, Della-Morte D, Capuani B, Coppola A, Scioli MG, Donadel G, Andreadi A, Ciccosanti F, Fimia GM, Bellia A, Orlandi A, Lauro D. Peroxiredoxin 6 Modulates Insulin Secretion and Beta Cell Death via a Mitochondrial Dynamic Network. Front Endocrinol (Lausanne) 2022;13:842575. https://doi.org/10.3389/fendo.2022.842575
82. Vivoli A, Ghislain J, Filali-Mouhim A, Angeles ZE, Castell AL, Sladek R, Poitout V. Single-Cell RNA Sequencing Reveals a Role for Reactive Oxygen Species and Peroxiredoxins in Fatty Acid-Induced Rat β-Cell Proliferation. Diabetes 2023;72:45-58. https://doi.org/10.2337/db22-0121
83. Lorenzen I, Eble JA, Hanschmann EM. Thiol switches in membrane proteins - Extracellular redox regulation in cell biology. Biological chemistry 2020;402:253-269. https://doi.org/10.1515/hsz-2020-0266
84. Hanschmann EM, Petry SF, Eitner S, Maresch CC, Lingwal N, Lillig CH, Linn T. Paracrine regulation and improvement of β-cell function by thioredoxin. Redox Biol 2020;34:101570. https://doi.org/10.1016/j.redox.2020.101570
85. Asami K, Inagaki A, Imura T, Sekiguchi S, Fujimori K, Masutani H, Yodoi J, Satomi S, Ohuchi N, Goto M. Thioredoxin-1 attenuates early graft loss after intraportal islet transplantation in mice. PLoS One 2013;8:e70259. https://doi.org/10.1371/journal.pone.0070259
86. Quesada I, Todorova MG, Soria B. Different metabolic responses in alpha-, beta-, and delta-cells of the islet of Langerhans monitored by redox confocal microscopy. Biophys J 2006;90:2641-2650. https://doi.org/10.1529/biophysj.105.069906
87. Miki A, Ricordi C, Sakuma Y, Yamamoto T, Misawa R, Mita A, Molano RD, Vaziri ND, Pileggi A, Ichii H. Divergent antioxidant capacity of human islet cell subsets: A potential cause of beta-cell vulnerability in diabetes and islet transplantation. PLoS One 2018;13:e0196570. https://doi.org/10.1371/journal.pone.0196570
88. Rahier J, Guiot Y, Goebbels RM, Sempoux C, Henquin JC. Pancreatic beta-cell mass in European subjects with type 2 diabetes. Diabetes Obes Metab 2008;10 Suppl 4:32-42. https://doi.org/10.1111/j.1463-1326.2008.00969.x
89. Marroqui L, Masini M, Merino B, Grieco FA, Millard I, Dubois C, Quesada I, Marchetti P, Cnop M, Eizirik DL. Pancreatic α Cells are Resistant to Metabolic Stress-induced Apoptosis in Type 2 Diabetes. EBioMedicine 2015;2:378-385. https://doi.org/10.1016/j.ebiom.2015.03.012
90. Gorasia DG, Dudek NL, Veith PD, Shankar R, Safavi-Hemami H, Williamson NA, Reynolds EC, Hubbard MJ, Purcell AW. Pancreatic beta cells are highly susceptible to oxidative and ER stresses during the development of diabetes. J Proteome Res 2015;14:688-699. https://doi.org/10.1021/pr500643h
91. Kim MK, Shin HM, Jung H, Lee E, Kim TK, Kim TN, Kwon MJ, Lee SH, Rhee BD, Park JH. Comparison of pancreatic beta cells and alpha cells under hyperglycemia: Inverse coupling in pAkt-FoxO1. Diabetes Res Clin Pract 2017;131:1-11. https://doi.org/10.1016/j.diabres.2017.05.017
92. Pipeleers DG. Heterogeneity in pancreatic beta-cell population. Diabetes 1992;41:777-781. https://doi.org/10.2337/diab.41.7.777
93. Gutierrez GD, Gromada J, Sussel L. Heterogeneity of the Pancreatic Beta Cell. Front Genet 2017;8:22. https://doi.org/10.3389/fgene.2017.00022
94. Da Silva Xavier G, Rutter GA. Metabolic and Functional Heterogeneity in Pancreatic β Cells. J Mol Biol 2020;432:1395-1406. https://doi.org/10.1016/j.jmb.2019.08.005
95. Kiekens R, In 't Veld P, Mahler T, Schuit F, Van De Winkel M, Pipeleers D. Differences in glucose recognition by individual rat pancreatic B cells are associated with intercellular differences in glucose-induced biosynthetic activity. J Clin Invest 1992;89:117-125. https://doi.org/10.1172/JCI115551
96. Van Schravendijk CF, Kiekens R, Pipeleers DG. Pancreatic beta cell heterogeneity in glucose-induced insulin secretion. J Biol Chem 1992;267:21344-21348. https://doi.org/10.1016/S0021-9258(19)36615-3

97. Van De Winkel M, Pipeleers D. Autofluorescence-activated cell sorting of pancreatic islet cells: purification of insulin-containing B-cells according to glucose-induced changes in cellular redox state. Biochem Biophys Res Commun 1983;114:835-842. https://doi.org/10.1016/0006-291X(83)90857-4
98. Benninger RKP, Kravets V. The physiological role of β-cell heterogeneity in pancreatic islet function. Nat Rev Endocrinol 2022;18:9-22. https://doi.org/10.1038/s41574-021-00568-0
99. Benáková Š, Holendová B, Plecitá-Hlavatá L. Redox Homeostasis in Pancreatic β-Cells: From Development to Failure. Antioxidants (Basel) 2021;10:526. https://doi.org/10.3390/antiox10040526
100. Hughes H, Hughes GE. The Effects of Prolonged Administration of Small Doses of Alloxan upon the Islet Tissue of the Rat Pancreas. Br J Exp Pathol 1944;25:126-130.
101. Hellerstrom C, Petersson B, Hellman B. Some properties of the B cells in the islet of Langerhans studied with regard to the position of the cells. Acta Endocrinol (Copenh) 1960;34:449-456. https://doi.org/10.1530/acta.0.XXXIV0449
102. Stefan Y, Meda P, Neufeld M, Orci L. Stimulation of insulin secretion reveals heterogeneity of pancreatic B cells in vivo. J Clin Invest 1987;80:175-183. https://doi.org/10.1172/JCI113045
103. Giordano E, Bosco D, Cirulli V, Meda P. Repeated glucose stimulation reveals distinct and lasting secretion patterns of individual rat pancreatic B cells. J Clin Invest 1991;87:2178-2185. https://doi.org/10.1172/JCI115251
104. Jetton TL, Magnuson MA. Heterogeneous expression of glucokinase among pancreatic beta cells. Proc Natl Acad Sci U S A 1992;89:2619-2623. https://doi.org/10.1073/pnas.89.7.2619
105. Johnston NR, Mitchell RK, Haythorne E, Pessoa MP, Semplici F, Ferrer J, Piemonti L, Marchetti P, Bugliani M, Bosco D, Berishvili E, Duncanson P, Watkinson M, Broichhagen J, Trauner D, Rutter GA, Hodson DJ. Beta Cell Hubs Dictate Pancreatic Islet Responses to Glucose. Cell Metab 2016;24:389-401. https://doi.org/10.1016/j.cmet.2016.06.020
106. Bosco D, Rouiller DG, Halban PA. Differential expression of E-cadherin at the surface of rat beta-cells as a marker of functional heterogeneity. J Endocrinol 2007;194:21-29. https://doi.org/10.1677/JOE-06-0169
107. Karaca M, Castel J, Tourrel-Cuzin C, Brun M, Géant A, Dubois M, Catesson S, Rodriguez M, Luquet S, Cattan P, Lockhart B, Lang J, Ktorza A, Magnan C, Kargar C. Exploring functional beta-cell heterogeneity in vivo using PSA-NCAM as a specific marker. PLoS One 2009;4:e5555. https://doi.org/10.1371/journal.pone.0005555
108. Bader E, Migliorini A, Gegg M, Moruzzi N, Gerdes J, Roscioni SS, Bakhti M, Brandl E, Irmler M, Beckers J, Aichler M, Feuchtinger A, Leitzinger C, Zischka H, Wang-Sattler R, Jastroch M, Tschöp M, Machicao F, Staiger H, Häring HU, Chmelova H, Chouinard JA, Oskolkov N, Korsgren O, Speier S, Lickert H. Identification of proliferative and mature β-cells in the islets of Langerhans. Nature 2016;535:430-434. https://doi.org/10.1038/nature18624
109. Li X, Yang KY, Chan VW, Leung KT, Zhang XB, Wong AS, Chong CCN, Wang CC, Ku M, Lui KO. Single-Cell RNA-Seq Reveals that CD9 Is a Negative Marker of Glucose-Responsive Pancreatic β-like Cells Derived from Human Pluripotent Stem Cells. Stem Cell Reports 2020;15:1111-1126. https://doi.org/10.1016/j.stemcr.2020.09.009
110. Dorrell C, Schug J, Canaday PS, Russ HA, Tarlow BD, Grompe MT, Horton T, Hebrok M, Streeter PR, Kaestner KH, Grompe M. Human islets contain four distinct subtypes of β cells. Nat Commun 2016;7:11756. https://doi.org/10.1038/ncomms11756
111. Hermann M, Pirkebner D, Draxl A, Berger P, Untergasser G, Margreiter R, Hengster P. Dickkopf-3 is expressed in a subset of adult human pancreatic beta cells. Histochem Cell Biol 2007;127:513-521. https://doi.org/10.1007/s00418-007-0278-6
112. Saisho Y, Harris PE, Butler AE, Galasso R, Gurlo T, Rizza RA, Butler PC. Relationship between pancreatic vesicular monoamine transporter 2 (VMAT2) and insulin expression in human pancreas. J Mol Histol 2008;39:543-551. https://doi.org/10.1007/s10735-008-9195-9
113. Elksnis A, Cen J, Wikström P, Carlsson PO, Welsh N. Pharmacological Inhibition of NOX4 Improves Mitochondrial Function and Survival in Human Beta-Cells. Biomedicines 2021;9:1865. https://doi.org/10.3390/biomedicines9121865
114. Campbell SA, Golec DP, Hubert M, Johnson J, Salamon N, Barr A, MacDonald PE, Philippaert K, Light PE. Human islets contain a subpopulation of glucagon-like peptide-1 secreting α cells that is increased in type 2 diabetes. Mol Metab 2020;39:101014. https://doi.org/10.1016/j.molmet.2020.101014

Physiol. Res. 73 (Suppl. 1): S153-S163, 2024 *https://doi.org/10.33549/physiolres.935261*

REVIEW

Metabolic Pathways of Acylcarnitine Synthesis

Jana BREJCHOVA[1], Kristyna BREJCHOVA[1], Ondrej KUDA[1]

[1]Laboratory of Metabolism of Bioactive Lipids, Institute of Physiology of the Czech Academy of Sciences, Prague, Czech Republic

Received October 22, 2023
Accepted March 22, 2024

Summary

Acylcarnitines are important markers in metabolic studies of many diseases, including metabolic, cardiovascular, and neurological disorders. We reviewed analytical methods for analyzing acylcarnitines with respect to the available molecular structural information, the technical limitations of legacy methods, and the potential of new mass spectrometry-based techniques to provide new information on metabolite structure. We summarized the nomenclature of acylcarnitines based on historical common names and common abbreviations, and we propose the use of systematic abbreviations derived from the shorthand notation for lipid structures. The transition to systematic nomenclature will facilitate acylcarnitine annotation, reporting, and standardization in metabolomics. We have reviewed the metabolic origins of acylcarnitines important for the biological interpretation of human metabolomic profiles. We identified neglected isomers of acylcarnitines and summarized the metabolic pathways involved in the synthesis and degradation of acylcarnitines, including branched-chain lipids and amino acids. We reviewed the primary literature, mapped the metabolic transformations of acyl-CoAs to acylcarnitines, and created a freely available WikiPathway WP5423 to help researchers navigate the acylcarnitine field. The WikiPathway was curated, metabolites and metabolic reactions were annotated, and references were included. We also provide a table for conversion between common names and abbreviations and systematic abbreviations linked to the LIPID MAPS or Human Metabolome Database.

Key words

Acylcarnitines • Mass spectrometry • Beta oxidation • Branched fatty acids • Branched lipids • Nomenclature • Standardization • Shorthand notation for lipid structures • LIPID MAPS

Corresponding author

O. Kuda, Laboratory of Metabolism of Bioactive Lipids, Institute of Physiology of the Czech Academy of Sciences, Videnska 1083, 14200 Prague, Czech Republic. E-mail: ondrej.kuda@fgu.cas.cz

Introduction

Acylcarnitines are acyl esters of carnitine (L-3-hydroxy-4-aminobutyrobetaine) and are essential for the oxidative catabolism of fatty acids in mitochondria and peroxisomes. They are necessary for healthy and sustainable cellular energy homeostasis, involved in the metabolism of branched-chain amino acids and related metabolic pathways, and serve as a detoxification pathway [1,2]. There are many acylcarnitine molecules described in public databases of metabolites, for instance, 114 records in LIPID MAPS, 2359 records in the Human Metabolome Database, and 308 entries on the ChEBI database, measured in plasma/serum, dried blood spots, urine, bile and amniotic fluid [3], but very little is published about their metabolic origins.

We aimed to help researchers interpret metabolomics data containing acylcarnitines. We reviewed the biologically important acylcarnitines [1] concerning their biochemical origins and generated a pathway map summarizing the reactions. We focused on the isomers and nomenclature and annotated the enzymatic reactions involved in their metabolism. This review should facilitate orientation in the acylcarnitine datasets and link the measured analytes with the correct enzymatic reactions.

Analytical methods using mass spectrometry

Critical evaluation of the limitations of the analytical techniques used to measure acylcarnitine is the basis for correct annotation and biological interpretation.

Sample extraction should consider that the polarity of acylcarnitines can vary by more than 10 orders of magnitude on the log octanol-water partition coefficient (logP) scale. In commonly employed bi-phase extraction methods like methyl *tert*-butyl ether/methanol/water, chloroform/methanol/water, and dichloromethane/methanol/water, it is crucial to analyze both fractions to cover these metabolites [4].

Direct-infusion tandem mass spectrometry (DI-MS/MS) remains a valid approach for identifying patients with inborn errors of metabolism, problems in mitochondrial fatty acid β-oxidation, and certain types of acidemias (reviewed by Miller *et al.* [3]). However, this legacy technique provides only limited information about the analytes, usually the number of carbon atoms and double bonds.

Currently, liquid chromatography-mass spectrometry (LC-MS/MS) is the most common technique for metabolomics profiling, which allows the separation of acylcarnitine isomeric species and improves the sensitivity and selectivity of their detection [1,3]. Although LC-MS/MS provides an insight into the analyte's structure, it does not yield unambiguous molecular identity.

Recent advances in analytical techniques push forward our ability to provide a full structural characterization of lipid species in complex biological matrices. These include ion mobility spectrometry (separating stereoisomers, reducing background), ion activation techniques (targeting double bonds by UV photodissociation, providing specific fragment *via* electron capture dissociation), and derivatizations (increasing sensitivity using charged modifiers, separating isomers, localizing double bonds using O_3), [5-9], which allow quantification of isomeric and odd-numbered acylcarnitines, identification of acyl double bond position and configuration, stereochemistry, etc. In the future, these specialized techniques will become a part of routine pipelines, producing hundreds of acylcarnitine species structurally identified at 'Complete structure level'. New tools will be needed to mine these information-rich datasets. Implementation of the Lipidomics Minimal Reporting Checklist, which summarizes all technical details of the analytical technique and defines the level of molecular structural information, would facilitate the interpretation of the acylcarnitine data [10].

Acylcarnitine nomenclature

Common names

According to IUPAC, the common names of acyl groups are typically derived by replacing the **-ic** acid suffix of the corresponding carboxylic acid's common name with **-yl** or the **-oic** acid suffix with **-oyl**, (acetic acid > acetyl- or palmitic acid > palmitoyl-). Systematic names based on hydrocarbon chains are derived similarly (hexadecanoic acid > hexadecanoylcarnitine).

Common abbreviations

Common name acylcarnitine abbreviations in the field of newborn screening are simple and follow these rules: a) a number of all carbon atoms is used to describe the chain length regardless of the branching or functional groups (e.g., glutarylcarnitine as C5-DC); b) unsaturation degree is used only when present (e.g., oleoylcarnitine as C18:1); c) functional groups are used without the positional information (e.g. 3(*S*)-hydroxybutyrylcarnitine as C4-OH) [3,11]. Alternative grammar distinguishes isomeric species, e.g., 3-hydroxybutyrylcarnitine and 3-hydroxyisobutyrylcarnitine as C4-OH and C4-OH-I, respectively [1]. The *iso* prefix can be used for structures where the saturated chain has a branching point on the penultimate (one from the end) carbon atom (e.g., isobutyrylcarnitine). The *anteiso* prefix marks the branching point located on the antepenultimate carbon atom (two from the end). The prefixes cannot be used with unsaturated or modified chains, and the position of the methyl branching group is used instead (e.g., tiglylcarnitine as C5:1-M).

Systematic abbreviations

Common names and abbreviations will soon reach their limit of usability. Abbreviations based on systematic names are needed due to the advent of more powerful analytical techniques. Nowadays, rules designed for unit-resolution mass spectrometers cannot describe structural diversity. Shorthand notation for lipid structures [12-14] allows annotation of the measured analytes based on the level of structural information provided by the analytical technique (Table 1). It combines predefined class (CAR) followed by the acyl chain characteristics, including all available structural information. For instance, there are at least four different decenoylcarnitines: CAR 10:2(2*E*), CAR 10:1(3*E*), CAR 10:1(3*Z*), and CAR 10:1(4*Z*)

Table 1. Example of structural hierarchy representation of '3-Hydroxyoleoylcarnitine' according to Shorthand notation for lipid structures [12-14].

Level	Name	Description (information gain)
Category	Fatty acyls [FA]	Lipid category
Class	Fatty acyl carnitines [FA0707]	+ lipid class
Species	CAR 18:1;O	+ headgroup, fatty *Acyl* identity, oxidation
Molecular species	CAR 18:1;O1	+ one oxygen
sn-Position	CAR 18:1;O1	(not applicable)
Structure defined	CAR 18:1(9*Z*);OH	+ double bond position, type of oxidation
Full structure	CAR 18:1(9*Z*);3OH	+ position of the oxidation
Complete structure	CAR 18:1(9*Z*);3OH[*S*]	+ stereo configuration

in the β-oxidation pathways of common fatty acids (Fig. 1). Two of them, CAR 10:1(3*Z*) and CAR 10:1(2*E*), come from β-oxidation of palmitoleic acid (9*Z*). However, there are at least 15 different isomers of fatty acid 16:1 in human plasma, four containing a double bond at positions 9, 10, and 11 [6]. Therefore, many more CAR 10:1 isomers from the FA 16:1 or other longer FAs could be present in plasma as yet unidentified but describable by shorthand notation. Other examples are quantification of C14:1 acylcarnitine n-5 and n-9 in human and mouse fibroblasts, which levels reflect differences in the expression of long chain acyl-CoA dehydrogenase [15] and quantification of *cis*-3-C12:1 and *cis*-5-C14:1 acylcarnitine in plasma of enoyl-CoA delta isomerase 1-deficient mice [16]. In both examples, the acyl chain identity is crucial for proper interpretation of long chain acyl-CoA dehydrogenase and enoyl-CoA isomerase activities. However, this approach is also limited based on predefined classes. It is impossible to distinguish the L-/D- isomers within the CAR class definition, and a full IUPAC name is the ultimate option.

The systematic abbreviations are backward compatible. Newborn screening acylcarnitine data can be correctly annotated, and metabolomic profiling data, acquired using innovative derivatization or fragmentation techniques, can be annotated with all structural details [6,7]. Broader acceptance of the shorthand notation by major databases would facilitate acylcarnitine annotations, standardization, and further data processing *via* overrepresentation analysis [17].

Lipid databases and metabolite identities

When discussing the biological effect of acylcarnitines, we need to find the most appropriate identifiers in a database considering the analytical limitations and the biological knowledge. This task is challenging and sometimes possible. For instance, an optimized analytical technique can measure the carnitine ester of palmitic acid at the 'Complete structure level' according to shorthand notation for lipid structures [12,13]. We need to find an identifier for (*S*)-3-(palmitoyloxy)-4-(trimethylammo-nio)butanoate, which is the biologically important molecule commonly known as ‘palmitoylcarnitine.’ First, L-carnitine is essential for the transportation of long-chain fatty acids into mitochondria for β-oxidation, and its optimal isomer, D-carnitine, is a xenobiotic compound [18,19]. Therefore, in most cases, only 'L'-acylcarnitines (or (*R*)- according to Cahn-Ingold-Prelog rules) are biologically relevant for human metabolism. Second, metabolite databases contain records covering different levels of knowledge of metabolite structure (Table 2). Some records lack stereochemistry, and some databases contain the 'D-' forms. Pre-calculated and non-curated databases might also contain wrong records, e.g., LIPID MAPS record LMFA07070079 was up to recently called L-palmitoylcarnitine, which was an incorrect common name for (*S*)-3-(palmitoyloxy)-4-(trimethyl-ammonio) butanoate aka D-palmitoylcarnitine. The involvement of the community is needed to report and curate database records. Another example would be the identity of ‘hydroxybutyrylcarnitine’ – deficiency of a short-chain-3-hydroxyacyl-coenzyme A dehydrogenase leads to the accumulation of CAR 4:0;3OH[S] [20] while ketosis leads to the accumulation of CAR 4:0;3OH[R] [19]. The incorrect mapping of database identifiers can affect further data processing, like over-representation or pathway analysis. For instance, the Rhea database contains only 'L'-acylcarnitine reactions (https://www.rhea-db.org/rhea/12663), and 'D'-identifiers would produce false negative results.

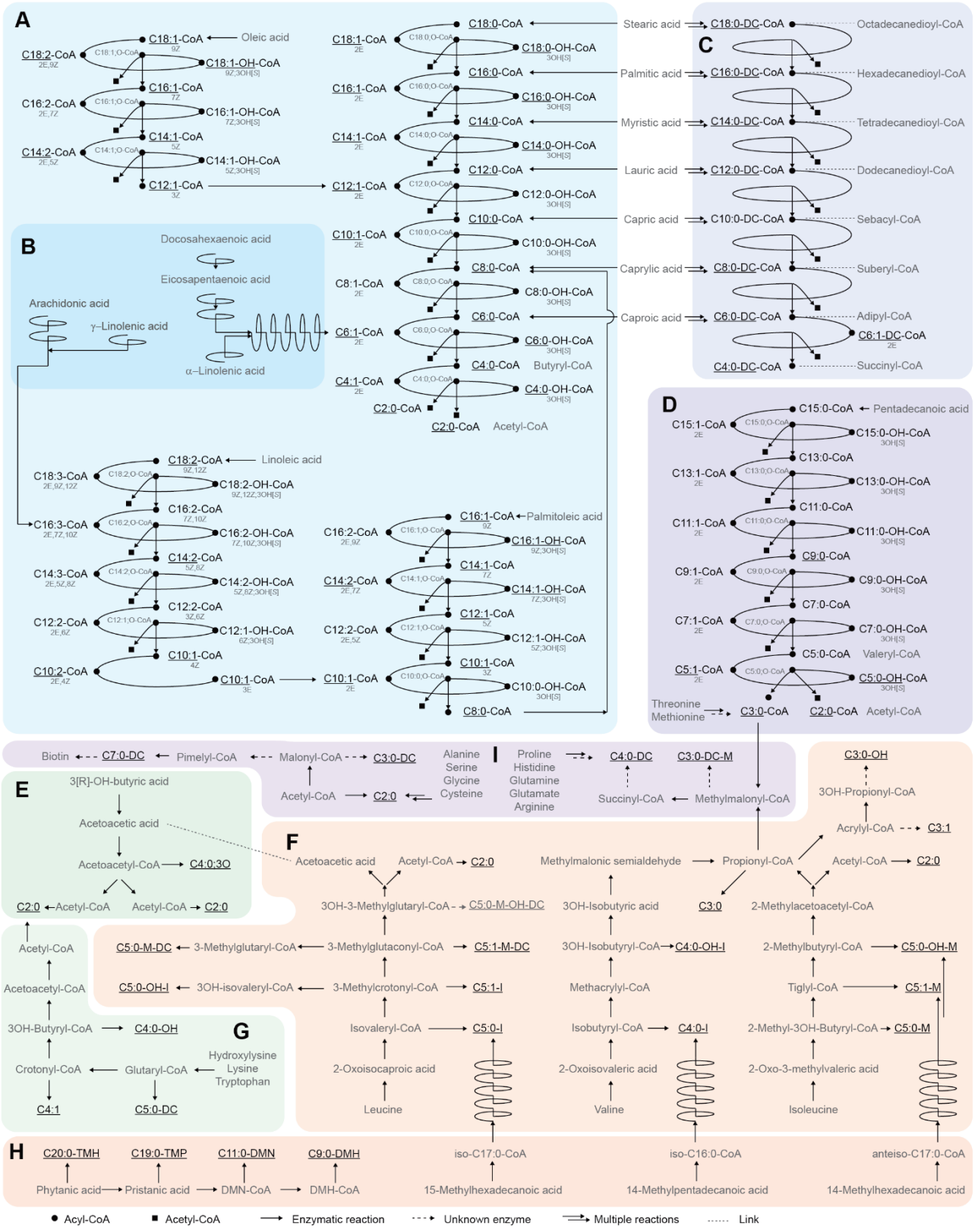

Fig. 1. Acylcarnitine pathways. (**A**) β-oxidation of straight fatty acids; (**B**) β-oxidation of straight polyunsaturated fatty acids; (**C**) β-oxidation of dicarboxylic fatty acids; (**D**) β-oxidation of odd-chain fatty acids; (**E**) Ketogenic pathway; (**F**) Metabolism of branched-chain amino acids; (**G**) Degradation of amino acids; (**H**) β-oxidation of branched-chain fatty acids; (**I**) Metabolism of amino acids and short-chain acylcarnitines. See Table 1 for annotations and WikiPathway WP5423 for details.

Table 1. Biologically important acylcarnitines.

Group	Panel	Common abbreviation	Common name	Systematic abbreviation	LIPID MAPS ID
Saturated straight	NBS	C2:0	Acetylcarnitine	CAR 2:0	LMFA07070050
	NBS	C3:0	Propionylcarnitine	CAR 3:0	LMFA07070005
	NBS	C4:0	Butyrylcarnitine	CAR 4:0	LMFA07070003
		C5:0	Valerylcarnitine	CAR 5:0	LMFA07070111
	NBS	C6:0	Caproylcarnitine	CAR 6:0	LMFA07070001
	NBS	C7:0	Heptanoylcarnitine	CAR 7:0	LMFA07070068
	NBS	C8:0	Octanoylcarnitine	CAR 8:0	LMFA07070002
		C9:0	Nonanoylcarnitine	CAR 9:0	LMFA07070082
	NBS	C10:0	Decanoylcarnitine	CAR 10:0	LMFA07070006
		C11:0	Undecanoylcarnitine	CAR 11:0	LMFA07070110
	NBS	C12:0	Lauroylcarnitine	CAR 12:0	LMFA07070062
		C13:0	Tridecanoylcarnitine	CAR 13:0	
	NBS	C14:0	Myristoylcarnitine	CAR 14:0	LMFA07070107
		C15:0	Pentadecanoylcarnitine	CAR 15:0	
	NBS	C16:0	Palmitoylcarnitine	CAR 16:0	LMFA07070004
	NBS	C18:0	Stearoylcarnitine	CAR 18:0	LMFA07070008
		C22:0	Behenoylcarnitine	CAR 22:0	LMFA07070089
		C24:0	Lignoceroylcarnitine	CAR 24:0	
		C26:0	Cerotoylcarnitine	CAR 26:0	LMFA07070069
Unsaturated straight	NBS	C3:1	Propenoylcarnitine	CAR 3:1(2*E*)	LMFA07070104
		C4:1	Butenylcarnitine	CAR 4:1(2*E*)	LMFA07070053
		C5:1	2-Pentenoylcarnitine	CAR 5:1(2*E*)	
		C6:1	Hexenoylcarnitine	CAR 6:1(2*E*)	LMFA07070031
	NBS	C8:1	Octenoylcarnitine	CAR 8:1(2*E*)	LMFA07070035
				CAR 10:1(2*E*)	
	NBS	C10:1	Decenoylcarnitine	CAR 10:1(3*E*)	
				CAR 10:1(3*Z*)	
				CAR 10:1(4*Z*)	LMFA07070017
	NBS	C10:2	Decadienoylcarnitine	CAR 10:2(2*E*,4*Z*)	LMFA07070015
				CAR 12:1(2*E*)	
	NBS	C12:1	Dodecenoylcarnitine	CAR 12:1(3*Z*)	
				CAR 12:1(5*Z*)	
				CAR 12:2(2*E*,5*Z*)	
		C12:2	Dodecadienoylcarnitine	CAR 12:2(2*E*,6*Z*)	
				CAR 12:2(3*Z*,6*Z*)	
				CAR 14:1(2*E*)	
	NBS	C14:1	Tetradecenoylcarnitine	CAR 14:1(5*Z*)	LMFA07070057
				CAR 14:1(7*Z*)	
				CAR 14:2(2*E*,5*Z*)	
	NBS	C14:2	Tetradecedienoylcarnitine	CAR 14:2(2*E*,7*Z*)	
				CAR 14:2(5*Z*,8*Z*)	LMFA07070020
				CAR 16:1(2*E*)	LMFA07070109
	NBS	C16:1	Hexadecenoylcarnitine	CAR 16:1(7*Z*)	
				CAR 16:1(9*Z*)	LMFA07070097

		C16:2	Hexadecadienoylcarnitine	CAR 16:2(2*E*,7*Z*) CAR 16:2(2*E*,9*Z*) CAR 16:2(7*Z*,10*Z*)	LMFA07070021
	NBS	C18:1	Octadecenoylcarnitine	CAR 18:1(2*E*) CAR 18:1(9*Z*)	LMFA07070096
	NBS	C18:2	Octadecadienylcarnitine	CAR 18:2(2*E*,9*Z*) CAR 18:2(9*Z*,12*Z*)	LMFA07070092
Branched	NBS	C4:0-I	Isobutyrylcarnitine	CAR 3:0;2Me	LMFA07070075
	NBS	C5:0-I	Isovalerylcarnitine	CAR 4:0;3Me	LMFA07070077
	NBS	C5:0-M	2-Methylbutyrylcarnitine	CAR 4:0;2Me	LMFA07070034
		C5:1-I	3-Methylcrotonylcarnitine	CAR 4:1(2*E*);3Me	
	NBS	C5:1-M	Tiglylcarnitine	CAR 4:1(2*E*);2Me	LMFA07070108
		C20:0-TMH	Phytanoylcarnitine*	CAR 16:0;3Me;7Me; 11Me;15Me	
		C19:0-TMP	Pristanoylcarnitine*	CAR 15:0;2Me;6Me; 10Me;14Me	
		C11:0-DMN	4,8-dimethylnonanoyl carnitine*	CAR 9:0;4Me;8Me	
		C9:0-DMH	2,6-dimethylheptanoyl carnitine*	CAR 7:0;2Me;6Me	
Oxidized		C3:0-OH	3-Hydroxypropionyl carnitine	CAR 3:0;3OH[*S*]	LMFA07070074
	NBS	C3:0-DC	Malonylcarnitine	CAR 2:0;2COOH	LMFA07070093
	NBS	C3:0-DC-M	Methylmalonylcarnitine	CAR 2:0;2Me;2COOH	LMFA07070094
	NBS	C4:0-OH	3-Hydroxybutyrylcarnitine	CAR 4:0;3OH[*S*]	LMFA07070037
		C4:0-OH-I	3-Hydroxyisobutyryl carnitine	CAR 3:0;2Me;3OH[*S*]	
		C4:0;O	Acetoacetylcarnitine	CAR 4:0;3oxo	
		C4:0-DC	Succinylcarnitine	CAR 3:0;3COOH	LMFA07070101
		C5:0-OH	3-Hydroxyvaleryl carnitine	CAR 5:0;3OH[*S*]	
	NBS	C5:0-OH-I	3-Hydroxyisovaleryl carnitine	CAR 4:0;3Me;3OH[*S*]	LMFA07070041
	NBS	C5:0-OH-M	2-Methyl-3-hydroxybutyrylcarnitine	CAR 4:0;2Me;3OH[*S*]	
	NBS	C5:0-DC	Glutarylcarnitine	CAR 4:0;4COOH	LMFA07070091
		C5:0-M-DC	3-Methylglutarylcarnitine	CAR 4:0;3Me[*R*]; 4COOH	
		C5:1-M-DC	3-Methylglutaconyl carnitine	CAR 4:1(2*E*);3Me; 4COOH	
		C5:0-M-OH-DC	3-Hydroxy-3-methylglutarylcarnitine	CAR 4:0;3OH[*S*]; 3Me;4COOH	
	NBS	C6:0-OH	3-Hydroxy-hexanoylcarnitine	CAR 6:0;3OH[*S*]	LMFA07070072
		C6:0-DC	Adipylcarnitine	CAR 5:0;5COOH	LMFA07070087
		C6:1-DC	Dehydroadipylcarnitine	CAR 5:1(2*E*);5COOH	LMFA07070013
		C7:0-DC	Pimelylcarnitine	CAR 6:0;6COOH	

		C8:0-DC	Suberylcarnitine	CAR 7:0;7COOH	
	NBS	C10:0-OH	3-Hydroxydecanoyl carnitine	CAR 10:0;3OH[*S*]	
	NBS	C10:1-OH	3-Hydroxydecenoyl carnitine	CAR 10:1;OH	
	NBS	C12:0-OH	3-Hydroxydodecanoyl carnitine	CAR 12:0;3OH[*S*]	LMFA07070039
		C12:0-DC	Dodecanedioylcarnitine	CAR 11:0;11COOH	LMFA07070083
	NBS	C12:1-OH	3-Hydroxydodecenoyl carnitine	CAR 12:1(5*Z*);3OH[*S*]	
	NBS	C14:0-OH	3-Hydroxytetradecanoyl carnitine	CAR 14:0;3OH[*S*]	LMFA07070045
		C14:0-DC	Tetradecanedioylcarnitine	CAR 13:0;13COOH	LMFA07070084
	NBS	C14:1-OH	3-Hydroxytetradecenoyl carnitine	CAR 14:1(5*Z*);3OH[*S*] CAR 14:1(7*Z*);3OH[*S*]	
	NBS	C16:0-OH	3-Hydroxyhexadecanoyl carnitine	CAR 16:0;3OH[*S*]	
	NBS	C16:1-OH	3-Hydroxyhexadecenoyl carnitine	CAR 16:1(7*Z*);3OH[*S*] CAR 16:1(9*Z*);3OH[*S*]	LMFA07070044
		C16:0-DC	Hexadecanedioylcarnitine	CAR 15:0;15COOH	LMFA07070007
	NBS	C18:0-OH	3-Hydroxystearoyl carnitine	CAR 18:0;3OH[*S*]	LMFA07070043
	NBS	C18:1-OH	3-Hydroxyoleoylcarnitine	CAR 18:1(9*Z*);3OH[*S*]	LMFA07070025
		C18:0-DC	Octadecanedioylcarnitine	CAR 17:0;17COOH	LMFA07070085
	NBS	C18:2-OH	3-Hydroxyoctadecadienoyl carnitine	CAR 18:2(9*Z*,12*Z*); 3OH[*S*]	LMFA07070042

Note: Zero (':0') was included in newborn screening (NBS) names to unify various dialects. * denotes mixture of unknown isomers.

In parallel, acylcarnitine data measured using direct infusion unit-resolution mass spectrometry yield annotations at 'Species level' [12,13], and careful identifier mapping should be performed to prevent over-interpretation. For instance, 3-hydroxyisovalerylcarnitine (C5-OH-I), LIPID MAPS identification LMFA07070041, is abbreviated as CAR 5:0;O and the same systematic abbreviation is used for 3-hydroxyvalerylcarnitine. However, these two metabolites come from entirely different pathways and precursors (leucine degradation and odd-chain fatty acid degradation, Fig. 1).

Acylcarnitines important for biological interpretation of human metabolomic profiles

Recently, Dambrova *et al.* published an excellent review on acylcarnitines [1]. We decided to update the older acylcarnitine nomenclature (based on newborn screening rules) into systematic nomenclature and map the metabolites associated with a disease or necessary for the biological interpretation of datasets into identifiers and pathways (Table 2, Fig. 1). We primarily focused on the identity and source of acylcarnitines and successfully mapped most of the metabolites. However, some acylcarnitines defined by newborn screening methods cannot be unambiguously identified [11].

Although the 3-hydroxydecenoylcarnitine (C10:1-OH) has been officially part of the newborn screening panel [3,11], we could not find its molecular identity. It is not a product of the major metabolic pathways, and the position of the double bond is unknown. Violante *et al.* performed a detailed analysis of mitochondrial carnitine acyltransferase substrate preference and showed that the acyltransferase enzyme for some short-chain-CoAs is still unknown. For instance, an enzyme(s) responsible for the synthesis of succinylcarnitine, malonylcarnitine, or 3-hydroxy-3-methylglutarylcarnitine is still unknown [21-23]. 3-Hydroxy-3-methylglutarylcarnitine (C5:1-M-OH-DC) was observed only using low-resolution MS, and its

molecular identity was not confirmed by other techniques [24].

Limitations of analytical techniques often prevent accurate identification of the compounds. For instance, isovalerylcarnitine (C5:0-I), which is a diagnostic indicator of isovaleric acidemia, is isobaric with pivaloylcarnitine, 2-methylbutyrylcarnitine, and *n*-valerylcarnitine [25,26]. Pivaloylcarnitine derived from antibiotics and pimeloylcarnitine synthesized by microbiota are typical members of exposome [25,27]. Mixtures of straight and branched saturated acylcarnitines (e.g., CAR 20:0 as arachidylcarnitine or phytanoyl-carnitine) should be considered when annotating unknown features [28,29].

Acylcarnitine pathways

We designed a map of acylcarnitine metabolism in WikiPathways format (WP5423) to facilitate data interpretation and better orientation in various acylcarnitines' metabolic origins. It is important to interpret the data and pathways carefully based on the type of the sample (isolated mitochondria, cells, tissue biopsies, serum/plasma, urine). Not all pathways are active in all cell types, inborn errors of metabolism have specific signs, and the circulating acylcarnitines reflect tissue acylcarnitine metabolism only transiently and inadequately [2,30,31]. The map is divided into three sections: straight-chain fatty acids, branched-chain lipids, and odd-chain fatty acids.

The straight-chain fatty acid part describes the intermediates of β-oxidation from stearic acid to acetyl-CoA, intermediates of oleic acid, linoleic acid, α- and γ-linolenic acids, palmitoleic acid, docosahexaenoic and eicosapentaenoic acid complete degradation leading to acetyl-CoA, ω- and β-oxidation of dicarboxylic fatty acids, and partial β-oxidation of eicosanoids and docosanoids illustrated by prostaglandin E_2 path [16,32-37].

The branched-chain lipids part includes α- and β-oxidation of phytanic and pristanic acids and degradation of branched-chain fatty acids of the iso and *anteiso* series leading to intermediates of branched-chain amino acid degradation [29,38,39]. Amino acid-related metabolism, including ketogenesis and biotin synthesis [19,27], is included to cover all metabolic origins of short-chain acylcarnitines [1] and branched acyl side chains of cholestanoic acids are β-oxidized in the pathway of bile acid synthesis [40]. Degradation of branched-acyls leads to the production of both acetyl-CoA and propionyl-CoA and their respective acylcarnitines.

The odd-chain fatty acids part illustrates the metabolic fate of pentadecanoic acid *via* β-oxidation, leading to six molecules of acetyl-CoA and one propionyl-CoA and their acylcarnitine counterparts.

All metabolites are annotated using shorthand notation for lipid structures [12,13], common names, and the most appropriate database identifiers from LIPID MAPS or the Human metabolome database. When the database contained records with (un)defined stereochemistry, the closest structure was selected. Acylcarnitines discussed in the review by Dambrova *et al.* [1] and acylcarnitines important for the pathway flow are highlighted in bold font and provided with literature citations. Metabolic conversions are depicted by arrows and enzymatic reactions yielding acylcarnitines are highlighted in red. Five acylcarnitine transferases: carnitine acetyltransferase (CRAT), carnitine O-octanoyl-transferase (CROT), carnitine palmitoyltransferase 1A (CPT1A), carnitine palmitoyltransferase 1B (CPT1B), and carnitine palmitoyltransferase 2 (CPT2) convert acyl-CoAs into acylcarnitines according to their substrate specificity, which is documented by references linked to the red arrows (and reviewed in Dambrova *et al.* [1]). Most of the pathways contain the β-oxidation catabolic spiral, which is composed of acyl-CoA dehydrogenase and the mitochondrial trifunctional protein (TFP) [41,42]. The fatty acyl-CoA dehydrogenase produces 2,3-enoyl-CoA, the TFP 2,3-enoyl-CoA hydratase adds water and yields 3-hydroxyacyl-CoA, the TFP 3-hydroxyacyl-CoA dehydrogenase oxidizes the intermediate to 3-ketoacyl-CoA, and the TFP 3-ketoacyl-CoA thiolase releases a two-carbon unit in the form of acetyl-CoA [41]. Carnitine-dependent peroxisomal oxidation reactions, starting with acyl-CoA oxidase, have been reviewed by Houten *et al.* [38,40].

Carnitine acyltransferases ensure the reversible shuttling of acyl groups between free CoA and carnitine, and even the acylcarnitine forms of the intermediates can be detected using very specific and targeted techniques [43]. However, the stability and enzymatic accessibility of the 3-ketoacyl intermediates is much lower compared to the final acyl-CoAs and acylcarnitines, and the 3-ketoacylcarnitines are not depicted in the map for clarity. To further reduce the complexity of the pathways, enzymes involved in α-, β-, and ω-oxidations are omitted but can be explored in the linked WikiPathways or Reactome maps [36,37]. Reactions populated in the Rhea

knowledgebase are annotated with a Rhea identifier [44].

We created a simplified poster version of the WP5423, which can be printed on A3 format paper (Fig. S1). The poster uses newborn screening-based acylcarnitine nomenclature, and the alternative systematic metabolite names can be found in Table 1.

Conclusions

We reviewed the metabolic origins of acylcarnitines, mapped their metabolic conversions, and created a freely available WikiPathway and a poster scheme to help researchers orient themselves in the acylcarnitine realm. We propose the use of shorthand notation for lipid structures [12,13] as a way to standardize the acylcarnitine reporting.

Availability of data and materials

WikiPathway WP5423 is freely available online at https://classic.wikipathways.org/index.php/Pathway:WP5423

Conflict of Interest

There is no conflict of interest.

Acknowledgements

This study was supported by a grant from the Czech Academy of Sciences [Lumina Quaeruntur LQ200111901], by the project National Institute for Research of Metabolic and Cardiovascular Diseases (Programme EXCELES, ID Project No. LX22NPO5104) – Funded by the European Union – Next Generation EU, and by Czech Ministry of Education, Youth and Sports [LUABA22010].

References

1. Dambrova M, Makrecka-Kuka M, Kuka J, Vilskersts R, Nordberg D, Attwood MM, Smesny S, Sen ZD, Guo AC, Oler E, Tian S, Zheng J, Wishart, DS, Liepinsh E, Schioth HB. Acylcarnitines: Nomenclature, Biomarkers, Therapeutic Potential, Drug Targets, and Clinical Trials. Pharmacol Rev 2022;74:506-551. https://doi.org/10.1124/pharmrev.121.000408
2. Schooneman MG, Vaz FM, Houten SM, Soeters MR. Acylcarnitines: reflecting or inflicting insulin resistance? Diabetes 2013;62:1-8. https://doi.org/10.2337/db12-0466
3. Miller MJ, Cusmano-Ozog K, Oglesbee D, Young S, Committee ALQA. Laboratory analysis of acylcarnitines, 2020 update: a technical standard of the American College of Medical Genetics and Genomics (ACMG). Genet Med 2021;23:249-258. https://doi.org/10.1038/s41436-020-00990-1
4. Cajka T. Towards Merging Targeted and Untargeted Analysis of the Lipidome, Metabolome, and Exposome. LCGC Eur 2019;32:314-316.
5. Hancock SE, Poad BL, Batarseh A, Abbott SK, Mitchell TW. Advances and unresolved challenges in the structural characterization of isomeric lipids. Anal Biochem 2017;24:45-55. https://doi.org/10.1016/j.ab.2016.09.014
6. Menzel JP, Young RSE, Benfield AH, Scott JS, Wongsomboon P, Cudlman L, Cvacka J, Butler LM, Henriques ST, Poad BLJ, Blanksby SJ. Ozone-enabled fatty acid discovery reveals unexpected diversity in the human lipidome. Nat Commun 2023;14:3940. https://doi.org/10.1038/s41467-023-39617-9
7. Yu D, Zhou L, Xuan Q, Wang L, Zhao X, Lu X, Xu G. Strategy for Comprehensive Identification of Acylcarnitines Based on Liquid Chromatography-High-Resolution Mass Spectrometry. Anal Chem 2018;90:5712-5718. https://doi.org/10.1021/acs.analchem.7b05471
8. Giesbertz P, Ecker J, Haag A, Spanier B, Daniel H. An LC-MS/MS method to quantify acylcarnitine species including isomeric and odd-numbered forms in plasma and tissues. J Lipid Res 2015;56:2029-2039. https://doi.org/10.1194/jlr.D061721
9. Minkler PE, Stoll MS, Ingalls ST, Yang S, Kerner J, Hoppel CL. Quantification of carnitine and acylcarnitines in biological matrices by HPLC electrospray ionization-mass spectrometry. Clin Chem 2008;54:1451-1462. https://doi.org/10.1373/clinchem.2007.099226
10. McDonald JG, Ejsing CS, Kopczynski D, Holčapek M, Aoki J, Arita M, Arita M, Baker ES, Bertrand-Michel J, Bowden JA, Brügger B, Ellis SR, Fedorova M, Griffiths WJ, Han X, Hartler J, Hoffmann N, Koelmel JP, Köfeler HC, Mitchell TW, ET AL. Introducing the Lipidomics Minimal Reporting Checklist. Nature Metabolism 2022;4:1086-1088. https://doi.org/10.1038/s42255-022-00628-3

11. Dietzen DJ, Rinaldo P, Whitley RJ, Rhead WJ, Hannon WH, Garg UC, Lo SF, Bennett MJ. National academy of clinical biochemistry laboratory medicine practice guidelines: follow-up testing for metabolic disease identified by expanded newborn screening using tandem mass spectrometry; executive summary. Clin Chem 2009;55:1615-1626. https://doi.org/10.1373/clinchem.2009.131300
12. Liebisch G, Fahy E, Aoki J, Dennis EA, Durand T, Ejsing CS, Fedorova M, Feussner I, Griffiths WJ, Kofeler H, Merrill AH, Jr, Murphy RC, O'Donnell VB, Oskolkova O, Subramaniam S, Wakelam MJO, Spener F. Update on LIPID MAPS classification, nomenclature, and shorthand notation for MS-derived lipid structures. J Lipid Res 2020;61:1539-1555. https://doi.org/10.1194/jlr.S120001025
13. Kopczynski D, Hoffmann N, Peng B, Liebisch G, Spener F, Ahrends R. Goslin 2.0 Implements the Recent Lipid Shorthand Nomenclature for MS-Derived Lipid Structures. Anal Chem 2022;94:6097-6101. https://doi.org/10.1021/acs.analchem.1c05430
14. Liebisch G, Vizcaino JA, Kofeler H, Trotzmuller M, Griffiths WJ, Schmitz G, Spener F, Wakelam MJO. Shorthand notation for lipid structures derived from mass spectrometry. J Lipid Res 2013;54:1523-1530. https://doi.org/10.1194/jlr.M033506
15. Chegary M, Brinke H, Ruiter JP, Wijburg FA, Stoll MS, Minkler PE, van Weeghel M, Schulz H, Hoppel CL, Wanders RJ, Houten SM. Mitochondrial long chain fatty acid beta-oxidation in man and mouse. Biochim Biophys Acta 2009;1791:806-815. https://doi.org/10.1016/j.bbalip.2009.05.006
16. van Weeghel M, te Brinke H, van Lenthe H, Kulik W, Minkler PE, Stoll MS, Sass JO, Janssen U, Stoffel W, Schwab KO, Wanders RJ, Hoppel CL, Houten SM. Functional redundancy of mitochondrial enoyl-CoA isomerases in the oxidation of unsaturated fatty acids. FASEB J 2012;26:4316-4326. https://doi.org/10.1096/fj.12-206326
17. Vondrackova M, Kopczynski D, Hoffmann N, Kuda O. LORA, Lipid Over-Representation Analysis Based on Structural Information. Anal Chem 2023;95:12600-12604. https://doi.org/10.1021/acs.analchem.3c02039
18. Li JM, Li LY, Zhang YX, Jiang ZY, Limbu SM, Qiao F, Degrace P, Chen LQ, Zhang ML, Du ZY. Functional differences between l- and d-carnitine in metabolic regulation evaluated using a low-carnitine Nile tilapia model. Br J Nutr 2019;122:625-638. https://doi.org/10.1017/S000711451900148X
19. Soeters MR, Serlie MJ, Sauerwein HP, Duran M, Ruiter JP, Kulik W, Ackermans MT, Minkler PE, Hoppel CL, Wanders RJ, Houten SM. Characterization of D-3-hydroxybutyrylcarnitine (ketocarnitine): an identified ketosis-induced metabolite. Metabolism 2012;61:966-973. https://doi.org/10.1016/j.metabol.2011.11.009
20. Schulz N, Himmelbauer H, Rath M, van Weeghel M, Houten S, Kulik W, Suhre K, Scherneck S, Vogel H, Kluge, R, Wiedmer P, Joost HG, Schurmann A. Role of medium- and short-chain L-3-hydroxyacyl-CoA dehydrogenase in the regulation of body weight and thermogenesis. Endocrinology 2011;152:4641-4651. https://doi.org/10.1210/en.2011-1547
21. Liu H, Tan D, Han L, Ye J, Qiu W, Gu X, Zhang H. A new case of malonyl-CoA decarboxylase deficiency with mild clinical features. Am J Med Genet A 2016;170A:1347-1351. https://doi.org/10.1002/ajmg.a.37590
22. Roe CR, Millington DS, Maltby DA. Identification of 3-methylglutarylcarnitine. A new diagnostic metabolite of 3-hydroxy-3-methylglutaryl-coenzyme A lyase deficiency. J Clin Invest 1986;77:1391-1394. https://doi.org/10.1172/JCI112446
23. Peters H, Ferdinandusse S, Ruiter JP, Wanders RJ, Boneh A, Pitt J. Metabolite studies in HIBCH and ECHS1 defects: Implications for screening. Mol Genet Metab 2015;115:168-173. https://doi.org/10.1016/j.ymgme.2015.06.008
24. Vaclavik J, Madrova L, Kouril S, de Sousa J, Brumarova R, Janeckova H, Jacova J, Friedecky D, Knapkova M, Kluijtmans LAJ, Grunert SC, Vaz FM, Janzen N, Wanders RJA, Wevers RA, Adam T. A newborn screening approach to diagnose 3-hydroxy-3-methylglutaryl-CoA lyase deficiency. JIMD Rep 2020;54:79-86. https://doi.org/10.1002/jmd2.12118
25. Hattori T, Notsu Y, Tanaka M, Matsui M, Iida T, Watanabe J, Osawa Y, Yamaguchi S, Yano S, Taketani T, Kobayashi H. A Simple Flow Injection Analysis-Tandem Mass Spectrometry Method to Reduce False Positives of C5-Acylcarnitines Due to Pivaloylcarnitine Using Reference Ions. Children (Basel) 2022;9:694. https://doi.org/10.3390/children9050694

26. Minkler PE, Stoll MSK, Ingalls ST, Hoppel CL. Selective and accurate C5 acylcarnitine quantitation by UHPLC-MS/MS: Distinguishing true isovaleric acidemia from pivalate derived interference. J Chromatogr B Analyt Technol Biomed Life Sci 2017;1061-1062:128-133. https://doi.org/10.1016/j.jchromb.2017.07.018
27. Lin S, Hanson RE, Cronan JE. Biotin synthesis begins by hijacking the fatty acid synthetic pathway. Nat Chem Biol 2010;6:682-688. https://doi.org/10.1038/nchembio.420
28. Taormina VM, Unger AL, Schiksnis MR, Torres-Gonzalez M, Kraft J. Branched-Chain Fatty Acids-An Underexplored Class of Dairy-Derived Fatty Acids. Nutrients 2020;12:2875. https://doi.org/10.3390/nu12092875
29. Wallace M, Green CR, Roberts LS, Lee YM, McCarville JL, Sanchez-Gurmaches J, Meurs N, Gengatharan JM, Hover JD, Phillips SA, Ciaraldi TP, Guertin DA, Cabrales P, Ayres JS, Nomura DK, Loomba R, Metallo CM. Enzyme promiscuity drives branched-chain fatty acid synthesis in adipose tissues. Nat Chem Biol 2018;14:1021-1031. https://doi.org/10.1038/s41589-018-0132-2
30. Schooneman MG, Achterkamp N, Argmann CA, Soeters MR, Houten SM. Plasma acylcarnitines inadequately reflect tissue acylcarnitine metabolism. Biochim Biophys Acta 2014;1841:987-994. https://doi.org/10.1016/j.bbalip.2014.04.001
31. Makrecka-Kuka M, Sevostjanovs E, Vilks K, Volska K, Antone U, Kuka J, Makarova E, Pugovics O, Dambrova M, Liepinsh E. Plasma acylcarnitine concentrations reflect the acylcarnitine profile in cardiac tissues. Sci Rep 2017;7:17528. https://doi.org/10.1038/s41598-017-17797-x
32. Hadjiagapiou C, Sprecher H, Kaduce TL, Figard PH, Spector AA. Formation of 8-hydroxyhexadecatrienoic acid by vascular smooth muscle cells. Prostaglandins 1987;34:579-589. https://doi.org/10.1016/0090-6980(87)90100-6
33. Diczfalusy U. Beta-oxidation of eicosanoids. Prog Lipid Res 1994;33:403-428. https://doi.org/10.1016/0163-7827(94)90025-6
34. Johnson M, Davison P, Ramwell PW. Carnitine-dependent β Oxidation of Prostaglandins. J Biol Chem 1972;247:5656-5658. https://doi.org/10.1016/S0021-9258(20)81155-7
35. Balas L, Rise P, Gandrath D, Rovati G, Bolego C, Stellari F, Trenti A, Buccellati C, Durand T, Sala A. Rapid Metabolization of Protectin D1 by beta-Oxidation of Its Polar Head Chain. J Med Chem 2019;62:9961-9975. https://doi.org/10.1021/acs.jmedchem.9b01463
36. Gillespie ME. Reactome, release 86, 10.3180/REACT_1473.1, 2003.
37. Jassal B. Reactome, release 86, 10.3180/REACT_16880.1, 2009.
38. Houten SM, Wanders RJA, Ranea-Robles P. Metabolic interactions between peroxisomes and mitochondria with a special focus on acylcarnitine metabolism. Biochim Biophys Acta Mol Basis Dis 2020;1866:165720. https://doi.org/10.1016/j.bbadis.2020.165720
39. van den Brink DM, Wanders RJ. Phytanic acid: production from phytol, its breakdown and role in human disease. Cell Mol Life Sci 2006;63:1752-1765. https://doi.org/10.1007/s00018-005-5463-y
40. Ferdinandusse S, Houten SM. Peroxisomes and bile acid biosynthesis. Biochim. Biophys Acta 2006;1763:1427-1440. https://doi.org/10.1016/j.bbamcr.2006.09.001
41. Wang Y, Palmfeldt J, Gregersen N, Makhov AM, Conway JF, Wang M, McCalley SP, Basu S, Alharbi H, St Croix C, Calderon MJ, Watkins S, Vockley J. Mitochondrial fatty acid oxidation and the electron transport chain comprise a multifunctional mitochondrial protein complex. J Biol Chem 2019;294:12380-12391. https://doi.org/10.1074/jbc.RA119.008680
42. Houten SM, Wanders RJ. A general introduction to the biochemistry of mitochondrial fatty acid beta-oxidation. J Inherit Metab Dis 2010;33:469-477. https://doi.org/10.1007/s10545-010-9061-2
43. Kuerschner L, Leyendecker P, Klizaite K, Fiedler M, Saam J, Thiele C. Development of oxaalkyne and alkyne fatty acids as novel tracers to study fatty acid beta-oxidation pathways and intermediates. J Lipid Res 2022;63:100188. https://doi.org/10.1016/j.jlr.2022.100188
44. Bansal P, Morgat A, Axelsen KB, Muthukrishnan V, Coudert E, Aimo L, Hyka-Nouspikel N, Gasteiger E, Kerhornou A, Neto TB, Pozzato M, Blatter MC, Ignatchenko A, Redaschi N, Bridge A. Rhea, the reaction knowledgebase in 2022. Nucleic Acids Res 2022;50:D693-D700. https://doi.org/10.1093/nar/gkab1016

Physiol. Res. 73 (Suppl. 1): S165-S183, 2024 *https://doi.org/10.33549/physiolres.935443*

REVIEW

Metabolomics and Lipidomics for Studying Metabolic Syndrome: Insights into Cardiovascular Diseases, Type 1 & 2 Diabetes, and Metabolic Dysfunction-Associated Steatotic Liver Disease

Stanislava RAKUSANOVA[1], Tomas CAJKA[1]

[1]Laboratory of Translational Metabolism, Institute of Physiology of the Czech Academy of Sciences, Prague, Czech Republic

Received July 8, 2024
Accepted July 18, 2024

Summary

Metabolomics and lipidomics have emerged as tools in understanding the connections of metabolic syndrome (MetS) with cardiovascular diseases (CVD), type 1 and type 2 diabetes (T1D, T2D), and metabolic dysfunction-associated steatotic liver disease (MASLD). This review highlights the applications of these omics approaches in large-scale cohort studies, emphasizing their role in biomarker discovery and disease prediction. Integrating metabolomics and lipidomics has significantly advanced our understanding of MetS pathology by identifying unique metabolic signatures associated with disease progression. However, challenges such as standardizing analytical workflows, data interpretation, and biomarker validation remain critical for translating research findings into clinical practice. Future research should focus on optimizing these methodologies to enhance their clinical utility and address the global burden of MetS-related diseases.

Key words

Metabolomics • Lipidomics • Mass spectrometry • Metabolic syndrome • Cardiovascular diseases • Type 1 diabetes • Type 2 diabetes • Metabolic dysfunction-associated steatotic liver disease

Corresponding author

T. Cajka, Laboratory of Translational Metabolism, Institute of Physiology of the Czech Academy of Sciences, Videnska 1083, 14200 Prague, Czech Republic. E-mail: tomas.cajka@fgu.cas.cz

Introduction

Metabolic syndrome (MetS), also known as insulin resistance syndrome, is defined as a cluster of risk factors for cardiovascular disease and diabetes. The main risk factors include raised blood pressure, visceral obesity, hyperglycemia, and dyslipidemia (reduced high-density lipoprotein cholesterol or raised triacylglycerols) [1-3]. These features are often related to insulin resistance, which can lead to prediabetes or type 2 diabetes [4]. Recent studies have shown that even non-obese patients may suffer from insulin resistance, with visceral adiposity being considered the primary contributor to MetS pathology. Visceral adiposity is strongly associated with hepatic fatty infiltration, indicating that the amount of fatty acids in the liver is indirectly linked with MetS, both as a cause and a consequence of the syndrome [5]. Furthermore, in recent decades, MetS has become a significant health concern with a high prevalence worldwide [4,6-8]. To properly understand MetS metabolism and the relationships between the aforementioned risk factors [9,10], metabolomics and lipidomics can be applied.

Metabolite profiling is conducted using either untargeted or targeted approaches, applied to biological samples through various analytical methods and platforms [11]. Large-scale metabolomics and lipidomics studies, which involve extensive populations or numerous samples (over 1000), have demonstrated their effectiveness in various scientific fields. These studies have defined individual phenotypes and shown the effects of genetic, environmental, intervention, or aging factors. They have also discovered biomarkers and validated metabolite patterns associated with specific biological

states [11]. Integrating newly identified metabolite biomarkers with clinical characteristics can potentially enhance the prediction of disease development [12].

In this review, we examine metabolomics and lipidomics human cohort studies and their application in MetS research. We introduce the analytical workflow and provide examples of recent MetS studies on cardiovascular diseases, type 1 and type 2 diabetes, and metabolic dysfunction-associated steatotic liver disease.

Metabolomics and lipidomics in large cohort studies

Large-scale metabolomics and lipidomics studies analyze hundreds to thousands of human samples containing thousands of metabolites. These samples are often processed in multiple batches over several weeks or months. No single analytical platform can cover all metabolites in a biological sample due to the complexity, diversity, and size of the human metabolome and lipidome. Therefore, multiple analytical platforms are employed to increase metabolite coverage [13]. Figure 1 shows metabolomics and lipidomics workflow, consisting of sample handling, instrumental analysis, data processing, and bioinformatics.

Sample handling

The first step in metabolomics and lipidomics studies is creating a proper experimental design, including sample size, sample collection and storage, sample preparation, quality control, and analytical techniques [14].

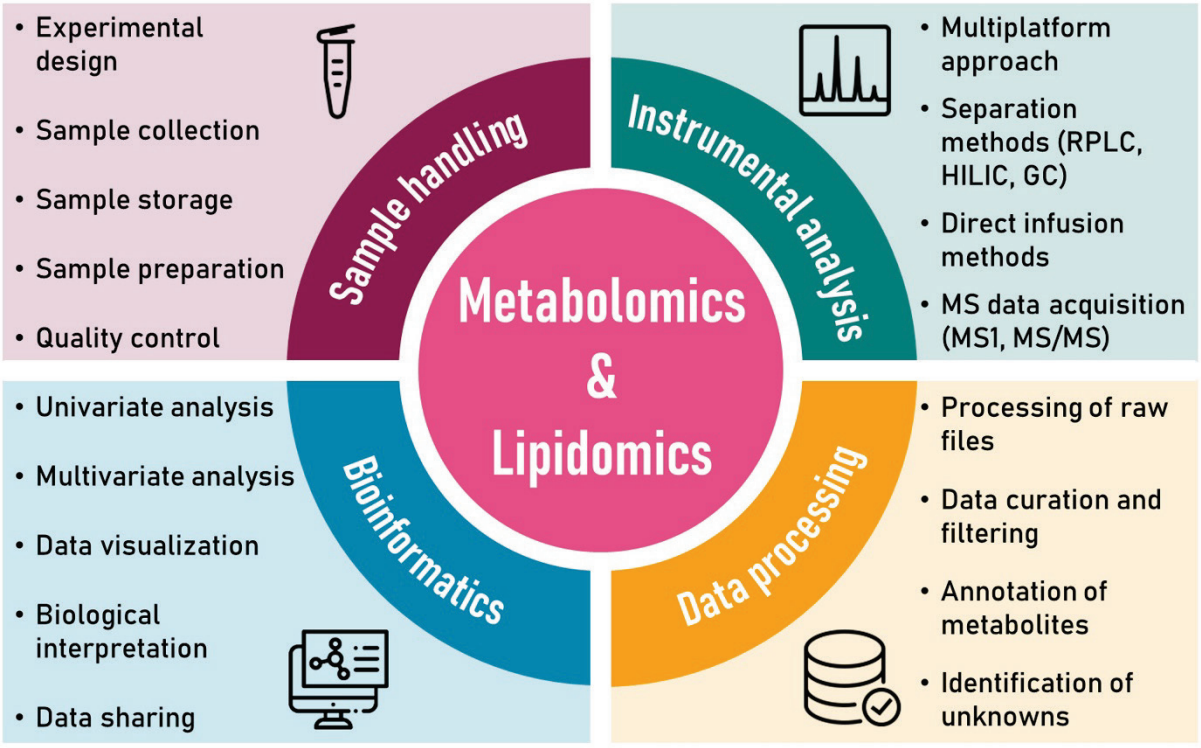

Fig. 1. Metabolomics and lipidomics workflow.

Determining the appropriate sample size, both overall and for each group, is essential. Insufficient sample size can lead to errors and lack of precision. Conversely, even small, insignificant differences might appear statistically significant with a larger sample size, while clinically important effects might seem statistically non-significant with a small sample size [15]. A high sample size may also waste resources for minimal information gain [16]. The minimal sample size is calculated using power analysis, taking into account the significance level (e.g., α=0.05), statistical power (e.g., 0.8), and effect size (d=0.8, 0.5, 0.2 for large, medium, small effect size, respectively) [17]. To this end, freely available software such as G*Power can be used [18]. However, for untargeted metabolomics and lipidomics studies with *a priori* unknown number of measured metabolites [19], alternative strategies have become available, such as the Data-driven Sample size Determination (DSD) algorithm

for MATLAB and GNU Octave [20], MetSizeR [21], or the online tool SSizer (idrblab.org/ssizer) [22].

Generally, at least 20-30 samples per group are advised for human studies, although the number of samples can range from hundreds to even thousands to achieve reasonable statistical power. On the other hand, for cell and animal studies with tightly controlled conditions, 3-6 and 5-10 samples per group, respectively, are recommended [23-25].

Another crucial aspect to consider is sample collection and storage. These steps must be decided during preanalytical processing to ensure reliable results [26]. Collection procedures differ based on the type of samples and planned analysis. For human cohort studies, samples typically consist of plasma or serum. The selection of a specific anticoagulant for plasma (e.g., EDTA, citrate, heparin) should be decided in advance and maintained consistently throughout the study. Inaccurate sample collection or improper storage may cause metabolite degradation, increased variability, or interference with instrumentation [27].

It is important to quench the metabolism of samples as soon as possible prior to their storage. Quenching should stop all enzymatic and chemical activities and maintain the current metabolite levels during harvesting [28]. The recommended method for quenching is to rapidly freeze the samples using liquid nitrogen, dry ice, or freeze clamping. After that, samples should be stored at -80 °C [29].

The next step is sample extraction to capture as many metabolites as possible in the sample. Various sample preparation techniques are available [30]. Minimal sample preparation methods, such as dilution, are sufficient for some matrices like urine. Water is a suitable diluent for reversed-phase liquid chromatography platforms, which start with a high percentage of water in the mobile phase. On the other hand, acetonitrile as a diluent is preferred for hydrophilic interaction chromatography, which begins with a high percentage of organic solvent (acetonitrile). Additionally, normalization to creatinine or osmolality values is a common strategy for urine due to its high variability in concentration, which correlates with metabolite composition [31]. On the other hand, plasma and serum, often used in large human cohort studies, contain many interfering proteins and require an extraction step to remove these before instrumental analysis. Common preparation methods like buffering, dilution, evaporation, and centrifugation may lead to metabolite losses and issues such as high salt concentration and instrument disruption, which can be reduced by adding an extraction step [32].

Extraction techniques in metabolomics and lipidomics commonly include organic solvent-based protein precipitation, liquid–liquid extraction (LLE), or solid-phase extraction (SPE). Isolation can also be performed in single or multiple fractions [33]. Single-phase extraction uses methanol, acetonitrile, isopropanol, a mixture of isopropanol/acetonitrile/water, acetonitrile/methanol, butanol/methanol [27,34,35]. This method enables simultaneous extraction of lipids and polar metabolites, but such extracts are very complex and can be challenging during instrumental analysis.

The most utilized method for reducing extract complexity is two-phase liquid extraction, where the separate phases are created by combining immiscible solvents: methyl *tert*-butyl ether (MTBE)/methanol/water [36], chloroform/methanol/water [37], and dichloromethane/methanol/water [38]. After centrifugation, the organic phase primarily contains nonpolar metabolites, such as lipids, while the polar (water) phase mainly consists of polar metabolites (Fig. 2A). In 2019, Vale *et al.* [39] introduced three-phase extraction using hexane, methyl acetate, acetonitrile, and water. After centrifugation, the upper organic phase is enriched with neutral lipids such as triacylglycerols and cholesteryl esters; the middle organic phase contains the glycerophospholipids, and the bottom aqueous phase contains polar metabolites.

While organic solvent-based protein precipitation and LLE methods are typically used for untargeted methods, SPE is the first choice for targeted methods, usually covering trace concentrations of metabolites [40].

The success of any research study also depends on an effective quality control (QC) process. Using internal standards in the extraction and resuspension solvents helps control the method's performance. These standards verify that aliquots are collected correctly from all extracts, the autosampler injects the correct volume, chromatographic and mass accuracy drifts are monitored, signal intensity fluctuations are tracked, and the quality of generated data is assessed during data processing [29]. They can also be used for quantification using a single-point calibration approach if added during the extraction step. Internal standards are essential because they represent true positives in the sample.

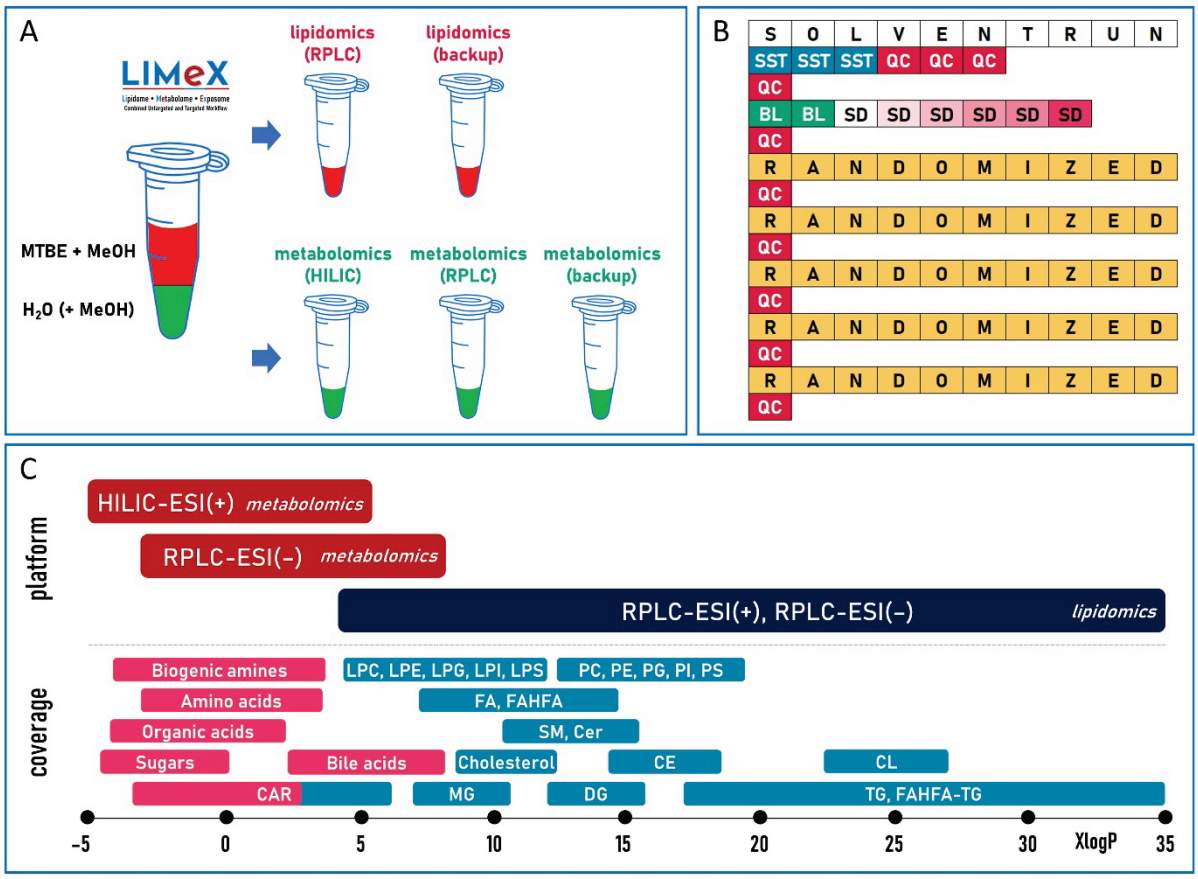

Fig. 2. (**A**) Example of sample extraction using MTBE, methanol, and water [41], leading to two phases for subsequent metabolomics and lipidomics platforms. (**B**) Example of a typical LC-MS sequence during metabolomics and lipidomic analysis, consisting of solvent injection for general platform equilibration, followed by a system suitability test (SST), platform equilibration using pooled QC samples, analysis of method blanks (BL), a diluted series of QC samples (SD), randomized study samples with regular QC sample injections after every 10 study samples. (**C**) Example of different LC-MS platforms [41,42] for metabolomic and lipidomic analysis in relation to the XlogP (predicted octanol/water partition coefficient) range of subgroups of polar metabolites and complex lipids.

QC samples are crucial for obtaining high-quality data in high-throughput analytical chemistry laboratories [43]. They help assess the precision and stability of the analysis. QC samples are used to equilibrate the analytical platform, monitor signals for precision (within and between days), correct signals (normalization), and standardize methods. QC data can also help indicate random errors or fluctuations during the analytical run [44].

QC samples can be created by pooling aliquots of each study sample, reflecting the composition of all samples during analysis. Another option is to employ external QC using a matrix that matches the study samples, which can be useful in large-scale studies where pooling is challenging. In such studies, pooling QC samples can be simplified by using pooled aliquots from only a portion of the samples. Additionally, commercially accessible QC samples (e.g., human plasma NIST SRM 1950 standard reference material [45]) can be applied, though there is a risk of missing some metabolites compared to pooled QC samples [46]. These approaches can be combined; however, they should be planned in advance and not modified during the study.

As Figure 2B shows, a typical metabolomics and lipidomics sequence consists of pre-injection steps (injection of solvents, QC sample) to equilibrate a particular platform, followed by a system suitability test (e.g., a mixture of selected metabolites or biological samples with known composition), analysis of method blanks, a diluted series of QC samples, randomized samples, and regular injection of QC samples [42]. All these steps are essential to generate reliable metabolomics and lipidomics data.

Instrumental analysis

A multiplatform approach using various analytical techniques and platforms is necessary due to the diversity and complexity of the metabolome and lipidome. This approach can improve the overall coverage and reliability of detected metabolites [47].

Liquid chromatography-mass spectrometry (LC-MS) dominates metabolomics and lipidomics. Other commonly applied platforms are gas chromatography-mass spectrometry (GC-MS), capillary electrophoresis-mass spectrometry (CE-MS), and nuclear magnetic resonance (NMR). However, NMR does not offer as broad metabolite coverage as MS-based approaches [29].

LC-MS separates metabolites with a wide range of polarities due to its versatility in stationary phases, column dimensions, mobile phase modifiers, and solvents [48]. Commonly used LC-MS separation platforms are reversed-phase LC (RPLC) and hydrophilic interaction chromatography (HILIC). RPLC separates polar to semi-polar metabolites using C18, C8, or C30 columns, whereas HILIC separates highly polar metabolites using silica, alkyl amide, aminopropylsilane, or sulfobetaine groups as the stationary phase [48]. Efficient chromatographic separation enhances the sensitivity of MS detection, while background noise reduction improves the quality of MS data [49]. For the analysis of polar metabolites (Fig. 2C), RPLC and HILIC are preferred, with mobile phases containing water, acetonitrile, and methanol. On the other hand, for RPLC-based lipidomics, stronger mobile phases are needed, typically containing a high percentage of isopropanol [41,42]. The column formats vary around 50-150 mm in length, with an internal diameter of 2.1 mm, packed with sub-2 μm particles. The separation process takes between 10 and 30 min [50]. However, fast, high-throughput LC-MS methods (<5 min), combined with 96-well plate sample preparation, are preferred for large cohort studies since they allow for hundreds of injections to be performed daily [29,42].

Once separated, analytes are ionized in an ion source to create charged particles. In LC-MS, electrospray ionization (ESI) is typically used, allowing ion formation for small molecules (<2,000 Da) and large molecules, such as peptides and proteins. Due to the chemical diversity of the metabolome and lipidome, ESI is usually applied in both positive and negative modes for more efficient coverage. ESI is a soft ionization technique, minimizing the fragmentation of molecular ions compared to electron ionization (EI) in GC-MS. However, ESI is sensitive to non-volatile salts, leading to limited use of only volatile mobile phase modifiers (e.g., formic acid, acetic acid, ammonium formate, ammonium acetate) in the chromatography part of the method. Due to the possible occurrence of ion suppression, metabolites with lower affinity for electrons or protons can be masked or undetected when competing for ionization [51].

MS techniques used for analyte detection can be either in a simple MS system with a single mass analyzer or in a tandem MS/MS system with multiple analyzers. These systems fall into low-resolution (LRMS) and high-resolution (HRMS) techniques. The main difference between LRMS and HRMS is their mass accuracy, i.e., the precision in determining the mass. HRMS can reach the accurate mass and increase confidence during metabolite annotation, whereas LRMS can only differentiate compounds based on nominal mass, which can cause false positives for compounds that share mass but are structurally unrelated [52]. Therefore, untargeted metabolomics and lipidomics rely on HRMS and HR-MS/MS using time-of-flight or orbital ion trap analyzers and operating in data-dependent acquisition (DDA) or data-independent acquisition (DIA) modes. In DDA mode, precursor ions above a pre-set threshold are selected using a narrow isolation window, making connecting product and precursor ions easier. However, low-abundance ions can be missed, and the settings are more complex than in DIA, which may lead to errors [53,54]. Conversely, in DIA mode, all precursor ions within the wide isolation window are fragmented, covering more low-abundance ions; however, this results in more complex spectra that are harder to interpret [55]. Tools like MS-DIAL [56], DecoMetDIA [57], and DecoID [58] help to deconvolute these complex MS/MS spectra. For the targeted LC-MS method, LRMS triple-quadrupole (QqQ) and quadrupole/linear ion trap (QLIT) are used, usually operating in a multiple reaction monitoring (MRM) mode to improve sensitivity and selectivity of monitored ions [50].

In general, untargeted methods provide semi-quantitative data, meaning that the results are reported as peak areas or heights in arbitrary units within the linear dynamic range of the detector. In contrast, targeted methods report quantitative data in molar concentrations [29]. Although quantification is often requested, it is not necessary for many studies since both semi-quantitative and quantitative data can be used for statistical analysis. However, the advantage of quantitative data is that it allows for the immediate distinction between major and minor metabolites and enables direct comparisons of results between laboratories and studies.

Data processing

Properly handling complex datasets produced by metabolomics and lipidomics experiments is crucial, as

this process significantly impacts metabolite annotation and quantification, consequently affecting the biological interpretation of results [59]. A standard untargeted metabolomics and lipidomics study can generate hundreds of annotated metabolites and numerous unknown features characterized by retention time and mass-to-charge ratio (*m*/*z*). Data handling can be divided into data processing and data analysis. Data processing uses signal processing methods to refine the raw data and combine them between measurements, converting data into a format that is easier for further analysis. This includes feature detection, chromatogram building, deisotoping, peak alignment, and gap-filling. Data analysis involves examining and interpreting processed data from previous steps, using methods like clustering metabolic profiles or finding key differences between sample groups [59]. Over the last decade, numerous processing tools have been introduced, such as MarkerLynx, MarkerView, MassHunter Profiling, Compound Discoverer, MS-DIAL (Fig. 3A), MZmine, XCMS, MetAlign, GeneDATA, Matlab and R scripts [29].

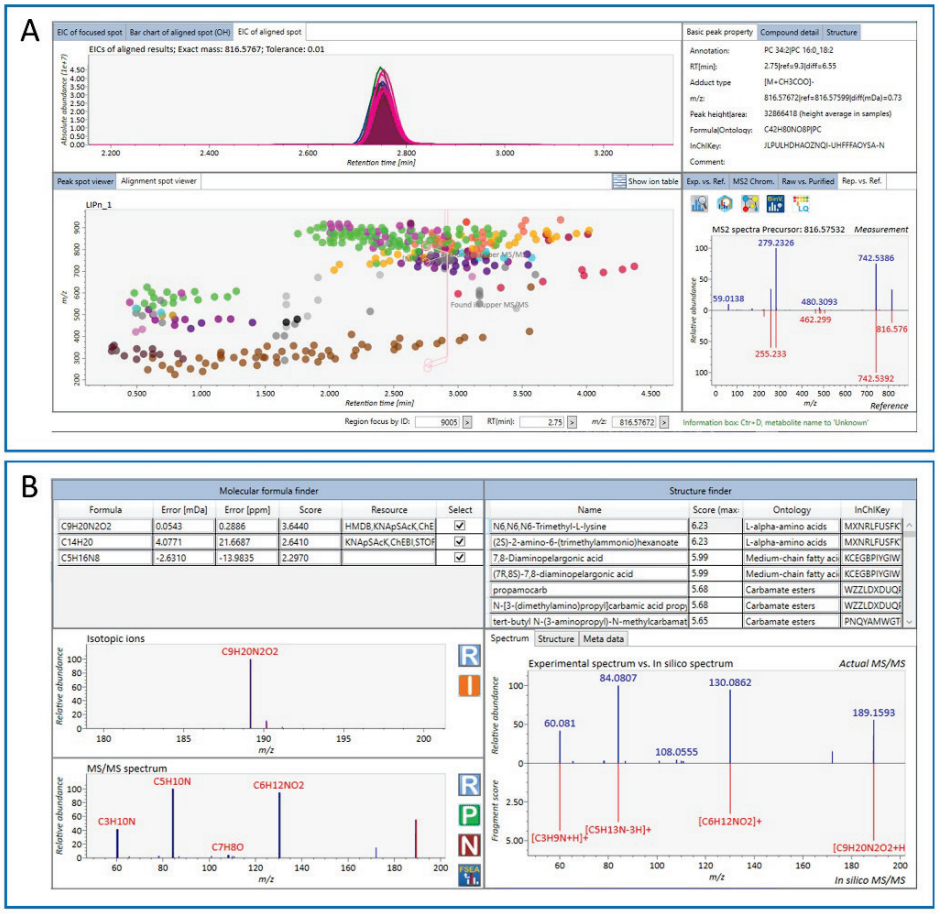

Fig. 3. (**A**) Example of MS-DIAL software [56] used for processing lipidomics data acquired using the RPLC-ESI(−)-MS [41], with annotated PC 16:0_18:2 in human serum. Using ammonium acetate and acetic acid as mobile phase modifiers led to the detection PC 34:2 as an acetate adduct ($[M+CH_3COO]^-$) (*m*/*z* 816.576). The MS/MS spectrum of PC 34:2 provided a fragment ion $[M–CH_3]^-$ (*m*/*z* 742.539) and a series of fragments for elucidating fatty acyl chains (e.g., *m*/*z* 255.233 for 16:0 and *m*/*z* 279.233 for 18:2). The use of the underscore "_" indicates certainty in the composition of the fatty acyl constituents but not their specific placement on the glycerol backbone. (**B**) Example of MS-FINDER software [60] used for the structure elucidation of an unknown compound (*m*/*z* 189.1597, retention time 4.57 min) in human serum acquired using the HILIC-ESI(+)-MS platform [41], with tentative annotation as N^{δ},N^{δ},N^{δ}-trimethyl-L-lysine.

Due to the structural variability and diversity of metabolites, detecting and annotating metabolites can be challenging. On average, successful annotation occurs for only approximately 10 % of the molecules, underscoring the importance of accurately identifying most molecular structures [61]. It should also be noted that in LC-MS, each metabolite can be detected in multiple ion forms, which can be annotated if present in spectral libraries or based on accurate mass differences. For instance, phosphatidylcholines (PC) can be detected during

lipidomics profiling in positive ESI as $[M+H]^+$ (major peak) and $[M+Na]^+$ (minor peak), while negative ESI provides $[M+CH_3COO]^-$ (major peak in the presence of ammonium acetate in the mobile phase [41]) and $[M+Cl]^-$ (minor peak). Depending on the data processing workflow, various options are possible for reporting these ion forms, such as providing all annotated species separately, species from one ionization mode only (e.g., the one with a lower relative standard deviation in QC samples), or combining adducts (summing peak intensities) for each ionization mode.

The Metabolomics Standardization Initiative (MSI) describes community-based guidelines for reporting and performing metabolomics workflows, proposing four confidence levels [62]: Level 1 – matching based on retention time, MS1, and MS/MS spectrum; Level 2 – matching based on MS1 and MS/MS spectrum; Level 3 – annotation based on matching MS1 accurate mass only; Level 4 – unknown compound characterized by retention time and *m*/*z*. However, multiple researchers have suggested revisions and modifications [63-65]. The Lipidomics Standards Initiative (LSI) has recently been introduced to create standardized lipid species annotations and unify community efforts [66].

The most reliable approach for metabolite annotation represents the use of spectral libraries containing retention time, *m*/*z* (MS1 accurate mass), and MS/MS fragmentation spectra (MSI – Level 1). However, it is virtually impossible to obtain all three pieces of information for every possible metabolite. Thus, commercial or open-access MS/MS libraries (with MS1 precursor ions and MS/MS spectra) are crucial in confident compound annotation in metabolomics and lipidomics (MSI – Level 2). In recent years, spectral libraries and databases have grown in both coverage and diversity [67]. METLIN Gen2 is the most extensive spectral library (metlin.scripps.edu), containing over 900,000 molecular standards and MS/MS data, comprising over 4 million tandem spectra [68]. Other extensive MS/MS libraries include the National Institute of Standards and Technology (NIST) MS/MS library (chemdata.nist.gov) and MassBank of North America (MoNA, massbank.us). Additional resources include MassBank (massbank.jp), ReSpect (spectra.psc.riken.jp), RIKEN PlaSMA (plasma.riken.jp), mzCloud (mzcloud.org), GNPS (gnps.ucsd.edu), MSforID (msforid.com), and HMBD (hmdb.ca).

Furthermore, numerous software and tools have been developed to help annotate unknown compounds, such as MS-FINDER (Fig. 3B), CFM-ID, MetFrag, ChemDistiller, and CSI:FingerID. These tools convert mass data into molecular fragments using combinatorial structure generation techniques and search against existing structures in various databases. Potential candidates can be filtered using additional orthogonal filters based on retention time prediction [69] or hydrogen/deuterium exchange mass spectrometry (HDX-MS) [70,71]. Nevertheless, confirmation should always follow by analyzing an analytical standard under identical instrumental conditions [72].

Bioinformatics

Statistical analysis is essential to properly extract relevant information from the obtained data. Statistical analyses can be categorized as univariate and multivariate methods. Univariate statistical methods include *t*-test, ANOVA, and fold-change analysis to compare different sets of samples. These methods are used for sets of tens to hundreds of metabolites, which increases the chances of false positives [73]. Therefore, correction methods such as Bonferroni correction [74] or the Benjamini-Hochberg [75] false discovery rate should be applied. These corrections have been addressed in multiple studies [74-76]. Commonly used multivariate methods include principal component analysis (PCA), partial least squares discriminant analysis (PLS-DA), and hierarchical cluster analysis (HCA) [77]. A routinely employed web-based platform for comprehensive metabolomics and lipidomics data analysis and interpretation is MetaboAnalyst (metaboanalyst.ca) [78].

Next, the biological relevance of the measured metabolites is interpreted using pathway and enrichment analysis. Enrichment analysis identifies functionally relevant metabolites and links their changes to biological contexts, suggesting key pathways or disease conditions for further study. Pathway analysis, on the other hand, finds pathways that significantly affect specific biological processes [79]. Both analyses are performed using various software tools such as MetaMapR, MetabNet, GNPS, MS2LDA, MetaboAnalyst, or MetFlow to map the metabolic pathways. New tools, such as an ontology database and enrichment analysis (LION, lipidontology.com) and lipid over-representation analysis (LORA, lora.metabolomics.fgu.cas.cz), are also available to interpret complex lipids [80].

An important part of every experiment is data sharing. Data should be shared following the Findable,

Accessible, Interoperable, and Reusable (FAIR) Guiding Principles for scientific data management and stewardship [81]. Public repositories such as Metabolomics Workbench (metabolomicsworkbench.org), MetaboLights (ebi.ac.uk/metabolights), and MassIVE (massive.ucsd.edu/ProteoSAFe/static/massive.jsp) enable data sharing. A newly introduced dynamic checklist (lipidomicstandards.org/reporting_checklist) summarizing key details of lipidomic analyses can be stored or shared in the supporting materials of papers or at a general-purpose open repository Zenodo (zenodo.org).

Recently introduced metabolomics and lipidomics atlases should also serve as open-access resources [29]. These atlases monitor the quantities and relationships of metabolites in different biological matrices, highlighting the importance of reusing and sharing data [82].

Metabolomics and lipidomics for studying metabolic syndrome

In recent years, MetS has become a major health risk with its increasing prevalence, reaching pandemic proportions [83]. The disease affects around 25 % of the global population, making prevention and management essential [84]. Understanding its pathophysiology is crucial in this effort. Metabolomics and lipidomics have been employed to investigate various diseases by identifying diagnostic biomarkers. Recently, research efforts have focused on cardiovascular diseases (CVD), type 2 diabetes (T2D), and metabolic dysfunction-associated steatotic liver disease (MASLD), all of which are associated with MetS. Wishart's comprehensive review in 2019 further underscored the significance of metabolomics studies in understanding physiological and pathophysiological processes [19]. Supplementary Tables S1-S3 overview metabolomics and lipidomics large-cohort studies focusing on CVD, T1D/T2D, and MASLD. Next, we briefly highlight some of these studies to elucidate key findings and advancements, emphasizing how metabolomic and lipidomic profiles have provided deeper insights into disease mechanisms and potential therapeutic targets.

Cardiovascular diseases

CVDs are the leading cause of death globally. In 2022, CVDs caused approximately 19.8 million deaths, accounting for about one-third of all global mortality that year. Major contributors to this toll were ischemic heart disease (9.2 million deaths) and ischemic stroke (3.5 million deaths) [85]. More than three-quarters of CVD deaths occur in low- and middle-income countries, compared to high-income countries, where the CVD death rate has declined [86,87].

CVDs are disorders of the heart and blood vessels, including coronary heart disease, cerebrovascular disease, peripheral arterial disease, rheumatic heart disease, congenital heart disease, deep vein thrombosis, and pulmonary embolism. Heart attacks and strokes are usually considered acute events, primarily resulting from a blockage that obstructs blood flow to the heart or brain [86]. The risk factors for cardiovascular diseases often include an unhealthy diet, physical inactivity, tobacco use, and harmful use of alcohol. These factors can be controlled, reducing the risk of CVD occurrence [86].

One area in CVD research involves exploring the role of different metabolites in disease promotion and progression. For instance, amino acids (alanine, glutamine, glycine, histidine, isoleucine, leucine, lysine, valine, phenylalanine, and tyrosine) have been identified as predictors of incident CVD risks [88-92]. Other discovered biomarkers of CVD are choline, trimethylamine *N*-oxide (TMAO), and betaine [93-96]. Similarly, compounds such as trimethyllysine [97], phenylacetyl glutamine [98], and niacin metabolites (N^1-methyl-2-pyridone-5-carboxamide and N^1-methyl-4-pyridone-3-carboxamide) [99] have been linked to CVD risks. Moreover, in recent studies, the endogenous sugar alcohols erythritol and xylitol were both clinically and mechanistically linked to CVD [100,101].

The association of diet-linked metabolites with CVD has also been explored. Fu *et al.* [102] investigated metabolites connected with a healthy lifestyle and their effect on CVD incidence. They identified and validated 111 metabolites associated with overall lifestyle, 65 of which were related to CVD risk. Healthy lifestyle-linked metabolites were also studied by Lu *et al.* [90]. Diabetes patients free of CVD were divided into groups based on the healthy level of five lifestyle factors and observed. Adherence to healthy lifestyle factors was associated with 44 plasma metabolites (e.g., 3-hydroxybutyrate, alanine, glutamine, glycine, branched-chain amino acids), and approximately half of them mediated between at least one lifestyle factor and CVD risk. Both studies suggest that a healthy diet positively affects the incidence of CVD.

Additionally, the effects of legume [103] and walnut [104] consumption on CVD risk were researched.

Walnut consumption was found to lower the risk of incident CVD and T2D, while legume consumption was associated with a lower risk of T2D but not CVD. Furthermore, gut microbiome-derived metabolites such as *p*-cresol sulfate and indoxyl sulfate have garnered attention [105]. This study shows that these abundant microbiome-derived metabolites have a greater impact on CVD than previously thought. It also suggests targeting the gut microbial pathways that produce *p*-cresol and indole as a potential strategy for treating CVD.

Lipidomics profiling also reveals characteristic lipid signatures associated with increased CVD risk. Harm *et al.* [106] focused on the platelet lipidome of coronary artery disease patients and found alterations in the lipid composition of patients with adverse cardiovascular events. The results showed that the platelet lipidome of CVD patients with increased cardiovascular risk is changed, and specific platelet lipids may indicate adverse events. These findings may help discriminate the individual risk of patients with coronary artery disease. Eichelmann *et al.* [88] investigated associations of plasma lipid alterations with incident cardiometabolic diseases and studied the effect of dietary fat modulation on discovered risk-associated lipids. The results suggest that dietary fat intervention can alter lipids, which may serve as a potential tool for primary disease prevention. Furthermore, Seah *et al.* [107] suggested that certain classes of sphingolipids may also affect CVD risk.

Type 1 & 2 diabetes

As of 2021, the global prevalence of diabetes was estimated at 10.5 % (537 million people), projected to rise to 12.2 % (783 million people) by 2045. Diabetes was responsible for approximately 6.7 million deaths worldwide in 2021, with global healthcare expenditures amounting to approximately USD 966 billion [108]. However, the majority of these cases are attributed to T2D, while T1D affected approximately 8.4 million individuals globally in 2021 [109]. In the future, access to and affordability of insulin may become challenging, particularly in underdeveloped and developing countries, due to the increasing prevalence and incidence of T1D [110].

Diabetes is a complex chronic metabolic disease characterized by high prevalence and mortality, encompassing T1D, T2D, and gestational diabetes occurring during pregnancy. T1D results from insufficient insulin production by the pancreas, necessitating daily insulin administration. T2D arises from inadequate insulin secretion and the body's ineffective use of insulin, leading to elevated blood sugar levels. T2D impacts the metabolism of glucose, lipids, and amino acids [111,112].

Metabolomics and lipidomics studies of T1D aim to identify biomarkers for predicting T1D risk and aiding in early disease detection. Orešič *et al.* [113] analyzed the lipidome profile of cord serum samples to investigate associations between lipid profile changes and β-cell autoimmunity development or clinical T1D. Their study found that progression to T1D correlated with decreased concentrations of major choline-containing phospholipids (sphingomyelins and phosphatidylcholines) in cord blood. The study also indicated that phospholipid reduction is associated explicitly with T1D progression rather than general β-cell autoimmunity.

La Torre [89] and Tapia [90] also studied cord blood samples. La Torre *et al.* [114] discovered that decreased levels of phospholipids at birth, especially phosphatidylcholines and phosphatidylethanolamines, may contribute to early induction of islet autoimmunity and increased T1D risk. Conversely, Tapia *et al.* [115] focused more on changes in the metabolome profile than lipidome alterations. However, the research showed no strong associations of selected polar metabolites with T1D. Nevertheless, Webb-Robertson *et al.* [116] identified multiple metabolites associated with T1D progression by age 6, primarily comprising sugar metabolism compounds such as fructose, levoglucosan, glycerol-α-phosphate, and xylulose.

Recent studies have explored metabolomics' potential in predicting T2D risk based on dietary patterns and corresponding biomarkers. One study involving nearly 6,000 participants identified 29 plasma metabolites associated with inflammatory and insulinemic dietary patterns [117]. The top five biomarkers included PE 36:4, CAR 5:0, PC 34:4, 1-methylguanosine, and N^4-acetyl-cytidine. Additionally, investigations into the lipid profile of lean and obese individuals with T2D revealed significant lipidome changes (lyso-, diacyl- and ether-phospholipids, and 1-deoxyceramides), aiding in T2D diagnosis [118].

Lipid profiles containing 69 odd-chain saturated fatty acids (OCFA) among 15 lipid subclasses were also examined for their potential as T2D biomarkers [119], revealing variations dependent on lipid class and sex, correlating with food consumption. Sun *et al.* [120] investigated plasma acylcarnitines' role in early

T2D prediction, identifying long-chain acylcarnitines as significantly linked to future T2D risk.

Moreover, interventions targeting weight loss have shown promise in altering metabolite signatures associated with T2D. Studies have noted positive associations between changes in branched-chain amino acids (valine, leucine, isoleucine) and branched-chain ketoacids (α-ketoisovalerate, α-ketoisocaproate, α-keto-β-methylvalerate) with glycated hemoglobin (HbA1c) levels following weight loss [121]. Branched-chain amino acids are frequently studied due to their association with increased T2D risk [122-127]. 3-Hydroxybutyrate is another frequently studied metabolite, often alongside branched-chain amino acids [122-126,128]. Similar to its association with CVD, TMAO has also been investigated in relation to T2D [129]. Lemaitre *et al.* [129] explored the connections of TMAO, carnitine, crotonobetaine, and γ-butyrobetaine with insulin resistance, and betaine and choline with enhanced insulin sensitivity. However, they did not establish a definitive association.

Metabolic dysfunction-associated steatotic liver disease

MASLD is the latest term used to describe steatotic liver disease associated with MetS, encompassing various metabolic risk factors and often coexisting with other chronic liver conditions [130]. Historically, the term nonalcoholic fatty liver disease (NAFLD) was used. In 2020, Eslam *et al.* [131] proposed the term metabolic dysfunction-associated fatty liver disease (MAFLD), which was further modified to MASLD in 2023 [132]. Both MAFLD and MASLD identify patients with hepatic steatosis and metabolic dysfunction [133]. There are slight differences in the definitions of MASLD and MAFLD, which have been discussed in several articles [130,132-134]. Notably, MAFLD encompasses patients with fatty liver regardless of alcohol consumption pattern or amount [132], whereas MASLD introduces the term MetALD for patients who meet alcohol-related fatty liver disease criteria [134]. MASLD diagnosis requires meeting one of five cardiometabolic risk factors [132], while MAFLD requires meeting two out of seven metabolic dysfunction parameters [131]. De *et al.* [135] suggest that MASLD and SLD (steatotic liver disease) criteria may better suit lean patients with NAFLD than MAFLD criteria. Consequently, both MASLD and MAFLD terms are used in literature to classify liver diseases associated with metabolic dysfunction, although NAFLD remains prevalent in many studies since the new nomenclature's introduction.

The global prevalence of NAFLD was estimated to be approximately 30 % between 1990 and 2019, with a continuing upward trend [136]. This increasing prevalence of NAFLD is likely associated with rising rates of diabetes and obesity. However, the global mortality rate declined from 2.39 per 100,000 population in 1990 to 2.09 per 100,000 population in 2019 [137].

MASLD includes a range of steatotic liver conditions, from isolated hepatic steatosis to metabolic dysfunction-associated steatohepatitis (MASH), with varying levels of liver fibrosis that can potentially lead to cirrhosis. MASLD is associated with a higher risk of liver complications (e.g., cirrhosis), end-stage liver disease, and hepatocellular carcinoma, as well as an increased risk of developing extrahepatic issues such as cardiovascular disease (CVD), chronic kidney disease, and certain extrahepatic cancers [138].

Recent large-scale cohort studies aim to identify risk factors and biomarkers for MASLD, aiding in its challenging diagnosis. Commonly identified biomarkers include amino acids, particularly aromatic amino acids (tyrosine, tryptophan) and branched-chain amino acids (isoleucine, leucine, valine) [139-143]. Studies by Hirata [142] and Martínez-Arranz [144] examined the association of NAFLD with cardiovascular risk, identifying metabolomic signatures aligning with known CVD risk factors. Hirata *et al.* [142] found that NAFLD was positively associated with the cardio-ankle vascular index (CAVI), an indicator of subclinical atherosclerosis, and identified ten metabolites involved in both NAFLD and CAVI: branched-chain amino acids (valine, leucine, and isoleucine), aromatic amino acids (tyrosine and tryptophan), alanine, proline, glutamic acid, glycerophosphorylcholine, and 4-methyl-2-oxopentanoate. Martínez-Arranz *et al.* [144] investigated lipidomic profile changes, particularly in triacylglycerols, phosphatidylcholines, and sphingomyelins, providing evidence of distinct metabolic mechanisms associated with NAFLD progression that vary between subtypes.

McGlinchey *et al.* [145] observed lipidomic and metabolomic profile changes across different stages of NAFLD progression, highlighting unique metabolites and 27 common metabolites across all stages, including significant alterations in cholesteryl esters, ceramides, lysophosphatidylcholines, phosphatidylcholines, phosphatidylethanolamine, sphingomyelins, and triacylglycerols. Hu *et al.* [146] discovered correlations between NAFLD and uric acid, as well as oleic acid-hydroxy oleic acid

(OAHOA), identifying OAHOA as a novel biomarker for NAFLD prevalence in a cohort of 1,479 patients (aged 18-80 years). Other studies have explored potential biomarkers, such as anandamide [147] or taurochloric acid [148].

Conclusions

Metabolomics and lipidomics represent effective tools for studying MetS and related disorders. The comprehensive multiplatform-based profiling of polar metabolites and complex lipids in large cohorts has enabled the identification of novel biomarkers and enhanced our understanding of disease mechanisms. Key advancements include the discovery of metabolic signatures associated with CVD, T1D, T2D, and MASLD.

Regarding polar metabolites, branched-chain amino acids (valine, leucine, isoleucine), TMAO, betaine, choline, and 3-hydroxybutyrate have been identified in multiple studies as promising biomarkers. For complex lipids, a panel or combination of affected lipids is expected to be useful as biomarkers, including acylcarnitines, phospholipids, sphingomyelins, and triacylglycerols as key lipid subclasses.

Further research is needed to validate these reported biomarkers in diverse populations and clinical settings, ensuring their robustness and clinical utility. Standardization of experimental protocols and data analysis methods will be critical to facilitate data comparability and reproducibility across studies. Based on a review of multiple studies, we also advocate for the inclusion of authoritative identifiers such as InChI keys or identifiers from bioinformatics resources such as the Human Metabolome Database (hmdb.ca) and LIPID MAPS (lipidmaps.org). This will expedite the comparison of potential biomarkers within studies, making the process faster and more effective.

In addition, further advances in analytical technologies and computational tools will continue to drive innovation in metabolomics and lipidomics, offering new opportunities for early disease detection and personalized therapeutic interventions.

Supplementary Materials

The supporting information (Table S1-S3) can be downloaded at:
https://www.biomed.cas.cz/physiolres/pdf/73_Suppl_1/Rakusanova_Supl_Tables_1-3.pdf

Conflict of Interest

There is no conflict of interest.

Acknowledgements

This research was funded by the Czech Health Research Council (NU20-01-00186), the Ministry of Education, Youth and Sport of the Czech Republic (LUAUS24169), and the National Institute for Research of Metabolic and Cardiovascular Diseases (Programme EXCELES, ID Project No. LX22NPO5104) funded by the European Union - Next Generation EU. Examples of LC-MS chromatographic records (Vanquish UHPLC & Q Exactive Plus, Vanquish UHPLC & Orbitrap Exploris 480) processed in MS-DIAL and MS-FINDER software were provided by the Metabolomics Core Facility at the Institute of Physiology of the Czech Academy of Sciences (metabolomics.fgu.cas.cz).

References

1. Alberti KG, Eckel RH, Grundy SM, Zimmet PZ, Cleeman JI, Donato KA, Fruchart JC, ET AL. Harmonizing the metabolic syndrome: a joint interim statement of the International Diabetes Federation Task Force on Epidemiology and Prevention; National Heart, Lung, and Blood Institute; American Heart Association; World Heart Federation; International Atherosclerosis Society; and International Association for the Study of Obesity. Circulation 2009;120:1640-1645. https://doi.org/10.1161/CIRCULATIONAHA.109.192644
2. Alberti KG, Zimmet P, Shaw J. The metabolic syndrome - a new worldwide definition. Lancet 2005;366:1059-1062. https://doi.org/10.1016/S0140-6736(05)67402-8
3. Han TS, Lean MEJ. Metabolic syndrome. Medicine 2015;43:80-87. https://doi.org/10.1016/j.mpmed.2014.11.006
4. Grundy SM. Metabolic Syndrome Pandemic. Arterioscler Thromb Vasc Biol 2008;28:629-636. https://doi.org/10.1161/ATVBAHA.107.151092
5. Radu F, Potcovaru C-G, Salmen T, Filip PV, Pop C, Fierbințeanu-Braticievici C. The link between NAFLD and metabolic syndrome. Diagnostics 2023;13:614. https://doi.org/10.3390/diagnostics13040614

6. Noubiap JJ, Nansseu JR, Lontchi-Yimagou E, Nkeck JR, Nyaga UF, Ngouo AT, Tounouga DN, Tianyi F-L, Foka AJ, Ndoadoumgue AL, ET AL. Geographic distribution of metabolic syndrome and its components in the general adult population: A meta-analysis of global data from 28 million individuals. Diabetes Res Clin Pr 2022;188:109924. https://doi.org/10.1016/j.diabres.2022.109924
7. Reisinger C, Nkeh-Chungag BN, Fredriksen PM, Goswami N. The prevalence of pediatric metabolic syndrome-a critical look on the discrepancies between definitions and its clinical importance. Int J Obes 2021;45:12-24. https://doi.org/10.1038/s41366-020-00713-1
8. Cameron AJ, Shaw JE, Zimmet PZ. The metabolic syndrome: prevalence in worldwide populations. Endocrinol Metab Clin North Am 2004;33:351-375. https://doi.org/10.1016/j.ecl.2004.03.005
9. Allam-Ndoul B, Guénard F, Garneau V, Cormier H, Barbier O, Pérusse L, Vohl MC. Association between metabolite profiles, metabolic syndrome and obesity status. Nutrients 2016;8:324. https://doi.org/10.3390/nu8060324
10. Gong L-L, Yang S, Zhang W, Han F-F, Lv Y-L, Xuan L-L, Liu H, Liu L-H. Discovery of metabolite profiles of metabolic syndrome using untargeted and targeted LC-MS based lipidomics approach. J Pharm Biomed 2020;177:112848. https://doi.org/10.1016/j.jpba.2019.112848
11. Hajjar G, Barros Santos MC, Bertrand-Michel J, Canlet C, Castelli F, Creusot N, Dechaumet S, ET AL. Scaling-up metabolomics: Current state and perspectives. Trends Analyt Chem 2023;167:117225. https://doi.org/10.1016/j.trac.2023.117225
12. Pujos-Guillot E, Brandolini M, Pétéra M, Grissa D, Joly C, Lyan B, Herquelot É, ET AL. Systems metabolomics for prediction of metabolic syndrome. J Proteome Res 2017;16:2262-2272. https://doi.org/10.1021/acs.jproteome.7b00116
13. Dunn WB, Broadhurst D, Begley P, Zelena E, Francis-McIntyre S, Anderson N, Brown M, ET AL. Procedures for large-scale metabolic profiling of serum and plasma using gas chromatography and liquid chromatography coupled to mass spectrometry. Nat Protoc 2011;6:1060-1083. https://doi.org/10.1038/nprot.2011.335
14. Salek R, Emery L, Beisken S. Metabolomics: an introduction. EMBL-EMI 2014. https://doi.org/10.6019/TOL.MBS.2014.00001.1
15. Gardner MJ, Altman DG. Confidence intervals rather than P values: Estimation rather than hypothesis testing. Br Med J (Clin Res Ed) 1986;292:746-750. https://doi.org/10.1136/bmj.292.6522.746
16. Vinaixa M, Samino S, Saez I, Duran J, Guinovart JJ, Yanes O. A guideline to univariate statistical analysis for LC/MS-based untargeted metabolomics-derived data. Metabolites 2012;2:775-795. https://doi.org/10.3390/metabo2040775
17. Serdar CC, Cihan M, Yücel D, Serdar MA. Sample size, power and effect size revisited: simplified and practical approaches in pre-clinical, clinical and laboratory studies. Biochem Med 2021;31:010502. https://doi.org/10.11613/BM.2021.010502
18. Faul F, Erdfelder E, Buchner A, Lang AG. Statistical power analyses using G*Power 3.1: Tests for correlation and regression analyses. Behav Res Methods 2009;41:1149-1160. https://doi.org/10.3758/BRM.41.4.1149
19. Zhao X, Niu L, Clerici C, Russo R, Byrd M, Setchell KDR. Data analysis of MS-based clinical lipidomics studies with crossover design: A tutorial mini-review of statistical methods. Clin Mass Spectrom 2019;13:5-17. https://doi.org/10.1016/j.clinms.2019.05.002
20. Billoir E, Navratil V, Blaise BJ. Sample size calculation in metabolic phenotyping studies. Brief Bioinform 2015;16:813-819. https://doi.org/10.1093/bib/bbu052
21. Nyamundanda G, Gormley IC, Fan Y, Gallagher WM, Brennan L. MetSizeR: Selecting the optimal sample size for metabolomic studies using an analysis based approach. BMC Bioinform 2013;14:338. https://doi.org/10.1186/1471-2105-14-338
22. Li F, Zhou Y, Zhang X, Tang J, Yang Q, Zhang Y, Luo Y, ET AL. SSizer: Determining the sample sufficiency for comparative biological study. J Mol Biol 2020;432:3411-3421. https://doi.org/10.1016/j.jmb.2020.01.027
23. Ivanisevic J, Want EJ. From samples to insights into metabolism: Uncovering biologically relevant information in LC-HRMS metabolomics data. Metabolites 2019;9:308. https://doi.org/10.3390/metabo9120308
24. Lenth RV. Some practical guidelines for effective sample size determination. Am Stat 2001;55:187-193. https://doi.org/10.1198/000313001317098149

25. Arifin WN, Zahiruddin WM. Sample size calculation in animal studies using resource equation approach. Malays J Med Sci 2017;24:101-105. https://doi.org/10.21315/mjms2017.24.5.11
26. Dunn WB, Wilson ID, Nicholls AW, Broadhurst D. The importance of experimental design and QC samples in large-scale and MS-driven untargeted metabolomic studies of humans. Bioanalysis 2012;4:2249-2264. https://doi.org/10.4155/bio.12.204
27. Smith L, Villaret-Cazadamont J, Claus SP, Canlet C, Guillou H, Cabaton NJ, Ellero-Simatos S. Important considerations for sample collection in metabolomics studies with a special focus on applications to liver functions. Metabolites 2020;10:104. https://doi.org/10.3390/metabo10030104
28. Alseekh S, Aharoni A, Brotman Y, Contrepois K, D'Auria J, Ewald J, Ewald JC, ET AL. Mass spectrometry-based metabolomics: A guide for annotation, quantification and best reporting practices. Nat Methods 2021;18:747-756. https://doi.org/10.1038/s41592-021-01197-1
29. Rakusanova S, Fiehn O, Cajka T. Toward building mass spectrometry-based metabolomics and lipidomics atlases for biological and clinical research. Trends Anal Chem 2023;158:116825. https://doi.org/10.1016/j.trac.2022.116825
30. Mushtaq MY, Choi YH, Verpoorte R, Wilson EG. Extraction for metabolomics: Access to the metabolome. Phytochem Anal 2014;25:291-306. https://doi.org/10.1002/pca.2505
31. Khamis MM, Holt T, Awad H, El-Aneed A, Adamko DJ. Comparative analysis of creatinine and osmolality as urine normalization strategies in targeted metabolomics for the differential diagnosis of asthma and COPD. Metabolomics 2018;14:115. https://doi.org/10.1007/s11306-018-1418-9
32. Álvarez-Sánchez B, Priego-Capote F, Castro MDL. Metabolomics analysis II. Preparation of biological samples prior to detection. Trends Anal Chem 2010;29:120-127. https://doi.org/10.1016/j.trac.2009.12.004
33. Dunn WB. Mass spectrometry in systems biology an introduction. Methods Enzymol 2011;500:15-35. https://doi.org/10.1016/B978-0-12-385118-5.00002-5
34. Showalter MR, Nonnecke EB, Linderholm AL, Cajka T, Sa MR, Lönnerdal B, Kenyon NJ, Fiehn O. Obesogenic diets alter metabolism in mice. PLoS One 2018;13:e0190632. https://doi.org/10.1371/journal.pone.0190632
35. Lepoittevin M, Blancart-Remaury Q, Kerforne T, Pellerin L, Hauet T, Thuillier R. Comparison between 5 extractions methods in either plasma or serum to determine the optimal extraction and matrix combination for human metabolomics. Cell Mol Biol Lett 2023;28:43. https://doi.org/10.1186/s11658-023-00452-x
36. Matyash V, Liebisch G, Kurzchalia TV, Shevchenko A, Schwudke D. Lipid extraction by methyl-tert-butyl ether for high-throughput lipidomics. J Lipid Res 2008;49:1137-1146. https://doi.org/10.1194/jlr.D700041-JLR200
37. Folch J, Lees M, Sloane Stanley GH. A simple method for the isolation and purification of total lipides from animal tissues. J Biol Chem 1957;226:497-509. https://doi.org/10.1016/S0021-9258(18)64849-5
38. Southam AD, Haglington LD, Najdekr L, Jankevics A, Weber RJM, Dunn WB. Assessment of human plasma and urine sample preparation for reproducible and high-throughput UHPLC-MS clinical metabolic phenotyping. Analyst 2020;145:6511-6523. https://doi.org/10.1039/D0AN01319F
39. Vale G, Martin SA, Mitsche MA, Thompson BM, Eckert KM, McDonald JG. Three-phase liquid extraction: a simple and fast method for lipidomic workflows. J Lipid Res 2019;60:694-706. https://doi.org/10.1194/jlr.D090795
40. Gasperotti M, Masuero D, Guella G, Mattivi F, Vrhovsek U. Development of a targeted method for twenty-three metabolites related to polyphenol gut microbial metabolism in biological samples, using SPE and UHPLC-ESI-MS/MS. Talanta 2014;128:221-230. https://doi.org/10.1016/j.talanta.2014.04.058
41. Cajka T, Hricko J, Rudl Kulhava L, Paucova M, Novakova M, Kuda O. Optimization of mobile phase modifiers for fast LC-MS-based untargeted metabolomics and lipidomics. Int J Mol Sci 2023;24:1987. https://doi.org/10.3390/ijms24031987
42. Hricko J, Rudl Kulhava L, Paucova M, Novakova M, Kuda O, Fiehn O, Cajka T. Short-term stability of serum and liver extracts for untargeted metabolomics and lipidomics. Antioxidants 2023;12:986. https://doi.org/10.3390/antiox12050986
43. Broadhurst D, Goodacre R, Reinke SN, Kuligowski J, Wilson ID, Lewis MR, Dunn WB. Guidelines and considerations for the use of system suitability and quality control samples in mass spectrometry assays applied in untargeted clinical metabolomic studies. Metabolomics 2018;14:72. https://doi.org/10.1007/s11306-018-1367-3

44. Begou O, Gika HG, Theodoridis GA, Wilson ID. Quality control and validation issues in LC-MS metabolomics. Methods Mol Biol 2018;1738:15-26. https://doi.org/10.1007/978-1-4939-7643-0_2
45. Bowden JA, Heckert A, Ulmer CZ, Jones CM, Koelmel JP, Abdullah L, Ahonen L, ET AL. Harmonizing lipidomics: NIST interlaboratory comparison exercise for lipidomics using SRM 1950-Metabolites in frozen human plasma. J Lipid Res 2017;58:2275-2288. https://doi.org/10.1194/jlr.M079012
46. Dudzik D, Barbas-Bernardos C, García A, Barbas C. Quality assurance procedures for mass spectrometry untargeted metabolomics. A review. J Pharm Biomed Anal 2018;147:149-173. https://doi.org/10.1016/j.jpba.2017.07.044
47. Jeppesen MJ, Powers R. Multiplatform untargeted metabolomics. Magn Reson Chem 2023;61:628-653. https://doi.org/10.1002/mrc.5350
48. Harrieder EM, Kretschmer F, Böcker S, Witting M. Current state-of-the-art of separation methods used in LC-MS based metabolomics and lipidomics. J Chromatogr B 2022;1188:123069. https://doi.org/10.1016/j.jchromb.2021.123069
49. Zhou B, Xiao JF, Tuli L, Ressom HW. LC-MS-based metabolomics. Mol Biosyst 2012;8:470-81. https://doi.org/10.1039/C1MB05350G
50. Cajka T, Fiehn O. Toward merging untargeted and targeted methods in mass spectrometry-based metabolomics and lipidomics. Anal Chem 2016;88:524-545. https://doi.org/10.1021/acs.analchem.5b04491
51. Gowda GAN, Djukovic D. Overview of mass spectrometry-based metabolomics: Opportunities and challenges. In: *Mass Spectrometry in Metabolomics: Methods and Protocols*. RAFTERY D (ed.), New York, NY, 2014, pp 3-12. https://doi.org/10.1007/978-1-4939-1258-2_1
52. Zarrouk E, El Balkhi S, Saint-Marcoux F. Low-resolution or high-resolution MS for clinical and forensic toxicology: some considerations from two real cases. LCGC Supplements 2023;41:24-27. https://doi.org/10.56530/lcgc.na.ez3089i6
53. Defossez E, Bourquin J, von Reuss S, Rasmann S, Glauser G. Eight key rules for successful data-dependent acquisition in mass spectrometry-based metabolomics. Mass Spectrom Rev 2023;42:131-143. https://doi.org/10.1002/mas.21715
54. Nash WJ, Dunn WB. From mass to metabolite in human untargeted metabolomics: Recent advances in annotation of metabolites applying liquid chromatography-mass spectrometry data. Trends Anal Chem 2019;120:115324. https://doi.org/10.1016/j.trac.2018.11.022
55. Guo J, Huan T. Comparison of full-scan, data-dependent, and data-independent acquisition modes in liquid chromatography-mass spectrometry based untargeted metabolomics. Anal Chem 2020;92:8072-8080. https://doi.org/10.1021/acs.analchem.9b05135
56. Tsugawa H, Ikeda K, Takahashi M, Satoh A, Mori Y, Uchino H, Okahashi N, ET AL. A lipidome atlas in MS-DIAL 4. Nat Biotechnol 2020;38:1159-1163. https://doi.org/10.1038/s41587-020-0531-2
57. Yin Y, Wang R, Cai Y, Wang Z, Zhu Z-J. DecoMetDIA: Deconvolution of multiplexed MS/MS spectra for metabolite identification in SWATH-MS-based untargeted metabolomics. Anal Chem 2019;91:11897-11904. https://doi.org/10.1021/acs.analchem.9b02655
58. Stancliffe E, Schwaiger-Haber M, Sindelar M, Patti GJ. DecoID improves identification rates in metabolomics through database-assisted MS/MS deconvolution. Nat Methods 2021;18:779-787. https://doi.org/10.1038/s41592-021-01195-3
59. Katajamaa M, Oresic M. Data processing for mass spectrometry-based metabolomics. J Chromatogr A 2007;1158:318-28. https://doi.org/10.1016/j.chroma.2007.04.021
60. Tsugawa H, Kind T, Nakabayashi R, Yukihira D, Tanaka W, Cajka T, Saito K, Fiehn O, Arita M. Hydrogen rearrangement rules: Computational MS/MS fragmentation and structure elucidation using MS-FINDER software. Anal Chem 2016;88:7946-7958. https://doi.org/10.1021/acs.analchem.6b00770
61. de Jonge NF, Mildau K, Meijer D, Louwen JJR, Bueschl C, Huber F, van der Hooft JJJ. Good practices and recommendations for using and benchmarking computational metabolomics metabolite annotation tools. Metabolomics 2022;18:103. https://doi.org/10.1007/s11306-022-01963-y
62. Sumner LW, Amberg A, Barrett D, Beale MH, Beger R, Daykin CA, Fan TWM, ET AL. Proposed minimum reporting standards for chemical analysis. Metabolomics 2007;3:211-221. https://doi.org/10.1007/s11306-007-0082-2

63. Creek DJ, Dunn WB, Fiehn O, Griffin JL, Hall RD, Lei Z, Mistrik R, ET AL. Metabolite identification: Are you sure? And how do your peers gauge your confidence? Metabolomics 2014;10:350-353. https://doi.org/10.1007/s11306-014-0656-8
64. Spicer RA, Salek R, Steinbeck C. A decade after the metabolomics standards initiative it's time for a revision. Sci Data 2017;4:170138. https://doi.org/10.1038/sdata.2017.138
65. Salek RM, Steinbeck C, Viant MR, Goodacre R, Dunn WB. The role of reporting standards for metabolite annotation and identification in metabolomic studies. Gigascience 2013;2:13. https://doi.org/10.1186/2047-217X-2-13
66. Liebisch G, Fahy E, Aoki J, Dennis EA, Durand T, Ejsing CS, Fedorova M, ET AL. Update on LIPID MAPS classification, nomenclature, and shorthand notation for MS-derived lipid structures. J Lipid Res 2020;61:1539-1555. https://doi.org/10.1194/jlr.S120001025
67. Kind T, Tsugawa H, Cajka T, Ma Y, Lai Z, Mehta SS, Wohlgemuth G, ET AL. Identification of small molecules using accurate mass MS/MS search. Mass Spectrom Rev 2018;37:513-532. https://doi.org/10.1002/mas.21535
68. Xue J, Guijas C, Benton HP, Warth B, Siuzdak G. METLIN MS2 molecular standards database: a broad chemical and biological resource. Nat Methods 2020;17:953-954. https://doi.org/10.1038/s41592-020-0942-5
69. Witting M, Böcker S. Current status of retention time prediction in metabolite identification. J Sep Sci 2020;43:1746-1754. https://doi.org/10.1002/jssc.202000060
70. Damont A, Legrand A, Cao C, Fenaille F, Tabet J-C. Hydrogen/deuterium exchange mass spectrometry in the world of small molecules. Mass Spectrom Rev 2023;42:1300-1331. https://doi.org/10.1002/mas.21765
71. Cajka T, Hricko J, Rakusanova S, Brejchova K, Novakova M, Rudl Kulhava L, Hola V, ET AL. Hydrophilic interaction liquid chromatography-hydrogen/deuterium exchange-mass spectrometry (HILIC-HDX-MS) for untargeted metabolomics. Int J Mol Sci 2024;25:2899. https://doi.org/10.3390/ijms25052899
72. Blaženović I, Kind T, Ji J, Fiehn O. Software tools and approaches for compound identification of LC-MS/MS data in metabolomics. Metabolites 2018;8:31. https://doi.org/10.3390/metabo8020031
73. Saccenti E, Hoefsloot HCJ, Smilde AK, Westerhuis JA, Hendriks MMWB. Reflections on univariate and multivariate analysis of metabolomics data. Metabolomics 2014;10:361-374. https://doi.org/10.1007/s11306-013-0598-6
74. Sedgwick P. Multiple significance tests: the Bonferroni correction. BMJ 2012;344:e509. https://doi.org/10.1136/bmj.e509
75. Benjamini Y, Hochberg Y. Controlling the false discovery rate: A practical and powerful approach to multiple testing. J R Stat Soc Ser B 1995;57:289-300. https://doi.org/10.1111/j.2517-6161.1995.tb02031.x
76. Storey JD. A direct approach to false discovery rates. J R Stat Soc Ser B Stat Method 2002;64:479-498. https://doi.org/10.1111/1467-9868.00346
77. Bartel J, Krumsiek J, Theis FJ. Statistical methods for the analysis of high-throughput metabolomics data. Comput Struct Biotechnol J 2013;4:e201301009. https://doi.org/10.5936/csbj.201301009
78. Pang Z, Chong J, Zhou G, de Lima Morais DA, Chang L, Barrette M, Gauthier C, ET AL. MetaboAnalyst 5.0: Narrowing the gap between raw spectra and functional insights. Nucleic Acids Res 2021;49:W388-W396. https://doi.org/10.1093/nar/gkab382
79. Chen Y, Li EM, Xu LY. Guide to metabolomics analysis: a bioinformatics workflow. Metabolites 2022;12:357 https://doi.org/10.3390/metabo12040357
80. Vondrackova M, Kopczynski D, Hoffmann N, Kuda O. LORA, Lipid Over-Representation Analysis based on structural information. Anal Chem 2023;95:12600-12604. https://doi.org/10.1021/acs.analchem.3c02039
81. Wilkinson MD, Dumontier M, Aalbersberg IJ, Appleton G, Axton M, Baak A, Blomberg N, ET AL. The FAIR Guiding Principles for scientific data management and stewardship. Sci Data 2016;3:160018. https://doi.org/10.1038/sdata.2016.18
82. Witting M. (Re-)use and (re-)analysis of publicly available metabolomics data. Proteomics 2023;23:2300032. https://doi.org/10.1002/pmic.202300032
83. Rus M, Crisan S, Andronie-Cioara FL, Indries M, Marian P, Pobirci OL, Ardelean AI. Prevalence and risk factors of metabolic syndrome: a prospective study on cardiovascular health. Medicina 2023;59:1711. https://doi.org/10.3390/medicina59101711

84. Madan K, Paliwal S, Sharma S, Kesar S, Chauhan N, Madan M. Metabolic syndrome: the constellation of co-morbidities, a global threat. Endocr Metab Immune Disord Drug 2023;23:1491-1504. https://doi.org/10.2174/1871530323666230309144825
85. Mensah GA, Fuster V, Murray CJL, Roth GA, Mensah GA, Abate YH, Abbasian M, ET AL. Global burden of cardiovascular diseases and risks, 1990-2022. J Am Coll Cardiol 2023;82:2350-2473. https://doi.org/10.1016/j.jacc.2023.11.007
86. World Health Organization. 2021, Cardiovascular diseases (CVDs). 28 May 2024. https://www.who.int/news-room/fact-sheets/detail/cardiovascular-diseases-(cvds)
87. Di Cesare M, Perel P, Taylor S, Kabudula C, Bixby H, Gaziano TA, McGhie DV, ET AL. The Heart of the World. Glob Heart 2024;19:11. https://doi.org/10.5334/gh.1288
88. Eichelmann F, Sellem L, Wittenbecher C, Jäger S, Kuxhaus O, Prada M, Cuadrat R, ET AL. Deep lipidomics in human plasma: Cardiometabolic disease risk and effect of dietary fat modulation. Circulation 2022;146:21-35. https://doi.org/10.1161/CIRCULATIONAHA.121.056805
89. Huang Z, Klaric L, Krasauskaite J, Khalid W, Strachan MWJ, Wilson JF, Price JF. Combining serum metabolomic profiles with traditional risk factors improves 10-year cardiovascular risk prediction in people with type 2 diabetes. Eur J Prev Cardiol 2023;30:1255-1262. https://doi.org/10.1093/eurjpc/zwad160
90. Lu Q, Chen J, Li R, Wang Y, Tu Z, Geng T, Liu L, Pan A, Liu G. Healthy lifestyle, plasma metabolites, and risk of cardiovascular disease among individuals with diabetes. Atherosclerosis 2023;367:48-55. https://doi.org/10.1016/j.atherosclerosis.2022.12.008
91. Tzoulaki I, Castagné R, Boulangé CL, Karaman I, Chekmeneva E, Evangelou E, Ebbels TMD, ET AL. Serum metabolic signatures of coronary and carotid atherosclerosis and subsequent cardiovascular disease. Eur Heart J 2019;40:2883-2896. https://doi.org/10.1093/eurheartj/ehz235
92. Würtz P, Havulinna AS, Soininen P, Tynkkynen T, Prieto-Merino D, Tillin T, Ghorbani A, ET AL. Metabolite profiling and cardiovascular event risk: A prospective study of 3 population-based cohorts. Circulation 2015;131:774-85. https://doi.org/10.1161/CIRCULATIONAHA.114.013116
93. Wang Z, Klipfell E, Bennett BJ, Koeth R, Levison BS, DuGar B, Feldstein AE, ET AL. Gut flora metabolism of phosphatidylcholine promotes cardiovascular disease. Nature 2011;472:57-63. https://doi.org/10.1038/nature09922
94. Benson TW, Conrad KA, Li XS, Wang Z, Helsley RN, Schugar RC, Coughlin TM, ET AL. Gut microbiota-derived trimethylamine N-oxide contributes to abdominal aortic aneurysm through inflammatory and apoptotic mechanisms. Circulation 2023;147:1079-1096. https://doi.org/10.1161/CIRCULATIONAHA.122.060573
95. Tang WHW, Wang Z, Levison BS, Koeth RA, Britt EB, Fu X, Wu Y, Hazen SL. Intestinal microbial metabolism of phosphatidylcholine and cardiovascular risk. N Engl J Med 2013;368:1575-1584. https://doi.org/10.1056/NEJMoa1109400
96. Zhu W, Gregory JC, Org E, Buffa JA, Gupta N, Wang Z, Li L, ET AL. Gut microbial metabolite TMAO enhances platelet hyperreactivity and thrombosis risk. Cell 2016;165:111-124. https://doi.org/10.1016/j.cell.2016.02.011
97. Li XS, Wang Z, Cajka T, Buffa JA, Nemet I, Hurd AG, Gu X, ET AL. Untargeted metabolomics identifies trimethyllysine, a TMAO-producing nutrient precursor, as a predictor of incident cardiovascular disease risk. JC Insight 2018;3:e99096. https://doi.org/10.1172/jci.insight.99096
98. Nemet I, Saha PP, Gupta N, Zhu W, Romano KA, Skye SM, Cajka T, ET AL. A cardiovascular disease-linked gut microbial metabolite acts via adrenergic receptors. Cell 2020;180:862-877.e22. https://doi.org/10.1016/j.cell.2020.02.016
99. Ferrell M, Wang Z, Anderson JT, Li XS, Witkowski M, DiDonato JA, Hilser JR, ET AL. A terminal metabolite of niacin promotes vascular inflammation and contributes to cardiovascular disease risk. Nat Med 2024;30:424-434. https://doi.org/10.1038/s41591-023-02793-8
100. Witkowski M, Nemet I, Alamri H, Wilcox J, Gupta N, Nimer N, Haghikia A, ET AL. The artificial sweetener erythritol and cardiovascular event risk. Nat Med 2023;29:710-718. https://doi.org/10.1038/s41591-023-02223-9
101. Witkowski M, Nemet I, Li XS, Wilcox J, Ferrell M, Alamri H, Gupta N, ET AL. Xylitol is prothrombotic and associated with cardiovascular risk. Eur Heart J 2024;45:2439-2452 https://doi.org/10.1093/eurheartj/ehae244

102. Fu Z, Liu Q, Liang J, Weng Z, Li W, Xu J, Zhang X, Xu C, Gu A. Association between NMR metabolomic signatures of healthy lifestyle and incident coronary artery disease. Eur J Prev Cardiol 2022;30:243-253. https://doi.org/10.1093/eurjpc/zwac252
103. Margara-Escudero HJ, Paz-Graniel I, García-Gavilán J, Ruiz-Canela M, Sun Q, Clish CB, Toledo E, ET AL. Plasma metabolite profile of legume consumption and future risk of type 2 diabetes and cardiovascular disease. Cardiovasc Diabetol 2024;23:38. https://doi.org/10.1186/s12933-023-02111-z
104. Guasch-Ferré M, Hernández-Alonso P, Drouin-Chartier JP, Ruiz-Canela M, Razquin C, Toledo E, Li J, ET AL. Walnut consumption, plasma metabolomics, and risk of type 2 diabetes and cardiovascular disease. J Nutr 2021;151:303-311. https://doi.org/10.1093/jn/nxaa374
105. Nemet I, Funabashi M, Li XS, Dwidar M, Sangwan N, Skye SM, Romano KA, ET AL. Microbe-derived uremic solutes enhance thrombosis potential in the host. mBio 2023;14:e0133123. https://doi.org/10.1128/mbio.01331-23
106. Harm T, Dittrich K, Brun A, Fu X, Frey M, Petersen Uribe A, Schwarz F-J, ET AL. Large-scale lipidomics profiling reveals characteristic lipid signatures associated with an increased cardiovascular risk. Clin Res Cardiol 2023;112:1664-1678. https://doi.org/10.1007/s00392-023-02260-x
107. Seah JYH, Chew WS, Torta F, Khoo CM, Wenk MR, Herr DR, Choi H, Tai ES, van Dam RM. Plasma sphingolipids and risk of cardiovascular diseases: a large-scale lipidomic analysis. Metabolomics 2020;16:89. https://doi.org/10.1007/s11306-020-01709-8
108. Sun H, Saeedi P, Karuranga S, Pinkepank M, Ogurtsova K, Duncan BB, Stein C, ET AL. IDF Diabetes Atlas: Global, regional and country-level diabetes prevalence estimates for 2021 and projections for 2045. Diabetes Res Clin Pract 2022;183:109119. https://doi.org/10.1016/j.diabres.2021.109119
109. Gregory GA, Robinson TIG, Linklater SE, Wang F, Colagiuri S, de Beaufort C, Donaghue KC, ET AL. Global incidence, prevalence, and mortality of type 1 diabetes in 2021 with projection to 2040: a modelling study. Lancet Diabetes Endocrinol 2022;10:741-760. https://doi.org/10.1016/S2213-8587(22)00218-2
110. Mobasseri M, Shirmohammadi M, Amiri T, Vahed N, Hosseini Fard H, Ghojazadeh M. Prevalence and incidence of type 1 diabetes in the world: a systematic review and meta-analysis. Health Promot Perspect 2020;10:98-115. https://doi.org/10.34172/hpp.2020.18
111. Rakusanova S, Cajka T. Current analytical methods to monitor type 2 diabetes medication in biological samples. Trends Anal Chem 2023;158:116831. https://doi.org/10.1016/j.trac.2022.116831
112. World Health Organization. 2023, Diabetes. 5 April 2023. https://www.who.int/news-room/fact-sheets/detail/diabetes
113. Sen P, Hyötyläinen T, Orešič M. 1-Deoxyceramides - Key players in lipotoxicity and progression to type 2 diabetes? Acta Physiol 2021;232:e13635. https://doi.org/10.1111/apha.13635
114. La Torre D, Seppänen-Laakso T, Larsson HE, Hyötyläinen T, Ivarsson SA, Lernmark Å, Orešič M, Group atDS. Decreased cord-blood phospholipids in young age-at-onset type 1 diabetes. Diabetes 2013;62:3951-3956. https://doi.org/10.2337/db13-0215
115. Tapia G, Suvitaival T, Ahonen L, Lund-Blix NA, Njølstad PR, Joner G, Skrivarhaug T, ET AL. Prediction of type 1 diabetes at birth: Cord blood metabolites vs genetic risk score in the Norwegian Mother, Father, and Child cohort. J Clin Endocrinol Metab 2021;106:e4062-e4071. https://doi.org/10.1210/clinem/dgab400
116. Webb-Robertson B-JM, Nakayasu ES, Frohnert BI, Bramer LM, Akers SM, Norris JM, Vehik K, ET AL. Integration of infant metabolite, genetic, and islet autoimmunity signatures to predict type 1 diabetes by age 6 years. J Clin Endocrinol Metab 2022;107:2329-2338. https://doi.org/10.1210/clinem/dgac225
117. Lee DH, Jin Q, Shi N, Wang F, Bever AM, Liang L, Hu FB, ET AL. The metabolic potential of inflammatory and insulinaemic dietary patterns and risk of type 2 diabetes. Diabetologia 2024;67:88-101. https://doi.org/10.1007/s00125-023-06021-3
118. Hannich JT, Loizides-Mangold U, Sinturel F, Harayama T, Vandereycken B, Saini C, Gosselin P, ET AL. Ether lipids, sphingolipids and toxic 1-deoxyceramides as hallmarks for lean and obese type 2 diabetic patients. Acta Physiol 2021;232:e13610. https://doi.org/10.1111/apha.13610
119. Prada M, Wittenbecher C, Eichelmann F, Wernitz A, Drouin-Chartier J-P, Schulze MB. Association of the odd-chain fatty acid content in lipid groups with type 2 diabetes risk: A targeted analysis of lipidomics data in the EPIC-Potsdam cohort. Clin Nutr 2021;40:4988-4999. https://doi.org/10.1016/j.clnu.2021.06.006

120. Sun L, Liang L, Gao X, Zhang H, Yao P, Hu Y, Ma Y, Wang F, Jin Q, Li H, ET AL. Early prediction of developing type 2 diabetes by plasma acylcarnitines: A population-based study. Diabetes Care 2016;39:1563-1570. https://doi.org/10.2337/dc16-0232
121. Thaker VV, Kwee LC, Chen H, Bahnson J, Ilkayeva O, Muehlbauer MJ, Wolfe B, ET AL. Metabolite signature of diabetes remission in individuals with obesity undergoing weight loss interventions. Obesity 2024;32:304-314. https://doi.org/10.1002/oby.23943
122. Ahola-Olli AV, Mustelin L, Kalimeri M, Kettunen J, Jokelainen J, Auvinen J, Puukka K, ET AL. Circulating metabolites and the risk of type 2 diabetes: a prospective study of 11,896 young adults from four Finnish cohorts. Diabetologia 2019;62:2298-2309. https://doi.org/10.1007/s00125-019-05001-w
123. Delgado-Velandia M, Gonzalez-Marrachelli V, Domingo-Relloso A, Galvez-Fernandez M, Grau-Perez M, Olmedo P, Galan I, ET AL. Healthy lifestyle, metabolomics and incident type 2 diabetes in a population-based cohort from Spain. Int J Behav Nutr Phys Act 2022;19:8. https://doi.org/10.1186/s12966-021-01219-3
124. Liu J, Semiz S, van der Lee SJ, van der Spek A, Verhoeven A, van Klinken JB, Sijbrands E, ET AL. Metabolomics based markers predict type 2 diabetes in a 14-year follow-up study. Metabolomics 2017;13:104. https://doi.org/10.1007/s11306-017-1239-2
125. Menni C, Fauman E, Erte I, Perry JR, Kastenmüller G, Shin SY, Petersen AK, ET AL. Biomarkers for type 2 diabetes and impaired fasting glucose using a nontargeted metabolomics approach. Diabetes 2013;62:4270-4276. https://doi.org/10.2337/db13-0570
126. Peddinti G, Cobb J, Yengo L, Froguel P, Kravić J, Balkau B, Tuomi T, Aittokallio T, Groop L. Early metabolic markers identify potential targets for the prevention of type 2 diabetes. Diabetologia 2017;60:1740-1750. https://doi.org/10.1007/s00125-017-4325-0
127. Rebholz CM, Yu B, Zheng Z, Chang P, Tin A, Köttgen A, Wagenknecht LE, Coresh J, Boerwinkle E, Selvin E. Serum metabolomic profile of incident diabetes. Diabetologia 2018;61:1046-1054. https://doi.org/10.1007/s00125-018-4573-7
128. Ferrannini E, Natali A, Camastra S, Nannipieri M, Mari A, Adam KP, Milburn MV, ET AL. Early metabolic markers of the development of dysglycemia and type 2 diabetes and their physiological significance. Diabetes 2013;62:1730-1737. https://doi.org/10.2337/db12-0707
129. Lemaitre RN, Jensen PN, Wang Z, Fretts AM, McKnight B, Nemet I, Biggs ML, Sotoodehnia N, de Oliveira Otto MC, Psaty BM, ET AL. Association of Trimethylamine N-Oxide and Related Metabolites in Plasma and Incident Type 2 Diabetes: The Cardiovascular Health Study. JAMA Netw Open 2021;4:e2122844-e2122844. https://doi.org/10.1001/jamanetworkopen.2021.22844
130. Song R, Li Z, Zhang Y, Tan J, Chen Z. Comparison of NAFLD, MAFLD and MASLD characteristics and mortality outcomes in United States adults. Liver Int 2024;44:1051-1060. https://doi.org/10.1111/liv.15856
131. Eslam M, Newsome PN, Sarin SK, Anstee QM, Targher G, Romero-Gomez M, Zelber-Sagi S, ET AL. A new definition for metabolic dysfunction-associated fatty liver disease: An international expert consensus statement. J Hepatol 2020;73:202-209. https://doi.org/10.1016/j.jhep.2020.03.039
132. Rinella ME, Lazarus JV, Ratziu V, Francque SM, Sanyal AJ, Kanwal F, Romero D, ET AL. A multisociety Delphi consensus statement on new fatty liver disease nomenclature. Hepatology 2023;78:1966-1986. https://doi.org/10.1097/HEP.0000000000000520
133. Ramírez-Mejía MM, Jiménez-Gutiérrez C, Eslam M, George J, Méndez-Sánchez N. Breaking new ground: MASLD vs. MAFLD-which holds the key for risk stratification? Hepatol Int 2024;18:168-178. https://doi.org/10.1007/s12072-023-10620-y
134. Chen L, Tao X, Zeng M, Mi Y, Xu L. Clinical and histological features under different nomenclatures of fatty liver disease: NAFLD, MAFLD, MASLD and MetALD. J Hepatol 2024;80:e64-e66. https://doi.org/10.1016/j.jhep.2023.08.021
135 De A, Bhagat N, Mehta M, Taneja S, Duseja A. Metabolic dysfunction-associated steatotic liver disease (MASLD) definition is better than MAFLD criteria for lean patients with NAFLD. J Hepatol 2024;80:e61-e62. https://doi.org/10.1016/j.jhep.2023.07.031

136. Younossi ZM, Golabi P, Paik JM, Henry A, Van Dongen C, Henry L. The global epidemiology of nonalcoholic fatty liver disease (NAFLD) and nonalcoholic steatohepatitis (NASH): a systematic review. Hepatology 2023;77:1335-1347. https://doi.org/10.1097/HEP.0000000000000004
137. Wang D, Xu Y, Zhu Z, Li Y, Li X, Li Y, Shen H, ET AL. Changes in the global, regional, and national burdens of NAFLD from 1990 to 2019: A systematic analysis of the global burden of disease study 2019. Front Nutr 2022;9:1047129. https://doi.org/10.3389/fnut.2022.1047129
138. Miao L, Targher G, Byrne CD, Cao YY, Zheng MH. Current status and future trends of the global burden of MASLD. Trends Endocrinol Metab 2024;S1043-2760(24)00036-5. https://doi.org/10.1016/j.tem.2024.02.007
139. Gagnon E, Manikpurage HD, Mitchell PL, Girard A, Gobeil É, Bourgault J, Bégin F, ET AL. Large-scale metabolomic profiling and incident non-alcoholic fatty liver disease. iScience 2023;26:107127. https://doi.org/10.1016/j.isci.2023.107127
140. Gobeil É, Maltais-Payette I, Taba N, Brière F, Ghodsian N, Abner E, Bourgault J, ET AL. Mendelian randomization analysis identifies blood tyrosine levels as a biomarker of non-alcoholic fatty liver disease. Metabolites 2022;12:440. https://doi.org/10.3390/metabo12050440
141. Hartley A, Santos Ferreira DL, Anderson EL, Lawlor DA. Metabolic profiling of adolescent non-alcoholic fatty liver disease [version 2; peer review: 2 approved]. Wellcome Open Res 2019;3:166. https://doi.org/10.12688/wellcomeopenres.14974.2
142. Hirata A, Harada S, Iida M, Kurihara A, Fukai K, Kuwabara K, Kato S, ET AL. Association of Nonalcoholic Fatty Liver Disease with Arterial Stiffness and its Metabolomic Profiling in Japanese Community-Dwellers. J Atheroscler Thromb 2024;31:1-17. https://doi.org/10.5551/jat.64616
143. Khusial R, Cioffi C, Caltharp S, Krasinskas A, Alazraki A, Knight-Scott J, Cleeton R, ET AL. Development of a plasma screening panel for pediatric nonalcoholic fatty liver disease using metabolomics. Hepatol Commun 2019;3:1311-1321. https://doi.org/10.1002/hep4.1417
144. Martínez-Arranz I, Bruzzone C, Noureddin M, Gil-Redondo R, Mincholé I, Bizkarguenaga M, Arretxe E, ET AL. Metabolic subtypes of patients with NAFLD exhibit distinctive cardiovascular risk profiles. Hepatology 2022;76:1121-1134. https://doi.org/10.1002/hep.32427
145. McGlinchey AJ, Govaere O, Geng D, Ratziu V, Allison M, Bousier J, Petta S, ET AL. Metabolic signatures across the full spectrum of non-alcoholic fatty liver disease. JHEP Rep 2022;4:100477. https://doi.org/10.1016/j.jhepr.2022.100477
146. Hu X-Y, Li Y, Li L-Q, Zheng Y, Lv J-H, Huang S-C, Zhang W, Liu L, Zhao L, Liu Z, ET AL. Risk factors and biomarkers of non-alcoholic fatty liver disease: an observational cross-sectional population survey. BMJ Open 2018;8:e019974. https://doi.org/10.1136/bmjopen-2017-019974
147. Kimberly WT, O'Sullivan JF, Nath AK, Keyes M, Shi X, Larson MG, Yang Q, ET AL. Metabolite profiling identifies anandamide as a biomarker of nonalcoholic steatohepatitis. JCI Insight 2017;2:e92989. https://doi.org/10.1172/jci.insight.92989
148. Zeng F, Su X, Liang X, Liao M, Zhong H, Xu J, Gou W, Zhang X, Shen L, Zheng J-S, ET AL. Gut microbiome features and metabolites in non-alcoholic fatty liver disease among community-dwelling middle-aged and older adults. BMC Med 2024;22:104. https://doi.org/10.1186/s12916-024-03317-y

REVIEW

Epitranscriptomic Regulations in the Heart

Daniel BENAK[1,2], Frantisek KOLAR[1], Marketa HLAVACKOVA[1]

[1]Laboratory of Developmental Cardiology, Institute of Physiology of the Czech Academy of Sciences, Prague, Czech Republic, [2]Department of Physiology, Faculty of Science, Charles University, Prague, Czech Republic

Received October 25, 2023
Accepted March 6, 2024

Summary

RNA modifications affect key stages of the RNA life cycle, including splicing, export, decay, and translation. Epitranscriptomic regulations therefore significantly influence cellular physiology and pathophysiology. Here, we selected some of the most abundant modifications and reviewed their roles in the heart and in cardiovascular diseases: N^6-methyladenosine (m^6A), N^6,2`-O-dimethyladenosine (m^6Am), N^1-methyladenosine (m^1A), pseudouridine (Ψ), 5-methylcytidine (m^5C), and inosine (I). Dysregulation of epitranscriptomic machinery affecting these modifications vastly changes the cardiac phenotype and is linked with many cardiovascular diseases such as myocardial infarction, cardiomyopathies, or heart failure. Thus, a deeper understanding of these epitranscriptomic changes and their regulatory mechanisms can enhance our knowledge of the molecular underpinnings of prevalent cardiac diseases, potentially paving the way for novel therapeutic strategies.

Keywords

Epitranscriptomics • RNA modifications • Epigenetics • m^6A • RNA • Heart

Corresponding author

Benak Daniel, Laboratory of Developmental Cardiology, Institute of Physiology of the Czech Academy of Sciences, 142 00 Prague, Czech Republic. E-mail: daniel.benak@fgu.cas.cz

Introduction

The original central dogma of molecular biology states that DNA is transcribed into RNA, which is subsequently translated into proteins [1]. However, the whole process is under the control of epigenetic mechanisms. Epigenetic mechanisms involve chemical modifications to the DNA itself, to the proteins that package DNA into chromatin (histones), or to the RNA molecules transcribed from the DNA (Fig. 1). Importantly, the epigenome is responsive to various environmental factors (diet, stress, exposure to toxins, etc.) and can produce heritable phenotypic changes without altering the DNA sequence [2,3].

RNA modifications are specifically known as the epitranscriptome. The research field of epitranscriptomics is rapidly developing. Currently, over 170 chemical RNA modifications are known (common RNA modifications overviewed in Fig. 2) [4]. The largest number of modifications with the widest chemical diversity is present in tRNA; however, various modifications also occur in other RNA types, including mRNA [5]. These modifications may be either irreversible or reversible [6]. Epitranscriptomic regulators can be described according to their function as writers (addition of the epitranscriptomic mark), erasers (removal of the epitranscriptomic mark), and readers (binding to the modified nucleotide). Dynamic regulation of epitranscriptomic modifications can affect key stages of the RNA life cycle, including splicing, export, decay, and translation [7,8].

Remodeling of the cardiac epitranscriptome has been described in several physiological as well as pathological states. This review summarizes the current knowledge and gaps about RNA modifications in cardiac biology and cardiovascular diseases (CVDs). A better understanding of epitranscriptomic regulations in the healthy and diseased heart opens the door for clinically relevant discoveries in the future.

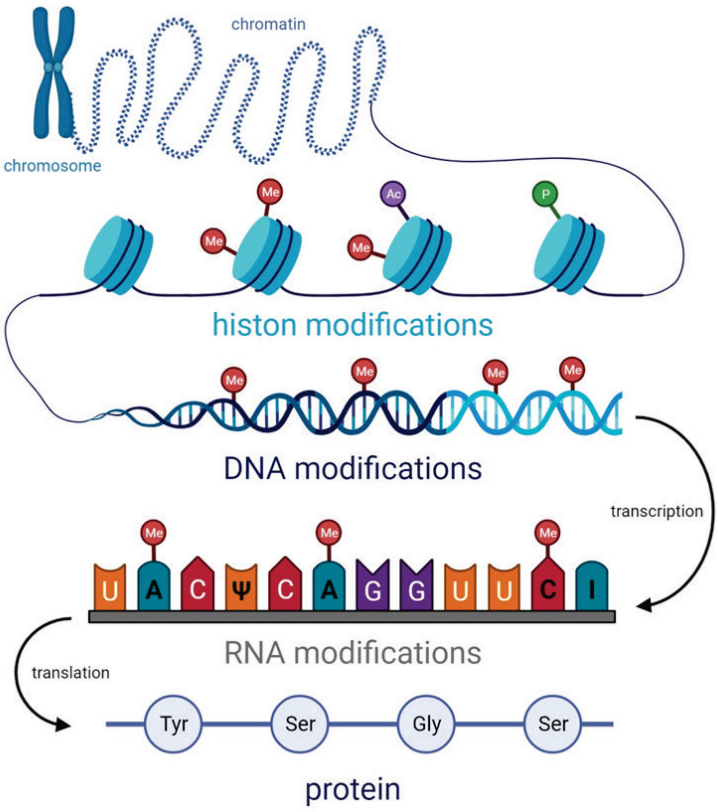

Fig. 1. Basic overview of epigenetic modifications. Created with BioRender.com

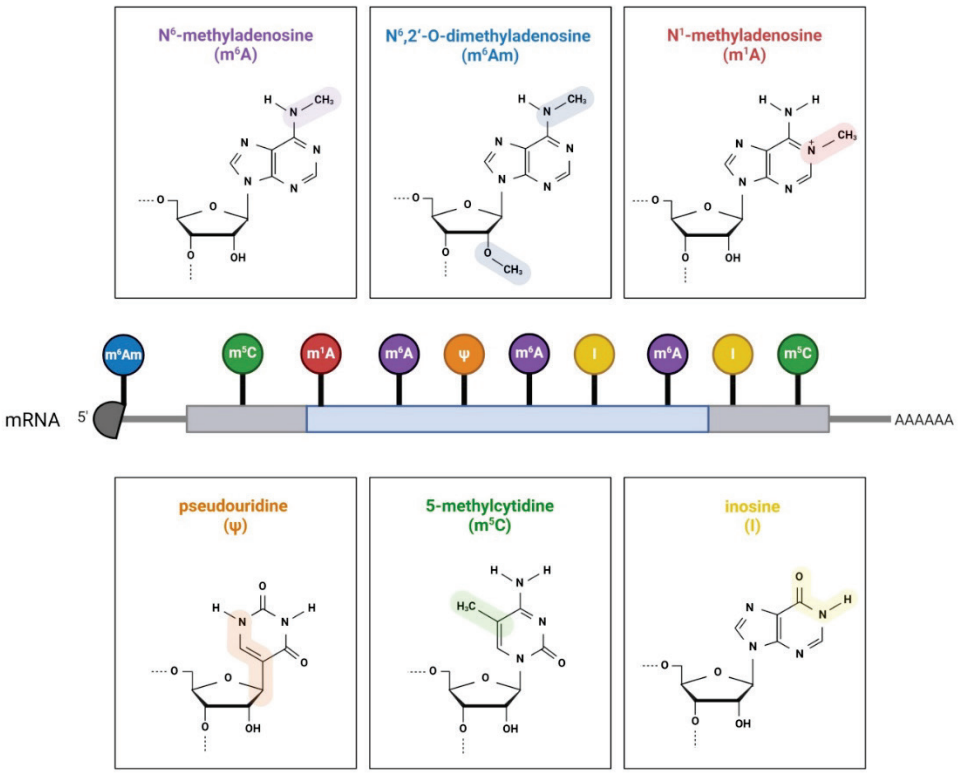

Fig. 2. Common RNA modifications. Created with BioRender.com

Common RNA modifications and their role in cardiac physiology

N^6-methyladenosine

N^6-methyladenosine (m^6A) is the most numerous modification in eukaryotic mRNA; however, it also occurs in other RNA types [9-12]. Multicomponent methyltransferase complex (MTC) is responsible for the deposition of the methyl group to adenosine, forming m^6A. The two main regulatory subunits of the MTC are methyltransferase-like 3 (METTL3) and methyltransferase-like 14 (METTL14). The catalytic function of the MTC is carried by METTL3 while METTL14 facilitates RNA binding [13,14]. The removal of the methyl group is mediated by two main demethylases. AlkB homolog 5 (ALKBH5) is the primary m^6A eraser [15]. Fat mass and obesity-associated protein (FTO) is not an m^6A-specific demethylase, however, m^6A is the preferable target of FTO in the nucleus [16-18]. There are many described m^6A readers. The most characterized include YTH domain-containing family proteins 1-3 (YTHDF1-3) and YTH domain-containing proteins 1-2 (YTHDC1-2). While readers YTHDF1-3 mediate primarily mRNA degradation, YTHDC1 regulates mRNA splicing and YTHDC2 promotes translation [19-25].

The heart is affected by m^6A already during its ontogenetic development as m^6A machinery regulates cardiomyocyte growth, proliferation, and differentiation [26-29]. Children born with a loss-of-function mutation in the *FTO* gene (m^6A demethylase) exhibited heart defects (ventricular septal defect, atrioventricular defect, patent ductus arteriosus), hypertrophic cardiomyopathy and died before 3 years of age [30]. Moreover, various gene variants of m^6A regulators were linked with CVDs, including myocardial infarction, acute coronary syndrome, increased risk of rejection in heart transplant patients, and sudden cardiac death [31-37]. It has been reported that m^6A also controls cardiac hypertrophy [38-40]. Dorn et al. [41] suggested that enhanced m^6A RNA methylation results in compensated cardiac hypertrophy, whereas diminished m^6A drives eccentric cardiomyocyte remodeling and dysfunction. Changes in m^6A methy-lation and dysregulation of m^6A machinery can contribute to the progression of heart failure [42-47]. Altered cardiac m^6A patterns were detected also in diabetic cardio-myopathy with distinct dysregulation of m^6A machinery in the two types of diabetes [48-50]. The heterogeneous role of m^6A modification in CVDs has been reviewed in several recent publications [51-60].

Altered m^6A levels in different CVDs might also serve as useful biomarkers. For instance, it has been described that patients with coronary artery disease (CAD) had significantly lower urine m^6A levels compared to healthy individuals [61].

Since cardiac m^6A machinery is dysregulated under many pathophysiological conditions, targeting m^6A modifiers can also induce cardioprotection. Several studies showed that demethylases FTO and ALKBH5 can protect cardiomyocytes against detrimental effects, such as treatment with cardiotoxic compounds or hypoxia/reoxygenation injury [43,62-69]. On the contrary, loss of METTL3 or METTL14 can alleviate myocardial injury and promote heart regeneration [70,71]. Thus, improving our knowledge of the m^6A regulations in the heart may lead to novel cardioprotective strategies using specific pharmacological activators or inhibitors targeting m^6A modifiers.

N^6,2'-O-dimethyladenosine

N^6,2'-O-dimethyladenosine (m^6Am) is formed by N^6-methylation of 2'-O-methyladenosine (Am). It has been described only in mRNA and snRNA [50,72]. This modification is present at the first transcribed nucleotide and forms the extended cap structure in at least 30-40 % of all vertebrate mRNA [73,74]. Moreover, m^6Am is also present at the internal sites of snRNAs [17]. The formation of m^6Am in the cap is mediated by phosphorylated CTD interacting factor 1 (PCIF1), while methyl-transferase-like 4 (METTL4) is responsible for internal m^6Am formation [75-78]. The demethylation of m^6Am takes place mainly in the cytosol where it is mediated by FTO, the same eraser that targets m^6A in the nucleus [17,18,79,80]. There are currently no m^6Am readers mediating the biological functions of this modification described, but it is known that the presence of m^6Am in the cap structure markedly enhances mRNA stability (in mRNA cap) and splicing (in snRNA cap) [79,81].

The function of m^6Am modification in the heart is mostly unknown. There are several problems associated with m^6Am research: 1) many m^6A detection methods do not distinguish between m^6A and m^6Am; 2) FTO is not a specific eraser because it demethylates also m^6A and m^1A; 3) METTL4 can also catalyze 6mA methylation. Thus, the potential effect of m^6Am on cardiac function could be masked as m^6A in many studies [72]. Besides the non-specific demethylase FTO covered in the previous chapter, not much is known about the role

of m^6Am and its regulators in the heart. Publicly available RNA-seq datasets generated from human left ventricles of failing and non-failing hearts reported some degree of regulation of *METTL4* (down-regulation) and *PCIF1* (up-regulation) [72]. Besides that, we recently found that m^6Am writers were regulated also in cardioprotective interventions. METTL4 was decreased in the hearts of rats adapted to chronic hypoxia and PCIF1 was increased in the hearts of rats subjected to fasting [69,72].

N^1-methyladenosine

N^1-methyladenosine (m^1A) is found mainly in tRNA and rRNA, but less numerously also in mRNA [82-85]. The writer proteins responsible for m^1A methylation include tRNA methyltransferase 6 (TRMT6), TRMT61A, TRMT61B, TRMT10C or ribosomal RNA-processing protein 8 (RRP8; also known as NML) [86-90]. Demethylation of m^1A is catalyzed by erasers ALKBH1, and ALKBH3 [85,91-93]. Moreover, FTO (m^6A and m^6Am eraser) also works as a demethylase of m^1A in tRNA [17]. The m^1A modification affects the structure and stability of tRNA and rRNA and its presence in mRNA regulates translation [85,86,94-96].

So far, no association between m^1A and CVDs has been found [97]. Analysis of methylated nucleosides in urine that revealed altered m^6A levels in CAD patients did not find any changes in the case of m^1A [61].

Pseudouridine

Pseudouridine (Ψ), the C5-glycoside isomer of uridine (U), is the first discovered and overall the most prevalent RNA modification that has been identified in almost all known RNA types [98-100]. The conversion of U to Ψ is mediated by the diverse pseudouridine synthase (PUS) family [101]. So far, 13 members of PUSs have been described in eukaryotes [100]. The human homologs of PUSs include PUS1, PUS3, PUS7, PUS10, PUSL1, PUSL7, TRUB1-2 (TruB pseudouridine synthase 1-2), RPUSD1-4 (RNA pseudouridine synthase D1-4), and DKC1 (dyskerin pseudouridine synthase 1) [102]. The formation of Ψ is irreversible (unlike the aforementioned modifications) [103]. The only known Ψ reader is a yeast RNA helicase Prp5 interacting with snRNA [104,105]. The molecular functions of Ψ include stabilization of RNA conformations and destabilization of interactions with RNA-binding proteins; the most well-characterized function of Ψ in mRNA is the promotion of a stop codon read-through [100,106].

Plasma and urine levels of Ψ were linked to CVDs [107]. Patients with heart failure exhibited higher plasma concentrations of Ψ than healthy controls and this modification was suggested as a suitable biomarker for heart failure diagnosis [108-110]. Tetralogy of Fallot, the most common cyanotic congenital heart defect, is associated with decreased Ψ levels in ventricular myocardial tissues, which is under the control of small Cajal body-specific RNAs [111,112].

5-methylcytidine

5-methylcytidine (m^5C) is an abundant RNA modification present in a wide variety of RNA types. The writers responsible for the installation of m^5C in humans are NOL1/NOP2/SUN domain proteins 1-7 (NSUN1-7) and DNA methyltransferase homolog DNMT2 [113,114]. Ten-eleven translocation proteins 1-3 (TET1-3) and ALKBH1 are known as m^5C erasers. TET-mediated oxidation results in a formation of 5-hydroxy-methylcytidine (hm^5C), while ALKBH1 is responsible for the oxidation of m^5C in mitochondrial tRNA generating 5-formylcytidine (f^5C) [115,116]. The readers of m^5C include Aly/REF export factor (ALYREF), which influences nuclear-cytoplasmic shuttling [117], and Y-box-binding protein 1 (YBX1), which preserves the stability of its target mRNA by recruiting ELAVL1 [118]. This modification is an important regulator of RNA export, ribosome assembly, translation, and RNA stability [113,119,120].

In mammals, m^5C modification occurs more frequently in the myocardium and skeletal muscle compared to other organs. The enrichment of m^5C is especially present in mitochondrial-related genes, suggesting a particularly important function of m^5C in the high-energy demanding myocardium [121]. Indeed, specific inactivation of the methyltransferase NSUN4 in the heart caused cardiomyopathy with mitochondrial dysfunction [122]. Deficiency of methyltransferase *Dnmt2* gene in mice resulted in cardiac hypertrophy [123]. RNA binding protein and known m^5C reader YBX1 was also identified as a cardiac hypertrophy regulator [124,125]. NSUN2 was found to increase *Nrf2* expression by promoting m^5C methylation of its mRNA and enhancing its antioxidant stress effect, which attenuates doxorubicin-induced myocardial damage [126].

RNA editing

RNA editing includes nucleoside modifications

such as adenosine deamination to inosine (A-to-I editing) or cytosine deamination to uridine (C-to-U editing), as well as insertion and deletion of nucleotides [127,128]. Deamination of A to I is irreversible and it is performed by enzymes belonging to the adenosine deaminase acting on RNA (ADAR) family, which is represented by three ADAR orthologs (ADAR1-3) in mammals. ADAR1 and ADAR2 are widely expressed, while ADAR3 was detected only in the brain [129,130]. C-to-U editing is not as common as A-to-I editing [131]. The deamination of C to U is performed by a multiple-protein editosome, which includes the catalytic subunit apolipoprotein B mRNA editing enzyme catalytic subunit 1 (APOBEC1) and an RNA-binding protein APOBEC1 complementation factor (A1CF) [132]. RNA editing in protein-coding regions of mRNAs can result in the expression of functionally altered proteins while editing in microRNA (miRNA) precursors leads to reduced expression or altered function of mature miRNAs [133].

ADAR1 is an essential enzyme for normal embryonic cardiac growth and development [134]. Cardiomyocyte-specific deletion of *Adar1* in adult mice caused severe ventricular remodeling and spontaneous cardiac dysfunction associated with a significant rise in lethality [135]. ADAR1 was also shown to prevent autoinflammatory processes in the heart [136]. A-to-I RNA editing has been significantly increased among children with cyanotic congenital heart disease compared to acyanotic controls [137]. On the contrary, reduction of A-to-I editing and decreased levels of ADAR2 have been described in the failing human heart [138]. Strong down-regulation of ADAR2 and up-regulation of ADAR1 expression was observed in blood samples of patients with congenital heart disease. The decrease in ADAR2 levels was in line with its down-regulation in ventricular tissues of dilated cardiomyopathy patients. Thus, it has been suggested that ADAR2 activity might play a critical role in preventing cardiovascular disorders [139]. Indeed, Wu et al. [140] described that ADAR2 was up-regulated in the heart during exercise and that this enzyme protects the heart against myocardial infarction as well as doxorubicin-induced cardiotoxicity, supporting the hypothesis of the beneficial effect of ADAR2 on the heart. So far, RNA editing therapeutics have not been established for the treatment of CVDs, however, it is a prospective therapeutic approach that could be implemented in the near future [141].

Conclusion

CVDs remain the leading cause of death worldwide. The search for appropriate cardioprotective strategies is therefore of crucial importance. The significant role of epitranscriptomics in cellular physiology and pathophysiology has been already accepted by the scientific community in the past few years. However, the exact role of complex epitranscriptomic regulations in the heart and CVDs is still far from being understood. It is becoming clear that RNA modifications and their regulators play a vital role in the ontogenetic development of the heart. Many CVDs, such as myocardial infarction, cardiomyopathies, or heart failure, have been also associated with dysregulated epitranscriptomic machinery (Fig. 3). Most importantly, targeting the enzymes responsible for regulating the RNA modifications affected by these diseases proved to be beneficial for the heart. Thus, it is only a matter of time before targeting epitranscriptomic regulations becomes a part of clinical practice.

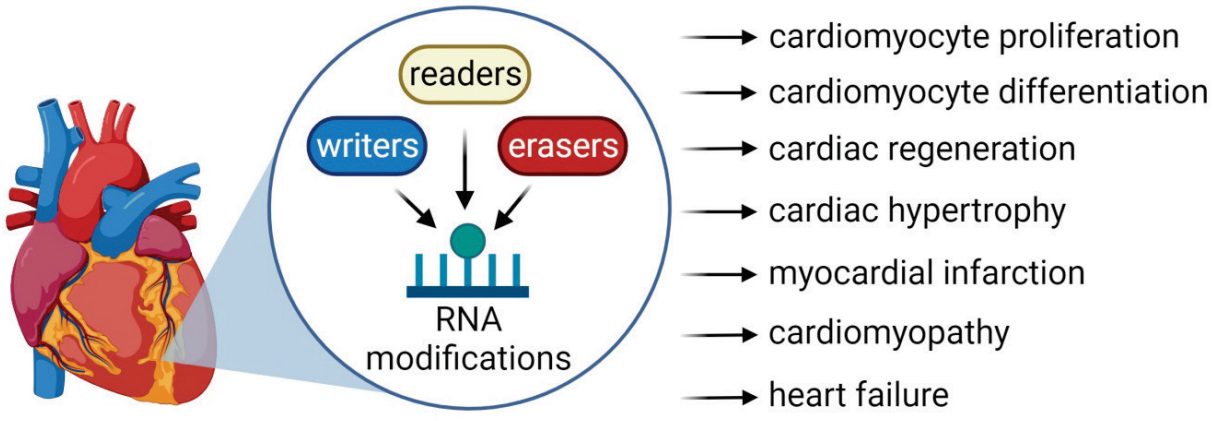

Fig. 3. Role of RNA modifications in the heart. Created with BioRender.com

Authors' contributions

D.B. drafted the article, F.K. and M.H. provided substantive revisions.

Conflict of Interest

There is no conflict of interest.

Acknowledgements

This work was supported by the Czech Science Foundation under Grant (24-10497S) to H.M.; the Charles University Grant Agency under Grant (GA UK 668220) to B.D.; and the project National Institute for Research of Metabolic and Cardiovascular Diseases (Programme EXCELES, ID Project No. LX22NPO5104) to K.F. - Funded by the European Union – Next Generation EU.

Figures were created with BioRender.com.

References

1. Crick FH. On protein synthesis. Symp Soc Exp Biol 1958;12:138-163.
2. Devaux Y, Robinson EL. Preface. In: Devaux Y, Robinson EL, editors. Epigenetics in Cardiovascular Disease: Academic Press; 2021. p. XXI-XXVI. https://doi.org/10.1016/B978-0-12-822258-4.00018-3
3. Zhang L, Lu Q, Chang C. Epigenetics in Health and Disease. In: Chang C, Lu Q, editors. Epigenetics in Allergy and Autoimmunity. Singapore: Springer Singapore; 2020. p. 3-55. https://doi.org/10.1007/978-981-15-3449-2_1
4. Boccaletto P, Machnicka MA, Purta E, Piatkowski P, Baginski B, Wirecki TK, de Crécy-Lagard V, Ross R, Limbach PA, Kotter A, Helm M, Bujnicki JM. MODOMICS: a database of RNA modification pathways. 2017 update. Nucleic Acids Res 2018;46:D303-d307. https://doi.org/10.1093/nar/gkx1030
5. Roundtree IA, Evans ME, Pan T, He C. Dynamic RNA Modifications in Gene Expression Regulation. Cell 2017;169:1187-1200. https://doi.org/10.1016/j.cell.2017.05.045
6. Dieterich C, Völkers M. Chapter 6 - RNA modifications in cardiovascular disease-An experimental and computational perspective. In: Devaux Y, Robinson EL, editors. Epigenetics in Cardiovascular Disease: Academic Press; 2021. p. 113-125. https://doi.org/10.1016/B978-0-12-822258-4.00003-1
7. Lee Y, Choe J, Park OH, Kim YK. Molecular Mechanisms Driving mRNA Degradation by m(6)A Modification. Trends Genet 2020;36:177-188. https://doi.org/10.1016/j.tig.2019.12.007
8. Boo SH, Kim YK. The emerging role of RNA modifications in the regulation of mRNA stability. Exp Mol Med 2020;52:400-408. https://doi.org/10.1038/s12276-020-0407-z
9. Desrosiers R, Friderici K, Rottman F. Identification of methylated nucleosides in messenger RNA from Novikoff hepatoma cells. Proc Natl Acad Sci U S A 1974;71:3971-3975. https://doi.org/10.1073/pnas.71.10.3971
10. Dominissini D, Moshitch-Moshkovitz S, Salmon-Divon M, Amariglio N, Rechavi G. Transcriptome-wide mapping of N(6)-methyladenosine by m(6)A-seq based on immunocapturing and massively parallel sequencing. Nat Protoc 2013;8:176-189. https://doi.org/10.1038/nprot.2012.148
11. Meyer KD, Saletore Y, Zumbo P, Elemento O, Mason CE, Jaffrey SR. Comprehensive analysis of mRNA methylation reveals enrichment in 3' UTRs and near stop codons. Cell 2012;149:1635-1646. https://doi.org/10.1016/j.cell.2012.05.003
12. Oerum S, Meynier V, Catala M, Tisné C. A comprehensive review of m6A/m6Am RNA methyltransferase structures. Nucleic Acids Res 2021;49:7239-7255. https://doi.org/10.1093/nar/gkab378
13. Wang P, Doxtader KA, Nam Y. Structural Basis for Cooperative Function of Mettl3 and Mettl14 Methyltransferases. Mol Cell 2016;63:306-317. https://doi.org/10.1016/j.molcel.2016.05.041
14. Wang X, Feng J, Xue Y, Guan Z, Zhang D, Liu Z, Gong Z, Wang Q, Huang J, Tang C, Zou T, Yin P. Structural basis of N(6)-adenosine methylation by the METTL3-METTL14 complex. Nature 2016;534:575-578. https://doi.org/10.1038/nature18298
15. Zheng G, Dahl JA, Niu Y, Fedorcsak P, Huang CM, Li CJ, Vågbø CB, Shi Y, Wang WL, Song SH, Lu Z, Bosmans RP, Dai Q, Hao YJ, Yang X, Zhao WM, Tong WM, Wang XJ, Bogdan F, Furu K, Fu Y, Jia G, Zhao X, Liu J, Krokan HE, Klungland A, Yang YG, He C. ALKBH5 is a mammalian RNA demethylase that impacts RNA metabolism and mouse fertility. Mol Cell 2013;49:18-29. https://doi.org/10.1016/j.molcel.2012.10.015

16. Jia G, Fu Y, Zhao X, Dai Q, Zheng G, Yang Y, Yi C, Lindahl T, Pan T, Yang YG, He C. N6-methyladenosine in nuclear RNA is a major substrate of the obesity-associated FTO. Nat Chem Biol 2011;7:885-887. https://doi.org/10.1038/nchembio.687
17. Wei J, Liu F, Lu Z, Fei Q, Ai Y, He PC, Shi H, Cui X, Su R, Klungland A, Jia G, Chen J, He C. Differential m(6)A, m(6)A(m), and m(1)A Demethylation Mediated by FTO in the Cell Nucleus and Cytoplasm. Mol Cell 2018;71:973-985.e975. https://doi.org/10.1016/j.molcel.2018.08.011
18. Relier S, Ripoll J, Guillorit H, Amalric A, Achour C, Boissière F, Vialaret J, Attina A, Debart F, Choquet A, Macari F, Marchand V, Motorin Y, Samalin E, Vasseur JJ, Pannequin J, Aguilo F, Lopez-Crapez E, Hirtz C, Rivals E, Bastide A, David A. FTO-mediated cytoplasmic m(6)A(m) demethylation adjusts stem-like properties in colorectal cancer cell. Nat Commun 2021;12:1716. https://doi.org/10.1038/s41467-021-21758-4
19. Zaccara S, Jaffrey SR. A Unified Model for the Function of YTHDF Proteins in Regulating m(6)A-Modified mRNA. Cell 2020;181:1582-1595.e1518. https://doi.org/10.1016/j.cell.2020.05.012
20. Lasman L, Krupalnik V, Viukov S, Mor N, Aguilera-Castrejon A, Schneir D, Bayerl J, Mizrahi O, Peles S, Tawil S, Sathe S, Nachshon A, Shani T, Zerbib M, Kilimnik I, Aigner S, Shankar A, Mueller JR, Schwartz S, Stern-Ginossar N, Yeo GW, Geula S, Novershtern N, Hanna JH. Context-dependent functional compensation between Ythdf m(6)A reader proteins. Genes Dev 2020;34:1373-1391. https://doi.org/10.1101/gad.340695.120
21. Wang X, Lu Z, Gomez A, Hon GC, Yue Y, Han D, Fu Y, Parisien M, Dai Q, Jia G, Ren B, Pan T, He C. N6-methyladenosine-dependent regulation of messenger RNA stability. Nature 2014;505:117-120. https://doi.org/10.1038/nature12730
22. Wang X, Zhao BS, Roundtree IA, Lu Z, Han D, Ma H, Weng X, Chen K, Shi H, He C. N(6)-methyladenosine Modulates Messenger RNA Translation Efficiency. Cell 2015;161:1388-1399. https://doi.org/10.1016/j.cell.2015.05.014
23. Xiao W, Adhikari S, Dahal U, Chen YS, Hao YJ, Sun BF, Sun HY, Li A, Ping XL, Lai WY, Wang X, Ma HL, Huang CM, Yang Y, Huang N, Jiang GB, Wang HL, Zhou Q, Wang XJ, Zhao YL, Yang YG. Nuclear m(6)A Reader YTHDC1 Regulates mRNA Splicing. Mol Cell 2016;61:507-519. https://doi.org/10.1016/j.molcel.2016.01.012, https://doi.org/10.1016/j.molcel.2016.03.004
24. Hsu PJ, Zhu Y, Ma H, Guo Y, Shi X, Liu Y, Qi M, Lu Z, Shi H, Wang J, Cheng Y, Luo G, Dai Q, Liu M, Guo X, Sha J, Shen B, He C. Ythdc2 is an N(6)-methyladenosine binding protein that regulates mammalian spermatogenesis. Cell Res 2017;27:1115-1127. https://doi.org/10.1038/cr.2017.99
25. Shi H, Wang X, Lu Z, Zhao BS, Ma H, Hsu PJ, Liu C, He C. YTHDF3 facilitates translation and decay of N(6)-methyladenosine-modified RNA. Cell Res 2017;27:315-328. https://doi.org/10.1038/cr.2017.15
26. Liu XH, Liu Z, Ren ZH, Chen HX, Zhang Y, Zhang Z, Cao N, Luo GZ. Co-effects of m6A and chromatin accessibility dynamics in the regulation of cardiomyocyte differentiation. Epigenetics Chromatin 2023;16:32. https://doi.org/10.1186/s13072-023-00506-6
27. Han Z, Wang X, Xu Z, Cao Y, Gong R, Yu Y, Yu Y, Guo X, Liu S, Yu M, Ma W, Zhao Y, Xu J, Li X, Li S, Xu Y, Song R, Xu B, Yang F, Bamba D, Sukhareva N, Lei H, Gao M, Zhang W, Zagidullin N, Zhang Y, Yang B, Pan Z, Cai B. ALKBH5 regulates cardiomyocyte proliferation and heart regeneration by demethylating the mRNA of YTHDF1. Theranostics 2021;11:3000-3016. https://doi.org/10.7150/thno.47354
28. Yang C, Zhao K, Zhang J, Wu X, Sun W, Kong X, Shi J. Comprehensive Analysis of the Transcriptome-Wide m6A Methylome of Heart via MeRIP After Birth: Day 0 vs. Day 7. Front Cardiovasc Med 2021;8:633631. https://doi.org/10.3389/fcvm.2021.633631
29. Semenovykh D, Benak D, Holzerova K, Cerna B, Telensky P, Vavrikova T, Kolar F, Neckar J, Hlavackova M. Myocardial m6A regulators in postnatal development: effect of sex. Physiol Res 2022;71:877-882. https://doi.org/10.33549/physiolres.934970
30. Boissel S, Reish O, Proulx K, Kawagoe-Takaki H, Sedgwick B, Yeo GS, Meyre D, Golzio C, Molinari F, Kadhom N, Etchevers HC, Saudek V, Farooqi IS, Froguel P, Lindahl T, O'Rahilly S, Munnich A, Colleaux L. Loss-of-function mutation in the dioxygenase-encoding FTO gene causes severe growth retardation and multiple malformations. Am J Hum Genet 2009;85:106-111. https://doi.org/10.1016/j.ajhg.2009.06.002
31. Liu C, Mou S, Pan C. The FTO gene rs9939609 polymorphism predicts risk of cardiovascular disease: a systematic review and meta-analysis. PLoS One 2013;8:e71901. https://doi.org/10.1371/journal.pone.0071901

32. Doney AS, Dannfald J, Kimber CH, Donnelly LA, Pearson E, Morris AD, Palmer CN. The FTO gene is associated with an atherogenic lipid profile and myocardial infarction in patients with type 2 diabetes: a Genetics of Diabetes Audit and Research Study in Tayside Scotland (Go-DARTS) study. Circ Cardiovasc Genet 2009;2:255-259. https://doi.org/10.1161/CIRCGENETICS.108.822320
33. Hubacek JA, Vrablik M, Dlouha D, Stanek V, Gebauerova M, Adamkova V, Ceska R, Dostálová G, Linhart A, Vitek L, Pitha J. Gene variants at FTO, 9p21, and 2q36.3 are age-independently associated with myocardial infarction in Czech men. Clin Chim Acta 2016;454:119-123. https://doi.org/10.1016/j.cca.2016.01.005
34. Hubacek JA, Stanek V, Gebauerová M, Pilipcincová A, Dlouhá D, Poledne R, Aschermann M, Skalická H, Matousková J, Kruger A, Penicka M, Hrabáková H, Veselka J, Hájek P, Lánská V, Adámková V, Pitha J. A FTO variant and risk of acute coronary syndrome. Clin Chim Acta 2010;411:1069-1072. https://doi.org/10.1016/j.cca.2010.03.037
35. Hubacek JA, Vymetalova J, Lanska V, Dlouha D. The fat mass and obesity related gene polymorphism influences the risk of rejection in heart transplant patients. Clin Transplant 2018;32:e13443. https://doi.org/10.1111/ctr.13443
36. Zhen X, Zhao W, Wang J, Li L, He Y, Zhang J, Li C, Zhang S, Huang J, Luo B, Gao Y. Genetic variations within METTL16 and susceptibility to sudden cardiac death in chinese populations with coronary artery disease. Am J Cardiol 2023;202:90-99. https://doi.org/10.1016/j.amjcard.2023.06.062
37. Wakil SM, Ram R, Muiya NP, Mehta M, Andres E, Mazhar N, Baz B, Hagos S, Alshahid M, Meyer BF, Morahan G, Dzimiri N. A genome-wide association study reveals susceptibility loci for myocardial infarction/coronary artery disease in Saudi Arabs. Atherosclerosis 2016;245:62-70. https://doi.org/10.1016/j.atherosclerosis.2015.11.019
38. Zhang R, Qu Y, Ji Z, Hao C, Su Y, Yao Y, Zuo W, Chen X, Yang M, Ma G. METTL3 mediates Ang-II-induced cardiac hypertrophy through accelerating pri-miR-221/222 maturation in an m6A-dependent manner. Cell Mol Biol Lett 2022;27:55. https://doi.org/10.1186/s11658-022-00349-1
39. Carnevali L, Graiani G, Rossi S, Al Banchaabouchi M, Macchi E, Quaini F, Rosenthal N, Sgoifo A. Signs of cardiac autonomic imbalance and proarrhythmic remodeling in FTO deficient mice. PLoS One 2014;9:e95499. https://doi.org/10.1371/journal.pone.0095499
40. Gan XT, Zhao G, Huang CX, Rowe AC, Purdham DM, Karmazyn M. Identification of fat mass and obesity associated (FTO) protein expression in cardiomyocytes: regulation by leptin and its contribution to leptin-induced hypertrophy. PLoS One 2013;8:e74235. https://doi.org/10.1371/journal.pone.0074235
41. Dorn LE, Lasman L, Chen J, Xu X, Hund TJ, Medvedovic M, Hanna JH, van Berlo JH, Accornero F. The N(6)-methyladenosine mRNA methylase METTL3 controls cardiac homeostasis and hypertrophy. Circulation 2019;139:533-545. https://doi.org/10.1161/CIRCULATIONAHA.118.036146
42. Kmietczyk V, Riechert E, Kalinski L, Boileau E, Malovrh E, Malone B, Gorska A, Hofmann C, Varma E, Jürgensen L, Kamuf-Schenk V, Altmüller J, Tappu R, Busch M, Most P, Katus HA, Dieterich C, Völkers M. m(6)A-mRNA methylation regulates cardiac gene expression and cellular growth. Life Sci Alliance 2019;2:e201800233. https://doi.org/10.26508/lsa.201800233
43. Mathiyalagan P, Adamiak M, Mayourian J, Sassi Y, Liang Y, Agarwal N, Jha D, Zhang S, Kohlbrenner E, Chepurko E, Chen J, Trivieri MG, Singh R, Boucharеb R, Fish K, Ishikawa K, Lebeche D, Hajjar RJ, Sahoo S. FTO-dependent N(6)-methyladenosine regulates cardiac function during remodeling and repair. Circulation 2019;139:518-532. https://doi.org/10.1161/CIRCULATIONAHA.118.033794
44. Berulava T, Buchholz E, Elerdashvili V, Pena T, Islam MR, Lbik D, Mohamed BA, Renner A, von Lewinski D, Sacherer M, Bohnsack KE, Bohnsack MT, Jain G, Capece V, Cleve N, Burkhardt S, Hasenfuss G, Fischer A, Toischer K. Changes in m6A RNA methylation contribute to heart failure progression by modulating translation. Eur J Heart Fail 2020;22:54-66. https://doi.org/10.1002/ejhf.1672
45. Zhang B, Xu Y, Cui X, Jiang H, Luo W, Weng X, Wang Y, Zhao Y, Sun A, Ge J. Alteration of m6A RNA methylation in heart failure with preserved ejection fraction. Front Cardiovasc Med 2021;8:647806. https://doi.org/10.3389/fcvm.2021.647806
46. Zhang B, Jiang H, Wu J, Cai Y, Dong Z, Zhao Y, Hu Q, Hu K, Sun A, Ge J. m6A demethylase FTO attenuates cardiac dysfunction by regulating glucose uptake and glycolysis in mice with pressure overload-induced heart failure. Signal Transduct Target Ther 2021;6:377. https://doi.org/10.1038/s41392-021-00699-w

47. Komal S, Gohar A, Althobaiti S, Ahmad Khan I, Cui LG, Zhang LR, Han SN, Shakeel M. ALKBH5 inhibitors as a potential treatment strategy in heart failure-inferences from gene expression profiling. Front Cardiovasc Med 2023;10:1194311. https://doi.org/10.3389/fcvm.2023.1194311
48. Ju W, Liu K, Ouyang S, Liu Z, He F, Wu J. Changes in N6-methyladenosine modification modulate diabetic cardiomyopathy by reducing myocardial fibrosis and myocyte hypertrophy. Front Cell Dev Biol 2021;9:702579. https://doi.org/10.3389/fcell.2021.702579
49. Shao Y, Li M, Yu Q, Gong M, Wang Y, Yang X, Liu L, Liu D, Tan Z, Zhang Y, Qu Y, Li H, Wang Y, Jiao L, Zhang Y. CircRNA CDR1as promotes cardiomyocyte apoptosis through activating hippo signaling pathway in diabetic cardiomyopathy. Eur J Pharmacol 2022;922:174915. https://doi.org/10.1016/j.ejphar.2022.174915
50. Benak D, Benakova S, Plecita-Hlavata L, Hlavackova M. The role of m6A and m6Am RNA modifications in the pathogenesis of diabetes mellitus. Front Endocrinol (Lausanne) 2023;14:1223583. https://doi.org/10.3389/fendo.2023.1223583
51. Zhang B, Jiang H, Dong Z, Sun A, Ge J. The critical roles of m6A modification in metabolic abnormality and cardiovascular diseases. Genes Dis 2021;8:746-758. https://doi.org/10.1016/j.gendis.2020.07.011
52. Longenecker JZ, Gilbert CJ, Golubeva VA, Martens CR, Accornero F. Epitranscriptomics in the Heart: a Focus on m(6)A. Curr Heart Fail Rep 2020;17:205-212. https://doi.org/10.1007/s11897-020-00473-z
53. Wu S, Zhang S, Wu X, Zhou X. m(6)A RNA Methylation in Cardiovascular Diseases. Mol Ther 2020;28:2111-2119. https://doi.org/10.1016/j.ymthe.2020.08.010
54. Qin Y, Li L, Luo E, Hou J, Yan G, Wang D, Qiao Y, Tang C. Role of m6A RNA methylation in cardiovascular disease (Review). Int J Mol Med 2020;46:1958-1972. https://doi.org/10.3892/ijmm.2020.4746
55. Paramasivam A, Vijayashree Priyadharsini J, Raghunandhakumar S. N6-adenosine methylation (m6A): a promising new molecular target in hypertension and cardiovascular diseases. Hypertens Res 2020;43:153-154. https://doi.org/10.1038/s41440-019-0338-z
56. Kumari R, Ranjan P, Suleiman ZG, Goswami SK, Li J, Prasad R, Verma SK. mRNA modifications in cardiovascular biology and disease: with a focus on m6A modification. Cardiovasc Res 2022;118:1680-1692. https://doi.org/10.1093/cvr/cvab160
57. Leptidis S, Papakonstantinou E, Diakou KI, Pierouli K, Mitsis T, Dragoumani K, Bacopoulou F, Sanoudou D, Chrousos GP, Vlachakis D. Epitranscriptomics of cardiovascular diseases (Review). Int J Mol Med 2022;49. https://doi.org/10.3892/ijmm.2021.5064
58. Chen YS, Ouyang XP, Yu XH, Novák P, Zhou L, He PP, Yin K. N6-Adenosine Methylation (m(6)A) RNA Modification: an Emerging Role in Cardiovascular Diseases. J Cardiovasc Transl Res 2021;14:857-872. https://doi.org/10.1007/s12265-021-10108-w
59. Zhou W, Wang C, Chang J, Huang Y, Xue Q, Miao C, Wu P. RNA Methylations in Cardiovascular Diseases, Molecular Structure, Biological Functions and Regulatory Roles in Cardiovascular Diseases. Front Pharmacol 2021;12:722728. https://doi.org/10.3389/fphar.2021.722728
60. Xu Z, Lv B, Qin Y, Zhang B. Emerging Roles and Mechanism of m6A Methylation in Cardiometabolic Diseases. Cells 2022;11. https://doi.org/10.3390/cells11071101
61. Li Y, Yu H, Zhao W, Xu X, Zhou J, Xu M, Gao W, Yuan G. Analysis of urinary methylated nucleosides of patients with coronary artery disease by high-performance liquid chromatography/electrospray ionization tandem mass spectrometry. Rapid Commun Mass Spectrom 2014;28:2054-2058. https://doi.org/10.1002/rcm.6986, https://doi.org/10.1007/s13361-017-1735-7
62. Ma Y, Liu X, Bi Y, Wang T, Chen C, Wang Y, Han D, Cao F. Alteration of N(6)-Methyladenosine mRNA Methylation in a Human Stem Cell-Derived Cardiomyocyte Model of Tyrosine Kinase Inhibitor-Induced Cardiotoxicity. Front Cardiovasc Med 2022;9:849175. https://doi.org/10.3389/fcvm.2022.849175
63. Deng W, Jin Q, Li L. Protective mechanism of demethylase fat mass and obesity-associated protein in energy metabolism disorder of hypoxia-reoxygenation-induced cardiomyocytes. Exp Physiol 2021;106:2423-2433. https://doi.org/10.1113/EP089901
64. Shen W, Li H, Su H, Chen K, Yan J. FTO overexpression inhibits apoptosis of hypoxia/reoxygenation-treated myocardial cells by regulating m6A modification of Mhrt. Mol Cell Biochem 2021;476:2171-2179. https://doi.org/10.1007/s11010-021-04069-6

65. Ke WL, Huang ZW, Peng CL, Ke YP. m(6)A demethylase FTO regulates the apoptosis and inflammation of cardiomyocytes via YAP1 in ischemia-reperfusion injury. Bioengineered 2022;13:5443-5452. https://doi.org/10.1080/21655979.2022.2030572
66. Zhang X, Fu Q, Xu L, Yang Y, Zhao W, Zhang Y, Li H, Mi W. Dexmedetomidine Postconditioning Alleviates Hypoxia/Reoxygenation Injury in Senescent Myocardial Cells by Regulating lncRNA H19 and m(6)A Modification. Oxidative Medicine and Cellular Longevity 2020;2020:9250512. https://doi.org/10.1155/2020/9250512
67. Cui Y, Wang P, Li M, Wang Y, Tang X, Cui J, Chen Y, Zhang T. Cinnamic acid mitigates left ventricular hypertrophy and heart failure in part through modulating FTO-dependent N(6)-methyladenosine RNA modification in cardiomyocytes. Biomed Pharmacother 2023;165:115168. https://doi.org/10.1016/j.biopha.2023.115168
68. Yu P, Wang J, Xu GE, Zhao X, Cui X, Feng J, Sun J, Wang T, Spanos M, Lehmann HI, Li G, Xu J, Wang L, Xiao J. RNA m(6)A-Regulated circ-ZNF609 Suppression Ameliorates Doxorubicin-Induced Cardiotoxicity by Upregulating FTO. JACC Basic Transl Sci 2023;8:677-698. https://doi.org/10.1016/j.jacbts.2022.12.005
69. Benak D, Holzerova K, Hrdlicka J, Kolar F, Olsen M, Karelson M, Hlavackova M. Epitranscriptomic regulation in fasting hearts: implications for cardiac health. RNA Biol 2024;21:1-14. https://doi.org/10.1080/15476286.2024.2307732
70. Gong R, Wang X, Li H, Liu S, Jiang Z, Zhao Y, Yu Y, Han Z, Yu Y, Dong C, Li S, Xu B, Zhang W, Wang N, Li X, Gao X, Yang F, Bamba D, Ma W, Liu Y, Cai B. Loss of m(6)A methyltransferase METTL3 promotes heart regeneration and repair after myocardial injury. Pharmacol Res 2021;174:105845. https://doi.org/10.1016/j.phrs.2021.105845
71. Wu C, Chen Y, Wang Y, Xu C, Cai Y, Zhang R, Peng F, Wang S. The m(6)A methylation enzyme METTL14 regulates myocardial ischemia/reperfusion injury through the Akt/mTOR signaling pathway. Mol Cell Biochem 2023. https://doi.org/10.1007/s11010-023-04808-x
72. Benak D, Kolar F, Zhang L, Devaux Y, Hlavackova M. RNA modification m(6)Am: the role in cardiac biology. Epigenetics 2023;18:2218771. https://doi.org/10.1080/15592294.2023.2218771
73. Wei C, Gershowitz A, Moss B. N6, O2'-dimethyladenosine a novel methylated ribonucleoside next to the 5' terminal of animal cell and virus mRNAs. Nature 1975;257:251-253. https://doi.org/10.1038/257251a0
74. Bokar JA. The biosynthesis and functional roles of methylated nucleosides in eukaryotic mRNA. In: Grosjean H, editor. Fine-Tuning of RNA Functions by Modification and Editing. Berlin, Heidelberg: Springer Berlin Heidelberg; 2005. p. 141-177. https://doi.org/10.1007/b106365
75. Akichika S, Hirano S, Shichino Y, Suzuki T, Nishimasu H, Ishitani R, Sugita A, Hirose Y, Iwasaki S, Nureki O, Suzuki T. Cap-specific terminal N (6)-methylation of RNA by an RNA polymerase II-associated methyltransferase. Science 2019;363. https://doi.org/10.1126/science.aav0080
76. Sun H, Zhang M, Li K, Bai D, Yi C. Cap-specific, terminal N(6)-methylation by a mammalian m(6)Am methyltransferase. Cell Res 2019;29:80-82. https://doi.org/10.1038/s41422-018-0117-4
77. Chen H, Gu L, Orellana EA, Wang Y, Guo J, Liu Q, Wang L, Shen Z, Wu H, Gregory RI, Xing Y, Shi Y. METTL4 is an snRNA m(6)Am methyltransferase that regulates RNA splicing. Cell Res 2020;30:544-547. https://doi.org/10.1038/s41422-019-0270-4
78. Goh YT, Koh CWQ, Sim DY, Roca X, Goh WSS. METTL4 catalyzes m6Am methylation in U2 snRNA to regulate pre-mRNA splicing. Nucleic Acids Res 2020;48:9250-9261. https://doi.org/10.1093/nar/gkaa684
79. Mauer J, Luo X, Blanjoie A, Jiao X, Grozhik AV, Patil DP, Linder B, Pickering BF, Vasseur JJ, Chen Q, Gross SS, Elemento O, Debart F, Kiledjian M, Jaffrey SR. Reversible methylation of m(6)A(m) in the 5' cap controls mRNA stability. Nature 2017;541:371-375. https://doi.org/10.1038/nature21022
80. Mauer J, Jaffrey SR. FTO, m(6) A(m), and the hypothesis of reversible epitranscriptomic mRNA modifications. FEBS Lett 2018;592:2012-2022. https://doi.org/10.1002/1873-3468.13092
81. Mauer J, Sindelar M, Despic V, Guez T, Hawley BR, Vasseur JJ, Rentmeister A, Gross SS, Pellizzoni L, Debart F, Goodarzi H, Jaffrey SR. FTO controls reversible m(6)Am RNA methylation during snRNA biogenesis. Nat Chem Biol 2019;15:340-347. https://doi.org/10.1038/s41589-019-0231-8

82. Dunn DB. The occurrence of 1-methyladenine in ribonucleic acid. Biochim Biophys Acta 1961;46:198-200. https://doi.org/10.1016/0006-3002(61)90668-0
83. Helm M, Giegé R, Florentz C. A Watson-Crick base-pair-disrupting methyl group (m1A9) is sufficient for cloverleaf folding of human mitochondrial tRNALys. Biochemistry 1999;38:13338-13346. https://doi.org/10.1021/bi991061g
84. Sharma S, Watzinger P, Kötter P, Entian KD. Identification of a novel methyltransferase, Bmt2, responsible for the N-1-methyl-adenosine base modification of 25S rRNA in Saccharomyces cerevisiae. Nucleic Acids Res 2013;41:5428-5443. https://doi.org/10.1093/nar/gkt195
85. Dominissini D, Nachtergaele S, Moshitch-Moshkovitz S, Peer E, Kol N, Ben-Haim MS, Dai Q, Di Segni A, Salmon-Divon M, Clark WC, Zheng G, Pan T, Solomon O, Eyal E, Hershkovitz V, Han D, Doré LC, Amariglio N, Rechavi G, He C. The dynamic N(1)-methyladenosine methylome in eukaryotic messenger RNA. Nature 2016;530:441-446. https://doi.org/10.1038/nature16998
86. Safra M, Sas-Chen A, Nir R, Winkler R, Nachshon A, Bar-Yaacov D, Erlacher M, Rossmanith W, Stern-Ginossar N, Schwartz S. The m1A landscape on cytosolic and mitochondrial mRNA at single-base resolution. Nature 2017;551:251-255. https://doi.org/10.1038/nature24456
87. Li X, Xiong X, Zhang M, Wang K, Chen Y, Zhou J, Mao Y, Lv J, Yi D, Chen XW, Wang C, Qian SB, Yi C. Base-Resolution Mapping Reveals Distinct m(1)A Methylome in Nuclear- and Mitochondrial-Encoded Transcripts. Mol Cell 2017;68:993-1005.e1009. https://doi.org/10.1016/j.molcel.2017.10.019
88. Chujo T, Suzuki T. Trmt61B is a methyltransferase responsible for 1-methyladenosine at position 58 of human mitochondrial tRNAs. Rna 2012;18:2269-2276. https://doi.org/10.1261/rna.035600.112
89. Bar-Yaacov D, Frumkin I, Yashiro Y, Chujo T, Ishigami Y, Chemla Y, Blumberg A, Schlesinger O, Bieri P, Greber B, Ban N, Zarivach R, Alfonta L, Pilpel Y, Suzuki T, Mishmar D. Mitochondrial 16S rRNA Is Methylated by tRNA Methyltransferase TRMT61B in All Vertebrates. PLoS Biol 2016;14:e1002557. https://doi.org/10.1371/journal.pbio.1002557
90. Waku T, Nakajima Y, Yokoyama W, Nomura N, Kako K, Kobayashi A, Shimizu T, Fukamizu A. NML-mediated rRNA base methylation links ribosomal subunit formation to cell proliferation in a p53-dependent manner. J Cell Sci 2016;129:2382-2393. https://doi.org/10.1242/jcs.183723
91. Liu F, Clark W, Luo G, Wang X, Fu Y, Wei J, Wang X, Hao Z, Dai Q, Zheng G, Ma H, Han D, Evans M, Klungland A, Pan T, He C. ALKBH1-mediated tRNA demethylation regulates translation. Cell 2016;167:816-828.e816. https://doi.org/10.1016/j.cell.2016.09.038
92. Li X, Xiong X, Wang K, Wang L, Shu X, Ma S, Yi C. Transcriptome-wide mapping reveals reversible and dynamic N(1)-methyladenosine methylome. Nat Chem Biol 2016;12:311-316. https://doi.org/10.1038/nchembio.2040
93. Chen Z, Qi M, Shen B, Luo G, Wu Y, Li J, Lu Z, Zheng Z, Dai Q, Wang H. Transfer RNA demethylase ALKBH3 promotes cancer progression via induction of tRNA-derived small RNAs. Nucleic Acids Res 2019;47:2533-2545. https://doi.org/10.1093/nar/gky1250
94. Oerum S, Dégut C, Barraud P, Tisné C. m1A Post-Transcriptional Modification in tRNAs. Biomolecules 2017;7. https://doi.org/10.3390/biom7010020
95. Shima H, Igarashi K. N 1-methyladenosine (m1A) RNA modification: the key to ribosome control. J Biochem 2020;167:535-539. https://doi.org/10.1093/jb/mvaa026
96. Zhao BS, Roundtree IA, He C. Post-transcriptional gene regulation by mRNA modifications. Nat Rev Mol Cell Biol 2017;18:31-42. https://doi.org/10.1038/nrm.2016.132
97. Wu Y, Zhan S, Xu Y, Gao X. RNA modifications in cardiovascular diseases, the potential therapeutic targets. Life Sci 2021;278:119565. https://doi.org/10.1016/j.lfs.2021.119565
98. Cohn WE. Some results of the applications of ion-exchange chromatography to nucleic acid chemistry. J Cell Physiol Suppl 1951;38:21-40. https://doi.org/10.1002/jcp.1030380405
99. Xue C, Chu Q, Zheng Q, Jiang S, Bao Z, Su Y, Lu J, Li L. Role of main RNA modifications in cancer: N(6)-methyladenosine, 5-methylcytosine, and pseudouridine. Signal Transduct Target Ther 2022;7:142. https://doi.org/10.1038/s41392-022-01003-0

100. Sun H, Li K, Liu C, Yi C. Regulation and functions of non-m(6)A mRNA modifications. Nat Rev Mol Cell Biol 2023. https://doi.org/10.1038/s41580-023-00622-x
101. Rintala-Dempsey AC, Kothe U. Eukaryotic stand-alone pseudouridine synthases - RNA modifying enzymes and emerging regulators of gene expression? RNA Biol 2017;14:1185-1196. https://doi.org/10.1080/15476286.2016.1276150
102. Li X, Ma S, Yi C. Pseudouridine: the fifth RNA nucleotide with renewed interests. Curr Opin Chem Biol 2016;33:108-116. https://doi.org/10.1016/j.cbpa.2016.06.014
103. Zhao BS, He C. Pseudouridine in a new era of RNA modifications. Cell Res 2015;25:153-154. https://doi.org/10.1038/cr.2014.143
104. Wu G, Adachi H, Ge J, Stephenson D, Query CC, Yu YT. Pseudouridines in U2 snRNA stimulate the ATPase activity of Prp5 during spliceosome assembly. Embo j 2016;35:654-667. https://doi.org/10.15252/embj.201593113
105. Levi O, Arava YS. Pseudouridine-mediated translation control of mRNA by methionine aminoacyl tRNA synthetase. Nucleic Acids Res 2021;49:432-443. https://doi.org/10.1093/nar/gkaa1178
106. Borchardt EK, Martinez NM, Gilbert WV. Regulation and Function of RNA Pseudouridylation in Human Cells. Annu Rev Genet 2020;54:309-336. https://doi.org/10.1146/annurev-genet-112618-043830
107. Jalan A, Jayasree PJ, Karemore P, Narayan KP, Khandelia P. Decoding the 'Fifth' Nucleotide: Impact of RNA Pseudouridylation on Gene Expression and Human Disease. Mol Biotechnol 2023. https://doi.org/10.1007/s12033-023-00792-1
108. Razavi AC, Bazzano LA, He J, Li S, Fernandez C, Whelton SP, Krousel-Wood M, Nierenberg JL, Shi M, Li C, Mi X, Kinchen J, Kelly TN. Pseudouridine and N-formylmethionine associate with left ventricular mass index: Metabolome-wide association analysis of cardiac remodeling. J Mol Cell Cardiol 2020;140:22-29. https://doi.org/10.1016/j.yjmcc.2020.02.005
109. Alexander D, Lombardi R, Rodriguez G, Mitchell MM, Marian AJ. Metabolomic distinction and insights into the pathogenesis of human primary dilated cardiomyopathy. Eur J Clin Invest 2011;41:527-538. https://doi.org/10.1111/j.1365-2362.2010.02441.x
110. Dunn WB, Broadhurst DI, Deepak SM, Buch MH, McDowell G, Spasic I, Ellis DI, Brooks N, Kell DB, Neyses L. Serum metabolomics reveals many novel metabolic markers of heart failure, including pseudouridine and 2-oxoglutarate. Metabolomics 2007;3:413-426. https://doi.org/10.1007/s11306-007-0063-5
111. Nagasawa CK, Kibiryeva N, Marshall J, O'Brien JE, Bittel DC. scaRNA1 levels alter pseudouridylation in spliceosomal RNA U2 affecting alternative mRNA splicing and embryonic development. Pediatric Cardiology 2020;41:341-349. https://doi.org/10.1007/s00246-019-02263-4
112. Patil P, Kibiryeva N, Uechi T, Marshall J, O'Brien JE, Jr., Artman M, Kenmochi N, Bittel DC. scaRNAs regulate splicing and vertebrate heart development. Biochim Biophys Acta 2015;1852:1619-1629. https://doi.org/10.1016/j.bbadis.2015.04.016
113. Bohnsack KE, Höbartner C, Bohnsack MT. Eukaryotic 5-methylcytosine (m^5C) RNA methyltransferases: mechanisms, cellular functions, and links to disease. Genes (Basel) 2019;10. https://doi.org/10.3390/genes10020102
114. Wang YY, Tian Y, Li YZ, Liu YF, Zhao YY, Chen LH, Zhang C. The role of m5C methyltransferases in cardiovascular diseases. Front Cardiovasc Med 2023;10:1225014. https://doi.org/10.3389/fcvm.2023.1225014
115. Haag S, Sloan KE, Ranjan N, Warda AS, Kretschmer J, Blessing C, Hübner B, Seikowski J, Dennerlein S, Rehling P, Rodnina MV, Höbartner C, Bohnsack MT. NSUN3 and ABH1 modify the wobble position of mt-tRNAMet to expand codon recognition in mitochondrial translation. Embo j 2016;35:2104-2119. https://doi.org/10.15252/embj.201694885
116. Fu L, Guerrero CR, Zhong N, Amato NJ, Liu Y, Liu S, Cai Q, Ji D, Jin SG, Niedernhofer LJ, Pfeifer GP, Xu GL, Wang Y. Tet-mediated formation of 5-hydroxymethylcytosine in RNA. J Am Chem Soc 2014;136:11582-11585. https://doi.org/10.1021/ja505305z
117. Yang X, Yang Y, Sun BF, Chen YS, Xu JW, Lai WY, Li A, Wang X, Bhattarai DP, Xiao W, Sun HY, Zhu Q, Ma HL, Adhikari S, Sun M, Hao YJ, Zhang B, Huang CM, Huang N, Jiang GB, Zhao YL, Wang HL, Sun YP, Yang YG. 5-methylcytosine promotes mRNA export - NSUN2 as the methyltransferase and ALYREF as an m(5)C reader. Cell Res 2017;27:606-625. https://doi.org/10.1038/cr.2017.55

118. Chen X, Li A, Sun BF, Yang Y, Han YN, Yuan X, Chen RX, Wei WS, Liu Y, Gao CC, Chen YS, Zhang M, Ma XD, Liu ZW, Luo JH, Lyu C, Wang HL, Ma J, Zhao YL, Zhou FJ, Huang Y, Xie D, Yang YG. 5-methylcytosine promotes pathogenesis of bladder cancer through stabilizing mRNAs. Nat Cell Biol 2019;21:978-990. https://doi.org/10.1038/s41556-019-0361-y
119. Squires JE, Preiss T. Function and detection of 5-methylcytosine in eukaryotic RNA. Epigenomics 2010;2:709-715. https://doi.org/10.2217/epi.10.47
120. Chen YS, Yang WL, Zhao YL, Yang YG. Dynamic transcriptomic m(5) C and its regulatory role in RNA processing. Wiley Interdiscip Rev RNA 2021;12:e1639. https://doi.org/10.1002/wrna.1639
121. Huang T, Chen W, Liu J, Gu N, Zhang R. Genome-wide identification of mRNA 5-methylcytosine in mammals. Nature Structural & Molecular Biology 2019;26:380-388. https://doi.org/10.1038/s41594-019-0218-x
122. Metodiev MD, Spåhr H, Loguercio Polosa P, Meharg C, Becker C, Altmueller J, Habermann B, Larsson NG, Ruzzenente B. NSUN4 is a dual function mitochondrial protein required for both methylation of 12S rRNA and coordination of mitoribosomal assembly. PLoS Genet 2014;10:e1004110. https://doi.org/10.1371/journal.pgen.1004110
123. Ghanbarian H, Wagner N, Polo B, Baudouy D, Kiani J, Michiels JF, Cuzin F, Rassoulzadegan M, Wagner KD. Dnmt2/Trdmt1 as mediator of RNA polymerase II transcriptional activity in cardiac growth. PLoS One 2016;11:e0156953. https://doi.org/10.1371/journal.pone.0156953
124. Varma E, Burghaus J, Schwarzl T, Sekaran T, Gupta P, Górska AA, Hofmann C, Stroh C, Jürgensen L, Kamuf-Schenk V, Li X, Medert R, Leuschner F, Kmietczyk V, Freichel M, Katus HA, Hentze MW, Frey N, Völkers M. Translational control of Ybx1 expression regulates cardiac function in response to pressure overload in vivo. Basic Res Cardiol 2023;118:25. https://doi.org/10.1007/s00395-023-00996-1
125. Yang R, Li L, Hou Y, Li Y, Zhang J, Yang N, Zhang Y, Ji W, Yu T, Lv L, Liang H, Li X, Li T, Shan H. Long non-coding RNA KCND1 protects hearts from hypertrophy by targeting YBX1. Cell Death Dis 2023;14:344. https://doi.org/10.1038/s41419-023-05852-7
126. Wang Y, Zan Y, Huang Y, Peng X, Ma S, Ren J, Li X, Wei L, Wang X, Yuan Y, Tang J, Zhan Z, Wang Z, Ding Y. NSUN2 alleviates doxorubicin-induced myocardial injury through Nrf2-mediated antioxidant stress. Cell Death Discov 2023;9:43. https://doi.org/10.1038/s41420-022-01294-w
127. Brennicke A, Marchfelder A, Binder S. RNA editing. FEMS Microbiol Rev 1999;23:297-316. https://doi.org/10.1111/j.1574-6976.1999.tb00401.x
128. Gott JM, Emeson RB. Functions and mechanisms of RNA editing. Annu Rev Genet 2000;34:499-531. https://doi.org/10.1146/annurev.genet.34.1.499
129. Ganem NS, Lamm AT. A-to-I RNA editing - thinking beyond the single nucleotide. RNA Biol 2017;14:1690-1694. https://doi.org/10.1080/15476286.2017.1364830
130. Dominissini D, Moshitch-Moshkovitz S, Amariglio N, Rechavi G. Adenosine-to-inosine RNA editing meets cancer. Carcinogenesis 2011;32:1569-1577. https://doi.org/10.1093/carcin/bgr124
131. Bhakta S, Tsukahara T. C-to-U RNA Editing: A Site Directed RNA Editing Tool for Restoration of Genetic Code. Genes (Basel) 2022;13. https://doi.org/10.3390/genes13091636
132. Sowden MP, Ballatori N, Jensen KL, Reed LH, Smith HC. The editosome for cytidine to uridine mRNA editing has a native complexity of 27S: identification of intracellular domains containing active and inactive editing factors. J Cell Sci 2002;115:1027-1039. https://doi.org/10.1242/jcs.115.5.1027
133. Nishikura K. A-to-I editing of coding and non-coding RNAs by ADARs. Nat Rev Mol Cell Biol 2016;17:83-96. https://doi.org/10.1038/nrm.2015.4
134. Moore JBt, Sadri G, Fischer AG, Weirick T, Militello G, Wysoczynski M, Gumpert AM, Braun T, Uchida S. The A-to-I RNA editing enzyme adar1 is essential for normal embryonic cardiac growth and development. Circ Res 2020;127:550-552. https://doi.org/10.1161/CIRCRESAHA.120.316932
135. El Azzouzi H, Vilaça AP, Feyen DAM, Gommans WM, de Weger RA, Doevendans PAF, Sluijter JPG. Cardiomyocyte Specific Deletion of ADAR1 Causes Severe Cardiac Dysfunction and Increased Lethality. Front Cardiovasc Med 2020;7:30. https://doi.org/10.3389/fcvm.2020.00030

136. Garcia-Gonzalez C, Dieterich C, Maroli G, Wiesnet M, Wietelmann A, Li X, Yuan X, Graumann J, Stellos K, Kubin T, Schneider A, Braun T. ADAR1 prevents autoinflammatory processes in the heart mediated by IRF7. Circ Res 2022;131:580-597. https://doi.org/10.1161/CIRCRESAHA.122.320839
137. Borik S, Simon AJ, Nevo-Caspi Y, Mishali D, Amariglio N, Rechavi G, Paret G. Increased RNA editing in children with cyanotic congenital heart disease. Intensive Care Med 2011;37:1664-1671. https://doi.org/10.1007/s00134-011-2296-z
138. Kokot KE, Kneuer JM, John D, Rebs S, Möbius-Winkler MN, Erbe S, Müller M, Andritschke M, Gaul S, Sheikh BN, Haas J, Thiele H, Müller OJ, Hille S, Leuschner F, Dimmeler S, Streckfuss-Bömeke K, Meder B, Laufs U, Boeckel JN. Reduction of A-to-I RNA editing in the failing human heart regulates formation of circular RNAs. Basic Res Cardiol 2022;117:32. https://doi.org/10.1007/s00395-022-00940-9
139. Altaf F, Vesely C, Sheikh AM, Munir R, Shah STA, Tariq A. Modulation of ADAR mRNA expression in patients with congenital heart defects. PLoS One 2019;14:e0200968. https://doi.org/10.1371/journal.pone.0200968
140. Wu X, Wang L, Wang K, Li J, Chen R, Wu X, Ni G, Liu C, Das S, Sluijter JPG, Li X, Xiao J. ADAR2 increases in exercised heart and protects against myocardial infarction and doxorubicin-induced cardiotoxicity. Mol Ther 2022;30:400-414. https://doi.org/10.1016/j.ymthe.2021.07.004
141. Birgaoanu M, Sachse M, Gatsiou A. RNA editing therapeutics: advances, challenges and perspectives on combating heart disease. Cardiovasc Drugs Ther 2023;37:401-411. https://doi.org/10.1007/s10557-022-07391-3

Physiol. Res. 73 (Suppl. 1): S199-S215, 2024 *https://doi.org/10.33549/physiolres.935406*

REVIEW

The Role of Cornichons in the Biogenesis and Functioning of Monovalent-Cation Transport Systems

Klára PAPOUŠKOVÁ[1], Karolína ČERNÁ[1], Viktorie RADOVÁ[1], Olga ZIMMERMANNOVÁ[1]

[1]Laboratory of Membrane Transport, Institute of Physiology of the Czech Academy of Sciences, Prague, Czech Republic

Received May 14, 2024
Accepted May 16, 2024

Summary

Monovalent-cation homeostasis, crucial for all living cells, is ensured by the activity of various types of ion transport systems located either in the plasma membrane or in the membranes of organelles. A key prerequisite for the functioning of ion-transporting proteins is their proper trafficking to the target membrane. The cornichon family of COPII cargo receptors is highly conserved in eukaryotic cells. By simultaneously binding their cargoes and a COPII-coat subunit, cornichons promote the incorporation of cargo proteins into the COPII vesicles and, consequently, the efficient trafficking of cargoes *via* the secretory pathway. In this review, we summarize current knowledge about cornichon proteins (CNIH/Erv14), with an emphasis on yeast and mammalian cornichons and their role in monovalent-cation homeostasis. *Saccharomyces cerevisiae* cornichon Erv14 serves as a cargo receptor of a large portion of plasma-membrane proteins, including several monovalent-cation transporters. By promoting the proper targeting of at least three housekeeping ion transport systems, Na^+, K^+/H^+ antiporter Nha1, K^+ importer Trk1 and K^+ channel Tok1, Erv14 appears to play a complex role in the maintenance of alkali-metal-cation homeostasis. Despite their connection to serious human diseases, the repertoire of identified cargoes of mammalian cornichons is much more limited. The majority of current information is about the structure and functioning of CNIH2 and CNIH3 as auxiliary subunits of AMPAR multi-protein complexes. Based on their unique properties and easy genetic manipulation, we propose yeast cells to be a useful tool for uncovering a broader spectrum of human cornichons´ cargoes.

Key words

Cornichon • Cation homeostasis • Transporters • Yeast • AMPAR

Corresponding author

O. Zimmermannová, Laboratory of Membrane Transport, Institute of Physiology of the Czech Academy of Sciences, Videnska 1083, 142 00 Prague 4 – Krč, Czech Republic. E-mail: olga.zimmermannova@fgu.cas.cz

Introduction

Cells need to incessantly adapt to gradual or sudden changes in cation concentrations in the extracellular milieu to maintain intracellular conditions that are suitable for their fitness (Fig. 1A). K^+, H^+, and Na^+ are the most important monovalent cations, required for all physiological processes [1]. From bacteria to mammals, cells need to maintain a stable cytosolic pH of 7.0 (the H^+ concentration) and accumulate a high concentration of K^+ (Fig. 1A), as it is essential for many physiological functions, including the regulation of cell volume and intracellular pH, and the maintenance of membrane potential [1]. Adequate K^+ content is also a pivotal signal for cell division and a prerequisite for resistance to various stresses [1,2]. A high intracellular concentration of Na^+ is generally toxic [1]. However, the electrochemical gradients of Na^+ and H^+ across the membranes are a driving force for secondary active transport systems. In mammals, Na^+ is the major cation in extracellular space, and both Na^+ and K^+ are also employed to generate membrane-potential changes in

A

Concentration (mM)	Sea water	Yeast	Plant cells	Animal cells	Blood plasma
K^+	≈ 10	300	200	100	4
Na^+	≈ 500	< 30	< 10	10	100-200

B

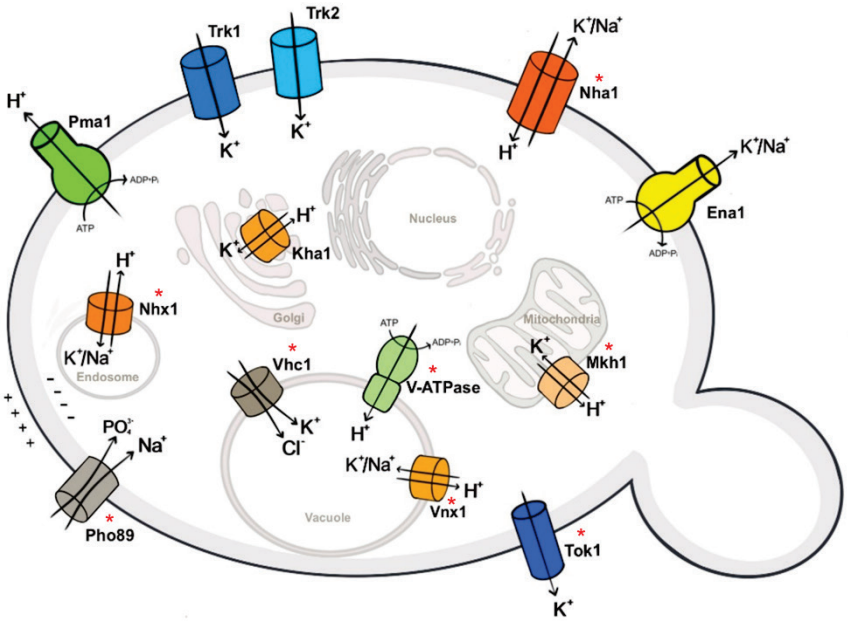

Fig. 1. Monovalent-cation homeostasis in eukaryotic cells. (**A**) Concentrations of K^+ and Na^+ in various representative organisms and extracellular environments. All cells accumulate K^+, keep low content of toxic Na^+, and preserve neutral cytosolic pH [1,11-13]. (**B**) An overview of transport systems for monovalent cations in *S. cerevisiae* (* transport systems with orthologues in humans [14]).

excitable cells, such as neurons. The intracellular concentrations of K^+, Na^+ and H^+ are strictly regulated *via* the activity of a series of membrane proteins – transporters and channels – mediating the fluxes of these cations across the membranes. In the model organism of eukaryotic cells, the yeast *Saccharomyces cerevisiae*, more than ten transport systems for monovalent cations have been characterized in the plasma membrane and in intracellular membranes (Fig. 1B, [3]). Some are fungi-specific, but many yeast transporters have orthologues in mammalian cells (Fig. 1B). Disturbances in H^+, Na^+ and/or K^+ concentrations result in many pathological conditions in humans, such as neuro-degenerative diseases, metabolic disorders and malignant transformations [4]. Hence, the investigation of regulatory mechanisms that ensure cationic homeostasis is receiving increasing attention in biomedical sciences.

Cation transporters are complex membrane proteins with hydrophobic parts embedded in cellular membranes, and in many cases, large hydrophilic regions positioned on both sides of the membrane. The activity of transporters is tightly regulated at several levels, e.g., the level of their expression and/or post-translational modifications. Moreover, the correct function of each membrane protein depends on its effective delivery into the target membrane. In eukaryotic cells, approximately one-third of nascent polypeptides undergo maturation during proteosynthesis *via* their passing through the secretory pathway [5]. An important group of proteins that interact with maturing proteins and ensure their passage through the secretory pathway are cargo receptors that help to insert their interaction partners into COPII vesicles, which are exported from the endoplasmic reticulum (ER) to the Golgi apparatus (Fig. 2A). The goal of this overview is to summarize current findings about the structures and physiological roles of the cornichon family of cargo receptors, with the emphasis on *S. cerevisiae* Erv14 protein and its mammalian homologues CNIH1-4, and their particular importance for the biogenesis of monovalent-cation transporters. Characterizing the physiological functions of cargo receptors from yeasts and humans and their importance for the maintenance of monovalent-cation homeostasis is one of the research topics investigated in the

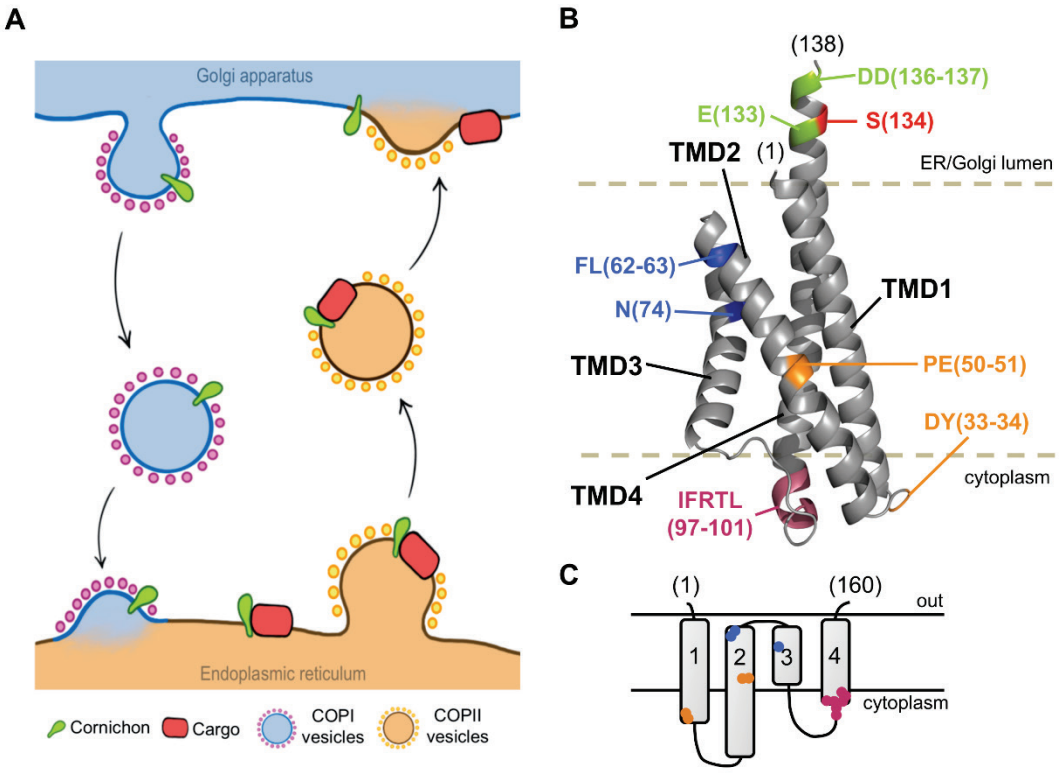

Fig. 2. Basic properties of cornichons. (**A**) Scheme of functioning of cornichons as COPII cargo receptors. (**B**) AlphaFold [23] structural model of Erv14. Regions important for the functioning of the protein (see the text) are depicted in different colors. (**C**) Scheme of topology of mammalian CNIH2/3 proteins. Positions of amino-acid residues homologous to Erv14 regions highlighted in (B) are depicted.

Laboratory of Membrane Transport at the Institute of Physiology CAS. It has arisen from a fruitful collaboration with the Laboratory of Prof. Omar Pantoja from the Institute of Biotechnology at the National Autonomous University of Mexico [6-10], within which we also employed the yeast *S. cerevisiae* and its mutated strains to investigate the interaction between the cornichon CNIH1 and the Na^+ transporter HKT1;3 from *Oryza sativa* [7].

Cargo-receptor function and structure of cornichon proteins

The cornichon family of COPII cargo receptors is highly conserved in eukaryotic organisms. The first characterized member, *Drosophila* cornichon Cni, which was reported to be necessary for the proper delivery of the transforming growth factor α (TGFα) from the ER to the oocyte surface during *Drosophila* oogenesis, gave the name to the whole family of proteins [15,16]. The absence of either the TGFα Gurken (Grk) or cornichon Cni results in an altered shape of the fly´s eggs, which are elongated (Gurken means "cucumbers" in German) [16-18]. However, the most characterized cornichon is the *S. cerevisiae* Erv14 protein. It is a 14 kDa, 138-amino-acid-residue-long protein that was originally found in isolated ER-derived vesicles [19]. Erv14 is predicted to be an integral membrane protein that localizes to the ER and Golgi apparatus [19]. By binding both the cargo protein and also a COPII coat subunit, Sec24 [20,21], Erv14 promotes the incorporation of its cargoes into COPII vesicles (Fig. 2A).

Previously, three transmembrane domains were predicted in Erv14 and, applying the "positive-inside rule", the N-terminus of the protein was expected to be located in the cytoplasm and the C-terminus in the lumen of the ER/Golgi apparatus [21,22]. Although some experimental evidence has further supported this predicted topology of Erv14 [21], a more recent AlphaFold [23,24] model of Erv14 suggests a topology with four transmembrane domains and both termini located in the lumen of the ER (Fig. 2B). This model is in full agreement with experimentally discovered structures of mammalian homologues, cornichon proteins CNIH2 and CNIH3, which act as auxiliary subunits of AMPA-type ionotropic glutamate receptors in the plasma membrane [25-28]. In both CNIH2 and CNIH3, cryo-electron microscopy revealed that the N- and C-termini

are located in the extracellular space (Fig. 2C). The first transmembrane domain spans the membrane, and after a short loop in the cytoplasm, the second α-helical segment, which already starts in the cytoplasm, again enters the membrane bilayer. There, the amino-acid chain turns back, the third transmembrane domain crosses the lipid bilayer and finally, after a cytoplasmic loop, the fourth transmembrane domain once more fully spans the membrane (Fig. 2C). Thus, the majority of mammalian cornichons CNIH2 and CNIH3 seems to be buried in the membrane, and only small portions of the proteins are located in the cytoplasm [26,28].

Characteristics of *S. cerevisiae* cornichons

S. cerevisiae Erv14 helps its binding partners to be efficiently transported through the secretory pathway (Fig. 2A). When Erv14 is not present in cells, its cargoes are typically partially accumulated in the ER (Fig. 3, [10,19,29]). The first known cargoes of Erv14, such as Axl2, which is required for the axial budding pattern of haploid cells, or Sma2, which plays a role in the formation of prospore membrane during sporulation, were discovered based on phenotypes of cells lacking the *ERV14* gene [19,21,30]. Later, to study the cargo spectrum of individual yeast cargo receptors more systematically, Herzig and colleagues [29] developed a "PAIRS" (pairing analysis of cargo receptors) approach. The methodology was based on the crossing of strains with deletions of individual non-essential genes encoding cargo receptors, such as Erv14, with strains from the library of *S. cerevisiae* with GFP-tagged putative cargoes (proteins from post-ER compartments). The newly created libraries of strains lacking cargo receptors and simultaneously harboring GFP-tagged putative cargoes were then inspected using automated microscopy screening. The PAIRS approach revealed that Erv14 serves as a cargo receptor of a large proportion (18 of 57) of the tested plasma-membrane proteins [29]. So far, approx. 40 diverse cargoes whose ER exit is dependent on the presence of Erv14 have been identified. Erv14´s cargoes are proteins with various physiological functions; membrane transporters, including several monovalent-cation transporters, flippases or proteins involved in budding, sporulation and other processes belong among them (see below, [9,10,19,21,29,30]).

A paralogue of *ERV14*, *ERV15*, is also present in *S. cerevisiae* genome [19]. Erv15 is 142 amino-acid residues long and shares 63 % identity with Erv14. No cargo whose trafficking through the secretory pathway would depend on the presence of Erv15 was identified using the PAIRS method [29]. However, Erv15 could cooperate with Erv14 in supporting the proper trafficking of some cargoes, such as the ABC transporter Yor1 [20]. When the packaging of Yor1 to COPII vesicles was studied in *in vitro* vesicle-formation assays, Erv15 alone was insufficient to compensate for the packaging defects associated with the lack of Erv14. However, the deletion of both *ERV14* and *ERV15* in cells resulted in a more pronounced defect than in cells that only lacked Erv14 [20]. The lower importance of Erv15 for the trafficking of various cargoes compared to Erv14 might be connected to the differences in the expression levels of both proteins. In agreement, when *ERV15* was expressed under the control of *ERV14* promoter in *erv14Δ* and *erv14Δ erv15Δ* cells, the protein gained the ability to restore packaging of Yor1 to COPII vesicles [20].

The binding partners of Erv14 do not seem to share any amino-acid motif which would be responsible for their recognition by Erv14 [29]. However, since the transmembrane domains of integral membrane proteins residing in post-Golgi compartments are longer [31], it was suggested that Erv14 might recognize its cargoes based on the length of their membrane-spanning segments [29]. Indeed, a replacement of the only endogenous transmembrane domain of Mid2, a known Erv14 cargo, with a chain of 14-26 leucines (with two-amino-acid increments) showed that longer versions of Mid2 exit the ER more efficiently and in an Erv14-dependent manner. Thus, these findings supported the idea that the length of transmembrane domains is a determining factor for Erv14-dependent sorting [29].

Several amino-acid residues of Erv14 have been identified to be important for its proper functioning. The stretch of amino-acid residues 97-101 (IFRTL, Fig. 2B) was found to be necessary for the efficient packaging of Erv14 into COPII vesicles and for the binding of COPII-coat components *in vitro*. The mutations of amino-acid residues 97-IFRTL-101 to alanine residues also resulted in defects in axial bud selection, which is typical for *erv14Δ* cells [19,21]. Thus, amino acids 97-101 were suggested to play a role in the direct binding of Erv14 to COPII coat [21]. According to the most recent structural prediction of Erv14 and analogously to the topology of mammalian cornichons (Fig. 2), the IFRTL motif is supposed to be located on the cytosolic side of the membrane at the beginning of the fourth α-helix of Erv14,which is in full agreement with its

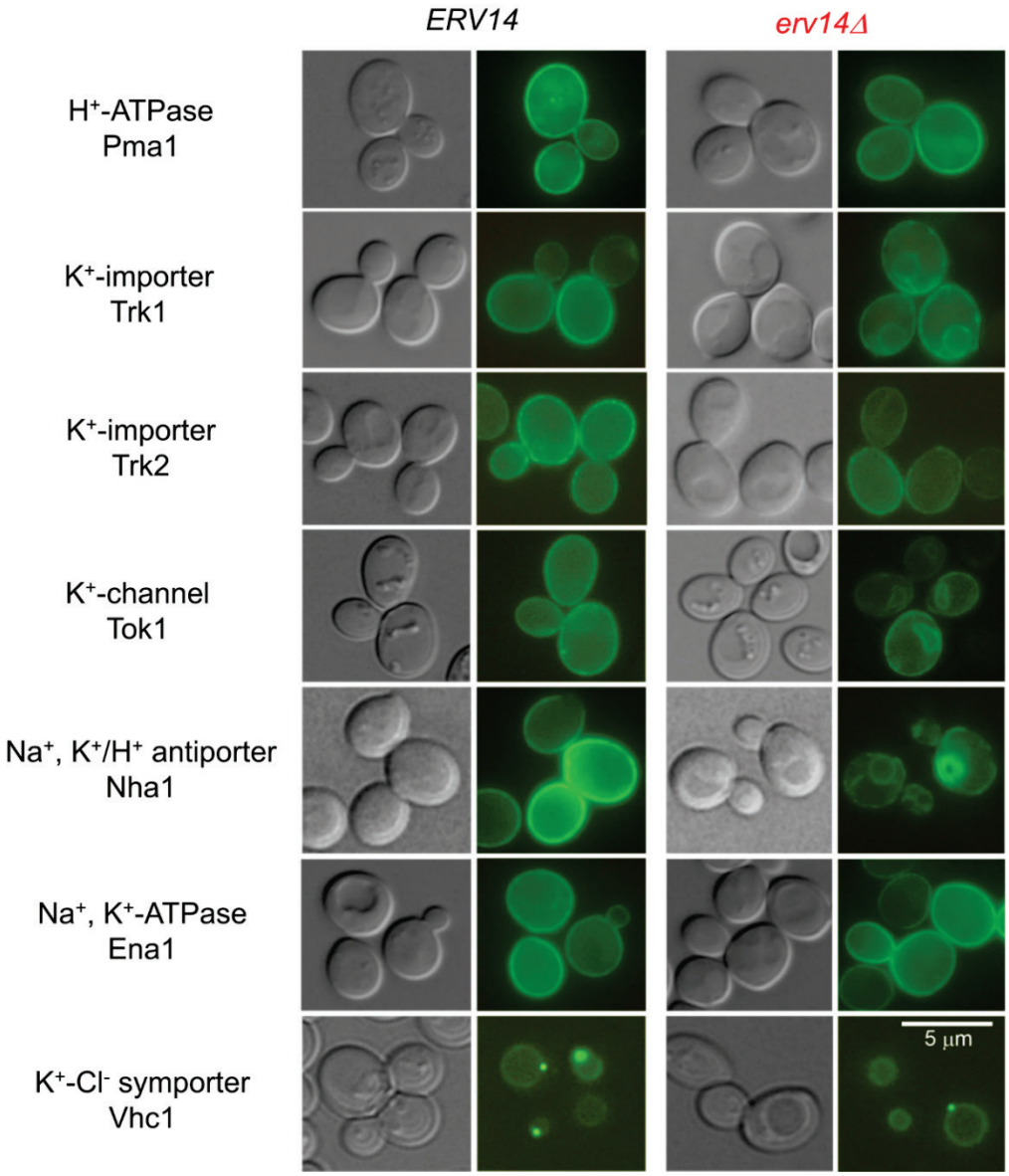

Fig. 3. Role of Erv14 in the targeting of various yeast cation transporters. Deletion of *ERV14* in *S. cerevisiae* results in retention of housekeeping K^+ transporters Trk1, Tok1 and Nha1 in endoplasmic reticulum. On the other hand, the localization of Pma1, Trk2, Ena1 and Vhc1 is not affected in *erv14Δ* cells. Nomarski (left) and fluorescence (right) micrographs of cells with or without Erv14 producing seven GFP-tagged membrane transporters as indicated. Cells were grown to the early exponential phase. The image was prepared using our results published in [9,10].

proposed role in binding the COPII complex. The incorporation of Erv14 into ER-derived vesicles was also affected by mutations of the DYPE (DY33-34, PE50-51) site (Fig. 2B, [20]). These amino-acid residues are located in the cytoplasmic short loop connecting the first and second α-helix of Erv14 (DY33-34) and in the second transmembrane domain of the cargo receptor (PE50-51), according to the most recent model of Erv14 (Fig. 2B).

On the other hand, mutations of three amino-acid residues, F62, L63, and N74, which are predicted to be located in the second or third transmembrane domain of Erv14, respectively (Fig. 2B), only affected *in vitro* packaging of the Erv14 substrate Yor1 into ER-derived vesicles, while the packaging of Erv14 itself remained unchanged [20]. These results suggested that the FLN motif might be involved in the binding of cargo proteins by Erv14. Indeed, mutations F62A and L63A impaired the binding of Erv14 to at least some of its cargoes, as observed by the yeast two-hybrid system and co-immunoprecipitation from microsomal membranes [20].

In the C-terminal parts of fungal and plant (but not animal) cornichons, a conserved acidic motif containing at least three aspartic or glutamic amino acids has been identified [8]. In *S. cerevisiae* Erv14, the motif

is formed by amino-acid residues 133-137 (ESGDD, Fig. 2B). The mutations of the acidic amino-acid residues in the motif (E133A, D136A and D137A) did not influence the localization of Erv14 in the ER/Golgi apparatus. However, Erv14 with these mutations did not fully support the proper trafficking of at least some of its cargoes to the plasma membrane, and the yeast two-hybrid system, supported by co-immunoprecipitation assays, suggested that the C-terminal EDD motif is involved in the binding of cargo proteins by Erv14 [8]. S134 from the same Erv14´s C-terminal motif (Fig. 2B) was suggested to be phosphorylated [32]. The mutations of S134 to aspartate or to alanine (mimicking the phosphorylated or dephosphorylated state of Erv14, respectively) resulted in changes in the ER structure as observed by electron microscopy. While Erv14´s cargo proteins were properly localized to the plasma membrane in cells with Erv14-S134A, they were partially accumulated in the ER of cells with Erv14-S134D [32]. In contrast to the C-terminal acidic amino-acid residues, S134 does not seem to be involved in the interaction between Erv14 and its cargoes [32]. However, the phosphor-mimetic mutation S134D caused both an ER retention of Erv14 and also affected its packaging to COPII vesicles *in vitro*. Based on these results, it was suggested that a cycle of phosphorylation and dephosphorylation of serine at position 134 is important for the proper functioning of Erv14 as a COPII cargo receptor that ensures the exit of its cargoes from the ER [32].

Role of cornichons in monovalent-cation homeostasis of yeast and plant cells

Comparisons of several physiological parameters of *S. cerevisiae* cells with or without Erv14 revealed that the lack of Erv14 decreases cell tolerance to high NaCl, KCl and cationic-drug (hygromycin B, tetramethylammonium) concentrations, and also the ability of cells to cope with low-K^+ conditions. Moreover, the deletion of *ERV14* influences cell volume and results in a relative plasma-membrane hyperpolarization as well as in a lower intracellular pH level [9,10]. Taken together, these results suggested that Erv14 plays a complex role in the maintenance of monovalent-cation homeostasis in yeast cells, most likely *via* assisting several transporters in their trafficking through the secretory pathway.

The first alkali-metal-cation transporter whose proper plasma-membrane targeting was shown to be Erv14-dependent was the Na^+, K^+/H^+ antiporter Nha1 [9,29]. Nha1 is a house-keeping protein whose cation-export activity is driven by the electrochemical gradient of H^+, which is generated by the H^+-ATPase Pma1 (Fig. 1B). It mainly contributes to the tolerance of *S. cerevisiae* cells to high external concentrations of Na^+ and K^+ at low external pH levels [33,34]. In the absence of the Erv14 cargo receptor, Nha1 is partially stacked in the ER of cells (Fig. 3), and the consequent decreased Na^+ or K^+ efflux *via* Nha1 results in a lower ability of *erv14Δ* cells to cope with high amounts of NaCl and KCl in the environment [9,29]. The physical interaction of both proteins was proved by the yeast two-hybrid system as well as co-immunoprecipitation assays [9].

Nha1 is a large (985 amino-acid residues long) polytopic membrane protein with a short N-terminus, 13 predicted transmembrane domains, and a long hydrophilic highly disordered cytoplasmic C-terminus that forms more than half of the entire protein (Fig. 4, [23]). The majority of Nha1´s C-terminal portion is neither necessary for the antiporter´s cation-translocation function nor for its plasma-membrane localization. However, an increasing amount of evidence shows the importance of this large hydrophilic portion of the antiporter in the regulation of Nha1´s activity [35-38]. Surprisingly, a truncated version of Nha1 that is shortened to 472 amino-acid residues and that lacks the majority of its C-terminal part, Nha1-472 (Fig. 4), does not require Erv14 for its trafficking to the plasma membrane *via* the secretory pathway, though it still binds the cargo receptor [9].

In various yeast Nha1 homologues, the C-termini are the least conserved parts, both in terms of their sequence and length [35,39]. However, our recent broad bioinformatic analysis of fungal Nha1 homologues that estimated the evolutionary conservation of the amino-acid positions of 286 sequences [6] specified the presence of seven approximately 15-30-amino-acid-residue-long conserved regions in the C-termini (C1-C6 described previously [35], and a new one, NC3, Fig. 4). The comparison of the localization and functioning of Nha1 versions gradually truncated from the end of the C-terminus in cells with or without Erv14 showed that only Nha1 versions that possess the C5 conserved region in their C-termini require Erv14 for their proper trafficking through the secretory pathway (Fig. 4, [6]). Thus, besides the long transmembrane domains [29], also a short hydrophilic portion of a cargo protein can underlie its need for Erv14´s assistance for its proper export from the ER.

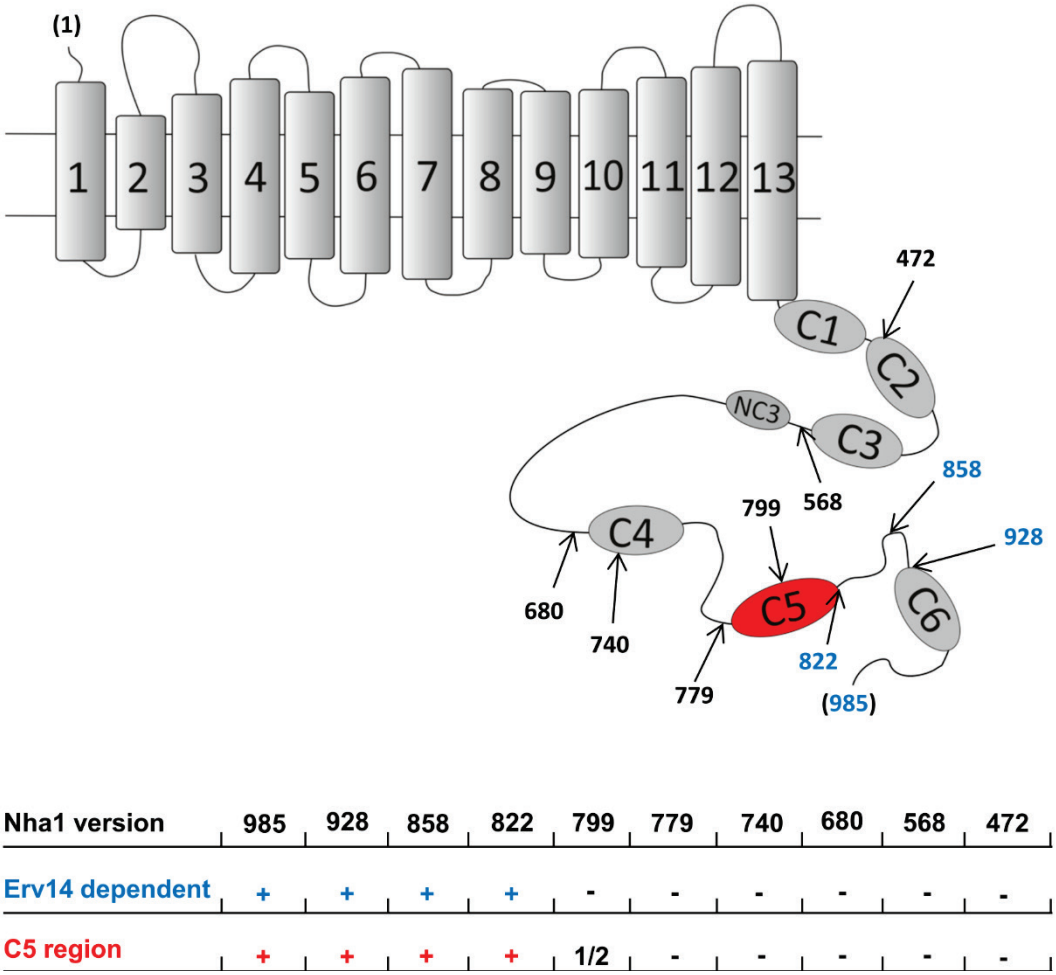

Fig. 4. Erv14 requirement of Na^+, K^+/H^+ antiporter Nha1. Only Nha1 versions that possess the C5 C-terminal conserved domain (in red) require Erv14 for their proper trafficking. Various C-terminally truncated versions of Nha1 were prepared, and their localization and functioning were studied in cells with or without Erv14. The arrows in the topological model of Nha1 point to the sites of C-terminal truncations, and the numbers correspond to the lengths of the Nha1 versions in amino-acid residues. The image was prepared using our results published in [6,9].

Nha1 was shown to form dimers, and this dimerization seems to be important for the antiporter´s cation-translocation activity [40]. The higher abundance of Nha1 dimers in both plasma and ER membranes of cells with Erv14 when compared to *erv14Δ* cells and also the lack of evidence of oligomerization of the truncated Erv14-independent Nha1-472 version suggested a possible importance of Erv14 for the formation of Nha1 dimers [9]. Whether the C-terminal region C5, whose presence determines the antiporter´s requirement of Erv14, plays a role in Nha1´s oligomerization, is not currently known.

In a systematic study addressing the role of Erv14 in the proper intracellular trafficking of various monovalent-cation transporting proteins, the localization of six transporters, namely of plasma-membrane H^+-ATPase Pma1, Na^+, K^+-efflux ATPase Ena1, K^+ importers Trk1 and Trk2, K^+ channel Tok1 and vacuolar K^+, Cl^- co-transporter Vhc1, was compared in cells with or without Erv14 (Fig. 3, [10]). In agreement with the decreased ability of *erv14Δ* cells to grow in the presence of low K^+, the main *S. cerevisiae* K^+ importer, Trk1 [41,42], was identified as a new cargo of Erv14. The lack of Erv14 results in a partial ER accumulation of Trk1 (Fig. 3), and consequently in a lower import of K^+ cations to cells. This phenomenon explains the inhibition of the growth of *erv14Δ* cells under conditions when K^+ is scarce [10]. In addition to Trk1, the evolutionarily highly conserved voltage-gated K^+ channel Tok1 was also found to be partially mislocalized in cells without Erv14 (Fig. 3). Tok1 is an outwardly rectifying channel that has been thoroughly described by electrophysiological methods [43-45]. The only known growth-related Tok1-specific phenotype is that *TOK1* overexpression improves the growth of a strain that lacks K^+ importers Trk1 and Trk2 under K^+-limiting conditions

[46]. This positive effect of the overproduction of Tok1 on the growth of *trk1Δ trk2Δ* cells at low K^+ was diminished when Erv14 was not present in cells [10]. This finding provides evidence that Tok1´s role in K^+ supply is dependent on the presence of the Erv14 cargo receptor, which assists with the delivery of Tok1 to the plasma membrane. Besides the microscopy and physiological evidence of the influence of the lack of Erv14 on the localization and functioning of both plasma-membrane K^+ transporting proteins, the physical interaction between Trk1 or Tok1 and Erv14 was confirmed in protein-protein interaction assays [10]. However, the signal for Erv14 binding in the structures of Trk1 or Tok1 has not yet been elucidated.

The lack of Erv14´s requirement of the Trk2 K^+ importer (Fig. 3) was somewhat surprising, as Trk1 and Trk2 share a high degree of identity, especially in the transmembrane parts of the proteins. Thus, differences between so-far unidentified structural features of both K^+ importers may explain why the main yeast K^+ importer Trk1 requires Erv14 for its exit from the ER, while its paralogue, Trk2, is not an Erv14 cargo. In addition to Trk2, neither the main Na^+ and K^+ efflux system that is inducible at high-salt concentrations, ATPase Ena1, nor the vacuolar K^+-Cl^- cotransporter Vhc1, were identified as Erv14 binding partners (Fig. 3, [10]). Interestingly, the targeting of the essential H^+-ATPase Pma1 to the plasma membrane does not require Erv14 in vegetative yeast cells (Fig. 3, [10,30]). However, during sporulation, the proper trafficking of Pma1 from the ER to the prospore membrane is strongly dependent on the presence of Erv14 [30].

The number of genes encoding cornichon proteins in plants is variable (e.g., two *CNIH* genes in *O. sativa*, six in *Cucurbita moschata* or five in *Arabidopsis thaliana* [7,47,48]). Due to the presence of the C-terminal acidic motif that is involved in the binding of cargoes, plant cornichons seem to be structurally more related to fungal than to animal homologues [32]. Although much less is known about the functional importance of cornichons in plant cells, the role of these COPII cargo receptors in the proper trafficking of cation transporters seems to be conserved even in plants. Similarly to yeast Erv14, the rice (*O. sativa*) cornichon *Os*CNIH1 localizes to both the ER and Golgi apparatus. It was found to physically interact with *Os*HKT1;3, a Golgi-apparatus Na^+ transporter from the vascular tissue of roots and leaves [7,49]. Both proteins seem to bind to each other in the membranes of the ER. The ER/Golgi apparatus localization of CNIH1 is also preserved in pumpkin (*C. moschata*) [47]. The *CmCNIH1* gene is upregulated under salt-stress conditions. Moreover, the growth of seedlings of the pumpkin mutant *cmcnih1* is inhibited in the presence of salt stress, and the mutants also exhibit higher Na^+ and lower K^+ levels in shoots [47]. The key binding partner of *Cm*CNIH1 that seems to underlie the importance of the *Cm*CNIH1 cornichon in the ability of pumpkin to cope with the presence of salt stress is *Cm*HKT1;1, a Na^+-selective transporter, which can enhance plant salt tolerance [50]. In agreement with the role of *Cm*CNIH1 as a typical COPII cargo receptor, *Cm*CNIH1 contributes to the proper plasma-membrane localization of *Cm*HKT1;1, but its presence does not impact ion-transport activity/ properties of the transporter [47]. Plant HKT transporters belong to the same family as yeast Trk proteins, and share a similar structure with them [51]. Thus, the involvement of plant cornichons and *S. cerevisiae* Erv14 in the ER exit of the same type of cation transporters suggests that the mechanisms of specific cargo recognition are at least partially conserved in both yeast and plant cornichons. Interestingly, *A. thaliana* cornichons were identified as cargo receptors that bind glutamate receptor-like (GLR) channels [48] that are involved in Ca^{2+} homeostasis. The GLR channels are related to mammalian ionotropic glutamate receptors, and even in mammalian cells, a type of these transporters, AMPA receptors, are binding partners of cornichon proteins (see below). These data demonstrate structural and functional conservation of the whole cornichon family.

Mammalian cornichon proteins and their role as auxiliary subunits of ionotropic AMPA receptors

Vertebrate genomes contain four *CNIH* genes encoding cornichon proteins [52]. The lengths of human cornichons, CNIH1-4, vary from 139-160 amino-acid residues (Fig. 5A). The multiple sequence alignments show the highest percentage identity between CNIH2 and CNIH3 (almost 82 %). Moreover, these two proteins share an additional unique sequence in the second transmembrane domain that is absent in CNIH1 or CNIH4 (Fig. 5A). CNIH4 appears to be quite distant from the other human cornichons (it shares approximately 32 to 37 % identity with CNIH1, -2 or -3) and at the same time it is the most similar (≈ 44 % identity) to the yeast Erv14 of all human CNIH proteins. Phylogenetic analyses of

metazoan cornichons indicate that vertebrate CNIH1/2/3 and CNIH4 belong to different cornichon subfamilies; *CNIH1*, *-2* and *-3* genes probably appeared by duplication of an ancestor gene [52]. According to an analysis of evolutionary relationships among cornichons from various yeast, plant and animal species, vertebrate CNIH4 proteins belong to the same group of cornichons as *S. cerevisiae* Erv14 [47].

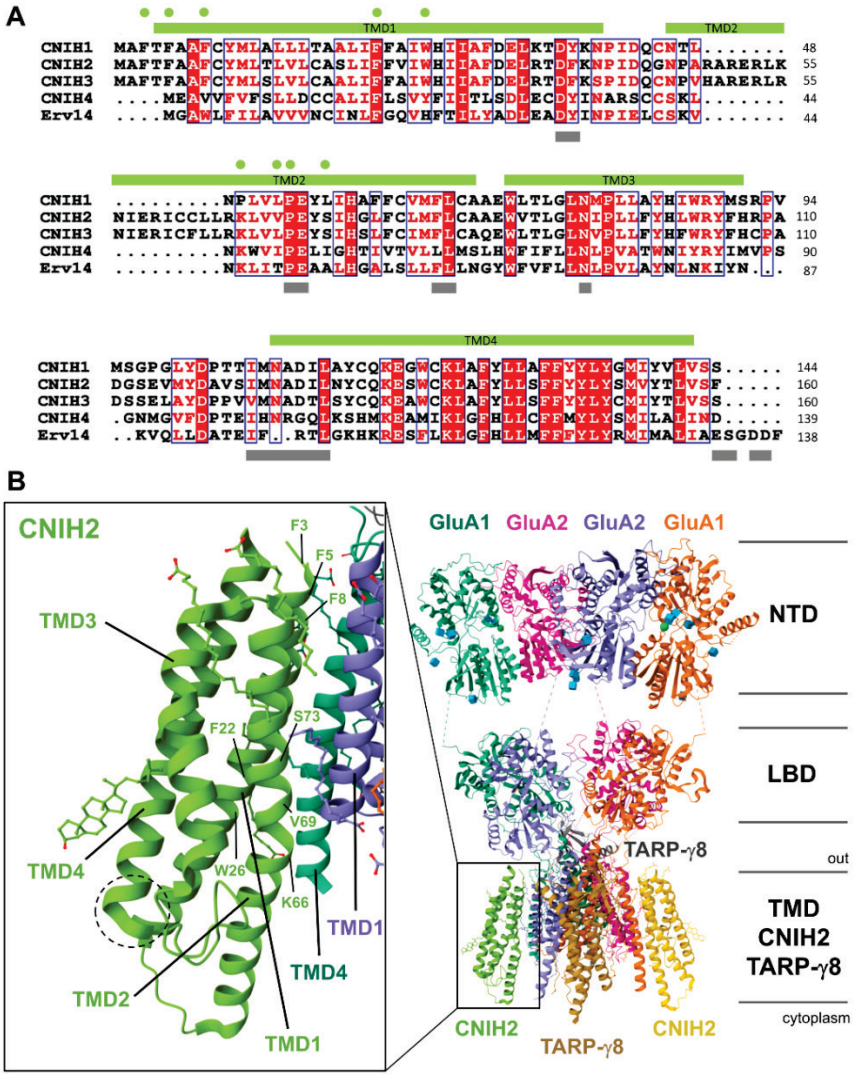

Fig. 5. Mammalian cornichon proteins. (**A**) Multiple sequence alignment of human cornichons and yeast Erv14 was created using ClustalO [70] and visualized with ESPript 3.0 tool [71]. Green lines highlight transmembrane domains of CNIH2, green dots depict amino-acid residues identified to be important for the functioning of CNIH2/3 as indicated in the text. Grey lines highlight functionally important motifs identified in Erv14 (see Fig. 2 and the text). (**B**) Structure of GluA1/A2 AMPA receptor in complex with pairs of CNIH2 and TARP-γ8 auxiliary subunits (PDB model 7OCA [28]). The proteins forming the AMPAR complex are visualized using different colors. NTD – N-terminal domains, LBD – ligand binding domains, TMD – transmembrane domains of GluA subunits. The second TARP-γ8 (in grey) is behind the complex. A detail of CNIH2 and the interaction interface with GluA subunits (left). Amino-acid residues that are in contact with GluAs are highlighted. The putative COPII-binding site (122-IMNADIL-128) is shown with a dashed-line oval.

The first experimental evidence of human cornichons was for the CNIH1 protein [53]. In HeLa cells, CNIH1 colocalized with both ER and Golgi apparatus markers, in agreement with its predicted function as a COPII cargo receptor. Analogous to the results obtained in *Drosophila*, CNIH1 was shown to be involved in the trafficking and also maturation of TGFα [53]. CNIH4 is known to be involved in the ER exit of G-protein coupled receptors [54]. However, the majority of current available information about mammalian cornichons concerns the proteins CNIH2 and CNIH3.

Proteomic and biochemical analyses of protein complexes from rat brains identified for the first time CNIH2 and CNIH3 as binding partners and new auxiliary subunits of pore-forming GluA subunits of AMPA (α-amino-3-hydroxy-5-methyl-4-isoxazole propionic acid)

glutamate-gated ionotropic receptors (AMPARs) [55]. AMPARs, which have characteristic fast kinetics, are concentrated at the postsynaptic membrane of excitatory synapses. In the central nervous system, AMPARs play a key role in excitatory synaptic transmission [56]. The core of AMPARs is formed of GluA1-4 subunits (Fig. 5B). They consist of a cytoplasmically-localized C-terminal domain, transmembrane domains (three membrane-spanning segments and a helix loop) that form the ion channel, a ligand-binding domain, and finally an N-terminal domain, which is the most distant from the membrane [57]. AMPARs are homo- or heterotetramers of GluA subunits. While the trans-membrane-domain part of the complex is tetrameric, both ligand-binding domains and N-terminal domains form dimers [57]. The particular GluA composition of an AMPA receptor then determines its basic properties, including cation (Na^+, K^+, Ca^{2+}) permeation [58]. AMPARs additionally form multi-protein complexes with up to four various auxiliary subunits: transmembrane AMPAR regulatory proteins (TARPs), cornichons, or GSG1l (Fig. 5B). They are all transmembrane proteins that bind to GluA tetramers at two distinct pairs of sites. The variable composition of the entire multi-protein complex adds more functional and also spatiotemporal diversity to AMPARs [57,58].

As is typical for cornichon-family proteins, CNIH2 and CNIH3 enhance the plasma-membrane localization and also promote the tetramerization, intracellular trafficking and maturation of AMPAR GluA subunits [55,59-64]. Thus, both cornichons seem to work as ordinary COPII cargo receptors and to promote the ER exit of AMPARs. However, and very differently from what was found so far for yeast or plant cornichons, when CNIH2 or CNIH3 become auxiliary subunits of an AMPA receptor, they do not recycle back to the ER, but together with the entire AMPAR protein complex, they are delivered to the plasma membrane and become plasma-membrane proteins [60-62,65,66].

Recently, the first experimental evidence of a cornichon structure came from cryo-electron microscopy analysis of rat GluA2 AMPAR subunits in complex with mouse CNIH3 at a stoichiometry of 4:4 [26]. In the protein complex which was obtained upon heterologous expression in human embryonic kidney (HEK) cells the interaction interface is formed by the first and fourth transmembrane domains of adjacent GluA2 subunits and the first and second transmembrane domains of CNIH3. Three phenylalanines (F3, F5 and F8) from the N-terminal part of CNIH3 make contacts with the transmembrane domains of GluA2 subunits [26]. These amino-acid residues are conserved in CNIH1, 2 and 3 proteins, but absent in CNIH4 (Fig. 5A). Their importance for the interaction between GluA and cornichons was also confirmed in structural analyses of either rat GluA1/A2 AMPARs in complex with CNIH2 and TARP-γ8 after their production in HEK cells, or in native hippocampal mouse AMPARs in complex with the same auxiliary subunits [27,28]. In both studies, CNIH2 and TARP-γ8 proteins were present in AMPAR complexes in two diagonally located pairs with CNIH2 being in contact with the first transmembrane domain of GluA2 and the fourth transmembrane domain of GluA1 (Fig. 5B). In addition to the phenylalanine residues from the N-terminal part of CNIH2, which are located near the extracellular boundary of the TMD pore of the receptor (Fig. 5B), other amino-acid residues from the opposite side of the membrane were shown to make contacts with GluA subunits, namely K66, V69 and S73 located in the second transmembrane domain of CNIH2 and F22 together with W26 from the first transmembrane domain of the cornichon (Fig. 5B, [27,28]). Moreover, the analyses of the interface of CNIH2/3-AMPAR interaction also suggest the involvement of lipids in the formation of interactions between AMPARs and cornichons [26-28].

Being auxiliary subunits of AMPAR protein complexes, cornichons not only promote the trafficking of the complex to the cell surface, but there is also substantial evidence of the ability of CNIH2 and CNIH3 to modulate the gating of the receptor. Depending on the protein composition of the entire receptor complex, CNIH2 and CNIH3 were shown to influence AMPAR functioning by e.g. slowing its deactivation and desensitization kinetics or blocking its TARP-γ8-mediated resensitization [25,55,63,65-68]. In early stages of ontogeny, there is an excess amount of AMPAR-free CNIH2/3 in rat brains. These cornichon molecules most probably function as typical COPII cargo receptors. However the amount of CNIH2/3 bound into AMPAR complexes increases with the progress of development. Thus the importance of cornichons as AMPAR auxiliary subunits seems to be higher later in the brain development [69]. Based on the topology of cornichons (Fig. 2C, 5B), their modulatory effects must be mediated by the intramembrane and cytoplasmic interactions between GluA and CNIH proteins. The activation of an AMPA receptor results in global structural changes to the whole protein complex, as shown by structural studies

of the GluA1/A2 receptor in complex with CNIH2 and TARP-γ8 [28]. The two pairs of auxiliary subunits undergo counter-rotations, and the structural change to CNIH2 was suggested to stabilize the active state of the channel [28].

The ability of CNIH2 and CNIH3 to modulate AMPAR functioning seems to be dependent on the amino-acid region that is specific for these cornichons and that forms the cytoplasmically localized beginning of the second α-helix in these proteins (Figs 2C, 5). Using high-resolution mass spectrometry, all four human cornichons were identified as being interacting partners of GluA2 in the human brain [62]. Moreover, rat CNIH1 co-immunoprecipitates with rat GluA2 when both proteins are expressed in HEK cells [62]. However, although CNIH1 can physically bind the AMPAR complex, it is not efficient at modulating its gating properties [62,65]. Interestingly, insertion of the CNIH2/3 specific region into the sequence of CNIH1 results in a more pronounced modulatory efficiency of this cornichon [28]. On the other hand, the deletion of the entire CNIH2/3 specific region or especially amino-acid residues from the second half of this region resulted in CNIH3 with a reduced ability to both bind and modulate the functioning of the AMPA receptor [62]. The conserved amino-acid residue P70 in the second α-helical structure of CNIH2 appears to be connected to the structural flexibility of the CNIH2/3 specific region, which tilts toward the pore of the channel upon AMPAR activation [28].

Evolutionary conservation of the cornichon family´s functioning

Cornichon COPII cargo receptors are highly conserved in fungi, plants and animals. Several pieces of evidence also suggest that even the way in which they recognize their cargoes and other interaction partners might be conserved among cornichons from various groups of organisms: (i) *S. cerevisiae* Erv14 promotes the ER exit of rice cation transporter *Os*HKT1;3 in yeast cells, (ii) *O. sativa Os*CNIH1 and *A. thaliana At*CNIH1, -3 and -4 promote the proper trafficking of Erv14´s cargoes in yeast cells without Erv14, and (iii) human cornichon CNIH1 is able to rescue the non-axial budding phenotype of yeast *erv14Δ* cells [7,8,48,53].

Erv14´s amino-acid residues 97-IFRTL-101 are supposed to be involved in the binding of COPII-coat components [21]. Although at the level of primary structure, this motif is not fully conserved in mammalian cornichons (Fig. 5A, 122-IMNADIL-128 in CNIH2), at the structural level, it seems to be located at the cytoplasmic beginning of the fourth α-helical structure in both yeast and mammalian cornichons (Figs 2, 5). Moreover, the localization of this motif being on the opposite side of CNIH2/3 to that of the binding interface with AMPAR GluA subunits (Fig. 5B) is in agreement with the accessibility of the motif for interaction with COPII coat. The DYPE (DY33-34, PE50-51) site of Erv14 was also suggested to play a role in the incorporation of Erv14 into COPII vesicles [20]. While the first two amino-acid residues of this motif (DF37-38 in CNIH2/3) are located in proximity to the above-discussed putative COPII binding site in mammalian cornichon CNIH2, at the cytoplasmic end of the first transmembrane domain (Figs 2, 5), residues corresponding to the second part of the putative motif (PE70-71 in CNIH2/3) seem to have a different function in CNIH2. The conserved proline (P70, Fig. 5A) should be responsible for the structural flexibility of the specific CNIH2/3 region that is important for the gating modulation of the AMPAR channel [28]. Amino-acid residues F82 and L83 of CNIH2 and CNIH3, which correspond to the phenylalanine and leucine from the Erv14´s FLN site (FL62-63) that are likely involved in the binding of cargo proteins by Erv14 [20], are located in the second transmembrane domain of mammalian cornichons (Figs 2, 5). Interestingly, this transmembrane domain indeed forms the interaction interface between cornichons and AMPA receptors (Fig. 5B, [25-28]). Although FL82-83 are not directly in contact with AMPAR GluA subunits, it might suggest that both yeast and mammalian cornichons involve similar regions in their interaction with cargoes.

Cornichons in medicine

The proper functioning of cornichon-family proteins is of high importance for human health. Abnormal vesicle-mediated transport plays a key role in cancer development [72]. Importantly, there is growing evidence of cornichons being prognostic markers and also putative therapeutic targets in various types of cancer. The gene encoding CNIH1, which plays a role in the trafficking and maturation of TGFα [53], was found to be highly expressed in lung-adenocarcinoma tissues, and knockdown of the *CNIH1* gene inhibited the growth and

migration of cancer cells in *in vitro* experiments [73]. CNIH4, so far known as a cargo receptor of G-protein coupled receptors [54], has been associated with an increased risk and changes in the immune microenvironment in several types of cancer (e.g. colon cancer, head and squamous carcinoma, hepatocellular carcinoma, glioma, cervical, ovarian and gastric cancer) [74-81]. *In vitro*, the downregulation of *CNIH4* inhibited cell proliferation and migration and increased drug sensitivity in cancer cell lines [74,76,79,81]. The growth of glioma cells was also slower in mice after *CNIH4* silencing [79]. In cervical cancer cells, the CNIH4-mediated reduction in ferroptosis is connected to the expression of the gene encoding the cystine/glutamate transporter SLC7A11. However, the functional relationship between both genes/proteins remains to be elucidated [77].

As for neurological disorders, *CNIH1*, *-2* and *-3* were found to be significantly upregulated in the dorsolateral prefrontal cortex of patients with schizophrenia [82]. A *de novo* deletion of a 1 Mbp region that also contained the gene encoding CNIH2 has been associated with intellectual disability [83], and moreover, *CNIH4* was identified as the target gene of an Alzheimer-disease risk-associated CpG site [84]. The polymorphisms of the *CNIH3* gene were also implicated to be involved in the pathophysiology of opioid dependence, with some SNPs having a robust protective effect [85]. Last, but not least, AMPAR auxiliary subunits, including CNIH2 and CNIH3, may serve as potential therapeutic targets for controlling AMPAR functioning in individual regions of the brain [57].

Conclusions

As COPII cargo receptors, cornichons play a role in the proper targeting of a variety of proteins, including several cation transport systems. Monovalent-cation transporters of eukaryotic cells have a fundamental importance for the fitness of both single cells and multicellular organisms. In addition, their malfunctioning in humans results in many pathologies. Thus, understanding their functioning and biogenesis is relevant to a range of human occupations, such as biotechnology, agriculture or medicine. *S. cerevisiae* cornichon Erv14 assists with the proper trafficking of several monovalent-cation translocating proteins, and its role in the maintenance of ion homeostasis in yeast cells seems to be complex. However, our current knowledge of the cargo repertoire of human cornichons is much more limited, despite the fact that changes in their expression/functioning are connected to severe diseases. The only cornichons' cargoes involved in cation homeostasis of mammalian cells known so far are ionotropic AMPA receptors, whose gating is also modulated by direct interaction with CNIH proteins. Thus, there seems to be an urgent need to uncover cornichons´ so-far unknown interacting partners and at the same time new putative treatment targets. Taking into account the easy genetic manipulation and low-cost and fast cultivation of yeast cells together with the possibility of heterologous expression of functional mammalian ion transporters and cornichons ([53,86-89], our unpublished results), *S. cerevisiae* appears to be a useful tool not only to deepen our knowledge of the basic properties of cornichon-family proteins, but also to study the physical interactions of human CNIH proteins with their putative binding partners and thus to broaden the list of cornichons´ known cargoes. Such an approach has been already successfully used to uncover the interactions between fungal or plant cornichons and their binding partners [7,47,48,90].

Conflict of Interest

There is no conflict of interest.

Acknowledgements

We wish to thank Dr. Hana Sychrová for critical reading of the manuscript. This work was supported by a grant from the Czech Science Foundation [grant number GAČR 21-08985S].

References

1. Arino J, Ramos J, Sychrova H. Alkali metal cation transport and homeostasis in yeasts. Microbiol Mol Biol Rev 2010;74:95-120. https://doi.org/10.1128/MMBR.00042-09
2. Arino J, Ramos J, Sychrova H. Monovalent cation transporters at the plasma membrane in yeasts. Yeast 2019;36:177-193. https://doi.org/10.1002/yea.3355
3. Cyert MS, Philpott CC. Regulation of cation balance in *Saccharomyces cerevisiae*. Genetics 2013;193:677-713. https://doi.org/10.1534/genetics.112.147207

4. Pedersen SF, Counillon L. The SLC9A-C mammalian Na^+/H^+ exchanger family: molecules, mechanisms, and physiology. Physiol Rev 2019;99:2015-2113. https://doi.org/10.1152/physrev.00028.2018
5. Aviram N, Ast T, Costa EA, Arakel EC, Chuartzman SG, Jan CH, Hassdenteufel S, ET AL. The SND proteins constitute an alternative targeting route to the endoplasmic reticulum. Nature 2016;540:134-138. https://doi.org/10.1038/nature20169
6. Papouskova K, Moravcova M, Masrati G, Ben-Tal N, Sychrova H, Zimmermannova O. C5 conserved region of hydrophilic C-terminal part of *Saccharomyces cerevisiae* Nha1 antiporter determines its requirement of Erv14 COPII cargo receptor for plasma-membrane targeting. Mol Microbiol 2021;115:41-57. https://doi.org/10.1111/mmi.14595
7. Rosas-Santiago P, Lagunas-Gomez D, Barkla BJ, Vera-Estrella R, Lalonde S, Jones A, Frommer WB, ET AL. Identification of rice cornichon as a possible cargo receptor for the Golgi-localized sodium transporter *Os*HKT1;3. J Exp Bot 2015;66:2733-2748. https://doi.org/10.1093/jxb/erv069
8. Rosas-Santiago P, Lagunas-Gomez D, Yanez-Dominguez C, Vera-Estrella R, Zimmermannova O, Sychrova H, Pantoja O. Plant and yeast cornichon possess a conserved acidic motif required for correct targeting of plasma membrane cargos. Biochim Biophys Acta 2017;1864:1809-1818. https://doi.org/10.1016/j.bbamcr.2017.07.004
9. Rosas-Santiago P, Zimmermannova O, Vera-Estrella R, Sychrova H, Pantoja O. Erv14 cargo receptor participates in yeast salt tolerance via its interaction with the plasma-membrane Nha1 cation/proton antiporter. Biochim Biophys Acta 2016;1858:67-74. https://doi.org/10.1016/j.bbamem.2015.09.024
10. Zimmermannova O, Felcmanova K, Rosas-Santiago P, Papouskova K, Pantoja O, Sychrova H. Erv14 cargo receptor participates in regulation of plasma-membrane potential, intracellular pH and potassium homeostasis via its interaction with K+-specific transporters Trk1 and Tok1. Biochim Biophys Acta 2019;1866:1376-1388. https://doi.org/10.1016/j.bbamcr.2019.05.005
11. Casey JR, Grinstein S, Orlowski J. Sensors and regulators of intracellular pH. Nat Rev Mol Cell Biol 2010;11:50-61. https://doi.org/10.1038/nrm2820
12. Milo R, Phillips R. *Cell Biology by the Numbers*. Garland Science, New York, 2015, 400 p. https://doi.org/10.1201/9780429258770
13. Volkov V. Salinity tolerance in plants. Quantitative approach to ion transport starting from halophytes and stepping to genetic and protein engineering for manipulating ion fluxes. Front Plant Sci 2015;6:873. https://doi.org/10.3389/fpls.2015.00873
14. Wong ED, Miyasato SR, Aleksander S, Karra K, Nash RS, Skrzypek MS, Weng S, ET AL. *Saccharomyces* genome database update: server architecture, pan-genome nomenclature, and external resources. Genetics 2023;224:iyac191. https://doi.org/10.1093/genetics/iyac191
15. Bokel C, Dass S, Wilsch-Brauninger M, Roth S. *Drosophila* Cornichon acts as cargo receptor for ER export of the TGFalpha-like growth factor Gurken. Development 2006;133:459-470. https://doi.org/10.1242/dev.02219
16. Roth S, Neuman-Silberberg FS, Barcelo G, Schupbach T. Cornichon and the EGF receptor signaling process are necessary for both anterior-posterior and dorsal-ventral pattern formation in *Drosophila*. Cell 1995;81:967-978. https://doi.org/10.1016/0092-8674(95)90016-0
17. Berg CA. The *Drosophila* shell game: patterning genes and morphological change. Trends Genet 2005;21:346-355. https://doi.org/10.1016/j.tig.2005.04.010
18. Neuman-Silberberg FS, Schupbach T. The *Drosophila* dorsoventral patterning gene gurken produces a dorsally localized RNA and encodes a TGF alpha-like protein. Cell 1993;75:165-174. https://doi.org/10.1016/S0092-8674(05)80093-5
19. Powers J, Barlowe C. Transport of Axl2p depends on Erv14p, an ER-vesicle protein related to the *Drosophila* cornichon gene product. J Cell Biol 1998;142:1209-1222. https://doi.org/10.1083/jcb.142.5.1209
20. Pagant S, Wu A, Edwards S, Diehl F, Miller EA. Sec24 is a coincidence detector that simultaneously binds two signals to drive ER export. Curr Biol 2015;25:403-412. https://doi.org/10.1016/j.cub.2014.11.070
21. Powers J, Barlowe C. Erv14p directs a transmembrane secretory protein into COPII-coated transport vesicles. Mol Biol Cell 2002;13:880-891. https://doi.org/10.1091/mbc.01-10-0499
22. von Heijne G, Gavel Y. Topogenic signals in integral membrane proteins. Eur J Biochem 1988;174:671-678. https://doi.org/10.1111/j.1432-1033.1988.tb14150.x

23. Jumper J, Evans R, Pritzel A, Green T, Figurnov M, Ronneberger O, Tunyasuvunakool K, ET AL. Highly accurate protein structure prediction with AlphaFold. Nature 2021;596:583-589. https://doi.org/10.1038/s41586-021-03819-2
24. Varadi M, Anyango S, Deshpande M, Nair S, Natassia C, Yordanova G, Yuan D, ET AL. AlphaFold Protein Structure Database: massively expanding the structural coverage of protein-sequence space with high-accuracy models. Nucleic Acids Res 2022;50:D439-D444. https://doi.org/10.1093/nar/gkab1061
25. Gangwar SP, Yen LY, Yelshanskaya MV, Korman A, Jones DR, Sobolevsky AI. Modulation of GluA2-gamma5 synaptic complex desensitization, polyamine block and antiepileptic perampanel inhibition by auxiliary subunit cornichon-2. Nat Struct Mol Biol 2023;30:1481-1494. https://doi.org/10.1038/s41594-023-01080-x
26. Nakagawa T. Structures of the AMPA receptor in complex with its auxiliary subunit cornichon. Science 2019;366:1259-1263. https://doi.org/10.1126/science.aay2783
27. Yu J, Rao P, Clark S, Mitra J, Ha T, Gouaux E. Hippocampal AMPA receptor assemblies and mechanism of allosteric inhibition. Nature 2021;594:448-453. https://doi.org/10.1038/s41586-021-03540-0
28. Zhang D, Watson JF, Matthews PM, Cais O, Greger IH. Gating and modulation of a hetero-octameric AMPA glutamate receptor. Nature 2021;594:454-458. https://doi.org/10.1038/s41586-021-03613-0
29. Herzig Y, Sharpe HJ, Elbaz Y, Munro S, Schuldiner M. A systematic approach to pair secretory cargo receptors with their cargo suggests a mechanism for cargo selection by Erv14. PLoS Biol 2012;10:e1001329. https://doi.org/10.1371/journal.pbio.1001329
30. Nakanishi H, Suda Y, Neiman AM. Erv14 family cargo receptors are necessary for ER exit during sporulation in *Saccharomyces cerevisiae*. J Cell Sci 2007;120:908-916. https://doi.org/10.1242/jcs.03405
31. Sharpe HJ, Stevens TJ, Munro S. A comprehensive comparison of transmembrane domains reveals organelle-specific properties. Cell 2010;142:158-169. https://doi.org/10.1016/j.cell.2010.05.037
32. Lagunas-Gomez D, Yanez-Dominguez C, Zavala-Padilla G, Barlowe C, Pantoja O. The C-terminus of the cargo receptor Erv14 affects COPII vesicle formation and cargo delivery. J Cell Sci 2023;136:jcs260527. https://doi.org/10.1242/jcs.260527
33. Banuelos MA, Sychrova H, Bleykasten-Grosshans C, Souciet JL, Potier S. The Nha1 antiporter of *Saccharomyces cerevisiae* mediates sodium and potassium efflux. Microbiology 1998;144:2749-2758. https://doi.org/10.1099/00221287-144-10-2749
34. Prior C, Potier S, Souciet JL, Sychrova H. Characterization of the *NHA1* gene encoding a Na^+/H^+-antiporter of the yeast Saccharomyces cerevisiae. FEBS Lett 1996;387:89-93. https://doi.org/10.1016/0014-5793(96)00470-X
35. Kamauchi S, Mitsui K, Ujike S, Haga M, Nakamura N, Inoue H, Sakajo S, ET AL. Structurally and functionally conserved domains in the diverse hydrophilic carboxy-terminal halves of various yeast and fungal Na^+/H^+ antiporters (Nha1p). J Biochem 2002;131:821-831. https://doi.org/10.1093/oxfordjournals.jbchem.a003171
36. Kinclova O, Ramos J, Potier S, Sychrova H. Functional study of the *Saccharomyces cerevisiae* Nha1p C-terminus. Mol Microbiol 2001;40:656-668. https://doi.org/10.1046/j.1365-2958.2001.02412.x
37. Smidova A, Stankova K, Petrvalska O, Lazar J, Sychrova H, Obsil T, Zimmermannova O, Obsilova V. The activity of *Saccharomyces cerevisiae* Na^+, K^+/H^+ antiporter Nha1 is negatively regulated by 14-3-3 protein binding at serine 481. Biochim Biophys Acta 2019;1866:118534. https://doi.org/10.1016/j.bbamcr.2019.118534
38. Zimmermannova O, Velazquez D, Papouskova K, Prusa V, Radova V, Falson P, Sychrova H. The hydrophilic C-terminus of yeast plasma-membrane Na^+/H^+ antiporters impacts their ability to transport K^+. J Mol Biol 2024;436:168443. https://doi.org/10.1016/j.jmb.2024.168443
39. Pribylova L, Papouskova K, Zavrel M, Souciet JL, Sychrova H. Exploration of yeast alkali metal cation/H^+ antiporters: sequence and structure comparison. Folia Microbiol 2006;51:413-424. https://doi.org/10.1007/BF02931585
40. Mitsui K, Kamauchi S, Nakamura N, Inoue H, Kanazawa H. A conserved domain in the tail region of the *Saccharomyces cerevisiae* Na^+/H^+ antiporter (Nha1p) plays important roles in localization and salinity-resistant cell-growth. J Biochem 2004;135:139-148. https://doi.org/10.1093/jb/mvh016
41. Bertl A, Ramos J, Ludwig J, Lichtenberg-Frate H, Reid J, Bihler H, Calero F, ET AL. Characterization of potassium transport in wild-type and isogenic yeast strains carrying all combinations of *trk1*, *trk2* and *tok1* null mutations. Mol Microbiol 2003;47:767-780. https://doi.org/10.1046/j.1365-2958.2003.03335.x

42. Gaber RF, Styles CA, Fink GR. *TRK1* encodes a plasma membrane protein required for high-affinity potassium transport in *Saccharomyces cerevisiae*. Mol Cell Biol 1988;8:2848-2859. https://doi.org/10.1128/MCB.8.7.2848
43. Bertl A, Slayman CL, Gradmann D. Gating and conductance in an outward-rectifying K^+ channel from the plasma membrane of Saccharomyces cerevisiae. J Membr Biol 1993;132:183-199. https://doi.org/10.1007/BF00235737
44. Ketchum KA, Joiner WJ, Sellers AJ, Kaczmarek LK, Goldstein SA. A new family of outwardly rectifying potassium channel proteins with two pore domains in tandem. Nature 1995;376:690-695. https://doi.org/10.1038/376690a0
45. Lewis A, McCrossan ZA, Manville RW, Popa MO, Cuello LG, Goldstein SAN. TOK channels use the two gates in classical K^+ channels to achieve outward rectification. FASEB J 2020;34:8902-8919. https://doi.org/10.1096/fj.202000545R
46. Fairman C, Zhou X, Kung C. Potassium uptake through the TOK1 K^+ channel in the budding yeast. J Membr Biol 1999;168:149-157. https://doi.org/10.1007/s002329900505
47. Wei L, Liu L, Chen Z, Huang Y, Yang L, Wang P, Xue S, Bie Z. CmCNIH1 improves salt tolerance by influencing the trafficking of CmHKT1;1 in pumpkin. Plant J 2023;114:1353-1368. https://doi.org/10.1111/tpj.16197
48. Wudick MM, Portes MT, Michard E, Rosas-Santiago P, Lizzio MA, Nunes CO, Campos C, ET AL. CORNICHON sorting and regulation of GLR channels underlie pollen tube Ca^{2+} homeostasis. Science 2018;360:533-536. https://doi.org/10.1126/science.aar6464
49. Jabnoune M, Espeout S, Mieulet D, Fizames C, Verdeil JL, Conejero G, Rodriguez-Navarro A, ET AL. Diversity in expression patterns and functional properties in the rice HKT transporter family. Plant Physiol 2009;150:1955-1971. https://doi.org/10.1104/pp.109.138008
50. Sun J, Cao H, Cheng J, He X, Sohail H, Niu M, Huang Y, Bie Z. Pumpkin CmHKT1;1 controls shoot Na^+ accumulation via limiting Na^+ transport from rootstock to scion in grafted cucumber. Int J Mol Sci 2018;19:2648. https://doi.org/10.3390/ijms19092648
51. Rodriguez-Navarro A. Potassium transport in fungi and plants. Biochim Biophys Acta 2000;1469:1-30. https://doi.org/10.1016/S0304-4157(99)00013-1
52. Ramos-Vicente D, Bayes A. AMPA receptor auxiliary subunits emerged during early vertebrate evolution by neo/subfunctionalization of unrelated proteins. Open Biol 2020;10:200234. https://doi.org/10.1098/rsob.200234
53. Castro CP, Piscopo D, Nakagawa T, Derynck R. Cornichon regulates transport and secretion of TGFalpha-related proteins in metazoan cells. J Cell Sci 2007;120:2454-2466. https://doi.org/10.1242/jcs.004200
54. Sauvageau E, Rochdi MD, Oueslati M, Hamdan FF, Percherancier Y, Simpson JC, Pepperkok R, Bouvier M. CNIH4 interacts with newly synthesized GPCR and controls their export from the endoplasmic reticulum. Traffic 2014;15:383-400. https://doi.org/10.1111/tra.12148
55. Schwenk J, Harmel N, Zolles G, Bildl W, Kulik A, Heimrich B, Chisaka O, ET AL. Functional proteomics identify cornichon proteins as auxiliary subunits of AMPA receptors. Science 2009;323:1313-1319. https://doi.org/10.1126/science.1167852
56. Royo M, Escolano BA, Madrigal MP, Jurado S. AMPA receptor function in hypothalamic synapses. Front Synaptic Neurosci 2022;14:833449. https://doi.org/10.3389/fnsyn.2022.833449
57. Kamalova A, Nakagawa T. AMPA receptor structure and auxiliary subunits. J Physiol 2021;599:453-469. https://doi.org/10.1113/JP278701
58. Schwenk J, Fakler B. Building of AMPA-type glutamate receptors in the endoplasmic reticulum and its implication for excitatory neurotransmission. J Physiol 2021;599:2639-2653. https://doi.org/10.1113/JP279025
59. Certain N, Gan Q, Bennett J, Hsieh H, Wollmuth LP. Differential regulation of tetramerization of the AMPA receptor glutamate-gated ion channel by auxiliary subunits. J Biol Chem 2023;299:105227. https://doi.org/10.1016/j.jbc.2023.105227
60. Harmel N, Cokic B, Zolles G, Berkefeld H, Mauric V, Fakler B, Stein V, Klocker N. AMPA receptors commandeer an ancient cargo exporter for use as an auxiliary subunit for signaling. PLoS One 2012;7:e30681. https://doi.org/10.1371/journal.pone.0030681
61. Herring BE, Shi Y, Suh YH, Zheng CY, Blankenship SM, Roche KW, Nicoll RA. Cornichon proteins determine the subunit composition of synaptic AMPA receptors. Neuron 2013;77:1083-1096. https://doi.org/10.1016/j.neuron.2013.01.017

62. Shanks NF, Cais O, Maruo T, Savas JN, Zaika EI, Azumaya CM, Yates III JR, ET AL. Molecular dissection of the interaction between the AMPA receptor and cornichon homolog-3. J Neurosci 2014;34:12104-12120. https://doi.org/10.1523/JNEUROSCI.0595-14.2014
63. Shi Y, Suh YH, Milstein AD, Isozaki K, Schmid SM, Roche KW, Nicoll RA. Functional comparison of the effects of TARPs and cornichons on AMPA receptor trafficking and gating. Proc Natl Acad Sci U S A 2010;107:16315-16319. https://doi.org/10.1073/pnas.1011706107
64. Schwenk J, Boudkkazi S, Kocylowski MK, Brechet A, Zolles G, Bus T, Costa K, ET AL. An ER assembly line of AMPA-receptors controls excitatory neurotransmission and its plasticity. Neuron 2019;104:680-692e689. https://doi.org/10.1016/j.neuron.2019.08.033
65. Coombs ID, Soto D, Zonouzi M, Renzi M, Shelley C, Farrant M, Cull-Candy SG. Cornichons modify channel properties of recombinant and glial AMPA receptors. J Neurosci 2012;32:9796-9804. https://doi.org/10.1523/JNEUROSCI.0345-12.2012
66. Kato AS, Gill MB, Ho MT, Yu H, Tu Y, Siuda ER, Wang H, ET AL. Hippocampal AMPA receptor gating controlled by both TARP and cornichon proteins. Neuron 2010;68:1082-1096. https://doi.org/10.1016/j.neuron.2010.11.026
67. Boudkkazi S, Brechet A, Schwenk J, Fakler B. Cornichon2 dictates the time course of excitatory transmission at individual hippocampal synapses. Neuron 2014;82:848-858. https://doi.org/10.1016/j.neuron.2014.03.031
68. Hawken NM, Zaika EI, Nakagawa T. Engineering defined membrane-embedded elements of AMPA receptor induces opposing gating modulation by cornichon 3 and stargazin. J Physiol 2017;595:6517-6539. https://doi.org/10.1113/JP274897
69. Mauric V, Molders A, Harmel N, Heimrich B, Sergeeva OA, Klocker N. Ontogeny repeats the phylogenetic recruitment of the cargo exporter cornichon into AMPA receptor signaling complexes. Mol Cell Neurosci 2013;56:10-17. https://doi.org/10.1016/j.mcn.2013.02.001
70. Madeira F, Pearce M, Tivey ARN, Basutkar P, Lee J, Edbali O, Madhusoodanan N, ET AL. Search and sequence analysis tools services from EMBL-EBI in 2022. Nucleic Acids Res 2022;50:W276-W279. https://doi.org/10.1093/nar/gkac240
71. Robert X, Gouet P. Deciphering key features in protein structures with the new ENDscript server. Nucleic Acids Res 2014;42:W320-W324. https://doi.org/10.1093/nar/gku316
72. Aber R, Chan W, Mugisha S, Jerome-Majewska LA. Transmembrane emp24 domain proteins in development and disease. Genet Res 2019;101:e14. https://doi.org/10.1017/S0016672319000090
73. Qian C, Jiang Z, Zhou T, Wu T, Zhang Y, Huang J, Ouyang J, ET AL. Vesicle-mediated transport-related genes are prognostic predictors and are associated with tumor immunity in lung adenocarcinoma. Front Immunol 2022;13:1034992. https://doi.org/10.3389/fimmu.2022.1034992
74. Wang J, Wang S, Wang J, Huang J, Lu H, Pan B, Pan H, ET AL. Comprehensive analysis of clinical prognosis and biological significance of CNIH4 in cervical cancer. Cancer Med 2023;12:22381-22394. https://doi.org/10.1002/cam4.6734
75. Wang Z, Pan L, Guo D, Luo X, Tang J, Yang W, Zhang Y, ET AL. A novel five-gene signature predicts overall survival of patients with hepatocellular carcinoma. Cancer Med 2021;10:3808-3821. https://doi.org/10.1002/cam4.3900
76. Xiao F, Sun G, Zhu H, Guo Y, Xu F, Hu G, Huang K, Guo H. CNIH4: a novel biomarker connected with poor prognosis and cell proliferation in patients with lower-grade glioma. Am J Cancer Res 2023;13:2135-2154. https://doi.org/10.18632/aging.204821
77. Yang JY, Ke D, Li Y, Shi J, Wan SM, Wang AJ, Zhao MN, Gao H. CNIH4 governs cervical cancer progression through reducing ferroptosis. Chem Biol Interact 2023;384:110712. https://doi.org/10.1016/j.cbi.2023.110712
78. Mishra S, Bernal C, Silvano M, Anand S, Ruiz IAA. The protein secretion modulator TMED9 drives CNIH4/TGFalpha/GLI signaling opposing TMED3-WNT-TCF to promote colon cancer metastases. Oncogene 2019;38:5817-5837. https://doi.org/10.1038/s41388-019-0845-z
79. Fang Z, Kong F, Zeng J, Zhang Z, Wang Y, Wang Y, Duan J, ET AL. Integrated analysis based on vesicle trafficking-related genes identifying CNIH4 as a novel therapeutic target for glioma. Cancer Med 2023;12:12943-12959. https://doi.org/10.1002/cam4.5947

80. Kasavi C. Gene co-expression network analysis revealed novel biomarkers for ovarian cancer. Front Genet 2022;13:971845. https://doi.org/10.3389/fgene.2022.971845
81. Zhang H, Lin Y, Zhuang M, Zhu L, Dai Y, Lin M. Screening and identification of CNIH4 gene associated with cell proliferation in gastric cancer based on a large-scale CRISPR-Cas9 screening database DepMap. Gene 2023;850:146961. https://doi.org/10.1016/j.gene.2022.146961
82. Drummond JB, Simmons M, Haroutunian V, Meador-Woodruff JH. Upregulation of cornichon transcripts in the dorsolateral prefrontal cortex in schizophrenia. Neuroreport 2012;23:1031-1034. https://doi.org/10.1097/WNR.0b013e32835ad229
83. Floor K, Baroy T, Misceo D, Kanavin OJ, Fannemel M, Frengen E. A 1 Mb de novo deletion within 11q13.1q13.2 in a boy with mild intellectual disability and minor dysmorphic features. Eur J Med Genet 2012;55:695-699. https://doi.org/10.1016/j.ejmg.2012.08.002
84. Sun Y, Zhu J, Yang Y, Zhang Z, Zhong H, Zeng G, Zhou D, ET AL. Identification of candidate DNA methylation biomarkers related to Alzheimer's disease risk by integrating genome and blood methylome data. Transl Psychiatry 2023;13:387. https://doi.org/10.1038/s41398-023-02695-w
85. Nelson EC, Agrawal A, Heath AC, Bogdan R, Sherva R, Zhang B, Al-Hasani R, ET AL. Evidence of CNIH3 involvement in opioid dependence. Mol Psychiatry 2016;21:608-614. https://doi.org/10.1038/mp.2015.102
86. Flegelova H, Sychrova H. Mammalian NHE2 Na^+/H^+ exchanger mediates efflux of potassium upon heterologous expression in yeast. FEBS Lett 2005;579:4733-4738. https://doi.org/10.1016/j.febslet.2005.07.046
87. Kolacna L, Zimmermannova O, Hasenbrink G, Schwarzer S, Ludwig J, Lichtenberg-Frate H, Sychrova H. New phenotypes of functional expression of the mKir2.1 channel in potassium efflux-deficient Saccharomyces cerevisiae strains. Yeast 2005;22:1315-1323. https://doi.org/10.1002/yea.1333
88. Schwarzer S, Kolacna L, Lichtenberg-Frate H, Sychrova H, Ludwig J. Functional expression of the voltage-gated neuronal mammalian potassium channel rat ether à go-go1 in yeast. FEMS Yeast Res 2008;8:405-413. https://doi.org/10.1111/j.1567-1364.2007.00351.x
89. Velazquez D, Prusa V, Masrati G, Yariv E, Sychrova H, Ben-Tal N, Zimmermannova O. Allosteric links between the hydrophilic N-terminus and transmembrane core of human Na^+/H^+ antiporter NHA2. Protein Sci 2022;31:e4460. https://doi.org/10.1002/pro.4460
90. Zheng J, Yao L, Zeng X, Wang B, Pan L. ERV14 receptor impacts mycelial growth via its interactions with cell wall synthase and transporters in *Aspergillus niger*. Front Microbiol 2023;14:1128462. https://doi.org/10.3389/fmicb.2023.1128462

REVIEW

Mitochondrial Physiology of Cellular Redox Regulations

Petr JEŽEK[1], Andrea DLASKOVÁ[1], Hana ENGSTOVÁ[1], Jitka ŠPAČKOVÁ[1], Jan TAUBER[1], Pavla PRŮCHOVÁ[1], Eduardo KLOPPEL[1], Oleksandra MOZHEITOVA[1], Martin JABŮREK[1]

[1]Laboratory of Mitochondrial Physiology, Institute of Physiology of the Czech Academy of Sciences, Prague, Czech Republic

Received October 31, 2023
Accepted February 24, 2024

Summary

Mitochondria (mt) represent the vital hub of the molecular physiology of the cell, being decision-makers in cell life/death and information signaling, including major redox regulations and redox signaling. Now we review recent advances in understanding mitochondrial redox homeostasis, including superoxide sources and H_2O_2 consumers, i.e., antioxidant mechanisms, as well as exemplar situations of physiological redox signaling, including the intramitochondrial one and mt-to-cytosol redox signals, which may be classified as acute and long-term signals. This review exemplifies the acute redox signals in hypoxic cell adaptation and upon insulin secretion in pancreatic β-cells. We also show how metabolic changes under these circumstances are linked to mitochondrial cristae narrowing at higher intensity of ATP synthesis. Also, we will discuss major redox buffers, namely the peroxiredoxin system, which may also promote redox signaling. We will point out that pathological thresholds exist, specific for each cell type, above which the superoxide sources exceed regular antioxidant capacity and the concomitant harmful processes of oxidative stress subsequently initiate etiology of numerous diseases. The redox signaling may be impaired when sunk in such excessive pro-oxidative state.

Key words

Mitochondrial superoxide formation • Redox regulations • Redox signaling • Pancreatic β-cells • β-oxidation • Peroxiredoxins

Corresponding author

P. Ježek, Laboratory of Mitochondrial Physiology, Institute of Physiology of the Czech Academy of Sciences, Vídeňská 1083, CZ 14220 Prague, Czech Republic. E-mail: jezek@biomed.cas.cz

Mitochondrial reactive oxygen species (ROS) sources

Primary sources of mitochondrial superoxide

According to the classification of M. Brand [1-4], flavin (F) and ubiquinone (Q) containing binding sites, typically within structures of respiratory chain (RC) complexes, belong to the most critical superoxide formation sites in mitochondria [5-7], besides particular *loci* of dehydrogenases [1,2] (Fig. 1). Recent progress in understanding mechanisms involved in proton-coupled electron transfer *via* the RC and in resolving supercomplexes formation and single crista architecture [7-9] then calls for reconsiderations of these mechanisms and more precise determination of superoxide formation sites within the given and already resolved protein structures.

A general requirement for *superoxide* ($O_2^{\bullet-}$; and its conjugated acid – hydroperoxyl radical, $HO_2^{\bullet}$, pKa 4.9) to be formed is a local retardation of the electron transfer or an enzyme reaction process so that intermediate radicals have enough lifetime to react with oxygen. These intermediates are typically semiquinone anion radical ($Q^{\bullet-}$; or semiquinol $QH^{\bullet}$) for Q sites and flavosemiquinone radical $FMNH^{\bullet}$ for F sites. Thus, the flavin site on Complex I (termed I_F) can produce superoxide at a higher $NADH/NAD^+$ ratio after the direct H^- transfer between NADH and FMN [10]. When an excessive electron cannot pass through the existing FeS chain within the Complex I matrix arm, the NAD^+ binding is interrupted, and the pairing of $FMNH^-$ and NADH form $FMNH^{\bullet}$. At lower NADH, indeed, NAD^+ can pair with $FMNH^{\bullet}$, and superoxide cannot be formed [11].

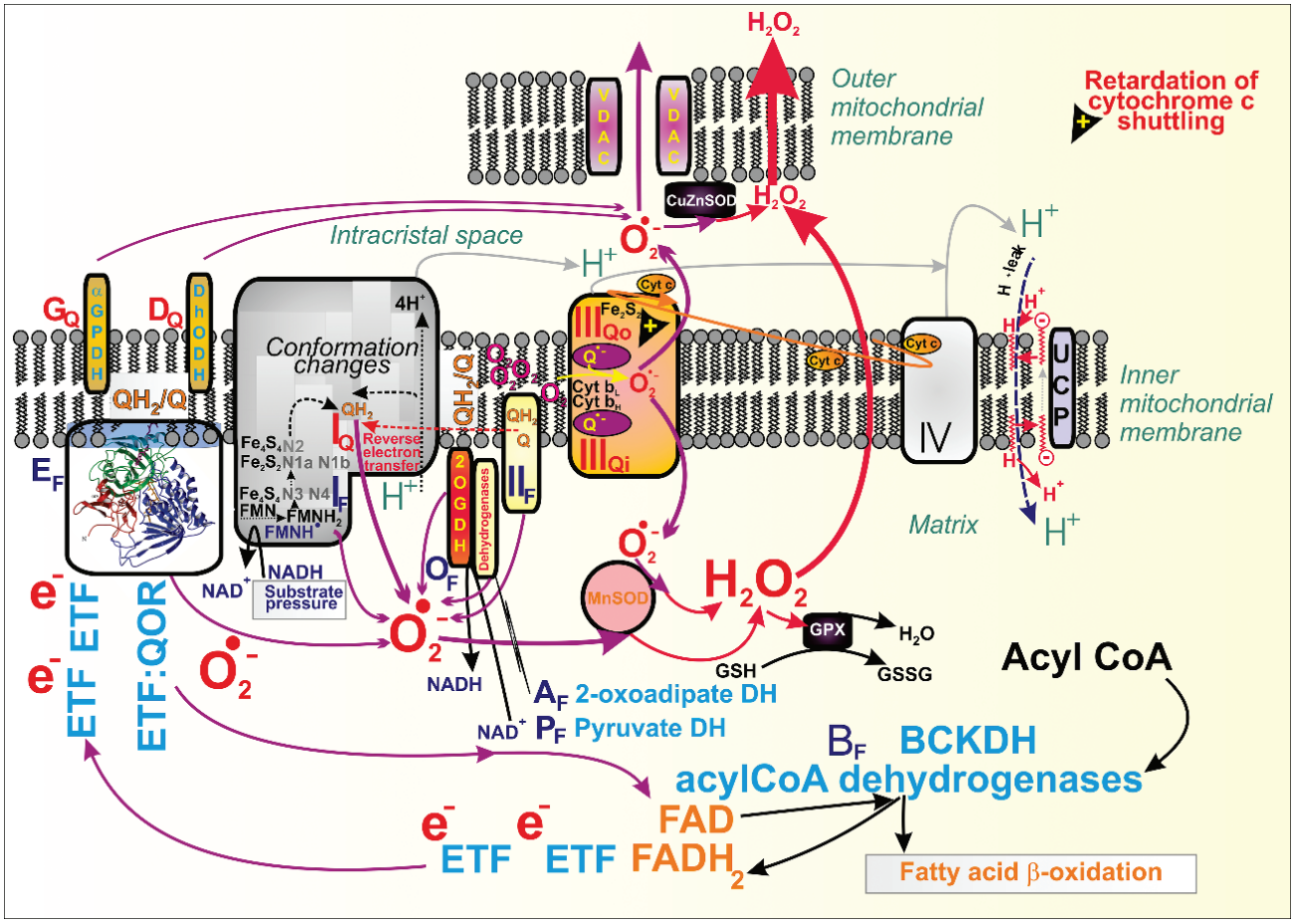

Fig. 1. Sites of superoxide formation in mitochondria. Schema depicts locations for the identified sites of superoxide formation, acting at the ~280 mV redox potential of the NADH/NAD$^+$ iso-potential pool (index F, flavin; dark blue capitalized fonts) and sites acting at the ~20 mV redox potential of the ubiquinol/ubiquinone (QH_2/Q) iso-potential pool (index Q; red capitalized fonts), according to the Brand's nomenclature introduced by Martin Brand [1]. Thus the major sites I_F, I_Q and III_{Qo} exists for Complex I and III, respectively; at certain circumstances also Complex II/succinate dehydrogenase forms superoxide at site II_F; and sites for probable superoxide formation by dehydrogenases (DH) are shown (G_Q for α-glycerolphosphate dehydrogenase, GPDH; D_Q for dihydroorotate DH; A_F for 2-oxoadipated DH; B_F for branched-chain ketaoacid DH, BCKDH; O_F for 2-oxoglutarate DH, 2OGDH; P_F for pyruvate DH. In case of acylCoA dehydrogenases acting in fatty acid β-oxidation, two electron transfer flavoproteins (ETF) are required to transfer electrons to the membrane-attached ETF:ubiquionone oxidoraductase (ETF:QOR, depicted by its structure) containing a site E_F (though a site E_Q also potentially exists). The scheme also depicts a situation when retardation fo cytochrome c shuttling induces superoxide formation on site III_{Qo}; as well as attenuation of superoxide formation by uncoupling proteins (UCP) based on the fatty acid-cycling mechanism [119]. Finally, formed superoxide is converted to H_2O_2 by MnSOD in the matrix or by CuZnSOD within the intermembrane space. H_2O_2 may readily penetrate to the cell cytosol (for special relations of such diffusion, see Reference [7].

Complex I, as an H$^+$-pumping NADH:quinone oxidoreductase, possesses a Q-tunnel structure, where an ongoing inhibition by a product (ubiquinol, QH_2) can form superoxide at the phenomenologically defined site I_Q [1] (Fig. 1). This typically occurs when the whole Complex I runs backward during so-called reversed electron transfer (RET). Disputes still exist whether under conditions of e.g. reperfusion after ischemic accu-mulation of succinate, superoxide is formed at I_Q or I_F site [12,13]. Due to the suppression of the electron leak to oxygen at site I_Q by a specific antioxidant S1QEL, the site I_Q is more plausible to act in RET-derived superoxide formation [1].

We have also revealed that the maximum superoxide was formed only when electron transport and H$^+$ pumping were retarded [14,15]. H$^+$ pumping may be attenuated by a high electrochemical gradient of protons established at the inner mitochondrial membrane (IMM), termed protonmotive force, Δp (when expressed in mV units) [16-18]. In pathologies this can be induced by mutations of the ND5 subunit (or other mitochondrion-encoded subunits) of the Complex I membrane arm.

Complex III, a ubiquinol-cytochrome c reductase, contributes to $O_2^{\bullet-}$ generation by autooxidation of the semiquinone anion radical ($Q^{\bullet-}$) within the so-called Q cycle [1,5,7,19,20], while it releases $O_2^{\bullet-}$ about equally to both sides of IMM [20,21]. Typically, when cytochrome c turnover is delayed for some reason, then a feedback inhibition of the Q-cycle within CIII is induced,

causing the superoxide formation at the Complex III site, termed III_{Qo} („o“ for outer, which is located in proximity to the intracristal space, [1]) (Fig. 1). This is because of the increased lifetime of $QH^{\bullet}$ and oxygen diffusion into this site [22]. *In vivo*, a physiological delay of the Q-cycle occurs at hypoxia or pathological one with specific mutations in Complex IV [23]. Retardation of the cytochrome c cycling automatically exists at the escape of cytochrome c from the cristae lumen during initiation of mitochondria-related apoptosis.

Also, Complex II (succinate dehydrogenase, SDH) may form superoxide under specific conditions but not at high succinate concentrations [24,25]. But superoxide is formed when the flavin site II_F within the SDHA subunit is less occupied, such as when succinate concentrations approach to K_m of 100-500 μM [26-28]. Pathologically, with the blocked SDHD subunit and hence interrupted electron transfer to Q, Complex II/SDH produces H_2O_2 (with a 70 % capacity) directly due to the ability of existing three FeS clusters to provide two-electron transfer to oxygen [29]. The 3Fe-4S cluster may also theoretically provide superoxide [30].

Evidence was also reported for superoxide formation within the dehydrogenase (DH) complexes in isolated mitochondria when excessive particular substrates for given DHs were used. Hence with excessive 2-oxoglutarate (2OG, 2-ketoglutarate) for OGDH, pyruvate for pyruvate dehydrogenase (PDH) and substrates of branched-chain 2-ketoacid (2-oxoacid) dehydrogenase (BCKDH) superoxide/H_2O_2 formation in skeletal muscle mitochondria was eightfold, fourfold, and twofold higher, respectively, than that one ascribed to the site I_F [31]. Phenomenological sites were termed as site O_F, P_F, and B_F, respectively, but mechanisms and occurrence *in vivo* must be further investigated.

Also, isolated mitochondria respiring with glycerol-3-phosphate partly produced superoxide at site G_Q of the glycerol-3-phosphate dehydrogenase [4,26, 32-34]. Analogously, dihydroorotate dehydrogenase was reported to form superoxide at side D_Q [1,4,33,35]. Moreover, ongoing fatty acid (FA) β-oxidation also produces superoxide. Its portion may originate from the site E_F of the electron-transferring flavoprotein – ubiquinone oxido reductase (ETFQOR) [27] (Fig. 1).

Superoxide dismutation into H_2O_2

Manganese superoxide dismutase (MnSOD or SOD2) is localized in the mitochondrial matrix, whereas CuZnSOD (SOD1) localizes to the mitochondrial intermembrane space, besides residing in the cell cytosol. MnSOD dismutates the majority of superoxide released to the matrix into H_2O_2. It is not known whether CuZnSOD is exclusively located between the outer mitochondrial membrane (OMM) and the inner boundary membrane (IBM, the unfolded part of IMM) in the so-called intermembrane space peripheral (IMSp), or whether in also resides in the intracristal space (ICS). In the latter case, it could more effectively convert superoxide therein [36], namely the part released from the site III_{Qo}.

MnSOD activity was found to be regulated. Rather fast posttranslational modifications (PTMs) were reported for NAD^+-dependent sirtuin-3- (SIRT3-) mediated deacetylation of MnSOD, activating the enzyme [37-40]. These results and derived conclusions need to be validated since not always a large population of MnSOD molecules in the matrix is acetylated/deacetylated. Only a fraction is affected, therefore, one should expect that this particular MnSOD molecule fraction is activated and, for example, only the resulting fraction of H_2O_2 may thus participate in intramitochondrial redox signaling or a weak redox signal directed to the cytosol. MnSOD regulations rather proceeded within an hour-time frame and could be regarded as chronic regulations [41-45]. Thus a subtle change in H_2O_2 release, accumulated during sufficient time, can be effective.

Ultrastructure of mitochondrion vs. H_2O_2 diffusion to the cell cytosol

We have published several reviews on how mitochondrial morphology and ultrastructure affect the diffusion of H_2O_2 into the cell cytosol and/or other organelles and up to the plasma membrane or even diffusion into the extracellular space [5-9,46-48]. Hence, let’s briefly summarize 3D architecture of mitochondria (Fig. 2). Actually the plural is adequate for isolated fragments of the original mitochondrial network, the mitochondrion [6-8,49-51]. Note that such a network also exists in skeletal muscle and the heart [52,53]. Small fragments are constantly separated from the main mitochondrial network by fission machinery (Fig. 2E), while at the same time, fragments join the main network by fusion (Fig. 2D), which is aided by the pro-fusion proteins [54,55]. This process is important, since mitochondrial-specific autophagy, termed mito-phagy, eliminates those fragments that do not possess a sufficient IMM membrane potential (or Δp) as a result

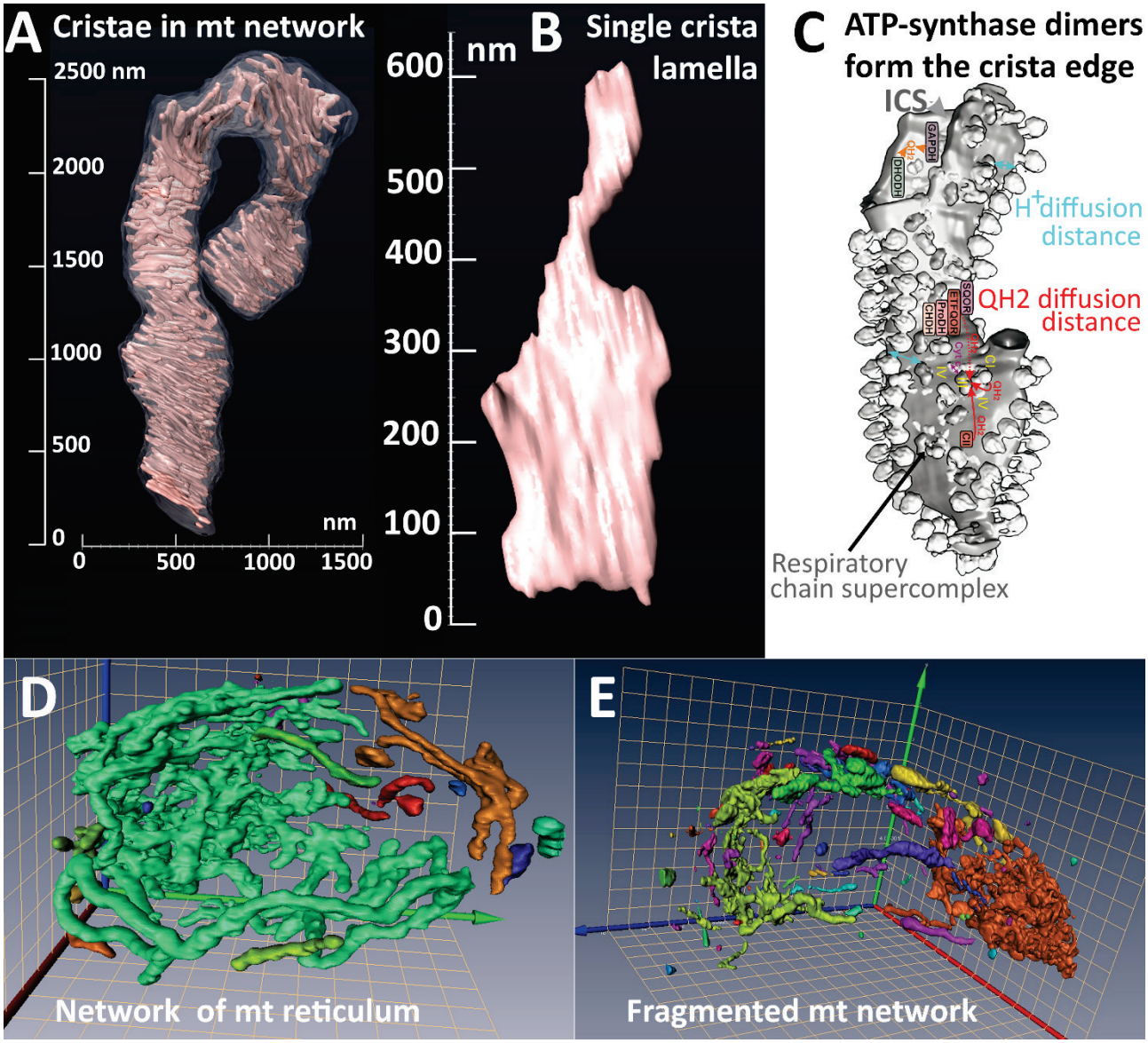

Fig. 2. Cristae in mitochondrial network of pancreatic islet β-cells. (**A**) An exemplar 3D image of crista lamellae within a 4-μm segment of the mitochondrial tubule, obtained by the focused ion beam/scanning electron microscopy (FIB/SEM); (**B**) detail of the single crista lamella from A). (**C**) Comparison with the 3D image of a single crista with resolved ATP-synthase dimers at the lamella edge, adapted from Ref. [67]. Also, structures of respiratory chain supercomplexes are visible on a lamella flank, which represents the crista membrane lipid bilayer leaflet oriented toward the matrix. The distances are marked for a minimum path of proton diffusion (mild blue arrows), providing a substantial coupling between the respiratory chain proton pumping and the ATP-synthase. The purple arrow indicates a shuttling of cytochrome c at the supercomplex surface. The distances are also marked for a short ubiquinol QH_2 (or ubiquionone Q) diffusion between Complex I (CI) and Complex III (CIII) around supercomplexes (red arrow) and a much longer diffusion path from Complex II (red arrow) to CIII or from oxidoreductases and dehydrogenases to CIII (dashed red arrows). Inside the broken portion of crista lamella at the inner (intracristal space) surface, a QH_2-diffusion path is indicated by orange arrows. This path must be followed by the flip across the membrane to CIII. (**D, E**) Mitochondrial reticular network in pancreatic islet β-cells of Wistar (**D**) and diabetic Goto-Kakizaki rats (**E**) in 3D images adopted from Ref. [49]. Note the nearly continuous mitochondrial network in intact β-cells (**D**), but the fragmented network in diabetic β-cells (**E**).

of local predominance of the mutated mt-DNA-encoded RC and ATP synthase subunits.

The mitochondrial tubular network possesses a complex ultrastructural organization of mt cristae, i.e., rich invaginations of IMM from the IBM, which shrink or inflate according to the metabolic performance or other reasons [7] and might exhibit dynamics in a short time scale [56]. To understand mitochondrial compartments, one must recognize their three-dimensional (3D) architecture. The cristae form rather lamellae with bottleneck connections to the IBM, where ICS meets IMSp (Fig. 2A, B). The mitochondrial cristae organization system (MICOS) complex is attached to the OMM SAM complex and thus forms crista junctions

(CJs) [57-59] around the crista outlets [7,60]. Note that at the edges of single crista lamella, the ATP-synthase dimers form rows or arrays [61-67] (Fig. 2C), the dynamic of which may also affect the cristae morphology [68-70]. Small MICOS subunits may intercalate between ATP-synthase dimers, such as Mic10, bound to the ATP-synthase membrane subunit e [71]; or Mic27 [72].

RC supercomplexes (typically CI $CIII_2$ CIV_1 [73-75] then reside at flanks of crista lamellae [61,67] (Fig. 2C). Just below CJs (crista outlets) other cristae-shaping proteins reside within cristae membranes (CM) facing ICS (crista lumen), such as various oligomers of OPA1 [76,77] or even filaments of OPA1 ortholog MGM1 [78]; and scaffolding proteins prohibitins, forming hetero-oligomeric 20-27 nm rings [79]. Positive curvature of 90° bends of the crista outlets, when IBM meets CM, is provided by oligomers of MICOS subunit MIC10 [80,81], while the negative curvature of crista lamellae is established by FAM92A1 protein, which binds cardiolipin and phosphatidylinositol 4,5-bisphosphate [82].

The rich lamellar cristae organization affects H_2O_2 diffusion into the cytosol [6]. If even H_2O_2 released into ICS (crista lumen) diffuses across the crista membrane, it will still reach the mt matrix in ~99 % of CM surface. Only at the proximity of CJs the ICS-located H_2O_2 might escape into the IMSp, across CM or IBM or through the crista outlet; and subsequently to the cytosol *via* the OMM. So, taking into account the mitochondrion ultrastructure, we see the limitations of H_2O_2 diffusion from ICS to the cytosol. On the contrary, such H_2O_2 diffusion is allowed upon initiation of mt-related apoptosis, when CJs (or crista outlets) are widened or broken, and this is accelerated by the cytochrome c escape [76,77,83] and concomitant increased superoxide formation.

Nevertheless, cristae lamellae inflate physiologically under hypoxic conditions due to partial losses of MIC60/mitofilin subunit of MICOS complex [60] or in pancreatic β-cells at low glucose (insulin non-stimulating) [46]. On the contrary, with a sudden excess of respiration substrate, the inflated cristae shrink. Such a narrowing of cristae was observed after dimethyl-2-oxoglutarate addition to hypoxia-preadapted HEPG2 cells [63] or upon glucose-stimulated insulin secretion (GSIS) in pancreatic β-cells, i.e., when high glucose was set [46].

Mitochondrial redox buffers and/or anti-oxidant systems

Mitochondrial glutathione reductase & glutathione peroxidase system

Redox buffers and antioxidant enzymes detoxify the produced ROS and may exert specific roles in redox signaling. Similarly to the cell cytosol, in addition to small antioxidant molecules such as vitamin E (α-tocopherol), ascorbate, and uric acid, enzyme systems of glutathione peroxidase (GPX) and peroxiredoxin represent the most critical intracellular antioxidants and a primary defense system. Catalase is absent in mitochondria except in the heart [5,9].

Glutathione is present in a reduced (GSH) or oxidized (GSSG, glutathione disulfide) form. Glutathione reductase (GRX; EC 1.8.1.7) catalyzes the NADPH-dependent reduction of GSSG to GSH [84], and hence oxidized glutathione is regenerated. Glutathione provides/GRX a major mt matrix redox buffer in numerous cells [85]. On the contrary, pancreatic β-cells exhibit a less abundant glutathione/GRX system [6,18,86-88].

GSH is also a cofactor of enzymes of the glutathione peroxidase (GPX) family. These enzymes reduce H_2O_2 to water, and some isoforms (e.g. GPX4) also reduce lipid hydroperoxides to their corresponding alcohols. The GPX family contains five enzymes with seleno-cysteine active sites (GPX1 to 4, and GPX6) and three other enzymes, acting as redox sensors (GPX5, GPX7, GPX8) [89,90]. The latter possess cysteine residues in their active sites and modest peroxidase activity [91]. The cytosolic and mt-residing GPX1 and plasma membrane and cytosolic GPX4 are abundant in all tissues and cell types. GPX1, GPX2, and GPX3 are homo-tetrameric proteins. GPX4 has a monomeric structure.

Mitochondrial vs. cytosolic peroxiredoxin system

Peroxiredoxins (PRDX) are hydroperoxide reductases, either of the 2-Cys type (cytosolic peroxiredoxins PRDX1 and PRDX2 (Fig. 3); PRDX3 residing in the mt matrix; and PRDX4 of the endoplasmic reticulum) or 1-Cys type (PRDX6) [92-98]. The second mitochondrial PRDX, PRDX5, also contains two cysteines in the monomer [99] but allows an atypical mechanism, while forming the intra-subunit S-S bridge within the single monomeric subunit [92-96,98]. However, PRDX5 is located also in the cytosol

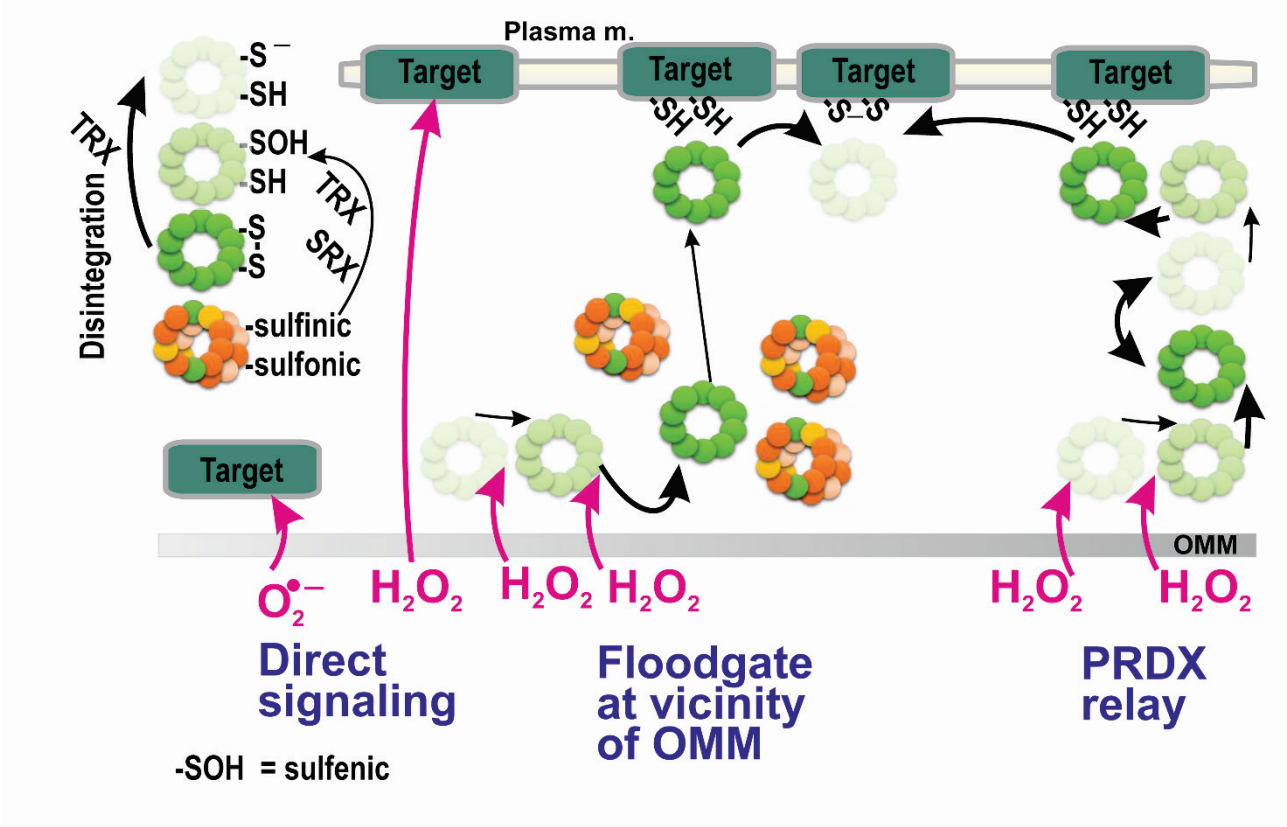

Fig. 3. Possible modes of peroxiredoxin participation in redox signaling. Possible ways of redox signal spreading from vicinity of the outer mitochondrial membrane (OMM) to the plasma membrane – from left to right: *i*) direct superoxide diffusion (range only in OMM proximity); *ii*) direct H_2O_2 diffusion; *iii*) peroxiredoxin-mediated redox signal transfer, including diffusion of peroxiredoxin decamers allowed by the flood-gate model mechanism; *iv*) hypothetical redox relay *via* an array of peroxiredoxins. Note, that according to the flood-gate model, H_2O_2 oxidizes PRDX to higher states than a sulfenic state, allowing distant decamers in a S-S state to migrate to the target and exchange the two target sulfhydryls for PRDX S-S bridge. In (*iv*) the target is the PRDX itself. **Left inset**: color coding of PRDX monomers: *green* – PRDX S-S bridge; *the very light green* – basic reduced state (sulfhydryl and thiolate anionic form); *the light green* – the first-degree of oxidation, i.e., sulfenic state; *yellow* – oxidation into the second degree, i.e., sulfinic state; *orange* – oxidation into the third degree, irreversible, sulfonic state. Note, thioredoxin (TRX) converts either disassembled S-S state dodecamers to the basic sate; and, together with sulfiredoxin (SRX), TRX regenerates PRDX in sulfinic state into the sulfenyl state.

and peroxisomes and prefers lipid peroxides and peroxynitrite over H_2O_2. Artificial PRDX5 expression in IMSp attenuated hypoxic transcriptome reprogramming [100] and cancerogenesis [101].

PRDX6 is a 1-cys-PRDX, which can also be recruited to mitochondria (probably to OMM) [102-104]. PRDX6 forms only homodimers, cannot form disulfide bonds, and is not reduced by sulfinyl reductase (SRX). PRDX6 reduces oxidized phospholipids. The sulfenic moiety of PRDX6 is subsequently reduced with GSH/GRX system but not with thioredoxins. PRDX6 also exerts Ca^{2+}-independent phospholipase A2 activity.

Cytosolic peroxiredoxins are decameric, containing five homodimers. Mitochondrial PRDX3 is dodecameric, consisting of six homodimers. Thus, PRDX1, PRDX2, and PRDX3 form a toroid (doughnut-like) structure of five (six) homodimers, which can split from the toroid in an unstable disulfide conformation (see below). Such mechanism allows disulfide regeneration.

Peroxiredoxin catalytic cycle

PRDX monomers of the 2-Cys type contain the peroxidatic cysteine, C_P and the resolving cysteine, C_R. After reaction with H_2O_2, the peroxidatic cysteine C_P of the first monomer within a homodimer forms an inter-subunit disulfide bond with the resolving cysteine C_R of the second homodimer subunit [92-98]. As an intermediate, sulfenic acid (R-SOH) is first formed by two-electron reversible oxidation of the C_P. Subsequently, the disulfide (S-S bridge) between C_P and C_R is formed. Interestingly, the PRDX ring is destabilized when such disulfide bonds are formed [92,94], thus allowing homodimers (monomers) to interact with their regenerating enzyme systems, completing the cycle. Such regeneration is catalyzed either by a couple of

thioredoxin (TRX) plus NADPH-dependent TRX reductase (TRXR) [105] or by glutathione (GSH)/glutaredoxin (GRX) [92-98]. The disulfide bonds of homodimers are thus converted back to two cysteines.

PRDXs react with H_2O_2 faster than other peroxidases (catalases and GPX); hence they outcompete them and serve as the primary regulators of cytosolic H_2O_2 and in specific tissues also of the mt matrix H_2O_2. The latter is valid for pancreatic β-cells. Therefore PRDXs have been considered major players in cancerogenesis [93,97] and are promising targets for therapies of cardiovascular [106] or neurodegenerative diseases [107] and for defense against oxidative stress in pancreatic β-cells [108].

Peroxiredoxins enable redox signaling

There are two other unique PRDX properties, making them essential players in the redox homeostasis regulations and even redox signaling. The first such property is the formation of stacks of decamers/dodecamers, thus establishing high molecular weight complexes (HMW), which can even form filaments with chaperone function [109]. Since this formation happens only with PRDXs oxidized into higher oxidation state (sulfinyl and sulfonyl), the HMW formation effectively withdraws PRDX molecules from their entire population. This instantly leads to a higher local H_2O_2 concentration in the HMW *loci*.

The second property lies in the specific interaction of PRDXs with other proteins containing the two proximal cysteines, which enables their direct redox regulation (targeting the redox signal). The PRDX disulfides (S-S bridges) oxidize those proximal cysteines of the target protein into the S-S bridge between them, while PRDX homodimer become reduced back into two cysteines, C_P and C_R.

Indeed, when sulfenyls of PRDX1,2 and PRDX3 are oxidized into higher oxidized states, i.e., sulfinyls or sulfonyls, HMW complexes are formed [109]. The sulfinyls within HMW complexes or filaments can still be reduced by ATP-dependent sulfinyl reductase (SRX) enzymes [109,110]. However, hyperoxidation into sulfonyls is irreversible and can be regarded as a sign of oxidative stress. Mitochondrial PRDX3 underlies hyperoxidation about twice as slower when compared to PRDX2 [109].

In summary, the redox signal can be initiated by peroxiredoxins, by two mechanisms, which can even be considered as the two different interpretations of the same phenomenon. So we can point out that the formation of HMW complexes withdraws PRDX molecule from the catalytic cycle reaction, otherwise consuming H_2O_2. Despite that, the prerequisite for such a withdrawal is oxidation into sulfinyls or sulfonyls. Due to their formation, still consuming H_2O_2, the local PRDX molecules can no longer react with the local H_2O_2 after a certain time period. Hence, if such a locus still contains the H_2O_2 source, the local H_2O_2 concentration is elevated.

An alternative interpretation considers the so-called floodgate model (Fig. 3). This model has been predicted to describe the shift of the oxidation from the original to distant locations [6,9,111,112]. According to the floodgate model, the HMWs formed in the original locations upon a sustained H_2O_2 flux allow oxidation in the distant *loci*, proximal to target proteins, enabling execution of the redox signal. This can happen simply by the direct interaction of H_2O_2 with target proteins or *via* oxidation of distant PRDX molecules, which subsequently oxidize proximal cysteines in the target protein. The latter mechanism can be regarded literally as a "redox kiss". Cytosolic peroxiredoxins convey their oxidation by H_2O_2 to the terminal target proteins (Fig. 3), typically phosphatases or transcription factors [92,94,113, 114-118]. It still remains to be investigated whether mitochondrial PRDX3 exhibits its own specific mitochondrial targets.

Mitochondrial redox signaling enabled by peroxiredoxins

However, sulfinyls in PRDX decamers/ dodecamers or HMW complexes can still be slowly reduced back to cysteines after their reduction by the SRX system. Mitochondrial SRXs were reported to act even in the transfer of circadian rhythms to the mt matrix. This is enabled by periodically enhanced SRX expression intermittent with enhanced SRX degradation by LON-protease under control of the clock genes in the adrenal gland, brown adipose tissue and heart [109,119,120]. It should be further investigated whether such elegant circadian regulation of the mitochondrial matrix redox homeostasis exists in pancreatic β-cells.

Mild uncoupling attenuates mitochondrial ROS generation at intact mtDNA

Oxidative phosphorylation (OXPHOS) represents an ATP synthesis by the mt ATP-synthase (Complex V), which is driven by the protonmotive force, Δp. Δp is formed by the respiratory chain H^+ pumping at Complex I, III, and IV [7,16-18,119]. The IMM domain

(membrane domain) of the ATP-synthase ($F_OATPase$) consumes an adequate Δp portion in a state, historically termed state-3, for isolated mitochondria with an ADP excess. *In vivo,* cellular respiration is governed by the metabolic state and/or availability of substrates. Hence, a finely tuned spectrum of various states-3 can be established, depending on the substrate load (e.g., increasing glucose). A state-4, is then given by zero ATP synthesis, when zero H^+ backflux *via* the $F_OATPase$ exists, while respiration and H^+ pumping are given by so-called H^+ leak, mediated by mitochondrial carrier proteins, as their side-function and by the native H^+ permeability of IMM. Since Δp exists predominantly in the form of Ψ_m (IMM electrical potential), Ψ_m is maximum at state-4 with the maximum substrate load.

Besides other proteins, such as the ADP/ATP carrier, Δp dissipation by a protonophoric short-circuit, termed uncoupling, can be physiologically provided by mitochondrial uncoupling proteins (UCPs) [119], frequently in synergy with mitochondrial phospholipases cleaving nascent fatty acids [120-123]. A mild uncoupling exists when carrier-mediated protonophore activity plus the native IMM H^+ leak do not overwhelm the $F_OATPase$ protonophoric activity, and hence, ATP synthesis still takes place. This contrasts to a complete uncoupling when Δp approaches zero, such as established by agents termed uncouplers. The mild uncoupling is able to decrease mitochondrial $O_2^{\bullet-}$ formation at Complex I [62,63] and Complex III [124]. In cell types where such mitochondrial ROS source predominates, even redox homeostasis in the cytosol may be more pro-oxidant. However, oxidative stress originating from irreversible changes, such as stress due to mutated subunits encoded by mitochondrial DNA (mtDNA), cannot be counteracted by mild uncoupling [62].

Previously, an antioxidant role for UCP2 has been demonstrated *in vivo* [123,125,126]. For example, Duval *et al*. [127] have shown that UCP2-mediated uncoupling in endothelial cells is able to decrease extracellular ROS in co-incubated low-density-lipoproteins (LDL). Mice with deleted LDL receptors exhibited extensive diet-induced atherosclerotic plaques when they received bone marrow transplanted from UCP2 (-/-) mice, and the appearance of these plaques was prevented when they received bone marrow transplants from UCP2 (+/+) mice [128]. We have also demonstrated that UCP2 function suppresses mitochondrial superoxide production *in vitro* [121,123, 129,130].

Physiological redox signaling vs. oxidative stress

Oxidative stress

In principle, there exists no net oxidative stress without the other consequences, such as proteinaceous stress due to the disrupted turnover of intact proteins, concomitantly impaired autophagy and/or mitochondria-specific authophagy, i.e., mitophagy, or without the endoplasmic reticulum stress. Oxidative stress cannot be separated from the possible initiation of apoptosis, ferroptosis, or other forms of the cell death, as well as from impaired mitochondrial biogenesis. Moreover, all these phenomena are projected to an abnormal mt network morphology, frequently also to an abnormal cristae morphology (e.g., apoptosis). Redox-sensitive transcriptomic reprogramming sets altered metabolism and changes in epigenetics, which may further accelerate pathogenesis. In addition, the internal causes should be distinguished from the external ones, such as macrophage attacks and other immune system stimuli. That is why oxidative-stress-related pathologies must always be analyzed in a complex way, and frequently it is difficult to establish the primary cause. The reason is that under oxidative stress, cellular constituents are oxidized, i.e., covalently modified, deteriorating function and/or quality with serious consequences. To avoid the encyclopedic description, next, we will only briefly describe the oxidative stress of mitochondrial origin and how we can distinguish it from the redox signaling.

Moreover, recently, mitochondria are regarded as signaling organelles when signals of different origins are produced, not only the redox signals [55,130,131]. The evoked signals affects not only cells and tissues but also the systemic levels of the organism. The latter exists with the metabokine/mitokine signaling [133-135], mt-nuclear crosstalk [136-139], and mt-initiated epigenome remodeling [140-143].

Oxidative stress of mitochondrial origin

Theoretically, when an overly excessive superoxide/H_2O_2 formation exceeds the mitochondrial redox buffering, i.e., antioxidant capacity in the mt matrix, local oxidative stress in the matrix takes place. When concomitant H_2O_2 diffusion into the cytosol and/or other cell constituents exceeds the cellular antioxidant buffers and defense mechanisms, cellular oxidative stress is developed. We should admit that the frequent causes of such disequilibria are consequences of certain

mutations in mtDNA and changes resulting from the impaired mt network morphology and/or cristae architecture. The extracellular origins or cytosolic oxidative stress acting on mitochondrial constituents also belong to frequently occurring pathologies.

The typical example of oxidative stress of mt origin is RET due to a previous accumulation of succinate, such as during heart reperfusion after ischemia [12]. Artificially induced mt oxidative stress resulted in chromatin release into the cytosol when mediated by MAPK/JNK signaling [144]. Similar manipulations induced telomere damage [145] or altered nuclear DNA methylation [146]. Senescent signaling due to increased mt ROS production activating NFκB pathway belongs to other examples [147-149].

Typically, proteinaceous stress and impairments of mitophagy and/or induction of all distinct types of cell death are developed when these thresholds are overcome. These mechanisms are out the scope of this review. We exemplified these phenomena in cases of normal physiology of pancreatic β-cells and the effects of lipotoxicity, glucotoxicity and glucolipotoxicity in the etiology of type 2 diabetes [150].

Mitochondrial redox signaling

Mitochondrial redox signaling of any time range was previously reviewed in References [151,152]. Here, we deal specifically with the acute redox signals. The triggering of redox-sensitive gene-regulatory processes (e.g. [153,154]) is beyond the scope of this review. We will discuss in detail redox signals in pancreatic β-cells in the next chapter. Now, we will list a few examples of rather acute redox signals of mitochondrial origin.

The uncoupling protein UCP1 was reported to be activated in order to switch on heat production and, therefore, nonshivering thermogenesis in brown adipose tissue (BAT) by oxidation of its Cys253 due to the elevated mt superoxide/H_2O_2 [155]. We speculated that H_2O_2-activated mt phospholipase iPLA2γ can also participate in this process by providing free fatty acids required for the UCP1-mediated uncoupling (thermogenic and not mild one) [156]. Mitochondrial superoxide/H_2O_2 may influence the local synaptic activity of neurons [157], and increased ROS upon mt fission provided a repair signal [158].

Mitochondrial redox signaling at hypoxia

One would not expect increasing ROS with a lowering oxygen. This paradox has been investigated, and mitochondrial contribution to oxygen sensing and hypoxic transcriptome reprogramming is still debated [159,160]. The central cytosolic mechanism of oxygen sensing is based on prolyl hydroxylases (PHD1 to 3, or Egl nine homolog 1 proteins, GLNs)[159,161-163], which catalyze hydroxylation of hypoxia-induced factor HIF-1α, -2α or -3α in a ferrous iron- (Fe^{II}-) plus 2OG- plus O_2-dependent manner. The resulting hydroxylation promotes its constant proteasome degradation after ubiquitination by pVHL ubiquitin ligase (Von Hippel-Lindau tumor suppressor protein) [164-166]. Therefore, by decreasing O_2, by lowering 2OG and by oxidation of Fe^{II} to Fe^{III} due to increasing cytosolic ROS, PHDs are inhibited, and HIF-1α stabilization occurs. Also, another O_2- and 2OG-dependent dioxygenase, termed factor inhibiting HIF (FIH), hydroxylates HIFα, but at asparagines. This blocks the binding of the coactivators CBP (CREB-binding protein) and p300, and thereby disables HIF-1-mediated transcription. Upon hypoxia, both PHD and FIH are inhibited; hence, HIF-α is stabilized and binds HIF-β plus coactivators VBP and p300, which allows activation of transcription of >400 genes [167-172]. In this way, the HIF system is activated, resulting in transcriptome reprogramming important in cancerogenesis and numerous physiological and pathological situations.

Since both PHD and FIH are affected by ROS, both can be targets of redox signaling. Various ROS may oxidize Fe^{II} of PHD to Fe^{III} [173]. Still, also reactive cysteines were recognized in PHD2, which, after oxidation, inactivate the enzyme (probably inactive PHD homodimers are formed due to S-S bridges) and initiate HIF-response upon oxidation [174-176]. Cytosolic peroxiredoxins may also be involved. In any case, PHDs sense oxygen independently of mitochondria, however, mitochondrial metabolism and mt redox signaling may also independently participate. Since PHDs are also inhibited by the lack of 2OG-related substrates, such as fumarate, succinate, malate isocitrate, and lactate [177,178], suppression of mitochondrial metabolism may stimulate HIF system.

Moreover, participation of mt redox signaling linked to HIF-1α stabilization was suggested by the $\Delta\Psi_m$ restoration, which returned a higher mt superoxide formation in cells with deleted mtDNA polymerase when respiration and hence Krebs cycle turnover was largely abolished [179]. After an instant hypoxia switch-on, a hypoxic burst of mt matrix superoxide release was

observed [180] but delayed by several hours [181,182]. Other reports described an instant hypoxic ROS burst in endothelial, HeLa, and HK2 cells [183]. Originally, the Complex III site III_{Qo} was considered as the superoxide source for the mt hypoxic ROS burst [180,184-188]. A similar hypoxic mt ROS burst was also detected for normoxic HIF activation [189]. The emanated mt H_2O_2 to the cytosol was suggested to oxidize Fe^{II} in PHDs. When certain Complex III subunits, such as Rieske iron-sulfur protein [190] or others were ablated, HIF-1α was stabilized [180], unlike in anoxia [187]. Moreover, suppressors of site III_{Qo} electron leak (S3QELs) prevented the HIF response [34]. The key evidence for mt redox signal participation in HIF-system signaling was provided by PRDX5 overexpression in the mt intermembrane space, which abolished HIF-1α stabilization [100].

HIF strikes back on mitochondria

The chicken-and-egg problem of the steady-state established upon HIF-signaling can be solved by precisely time-resolved events. This is because the execution of HIF-mediated transcriptome reprogramming affects redox homeostasis, which is then different than that one allowing HIF-system initiation. Indeed, HIF activates transcription for the expression of proteins, decreasing ROS formation or scavenging ROS [171].

Mitochondrial cristae inflate with dormant ATP synthesis in hypoxic cells and shrink with its restoration

We have also encountered that mitochondrial cristae inflate after adaptation of HepG2 cells to hypoxia [60] (Fig. 4). It is recognized as cristae widening in transmission electron microscopic (TEM) images (Fig. 4A) and as inflation (widening in 2D projections) of 3D super-resolution images of mitochondrial cristae stained with Eos-Lactamase-β (Fig. 4B,D). Due to the HIF transcriptome reprogramming, hypoxic HepG2 cells exhibited a low-intensity (dormant) ATP synthesis and respiration [60,182]. Partial degradation of mitofilin/MIC60 protein led to the decrease of crista junctions and the widening of crista outlets from the inflated crista to the intermembrane space [60,63].

In contrast, after addition of respiratory substrate to the hypoxia-adapted HepG2 cells, a sudden narrowing of cristae in 2D projections (shrinkage of crista lamellae in a space) resulted from the restored respiration and ATP-synthesis [63,188] (Fig. 4B). We have observed similar changes in rat pancreatic β-cells, INS-1E, after the addition of a substrate, i.e. glucose (which stimulates secretion of insulin) [46]. This observation led us to a hypothesis assuming that strengthening and ordering the ATP-synthase dimers at the crista lamellar edges leads to sharpening of these edges and that the two lamellae flanks mechanistically come close together [46,63]. When metabolic conditions and signaling allow disordering of the ATP-synthase dimers at the crista lamellar edges, this allows a more flat edge, which mechanistically puts apart the two lamellae flanks of the crista, resulting in cristae inflation [7,46,63].

However, considering that individual mechanistic tension within the single crista is responsible for the lamella inflation and shrinkage seems insufficient. Hence, recently, we came up with a novel hypothesis [7], which may be valid simultaneously, that the osmotic forces are the real engines of the crista lamellae inflation and shrinkage (Fig. 4E). The hypothesis expects that at low ATP-synthesis and low Δp, ion fluxes allow the salt to be extruded from the matrix (cations such as K^+ and Na^+ and anions such as phosphate and Krebs cycle intermediates). After a switch-on of the ATP synthesis and before the built-up of the high ATP concentration, i.e., at the beginning of cristae morphology changes, the open mitochondrial ATP-sensitive K^+ channel (mtK_{ATP}) allows an influx of K^+ from the intracristal space to the matrix. Since simultaneous phosphate uptake to the matrix diminishes a salt content in the ICS and enriches it in the matrix, water uptake to the matrix occurs concomitantly to the salt influx. As a result, this osmotic force shrinks the ICS. However, to prevent an infinite cristae shrinkage, a built-up of ATP closes the mtK_{ATP}, stopping salt leakage from the ICS and water transport to the matrix. Also, mt K^+/H^+ and Na^+/H^+ antiporters, being driven by Δp, prevent the infinite shrinkage of cristae.

We have already obtained the first evidence supporting the relevance of the osmotic hypothesis of cristae morphology changes. In hypoxia-adapted HepG2 cells where the addition of dimethyl-2-oxoglutarate initiated respiration and cristae shrinkage, glibenclamide, an inhibitor of the mtK_{ATP}, blocked such shrinkage [60] (Fig. 4C). Further investigations are required to reveal whether the mechanistic or osmotic hypothesis is relevant, or whether both are relevant; as well as to describe possible regulations which transfer metabolic changes to the activation of relevant proteins which initiate cristae morphology changes.

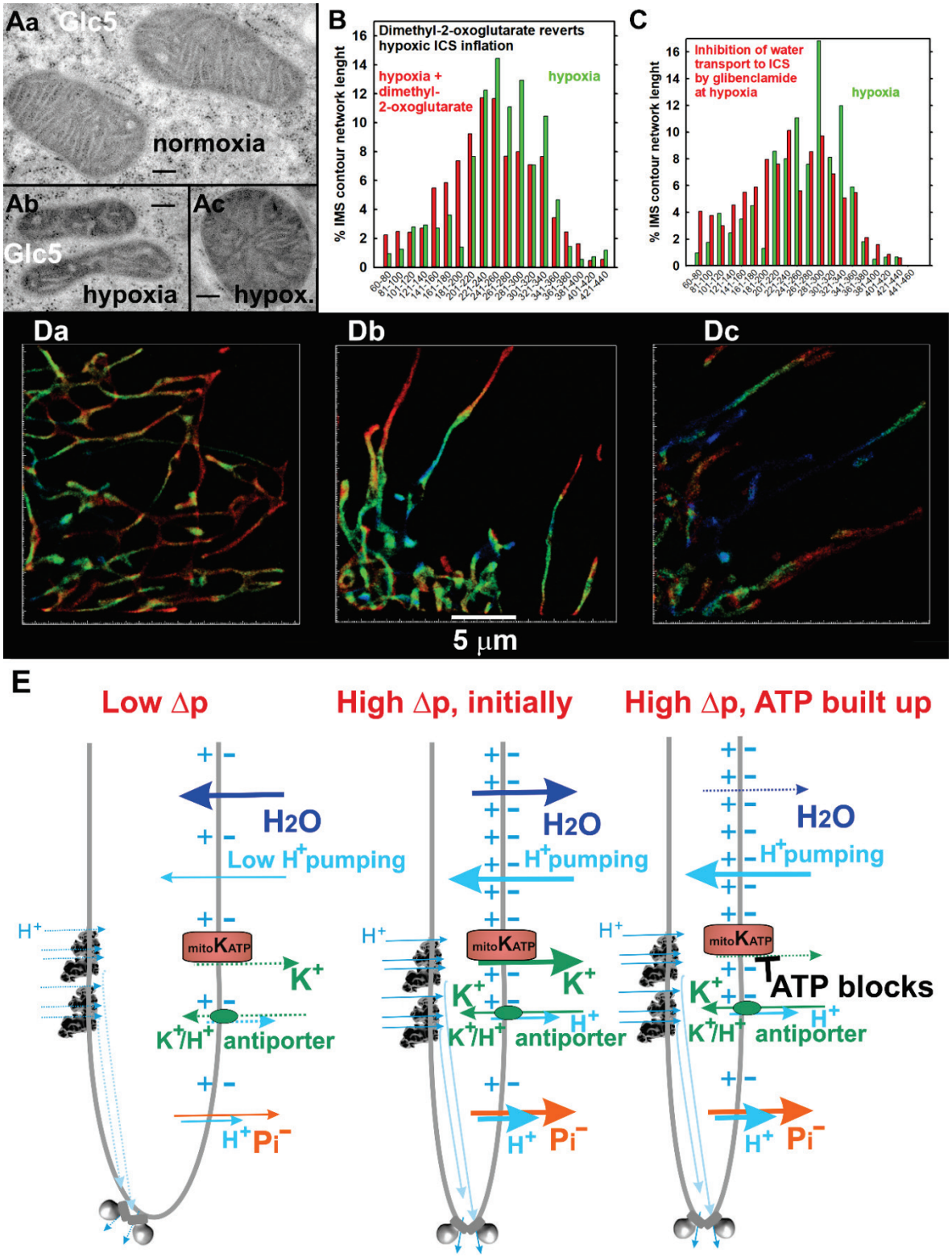

Fig. 4. Hypoxic cristae inflation, its reversal at restored respiration and ATP synthesis and possible osmotic mechanism involving mitochondrial ATP-sensitive K^+ channel. (**A**) Illustration of mitochondrial cristae widening after adaptation of HepG2 cells to hypoxia in transmission electron microscopic (TEM) sections (adapted from Ref. [60]). (**B-D**) Mitochondrial cristae widening indicated by the Eos-Lactamase-β 3D-superresolution fluorescence microscopy (adapted from Ref. [60]). Since Lactamase-β stains the intracristal space, an apparent width of its fluorescence contour on 2D sections of 3D images (panels **Da** for normoxia, **Db**, **Dc** for hypoxia) semi-quantifies the volume of crista lamellae. Thus, panel (**B**) illustrates on histograms of such width the existence of bulky cristae after hypoxic adaptation and their shrinkage after the addition of respiratory substrate, dimethyl-2-oxoglutarate. In contrast, panel (**C**) shows inhibition of the cristae lamellae shrinkage by glibenclamide, a known inhibitor of ATP-sensitive K^+ channel, including its mitochondrial form (mtK_{ATP}). (**E**) Osmotic hypothesis for participation of mtK_{ATP} in cristae shrinkage. For an explanation, see text (Chapter Mitochondrial cristae inflate with dormant ATP synthesis in hypoxic cells and shrink with its restoration).

Pancreatic β-cells as an exemplar mitochondrial redox system

Oxidative phosphorylation and NADPH-oxidase-4-mediated redox signaling as essential determinant of glucose-stimulated insulin secretion

Previously, an effect of antioxidants upon exhausted glutathione in pancreatic β-cells has been reported as an unspecified link between glucose-stimulated insulin secretion (GSIS) and external H_2O_2 [191]. Recently, it has been established that the essential conditions for GSIS involve the elevated OXPHOS and consequent ATP/ADP elevation in the peri-plasma membrane space [87,192,193] plus essential redox signaling, mediated by the NADPH-oxidase 4 (NOX4) [18,88,194] (Fig. 5). Together with ATP, the cytosolic redox (H_2O_2) signal closes the plasma membrane ATP-sensitive K^+ channels (K_{ATP}), together with the elevated ATP [18,88,194]. For a closing of the entire K_{ATP} population and setting a threshold membrane potential to -50 mV, opening of other non-specific calcium channels (NSCCs, such as TRMP2 channels, [195]) or Cl^- channels is required [87]. At -50 mV an intermittent opening of voltage-dependent Ca^{2+} channels (Ca_V) is initiated, being instantly counteracted by voltage-dependent K^+ channels (K_V). This leads to a pulsatile Ca^{2+} entry into the cytosol and in-phase exocytosis of insulin granule vesicles (IGV) [18,87].

Upon GSIS, an NADPH supply to the constitutively expressed NOX4 originates from the two enzymes of the pentose phosphate pathway (PPP), producing NADPH, i.e., glucose-6-phosphate dehydrogenase (G6PDH) 6-phosphogluconate dehydrogenase (6PGDH) [196]; plus from so-called (pyruvate redox) shuttles [18,88,193,197]. Interestingly, these shuttles do not allow synthesis of one NADH molecule in the mt matrix, but instead, NADPH is formed in the cytosol after a few transport steps and enzyme reactions [197]. As a result, production of superoxide released to the mt matrix is slowed down, most probably due to the decreased NADH/NAD^+ ratio affecting the Complex I superoxide formation site I_F [7,197]. We have linked two redox shuttles with the decreasing superoxide formation upon GSIS, the pyruvate-malate shuttle and the pyruvate-isocitrate shuttle [197]. Other shuttles were also reported [193,198]. The pyruvate-malate shuttle is allowed by the pyruvate carboxylase (PC). Such a bypass of pyruvate dehydrogenase makes possible a reverse reaction of malate dehydrogenase (MDH2), consuming NADH. A concomitant malate export from the mt matrix enables the cytosolic malic enzyme (ME1) to convert malate into pyruvate while yielding NADPH. The pyruvate-isocitrate shuttle stems from a truncated Krebs cycle after citrate synthase so that isocitrate dehydrogenase 3 (IDH3) does not form NADH. Instead, matrix NADPH is converted by IDH2 together with 2-oxoglutarate (2OG) into isocitrate, allowing its export from the mt matrix and subsequent reaction of cytosolic IDH1, transforming cytosolic isocitrate back to 2OG and synthesizing NADPH. ^{13}C-glutamine-assisted isotope tracing enabled to verify the existence of this redox shuttle [197,199].

Relative easy spread of redox changes in pancreatic β-cells is possible due to a rather weak antioxidant defense system and low capacity of redox buffers [200,201]. Such a delicate redox homeostasis is then disturbed by a rather weak insult. Expression and activity of antioxidant enzymes is low in rodent β-cells as compared to other organs [202].

Oxidative phosphorylation and mitochondrial redox signaling as essential determinant of branched-chain-ketoacid- and fatty-acid-stimulated insulin secretion

Insulin is also stimulated by other metabolites, collectively termed secretagogues [7,88] (Fig. 5). Thus, a leucine metabolite, keto-isocaproate (KIC) was demonstrated to stimulate insulin secretion, while its oxidation (termed commonly as β-like oxidation) provides both elevated ATP and redox (H_2O_2) signal [194]. The mitochondrial origin of this redox signal was suggested by the blockage of KIC-stimulated insulin secretion with mt-matrix-targeted antioxidant SkQ1 [194]. This excludes the previous hypothesis that leucine itself stimulate IGV exocytosis.

Also, free fatty acids (FAs) have been regarded to augment GSIS [203], meaning that insulin secretion in the presence of FAs required certain higher glucose concentrations [204-206]. Nevertheless, we and others have demonstrated that the net FA-stimulated insulin secretion (FASIS) exists [18,88,123,207-210], i.e., insulin secretion stimulated by FAs at low glucose concentration, which otherwise does not stimulate insulin release alone. Similarly to KIC, FA β-oxidation [123] provides both elevated ATP and increased mt superoxide formation transformed into the redox (H_2O_2) signal, which is subsequently spread up to the plasma membrane [9]. Previously, mitochondrial ROS resulting from the addition of monooleoyl-glycerol [211] have been suggested to modulate insulin secretion, and mt-derived

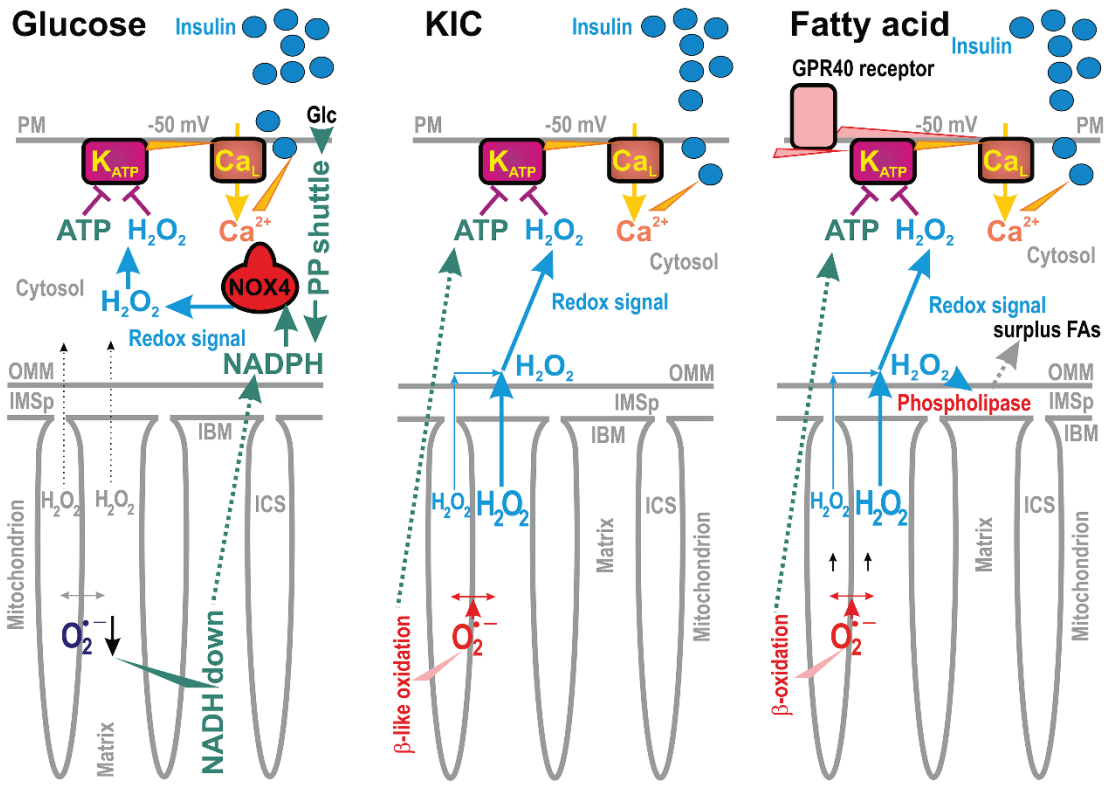

Fig. 5. Redox signaling upon insulin secretion stimulated with glucose or ketoisocaproate (KIC) or fatty acid. Redox signaling is depicted for insulin secretion stimulated with three distinct secretagogues. In all cases, the plasma membrane ATP-sensitive K^+ channel (K_{ATP}) is synergically closed only when both ATP and H_2O_2 (redox signaling) are elevated [194]. This predetermines plasma membrane depolarization to -50 mV and concomitant opening of the voltage-dependent Ca^{2+} channels (typically Ca_L), allowing the Ca^{2+} entry and exocytosis of insulin granule vesicles [88]. For the glucose-stimulated insulin secretion (GSIS) the constitutively expressed NADPH-oxidase isoform 4 (NOX4) substantiates cytosolic redox signaling, while NADPH is supplied by pentose phosphate (PP) shuttle [194] and by redox pyruvate transport shuttles (causing matrix NADH to be down and increased cytosolic NADPH, [197]). For ketoisocaproate stimulation of insulin secretion, KIC oxidation (termed β-like oxidation) generates both ATP and H_2O_2, which now originates from the mt-matrix-formed superoxide/H_2O_2 [194]. For fatty acid, stimulating insulin secretion even at low glucose [123], fatty acid β-oxidation also provides both ATP and H_2O_2 [88]. Similarly, as for KIC, H_2O_2 substantiates the redox signal from the mitochondrial matrix directed to the plasma membrane. Simultaneously, H_2O_2 also activates mitochondrial phospholipase iPLA2γ ("phospholipase"), which adds a surplus of mitochondrial fatty acids for both β-oxidation and the metabotropic GPR40 receptor on the plasma membrane [123]. The downstream pathways of the GPR40 receptor further stimulate insulin secretion.

ROS were regarded as obligatory signals for insulin secretion [212].

FASIS is more complex than the KIC-stimulated insulin secretion (Fig. 5), since also metabotropic GPR40 receptors, residing presumably on the plasma membrane, sense FAs and initiate a complex downstream signaling. When this proceeds *via* Gαq/11 heterotrimeric G-proteins, followed by the Ca^{2+}-dependent phospholipase-C-(PLC)-mediated hydrolysis of phosphatidylinositol-4,5-bisphosphate (PIP2) into diacyl-glycerol (DAG) and inositol-3-phosphate (IP3), a non-metabolizable GPR40 agonist can stimulate insulin secretion even at low glucose and ATP (Jezek *et al.*, unpublished). Indeed, PIP2 was known to stabilize the open K_{ATP}, hence its degradation by PLC-hydrolysis facilitates the K_{ATP} closure [213]. The reaction product DAG stimulates protein kinase-C (PKC) iso-enzymes, some of which phosphorylate TRPM4 and TRPM5 [214], which opens these channels, enabling them to activate Ca_V channels, similarly to the TRPM2 action upon GSIS.

Moderately elevated cytosolic [Ca^{2+}] should be required for PLC activity, however, DAG could also originate from the so-called glycerol/FA cycle [203], if it exists at "fasting" glucose. Interestingly, novel PKCs (nPKCs) are activated by DAG alone, but not by Ca^{2+} [215]. Hence, GPR40-signaling to final targets *via* nPKCs, promoting IGV-exocytosis, could exist even at low glucose.

The other product IP3 acts in the Ca^{2+}-induced Ca^{2+}-release from endoplasmic reticulum, enabled by the IP3-receptor (IP3R), functioning as a Ca^{2+} channel. Note also that *in vivo*, FASIS is not separated but acts in parallel with the signaling by monoacyl-glycerols (MAG) *via* the GPR119-Gαs-PKA(EPAC2) pathway. The PKA and EPAC2 pathways also serve as a biased pathways for

certain GPR40 agonists. The protein kinase A (PKA) phosphorylates glucose transporter GLUT2 to facilitate glucose entry. PKA also phosphorylates K_{ATP} and Ca_V to ease action potential triggering. The EPAC pathway acts similarly by phosphorylating TRPM2, releasing PIP2 from K_{ATP} and affecting Rim2a interaction with SNARE proteins, thus facilitating IGV exocytosis [18,87,88].

Yet another phenomenon is concomitant to FASIS. Interestingly not the extracellular FAs, but FAs cleaved from the mt phospholipids by the redox-activated mt phospholipase A2, isoform γ (iPLA2γ) stimulate the GPR40 receptors [123]. Silencing of iPLA2γ led to a profound decrease of FASIS [123] despite the redox signaling up to the plasma membrane was not attenuated (Jabůrek *et al.*, unpublished). There was a paradox encountered which has to be resolved. Due to the antioxidant synergy provided by a couple of iPLA2γ and uncoupling protein 2 (UCP2), the FA addition to pancreatic β-cells first attenuates mitochondrial superoxide formation released to the matrix. This mechanism exists since the redox-activated iPLA2γ provides nascent free FAs for UCP2 to initiate a mild uncoupling and thus reduce the mt superoxide formation [123]. However, when H_2O_2 is monitored in the cell cytosol or extracellularly at the same time, it is elevated (MJ, unpublished data). This paradox could be speculatively explained by MnSOD activation or by the involvement of the peroxiredoxin system [9]. Indeed PRDX3 silencing in INS-1E cells partly inhibited FASIS (MJ, unpublished data).

Future perspectives

It is an experimental challenge to track or monitor acute redox signaling by observing changes in particular reactive oxygen species in a given compartment [9]. Any event has to be studied to reliably identify the source, the path, and the target of redox signaling. Tracking changes in the surrounding proteins, e.g., in cysteine oxidation, cannot frequently distinguish the real target from those collateral ones. Correlations must be found for the initiation of the signal with the initiation of the effect and particular molecular changes in the effector proteins. It has to be investigated, for example, whether the changes in mitochondrial cristae morphology are governed by certain redox signals. With already identified redox signals, such as NADPH-oxidase 4 essential participation in glucose-stimulated insulin secretion (GSIS), it must be further studied, whether a cytosol-targeted antioxidant therapy would not rather promote a certain harm. Strong artificial suppression of redox signals could inevitably suppress GSIS and even redox signals, which otherwise contribute to the fitness of pancreatic β-cells [194]. Thus, instead of healing, this would amplify symptoms of prediabetes. In contrast, mitochondria-targeted antioxidants would not harm physiological redox signaling (except that of oxoacids and fatty acids) and might avoid the premature oxidative stress in the matrix of β-cells at the prediabetes stage. In conclusion, future studies of redox signaling should answer not only the basic questions of molecular physiology, but will also lead to novel translational aspects.

Conflict of Interest

There is no conflict of interest.

Acknowledgements

This work has been supported by Grant Agency of the Czech Republic, grant No. 21-01205S and No. 24-10132S to PJ, 23-05798S to HE, 22-02203S to AD, 22-17173S to MJ and by the project National Institute for Research of Metabolic and Cardiovascular Diseases (Programme EXCELES, ID Project No. LX22NPO5104) – Funded by the European Union – Next Generation EU.

References

1. Brand MD. Mitochondrial generation of superoxide and hydrogen peroxide as the source of mitochondrial redox signaling. Free Radic Biol Med 2016;100:14-31. https://doi.org/10.1016/j.freeradbiomed.2016.04.001
2. Brand MD. Riding the tiger - physiological and pathological effects of superoxide and hydrogen peroxide generated in the mitochondrial matrix. Crit Rev Biochem Mol Biol 2020;55:592-661. https://doi.org/10.1080/10409238.2020.1828258
3. Fang J, Wong HS, Brand MD. Production of superoxide and hydrogen peroxide in the mitochondrial matrix is dominated by site IQ of complex I in diverse cell lines. Redox Biol 2020;37:101722. https://doi.org/10.1016/j.redox.2020.101722

4. Quinlan CL, Perevoshchikova IV, Hey-Mogensen M, Orr AL, Brand MD. Sites of reactive oxygen species generation by mitochondria oxidizing different substrates. Redox Biol 2013;1:304-312. https://doi.org/10.1016/j.redox.2013.04.005
5. Ježek P, Hlavatá L. Mitochondria in homeostasis of reactive oxygen species in cell, tissues, and organism. Int J Biochem Cell Biol 2005;37:2478-2503. https://doi.org/10.1016/j.biocel.2005.05.013
6. Ježek P, Holendová B, Plecitá-Hlavatá L. Redox Signaling from Mitochondria: Signal Propagation and Its Targets. Biomolecules 2020;10:93. https://doi.org/10.3390/biom10010093
7. Ježek P, Jabůrek M, Holendová B, Engstová H, Dlasková A. Mitochondrial Cristae Morphology Reflecting Metabolism, Superoxide Formation, Redox Homeostasis, and Pathology. Antioxid Redox Signal 2023;39:635-683. https://doi.org/10.1089/ars.2022.0173
8. Kawano I, Bazila B, Ježek P, Dlasková A. Mitochondrial dynamics and cristae shape changes during metabolic re-programming. Antioxid Redox Signal 2023;39:684-707. https://doi.org/10.1089/ars.2023.0268
9. Ježek P. Pitfalls of Mitochondrial Redox Signaling Research. Antioxidants (Basel) 2023;12:1696. https://doi.org/10.3390/antiox12091696
10 Ohnishi ST, Shinzawa-Itoh K, Ohta K, Yoshikawa S, Ohnishi T. New insights into the superoxide generation sites in bovine heart NADH-ubiquinone oxidoreductase (Complex I): the significance of protein-associated ubiquinone and the dynamic shifting of generation sites between semiflavin and semiquinone radicals. Biochim Biophys Acta 2010;1797:1901-1909. https://doi.org/10.1016/j.bbabio.2010.05.012
11. Hirst J, Roessler MM. Energy conversion, redox catalysis and generation of reactive oxygen species by respiratory complex I. Biochim Biophys Acta 2016;1857:872-883. https://doi.org/10.1016/j.bbabio.2015.12.009
12. Chouchani ET, Pell VR, Gaude E, Aksentijević D, Sundier SY, Robb EL, Logan A, Nadtochiy SM, Ord ENJ, Smith AC, Eyassu F, Shirley R, Hu CH, Dare AJ, James AM, Rogatti S, Hartley RC, Eaton S, Costa ASH, Brookes PS, Davidson SM, Duchen MR, Saeb-Parsy K, Shattock MJ, Robinson AJ, Work LM, Frezza C, Krieg T, Murphy MP. Ischaemic accumulation of succinate controls reperfusion injury through mitochondrial ROS. Nature 2014;515:431-435. https://doi.org/10.1038/nature13909
13. Robb EL, Hall AR, Prime TA, Eaton S, Szibor M, Viscomi C, James AM, Murphy MP. Control of mitochondrial superoxide production by reverse electron transport at complex I. J Biol Chem 2018;293:9869-9879. https://doi.org/10.1074/jbc.RA118.003647
14. Dlasková A, Hlavatá L, Ježek P. Oxidative stress caused by blocking of mitochondrial complex I H(+) pumping as a link in aging/disease vicious cycle. Int J Biochem Cell Biol 2008;40:1792-1805. https://doi.org/10.1016/j.biocel.2008.01.012
15. Dlasková A, Hlavatá L, Ježek J, Ježek P. Mitochondrial Complex I superoxide production is attenuated by uncoupling. Int J Biochem Cell Biol 2008;40:2098-2109. https://doi.org/10.1016/j.biocel.2008.02.007
16. Ježek P, Žáčková M, Růžička M, Škobisová E, Jabůrek M. Mitochondrial uncoupling proteins--facts and fantasies. Physiol Res 2004;53(Suppl 1):S199-S211. https://doi.org/10.33549/physiolres.930000.53.S199
17. Ježek P, Olejár T, Smolková K, Ježek J, Dlasková A, Plecitá-Hlavatá L, Zelenka J, Špaček T, Engstová H, Pajuelo Reguera D, Jabůrek M. Antioxidant and regulatory role of mitochondrial uncoupling protein UCP2 in pancreatic beta-cells. Physiol Res 2014;63(Suppl 1):S73-S91. https://doi.org/10.33549/physiolres.932633
18. Ježek P, Holendová B, Jabůrek M, Dlasková A, Plecitá-Hlavatá L. Contribution of Mitochondria to Insulin Secretion by Various Secretagogues. Antioxid Redox Signal 2022;36:920-952. https://doi.org/10.1089/ars.2021.0113
19. Brand MD, Affourtit C, Esteves TC, Green K, Lambert AJ, Miwa S, Pakay JL, Parker N. Mitochondrial superoxide: production, biological effects, and activation of uncoupling proteins. Free Radic Biol Med 2004;37:755-767. https://doi.org/10.1016/j.freeradbiomed.2004.05.034
20. Muller FL, Roberts AG, Bowman MK, Kramer DM. Architecture of the Qo site of the cytochrome bc1 complex probed by superoxide production. Biochemistry 2003;42:6493-6499. https://doi.org/10.1021/bi0342160
21. Muller FL, Liu Y, Van Remmen H. Complex III releases superoxide to both sides of the inner mitochondrial membrane. J Biol Chem 2004;279:49064-49073. https://doi.org/10.1074/jbc.M407715200
22. Husen P, Nielsen C, Martino CF, Solov'yov IA. Molecular Oxygen Binding in the Mitochondrial Electron Transfer Flavoprotein. J Chem Inf Model 2019;59:4868-4879. https://doi.org/10.1021/acs.jcim.9b00702

23. Reichart G, Mayer J, Zehm C, Kirschstein T, Tokay T, Lange F, Baltrusch S, Tiedge M, Fuellen G, Ibrahim S, Köhling R. Mitochondrial complex IV mutation increases reactive oxygen species production and reduces lifespan in aged mice. Acta Physiol (Oxf) 2019;225:e13214. https://doi.org/10.1111/apha.13214
24. Grivennikova VG, Kozlovsky VS, Vinogradov AD. Respiratory complex II: ROS production and the kinetics of ubiquinone reduction. Biochim Biophys Acta 2017;1858:109-117. https://doi.org/10.1016/j.bbabio.2016.10.008
25. St-Pierre J, Buckingham JA, Roebuck SJ, Brand MD. Topology of superoxide production from different sites in the mitochondrial electron transport chain. J Biol Chem 2002;277:44784-44790. https://doi.org/10.1074/jbc.M207217200
26. Perevoshchikova IV, Quinlan CL, Orr AL, Gerencser AA, Brand MD. Sites of superoxide and hydrogen peroxide production during fatty acid oxidation in rat skeletal muscle mitochondria. Free Radic Biol Med 2013;61:298-309. https://doi.org/10.1016/j.freeradbiomed.2013.04.006
27. Quinlan CL, Treberg JR, Perevoshchikova IV, Orr AL, Brand MD. Native rates of superoxide production from multiple sites in isolated mitochondria measured using endogenous reporters. Free Radic Biol Med 2012;53:1807-1817. https://doi.org/10.1016/j.freeradbiomed.2012.08.015
28. Trewin AJ, Bahr LL, Almast A, Berry BJ, Wei AY, Foster TH, Wojtovich AP. Mitochondrial Reactive Oxygen Species Generated at the Complex-II Matrix or Intermembrane Space Microdomain Have Distinct Effects on Redox Signaling and Stress Sensitivity in Caenorhabditis elegans. Antioxid Redox Signal 2019;31:594-607. https://doi.org/10.1089/ars.2018.7681
29. Siebels I, Dröse S. Q-site inhibitor induced ROS production of mitochondrial complex II is attenuated by TCA cycle dicarboxylates. Biochim Biophys Acta 2013;1827:1156-1164. https://doi.org/10.1016/j.bbabio.2013.06.005
30. Manhas N, Duong QV, Lee P, Richardson JD, Robertson JD, Moxley MA, Bazil JN. Computationally modeling mammalian succinate dehydrogenase kinetics identifies the origins and primary determinants of ROS production. J Biol Chem 2020;295:15262-15279. https://doi.org/10.1074/jbc.RA120.014483
31. Quinlan CL, Goncalves RL, Hey-Mogensen M, Yadava N, Bunik VI, Brand MD. The 2-oxoacid dehydrogenase complexes in mitochondria can produce superoxide/hydrogen peroxide at much higher rates than complex I. J Biol Chem 2014;289:8312-8325. https://doi.org/10.1074/jbc.M113.545301
32. McDonald AE, Pichaud N, Darveau CA. "Alternative" fuels contributing to mitochondrial electron transport: Importance of non-classical pathways in the diversity of animal metabolism. Comp Biochem Physiol B Biochem Mol Biol 2018;224:185-194. https://doi.org/10.1016/j.cbpb.2017.11.006
33. Orr AL, Quinlan CL, Perevoshchikova IV, Brand MD. A refined analysis of superoxide production by mitochondrial sn-glycerol 3-phosphate dehydrogenase. J Biol Chem 2012;287:42921-42935. https://doi.org/10.1074/jbc.M112.397828
34. Orr AL, Vargas L, Turk CN, Baaten JE, Matzen JT, Dardov VJ, Attle SJ, Li J, Quackenbush DC, Goncalves RL, Perevoshchikova IV, Petrassi HM, Meeusen SL, Ainscow EK, Brand MD. Suppressors of superoxide production from mitochondrial complex III. Nat Chem Biol 2015;11:834-836. https://doi.org/10.1038/nchembio.1910
35. Boukalova S, Hubackova S, Milosevic M, Ezrova Z, Neuzil J, Rohlena J. Dihydroorotate dehydrogenase in oxidative phosphorylation and cancer. Biochim Biophys Acta 2020;1866:165759. https://doi.org/10.1016/j.bbadis.2020.165759
36. Valentine JS, Doucette PA, Zittin Potter S. Copper-zinc superoxide dismutase and amyotrophic lateral sclerosis. Annu Rev Biochem 2005;74:563-593. https://doi.org/10.1146/annurev.biochem.72.121801.161647
37. Ozden O, Park SH, Kim HS, Jiang H, Coleman MC, Spitz DR, Gius D. Acetylation of MnSOD directs enzymatic activity responding to cellular nutrient status or oxidative stress. Aging 2011;3:102-107. https://doi.org/10.18632/aging.100291
38. Park SH, Ozden O, Jiang H, Cha YI, Pennington JD, Aykin-Burns N, Spitz DR, Gius D, Kim HS. Sirt3, mitochondrial ROS, ageing, and carcinogenesis. Int J Mol Sci 2011;12:6226-6239. https://doi.org/10.3390/ijms12096226
39. Salvatori I, Valle C, Ferri A, Carrì MT. SIRT3 and mitochondrial metabolism in neurodegenerative diseases. Neurochem Int 2017;109:184-192. https://doi.org/10.1016/j.neuint.2017.04.012
40. Tao R, Vassilopoulos A, Parisiadou L, Yan Y, Gius D. Regulation of MnSOD enzymatic activity by Sirt3 connects the mitochondrial acetylome signaling networks to aging and carcinogenesis. Antioxid Redox Signal 2014;20:1646-1654. https://doi.org/10.1089/ars.2013.5482

41. Anamika Roy A, Trigun SK. Hippocampus mitochondrial MnSOD activation by a SIRT3 activator, honokiol, correlates with its deacetylation and upregulation of FoxO3a and PGC1α in a rat model of ammonia neurotoxicity. J Cell Biochem 2023;124:606-618. https://doi.org/10.1002/jcb.30393
42. Gao E, Sun X, Thorne RF, Zhang XD, Li J, Shao F, Ma J, Wu M. NIPSNAP1 directs dual mechanisms to restrain senescence in cancer cells. J Transl Med 2023;21:401. https://doi.org/10.1186/s12967-023-04232-1
43. Liu X, Xie X, Li D, Liu Z, Zhang B, Zang Y, Yuan H, Shen C. Sirt3-dependent regulation of mitochondrial oxidative stress and apoptosis contributes to the dysfunction of pancreatic islets after severe burns. Free Radic Biol Med 2023;198:59-67. https://doi.org/10.1016/j.freeradbiomed.2023.01.027
44. Ma C, Sun Y, Pi C, Wang H, Sun H, Yu X, Shi Y, He X. Sirt3 Attenuates Oxidative Stress Damage and Rescues Cellular Senescence in Rat Bone Marrow Mesenchymal Stem Cells by Targeting Superoxide Dismutase 2. Front Cell Dev Biol 2020;8:599376. https://doi.org/10.3389/fcell.2020.599376
45. Mohan MS, Aswani SS, Aparna NS, Boban PT, Sudhakaran PR, Saja K. Effect of acute cold exposure on cardiac mitochondrial function: role of sirtuins. Mol Cell Biochem 2023;478:2257-2270. https://doi.org/10.1007/s11010-022-04656-1
46. Dlasková A, Engstová H, Špaček T, Kahancová A, Pavluch V, Smolková K, Špačková J, Bartoš M, Hlavatá L, Ježek P. 3D super-resolution microscopy reflects mitochondrial cristae alternations and mtDNA nucleoid size and distribution. Biochim Biophys Acta 2018;1859:829-844. https://doi.org/10.1016/j.bbabio.2018.04.013
47. Ježek P, Plecitá-Hlavatá L. Mitochondrial reticulum network dynamics in relation to oxidative stress, redox regulation, and hypoxia. Int J Biochem Cell Biol 2009;41:1790-1804. https://doi.org/10.1016/j.biocel.2009.02.014
48. Plecitá-Hlavatá L, Ježek P. Integration of superoxide formation and cristae morphology for mitochondrial redox signaling. Int J Biochem Cell Biol 2016;80:31-50. https://doi.org/10.1016/j.biocel.2016.09.010
49. Dlasková A, Špaček T, Šantorová J, Plecitá-Hlavatá L, Berková Z, Saudek F, Lessard M, Bewersdorf J, Ježek P. 4Pi microscopy reveals an impaired three-dimensional mitochondrial network of pancreatic islet beta-cells, an experimental model of type-2 diabetes. Biochim Biophys Acta 2010;1797:1327-1341. https://doi.org/10.1016/j.bbabio.2010.02.003
50. Dlasková A, Engstová H, Plecitá-Hlavatá L, Lessard M, Alán L, Reguera DP, Jabůrek M, Ježek P. Distribution of mitochondrial DNA nucleoids inside the linear tubules vs. bulk parts of mitochondrial network as visualized by 4Pi microscopy. J Bioenerg Biomembr 2015;47:255-263. https://doi.org/10.1007/s10863-015-9610-3
51. Plecitá-Hlavatá L, Lessard M, Šantorová J, Bewersdorf J, Ježek P. Mitochondrial oxidative phosphorylation and energetic status are reflected by morphology of mitochondrial network in INS-1E and HEP-G2 cells viewed by 4Pi microscopy. Biochim Biophys Acta 2008;1777:834-846. https://doi.org/10.1016/j.bbabio.2008.04.002
52. Glancy B, Hartnell LM, Malide D, Yu ZX, Combs CA, Connelly PS, Subramaniam S, Balaban RS. Mitochondrial reticulum for cellular energy distribution in muscle. Nature 2015;523:617-620. https://doi.org/10.1038/nature14614
53. Eisner V, Cupo RR, Gao E, Csordás G, Slovinsky WS, Paillard M, Cheng L, Ibetti J, Chen SR, Chuprun JK, Hoek JB, Koch WJ, Hajnóczky G. Mitochondrial fusion dynamics is robust in the heart and depends on calcium oscillations and contractile activity. Proc Natl Acad Sci U S A 2017;114:E859-E868. https://doi.org/10.1073/pnas.1617288114
54. Twig G, Elorza A, Molina AJ, Mohamed H, Wikstrom JD, Walzer G, Stiles L, Haigh SE, Katz S, Las G, Alroy J, Wu M, Py BF, Yuan J, Deeney JT, Corkey BE, Shirihai OS. Fission and selective fusion govern mitochondrial segregation and elimination by autophagy. EMBO J 2008;27:433-446. https://doi.org/10.1038/sj.emboj.7601963
55. Picard M, Shirihai OS. Mitochondrial signal transduction. Cell Metab 2022;34:1620-1653. https://doi.org/10.1016/j.cmet.2022.10.008
56. Kondadi AK, Anand R, Hänsch S, Urbach J, Zobel T, Wolf DM, Segawa M, Liesa M, Shirihai OS, Weidtkamp-Peters S, Reichert AS. Cristae undergo continuous cycles of membrane remodelling in a MICOS-dependent manner. EMBO Rep 2020;21:e49776. https://doi.org/10.15252/embr.201949776
57. Bohnert M, Wenz LS, Zerbes RM, Horvath SE, Stroud DA, von der Malsburg K, Müller JM, Oeljeklaus S, Perschil I, Warscheid B, Chacinska A, Veenhuis M, van der Klei IJ, Daum G, Wiedemann N, Becker T, Pfanner N, van der Laan M. Role of mitochondrial inner membrane organizing system in protein biogenesis of the mitochondrial outer membrane. Mol Biol Cell 2012;23:3948-3956. https://doi.org/10.1091/mbc.e12-04-0295

58. Pfanner N, van der Laan M, Amati P, Capaldi RA, Caudy AA, Chacinska A, Darshi M, Deckers M, Hoppins S, Icho T, Jakobs S, Ji J, Kozjak-Pavlovic V, Meisinger C, Odgren PR, Park SK, Rehling P, Reichert AS, Sheikh MS, Taylor SS, Tsuchida N, van der Bliek AM, van der Klei IJ, Weissman JS, Westermann B, Zha J, Neupert W, Nunnari J. Uniform nomenclature for the mitochondrial contact site and cristae organizing system. J Cell Biol 2014;204:1083-1086. https://doi.org/10.1083/jcb.201401006
59. Zerbes RM, Bohnert M, Stroud DA, von der Malsburg K, Kram A, Oeljeklaus S, Warscheid B, Becker T, Wiedemann N, Veenhuis M, van der Klei IJ, Pfanner N, van der Laan M. Role of MINOS in mitochondrial membrane architecture: cristae morphology and outer membrane interactions differentially depend on mitofilin domains. J Mol Biol 2012;422:183-191. https://doi.org/10.1016/j.jmb.2012.05.004
60. Plecitá-Hlavatá L, Engstová H, Alán L, Špaček T, Dlasková A, Smolková K, Špačková J, Tauber J, Strádalová V, Malínský J, Lessard M, Bewersdorf J, Ježek P. Hypoxic HepG2 cell adaptation decreases ATP synthase dimers and ATP production in inflated cristae by mitofilin down-regulation concomitant to MICOS clustering. FASEB J 2016;30:1941-1957. https://doi.org/10.1096/fj.201500176
61. Davies KM, Strauss M, Daum B, Kief JH, Osiewacz HD, Rycovska A, Zickermann V, Kühlbrandt W. Macromolecular organization of ATP synthase and complex I in whole mitochondria. Proc Natl Acad Sci U S A 2011;108:14121-14126. https://doi.org/10.1073/pnas.1103621108
62. Davies KM, Anselmi C, Wittig I, Faraldo-Gómez JD, Kühlbrandt W. Structure of the yeast F1Fo-ATP synthase dimer and its role in shaping the mitochondrial cristae. Proc Natl Acad Sci U S A 2012;109:13602-13607. https://doi.org/10.1073/pnas.1204593109
63. Dlasková A, Špaček T, Engstová H, Špačková J, Schröfel A, Holendová B, Smolková K, Plecitá-Hlavatá L, Ježek P. Mitochondrial cristae narrowing upon higher 2-oxoglutarate load. Biochim Biophys Acta 2019;1860:659-678. https://doi.org/10.1016/j.bbabio.2019.06.015
64. Dudkina NV, Oostergetel GT, Lewejohann D, Braun HP, Boekema EJ. Row-like organization of ATP synthase in intact mitochondria determined by cryo-electron tomography. Biochim Biophys Acta 2010;1797:272-277. https://doi.org/10.1016/j.bbabio.2009.11.004
65. Gu J, Zhang L, Zong S, Guo R, Liu T, Yi J, Wang P, Zhuo W, Yang M. Cryo-EM structure of the mammalian ATP synthase tetramer bound with inhibitory protein IF1. Science 2019;364:1068-1075. https://doi.org/10.1126/science.aaw4852
66. Guo H, Bueler SA, Rubinstein JL. Atomic model for the dimeric FO region of mitochondrial ATP synthase. Science 2017;358:936-940. https://doi.org/10.1126/science.aao4815
67. Nesterov S, Chesnokov Y, Kamyshinsky R, Panteleeva A, Lyamzaev K, Vasilov R, Yaguzhinsky L. Ordered Clusters of the Complete Oxidative Phosphorylation System in Cardiac Mitochondria. Int J Mol Sci 2021;22:1462. https://doi.org/10.3390/ijms22031462
68. Blum TB, Hahn A, Meier T, Davies KM, Kühlbrandt W. Dimers of mitochondrial ATP synthase induce membrane curvature and self-assemble into rows. Proc Natl Acad Sci U S A 2019;116:4250-4255. https://doi.org/10.1073/pnas.1816556116
69. Daum B, Walter A, Horst A, Osiewacz HD, Kühlbrandt W. Age-dependent dissociation of ATP synthase dimers and loss of inner-membrane cristae in mitochondria. Proc Natl Acad Sci U S A 2013;110:15301-15306. https://doi.org/10.1073/pnas.1305462110
70. Spikes TE, Montgomery MG, Walker JE. Structure of the dimeric ATP synthase from bovine mitochondria. Proc Natl Acad Sci U S A 2020;117:23519-23526. https://doi.org/10.1073/pnas.2013998117
71. Rampelt H, Bohnert M, Zerbes RM, Horvath SE, Warscheid B, Pfanner N, van der Laan M. Mic10, a Core Subunit of the Mitochondrial Contact Site and Cristae Organizing System, Interacts with the Dimeric F1Fo-ATP Synthase. J Mol Biol 2017;429:1162-1170. https://doi.org/10.1016/j.jmb.2017.03.006
72. Eydt K, Davies KM, Behrendt C, Wittig I, Reichert AS. Cristae architecture is determined by an interplay of the MICOS complex and the F1FO ATP synthase via Mic27 and Mic10. Microb Cell 2017;4:259-272. https://doi.org/10.15698/mic2017.08.585
73. Lenaz G, Tioli G, Falasca AI, Genova ML. Complex I function in mitochondrial supercomplexes. Biochim Biophys Acta 2016;1857:991-1000. https://doi.org/10.1016/j.bbabio.2016.01.013

74. Letts JA, Fiedorczuk K, Sazanov LA. The architecture of respiratory supercomplexes. Nature 2016;537:644-648. https://doi.org/10.1038/nature19774
75. Lobo-Jarne T, Ugalde C. Respiratory chain supercomplexes: Structures, function and biogenesis. Semin Cell Dev Biol 2018;76:179-190. https://doi.org/10.1016/j.semcdb.2017.07.021
76. Giacomello M, Pyakurel A, Glytsou C, Scorrano L. The cell biology of mitochondrial membrane dynamics. Nat Rev Mol Cell Biol 2020;21:204-224. https://doi.org/10.1038/s41580-020-0210-7
77. Pernas L, Scorrano L. Mito-Morphosis: Mitochondrial Fusion, Fission, and Cristae Remodeling as Key Mediators of Cellular Function. Annu Rev Physiol 2016;78:505-531. https://doi.org/10.1146/annurev-physiol-021115-105011
78. Faelber K, Dietrich L, Noel JK, Wollweber F, Pfitzner AK, Mühleip A, Sánchez R, Kudryashev M, Chiaruttini N, Lilie H, Schlegel J, Rosenbaum E, Hessenberger M, Matthaeus C, Kunz S, von der Malsburg A, Noé F, Roux A, van der Laan M, Kühlbrandt W, Daumke O. Structure and assembly of the mitochondrial membrane remodelling GTPase Mgm1. Nature 2019;571:429-433. https://doi.org/10.1038/s41586-019-1372-3
79. Tatsuta T, Langer T. Prohibitins. Curr Biol 2017;27:R629-R631. https://doi.org/10.1016/j.cub.2017.04.030
80. Barbot M, Jans DC, Schulz C, Denkert N, Kroppen B, Hoppert M, Jakobs S, Meinecke M. Mic10 oligomerizes to bend mitochondrial inner membranes at cristae junctions. Cell Metab 2015;21:756-763. https://doi.org/10.1016/j.cmet.2015.04.006
81. Bohnert M, Zerbes RM, Davies KM, Mühleip AW, Rampelt H, Horvath SE, Boenke T, Kram A, Perschil I, Veenhuis M, Kühlbrandt W, van der Klei IJ, Pfanner N, van der Laan M. Central role of Mic10 in the mitochondrial contact site and cristae organizing system. Cell Metab 2015;21:747-755. https://doi.org/10.1016/j.cmet.2015.04.007
82. Wang L, Yan Z, Vihinen H, Eriksson O, Wang W, Soliymani R, Lu Y, Xue Y, Jokitalo E, Li J, Zhao H. FAM92A1 is a BAR domain protein required for mitochondrial ultrastructure and function. J Cell Biol 2019;218:97-111. https://doi.org/10.1083/jcb.201806191
83. Frezza C, Cipolat S, Martins de Brito O, Micaroni M, Beznoussenko GV, Rudka T, Bartoli D, Polishuck RS, Danial NN, De Strooper B, Scorrano L. OPA1 controls apoptotic cristae remodeling independently from mitochondrial fusion. Cell 2006;126:177-189. https://doi.org/10.1016/j.cell.2006.06.025
84. Deponte M. Glutathione catalysis and the reaction mechanisms of glutathione-dependent enzymes. Biochim Biophys Acta 2013;1830:3217-3266. https://doi.org/10.1016/j.bbagen.2012.09.018
85. Sies H, Jones DP. Reactive oxygen species (ROS) as pleiotropic physiological signalling agents. Nat Rev Mol Cell Biol 2020;21:363-383. https://doi.org/10.1038/s41580-020-0230-3
86. Merrins MJ, Corkey BE, Kibbey RG, Prentki M. Metabolic cycles and signals for insulin secretion. Cell Metab 2022;34:947-968. https://doi.org/10.1016/j.cmet.2022.06.003
87. Rorsman P, Ashcroft FM. Pancreatic β-Cell Electrical Activity and Insulin Secretion: Of Mice and Men. Physiol Rev 2018;98:117-214. https://doi.org/10.1152/physrev.00008.2017
88. Ježek P, Holendová B, Jabůrek M, Tauber J, Dlasková A, Plecitá-Hlavatá L. The Pancreatic β-Cell: The Perfect Redox System. Antioxidants 2021;10:197. https://doi.org/10.3390/antiox10020197
89. Brigelius-Flohe R, Maiorino M. Glutathione peroxidases. Biochim Biophys Acta 2013;1830:3289-3303. https://doi.org/10.1016/j.bbagen.2012.11.020
90. Ighodaro OM, Akinloye OA. First line defence antioxidants-superoxide dismutase (SOD), catalase (CAT) and glutathione peroxidase (GPX): Their fundamental role in the entire antioxidant defence grid. Alex J Med 2018;54:287-293. https://doi.org/10.1016/j.ajme.2017.09.001
91. Herbette S, Roeckel-Drevet P, Drevet JR. Seleno-independent glutathione peroxidases. More than simple antioxidant scavengers. FEBS J 2007;274:2163-2180. https://doi.org/10.1111/j.1742-4658.2007.05774.x
92. Bolduc J, Koruza K, Luo T, Malo Pueyo J, Vo TN, Ezeriņa D, Messens J, Peroxiredoxins wear many hats: Factors that fashion their peroxide sensing personalities. Redox Biol 2021;42:101959. https://doi.org/10.1016/j.redox.2021.101959
93. Liu Y, Wang P, Hu W, Chen D. New insights into the roles of peroxiredoxins in cancer. Biomed Pharmacother 2023;164:114896. https://doi.org/10.1016/j.biopha.2023.114896
94. Rhee SG. Overview on Peroxiredoxin. Mol Cells 2016;39:1-5. https://doi.org/10.14348/molcells.2016.2368
95. Rhee SG, Kang SW, Chang TS, Jeong W, Kim K. Peroxiredoxin, a novel family of peroxidases. IUBMB Life 2001;52:35-41. https://doi.org/10.1080/15216540252774748

96. Rhee SG, Woo HA. Multiple functions of 2-Cys peroxiredoxins, I and II, and their regulations via post-translational modifications. Free Radic Biol Med 2020;152:107-115. https://doi.org/10.1016/j.freeradbiomed.2020.02.028
97. Thapa P, Jiang H, Ding N, Hao Y, Alshahrani A, Wei Q. The Role of Peroxiredoxins in Cancer Development. Biology (Basel) 2023;12:666. https://doi.org/10.3390/biology12050666
98. Villar SF, Ferrer-Sueta G, Denicola A. The multifaceted nature of peroxiredoxins in chemical biology. Curr Opin Chem Biol 2023;76:102355. https://doi.org/10.1016/j.cbpa.2023.102355
99. Knoops B, Goemaere J, Van der Eecken V, Declercq JP. Peroxiredoxin 5: structure, mechanism, and function of the mammalian atypical 2-Cys peroxiredoxin. Antioxid Redox Signal 2011;15:817-829. https://doi.org/10.1089/ars.2010.3584
100. Sabharwal SS, Waypa GB. Marks JD, Schumacker PT. Peroxiredoxin-5 targeted to the mitochondrial intermembrane space attenuates hypoxia-induced reactive oxygen species signalling. Biochem J 2013;456:337-346. https://doi.org/10.1042/BJ20130740
101. Sabharwal SS, Dudley VJ, Landwerlin C, Schumacker PT. H2O2 transit through the mitochondrial intermembrane space promotes tumor cell growth in vitro and in vivo. J Biol Chem 2023;299:104624. https://doi.org/10.1016/j.jbc.2023.104624
102. López-Grueso MJ, Lagal DJ, García-Jiménez ÁF, Tarradas RM, Carmona-Hidalgo B, Peinado J, Requejo-Aguilar R, Bárcena JA, Padilla CA. Knockout of PRDX6 induces mitochondrial dysfunction and cell cycle arrest at G2/M in HepG2 hepatocarcinoma cells. Redox Biol 2020;37:101737. https://doi.org/10.1016/j.redox.2020.101737
103. Ma S, Zhang X, Zheng L, Li Z, Zhao X, Lai W, Shen H, Lv J, Yang G, Wang Q, Ji J. Peroxiredoxin 6 Is a Crucial Factor in the Initial Step of Mitochondrial Clearance and Is Upstream of the PINK1-Parkin Pathway. Antioxid Redox Signal 2016;24:486-501. https://doi.org/10.1089/ars.2015.6336
104. Pacifici F, Della-Morte D, Capuani B, Coppola A, Scioli MG, Donadel G, Andreadi A, Ciccosanti F, Fimia GM, Bellia A, Orlandi A, Lauro, D. Peroxiredoxin 6 Modulates Insulin Secretion and Beta Cell Death via a Mitochondrial Dynamic Network. Front Endocrinol 2022;13:842575. https://doi.org/10.3389/fendo.2022.842575
105. Bachnoff N, Trus M, Atlas D. Alleviation of oxidative stress by potent and selective thioredoxin-mimetic peptides. Free Radic Biol Med 2011;50:1355-1367. https://doi.org/10.1016/j.freeradbiomed.2011.02.026
106. Jeong SJ, Park JG, Oh GT. Peroxiredoxins as Potential Targets for Cardiovascular Disease. Antioxidants 2021;10:1244. https://doi.org/10.3390/antiox10081244
107. Szeliga M. Peroxiredoxins in Neurodegenerative Diseases. Antioxidants 2020;9:1203. https://doi.org/10.3390/antiox9121203
108. Stancill JS, Corbett JA. The Role of Thioredoxin/Peroxiredoxin in the β-Cell Defense Against Oxidative Damage. Front Endocrinol 2021;12:718235. https://doi.org/10.3389/fendo.2021.718235
109. Rhee SG, Kil IS. Mitochondrial H2O2 signaling is controlled by the concerted action of peroxiredoxin III and sulfiredoxin: Linking mitochondrial function to circadian rhythm. Free Radic Biol Med 2016;100:73-80. https://doi.org/10.1016/j.freeradbiomed.2016.10.011
110. Mishra M, Jiang H, Wu L, Chawsheen HA, Wei Q. The sulfiredoxin-peroxiredoxin (Srx-Prx) axis in cell signal transduction and cancer development. Cancer Lett 2015;366:150-159. https://doi.org/10.1016/j.canlet.2015.07.002
111. Reczek CR, Chandel NS. ROS-dependent signal transduction. Curr Opin Cell Biol 2015;33:8-13. https://doi.org/10.1016/j.ceb.2014.09.010
112. Woo HA, Yim SH, Shin DH, Kang D, Yu DY, Rhee SG. Inactivation of peroxiredoxin I by phosphorylation allows localized H(2)O(2) accumulation for cell signaling. Cell 2010;140:517-528. https://doi.org/10.1016/j.cell.2010.01.009
113. Heo S, Kim S, Kang D. The Role of Hydrogen Peroxide and Peroxiredoxins throughout the Cell Cycle. Antioxidants 2020;9:280. https://doi.org/10.3390/antiox9040280
114. Jarvis RM, Hughes SM, Ledgerwood EC. Peroxiredoxin 1 functions as a signal peroxidase to receive, transduce, and transmit peroxide signals in mammalian cells. Free Radic Biol Med 2012;53:1522-1530. https://doi.org/10.1016/j.freeradbiomed.2012.08.001
115. Rhee SG, Woo HA, Kang D. The Role of Peroxiredoxins in the Transduction of H2O2 Signals. Antioxid Redox Signal 2018;28:537-557. https://doi.org/10.1089/ars.2017.7167

116. Rhee SG. A catalytic career: Studies spanning glutamine synthetase, phospholipase C, peroxiredoxin, and the intracellular messenger role of hydrogen peroxide. J Biol Chem 2019;294:5169-5180. https://doi.org/10.1074/jbc.X119.007975
117. Sobotta MC, Liou W, Stocker S, Talwar D, Oehler M, Ruppert T, Scharf AN, Dick TP. Peroxiredoxin-2 and STAT3 form a redox relay for H2O2 signaling. Nat Chem Biol 2015;11:64-70. https://doi.org/10.1038/nchembio.1695
118. Stocker S, Van Laer K, Mijuskovic A, Dick TP. The Conundrum of Hydrogen Peroxide Signaling and the Emerging Role of Peroxiredoxins as Redox Relay Hubs. Antioxid Redox Signal 2018;28:558-573. https://doi.org/10.1089/ars.2017.7162
119. Ježek P, Holendová B, Garlid KD, Jabůrek M. Mitochondrial Uncoupling Proteins: Subtle Regulators of Cellular Redox Signaling. Antioxid Redox Signal 2018;29:667-714. https://doi.org/10.1089/ars.2017.7225
120. Jabůrek M, Průchová P, Holendová B, Galkin A, Ježek P. Antioxidant Synergy of Mitochondrial Phospholipase PNPLA8/iPLA2γ with Fatty Acid-Conducting SLC25 Gene Family Transporters. Antioxidants 2021;10:678. https://doi.org/10.3390/antiox10050678
121. Průchová P, Gotvaldová K, Smolková K, Alán L, Holendová B, Tauber J, Galkin A, Ježek P, Jabůrek M. Antioxidant Role and Cardiolipin Remodeling by Redox-Activated Mitochondrial Ca2+-Independent Phospholipase A2γ in the Brain. Antioxidants 2022;11:198. https://doi.org/10.3390/antiox11020198
122. Fedorenko A, Lishko PV, Kirichok Y. Mechanism of fatty-acid-dependent UCP1 uncoupling in brown fat mitochondria. Cell 2012;151:400-413. https://doi.org/10.1016/j.cell.2012.09.010
123. Ježek J, Dlasková A, Zelenka J, Jabůrek M, Ježek P. H_2O_2-Activated Mitochondrial Phospholipase $iPLA_2\gamma$ Prevents Lipotoxic Oxidative Stress in Synergy with UCP2, Amplifies Signaling via G-Protein-Coupled Receptor GPR40, and Regulates Insulin Secretion in Pancreatic β-Cells. Antioxid Redox Signal 2015;23:958-972. https://doi.org/10.1089/ars.2014.6195
124. Korshunov SS, Skulachev VP, Starkov AA. High protonic potential actuates a mechanism of production of reactive oxygen species in mitochondria. FEBS Lett 1997;416:15-18. https://doi.org/10.1016/S0014-5793(97)01159-9
125. Arsenijevic D, Onuma H, Pecqueur C, Raimbault S, Manning BS, Miroux B, Couplan E, Alves-Guerra MC, Goubern M, Surwit R, Bouillaud F, Richard D, Collins S, Ricquier D. Disruption of the uncoupling protein-2 gene in mice reveals a role in immunity and reactive oxygen species production. Nat Genet 2000;26:435-439. https://doi.org/10.1038/82565
126. Nègre-Salvayre A, Hirtz C, Carrera G, Cazenave R, Troly M, Salvayre R, Pénicaud L, Casteilla L. A role for uncoupling protein-2 as a regulator of mitochondrial hydrogen peroxide generation. FASEB J 1997;11:809-815. https://doi.org/10.1096/fasebj.11.10.9271366
127. Duval C, Nègre-Salvayre A, Dogilo A, Salvayre R, Pénicaud L, Casteilla L. Increased reactive oxygen species production with antisense oligonucleotides directed against uncoupling protein 2 in murine endothelial cells. Biochem Cell Biol 2002;80:757-764. https://doi.org/10.1139/o02-158
128. Blanc J, Alves-Guerra MC, Esposito B, Rousset S, Gourdy P, Ricquier D, Tedgui A, Miroux B, Mallat Z. Protective role of uncoupling protein 2 in atherosclerosis. Circulation 2003;107:388-390. https://doi.org/10.1161/01.CIR.0000051722.66074.60
129. Ježek J, Jabůrek M, Zelenka J, Ježek P. Mitochondrial phospholipase A2 activated by reactive oxygen species in heart mitochondria induces mild uncoupling. Physiol Res 2010;59:737-747. https://doi.org/10.33549/physiolres.931905
130. Jabůrek M, Ježek J, Zelenka J, Ježek P. Antioxidant activity by a synergy of redox-sensitive mitochondrial phospholipase A2 and uncoupling protein-2 in lung and spleen. Int J Biochem Cell Biol 2013;45:816-825. https://doi.org/10.1016/j.biocel.2013.01.010
131. Chandel N. Evolution of mitochondria as signaling organelles. Cell Metab 2015;22:204-206. https://doi.org/10.1016/j.cmet.2015.05.013
132. Nunnari J, Suomalainen A. Mitochondria: in sickness and in health. Cell 2012;148:1145-1159. https://doi.org/10.1016/j.cell.2012.02.035
133. Durieux J, Wolff S, Dillin A. The cell-non-autonomous nature of electron transport chain-mediated longevity. Cell 2011;144:79-91. https://doi.org/10.1016/j.cell.2010.12.016

134. Forsstrom S, Jackson CB, Carroll CJ, Kuronen M, Pirinen E, Pradhan S, Marmyleva A, Auranen M, Kleine IM, Khan NA, Roivainen A, Marjamäki P, Liljenbäck H, Wang L, Battersby BJ, Richter U, Velagapudi V, Nikkanen J, Euro L, Suomalainen A. Fibroblast growth factor 21 drives dynamics of local and systemic stress responses in mitochondrial myopathy with mtDNA deletions. Cell Metab 2019;30:1040-1054.e7. https://doi.org/10.1016/j.cmet.2019.08.019
135. Tyynismaa H, Carroll CJ, Raimundo N, Ahola-Erkkila S, Wenz T, Ruhanen H, Guse K, Hemminki A, Peltola-Mjosund KE, Tulkki V, Oresic M, Moraes CT, Pietiläinen K, Hovatta I, Suomalainen A. Mitochondrial myopathy induces a starvation-like response. Hum Mol Genet 2010;19:3948-3958. https://doi.org/10.1093/hmg/ddq310
136. Cardamone MD, Tanasa B, Cederquist CT, Huang J, Mahdaviani K, Li W, Rosenfeld MG, Liesa M, Perissi V. Mitochondrial retrograde signaling in mammals is mediated by the transcriptional cofactor GPS2 via direct mitochondria-to-nucleus translocation. Mol Cell 2018;69:757-772.e7. https://doi.org/10.1016/j.molcel.2018.01.037
137. Kim KH, Son JM, Benayoun BA, Lee C. The mitochondrial-encoded peptide MOTS-c translocates to the nucleus to regulate nuclear gene expression in response to metabolic stress. Cell Metab 2018;28;516-524.e7. https://doi.org/10.1016/j.cmet.2018.06.008
138. Nargund AM, Pellegrino MW, Fiorese CJ, Baker BM, Haynes CM. Mitochondrial import efficiency of ATFS-1 regulates mitochondrial UPR activation. Science 2012;337:587-590. https://doi.org/10.1126/science.1223560
139. West AP, Khoury-Hanold W, Staron M, Tal MC, Pineda CM, Lang SM, Bestwick M, Duguay BA, Raimundo N, MacDuff DA, Kaech SM, Smiley JR, Means RE, Iwasaki A, Shadel GS. Mitochondrial DNA stress primes the antiviral innate immune response. Nature 2015;520:553-557. https://doi.org/10.1038/nature14156
140. Lozoya OA, Martinez-Reyes I, Wang T, Grenet D, Bushel P, Li J, Chandel N, Woychik RP, Santos JH. Mitochondrial nicotinamide adenine dinucleotide reduced (NADH) oxidation links the tricarboxylic acid (TCA) cycle with methionine metabolism and nuclear DNA methylation. PLoS Biol 2018;16:e2005707. https://doi.org/10.1371/journal.pbio.2005707
141. Picard M, Zhang J, Hancock S, Derbeneva O, Golhar R, Golik P, O'Hearn S, Levy S, Potluri P, Lvova M, Davila A, Lin CS, Perin JC, Rappaport EF, Hakonarson H, Trounce IA, Procaccio V, Wallace DC. Progressive increase in mtDNA 3243A>G heteroplasmy causes abrupt transcriptional reprogramming. Proc Natl Acad Sci U S A 2014;111:E4033-E4042. https://doi.org/10.1073/pnas.1414028111
142. Smiraglia D, Kulawiec M, Bistulfi GL, Ghoshal S, Singh KK. A novel role for mitochondria in regulating epigenetic modifications in the nucleus. Cancer Biol Ther 2008;7:1182-1190. https://doi.org/10.4161/cbt.7.8.6215
143. Tian Y, Garcia G, Bian Q, Steffen K, Joe L, Wolff S, Meyer B, Dillin A. Mitochondrial stress induces chromatin reorganization to promote longevity and UPR(mt). Cell 2016;165:1197-1208. https://doi.org/10.1016/j.cell.2016.04.011
144. Vizioli MG, Liu T, Miller KN, Robertson NA, Gilroy K, Lagnado AB, Perez-Garcia A, Kiourtis C, Dasgupta N, Lei X, Kruger PJ, Nixon C, Clark W, Jurk D, Bird TG, Passos JF, Berger SL, Dou Z, Adams PD. Mitochondria-to-nucleus retrograde signaling drives formation of cytoplasmic chromatin and inflammation in senescence. Genes Dev 2020;34:428-445. https://doi.org/10.1101/gad.331272.119
145. Qian W, Kumar N, Roginskaya V, Fouquerel E, Opresko PL, Shiva S, Watkins SC, Kolodieznyi D, Bruchez MP, Van Houten B. Chemoptogenetic damage to mitochondria causes rapid telomere dysfunction. Proc Natl Acad Sci U S A 2019;116:18435-18444. https://doi.org/10.1073/pnas.1910574116
146. Lozoya OA, Xu F, Grenet D, Wang T, Grimm SA, Godfrey V, Waidyanatha S, Woychik RP, Santos JH. Single nucleotide resolution analysis reveals pervasive, long-lasting DNA methylation changes by developmental exposure to a mitochondrial toxicant. Cell Rep 2020;32:108131. https://doi.org/10.1016/j.celrep.2020.108131
147. Correia-Melo C, Marques FD, Anderson R, Hewitt G, Hewitt R, Cole J, Carroll BM, Miwa S, Birch J, Merz A, Rushton MD, Charles M, Jurk D, Tait SW, Czapiewski R, Greaves L, Nelson G, Bohlooly-Y M, Rodriguez-Cuenca S, Vidal-Puig A, Mann D, Saretzki G, Quarato G, Green DR, Adams PD, von Zglinicki T, Korolchuk VI, Passos JF.Mitochondria are required for pro-ageing features of the senescent phenotype. EMBO J 2016;35:724-742. https://doi.org/10.15252/embj.201592862
148. Nelson G, Kucheryavenko O, Wordsworth J, von Zglinicki T. The senescent bystander effect is caused by ROS-activated NF-kB signalling. Mech Ageing Dev 2018;170:30-36. https://doi.org/10.1016/j.mad.2017.08.005

149. da Silva PFL, Ogrodnik M, Kucheryavenko O, Glibert J, Miwa S, Cameron K, Ishaq A, Saretzki G, Nagaraja-Grellscheid S, Nelson G, von Zglinicki T. The bystander effect contributes to the accumulation of senescent cells in vivo. Aging Cell 2019;18:e12848. https://doi.org/10.1111/acel.12848
150. Ježek P, Jabůrek M. Plecitá-Hlavatá L. Contribution of oxidative stress and impaired biogenesis of pancreatic beta-cells to type 2 diabetes. Antioxid Redox Signal 2019;31:722-751. https://doi.org/10.1089/ars.2018.7656
151. Balaban RS, Nemoto S, Finkel T. Mitochondria, oxidants, and aging. Cell 2005;120:483-495. https://doi.org/10.1016/j.cell.2005.02.001
152. Shadel G, Horvath T. Mitochondrial ROS signaling in organismal homeostasis. Cell 2015;163:560-569. https://doi.org/10.1016/j.cell.2015.10.001
153. Al-Mehdi AB, Pastukh VM, Swiger BM, Reed DJ, Patel MR, Bardwell GC, Pastukh VV, Alexeyev MF, Gillespie MN. Perinuclear mitochondrial clustering creates an oxidant-rich nuclear domain required for hypoxia-induced transcription. Sci Signal 2012;5:ra47. https://doi.org/10.1126/scisignal.2002712
154. Desai R, East DA, Hardy L, Faccenda D, Rigon M, Crosby J, Alvarez MS, Singh A, Mainenti M, Hussey LK, Bentham R, Szabadkai G, Zappulli V, Dhoot GK, Romano LE, Xia D, Coppens I, Hamacher-Brady A, Chapple JP, Abeti R, Fleck RA, Vizcay-Barrena G, Smith K, Campanella M.Mitochondria form contact sites with the nucleus to couple prosurvival retrograde response. Sci Adv 2020;6:eabc9955. https://doi.org/10.1126/sciadv.abc9955
155. Chouchani ET, Kazak L, Jedrychowski MP, Lu GZ, Erickson BK, Szpyt J, Pierce KA, Laznik-Bogoslavski D, Vetrivelan R, Clish CB, Robinson AJ, Gygi SP, Spiegelman BM. Mitochondrial ROS regulate thermogenic energy expenditure and sulfenylation of UCP1. Nature 2016;532:112-116. https://doi.org/10.1038/nature17399
156. Ježek P, Jabůrek M, Porter RK. Uncoupling mechanism and redox regulation of mitochondrial uncoupling protein 1 (UCP1). Biochim Biophys Acta 2019;1860:259-269. https://doi.org/10.1016/j.bbabio.2018.11.007
157. Fu ZX, Tan X, Fang H, Lau PM, Wang X, Cheng H, Bi GQ. Dendritic mitoflash as a putative signal for stabilizing long-term synaptic plasticity. Nat Commun 2017;8:31. https://doi.org/10.1038/s41467-017-00043-3
158. Horn A, Raavicharla S, Shah S, Cox D, Jaiswal JK. Mitochondrial fragmentation enables localized signaling required for cell repair. J Cell Biol 2020;219:e201909154. https://doi.org/10.1083/jcb.201909154
159. Fuhrmann DC, Brune B. Mitochondrial composition and function under the control of hypoxia. Redox Biol 2017;12:208-215. https://doi.org/10.1016/j.redox.2017.02.012
160. Pan Y, Mansfield KD, Bertozzi CC, Rudenko V, Chan DA, Giaccia AJ, Simon MC. Multiple factors affecting cellular redox status and energy metabolism modulate hypoxia-inducible factor prolyl hydroxylase activity in vivo and in vitro. Mol Cell Biol 2007;27:912-925. https://doi.org/10.1128/MCB.01223-06
161. Appelhoff RJ, Tian YM, Raval RR, Turley H, Harris AL, Pugh CW, Ratcliffe PJ, Gleadle JM. Differential function of the prolyl hydroxylases PHD1, PHD2, and PHD3 in the regulation of hypoxia-inducible factor. J Biol Chem 2004;279:38458-38465. https://doi.org/10.1074/jbc.M406026200
162. Lu H, Dalgard CL, Mohyeldin A, McFate T, Tait AS, Verma A. Reversible inactivation of HIF-1 prolyl hydroxylases allows cell metabolism to control basal HIF-1. J Biol Chem 2005;280:41928-41939. https://doi.org/10.1074/jbc.M508718200
163. Samanta D, Semenza GL. Maintenance of redox homeostasis by hypoxia-inducible factors. Redox Biol 2017;13:331-335. https://doi.org/10.1016/j.redox.2017.05.022
164. Ivan M, Kondo K, Yang H, Kim W, Valiando J, Ohh M, Salic A, Asara JM, Lane WS, Kaelin WG, Jr. HIFalpha targeted for VHL-mediated destruction by proline hydroxylation: Implications for O2 sensing. Science 2001;292:464-468. https://doi.org/10.1126/science.1059817
165. Jaakkola P, Mole DR, Tian YM, Wilson MI, Gielbert J, Gaskell SJ, von Kriegsheim A, Hebestreit HF, Mukherji M, Schofield CJ, Maxwell PH, Pugh CW, Ratcliffe PJ. Targeting of HIF-alpha to the von Hippel-Lindau ubiquitylation complex by O2-regulated prolyl hydroxylation. Science 2001;292:468-472. https://doi.org/10.1126/science.1059796
166. Semenza GL. Regulation of Erythropoiesis by the Hypoxia-Inducible Factor Pathway: Effects of Genetic and Pharmacological Perturbations. Annu Rev Med 2023;74:307-319. https://doi.org/10.1146/annurev-med-042921-102602
167. Brocato J, Chervona Y, Costa M. Molecular responses to hypoxia-inducible factor 1alpha and beyond. Mol Pharmacol 2014;85:651-657. https://doi.org/10.1124/mol.113.089623
168. Schodel J, Oikonomopoulos S, Ragoussis J, Pugh CW, Ratcliffe PJ, Mole DR. High-resolution genome-wide mapping of HIF-binding sites by ChIP-seq. Blood 2011;117:e207-e217. https://doi.org/10.1182/blood-2010-10-314427

169. Semenza GL. Hypoxia-inducible factors in physiology and medicine. Cell 2012;148:399-408. https://doi.org/10.1016/j.cell.2012.01.021
170. Semenza GL. The Genomics and Genetics of Oxygen Homeostasis. Annu Rev Genomics Hum Genet 2020;21:183-204. https://doi.org/10.1146/annurev-genom-111119-073356
171. Wicks EE, Semenza GL. Hypoxia-inducible factors: cancer progression and clinical translation. J Clin Invest 2022;132:e159839. https://doi.org/10.1172/JCI159839
172. Zepeda AB, Pessoa A Jr, Castillo RL, Figueroa CA, Pulgar VM, Farias JG. Cellular and molecular mechanisms in the hypoxic tissue: Role of HIF-1 and ROS. Cell Biochem Funct 2013;31:451-459. https://doi.org/10.1002/cbf.2985
173. Gerald D, Berra E, Frapart YM, Chan DA, Giaccia AJ, Mansuy D, Pouyssegur J, Yaniv M, Mechta-Grigoriou F. JunD reduces tumor angiogenesis by protecting cells from oxidative stress. Cell 2004;118:781-794. https://doi.org/10.1016/j.cell.2004.08.025
174. Briggs KJ, Koivunen P, Cao S, Backus KM, Olenchock BA, Patel H, Zhang Q, Signoretti S, Gerfen GJ, Richardson AL, Witkiewicz AK, Cravatt BF, Clardy J, Kaelin WG Jr. Paracrine Induction of HIF by Glutamate in Breast Cancer: EglN1 Senses Cysteine. Cell 2016;166:126-139. https://doi.org/10.1016/j.cell.2016.05.042
175. Chowdhury R, Flashman E, Mecinovic J, Kramer HB, Kessler BM, Frapart YM, Boucher JL, Clifton IJ, McDonough MA, Schofield CJ. Studies on the reaction of nitric oxide with the hypoxia-inducible factor prolyl hydroxylase domain 2 (EGLN1). J Mol Biol 2011;410:268-279. https://doi.org/10.1016/j.jmb.2011.04.075
176. Lee G, Won HS, Lee YM, Choi JW, Oh TI, Jang JH, Choi DK, Lim BO, Kim YJ, Park JW, Puigserver P, Lim JH. Oxidative Dimerization of PHD2 is Responsible for its Inactivation and Contributes to Metabolic Reprogramming via HIF-1alpha Activation. Sci Rep 2016;6:18928. https://doi.org/10.1038/srep18928
177. Hewitson KS, Lienard BM, McDonough MA, Clifton IJ, Butler D, Soares AS, Oldham NJ, McNeill LA, Schofield CJ. Structural and mechanistic studies on the inhibition of the hypoxia-inducible transcription factor hydroxylases by tricarboxylic acid cycle intermediates. J Biol Chem 2007;282:3293-3301. https://doi.org/10.1074/jbc.M608337200
178. Koivunen P, Hirsila M, Remes AM, Hassinen IE, Kivirikko KI, Myllyharju J. Inhibition of hypoxia-inducible factor (HIF) hydroxylases by citric acid cycle intermediates: Possible links between cell metabolism and stabilization of HIF. J Biol Chem 2007;282:4524-4532. https://doi.org/10.1074/jbc.M610415200
179. Martínez-Reyes I, Diebold LP, Kong H, Schieber M, Huang H, Hensley CT, Mehta MM, Wang T, Santos JH, Woychik R, Dufour E, Spelbrink JN, Weinberg SE, Zhao Y, DeBerardinis RJ, Chandel NS. TCA Cycle and Mitochondrial Membrane Potential Are Necessary for Diverse Biological Functions. Mol Cell 2016;61:199-209. https://doi.org/10.1016/j.molcel.2015.12.002
180. Bell EL, Klimova TA, Eisenbart J, Moraes CT, Murphy MP, Budinger GR, Chandel NS. The Qo site of the mitochondrial complex III is required for the transduction of hypoxic signaling via reactive oxygen species production. J Cell Biol 2007;177:1029-1036. https://doi.org/10.1083/jcb.200609074
181. Nguyen LK, Cavadas MA, Scholz CC, Fitzpatrick SF, Bruning U, Cummins EP, Tambuwala MM, Manresa MC, Kholodenko BN, Taylor CT, Cheong A. A dynamic model of the hypoxia-inducible factor 1alpha (HIF-1alpha) network. J Cell Sci 2013;126:1454-1463. https://doi.org/10.1242/jcs.119974
182. Plecitá-Hlavatá L, Ježek J. Ježek P. Aglycemia keeps mitochondrial oxidative phosphorylation under hypoxic conditions in HepG2 cells. J Bioenerg Biomembr 2015;47:467-476. https://doi.org/10.1007/s10863-015-9628-6
183. Hernansanz-Agustín P, Ramos E, Navarro E, Parada E, Sánchez-López N, Peláez-Aguado L, Cabrera-García JD, Tello D, Buendia I, Marina A, Egea J, López MG, Bogdanova A, Martínez-Ruiz A. Mitochondrial complex I deactivation is related to superoxide production in acute hypoxia. Redox Biol 2017;12:1040-1051. https://doi.org/10.1016/j.redox.2017.04.025
184. Chandel NS, Maltepe E, Goldwasser E, Mathieu CE, Simon MC, Schumacker PT. Mitochondrial reactive oxygen species trigger hypoxia-induced transcription. Proc Natl Acad Sci U S A 1998;95:11715-11720. https://doi.org/10.1073/pnas.95.20.11715
185. Comito G, Calvani M, Giannoni E, Bianchini F, Calorini L, Torre E, Migliore C, Giordano S, Chiarugi P. HIF-1alpha stabilization by mitochondrial ROS promotes Met-dependent invasive growth and vasculogenic mimicry in melanoma cells. Free Radic Biol Med 2011;51:893-904. https://doi.org/10.1016/j.freeradbiomed.2011.05.042

186. Guzy RD, Hoyos B, Robin E, Chen H, Liu L, Mansfield KD, Simon MC, Hammerling U, Schumacker PT. Mitochondrial complex III is required for hypoxia-induced ROS production and cellular oxygen sensing. Cell Metab 2005;1:401-408. https://doi.org/10.1016/j.cmet.2005.05.001
187. Schroedl C, McClintock DS, Budinger GR, Chandel NS. Hypoxic but not anoxic stabilization of HIF-1alpha requires mitochondrial reactive oxygen species. Am J Physiol 2002;283:L922-L931. https://doi.org/10.1152/ajplung.00014.2002
188. Ježek J, Plecitá-Hlavatá L, Ježek P. Aglycemic HepG2 cells switch from aminotransferase glutaminolytic pathway of pyruvate utilization to complete Krebs cycle at hypoxia. Front Endocrinol 2018;9:637. https://doi.org/10.3389/fendo.2018.00637
189. Patten DA, Lafleur VN, Robitaille GA, Chan DA, Giaccia AJ, Richard DE. Hypoxia-inducible factor-1 activation in nonhypoxic conditions: The essential role of mitochondrial-derived reactive oxygen species. Mol Biol Cell 2010;21:3247-3257. https://doi.org/10.1091/mbc.e10-01-0025
190. Brunelle JK, Bell EL, Quesada NM, Vercauteren K, Tiranti V, Zeviani M, Scarpulla RC, Chandel NS. Oxygen sensing requires mitochondrial ROS but not oxidative phosphorylation. Cell Metab 2005;1:409-414. https://doi.org/10.1016/j.cmet.2005.05.002
191. Pi J, Bai Y, Zhang Q, Wong V, Floering LM, Daniel K, Reece JM, Deeney JT, Andersen ME, Corkey BE, Collins S. Reactive oxygen species as a signal in glucose-stimulated insulin secretion. Diabetes 2007;56:1783-1791. https://doi.org/10.2337/db06-1601
192. Ashcroft FM, Rorsman P. Diabetes mellitus and the β cell: the last ten years. Cell 2012;148:1160-1171. https://doi.org/10.1016/j.cell.2012.02.010
193. Ho T, Potapenko E, Davis DB, Merrins MJ. A plasma membrane-associated glycolytic metabolon is functionally coupled to KATP channels in pancreatic α and β cells from humans and mice. Cell Rep 2023;42:112394. https://doi.org/10.1016/j.celrep.2023.112394
194. Plecitá-Hlavatá L, Jabůrek M, Holendová B, Tauber J, Pavluch V, Berková Z, Cahová M, Schröder K, Brandes RP, Siemen D, Ježek P. Glucose-Stimulated Insulin Secretion Fundamentally Requires H2O2 Signaling by NADPH Oxidase 4. Diabetes 2020;69:1341-1354. https://doi.org/10.2337/db19-1130
195. Yosida M, Dezaki K, Uchida K, Kodera S, Lam NV, Ito K, Rita RS, Yamada H, Shimomura K, Ishikawa SE, Sugawara H, Kawakami M, Tominaga M, Yada T, Kakei M. Involvement of cAMP/EPAC/TRPM2 activation in glucose- and incretin-induced insulin secretion. Diabetes 2014;63:3394-3403. https://doi.org/10.2337/db13-1868
196. Spégel P, Sharoyko VV, Goehring I, Danielsson AP, Malmgren S, Nagorny CL, Andersson LE, Koeck T, Sharp GW, Straub SG, Wollheim CB, Mulder H. Time-resolved metabolomics analysis of β-cells implicates the pentose phosphate pathway in the control of insulin release. Biochem J 2013;450:595-605. https://doi.org/10.1042/BJ20121349
197. Plecitá-Hlavatá L, Engstová H, Holendová B, Tauber J, Špaček T, Petrásková L, Křen V, Špačková J, Gotvaldová K, Ježek J, Dlasková A, Smolková K, Ježek P. Mitochondrial Superoxide Production Decreases on Glucose-Stimulated Insulin Secretion in Pancreatic β Cells Due to Decreasing Mitochondrial Matrix NADH/NAD+ Ratio. Antioxid Redox Signal 2020;33:789-815. https://doi.org/10.1089/ars.2019.7800
198. Jitrapakdee S, Wutthisathapornchai A, Wallace JC, MacDonald MJ. Regulation of insulin secretion: role of mitochondrial signalling. Diabetologia 2010;53:1019-1032. https://doi.org/10.1007/s00125-010-1685-0
199. Smolková K, Dvořák A, Zelenka J, Vítek L, Ježek P. Reductive carboxylation and 2-hydroxyglutarate formation by wild-type IDH2 in breast carcinoma cells. Int J Biochem Cell Biol 2015;65:125-133. https://doi.org/10.1016/j.biocel.2015.05.012
200. Lenzen S, Drinkgern J, Tiedge M. Low antioxidant enzyme gene expression in pancreatic islets compared with various other mouse tissues. Free Radic Biol Med 1996;20:463-466. https://doi.org/10.1016/0891-5849(96)02051-5
201. Ježek P, Dlasková A, Plecitá-Hlavatá L. Redox Homeostasis in Pancreatic β Cells. Oxid Med Cell Longev 2012;2012:932838. https://doi.org/10.1155/2012/932838
202. Lenzen S. Oxidative stress: the vulnerable beta-cell. Biochem Soc Trans 2008;36:343-347. https://doi.org/10.1042/BST0360343
203. Prentki M, Matschinsky FM, Madiraju SR. Metabolic signaling in fuel-induced insulin secretion. Cell Metab 2013;18:162-185. https://doi.org/10.1016/j.cmet.2013.05.018
204. Carpinelli AR, Picinato MC, Stevanato E, Oliveira HR, Curi, R. Insulin secretion induced by palmitate-a process fully dependent on glucose concentration. Diabetes Metab 2002;28:3S37-44.

205. Gehrmann W, Elsner M, Lenzen S. Role of metabolically generated reactive oxygen species for lipotoxicity in pancreatic β-cells. Diab Obes Metab 2010;12(Suppl 2):149-158. https://doi.org/10.1111/j.1463-1326.2010.01265.x
206. Graciano MF, Valle MM, Kowluru A, Curi R, Carpinelli AR. Regulation of insulin secretion and reactive oxygen species production by free fatty acids in pancreatic islets. Islets 2011;3:213-223. https://doi.org/10.4161/isl.3.5.15935
207. Cen J, Sargsyan E, Bergsten P. Fatty acids stimulate insulin secretion from human pancreatic islets at fasting glucose concentrations via mitochondria-dependent and -independent mechanisms. Nutr Metab (Lond) 2016;13:59. https://doi.org/10.1186/s12986-016-0119-5
208. Fernandez J, Valdeolmillos M. Increased levels of free fatty acids in fasted mice stimulate in vivo beta-cell electrical activity. Diabetes 1998;47:1707-1712. https://doi.org/10.2337/diabetes.47.11.1707
209. Hauke S, Keutler K, Phapale P, Yushchenko DA, Schultz C. Endogenous Fatty Acids Are Essential Signaling Factors of Pancreatic β-Cells and Insulin Secretion. Diabetes 2018;67:1986-1998. https://doi.org/10.2337/db17-1215
210. Ježek P, Jabůrek M, Holendová B, Plecitá-Hlavatá L. Fatty Acid-Stimulated Insulin Secretion vs. Lipotoxicity. Molecules 2018;23:1483. https://doi.org/10.3390/molecules23061483
211. Saadeh M, Ferrante TC, Kane A, Shirihai O, Corkey BE, Deeney JT. Reactive oxygen species stimulate insulin secretion in rat pancreatic islets: studies using mono-oleoyl-glycerol. PLoS One 2012;7:e30200. https://doi.org/10.1371/journal.pone.0030200
212. Leloup C, Tourrel-Cuzin C, Magnan C, Karaca M, Castel J, Carneiro L, Colombani AL, Ktorza A, Casteilla L, Pénicaud, L. Mitochondrial reactive oxygen species are obligatory signals for glucose-induced insulin secretion. Diabetes 2009;58,673-681. https://doi.org/10.2337/db07-1056
213. Yang HQ, Martinez-Ortiz W, Hwang J, Fan X, Cardozo TJ, Coetzee WA. Palmitoylation of the K(ATP)channel Kir6.2 subunit promotes channel opening by regulating PIP(2) sensitivity. Proc Natl Acad Sci U S A 2020;117:10593-10602. https://doi.org/10.1073/pnas.1918088117
214. Shigeto M, Ramracheya R, Tarasov AI, Cha CY, Chibalina MV, Hastoy B, Philippaert K, Reinbothe T, Rorsman N, Salehi A, Sones WR, Vergari E, Weston C, Gorelik J, Katsura M, Nikolaev VO, Vennekens R, Zaccolo M, Galione A, Johnson PR, Kaku K, Ladds G, Rorsman P. GLP-1 stimulates insulin secretion by PKC-dependent TRPM4 and TRPM5 activation. J Clin Invest 2015;125:4714-4728. https://doi.org/10.1172/JCI81975

Physiol. Res. 73 (Suppl. 1): S243-S278, 2024 *https://doi.org/10.33549/physiolres.935407*

REVIEW

Variability of Clinical Phenotypes Caused by Isolated Defects of Mitochondrial ATP Synthase

Kateřina TAUCHMANNOVÁ[1], Alena PECINOVÁ[1], Josef HOUŠTĚK[1], Tomáš MRÁČEK[1]

[1]Laboratory of Bioenergetics, Institute of Physiology of the Czech Academy of Sciences, Prague, Czech Republic

Received May 14, 2024
Accepted June 28, 2024

Summary
Disorders of ATP synthase, the key enzyme in mitochondrial energy supply, belong to the most severe metabolic diseases, manifesting as early-onset mitochondrial encephalo-cardiomyopathies. Since ATP synthase subunits are encoded by both mitochondrial and nuclear DNA, pathogenic variants can be found in either genome. In addition, the biogenesis of ATP synthase requires several assembly factors, some of which are also hotspots for pathogenic variants. While variants of *MT-ATP6* and *TMEM70* represent the most common cases of mitochondrial and nuclear DNA mutations respectively, the advent of next-generation sequencing has revealed new pathogenic variants in a number of structural genes and *TMEM70*, sometimes with truly peculiar genetics. Here we present a systematic review of the reported cases and discuss biochemical mechanisms, through which they are affecting ATP synthase. We explore how the knowledge of pathophysiology can improve our understanding of enzyme biogenesis and function.

Keywords
Mitochondrial diseases • ATP synthase • Nuclear DNA • Mitochondrial DNA • TMEM70

Corresponding author
Tomáš Mráček, Institute of Physiology of the Czech Academy of Sciences, Vídeňská 1083, 140 00 Prague 4, Czech Republic. E-mail: tomas.mracek@fgu.cas.cz

ATP synthase

Mammalian F_1F_o-ATP synthase (complex V) is mitochondrial enzyme, that is responsible for the production of more than 90 % of cellular ATP. To produce ATP, F_1F_o-ATP synthase operates in synthetic mode. In this mode, energy from the proton gradient, generated by the respiratory chain complexes, is used for phosphorylation of ADP to ATP. However, since it belongs to the family of ATPases, it can also catalyze ATP hydrolysis. In the so-called reverse mode, hydrolysis of ATP to ADP powers the proton pumping from mitochondrial matrix to inter-membrane space [1]. Human ATP synthase is composed of 18 different subunits, encoded by both nuclear DNA (nDNA) and mitochondrial DNA (mtDNA). Structurally it can be divided into three parts (Fig. 1A). Subunits α and β form $\alpha_3\beta_3$ hexamer, where the ADP↔ATP conversion takes place, and together with γ, δ and ε subunits, they constitute F_1 catalytic part. Membrane-embedded F_o part is composed of a bunch of small subunits, including *e*, *f*, *g*, DAPIT (diabetes-associated protein in insulin sensitive tissues), MLQ, 8 copies of subunit *c* (c_8 ring), and two mtDNA-encoded subunits *a* and A6L. Proton translocation across the inner mitochondrial membrane occurs within the F_o domain, on the interface between the ring of subunits *c* and subunit *a*. The third structural component, so-called peripheral stalk, contains subunits *b*, *d*, F_6 and OSCP (oligomycin-sensitivity conferring protein) [2]. The pe-ripheral stalk is stationary and immobilizes the $\alpha_3\beta_3$ hexamer. In contrast, the central stalk (composed of γ, δ, and ε subunits) and c_8 represent the rotor – it transfers the torque between F_1 and F_o domains and, depending on the direction, allows ADP phosphorylation or ATP hydrolysis. The last subunit associated with F_1F_o-ATP synthase is inhibitory factor IF_1. IF_1 binds to the F_1 part under certain circumstances, for example, under low pH or during assembly, and inhibits the hydrolytic activity of ATP synthase [3,4].

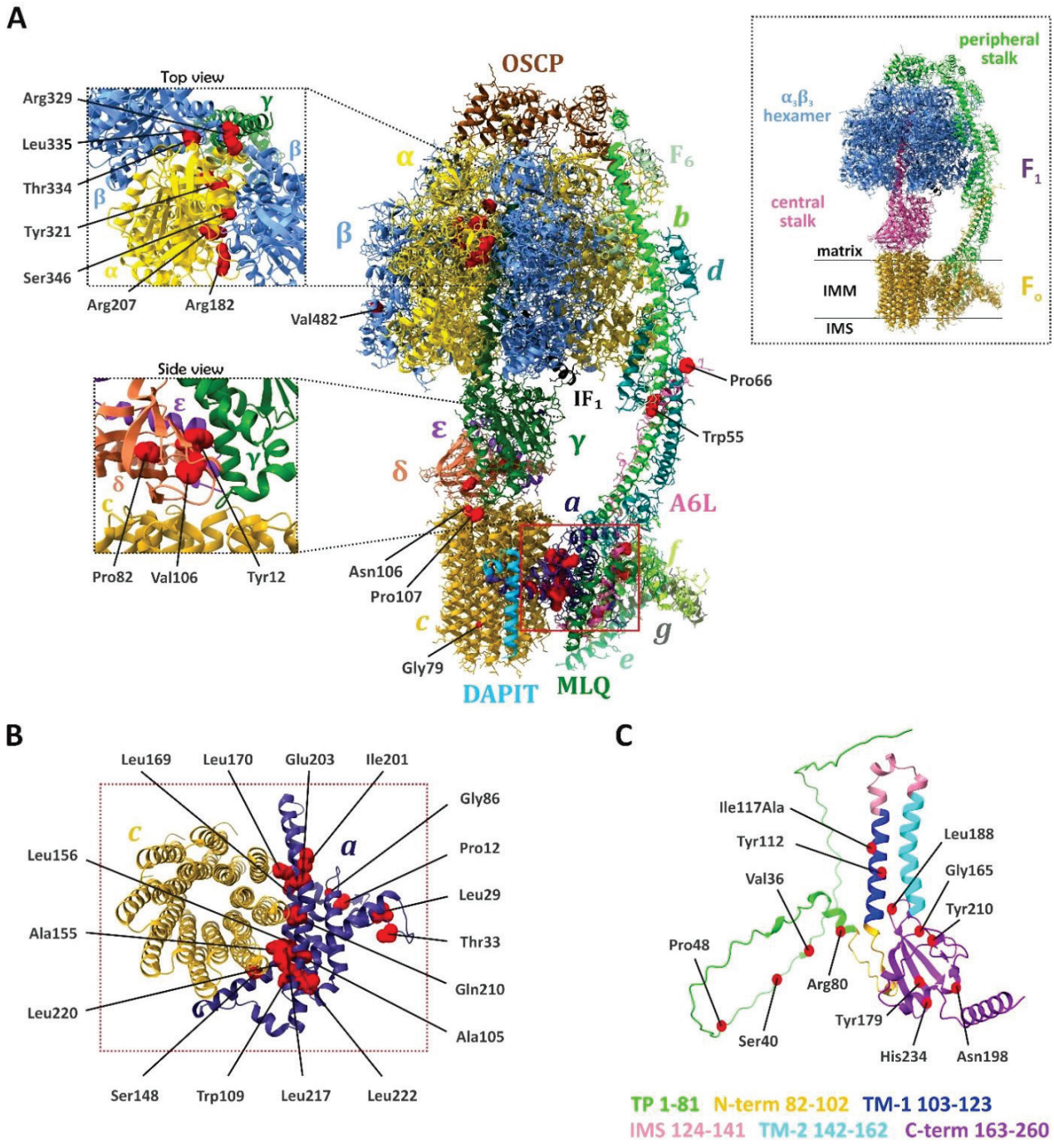

Fig. 1. Human ATP synthase and its pathogenic variants. **(A)** Structure of human ATP synthase, created in UCSF ChimeraX version 1.7.1, adapted from cryo-EM structure, model 8h9s Human ATP synthase state 1 (combined), https://doi.org/10.2210/pdb8H9S/pdb [2]. DAPIT protein is added from the cryo-EM structure of bovine F_o part, model 6zbb Bovine ATP synthase Fo domain, https://doi.org/10.2210/pdb6ZBB/pdb [184]. C-terminal part of subunit A6L (AA 52-68) is from AlphaFold computed structure, model AF-P03928-F1 [185,186]. Subunits of ATP synthase affected by both nDNA or mtDNA pathogenic variants are in color – α (yellow), β (blue), δ (coral), ε (purple), OSCP (brown), *c* (gold), DAPIT (cyan), *a* (dark blue) and A6L (pink). The remaining subunits are in various shades of green. Affected amino acids (red) are in sphere mode, remaining residues in stick mode. Only name and number of the residue is listed, for details about AA change and respective pathogenic variant see Table 2+3. Pathogenic variants of α, β, δ, and ε subunits are visualized in detail in black dashed boxes on the left (top view for α and β; side view for δ and ε). Black dashed box on the right: ATP synthase complex divided into structural parts: $α_3β_3$ hexamer (blue) together with central stalk (pink) form F_1 catalytic part; peripheral stalk (green); F_o membrane-embedded part (gold). IMM – inner mitochondrial membrane, IMS – intermembrane space. Pathogenic variants of subunit *a* (red box) are visualized in detail in red dashed box in part **(B)** of the figure (top view). Affected regions of DAPIT and OSCP subunits are not visualized since they lead to the loss of full-length mature protein. **(C)** Structure of human TMEM70 protein and its pathogenic variants. AlphaFold computed structure, model AF-Q9BUB7-F1 [185,186]. Transit peptide (TP) in green, N-terminal part (N-term) in yellow, transmembrane domain 1 (TM-1) in dark blue, intermembrane space loop (IMS) in pink, transmembrane domain 2 (TM-2) in light blue, C-terminal part (C-term) in purple. Affected positions labeled with red bal. Only name and number of the residue is listed, for details about amino acid change and respective pathogenic variant see Table 4.

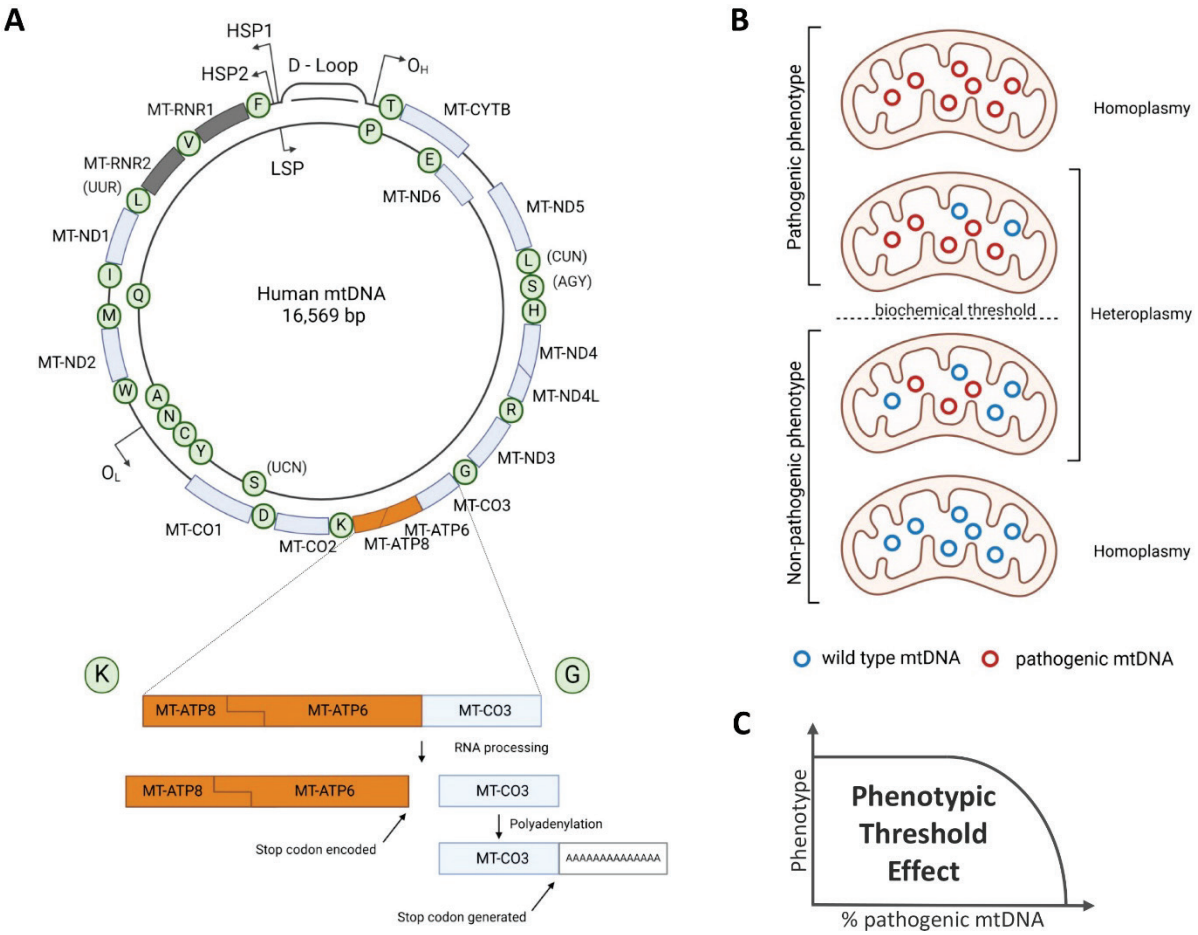

Fig. 2. (A) Human mitochondrial DNA encodes for 13 protein coding genes (light blue), the 22 tRNAs (green) and 2 rRNAS (grey). The origin of outer heavy strand (OH) and inner light strand (OL) are depicted. Transcription is bidirectional, initiated in D-loop control region from three promoters HSP1, HSP2 and LSP. Scheme of polycistronic MT-ATP8/MT-ATP6/MT-CO3 mRNA transcript is shown in detail (adapted from Ng 2022, 36399564). **(B)** Scheme of mtDNA heteroplasmy. The mtDNA in mitochondria are homoplasmic when all mtDNA copies are either wild type or mutant, the percentage of pathogenic mtDNA determines the mtDNA heteroplasmy. Biochemical threshold indicates the limiting amount of the pathogenic mtDNA above which the pathogenic phenotype manifests **(C).** Part **(A)** and **(B)** Created with BioRender.com. Part **(C)** adopted from Rossignol et al. [25].

The biogenesis and assembly of F_1F_o-ATP synthase is a complex process, due to its multisubunit composition, localization in the inner mitochondrial membrane, and two genomes-origin. In yeast, numerous assembly factors were described, with only a subset of them having mammalian homologs. Those conserved from yeast to humans include ATPAF1 and ATPAF2 (ATP11 and ATP12 in yeast), which are necessary for $\alpha_3\beta_3$ hexamer formation [5], and FMC1 homolog (or c7orf55, homolog of yeast FMC1 protein), which was suggested to play a role in this process as well [6]. On the other hand, two described assembly factors are specific for higher eukaryotes. TMEM70 and TMEM242 proteins are involved in the assembly of c_8 ring and its association with ATP synthase complex. However, the exact mechanism of their function is still not completely explained [7,8]. The last factor presumed to be involved in the assembly of ATP synthase in mammals is Prickle planar cell polarity protein 3 encoded by *PRICKLE3* gene [9].

Mitochondrial diseases

From an organismal perspective, mitochondria are the predominant source of ATP. Glycolysis can substitute for mitochondrial ATP production, but only in an organ or time limited fashion. Therefore, mitochondrial dysfunctions manifest in the tissues with high energy demands such as heart, brain, liver, or skeletal muscle, and frequently lead to metabolic diseases. Another consequence of defective oxidative phosphorylation system (OXPHOS) is increased oxidative stress, a condition also linked with human pathologies [10]. As a consequence of this, mitochondrial defects are associated with a broad range of clinical phenotypes. They range from early-onset,

severe and devastating encephalo-cardiomyopathies to late-onset and milder forms of mitochondrial diseases. However, they also include polygenic neuro-degenerative diseases, such as Alzheimer's disease, Parkinson's disease, multiple sclerosis; motor neuron diseases (amyotrophic lateral sclerosis); metabolic disorders, such as obesity and diabetes; metabolic syndrome; cancer; and aging [10-18]. Due to the dual genetic origin of OXPHOS system, mitochondrial diseases can be caused by pathogenic variants/mutations of either nuclear or mitochondrial genomes. Historically, maternally transmitted mtDNA (Fig. 2A) was more accessible for genetic studies, which led to extensive characterization of its mutational landscape. To date, over a thousand pathogenic variants in mtDNA have been described (MITOMAP: A Human Mitochondrial Genome Database http://mitomap.org, 2023, [19]) and their detection have become rather routine task [20,21]. However, according to current estimates, mtDNA variants are responsible for only ~15 % of mitochondrial diseases in the pediatric population [22]. Consequently, pathogenic variants of nuclear genes are more prevalent, while their identification and especially functional validation still represent a challenge.

Pathogenic variants of genes associated with isolated ATP synthase deficiency are summarized in Table 1. Approximately 60 % (38 out of 63) of the variants are encoded by nDNA, but this may be skewed by the fact, that only truly pathogenic variants of mtDNA are considered (for criteria, please see section "ATP synthase deficiencies associated with pathogenic variants of mtDNA"). Of these, 20 are localized in *TMEM70* gene, which encodes ATP synthase assembly factor, representing a slight majority of nDNA pathogenic variants.

The remaining nDNA pathogenic variants are in genes encoding seven structural subunits, three of which are directly involved in the production of ATP. This means that to date, no pathogenic variant has been described for nine nDNA genes encoding structural subunits of ATP synthase. We can only speculate, whether this suggests greater level of sequence flexibility for structural subunits compared to catalytic ones or

Table 1. The number of pathogenic variants of genes related to isolated ATP synthase deficiency. For mtDNA genes encoding structural subunits of ATP synthase, the number of pathogenic variants discussed in this review is given, along with the total number of variants reported according to MITOMAP in parentheses. *MT-ATP8* variants include one in *MT-ATP8/MT-ATP6* overlapping region affecting only A6L subunit, similarly *MT-ATP6* variants include one in *MT-ATP8/MT-ATP6* overlapping region affecting only subunit *a*, *MT-ATP8/MT-ATP6* variants include those affecting both subunits. For nDNA genes, the total number of pathogenic variants reported is given, with compound heterozygous combinations counted as one variant (or being counted as a single variant).

mtDNA: structural subunits		**nDNA: structural subunits**		**nDNA: assembly factors**	
Gene	**No. of pathogenic variants (MITOMAP)**	**Gene**	**No. of pathogenic variants**	**Gene**	**No. of pathogenic variants**
MT-ATP8	1 (13)	*ATP5F1A*	5	*ATPAF1*	0
MT-ATP8/MT-ATP6	3 (5)	*ATP5F1B*	3	*ATPAF2*	1
MT-ATP6	21 (78)	*ATP5F1C*	0	*TMEM70*	20
		ATP5F1D	2	*TMEM242*	0
		ATP5F1E	1	*FMC1*	0
		ATP5PB	0		
		ATP5PD	0		
		ATP5PF	0		
		ATP5PO	2		
		ATP5MC	3		
		ATP5ME	0		
		ATP5MF	0		
		ATP5MG	0		
		ATP5MJ	0		
		ATP5MK	1		
		ATP5IF1	0		

whether pathogenic variants in the remaining subunits will be identified in the future. However, in the case of the only two mtDNA-encoded structural subunits of ATP synthase, it seems that the functional versus structural significance could really be the key factor. For *MT-ATP6* gene, which encodes the subunit directly involved in the production of ATP, approximately 80 variants have been described to date. However, the majority of these have not yet been confirmed as pathogenic. In contrast, for *MT-ATP8* gene, which encodes a subunit with an unknown function, only 13 variants with a predominantly unclear pathogenicity have been described. Moreover, in the case of *MT-ATP6*, pathogenic variants are distributed throughout the entire sequence, while *MT-ATP8* variants with the strongest pathogenic potential are localized at the end of the gene. This suggests that the C-terminal part of this subunit requires more specific fold without the room for any wobble. It is also noteworthy that five pathogenic variants, affecting both subunits, have been reported in *MT-ATP8/MT-ATP6* overlapping region (Fig. 2A).

Mitochondrial DNA pathogenic variants

In pediatric cases, pathogenic variants in mtDNA are often associated with severe metabolic defects, and to a lesser extent also with neurodegenerative syndromes, deafness, optic neuropathy, and other diseases. Approximately 550 of mtDNA pathogenic variants in structural genes for subunits of respiratory complex I, III and IV, as well as of ATP synthase, and more than 450 pathogenic variants in tRNAs or rRNAs, have been described. These include point substitutions and simple deletions or insertions (MITOMAP). The majority of mtDNA pathogenic variants are single nucleotide substitutions that result in a missense codon and replacement of respective amino acid (AA) with a different one. Less often, a premature stop codon is created, or a shift in the reading frame may occur due to nonsense or frameshift variants. In addition to maternally inherited point variants, more than a hundred mainly somatic deletions or insertions of large mtDNA regions were described (MITOMAP).

Clinical and biochemical phenotypes of the patients with mtDNA pathogenic variants can vary considerably between individuals harboring the same variant. This may reflect different nuclear genetic background of the patients since similar symptoms or group of symptoms can be observed within one family but vary between different families. Physiological variability in mtDNA may also influence the clinical presentation of a pathogenic variant in either way. Some mtDNA variants may serve as disease modifiers in a negative [23] or positive [24] manner. It is not uncommon for members of the same family carrying the same variant(s) to present with phenotypes ranging from none or very mild to severe. This variability can be explained by the phenomenon of mtDNA heteroplasmy, which refers the percentage of pathogenic mtDNA within a single cell, which typically contains several thousands of copies of mtDNA (Fig. 2B). In many cases, the degree of mu-tational load determines the pathogenic phenotype. In the most severe cases, all copies of mtDNA are pathogenic (also known as mtDNA homoplasmy). It is important to note that the relationship between heteroplasmy and disease progression is often not linear and exerts a phenotypic threshold effect when the disease starts to manifest (Fig. 2C) [25]. The key factor may not be just the level of heteroplasmy itself, but rather its variability across tissues. Individuals carrying similar mutational loads throughout the whole body, as well as patients with a broad span of heteroplasmy levels between tissues, are well described. For instance, m.8618-8619insT, which was identified in two patients exhibiting a predominantly neuro-muscular phenotype, was detected at relatively low levels in the blood (approximately 20 %), yet hetero-plasmy levels of 65 % and 85 % were observed in skeletal muscle [26,27]. Another aspect blurring the relationship between heteroplasmy levels and the severity of the symptoms is the determination of mutational load itself. Here, we face the problems of methodological limitations, tissue availability for analysis, but also features of the analyzed material. For example, very rare m.9205delTA variant of *MT-ATP6* gene was reported only in the two cases with completely different phenotypes but both patients were originally reported as homoplasmic in fibroblasts [28,29]. Prolonged cultivation of the patients' fibroblasts with very mild phenotype revealed that the variant was present as heteroplasmic, albeit at a very high mutational load. Therefore, the mild phenotype may be explained by the selection against the pathogenic variant in different tissues (which were not available for analysis) [30].

ATP synthase deficiencies associated with pathogenic variants of mtDNA

Of the two ATP synthase subunits encoded by mtDNA, pathogenic variants of subunit *a* (*MT-ATP6*) are much more frequent, while subunit A6L (*MT-ATP8*) is only rarely affected (Table 1). The most prevalent are missense variants of mtDNA *MT-ATP6* gene. Altogether, around 80 disease-causing variants of *MT-ATP6* have been described, including small-scale deletions and insertions. These variants were associated with a range of severe disorders affecting brain, heart, and muscles, but also with deafness, multiple sclerosis, autism, optic neuropathy, and diabetes, usually in combination with other mtDNA variants (MITOMAP). Twelve variants of *MT-ATP8* gene were associated with heart and brain defects, but they were also linked to type II diabetes mellitus, again typically in combination with other possible pathogenic variants. Finally, eight cardiomyopathic or neuromuscular variants of *MT-ATP8*/*MT-ATP6* overlapping region (Fig. 2A) affecting either both genes or only *MT-ATP8* were described. Taken together, approximately 100 variants of mtDNA genes coding for ATP synthase subunits were reported to be (potentially) linked with human diseases (reported vs confirmed pathogenicity). Due to the high number of cases, in the following section, we will discuss only mtDNA variants with known phenotype that 1) are confirmed as disease-causing in MITOMAP, 2) were found in more than one patient as the single variant, or 3) were associated with aberrant ATP synthase structure and function as a possible explanation of the disease phenotype (Table 2).

MT-ATP8/MT-ATP6 pathogenic variants

As previously stated, pathogenic variants of *MT-ATP8* gene are extremely rare with only a few patients described for each variant. This renders the discussion about their potential pathogenicity rather unsatisfactory. The majority of patients carry m.8528T>C missense variant of *MT-ATP8/MT-ATP6* overlapping region, which affects both subunits. This variant replaces highly conserved tryptophan 55 to arginine in A6L subunit and methionine 1 to threonine in the case of subunit *a*, potentially disrupting the initiation of translation of the subunit [31]. Hypertrophic cardiomyopathy (HCMP) or biventricular hypertrophy was found in almost all patients, with an early onset from prenatal to five months of life. Other life-threatening symptoms, including heart failure, metabolic crises, hypotonia, failure to thrive (FTT), and feeding difficulties, developed, and two patients died within a few months of life. The variant is typically present at a high heteroplasmy level, exceeding 90 % [31,32]. However, in the blood of one patient with HCMP, only 59 % of pathogenic mtDNA was detected [33].

Table 2. Single *MT-ATP8/MT-ATP6* and *MT-ATP6* pathogenic variants, associated with isolated ATP synthase disorders. In the case of substitutions in position 8993, only papers describing specific phenotype as the first, and studies describing unusual phenotypes, are listed.

Gene Variant (Protein)	Clinical phenotype	Biochemical phenotype	Refs.
MT-ATP8/MT-ATP6			
m.8528T>C **(p.Trp55Arg/p.Met1Thr)**	**HCMP/biventricular hypertrophy**, 3-MGA, HA, LA, hyperketonemia, LVNC, arrythmia, WPW, HF, PAH, hypotonia, exercise intolerance, myopathy, anemia, thrombocytopenia, PMR, FTT	↓↓↓ synthesis of both *a* and A6L subunits, ↓↓↓ cV complex levels, ↓↓↓ synthesis of ATP	[31-34]
m.8529G>A (p.Trp55Ter/-)	HCMP, neuropathy, ataxia, ophthalmoplegia, PMR (1P)	↓ cV complex levels, ↑↑ F_1 subcomplexes	[35]
m. 8561C>T **(p.Pro66Ser/p.Pro12Leu)**	Hypotonia, microcephaly, ataxia, lesions in the basal ganglia, bilateral retinal hypoplasia, PMR (1P)	↓ cV complex levels, ↑↑ F_1 subcomplexes, ↓ ATP hydrolytic activity	[37]
m. 8561C>G **(p.Pro66Ala/p.Pro12Arg)**	**hypergonadotropic hypogonadism**, **ataxia**, **neuropathy**, **brain atrophy,** sensorineural hearing impairment	↑ F_1 subcomplexes	[36]

MT-ATP6			
m.8611_8612insC (p.Leu29ProfsTer36)	LA, gallstones, ataxia, encephalopathy, myopathy, PMR (1P)	↓↓↓ content of subunit *a,* ↓↓↓ complex V stability, ↓↓↓ ATP hydrolytic activity	[92]
m.8612T>C (p.Leu29Pro)	HSP, LS, volatile anesthetic hypersensitivity, PMR	n.a.	[86,93]
m.8618-8619insT (p.Thr33HisfsTer63)	**cerebellar atrophy, hearing loss, PMR,** NARP, impaired renal function, myopathy, ophthalmologic defects, diabetes, FTT	↓↓↓ ATP hydrolytic activity, ↓↓ cV complex levels, ↑ F_1 subcomplexes, ↑ ROS	[26,27]
m.8782G>A (p.Gly86Ter)	IUGR, **cerebellar ataxia, hearing loss,** myoclonic epilepsy, short stature, kidney disease, diabetes, speech impairment	↓↓ ATP synthase activity, ↓↓ basal OCR, ↑ ROS, ↑↑ F_1 subcomplexes	[26]
m.8839G>C (p.Ala105Pro)	NARP (1P)	↓↓ $\Delta\Psi_m$	[88]
m.8851T>C (p.Trp109Arg)	BSN, LS, microcephaly, brain malformations, encephalopathy, stroke, myopathy, hypotonia, neuropathy	↓↓ cV complex levels	[41,87,94]
m.8969G>A (p.Ser148Asn)	MLASA, LA, HCMP, WPW, patent foramen ovale, epilepsy, brain atrophy, myoclonic seizures, IgA nephropathy, liver steatosis, hypospadias, hearing impairment, PMR, FTT	Normal cV complex levels, ↓↓ ATP synthase activity, ↑ ROS	[98,99, 101,102]
m.8989G>C (p.Ala155Pro)	NARP (1P)	↓↓ ATP hydrolytic activity	[89]
m.8993T>C (p.Leu156Pro)	LS, NARP, neuropathy, ataxia, brain atrophy, pyramidal signs, dystonia, muscle weakness, optic atrophy, hearing impairment	↓ ATP synthase activity, ↑↑ ROS	[21,40,47, 50,51,53,55,6 0,61,112]
m.8993_8994TG>CA (p.Leu156Pro)	developmental delay and myopathy (1P)	n.a.	[41]
m.8993T>G (p.Leu156Arg)	LS, NARP, HCMP, seizures, ataxia, muscle weakness, glomerular proteinuria, sensorineural hearing loss, PMR	↓↓↓ ATP synthase activity, ↑↑ ROS	[39,42,43, 45,49,51,53,5 4,56-58,62, 63,66,112]
m.9032T>C (p.Leu169Pro)	NARP, LA, epilepsy, ataxia, cerebellar atrophy, microcephaly, sensorineural hearing loss, PMR	↓ ATP synthase activity, ↑ ROS, ↑ F_1 subcomplexes	[90,97]
m.9035T>C (p.Leu170Pro)	**Ataxia,** LS, cerebellar atrophy, neuropathy, dystonia, hypotonia, hypertonicity, visual impairment, retinitis pigmentosa, learning disability, PMR	↓↓ ATP hydrolytic activity, ↑↑↑ ROS	[51,84,95, 96]
m.9127-9128delAT (p. Ile201ProfsTer2)	NARP (1P)	↓↓ ATP hydrolytic activity	[91]
m.9134A>G (p.Glu203Gly)	IUGR, LA, HCMP, hypotonia (1P)	↓↓ ATP hydrolytic activity	[100]
m.9155A>G (p.Gln210Arg)	**MIDD**, metabolic syndrome, focal segmental glomerulosclerosis	Normal cV complex levels and activity	[103,104]
m.9176T>C (p.Leu217Pro)	FBSN, LS, CMT, HSP, LA, HCMP, ataxia, dystonia, external ophthalmoparesis, episodic muscle weakness and neuropathy, PMR	Normal cV complex levels, ↓↓ ATP synthase activity, ↑ ROS	[38,47,48, 51,53,67,73, 77,79,81,82]
m.9176T>G (p.Leu217Arg)	LS, seizures, epilepsy, ataxia, spastic paraparesis, polyneuropathy, PMR	↓↓↓ ATP synthase activity	[57,68,69]

m.9185T>C (p.Leu220Pro)	LS, LS-like, NARP, CMT, WPW, HCMP, arrhythmia, brain atrophy, epilepsy, ataxia, hypotonia, neuropathy, neuropathy, muscle weakness, respiratory and renal failure, ptosis, sensorineural hearing loss, learning difficulties	↓ cV complex levels, ↓ ATP hydrolytic activity, ↑ ROS	[47,51-53, 55,70-76, 78,80,83,84]
m.9191T>C (p.Leu222Pro)	LS (1P)	↓ ATP hydrolytic activity	[76]
m.9205delTA (Ter-Met)	transient LA with seizures, severe encephalopathy and LA	↓↓↓ cV complex levels	[28,29]

1P – data available for 1 patient only; n.a. – biochemical phenotype for the patient is not available, in the case of m.8993_8994TG>CA expected to be similar to m.8993T>C, resulting in the same amino acid exchange; $\Delta\Psi_m$ – mitochondrial membrane potential; cV – complex V (ATP synthase); OCR – oxygen consumption rate; ROS – reactive oxygen species. Clinical phenotype in bold – shared symptoms if more than one patient; 3-MGA – 3-methylglutaconic aciduria; CMT – Charcot-Marie-Tooth disease; DF – dysmorphic features; (F)BSN – (familiar) bilateral striatal necrosis; FTT – failure to thrive; HCMP – hypertrophic cardiomyopathy; HA – hyperammonemia; HF – heart failure; HSP – hereditary spastic paraplegia; IUGR – intrauterine growth restriction; LA – lactic acidosis; LS – Leigh syndrome; LVNC – left ventricular non-compaction; MIDD – maternally inherited diabetes and deafness; MLASA – mitochondrial myopathy, lactic acidosis and sideroblastic anemia; NARP – neurogenic muscle weakness (neuropathy), ataxia and retinitis pigmentosa syndrome; PAH – pulmonary arterial hypertension; PMR – psychomotor retardation (in general, details in references and text); WPW – Wolf-Parkinson-White syndrome.

Zigman *et al.* [34] described another patient with myocardial hypertrophy carrying homoplasmic m.8528T>C variant, who suffered from severe neonatal hyperammonemia requiring hemodialysis during the first days of life. The mother of the patient was the first asymptomatic carrier with high heteroplasmy (82 % in the blood) of m.8528T>C variant described while in the previous cases, very low levels of the variant were found in patients' relatives. This pathogenic variant was shown to cause impaired synthesis of both subunits *a* and A6L, with low levels of complete ATP synthase detected in patient samples. Based on the experience with m.9205delTA *MT-ATP6* variant [30], one would expect that the lack of subunit *a* is the primary driver of diminished assembly/stability of complex V in the case of m.8528T>C substitution. However, in a patient with similar phenotype of HCMP, neuropathy, ataxia, ophthalmoplegia, and psychomotor retardation carrying m.8529G>A variant (one base next to the previous one), only subunit A6L (p.Trp55Ter) is affected. Still, this leads to the decreased stability of ATP synthase complex [35]. As illustrated in Figure 1A, all A6L pathogenic variants described in this review are situated in the extra-membrane part of the protein, where it interacts with subunits of the peripheral stalk. Consequently, these variants can influence the connection between membrane part and the peripheral stalk. Similar to previously discussed cases, m.8529G>A variant exhibited a high degree of heteroplasmy (over 90 %), yet the disease course was rather milder, with later onset at 4 years of age. Excessive mutational load was determined also in patients with other two variants in *MT-ATP8/MT-ATP6* overlapping region, affecting the stability of ATP synthase, both in position 8561. These patients presented with neurological symptoms, including hypotonia, ataxia, microcephaly/brain atrophy, and neuropathy, without cardiac involvement [36,37]. In addition, variant m.8561C>G was associated with a very unusual mitochondrial disease phenotype of hyper-gonadotropic hypogonadism [36].

Most frequent MT-ATP6 pathogenic variants

Contrary to the above-mentioned variants, which affect both subunit *a* and A6L, variants affecting only *MT-ATP6* gene are predominantly linked with neuro-degenerative phenotypes. The most common is devastating Leigh syndrome (LS), subacute, necrotizing encephalo-pathy characterized by bilateral symmetrical necrotic lesions of grey matter nuclei in the basal ganglia, diencephalon, cerebellum, or brainstem. The onset of the disease is typically in early infancy, and patients manifest a heterogeneous set of symptoms, including regression or psychomotor delay, optic atrophy, ophthalmoplegia, ptosis, nystagmus, respiratory abnormalities due to brainstem dysfunction, and pyramidal signs. In addition, patients may exhibit signs of dystonia, ataxia, peripheral neuropathy, and intention tremor associated with lactic acidosis (LA) in the blood, cerebrospinal fluid, or urine [38]. The second relatively common presentation of *MT-ATP6* pathogenic variants is less severe neurogenic muscle weakness (or neuropathy), ataxia, and retinitis pigmentosa (NARP) syndrome. However, the clinical picture of *MT-ATP6* patients is not limited only to these two syndromes.

The most prevalent is m.8993T>G missense variant, which was first described by Holt *et al.* in 1990. This variant replaces highly conserved leucine 156 with arginine [39]. To date, several hundred or even thousands of patients with m.8993T>G variant have been diagnosed. At the same position, another two pathogenic variants were identified. The second most common disease-causing variant of *MT-ATP6* gene is m.8993T>C, which changes leucine 156 to proline [40]. In a single patient, m.8993_8994TG>CA was also observed, resulting in the same amino acid substitution [41].

In accordance with the prevailing consensus, patients exhibiting heteroplasmy levels of up to ~70 % are typically asymptomatic or present with relatively mild symptoms. Heteroplasmy levels between 70 % and 90 % are associated with NARP, while levels above 90 % are associated with the typical presentation of LS [39,40,42-49]. The m.8993T>G substitution typically presents in the first months of life, while in the patients with m.8993T>C, the onset is delayed, with a milder disease course [47,50-53]. However, while this is the general pattern, exceptions can be found. Thus, there are reports of patients with heteroplasmy above 90 % or even homoplasmy manifesting a milder phenotype than LS [41,51,53-57]. Conversely, individuals suffering from LS but harboring heteroplasmy under 90 % have been documented [51,53]. Another group includes patients with late or adult onset of the disease that harbor both very low or very high heteroplasmy [42,45,51,53,58,59] or mainly adults carrying m.8993T>C with a phenotype similar to NARP but possessing ophthalmologic disorders [60,61]. Exceptionally, m.8993T>G and m.8993T>C variants have been linked with a number of conditions, including renal disease [62], sensorineural hearing loss/deafness [21,50,63-65], epilepsy [65], and cardiomyopathy [66].

In addition, common *MT-ATP6* disease-causing variants include transitions at positions 9176 and 9185: m.9176T>G (p.Leu217Arg), m.9176T>C (p.Leu217Pro), and m.9185T>C (p.Leu220Pro). The clinical picture of the patients encompasses mainly neurodegenerative phenotypes with rather late onset, but the symptoms differ more than in the case of 8993 variants. The severity of symptoms is not heteroplasmy dependent, and almost all the patients possess very high mutational loads ranging from 90 % to homoplasmy. Once again, the most severe presentation is LS [38,47,48,51-53,67-75]. In some patients, the LS was accompanied by cardiac phenotype, epileptic seizures, renal failure [70,71,75], or with some features of poliodystrophy [68]. Interestingly, three patients with mild and reversible phenotype of LS were described [74,76].

Conversely, the Charcot-Marie-Tooth syndrome represents a condition of minimal severity. It is characterized by (but not limited to) muscle weakness and neuropathy, often associated with T>C transition at positions 9176 and 9185 [77-79]. In some patients, it is accompanied by ataxia or sensorineural hearing loss [70,78,80].

Another group of patients presents with milder symptoms, exceptionally linked with T>C substitutions. These include NARP [51,53,71], familial bilateral striatal necrosis (FBSN), which is characterized by devel-opmental regression, choreoathetosis and dystonia progressing to spastic quadriparesis [81], and hereditary spastic paraplegia (HSP), a group of inherited disorders that involves weakness and spasticity [82]. FBSN and HSP were described only in patients with m.9176T>C [81,82]. Symptoms mimicking periodic paralyses due to channelopathies or spinal muscular atrophy, but were ultimately diagnosed as mitochondriopathy due to m.9185T>C transition, were described in few patients [55,83].

A significant proportion of patients carrying one of the common pathogenic variants present with a spectrum of neurological and neuromuscular disorders that do not fit into any specific syndrome. These include hypotonia, muscle weakness, neuropathy, ataxia, paresis, epilepsy, seizures, ptosis, and pyramidal signs, with varying severity [51,53,55,57,65,68,70,71,80,84,85], sometimes accompanied by mental retardation [67,68], LA, and cerebellar atrophy [83]. For all the common pathogenic variants, carriers with lower mutational load [38,51,53,60,69,74,78] as well as asymptomatic individuals with high heteroplasmy or even homoplasmy have been described [51,53,67,71,76]. However, they could just be identified before the disease onset since patients with very late onset of the disease are occasionally described for all the variants discussed above [58,61,74,82].

Less frequent MT-ATP6 pathogenic variants

The clinical presentation of remaining *MT-ATP6* pathogenic variants is highly diverse, encompassing the entire spectrum of symptoms commonly associated with mitochondrial diseases. LS is relatively rare presentation observed in patients with m.8612T>C, m.8851T>C,

m.9035T>C, and m.9191T>C transitions [51,76,86,87]. Similarly, NARP is associated with m.8618-8619insT, m.8839G>C, m.8989G>C, m.9032T>C, and m.9127–9128delAT variants [27,88-91]. Still, the neuro-logical signs such as encephalopathy, brain atrophy, epilepsy, stroke, and microcephaly, or neuromuscular symptoms of ataxia, hypotonia, BSN, neuropathy, and myopathy in general are the main clinical characteristics of rare *MT-ATP6* variants m.8611_8612insC, m.8612 T>C, m.8851T>C, and m.9035T>C [41,84,92-96]. In addition to the previously mentioned symptoms, various visual and hearing defects are also observed in individuals with m.8618-8619insT, m.8782G>A, m.9032T>C, and m.9035T>C variants, in the first two also kidney disease was reported [26,96,97]. The patient carrying m.8611_8612insC insertion was originally diagnosed at the age of four months with gallstones that persisted during follow-up [92]. The severity of the disease course does not seem to be heteroplasmy dependent since the majority of patients have very high heteroplasmy above 90 % or even homoplasmy.

Slightly different spectrum of symptoms was found in the group of patients with m.8969G>A and one patient with m.9134A>G. In one case, MLASA plus syndrome was diagnosed (mitochondrial myopathy, LA and sideroblastic anemia plus developmental delay, sensorineural hearing loss, epilepsy, agenesis of the corpus callosum, FTT, and stroke-like episodes, [98]). Similarly, another individual exhibited epileptic episodes and decreased muscle strength, brain atrophy, severe hearing impairment together with kidney disease (IgA nephropathy) and cardiac involvement (Wolf-Parkinson-White syndrome) [99]. Remaining patients suffer from various combinations of cardiac symptoms (HCMP, patent foramen ovale), LA, anemia, hypotonia, myoclonic seizures, facial dysmorphism, hypospadias, tortuosity of the retinal vessels, liver steatosis, and psychomotor retardation [100-102].

Only two patients were described carrying m.9205delTA, two-base deletion that affects not only ATP synthase but also complex IV (cytochrome *c* oxidase). This mutation results in the removal of the stop codon of *MT-ATP6* gene, thereby altering the processing of MT-ATP8/MT-ATP6/MT-CO3 poly-cistronic tran-script (Fig. 2A). Consequently, the biosynthesis of both subunit *a* of ATP synthase and of subunit Cox3 of cytochrome *c* oxidase is markedly diminished [30]. Transient LA and seizures were the only symptoms in the first patient with more than 90 % heteroplasmy [28], while the second homoplasmic patient suffered from severe encephalopathy and LA [29]. Finally, two adult patients were described with the m.9155A>G variant. They presented with maternally inherited diabetes and deafness syndrome (MIDD), with one of them also having metabolic syndrome and focal segmental glomerulosclerosis [103,104].

The specific type of the disease based on mitochondrial dysfunction is Leber's hereditary optic neuropathy (LHON), maternally inherited disease that can lead to acute bilateral blindness due to the loss of the optic nerve and papillomacular bundle nerve fibers, predominantly in young men [105]. The patients usually carry one of the so-called primary mutations in mtDNA genes encoding subunits of complex I. However, they may also carry additional, so-called secondary mutations that modify the disease course. Such secondary variants can be identified in the *MT-ATP6* gene as well. In sporadic cases, patients with LHON were described who carried only the substitution in *MT-ATP6* as a single variant (e.g. m.8836A>G and m.9101T>C). These variants were possibly causal for the disease development [106-108].

Functional and structural consequences of MT-ATP6 pathogenic variants

As the key subunit for proton translocation, subunit *a* plays a pivotal role in ATP synthesis and ATP synthase stabilization [30,109]. Missense variants of *MT-ATP6* typically affect the efficiency of proton translocation, resulting in reduced ATP production and eventually to increased reactive oxygen species (ROS) production [68,76,88-90,95,97,99,101,110-113]. In some cases, when ATP synthase activity is only slightly affected, increased ROS production itself may serve as the underlying pathological mechanism [55,82,95,112]. In contrast to the synthetic activity of ATP synthase, the hydrolytic activity of this enzyme is not altered in most patient samples. The reason for this is, that the reverse reaction of ATP hydrolysis is not dependent on the proton flux. Moreover, it was demonstrated that in the reverse mode, protons could be transported normally even when a pathogenic variant of subunit *a* was present [114]. ATP hydrolytic activity is therefore an inadequate diagnostic tool for isolated ATP synthase deficiency caused by pathogenic variants of mtDNA. Nevertheless, in certain set of mutations, even ATP hydrolysis has been observed to be reduced [70,76,91,100]. The literature contains conflicting reports regarding the impact of the

most common variant, m.8993T>G, and the relatively rare m.9035T>C variant on ATP hydrolytic activity. Some studies have documented a reduction in ATP hydrolysis in a few patients [95,113,115], while others have observed no change [42,46,96,116]. The discrepancies observed may be attributed to differences in methodology and the use of different assay protocols, which can lead to disparate outcomes. Moreover, the hydrolytic activity specific for ATP synthase is typically determined as the oligomycin-sensitive portion of the total hydrolytic activity of the sample. It is questionable how variants of subunit *a* can alter the sensitivity of ATP synthase to oligomycin, which is bound to subunit *c* in close proximity to subunit *a*. Some studies suggest that m.8993T>G variant may result in increased sensitivity to oligomycin [116,117]. However, in the case of m.9035T>C, total hydrolytic activity was found to be decreased to the same extent as the oligomycin-sensitive portion [95]. Another aspect to consider is the stability of the enzyme. In condition of activity measurement, F_1 can be (partially) dissociated from F_o, which results in a loss of sensitivity to oligomycin. For instance, some studies have indicated that normal ATP hydrolytic activity in muscle was preserved in some patients, yet it was decreased in fibroblasts of the same patient [45,65]. This suggests that the enzyme in fibroblasts may be more fragile. A reduction in ATP hydrolysis can be causally linked with a reduction in the levels of ATP synthase complex [70,76,78].

Previously, disease-causing substitutions and potential mechanism by which they can affect ATP synthase function were discussed in the context of available yeast [118] or bovine [65] structures. When we take into consideration the recently reported cryo-EM structure of human ATP synthase [2], we can now map all the reported variants on it (Fig. 1A), as recently demonstrated here [119]. It is evident that the majority of the disease-causing variants of *MT-ATP6* discussed here are changing residues around c_8 ring, in proximity with residues crucial for proton translocation (Fig. 1B). Residues 169, 170 and 203 are located in the region of subunit *a*, involved in the entry of protons from intermembrane space, while 109, 217, 220 and 222 are close to the exit site towards matrix. Positions 105, 155, 156, and 148 are in close proximity to residues, where exchange of protons between subunits *a* and *c* occur [118]. Residue 210 is rather far from active sites, yet its involvement in the proton flow through subunit *a* is probable. Transitions at positions 12 and 29 were accompanied by higher levels of F_1 part, suggesting that these residues could be involved in the connection of subunit *a* with peripheral stalk of ATP synthase complex.

In the case of frameshift variants and one nonsense variant creating premature stop codon, ATP production is strongly reduced. In addition, ATP synthase complex is significantly more labile due to the lack of full-length subunit *a* [26,27,29,92]. Decreased complex stability leads to higher levels of free F_1 part of the enzyme, which still possesses hydrolytic activity and may further exacerbate the biochemical phenotype.

Nuclear DNA pathogenic variants

As mentioned above, nuclear DNA variants are a frequent cause of mitochondrial disorders. Since the advent of next-generation sequencing (NGS), the number of recognized nuclear disease-causing genes has increased rapidly, and nuclear genetic defects in all respiratory chain complexes, including ATP synthase, have been reported. In most cases, defects in OXPHOS complexes present as autosomal recessive traits [120]. In other words, the patients are homozygous for one pathogenic variant, or compound heterozygotes carrying two different pathogenic variants of the same gene, one in each allele. The parents of the patients are usually healthy heterozygous carriers of the variant. Pathogenic variants have been identified either in genes encoding structural proteins or in the biogenetic and regulatory factors of OXPHOS machinery – so-called “direct and indirect hits” [121]. The spectrum of affected pathways, which ultimately result in the defect of OXPHOS apparatus is very broad. Pathogenic variants have been described in proteins involved in mtDNA stability, replication, and expression. Similarly, proteins involved in the metabolism of cofactors and toxic compounds may also affect OXPHOS system, and finally, proteins involved in mitochondrial dynamics, homeostasis, and quality control represent another broad group of targets [120].

Nuclear DNA pathogenic variants associated with isolated deficiency of ATP synthase

The first evidence that a nuclear gene variant may be associated with inborn ATP synthase dysfunction was published by Holme *et al.* [122], who described a child with cardiomyopathy, LA, persisting 3-methylglutaconic aciduria (3-MGA) and severely

decreased activity of ATP synthase without any underlying mtDNA variant. A few years later, another patient with early onset neonatal and fatal LA, cardiomyopathy, and hepatomegaly was reported by Houštěk *et al.* [123]. In patient tissues, an isolated 70 % decrease of ATP synthase complex was found. However, transmitochondrial cybrids containing patients' mtDNA contained normal levels of the complex, confirming the nuclear origin of the disease. A number of similar patients with isolated ATP synthase deficiency lacking pathogenic mtDNA variants were later described [124]. However, the pathogenic variant of *ATPAF2* gene encoding ATP synthase assembly factor ATP12 was identified in only one of these patients [125]. In 2008, using the homozygosity mapping and sequencing of candidate genes in the group of 24 patients with ATP synthase deficiency, severe neonatal LA and encephalo-cardiomyopathy, *TMEM70* was identified as another disease-causing gene [126]. Since then, the number of new patients carrying *TMEM70* pathogenic variants has steadily increased, with more than 80 cases described to date. Apparently, *TMEM70* gene is highly susceptible to mutagenesis, and this type of rare mitochondrial disease has rather frequent incidence.

The first pathogenic variant in ATP synthase structural gene was described two years later, when disease-associated variant of *ATP5F1E* gene encoding ε subunit was found in the patient with milder mitochondrial disease phenotype [127]. In contrast, four patients with two different *ATP5F1A* (α subunit) pathogenic variants with fatal disease course and premature death in early childhood (one week or several months) were reported at the same time [128,129]. With the development of sequencing techniques, several novel pathogenic variants of ATP synthase structural genes have recently been characterized. These include variants of genes encoding α, β, δ, ε, *c*, DAPIT and OSCP subunits [130-137]. It is noteworthy that a considerable number of the recently identified pathogenic variants of ATP synthase structural genes are heterozygous, yet still result in the manifestation of disease phenotypes. The autosomal dominant mode of inheritance is rather unusual in the context of mitochondrial diseases. Similarly, two heterozygous patients with *PEX14* pathogenic variant were recently described with a peroxisomal disorder, a condition normally linked with the autosomal recessive mode of inheritance [138]. These findings indicate the necessity for a change in the approach to the diagnostic process for genetic diseases, with a greater focus on these dominant pathogenic variants. Pathogenic variants of ATP synthase structural genes and their associated phenotypes are summarized in Table 3 and visualized in Fig. 1A. The severity of the clinical manifestation and biochemical consequences are highly variable, ranging from asymptomatic patients to premature death.

Although the number of genes involved in inborn and isolated ATP synthase deficiency has increased significantly, the pathogenic variants of structural genes still represent a very rare cause of the disease. In the following section, we will examine pathogenic variants and their clinical manifestations. For the purposes of this review, we have divided these rare pathogenic variants according to the severity of the phenotypes observed in a small group of patients. While this classification makes easier the discussion of phenotypes in the context of this review, it should be kept in mind, that it is highly subjective. It should be noted, that the current prevailing consensus is to see the severity as a continuous spectrum, where even the same pathogenic variant can present with different degree of severity in two different patients.

nDNA pathogenic variants in structural genes of ATP synthase with mild phenotype

In general, the less severe phenotype can be observed in the individuals carrying heterozygous substitutions in *ATP5F1A* [130,131], *ATP5F1B* [133], and *ATP5MC3* [131,135] genes.

Recently, *de novo* heterozygous pathogenic variant c.620G>A (p.His207Arg) of *ATP5F1A* gene coding for α subunit was found in four independent patients [130,131]. All the patients suffered from early-onset mitochondrial disease and presented with psychomotor delay, failure to thrive and LA, accompanied by feeding intolerance, chronic diarrhea, anemia, hyperammonemia, and in some cases, acute encephalopathy. Although the initial manifestation suggests a typical mitochondrial disease course with metabolic imbalance, the severity of the phenotype for this variant is rather mild, and the major clinical findings recovered by late infancy in all the cases.

Table 3. Nuclear DNA pathogenic variants of structural genes for ATP synthase subunits associated with isolated deficiency of ATP synthase.

Gene Variant (Protein)	Clinical phenotype	Biochemical phenotype	No. of patients	Refs.
ATP5F1A				
c.545G>A Ht **(p.Arg182Gln)**	ataxia, spastic paraparesis, dystonia, PMR	n.a.	1	[131]
c.620G>A Ht **(p.Arg207His)**	**LA, FTT**, HA, anemia, metabolic imbalance, encephalopathy, feeding intolerance, PMR, #	Normal cV complex levels, ↓↓↓ ATP hydrolytic activity, ↓ OCR	4	[130, 131]
c.962A>G Hm **(p.Tyr321Cys)**	**microcephaly, hypotonia,** IUGR, HF, encephalopathy, seizures, pulmonary hypertension, FTT	mtDNA depletion, ↓↓ ETC activity	2	[128]
c.985C>T + c.-49+418C>T* **(p.Arg329Cys + *)**	**severe encephalopathy, small renal cysts hypoplastic lungs**	↓↓↓ cV complex levels, ↓↓ ATP hydrolytic activity, ↓ OCR	2	[129]
c.1037C>T Ht **(p.Ser346Phe)**	LA, cerebral palsy, dystonia, spastic tetraparesis, absent speech, PMR	n.a.	1	[131]
ATP5F1B				
c.1000A>C Ht **(p.Thr334Pro)**	generalized dystonia	Normal cV complex levels, ↓↓↓ ATP hydrolytic activity, ↓ $\Delta\Psi_m$	3 (+2)	[133]
c.1004 T>C Ht **(p.Leu335Pro)**	hyperphagia, tachypnea, episodic hyperthermia, euthyroid hypermetabolism, FTT, PMR	↑ basal OCR, ↓basal $\Delta\Psi_m$, ↓ coupling of RCC and cV	2	[132]
c.1445T>C Ht **(p.Val482Ala)**	generalized dystonia	Normal cV complex levels, ↓ ATP hydrolytic activity, ↓↓↓ $\Delta\Psi_m$	1 (+1)	[133]
ATP5F1D				
c.245C>T Hm **(p.Pro82Leu)**	3-MGA, LA, HA, dilated CMP, rhabdomyolysis, PMR	↓ cV complex levels, ↓↓↓ ATP hydrolytic activity	1	[134]
c.317T>G Hm **(p.Val106Gly)**	3-MGA, HA, ketoacidosis, mild exercise intolerance, PMR	↓↓ cV complex levels, ↓↓ ATP hydrolytic activity	1	[134]
ATP5F1E				
c.35A>G Hm **(p.Tyr12Cys)**	**LA, PMR**, 3-MGA, HCMP, ataxia, seizures, hypotonia, dystonia, neuropathy, visual and hearing deficit, #	↓↓↓ cV complex levels, ↓↓↓ ATP synthase activity, ↓OCR	3	[127]
ATP5PO				
c.34C>T + c.329-20A>G **(p.Gln12Ter + §)**	LA, seizures, microcephaly, brain atrophy, dystonia, hypotonia encephalopathy, restlessness, sleep disturbances, PMR	↓↓ cV complex levels, ↑↑ F_1 subcomplexes	1	[131]
c.87+3A>G Hm **(exon 2 skipped)**	**LS**, **HCMP**, **hypotonia**, **hypospadias**, 3-MGA, bradycardia, seizures, epilepsy, hypothrophic muscles, renal insufficiency, DF, cryptorchidism, PMR	↓↓ cV complex levels, ↑↑ F_1 subcomplexes, ↓↓↓ ATP hydrolytic activity	3	[137]

ATP5MK				
c.87+1G>C Hm (exon 3 skipped)	**LS, febrile illness,** HCMP, accessory spleen, testicular atrophy, fatty liver	normal cV monomer levels but no dimer, ↓↓ ATP synthase activity	4	[136]
ATP5MC3				
c.236G>T Ht (p.Gly79Val)	LA, lower-extremity spasticity, PMR	↓↓ cV complex levels, ↓↓ ATP hydrolytic activity	1	[131]
c.318C>G Ht (p.Asn106Lys)	dystonia [dystonia or HSP]	↓ ATP synthase activity	2 [+17]	[131, 135]
c.319C>G Ht (p.Pro107Ala)	pyramidal signs, generalized dystonia, PMR	n.a.	1	[131]

Hm – homozygous variant; Ht – heterozygous variant; * – pathogenic substitution in the first intron disrupting expression of *ATP5F1A* gene from this variant; § – loss-of function allele associated with abnormal gene splicing and reduced ATP5PO mRNA levels; # – major clinical findings recovered during life; ΔΨm – mitochondrial membrane potential; cV – complex V (ATP synthase); ETC – electron transport chain; OCR – oxygen consumption rate; RCC – respiratory chain complexes. No. of patients in round brackets means healthy individuals carrying the pathogenic variant, in square brackets family members suffering from dystonia of HSP supposed to have the same *ATP5MC3* pathogenic variant. Clinical phenotype in bold – shared symptoms if more than one patient; 3-MGA – 3-methylglutaconic aciduria; DF – dysmorphic features; FTT – failure to thrive; (H)CMP – (hypertrophic) cardiomyopathy; HA – hyperammonemia; HF – heart failure; HSP – hereditary spastic paraplegia; IUGR – intrauterine growth restriction; LA – lactic acidosis; LS – Leigh syndrome; PMR – psychomotor retardation (in general, details in the references and text).

Heterozygous disease-causing variants have also been reported in *ATP5F1B* gene encoding β subunit, bringing new and exciting insights into the pathogenesis of isolated ATP synthase deficiency. Two of them, c.1000A>C (p.Thr334Pro) and c.1445T>C (p.Val482Ala) were recently described by Nasca *et al.* in two unrelated families [133]. All the patients presented with isolated and slowly progressive dystonia without any additional neurological or systemic features, with early or late onset, ranging from infancy to adolescence. Although dominant, these variants have incomplete penetrance, as asymptomatic carriers (aged 22, 57, and 76 years) were identified in both families.

Similarly, the very mild course of the disease, which preferentially affects muscle tissue, has been associated with heterozygous pathogenic variants of *ATP5MC3* gene coding for subunit *c* [131,135]. Variant c.318C>G (p.Asn106Lys) was found in two unrelated individuals, one patient, carrying *de novo* substitution, presented with late onset (7 years) isolated dystonia, while the second patient presented with earlier onset (2 years) generalized dystonia, and the family history shows autosomal dominant form of the disease [135]. Adult-onset cases tend to develop predominantly uncomplicated, gradually progressive HSP, early childhood-onset patients have severe progressive generalized dystonia, and later childhood cases have intermediate segmental dystonia or spasmodic dysphonia. Three branches of the family show a tendency for successive generations to develop earlier and more severe symptoms than their affected parents (genetic anticipation) [139]. *De novo* heterozygous substitution in the next bp, c.319C>G (p.Pro107Ala), was described in the patient who presented with milestone delay and pyramidal signs in addition to generalized dystonia, but with late onset of 7 years [131]. Finally, the c.236G>T (p.Gly79Val) *ATP5MC3* variant was reported in one patient with delayed psychomotor development, lower-extremity spasticity, and LA [131].

nDNA pathogenic variants in structural genes of ATP synthase with moderate phenotype

Mild to moderate severity of the phenotype is associated with other heterozygous variants of *ATP5F1A* [131] and *ATP5F1B* gene [132], but also with homozygous variants of *ATP5F1D* [134] and *ATP5F1E* gene [127,131].

Within multicenter collaboration and community data sharing, Zech *et al.* [131] found and described two additional patients carrying *de novo* heterozygous substitution in *ATP5F1A*, c.545G>A (p.Arg182Gln) and c.1037C>T (p.Ser346Phe). Patients carrying these variants presented with psychomotor delay, dystonia, spastic paraplegia or tetraparesis, intellectual disability, ataxia, or cerebral palsy, the later also with swallowing problems and LA. At the last follow-up, the patients were 17 and 12 years old, respectively.

ATP5F1B de novo heterozygous c.1004T>C variant (p.Leu335Pro) was found in monozygotic twin boys, who were born with intrauterine growth restriction (IUGR) and developed failure to thrive at two months of

age, later accompanied by hyperphagia, developmental delay, euthyroid hypermetabolism characterized by excessive caloric intake, inability to gain weight, and tachypnea [132]. Both patients had unexplained episodic hyperthermia, a condition similar to Luft syndrome [140,141].

Two homozygous substitutions with biparental inheritance were found in *ATP5F1D* gene encoding δ subunit, c.245C>T (p.Pro82Leu) and c.317T>G (p.Val106Gly), each in one patient [134]. Both patients underwent episodes of metabolic decompensations with LA, 3-MGA and hyperammonemia, both suffered from muscle weakness and their psychomotor development tended to be slightly delayed. They differ in the onset of the disease, c.245C>T manifested on the second day of life, with additional phenotypes of rhabdomyolysis and dilated cardiomyopathy (normalized between first and fourth years of life), whereas in the case of c.317T>G, the patient was healthy until almost five years of age, with no further cardiologic or neurologic symptoms until the last follow-up at six years of age.

The first nuclear pathogenic variant of ATP synthase structural gene was identified in a patient who was 22 years old at the time of diagnosis (P13 in [124]). This patient developed early-onset LA and 3-MGA but without cardiac involvement. This was followed by mild mental retardation, exercise intolerance, ataxia, peripheral neuropathy, and dystonia. Targeted sequencing of *ATP5F1E* gene encoding ε subunit revealed homozygous missense variant *c.35A>G* replacing tyrosine 12 with cysteine [127]. The same substitution was later found in two unrelated patients [131]. A 13-year-old girl presented with a similar phenotype of intellectual disability, developmental delay, LA, ataxia, seizures, peripheral neuropathy, and transient respiratory failure. Severe respiratory distress at birth was one of the initial phenotypes of the third patient, along with vomiting, seizures, and LA, followed by developmental delay, progressive generalized dystonia, and visual and hearing deficits. In all three patients, the metabolic abnormalities improved or normalized later in life [131].

nDNA pathogenic variants in structural genes of ATP synthase with severe phenotype

Remaining homozygous pathogenic variants of structural genes of ATP synthase subunits, namely of *ATP5F1A* [128,129], *ATP5MK* [136], and *ATP5PO* [131,137] manifested with severe, usually lethal phenotype, and most of the patients died within the first year of life (mainly *ATP5F1A* and *ATP5PO* patients), or during childhood (*ATP5MK* patients).

First disease-causing variants of *ATP5F1A* gene were described almost simultaneously in 2013, with both papers describing unexpected features. The first study found *ATP5F1A* variant in a patient who presented with microcephaly, pulmonary hypertension, hypotonia, and heart failure at birth and died at three months of age [128]. The authors identified homozygous c.962A>G substitution (p.Tyr321Cys) in *ATP5F1A* gene in the index patient and her older sister, who previously died at 15 months of age with a diagnosis of microcephaly, hypotonia, and seizures, while their mother was healthy carrier of the variant. The study of Jonckheere *et al.* [129] describes two siblings with severe neonatal encephalopathy, both died in the first week of life. In this case, compound heterozygous variants c.985C>T + c.-49 + 418C>T of *ATP5F1A* were found. The missense variant c.985C>T leads to the replacement of arginine 329 with cysteine. However, this replacement in heterozygous form cannot explain the severity of the patients' phenotype, since their father was heterozygous healthy carrier of the variant. Indeed, the authors found that healthy mother of the patients carried heterozygous substitution c.-49 + 418C>T localized in the first intron of *ATP5F1A* gene resulting in the decreased levels of ATP5F1A mRNA (60 % of controls) in her fibroblasts. This suggests that the synthesis of α subunit from this variant is partially disrupted, and only pathogenic allele is expressed in both patients.

Four patients from three unrelated families were described by Barca *et al.* with c.87+1G>C pathogenic variant of *ATP5MK* gene encoding DAPIT protein [136]. All of them were diagnosed with severe LS between 6 and 18 months of age. The disease manifested with developmental delay and ataxia in all patients, other symptoms included movement disorders, various types of brain lesions, ophthalmoplegia, accessory spleen, testicular atrophy, fatty liver, and HCMP. Two patients died at six and nine years of age, while the other two aged six years were still alive at the time of reporting. This splice site variant resulted in the loss of DAPIT protein due to skipping of exon 3.

Last subunit of ATP synthase, whose variants have been associated with ATP synthase deficiency, is subunit OSCP. Zech *et al.* described one patient with compound heterozygous variant of *ATP5MO* gene, c.34C>T + c.329-20A>G [131]. As a result of c.34C>T nonsense variant, 12 AAs long OSCP protein is produced, representing only the first half of transit peptide, while

c.329-20A>G splice site variant resulted in the skipping of exon 5 and exon 4 plus 5 and to a drastic reduction in ATP5MO mRNA levels. The patient with neonatal onset died at age of six years after several epileptic episodes. She suffered from severe symptoms including fever-induced partial seizures, hypotonia, LA, acquired microcephaly, global developmental delay, dystonia, progressive brain atrophy, seizure deterioration, epilepsy, restlessness, sleep disturbances, and speech abnormality. Another splice site c.87+3A>G variant of *ATP5MO* gene, resulting in the skipping of exon 2 of OSCP protein, has been reported in three LS patients from two unrelated families. Since exon 2 encodes the last 11 AA (out of 23) of transit peptide, this variant is associated with drastic reduction of OSCP levels in the mitochondria. Two male patients died in the first six months of life, while the only female patient was three years old at the time of publication [137]. They all shared common symptoms of LS, such as hypotonia, developmental delay, HCMP, LA, progressive epileptic encephalopathy, and progressive brain atrophy. In addition, facial dysmorphism was present in two siblings, and both boys had hypospadias, in one of them accompanied with cryptorchidism and enlarged kidneys.

Functional consequences of structural subunits pathogenic variants

Huge variability is associated not only with the clinical features of patients, but also with the underlying biochemical phenotype. Some variants cause defects in the structure and stability of the enzyme, accompanied with severe reduction of ATP synthase levels and activity, while others affect only the activity, but not the content of the enzyme. In some cases, however, the relevant biochemical data are not available, and in others they are scarce. Significantly decreased activity of ATP synthase, mainly determined as hydrolytic activity, but normal levels of ATP synthase have usually been found in the tissues of patients with milder or reversible phenotype, namely in patients with heterozygous substitutions in *ATP5F1A* (c.620G>A) [130] and in *ATP5F1B* (c.1000A>C and c.1445T>C) [133], but also in patient with homozygous c.87+1G>C variant of *ATP5MK* suffering from Leigh syndrome [136]. Strong reduction of both activity and content of ATP synthase complex has been found in samples from patients with severe or even lethal phenotype, carrying pathogenic variants of *ATP5F1A* [129] or of *ATP5PO* [131,137], but it has also been described in case of *ATP5F1E* [127,131], *ATP5F1D* [134], and *ATP5MC3* [131] variants, resulting in mild phenotype.

In the case of pathogenic *ATP5MK* and *ATP5PO* variants, the affected proteins are key structural ATP synthase subunits, DAPIT and OSCP, respectively. OSCP is essential for the assembly of the peripheral stalk, which stabilizes enzyme structure, but also regulates the activity of catalytic F_1 part [142]. It is highly probable that aberrant or completely missing OSCP protein has a strong effect on the whole enzyme. Indeed, the levels of ATP synthase complex were drastically reduced in fibroblasts of patients, causing a strong decrease in hydrolytic activity of ATP synthase [131,137]. DAPIT protein has been shown to affect dimerization of ATP synthase complex [143], but its exact role in enzyme function is not known because it does not form dimerization interface between ATP synthase monomers [2,65]. In patient fibroblasts, the absence of DAPIT protein biochemically resulted in a severe reduction of ATP levels and the absence of dimeric form of ATP synthase, altering mitochondrial cristae structure [136].

Not surprisingly, all the missense variants that manifest as the ATP synthase defects affect highly conserved residues. Most of them are located in genes for subunits of F_1 domain (Fig. 1A). As already mentioned, homozygous variants of *ATP5F1D* and *ATP5F1E* (δ and ε subunits, respectively) share the same biochemical phenotype with significant and rather severe reduction of ATP synthase content and thus with reduced activity of the complex, resulting in similar mild and rather non-progressive disease course [127,131,134]. Together with γ subunit, they form central stalk that stabilizes γ subunit connection with the *c* ring and they are important for the complex stability [2]. Both *ATP5F1D* pathogenic variants lead to changes in the predicted protein structure of δ subunit, associated with its inability to properly bind other F_1 subunits. This results in reduced assembly of ATP synthase complex, but normal levels of free δ subunit [134]. In contrast, amount of ε subunit is significantly reduced as a result of pathogenic *ATP5F1E* variant, and the remaining ε subunit is assembled into ATP synthase complex without affecting its stability, even when pathogenic [127].

Since α subunit forms catalytic $\alpha_3\beta_3$ hexamer, the severe phenotype of homozygous variant c.962A>G in *ATP5F1A* is expected. Furthermore, this substitution is located in highly conserved region associated with mitochondrial genomic integrity (*mgi*) in yeast [144]. Although the levels of ATP synthase in patient samples are not discussed in the original report, based on the yeast model the authors suggest that this variant led to reduced

synthesis of all OXPHOS mtDNA-encoded subunits, and thus to decreased membrane potential and uncoupling of ATP synthase. This is in accordance with significant decline in activity of complex I, III and IV in the patient's muscle tissue and with mitochondrial DNA depletion in muscle and liver (app. 40 % of controls) [128]. Similarly, in patients with compound heterozygous c.985C>T + c.-49 + 418C>T *ATP5F1A* variant, where only pathogenic variant of the subunit is produced, the interaction between α and β subunits is disturbed, leading to drastic reduction in the level of assembled ATP synthase and fatal course of the disease [129].

On the contrary, the heterozygous variants of α or β subunits genes result in decreased activity but normal levels of ATP synthase complex, leading to mild or moderate disease phenotype. All three substitutions in *ATP5F1A*, c.545G>A, c.620G>A and c.1037C>T, are localized at the interface between α and β subunits (Fig. 1A), as clearly shown by authors using 3D modelling [130,131]. Since ATP synthesis takes place at α/β interface [145], these variants may affect assembly/stability of $\alpha_3\beta_3$ hexamer and of the whole complex, but also functional properties of the enzyme. However, decreased hydrolytic activity of ATP synthase but normal levels of ATP synthase complex were found only in the case of c.620G>A variant, since it was not analyzed in detail in the others. At the α/β interface and close to the pocket for γ subunit, heterozygous c.1000A>C *ATP5F1B* substitution is also localized (Fig. 1A). Interestingly, c.1445T>C variant has exactly the same clinical presentation as c.1000A>C, but c.1445T>C is not located at α/β interface, but on the outer surface of β subunit (Fig. 1A), far away from any contact site [133]. All these heterozygous substitutions affect synthesis of ATP everywhere, but only specific cell types and tissues, such as neurons and muscle, appear to be sensitive to this mild energetic deprivation [133]. Since heterozygous variants produce about 50 % of defective subunit (α or β) and one ATP synthase complex contains three copies of each in its F_1 domain, it is questionable how many pathogenic copies are present in one fully assembled enzyme and thus how the enzyme activity is affected. Interestingly, in patients with c.620G>A variant of *ATP5F1A*, the symptoms remitted and patients later developed normally [130,131], suggesting that cells can either adapt their metabolism to reduced ATP supply or to assemble the enzyme preferentially using the non-defective subunits.

Slightly exceptional are the patients with heterozygous *ATP5F1B* variant, c.1004T>C, who present with more severe Luft-like phenotype [132]. Luft syndrome is a very rare disease, belonging to the category of "mitochondrial uncoupling syndromes" presenting with high caloric intake and hyperthermia caused by uncoupled proton translocation and ATP synthesis, with only a few patients described worldwide [140,141]. Analysis of patient fibroblasts confirmed that the mitochondrial respiration is not fully coupled to ATP synthesis, and membrane potential is dissipated in the form of heat. It is of interest that this variant lies in the region of *mgi* variants in yeast, as discussed above [132].

Another example of pathogenic heterozygous variant in a subunit present in multiple copies per enzyme monomer are substitutions in *ATP5MC3* gene encoding subunit *c*. It plays a crucial role in energy transduction, since *c* ring harnesses the energy released from the translocation of protons across the mitochondrial inner membrane (from intermembrane space to matrix) and couples it to its rotation. Subunit *c* is tightly connected with γ subunit, which fits between α and β interface and the rotation results in structural changes in $\alpha_3\beta_3$ hexamer necessary for binding and phosphorylation of ADP (and P_i) and release of generated ATP. Variant c.236G>T affects amino acid at the interface of the two adjacent helixes (Fig. 1A), potentially disturbing its interaction [131]. c.318C>G and c.319C>G affect highly conserved loop structure that interacts directly with the F_1 subunits (Fig. 1A) [131,135]. Biochemically, all these variants lead to decreased hydrolytic activity of ATP synthase and, in the case of c.236G>T, to a significant decrease in the amount of fully assembled ATP synthase. For the remaining two variants, the level of assembled ATP synthase was not determined in the original report, so no general conclusions can be drawn. However, even in the cells completely lacking all three isoforms of subunit *c*, vestigial complex remains present in the membrane [146]. An interesting aspect is, that subunit *c* is encoded by three genes *ATP5MC1, ATP5MC2,* and *ATP5MC3*, which do not show any strong tissue-specific expression and ultimately produce identical mature protein. The requirement for the presence of 8 copies of subunit *c* per assembled *c* ring may explain the dominant presentation of the heterozygous *ATP5MC3* variant even under such conditions. However, the low penetrance of the c.318C>G variant is peculiar. It would be attractive to speculate that non-symptomatic carriers express subunit *c* from its other isoforms.

Table 4. Nuclear DNA pathogenic variants in ATP synthase assembly factors associated with isolated deficiency of ATP synthase

Gene Variant (Protein)	Clinical phenotype	Biochemical phenotype	No. of patients	Refs.
ATPAF2				
c.280T>A Hm (p.Trp94Arg)	encephalopathy, 3-MGA, LA, DF	↓↓↓ levels of cV complex, ↓↓ ATP hydrolytic activity	1	[125]
TMEM70				
c.105dupT Hm (p.Val36CysfsTer52)	**IUGR, LA, HCMP, hypotonia, DF**, 3-MGA, HA, hypoglycemia, hypercitrullinemia, encephalopathy, buphthalmos, PMR, FTT, gastrostomy	n.a.	2	[161]
c.141delG/c.316+1G>A (p.Pro48ArgfsTer2/ exon 2 skipped)	**LVNC, PMR**, 3-MGA, LA, metabolic acidosis, HA, hypoglycemia, hyperketonemia, tachypnea, hernia, undescended testicle, FTT	↓↓↓ levels of cV complex	2	[166]
c.211–450_317–568del Hm (2290bp deletion – exon 2)	IUGR, 3-MGA, LA, HCMP, PMR	↓↓↓ levels of cV complex	1	[150]
c.238C>T Hm (p.Arg80Ter)	oligohydramnios, **IUGR, 3-MGA, LA, HA, encephalopathy**, **hypotonia,** metabolic acidosis, HCMP, multiorgan failure, DF, PMR, FTT, apnea	↓↓ ATP hydrolytic activity	2	[154,156, 159]
g.2436–3789 in-frame deletion Hm (exon 2 skipped)	oligohydramnios, IUGR, LA, HA, HHH-syndrome, HCMP, encephalopathy, ataxia, ptosis, PMR, FTT, gastrostomy	↓↓↓ levels of cV complex	1	[160]
c.316+1G>T Hm (exon 2 skipped)	IUGR, in utero cardiac thickening, **oligohydramnios, LA**, **encephalopathy, hypotonia**, **hypospadias**, **DF**, aminoaciduria, HCMP, HF, hernia, PMR, FTT, feeding difficulties, intestinal pseudo-obstructions and delayed gastric emptying	n.a.	2	[154,159]
c.317–2A>G Hm (exon 2 skipped)	oligohydramnios, IUGR, **3-MGA, LA**, **HA**, **HCMP/NCCM/LVNC**, **hypotonia**, **DF, PMR**, **FTT**, HF, hypoglycemia, cardiomegaly, WPW, tachycardia, epilepsy, PPHN/AH, microcephaly, ataxia, brain atrophy, extrapyramidal signs, liver failure, hepatomegaly, microphthalmia, cataract, ptosis, strabismus, hypospadias, cryptorchidism, hernia, feeding difficulties, apnoea	↓↓↓ levels of cV complex, ↓↓↓ ATP synthase activity	52	[123,124, 126, 148-158]
c.3172A>G/c.118_119insGT (exon 2 skipped/ p.Ser40CysfsTer11)	oligohydramnios, poor fetal movement, **3-MGA, HCMP**, LA, hernia, diastases recti, DF, FTT	↓↓↓ levels of cV complex, ↓↓↓ ATP hydrolytic activity	2	[126,148, 154,164]
c.317–2A>G/c.251delC (exon 2 skipped/n.a.)	late-onset epilepsy and mild intellectual disability	n.a.	1	[154]

c.317–2A>G/c.349_352del (exon 2 skipped/ p.Ile117AlafsTer36)	oligohydramnios, IUGR, LA, HA, HCMP, epilepsy, hypotonia, DF, PMR, apnea	↓↓↓ levels of cV complex, ↓↓ ATP hydrolytic activity	1	[156]
c.317–2A>G/c.470T>A (exon 2 skipped/n.a.)	n.a.	n.a.	1	[154]
c.317–2A>G/c.494G>A (exon 2 skipped/p.Gly165Asp)	3-MGA, LA, HA, Reye-like syndrome, tachycardia, HCMP, brain abnormalities, exercise intolerance	↓↓↓ levels of cV complex	1	[165,170]
c.317–2A>G/c.628A>C (exon 2 skipped/p.Tyr210Pro)	**3-MGA, LA, HA, hypotonia, PMR, growth retardation**, patent foramen ovale, HCMP, pneumothorax, PPHN, WPW	↓↓↓ levels of cV complex, ↓↓ ATP synthase activity	2	[153]
c.317–2A>G/c.783A>G (exon 2 skipped/p.Ter261Trpext17)	oligohydramnios, IUGR, LA, HCMP, epilepsy, DF, PMR, apnea	↓↓↓ levels of cV complex, ↓ ATP hydrolytic activity	1	[156]
c.336T>A Hm (p.Tyr112Ter)	oligohydramnios, IUGR, in utero cardiac thickening, LA, HA, HCMP, hypertonia, limb deformations, hernia, undescended testicles, hypospadias, DF, PMR, FTT	↓↓↓ ATP hydrolytic activity	1	[159]
c.359delC Hm (n.a.)	n.a.	n.a.	1	[154]
c.535C>T Hm (p.Tyr179His)	IUGR, 3-MGA, HA, LA, HCMP, hypotonia, DF, hernia, bilateral cataract, undescended testis, hypospadias, PMR	n.a.	1	[154,162]
c.563T>C Hm (p.Leu188Pro)	IUGR, 3-MGA, LA, HCMP, LVNC, dilated aortic root + sinotubular junction + ascending aorta, hypotonia, DF, FTT	n.a.	1	[163]
c.578_579delCA Hm (p.Asn198Ter)	**IUGR, 3-MGA, LA, HCMP, encephalopathy, hypotonia, cataract, DF, hypospadias, PMR, FTT,** ataxia, brain atrophy, epilepsy, hernia, vomiting, undescended testis, delayed gastric emptying,	↓↓↓ ATP hydrolytic activity	2	[154,159]
c.701A>C Hm (p.His234Pro)	oligohydramnios, IUGR, **3-MGA, LA, HCMP, hypotonia, PMR,** HA, encephalopathy, epileptic spasm, PPHN, leukoencephalopathy, DF, FTT, feeding difficulties, apnea	↓↓ ATP hydrolytic activity	2	[152,156]

Hm – homozygous variant, Ht – heterozygous variant; as – altered splicing; cV – complex V (ATP synthase). n.a. – data not available. Clinical phenotype in bold – symptoms described in most of the patients if more than one; 3-MGA – 3-methylglutaconic aciduria; AH – arterial hypertension; DF – dysmorphic features; FTT – failure to thrive; HA – hyperammonemia; HCMP – hypertrophic cardiomyopathy; HF – heart failure; HHH-syndrome – hyperornithinemia-hyperammonemia-homocitrullinuria syndrome; HSP – hereditary spastic paraplegia; IUGR – intrauterine growth restriction; LA – lactic acidosis; LS – Leigh syndrome; LVNC – left ventricular non-compaction; NCCM – non-compaction cardiomyopathy; PPHN – persistent pulmonary hypertension of the newborn; PMR – psychomotor retardation (in general, details in the references and text).

nDNA pathogenic variants in assembly factors of ATP synthase

ATPAF2

In 2004, De Meirleir *et al.* [125] described a patient with severe neonatal encephalopathy harboring missense variant of ATPAF2 protein, an assembly factor essential for incorporation of α subunit into F_1 domain of ATP synthase. A homozygous c.280T>A substitution in *ATPAF2* gene was found in a girl with dysmorphic features, cortical-subcortical brain atrophy followed by basal ganglia atrophy and metabolic acidosis, who died at the age of 14 months. The TGG>AGG transition caused replacement of evolutionary conserved neutral tryptophan

at position 94 to a basic arginine (Table 4), probably affecting the interaction of ATPAF2 with α subunit and leading to a severe reduction of native complex V without accumulation of F_1-containing subcomplexes.

TMEM70

Pathogenic variants of *TMEM70* gene, which encodes TMEM70 protein, represent the most common cause of isolated ATP synthase deficiency in newborns (Table 4). *TMEM70* was first described in 2006 by Calvo *et al.* [147] as a gene encoding potentially mitochondrial protein. TMEM70 protein was recognized as a new biogenetic factor of ATP synthase based on the findings in cells of patients carrying *TMEM70* pathogenic variants, which in most cases led to a drastic reduction in the level of fully assembled ATP synthase with a slight accumulation of F_1 subassemblies [126]. First two pathogenic variants of T*MEM70* gene were found in the group of patients with severe neonatal LA and encephalo-cardiomyopathy.

c.317–2A>G: the most common TMEM70 pathogenic variant

Homozygous splice site c.317–2A>G variant at the end of the second intron of *TMEM70* gene, which prevents the synthesis of TMEM70 protein, has been found in 24 cases including the first patient reported in 1999 [123,126,148]. Later on, another 28 patients carrying this variant in bi-allelic form were described [149-158]. The absence of TMEM70 protein in patients typically presented prenatally as IUGR, sometimes accompanied with oligohydramnios. Alternatively, symptoms may appear soon after birth. Early phenotypes include severe metabolic disbalance with LA, 3-MGA, hyperammonemia, hypotonia, and HCMP. During the life, other typical symptoms develop, less severe malformations and abnormalities such as facial dysmorphism, hernias (including the most severe diaphragmatic hernia), hypospadias and cryptorchidism in boys, but also neuromuscular disorders (ataxia, extrapyramidal signs, ptosis), strabismus, hepatomegaly, brain defects including encephalopathy, atrophy, microcephaly, and epilepsy, and general developmental delay with failure to thrive and psychomotor retardation. In a subset of patients, the disease course was accompanied with persistent pulmonary artery hypertension in the neonatal period [149,152-154]. Although the metabolic crisis is usually one of the initial phenotypes, Baban *et al.* described 3 patients suffering from early-onset metabolic cardiomyopathies, one with *TMEM70* c.317–2A>G variant and with 3-MGA development only at later stage [158]. Rarely, the cardiac presentation is not limited to HCMP, but also leads to another type of cardiomyopathy, left ventricular non-compaction (LVNC) [155], and in one case in combination with HCMP, progressing to dilated form [158]. Heart rate abnormalities are also uncommon, presenting mainly as tachycardia or Wolf-Parkinson-White syndrome [149,152-154,157,158]. Six patients out of 51 were not diagnosed with any form of cardiac involvement [148]. As mitochondrial defects can be associated with ophthalmologic defects, these were found also in patients carrying *TMEM70* c.317–2A>G variant, except for strabismus as a rather rare condition of chronic progressive external ophthalmoplegia, cataract and microphthalmia [148,152-154].

More than half of the patients died, usually from a severe acute metabolic crisis or heart failure. They can be divided into two groups according to the age at death – most of the patients died in the first few days or months of life at most, and the rest between one and five years. Interestingly, some patients can survive significantly longer, with one of them reaching 12 years and two reaching 13 years when they were last reported [148,150,155]. As pointed out by Honzík *et al.* in a detailed retrospective clinical study, if the patients survive the critical postnatal period of the first weeks and months of life, the metabolic problems and cardiac disorders may at least partially recede [148]. Interestingly, none of the TMEM70 patients with neonatal onset surviving to the age five years, nor any of the patients with later onset, have died to date.

Other TMEM70 pathogenic variants

Discovery of *TMEM70* as disease-causing gene in patients with a previously unknown cause of isolated ATP synthase deficiency of nuclear origin allowed the diagnosis of other patients, and indeed the patients carrying the novel *TMEM70* pathogenic variants were reported. In most cases, the clinical picture shared the same typical features as the common variant, but the genetic background was different.

Three homozygous pathogenic variants have been reported, skipping exon 2 of *TMEM70* gene and resulting in putative aberrant TMEM70 protein lacking functional N-terminal targeting sequence, affecting import of TMEM70 into mitochondria or its membrane assembly. Patients presented with typical features described above, but without 3-MGA in most of them.

TMEM70 c.316+1G>T splice site variant was found in two siblings, who died at ten days and five months of age, respectively [159]. In contrast to these patients, the patient carrying g.2436–3789 in-frame deletion as well as the patient with c.211–450_317–568del variant (who presented also with 3-MGA), survived much longer, being reported at six and seven years of age, respectively [150,160].

Synthesis of potentially truncated TMEM70 has been reported to be associated with four additional homozygous nonsense or frameshift variants, creating premature stop codon. Two siblings harbored frameshift c.578_579delCA deletion resulting in a putative 197 AA long protein lacking almost two thirds of the C-terminus with remarkably different survival; one is 24 years old while the second died at 3.5 years [159]. Three *TMEM70* variants predicted to result in very short TMEM70 protein (112 AA at maximum) have been described in five patients. One patient with nonsense c.336T>A variant was identified at 11 months of age [159], while of the two patients with nonsense c.238C>T variant, one died at seven days postnatally [159] and the second was reported at one year of age [156]. Frameshift c.105dupT variant has been described in two siblings with transiently elevated levels citrulline [161], a condition previously reported only in two living TMEM70 patients with the common variant [148].

So far, only three homozygous missense variants have been described. The first is c.535C>T substitution that changes the highly conserved tyrosine to a histidine at position 179 at the beginning of the C-terminus [162]. The second missense variant c.701A>C changes conserved histidine 234 to proline [152,156]. Both patients presented with typical phenotypes such as cardiomyopathy, hypotonia, and metabolic crisis, and less frequently arterial hypertension. Recently, third missense c.563T>C *TMEM70* variant, changing highly conserved leucine 188 to proline, was described in a boy with HCMP and LVNC, moderately dilated aortic root, severely dilated sinotubular junction, and severely dilated ascending aorta, failure to thrive, facial dysmorphism, and hypotonia. Although cardiomyopathy was present at birth, the patient did not show typical early-onset metabolic decompensation, but rather later decompensation triggered by infectious disease [163].

The common c.317–2A>G variant can also be found as compound heterozygous in combination with other *TMEM70* pathogenic variants. Two patients with typical TMEM70 symptoms but in a milder form have been described to carry c.317–2A>G and c.118_119insGT frameshift variant resulting in premature stop codon and truncated TMEM70 protein p.Ser40CysfsTer11 [126,164]. Two combinations of common c.317–2A>G and missense variants have been reported. Clinical outcome of the patient with c.494G>A variant, which changes neutral glycine 165 to acidic aspartate at the C-terminus, was mild with Reye-like syndrome and long survival of at least 14 years [165], while both patients reported by Torraco *et al.* are severely affected by metabolic acidosis and cardiomyopathy based on the combination of c.317–2A>G and c.628A>G, which changes highly conserved threonine 210 to proline [152,153]. Two other compound heterozygous variants affecting the C-terminus of TMEM70 protein have been found in combination with the common variant [156]. Frameshift microdeletion c.349_352delC is predicted to change isoleucine 117 to alanine and result in a truncated protein shortened to 36 AA, while missense variant c.783A>G is predicted to change the stop codon to tryptophan, resulting in an aberrant protein with 17 extra AA at the C-terminus. Although the patients suffer from severe encephalo-cardiomyopathy without 3-MGA, the onset of the disease was quite late (eight months and two years, respectively). A unique combination of the novel c.141delG *TMEM70* deletion with c.316+1G>A variant previously described as homozygous was reported by Hirono *et al.* being the first *TMEM70* bi-allelic variant in Japanese patients [166]. Both variants are predicted to result in the loss-of-function phenotype. Two brothers were diagnosed with LVNC and psychomotor delay, the younger also with LA, 3-MGA, inguinal hernia, undescended testis, and failure to thrive, typical clinical picture of TMEM70 patients.

In the study of Magner *et al.* [154], several novel *TMEM70* pathogenic variants were mentioned, including homozygous c.359delC microdeletion, and compound heterozygotes, harboring two novel variants in combination with the common one: c.251delC microdeletion and c.470T>A substitution. No specific information about the patients was given, only the fact that the patient carrying c.317–2A>G and c.251delC was 25 years old with very mild phenotype of epilepsy and mild intellectual disability. The last five TMEM70 patients not mentioned before, are those reported by Brambilla *et al.* [167], diagnosed with primary mitochondrial disorder, all with cardiovascular involvement. However, information on the clinical course or type of *TMEM70* variant was lacking (these patients

are not included in Table 4).

Pathogenic *TMEM70* variants found in patients with isolated ATP synthase deficiency can also be distinguished according to the sequence regions affected. First are variants localized in transit peptide [126,159,161,166] or in the first transmembrane domain [156,159] of the protein, generating premature stop codon, with the longest version of the protein consisting of 112 AA, containing only N-terminus and approximately half of the first transmembrane domain (Fig. 2C). The second group represents variants affecting TMEM70 C-terminus, mostly altering highly conserved residues [152,153,156,162,163,165] or creating premature stop codon where the majority of the C-terminus is missing [159]. Remaining variants, including the most common c.317–2A>G variant, are splice site variants that skip exon 2 (coding for AA 71-105), usually resulting in the loss of TMEM70 transcript and thus of the protein [126,150,159,160]. Taken together, C-terminus of TMEM70, which is directed into the mitochondrial matrix, is most likely the key part of protein that functions in the assembly of ATP synthase complex. This is consistent with the findings that TMEM70 is involved in the incorporation of subunit *c* into inner mitochondrial membrane, in the formation of c_8 ring, and in its association with F_1 part of the complex [7,8]. Furthermore, its role in translation and membrane insertion of mtDNA encoded subunits of ATP synthase cannot be excluded [8].

Discussion and Conclusions

Since mitochondria play a crucial role in energetic metabolism of the living cells, defects of their function are linked to many pathologies. In most of them, for example in neurodegenerative diseases such as Parkinson and Alzheimer, or systemic diabetes mellitus, as well as in cancer, mitochondrial dysfunction is not the only underlying mechanisms, but the basis of these polygenic diseases is often a combination of more pathological factors. Moreover, in these pathologies the mitochondrial function is only partially affected and usually linked with another condition, such as increased ROS production [10]. Unsurprisingly, strong reduction in ATP levels is usually embryonically lethal and thus cannot represent relevant pathological mechanism in these diseases. On the other side of the spectrum are rare inherited isolated defects of oxidative phosphorylation apparatus including disorders of the mitochondrial ATP synthase, where profound dysfunction of mitochondrial energy provision is the driver of pathological presentation. NGS strategies highly accelerated the discovery of new disease-causing genes and the diagnosis of clinically affected patients with mitochondrial disease, but causative and effective treatment of mitochondrial disorders with high heterogeneity of symptoms still does not exist yet. Thus, the therapy remains largely symptomatic, although, in many cases, it is crucial for the survival and quality of life of the patients.

In large number of cases with proven mitochondrial disorder the affected gene remains unknown, and the diagnostic and screening depend on clinical and biochemical phenotyping. It would be nice to have some specific marker for ATP synthase diseases, which could reveal the defect before first symptoms occur (if the onset is not at birth), but unfortunately, any such marker doesn´t exists. In 2014, Mori *et al.* described a homoplasmic patient with LS started at 4 months of age, but the initial sign was hypocitrullinemia, which was revealed during neonatal screening [49]. The mother of the patient with lover levels of pathogenic variant and diagnosed with NARP syndrome at age 24 years had low levels of citrulline as well. These findings strengthen the suggestion of Rabier *et al.* [168] that hypocitrullinemia should be used as a marker of mitochondrial disorders and patients can benefit from early diagnosis. Elevated levels of ammonia in the blood are a common biochemical finding in patients suffering from mitochondrial diseases of ATP synthase. The majority of cases are attributed to pathogenic variants of *TMEM70* (Table 2-4). Hyperammonemia may therefore be regarded as a further potential marker for this disorder. Both citrulline synthesis and detoxification of ammonium are linked with the urea cycle, which occurs in mitochondria [169]. Given that carbamoylphosphate synthetase 1 is a urea cycle enzyme that depends on ATP, it can be postulated that ATP synthase defects can result in hypocitrullinemia and hyperammonemia. Nevertheless, there are at least three clearly documented cases of TMEM70 patients with hyperammonemia accompanied by hypercitrullinemia during metabolic crises, yet with normal citrulline levels at follow-up [148,161], questioning the real diagnostic utility of this marker. The combination of hyperammonemia and hypercitrullinemia may be explained by a defect in argininosuccinate synthase 1, another urea cycle

ATP-dependent enzyme that converts citrulline to arginine in the cytosol [148,161,169]. The next potential marker is 3-methylglutaconic acid aciduria (3-MGA), as elevated levels of this compound are frequently associated with nDNA pathogenic variants of ATP synthase-linked genes [125,127,134,137, 150,154,156,161-163,166,170]. There are two classes of 3-MGA [171]. Primary 3-MGA is caused directly by defects in the leucine catabolism pathway. Secondary 3-MGA is not linked with defective catabolism of leucine; however, a pathogenic variant in some mitochondrial gene was identified in nearly all cases. It was proposed that defects in the OXPHOS pathway led to the inhibition of the TCA cycle. Consequently, acetyl-CoA is unable to enter the TCA cycle, resulting in the accumulation of this intermediate metabolite. This accumulation activates a divergent pathway that ultimately leads to the synthesis of 3-MGA [171]. However, not every patient with mitochondrial disease, even with isolated ATP synthase deficiency, has elevated levels of 3-MGA, and patients with delayed increase of 3-MGA are reported [163]. Furthermore, 3-MGA aciduria is linked with metabolic diseases in general, not only with defective mitochondrial metabolism [172].

As summarized in this review, clinical pictures of the patients with isolated ATP synthase deficiency represent a diverse spectrum of phenotypes, even if the same gene is affected. At the same time, the symptoms range from very mild to fatal, making the situation even more complicated. Moreover, some of the patients display atypical clinical features [173], and mitochondrial disorders mimicking others (usually neuromuscular), and *vice versa*, were described [55,83,174]. On the other hand, the knowledge of the disease-causing genes in combination with initial disease phenotype can help the clinicians to predict the disease course and better target the therapy. In any case, identification of the causative variant even in the genes that are known to be linked with mitochondrial disorders is a long-distance run. Thanks to the advances in methodology of NGS, namely whole exome sequencing (WES) and whole genome sequencing (WGS), revealing of mitochondrial disease-causing genes became a lot easier. In 2012, a key study of Calvo *et al.* [175] described the use of WES in a clinical trial, and they identified several disease-causing genes not to be linked with mitochondrial diseases before. This study was, however, limited only to “Mitoexome”, it means only to the genes that were known to be coding for mitochondrial proteins. From that time, several other studies on cohorts of patients suffering from mitochondrial diseases with unknown underlying genetic variant were performed, describing novel genes involved in these disorders [173,176,177], in some cases encoding non mitochondrial proteins [174], or mitochondrial proteins not included in Mitocarta database [178]. During eight years, from 2012 till 2020, the number of mitochondrial disease-related genes increased from about 100 to more than 300 [179]. It is obvious, that even if NGS technology itself is more and more accessible for clinicians methodologically, and cost-effective methods and kits are developed [180], still the key aspect is the setup of the studies. It means not only the criteria according to which the patients are selected for the study, but especially bioinformatic restrains defined in the pipeline (how to further sort the patients, which gene database to use, how to confirm the pathogenicity, etc.) [179]. It is obvious, that freely accessible and up to date databases of genes, linked with mitochondrial diseases, could significantly increase the chances of mitopatients to effective therapy. It can help to associate patients with similar phenotypes for therapeutic trials and speed up the diagnosis of those still waiting for it. Such databases could also help with the proper classification of the variants according to their pathogenicity, as many of the variants are undergoing reclassification [181].

Another interesting question is the possibility to prevent mitochondrial diseases by genetic counselling. Of course, in the families with known pathogenic variants of nuclear origin, prenatal diagnostics is commonly used. Regarding the mtDNA variants, the prenatal diagnosis is much more difficult. In cases of inherited variants, the risk for the disease prevalence is very high, because of the bottleneck phenotype [182]. In the study of Sallevelt *et al.* [183], several families with previous appearance of *de novo* mtDNA *MT-ATP6* pathogenic variants were described. Using prenatal diagnosis in the following pregnancies the authors suggested that the risk that defect will occur *de novo* again is very low, and all the families with negative findings of the mutation in second pregnancy had healthy children.

Abbreviations

3-MGA, 3-methylglutaconic aciduria; AA, amino

acid(s); DAPIT, diabetes-associated protein in insulin sensitive tissues; (F)BSN, (familial) bilateral striatal necrosis; FTT, failure to thrive; HCMP, hypertrophic cardiomyopathy; HSP, hereditary spastic paraplegia; IUGR, intrauterine growth restriction; LA, lactic acidosis; LHON, Leber's hereditary optic neuropathy; LS, Leigh syndrome; LVNC, left ventricular non-compaction; mtDNA, mitochondrial DNA; NARP, neurogenic muscle weakness (or neuropathy), ataxia and retinitis pigmentosa syndrome; nDNA, nuclear DNA; NGS, next-generation sequencing; OSCP, oligomycin-sensitivity conferring protein; OXPHOS, oxidative phosphorylation system; PMR, psychomotor retardation; ROS, reactive oxygen species; WES, whole exome sequencing; WGS, whole genome sequencing.

Conflict of Interest

There is no conflict of interest.

Acknowledgements

This research was supported by the project National Institute for Research of Metabolic and Cardiovascular Diseases (Programme EXCELES, ID Project No. LX22NPO5104) – Funded by the European Union – Next Generation EU, by the Czech Science Foundation GACR 21-18993S and by the Czech Health Research Council NU21-07-00550. Institutional funding to the Institute of Physiology of the Czech Academy of Sciences is provided through the RVO:67985823.

References

1. Kobayashi R, Ueno H, Li CB, Noji H. Rotary catalysis of bovine mitochondrial F(1)-ATPase studied by single-molecule experiments. Proc Natl Acad Sci U S A 2020;117:1447-1456. https://doi.org/10.1073/pnas.1909407117
2. Lai Y, Zhang Y, Zhou S, Xu J, Du Z, Feng Z, Yu L, Zhao Z, Wang W, Tang Y, Yang X, Guddat LW, Liu F, Gao Y, Rao Z, Gong H. Structure of the human ATP synthase. Mol Cell 2023;83:2137-2147 e2134. https://doi.org/10.1016/j.molcel.2023.04.029
3. Green DW, Grover GJ. The IF(1) inhibitor protein of the mitochondrial F(1)F(0)-ATPase. Biochim Biophys Acta 2000;1458:343-355. https://doi.org/10.1016/S0005-2728(00)00085-2
4. Wittig I, Meyer B, Heide H, Steger M, Bleier L, Wumaier Z, Karas M, Schagger H. Assembly and oligomerization of human ATP synthase lacking mitochondrial subunits a and A6L. Biochim Biophys Acta 2010;1797:1004-1011. https://doi.org/10.1016/j.bbabio.2010.02.021
5. Wang ZG, White PS, Ackerman SH. Atp11p and Atp12p are assembly factors for the F(1)-ATPase in human mitochondria. J Biol Chem 2001;276:30773-30778. https://doi.org/10.1074/jbc.M104133200
6. Li Y, Jourdain AA, Calvo SE, Liu JS, Mootha VK. CLIC, a tool for expanding biological pathways based on co-expression across thousands of datasets. PLoS Comput Biol 2017;13:e1005653. https://doi.org/10.1371/journal.pcbi.1005653
7. Kovalcikova J, Vrbacky M, Pecina P, Tauchmannova K, Nuskova H, Kaplanova V, Brazdova A, Alan L, Elias J, Cunatova K, Korinek V, Sedlacek R, Mracek T, Houstek J. TMEM70 facilitates biogenesis of mammalian ATP synthase by promoting subunit c incorporation into the rotor structure of the enzyme. FASEB J 2019;33:14103-14117. https://doi.org/10.1096/fj.201900685RR
8. Carroll J, He J, Ding S, Fearnley IM, Walker JE. TMEM70 and TMEM242 help to assemble the rotor ring of human ATP synthase and interact with assembly factors for complex I. Proc Natl Acad Sci U S A 2021;118. https://doi.org/10.1073/pnas.2100558118
9. Yu J, Liang X, Ji Y, Ai C, Liu J, Zhu L, Nie Z, Jin X, Wang C, Zhang J, Zhao F, Mei S, Zhao X, Zhou X, Zhang M, Wang M, Huang T, Jiang P, Guan MX. PRICKLE3 linked to ATPase biogenesis manifested Leber's hereditary optic neuropathy. J Clin Invest 2020;130:4935-4946. https://doi.org/10.1172/JCI134965
10. Harrington JS, Ryter SW, Plataki M, Price DR, Choi AMK. Mitochondria in health, disease, and aging. Physiol Rev 2023;103:2349-2422. https://doi.org/10.1152/physrev.00058.2021
11. Rahman S. Mitochondrial disease in children. J Intern Med 2020;287:609-633. https://doi.org/10.1111/joim.13054
12. Ng YS, Bindoff LA, Gorman GS, Klopstock T, Kornblum C, Mancuso M, McFarland R, Sue CM, Suomalainen A, Taylor RW, Thorburn DR, Turnbull DM. Mitochondrial disease in adults: recent advances and future promise. Lancet Neurol 2021;20:573-584. https://doi.org/10.1016/S1474-4422(21)00098-3

13. Al-Kafaji G, Bakheit HF, AlAli F, Fattah M, Alhajeri S, Alharbi MA, Daif A, Alsabbagh MM, Alwehaidah MS, Bakhiet M. Next-generation sequencing of the whole mitochondrial genome identifies functionally deleterious mutations in patients with multiple sclerosis. PLoS One 2022;17:e0263606. https://doi.org/10.1371/journal.pone.0263606
14. de Mello AH, Costa AB, Engel JDG, Rezin GT. Mitochondrial dysfunction in obesity. Life Sci 2018;192:26-32. https://doi.org/10.1016/j.lfs.2017.11.019
15. Yaribeygi H, Sathyapalan T, Atkin SL, Sahebkar A. Molecular mechanisms linking oxidative stress and diabetes mellitus. Oxid Med Cell Longev 2020;2020:8609213. https://doi.org/10.1155/2020/8609213
16. Prasun P. Mitochondrial dysfunction in metabolic syndrome. Biochim Biophys Acta Mol Basis Dis 2020;1866:165838. https://doi.org/10.1016/j.bbadis.2020.165838
17. Wallace DC. Mitochondria and cancer. Nat Rev Cancer 2012;12:685-698. https://doi.org/10.1038/nrc3365
18. Park CB, Larsson NG. Mitochondrial DNA mutations in disease and aging. J Cell Biol 2011;193:809-818. https://doi.org/10.1083/jcb.201010024
19. Lott MT, Leipzig JN, Derbeneva O, Xie HM, Chalkia D, Sarmady M, Procaccio V, Wallace DC. mtDNA Variation and Analysis Using Mitomap and Mitomaster. Curr Protoc Bioinformatics 2013;44:1 23 21-26. https://doi.org/10.1002/0471250953.bi0123s44
20. DiMauro S, Mancuso M. Mitochondrial diseases: therapeutic approaches. Biosci Rep 2007;27:125-137. https://doi.org/10.1007/s10540-007-9041-4
21. Ardissone A, Ferrera G, Lamperti C, Tiranti V, Ghezzi D, Moroni I, Lamantea E. Phenotyping mitochondrial DNA-related diseases in childhood: A cohort study of 150 patients. Eur J Neurol 2023;30:2079-2091. https://doi.org/10.1111/ene.15814
22. Galber C, Carissimi S, Baracca A, Giorgio V. The ATP Synthase Deficiency in Human Diseases. Life (Basel) 2021;11. https://doi.org/10.3390/life11040325
23. D'Aurelio M, Vives-Bauza C, Davidson MM, Manfredi G. Mitochondrial DNA background modifies the bioenergetics of NARP/MILS ATP6 mutant cells. Hum Mol Genet 2010;19:374-386. https://doi.org/10.1093/hmg/ddp503
24. Mkaouar-Rebai E, Chaari W, Younes S, Bousoffara R, Sfar MT, Fakhfakh F. Maternally inherited Leigh syndrome: T8993G mutation in a Tunisian family. Pediatr Neurol 2009;40:437-442. https://doi.org/10.1016/j.pediatrneurol.2009.01.004
25. Rossignol R, Faustin B, Rocher C, Malgat M, Mazat JP, Letellier T. Mitochondrial threshold effects. Biochem J 2003;370:751-762. https://doi.org/10.1042/bj20021594
26. Bugiardini E, Bottani E, Marchet S, Poole OV, Beninca C, Horga A, Woodward C, Lam A, Hargreaves I, Chalasani A, Valerio A, Lamantea E, Venner K, Holton JL, Zeviani M, Houlden H, Quinlivan R, Lamperti C, Hanna MG, Pitceathly RDS. Expanding the molecular and phenotypic spectrum of truncating MT-ATP6 mutations. Neurol Genet 2020;6:e381. https://doi.org/10.1212/NXG.0000000000000381
27. Lopez-Gallardo E, Solano A, Herrero-Martin MD, Martinez-Romero I, Castano-Perez MD, Andreu AL, Herrera A, Lopez-Perez MJ, Ruiz-Pesini E, Montoya J. NARP syndrome in a patient harbouring an insertion in the MT-ATP6 gene that results in a truncated protein. J Med Genet 2009;46:64-67. https://doi.org/10.1136/jmg.2008.060616
28. Seneca S, Abramowicz M, Lissens W, Muller MF, Vamos E, de Meirleir L. A mitochondrial DNA microdeletion in a newborn girl with transient lactic acidosis. J Inherit Metab Dis 1996;19:115-118. https://doi.org/10.1007/BF01799407
29. Jesina P, Tesarova M, Fornuskova D, Vojtiskova A, Pecina P, Kaplanova V, Hansikova H, Zeman J, Houstek J. Diminished synthesis of subunit a (ATP6) and altered function of ATP synthase and cytochrome c oxidase due to the mtDNA 2 bp microdeletion of TA at positions 9205 and 9206. Biochem J 2004;383:561-571. https://doi.org/10.1042/BJ20040407
30. Hejzlarova K, Kaplanova V, Nuskova H, Kovarova N, Jesina P, Drahota Z, Mracek T, Seneca S, Houstek J. Alteration of structure and function of ATP synthase and cytochrome c oxidase by lack of Fo-a and Cox3 subunits caused by mitochondrial DNA 9205delTA mutation. Biochem J 2015;466:601-611. https://doi.org/10.1042/BJ20141462

31. Ware SM, El-Hassan N, Kahler SG, Zhang Q, Ma YW, Miller E, Wong B, Spicer RL, Craigen WJ, Kozel BA, Grange DK, Wong LJ. Infantile cardiomyopathy caused by a mutation in the overlapping region of mitochondrial ATPase 6 and 8 genes. J Med Genet 2009;46:308-314. https://doi.org/10.1136/jmg.2008.063149
32. Imai A, Fujita S, Kishita Y, Kohda M, Tokuzawa Y, Hirata T, Mizuno Y, Harashima H, Nakaya A, Sakata Y, Takeda A, Mori M, Murayama K, Ohtake A, Okazaki Y. Rapidly progressive infantile cardiomyopathy with mitochondrial respiratory chain complex V deficiency due to loss of ATPase 6 and 8 protein. Int J Cardiol 2016;207:203-205. https://doi.org/10.1016/j.ijcard.2016.01.026
33. Imai-Okazaki A, Kishita Y, Kohda M, Mizuno Y, Fushimi T, Matsunaga A, Yatsuka Y, Hirata T, Harashima H, Takeda A, Nakaya A, Sakata Y, Kogaki S, Ohtake A, Murayama K, Okazaki Y. Cardiomyopathy in children with mitochondrial disease: Prognosis and genetic background. Int J Cardiol 2019;279:115-121. https://doi.org/10.1016/j.ijcard.2019.01.017
34. Zigman T, Sikic K, Petkovic Ramadza D, Mayr J, Wortmann S, Prokisch H, Ninkovic D, Dilber D, Saric D, Rubic F, Galic S, Slavicek J, Belina D, Fumic K, Baric I. ATP synthase deficiency due to m.8528T>C mutation - a novel cause of severe neonatal hyperammonemia requiring hemodialysis. J Pediatr Endocrinol Metab 2021;34:389-393. https://doi.org/10.1515/jpem-2020-0396
35. Jonckheere AI, Hogeveen M, Nijtmans LG, van den Brand MA, Janssen AJ, Diepstra JH, van den Brandt FC, van den Heuvel LP, Hol FA, Hofste TG, Kapusta L, Dillmann U, Shamdeen MG, Smeitink JA, Rodenburg RJ. A novel mitochondrial ATP8 gene mutation in a patient with apical hypertrophic cardiomyopathy and neuropathy. J Med Genet 2008;45:129-133. https://doi.org/10.1136/jmg.2007.052084
36. Kytovuori L, Lipponen J, Rusanen H, Komulainen T, Martikainen MH, Majamaa K. A novel mutation m.8561C>G in MT-ATP6/8 causing a mitochondrial syndrome with ataxia, peripheral neuropathy, diabetes mellitus, and hypergonadotropic hypogonadism. J Neurol 2016;263:2188-2195. https://doi.org/10.1007/s00415-016-8249-2
37. Fragaki K, Chaussenot A, Serre V, Acquaviva C, Bannwarth S, Rouzier C, Chabrol B, Paquis-Flucklinger V. A novel variant m.8561C>T in the overlapping region of MT-ATP6 and MT-ATP8 in a child with early-onset severe neurological signs. Mol Genet Metab Rep 2019;21:100543. https://doi.org/10.1016/j.ymgmr.2019.100543
38. Ronchi D, Bordoni A, Cosi A, Rizzuti M, Fassone E, Di Fonzo A, Servida M, Sciacco M, Collotta M, Ronzoni M, Lucchini V, Mattioli M, Moggio M, Bresolin N, Corti S, Comi GP. Unusual adult-onset Leigh syndrome presentation due to the mitochondrial m.9176T>C mutation. Biochem Biophys Res Commun 2011;412:245-248. https://doi.org/10.1016/j.bbrc.2011.07.076
39. Holt IJ, Harding AE, Petty RK, Morgan-Hughes JA. A new mitochondrial disease associated with mitochondrial DNA heteroplasmy. Am J Hum Genet 1990;46:428-433.
40. de Vries DD, van Engelen BG, Gabreels FJ, Ruitenbeek W, van Oost BA. A second missense mutation in the mitochondrial ATPase 6 gene in Leigh's syndrome. Ann Neurol 1993;34:410-412. https://doi.org/10.1002/ana.410340319
41. Wong LC, Chen T, Schmitt ES, Wang J, Tang S, Landsverk M, Li F, Zhang S, Wang Y, Zhang VW, Craigen WJ. Clinical and laboratory interpretation of mitochondrial mRNA variants. Hum Mutat 2020;41:1783-1796. https://doi.org/10.1002/humu.24082
42. Tatuch Y, Christodoulou J, Feigenbaum A, Clarke JT, Wherret J, Smith C, Rudd N, Petrova-Benedict R, Robinson BH. Heteroplasmic mtDNA mutation (T----G) at 8993 can cause Leigh disease when the percentage of abnormal mtDNA is high. Am J Hum Genet 1992;50:852-858.
43. Fryer A, Appleton R, Sweeney MG, Rosenbloom L, Harding AE. Mitochondrial DNA 8993 (NARP) mutation presenting with a heterogeneous phenotype including 'cerebral palsy'. Arch Dis Child 1994;71:419-422. https://doi.org/10.1136/adc.71.5.419
44. Houstek J, Klement P, Hermanska J, Houstkova H, Hansikova H, Van den Bogert C, Zeman J. Altered properties of mitochondrial ATP-synthase in patients with a T-->G mutation in the ATPase 6 (subunit a) gene at position 8993 of mtDNA. Biochim Biophys Acta 1995;1271:349-357. https://doi.org/10.1016/0925-4439(95)00063-A
45. Uziel G, Moroni I, Lamantea E, Fratta GM, Ciceri E, Carrara F, Zeviani M. Mitochondrial disease associated with the T8993G mutation of the mitochondrial ATPase 6 gene: a clinical, biochemical, and molecular study in six families. J Neurol Neurosurg Psychiatry 1997;63:16-22. https://doi.org/10.1136/jnnp.63.1.16

46. Carelli V, Baracca A, Barogi S, Pallotti F, Valentino ML, Montagna P, Zeviani M, Pini A, Lenaz G, Baruzzi A, Solaini G. Biochemical-clinical correlation in patients with different loads of the mitochondrial DNA T8993G mutation. Arch Neurol 2002;59:264-270. https://doi.org/10.1001/archneur.59.2.264
47. Wei Y, Cui L, Peng B. Mitochondrial DNA mutations in late-onset Leigh syndrome. J Neurol 2018;265:2388-2395. https://doi.org/10.1007/s00415-018-9014-5
48. Hu C, Li X, Zhao L, Shi Y, Zhou S, Wu B, Wang Y. Clinical and molecular characterization of pediatric mitochondrial disorders in south of China. Eur J Med Genet 2020;63:103898. https://doi.org/10.1016/j.ejmg.2020.103898
49. Mori M, Mytinger JR, Martin LC, Bartholomew D, Hickey S. m.8993T>G-Associated Leigh Syndrome with Hypocitrullinemia on Newborn Screening. JIMD Rep 2014;17:47-51. https://doi.org/10.1007/8904_2014_332
50. Morava E, Rodenburg RJ, Hol F, de Vries M, Janssen A, van den Heuvel L, Nijtmans L, Smeitink J. Clinical and biochemical characteristics in patients with a high mutant load of the mitochondrial T8993G/C mutations. Am J Med Genet A 2006;140:863-868. https://doi.org/10.1002/ajmg.a.31194
51. Ng YS, Martikainen MH, Gorman GS, Blain A, Bugiardini E, Bunting A, Schaefer AM, Alston CL, Blakely EL, Sharma S, Hughes I, Lim A, de Goede C, McEntagart M, Spinty S, Horrocks I, Roberts M, Woodward CE, Chinnery PF, Horvath R, Nesbitt V, Fratter C, Poulton J, Hanna MG, Pitceathly RDS, Taylor RW, Turnbull DM, McFarland R. Pathogenic variants in MT-ATP6: A United Kingdom-based mitochondrial disease cohort study. Ann Neurol 2019;86:310-315. https://doi.org/10.1002/ana.25525
52. Yu XL, Yan CZ, Ji KQ, Lin PF, Xu XB, Dai TJ, Li W, Zhao YY. Clinical, Neuroimaging, and Pathological Analyses of 13 Chinese Leigh Syndrome Patients with Mitochondrial DNA Mutations. Chin Med J (Engl) 2018;131:2705-2712. https://doi.org/10.4103/0366-6999.245265
53. Stendel C, Neuhofer C, Floride E, Yuqing S, Ganetzky RD, Park J, Freisinger P, Kornblum C, Kleinle S, Schols L, Distelmaier F, Stettner GM, Buchner B, Falk MJ, Mayr JA, Synofzik M, Abicht A, Haack TB, Prokisch H, Wortmann SB, Murayama K, Fang F, Klopstock T, Group ATPS. Delineating MT-ATP6-associated disease: From isolated neuropathy to early onset neurodegeneration. Neurol Genet 2020;6:e393. https://doi.org/10.1212/NXG.0000000000000393
54. Tsao CY, Mendell JR, Bartholomew D. High mitochondrial DNA T8993G mutation (<90%) without typical features of Leigh's and NARP syndromes. J Child Neurol 2001;16:533-535. https://doi.org/10.1177/088307380101600716, https://doi.org/10.2310/7010.2001.16972
55. Aure K, Dubourg O, Jardel C, Clarysse L, Sternberg D, Fournier E, Laforet P, Streichenberger N, Petiot P, Gervais-Bernard H, Vial C, Bedat-Millet AL, Drouin-Garraud V, Bouillaud F, Vandier C, Fontaine B, Lombes A. Episodic weakness due to mitochondrial DNA MT-ATP6/8 mutations. Neurology 2013;81:1810-1818. https://doi.org/10.1212/01.wnl.0000436067.43384.0b
56. Claeys KG, Abicht A, Hausler M, Kleinle S, Wiesmann M, Schulz JB, Horvath R, Weis J. Novel genetic and neuropathological insights in neurogenic muscle weakness, ataxia, and retinitis pigmentosa (NARP). Muscle Nerve 2016;54:328-333. https://doi.org/10.1002/mus.25125
57. Larson AA, Balasubramaniam S, Christodoulou J, Burrage LC, Marom R, Graham BH, Diaz GA, Glamuzina E, Hauser N, Heese B, Horvath G, Mattman A, van Karnebeek C, Lane Rutledge S, Williamson A, Estrella L, Van Hove JKL, Weisfeld-Adams JD. Biochemical signatures mimicking multiple carboxylase deficiency in children with mutations in MT-ATP6. Mitochondrion 2019;44:58-64. https://doi.org/10.1016/j.mito.2018.01.001
58. Porto FB, Mack G, Sterboul MJ, Lewin P, Flament J, Sahel J, Dollfus H. Isolated late-onset cone-rod dystrophy revealing a familial neurogenic muscle weakness, ataxia, and retinitis pigmentosa syndrome with the T8993G mitochondrial mutation. Am J Ophthalmol 2001;132:935-937. https://doi.org/10.1016/S0002-9394(01)01187-4
59. Puddu P, Barboni P, Mantovani V, Montagna P, Cerullo A, Bragliani M, Molinotti C, Caramazza R. Retinitis pigmentosa, ataxia, and mental retardation associated with mitochondrial DNA mutation in an Italian family. Br J Ophthalmol 1993;77:84-88. https://doi.org/10.1136/bjo.77.2.84
60. Rantamaki MT, Soini HK, Finnila SM, Majamaa K, Udd B. Adult-onset ataxia and polyneuropathy caused by mitochondrial 8993T-->C mutation. Ann Neurol 2005;58:337-340. https://doi.org/10.1002/ana.20555

61. Craig K, Elliott HR, Keers SM, Lambert C, Pyle A, Graves TD, Woodward C, Sweeney MG, Davis MB, Hanna MG, Chinnery PF. Episodic ataxia and hemiplegia caused by the 8993T->C mitochondrial DNA mutation. J Med Genet 2007;44:797-799. https://doi.org/10.1136/jmg.2007.052902
62. Lemoine S, Panaye M, Rabeyrin M, Errazuriz-Cerda E, Mousson de Camaret B, Petiot P, Juillard L, Guebre-Egziabher F. Renal Involvement in Neuropathy, Ataxia, Retinitis Pigmentosa (NARP) Syndrome: A Case Report. Am J Kidney Dis 2018;71:754-757. https://doi.org/10.1053/j.ajkd.2017.09.020
63. Santorelli FM, Tanji K, Shanske S, DiMauro S. Heterogeneous clinical presentation of the mtDNA NARP/T8993G mutation. Neurology 1997;49:270-273. https://doi.org/10.1212/WNL.49.1.270
64. Chinnery PF, Elliott C, Green GR, Rees A, Coulthard A, Turnbull DM, Griffiths TD. The spectrum of hearing loss due to mitochondrial DNA defects. Brain 2000;123 (Pt 1):82-92. https://doi.org/10.1093/brain/123.1.82
65. Rucheton B, Jardel C, Filaut S, Amador MDM, Maisonobe T, Serre I, Romero NB, Leonard-Louis S, Haraux F, Lombes A. Homoplasmic deleterious MT-ATP6/8 mutations in adult patients. Mitochondrion 2020;55:64-77. https://doi.org/10.1016/j.mito.2020.08.004
66. Pastores GM, Santorelli FM, Shanske S, Gelb BD, Fyfe B, Wolfe D, Willner JP. Leigh syndrome and hypertrophic cardiomyopathy in an infant with a mitochondrial DNA point mutation (T8993G). Am J Med Genet 1994;50:265-271. https://doi.org/10.1002/ajmg.1320500310
67. Campos Y, Martin MA, Rubio JC, Solana LG, Garcia-Benayas C, Terradas JL, Arenas J. Leigh syndrome associated with the T9176C mutation in the ATPase 6 gene of mitochondrial DNA. Neurology 1997;49:595-597. https://doi.org/10.1212/WNL.49.2.595
68. Carrozzo R, Tessa A, Vazquez-Memije ME, Piemonte F, Patrono C, Malandrini A, Dionisi-Vici C, Vilarinho L, Villanova M, Schagger H, Federico A, Bertini E, Santorelli FM. The T9176G mtDNA mutation severely affects ATP production and results in Leigh syndrome. Neurology 2001;56:687-690. https://doi.org/10.1212/WNL.56.5.687
69. Akagi M, Inui K, Tsukamoto H, Sakai N, Muramatsu T, Yamada M, Matsuzaki K, Goto Y, Nonaka I, Okada S. A point mutation of mitochondrial ATPase 6 gene in Leigh syndrome. Neuromuscul Disord 2002;12:53-55. https://doi.org/10.1016/S0960-8966(01)00242-5
70. Castagna AE, Addis J, McInnes RR, Clarke JT, Ashby P, Blaser S, Robinson BH. Late onset Leigh syndrome and ataxia due to a T to C mutation at bp 9,185 of mitochondrial DNA. Am J Med Genet A 2007;143A:808-816. https://doi.org/10.1002/ajmg.a.31637
71. Childs AM, Hutchin T, Pysden K, Highet L, Bamford J, Livingston J, Crow YJ. Variable phenotype including Leigh syndrome with a 9185T>C mutation in the MTATP6 gene. Neuropediatrics 2007;38:313-316. https://doi.org/10.1055/s-2008-1065355
72. Saneto RP, Singh KK. Illness-induced exacerbation of Leigh syndrome in a patient with the MTATP6 mutation, m. 9185 T>C. Mitochondrion 2010;10:567-572. https://doi.org/10.1016/j.mito.2010.05.006
73. Ogawa E, Shimura M, Fushimi T, Tajika M, Ichimoto K, Matsunaga A, Tsuruoka T, Ishige M, Fuchigami T, Yamazaki T, Mori M, Kohda M, Kishita Y, Okazaki Y, Takahashi S, Ohtake A, Murayama K. Clinical validity of biochemical and molecular analysis in diagnosing Leigh syndrome: a study of 106 Japanese patients. J Inherit Metab Dis 2017;40:685-693. https://doi.org/10.1007/s10545-017-0042-6
74. Piekutowska-Abramczuk D, Rutyna R, Czyzyk E, Jurkiewicz E, Iwanicka-Pronicka K, Rokicki D, Stachowicz S, Strzemecka J, Guz W, Gawronski M, Kosierb A, Ligas J, Puchala M, Drelich-Zbroja A, Bednarska-Makaruk M, Dabrowski W, Ciara E, Ksiazyk JB, Pronicka E. Leigh syndrome in individuals bearing m.9185T>C MTATP6 variant. Is hyperventilation a factor which starts its development? Metab Brain Dis 2018;33:191-199. https://doi.org/10.1007/s11011-017-0122-1
75. Takada R, Tozawa T, Kondo H, Kizaki Z, Kishita Y, Okazaki Y, Murayama K, Ohtake A, Chiyonobu T. Early infantile-onset Leigh syndrome complicated with infantile spasms associated with the m.9185 T > C variant in the MT-ATP6 gene: Expanding the clinical spectrum. Brain Dev 2020;42:69-72. https://doi.org/10.1016/j.braindev.2019.08.006
76. Moslemi AR, Darin N, Tulinius M, Oldfors A, Holme E. Two new mutations in the MTATP6 gene associated with Leigh syndrome. Neuropediatrics 2005;36:314-318. https://doi.org/10.1055/s-2005-872845

77. Synofzik M, Schicks J, Wilhelm C, Bornemann A, Schols L. Charcot-Marie-Tooth hereditary neuropathy due to a mitochondrial ATP6 mutation. Eur J Neurol 2012;19:e114-116. https://doi.org/10.1111/j.1468-1331.2012.03812.x
78. Pitceathly RD, Murphy SM, Cottenie E, Chalasani A, Sweeney MG, Woodward C, Mudanohwo EE, Hargreaves I, Heales S, Land J, Holton JL, Houlden H, Blake J, Champion M, Flinter F, Robb SA, Page R, Rose M, Palace J, Crowe C, Longman C, Lunn MP, Rahman S, Reilly MM, Hanna MG. Genetic dysfunction of MT-ATP6 causes axonal Charcot-Marie-Tooth disease. Neurology 2012;79:1145-1154. https://doi.org/10.1212/WNL.0b013e3182698d8d
79. Bardakjian T, Scherer SS. A MT-ATP6 mutation causes a slowly progressive myeloneuropathy. J Neuromuscul Dis 2019;6:385-387. https://doi.org/10.3233/JND-190400
80. Panosyan FB, Tawil R, Herrmann DN. Episodic weakness and Charcot-marie-tooth disease due to a mitochondrial MT-ATP6 mutation. Muscle Nerve 2017;55:922-927. https://doi.org/10.1002/mus.25453
81. Thyagarajan D, Shanske S, Vazquez-Memije M, De Vivo D, DiMauro S. A novel mitochondrial ATPase 6 point mutation in familial bilateral striatal necrosis. Ann Neurol 1995;38:468-472. https://doi.org/10.1002/ana.410380321
82. Verny C, Guegen N, Desquiret V, Chevrollier A, Prundean A, Dubas F, Cassereau J, Ferre M, Amati-Bonneau P, Bonneau D, Reynier P, Procaccio V. Hereditary spastic paraplegia-like disorder due to a mitochondrial ATP6 gene point mutation. Mitochondrion 2011;11:70-75. https://doi.org/10.1016/j.mito.2010.07.006
83. Brum M, Semedo C, Guerreiro R, Pinto Marques J. Motor Neuron Syndrome as a New Phenotypic Manifestation of Mutation 9185T>C in Gene MTATP6. Case Rep Neurol Med 2014;2014:701761. https://doi.org/10.1155/2014/701761
84. Pfeffer G, Blakely EL, Alston CL, Hassani A, Boggild M, Horvath R, Samuels DC, Taylor RW, Chinnery PF. Adult-onset spinocerebellar ataxia syndromes due to MTATP6 mutations. J Neurol Neurosurg Psychiatry 2012;83:883-886. https://doi.org/10.1136/jnnp-2012-302568
85. Nolte D, Kang JS, Hofmann A, Schwaab E, Kramer HH, Muller U. Mutations in MT-ATP6 are a frequent cause of adult-onset spinocerebellar ataxia. J Neurol 2021;268:4866-4873. https://doi.org/10.1007/s00415-021-10607-5
86. Ganetzky RD, Stendel C, McCormick EM, Zolkipli-Cunningham Z, Goldstein AC, Klopstock T, Falk MJ. MT-ATP6 mitochondrial disease variants: Phenotypic and biochemical features analysis in 218 published cases and cohort of 14 new cases. Hum Mutat 2019;40:499-515. https://doi.org/10.1002/humu.23723
87. Honzik T, Tesarova M, Vinsova K, Hansikova H, Magner M, Kratochvilova H, Zamecnik J, Zeman J, Jesina P. Different laboratory and muscle biopsy findings in a family with an m.8851T>C mutation in the mitochondrial MTATP6 gene. Mol Genet Metab 2013;108:102-105. https://doi.org/10.1016/j.ymgme.2012.11.002
88. Blanco-Grau A, Bonaventura-Ibars I, Coll-Canti J, Melia MJ, Martinez R, Martinez-Gallo M, Andreu AL, Pinos T, Garcia-Arumi E. Identification and biochemical characterization of the novel mutation m.8839G>C in the mitochondrial ATP6 gene associated with NARP syndrome. Genes Brain Behav 2013;12:812-820. https://doi.org/10.1111/gbb.12089
89. Duno M, Wibrand F, Baggesen K, Rosenberg T, Kjaer N, Frederiksen AL. A novel mitochondrial mutation m.8989G>C associated with neuropathy, ataxia, retinitis pigmentosa - the NARP syndrome. Gene 2013;515:372-375. https://doi.org/10.1016/j.gene.2012.12.066
90. Lopez-Gallardo E, Emperador S, Solano A, Llobet L, Martin-Navarro A, Lopez-Perez MJ, Briones P, Pineda M, Artuch R, Barraquer E, Jerico I, Ruiz-Pesini E, Montoya J. Expanding the clinical phenotypes of MT-ATP6 mutations. Hum Mol Genet 2014;23:6191-6200. https://doi.org/10.1093/hmg/ddu339
91. Mordel P, Schaeffer S, Dupas Q, Laville MA, Gerard M, Chapon F, Allouche S. A 2 bp deletion in the mitochondrial ATP 6 gene responsible for the NARP (neuropathy, ataxia, and retinitis pigmentosa) syndrome. Biochem Biophys Res Commun 2017;494:133-137. https://doi.org/10.1016/j.bbrc.2017.10.066
92. Jackson CB, Hahn D, Schroter B, Richter U, Battersby BJ, Schmitt-Mechelke T, Marttinen P, Nuoffer JM, Schaller A. A novel mitochondrial ATP6 frameshift mutation causing isolated complex V deficiency, ataxia and encephalomyopathy. Eur J Med Genet 2017;60:345-351. https://doi.org/10.1016/j.ejmg.2017.04.006

93. Panwala TF, Garcia-Santibanez R, Vizcarra JA, Garcia AG, Verma S. Childhood-Onset Hereditary Spastic Paraplegia (HSP): A Case Series and Review of Literature. Pediatr Neurol 2022;130:7-13. https://doi.org/10.1016/j.pediatrneurol.2022.02.007
94. De Meirleir L, Seneca S, Lissens W, Schoentjes E, Desprechins B. Bilateral striatal necrosis with a novel point mutation in the mitochondrial ATPase 6 gene. Pediatr Neurol 1995;13:242-246. https://doi.org/10.1016/0887-8994(95)00184-H
95. Sikorska M, Sandhu JK, Simon DK, Pathiraja V, Sodja C, Li Y, Ribecco-Lutkiewicz M, Lanthier P, Borowy-Borowski H, Upton A, Raha S, Pulst SM, Tarnopolsky MA. Identification of ataxia-associated mtDNA mutations (m.4052T>C and m.9035T>C) and evaluation of their pathogenicity in transmitochondrial cybrids. Muscle Nerve 2009;40:381-394. https://doi.org/10.1002/mus.21355
96. Capiau S, Smet J, De Paepe B, Yildiz Y, Arslan M, Stevens O, Verschoore M, Stepman H, Seneca S, Vanlander A. Clinical heterogeneity in MT-ATP6 pathogenic variants: same genotype-different onset. Cells 2022;11. https://doi.org/10.3390/cells11030489
97. Knight KM, Shelkowitz E, Larson AA, Mirsky DM, Wang Y, Chen T, Wong LJ, Friederich MW, Van Hove JLK. The mitochondrial DNA variant m.9032T > C in MT-ATP6 encoding p.(Leu169Pro) causes a complex mitochondrial neurological syndrome. Mitochondrion 2020;55:8-13. https://doi.org/10.1016/j.mito.2020.08.009
98. Burrage LC, Tang S, Wang J, Donti TR, Walkiewicz M, Luchak JM, Chen LC, Schmitt ES, Niu Z, Erana R, Hunter JV, Graham BH, Wong LJ, Scaglia F. Mitochondrial myopathy, lactic acidosis, and sideroblastic anemia (MLASA) plus associated with a novel de novo mutation (m.8969G>A) in the mitochondrial encoded ATP6 gene. Mol Genet Metab 2014;113:207-212. https://doi.org/10.1016/j.ymgme.2014.06.004
99. Wen S, Niedzwiecka K, Zhao W, Xu S, Liang S, Zhu X, Xie H, Tribouillard-Tanvier D, Giraud MF, Zeng C, Dautant A, Kucharczyk R, Liu Z, di Rago JP, Chen H. Identification of G8969>A in mitochondrial ATP6 gene that severely compromises ATP synthase function in a patient with IgA nephropathy. Sci Rep 2016;6:36313. https://doi.org/10.1038/srep36313
100. Honzik T, Tesarova M, Magner M, Mayr J, Jesina P, Vesela K, Wenchich L, Szentivanyi K, Hansikova H, Sperl W, Zeman J. Neonatal onset of mitochondrial disorders in 129 patients: clinical and laboratory characteristics and a new approach to diagnosis. J Inherit Metab Dis 2012;35:749-759. https://doi.org/10.1007/s10545-011-9440-3
101. Isohanni P, Carroll CJ, Jackson CB, Pohjanpelto M, Lonnqvist T, Suomalainen A. Defective mitochondrial ATPase due to rare mtDNA m.8969G>A mutation-causing lactic acidosis, intellectual disability, and poor growth. Neurogenetics 2018;19:49-53. https://doi.org/10.1007/s10048-018-0537-9
102. Berhe S, Heeney MM, Campagna DR, Thompson JF, White EJ, Ross T, Peake RWA, Hanrahan JD, Rodriguez V, Renaud DL, Patnaik MS, Chang E, Bottomley SS, Fleming MD. Recurrent heteroplasmy for the MT-ATP6 p.Ser148Asn (m.8969G>A) mutation in patients with syndromic congenital sideroblastic anemia of variable clinical severity. Haematologica 2018;103:e561-e563. https://doi.org/10.3324/haematol.2018.199109
103. Adema AY, Janssen MC, van der Heijden JW. A novel mutation in mitochondrial DNA in a patient with diabetes, deafness and proteinuria. Neth J Med 2016;74:455-457.
104. Bergs PMJ, Maas DM, Janssen MCH, Groothuis JT. Feasible and clinical relevant outcome measures for adults with mitochondrial disease. Mol Genet Metab 2022;135:102-108. https://doi.org/10.1016/j.ymgme.2021.12.010
105. Kumar M, Tanwar M, Saxena R, Sharma P, Dada R. Identification of novel mitochondrial mutations in Leber's hereditary optic neuropathy. Mol Vis 2010;16:782-792.
106. Abu-Amero KK, Bosley TM. Mitochondrial abnormalities in patients with LHON-like optic neuropathies. Invest Ophthalmol Vis Sci 2006;47:4211-4220. https://doi.org/10.1167/iovs.06-0295
107. Dawod PGA, Jancic J, Marjanovic A, Brankovic M, Jankovic M, Samardzic J, Potkonjak D, Djuric V, Mesaros S, Novakovic I, Abdel Motaleb FI, Kostic VS, Nikolic D. Whole Mitochondrial Genome Analysis in Serbian Cases of Leber's Hereditary Optic Neuropathy. Genes (Basel) 2020;11. https://doi.org/10.3390/genes11091037
108. Lamminen T, Majander A, Juvonen V, Wikstrom M, Aula P, Nikoskelainen E, Savontous ML. A mitochondrial mutation at nt 9101 in the ATP synthase 6 gene associated with deficient oxidative phosphorylation in a family with Leber hereditary optic neuroretinopathy. Am J Hum Genet 1995;56:1238-1240.

109. Pinke G, Zhou L, Sazanov LA. Cryo-EM structure of the entire mammalian F-type ATP synthase. Nat Struct Mol Biol 2020;27:1077-1085. https://doi.org/10.1038/s41594-020-0503-8
110. Pallotti F, Baracca A, Hernandez-Rosa E, Walker WF, Solaini G, Lenaz G, Melzi D'Eril GV, Dimauro S, Schon EA, Davidson MM. Biochemical analysis of respiratory function in cybrid cell lines harbouring mitochondrial DNA mutations. Biochem J 2004;384:287-293. https://doi.org/10.1042/BJ20040561
111. Sgarbi G, Baracca A, Lenaz G, Valentino LM, Carelli V, Solaini G. Inefficient coupling between proton transport and ATP synthesis may be the pathogenic mechanism for NARP and Leigh syndrome resulting from the T8993G mutation in mtDNA. Biochem J 2006;395:493-500. https://doi.org/10.1042/BJ20051748
112. Baracca A, Sgarbi G, Mattiazzi M, Casalena G, Pagnotta E, Valentino ML, Moggio M, Lenaz G, Carelli V, Solaini G. Biochemical phenotypes associated with the mitochondrial ATP6 gene mutations at nt8993. Biochim Biophys Acta 2007;1767:913-919. https://doi.org/10.1016/j.bbabio.2007.05.005
113. Vazquez-Memije ME, Rizza T, Meschini MC, Nesti C, Santorelli FM, Carrozzo R. Cellular and functional analysis of four mutations located in the mitochondrial ATPase6 gene. J Cell Biochem 2009;106:878-886. https://doi.org/10.1002/jcb.22055
114. Baracca A, Barogi S, Carelli V, Lenaz G, Solaini G. Catalytic activities of mitochondrial ATP synthase in patients with mitochondrial DNA T8993G mutation in the ATPase 6 gene encoding subunit a. J Biol Chem 2000;275:4177-4182. https://doi.org/10.1074/jbc.275.6.4177
115. Tatuch Y, Pagon RA, Vlcek B, Roberts R, Korson M, Robinson BH. The 8993 mtDNA mutation: heteroplasmy and clinical presentation in three families. Eur J Hum Genet 1994;2:35-43. https://doi.org/10.1159/000472339
116. Vazquez-Memije ME, Shanske S, Santorelli FM, Kranz-Eble P, DeVivo DC, DiMauro S. Comparative biochemical studies of ATPases in cells from patients with the T8993G or T8993C mitochondrial DNA mutations. J Inherit Metab Dis 1998;21:829-836. https://doi.org/10.1023/A:1005418718299
117. Cortes-Hernandez P, Vazquez-Memije ME, Garcia JJ. ATP6 homoplasmic mutations inhibit and destabilize the human F1F0-ATP synthase without preventing enzyme assembly and oligomerization. J Biol Chem 2007;282:1051-1058. https://doi.org/10.1074/jbc.M606828200
118. Dautant A, Meier T, Hahn A, Tribouillard-Tanvier D, di Rago JP, Kucharczyk R. ATP Synthase Diseases of Mitochondrial Genetic Origin. Front Physiol 2018;9:329. https://doi.org/10.3389/fphys.2018.00329
119. Del Dotto V, Musiani F, Baracca A, Solaini G. Variants in Human ATP Synthase Mitochondrial Genes: Biochemical Dysfunctions, Associated Diseases, and Therapies. Int J Mol Sci 2024;25. https://doi.org/10.3390/ijms25042239
120. Stenton SL, Prokisch H. Genetics of mitochondrial diseases: Identifying mutations to help diagnosis. EBioMedicine 2020;56:102784. https://doi.org/10.1016/j.ebiom.2020.102784
121. Dimauro S. A history of mitochondrial diseases. J Inherit Metab Dis 2011;34:261-276. https://doi.org/10.1007/s10545-010-9082-x
122. Holme E, Greter J, Jacobson CE, Larsson NG, Lindstedt S, Nilsson KO, Oldfors A, Tulinius M. Mitochondrial ATP-synthase deficiency in a child with 3-methylglutaconic aciduria. Pediatr Res 1992;32:731-735. https://doi.org/10.1203/00006450-199212000-00022
123. Houstek J, Klement P, Floryk D, Antonicka H, Hermanska J, Kalous M, Hansikova H, Hout'kova H, Chowdhury SK, Rosipal T, Kmoch S, Stratilova L, Zeman J. A novel deficiency of mitochondrial ATPase of nuclear origin. Hum Mol Genet 1999;8:1967-1974. https://doi.org/10.1093/hmg/8.11.1967
124. Sperl W, Jesina P, Zeman J, Mayr JA, Demeirleir L, VanCoster R, Pickova A, Hansikova H, Houst'kova H, Krejcik Z, Koch J, Smet J, Muss W, Holme E, Houstek J. Deficiency of mitochondrial ATP synthase of nuclear genetic origin. Neuromuscul Disord 2006;16:821-829. https://doi.org/10.1016/j.nmd.2006.08.008
125. De Meirleir L, Seneca S, Lissens W, De Clercq I, Eyskens F, Gerlo E, Smet J, Van Coster R. Respiratory chain complex V deficiency due to a mutation in the assembly gene ATP12. J Med Genet 2004;41:120-124. https://doi.org/10.1136/jmg.2003.012047
126. Cizkova A, Stranecky V, Mayr JA, Tesarova M, Havlickova V, Paul J, Ivanek R, Kuss AW, Hansikova H, Kaplanova V, Vrbacky M, Hartmannova H, Noskova L, Honzik T, Drahota Z, Magner M, Hejzlarova K, Sperl W, Zeman J, Houstek J, Kmoch S. TMEM70 mutations cause isolated ATP synthase deficiency and neonatal mitochondrial encephalocardiomyopathy. Nat Genet 2008;40:1288-1290. https://doi.org/10.1038/ng.246

127. Mayr JA, Havlickova V, Zimmermann F, Magler I, Kaplanova V, Jesina P, Pecinova A, Nuskova H, Koch J, Sperl W, Houstek J. Mitochondrial ATP synthase deficiency due to a mutation in the ATP5E gene for the F1 epsilon subunit. Hum Mol Genet 2010;19:3430-3439. https://doi.org/10.1093/hmg/ddq254
128. Lieber DS, Calvo SE, Shanahan K, Slate NG, Liu S, Hershman SG, Gold NB, Chapman BA, Thorburn DR, Berry GT, Schmahmann JD, Borowsky ML, Mueller DM, Sims KB, Mootha VK. Targeted exome sequencing of suspected mitochondrial disorders. Neurology 2013;80:1762-1770. https://doi.org/10.1212/WNL.0b013e3182918c40
129. Jonckheere AI, Renkema GH, Bras M, van den Heuvel LP, Hoischen A, Gilissen C, Nabuurs SB, Huynen MA, de Vries MC, Smeitink JA, Rodenburg RJ. A complex V ATP5A1 defect causes fatal neonatal mitochondrial encephalopathy. Brain 2013;136:1544-1554. https://doi.org/10.1093/brain/awt086
130. Lines MA, Cuillerier A, Chakraborty P, Naas T, Duque Lasio ML, Michaud J, Pileggi C, Harper ME, Burelle Y, Toler TL, Sondheimer N, Crawford HP, Millan F, Geraghty MT. A recurrent de novo ATP5F1A substitution associated with neonatal complex V deficiency. Eur J Hum Genet 2021;29:1719-1724. https://doi.org/10.1038/s41431-021-00956-0
131. Zech M, Kopajtich R, Steinbrucker K, Bris C, Gueguen N, Feichtinger RG, Achleitner MT, Duzkale N, Perivier M, Koch J, Engelhardt H, Freisinger P, Wagner M, Brunet T, Berutti R, Smirnov D, Navaratnarajah T, Rodenburg RJT, Pais LS, Austin-Tse C, O'Leary M, Boesch S, Jech R, Bakhtiari S, Jin SC, Wilbert F, Kruer MC, Wortmann SB, Eckenweiler M, Mayr JA, Distelmaier F, Steinfeld R, Winkelmann J, Prokisch H. Variants in Mitochondrial ATP Synthase Cause Variable Neurologic Phenotypes. Ann Neurol 2022;91:225-237. https://doi.org/10.1002/ana.26293
132. Ganetzky RD, Markhard AL, Yee I, Clever S, Cahill A, Shah H, Grabarek Z, To TL, Mootha VK. Congenital Hypermetabolism and Uncoupled Oxidative Phosphorylation. N Engl J Med 2022;387:1395-1403. https://doi.org/10.1056/NEJMoa2202949
133. Nasca A, Mencacci NE, Invernizzi F, Zech M, Keller Sarmiento IJ, Legati A, Frascarelli C, Bustos BI, Romito LM, Krainc D, Winkelmann J, Carecchio M, Nardocci N, Zorzi G, Prokisch H, Lubbe SJ, Garavaglia B, Ghezzi D. Variants in ATP5F1B are associated with dominantly inherited dystonia. Brain 2023;146:2730-2738. https://doi.org/10.1093/brain/awad068
134. Olahova M, Yoon WH, Thompson K, Jangam S, Fernandez L, Davidson JM, Kyle JE, Grove ME, Fisk DG, Kohler JN, Holmes M, Dries AM, Huang Y, Zhao C, Contrepois K, Zappala Z, Fresard L, Waggott D, Zink EM, Kim YM, Heyman HM, Stratton KG, Webb-Robertson BM, Undiagnosed Diseases N, Snyder M, Merker JD, Montgomery SB, Fisher PG, Feichtinger RG, Mayr JA, Hall J, Barbosa IA, Simpson MA, Deshpande C, Waters KM, Koeller DM, Metz TO, Morris AA, Schelley S, Cowan T, Friederich MW, McFarland R, Van Hove JLK, Enns GM, Yamamoto S, Ashley EA, Wangler MF, Taylor RW, Bellen HJ, Bernstein JA, Wheeler MT. Biallelic Mutations in ATP5F1D, which Encodes a Subunit of ATP Synthase, Cause a Metabolic Disorder. Am J Hum Genet 2018;102:494-504. https://doi.org/10.1016/j.ajhg.2018.01.020
135. Neilson DE, Zech M, Hufnagel RB, Slone J, Wang X, Homan S, Gutzwiller LM, Leslie EJ, Leslie ND, Xiao J, Hedera P, LeDoux MS, Gebelein B, Wilbert F, Eckenweiler M, Winkelmann J, Gilbert DL, Huang T. A novel variant of ATP5MC3 associated with both dystonia and spastic paraplegia. Mov Disord 2022;37:375-383. https://doi.org/10.1002/mds.28821
136. Barca E, Ganetzky RD, Potluri P, Juanola-Falgarona M, Gai X, Li D, Jalas C, Hirsch Y, Emmanuele V, Tadesse S, Ziosi M, Akman HO, Chung WK, Tanji K, McCormick EM, Place E, Consugar M, Pierce EA, Hakonarson H, Wallace DC, Hirano M, Falk MJ. USMG5 Ashkenazi Jewish founder mutation impairs mitochondrial complex V dimerization and ATP synthesis. Hum Mol Genet 2018;27:3305-3312. https://doi.org/10.1093/hmg/ddy231
137. Ganapathi M, Friocourt G, Gueguen N, Friederich MW, Le Gac G, Okur V, Loaec N, Ludwig T, Ka C, Tanji K, Marcorelles P, Theodorou E, Lignelli-Dipple A, Voisset C, Walker MA, Briere LC, Bourhis A, Blondel M, LeDuc C, Hagen J, Cooper C, Muraresku C, Ferec C, Garenne A, Lelez-Soquet S, Rogers CA, Shen Y, Strode DK, Bizargity P, Iglesias A, Goldstein A, High FA, Network UD, Sweetser DA, Ganetzky R, Van Hove JLK, Procaccio V, Le Marechal C, Chung WK. A homozygous splice variant in ATP5PO, disrupts mitochondrial complex V function and causes Leigh syndrome in two unrelated families. J Inherit Metab Dis 2022;45:996-1012. https://doi.org/10.1002/jimd.12526

138. Waterham HR, Koster J, Ebberink MS, Jesina P, Zeman J, Noskova L, Kmoch S, Devic P, Cheillan D, Wanders RJA, Ferdinandusse S. Autosomal dominant Zellweger spectrum disorder caused by de novo variants in PEX14 gene. Genet Med 2023;25:100944. https://doi.org/10.1016/j.gim.2023.100944
139. Gilbert DL, Leslie EJ, Keddache M, Leslie ND. A novel hereditary spastic paraplegia with dystonia linked to chromosome 2q24-2q31. Mov Disord 2009;24:364-370. https://doi.org/10.1002/mds.22363
140. Luft R, Ikkos D, Palmieri G, Ernster L, Afzelius B. A case of severe hypermetabolism of nonthyroid origin with a defect in the maintenance of mitochondrial respiratory control: a correlated clinical, biochemical, and morphological study. J Clin Invest 1962;41:1776-1804. https://doi.org/10.1172/JCI104637
141. DiMauro S, Bonilla E, Lee CP, Schotland DL, Scarpa A, Conn H, Jr., Chance B. Luft's disease. Further biochemical and ultrastructural studies of skeletal muscle in the second case. J Neurol Sci 1976;27:217-232. https://doi.org/10.1016/0022-510X(76)90063-0
142. Giorgio V, Fogolari F, Lippe G, Bernardi P. OSCP subunit of mitochondrial ATP synthase: role in regulation of enzyme function and of its transition to a pore. Br J Pharmacol 2019;176:4247-4257. https://doi.org/10.1111/bph.14513
143. He J, Ford HC, Carroll J, Douglas C, Gonzales E, Ding S, Fearnley IM, Walker JE. Assembly of the membrane domain of ATP synthase in human mitochondria. Proc Natl Acad Sci U S A 2018;115:2988-2993. https://doi.org/10.1073/pnas.1722086115
144. Wang Y, Singh U, Mueller DM. Mitochondrial genome integrity mutations uncouple the yeast Saccharomyces cerevisiae ATP synthase. J Biol Chem 2007;282:8228-8236. https://doi.org/10.1074/jbc.M609635200
145. Kuhlbrandt W. Structure and Mechanisms of F-Type ATP Synthases. Annu Rev Biochem 2019;88:515-549. https://doi.org/10.1146/annurev-biochem-013118-110903
146. He J, Ford HC, Carroll J, Ding S, Fearnley IM, Walker JE. Persistence of the mitochondrial permeability transition in the absence of subunit c of human ATP synthase. Proc Natl Acad Sci U S A 2017;114:3409-3414. https://doi.org/10.1073/pnas.1702357114, https://doi.org/10.1073/pnas.1711201114
147. Calvo S, Jain M, Xie X, Sheth SA, Chang B, Goldberger OA, Spinazzola A, Zeviani M, Carr SA, Mootha VK. Systematic identification of human mitochondrial disease genes through integrative genomics. Nat Genet 2006;38:576-582. https://doi.org/10.1038/ng1776
148. Honzik T, Tesarova M, Mayr JA, Hansikova H, Jesina P, Bodamer O, Koch J, Magner M, Freisinger P, Huemer M, Kostkova O, van Coster R, Kmoch S, Houstek J, Sperl W, Zeman J. Mitochondrial encephalocardio-myopathy with early neonatal onset due to TMEM70 mutation. Arch Dis Child 2010;95:296-301. https://doi.org/10.1136/adc.2009.168096
149. Wortmann SB, Rodenburg RJ, Jonckheere A, de Vries MC, Huizing M, Heldt K, van den Heuvel LP, Wendel U, Kluijtmans LA, Engelke UF, Wevers RA, Smeitink JA, Morava E. Biochemical and genetic analysis of 3-methylglutaconic aciduria type IV: a diagnostic strategy. Brain 2009;132:136-146. https://doi.org/10.1093/brain/awn296
150. Tort F, Del Toro M, Lissens W, Montoya J, Fernandez-Burriel M, Font A, Bujan N, Navarro-Sastre A, Lopez-Gallardo E, Arranz JA, Riudor E, Briones P, Ribes A. Screening for nuclear genetic defects in the ATP synthase-associated genes TMEM70, ATP12 and ATP5E in patients with 3-methylglutaconic aciduria. Clin Genet 2011;80:297-300. https://doi.org/10.1111/j.1399-0004.2011.01650.x
151. Stojanovic V, Doronjski A. Mild form of 3-methylglutaconic aciduria type IV and mutation in the TMEM70 genes. J Pediatr Endocrinol Metab 2013;26:151-154. https://doi.org/10.1515/jpem-2012-0291
152. Catteruccia M, Verrigni D, Martinelli D, Torraco A, Agovino T, Bonafe L, D'Amico A, Donati MA, Adorisio R, Santorelli FM, Carrozzo R, Bertini E, Dionisi-Vici C. Persistent pulmonary arterial hypertension in the newborn (PPHN): a frequent manifestation of TMEM70 defective patients. Mol Genet Metab 2014;111:353-359. https://doi.org/10.1016/j.ymgme.2014.01.001
153. Torraco A, Verrigni D, Rizza T, Meschini MC, Vazquez-Memije ME, Martinelli D, Bianchi M, Piemonte F, Dionisi-Vici C, Santorelli FM, Bertini E, Carrozzo R. TMEM70: a mutational hot spot in nuclear ATP synthase deficiency with a pivotal role in complex V biogenesis. Neurogenetics 2012;13:375-386. https://doi.org/10.1007/s10048-012-0343-8

154. Magner M, Dvorakova V, Tesarova M, Mazurova S, Hansikova H, Zahorec M, Brennerova K, Bzduch V, Spiegel R, Horovitz Y, Mandel H, Eminoglu FT, Mayr JA, Koch J, Martinelli D, Bertini E, Konstantopoulou V, Smet J, Rahman S, Broomfield A, Stojanovic V, Dionisi-Vici C, van Coster R, Morava E, Sperl W, Zeman J, Honzik T. TMEM70 deficiency: long-term outcome of 48 patients. J Inherit Metab Dis 2015;38:417-426. https://doi.org/10.1007/s10545-015-9833-9, https://doi.org/10.1007/s10545-014-9774-8
155. Braczynski AK, Vlaho S, Muller K, Wittig I, Blank AE, Tews DS, Drott U, Kleinle S, Abicht A, Horvath R, Plate KH, Stenzel W, Goebel HH, Schulze A, Harter PN, Kieslich M, Mittelbronn M. ATP synthase deficiency due to TMEM70 mutation leads to ultrastructural mitochondrial degeneration and is amenable to treatment. Biomed Res Int 2015;2015:462592. https://doi.org/10.1155/2015/462592
156. Diodato D, Invernizzi F, Lamantea E, Fagiolari G, Parini R, Menni F, Parenti G, Bollani L, Pasquini E, Donati MA, Cassandrini D, Santorelli FM, Haack TB, Prokisch H, Ghezzi D, Lamperti C, Zeviani M. Common and novel TMEM70 mutations in a cohort of italian patients with mitochondrial encephalocardiomyopathy. JIMD Rep 2015;15:71-78. https://doi.org/10.1007/8904_2014_300
157. Sarajlija A, Magner M, Djordjevic M, Kecman B, Grujic B, Tesarova M, Minic P. Late-presenting congenital diaphragmatic hernia in a child with TMEM70 deficiency. Congenit Anom (Kyoto) 2017;57:64-65. https://doi.org/10.1111/cga.12194
158. aban A, Adorisio R, Corica B, Rizzo C, Cali F, Semeraro M, Taurisano R, Magliozzi M, Carrozzo R, Parisi F, Dallapiccola B, Vaz FM, Drago F, Dionisi-Vici C. Delayed appearance of 3-methylglutaconic aciduria in neonates with early onset metabolic cardiomyopathies: A potential pitfall for the diagnosis. Am J Med Genet A 2020;182:64-70. https://doi.org/10.1002/ajmg.a.61383
159. Spiegel R, Khayat M, Shalev SA, Horovitz Y, Mandel H, Hershkovitz E, Barghuti F, Shaag A, Saada A, Korman SH, Elpeleg O, Yatsiv I. TMEM70 mutations are a common cause of nuclear encoded ATP synthase assembly defect: further delineation of a new syndrome. J Med Genet 2011;48:177-182. https://doi.org/10.1136/jmg.2010.084608
160. Jonckheere AI, Huigsloot M, Lammens M, Jansen J, van den Heuvel LP, Spiekerkoetter U, von Kleist-Retzow JC, Forkink M, Koopman WJ, Szklarczyk R, Huynen MA, Fransen JA, Smeitink JA, Rodenburg RJ. Restoration of complex V deficiency caused by a novel deletion in the human TMEM70 gene normalizes mitochondrial morphology. Mitochondrion 2011;11:954-963. https://doi.org/10.1016/j.mito.2011.08.012
161. Staretz-Chacham O, Wormser O, Manor E, Birk OS, Ferreira CR. TMEM70 deficiency: Novel mutation and hypercitrullinemia during metabolic decompensation. Am J Med Genet A 2019;179:1293-1298. https://doi.org/10.1002/ajmg.a.61138
162. Atay Z, Bereket A, Turan S, Haliloglu B, Memisoglu A, Khayat M, Shalev SA, Spiegel R. A novel homozygous TMEM70 mutation results in congenital cataract and neonatal mitochondrial encephalo-cardiomyopathy. Gene 2013;515:197-199. https://doi.org/10.1016/j.gene.2012.11.044
163. Mackay L, Gijavanekar C, Streff H, Price JF, Elsea SH, Scaglia F. Novel phenotype of aortic root dilatation and late-onset metabolic decompensation in a patient with TMEM70 deficiency. Am J Med Genet A 2023;191:1366-1372. https://doi.org/10.1002/ajmg.a.63131
164. Cameron JM, Levandovskiy V, Mackay N, Ackerley C, Chitayat D, Raiman J, Halliday WH, Schulze A, Robinson BH. Complex V TMEM70 deficiency results in mitochondrial nucleoid disorganization. Mitochondrion 2011;11:191-199. https://doi.org/10.1016/j.mito.2010.09.008
165. Shchelochkov OA, Li FY, Wang J, Zhan H, Towbin JA, Jefferies JL, Wong LJ, Scaglia F. Milder clinical course of Type IV 3-methylglutaconic aciduria due to a novel mutation in TMEM70. Mol Genet Metab 2010;101:282-285. https://doi.org/10.1016/j.ymgme.2010.07.012
166. Hirono K, Ichida F, Nishio N, Ogawa-Tominaga M, Fushimi T, Feichtinger RG, Mayr JA, Kohda M, Kishita Y, Okazaki Y, Ohtake A, Murayama K. Mitochondrial complex deficiency by novel compound heterozygous TMEM70 variants and correlation with developmental delay, undescended testicle, and left ventricular noncompaction in a Japanese patient: A case report. Clin Case Rep 2019;7:553-557. https://doi.org/10.1002/ccr3.2050

167. Brambilla A, Olivotto I, Favilli S, Spaziani G, Passantino S, Procopio E, Morrone A, Donati MA. Impact of cardiovascular involvement on the clinical course of paediatric mitochondrial disorders. Orphanet J Rare Dis 2020;15:196. https://doi.org/10.1186/s13023-020-01466-w
168. Rabier D, Diry C, Rotig A, Rustin P, Heron B, Bardet J, Parvy P, Ponsot G, Marsac C, Saudubray JM, Munnich A, Kamoun P. Persistent hypocitrullinaemia as a marker for mtDNA NARP T 8993 G mutation? J Inherit Metab Dis 1998;21:216-219. https://doi.org/10.1023/A:1005391300203
169. Ribas GS, Lopes FF, Deon M, Vargas CR. Hyperammonemia in Inherited Metabolic Diseases. Cell Mol Neurobiol 2022;42:2593-2610. https://doi.org/10.1007/s10571-021-01156-6
170. Scaglia F, Scheuerle AE, Towbin JA, Armstrong DL, Sweetman L, Wong LJ. Neonatal presentation of ventricular tachycardia and a Reye-like syndrome episode associated with disturbed mitochondrial energy metabolism. BMC Pediatr 2002;2:12. https://doi.org/10.1186/1471-2431-2-12
171. Jones DE, Klacking E, Ryan RO. Inborn errors of metabolism associated with 3-methylglutaconic aciduria. Clin Chim Acta 2021;522:96-104. https://doi.org/10.1016/j.cca.2021.08.016
172. Wortmann SB, Duran M, Anikster Y, Barth PG, Sperl W, Zschocke J, Morava E, Wevers RA. Inborn errors of metabolism with 3-methylglutaconic aciduria as discriminative feature: proper classification and nomenclature. J Inherit Metab Dis 2013;36:923-928. https://doi.org/10.1007/s10545-012-9580-0
173. Taylor RW, Pyle A, Griffin H, Blakely EL, Duff J, He L, Smertenko T, Alston CL, Neeve VC, Best A, Yarham JW, Kirschner J, Schara U, Talim B, Topaloglu H, Baric I, Holinski-Feder E, Abicht A, Czermin B, Kleinle S, Morris AA, Vassallo G, Gorman GS, Ramesh V, Turnbull DM, Santibanez-Koref M, McFarland R, Horvath R, Chinnery PF. Use of whole-exome sequencing to determine the genetic basis of multiple mitochondrial respiratory chain complex deficiencies. JAMA 2014;312:68-77. https://doi.org/10.1001/jama.2014.7184
174. Wortmann SB, Koolen DA, Smeitink JA, van den Heuvel L, Rodenburg RJ. Whole exome sequencing of suspected mitochondrial patients in clinical practice. J Inherit Metab Dis 2015;38:437-443. https://doi.org/10.1007/s10545-015-9823-y
175. Calvo SE, Compton AG, Hershman SG, Lim SC, Lieber DS, Tucker EJ, Laskowski A, Garone C, Liu S, Jaffe DB, Christodoulou J, Fletcher JM, Bruno DL, Goldblatt J, Dimauro S, Thorburn DR, Mootha VK. Molecular diagnosis of infantile mitochondrial disease with targeted next-generation sequencing. Sci Transl Med 2012;4:118ra110. https://doi.org/10.1126/scitranslmed.3003310
176. Carroll CJ, Brilhante V, Suomalainen A. Next-generation sequencing for mitochondrial disorders. Br J Pharmacol 2014;171:1837-1853. https://doi.org/10.1111/bph.12469
177. Alston CL, Rocha MC, Lax NZ, Turnbull DM, Taylor RW. The genetics and pathology of mitochondrial disease. J Pathol 2017;241:236-250. https://doi.org/10.1002/path.4809
178. Theunissen TEJ, Nguyen M, Kamps R, Hendrickx AT, Sallevelt S, Gottschalk RWH, Calis CM, Stassen APM, de Koning B, Mulder-Den Hartog ENM, Schoonderwoerd K, Fuchs SA, Hilhorst-Hofstee Y, de Visser M, Vanoevelen J, Szklarczyk R, Gerards M, de Coo IFM, Hellebrekers D, Smeets HJM. Whole exome sequencing is the preferred strategy to identify the genetic defect in patients with a probable or possible mitochondrial cause. Front Genet 2018;9:400. https://doi.org/10.3389/fgene.2018.00400
179. Thompson K, Collier JJ, Glasgow RIC, Robertson FM, Pyle A, Blakely EL, Alston CL, Olahova M, McFarland R, Taylor RW. Recent advances in understanding the molecular genetic basis of mitochondrial disease. J Inherit Metab Dis 2020;43:36-50. https://doi.org/10.1002/jimd.12104
180. Abicht A, Scharf F, Kleinle S, Schon U, Holinski-Feder E, Horvath R, Benet-Pages A, Diebold I. Mitochondrial and nuclear disease panel (Mito-aND-Panel): Combined sequencing of mitochondrial and nuclear DNA by a cost-effective and sensitive NGS-based method. Mol Genet Genomic Med 2018;6:1188-1198. https://doi.org/10.1002/mgg3.500
181. Walsh N, Cooper A, Dockery A, O'Byrne JJ. Variant reclassification and clinical implications. J Med Genet 2024;61:207-211. https://doi.org/10.1136/jmg-2023-109488
182. Zhang H, Burr SP, Chinnery PF. The mitochondrial DNA genetic bottleneck: inheritance and beyond. Essays Biochem 2018;62:225-234. https://doi.org/10.1042/EBC20170096

183. Sallevelt SC, de Die-Smulders CE, Hendrickx AT, Hellebrekers DM, de Coo IF, Alston CL, Knowles C, Taylor RW, McFarland R, Smeets HJ. De novo mtDNA point mutations are common and have a low recurrence risk. J Med Genet 2017;54:73-83. https://doi.org/10.1136/jmedgenet-2016-103876
184. Spikes TE, Montgomery MG, Walker JE. Structure of the dimeric ATP synthase from bovine mitochondria. Proc Natl Acad Sci U S A 2020;117:23519-23526. https://doi.org/10.1073/pnas.2013998117
185. Jumper J, Evans R, Pritzel A, Green T, Figurnov M, Ronneberger O, Tunyasuvunakool K, Bates R, Zidek A, Potapenko A, Bridgland A, Meyer C, Kohl SAA, Ballard AJ, Cowie A, Romera-Paredes B, Nikolov S, Jain R, Adler J, Back T, Petersen S, Reiman D, Clancy E, Zielinski M, Steinegger M, Pacholska M, Berghammer T, Bodenstein S, Silver D, Vinyals O, Senior AW, Kavukcuoglu K, Kohli P, Hassabis D. Highly accurate protein structure prediction with AlphaFold. Nature 2021;596:583-589. https://doi.org/10.1038/s41586-021-03819-2
186. Varadi M, Anyango S, Deshpande M, Nair S, Natassia C, Yordanova G, Yuan D, Stroe O, Wood G, Laydon A, Zidek A, Green T, Tunyasuvunakool K, Petersen S, Jumper J, Clancy E, Green R, Vora A, Lutfi M, Figurnov M, Cowie A, Hobbs N, Kohli P, Kleywegt G, Birney E, Hassabis D, Velankar S. AlphaFold Protein Structure Database: massively expanding the structural coverage of protein-sequence space with high-accuracy models. Nucleic Acids Res 2022;50:D439-D444. https://doi.org/10.1093/nar/gkab1061

Physiol. Res. 73 (Suppl. 1): S279-S294, 2024 *https://doi.org/10.33549/physiolres.935361*

REVIEW

This paper is a tribute to Leslie Paul Kozak, PhD (1940-2023)

Adaptive Induction of Nonshivering Thermogenesis in Muscle Rather Than Brown Fat Could Counteract Obesity

Kristina BARDOVA[1], Petra JANOVSKA[1], Anna VAVROVA[1], Jan KOPECKY[1], Petr ZOUHAR[1]

[1]Laboratory of Adipose Tissue Biology, Institute of Physiology of the Czech Academy of Sciences, Prague, Czech Republic

Received March 19, 2024
Accepted April 2, 2024

Summary

Warm-blooded animals such as birds and mammals are able to protect stable body temperature due to various thermogenic mechanisms. These processes can be facultative (occurring only under specific conditions, such as acute cold) and adaptive (adjusting their capacity according to long-term needs). They can represent a substantial part of overall energy expenditure and, therefore, affect energy balance. Classical mechanisms of facultative thermogenesis include shivering of skeletal muscles and (in mammals) non-shivering thermogenesis (NST) in brown adipose tissue (BAT), which depends on uncoupling protein 1 (UCP1). Existence of several alternative thermogenic mechanisms has been suggested. However, their relative contribution to overall heat production and the extent to which they are adaptive and facultative still needs to be better defined. Here we focus on comparison of NST in BAT with thermogenesis in skeletal muscles, including shivering and NST. We present indications that muscle NST may be adaptive but not facultative, unlike UCP1-dependent NST. Due to its slow regulation and low energy efficiency, reflecting in part the anatomical location, induction of muscle NST may counteract development of obesity more effectively than UCP1-dependent thermogenesis in BAT.

Key words

Regulation of thermogenesis • Warm-blooded animals • Body temperature • UCP1

Corresponding authors

J. Kopecky and P. Zouhar, Laboratory of Adipose Tissue Biology, Institute of Physiology of the Czech Academy of Sciences, Videnska 1083, Prague 4, 142 00, Czech Republic. E-mail: Jan.kopecky@fgu.cas.cz or Petr.zouhar@fgu.cas.cz

Introduction

Life is sustained by a constant supply of energy that propels cellular processes. However, no biochemical reaction is 100 % efficient, and portion of energy is inevitably "lost" as a heat [1]. Birds and mammals evolved an ability to utilize this metabolic inefficiency to keep stable body temperature. They are, therefore, endothermic, i.e. able to warm themselves using internal heat sources, and homeothermic, i.e. with stable body temperature. These enabled them to colonize environments with cold climates. Their basal metabolic rate is 5-10 times higher in comparison to other vertebrates with similar body weight but variable body temperature (poikilotherms), which depend mainly on ambient temperature (ectotherms) [2]. In the homeotherms, the heat dissipated by basal metabolism fully covers the cost of maintaining a stable body temperature under conditions of so called thermoneutral zone (i.e. ambient temperature typically in a range 20-25 °C for lightly dressed human, and 29-33 °C for standard laboratory mouse during day and night [3]). At temperatures below the thermoneutral zone, homeotherms turn on several heat-saving and heat-generating processes [4-7]. As ambient temperature can change rapidly, it is essential to control these thermoregulatory mechanisms tightly, switching them on and off as needed to prevent hypothermia or overheating. Thus, the thermogenesis is

acutely adjustable, i.e. facultative. It includes shivering and non-shivering thermogenesis (**NST**; Fig. 1). Shivering is defined as the involuntary contractile activity of skeletal muscles triggered by motor neurons, producing heat but no external work. It is activated especially in response to acute cold stimuli. NST includes all potential facultative heat-producing mechanisms independent on muscle contractile activity. NST is also adaptive: If a cold stimulus persists, the capacity for NST gradually increases, which allows cessation of shivering [7].

Thermoregulatory rather than diet-induced thermogenesis in brown fat

Placental mammals developed a unique and particularly efficient mechanism of NST, allowing them to use the maximum amount of dissipated energy for thermoregulation. This NST is mediated by mitochondrial uncoupling protein 1 (**UCP1**) in brown adipose tissue (**BAT**; Fig. 1) [7]. UCP1 is activated in the cold, by the sympathetic nervous system and adrenergic receptor signaling *via* cAMP-dependent lipolysis (Fig. 1). Liberated free fatty acids directly activate the protonophoric activity of UCP1 while overriding the opposite effect of intracellular purine nucleotides (reviewed e.g. in [7]). This results in the uncoupling of respiratory chain activity from ATP synthesis, maximizing respiratory rate and dissipating the energy of the transmembrane electrochemical gradient of protons as heat. The increase in energy expenditure follows the stimulus within dozens of minutes at the latest, depending also on the increased blood flow through BAT, which supplies oxygen and nutrients [7]. Long-term cold exposure also regulates UCP1 at the level of mRNA and protein content, resulting in increased thermogenic capacity of BAT, which also reflects BAT growth and oxidative capacity. Thus, UCP1-mediated NST is both facultative and adaptive (Fig. 1). Adaptation to cold is accompanied by increased lipogenesis [8], possibly in order to replenish lipid stores in BAT.

UCP1 is also present in inducible adipocytes interspersed in white adipose tissue (**WAT**) depots. These cells, later called brite or beige adipocytes [9,10], were described first by Leslie Paul Kozak, one of the most original and renowned scientists in the field of obesity and energy metabolism (see Table 1) [11,12]. L. P. Kozak has also characterized the mechanism of brown (brite/beige)-adipocyte-specific expression of *Ucp1* by discovering the unique enhancer in the 5′-flanking region of *Ucp1* [13,14], see also [15]. However, the capacity of these brite/beige cells for UCP1-dependent thermogenesis is somewhat limited compared to classical BAT [16,17].

It has been repeatedly and wishfully suggested that UCP1 plays a physiological role not only in protection against cold, but also against obesity [18-20]. This hypothesis is based on a concept of "diet-induced thermogenesis", which supposes that BAT burns excess calories in states of positive energy balance to maintain stable body weight. The existence of such a physiological mechanism was challenged by L. P. Kozak in 2010, in his important but long overlooked article entitled "Brown Fat and the Myth of Diet-Induced Thermogenesis" [21]. There, he brought several arguments to support this skepticism, based mainly on experiments in mice with germline inactivation of *Ucp1* in adipocytes (**UCP1-KO** mice) [22] or ectopic expression of *Ucp1* in WAT, which models were developed in his laboratory [23]. Notably, mice with partially ablated BAT develop obesity [24], but this may only be a consequence of hyperphagia. Both hyperphagia and the development of obesity are absent when these mice are reared at thermoneutrality [25]. Similarly, the propensity to obesity of UCP1-KO mice depends on ambient temperature. At laboratory temperature, UCP1-KO mice do not develop obesity [22] or they even show paradoxical obesity resistance [26], while some authors report that these mice develop obesity at thermoneutral temperature [27,28]. An increased level of UCP1, which indicates a high capacity for NST, is not directly associated with obesity resistance unless the biochemical (i.e. protonophoric) activity of the existing UCP1 is stimulated at the same time [29-31]. Thus, while diet-induced thermogenesis may be involved in acute control of food intake [32], UCP1 does not seem to play a physiological role in the prevention of body gain. Generally, it is not even clear to what extent body weight is under homeostatic control [33].

However, as already recognized by L. P. Kozak [21], artificial stimulation of both UCP1-mediated and UCP1-independent NST could be used clinically in body weight management, irrespective of the validity of the traditional concept of diet-induced thermogenesis. Induction of UCP1-mediated thermogenesis using β-adrenergic agonist can reduce obesity in mice [34] and even in humans [35], but cardiovascular side-effects prevented its clinical use [35]. Similarly, obesity development was counteracted by ectopic expression of *Ucp1* gene in WAT of mice and pigs [23,36].

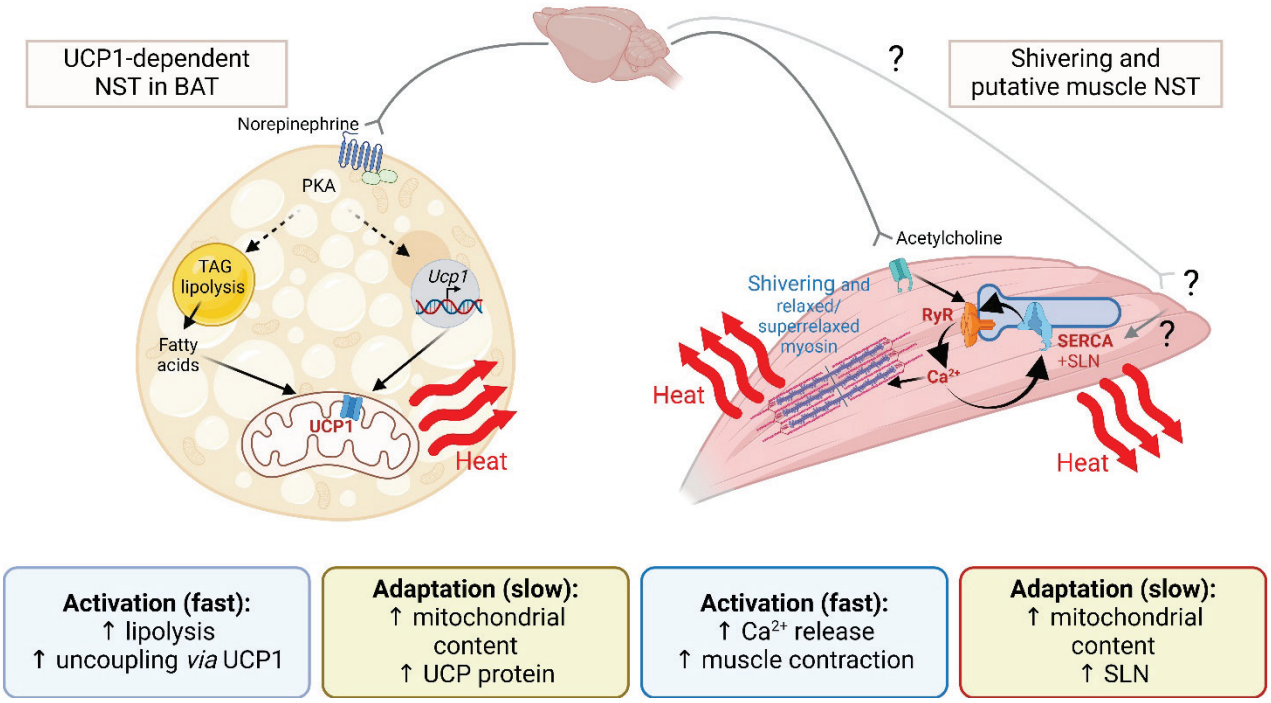

Fig. 1. Two-level regulation of thermogenesis in brown adipose tissue (BAT) and skeletal muscle. UCP1-dependent thermogenesis in BAT is activated by fatty acids released by lipolysis of intracellular triacylglycerols (TAG) in response to norepinephrine from sympathetic nerve endings. The same mechanism causes adaptive rise in *Ucp1* expression and UCP1 content. Shivering is acutely stimulated by acetylcholine from motor nerve endings, activation of acetylcholine receptors and consecutive calcium release from sarcoplasmic reticulum through ryanodine receptors (RyR). Efficiency of calcium recycling is affected by interaction between sarcoplasmic/endoplasmic reticulum Ca^{2+}-ATPase (SERCA) and sarcolipin (SLN). The activity of SLN is probably regulated mostly at the level of gene expression. SLN may represent a mechanism of adaptive, long-term tuning of regulatory pathway of shivering and/or shivering-independent mechanism of NST. Created with Biorender.com.

Table 1. Studies of Leslie Paul Kozak, PhD (1940 – 2023) focused on mechanism and role of NST.

1991 – 1995, early studies focused on UCP1-mediated NST: • Characterization of brown-fat specific enhancer in the 5'-upstream region of murine *Ucp1* [13,14] • Development of obesity in mice with genetic ablation of BAT [24] • Ectopic expression of *Ucp1* in white fat prevents obesity [23]
1997 – 2006, development of mice with germline inactivation of Ucp1 in adipocytes; results suggested that UCP1 was required for thermoregulatory thermogenesis but not for adaptive induction of NST by cold, resulting in obesity-resistance. UCP1-independent NST involved metabolism in white fat and possibly also other tissues: • UCP1-KO mice are cold-sensitive but partially resistant to dietary obesity [22,25,26] • Dependence of NST on genetic background in UCP1-KO mice [112] • Both leptin and thyroid hormones are required for UCP1-independent NST in the cold [78] • UCP1-independent NST in white fat of UCP1-KO mice [42]
1998 – 2011, brown fat cells could be induced in specific depots of white fat by cold: • Discovery of "inducible brown fat cells" in white fat [11,12]
2010, physiological role of brown fat is protection against cold but not against obesity: • Brown fat and the myth of diet-induced thermogenesis [21]
2015 – 2016, UCP1 and sarcolipin have complementary but distinct roles in NST: • Complementary roles of NST mediated by sarcolipin in skeletal muscle and UCP1 in BAT [99] • Sarcolipin and UCP1 play distinct roles in propensity to obesity and do not compensate for one another [28]

List of selected publications of L. P. Kozak. For Kozak's memories [120] and for a short biographical sketch and obituary, see [121].

In addition to the UCP1-dependent thermogenic mechanism bypassing ATP synthase, also other biochemical pathways could mediate NST in BAT by dissipating the metabolic energy of ATP [37]. Mechanisms such as creatine cycling controlled by creatine kinase b (**CKB**) [38,39], esterification/lipolysis of triacylglycerols [40] and some others [41,42] may be involved and need to be better characterized. Namely the CKB-dependent pathway was recently suggested to represent a complementary mechanism to that mediated by UCP1 in adipocytes, with functional redundancy providing a robust mechanism for heat production (reviewed in [39]). Similarly to UCP1, these mechanisms are usually believed to be under adrenergic control (e.g. [43]), which challenges the view that only UCP1 could mediate adrenergically regulated facultative and adaptive NST [44].

Mechanisms of thermoregulatory NST in other organs and tissues besides BAT and their control are relatively poorly characterized. Increased energy expenditure in response to adrenergic stimulation [45] or cold [46] has been reported in perigonadal WAT. Moreover, NST could also take place in subcutaneous WAT [10,42,47], or liver [48,49]. It could also result from inter-organ futile metabolic cycling [50]. Although all of these mechanisms need to be further characterized, this short review will focus specifically on the thermogenic mechanisms in skeletal muscle, their contribution to the maintenance of a stable body temperature, and their impact on the propensity to obesity.

Shivering and cold-induced changes in muscle

Skeletal muscles evolved primarily to enable locomotion. However, with the advent of endothermy in birds and mammals, skeletal muscle also became engaged in thermogenesis comprising both shivering and putative NST. Muscle function is based on sliding actin and myosin filaments organized in sarcomeres, which consume ATP and generate force and potentially subsequent changes in muscle length. However, typical muscle is able to convert only 20-30 % of ATP to work, while the most of the remaining part is dissipated as heat (reviewed in [51]), which may contribute to thermos-regulation. A major contribution of muscles to overall thermogenesis could be inferred from their high oxidative capacity. Thus, in adult humans, the capacity of skeletal muscles to burn fat energy stores is several-fold greater than that of BAT [52]. Blood flow through skeletal muscles can substantially increase during the transition from basal state to state of maximal physical activity. Even in the resting state, muscles can account for 20-30 % of the total oxygen consumption [5,7]. Muscle metabolism is one of the major contributors to resting energy expenditure with a clear potential to affect the pathogenesis of obesity [53]. Shivering can increase the whole-body energy expenditure up to five times its basal values, corresponding to approximately 40 % of maximal oxygen consumption ($\dot{V}O_2$max) during exercise [54]. The putative contribution of muscle NST has not been reliably quantified. However, it is to be inferred that even a slight relative increase in muscle energy expenditure, independent of physical activity or shivering, would have a profound effect on whole body energy balance, potentially affecting fat deposition.

Skeletal muscles are composed of long multinucleated cells (muscle fibers), which differ in their biochemical and functional properties: i) slow-twitch type I fibers have high content of mitochondria (causing dark red color), high oxidative capacity, and high fatigue resistance; ii) fast-twitch type IIa fibers have high content of mitochondria and rely both on glycolysis and oxidative metabolism; iii) fast-twitch type IIb fibers with low mitochondrial content (causing pale color) and high glycolytic activity, which are prone to rapid fatigue; and additionally iv) type IIx muscle fibers [55]. Fiber type composition of individual muscles is optimized for the typical work pattern of the respective muscle groups. It can be partially affected by muscle endurance training, which leads to increased mitochondrial biogenesis, as well as adaptation of mitochondrial network, contractile apparatus, and vasculature [56]. Some of these changes towards increased oxidative capacity have also been seen in animal models during prolonged cold exposure, suggesting a similar effect on muscle metabolism as endurance training and demonstrating a partially adaptive nature of shivering [57].

Skeletal muscles are relatively flexible in the utilization of various fuel mixtures under acute cold exposure [58], while chronic cold exposure leads to a proportional increase in the oxidation of lipids by the muscle [59]. The fiber composition is also a strong predictor of the shivering pattern evoked by acute cold [60]. While short-term activity can rely on glycolytic fast-twitch fibers, prolonged endurance activity requires a higher proportion of oxidative slow-twitch fibers. The changes in muscle metabolism and fiber composition in response to cold exposure may reflect the activation of both shivering and NST. Rapid changes in muscle

metabolism are likely associated with shivering, which is activated at the beginning of cold exposure [61]. These changes may vary between individuals and depend on severity of cold exposure (see below). Sustained low-intensity shivering in humans largely depends on lipid oxidation (50 %), while muscle glycogen and plasma glucose are used to a lesser extent (30 % and 10 %, respectively) [59]. Increased energy requirements during the transition from low to moderate shivering intensity are primarily met by increased glycogen consumption in humans [62]. Besides these changes in the biochemistry of muscle shivering, long-term exposure (i.e. acclimation) to cold environment results in an adaptive increase in the capacity for NST in BAT and possibly elsewhere, leading to the cessation of shivering [5-7,16,60,63].

Distinguishing between shivering and putative muscle NST is not straightforward, as the definition of shivering itself is ambiguous. There are at least two different types of muscle contractile thermogenic activities. Burst shivering ("classical shivering") is associated with fatigued type II muscle fibers and, therefore, cannot be sustained for a prolonged time [63]. On the other hand, muscle tone, also reported as resting muscle mechanical activity [64], shivering microvibrations, minor tremor, or thermoregulatory tonus [65], can be continuous and therefore associated with fatigue resistant, oxidative type I muscle fibers [63]. When assessed by electromyography, burst and continuous shivering in humans typically show frequencies of 0.1-0.2 Hz and 4-8 Hz, respectively ([63]; in general, the smaller the animal, the higher the frequency [64]). Burst shivering can be perceived visually, while continuous shivering may not be visually manifested.

The relative contribution of each of these types of contractile activity to overall shivering thermogenesis is debated. It also exhibits high inter-individual variability, perhaps corresponding to variability in muscle fiber composition [58]. The mutation causing a shift towards higher proportion of slow-twitch muscles results in increased muscle tone and higher resistance to cold [66]. It has been observed that the intensity of continuous shivering increases linearly with decreasing ambient temperature below thermoneutral zone [57,64,65], whereas burst shivering is only triggered at very low temperatures (below 7 °C in rats [57]), when thermogenic capacity of continuous shivering is presumably insufficient. On the other hand, some authors do not report any continuous shivering preceding shivering bursts [63]. Interestingly, contractile activity similar to continuous shivering is also detected after vigorous exercise [65], suggesting a common mechanism linking it to skeletal muscle training.

Assessment of shivering activity is further complicated by a broad range of muscle groups that can be involved in thermogenesis. Extensive continuous shivering was recorded e.g. in m. extensor digitorum longus, deep parts of m. tibialis, deep neck muscles and m. soleus (but not in the superficial part of m. tibialis and m. trapezius) [57]. The involvement of particular muscle groups can also considerably vary among individuals: While some humans rely on shivering in upper body muscles, others use upper leg muscles [54]. Hence, evaluating shivering activity in a specific muscle does not necessarily indicate the overall shivering activity. This complicates the quantification of the contribution of this mechanism to the total body heat production.

As reviewed by Blondin and Haman [63], muscle metabolic activity and the relative importance of individual muscles can be indirectly visualized using positron emission tomography (PET) and the glucose analogue [^{18}F]FDG. Shivering pattern of individual muscles can be characterized using electromyography (assessing regulatory muscle electric activity). While surface electromyography is widely used in humans, it is rarely applied to rodents (e.g. in [67]) because of technical constraints. Placing an electrode directly onto the muscle is more common in rodents [68-70]. However, it can produce misleading results due to the open surgery and prevailing effects of anaesthesia. Another way to collect data on whole-body shivering patterns is through mechanical methods, most commonly mechano-myography [16,71]. This technique is getting increasingly sensitive and provides output corresponding to electromyography [16]. However, a comprehensive comparison of the two techniques is missing. The least reliable and most subjective approach to assessing shivering is visual observation, which may fail to detect less striking forms of contractile activity.

Shivering is thus a phenomenon of underestimated complexity. Proper quantification of its contribution to thermogenesis and overall energy expenditure is a technically challenging task, which is rarely sufficiently addressed in studies attempting to uncover potential alternative mechanisms of NST. However, without evaluation of at least presence of shivering, results of the whole-body studies focused on NST, conducted at ambient temperatures below thermoneutrality, are difficult to interpret (see below).

Muscle NST: Major role of slippage of sarcoplasmic/endoplasmic reticulum Ca^{2+}-ATPase?

Prior to the identification of BAT as a major site of adrenergic thermogenesis, several investigators, including L. Jansky and his colleagues at the Charles University in Prague, suggested that adaptive NST occurs primarily in skeletal muscle [72-75]. Although the research focus later shifted predominantly towards BAT, several alternative mechanisms were proposed to play a role in NST in skeletal muscle, including i) UCP1-independent mitochondrial proton leak [60,63]; ii) impaired thermodynamic efficiency of Na^+/K^+-ATPase in the plasma membrane [76,77]; and iii) futile substrate cycling between *de novo* lipogenesis (DNL) and fatty acid (FA) oxidation (DNA/FAox cycle) controlled by leptin–AMP-activated protein kinase (AMPK) axis [78-81]. Also thermoregulatory tonus (continuous "shivering") should be considered here (see above). However, major attention has been paid recently to NST resulting from slippage of sarcoplasmic/endoplasmic reticulum Ca^{2+}-ATPase (**SERCA**) [42,63,82-84].

As stated above, only a relatively small proportion of ATP consumed in muscle is used directly to generate contractile force. Various muscles and organisms differ in contractile efficiency, which is the ratio of ATP consumed for contraction and for regulatory processes, particularly calcium cycling which requires SERCA. The regulatory processes can consume up to 45 % of ATP [51]. Muscle contraction is initiated by a well-established signaling cascade that involves acetylcholine release from motor nerve endings at the neuromuscular junction and the stimulation of nicotinic acetylcholine receptors on the muscle membrane (Fig. 1). Local depolarization triggers action potential, which is further propagated across the plasma membrane and its invaginations (T-tubules) to the vicinity of sarcoplasmic reticulum (**SER**). Activated voltage-gated dihydropyridine receptors in T-tubules open adjacent ryanodine receptors (**RyR**) in the membrane of SER, enabling the massive release of calcium from this reservoir to the cytoplasm. Elevated cytoplasmic calcium concentration is the critical signal to initiate the muscle contraction. In particular, calcium binding to regulatory protein troponin causes exposition of binding sites for myosin heads on actin filament and allows cross-bridge cycling, which hydrolyses ATP and generates the contraction force (see e.g. [85] for more detail). The single neural stimulus causes only short twitch contraction because calcium is rapidly removed from the cytoplasm by the activity of SERCA. If the second stimulus follows the first one before SERCA manages to remove calcium from the cytoplasm and reach resting calcium level, the twitches are partially summated, i.e. the cytoplasmic calcium concentration after the second twitch is higher and the generated tension is greater than those after a single twitch. A sequence of stimuli of sufficient frequency leads to complete summation of individual twitches into stronger and longer lasting tetanic contraction. Activity of SERCA is thus critical for regulation of strength of muscle contraction.

Two SERCA genes (*Atp2a1* for SERCA1 and *Atp2a2* for SERCA2) are expressed in mammalian skeletal muscle, producing several splice variants. Fast kinetic SERCA1a and 1b are found in adult fast-twitch muscles, and SERCA1b also in neonates [86,87]. SERCA2a with slow kinetics is found in slow-twitch fibres [88] and its expression is induced by cold [16,89]. During neonatal development, gradual changes from SERCA2a and SERCA1b to SERCA1a were reported [88,89].

The activity of SERCA is affected by interaction with micropeptides phospholamban (particularly in heart ventricles) and sarcolipin (**SLN**; both in heart and skeletal muscle). The normal working cycle of SERCA comprises the binding of 2 calcium ions and a molecule of ATP to the cytosolic side of the pump, hydrolysis of ATP, and subsequent conformational change causing the release of both calcium ions to the sarcoplasmic reticulum [90,91]. Phospholamban interaction with SERCA (preferentially SERCA2a [92]) depends on phospholamban phosphorylation [93] and only happens if the cytoplasmic calcium level is low [91,94]. In heart ventricles, adrenergic stimulation leads to phospholamban phosphorylation and subsequent disinhibition of SERCA resulting in prolonged periods of high calcium concentration and therefore in increased cardiac contractility [95]. A similar function was suggested for SLN in heart atria [96] but attention was later shifted to activity of SLN in skeletal muscle. The kinetics of SLN is different from that of phospholamban: SLN binds to SERCA (preferentially SERCA1a [92]) regardless of calcium concentration [94]. The binding of SLN reduces maximal rate of SERCA calcium pumping without affecting SERCA affinity for calcium, resulting in calcium ions slipping back to the cytoplasm and in uncoupling of ATP hydrolysis from calcium pumping; i.e. heat production [91,97]. As an alternative to the effect of SLN on SERCA calcium pumping, calcium leak

through RyR has also been suggested to regulate thermogenesis in murine resting skeletal muscle [98].

Mice lacking either UCP1 or SLN can survive in the cold probably due to compensatory upregulation of the remaining thermogenic mechanisms, while UCP1/SLN double knockout mice cannot sustain long-term cold exposure [99]. Thus, both SLN and UCP1 may be involved in thermogenesis in cold [99]. Muscle SLN level is increased in mice with ablation of either interscapular BAT or UCP1 [99-101]. Thus, BAT and muscle may represent synergistic and potentially even partially redundant components of thermoregulatory NST [60,82]. Importantly in this respect, our own data suggest that the relative contribution of the discussed thermogenic mechanisms varies among different murine strains. C57BL/6 mice, which are typically used in the majority of metabolic studies, rely mainly on BAT, while A/J mice, known for their resistance to obesity, use muscle thermogenesis to a greater extent [16]. While the burst shivering rate does not differ between C57BL/6 and A/J mice at cold, A/J mice recruit larger amount of SLN in their muscles [16].

Calcium cycling (involving RyR and SERCA) was shown to be the primary thermogenic mechanism in specialized heater organs of some species of marine fish (e.g. [102]). Although these organs were derived from extraocular muscles, they lost their contractile apparatus. In contrast, in mammals, SLN- and RyR-dependent mechanisms operate in fully functional muscles where the primary role of calcium is to regulate sarcomere contraction. In such a system, proof of functional independence of shivering and calcium cycling is quite methodologically challenging. Similarly to continuous shivering, also SLN-dependent thermogenesis is thought to be localized in slow-twitch oxidative fibers relying primarily on lipid oxidation [89].

Although attempts were made to demonstrate that stimulation of SLN can occur in the absence of corresponding changes in shivering (e.g. [94]), these reports need to be taken with caution considering the above mentioned complexity of shivering (not only burst shivering but also the thermoregulatory tonus) and pitfalls of its assessment. Without any doubt, SLN-induced calcium slippage in SERCA may generate heat, but it is unclear whether this effect is potent enough and can be sufficiently quickly adjusted to play a role in facultative thermogenesis [83]. As regulation of SERCA activity is a common mechanism how to adjust heart contractility (see above), it is possible that the primary function of SERCA regulation in skeletal muscle is also to adjust the calcium level in the long term, which determines the thresholds for muscle contraction. Therefore, SLN may play a role in both the adaptive tuning of shivering activity and muscle NST.

Regulation of the activity of SLN (and other putative muscle NST mechanisms) needs to be better understood (Fig. 2). Adrenergic signaling is for decades accepted as the mean of regulation of facultative NST [5].

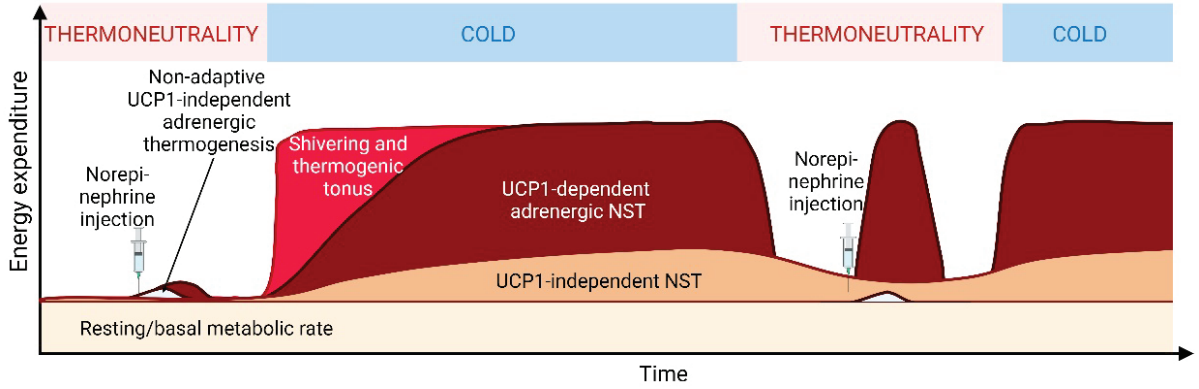

Fig. 2. Metabolic responses to acute and chronic cold exposure in mice (adapted from [7]). General increase of energy expenditure upon cold exposure reflects several thermogenic mechanisms. Muscle shivering and thermoregulatory tonus cover majority of heat production in response to acute cold stimulus. Continuing shivering leads to adaptation resembling exercise training, but shivering is gradually replaced by NST. NST mediated by UCP1 has a low capacity at thermoneutrality. However, if cold persist, capacity of UCP1-dependent NST adaptively rises and it gradually replaces shivering. It is facultative, i.e. it can be rapidly switched on and off due to its control by adrenergic nervous system (adrenergic thermogenesis). NST alternative to UCP1-mediated heat production, reflects several mechanisms, including NST in skeletal muscle. Preferential activation and adaptive increase of NST capacity in BAT or skeletal muscle depends on the genetic background of the mice. Control of muscle NST is probably relatively slow – it may not be facultative. Thus, when the contribution of muscle NST to total energy expenditure is relatively high compared to BAT (such as in A/J mice, see the main text), a substantial amount of energy is lost during the stay of cold-adapted mice in thermoneutral conditions. This phenomenon may contribute to resistance to obesity. Prolonged maintenance of cold-adapted animals at thermoneutral conditions results in reduction of the capacity of NST (not shown). Created with Biorender.com.

It was assumed that the adrenergic system also regulates SLN activity in skeletal muscles [103,104], similar to how phospholamban activity is regulated in the heart (see above). However, to our knowledge, this assumption has never been unambiguously proven. While adrenergic stimulation results also in some UCP1-independent rise in energy expenditure, this induction is not potentiated by cold adaptation in UCP1-KO animals [68]. Interestingly, while cold adaptation recruits adrenergic thermogenesis in C57BL/6 mice, A/J mice adapt to cold without recruiting capacity for adrenergic thermogenesis, presumably relying on muscle mechanisms that are regulated by different means [16]. Cold tolerance requires intact signaling including several hormones, namely leptin and thyroid hormones [78,105]. Similarly, corticotropin was suggested to mediate the thermogenic effect on muscle [106]. Thus, putative muscle NST may be under endocrine rather than sympathetic control. However, whether humoral regulation can be fast enough to govern facultative thermogenesis remains to be elucidated.

Additional research is required to verify the involvement of various potential mechanisms of NST in skeletal muscles, as well as to understand their interdependence, regulation, and functional importance. The extent to which these mechanisms are facultative and adaptive is still a matter of debate. When assessing their contribution to energy balance, it is challenging to separate NST activation from both classic shivering and thermogenic tonus. This is because they occur simultaneously with muscle contractile activity in the same organ.

States of myosin: The grey zone between shivering and NST

During the last decade, one more mechanism for increased muscle energy dissipation has been described in the grey zone between shivering and NST. During cross-bridge cycling, active myosin heads bind to the exposed myosin binding sites of the actin filament (see above) and, by conformational changes (driven by ATP hydrolysis), cause sliding of both filaments on each other, which results in muscle contraction. However, besides this active state, myosin heads can also exist in two different inactive states distinguished experimentally by following the kinetics of release of fluorescent ATP hydrolysis products from myosin [107]. Classical relaxed state (or disordered relaxed state; DRX) is characterized by low basal ATPase activity independent of binding to actin, while the newly identified super relaxed state (SRX) hydrolyzes nearly no ATP [107]. The ratios of these three states vary depending on parameters such as sarcomere length, phosphorylation of regulatory proteins, or calcium level [108]. The transition of part of myosin from SRX to DRX would significantly increase energy expenditure, and it was therefore suggested to play a role in cold adaptation [109]. Considerable effort is currently invested in identifying compounds that would affect the SRX/DRX ratio in order to treat pathologies including obesity by increasing muscle energy expenditure.

Cold-induced adaptive induction of the capacity of NST in skeletal muscles rather than in BAT is associated with obesity resistance

Experiments in mice suggest that putative SLN-dependent NST could affect the propensity to obesity, as SLN-deficient mice gain more weight than the control mice if exposed to high-fat diet [28,94] and muscle-specific *Sln* overexpression prevents diet-induced obesity [110]. Surprisingly, UCP1 and SLN double KO mice do not develop dietary obesity, possibly because of relying on less efficient mechanisms of NST [28]. Obesity-resistant inbred murine strains (such as A/J mice) exhibit higher muscle *Sln* expression than obesity-prone C57BL6 mice [16]. Besides SLN, another more generally expressed protein, neuronatin, was also recently claimed to cause SERCA uncoupling [111]. Neuronatin expression is affected by high-fat feeding [111], which is interpreted as an indication that SERCA-mediated NST is involved in a physiological negative feedback loop preventing the development of obesity.

Muscle NST and UCP1-mediated NST in BAT differ in important features that could affect their impact on both thermal and energy homeostasis. To achieve the same level of protection against cold, more energy is required by thermogenesis in skeletal muscle compared to UCP1-mediated thermogenesis in BAT [21,82]. This is consistent with the more recent evolution of BAT as a specialized and precisely controlled thermogenic organ, as compared with muscle. The different energy efficiency of thermoregulatory thermogenesis exerted by BAT and muscle could result from differences in i) location and/or ii) regulation.

Location of BAT depots in the center of the body, close to major arteries, allows relatively efficient transport of heat formed in BAT to the vital organs with

minimal losses, as compared with thermogenesis in the muscles, which are mostly somewhat peripherally located [6,21]. However, it was also noted that continuous shivering is often happening in highly vascularized deep muscles where heat losses are more minor, and muscle activity may efficiently heat venous blood returning from peripheral tissues [57].

Regulation of NST in BAT and muscle is very different. Thermogenesis in BAT is strictly activated during i) periods of cold exposure or ii) when animals are eating, i.e. during the dark phase of the day in mice [20]. On the other hand, muscle NST seems to be under a looser and less flexible control. When adaptively increased in response to long-lasting cold exposure, it could dissipate energy independent of actual energy intake (see below).

Collectively, the combined effect of the relative thermogenic inefficiency, and absence of rapid flexible regulation of muscle NST in comparison to BAT, results in relatively high energy cost of NST mediated by skeletal muscles, which could lead to reduced propensity to obesity. Indeed, we have observed that both obesity-prone C57BL/6 and obesity-resistant A/J mice were able to survive in the cold with only a slight decrease in body temperature, using muscle shivering for thermogenesis at the beginning of cold exposure (6 °C). Prolonged maintenance of mice at low temperature led to increased capacity of NST in BAT in obesity-prone mice. Surprisingly, however, obesity-resistant A/J mice failed to activate BAT, but instead increased oxidative capacity in skeletal muscle. This putative muscle NST may be mediated by the SLN-SERCA mechanism, consuming additional ATP and allowing for the acceleration of mitochondrial oxidation [16]. Thus, resistance to obesity was associated with cold-induced rise of the capacity of NST in skeletal muscles rather than in BAT (Fig. 2), which is in line with earlier opinions about the adaptivity of muscle NST [5,6]. That capacity for NST in skeletal muscles could be adaptively induced was also documented in mice with genetic ablation of SLN, in accordance with the notion that UCP1- and SLN-SERCA-mediated NST complement each other [99].

The importance of genetic background (particularly the potential role of heterosis) in cold resistance was earlier reported by Kozak's lab [12,112]. Our results suggest that A/J mice represent a model for characterizing UCP1-independent mechanisms of NST [21,45,113,114] and their physiological role. Reflecting the relatively low thermogenic activity of their BAT, these mice may provide a better model of the situation in humans compared with C57BL/6 mice and mixed-background mice, used in most of the previous studies in this field with the focus on the role of UCP1 [20,68], SERCA-SLN [82,99,101] or other mechanisms [26,40,42,45,78,115,116] of NST. To get further insight into the mechanisms engaged in NST, more inbred strains of mice differing in susceptibility to dietary obesity [117] should be characterized in future studies.

Two common approaches used in the prevention and treatment of obesity are reducing calorie intake and increasing physical activity. However, in both rodents and humans, weight loss imposed by fasting leads to i) decreased leptinaemia and sympathetic nervous system activity and ii) increased muscle energy efficiency, i.e. decreased energy expenditure [118]. This can be reversed by normalizing the leptin levels in the context of reversing the decline in sympathetic activity [118,119]. Besides showing the importance of the genetic background of experimental animals for the study of muscle NST, our results support the notion that NST in skeletal muscle may partially counteract weight gain, and its induction could be used to treat obesity. More studies are required in order to elucidate the (i) mechanisms behind adaptivity of NST in skeletal muscle, and (ii) its quantitative importance with respect to overall energy balance.

Conclusions

Although NST includes several alternative mechanisms, UCP1-dependent NST is widely considered the only means of facultative and adaptive NST involved in the homeostasis of both body temperature and possibly body weight. This traditional view has recently been challenged. The involvement of BAT in the maintenance of a constant body weight and prevention of obesity has become increasingly controversial. Compared to small rodents, humans are rarely exposed to chronic cold and can rely more on muscle shivering. Our understanding of both shivering and putative muscle NST is not sufficient. In addition to classic burst shivering, the muscle can produce significant amounts of heat by increasing tonus, a type of muscle contractile activity that may not be visually manifested. Muscle contractions are rapidly regulated by the release and removal of calcium. The efficiency of calcium removal by SERCA is affected by the peptide SLN, which is up-regulated by cold. We propose here that SLN plays a role in the long-term

tuning of shivering activity. SLN decreases the efficiency of calcium pumping by SERCA, and promotes thermogenesis. Even though the mechanisms behind NST in skeletal muscles are not fully characterized, it is to be inferred that the slow regulation of muscle NST and its adaptive induction in response to cold may result in increased muscle thermogenesis even when it is not acutely required for thermal homeostasis. The ability to activate NST in the muscle or in BAT depends on the genetic background, which could contribute to strain-specific differences in propensity to obesity in mice. Lower energy efficiency of muscle thermogenesis relative to that in BAT, reflecting the anatomic location, as well as the large oxidative capacity of the muscles, further augments the potential of muscle NST to reduce body fat. In adult humans, the capacity of skeletal muscle to burn fat energy stores is several-fold greater than in BAT. Thus, only a relatively small increase in thermogenesis in muscle could significantly reduce adipose tissue deposition. We propose that muscle NST represents a more promising target for weight-reducing therapies than the traditionally studied BAT.

Conflict of Interest

There is no conflict of interest.

Acknowledgements

Supported by project no. 22-07004S of Czech Science Foundation, and by the project National Institute for Research of Metabolic and Cardiovascular Diseases (Programme EXCELES, ID Project No. LX22NPO5104) – Funded by the European Union-Next Generation EU.

References

1. Himms-Hagen J. Role of thermogenesis in the regulation of energy balance in relation to obesity. Can J Physiol Pharmacol 1989;67:394-401. https://doi.org/10.1139/y89-063
2. Grigg G, Nowack J, Bicudo J, Bal NC, Woodward HN, Seymour RS. Whole-body endothermy: ancient, homologous and widespread among the ancestors of mammals, birds and crocodylians. Biol Rev Camb Philos Soc 2022;97:766-801. https://doi.org/10.1111/brv.12822
3. Skop V, Guo J, Liu N, Xiao C, Hall KD, Gavrilova O, Reitman ML. Mouse Thermoregulation: Introducing the Concept of the Thermoneutral Point. Cell Rep 2020;31:107501. https://doi.org/10.1016/j.celrep.2020.03.065
4. Girardier L. The regulation of the biological furnace of warm blooded animals. Experientia 1977;33:1121-1122. https://doi.org/10.1007/BF01922276
5. Jansky I. Humoral thermogenesis and its role in maintaining energy balance. Physiol Rev 1995;75:237-259. https://doi.org/10.1152/physrev.1995.75.2.237
6. Silva JE. Thermogenic mechanisms and their hormonal regulation. Physiol Rev 2006;86:435-464. https://doi.org/10.1152/physrev.00009.2005
7. Cannon B, Nedergaard J. Brown adipose tissue: function and physiological significance. Physiol Rev 2004;84:277-359. https://doi.org/10.1152/physrev.00015.2003
8. Masoro EJ. Role of lipogenesis in nonshivering thermogenesis. Fed Proc 1963;22:868-873.
9. Petrovic N, Walden TB, Shabalina IG, Timmons JA, Cannon B, Nedergaard J. Chronic peroxisome proliferator-activated receptor gamma (PPARgamma) activation of epididymally derived white adipocyte cultures reveals a population of thermogenically competent, UCP1-containing adipocytes molecularly distinct from classic brown adipocytes. J Biol Chem 2010;285:7153-7164. https://doi.org/10.1074/jbc.M109.053942
10. Wu J, Bostrom P, Sparks LM, Ye L, Choi JH, Giang AH, Khandekar M, ET AL. Beige adipocytes are a distinct type of thermogenic fat cell in mouse and human. Cell 2012;150:366-376. https://doi.org/10.1016/j.cell.2012.05.016
11. Guerra C, Koza RA, Yamashita H, King KW, Kozak LP. Emergence of brown adipocytes in white fat in mice is under genetic control. Effects on body weight and adiposity. J Clin Invest 1998;102:412-420. https://doi.org/10.1172/JCI3155
12. Kozak LP. The genetics of brown adipocyte induction in white fat depots. Front Endocrinol (Lausanne) 2011;2:64. https://doi.org/10.3389/fendo.2011.00064
13. Boyer BB, Kozak LP. The mitochondrial uncoupling protein gene in brown fat: correlation between DNase I hypersensitivity and expression in transgenic mice. Mol Cell Biol 1991;11:4147-4156. https://doi.org/10.1128/mcb.11.8.4147-4156.1991

14. Kozak UC, Kopecky J, Teisinger J, Enerback S, Boyer B, Kozak LP. An upstream enhancer regulating brown-fat-specific expression of the mitochondrial uncoupling protein gene. Mol Cell Biol 1994;14:59-67. https://doi.org/10.1128/mcb.14.1.59-67.1994
15. Cassard-Doulcier AM, Gelly C, Fox N, Schrementi J, Raimbault S, Klaus S, Forest C, Bouillaud F, Ricquier D. Tissue-specific and beta-adrenergic regulation of the mitochondrial uncoupling protein gene: control by cis -acting elements in the 5'-flanking region. Mol Endocrinol 1993;7:497-506. https://doi.org/10.1210/mend.7.4.8388995
16. Janovska P, Zouhar P, Bardova K, Otahal J, Vrbacky M, Mracek T, Adamcova K, ET AL. Impairment of adrenergically-regulated thermogenesis in brown fat of obesity-resistant mice is compensated by non-shivering thermogenesis in skeletal muscle. Mol Metab 2023;69:101683. https://doi.org/10.1016/j.molmet.2023.101683
17. Shabalina IG, Petrovic N, de Jong JM, Kalinovich AV, Cannon B, Nedergaard J. UCP1 in Brite/Beige Adipose Tissue Mitochondria Is Functionally Thermogenic. Cell Rep 2013;5:1196-1203. https://doi.org/10.1016/j.celrep.2013.10.044
18. Rothwell NJ, Stock MJ. Similarities between Cold-Induced and Diet-Induced Thermogenesis in the Rat. Can J Physiol Pharmacol 1980;58:842-848. https://doi.org/10.1139/y80-130
19. Wijers SL, Saris WH, Marken Lichtenbelt WD. Individual thermogenic responses to mild cold and overfeeding are closely related. J Clin Endocrinol Metab 2007;92:4299-4305. https://doi.org/10.1210/jc.2007-1065
20. von Essen G, Lindsund E, Cannon B, Nedergaard J. Adaptive facultative diet-induced thermogenesis in wild-type but not in UCP1-ablated mice. Am J Physiol Endocrinol Metab 2017;313:E515-E527. https://doi.org/10.1152/ajpendo.00097.2017
21. Kozak LP. Brown fat and the myth of diet-induced thermogenesis. Cell Metab 2010;11:263-267. https://doi.org/10.1016/j.cmet.2010.03.009
22. Enerback S, Jacobsson A, Simpson EM, Guerra C, Yamashita H, Harper ME, Kozak LP. Mice lacking mitochondrial uncoupling protein are cold-sensitive but not obese. Nature 1997;387:90-94. https://doi.org/10.1038/387090a0
23. Kopecky J, Clarke G, Enerback S, Spiegelman B, Kozak LP. Expression of the mitochondrial uncoupling protein gene from the aP2 gene promoter prevents genetic obesity. J Clin Invest 1995;96:2914-2923. https://doi.org/10.1172/JCI118363
24. Lowell BB, Susulic V, Hamann A, Lawitts JA, Himms-Hagen J, Boyer BB, Kozak LP, Flier JS. Development of obesity in transgenic mice after genetic ablation of brown adipose tissue. Nature 1993;366:740-742. https://doi.org/10.1038/366740a0
25. Melnyk A, Harper ME, Himms-Hagen J. Raising at thermoneutrality prevents obesity and hyperphagia in BAT-ablated transgenic mice. Am J Physiol 1997;272:R1088-R1093. https://doi.org/10.1152/ajpregu.1997.272.4.R1088
26. Liu X, Rossmeisl M, McClaine J, Kozak LP. Paradoxical resistance to diet-induced obesity in UCP1-deficient mice1. J Clin Invest 2003;111:399-407. https://doi.org/10.1172/JCI15737
27. Feldmann HM, Golozoubova V, Cannon B, Nedergaard J. UCP1 Ablation Induces Obesity and Abolishes Diet-induced Thermogenesis in Mice Exempt from Thermal Stress by Living at Thermoneutrality. Cell Metab 2009;9:203-209. https://doi.org/10.1016/j.cmet.2008.12.014
28. Rowland LA, Maurya SK, Bal NC, Kozak L, Periasamy M. Sarcolipin and uncoupling protein 1 play distinct roles in diet-induced thermogenesis and do not compensate for one another. Obesity 2016;24:1430-1433. https://doi.org/10.1002/oby.21542
29. Wang H, Willershauser M, Li Y, Fromme T, Schnabl K, Bast-Habersbrunner A, Ramisch S, Mocek S, Klingenspor M. Uncoupling protein 1 expression does not protect mice from diet-induced obesity. Am J Physiol Endocrinol Metab 2021;320:E333-E345. https://doi.org/10.1152/ajpendo.00285.2020
30. von Essen G, Lindsund E, Maldonado EM, Zouhar P, Cannon B, Nedergaard J. Highly recruited brown adipose tissue does not in itself protect against obesity. Mol Metab 2023;76:101782. https://doi.org/10.1016/j.molmet.2023.101782
31. Nedergaard J, von Essen G, Cannon B. Brown adipose tissue: can it keep us slim? A discussion of the evidence for and against the existence of diet-induced thermogenesis in mice and men. Philos Trans R Soc Lond B Biol Sci 2023;378:20220220. https://doi.org/10.1098/rstb.2022.0220
32. Li Y, Schnabl K, Gabler SM, Willershauser M, Reber J, Karlas A, Laurila S, ET AL. Secretin-Activated Brown Fat Mediates Prandial Thermogenesis to Induce Satiation. Cell 2018;175:1561-1574.e12. https://doi.org/10.1016/j.cell.2018.10.016

33. Speakman JR, Hall KD. Models of body weight and fatness regulation. Philos Trans R Soc Lond B Biol Sci 2023;378:20220231. https://doi.org/10.1098/rstb.2022.0231
34. Collins S, Daniel KW, Petro AE, Surwit RS. Strain-specific response to beta3-adrenergic receptor agonist treatment of diet-induced obesity in mice. Endocrinology 1997;138:405-413. https://doi.org/10.1210/endo.138.1.4829
35. Finlin BS, Memetimin H, Confides AL, Kasza I, Zhu B, Vekaria HJ, Harfmann B, ET AL. Human adipose beiging in response to cold and mirabegron. JCI Insight 2018;3:e121510. https://doi.org/10.1172/jci.insight.121510
36. Zheng Q, Lin J, Huang J, Zhang H, Zhang R, Zhang X, Cao C, ET AL. Reconstitution of UCP1 using CRISPR/Cas9 in the white adipose tissue of pigs decreases fat deposition and improves thermogenic capacity. Proc Natl Acad Sci U S A 2017;114:E9474-E9482. https://doi.org/10.1073/pnas.1707853114
37. Lindberg O, Prusiner SB, Cannon B, Ching TM, Eisenhardt RH. Metabolic control in isolated brown fat cells. Lipids 1970;5:204-209. https://doi.org/10.1007/BF02532470
38. Kazak L. Promoting metabolic inefficiency for metabolic disease. iScience 2023;26:107843. https://doi.org/10.1016/j.isci.2023.107843
39. Rahbani JF, Bunk J, Lagarde D, Samborska B, Roesler A, Xiao H, Shaw A, ET AL. Parallel control of cold-triggered adipocyte thermogenesis by UCP1 and CKB. Cell Metab 2024;36:526-540.e7. https://doi.org/10.1016/j.cmet.2024.01.001
40. Oeckl J, Janovska P, Adamcova K, Bardova K, Brunner S, Dieckmann S, Ecker J, ET AL. Loss of UCP1 function augments recruitment of futile lipid cycling for thermogenesis in murine brown fat. Mol Metab 2022;61:101499. https://doi.org/10.1016/j.molmet.2022.101499
41. Ikeda K, Kang Q, Yoneshiro T, Camporez JP, Maki H, Homma M, Shinoda K, ET AL. UCP1-independent signaling involving SERCA2b-mediated calcium cycling regulates beige fat thermogenesis and systemic glucose homeostasis. Nat Med 2017;23:1454-1465. https://doi.org/10.1038/nm.4429
42. Ukropec J, Anunciado RP, Ravussin Y, Hulver MW, Kozak LP. UCP1-independent thermogenesis in white adipose tissue of cold-acclimated Ucp1-/- mice. J Biol Chem 2006;281:31894-31908. https://doi.org/10.1016/S0021-9258(19)84104-2
43. Rahbani JF, Scholtes C, Lagarde DM, Hussain MF, Roesler A, Dykstra CB, Bunk J, ET AL. ADRA1A-Galpha(q) signalling potentiates adipocyte thermogenesis through CKB and TNAP. Nat Metab 2022;4:1459-1473. https://doi.org/10.1038/s42255-022-00667-w
44. Golozoubova V, Cannon B, Nedergaard J. UCP1 is essential for adaptive adrenergic nonshivering thermogenesis. Am J Physiol Endocrinol Metab 2006;291:E350-E357. https://doi.org/10.1152/ajpendo.00387.2005
45. Granneman JG, Burnazi M, Zhu Z, Schwamb LA. White adipose tissue contributes to UCP1-independent thermogenesis. Am J Physiol Endocrinol Metab 2003;285:E1230-E1236. https://doi.org/10.1152/ajpendo.00197.2003
46. Flachs P, Adamcova K, Zouhar P, Marques C, Janovska P, Viegas I, Jones JG, ET AL. Induction of lipogenesis in white fat during cold exposure in mice: link to lean phenotype. Int J Obes (Lond) 2017;41:372-380. https://doi.org/10.1038/ijo.2016.228
47. Meyer CW, Willershauser M, Jastroch M, Rourke BC, Fromme T, Oelkrug R, Heldmaier G, Klingenspor M. Adaptive thermogenesis and thermal conductance in wild-type and UCP1-KO mice. Am J Physiol Regul Integr Comp Physiol 2010;299:R1396-R1406. https://doi.org/10.1152/ajpregu.00021.2009
48. Poussin C, Ibberson M, Hall D, Ding J, Soto J, Abel ED, Thorens B. Oxidative phosphorylation flexibility in the liver of mice resistant to high-fat diet-induced hepatic steatosis. Diabetes 2011;60:2216-2224. https://doi.org/10.2337/db11-0338
49. Burcelin R, Crivelli V, Dacosta A, Roy-Tirelli A, Thorens B. Heterogeneous metabolic adaptation of C57BL/6J mice to high-fat diet. Am J Physiol Endocrinol Metab 2002;282:E834-E842. https://doi.org/10.1152/ajpendo.00332.2001
50. Hui S, Cowan AJ, Zeng X, Yang L, TeSlaa T, Li X, Bartman C, ET AL. Quantitative Fluxomics of Circulating Metabolites. Cell Metab 2020;32:676-688.e4. https://doi.org/10.1101/2020.03.02.973669
51. Barclay CJ, Curtin NA. Advances in understanding the energetics of muscle contraction. J Biomech 2023;156:111669. https://doi.org/10.1016/j.jbiomech.2023.111669
52. Blondin DP, Labbe SM, Phoenix S, Guerin B, Turcotte EE, Richard D, Carpentier AC, Haman F. Contributions of white and brown adipose tissues and skeletal muscles to acute cold-induced metabolic responses in healthy men. J Physiol 2015;593:701-714. https://doi.org/10.1113/jphysiol.2014.283598

53. Zurlo F, Larson K, Bogardus C, Ravussin E. Skeletal muscle metabolism is a major determinant of resting energy expenditure. J Clin Invest 1990;86:1423-1427. https://doi.org/10.1172/JCI114857
54. Haman F, Blondin DP. Shivering thermogenesis in humans: Origin, contribution and metabolic requirement. Temperature (Austin) 2017;4:217-226. https://doi.org/10.1080/23328940.2017.1328999
55. Schiaffino S. Fibre types in skeletal muscle: a personal account. Acta Physiol (Oxford) 2010;199:451-463. https://doi.org/10.1111/j.1748-1716.2010.02130.x
56. Booth FW, Ruegsegger GN, Toedebusch RG, Yan Z. Endurance Exercise and the Regulation of Skeletal Muscle Metabolism. Prog Mol Biol Transl Sci 2015;135:129-151. https://doi.org/10.1016/bs.pmbts.2015.07.016
57. Lomo T, Eken T, Bekkestad Rein E, Nja A. Body temperature control in rats by muscle tone during rest or sleep. Acta Physiol (Oxford) 2020;228:e13348. https://doi.org/10.1111/apha.13348
58. Haman F, Legault SR, Rakobowchuk M, Ducharme MB, Weber JM. Effects of carbohydrate availability on sustained shivering II. Relating muscle recruitment to fuel selection. J Appl Physiol 2004;96:41-49. https://doi.org/10.1152/japplphysiol.00428.2003
59. Haman F, Peronnet F, Kenny GP, Massicotte D, Lavoie C, Scott C, Weber JM. Effect of cold exposure on fuel utilization in humans: plasma glucose, muscle glycogen, and lipids. J Appl Physiol 2002;93:77-84. https://doi.org/10.1152/japplphysiol.00773.2001
60. Blondin DP, Daoud A, Taylor T, Tingelstad HC, Bezaire V, Richard D, Carpentier AC, ET AL. Four-week cold acclimation in adult humans shifts uncoupling thermogenesis from skeletal muscles to brown adipose tissue. J Physiol 2017;595:2099-2113. https://doi.org/10.1113/JP273395
61. Castellani JW, Young AJ. Human physiological responses to cold exposure: Acute responses and acclimatization to prolonged exposure. Auton Neurosci 2016;196:63-74. https://doi.org/10.1016/j.autneu.2016.02.009
62. Haman F, Peronnet F, Kenny GP, Massicotte D, Lavoie C, Weber JM. Partitioning oxidative fuels during cold exposure in humans: muscle glycogen becomes dominant as shivering intensifies. J Physiol 2005;566:247-256. https://doi.org/10.1113/jphysiol.2005.086272
63. Blondin DP, Haman F. Shivering and nonshivering thermogenesis in skeletal muscles. Handb Clin Neurol 2018;156:153-173. https://doi.org/10.1016/B978-0-444-63912-7.00010-2
64. Dulloo AG, Miles-Chan JL, Montani JP, Schutz Y. Isometric thermogenesis at rest and during movement: a neglected variable in energy expenditure and obesity predisposition. Obes Rev 2017;18(Suppl 1):56-64. https://doi.org/10.1111/obr.12505
65. McKay WP, Vargo M, Chilibeck PD, Daku BL. Effects of ambient temperature on mechanomyography of resting quadriceps muscle. Appl Physiol Nutr Metab 2013;38:227-233. https://doi.org/10.1139/apnm-2011-0358
66. Wyckelsma VL, Venckunas T, Houweling PJ, Schlittler M, Lauschke VM, Tiong CF, Wood HD, ET AL. Loss of alpha-actinin-3 during human evolution provides superior cold resilience and muscle heat generation. Am J Hum Genet 2021;108:446-457. https://doi.org/10.1016/j.ajhg.2021.01.013
67. Scholle HC, Biedermann F, Arnold D, Jinnah HA, Grassme R, Schumann NP. A surface EMG multi-electrode technique for characterizing muscle activation patterns in mice during treadmill locomotion. J Neurosci Methods 2005;146:174-182. https://doi.org/10.1016/j.jneumeth.2005.02.006
68. Golozoubova V, Hohtola E, Matthias A, Jacobsson A, Cannon B, Nedergaard J. Only UCP1 can mediate adaptive nonshivering thermogenesis in the cold. FASEB J 2001;15:2048-2050. https://doi.org/10.1096/fj.00-0536fje
69. Westerberg R, Mansson JE, Golozoubova V, Shabalina IG, Backlund EC, Tvrdik P, Retterstol K, Capecchi MR, Jacobsson A. ELOVL3 is an important component for early onset of lipid recruitment in brown adipose tissue. J Biol Chem 2006;281:4958-4968. https://doi.org/10.1074/jbc.M511588200
70. Chen Y, Ikeda K, Yoneshiro T, Scaramozza A, Tajima K, Wang Q, Kim K, ET AL. Thermal stress induces glycolytic beige fat formation via a myogenic state. Nature 2019;565:180-185. https://doi.org/10.1038/s41586-018-0801-z
71. Islam MA, Sundaraj K, Ahmad RB, Ahamed NU. Mechanomyogram for muscle function assessment: a review. PLoS One 2013;8:e58902. https://doi.org/10.1371/journal.pone.0058902
72. Jansky L, Hart JS. Participation of skeletal muscle and kidney during nonshivering thermogenesisin cold-acclimated rats. Can J Biochem Physiol 1963;41:953-964. https://doi.org/10.1139/y63-108

73. Jansky L, Hart JS. Cardiac output and organ blood flow in warm- and cold-acclimated rats exposed to cold. Can J Physiol Pharmacol 1968;46:653-659. https://doi.org/10.1139/y68-096
74. Mejsnar J, Jansky L. Means of noradrenalin action during non-shivering thermogenesis in a single muscle. Int J Biometeorol 1971;15:321-324. https://doi.org/10.1007/BF01803920
75. Jansky L. Contribution of striated muscles to regulatory heat production. Experientia 1977;33:1123-1124. https://doi.org/10.1007/BF01922277
76. Smith TJ, Edelman IS. The role of sodium transport in thyroid thermogenesis. Fed Proc 1979;38:2150-2153.
77. Clarke RJ, Catauro M, Rasmussen HH, Apell HJ. Quantitative calculation of the role of the Na(+),K(+)-ATPase in thermogenesis. Biochim Biophys Acta 2013;1827:1205-1212. https://doi.org/10.1016/j.bbabio.2013.06.010
78. Ukropec J, Anunciado RV, Ravussin Y, Kozak LP. Leptin is required for uncoupling protein-1-independent thermogenesis during cold stress. Endocrinology 2006;147:2468-2480. https://doi.org/10.1210/en.2005-1216
79. Solinas G, Summermatter S, Mainieri D, Gubler M, Pirola L, Wymann MP, Rusconi S, ET AL. The direct effect of leptin on skeletal muscle thermogenesis is mediated by substrate cycling between de novo lipogenesis and lipid oxidation. FEBS Lett 2004;577:539-544. https://doi.org/10.1016/j.febslet.2004.10.066
80. Kus V, Prazak T, Brauner P, Hensler M, Kuda O, Flachs P, Janovska P, ET AL. Induction of muscle thermogenesis by high-fat diet in mice: association with obesity-resistance. Am J Physiol Endocrinol Metab 2008;295:E356-E367. https://doi.org/10.1152/ajpendo.90256.2008
81. Minokoshi Y, Kim YB, Peroni OD, Fryer LG, Muller C, Carling D, Kahn BB. Leptin stimulates fatty-acid oxidation by activating AMP-activated protein kinase. Nature 2002;415:339-343. https://doi.org/10.1038/415339a
82. Bal NC, Periasamy M. Uncoupling of sarcoendoplasmic reticulum calcium ATPase pump activity by sarcolipin as the basis for muscle non-shivering thermogenesis. Philos Trans R Soc Lond B Biol Sci 2020;375:20190135. https://doi.org/10.1098/rstb.2019.0135
83. Campbell KL, Dicke AA. Sarcolipin Makes Heat, but Is It Adaptive Thermogenesis? Front Physiol 2018;9:714. https://doi.org/10.3389/fphys.2018.00714
84. Nowack J, Vetter SG, Stalder G, Painer J, Kral M, Smith S, Le MH, ET AL. Muscle nonshivering thermogenesis in a feral mammal. Sci Rep 2019;9:6378. https://doi.org/10.1038/s41598-019-42756-z
85. Gordon AM, Homsher E, Regnier M. Regulation of contraction in striated muscle. Physiol Rev 2000;80:853-924. https://doi.org/10.1152/physrev.2000.80.2.853
86. Nowack J, Giroud S, Arnold W, Ruf T. Muscle Non-shivering Thermogenesis and Its Role in the Evolution of Endothermy. Front Physiol 2017;8:889. https://doi.org/10.3389/fphys.2017.00889
87. Toth A, Fodor J, Vincze J, Olah T, Juhasz T, Zakany R, Csernoch L, Zador E. The Effect of SERCA1b Silencing on the Differentiation and Calcium Homeostasis of C2C12 Skeletal Muscle Cells. PLoS One 2015;10:e0123583. https://doi.org/10.1371/journal.pone.0123583
88. Periasamy M, Kalyanasundaram A. SERCA pump isoforms: their role in calcium transport and disease. Muscle Nerve 2007;35:430-442. https://doi.org/10.1002/mus.20745
89. Pant M, Bal NC, Periasamy M. Cold adaptation overrides developmental regulation of sarcolipin expression in mice skeletal muscle: SOS for muscle-based thermogenesis? J Exp Biol 2015;218:2321-2325. https://doi.org/10.1242/jeb.119164
90. Periasamy M, Bhupathy P, Babu GJ. Regulation of sarcoplasmic reticulum Ca2+ ATPase pump expression and its relevance to cardiac muscle physiology and pathology. Cardiovasc Res 2008;77:265-273. https://doi.org/10.1093/cvr/cvm056
91. Sahoo SK, Shaikh SA, Sopariwala DH, Bal NC, Periasamy M. Sarcolipin protein interaction with sarco(endo)plasmic reticulum Ca2+ ATPase (SERCA) is distinct from phospholamban protein, and only sarcolipin can promote uncoupling of the SERCA pump. J Biol Chem 2013;288:6881-6889. https://doi.org/10.1074/jbc.M112.436915
92. Fajardo VA, Bombardier E, Vigna C, Devji T, Bloemberg D, Gamu D, Gramolini AO, Quadrilatero J, Tupling AR. Co-expression of SERCA isoforms, phospholamban and sarcolipin in human skeletal muscle fibers. PLoS One 2013;8:e84304. https://doi.org/10.1371/journal.pone.0084304
93. Bhupathy P, Babu GJ, Periasamy M. Sarcolipin and phospholamban as regulators of cardiac sarcoplasmic reticulum Ca2+ ATPase. J Mol Cell Cardiol 2007;42:903-911. https://doi.org/10.1016/j.yjmcc.2007.03.738

94. Bal NC, Maurya SK, Sopariwala DH, Sahoo SK, Gupta SC, Shaikh SA, Pant M, ET AL. Sarcolipin is a newly identified regulator of muscle-based thermogenesis in mammals. Nat Med 2012;18:1575-1579. https://doi.org/10.1038/nm.2897
95. MacLennan DH, Kranias EG. Phospholamban: a crucial regulator of cardiac contractility. Nat Rev Mol Cell Biol 2003;4:566-577. https://doi.org/10.1038/nrm1151
96. Babu GJ, Bhupathy P, Timofeyev V, Petrashevskaya NN, Reiser PJ, Chiamvimonvat N, Periasamy M. Ablation of sarcolipin enhances sarcoplasmic reticulum calcium transport and atrial contractility. Proc Natl Acad Sci U S A 2007;104:17867-17872. https://doi.org/10.1073/pnas.0707722104
97. Shaikh SA, Sahoo SK, Periasamy M. Phospholamban and sarcolipin: Are they functionally redundant or distinct regulators of the Sarco(Endo)Plasmic Reticulum Calcium ATPase? J Mol Cell Cardiol 2016;91:81-91. https://doi.org/10.1016/j.yjmcc.2015.12.030
98. Meizoso-Huesca A, Pearce L, Barclay CJ, Launikonis BS. Ca(2+) leak through ryanodine receptor 1 regulates thermogenesis in resting skeletal muscle. Proc Natl Acad Sci U S A 2022;119:e2119203119. https://doi.org/10.1073/pnas.2119203119
99. Rowland LA, Bal NC, Kozak LP, Periasamy M. Uncoupling Protein 1 and Sarcolipin Are Required to Maintain Optimal Thermogenesis, and Loss of Both Systems Compromises Survival of Mice under Cold Stress. J Biol Chem 2015;290:12282-12289. https://doi.org/10.1074/jbc.M115.637603
100. Bal NC, Maurya SK, Singh S, Wehrens XH, Periasamy M. Increased Reliance on Muscle-based Thermogenesis upon Acute Minimization of Brown Adipose Tissue Function. J Biol Chem 2016;291:17247-17257. https://doi.org/10.1074/jbc.M116.728188
101. Bal NC, Singh S, Reis FCG, Maurya SK, Pani S, Rowland LA, Periasamy M. Both brown adipose tissue and skeletal muscle thermogenesis processes are activated during mild to severe cold adaptation in mice. J Biol Chem 2017;292:16616-16625. https://doi.org/10.1074/jbc.M117.790451
102. Morrissette JM, Franck JP, Block BA. Characterization of ryanodine receptor and Ca2+-ATPase isoforms in the thermogenic heater organ of blue marlin (Makaira nigricans). J Exp Biol 2003;206:805-812. https://doi.org/10.1242/jeb.00158
103. Shiuchi T, Haque MS, Okamoto S, Inoue T, Kageyama H, Lee S, Toda C, ET AL. Hypothalamic orexin stimulates feeding-associated glucose utilization in skeletal muscle via sympathetic nervous system. Cell Metab 2009;10:466-480. https://doi.org/10.1016/j.cmet.2009.09.013
104. Bombardier E, Smith IC, Gamu D, Fajardo VA, Vigna C, Sayer RA, Gupta SC, Bal NC, Periasamy M, Tupling AR. Sarcolipin trumps beta-adrenergic receptor signaling as the favored mechanism for muscle-based diet-induced thermogenesis. FASEB J 2013;27:3871-3878. https://doi.org/10.1096/fj.13-230631
105. Zekri Y, Flamant F, Gauthier K. Central vs. Peripheral Action of Thyroid Hormone in Adaptive Thermogenesis: A Burning Topic. Cells 2021;10:1327. https://doi.org/10.3390/cells10061327
106. Solinas G, Summermatter S, Mainieri D, Gubler M, Montani JP, Seydoux J, Smith SR, Dulloo AG. Corticotropin-releasing hormone directly stimulates thermogenesis in skeletal muscle possibly through substrate cycling between de novo lipogenesis and lipid oxidation. Endocrinology 2006;147:31-38. https://doi.org/10.1210/en.2005-1033
107. Stewart MA, Franks-Skiba K, Chen S, Cooke R. Myosin ATP turnover rate is a mechanism involved in thermogenesis in resting skeletal muscle fibers. Proc Natl Acad Sci U S A 2010;107:430-435. https://doi.org/10.1073/pnas.0909468107
108. Schmid M, Toepfer CN. Cardiac myosin super relaxation (SRX): a perspective on fundamental biology, human disease and therapeutics. Biol Open 2021;10:bio057646. https://doi.org/10.1242/bio.057646
109. Cooke R. The role of the myosin ATPase activity in adaptive thermogenesis by skeletal muscle. Biophys Rev 2011;3:33-45. https://doi.org/10.1007/s12551-011-0044-9
110. Maurya SK, Bal NC, Sopariwala DH, Pant M, Rowland LA, Shaikh SA, Periasamy M. Sarcolipin Is a Key Determinant of the Basal Metabolic Rate, and Its Overexpression Enhances Energy Expenditure and Resistance against Diet-induced Obesity. J Biol Chem 2015;290:10840-10849. https://doi.org/10.1074/jbc.M115.636878

111. Braun JL, Teng ACT, Geromella MS, Ryan CR, Fenech RK, MacPherson REK, Gramolini AO, Fajardo VA. Neuronatin promotes SERCA uncoupling and its expression is altered in skeletal muscles of high-fat diet-fed mice. FEBS Lett 2021;595:2756-2767. https://doi.org/10.1002/1873-3468.14213
112. Hofmann WE, Liu X, Bearden CM, Harper ME, Kozak LP. Effects of genetic background on thermoregulation and fatty acid- induced uncoupling of mitochondria in UCP1-deficient mice. J Biol Chem 2001;276:12460-12465. https://doi.org/10.1074/jbc.M100466200
113. Flachs P, Rossmeisl M, Kuda O, Kopecky J. Stimulation of mitochondrial oxidative capacity in white fat independent of UCP1: A key to lean phenotype. Biochim Biophys Acta 2013;1831:986-1003. https://doi.org/10.1016/j.bbalip.2013.02.003
114. Rohm M, Zeigerer A, Machado J, Herzig S. Energy metabolism in cachexia. EMBO Rep 2019;20:e47258. https://doi.org/10.15252/embr.201847258
115. Keipert S, Lutter D, Schroeder BO, Brandt D, Stahlman M, Schwarzmayr T, Graf E, ET AL. Endogenous FGF21-signaling controls paradoxical obesity resistance of UCP1-deficient mice. Nat Commun 2020;11:624. https://doi.org/10.1038/s41467-019-14069-2
116. Kazak L, Rahbani JF, Samborska B, Lu GZ, Jedrychowski MP, Lajoie M, Zhang S, ET AL. Ablation of adipocyte creatine transport impairs thermogenesis and causes diet-induced obesity. Nat Metab 2019;1:360-370. https://doi.org/10.1038/s42255-019-0035-x
117. West DB, Boozer CN, Moody DL, Atkinson RL. Dietary obesity in nine inbred mouse strains. Am J Physiol 1992;262:R1025-R1032. https://doi.org/10.1152/ajpregu.1992.262.6.R1025
118. Goldsmith R, Joanisse DR, Gallagher D, Pavlovich K, Shamoon E, Leibel RL, Rosenbaum M. Effects of experimental weight perturbation on skeletal muscle work efficiency, fuel utilization, and biochemistry in human subjects. Am J Physiol Regul Integr Comp Physiol 2010;298:R79-R88. https://doi.org/10.1152/ajpregu.00053.2009
119. Rosenbaum M, Goldsmith R, Bloomfield D, Magnano A, Weimer L, Heymsfield S, Gallagher D, ET AL. Low-dose leptin reverses skeletal muscle, autonomic, and neuroendocrine adaptations to maintenance of reduced weight. J Clin Invest 2005;115:3579-3586. https://doi.org/10.1172/JCI25977
120. Kozak LP. *Play Up! Play Up! And Play the Game! (First Edition)*. FriesenPress, 2020, 156 p.
121. Ravussin E, Enerback S, Koza R. Leslie Paul Kozak, PhD (1940-2023). Obesity 2023;31:2885-2886. https://doi.org/10.1002/oby.23919

REVIEW

Influence of Lipid Class Used for Omega-3 Fatty Acid Supplementation on Liver Fat Accumulation in MASLD

Isaiah SABINARI[1,2], Olga HORAKOVA[1], Tomas CAJKA[3], Veronika KLEINOVA[1,2], Mariusz R. WIECKOWSKI[4], Martin ROSSMEISL[1]

[1]Laboratory of Adipose Tissue Biology, Institute of Physiology of the Czech Academy of Sciences, Prague, Czech Republic, [2]Department of Physiology, Faculty of Science, Charles University, Prague, Czech Republic, [3]Laboratory of Translational Metabolism, Institute of Physiology of the Czech Academy of Sciences, Prague, Czech Republic, [4]Laboratory of Mitochondrial Biology and Metabolism, Nencki Institute of Experimental Biology, Polish Academy of Sciences, Warsaw, Poland

Received May 3, 2024
Accepted June 25, 2024

Summary

Metabolic dysfunction-associated steatotic liver disease (MASLD) occurs in subjects with obesity and metabolic syndrome. MASLD may progress from simple steatosis (i.e., hepatic steatosis) to steatohepatitis, characterized by inflammatory changes and liver cell damage, substantially increasing mortality. Lifestyle measures associated with weight loss and/or appropriate diet help reduce liver fat accumulation, thereby potentially limiting progression to steatohepatitis. As for diet, both total energy and macronutrient composition significantly influence the liver's fat content. For example, the type of dietary fatty acids can affect the metabolism of lipids and hence their tissue accumulation, with saturated fatty acids having a greater ability to promote fat storage in the liver than polyunsaturated ones. In particular, polyunsaturated fatty acids of *n*-3 series (omega-3), such as docosahexaenoic acid (DHA) and eicosapentaenoic acid (EPA), have been intensively studied for their antisteatotic effects, both in preclinical animal models of obesity and hepatic steatosis and in overweight/obese patients. Their effects may depend not only on the dose and duration of administration of omega-3, or DHA/EPA ratio, but also on the lipid class used for their supplementation. This review summarizes the available evidence from recent comparative studies using omega-3 supplementation *via* different lipid classes. Albeit the evidence is mainly limited to preclinical studies, it suggests that phospholipids and possibly wax esters could provide greater efficacy against MASLD compared to traditional chemical forms of omega-3 supplementation (i.e., triacylglycerols, ethyl esters). This cannot be attributed solely to improved EPA and/or DHA bioavailability, but other mechanisms may be involved.

Keywords

MASLD • Metabolic dysfunction-associated steatotic liver disease • NAFLD • Non-alcoholic fatty liver disease • n-3 polyunsaturated fatty acids

Corresponding author

Martin Rossmeisl, Laboratory of Adipose Tissue Biology, Institute of Physiology of the Czech Academy of Sciences, Vídeňská 1083 , 14200 Prague 4, Czech Republic. E-mail: martin.rossmeisl@fgu.cas.cz

Introduction

The increasing global prevalence of obesity goes hand in hand with an increased risk of metabolic disorders (i.e., metabolic syndrome), which are additionally associated with non-alcoholic fatty liver disease, currently affecting ~30 % of the global population [1]. In fact, the new term metabolic dysfunction-associated steatotic liver disease (MASLD) has recently been coined to reflect the important role of

cardiometabolic risk factors associated with the disease [2-4]. While increased intrahepatic fat accumulation (i.e., liver steatosis or fatty liver) is characteristic of the early stages of MASLD, the disease can progress to metabolic dysfunction-associated steatohepatitis (MASH; previously known as NASH), which is associated with hepatocellular damage and inflammatory changes that may be accompanied by some degree of fibrosis. MASH can further develop into serious conditions such as cirrhosis and hepatocellular carcinoma, but overall mortality is already increased at the stage of hepatic steatosis and progressively increases with worsening MASLD histology [5]. A number of promising drugs are currently being investigated for treating MASLD/MASH based on different mechanisms of action. These agents include, for example, long-acting fibroblast growth factor 21 analogs [6], peroxisome proliferator-activated receptor agonists [7], or glucagon-like peptide 1 receptor agonists [8].

Lifestyle measures leading to weight loss and/or appropriate dietary modifications can positively affect fat accumulation in the liver [9,10], thereby potentially limiting progression to steatohepatitis [11]. Regarding the influence of diet, both total energy content and macronutrient composition seem to play an important role in the above processes [12]. In particular, the type of fatty acids (FA) in the diet can affect lipid metabolism in the liver and thus their tissue deposition. Accordingly, saturated FA appear to have a greater ability to promote fat storage in the liver and also in visceral adipose tissue (AT) compared to polyunsaturated FA (PUFA; [13,14] and reviewed in [12,15]). In particular, long-chain PUFA of *n*-3 series (omega-3), such as docosahexaenoic acid (DHA; 22:6*n*-3) or eicosapentaenoic acid (EPA; 20:5*n*-3), which contain the first double bond between the 3rd and 4th carbon atoms, starting from the terminal methyl end of the molecule, have been extensively studied under a variety of MASLD-promoting conditions, primarily based on their well-documented hypolipidemic [16-20] and anti-inflammatory properties (reviewed in [21-23]). From the results of a number of MASLD studies conducted in both preclinical animal models (mainly laboratory mice or rats) and human subjects, a general conclusion can be drawn that dietary supplementation with DHA and/or EPA can reduce liver fat (see e.g. [24-26] for recent reviews), but the efficacy towards MASH appears to be limited ([27] and reviewed in [25,28-30]). On the other hand, as might be expected, the antisteatotic effects of omega-3 supplementation in the liver depend on various factors, such as dose, duration of administration, and the DHA/EPA ratio of the supplemented omega-3. Moreover, it is important to note that most published studies have used triacylglycerol (TG; i.e., the chemical form found in fish oil) - or ethyl ester (EE)-based concentrates for omega-3 supplementation. In contrast, there is much less evidence, particularly in human subjects with MASLD, of the effects of omega-3 when these PUFA are supplemented using other lipid classes such as phospholipids (PL) or wax esters (WE; [31,32]).

This article does not present an exhaustive review of the published literature regarding MASLD and obesity, but instead strongly focuses on the effects of omega-3 supplementation on liver steatosis, mainly studied in the context of obesity or weight gain. Emphasis is placed on more recent comparative studies in preclinical animal models or in humans where omega-3 bound in different lipid classes have been administered. Finally, we also provide a brief overview of possible mechanisms (including omega-3 bioavailability) that may be common or unique to the different lipid classes of omega-3 used for supplementation.

Lipid classes used for omega-3 supplementation and their common sources

Essential α-linolenic acid (18:3*n*-3) serves as a precursor for the synthesis of omega-3 in animals and humans, but its conversion to EPA and DHA in the body is relatively inefficient. On the other hand, marine phytoplankton, an integral part of the marine food chain, is the richest source of omega-3 [21,33]. Therefore, marine fatty fish, especially those that live in colder environments (e.g., herring, sardine, mackerel, salmon), represent a major source of omega-3 for human consumption. Oils from these marine sources provide omega-3 primarily in the chemical form of TG and typically contain ~12 % DHA and ~18 % EPA bound in the *sn*-2 position of TG molecules; however, these oils can be further processed, using an EE intermediate, to obtain re-esterified TGs (rTG) in which DHA or EPA can also be esterified in the *sn*-1/3 position [34]. In addition to TG-based marine oils or EE products, oils from Antarctic krill (*Euphausia superba*) and from the copepod *Calanus finmarchicus*, which contain EPA and DHA in the chemical forms of PL and WE, respectively, can also be an alternative source of omega-3 [31,32]. An overview of the most important sources of omega-3 in

which EPA and DHA are bound in different lipid classes, including TG, EE, WE and PL, is given in Figure 1. Existing data on the composition of marine oils in terms of the lipid classes contained and the distribution of DHA and EPA in these lipid types are limited [32,35]. In this regard, our recent LC-MS-based lipidomic analysis revealed five major lipid classes, i.e., diacylglycerols (DG), free FA, phosphatidylcholine (PC), TG and WE, which are present in varying amounts in marine oils of different origins (Table 1). As expected, TG-based oils (e.g. herring oil and the rTG product) contained largely TG molecules (~80 %), whereas WEs are the lipid class that predominates (~80 %) in Calanus oil; in contrast, the relative content of PC as the major PL species contained in krill oil is only ~50 % and other types of lipids, such as TG, contribute significantly (Table 1).

Regarding the distribution of omega-3 in the main lipid classes of the selected marine oils (Table 1, middle and lower part), in the rTG concentrate enriched with DHA, TG and DG are the main species that contained DHA (up to 85 %) and EPA (up to 45 %); however, herring oil, as an example of a natural fish oil, shows a more even distribution of omega-3 in all major lipid classes except WE. Calanus oil showed a significant representation of DHA and EPA in all five major lipid classes, but the biological significance of such a distribution is probably low due to the predominance of the WE class in this type of oil. In krill oil, a PL-based omega-3 concentrate representative, PC, DG and free FAs represent those lipid classes enriched primarily in EPA and less in DHA (Table 1, middle and lower part). Thus, in addition to the composition and position of omega-3 in a given lipid molecule, the distribution of omega-3 into different types of lipid classes likely affects bioavailability, especially when omega-3 are supplemented through complex products such as krill oil.

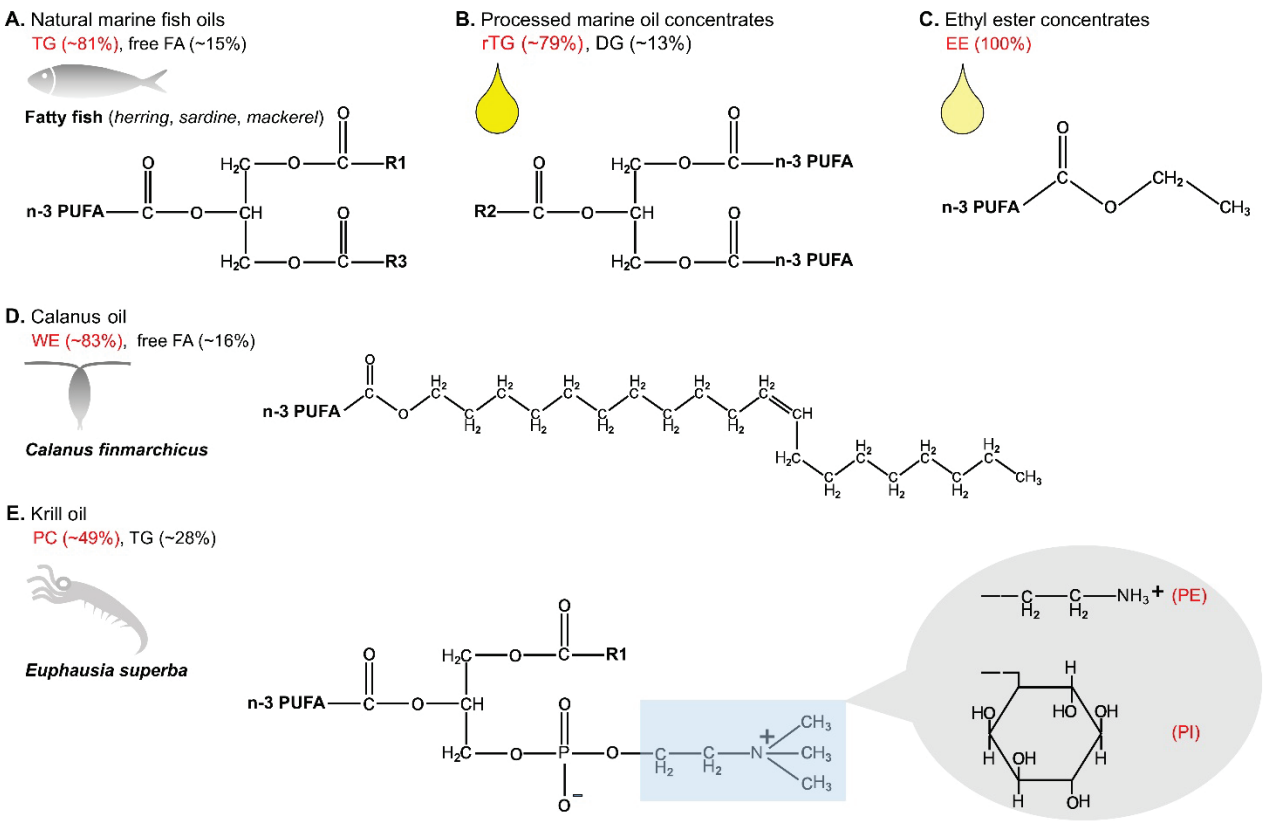

Fig. 1. Overview of marine sources of omega-3 with EPA and DHA bound in different lipid classes, including a schematic representation of the chemical formula of the main lipid class present in the respective product. Information on the relative abundance of the main lipid classes in the marine oils listed in A-E is based on the data given in Table 1. In the case of Calanus oil (D), a representative wax ester with fatty alcohol 20:1*n*-9 is shown, which together with 22:1*n*-11 are the main fatty alcohols contained in Calanus oil [32]. Krill oil (E) contains primarily phosphatidylcholine (PC) and triacylglycerols (TG), while other lipid classes including different types of phospholipids (e.g.; PE, PI,…) are only marginally present. DG, diacylglycerols; EE, ethyl esters; FA, fatty acids; PC, phosphatidylcholine; PE, phosphatidylethanolamine; PI, phosphatidylinositol; PUFA, polyunsaturated fatty acids; R1(2,3), other types of fatty acids in the *sn*-1, 2 and 3 position, respectively; TG, triacylglycerols; rTG, re-esterified triacylglycerols; WE, wax esters.

Table 1. Main lipid classes and their omega-3 occupancy in selected oils of marine origin

Lipid class composition distribution				
Lipid class (%)	Herring oil	Krill oil	Calanus oil	Epax 1050
DG	1.1	3.5	0.1	13.0
FA	15.0	4.9	15.5	1.7
PC	0.1	48.7	0.1	6.5
TG	80.5	28.3	0.8	78.7
WE	0.0	0.0	82.5	0.0
Distribution of omega-3 fatty acids in different lipid classes				
DHA (22:6n-3)				
DG	24.9	20.0	22.0	73.0
FA	35.8	24.2	34.2	25.4
PC	8.9	24.9	56.2	15.1
TG	13.6	5.3	19.3	85.4
WE	0.0	0.0	40.2	0.0
EPA (20:5n-3)				
DG	45.8	82.1	74.9	44.1
FA	10.3	35.2	28.7	13.8
PC	20.6	51.2	40.3	18.9
TG	17.4	12.9	34.5	44.8
WE	0.0	0.0	58.6	0.0

The results are based on LC-MS analysis of the oils listed. Relative content of the main lipid classes in oils (upper part) and the percentage of species containing DHA or EPA in the respective lipid fractions. The distribution of omega-3 (i.e., DHA and EPA) in lipid classes is determined by the cumulative sum of all distinct lipid species within a given lipid class, including DHA or EPA. These species may consist of identical omega-3 within their molecular structure (e.g., PC 22:6_22:6, TAG 22:6_22:6_22:6) or may be combined with other FA (e.g., PC 14:0_22:6, TAG 14:0_16:0_22:6). Abbreviations: DG, diacylglycerols; Epax 1050, concentrate of re-esterified triacylglycerols enriched with DHA from sources other than tuna (Epax Norway AS); FA, fatty acids; PC, phosphatidylcholines; TG, triacylglycerols; WE, wax esters.

Comparative studies using omega-3 concentrates based on different lipid classes

Original articles comparing the effects of omega-3 supplementation *via* different lipid classes on hepatic steatosis in MASLD were retrieved from the PubMed database using different keyword strings. While several existing review articles have summarized findings regarding the efficacy of omega-3 against MASLD [25,30], they do not specifically focus on studies using different lipid classes for omega-3 supplementation analyzed simultaneously in a single study. Our current review therefore focuses on comparative studies that included two or more lipid classes used for omega-3 administration, under conditions associated with weight gain and/or obesity. In addition, source articles were selected from those published in the last 15 years. We compiled specific search strings that combined keywords relevant to the focus of our review. These keywords thus encompassed the different ways in which (i) the disease of interest is described in the literature (e.g., NAFLD, MASLD, MAFLD), (ii) the primary phenotype (e.g., hepatic or liver steatosis, liver triacylglycerol(s)), and also (iii) the comparative nature of the retrieved studies involving different sources of omega-3 (e.g., fish oil, krill oil, Calanus oil) and different classes of lipids used for their supplementation (e.g., triacylglycerols, ethyl esters, phospholipids, wax esters). Regarding the retrieved studies, most of them were performed in rodents (38 in total), mainly in laboratory mice, but only 21 of these studies were included in the review because they fulfilled the condition where the liver phenotype is studied in the context of weight gain or obesity. In contrast, only five human studies that reported MASLD-related metabolic phenotypes were included in the review because comparative studies involving omega-3 supplementation *via* different lipid classes and direct quantification of liver fat content are lacking. In the reported studies, four lipid

classes, including TG, PL, WE and EE, were used for omega-3 supplementation, with the vast majority of studies comparing TG and PL forms of omega-3.

Based on a detailed examination of studies obtained in rodents, omega-3 PL from various marine sources (e.g., krill oil, herring meal extract, squid roe oil, algae oil) appear to be more effective in reducing liver fat compared to fish sources rich in omega-3 TG (see Table 2 for details). This was observed in both the preventive and reversal (i.e., treatment) experimental designs (e.g., [36-38]), using different types of high-fat diets (HFD; either based on corn oil or lard) and experimental conditions (e.g., 22 °C vs. 30 °C). Also, in KK-Ay mice, a genetic model of obesity and hyperglycemia, Sugimoto *et al.* [39] demonstrated greater efficacy of PL-rich scallop oil in reducing liver TG content than fish oil supplementation. Moreover, regarding different sources of omega-3 PL, a recent study on mice fed an HFD/high-cholesterol diet suggests that krill oil may have greater antisteatotic effects than squid oil extract [40]. Similarly, Wang *et al.* [41] show that omega-3 PL derived from Silver carp head is superior to Salmon head extract in reducing liver fat, suggesting that some other components of omega-3 PL concentrates are likely to contribute to antisteatotic effects in the liver ([37,38] and reviewed in [31]). On the other hand, there are studies where no significant reduction in liver fat was observed after administration of either form of omega-3 supplementation [42] or, alternatively, where there was a stronger effect when omega-3 was administered in the TG form compared to the PL form [43,44]. However, in a study by Botelho *et al.* [43], fish oil used for omega-3 supplementation in the form of TG contained both EPA and DHA, while algae oil as a source of omega-3 PLs was completely devoid of EPA. This certainly had a negative impact on the efficacy of omega-3 PL supplementation, which was reflected in significantly lower EPA content in the liver after algae oil supplementation compared to other forms of supplementation. Botelho *et al.* [43] and Gui *et al.* [44], moreover, did not accurately quantify liver fat after omega-3 supplementation (only histological images of the liver are presented), making it difficult to draw firm conclusions from these studies.

In terms of reducing liver TG content, other lipid classes used for omega-3 supplementation, such as highly purified EE or WE, have rarely been tested. Therefore, assessing their relative efficacies from the available studies is impossible, especially when compared to more commonly used classes such as TG or PL. One short-term prevention-type study compared the effects of DHA-rich omega-3 formulations based on EE, PL, free FA and TG forms in BALBc mice [45]; interestingly, at lower dietary fat levels (5 %), EE, PL and TG form reduced liver fat, but at higher dietary fat levels (22.5 %), all were ineffective. On the other hand, compared with omega-3 supplemented in the form of EE, Calanus oil-derived WE exhibited potent antisteatotic capabilities with respect to liver fat content while increasing adiponectin expression in AT [46].

Only five comparative human studies were found, where the effects of omega-3 supplementations on MASLD-related parameters (i.e., not directly on liver fat accumulation) were examined (Table 3). Compared to placebo-treated subjects, there was no difference in the effects of omega-3 supplemented for 14 weeks as PL (algae oil) or TG (fish oil) on reducing serum TG in statin-treated hypertriglyceridemic patients [60], and a similar effect was found in a 2-week crossover study using PLs from herring roe vs. fish oil in patients with hypertriglyceridemia [61]. When comparing omega-3 administered in the TG form with their EE form (i.e., using Omacor), a similar degree of reduction in plasma TG was observed with both forms of supplementation [62]. However, Schuchardt *et al.* [17,63] reported a reduction in serum TG in statin-treated dyslipidemic subjects who were given omega-3 in the form of rTG, whereas omega-3 EE had no effect. Comparisons of seal and tuna oils in subjects with hypertriglyceridemia suggest better effectiveness of tuna oil in reducing plasma TG [64]; however, the results are difficult to interpret due to the higher amounts of EPA and DHA supplemented *via* tuna oil.

In summary, based on an analysis of studies primarily in rodents, it can be concluded that in the context of obesity-related MASLD, PL-based omega-3 supplementation has stronger effects in terms of reducing liver fat compared with other lipid classes used for supplementation, with the possible exception of WE, whose relative efficacy to the PL form has not been tested in a comparative study. The absence of comparative human studies on the effects of omega-3 supplementation on liver fat precludes any conclusions regarding the greater efficacy of omega-3 PLs found in rodent studies. On the other hand, the very limited number of studies examining the effects of omega-3 supplementation on MASLD-related phenotypes, such as circulating TG levels, suggested similar efficacy of PL vs. TG or TG vs. EE.

Table 2. Comparative rodent studies on MASLD using omega-3 supplemented in different lipid classes

Omega-3 concentrates	EPA/DHA dose	Species	Age[a] (weeks)	Sex	Study design	Primary outcome (Liver TG/MASLD)	MASLD-related phenotypes	Reference
ω-3PL vs. ω-3TG	ω-3PL (Herring meal extract) EPA: 5.66 DHA: 24.34 ω-3TG (rTG) EPA: 6.78 DHA: 23.22 (g/kg diet)	Mouse C57BL/6J	12	Male	<u>Prevention</u> (9 weeks) Groups: CON HFD HFD + ω-3PL HFD + ω-3TG	Liver TG: ω-3PL ↓ (40% of HFD) ω-3TG ↓ (20% of HFD) (ω-3PL > ω-3TG)	Plasma TG: ↓ω-3PL Plasma NEFA: ↓ω-3PL	Rossmeisl *et al.*, 2012 [36]
		Mouse C57BL/6J	28	Male	<u>Reversal</u> HFD + metformin (16 weeks) then Treatments (9 weeks): HFD + metformin + ω-3PL HFD + metformin + ω-3TG	Liver TG: ω-3PL ↓ (77% of HFD) ω-3TG ↓ (52% of HFD) (ω-3PL > ω-3TG)	Weight gain: ↓↓ω-3PL ↓ω-3TG FBG: ↓↓ω-3PL ↓ω-3TG Adiponectin: ↑ω-3PL Plasma Insulin: ↓ω-3PL Plasma TG: ↓ω-3PL ↓ω-3TG Plasma TC: ↓ω-3PL ↓ω-3TG Plasma NEFA: ↓ω-3PL ↓ω-3TG	
	ω-3PL (Krill oil) EPA: 9.3 DHA: 4.1 ω-3TG (Fish oil) EPA: 17.5 DHA: 12.5 (g/kg diet)	Mouse C57BL/6J	9-10	Male	<u>Prevention</u> (6 weeks) Groups: HFD HFD + ω-3PL HFD + ω-3TG	Liver TG: ω-3PL ↑ (150% of HFD) ω-3TG ↑ (400% of HFD)	Body weight: ↑ω-3PL Plasma TG: ↓ ω-3PL ↓↓ω-3TG Plasma TC: ↓ω-3PL ↓↓ω-3TG Plasma NEFA: ↓ω-3PL ↓↓ω-3TG HDL: ↓↓ω-3TG Liver TC: ↑ω-3PL ↑ω-3TG	Tillander *et al.*, 2014 [48]
	ω-3PL (Krill oil) EPA: N/A DHA: N/A ω-3TG (Fish oil) EPA: N/A DHA: N/A (g/kg diet)	Mouse C57BL/6J	9-10	Male	<u>Prevention</u> (6 weeks) Groups: HFD HFD + ω-3PL HFD + ω-3TG	Liver TG: ω-3PL ↑ (200% of HFD) ω-3TG ↑ (196% of HFD)	Liver DG: ↓ω-3PL	Skorve *et al.*, 2015 [49]

	ω-3PL (Microalgae oil) EPA: N/A DHA: N/A ω-3TG (Fish oil) EPA: N/A DHA: N/A (g/kg diet)	Mouse C57BL/6J	14	Male	<u>Reversal</u> CON HFD (8 weeks) then Treatments (8 weeks): HFD + ω-3PL HFD + ω-3TG	Liver TG: ω-3PL ↓ (62% of HFD) ω-3TG ↓ (50% of HFD) (ω-3PL > ω-3TG)	Weight gain: ↓ω-3PL Serum TG: ↓↓ω-3PL↓ω-3TG Serum TC: ↓ω-3PL ↓↓ω-3TG	Yook *et al*., 2015 [50]
	ω-3PL-l (Algae oil-lower purity) EPA: 3.0 DHA: 97.0 ω-3PL-h (Algae oil-higher purity) EPA: 1.1 DHA: 98.1 ω-3TG (Fish oil) EPA: 52.0 DHA: 45.0 (mg/kg body weight by oral gavage)	Mouse C57BL/6J	3-4	Male	<u>Prevention</u> (16 weeks) Groups: CON HFD HFD + ω-3PL-l HFD + ω-3PL-h HFD + ω-3TG	Liver lipid droplets (HFD): ω-3PL-l (↓) ω-3PL-h (↓) ω-3TG (↓)	Weight gain: ↓ω-3PL-l ↓ω-3PL-h Serum TG: ↓ω-3PL-l ↓ω-3PL-h ↓ω-3TG Serum TC: ↓ω-3PL-l ↓ω-3PL-h ↓ω-3TG	Yu *et al*., 2017 [51]
	DHA (Algal oil) EPA: 13 DHA: 738 DHA/EPA-A [2:1 (Fish oil + Algal oil)] EPA: 252 DHA: 469 DHA/EPA-B [1:1 (Fish oil + Algal oil)] EPA: 358 DHA: 346	Mouse C57BL/6J	5	Male	<u>Prevention</u> (11 weeks) Groups: CON HFD HFD + DHA HFD + DHA/EPA-A HFD + DHA/EPA-B HFD + DHA/EPA-C	Liver TG: DHA ↓ (56% of HFD) DHA/EPA-A ↓ (31% of HFD) DHA/EPA-B ↓ (27% of HFD) DHA/EPA-C ↓ (27% of HFD) Liver lipid droplets (HFD): DHA (↓) DHA/EPA-A (↓↓) DHA/EPA-B (↓↓)	Serum TG: ↓↓DHA ↓DHA/EPA-A ↓DHA/EPA-B ↓DHA/EPA-C Serum TC: ↓↓DHA ↓DHA/EPA-A ↓DHA/EPA-B ↓↓DHA/EPA-C Serum LDL.: ↓DHA ↓DHA/EPA-A ↓DHA/EPA-B ↓↓DHA/EPA-C Serum HDL: ↑DHA ↑DHA/EPA-A ↑DHA/EPA-B ↑↑DHA/EPA-C	Shang *et al*., 2017 [52]

	DHA/EPA-C [1:2 (Fish oil + Algal oil)] EPA: 460 DHA: 244 (mg/kg body weight by oral gavage)					DHA/EPA-C (↓↓)	Liver TC: ↓↓DHA ↓DHA/EPA-A ↓DHA/EPA-B ↓DHA/EPA-C	
	ω-3PL (Algae oil) DHA + EPA: 4.5 ω-3TG (Fish oil) DHA + EPA: 4.5 (% of total energy intake)	Mouse C57BL/6J	7	Male	<u>Prevention</u> (12 weeks) Groups: CON HFD HFD + ω-3PL HFD + ω-3TG	Liver lipid droplets (HFD): ω-3PL (↓) ω-3TG (↓↓) (ω-3TG > ω-3PL)	Body weight: ↓ω-3PL ↓ω-3TG Serum TG: ↓ω-3PL ↓↓ω-3TG Serum TC: ↓ω-3PL ↓ω-3TG Serum LDL-C: ↓ω-3PL ↓ω-3TG Serum AST: ↓ω-3PL ↓ω-3TG Serum ALT: ↓ω-3PL ↓ω-3TG	Gui *et al*., 2019 [44]
	SCO-PL (Scallop oil phospholipid fraction) EPA: 2.6 DHA: 2.1 SCO-TG (Scallop oil triglyceride fraction) EPA: 2.6 DHA: 2.1 (g/kg diet)	Mouse C57BL/6J	4	Male	<u>Prevention</u> (4 weeks) Groups: HFD + SOY-TG HFD + SOY-PL HFD + SCO-PL HFD + SCO-TG	Liver TG: SCO-TG ↓ (17% of SOY-TG) SCO-PL ≈ SOY-PL (ω-3TG > ω-3PL)	Liver weight: ↓ SCO-PL Serum TG: ↓ SCO-PL Serum TC: ↓↓SCO-PL Serum HDL: ↓ SCO-PL	Sugimoto *et al*., 2021 [53]
	ω-3PL-K (Krill oil) EPA: 28 DHA: 13 ω-3PL-S (Squid roe oil) EPA: 28 DHA: 11	Mouse C57BL/6J	16	Male	<u>Reversal</u> CON HFD (9 weeks) then Treatments (9 weeks): HFD + ω-3PL-K HFD + ω-3PL-S HFD + ω-3TG	Liver TG: ω-3PL-K ↓ (23% of HFD) ω-3PL-S ↓ (21% of HFD) ω-3TG ↓ (21% of HFD) Liver lipid droplets (HFD): ω-3PL-K (↓↓↓) ω-3PL-S (↓↓) ω-3TG (↓)	Liver weight: ↓ω-3PL-K ↓ω-3PL-S ↓ω-3TG Liver TC: ↓↓ω-3PL-K ↓ω-3PL-S ↓ω-3TG HOMA-IR: ↓ω-3PL-K ↓ω-3PL-S ↓ω-3TG Serum TG: ↓ω-3PL-K	Chen *et al*., 2024 [40]

	ω-3TG (Fish oil) EPA: 22 DHA: 15 (mg per day by oral gavage)					(ω-3PL > ω-3TG)	↓ω-3PL-S ↓ω-3TG Serum TC: ↓ω-3PL-K ↓ω-3PL-S ↓ω-3TG Serum ALT: ↓↓ω-3PL-K ↓ω-3PL-S ↓ω-3TG Serum AST: ↓↓ω-3PL-K ↓ω-3PL-S ↓ω-3TG	
	ω-3PL (Microalgae oil) EPA: 1.08 DHA: 99.2 ω-3TG (Fish oil) EPA: 51.92 DHA: 44.98 (mg/kg body weight by oral gavage)	Mouse C57BL/6J	20	Male	<u>Reversal</u> CON HFD (8 weeks) then Treatments (16 weeks): HFD + ω-3PL HFD + ω-3TG	Liver lipid droplets (HFD): ω-3PL (↓↓) ω-3TG (↓) (ω-3PL > ω-3TG)	Body weight: ↓ω-3PL ↓ω-3TG Blood glucose: ↓ω-3PL ↓ω-3TG Serum TG: ↓↓ω-3PL ↓ω-3TG	Ran *et al*., 2022 [54]
	ω-3PL (Krill oil) EPA: 21 DHA: 12 ω-3TG (rTG) EPA: 8 DHA: 25 (g/kg diet)	Mouse C57BL/6N	12	Male	<u>Prevention</u> (8 weeks) Groups: HFD HFD + ω-3PL HFD + ω-3TG	Liver TG: ω-3PL ↓ (60% of HFD) ω-3TG ≈ HFD (ω-3PL > ω-3TG)	Body weight: ↓ω-3PL ↑ω-3TG Liver weight: ↓ω-3PL Plasma insulin: ↓ω-3PL Plasma TG: ↑ω-3PL Plasma TC: ↓ω-3PL ↓ω-3TG Plasma NEFA: ↑ω-3PL	Kroupova *et al*., 2020 [55]
	ω-3PL (Krill oil) EPA+DHA: 25 ω-3TG (rTG) EPA+DHA: 25 (g/kg diet)	Mouse C57BL/6N	10	Male	<u>Prevention</u> (8 weeks) Groups: HFD HFD + ω-3PL HFD + ω-3TG	Liver TG: ω-3PL ↓ (68% of HFD) ω-3TG ↓ (32% of HFD) (ω-3PL > ω-3TG)	Weight gain: ↓ω-3PL HOMA-IR: ↓↓ω-3PL ↓ω-3TG Adiponectin: ↑ω-3PL	Rossmeisl *et al*., 2020 [37]

	ω-3PL (Krill oil) EPA: 19.9 DHA: 12.1 ω-3TG (rTG) EPA: 19.0 DHA: 12.2 (g/kg diet)	Mouse C57BL/6N	18	Male	<u>Reversal</u> HFD (8 weeks) then Treatments (16 weeks): HFD + ω-3PL HFD + ω-3TG	Liver TG: ω-3PL ↓ (50% of HFD) ω-3TG ↓ (15% of HFD) (ω-3PL > ω-3TG)	Body weight: ↓ω-3PL ↓ω-3TG Blood glucose: ↓↓ω-3PL Plasma insulin: ↑ω-3TG Plasma TC: ↓ω-3PL Plasma AST: ↓ω-3PL Plasma ALT: ↓ω-3PL ↓↓ω-3TG Plasma adiponectin: ↑↑ω-3PL ↑ω-3TG	Sistilli *et al.*, 2021 [38]
	ω-3PL (Algae oil) EPA: 0.0 DHA: 0.77 ω-3TG (Fish oil) EPA: 0.44 DHA: 0.25 (mg per day by oral gavage)	Mouse LDLr KO C57BL/6	16 - 18	Male	<u>Prevention</u> (4 weeks) Groups: HFD HFD + ω-3PL HFD + ω-3TG	Liver lipid droplets (HFD): ω-3PL (≈) ω-3TG (↓↓) (ω-3TG > ω-3PL)	Weight gain: ↓ω-3TG Plasma TG: ↓↓ω-3PL ↓ω-3TG Plasma TC: ↓ω-3PL ↓↓ω-3TG	Botelho *et al.*, 2013 [43]
	ω-3PL (Scallop oil-Mutsu) EPA: 25.9 DHA: 4.1 ω-3PL (Scallop oil-Uchiura) EPA: 17.5 DHA: 9.8 ω-3TG (Fish oil) EPA: 4.3 DHA: 19.6 (g/kg diet)	Mouse KK-A^{y}	5	Male	<u>Prevention</u> (7 weeks) Groups: HFD HFD + ω-3PL(SCO-M) HFD + ω-3PL (SCO-U) HFD + ω-3TG	Liver TG: ω-3PL (SCO-M) ↓ (12% of HFD) ω-3PL (SCO-U) ↓ (20% of HFD) ω-3TG ↑ (22% of HFD) (ω-3PL > ω-3TG)	Serum TG: ↓ω-3PL (SCO-M) ↓ω-3PL (SCO-U) ↓↓ω-3TG Serum TC: ↓↓ω-3PL (SCO-M) ↓ω-3PL (SCO-U) ↓ω-3TG	Sugimoto *et al.*, 2020 [39]
	ω-3PL (Scallop oil) EPA: 21.4 DHA: 7.6 ω-3PL (Krill oil)	Mouse KK-A^{y}	5	Male	<u>Prevention</u> (6 weeks) Groups: CON CON + ω-3PL (SCO) CON + ω-3PL (KO) CON + ω-3TG	Liver TG: ω-3PL (SCO) ≈HFD ω-3PL (KO) ↑ (312% of HFD) ω-3TG ≈HFD	Serum TG: ↓↓ω-3PL (SCO) ↓↓ω-3PL (KO) ↓ω-3TG Serum TC: ↓ω-3PL (SCO) ↑ω-3PL (KO) Serum HDL: ↓↓ω-3PL (SCO) ↑ω-3PL (KO)	Sugimoto *et al.*, 2021 [56]

	EPA: 11.8 DHA: 8.4 ω-3TG (Fish oil) EPA: 20.7 DHA: 8.8 (g/kg diet)						↓ω-3TG Liver weight: ↑ω-3PL (KO)	
	ω-3PL (Krill oil) EPA: N/A DHA: N/A ω-3TG (Fish oil) EPA: N/A DHA: N/A (oral gavage)	Mouse ICR	10	Male	<u>Prevention</u> (12 weeks) Groups: CON HFD HFD + ω-3PL HFD + ω-3TG	N/A	Body weight: ↓ω-3PL ↓ω-3TG Serum TG: ↓ω-3PL Serum TC: ↓↓ω-3PL ↓ω-3TG Serum LDL: ↓↓ω-3PL ↓ω-3TG Serum HDL: ↑↑ω-3PL ↑ω-3TG	Cui *et al*., 2017 [57]
	ω-3PL (Krill oil) EPA: 3.0 DHA: 1.7 ω-3TG (Fish oil) EPA: 2.0 DHA: 2.9 (g/kg diet)	Wistar rats		Male	<u>Prevention</u> (6 weeks) Groups: HFD HFD + ω-3PL HFD + ω-3TG	Liver TG: ω-3PL ↓ (22% of HFD) ω-3TG ↓ (10% of HFD) (ω-3PL > ω-3TG)	Plasma TG: ↓ω-3PL ↓ω-3TG Plasma TC: ↓ω-3PL ↓ω-3TG Liver TC: ↓↓ω-3PL ↓ω-3TG	Ferramosca *et al.*, 2012 [47]
	ω-3PL (Squid meal) EPA: 6.9 DHA: 23.5 ω-3TG (Fish oil) EPA: 2.1 DHA: 7.7 (g/kg diet)	Wistar rats	4	Male	<u>Prevention</u> (6 weeks) Groups: CON + 7% SOY CON + 7% SOY + ω-3PH-PL CON + 7% SOY+ ω-3TG	Liver TG: ω-3PL ↓ (22% of CON) ω-3TG ↓ (35% of CON) (ω-3TG > ω-3PL)	Serum TG: ↓↓ω-3PL ↓ω-3TG Serum AST: ↓↓ω-3PL ↓ω-3TG Serum ALT: ↓↓ω-3PL ↓ω-3TG	Hosomi *et al.*, 2019 [58]
	ω-3PL (Krill oil) EPA: 3.0 DHA: 1.8	Wistar rats	8-10	Male	<u>Prevention</u> (8 weeks) Groups: CON	Liver TG: ω-3PL ≈ HFD ω-3TG ≈ HFD	Weight gain: ↓↓ω-3PL ↓ω-3TG Serum TG: ↓↓ω-3PL ↓ω-3TG Serum TC: ↓ω-3PL ↓ω-3TG	Aydin Cil *et al*., 2021 [42]

	ω-3TG (Fish oil) EPA: 3.1 DHA: 2.9 (g/kg diet)				HFD HFD+ ω-3PL HFD+ ω-3TG			
	ω-3PL (Krill oil) EPA: 13.2 DHA: 4.6 ω-3TG-M (Menhaden oil) EPA: 5.5 DHA: 2.0 ω-3TG-S (Salmon oil) EPA: 10.0 DHA: 1.9 ω-3TG-T (Tuna oil) EPA: 2.6 DHA: 2.9 (g/kg diet)	Sprague-Dawley rats	4	Female	Prevention (8 weeks) Groups: HFD HFD + ω-3PL HFD + ω-3TG-M HFD + ω-3TG-S HFD + ω-3TG-T	N/A	Weight gain: ↑ω-3PL ↑ ↑ω-3TG-M ↑ω-3TG-S ↑↑ω-3TG-T Liver weight: ↑ω-3TG-S ↑ω-3TG-T	Tou *et al.*, 2011 [59]
Salmon PL vs. Silver carp PL	ω-3PL-S (Salmon head extract) EPA: N/A DHA: N/A ω-3PL-SC (Silver carp head extract) EPA: N/A DHA: N/A (g/kg diet)	Mouse C57BL/6J	5	Male	Prevention (9 weeks) Groups: CON HFD HFD + ω-3PL-S HFD + ω-3PL-SC	Liver TG: ω-3PL-S ≈ HFD ω-3PL-SC ↓ (56% of HFD) Liver lipid droplets (HFD): ω-3PL-S (↓) ω-3PL-SC (↓) (ω-3PL-SC > ω-3PL-S)	Weight gain: ↓ω-3PL-S ↓↓ω-3PL-SC Serum TG: ↓ω-3PL-S ↓↓ω-3PL-SC Serum TC: ↓ω-3PL-S ↓↓ω-3PL-SC Liver TC: ↓ω-3PL-S ↓↓ω-3PL-SC	Wang *et al.*, 2023 [41]
ω-3PL vs. ω-3EE vs. ω-3FFA vs. ω-3TG	ω-3PL (Squid roe oil) EPA: 1.95 DHA: 5.13 ω-3EE EPA: 1.76 DHA: 5.13	Mouse BALBc	N/A	Male	Prevention (1 week) Groups: LFD LFD + ω-3PL LFD + ω-3EE LFD + ω-3FFA LFD + ω-3TG	Liver TG: ω-3PL ↓ (53% of LFD) ω-3EE ↓ (64% of LFD) ω-3 FFA ↓(34% of LFD) ω-3TG ↓ (45% of LFD) ω-3PL ≈ HFD ω-3EE ≈ HFD	LFD: Serum TG: ↓ω-3PL ↓ω-3EE ↑ω-3FFA ↑ω-3TG Serum TC: ↓↓ω-3PL ↓↓ω-3EE ↓ω-3FFA ↓ω-3TG Liver TC: ↓ω-3PL ↓↓ω-3EE ↓ω-3FFA ↓↓ω-3TG HFD:	Tang *et al.*, 2012 [45]

	ω-3FFA EPA: 1.86 DHA: 5.13 ω-3TG (Fish and algae oil mixture) EPA: 1.94 DHA: 5.13 (g/kg diet)				HFD HFD + ω-3PL HFD + ω-3EE HFD + ω-3FFA HFD + ω-3TG	ω-3FFA ≈ HFD ω-3TG ≈ HFD	Serum TG: ↑ω-3PL ↓↓ω-3EE ↑ω-3FFA Liver TC: ↓ω-3PL ↓ω-3EE	
ω-3WE vs. ω-3EE	ω-3WE (Calanus oil-derived) EPA: 3.5 DHA: 1.3 ω-3EE (Omacor) EPA+DHA: 4.7 (g/kg diet)	Mouse C57BL/6J	12	Male	<u>Reversal</u> HFD (7 weeks) then Treatments (20 weeks): HFD + ω-3WE HFD + ω-3EE	Liver TG: ω-3WE ↓ (55% of HFD) ω-3EE ≈ HFD (ω-3WE > ω-3EE)	Body weight: ↓ω-3WE AT adiponectin: ↑ω-3WE Plasma glucose: ↓ω-3WE ↓ω-3EE Plasma insulin: ↓↓ω-3WE ↓ω-3EE Plasma NEFA: ↓↓ω-3WE ↓ω-3EE	Hoper *et al.*, 2014 [46]

Only studies (n = 24) published in the last 15 years were included in the table. The "MASLD-related phenotypes" section contains only information on parameters differentially affected by the lipid classes used for omega-3 supplementation in a given study. The direction of effect of a given omega-3 supplementation compared to the respective control: ↑, increase; ↓, decrease; ≈, no effect (the size of the effect is expressed by the number of arrows). [a]Age at the beginning of omega-3 interventions. Abbreviations: ALT, alanine transaminase; AST, aspartate transaminase; CON, control (usually low-fat) diet; DG, diacylglycerols; DHA, docosahexaenoic acid; EE, ethyl esters; EPA, eicosapentaenoic acid; FFA, free fatty acids; HDL, high-density lipoprotein; HFD, high-fat diet; HOMA-IR, homeostatic model assessment for insulin resistance; LDL, low-density lipoprotein; LDLr KO, Low-density lipoprotein receptor knock-out mice; LFD, low fat diet; N/A, not applicable or not assessed; NEFA, non-esterified fatty acids; PL, phospholipids; rTG, re-esterified triacylglycerols; TC, total cholesterol; TG, triacylglycerols; WE, wax esters.

Table 3. Comparative human studies on MASLD using omega-3 supplemented in different lipid classes.

Omega-3 concentrates	EPA/DHA dose	Target	Age of subjects (years)	Study design	MASLD-related phenotypes	Reference
ω-3PL vs. ω-3TG	ω-3PL (Algae oil) EPA: 2400 DHA: 6480 ω-3TG (Fish oil) EPA: 1400 DHA: 2000 (mg per day)	Hypertriglyceridemic statin-treated subjects	18 - 79	14 weeks Double-blind, randomized, parallel trial	Serum TG: ↓ ω-3PL (to placebo) ↓ ω-3TG (to placebo)	Maki *et al.*, 2014 [60]
	EPA/DHA-PL (Herring roe + fish oil mixture) EPA: 628 DHA: 1810 EPA/DHA-TG (Fish oil) EPA: 1843 DHA: 178 (mg per day)	Mild hypertriglyceridemic subjects	43 - 48	2 weeks Randomized, single-blind, crossover trial (4 weeks washout)	Serum TG: ↓ EPA/DHA-PL (to baseline) ↓ EPA/DHA-TG (to baseline) Serum TC: ↓ EPA/DHA-PL (to baseline) ↓ EPA/DHA-TG (to baseline) Serum LDL: ↓ EPA/DHA-PL (to baseline) ↓ EPA/DHA-TG (to baseline)	Cook *et al.*, 2016 [61]
Seal Oil vs. Fish Oil	EPA/DHA-Seal oil EPA: 340 DHA: 450 EPA/DHA-Fish oil EPA: 210 DHA: 810 (mg per day)	Hypertriglyceridemic subjects	42 - 73	6 weeks Double-blind randomized, parallel, placebo-controlled trial	Plasma TG: ↓ EPA/DHA-Fish oil (to placebo) Systolic BP: ↓ EPA/DHA- Fish oil (to placebo) Mean arterial BP: ↓ EPA/DHA- Fish oil (to placebo)	Meyer *et al.*, 2009 [64]
ω-3rTG vs.	ω-3rTG (rTG) EPA: 1008	Dyslipidemic statin-treated subjects	30 - 75	6 months Double-blind, placebo-	Serum TG: ↓ ω-3rTG (to placebo)	Schuchardt *et al.*,

ω-3EE	DHA: 672 ω-3EE (Ethyl esters) EPA: 1008 DHA: 672 (mg per day)			controlled trial rTG vs. EE		2011 & 2014 [69,63]
	ω-3AG (rTG) EPA: 767 DHA: 1930 ω-3EE (Ethyl esters) EPA: 1702 DHA: 1382 (mg per day)	Hypertriglyceridemic subjects	≥ 18	8 ± 2 weeks Double-blind, randomized, placebo-controlled trial	Plasma TG/HDL: ↓ ω-3AG (to placebo) ↓ ω-3EE (to placebo) Plasma non-HDL/HDL: ↓ ω-3AG (to placebo)	Hedengran *et al.*, 2015 [62]

Only studies (n = 5) published in the last 15 years were included in the table. The primary outcome, liver fat content, was not assessed in these studies, while the section "MASLD-related phenotypes" contains only information on parameters differentially affected by the lipid classes used for omega-3 supplementation in a given study. Direction of effect of a given omega-3 supplementation compared to the respective control: ↑, increase; ↓, decrease; ≈, no effect. Abbreviations: AG: acylglycerols; BP, blood pressure; DHA, docosahexaenoic acid; EPA, eicosapentaenoic acid; HDL, high-density lipoprotein; LDL, low-density lipoprotein; PL, phospholipids; rTG, re-esterified triacylglycerols; TC, total cholesterol; TG, triacylglycerols.

Bioavailability and the mechanism of action of omega-3 in MASLD

The bioavailability of omega-3 from the diet, i.e., the rate of absorption and transport of EPA, DHA and other omega-3 into the circulation and/or site of action, is an important factor in determining the biological effects of these FA. The chemical binding form may influence the bioavailability of omega-3. However, other factors, such as the matrix effect, the galenic form, i.e., the method of preparing and compounding medicinal products, as well as inter-individual differences or age, also contribute to the final effect (discussed in detail in [34,65]). Interestingly, the liver already contains significant amounts of DHA in tissue PL under conditions when no extra EPA and DHA is supplemented *via* the diet; however, administration of varying amounts of omega-3 in the form of rTG (as part of HFD) resulted in saturable incorporation of DHA and, to a lesser extent, EPA into the hepatic PL fraction in C57BL/6J mice [65]. Regarding the assessment of omega-3 bioavailability, it should be noted that the gold standard for assessing omega-3 status in the body is the omega-3 index, i.e., the EPA+DHA content of erythrocytes expressed as a percentage of all FA analyzed [55,66]; however, studies investigating this topic have also used alternative and less accurate methods of assessment, which makes interpretation of published data significantly more difficult.

Results of preclinical mouse experiments on omega-3 supplementation under conditions of obesity/MASLD induced by HFD administration suggest improved bioavailability of EPA or DHA+EPA in plasma and liver (mainly at the level of hepatic PL fraction) when omega-3 are administered in the form of PLs from marine fish or krill oil compared to rTG [36-38,55]. No information is available on studies in rodents with dietary obesity examining the bioavailability of omega-3 from WE compared to other chemical forms. However, omega-3 from Calanus oil rich in WEs have been shown to be bioavailable in AT and liver of HFD-fed mice, despite some loss of free FA and fatty alcohols through feces [67]. Furthermore, despite the limitations resulting from the bioavailability analysis at the level of total plasma lipids, the study by Paluchova *et al.* [35] indicated improved plasma DHA bioavailability from Calanus oil compared to rTG when these oils were orally administered to C57BL/6N mice for 8 days and provided the same daily dose of 12 μg DHA.

In humans, the question of improved bio-availability when omega-3 are administered in a particular chemical form remains controversial. Earlier studies on healthy volunteers suggested better plasma bio-availability of omega-3 from PL (krill oil) compared to TG (fish oil) or EE form [68,69]. A 4-week study in obese subjects with insulin resistance suggested a greater increase in plasma EPA levels after omega-3 supplementation using krill oil compared to fish oil, where the EPA dose was very similar in both cases, i.e.,~0.21 g/day [70]. In addition, in a 6-month double-blind placebo-controlled trial in statin-treated hyperlipidemic subjects, the bioavailability of EPA+DHA, assessed as the omega-3 index, was better when omega-3 (~1.7 g dose) were administered *via* rTG compared to the EE concentrate [66]. This led to a significant reduction in fasting serum TG levels in the rTG but not in the EE group [17]. In contrast, a recent 12-week study on healthy volunteers found comparable increases in the omega-3 index (see above) after daily supplementation with ~250 mg of EPA+DHA either *via* fish oil (i.e., in the TG form), krill oil (PL) or Calanus oil (WE; [71]). This is consistent with the results of a previous randomized, two-period crossover study [72] that demonstrated similar increases in plasma EPA+DHA levels within 72 hours after a single administration of omega-3 *via* either Calanus oil (416 mg EPA+DHA) or omega-3 EE concentrate (Omacor/Lovaza; 840 mg EPA+DHA). Regardless of the controversy regarding the improved bioavailability of omega-3 in the circulation when these FAs are administered in a particular chemical form, the question of their tissue availability remains open, as there are no human studies investigating this phenomenon in the liver.

A number of mechanisms are involved in the accumulation of fat in the liver. Briefly, hepatocytes take up FAs from the diet and non-esterified FAs (NEFA) released from AT by lipolysis, while they can also synthesize FAs *via de novo* lipogenesis (DNL). It was found that 59 % of TG stored in the liver of obese MASLD patients originated from plasma NEFA, while DNL and diet contributed 26 and 15 %, respectively [73]. Thus, a therapeutic strategy based on affecting deregulated lipolysis in the hypertrophic AT of obese patients could favorably influence MASLD development, as demonstrated in HFD-fed mice with pharmacological inhibition of adipose triglyceride lipase [74]. In any case, hepatic steatosis may arise when the quantity of FAs taken up from plasma and/or DNL in the liver exceeds the ability of the tissue to oxidize FAs either *via* mitochondrial or

peroxisomal FA oxidation or to export TG *via* lipoprotein particles. Liver mitochondria exhibit increased rates of FA-driven respiration during the development of diet-induced MASLD, suggesting an adaptive response to overcome the FA load in the liver [75,76]. However, this appears to be related to the presence of an ER stress response and dysfunctional unfolded protein response [76] with subsequent activation of the transcription factor sterol regulatory element-binding protein 1c, leading to increased DNL [77]. Hepatic DNL may also be potentiated due to activation of CB1 receptors by endocannabinoids [78]. In addition, decreased autophagic flux associated with metabolic changes in hepatocytes may further contribute to the development of liver steatosis in MASLD [79,80]. In this regard, it appears that peroxisomes, not mitochondria, may be the major contributor to the production of reactive oxygen species that cause oxidative damage during MASLD development [75,81]. Given that peroxisomes seem to be crucial for inducing the oxidative insult necessary for the onset and/or progression of MASLD, a defective autophagy would not only impair the proper removal of oxidized molecules (lipids, proteins or DNA) but also the removal of damaged organelles involved in ROS production. Indeed, failed degradation of peroxisomes has been associated with defects in peroxisome dynamics and results in increased oxidative stress [82]. Moreover, a mechanism based on peroxisomal FA degradation with subsequent H_2O_2 production and peroxin PEX2 stabilization was identified that negatively modulates intracellular lipolysis *via* posttranslational modification of adipose triglyceride lipase, thereby contributing to the progression of steatosis [83]. Besides dysregulation of various lipid metabolism pathways, there are a number of other mechanisms that contribute to the development and progression of MASLD, such as changes in the gut microbiota and increased intestinal permeability, which are associated with increased energy extraction from food, metabolic endotoxemia (i.e., increased plasma lipopolysaccharide levels), and overproduction of ammonia [84-86]. However, a detailed description of these mechanisms is beyond the scope of this review article.

Dietary supplementation with omega-3 can positively affect intrahepatic TG accumulation in mice and humans with MASLD, as observed in a number of primary studies as well as meta-analyses (see e.g. [29,30,87] and the section “Comparative studies” in this review article). However, the magnitude of the reduction in liver fat induced by an omega-3 intervention may depend on a number of factors, including baseline % liver fat, change in omega-3 index, or weight loss in response to the omega-3 intervention [88,89]. In addition, predominantly preclinical studies suggest that the antisteatotic effects of omega-3 in the liver may also depend on the class of lipids used for their supplementation ([31] and this review). In terms of mechanisms, chronic omega-3 administration is associated with a whole-body metabolic adaptation that primarily involves a switch from glucose oxidation to FA oxidation, leading to inhibition of glucose utilization, especially in the postprandial state [18,20]. The involvement of FA oxidation in the antisteatotic effects of omega-3 supple-mentation was further demonstrated in carnitine-deficient mice with impaired mitochondrial β-oxidation of FA, in which EPA supplementation further exacerbated severe TG accumulation in the liver [90]. In this regard, a recent study in fat-1 transgenic mice with increased endogenous levels of omega-3 shows that specific DHA-derived lipid autacoids, such as resolvin D1 and maresin 1, can unblock TCA cycle flux and metabolic utilization of long-chain acyl-carnitines in hepatocytes [91], similar to the effect of combination therapy with omega-3 and 10 % caloric restriction on mitochondria of abdominal AT in HFD-fed mice [92]. On the other hand, omega-3 have been consistently shown to affect primarily peroxisomes, as evidenced by elevated hepatic markers of peroxisomal but not mitochondrial β-oxidation in mice fed omega-3-supplemented HFD [19,36,92,93]. Omega-3 can also inhibit the hepatic DNL pathway [20,94,95], although the degree of inhibition may vary depending on the lipid class used for their administration; indeed, omega-3 PL in the form of krill oil appear to be much more potent compared to omega-3 TG [38,95]. The detailed mechanisms of action of omega-3 supplementation, particularly in the form of PLs, on hepatic FA oxidation and DNL have recently been reviewed elsewhere [31]. Interestingly, in fat-1 transgenic mice fed HFD, pharmacological inhibition of soluble epoxide hydrolase stabilized hepatic levels of cytochrome P-450-derived omega-3 epoxides, which was associated with reduced ER stress and up-regulation of hepatic autophagy, along with more intense antisteatotic effects [96]. These data further suggest the involvement of ER stress and autophagy regulation in the effects of omega-3 interventions on liver fat accumulation in MASLD and potentially also on the transition from simple steatosis to MASH.

Regarding the involvement of extrahepatic tissues in the beneficial effects of omega-3 supplementation on hepatic steatosis, it is primarily changes in AT and the gut by which omega-3s may indirectly influence liver TG

content. Indeed, in the epididymal AT of mice fed a semisynthetic HFD based on α-linolenic acid and supplemented with EPA and DHA, increased expression of genes involved in mitochondrial biogenesis was observed along with an increase in β-oxidation of FA [92]; *in situ* catabolism of FA in abdominal fat could thus lead to their lower release and subsequent deposition in the liver. Furthermore, adiponectin, an adipokine with antilipotoxic and anti-inflammatory properties, may also contribute to the beneficial effects of omega-3 on liver fat accumulation and hepatic insulin sensitivity [97-99]; however, in patients with type 2 diabetes, the ability of omega-3 (in the form of rTG) to induce plasma adiponectin was relatively limited compared to the insulin sensitizer pioglitazone [18]. Nevertheless, omega-3 PLs had a greater potency to elevate circulating adiponectin levels when compared to similar doses of EPA/DHA supplemented *via* omega-3 TG [31,37,38]. Similarly, adiponectin expression was stimulated in the perirenal and epididymal AT of HFD-fed mice receiving omega-3 *via* Calanus oil (i.e., omega-3 in WE) but not in mice receiving an equivalent dose of EPA/DHA *via* EE (i.e., Omacor; [46]). In addition, AT is also a source of bioactive lipids that can be modulated in response to omega-3 administration and thus affect the immunometabolic properties of other tissues including the liver (reviewed in [100]). Accordingly, administration of an EPA/DHA concentrate based on rTG resulted in increased levels of 13-DHAHLA, an anti-inflammatory lipid from the family of fatty acid esters of hydroxy fatty acids, in both AT and circulation of HFD-fed mice [35,101]. We and others have also shown that AT levels of endocannabinoids such as anandamide and 2-arachidonoylglycerol were reduced in response to omega-3 PL supplementation in obese rodents [36,102,103]. Importantly, this effect of omega-3 PL was also seen in the circulation and was stronger compared to TG-based omega-3 [36,37]. Given the role of CB1 receptors in the potentiation of hepatic DNL (see above) and the impairment of mitochondrial function [104], the reduction of endocannabinoid levels in AT and plasma may contribute to the antisteatotic effects of omega-3 supplementation (especially in the form of PL) in MASLD.

Interestingly, the more potent effect of omega-3 PL (vs. TG-based omega-3 supplementation) in terms of reducing hepatic steatosis may also involve the induction of mitochondrial ß-oxidation in the small intestine, as evidenced by gene expression within this metabolic pathway, as well as palmitate oxidation, which were specifically increased in the proximal ileum of omega-3 PL-supplemented mice [55]. It is worth noting that the antisteatotic effects of alternative supplementation forms of omega-3, such as PL and WE, may be due in part to certain bioactive substances contained in complex preparations such as krill oil and Calanus oil, respectively. Examples are palmitoleic acid and plant alkaloids in the case of krill oil ([37,38] and reviewed in [31]) and omega-3 stearidonic acid in the case of Calanus oil, which is converted to EPA in humans [105].

Conclusions

Based on a majority of the comparative studies retrieved, mostly conducted in preclinical mouse models, it can be concluded that the class of lipids used for supplementation contributes largely to the efficacy with which dietary omega-3 can prevent or alleviate hepatic steatosis in MASLD. Regarding the efficacy of individual lipid classes used for omega-3 supplementation, in particular the PL class (e.g., in the form of fish meal extract, krill oil, algae oil) is associated with stronger antisteatotic effects in the liver compared to TG-based omega-3 supplementation (e.g., fish oil, rTG). In addition to improving the bioavailability of mainly EPA in the hepatic PL fraction, omega-3 PLs appear to more effectively reduce hepatic DNL and modulate the production of bioactive lipids in both AT and liver, which may contribute to enhancing mitochondrial function, stimulating autophagy and reducing ER stress. Considering the superior antisteatotic effects of marine omega-3 PL, the involvement of extrahepatic tissues such as AT and the gut with its microbiome cannot be excluded. On the other hand, conducting comparative studies based on the administration of similar amounts of omega-3 using different supplementation forms is often technically very challenging. This is due to differences in the omega-3 content of various formulations, but potentially also to differences in the length of dietary intervention required for the onset of action of a given formulation in the context of the chosen experimental model. This fact makes it difficult to draw strong conclusions when comparing the antisteatotic efficacy of the various omega-3 formulations.

Unfortunately, there are no studies in humans with MASLD where the effect of two or more lipid classes on fat accumulation in the liver has been compared as a primary outcome. Thus, randomized controlled trials of sufficient size and duration are needed

to test the efficacy of alternative lipid classes such as PL or WE used for omega-3 supplementation. Since omega-3 should ideally be part of our normal diet, identifying the optimal class of lipids for supplementation may also be important for their possible co-administration with different drugs to further enhance treatment efficacy.

Abbreviations

AG, acylglycerols; AT, adipose tissue; CON, control diet; DG, diacylglycerols; DHA, docosahexaenoic acid; DNL, *de novo* lipogenesis; EE, ethyl esters; EPA, eicosapentaenoic acid; HDL, high-density lipoprotein; LDL, low-density lipoprotein; MASH, metabolic dysfunction-associated steatohepatitis; MASLD, metabolic dysfunction-associated steatotic liver disease; NAFLD, non-alcoholic fatty liver disease; NEFA, non-esterified fatty acids; PC, phosphatidylcholine; PL, phospholipids; PUFA, polyunsaturated FA; rTG, reesterified triacylglycerols; TC, total cholesterol; TG, triacylglycerols; WE, wax esters.

Conflict of Interest

There is no conflict of interest.

Acknowledgements

This work was supported by the Czech Science Foundation (grant no. 22-04100L; recipient M.R.), National Science Centre Poland (grant no. UMO-2021/43/I/NZ3/00510; recipient M.R.W.), and by the project National Institute for Research of Metabolic and Cardiovascular Diseases (Programme EXCELES, ID Project no. LX22NPO5104) - funded by the European Union - Next Generation EU.

References

1. Younossi Z, Tacke F, Arrese M, Chander Sharma B, Mostafa I, Bugianesi E, Wai-Sun Wong V, Yilmaz Y, George J, Fan J, Vos MB. Global perspectives on nonalcoholic fatty liver disease and nonalcoholic steatohepatitis. Hepatology 2019;69:2672-2682. https://doi.org/10.1002/hep.30251
2. Eslam M, Sanyal AJ, George J, International Consensus P. MAFLD: A consensus-driven proposed nomenclature for metabolic associated fatty liver disease. Gastroenterology 2020;158:1999-2014 e1991. https://doi.org/10.1053/j.gastro.2019.11.312
3. Gofton C, Upendran Y, Zheng MH, George J. MAFLD: How is it different from NAFLD? Clin Mol Hepatol 2023;29:S17-S31. https://doi.org/10.3350/cmh.2022.0367
4. Rinella ME, Lazarus JV, Ratziu V, Francque SM, Sanyal AJ, Kanwal F, Romero D, Abdelmalek MF, Anstee QM, Arab JP, Arrese M, Bataller R, Beuers U, Boursier J, Bugianesi E, Byrne CD, Castro Narro GE, Chowdhury A, Cortez-Pinto H, Cryer DR, Cusi K, El-Kassas M, Klein S, Eskridge W, Fan J, Gawrieh S, Guy CD, Harrison SA, Kim SU, Koot BG, Korenjak M, Kowdley KV, Lacaille F, Loomba R, Mitchell-Thain R, Morgan TR, Powell EE, Roden M, Romero-Gomez M, Silva M, Singh SP, Sookoian SC, Spearman CW, Tiniakos D, Valenti L, Vos MB, Wong VW, Xanthakos S, Yilmaz Y, Younossi Z, Hobbs A, Villota-Rivas M, Newsome PN, group NNc. A multisociety Delphi consensus statement on new fatty liver disease nomenclature. J Hepatol 2023. https://doi.org/10.1097/HEP.0000000000000520
5. Simon TG, Roelstraete B, Khalili H, Hagstrom H, Ludvigsson JF. Mortality in biopsy-confirmed nonalcoholic fatty liver disease: results from a nationwide cohort. Gut 2021;70:1375-1382. https://doi.org/10.1136/gutjnl-2020-322786
6. Puengel T, Tacke F. Efruxifermin, an investigational treatment for fibrotic or cirrhotic nonalcoholic steatohepatitis (NASH). Expert Opin Investig Drugs 2023;32:451-461. https://doi.org/10.1080/13543784.2023.2230115
7. Francque SM, Bedossa P, Ratziu V, Anstee QM, Bugianesi E, Sanyal AJ, Loomba R, Harrison SA, Balabanska R, Mateva L, Lanthier N, Alkhouri N, Moreno C, Schattenberg JM, Stefanova-Petrova D, Vonghia L, Rouzier R, Guillaume M, Hodge A, Romero-Gomez M, Huot-Marchand P, Baudin M, Richard MP, Abitbol JL, Broqua P, Junien JL, Abdelmalek MF, Group NS. A randomized, controlled trial of the Pan-PPAR agonist lanifibranor in NASH. N Engl J Med 2021;385:1547-1558. https://doi.org/10.1056/NEJMoa2036205
8. Newsome PN, Buchholtz K, Cusi K, Linder M, Okanoue T, Ratziu V, Sanyal AJ, Sejling AS, Harrison SA, Investigators NN. A placebo-controlled trial of subcutaneous semaglutide in nonalcoholic steatohepatitis. N Engl J Med 2021;384:1113-1124. https://doi.org/10.1056/NEJMoa2028395

9. Golabi P, Locklear CT, Austin P, Afdhal S, Byrns M, Gerber L, Younossi ZM. Effectiveness of exercise in hepatic fat mobilization in non-alcoholic fatty liver disease: Systematic review. World J Gastroenterol 2016;22:6318-6327. https://doi.org/10.3748/wjg.v22.i27.6318
10. Katsagoni CN, Papatheodoridis GV, Ioannidou P, Deutsch M, Alexopoulou A, Papadopoulos N, Papageorgiou MV, Fragopoulou E, Kontogianni MD. Improvements in clinical characteristics of patients with non-alcoholic fatty liver disease, after an intervention based on the Mediterranean lifestyle: a randomised controlled clinical trial. Br J Nutr 2018;120:164-175. https://doi.org/10.1017/S000711451800137X
11. Hallsworth K, Adams LA. Lifestyle modification in NAFLD/NASH: Facts and figures. JHEP Rep 2019;1:468-479. https://doi.org/10.1016/j.jhepr.2019.10.008
12. Hodson L, Rosqvist F, Parry SA. The influence of dietary fatty acids on liver fat content and metabolism. Proc Nutr Soc 2020;79:30-41. https://doi.org/10.1017/S0029665119000569
13. Rosqvist F, Iggman D, Kullberg J, Cedernaes J, Johansson HE, Larsson A, Johansson L, Ahlstrom H, Arner P, Dahlman I, Riserus U. Overfeeding polyunsaturated and saturated fat causes distinct effects on liver and visceral fat accumulation in humans. Diabetes 2014;63:2356-2368. https://doi.org/10.2337/db13-1622
14. Luukkonen PK, Sadevirta S, Zhou Y, Kayser B, Ali A, Ahonen L, Lallukka S, Pelloux V, Gaggini M, Jian C, Hakkarainen A, Lundbom N, Gylling H, Salonen A, Oresic M, Hyotylainen T, Orho-Melander M, Rissanen A, Gastaldelli A, Clement K, Hodson L, Yki-Jarvinen H. Saturated fat is more metabolically harmful for the human liver than unsaturated fat or simple sugars. Diabetes Care 2018;41:1732-1739. https://doi.org/10.2337/dc18-0071
15. Bray GA, Krauss RM. Overfeeding of polyunsaturated versus saturated Fatty acids reduces ectopic fat. Diabetes 2014;63:2222-2224. https://doi.org/10.2337/db14-0493
16. Roche HM, Gibney MJ. Effect of long-chain n-3 polyunsaturated fatty acids on fasting and postprandial triacylglycerol metabolism1. Am J Clin Nutr 2000;71:232S-237. https://doi.org/10.1093/ajcn/71.1.232S
17. Schuchardt JP, Neubronner J, Kressel G, Merkel M, von SC, Hahn A. Moderate doses of EPA and DHA from re-esterified triacylglycerols but not from ethyl-esters lower fasting serum triacylglycerols in statin-treated dyslipidemic subjects: Results from a six month randomized controlled trial. Prostaglandins Leukot Essent Fatty Acids 2011;85:381-386. https://doi.org/10.1016/j.plefa.2011.07.006
18. Veleba J, Kopecky J, Jr., Janovska P, Kuda O, Horakova O, Malinska H, Kazdova L, Oliyarnyk O, Skop V, Trnovska J, Hajek M, Skoch A, Flachs P, Bardova K, Rossmeisl M, Olza J, de Castro GS, Calder PC, Gardlo A, Fiserova E, Jensen J, Bryhn M, Kopecky J, Sr., Pelikanova T. Combined intervention with pioglitazone and -3 fatty acids in metformin-treated type 2 diabetic patients: improvement of lipid metabolism. Nutr Metab (Lond) 2015;12:52. https://doi.org/10.1186/s12986-015-0047-9
19. Pavlisova J, Bardova K, Stankova B, Tvrzicka E, Kopecky J, Rossmeisl M. Corn oil versus lard: Metabolic effects of omega-3 fatty acids in mice fed obesogenic diets with different fatty acid composition. Biochimie 2016;124:150-162. https://doi.org/10.1016/j.biochi.2015.07.001
20. Green CJ, Pramfalk C, Charlton CA, Gunn PJ, Cornfield T, Pavlides M, Karpe F, Hodson L. Hepatic de novo lipogenesis is suppressed and fat oxidation is increased by omega-3 fatty acids at the expense of glucose metabolism. BMJ Open Diabetes Res Care 2020;8. https://doi.org/10.1136/bmjdrc-2019-000871
21. Flachs P, Rossmeisl M, Bryhn M, Kopecky J. Cellular and molecular effects of n-3 polyunsaturated fatty acids on adipose tissue biology and metabolism. Clin Sci (Lond) 2009;116:1-16. https://doi.org/10.1042/CS20070456
22. Glass CK, Olefsky JM. Inflammation and lipid signaling in the etiology of insulin resistance. Cell Metab 2012;15:635-645. https://doi.org/10.1016/j.cmet.2012.04.001
23. Calder PC. Marine omega-3 fatty acids and inflammatory processes: Effects, mechanisms and clinical relevance. Biochim Biophys Acta 2015;1851:469-484. https://doi.org/10.1016/j.bbalip.2014.08.010
24. de Castro GS, Calder PC. Non-alcoholic fatty liver disease and its treatment with n-3 polyunsaturated fatty acids. Clin Nutr 2018;37:37-55. https://doi.org/10.1016/j.clnu.2017.01.006
25. Spooner MH, Jump DB. Omega-3 fatty acids and nonalcoholic fatty liver disease in adults and children: where do we stand? Curr Opin Clin Nutr Metab Care 2019;22:103-110. https://doi.org/10.1097/MCO.0000000000000539
26. Lee CH, Fu Y, Yang SJ, Chi CC. Effects of Omega-3 polyunsaturated fatty acid supplementation on non-alcoholic fatty liver: a systematic review and meta-analysis. Nutrients 2020;12. https://doi.org/10.3390/nu12092769

27. Argo CK, Patrie JT, Lackner C, Henry TD, de Lange EE, Weltman AL, Shah NL, Al-Osaimi AM, Pramoonjago P, Jayakumar S, Binder LP, Simmons-Egolf WD, Burks SG, Bao Y, Taylor AG, Rodriguez J, Caldwell SH. Effects of n-3 fish oil on metabolic and histological parameters in NASH: a double-blind, randomized, placebo-controlled trial. J Hepatol 2015;62:190-197. https://doi.org/10.1016/j.jhep.2014.08.036
28. Caldwell S. NASH Therapy: omega 3 supplementation, vitamin E, insulin sensitizers and statin drugs. Clin Mol Hepatol 2017;23:103-108. https://doi.org/10.3350/cmh.2017.0103
29. Musa-Veloso K, Venditti C, Lee HY, Darch M, Floyd S, West S, Simon R. Systematic review and meta-analysis of controlled intervention studies on the effectiveness of long-chain omega-3 fatty acids in patients with nonalcoholic fatty liver disease. Nutr Rev 2018;76:581-602. https://doi.org/10.1093/nutrit/nuy022
30. Scorletti E, Byrne CD. Omega-3 fatty acids and non-alcoholic fatty liver disease: Evidence of efficacy and mechanism of action. Mol Aspects Med 2018;64:135-146. https://doi.org/10.1016/j.mam.2018.03.001
31. Mitrovic M, Sistilli G, Horakova O, Rossmeisl M. Omega-3 phospholipids and obesity-associated NAFLD: Potential mechanisms and therapeutic perspectives. Eur J Clin Invest 2022;52:e13650. https://doi.org/10.1111/eci.13650
32. Schots PC, Pedersen AM, Eilertsen KE, Olsen RL, Larsen TS. Possible health effects of a wax ester rich marine oil. Front Pharmacol 2020;11:961. https://doi.org/10.3389/fphar.2020.00961
33. Ruzickova J, Rossmeisl M, Prazak T, Flachs P, Sponarova J, Vecka M, Tvrzicka E, Bryhn M, Kopecky J. Omega-3 PUFA of marine origin limit diet-induced obesity in mice by reducing cellularity of adipose tissue. Lipids 2004;39:1177-1185. https://doi.org/10.1007/s11745-004-1345-9
34. Schuchardt JP, Hahn A. Bioavailability of long-chain omega-3 fatty acids. Prostaglandins Leukot Essent Fatty Acids 2013;89:1-8. https://doi.org/10.1016/j.plefa.2013.03.010
35. Paluchova V, Vik A, Cajka T, Brezinova M, Brejchova K, Bugajev V, Draberova L, Draber P, Buresova J, Kroupova P, Bardova K, Rossmeisl M, Kopecky J, Hansen TV, Kuda O. Triacylglycerol-rich oils of marine origin are optimal nutrients for induction of polyunsaturated docosahexaenoic acid ester of hydroxy linoleic acid (13-DHAHLA) with anti-inflammatory properties in mice. Mol Nutr Food Res 2020;64:e1901238. https://doi.org/10.1002/mnfr.201901238
36. Rossmeisl M, Jilkova ZM, Kuda O, Jelenik T, Medrikova D, Stankova B, Kristinsson B, Haraldsson GG, Svensen H, Stoknes I, Sjovall P, Magnusson Y, Balvers MG, Verhoeckx KC, Tvrzicka E, Bryhn M, Kopecky J. Metabolic effects of n-3 PUFA as phospholipids are superior to triglycerides in mice fed a high-fat diet: possible role of endocannabinoids. PLoS One 2012;7:e38834. https://doi.org/10.1371/journal.pone.0038834
37. Rossmeisl M, Pavlisova J, Bardova K, Kalendova V, Buresova J, Kuda O, Kroupova P, Stankova B, Tvrzicka E, Fiserova E, Horakova O, Kopecky J. Increased plasma levels of palmitoleic acid may contribute to beneficial effects of Krill oil on glucose homeostasis in dietary obese mice. Biochim Biophys Acta Mol Cell Biol Lipids 2020:158732. https://doi.org/10.1016/j.bbalip.2020.158732
38. Sistilli G, Kalendova V, Cajka T, Irodenko I, Bardova K, Oseeva M, Zacek P, Kroupova P, Horakova O, Lackner K, Gastaldelli A, Kuda O, Kopecky J, Rossmeisl M. Krill Oil Supplementation Reduces Exacerbated Hepatic Steatosis Induced by Thermoneutral Housing in Mice with Diet-Induced Obesity. Nutrients 2021;13. https://doi.org/10.3390/nu13020437
39. Sugimoto K, Hosomi R, Yoshida M, Fukunaga K. Effects of dietary oils prepared from the internal organs of the Japanese giant scallop (Patinopecten yessoensis) on cholesterol metabolism in obese type-II diabetic KK-A(y) mice. Food Sci Nutr 2020;8:6727-6737. https://doi.org/10.1002/fsn3.1967
40. Chen YF, Fan ZK, Gao X, Zhou F, Guo XF, Sinclair AJ, Li D. n-3 polyunsaturated fatty acids in phospholipid or triacylglycerol form attenuate nonalcoholic fatty liver disease *via* mediating cannabinoid receptor 1/adiponectin/ceramide pathway. J Nutr Biochem 2024;123:109484. https://doi.org/10.1016/j.jnutbio.2023.109484
41. Wang Q, Wang R, Zhao X, Lu H, Zhang P, Dong X, Wang Y. Comparison of the effect of phospholipid extracts from salmon and silver carp heads on high-fat-diet-induced metabolic syndrome in C57BL/6J Mice. Mar Drugs 2023;21. https://doi.org/10.3390/md21070409

42. Aydin Cil M, Ghosi Ghareaghaji A, Bayir Y, Buyuktuncer Z, Besler HT. Efficacy of krill oil versus fish oil on obesity-related parameters and lipid gene expression in rats: randomized controlled study. PeerJ 2021;9:e12009. https://doi.org/10.7717/peerj.12009
43. Botelho PB, Mariano Kda R, Rogero MM, de Castro IA. Effect of Echium oil compared with marine oils on lipid profile and inhibition of hepatic steatosis in LDLr knockout mice. Lipids Health Dis 2013;12:38. https://doi.org/10.1186/1476-511X-12-38
44. Gui L, Chen S, Wang H, Ruan M, Liu Y, Li N, Zhang H, Liu Z. omega-3 PUFAs alleviate high-fat diet-induced circadian intestinal microbes dysbiosis. Mol Nutr Food Res 2019;63:e1900492. https://doi.org/10.1002/mnfr.201900492
45. Tang X, Li ZJ, Xu J, Xue Y, Li JZ, Wang JF, Yanagita T, Xue CH, Wang YM. Short term effects of different omega-3 fatty acid formulation on lipid metabolism in mice fed high or low fat diet. Lipids Health Dis 2012;11:70. https://doi.org/10.1186/1476-511X-11-70
46. Hoper AC, Salma W, Sollie SJ, Hafstad AD, Lund J, Khalid AM, Raa J, Aasum E, Larsen TS. Wax esters from the marine copepod Calanus finmarchicus reduce diet-induced obesity and obesity-related metabolic disorders in mice. J Nutr 2014;144:164-169. https://doi.org/10.3945/jn.113.182501
47. Ferramosca A, Conte L, Zara V. A krill oil supplemented diet reduces the activities of the mitochondrial tricarboxylate carrier and of the cytosolic lipogenic enzymes in rats. J Anim Physiol Anim Nutr (Berl) 2012;96:295-306. https://doi.org/10.1111/j.1439-0396.2011.01135.x
48. Tillander V, Bjorndal B, Burri L, Bohov P, Skorve J, Berge RK, Alexson SE. Fish oil and krill oil supplementations differentially regulate lipid catabolic and synthetic pathways in mice. Nutr Metab (Lond) 2014;11:20. https://doi.org/10.1186/1743-7075-11-20
49. Skorve J, Hilvo M, Vihervaara T, Burri L, Bohov P, Tillander V, Bjorndal B, Suoniemi M, Laaksonen R, Ekroos K, Berge RK, Alexson SE. Fish oil and krill oil differentially modify the liver and brain lipidome when fed to mice. Lipids Health Dis 2015;14:88. https://doi.org/10.1186/s12944-015-0086-2
50. Yook JS, Kim KA, Park JE, Lee SH, Cha YS. Microalgal oil supplementation has an anti-obesity effect in C57BL/6J mice fed a high fat diet. Prev Nutr Food Sci 2015;20:230-237. https://doi.org/10.3746/pnf.2015.20.4.230
51. Yu J, Ma Y, Sun J, Ran L, Li Y, Wang N, Yu T, Gao W, Jia W, Jiang R, Guo M, Bi Y, Wu Y. Microalgal oil from schizochytrium sp. prevents HFD-induced abdominal fat accumulation in mice. J Am Coll Nutr 2017;36:347-356. https://doi.org/10.1080/07315724.2017.1302366
52. Shang T, Liu L, Zhou J, Zhang M, Hu Q, Fang M, Wu Y, Yao P, Gong Z. Protective effects of various ratios of DHA/EPA supplementation on high-fat diet-induced liver damage in mice. Lipids Health Dis 2017;16:65. https://doi.org/10.1186/s12944-017-0461-2
53. Sugimoto K, Hosomi R, Yoshida M, Fukunaga K. Dietary phospholipids prepared from scallop internal organs attenuate the serum and liver cholesterol contents by enhancing the expression of cholesterol hydroxylase in the liver of mice. Front Nutr 2021;8:761928. https://doi.org/10.3389/fnut.2021.761928
54. Ran L, Yu J, Ma R, Yao Q, Wang M, Bi Y, Yu Z, Wu Y. Microalgae oil from Schizochytrium sp. alleviates obesity and modulates gut microbiota in high-fat diet-fed mice. Food Funct 2022;13:12799-12813. https://doi.org/10.1039/D2FO01772E
55. Kroupova P, van Schothorst EM, Keijer J, Bunschoten A, Vodicka M, Irodenko I, Oseeva M, Zacek P, Kopecky J, Rossmeisl M, Horakova O. Omega-3 phospholipids from krill oil enhance intestinal fatty acid oxidation more effectively than omega-3 triacylglycerols in high-fat diet-fed obese mice. Nutrients 2020;12. https://doi.org/10.3390/nu12072037
56. Sugimoto K, Hosomi R, Shimono T, Kanda S, Nishiyama T, Yoshida M, Fukunaga K. Comparison of the Cholesterol-Lowering Effect of Scallop Oil Prepared from the Internal Organs of the Japanese Giant Scallop (Patinopecten yessoensis), Fish Oil, and Krill Oil in Obese Type II Diabetic KK-A (y) Mice. J Oleo Sci 2021;70:965-977. https://doi.org/10.5650/jos.ess21032
57. Cui C, Li Y, Gao H, Zhang H, Han J, Zhang D, Li Y, Zhou J, Lu C, Su X. Modulation of the gut microbiota by the mixture of fish oil and krill oil in high-fat diet-induced obesity mice. PLoS One 2017;12:e0186216. https://doi.org/10.1371/journal.pone.0186216

58. Hosomi R, Fukunaga K, Nagao T, Tanizaki T, Miyauchi K, Yoshida M, Kanda S, Nishiyama T, Takahashi K. Effect of dietary partial hydrolysate of phospholipids, rich in docosahexaenoic acid-bound lysophospholipids, on lipid and fatty acid composition in rat serum and liver. J Food Sci 2019;84:183-191. https://doi.org/10.1111/1750-3841.14416
59. Tou JC, Altman SN, Gigliotti JC, Benedito VA, Cordonier EL. Different sources of omega-3 polyunsaturated fatty acids affects apparent digestibility, tissue deposition, and tissue oxidative stability in growing female rats. Lipids Health Dis 2011;10:179. https://doi.org/10.1186/1476-511X-10-179
60. Maki KC, Yurko-Mauro K, Dicklin MR, Schild AL, Geohas JG. A new, microalgal DHA- and EPA-containing oil lowers triacylglycerols in adults with mild-to-moderate hypertriglyceridemia. Prostaglandins Leukot Essent Fatty Acids 2014;91:141-148. https://doi.org/10.1016/j.plefa.2014.07.012
61. Cook CM, Hallaraker H, Saebo PC, Innis SM, Kelley KM, Sanoshy KD, Berger A, Maki KC. Bioavailability of long chain omega-3 polyunsaturated fatty acids from phospholipid-rich herring roe oil in men and women with mildly elevated triacylglycerols. Prostaglandins Leukot Essent Fatty Acids 2016;111:17-24. https://doi.org/10.1016/j.plefa.2016.01.007
62. Hedengran A, Szecsi PB, Dyerberg J, Harris WS, Stender S. n-3 PUFA esterified to glycerol or as ethyl esters reduce non-fasting plasma triacylglycerol in subjects with hypertriglyceridemia: a randomized trial. Lipids 2015;50:165-175. https://doi.org/10.1007/s11745-014-3968-6
63. Schuchardt JP, Neubronner J, Block RC, von Schacky C, Hahn A. Associations between Omega-3 Index increase and triacylglyceride decrease in subjects with hypertriglyceridemia in response to six month of EPA and DHA supplementation. Prostaglandins Leukot Essent Fatty Acids 2014;91:129-134. https://doi.org/10.1016/j.plefa.2014.07.014
64. Meyer BJ, Lane AE, Mann NJ. Comparison of seal oil to tuna oil on plasma lipid levels and blood pressure in hypertriglyceridaemic subjects. Lipids 2009;44:827-835. https://doi.org/10.1007/s11745-009-3333-3
65. Kopecky J, Rossmeisl M, Flachs P, Kuda O, Brauner P, Jilkova Z, Stankova B, Tvrzicka E, Bryhn M. n-3 PUFA: bioavailability and modulation of adipose tissue function. Proc Nutr Soc 2009;68:361-369. https://doi.org/10.1017/S0029665109990231
66. Neubronner J, Schuchardt JP, Kressel G, Merkel M, von SC, Hahn A. Enhanced increase of omega-3 index in response to long-term n-3 fatty acid supplementation from triacylglycerides versus ethyl esters. Eur J ClinNutr 2011;65:247-254. https://doi.org/10.1038/ejcn.2010.239
67. Pedersen AM, Salma W, Hoper AC, Larsen TS, Olsen RL. Lipid profile of mice fed a high-fat diet supplemented with a wax ester-rich marine oil. Eur J Lipid Sci Tech 2014;116:1718-1726. https://doi.org/10.1002/ejlt.201400052
68. Ulven SM, Kirkhus B, Lamglait A, Basu S, Elind E, Haider T, Berge K, Vik H, Pedersen JI. Metabolic effects of krill oil are essentially similar to those of fish oil but at lower dose of EPA and DHA, in healthy volunteers. Lipids 2011;46:37-46. https://doi.org/10.1007/s11745-010-3490-4
69. Schuchardt JP, Schneider I, Meyer H, Neubronner J, von Schacky C, Hahn A. Incorporation of EPA and DHA into plasma phospholipids in response to different omega-3 fatty acid formulations - a comparative bioavailability study of fish oil vs. krill oil. Lipids Health Dis 2011;10:145. https://doi.org/10.1186/1476-511X-10-145
70. Maki KC, Reeves MS, Farmer M, Griinari M, Berge K, Vik H, Hubacher R, Rains TM. Krill oil supplementation increases plasma concentrations of eicosapentaenoic and docosahexaenoic acids in overweight and obese men and women. Nutr Res 2009;29:609-615. https://doi.org/10.1016/j.nutres.2009.09.004
71. Vosskotter F, Burhop M, Hahn A, Schuchardt JP. Equal bioavailability of omega-3 PUFA from Calanus oil, fish oil and krill oil: A 12-week randomized parallel study. Lipids 2023;58:129-138. https://doi.org/10.1002/lipd.12369
72. Cook CM, Larsen TS, Derrig LD, Kelly KM, Tande KS. Wax Ester Rich Oil From The Marine Crustacean, Calanus finmarchicus, is a Bioavailable Source of EPA and DHA for Human Consumption. Lipids 2016;51:1137-1144. https://doi.org/10.1007/s11745-016-4189-y
73. Donnelly KL, Smith CI, Schwarzenberg SJ, Jessurun J, Boldt MD, Parks EJ. Sources of fatty acids stored in liver and secreted *via* lipoproteins in patients with nonalcoholic fatty liver disease. J Clin Invest 2005;115:1343-1351. https://doi.org/10.1172/JCI23621

74. Schweiger M, Romauch M, Schreiber R, Grabner GF, Hutter S, Kotzbeck P, Benedikt P, Eichmann TO, Yamada S, Knittelfelder O, Diwoky C, Doler C, Mayer N, De Cecco W, Breinbauer R, Zimmermann R, Zechner R. Pharmacological inhibition of adipose triglyceride lipase corrects high-fat diet-induced insulin resistance and hepatosteatosis in mice. Nat Comm 2017;8:14859. https://doi.org/10.1038/ncomms14859, https://doi.org/10.1038/ncomms15490
75. Einer C, Hohenester S, Wimmer R, Wottke L, Artmann R, Schulz S, Gosmann C, Simmons A, Leitzinger C, Eberhagen C, Borchard S, Schmitt S, Hauck SM, von Toerne C, Jastroch M, Walheim E, Rust C, Gerbes AL, Popper B, Mayr D, Schnurr M, Vollmar AM, Denk G, Zischka H. Mitochondrial adaptation in steatotic mice. Mitochondrion 2018;40:1-12. https://doi.org/10.1016/j.mito.2017.08.015
76. Dewidar B, Mastrototaro L, Englisch C, Ress C, Granata C, Rohbeck E, Pesta D, Heilmann G, Wolkersdorfer M, Esposito I, Reina Do Fundo M, Zivehe F, Yavas A, Roden M. Alterations of hepatic energy metabolism in murine models of obesity, diabetes and fatty liver diseases. EBio Med 2023;94:104714. https://doi.org/10.1016/j.ebiom.2023.104714
77. Kammoun HL, Chabanon H, Hainault I, Luquet S, Magnan C, Koike T, Ferre P, Foufelle F. GRP78 expression inhibits insulin and ER stress-induced SREBP-1c activation and reduces hepatic steatosis in mice. J Clin Invest 2009;119:1201-1215. https://doi.org/10.1172/JCI37007
78. Osei-Hyiaman D, Liu J, Zhou L, Godlewski G, Harvey-White J, Jeong WI, Batkai S, Marsicano G, Lutz B, Buettner C, Kunos G. Hepatic CB1 receptor is required for development of diet-induced steatosis, dyslipidemia, and insulin and leptin resistance in mice. J Clin Invest 2008;118:3160-3169. https://doi.org/10.1172/JCI34827
79. Ramos VM, Kowaltowski AJ, Kakimoto PA. Autophagy in hepatic steatosis: a structured review. Front Cell Dev Biol 2021;9:657389. https://doi.org/10.3389/fcell.2021.657389
80. Sharma L, Lone NA, Knott RM, Hassan A, Abdullah T. Trigonelline prevents high cholesterol and high fat diet induced hepatic lipid accumulation and lipo-toxicity in C57BL/6J mice, *via* restoration of hepatic autophagy. Food Chem Toxicol 2018;121:283-296. https://doi.org/10.1016/j.fct.2018.09.011
81. Simoes ICM, Amorim R, Teixeira J, Karkucinska-Wieckowska A, Carvalho A, Pereira SP, Simoes RF, Szymanska S, Dabrowski M, Janikiewicz J, Dobrzyn A, Oliveira PJ, Potes Y, Wieckowski MR. The alterations of mitochondrial function during NAFLD progression-an independent effect of mitochondrial ROS production. Int J Mol Sci 2021;22. https://doi.org/10.3390/ijms22136848
82. Vasko R, Goligorsky MS. Dysfunctional lysosomal autophagy leads to peroxisomal oxidative burnout and damage during endotoxin-induced stress. Autophagy 2013;9:442-444. https://doi.org/10.4161/auto.23344
83. Ding L, Sun W, Balaz M, He A, Klug M, Wieland S, Caiazzo R, Raverdy V, Pattou F, Lefebvre P, Lodhi IJ, Staels B, Heim M, Wolfrum C. Peroxisomal beta-oxidation acts as a sensor for intracellular fatty acids and regulates lipolysis. Nat Metab 2021;3:1648-1661. https://doi.org/10.1038/s42255-021-00489-2
84. Cani PD, Bibiloni R, Knauf C, Waget A, Neyrinck AM, Delzenne NM, Burcelin R. Changes in gut microbiota control metabolic endotoxemia-induced inflammation in high-fat diet-induced obesity and diabetes in mice. Diabetes 2008;57:1470-1481. https://doi.org/10.2337/db07-1403
85. Winer DA, Winer S, Dranse HJ, Lam TK. Immunologic impact of the intestine in metabolic disease. J Clin Invest 2017;127:33-42. https://doi.org/10.1172/JCI88879
86. Delgado TC, de Las Heras J, Martinez-Chantar ML. Understanding gut-liver axis nitrogen metabolism in Fatty Liver Disease. Front Endocrinol (Lausanne) 2022;13:1058101. https://doi.org/10.3389/fendo.2022.1058101
87. Jump DB, Lytle KA, Depner CM, Tripathy S. Omega-3 polyunsaturated fatty acids as a treatment strategy for nonalcoholic fatty liver disease. Pharmacol Ther 2018;181:108-125. https://doi.org/10.1016/j.pharmthera.2017.07.007
88. Scorletti E, Bhatia L, McCormick KG, Clough GF, Nash K, Hodson L, Moyses HE, Calder PC, Byrne CD, Study W. Effects of purified eicosapentaenoic and docosahexaenoic acids in nonalcoholic fatty liver disease: results from the Welcome* study. Hepatology 2014;60:1211-1221. https://doi.org/10.1002/hep.27289
89. Smid V, Dvorak K, Sedivy P, Kosek V, Lenicek M, Dezortova M, Hajslova J, Hajek M, Vitek L, Bechynska K, Bruha R. Effect of Omega-3 Polyunsaturated Fatty Acids on Lipid Metabolism in Patients With Metabolic Syndrome and NAFLD. Hepatol Commun 2022;6:1336-1349. https://doi.org/10.1002/hep4.1906

90. Du ZY, Ma T, Liaset B, Keenan AH, Araujo P, Lock EJ, Demizieux L, Degrace P, Froyland L, Kristiansen K, Madsen L. Dietary eicosapentaenoic acid supplementation accentuates hepatic triglyceride accumulation in mice with impaired fatty acid oxidation capacity. Biochim Biophys Acta 2013;1831:291-299. https://doi.org/10.1016/j.bbalip.2012.10.002
91. Lopez-Vicario C, Sebastian D, Casulleras M, Duran-Guell M, Flores-Costa R, Aguilar F, Lozano JJ, Zhang IW, Titos E, Kang JX, Zorzano A, Arita M, Claria J. Essential lipid autacoids rewire mitochondrial energy efficiency in metabolic dysfunction-associated fatty liver disease. Hepatology 2023;77:1303-1318. https://doi.org/10.1002/hep.32647
92. Flachs P, Ruhl R, Hensler M, Janovska P, Zouhar P, Kus V, Macek JZ, Papp E, Kuda O, Svobodova M, Rossmeisl M, Tsenov G, Mohamed-Ali V, Kopecky J. Synergistic induction of lipid catabolism and anti-inflammatory lipids in white fat of dietary obese mice in response to calorie restriction and n-3 fatty acids. Diabetologia 2011;54:2626-2638. https://doi.org/10.1007/s00125-011-2233-2
93. Fiamoncini J, Turner N, Hirabara SM, Salgado TM, Marcal AC, Leslie S, da Silva SM, Deschamps FC, Luz J, Cooney GJ, Curi R. Enhanced peroxisomal beta-oxidation is associated with prevention of obesity and glucose intolerance by fish oil-enriched diets. Obesity 2013;21:1200-1207. https://doi.org/10.1002/oby.20132
94. Ferramosca A, Conte A, Burri L, Berge K, De NF, Giudetti AM, Zara V. A krill oil supplemented diet suppresses hepatic steatosis in high-fat fed rats. Plos One 2012;7:e38797. https://doi.org/10.1371/journal.pone.0038797
95. Rossmeisl M, Medrikova D, van Schothorst EM, Pavlisova J, Kuda O, Hensler M, Bardova K, Flachs P, Stankova B, Vecka M, Tvrzicka E, Zak A, Keijer J, Kopecky J. Omega-3 phospholipids from fish suppress hepatic steatosis by integrated inhibition of biosynthetic pathways in dietary obese mice. Biochim Biophys Acta 2014;1841:267-278. https://doi.org/10.1016/j.bbalip.2013.11.010
96. Lopez-Vicario C, Alcaraz-Quiles J, Garcia-Alonso V, Rius B, Hwang SH, Titos E, Lopategi A, Hammock BD, Arroyo V, Claria J. Inhibition of soluble epoxide hydrolase modulates inflammation and autophagy in obese adipose tissue and liver: role for omega-3 epoxides. Proc Natl Acad Sci U S A 2015;112:536-541. https://doi.org/10.1073/pnas.1422590112
97. Neschen S, Morino K, Rossbacher JC, Pongratz RL, Cline GW, Sono S, Gillum M, Shulman GI. Fish oil regulates adiponectin secretion by a peroxisome proliferator-activated receptor-gamma-dependent mechanism in mice. Diabetes 2006;55:924-928. https://doi.org/10.2337/diabetes.55.04.06.db05-0985
98. Flachs P, Mohamed-Ali V, Horakova O, Rossmeisl M, Hosseinzadeh-Attar MJ, Hensler M, Ruzickova J, Kopecky J. Polyunsaturated fatty acids of marine origin induce adiponectin in mice fed high-fat diet. Diabetologia 2006;49:394-397. https://doi.org/10.1007/s00125-005-0053-y
99. Jelenik T, Rossmeisl M, Kuda O, Jilkova ZM, Medrikova D, Kus V, Hensler M, Janovska P, Miksik I, Baranowski M, Gorski J, Hebrard S, Jensen TE, Flachs P, Hawley S, Viollet B, Kopecky J. AMP-activated protein kinase {alpha}2 subunit is required for the preservation of hepatic insulin sensitivity by n-3 polyunsaturated fatty acids. Diabetes 2010;59:2737-2746. https://doi.org/10.2337/db09-1716
100. Kuda O, Rossmeisl M, Kopecky J. Omega-3 fatty acids and adipose tissue biology. Mol Aspects Med 2018;64:147-160. https://doi.org/10.1016/j.mam.2018.01.004
101. Kuda O, Brezinova M, Rombaldova M, Slavikova B, Posta M, Beier P, Janovska P, Veleba J, Kopecky J, Jr., Kudova E, Pelikanova T, Kopecky J. Docosahexaenoic acid-derived fatty acid esters of hydroxy fatty acids (FAHFAs) with anti-inflammatory properties. Diabetes 2016;65:2580-2590. https://doi.org/10.2337/db16-0385
102. Batetta B, Griinari M, Carta G, Murru E, Ligresti A, Cordeddu L, Giordano E, Sanna F, Bisogno T, Uda S, Collu M, Bruheim I, Di Marzo V, Banni S. Endocannabinoids may mediate the ability of (n-3) fatty acids to reduce ectopic fat and inflammatory mediators in obese Zucker rats. J Nutr 2009;139:1495-1501. https://doi.org/10.3945/jn.109.104844
103. Rossmeisl M, Pavlisova J, Janovska P, Kuda O, Bardova K, Hansikova J, Svobodova M, Oseeva M, Veleba J, Kopecky J, Jr., Zacek P, Fiserova E, Pelikanova T, Kopecky J. Differential modulation of white adipose tissue endocannabinoid levels by n-3 fatty acids in obese mice and type 2 diabetic patients. Biochim Biophys Acta 2018;1863:712-725. https://doi.org/10.1016/j.bbalip.2018.03.011

104. Tedesco L, Valerio A, Dossena M, Cardile A, Ragni M, Pagano C, Pagotto U, Carruba MO, Vettor R, Nisoli E. Cannabinoid receptor stimulation impairs mitochondrial biogenesis in mouse white adipose tissue, muscle, and liver: the role of eNOS, p38 MAPK, and AMPK pathways. Diabetes 2010;59:2826-2836. https://doi.org/10.2337/db09-1881
105. Baker EJ, Miles EA, Burdge GC, Yaqoob P, Calder PC. Metabolism and functional effects of plant-derived omega-3 fatty acids in humans. Prog Lipid Res 2016;64:30-56. https://doi.org/10.1016/j.plipres.2016.07.002

REVIEW

Circadian Disruption as a Risk Factor for Development of Cardiovascular and Metabolic Disorders – From Animal Models to Human Population

Alena SUMOVÁ[1], Martin SLÁDEK[1]

[1]Laboratory of Biological Rhythms, Institute of Physiology of the Czech Academy of Sciences, Prague, Czech Republic

Received February 5, 2024
Accepted February 21, 2024

Summary

The lifestyle of human society is drifting apart from the natural environmental cycles that have influenced it since its inception. These cycles were fundamental in structuring the daily lives of people in the pre-industrial era, whether they were seasonal or daily. Factors that disrupt the regularity of human behaviour and its alignment with solar cycles, such as late night activities accompanied with food intake, greatly disturb the internal temporal organization in the body. This is believed to contribute to the rise of the so-called diseases of civilization. In this review, we discuss the connection between misalignment in daily (circadian) regulation and its impact on health, with a focus on cardiovascular and metabolic disorders. Our aim is to review selected relevant research findings from laboratory and human studies to assess the extent of evidence for causality between circadian clock disruption and pathology.

Keywords

Circadian clock • Chronodisruption • Metabolism • Cardiovascular disorders • Spontaneously hypertensive rat • Human • Social jetlag • Chronotype

Corresponding author

Alena Sumová, Institute of Physiology of the Czech Academy of Sciences, Videnska 1083, 14220 Prague, Czech Republic. Email: alena.sumova@fgu.cas.cz

Introduction

Physiological processes are controlled to maintain homeostasis, the basic principle that sustains a stable balance in the body under changing environmental conditions. Since some of these environmental changes are regularly repeated in cycles, organisms have evolved a mechanism that allows them to respond appropriately in anticipation of the changes in order to achieve homeostasis more effectively. Such a mechanism requires an internal timer, a "clock" that tracks time endogenously [1]. The best understood mechanism, called the circadian clock (from the Latin circa-diem; about a day), generates approximately 24-hour cycles that organize biological processes even in the absence of regular environmental cycles [2]. The circadian clock uses external signals that regularly oscillate with the period of the solar day to adjust its endogenous period to exactly 24 hours and achieve the correct phase relative to a particular time of day through a process known as entrainment [3]. The most important signal is the alternation of light and darkness, but other signals such as food availability, temperature, humidity, social interaction, the presence of predators, etc. are also relevant factors depending on the species. In everyday life, the human circadian clock is primarily controlled by exposure to light and food intake [2], i.e. by factors that are strongly dependent on the daily regime and lifestyle.

It is important to note that the presence of a circadian clock is not conditional for survival [4,5], especially for organisms that live in a constant environment where anticipation of environmental change is meaningless [6]. Such organisms are able to respond to a light/dark (LD) cycle and entrain to it in terms of behaviour and molecular rhythms, but become arrhythmic

immediately after transfer to constant darkness, as has been shown in the cavefish species Astyanax mexicanus [7]. However, organisms lacking the clock but living in a cyclic environment have been found to have shorter lifespans, whether in the laboratory [8] or in natural habitats [9]. The situation is even more detrimental when the clock is present but its resonance with the environmental and behavioral cycles is disturbed [10, 11]. This leads to the loss of internal synchrony between the clocks in our body, and eventually the circadian system cannot fulfill its role in predictive homeostasis. This situation applies to people living in contemporary societies where artificial light at night and unlimited access to food are predominant factors causing the internal desynchrony.

In this review, we contextualize data supporting the evidence that disruption of circadian regulation increases the risk of cardiometabolic disorders. The evidence comes mainly from experimental work in animal models, but also from studies in humans. Despite the exponential increase in our knowledge of these processes and the flood of reviews on this topic in the scientific literature, we argue that still more studies are needed to prove a causal relationship. Understanding the impact of our everyday lifestyle preferences on our health could pave the way to mitigate the detrimental effects of technological development on human health.

Complexity of the circadian system

There is a hierarchy between cellular circadian clocks in our body that determines their sensitivity to external signals and their role within the circadian system. Light is the dominant signal for the mammalian central clock in the suprachiasmatic nuclei of the hypothalamus (SCN), which is the only clock capable of perceiving it directly via a connection to the retina [12, 13]. The central clock entrains to a LD cycle and consequently drives 24-hour rhythms in multiple signals involving neural, hormonal and behavioral pathways to relay information about the time of day to peripheral clocks in other parts of the body (brain, liver, intestine, pancreas, heart, adipose tissue, etc.) (reviewed in [14-17]). The SCN has the most robust clock, whose sensitivity to non-photic rhythmic signals is much lower compared to light and depends on the signal, the species and the specific context (reviewed in [18]).

On the other hand, peripheral clocks depend on the non-photic signals derived from the SCN to maintain synchrony with the solar day (reviewed in [19]), although data suggest that individual clocks in the periphery may differ in their dependence on SCN signals [20]. For example, exposure of rats to constant light abolishes the rhythmic output of the SCN, as documented by behavioral arrythmicity, but affects clocks in the liver, duodenum and colon to a different extent [21]. One of the strongest entraining signals for most peripheral clocks are hormones such as glucocorticoids (reviewed in [22]), whose rhythmic production in the adrenal gland is under the control of the SCN [23, 24]. These hormones and their synthetic analog dexamethasone represent robust synchronizing cues for clocks not only in peripheral tissues [25], but also in extra-SCN brain regions [26, 27] and cell lines [28]. Nevertheless, even clocks in functionally related tissues of the gastrointestinal tract (jejunal mucosa, liver, renal cortex and epididymal adipose tissue) responded very differently to absence of circulating glucocorticoids due to adrenalectomy [29], demonstrating that signaling from the SCN to these clocks is tissue-specific and more complex. Changes in energy balance resulting from the feeding/fasting cycle controlled by the SCN clock are another example of a significant cue to which peripheral clocks in some tissues are highly sensitive [25, 30, 31]. However, similar to glucocorticoids, clocks in functionally related tissues of the gastrointestinal tract (liver, duodenum and colon) differ in their sensitivity to feeding [21]. Peripheral clocks also respond to other SCN-controlled signals such as body temperature cycles [32, 33] and autonomic nervous system activity (reviewed in [34]), but these are beyond the scope of our review.

All of these findings demonstrate that the synchrony between the clocks of the circadian system is fine-tuned to provide tissues with specific local temporal organizations in alignment with expected changes in the environment over the solar day. Understanding the complexity and specificity of the pathways that synchronize clocks in individual cells is one of the major challenges of chronobiology.

How do circadian clocks control cellular processes?

The interaction between the molecular clock machinery and a specific physiological process begins at the cellular level. The circadian signal results from a mechanism based on mutually interlocked transcriptional-translational feedback loops (TTFLs) that

autonomously activate and inhibit the expression of a set of clock genes in cycles with a circadian period. The protein products of these clock genes serve as transcription factors that rhythmically activate (positive elements) or inhibit (negative elements) the expression of genes inside and outside the feedback loop. In this way, the TTFL drives the rhythm of a large number of clock-controlled genes that encode either transcription factors or "functional" proteins directly involved in cell functions. The mechanism of mammalian TTFL has already been reviewed many times in detail [35-38], so we only provide a brief overview of the process here. At the core of the clock mechanism, a feedback loop is formed by *Clock, Npas2* and *Bmal1* (also known as *Arntl*) as positive elements and *Per1,2,3* and *Cry1,2* as negative elements. *Bmal1* is the only clock gene whose absence cannot be substituted, as its functional paralog's (*Bmal2*) expression is tissue-specific and dependent on *Bmal1*. Its rhythmic expression is controlled by a secondary feedback loop in which *Rorα,β,γ* and *Nr1d1,2* (also known as *Rev-Erbα,β*) participate as positive and negative elements, respectively. In additional feedback loops, the rhythmic expression of *Nr1d1,2* is directly controlled by *Clock, Npas2* and *Bmal1*, and the expression of *Rorα,β,γ* is controlled by *Dbp* (regulated by *Clock* and *Bmal1*) and *Nfil3* (also known as *E4bp4*, regulated by *Rorα,β,γ* and *Dbp*). All loops are interdependent, which enables their mutual coordination. The approximately 24-hour period of TTFL is maintained by complex posttranscriptional (e.g. RNA methylation) and posttranslational mechanisms mediated by several kinases (CK1ε, CK1δ, GSK3β, etc.), ubiquitin ligases (β-TrCP, FBXL3,21), enyzymes involved in protein glycosylation, acetylation or SUMOylation that modulate the activity, stability or dynamics of the bidirectional nuclear-cytoplasmic transport of clock proteins (reviewed in [39]). It is important to note that although the genes referred to as "clock genes" are necessary for the clock machinery, they also fulfil functions outside the circadian system. Therefore, genetic deletion of any of the clock genes can affect the function of the clock, but also disrupt other cellular functions *via* clock-independent mechanisms [40-42]. Conversely, since TTFL-indepen-dent [43] circadian regulation has been documented as a likely evolutionarily conserved mechanism even in human cells [44], deletion of the clock genes may theoretically not abolish rhythmicity at all levels of biological regulation.

While the vast majority of cells are capable of generating cellular circadian rhythms, there is great variability in the self-sustainability and robustness of the rhythms, which is largely determined by the level of the intercellular communication network that facilitates rhythmicity at both the cellular and tissue level. The SCN is a unique example of a clock built of cellular oscillators that are more or less self-sustaining when separated from each other [45], but generate much more robust rhythmicity when their intercellular communication is preserved (reviewed in [13]). The intercellular communication depends on sodium channel action potentials [46], interneuronal neuropeptide signaling [47-49] and neuron/glia interactions [50-52]. In addition, a recent study pointed to the involvement of cilia in a subpopulation of SCN neurons as an important subcellular component for their synchronization [53]. For synchronization of the peripheral clocks, inter-cellular communication was not expected to be important [54], as they were thought to be driven by SCN-related signals. However, recent research has shown that such communication, which is likely paracrine, can contribute to the rhythmicity of cellular oscillators in hepatocytes [55]. These results indicate that the circadian system must be synchronized at multiple levels – *level 1*: with the external environment, *level 2*: between central and peripheral clocks, and *level 3*: between cellular oscillators in the same tissue. This organization highlights the potential multiple targets where the coherence of the circadian system can be compromised.

What do we mean by chronodisruption?

The term chronodisruption was introduced as an equivalent to "circadian disruption" to refer to disrupted circadian regulation in consequence of misalignment of entraining signals with environmental cycles, causing internal desynchrony between oscillators in the organism. Many comprehensive reviews have been published on this topic [56-59].

In pre-industrial communities that were dependent on sunlight, chronodisruption was unlikely due to behavioral activities associated with daylight and the onset of sleep linked to sunset. The spectrum and intensity of light from fire or the moon, the only available light sources, were not efficient enough to disrupt synchrony with the solar cycle as people spent much time outdoors and were maximally exposed to natural daylight. Moreover, the journey across time zones, if happened, took much longer than necessary to resynchronize the clock to solar time at the destination. In

the real life of modern societies where electric light sources are available, chronodisruption may result from the decision to postpone our activities to the time interval that our clock determines as "subjective night". It happens due to personal choices related to work requirements or leisure activities. Additionally, the use of artificial light to extend our active time into the night appears to be facilitated by our personal preference for timing of activity/sleep, known as chronotype [60-62]. The combination of these factors leads to chrono-disruption.

Ambient electric light at night per se ("light pollution") is often blamed for chronodisruption and its health consequences. However, it is important to clarify that this light would not exist if there was no demand for people to be active at night and for most people in the population, unlike for animals and plants in the wild, exposure to light at night is actually controllable. Humans can adapt behavior to the conditions of life in urban society by exposing to outdoor light as much as possible during the day, shielding ambient light with blinds at night, and avoiding nighttime activities associated with light exposure whenever possible. Using the findings from chronobiology research provides us with a guide on how to properly synchronize our internal clock and points to the importance of such adaptation to the conditions of modern societal lifestyles. While light at night is massively medialized as a cause of chronodisruption, we hear much less about the lack of light during the day. City dwellers in particular spend most of the day indoors and are shielded from natural daylight [63]. Houses, schools and factory halls are often built with inadequate indoor lighting, and the intensity and spectral properties of light from electric bulbs cannot fully replace natural daylight. As a result, urban population is not exposed to sufficient natural daylight, which is crucial for proper entrainment of circadian clocks with solar cycle. Chronotype *per se* is also not the cause of chronodisruption, as people with late chronotype, who prefer to shift their activities to the late night hours, are able to entrain to the solar cycle by exposing themselves fully to natural daylight and avoiding light at night [64].

Furthermore, in real life, many people voluntarily place themselves in situations that lead to internal desynchronization when they are on trans-meridian flights that span more than six time zones. Under such conditions, most people experience jetlag symptoms because their internal time is dictated by the endogenous clock, that is out of sync with the social time at their destination [65, 66]. These symptoms persist until their clocks attain resonance with the new environmental cycles and begin to fulfill their role in the temporal organization of physiological processes. For the majority of the population, such a situation is not frequent and long-term impact on health is not documented. Nevertheless, this is probably the best evidence of the benefits of having our clocks well-synchronized that each person can experience individually.

Of course, modern society requires human-powered services around the clock, forcing part of the population to work during the night, expose themselves to intensive artificial light, and eat and sleep at inconvenient times of the day. Around 20 % of the world's population work night shifts, forcing them to be physically, mentally and metabolically active during their subjective night [67]. Despite progressive technological development, including robotization and artificial intelligence, many professions, such as healthcare, will continue to require human labour around the clock. Therefore, we need to understand the biological underpinnings of this altered human behavior and ascertain its link to pathology in order to reduce the detrimental impact on society's health.

How to study chronodisruption?

Using animal models, chronodisruption can be experimentally induced genetically (by disruption or alteration of molecular clocks in various organs), surgically (by removal of the suprachiasmatic nuclei as the site of the central clock) or by environmental conditions (by exposure to conditions that jeopardise synchrony between internal and social time). For the latter, several methods have been developed in chronobiological research that effectively induce internal desynchrony via various mechanisms, such as long-term exposure to constant light (LL), repeated shifts in the LD cycle, irregular LD regimen, a non-24-hour LD cycle, and decoupling access to food and sleep time. The research is mainly conducted with laboratory rodents, that are nocturnal species and differ in their sensitivity to the choronodisruption protocols [57, 68]. Therefore, the results can be translated to the human situation with limitations [69].

In experimental research on humans, it is a question of ethical standards whether and to what extent subjects can be exposed to unfavorable conditions that could affect their health. The gold standard for

experimentally inducing chronodisruption is the forced desynchrony protocol [70, 71], in which subjects are exposed to a 20- or 28-hour daily regimen of the scheduled sleep/wake cycle and mealtime in dim LD cycle. The period of this cycle is too extreme for the SCN clock to entrain, so that after a few days it becomes uncoupled from the imposed sleep/wake cycle and begins to run freely with the endogenous period. As a result, such subjects sleep when their clocks are preparing their bodies for activity and vice versa, as is the case with night shiftwork. These studies provided important insights into the impact of chronodisruption on circadian organization at the level of circadian regulation of the transcriptome [72] and the development of pathology [73]. Strikingly, hyperglycemia, insulin resistance, poor glucose tolerance, increased arterial pressure, and reversed cortisol rhythms developped in human participants exposed to a forced desynchrony protocol when they were approximately 12 hours out of phase with the environmental LD cycle [73]. The advantage of these studies is their well-controlled design and the ability to accurately capture the actual state of the circadian clock, but they are limited by high costs and a small sample size that cannot achieve population representativeness. Therefore, large-scale, population-representative studies are being conducted to analyze correlations between circadian misalignment and health parameters (see below).

Multilevel effect of chronodisruption on circadian regulation in our body

Chronodisruption disrupts synchrony in the circadian system at all levels defined above. This is because the clocks in cell populations that span anatomical boundaries are sensitive to the same entraining signals, and the clocks in cells of the same anatomical structure can be sensitive to different entraining signals (Fig. 1).

Food intake restricted to rest/sleep time only (mistimed feeding) impairs synchrony between the SCN clock and clocks in metabolically relevant tissues [25]. However, the desynchrony has more levels. An example from our recent study showed that desynchrony can occur even between functionally distinct cellular subpopulations of the same organ [74]. We found that restricting food intake to the light phase in nocturnal animals (sleep time) robustly shifted the circadian clock in the pancreatic islets to feeding time, just like the clock

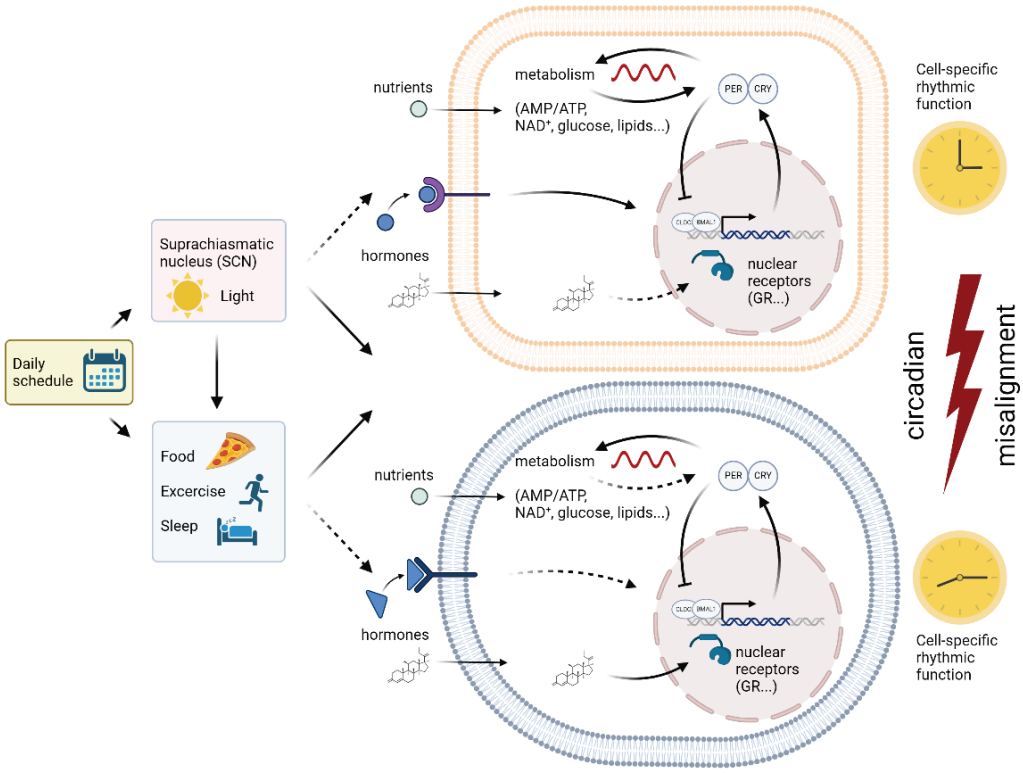

Fig. 1. Circadian misalignment results from desynchrony among cellular oscillators. Circadian clock in different cell types (depicted by different shapes and colour) may differ in their sensitivity to rhythmic cues, such as light-dark cycle entrained SCN cues, activity or food, resulting in circadian misalignment between their rhythmic functions when the cues are out of sync with each other (for example due to social jetlag). Full vs. dashed arrows indicate differences in relative strength of entrainment. Created with BioRender.com

in the liver, but severely dampened the clocks in the cells of the exocrine pancreatic tissue [74]. The mechanism behind this effect was attributed to a different sensitivity of the clocks in these two functionally distinct cellular subpopulations to two different hormones, insulin and corticosterone. These hormones are released rhythmically, with their peaks synchronized under *ad libitum* conditions, but uncoupled under the reversed feeding protocol [74]. The effect of mistimed feeding on the suppression of the rhythmicity of the exocrine pancreas is rather unexpected and may underlie its dysfunction. It gives rise to speculation about its initially potential adaptive value. If food is not provided at the opportune and predictable time for a short period, it might be more advantageous to turn off the clock, which is not needed to anticipate it, but to operate on an "as-needed" basis to supply the organism with energy as needed for survival. An analogous situation arises for organisms living in an environment where there are no daily cycles (high latitudes, deep water/caves), where anticipating daily cycles is not meaningful [7, 75]. However, in the case of presence of daily cycles, such a situation leads to pathology.

Experimental chronodisruption impairs cardiometabolic health – lessons from "old-fashioned" animal models

Research on the relationship between chronodisruption and cardiometabolic disorders has focused on revealing their causality. One of the “classic studies” demonstrating the impact of chronodisruption on cardiovascular health used tau mutant hamsters, an animal model with a spontaneously mutated clock. The hamsters carried a single autosomal mutation in the gene encoding the enzyme *casein kinase 1 epsilon* (CKIe), which resulted in a significant shortening of the period of free-running activity rhythms (to approximately 22 hours in heterozygotes and 20 hours in homozygotes) [76]. Keeping the tau mutant hamsters in LD12:12 shortened their survival time and led to the development of renal dysfunction and cardiomyopathy with fibrosis and impaired contractility. This effect occurred only in the heterozygotes but not in the homozygotes, which remained free-running because the LD cycle was out of entrainment range for their SCN clock [77, 78]. Survival and pathology was improved if the heterozygotes were either SCN lesioned and thus became arrhythmic, or if they were maintained on their endogenous day length of 22 hours (LD11:11). These studies paved the way for the current understanding that long-term maladaptation to environmental cycles, which is highly relevant to the human situation, has adverse health impact. Moreover, these studies showed that such a situation is more harmful than that resulting from the absence of the clock or its inability to predict environmental cycles [79]. In this case, when investigating the impact of a non-resonant clock on health, the tau mutant hamster was discovered not only as a model with a mutated clock, but also as an experimental model for the cardiovascular disease.

The opposite approach was based on the study of the circadian phenotype of an animal model already known for the spontaneous development of cardiometabolic disorders, namely the *spontaneously hypertensive rat* (SHR), that identified the rat strain as a model for a maladapted circadian system [80, 81]. The SHR strain has been used as a popular model to study the mechanism of hypertension since its introduction in the early sixties of the last century [82], and later it was also used as a model for *attention deficit hyperactivity disorder* (ADHD) [83] or metabolic syndrome [84]. From this perspective, and in comparison to mouse models with targeted deletion of a single gene, the model is considered outdated for studies on the mechanisms of disrupted circadian regulation. However, the pathophysiology of most disorders, including hypertension or ADHD, involves multiple genes and signaling pathways, so this model remains a valuable complementary tool for studying the complex mechanisms involved in the development of these disorders. Several earlier studies pointed to the possibility that circadian regulation in SHR differs from that of normotensive controls. In particular, the early discovery that the day/night ratio of blood pressure is reduced [85] and sleep patterns are modulated [86] prompted investigation of the circadian system in SHR. One study reported increased expression of the *vasoactive intestinal polypeptide* (VIP) gene in the SCN of SHR [87], which may influence SCN clock function by enhancing intercellular communication [49]. The finding fits with a recent report that SCN-driven behavioral rhythms are more stable and less fragmented in SHR [88]. However, the amplitude of clock gene expression profiles in the SCN of SHR was not reduced [80]. The period of the peripheral clock of SHR fibroblasts measured in vitro with real-time recordings of the *Bmal1-dLuc* reporter also did not differ from that of controls [32]. Furthermore, although SHR did not differ in level of locomotor activity in LD12:12 or constant

darkness compared to normotensive controls, the amplitudes of SHR activity rhythms were reduced in both conditions [80]. For the clock gene and clock-controlled gene expression profiles in the peripheral tissues of SHR, higher amplitudes were reported in the heart but not in the aorta [89] and liver [80], while a reduced amplitude was found in the colon [80]. In addition, the onset of behavioral activity and phases of clocks were significantly advanced in the SCN and colon in SHR compared to controls [80]. This reflects the positive phase angle of entrainment of their clocks relative to the LD cycle, which resembles an earlier chronotype in humans (see below).

Even more striking evidence of the abnormal circadian phenotype of SHR came from the finding that SHR were more sensitive to mistimed feeding compared to controls. SHR developed earlier and more pronounced anticipatory activity prior to the presence of food, and their activity profile shifted entirely to mealtime, in contrast to control rats, which only redistributed their activity into two bouts, one nocturnal and one associated with the anticipation and presence of food [81]. As a potential mechanism, the expression rhythm of clock gene *Bmal2* (a paralog of *Bmal1*) increased in the liver of SHR in contrast to controls and was advanced to a similar phase as *Bmal1* due to the altered feeding regime. It is tempting to speculate that the higher response of the *Bmal2* gene to mistimed feeding was likely the reason why the expression profiles of other clock genes were not attenuated as in controls and were more shifted to mealtime in SHR, because the facilitated BMAL2::CLOCK-mediated transactivation could assist the canonical BMAL1::CLOCK mechanism and enhance clock oscillations [81]. Since *Bmal2* expression in the liver is dependent on its paralog *Bmal1*, the data are consistent with other studies showing a possible direct link between the pathological phenotype of SHR and the circadian system through an association between *Bmal1* promoter polymorphisms and metabolic syndrome in SHR [90]. A better understanding of the mechanisms would be necessary as the *Bmal1* promoter acts as one of the major "hubs" linking the circadian system to metabolism (reviewed in [91]).

Surprisingly, despite the well-defined cardiometabolic pathology and circadian abnormality of SHR, evidence for their causal relationship is sparse, and the important question of whether circadian system dysfunction is involved in the development of the disease remains to be answered. Nevertheless, several studies suggest that strengthening circadian regulation may improve the pathologic phenotype of SHR. The introduction of a regular feeding regime at an appropriate time of day led to a restoration of the diurnal rhythm of blood pressure as well as clock- and metabolism-related gene expression in cardiovascular tissues [92]. In addition, caloric restriction prevented hypertension in SHR [93]. In our opinion, the most compelling evidence comes from a study in which both circadian disruption and pathology were reversed by aligning the developing clocks of SHR pups with LD cycle since birth [94]. Maternal care provided by a foster mother of a normotensive control strain (Wistar rat) promoted the development of rhythmic *Bmal1* expression in the SCN clock as well as the clock-driven activity/rest rhythm in SHR pups. Importantly, the activity/rest rhythm of the pups was aligned with the external LD cycle, thereby protecting the SHR pups from developing the typical phase-advanced phenotype. Surprisingly, proper entrainment of the circadian system by maternal care was able to improve the dampened rhythm of the colonic clock as well as certain cardiovascular functions. Specifically, the increase in heart rate that SHR spontaneously develops with age was not present in offspring raised with aligned circadian clocks [94]. The results provide evidence that modulation of circadian regulation can attenuate pathological symptoms in SHR, even when the development of heart rate is genetically programmed.

What can we learn from human population studies?

It is estimated that up to half of the population in industrialized societies have a circadian clock that is out of sync with their daily schedule [95], with cardiovascular [96, 97] and metabolic [98, 99] diseases being the most common consequences. As mentioned above, population-based studies are an alternative way of gaining insight into the relationship between chronodisruption and human health. Their advantage is that they reflect the real situation in a larger population sample, but their disadvantage is low level of their control and the fact that they cannot prove causality, but only correlation with a study-specific degree of statistical power, which makes the conclusions less straightforward. Here the postulate "*the larger the sample, the higher the statistical power*" appears to be even more relevant. It is also important to keep in mind that this type of study

requires multifactorial statistics. Let us give an example of a pitfall when the multifactorial complexity is underestimated. In the literature and in the media, we are confronted with statements such as "*light pollution causes cancer because it is more common in people who live in larger cities and thus are exposed to more light at night*". This statement is based on making a causal link between the light-induced suppression of nocturnal production of the hormone melatonin in the pineal gland and the results indicating a possible protective role of the hormone in the development of certain types of cancer. It may be true that there is more light pollution in larger cities, and it may also be true that cancer is more common in larger cities, but can we really approximate causality so simply? Although these two factors could hypothetically be related, their direct link is rather vague and supported by weak evidence. Urban populations are certainly more exposed to many other potent cancer risk factors than rural populations. Furthermore, there is insufficient evidence that the light-senstitive melatonin produced in the pineal gland is responsible for the anticancer effects, considering that its main physiological role is to transmit information to the organism about the changing ambient light. Instead, it is more likely that the presumably not photosensitive melatonin produced in various tissues plays a role in these processes [100]. As mentioned above, nocturnal light is undoubtedly a dominant factor that disrupts the synchrony of the circadian clock with the LD cycle, but the same is true for ambient lighting in the city and for indoor light emitted by overhead lamps or electronic devices such as televisions or computer monitors. It is well documented that constant light, when chronic, disrupts circadian regulation in nocturnal species that are highly light-sensitive, however, it does not affect their sleep but their activity during nocturnal wakefulness [101]. In humans, the opposite is true: light at night impairs sleep. In addition, recent evidence suggests that the mechanism by which the SCN clock perceives light from the retina differs between nocturnal rodents and humans [102]. These facts point to the limitations of simply transferring the data on the effects of light from nocturnal animals to humans.

Most population-based studies on the prevalence of chronodisruption are based on online internet surveys, which, although aimed at a large cross-national sample, are not fully representative (limited internet access, language barrier, level of interest, etc.). Filling out specialized questionnaires can also involve a bias resulting from knowledge of the purpose for which they are created. This can be overcome by a more difficult and more labor- and cost-intensive population-representative study, which may, however, be limited by political geography (country). Therefore, the results of both approaches are valuable for population-wide explorations.

Numerous studies that provided evidence of an association between chronodisruption and impaired health focused on pre-specified subpopulations, e.g., shift workers, specific employment types or extreme chronotypes. Rotational shift work is the most devastating factor associated with increased cardiovascular risk, obesity, high triglyceride and low HDL cholesterol levels as markers of the development of metabolic syndrome [103]. Interestingly, in the population of non-shift workers similar cardiovascular and metabolic health markers correlated with (1) an extreme chronotype, defined as a preference for sleep time on free days significantly deviating from the population mean [63, 104-106], and (2) social jetlag, defined as the extent of misalignment between sleep time on work days and free days [107-110]. Chronotype and social jetlag are closely inter-related and positively correlated, and both concepts have been described in more detail elsewhere [62, 111]. Therefore, population studies indicate that chronodisruption, resulting from the maladaptation of the internal clock to solar time, whether induced by shiftwork or other lifestyle factors, exerts a comparable impact on cardiometabolic health.

Conclusion

Technological development is accelerating rapidly and outpacing human evolutionary adaptation. There is strong evidence that chronodisruption results from this conflict and is associated with adverse health outcomes, of which cardiometabolic disorders are the most prevalent. To avoid the impact on our health, human society cannot return to preindustrial lifestyle. Instead, further research is needed to uncover the underlying mechanisms to propose strategies for knowledge-based adaptation of our everyday life and protection of human health in the face of rapidly evolving environmental changes.

Abbreviations

ADHD, Attention Deficit Hyperactivity Disorder; BMAL1,2, Brain and Muscle Arnt-Like protein 1, 2;

β-TrCP, Beta-Transducin Repeat Containing Protein; CK1ε, δ, Casein Kinase 1 epsilon, delta; CLOCK, Circadian Locomotor Output Cycle Kaput; *dLuc*, destabilized Luciferase; FBXL3, 21, F-Box And Leucine Rich Repeat Protein 3, 21; GSK3β, Glycogen Synthase Kinase 3 Beta; LD, Light-Dark cycle; LL, constant light; SHR, Spontaneously Hypertensive Rat; SCN, Suprachiasmatic Nucleus; TTFL, Transcriptional-Translational Feedabck Loop; VIP, Vasoactive Intestinal Polypeptide.

Conflict of Interest

There is no conflict of interest.

Acknowledgements

This research was supported by the project National Institute for Research of Metabolic and Cardiovascular Diseases (Programme EXCELES, ID Project No. LX22NPO5104) - Funded by the European Union-Next Generation EU.

References

1. Pittendrigh CS. Circadian rhythms and the circadian organization of living systems. Cold Spring Harb Symp Quant Biol 1960;25: 159-184. https://doi.org/10.1101/SQB.1960.025.01.015
2. Aschoff J, Fatransk.M, Giedke H, Doerr P, Stamm D, Wisser H. Human circadian rhythms in continuous darkness - entrainment by social cues. Science 1971;171: 213-215 https://doi.org/10.1126/science.171.3967.213
3. Pittendrigh CS. Circadian systems: Entrainment. In: *Handbook of Behavioural Neurobiology*, vol 4, Biological Rhythms, Aschoff J (ed) New York: Plenum, 1981, pp 95-124. https://doi.org/10.1007/978-1-4615-6552-9_7
4. Ruby NF, Dark J, Heller HC, Zucker I. Ablation of suprachiasmatic nucleus alters timing of hibernation in ground squirrels. Proc Natl Acad Sci U S A 1996;93: 9864-9868. https://doi.org/10.1073/pnas.93.18.9864
5. Menaker M, Vogelbaum MA. Mutant circadian period as a marker of suprachiasmatic nucleus function. J Biol Rhythms 1993;8 Suppl: S93-98.
6. 6. Reierth E, Stokkan KA. Biological rhythms in arctic animals. In: *Biological Rhythms*, Kumar V (ed) Berlin, Heidelberg: Springer Berlin Heidelberg, 2002, pp 216-223. https://doi.org/10.1007/978-3-662-06085-8_18
7. Beale A, Guibal C, Tamai TK, Klotz L, Cowen S, Peyric E, Reynoso VH, et al. Circadian rhythms in Mexican blind cavefish Astyanax mexicanus in the lab and in the field. Nat Commun 2013;4: 2769. https://doi.org/10.1038/ncomms3769
8. Kondratov RV, Kondratova AA, Gorbacheva VY, Vykhovanets OV, Antoch MP. Early aging and age-related pathologies in mice deficient in BMAL1, the core componentof the circadian clock. Genes Dev 2006;20: 1868-1873. https://doi.org/10.1101/gad.1432206
9. DeCoursey PJ, Krulas JR, Mele G, Holley DC. Circadian performance of suprachiasmatic nuclei (SCN)-lesioned antelope ground squirrels in a desert enclosure. Physiol Behav 1997;62: 1099-1108. https://doi.org/10.1016/S0031-9384(97)00263-1
10. Spoelstra K, Wikelski M, Daan S, Loudon AS, Hau M. Natural selection against a circadian clock gene mutation in mice. Proc Natl Acad Sci U S A 2016;113: 686-691. https://doi.org/10.1073/pnas.1516442113
11. Park N, Cheon S, Son GH, Cho S, Kim K. Chronic circadian disturbance by a shortened light-dark cycle increases mortality. Neurobiol Aging 2012;33: 1122 e1111-1122. https://doi.org/10.1016/j.neurobiolaging.2011.11.005
12. Klein DC, Moore RY, Reppert SM. Suprachiasmatic nucleus : the mind's clock. Oxford University Press, New York 1991.
13. Hastings MH, Maywood ES, Brancaccio M. Generation of circadian rhythms in the suprachiasmatic nucleus. Nat Rev Neurosci 2018;19: 453-469. https://doi.org/10.1038/s41583-018-0026-z
14. Menaker M, Murphy ZC, Sellix MT. Central control of peripheral circadian oscillators. Curr Opin Neurobiol 2013;23: 741-746. https://doi.org/10.1016/j.conb.2013.03.003
15. Mohawk JA, Takahashi JS. Cell autonomy and synchrony of suprachiasmatic nucleus circadian oscillators. Trends Neurosci 2011;34: 349-358. https://doi.org/10.1016/j.tins.2011.05.003
16. Panda S. Circadian physiology of metabolism. Science 2016;354: 1008-1015. https://doi.org/10.1126/science.aah4967

17. Begemann K, Neumann AM, Oster H. Regulation and function of extra-SCN circadian oscillators in the brain. Acta Physiol (Oxf) 2020: e13446. https://doi.org/10.1111/apha.13446
18. Jha PK, Bouaouda H, Kalsbeek A, Challet E. Distinct feedback actions of behavioural arousal to the master circadian clock in nocturnal and diurnal mammals. Neurosci Biobehav Rev 2021;123: 48-60. https://doi.org/10.1016/j.neubiorev.2020.12.011
19. Dibner C, Schibler U, Albrecht U. The mammalian circadian timing system: organization and coordination of central and peripheral clocks. Annu Rev Physiol 2010;72: 517-549. https://doi.org/10.1146/annurev-physiol-021909-135821
20. Yamazaki S, Numano R, Abe M, Hida A, Takahashi R, Ueda M, Block GD, et al. Resetting central and peripheral circadian oscillators in transgenic rats. Science 2000;288: 682-685. https://doi.org/10.1126/science.288.5466.682
21. Polidarova L, Sladek M, Sotak M, Pacha J, Sumova A. Hepatic, duodenal, and colonic circadian clocks differ in their persistence under conditions of constant light and in their entrainment by restricted feeding. Chronobiol Int 2011;28: 204-215. https://doi.org/10.3109/07420528.2010.548615
22. Dickmeis T. Glucocorticoids and the circadian clock. J Endocrinol 2009;200: 3-22. https://doi.org/10.1677/JOE-08-0415
23. Moore RY, Eichler VB. Loss of a circadian adrenal corticosterone rhythm following suprachiasmatic lesions in the rat. Brain Res 1972;42: 201-206. https://doi.org/10.1016/0006-8993(72)90054-6
24. Ishida A, Mutoh T, Ueyama T, Bando H, Masubuchi S, Nakahara D, Tsujimoto G, et al. Light activates the adrenal gland: timing of gene expression and glucocorticoid release. Cell Metab 2005;2: 297-307. https://doi.org/10.1016/j.cmet.2005.09.009
25. Damiola F, Le Minh N, Preitner N, Kornmann B, Fleury-Olela F, Schibler U. Restricted feeding uncouples circadian oscillators in peripheral tissues from the central pacemaker in the suprachiasmatic nucleus. Genes Dev 2000;14: 2950-2961. https://doi.org/10.1101/gad.183500
26. Liska K, Sladek M, Cecmanova V, Sumova A. Glucocorticoids reset circadian clock in choroid plexus via period genes. J Endocrinol 2021;248: 155-166. https://doi.org/10.1530/JOE-20-0526
27. Liska K, Sladek M, Houdek P, Shrestha N, Luzna V, Ralph MR, Sumova A. High sensitivity of circadian clock in the hippocampal dentate gyrus to glucocorticoid- and GSK3beta-dependent signals. Neuroendocrinology 2021;112: 384-398. https://doi.org/10.1159/000517689
28. So AY, Bernal TU, Pillsbury ML, Yamamoto KR, Feldman BJ. Glucocorticoid regulation of the circadian clock modulates glucose homeostasis. Proc Natl Acad Sci U S A 2009;106: 17582-17587. https://doi.org/10.1073/pnas.0909733106
29. Sotak M, Bryndova J, Ergang P, Vagnerova K, Kvapilova P, Vodicka M, Pacha J, et al. Peripheral circadian clocks are diversely affected by adrenalectomy. Chronobiol Int 2016;33: 520-529. https://doi.org/10.3109/07420528.2016.1161643
30. Hara R, Wan K, Wakamatsu H, Aida R, Moriya T, Akiyama M, Shibata S. Restricted feeding entrains liver clock without participation of the suprachiasmatic nucleus. Genes Cells 2001;6: 269-278. https://doi.org/10.1046/j.1365-2443.2001.00419.x
31. Vollmers C, Gill S, DiTacchio L, Pulivarthy SR, Le HD, Panda .S Time of feeding and the intrinsic circadian clock drive rhythms in hepatic gene expression. Proc Natl Acad Sci U S A 2009;106: 21453-21458. https://doi.org/10.1073/pnas.0909591106
32. Sladek M, Sumova A. Entrainment of spontaneously hypertensive rat fibroblasts by temperature cycles. PLoS One 2013;8: e77010. https://doi.org/10.1371/journal.pone.0077010
33. Buhr ED, Yoo SH, Takahashi JS. Temperature as a universal resetting cue for mammalian circadian oscillators. Science 2010;330: 379-385. https://doi.org/10.1126/science.1195262
34. Riganello F, Prada V, Soddu A, di Perri C, Sannita WG. Circadian Rhythms and Measures of CNS/Autonomic Interaction. Int J Environ Res Public Health 2019;16: 2336. https://doi.org/10.3390/ijerph16132336
35. Cox KH, Takahashi JS. Circadian clock genes and the transcriptional architecture of the clock mechanism. J Mol Endocrinol 2019;63: R93-R102. https://doi.org/10.1530/JME-19-0153
36. Patke A, Young MW, Axelrod S. Molecular mechanisms and physiological importance of circadian rhythms. Nat Rev Mol Cell Biol 2020;21: 67-84. https://doi.org/10.1038/s41580-019-0179-2

37. Reppert SM, Weaver DR. Molecular analysis of mammalian circadian rhythms. Annu Rev Physiol 2001;63: 647-676. https://doi.org/10.1146/annurev.physiol.63.1.647
38. Takahashi JS. Transcriptional architecture of the mammalian circadian clock. Nat Rev Genet 2017;18: 164-179. https://doi.org/10.1038/nrg.2016.150
39. Reinke H, Asher G. Crosstalk between metabolism and circadian clocks. Nat Rev Mol Cell Biol 2019;20: 227-241. https://doi.org/10.1038/s41580-018-0096-9
40. Ramos CA, Ouyang C, Qi Y, Chung Y, Cheng CT, LaBarge MA, Seewaldt VL, et al. A Non-canonical Function of BMAL1 Metabolically Limits Obesity-Promoted Triple-Negative Breast Cancer. iScience 2020;23: 100839. https://doi.org/10.1016/j.isci.2020.100839
41. McKee CA, Polino AJ, King MW, Musiek ES. Circadian clock protein BMAL1 broadly influences autophagy and endolysosomal function in astrocytes. Proc Natl Acad Sci U S A 2023;120: e2220551120. https://doi.org/10.1073/pnas.2220551120
42. Griffin P, Dimitry JM, Sheehan PW, Lananna BV, Guo C, Robinette ML, Hayes ME, et al. Circadian clock protein Rev-erbalpha regulates neuroinflammation. Proc Natl Acad Sci U S A 2019;116: 5102-5107. https://doi.org/10.1073/pnas.1812405116
43. Edgar RS, Green EW, Zhao Y, van Ooijen G, Olmedo M, Qin X, Xu Y, et al. Peroxiredoxins are conserved markers of circadian rhythms. Nature 2012;485: 459-464. https://doi.org/10.1038/nature11088
44. O'Neill JS, Reddy AB Circadian clocks in human red blood cells. Nature 2011;469: 498-503. https://doi.org/10.1038/nature09702
45. Welsh DK, Logothetis DE, Meister M, Reppert SM Individual neurons dissociated from rat suprachiasmatic nucleus express independently phased circadian firing rhythms. Neuron 1995;14: 697-706. https://doi.org/10.1016/0896-6273(95)90214-7
46. Yamaguchi S, Isejima H, Matsuo T, Okura R, Yagita K, Kobayashi M, Okamura H. Synchronization of cellular clocks in the suprachiasmatic nucleus. Science 2003;302: 1408-1412. https://doi.org/10.1126/science.1089287
47. Aton SJ, Colwell CS, Harmar AJ, Waschek J, Herzog ED. Vasoactive intestinal polypeptide mediates circadian rhythmicity and synchrony in mammalian clock neurons. Nat Neurosci 2005;8: 476-483. https://doi.org/10.1038/nn1419
48. Harmar AJ, Marston HM, Shen S, Spratt C, West KM, Sheward WJ, Morrison CF, et al. The VPAC(2) receptor is essential for circadian function in the mouse suprachiasmatic nuclei. Cell 2002;109: 497-508. https://doi.org/10.1016/S0092-8674(02)00736-5
49. Patton AP, Edwards MD, Smyllie NJ, Hamnett R, Chesham JE, Brancaccio M, Maywood ES, et al. The VIP-VPAC2 neuropeptidergic axis is a cellular pacemaking hub of the suprachiasmatic nucleus circadian circuit. Nat Commun 2020;11: 3394. https://doi.org/10.1038/s41467-020-17110-x
50. Brancaccio M, Edwards MD, Patton AP, Smyllie NJ, Chesham JE, Maywood ES, Hastings MH. Cell-autonomous clock of astrocytes drives circadian behavior in mammals. Science 2019;363: 187-192. https://doi.org/10.1126/science.aat4104
51. Brancaccio M, Patton AP, Chesham JE, Maywood ES, Hastings MH. Astrocytes Control Circadian Timekeeping in the Suprachiasmatic Nucleus via Glutamatergic Signaling. Neuron 2017;93: 1420-1435 e1425. https://doi.org/10.1016/j.neuron.2017.02.030
52. Tso CF, Simon T, Greenlaw AC, Puri T, Mieda M, Herzog ED. Astrocytes Regulate Daily Rhythms in the Suprachiasmatic Nucleus and Behavior. Curr Biol 2017;27: 1055-1061. https://doi.org/10.1016/j.cub.2017.02.037
53. Tu HQ, Li S, Xu YL, Zhang YC, Li PY, Liang LY, Song GP, et al. Rhythmic cilia changes support SCN neuron coherence in circadian clock. Science 2023;380: 972-979. https://doi.org/10.1126/science.abm1962
54. Yoo SH, Yamazaki S, Lowrey PL, Shimomura K, Ko CH, Buhr ED, Siepka SM, et al. PERIOD2::LUCIFERASE real-time reporting of circadian dynamics reveals persistent circadian oscillations in mouse peripheral tissues. Proc Natl Acad Sci U S A 2004;101: 5339-5346. https://doi.org/10.1073/pnas.0308709101
55. Sinturel F, Gos P, Petrenko V, Hagedorn C, Kreppel F, Storch KF, Knutti D, et al. Circadian hepatocyte clocks keep synchrony in the absence of a master pacemaker in the suprachiasmatic nucleus or other extrahepatic clocks. Genes Dev 2021;35: 329-334. https://doi.org/10.1101/gad.346460.120

56. Golombek DA, Casiraghi LP, Agostino PV, Paladino N, Duhart JM, Plano SA, Chiesa JJ. The times they're a-changing: effects of circadian desynchronization on physiology and disease. J Physiol Paris 2013;107: 310-322. https://doi.org/10.1016/j.jphysparis.2013.03.007
57. West AC, Smith L, Ray DW, Loudon ASI, Brown TM, Bechtold DA. Misalignment with the external light environment drives metabolic and cardiac dysfunction. Nat Commun 2017;8: 417. https://doi.org/10.1038/s41467-017-00462-2
58. Evans JA, Davidson AJ. Health consequences of circadian disruption in humans and animal models. Prog Mol Biol Transl Sci 2013;119: 283-323. https://doi.org/10.1016/B978-0-12-396971-2.00010-5
59. Logan RW, McClung CA. Rhythms of life: circadian disruption and brain disorders across the lifespan. Nat Rev Neurosci 2019;20: 49-65. https://doi.org/10.1038/s41583-018-0088-y
60. Roenneberg T, Wirz-Justice A, Merrow M. Life between clocks: daily temporal patterns of human chronotypes. J Biol Rhythms 2003;18: 80-90. https://doi.org/10.1177/0748730402239679
61. Horne JA, Ostberg O. Individual differences in human circadian rhythms. Biol Psychol 1977;5: 179-190. https://doi.org/10.1016/0301-0511(77)90001-1
62. Roenneberg T, Pilz LK, Zerbini G, Winnebeck EC. Chronotype and Social Jetlag: A (Self-) Critical Review. Biology (Basel) 2019;8: 54. https://doi.org/10.3390/biology8030054
63. Sladek M, Kudrnacova Roschova M, Adamkova V, Hamplova D, Sumova A. Chronotype assessment via a large scale socio-demographic survey favours yearlong Standard time over Daylight Saving Time in central Europe. Sci Rep 2020;10: 1419. https://doi.org/10.1038/s41598-020-58413-9
64. Wright KP, Jr., McHill AW, Birks BR, Griffin BR, Rusterholz T, Chinoy ED. Entrainment of the human circadian clock to the natural light-dark cycle. Curr Biol 2013;23: 1554-1558. https://doi.org/10.1016/j.cub.2013.06.039
65. Sack RL. Clinical practice. Jet lag. N Engl J Med 2010;362: 440-447. https://doi.org/10.1056/NEJMcp0909838
66. Waterhouse J, Reilly T, Atkinson G, Edwards B Jet lag: trends and coping strategies. Lancet 2007;369: 1117-1129. https://doi.org/10.1016/S0140-6736(07)60529-7
67. Cisse YM, Peng J, Nelson RJ. Dim light at night prior to adolescence increases adult anxiety-like behaviors. Chronobiol Int 2016;33: 1473-1480. https://doi.org/10.1080/07420528.2016.1221418
68. Tsang AH, Astiz M, Leinweber B, Oster H. Rodent Models for the Analysis of Tissue Clock Function in Metabolic Rhythms Research. Front Endocrinol (Lausanne) 2017;8: 27. https://doi.org/10.3389/fendo.2017.00027
69. Fishbein AB, Knutson KL, Zee PC Circadian disruption and human health. J Clin Invest 2021;131: e148286. https://doi.org/10.1172/JCI148286
70. Penev PD, Kolker DE, Zee PC, Turek FW. Chronic circadian desynchronization decreases the survival of animals with cardiomyopathic heart disease. Am J Physiol 1998;275: H2334-2337. https://doi.org/10.1152/ajpheart.1998.275.6.H2334
71. Casiraghi LP, Oda GA, Chiesa JJ, Friesen WO, Golombek DA. Forced desynchronization of activity rhythms in a model of chronic jet lag in mice. J Biol Rhythms 2012;27: 59-69. https://doi.org/10.1177/0748730411429447
72. Archer SN, Laing EE, Moller-Levet CS, van der Veen DR, Bucca G, Lazar AS, Santhi N, et al. Mistimed sleep disrupts circadian regulation of the human transcriptome. Proc Natl Acad Sci U S A 2014;111: E682-691. https://doi.org/10.1073/pnas.1316335111
73. Scheer FA, Hilton MF, Mantzoros CS, Shea SA. Adverse metabolic and cardiovascular consequences of circadian misalignment. Proc Natl Acad Sci U S A 2009;106: 4453-4458. https://doi.org/10.1073/pnas.0808180106
74. Honzlova P, Novosadova Z, Houdek P, Sladek M, Sumova A. Misaligned feeding schedule elicits divergent circadian reorganizations in endo- and exocrine pancreas clocks. Cell Mol Life Sci 2022;79: 318. https://doi.org/10.1007/s00018-022-04354-7
75. Lu W, Meng QJ, Tyler NJ, Stokkan KA, Loudon AS. A circadian clock is not required in an arctic mammal. Curr Biol 2010;20: 533-537. https://doi.org/10.1016/j.cub.2010.01.042
76. Ralph MR, Foster RG, Davis FC, Menaker M. Transplanted suprachiasmatic nucleus determines circadian period. Science 1990;247: 975-978. https://doi.org/10.1126/science.2305266
77. Hurd MW, Ralph MR. The significance of circadian organization for longevity in the golden hamster. J Biol Rhythms 1998;13: 430-436. https://doi.org/10.1177/074873098129000255

78. Martino TA, Oudit GY, Herzenberg AM, Tata N, Koletar MM, Kabir GM, Belsham DD, et al. Circadian rhythm disorganization produces profound cardiovascular and renal disease in hamsters. Am J Physiol Regul Integr Comp Physiol 2008;294: R1675-1683. https://doi.org/10.1152/ajpregu.00829.2007
79. Turek FW. Staying off the dance floor: when no rhythm is better than bad rhythm. Am J Physiol Regul Integr Comp Physiol 2008;294: R1672-1674. https://doi.org/10.1152/ajpregu.00160.2008
80. Sladek M, Polidarova L, Novakova M, Parkanova D, Sumova A. Early chronotype and tissue-specific alterations of circadian clock function in spontaneously hypertensive rats. PLoS One 2012;7: e46951. https://doi.org/10.1371/journal.pone.0046951
81. Polidarova L, Sladek M, Novakova M, Parkanova D, Sumova A. Increased sensitivity of the circadian system to temporal changes in the feeding regime of spontaneously hypertensive rats - a potential role for Bmal2 in the liver. PLoS One 2013;8: e75690. https://doi.org/10.1371/journal.pone.0075690
82. Okamoto K, Aoki K. Development of a strain of spontaneously hypertensive rats. Jpn Circ J 1963;27: 282-293. https://doi.org/10.1253/jcj.27.282
83. Sagvolden T, Johansen EB, Woien G, Walaas SI, Storm-Mathisen J, Bergersen LH, Hvalby O, et al. The spontaneously hypertensive rat model of ADHD--the importance of selecting the appropriate reference strain. Neuropharmacology 2009;57: 619-626. https://doi.org/10.1016/j.neuropharm.2009.08.004
84. Pravenec M, Zidek V, Landa V, Simakova M, Mlejnek P, Kazdova L, Bila V, et al. Genetic analysis of "metabolic syndrome" in the spontaneously hypertensive rat. Physiol Res 2004;53 Suppl 1: S15-22. https://doi.org/10.33549/physiolres.930000.53.S15
85. Lemmer B, Mattes A, Bohm M, Ganten D. Circadian blood pressure variation in transgenic hypertensive rats. Hypertension 1993;22: 97-101. https://doi.org/10.1161/01.HYP.22.1.97
86. Carley DW, Trbovic S, Radulovacki M. Sleep apnea in normal and REM sleep-deprived normotensive Wistar-Kyoto and spontaneously hypertensive (SHR) rats. Physiol Behav 1996;59: 827-831. https://doi.org/10.1016/0031-9384(95)02205-8
87. Peters RV, Zoeller RT, Hennessey AC, Stopa EG, Anderson G, Albers HE. The control of circadian rhythms and the levels of vasoactive intestinal peptide mRNA in the suprachiasmatic nucleus are altered in spontaneously hypertensive rats. Brain Res 1994;639: 217-227. https://doi.org/10.1016/0006-8993(94)91733-7
88. Yilmaz A, Li P, Kalsbeek A, Buijs RM, Hu K. Differential fractal and circadian patterns in motor activity in spontaneously hypertensive rats at the stage of prehypertension. Adv Biol (Weinh) 2023;7: e2200324. https://doi.org/10.1002/adbi.202200324
89. Naito Y, Tsujino T, Kawasaki D, Okumura T, Morimoto S, Masai M, Sakoda T, et al. Circadian gene expression of clock genes and plasminogen activator inhibitor-1 in heart and aorta of spontaneously hypertensive and Wistar-Kyoto rats. J Hypertens 2003;21: 1107-1115. https://doi.org/10.1097/00004872-200306000-00010
90. Woon PY, Kaisaki PJ, Braganca J, Bihoreau MT, Levy JC, Farrall M, Gauguier D. Aryl hydrocarbon receptor nuclear translocator-like (BMAL1) is associated with susceptibility to hypertension and type 2 diabetes. Proc Natl Acad Sci U S A 2007;104: 14412-14417. https://doi.org/10.1073/pnas.0703247104
91. Kim YH, Lazar MA. Transcriptional Control of Circadian Rhythms and Metabolism: A Matter of Time and Space. Endocr Rev 2020;41: 707-732. https://doi.org/10.1210/endrev/bnaa014
92. Cui H, Kohsaka A, Waki H, Bhuiyan ME, Gouraud SS, Maeda M Metabolic cycles are linked to the cardiovascular diurnal rhythm in rats with essential hypertension. PLoS One 2011;6: e17339. https://doi.org/10.1371/journal.pone.0017339
93. Dolinsky VW, Morton JS, Oka T, Robillard-Frayne I, Bagdan M, Lopaschuk GD, Des Rosiers C, et al. Calorie restriction prevents hypertension and cardiac hypertrophy in the spontaneously hypertensive rat. Hypertension 2010;56: 412-421. https://doi.org/10.1161/HYPERTENSIONAHA.110.154732
94. Olejnikova L, Polidarova L, Behuliak M, Sladek M, Sumova A. Circadian alignment in a foster mother improves the offspring's pathological phenotype. J Physiol 2018;596: 5757-5775. https://doi.org/10.1113/JP275585
95. Phillips ML Circadian rhythms: Of owls, larks and alarm clocks. Nature 2009;458: 142-144. https://doi.org/10.1038/458142a

96. Ekstrand K, Bostrom PA, Arborelius M, Nilsson JA, Lindell SE. Cardiovascular risk factors in commercial flight aircrew officers compared with those in the general population. Angiology 1996;47: 1089-1094. https://doi.org/10.1177/000331979604701109
97. Peters RW, McQuillan S, Gold MR. Interaction of septadian and circadian rhythms in life-threatening ventricular arrhythmias in patients with implantable cardioverter-defibrillators. Am J Cardiol 1999;84: 555-557. https://doi.org/10.1016/S0002-9149(99)00376-8
98. Al-Naimi S, Hampton SM, Richard P, Tzung C, Morgan LM. Postprandial metabolic profiles following meals and snacks eaten during simulated night and day shift work. Chronobiol Int 2004;21: 937-947. https://doi.org/10.1081/CBI-200037171
99. Karlsson BH, Knutsson AK, Lindahl BO, Alfredsson LS. Metabolic disturbances in male workers with rotating three-shift work. Results of the WOLF study. Int Arch Occup Environ Health 2003;76: 424-430. https://doi.org/10.1007/s00420-003-0440-y
100. Liu L, Labani N, Cecon E, Jockers R. Melatonin Target Proteins: Too Many or Not Enough? Front Endocrinol (Lausanne) 2019;10: 791. https://doi.org/10.3389/fendo.2019.00791
101. Polidarova L, Houdek P, Sumova A. Chronic disruptions of circadian sleep regulation induce specific proinflammatory responses in the rat colon. Chronobiol Int 2017;34: 1273-1287. https://doi.org/10.1080/07420528.2017.1361436
102. Schoonderwoerd RA, de Rover M, Janse JAM, Hirschler L, Willemse CR, Scholten L, Klop I, et al. The photobiology of the human circadian clock. Proc Natl Acad Sci U S A 2022;119: e2118803119. https://doi.org/10.1073/pnas.2118803119
103. Morris CJ, Purvis TE, Hu K, Scheer FA. Circadian misalignment increases cardiovascular disease risk factors in humans. Proc Natl Acad Sci U S A 2016;113: E1402-1411. https://doi.org/10.1073/pnas.1516953113
104. Arora T, Taheri S Associations among late chronotype, body mass index and dietary behaviors in young adolescents. Int J Obes (Lond) 2015;39: 39-44. https://doi.org/10.1038/ijo.2014.157
105. Reutrakul S, Hood MM, Crowley SJ, Morgan MK, Teodori M, Knutson KL. The relationship between breakfast skipping, chronotype, and glycemic control in type 2 diabetes. Chronobiol Int 2014;31: 64-71. https://doi.org/10.3109/07420528.2013.821614
106. Reutrakul S, Hood MM, Crowley SJ, Morgan MK, Teodori M, Knutson KL, Van Cauter E. Chronotype is independently associated with glycemic control in type 2 diabetes. Diabetes Care 2013;36: 2523-2529. https://doi.org/10.2337/dc12-2697
107. Sladek M, Klusacek J, Hamplova D, Sumova A. Population-representative study reveals cardiovascular and metabolic disease biomarkers associated with misaligned sleep schedules. Sleep 2023;46: zsad037. https://doi.org/10.1093/sleep/zsad037
108. Koopman ADM, Rauh SP, van 't Riet E, Groeneveld L, van der Heijden AA, Elders PJ, Dekker JM, et al. The Association between Social Jetlag, the Metabolic Syndrome, and Type 2 Diabetes Mellitus in the General Population: The New Hoorn Study. J Biol Rhythms 2017;32: 359-368. https://doi.org/10.1177/0748730417713572
109. Wong PM, Hasler BP, Kamarck TW, Muldoon MF, Manuck SB. Social Jetlag, Chronotype, and Cardiometabolic Risk. J Clin Endocrinol Metab 2015;100: 4612-4620. https://doi.org/10.1210/jc.2015-2923
110. Islam Z, Akter S, Kochi T, Hu H, Eguchi M, Yamaguchi M, Kuwahara K, et al. Association of social jetlag with metabolic syndrome among Japanese working population: the Furukawa Nutrition and Health Study. Sleep Med 2018;51: 53-58. https://doi.org/10.1016/j.sleep.2018.07.003
111. Wittmann M, Dinich J, Merrow M, Roenneberg T. Social jetlag: misalignment of biological and social time. Chronobiol Int 2006;23: 497-509. https://doi.org/10.1080/07420520500545979

REVIEW

Vascular Damage and Repair - Are Small-Diameter Vascular Grafts Still the "Holy Grail" of Tissue Engineering?

Lucie BAČÁKOVÁ[1], Jaroslav CHLUPÁČ[1,2], Elena FILOVÁ[1], Jana MUSÍLKOVÁ[1], Júlia TOMŠŮ[1], Yu-Chieh WU[1], Lucie SVOBODOVÁ[1], Šimon PRAŽÁK[1], Antonín BROŽ[1]

[1]Laboratory of Biomaterials and Tissue Engineering, Institute of Physiology of the Czech Academy of Sciences, Prague, Czech Republic, [2]Transplantation Surgery Department, Institute for Clinical and Experimental Medicine, Prague, Czech Republic

Received December 3, 2023
Accepted April 30, 2024

Summary

Cardiovascular diseases are the most important cause of morbidity and mortality in the civilized world. Stenosis or occlusion of blood vessels leads not only to events that are directly life-threatening, such as myocardial infarction or stroke, but also to a significant reduction in quality of life, for example in lower limb ischemia as a consequence of metabolic diseases. The first synthetic polymeric vascular replacements were used clinically in the early 1950s. However, they proved to be suitable only for larger-diameter vessels, where the blood flow prevents the attachment of platelets, pro-inflammatory cells and smooth muscle cells on their inner surface, whereas in smaller-diameter grafts (6 mm or less), these phenomena lead to stenosis and failure of the graft. Moreover, these polymeric vascular replacements, like biological grafts (decellularized or devitalized), are cell-free, i.e. there are no reconstructed physiological layers of the blood vessel wall, i.e. an inner layer of endothelial cells to prevent thrombosis, a middle layer of smooth muscle cells to perform the contractile function, and an outer layer to provide innervation and vascularization of the vessel wall. Vascular substitutes with these cellular components can be constructed by tissue engineering methods. However, it has to be admitted that even about 70 years after the first polymeric vascular prostheses were implanted into human patients, there are still no functional small-diameter vascular grafts on the market. The damage to small-diameter blood vessels has to be addressed by endovascular approaches or by autologous vascular substitutes, which leads to some skepticism about the potential of tissue engineering. However, new possibilities of this approach lie in the use of modern technologies such as 3D bioprinting and/or electrospinning in combination with stem cells and pre-vascularization of tissue-engineered vascular grafts. In this endeavor, sex-related differences in the removal of degradable biomaterials by the cells and in the behavior of stem cells and pre-differentiated vascular cells need to be taken into account.

Key words

Blood vessel prosthesis • Regenerative medicine • Stem cells • Footprint-free iPSCs • sr-RNA • Dynamic bioreactor • Sex-related differences

Corresponding author

L. Bačáková, Laboratory of Biomaterials and Tissue Engineering, Institute of Physiology of the Czech Academy of Sciences, Vídeňská 1083, 14200 Prague 4 – Krč, Czech Republic. E-mail: Lucie.Bacakova@fgu.cas.cz

Introduction

Cardiovascular diseases are the leading cause of illness and death in the civilized world [1]. According to the World Health Organization (WHO), more than 30 % of deaths worldwide are caused by these diseases [2]. This is also true for the Czech Republic, where circulatory diseases accounted for over 40 % of all deaths in 2019, while cancer accounted for 25 % [3].

Ischemia of tissues supplied by damaged blood vessels, i.e. vessels with a significantly narrowed or closed lumen, manifests itself not only in serious life-threatening disorders such as heart attack or stroke, but

also in a significant reduction in quality of life, e.g. the relatively frequent necrosis of lower limb tissues in diabetes. In the Czech Republic, there are more than 10 000 sudden deaths due to heart attacks every year, and already in 2010 the number of patients with diabetes was around 600 000 - with at least 5 000 of them developing the 'diabetic foot' syndrome, leading to amputation of a limb - and these figures are rising.

An interesting observation from clinical practice is that men are more susceptible to cardiovascular diseases than women, or at least more susceptible than women of childbearing age - after menopause, the susceptibility of women is equal to the susceptibility of men (for a review, see [4]). One of the reasons for the increased propensity of men to cardiovascular diseases is the increased readiness of vascular smooth muscle cells (VSMCs) to migrate and proliferate. In our earlier studies, VSMCs in cultures from male rats migrated and proliferated faster than VSMCs from female rats, even without the current presence of sex hormones in the culture medium (e.g. in a serum-free medium), or even in the case of VSMCs isolated from newborn rats. This difference also increased with the time of cell cultivation, i.e. with the number of passages in the culture (for a review, see [5]). However, some studies suggest that this VSMC behavior is androgen-dependent after all - i.e. it is established prenatally by the action of these hormones, which apparently induce irreversible changes in the expression of some genes. For example, it has been described that in spontaneously hypertensive rats (SHR), the blood pressure reaches significantly higher values in males than in females [6] and depends on prenatal androgen synthesis due to gene expression in the SRY locus on the Y chromosome [7]. Androgens, among other things, increase the sensitivity of VSMCs to adrenergic hormones, and this persists throughout the whole life of the animals, even without the current presence of physiological levels of androgens, e.g. after castration of rats [8]. In addition, VSMCs from the aorta of spontaneously hypertensive male rats were significantly more sensitive to proliferation stimulation by angiotensin II *in vitro* than female VSMCs [6]. In contrast, estrogens have a rather antiproliferative effect on VSMCs [9–11].

In healthy blood vessels under physiological circumstances, vascular smooth muscle cells (VSMCs) are in a quiescent, non-proliferative, differentiated contractile state. An important factor that keeps them in this state is the endothelial barrier. However, this barrier can be damaged – both mechanically, e.g. by hypertension, and also biochemically – e.g. due to metabolic disorders such as elevated levels of glucose, cholesterol or homocysteine, the presence of oxygen radicals, nicotine, etc. Substances that are not present in the vascular wall under physiological conditions then reach the VSMCs, such as growth factors from the blood, especially platelet-derived growth factor (PDGF), and also vascular endothelial growth factor (VEGF), epidermal growth factor (EGF), fibroblast growth factor (FGF), nerve growth factor (NGF), and insulin-like growth factor-1 (IGF-1) (for a review, see [1,5]). The blood vessel is further infiltrated by other proteins from the blood, such as albumin, immunoglobulins, and lipidic substances, and also by pro-inflammatory cells such as leukocytes, lymphocytes, monocytes, macrophages and mast cells. These cells synthesize chemokines and cytokines, e.g. interleukins (e.g. interleukin-1), tumor necrosis factors (TNFs, e.g. TNF-α) and monocyte chemoattractant protein-1 (MCP-1), as well as metalloproteases (MMPs, e.g. MMP-2, MMP-9 and MMP-13), degrading the extracellular matrix (ECM) of the vascular wall. All these factors then stimulate the so-called phenotypic modulation of VSMCs, manifested by the transition from the contractile phenotype to the synthetic phenotype and by activation of the migratory and proliferative activity of VSMCs (for a review, see [1,5]).

The migratory and proliferative activity of VSMCs can be so massive that, together with the synthesis of ECM molecules, their calcification and the deposition of lipidic substances (mainly cholesterol), it leads not only to narrowing of the lumen of the damaged vessel, but also to its complete closure. It is not without interest that for this reason some researchers, especially in the 1970s, equated VSMC proliferation with tumor cell growth and viewed atherosclerotic lesions as "benign VSMC tumors" [12,13]. The finding of a connection between viral infection (which is the cause of some tumors) and the subsequent proliferation of VSMCs contributed to this view [14]. Even one of our own earlier studies [15] indicated a connection between the increased proliferative activity of VSMCs and the presence of pathogens in the organism. VSMCs in cultures derived from the aorta of specific pathogen-free (SPF) rats migrated later from explants of the *tunica media* and *intima* complex and proliferated more slowly than VSMCs from rats reared under standard conditions in the presence of microorganisms in the surrounding environment and in the rat organism. Nevertheless, the

increased growth activity of VSMCs, rather than tumor growth, is a manifestation of high regenerative capacity of these cells, which exceeds the current need to repair the damaged vessel and becomes counterproductive, i.e. leading to irreversible damage and obstruction of the vessel and the need for its replacement. Furthermore, VSMCs are not the only proliferating cell type in the vessel wall – macrophages also proliferate there. Their proliferation is induced by the macrophage colony-stimulating factor (M-CSF), and some authors have attributed even greater importance to it in the pathology of the vascular wall (especially for the formation of atherosclerotic lesions) than to the proliferation of VSMCs themselves [16,17]; for a review, see [5]. There are also sex-related differences not only in the propensity to cardiovascular diseases but also in the manner of their manifestation. For example, an increase in vascular stiffness, which is associated with a higher risk of cardiovascular morbidity and mortality, is likely sex-specific. In Dahl salt-sensitive rats, the ultrastructure of mesenteric arteries showed significant increases in collagen and smooth muscle cell areas, which altered the mechanics and hemodynamics of these arteries and led to higher blood pressure in male rats than in female rats [18]. In coronary artery disease, men are more prone to lipid-rich and inflammatory plaques, while women are more likely to develop fibrous plaques, based on endothelial dysfunction and phenotypic modulation of VSMC [19]. It is widely accepted that during coronary artery disease (CAD), men develop less stable atherosclerosis plaques than women. In CAD, recent studies have revealed that genes more active in men were associated with the immune system, while genes more active in women were associated with mesenchymal cells and endothelial cells [20]. However, in mice with metabolic syndrome, VSMCs from male donors were more prone to dedifferentiation, i.e. loss of contractile markers (leiomodin 1 and calponin) than the cells from female donors. This loss was induced by thrombospondin-1, the expression of which depended on the level of testosterone [1]. In aortic valve stenosis, which is driven by fibrosis and calcification of the aortic valve leaflets, annexin A2 and cystatin C increased the osteoblast-like differentiation of valve interstitial cells (VICs) from male pigs, while in female VICs, these inflammatory proteins promoted activation to myofibroblasts, manifested by increased expression of genes for α-actin and type 1 collagen [21].

This review summarizes the possibilities of surgical treatment of blood vessel obstruction, especially of small and medium-diameter vessels, mainly by replacing them or bypassing them with synthetic and biological vascular substitutes. The review takes into account the experience of our group in this field, in the context of the worldwide trends in the design of vascular substitutes, especially in recent years (2022-2023), including different approaches to patients according to their sex.

Surgical treatment of blood vessel obstruction and vascular substitutes

Vessels affected by stenosis and obliteration can be treated with endovascular (catheterization) approaches, such as balloon angioplasty and stenting, or with surgical approaches such as endarterectomy of short arterial segments. However, if these approaches fail, it is necessary to replace the damaged vessel - either directly, i.e. by resection and interposition grafting with end-to-end anastomoses, or by bridging the damaged section of the vessel by a so-called by-pass with end-to-side anastomoses, i.e. another patent vascular structure. Important vascular replacements often used in current clinical practice are based on synthetic polymers - mainly on expanded polytetrafluoroethylene (ePTFE) and poly(ethylene terephthalate) (PET), or segmented polyurethane (PU), used mainly for the production of hemodialysis access grafts (for a review, see [22–24]). Synthetic polymeric vascular replacements have been used since 1954 when they were prepared from Vinyon N cloth; chemically poly(vinyl chloride). Vinyon N tubes were first tested on dogs in the form of tubular constructs bridging defects of the abdominal aorta [25], and then they were also used in human patients for replacements of resected aneurysms of the abdominal aorta [26].

However, it should be noted that past and present synthetic vascular replacements have been commonly clinically applied in a cell-free form, i.e. without reconstructed physiological layers of the blood vessel wall. These layers include the *tunica intima*, i.e. the inner layer containing endothelial cells; the *tunica media*, i.e. the middle layer formed by smooth muscle cells, and the *tunica adventitia*, i.e. the outer layer containing fibroblasts, adjacent nerve fibers, and also smaller vessels and capillaries, referred to as *vasa vasorum*. Synthetic polymeric vascular grafts therefore behave more or less passively – at least they lack an endothelial layer, which in its mature confluent state is

considered the best way to prevent graft thrombosis, and they also lack a layer of smooth muscle cells, ensuring the contractile and relaxing function of the vessels.

Expanded PTFE, PET and PU, used for the manufacture of currently clinically used vascular prostheses, are highly hydrophobic polymers, and are therefore primarily unsuitable for the adhesion and growth of cells that require moderately hydrophilic surfaces. However, the blood proteins mediating cell adhesion (e.g. fibronectin, vitronectin) are adsorbed on the inner surface of the prostheses, which is followed by the adhesion of platelets, inflammatory cells and VSMCs. VSMCs reach the vascular substitute from the margins of its anastomosis with the original vessel, from the *tunica adventitia*, and also arise from VSMC precursors present in the blood (for a review, see [24]). In larger-diameter replacements, the adhesion of platelets, immune cells and VSMCs is made difficult or impossible by the fast and strong blood flow, and such replacements may therefore remain patent for a long time. However, in small-diameter vascular grafts, usually 6 mm or less, these processes result in thrombosis, inflammation, and excessive proliferation of VSMCs in an attempt to regenerate the damage, and finally stenosis and failure of the vascular replacement.

Clinically-used small-diameter vascular replacements mostly include an aortocoronary bypass [27,28], then bypasses of the lower limb, especially below-knee bypasses [29], as well as extracranial-intracranial bypasses, e.g. between the middle cerebral artery and the superficial temporal artery or the vertebral artery [30]. Small-diameter vascular replacements are burdened with the highest incidence of complications, leading to stenosis or complete closure of the replacement. In principle, it can be said that there are currently practically no long-term functional replacements for vessels of small diameter (6 mm and less) on the market. Thus, even approximately 70 years since the first vascular replacements were implanted (1952-1954), the design of functional small-diameter vascular replacements remains literally a “search for the Holy Grail” in the field of vascular tissue engineering [31,32].

The “dead end” of tissue engineering

Some renowned authors believe that vascular tissue engineering has now come to a "dead end" or needs to cross a “death valley” [24]. This is explained by the fact that the leading force in this field is no longer exerted by vascular surgeons. Leading roles have been taken over by basic research scientists who are detached from clinical practice, and have been unaware that the construction small-diameter vascular replacements is no longer the "Holy Grail" of vascular tissue engineering! Endovascular treatments, such as percutaneous transluminal angioplasty and the introduction of an endovascular graft (i.e. a special fabric tube device framed with stainless steel self-expanding stents), are now considered to be sufficient, together with the replacement of damaged blood vessels by autologous arteries, which the patient's organism is considered able to provide in sufficient quantities. There may also be some frustration and disappointment, due to the inability, even after 70 years of designing vascular replacements, to construct functional and durable small-diameter vascular grafts. But should we not still try to construct these replacements - at least to have some backup in cases where endovascular treatment fails (e.g. due to fibrosis and calcifications), or where autologous vessels are not available (in elderly patients with comorbidities), or even just to avoid burdening the patient with additional surgery? Moreover, as Zilla *et al*. (2020) [24] point out, there is also a need for medium-diameter vascular grafts for dialysis patients, who are rapidly increasing in numbers with the development of medicine in modern times – and constructing these grafts would be another important task for vascular tissue engineering. In addition, vascular replacements are needed not only for the arterial system but also for the venous system – for example, lower limb vein diseases alone are very common, affecting approx. 25 % of adults in westernized societies (for a review, see [33]). Venous grafts are also needed to reconstruct the missing portal system in pediatric patients. For this purpose, human decellularized allogeneous veins recellularized using autologous blood have been used [33].

Autologous vascular replacements

What options do we have for the design of small- or medium-diameter vascular replacements? Autologous vessels are considered the gold standard in this respect. These replacements contain physiological layers of the vessel wall - primarily a continuous layer of mature endothelial cells, which is considered the best way to prevent thrombosis, immune cell activation, and excessive VSMC migration and proliferation. Autologous vessels also contain VSMCs of mature contractile phenotype, providing the contractile and relaxing

function of the vascular replacement. Furthermore, autologous replacements are not burdened by the risk of immune reaction and subsequent graft rejection, nor by the risk of pathogen transmission, especially viruses and prions, as is the case with allogeneic or even xenogeneic replacements (for a review, see [22,23,34]). On the other hand, autologous transplanted tissue generally has some serious disadvantages. Firstly, it is usually only available in limited quantities, and secondly, obtaining it places an additional burden on the patient due to the additional surgery and damage to another site in the body. Moreover, certain tissues, when transferred to a new site in the body, have mechanical, biochemical and other properties that do not fully meet the requirements for their new function. A typical example is when venous grafts are used as arterial replacements, e.g. saphenous veins in aortocoronary bypass surgery [28]. These grafts are suddenly exposed to much higher blood pressures than they have been permanently adapted to, leading to endothelial damage, vascular distension, mechanical and biochemical damage to VSMCs and their subsequent efforts to regenerate, manifested by excessive migration, proliferation and proteosynthesis in these cells. All this is accompanied by thrombosis and adhesion of immune cells. The consequence is obvious - again the risk of graft stenosis. Although stenosis is treated in clinical practice by the insertion of a stent inside the vessel, this stent, usually metallic, further aggravates the mechanical damage to the endothelium, and there is also a risk of loosening and migration of the stent through the vessel. If the stent releases a drug that inhibits the unwanted proliferation of VSMCs, such as sirolimus (rapamycin), the endothelium, where proliferation and rapid regeneration of the damage would be desirable, is the first to be affected [35]. More recent approaches, in which our group has also participated, have attempted to replace intravascular stents with perivascular drug-eluting systems that simultaneously "wrap" the venous graft, giving it mechanical support and limiting its undesirable initial distension. In our earlier studies, we constructed a synthetic polymer-based outer vessel coating that released sirolimus. This system significantly limited the proliferation of VSMCs even without the presence of sirolimus - only on the basis of mechanical support - while preserving the viability of VSMCs and not damaging the endothelial layer [36–38]. Nevertheless, even this situation is not ideal, and calls for a search for other new options to replace irreversibly damaged vessels.

History and present of tissue-engineered vascular replacements

New options for replacing irreversibly damaged vessels consist in the creation of small- or medium-diameter vascular grafts by tissue engineering methods, which will reconstruct at least the *tunica intima* and *tunica media* of the vascular wall (and optimally also the *tunica adventitia*). Standard tissue engineering methods include (1) the preparation of a suitable cell carrier or scaffold to act as an ECM analogue to anchor the cells, (2) the cellular component of the newly constructed tissue, and (3) appropriate signals (biochemical and mechanical) to induce the desired cell behavior. Researchers have been attempting to create vascular replacements using tissue engineering methods since the 1980s. The work of Weinberg and Bell (1986) [39], who created an *in vitro* model of a blood vessel using a tubular matrix of bovine collagen, reinforced with a Dacron (PET) mesh, and populated with bovine adventitial fibroblasts, smooth muscle cells, and endothelial cells, may be considered the most prominent in this regard. To date, however, these efforts have not been crowned with success in achieving routine clinical application of constructs of this type, i.e. with all three layers of the physiological vascular wall reconstructed. Usually, only one layer has been reconstructed on these substitutes - initially, most often the endothelial layer, although attempts have also been made to reconstruct other layers, namely using autologous stem cells and skin fibroblasts.

The first clinical use of tissue-engineered vascular grafts was reported by Herring *et al*. in 1984 [40]. They implanted synthetic vascular prostheses that were *in vitro* endothelialized in the lumen. The first human implantation of a totally engineered blood vessel (TEBV) without any permanent synthetic support was carried out by Shin'oka *et al*. (2001) [41] as a pediatric pulmonary artery replacement, i.e., in low-pressure circulation. The first human use of TEBV in high-pressure circulation was performed by L'Heureux *et al*. (2007) [42] as an arterio-venous (AV) hemodialysis access graft (Lifeline©, Cytograft, Inc.), and Wystrychowski *et al*. (2014) [43] reported the first implantation of an allogeneic nonliving AV graft within the Lifeline© study. Kato *et al*. (2016) [44] reported the first clinical application of an *in vivo* tissue-engineered graft composed of autologous subcutaneous encapsulation tissue (Biotube) used for patch repair of the pulmonary artery in a child. Gutowski *et al*. (2020;

a group of Laura Niklason) [45] first conducted a human trial for peripheral arterial occlusive disease (PAD) with totally bioengineered human acellular vessels (HAV; Humacyte©). As of 2023, HAV is being evaluated in seven trials to treat PAD and vascular trauma, and as a hemodialysis access conduit [46]. The implantation site for clinical evaluation of TEBVs has changed over the years from lower extremity bypass procedures to AV access grafts, for safety reasons and better surveillance opportunities. In the past, only a few trials were conducted on coronary artery bypass grafting [47,48]. Major clinical achievements in tissue engineering of vascular grafts together with landmark publications are summarized in Table 1 and are depicted in Fig. 1. It should be noted that these relatively successful implants have been used within limited clinical trials and are not widely available.

Table 1. Clinical achievements and landmark publications regarding tissue-engineered vascular grafts. Abbreviations: arterio-venous (AV), bone marrow (BM), endothelial cells (EC), expanded polytetrafluoroethylene (ePTFE), months (M), not applicable (N/A), number of implants (No, n), polycaprolactone (PCL), poly(glycolic acid) (PGA), poly(lactic acid) (PLA), reference(s) (ref.), and vascular smooth muscle cells (VSMC).

Author, year	Clinical use	Scaffold	Cell type	No	Country	Outcome	Ref.
Herring *et al*. 1984	Lower extremity bypass	Dacron	Autologous vein EC, one-stage seeding	n = 18	USA	Improved patency in non-smokers	[40]
Deutsch *et al*. 1990 Zilla et al 1994 Meinhart *et al*. 1997 Deutsch *et al*. 2009	Lower extremity bypass	ePTFE	Autologous vein EC, two-stage seeding, fibrin-glue	n = 341	Austria	Improved patency, closing the gap between prosthetic and vein grafts	[49–52]
Laube *et al*. 2000	Coronary bypass	ePTFE	Autologous EC	n=14	Germany	Improved patency	[47]
Lamm *et al*. 2001	Coronary bypass	Allogeneic saphenous vein	Autologous EC	n = 15	Germany	Patency 80 % at 3M	[48]
Shin'oka *et al*. 2001, 2005 Hibino *et al*. 2010 Sugiura *et al*. 2018	Cavo-pulmonary conduits in congenital heart disease	Bioabsorbable synthetic polymer: PCL-PLA, PGA	Initially autologous EC; then: BM cells; two-stage seeding	n = 25 grafts n = 19 patches	Japan	Patent grafts, no aneurysm, rupture, infection, or calcification, reconstituted by host cells, some growth, 7/25 (28 %) stenosis treated with angioplasty	[41,53–55]
Bockeria *el al*. 2017, 2020	Cavo-pulmonary conduits, in congenital heart disease (Xeltis© Switzerland)	Bioabsorbable synthetic polymer: PCL-2-U-4[1H]-pyrimidinone	N/A	n = 5	Russia	No graft-related adverse events, endogenous tissue restoration	[56,57]
Teebken *et al*. 2009	Replacement of iliac vein affected by a tumor	Allogeneic decellularized *vena cava*	Autologous EC	n = 1	Germany	Thrombosis at 4M due to recurrent disease and discontinuation of anticoagulation	[58]
Olausson *et al*. 2012, 2014	Pediatric portal vein Meso-Rex bypass	Allogeneic decellularized iliac vein	Autologous BM or blood cells, two-stage seeding	n = 3	Sweden	Patent; second graft needed twice	[33,59]
L'Heureux *et al*. 2007 McAllister *et al*. 2009 Peck *et al*. 2011	AV access for hemodialysis, Lifeline©, Cytograft, USA	N/A	Autologous skin fibroblasts, cell sheets, seeded with vein EC	n = 9	Argentina, Poland	Primary patency 78 % at 1M, 60 % at 6M, 108 patient-months of use	[42,60,61]
Wystrychowski *et al*. 2014	AV access for hemodialysis, Lifeline©, Cytograft, USA	N/A	Allogeneic fibroblasts, cell sheets, devitalized	n = 3	Poland	Primary patency 5M, 7 days (unrelated death), and 3M	[43]

Lawson *et al*. 2016 Kirkton *et al*. 2019 Jakimowicz et al. 2022	AV access for hemodialysis, human acellular vessel, HAV, Humacyte© USA	PGA	Allogeneic VSMC, decellularized	n = 60	USA, Poland	Secondary patency 89 % at 12M and 58 % at 60M, no infection or aneurysm	[62–64]
Gutowski *et al*. 2020, 2023	Lower extremity bypass, HAV, Humacyte© USA	PGA	Allogeneic VSMC, decellularized	n = 20	Poland	Secondary patency 74 % at 48M and 60 % at 72M, no infection or aneurysm	[45,46]
Kato *et al*. 2016	Pulmonary artery patch	Autologous encapsulation tissue, Biotube	N/A	n = 1	Japan	Patent graft at 7M	[44]
Nakayama *et al*. 2018, 2020	AV access for hemodialysis extension, Biotube Co, Ltd	Subcutaneous mandrel implant, in-body tissue architecture	N/A	n = 2	Japan	Stenosis at 24M and 7M, both treated with angioplasty	[65,66]
Higashita *et al*. 2022	Lower extremity bypass extension, Biotube Co, Ltd	Subcutaneous mandrel implant, in-body tissue architecture	N/A	n = 1	Japan	Patent at 12M	[67]

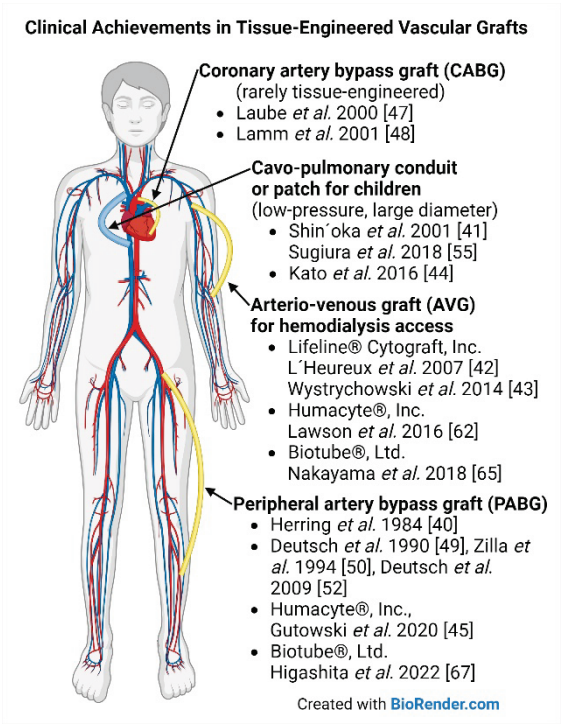

Fig. 1. Clinical achievements in tissue engineering of vascular grafts. Created with BioRender.com

However, commonly clinically used constructs that are declared on the market as "tissue-engineered vascular grafts" (TEVG) and that have been approved for current clinical practice include virtually only cell-free products based on decellularized allogeneic (i.e. human) matrices, such as Synergraft® or Cryovein® (CryoLife, Inc, Kennesaw, GA, USA) or on xenogeneic matrices, such as bovine Artegraft® or Procol® (both LeMaitre Vascular, Inc., Burlington, MA, USA; for a review, see [68]).

Several chemically stabilized and/or decellularized matrices are also used to produce vascular patches, i.e., needed to repair vascular defects caused by surgical procedures such as endarterectomy, thrombectomy or embolectomy, after vascular injuries or even after damage to blood vessels due to trauma or cancer. Currently, chemically stabilized matrices derived from bovine pericardium (XenoSure®), porcine pericardium (BioIntegral® NoReact®), or decellularized porcine small intestinal submucosa (SIS, CorMatrix®, Aziyo®) are used for vascular patches, and also synthetic matrices, namely ePTFE (Propaten® Gore®) and PET (Vascutek®), and matrices from autologous vessels, similar to those used for blood vessel replacement. However, synthetic and biological matrices are used in a cell-free form, i.e. in a form that does not fully correspond to the physiological tissue. In addition, biological matrices are often stabilized with glutaraldehyde, making them potentially cytotoxic (for a review, see [23,34]).

Newly-developed vascular grafts based on decellularized matrices

The idea of using decellularized matrices in an acellular form continues to be developed even today. There are at least two important reasons for this. First, the use of decellularized matrices is a kind of "renaissance" of the older idea of using allogeneic or even xenogeneic transplantation of blood vessels and other organs in general. Unlike synthetic substitutes, these biological

substitutes have similar mechanical properties, architecture and biochemical composition. However, the main immunogenic factor is the presence of a cellular component. It has been found that by removing this cellular component, i.e. by decellularization, the tissue then loses a substantial part of its immunogenicity - up to 90 % has been reported in the literature [69]. Second, acellular matrices are more easily approved for clinical use than cell-seeded matrices. Seeding matrices with cells usually requires processing the patient tissue outside the operating room, which is tightened prohibitively by new regulations [24]. EU legislation has become so strict that it is virtually impossible to implant constructs colonized with cells, not only allogeneic but also autologous cells from the patient. This is because it is usually necessary to remove the patient's cells from the operating room in order to seed, expand and differentiate them on the tissue-engineered constructs *in vitro*. Another problem is the cultivation and cryopreservation of cells in media containing components of xenogenic or allogenic origin (e.g. fetal bovine serum, human platelet lysate). EU legislation includes the following standards and regulations: ASTM F3225-17, ISO 10993-1:2018, ISO 7198:2016, EU 2017/745, EU 1394/2007 [70]. Therefore, in clinical practice, cell-free constructs are preferred, which could be colonized by cells only after their implantation into the patient's body. However, we believe that this situation is only temporary and that in the future, after the development of new technologies for the cultivation, preservation and further manipulation of cells, these rules will be adjusted to a more favorable form, tissue engineering will again find a place and all the efforts made for several decades will not be lost and will be crowned with success.

In recent years, decellularized tubular matrices have been prepared e.g. from rat aorta [71], porcine thoracic aorta [72], porcine carotid arteries [73], bovine internal mammary arteries [74], human umbilical artery [75,76], human saphenous vein [77], submillimeter vessels of the human placenta [78], or from rolled human amniotic membrane [79]. Decellularized plant leaves, namely of *Viburnum rhytidophyllum*, combined with gelatin were also an interesting non-traditional material [80]. The mechanical properties of decellularized matrices have been further improved by crosslinking with genipin, which proved to be better than the traditionally used glutaraldehyde in terms of matrix biocompatibility [81]. In our earlier study, we also achieved similar results with genipin-crosslinked pericardium, which proved to be more advantageous not only in comparison with glutaraldehyde but also in comparison with tannic acid and nordihydroguaiaretic acid [82]. Crosslinking also significantly reduces the residual immunogenicity of the decellularized matrices (for a review, see [24]). To strengthen the mechanical properties of decellularized matrices, they have been used in combination with synthetic polymers, especially degradable polymers such as polycaprolactone (PCL) [71] or poly(L-lactide-*co*-ε-caprolactone) (PLCL) [72]. Attempts have even been made to construct small-diameter blood vessels from synthetic polymers (e.g., PCL) seeded with cells (e.g., dermal fibroblasts) and secondarily decellularized, after the cells have deposited natural ECM proteins onto these polymers [83].

Decellularized matrices are important not only for the construction of small-diameter vascular grafts, but also in the context of Ross surgery. This is a cardiac surgical procedure in which the diseased aortic valve is replaced with the patient's own pulmonary valve, followed by the replacement of the pulmonary valve with a pulmonary homograft (i.e., allograft in more recent terminology). The valved homograft conduit was developed in the late 1960s, but its widespread use was limited by the lack of effective sterilization and preservation methods [84]. Modern cryopreservation methods have extended the shelf life of this conduit, but it is still at risk for degeneration and calcification, which is considered to be a result of immune rejection of this allogeneic implant [85]. In addition, conventional pulmonary homografts lack the additional growth capacity needed in pediatric patients. Therefore, a new and promising alternative approach has been to decellularize these homografts, which was expected to significantly reduce their immunogenicity and provide the possibility for spontaneous recellularization of these grafts with autologous host cells and their further growth [84,85].

In our studies, we also considered direct reconstruction of the aortic valve using decellularized autologous pericardium from the patients [82] or xenogenic (porcine) pericardium [86]. However, pericardium proved to have poor mechanical properties for these purposes - rather it could be used for vascular patches. However, some promising results were obtained in experiments in which autologous pericardium was "trained" in a dynamic bioreactor that stimulated the proliferation of its cellular component as well as the production and maturation of its ECM [87,88].

The biological activity of decellularized scaffolds, including those combined with synthetic polymers, has been further improved by endowing them with various biomolecules, such as heparin [77] or salidroside [72] to increase their antithrombogenic activity, and hepatocyte growth factor [73] or VEGF [74] to increase their spontaneous endothelialization after implantation in experimental animals *in vivo*, such as rats [71,72,78,79] or rabbits [73]. In such improved vascular replacements, not only spontaneous endothelialization but also regeneration of the smooth muscle layer has often occurred [72,77,83]. However, it is important to note that although these beneficial effects occur in animal models, including large animal models (pigs), they usually do not occur in human patients - especially when the vast majority of patients requiring vascular replacement are already elderly and also suffer from a number of concurrent diseases. In other words, spontaneous endothelialization of vascular replacements cannot be relied upon in human patients, especially in terms of trans-anastomotic endothelial outgrowth or retention of the endothelial cell precursors from the blood. Some hope is placed in the endothelialization of vascular substitutes by a transmural ingrowth of capillaries from the outside into the vascular substitute, facilitated by its porous structure or degradability. However, it should be taken into account that there will not always be enough of these capillaries or small vessels around the implant [24]. In addition, in the case of VSMCs, problems such as their hyperplasia, leading to stenosis of the vascular graft, must be anticipated. This problem has often been addressed by the release of agents inhibiting migration and proliferation of VSMCs, e.g. rapamycin [71], but it would be more physiological to bring the VSMC behavior under control by the presence of a confluent endothelial cell layer and appropriate biochemical and mechanical signals. In other words, to create tissue-engineered vascular grafts for human patients, it is necessary to incorporate the cellular component into the scaffold before it is implanted, i.e. not to wait for secondary spontaneous cell colonization after implantation into the organism.

Recellularization of decellularized matrices, reconstruction of the *tunica media*

In our studies, we have therefore tried to further develop the idea of using decellularized xenogeneic and allogeneic matrices for creating small-diameter vascular replacements and vascular patches after their preliminary in vitro recellularization. The decellularized tissue can be recellularized with the patient's own cells - especially stem cells. We have investigated the recellularization of decellularized tissues mainly with mesenchymal stem cells (MSCs). These cells can be obtained from patients from their subcutaneous adipose tissue in autologous form, in reasonable quantities and by a relatively minimally invasive method, namely liposuction (for a review, see [89]). This method is less demanding and less painful than, for example, bone marrow aspiration, by which MSCs can also be obtained - many patients undergo liposuction quite voluntarily for aesthetic reasons. The use of adipose tissue-derived stem cells (ADSCs) is generally preferable to the use of already differentiated VSMCs, which may have a lower proliferative capacity, may undergo senescence earlier, and, in particular, would require subcutaneous veins or other vessels to be harvested, which would burden the patient with another demanding surgical procedure. Another source of MSCs for our studies was Wharton's jelly of the umbilical cord. Wharton's jelly stem cells (WJSCs) are usually used in allogeneic form, but they can be obtained in relatively large quantities without any surgery on the patient, and de facto from “biological waste”. Moreover, WJSCs are considered less mature than adult MSCs, i.e. standing on the borderline between pluripotency and multipotency. At least some markers of pluripotency have been detected in them (for a review, see [90]), which offers the possibility to differentiate them into all cell types present in the vascular wall, including endothelial cells. Last but not least, MSCs are generally considered to be poorly immunogenic or even immunomodulatory (for a review, [89]). In our recent study, where decellularized allogeneic or xenogeneic pericardium was recellularized with allogeneic WJSCs and was implanted as vascular patches in laboratory pigs, these WJSCs reduced neo-adventitial inflammatory reaction, patch resorption, as well as neo-intimal hyperplasia on xenografts, suggesting immunomodulatory properties of WJSCs [23].

In our studies, we have used small-diameter porcine arteries for decellularization to create vascular substitutes (Fig. 2) and porcine pericardium to create vascular patches [23,86,91]. The attractiveness of these matrices for stem cell adhesion and growth was enhanced by modifying the matrices with fibrin, further endowed with heparin and VEGF. Differentiation of stem cells towards VSMCs was induced by the appropriate

composition of the culture medium, in particular by the presence of transforming growth factor-β1 (TGF-β1) and bone morphogenetic protein (BMP-4), and was further enhanced by mechanical stimulation in a lab-made dynamic bioreactor providing pulsatile pressure stress. The degree of stem cell differentiation towards VSMCs was assessed by the expression of α-actin, calponin-1 and myosin heavy chain at both mRNA and protein levels [23,86,91,92].

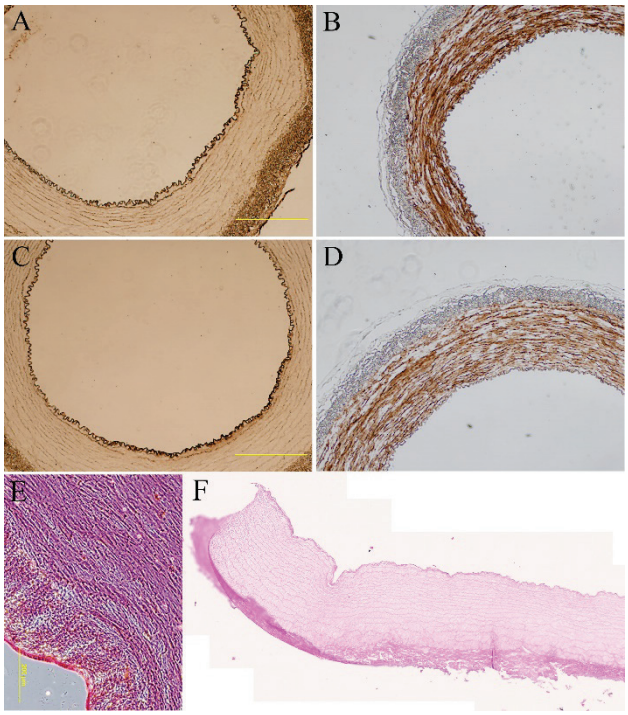

Fig. 2. Immunohistological staining of von Willebrand factor (**A, C**) and calponin (**B, D**) of endothelialized porcine carotid artery that had been decellularized and seeded with human adipose tissue-derived stem cells (**A, B**) or human bone marrow-derived stem cells (**C, D**) for 14 days and human umbilical vein endothelial cells for two days of in vitro culture. Hematoxylin-eosin staining of control native (**E**) and decellularized arteries, tile scan (**F**). **A-E**: Olympus IX 71 epifluorescence microscope, DP80 digital camera; **A-D**: obj.×4, scale bar = 500 μm; **E**: obj.×10, scale bar = 200 μm; **F**: ZEISS Axio Scan. Z1 Slide Scanner, obj.×20.

Differentiation of stem cells towards VSMCs can be induced not only by the composition of the culture medium and mechanical stimulation in a dynamic bioreactor, but also by the composition of the cultivation substrate. An interesting finding of our earlier experiments was that coating standard tissue culture polystyrene (PS) with collagen and fibronectin significantly increased the expression of calponin-1 and smoothelin, i.e. an intermediate and a late marker of VSMC differentiation, respectively, in ADSCs in comparison with the pure PS. The differentiation of ADSCs towards VSMCs was induced by a medium with TGF-β1 and BMP-4 (both in a concentration of 2.5 ng/mL). However, the expression of both markers showed a tendency to decrease with culture time (from 3 to 10 days), probably due to negative feedback from the synthesized protein (Fig. 3).

New options for endothelialization of vascular replacements

Pre-seeding decellularized matrices with stem cells facilitated proper endothelialization of these matrices. For this endothelialization under experimental conditions, we used already differentiated endothelial cells such as human umbilical vein endothelial cells (HUVECs). However, for clinical practice, it would be preferable to avoid the direct collection of differentiated endothelial cells from patients, which would again involve surgical removal of a blood vessel, e.g. a subcutaneous vein, followed by relatively demanding isolation of cells, lengthy propagation of the cells, and purification from other cell types. Even after the successful isolation and purification of endothelial cells, the proliferation of these cells takes a relatively long time, especially in elderly patients who are usually burdened by a number of comorbidities. When the endothelial cells are finally sufficiently proliferated, a special dynamic culture system is required to seed them onto the vascular prosthesis, often tens of centimetres long, where they are then cultured until they reach a confluent layer. Indeed, immature, non-confluent and proliferating endothelium can be thrombogenic and immunogenic. The whole process is quite time consuming and, as with any *in vitro* culture, there is a risk of microbial contamination or pathogen transmission due to the xenogenic components of conventional culture media. For these reasons, this technology referred to as two-stage endothelialization of vascular grafts is not routinely used in clinical practice, although it was developed years ago (for a review, see [22]), and even though Austria was able to comply with the existing strict European regulations and implement the two-stage endothelialization method of a vascular replacement at the Floridsdorf Clinic (see the newspaper article published on October 25, 2020; [93]). Previously, two-stage endothelialization of synthetic vascular prostheses has been clinically tested in infrainguinal prostheses in Vienna, Austria (Hospital Hietzing, [52]),

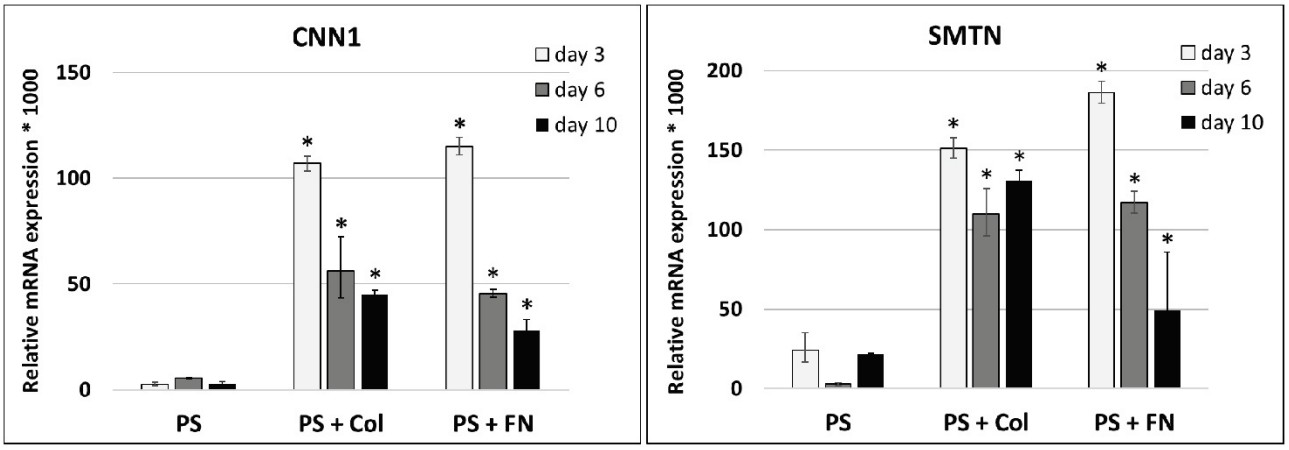

Fig. 3. The influence of the cultivation substrate on the differentiation of ADSCs towards VSMCs. The correlation of relative mRNA expression of genes for calponin 1 (CNN1) and smoothelin (SMTN) in human adipose-derived stem cells cultivated in differentiation medium on standard tissue culture polystyrene (PS), PS coated with type 1 collagen (PS + Col) or with fibronectin (PS + FN). Measured by real-time PCR. Arithmetic mean ± SD from 2-3 samples for each experimental group and time interval. ANOVA, Student-Newman-Keuls method. Statistical significance: * p≤0.05 in comparison with corresponding control PS samples.

but also at the Université Victor Segalen, Bordeaux, France [94], in Berlin (Charité Hospital, Provitro GmbH; [95]).

In the new era, however, as in the case of VSMCs, we have the opportunity to differentiate endothelial cells from MSCs, which can be isolated from the patient using less invasive methods (e.g., liposuction of subcutaneous fat, from blood or urine, or from the umbilical cord). However, such differentiation is difficult, incomplete or even impossible in the case of MSCs. MSCs are multipotent cells, i.e. (unlike totipotent and pluripotent cells), they are capable of differentiating into only a limited spectrum of cell types. They differentiate reluctantly towards endothelial cells, as common physiological biochemical and mechanical signals *in vitro* are usually not sufficient to induce polarization, i.e. functional specialization of the cytoplasmic cell membrane, typical for endothelial and epithelial cells (for a review, see [89]).

Direct differentiation of MSCs into endothelial cells by physiological biochemical and mechanical signals could perhaps be possible in WJSCs. Although these cells are counted among the multipotent MSCs, due to their origin from (extra)fetal tissue they are phenotypically more immature and express some markers of pluripotency, such as OCT4, SOX2, NANOG and SSEA4 (for a review, see [90]). Appropriate composition of the culture medium, e.g., the presence of VEGF, EGF, IGF-1, FGF-2, hydrocortisone, heparin and vitamin C, combined with laminar shear stress in a bioreactor, could induce differentiation of WJSCs to endothelial cells. The potential of WJSCs to differentiate into endothelial cells was already shown in a study by Alaminos *et al*. [96]. Also, in our recent study [23], after implantation of decellularized matrices seeded with WJSCs into a laboratory pig, cells positive for CD31, one of the markers of endothelial cells, were found on these matrices. However, it cannot be excluded that CD31-positive cells migrated to the matrices secondarily from the pig organism, e.g. from the adjacent vascular wall, or were captured from the blood.

For the purposes of vascular tissue engineering, endothelial cells can of course be generated from induced pluripotent stem cells (iPSCs) [97,98]. The iPSCs were first generated in 2006 from mouse embryonic or adult fibroblasts by introducing the genes for OCT4, SOX2, KLF4 and cMyc into these cells using a retroviral system [99]. Later, human dermal fibroblast-derived iPSCs were also generated in this way [100]. In 2007, human iPSCs were also generated from human fibroblasts by introducing genes for OCT4, SOX2, NANOG and LIN28 using a lentiviral system [101]. However, iPSCs generated in this way are burdened with many disadvantages such as low efficiency of the conversion to iPSCs (0.01-0.1 %), incomplete reprogramming, genomic insertion associated with a risk of mutations, tumorigenicity and also immunogenicity of iPSCs, which also hinder their potential introduction into clinical practice. For this reason, modern iPSCs of a new type are currently entering the scene. They are created not by DNA manipulation but by novel RNA technologies - specifically by inserting mRNA encoding transcription

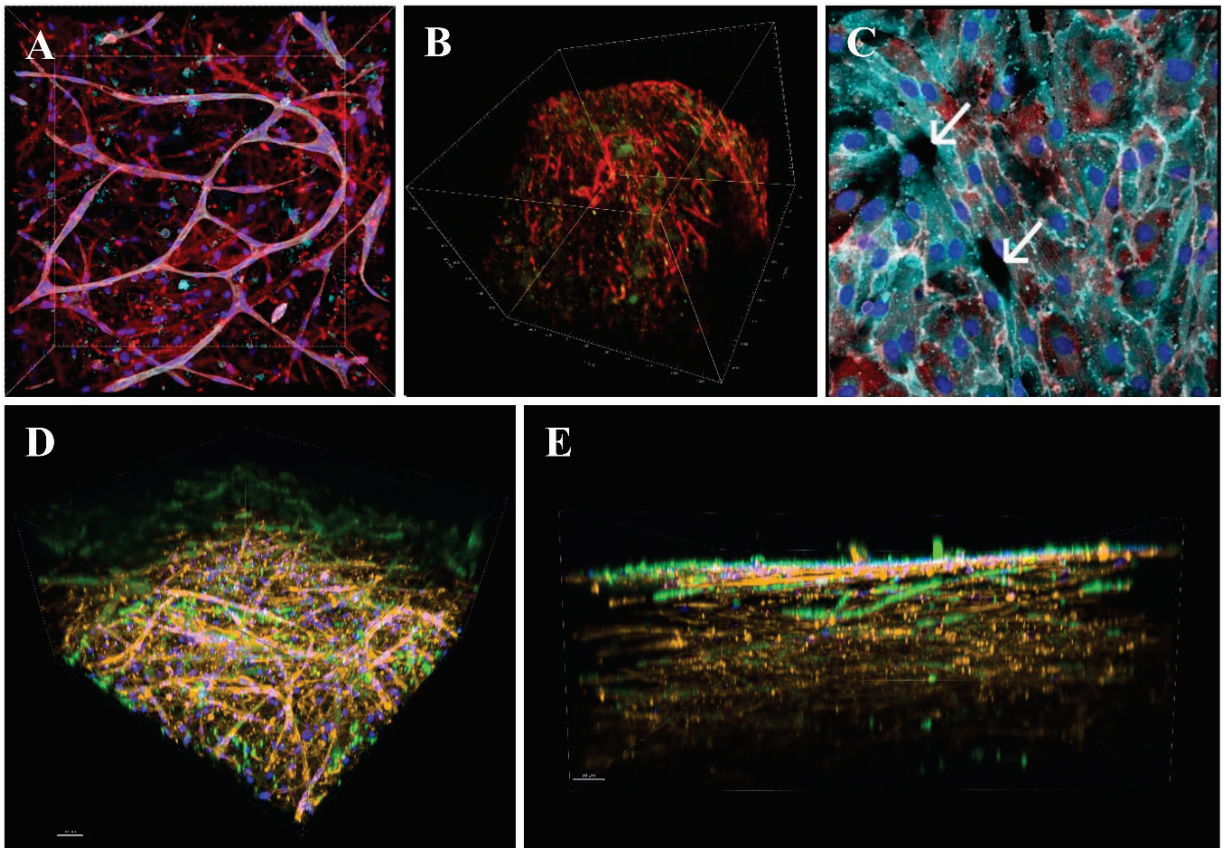

Fig. 4. A: Capillary-like network formation in a collagen hydrogel with embedded HUVECs and ADSCs immigrating from an underlying fibrin-modified electrospun nanofibrous polylactide membrane after 14 days in culture. **B**: Immunofluorescence staining of β-actin (red) and calponin (green) in human ADSCs in collagen gels on day 14 of culture in EGM-2 medium. **C**: A monolayer of HUVECs originating from the openings (arrows) of capillary-like structures on the surface of the collagen hydrogel. **A, C**: Both cell types were stained with phalloidin for cytoskeletal F-actin (conjugated with Atto 488; all images; red), and with DAPI for cell nuclei (all images; blue). The CD31 membrane marker of HUVECs was visualized by immunofluorescence (Alexa 633; turquoise). **D, E**: bottom and side view of the construct, where the collagen hydrogel was enriched with fibronectin (10 μg/ml). Both HUVECs and ADSCs were stained with phalloidin for the cytoskeletal F-actin (red), and with DAPI for the cell nuclei (blue). Von Willebrand factor, a marker of HUVECs, was visualized by immunofluorescence (green). Scale bar 50 μm. **A, C, D, E**: Dragonfly 503 spinning disk confocal microscope, obj. ×20 (A, D, E), obj. ×40 (C). **B**: Zeiss Z.1 light-sheet microscope, obj. ×10 for excitation, obj. ×20 for detection, zoom ×0.4 tile scans.

factors of pluripotent cells, such as OCT4, KLF4, c-Myc and SOX2, into cells. Moreover, this mRNA can be in the synthetic and self-replicating form (sr-RNA), which eliminates the need for repeated transfection of cells. The sr-RNA encoding transcription factors OCT4, KLF4, SOX2, and cMyc, together with internal ribosome entry site (IRES) and the reporter green fluorescent protein (GFP), were used to generate so-called footprint-free iPSC-derived cardiomyocytes [102,103] or vascular endothelial cells from renal epithelial cells [104]. These cells can be isolated from patients' urine, and thus in an autologous form and by a completely non-invasive method. It could even be assumed that endothelial cells might be generated directly from WJSCs expressing at least some pluripotency markers by introducing sr-RNA encoding directly endothelial markers such as CD31, VEGF receptor 2 (KDR), VE-cadherin or von Willebrand factor. Recently, mRNAs encoding VEGF or runt-related transcription factor 2 (RUNX2), prepared via *in vitro* transcription, were administered into primary osteoblast-like cells *in vitro*, derived from cranial bones of neonatal mice, or into rat mandible defects *in vivo* in order to promote osteogenic cell differentiation, vascularization and healing of the bone defect [105].

Creating *vasa vasorum*, and spontaneous endothelialization of vascular grafts through these structures

From the preceding text, it follows that from relatively readily available MSCs, such as ADSCs, WJSCs, and also bone marrow MSCs, VSMCs can be directly differentiated by biochemical stimulation with growth factors and other biomolecules and mechanical stimulation in a dynamic bioreactor. In addition, from these MSCs, endothelial cells could be differentiated

indirectly, i.e. using sr-RNA or mRNA for endothelial markers. Moreover, we can take advantage of another phenomenon that we have observed in MSCs (specifically ADSCs) and endothelial cells in a three-dimensional collagen hydrogel, namely that these two cell types self-assembled into tubular capillary-like structures in which endothelial cells form an inner layer, and ADSCs attach externally in a pericyte-like manner (Fig. 4A). Interestingly, even the ADSCs themselves were able to form elongated capillary-like structures in the collagen hydrogel environment (Fig. 4B, D). As soon as the capillary-like structures in our experiments reached the surface of the construct, they emerged on it, i.e. they created openings, from which endothelial cells subsequently grew (spread) over the entire surface of the construct and formed a continuous layer on it (Fig. 4C, E). In other words, it would be possible in this way to achieve not only an endothelialized, but also a pre-vascularized blood vessel replacement or patch, i.e., with a pre-formed "*vasa vasorum*". Thus, we do not have to rely only on transmural vascularization and endothelialization of the vascular substitute after it has been implanted *in vivo* from its surroundings. Instead, we can move towards these phenomena by pre-vascularization of the construct *in vitro*. Moreover, spontaneous outflow of newly-formed capillaries can be expected not only on the luminal surface of the vascular substitute or vascular patch, but also on the lateral and external sides. A phenomenon called inosculation, i.e. spontaneous connection of pre-capillaries to capillaries of adjacent tissues and thus to the systemic blood circulation, can then be expected at the sites of pre-capillary outflow [106,107]; for a review, see [24]. If ADSCs are in excess over endothelial cells in the matrix, only a fraction of them will be used for pericyte function, and the remaining fraction may be differentiated towards VSMCs - indeed, pericytes and VSMCs are similar incertain features, e.g. they express α-actin (for a review, see [89,92]). Similar phenomena were observed already in 1962 in the form of the penetration of the full wall thickness of knitted Dacron tubes, implanted into the abdominal aorta of baboons, by sprouting adventitial capillaries, which coalesced with the graft lumen and gave rise to expanding endothelial islands [108]. In another study, endothelial tubes formed in an agarose assay system were followed by multipotent murine embryonic cells, which then differentiated into VSMCs [109]; for a review, see [24].

The perspective of hydrogels for creating small-diameter vascular grafts

From the point of view of both pre-vascularization and transmural ingrowth of capillaries, hydrogels appear to be promising for the design of vascular replacements. However, they have rather weak mechanical properties, and are also prone to shrinkage by cells growing inside them. They therefore need to be strengthened and reinforced in some way - for example, with nanoparticles prepared by lyophilization and homogenization of collagen nanofibers created by electrospinning, as we have shown in our recent study [110]. In this study, we also took into account the appropriate composition of the media that would promote the endothelialization and also the differentiation of ADSCs towards VSMCs. In this respect, the so-called external drug delivery system, based on electrospun nanofibrous poly(vinyl alcohol) (PVA) nanofibers, releasing the platelet lysate continuously and for a long period of time, was the best option. Although the differentiation of ADSCs toward VSMCs was slower than in the “classical” differentiation medium for VSMCs containing TGF-β1 and BMP-4, the endothelialization of the construct was more homogeneous and continuous, which was accompanied by a minimum amount of gel shrinkage [110].

Synthetic hydrogels are also promising for the design of small-diameter vascular prostheses. In particular, vascular substitutes made of synthetic hydrogels, such as poly(N-acryloyl glycinamide) with an inner layer of zwitterionic fluorinated hydrogel [111], degradable poly(2-hydroxyethyl methacrylate) [112], and crosslinked PVA [113,114] have recently been experimentally tested. However, these substitutes were often acellular and bioinert in order to prevent the adhesion of platelets, pro-inflammatory cells and bacteria [111,112], or even to limit VSMC hyperplasia [113]. For incorporating a cellular component into these substitutes, such as endothelial cells [113] or VSMCs [115], a synthetic polymer was combined with a natural polymer, such as fucoidan, i.e. a sulfated polysaccharide with a similar structure to that of heparin [114], gelatin, e.g. in a gelatin-methacryloyl hydrogel (GelMa) [115], or a hydrogel prepared from vascular ECM and deposited on PCL scaffolds [116]. The mechanical properties of the hydrogels were further improved with various additives, e.g. graphene [112]. Hydrogel vascular substitutes have also been prepared by a modern method of 3D bioprinting the matrix together with cells [115].

Modern technology I – 3D (bio)printing in creating small-diameter vascular grafts

The modern technology of 3D bioprinting, i.e. simultaneous printing of a matrix, i.e. bioink, together with cells, is currently very popular for the construction of small-diameter vascular grafts, and provides hope for the commercialization of these products. For example, collagen, gelatin, hyaluronic acid, alginate, chitosan, GelMa, and poly(ethylene glycol) diacrylate (PEGDA), have been used as bioinks. Usually, only VSMCs have been printed together with the bioink, whereas endothelial cells have been seeded into the lumen of the tubular structure only secondarily. However, techniques capable of printing endothelial cells into the vascular substitute have already been developed (for a review, see [117]). In a recent study by some members of our group, a porcine collagen hydrogel was printed together with ADSCs [118]. Such constructs could then be used as vascular patches for pre-clinical studies on large animals (pigs), because, as known from other studies by our group, these cells can be differentiated towards VSMCs by an appropriate composition of the culture medium and mechanical training in a bioreactor [23,91].

Even the technology of simple 3D printing of various synthetic and nature-derived polymers is currently used to create small-diameter vascular replacements. For example, these replacements have been created from negatively charged PVA and alginate interpenetrating networks, immersed in a positively-charged chitosan solution. Moreover, these replacements also had antibacterial and angiogenic effects [119]. Antibacterial and angiogenic activity and endothelial regeneration were also promoted in 3D-printed vascular substitutes made of PCL, poly(glycerol sebacate) (PGS) with the addition of bioactive glass [120]. 3D printing technology has often been combined with another advanced technology, namely electrospinning, in the design of vascular prostheses [121,122], including prostheses triple-layered with inner, intermediate and outer layers, simulating the *tunica intima*, *media* and *adventitia* [123]. However, the resulting constructs of both technologies are usually cell-free, and are populated with cells only after they have been implanted into the body of experimental animals, such as sheep [121], dogs [122], or subcutaneously into mice [120], or seeded with HUVECs *in vitro* [123]. 3D prints of organs and their vasculature are also performed to assist surgeons in imaging and in decision-making in the preparation of live donor organ transplantation [34].

Modern technology II – electrospinning in creating small-diameter vascular grafts

Electrospinning itself is also a very widespread and promising technique for the preparation of small-diameter vascular substitutes. Similarly as for 3D printing, various synthetic and nature-derived polymers and combinations of polymers have been employed for this technology. The synthetic polymers included e.g. PCL [124,125], polylactide [111], poly(1,4-butylene succinate) (PBS) [126], PLCL [127], poly(lactide-*co*-glycolide) (PLGA) [128], poly-ε-caprolactone/polydioxanone (PCL/PDO) [129], poly(dimethylsiloxane) (PDMS) [130] and PU [131], including thermoplastic polyurethane (TPU) and a new self-reinforcing thermoplastic poly(urethane-urea) (TPUU) [132]. The main nature-derived polymers include collagen [133], gelatin [134], tropoelastin [135], PGS [136], chitosan [137] and silk fibroin [138]. The combinations include e.g. PCL with PU [139], PDMS with poly(methyl methacrylate) and TPU [130], PLCL with recombinant humanized collagen [81], and tropoelastin with PGS [135]. Bi-layered scaffolds with an inner electrospun PCL layer promoting the axial alignment of endothelial cells, and a GelMA cast outer layer promoting the circumferential alignment of VSMCs have also been constructed [140]. Another hybrid bi-layered vascular graft comprised the inner PCL/poly (ethylene glycol) methyl ether loaded with VEGF, promoting the adhesion and growth of endothelial cells, and the outer PCL/chitosan layer loaded with PDGF, promoting the differentiation of bone marrow MSCs towards VSMCs [137]. A tri-layered electrospun PCL-collagen/PCL/PCL-gelatin graft imitated the tri-layered architecture of the natural vascular wall and promoted the adhesion of endothelial cells on its inner surface [134].

The endothelialization of electrospun vascular grafts has been further improved by various physical and biochemical modifications. The physical factors include e.g. appropriate hydrophilicity [134], nanofibrous architecture [131] or microgroove patterning [127] of the luminal surface. Biochemical modifications include e.g. the presence of platelet-rich plasma [141], heparin, REDV-containing peptides and VEGF [142], endothelial progenitor cell-binding TPSLEQRTVYAK peptide [125], polydopamine-copper ion complexes, polylysine and

Cys-Ala-Gly peptides [127], an adenosine monophosphate-activated protein kinase (AMPK) activator, i.e. 5-aminoimidazole-4-carboxamide ribonucleotide (AICAR) [143], and epsin-mimetic endothelium-targeting chimeric (UPI) peptide [144]. Vascular scaffolds based on collagen nanofibers modified with hyaluronic acid oligosaccharides and loaded with apyrase and 5'-nucleotidase enzymes were successfully tested for antithrombosis and *in situ* endothelialization, although only in a rabbit model [133]. The adhesion, migration and growth of endothelial cells are also improved by loading vascular grafts with nitric oxide, which also prevents the overgrowth of VSMCs and bacterial infection [145]. Electrospun vascular scaffolds can also be loaded with antimicrobial substances, such as cobalt [124] or antibiotics, e.g. tobramycin [128], or anti-inflammatory substances, e.g. those modulating the phenotype of macrophages from pro-inflammatory to anti-inflammatory, such as AICAR mentioned above [143] or MCP-1 [146].

The experimental small-diameter vascular substitutes prepared by electrospinning in the above studies were usually prepared by directly depositing nanofibers around a rotating mandrel, usually metallic, e.g. stainless steel. However, it should be noted that the incorporation of cellular components into tubular structures is relatively difficult and usually requires a dynamic culture system, e.g., a flow-through bioreactor [83]. Therefore, small-diameter vascular substitutes can also be prepared by rolling planar sheets of nanofibers (e.g. PCL) [147] or even other materials (e.g. polymer films fabricated by dropping a polymer solution, such as PU, on water surface [148], after colonizing them with cells. Other important techniques include the self-assembly of elastin-like polypeptides into nanofibrous structures [149]) and so-called scaffold-free tissue engineering, based on cell-sheet technology, i.e. layer-by-layer assembly of continuous cell sheets, containing cells and their ECM, into tubular structures [61,150].

Even classical materials are not completely lost for creating small-diameter vascular grafts

Finally, it is even worth considering materials such as ePTFE and PET for the design of small-diameter vascular replacements. Although these materials are unsuitable for this purpose in their pristine unmodified state, they have long been established for the design of vascular substitutes, and further innovation and modification may have a beneficial effect on their endothelialization and on the reconstruction of the contractile VSMC layer. Recently, the inner surface of small-diameter ePTFE grafts with an inner diameter of 1 mm was modified with heparin and epigallocatechin gallate, while the outer surface was modified with polyethyleneimine and rapamycin. The inner surface then promoted the adhesion and growth of HUVECs, while the outer surface inhibited the proliferation of VSMCs [151]. In another study, the endothelialization of ePTFE vascular prostheses (either *in vitro* by pre-seeding with endothelial cells or *in vivo* by capture of endothelial progenitor cells from the blood) was improved by immobilization of antibodies against CD34 on the inner surface of these grafts [152].

In PET grafts, tannic acid-assisted immobilization of Cu^{2+}, carboxybetaine and argatroban improved the blood compatibility, endothelialization and also antimicrobial activity, while the migration and proliferation of VSMCs were attenuated [153]. In this context, it is also necessary to mention the pioneering work of Czech authors (namely Assoc. Prof. Milan Krajíček and his co-workers and followers), who also tried to innovate a material based on polyester (e.g. PET) so that it could be used for the construction of vascular substitutes of small diameter up to 6 mm. When designing small-diameter vascular grafts, these authors tried to mimic the physiological structure of the saphenous vein, which is often used for these grafts. These authors chose a knitted tubular scaffold made of non-resorbable polyester as the basis, which actually represented the *tunica media*. This scaffold was further enriched with a biologically resorbable component, namely with an inner and outer layer of collagen, which reconstituted the *tunica intima* and *tunica adventitia*, respectively. The resulting low-flow, small-diameter vascular grafts were then successfully tested in a large animal model, i.e. a sheep model [154]. These vascular grafts were developed not only on the basis of the commonly used bovine collagen [155], but also on the basis of fish collagen, specifically purified (delipidated) collagen from Czech carp, which was characterized by lower immunogenicity compared to bovine collagen [156] and promoted spontaneous endothelialization of the graft after its implantation in sheep [157]. These novel low-flow, small-diameter composite vascular grafts have also been patented [158].

However, it would also be advisable to introduce

physiological cellular components of the vessel wall into these types of vascular substitutes. This task was at least partially undertaken in our work. In our experiments, the inner surface of PET prostheses (VUP Joint-Stock Co., Brno, Czech Republic) was modified with fibrin and fibronectin [159] and was seeded with autologous porcine endothelial cells isolated from the jugular vein, which were expanded *in vitro* and purified from other cell types. Endothelialization of the grafts was performed in a tubular chamber of a commercially available dynamic culture system (Provitro GmbH, Berlin, Germany), and the grafts were implanted into pigs as iliac-femoral bypasses. On day 22 after implantation, the endothelialized graft was patent, while the unmodified graft was occluded with thrombosis. Immunofluorescence of the grafts after explantation revealed some "contamination" of the endothelial cell layer with VSMCs (Fig. 5). However, the presence of VSMCs gives hope that a neoarterial structure with mature, contractile VSMCs underneath the endothelium will be developed (for a review, see [24]).

Last but not least, even ePTFE and PET (Dacron) are promising for spontaneous endothelialization through *vasa vasorum*, including capillaries ingrowing transmurally into the vascular replacement from its surroundings after its implantation *in vivo*. A pre-requisite is that these implants must be thin-walled and of porous structure, with pores of an internal diameter of 60-90 μm, optimally as large as 5000-6000 μm^2 (for a review, see [24].

Taking into consideration sex-related differences in vascular tissue engineering

Not only when investigating the causes, the course and the clinical picture of cardiovascular diseases, but also when designing vascular replacements, it is necessary to take into account possible sex-related differences in the response of the organism to the implanted biomaterial and in the behavior of the cellular

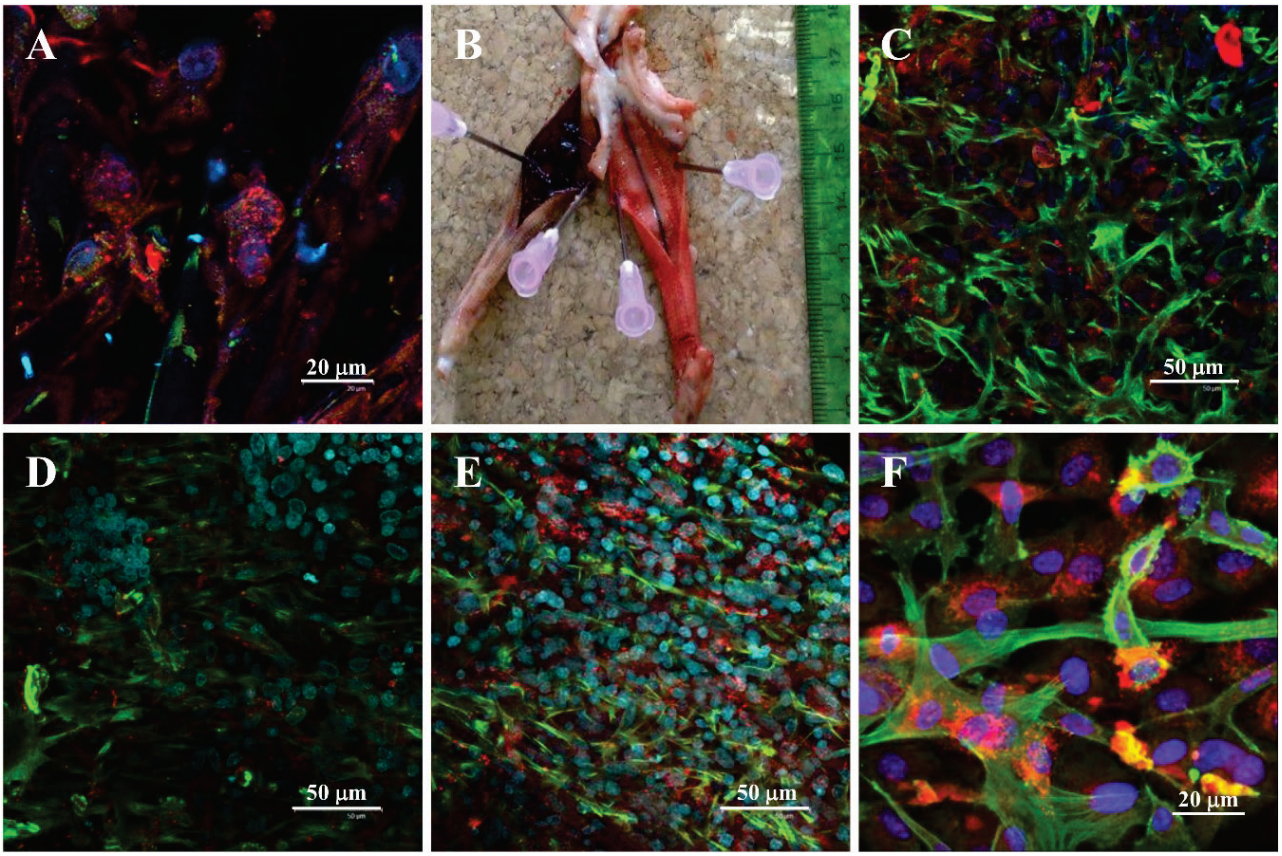

Fig. 5. Performance of a PET vascular prosthesis modified with fibrin and fibronectin, seeded with autologous endothelial cells and implanted into pigs. **A**: the inner surface pre-seeded with endothelial cells in vitro prior to the implantation; **B**: the gross morphology of explanted prostheses on day 22 after implantation: left – non-modified, right – pre-endothelialized; **C**, **D**, **E**: proximal, middle and distal parts of the prosthesis, respectively; **F**: control co-culture of endothelial cells and VSMCs on a glass coverslip. Immunofluorescence stain of von Willebrand factor, a marker of endothelial cells (red) and α-actin, a marker of VSMCs (green). The cell nuclei are counterstained with Hoechst 33342 (blue). Confocal microscope Leica SP2.

component of the vascular replacement. For example, in a study performed on PLGA vascular grafts with PLA and PCL sealant, implanted in mice, monocytes and macrophages of male and female recipients responded differently to the biomaterial. This has to be important for further evaluating various biomaterials as well as their translation to the clinic. Males, despite having similar levels of macrophages to females, degrade the implanted biomaterial much more rapidly, while females create more foreign body giant cells and produce more collagen [160]. Also, human pluripotent stem cells (hPSCs), whether embryonic stem cells or induced pluripotent stem cells (iPSCs), behaved differently when derived from male or female donors. Although hPSCs have a similar ability to differentiate towards VSMCs in males and in females, estrogens increase this ability only in females, not in males. Estrogens also promote the synthesis of ECM (collagen type 1 and 3) by hPSCs, and prevent its degradation [161].

Regarding the differentiation of hPSCs towards endothelial cells, male hPSCs efficiently differentiate into $CD34^+$ $CD31^+$ endothelial progenitors using the standard glycogen synthase kinase 3 (GSK3) inhibition protocol, while female hPSCs need the addition of VEGF to this protocol [162]. Another positive effect on endothelial cells is due to estrogens. These hormones mobilize endothelial progenitor cells from the bone marrow, which then have the opportunity to colonize the lumen of blood vessels and differentiate into endothelial cells (for a review, see [163]. Estrogens also stimulate the migration and proliferation of endothelial cells and have numerous other protective effects on these cells and on blood vessels in general, such as activating the synthesis of vasodilators (nitric oxide, hydrogen sulfide, prostacyclin), antioxidant, anti-inflammatory and antithrombotic effects, and reducing the transport of low-density lipoproteins through endothelial cells (for a review, see [4]). However, it should be taken into account that while estrogen can accelerate the endothelialization of denudated arteries or tissue-engineered vascular grafts, tamoxifen does not have this effect [160].

Conclusion and further perspectives

According to some authors, especially clinicians, tissue engineering of small-diameter vascular replacements has reached some kind of "dead end", because even 70 years since the first vascular prostheses were implanted in human patients, there are still no functional small-diameter vascular prostheses on the market. Stenosis and occlusion of small-diameter vessels have to be addressed by endovascular therapies or by the use of autologous vascular grafts. Moreover, neither polymeric nor biological vascular substitutes (decellularized or devitalized) contain a cellular component, especially the inner layer of endothelial cells. Unlike animal models, cell-free vascular substitutes do not spontaneously endothelialize in human patients. Some hope for their endothelialization is seen in the transmural vascularization of porous vascular substitutes by the ingrowth of blood vessels from the surrounding environment. We believe that this vascularization could be aided by pre-vascularization of tissue-engineered vascular constructs already under *in vitro* conditions by mixing mesenchymal stem cells (MSCs), e.g. derived from adipose tissue, and endothelial cells that are able to self-assemble into pre-capillaries in a 3D environment. Moreover, MSCs are able to differentiate into smooth muscle cells relatively easily by physiological biochemical and mechanical stimulation, and it would be also possible to generate endothelial cells from MSCs using so-called footprint-free iPSCs, obtained by introducing synthetic self-replicating RNA into these cells. Small-diameter vascular replacements could therefore be created by combining new modern tissue engineering techniques such as 3D bioprinting, electrospinning, differentiation of readily available stem cell types and RNA technologies, as well as through personalized medicine that would take into account potential sex and other differences in behavior and in the acceptance of vascular constructs. Even if tissue-engineered blood vessel constructs are not ultimately used as implants in the human body, they can serve as *in vitro* tissue models for a variety of developmental, physiological, pathophysiological, and pharmacological studies to replace the expensive and less ethical use of laboratory animals in modern 21st-century science according to the 3R principle.

Conflict of Interest

There is no conflict of interest.

Acknowledgements

This review article, summarizing results from several studies, has been supported by the National Institute for Research of Metabolic and Cardiovascular Diseases project (EXCELES Programme, ID Project

No. LX22NPO5104) - funded by the European Union - Next Generation EU. Further support was provided by the Czech Academy of Sciences, Praemium Academiae grant No. AP2202, by the Czech Health Research Council, Ministry of Health of the Czech Republic (grant No. NV19-02-00068), and also by OP JAC Project No. CZ.02.01.01/00/22_008/0004562, of the Ministry of Education, Youth and Sports (MEYS) of the Czech Republic, co-funded by the European Union. We also acknowledge the Light Microscopy Core Facility, Institute of Molecular Genetics, Prague, Czech Republic, supported by MEYS – LM2023050 and RVO – 68378050-KAV-NPUI, for their support with the confocal/widefield/super-resolution imaging/image analysis presented herein. Robin Healey (Czech Technical University in Prague, Czech Republic) is gratefully acknowledged for his language revision of the manuscript.

Abbreviations

ADSCs, adipose tissue-derived stem cells; AICAR, 5-aminoimidazole-4-carboxamide ribonucleotide; AMPK, adenosine monophosphate-activated protein kinase; ANOVA, analysis of variance; Atto 488, green-fluorescent dye from ATTO-TEC GmbH, Germany, with excitation suited to the 488 nm laser line; AV, arterio-venous; BM, bone marrow; BMP-4, bone morphogenetic protein-4; CAD, coronary artery disease; CD, cluster of differentiation; cMyc, cellular myelocytomatosis oncogene; *CNN1*, calponin 1 gene; Col, collagen; Cys-Ala-Gly, cysteine-alanine-glycine; DAPI, 4′,6-diamidine-2′-phenylindole dihydrochloride; DNA, deoxyribonucleic acid; ECM, extracellular matrix; EGF, epidermal growth factor; EGM-2, endothelial cell growth medium-2; ePTFE, expanded polytetrafluoroethylene; F-actin, filamentous actin; FGF, fibroblast growth factor; FN, fibronectin; GelMa, gelatin-methacryloyl hydrogel; GFP, green fluorescent protein; GSK3, glycogen synthase kinase 3; HAV, human acellular vessel; hPSCs, human pluripotent stem cells; HUVECs, human umbilical vein endothelial cells; IGF-1, insulin-like growth factor-1; iPSCs, induced pluripotent stem cells; IRES, internal ribosome entry site; KDR, kinase insert domain receptor; KLF4, Krüppel-like factor 4; LIN28, Lin-28 homolog A (an RNA-binding protein that binds to and enhances the translation of the insulin-like growth factor 2 mRNA); M, months; M-CSF, macrophage colony-stimulating factor; MCP-1, monocyte chemoattractant protein-1; MEYS, Ministry of Education, Youth and Sports; MMPs, metalloproteases; mRNA, messenger ribonucleic acid; MSCs, mesenchymal stem cells; N/A, not applicable; NANOG, Tír na nÓg (Irish for "Land of the Young"); NGF, nerve growth factor; OCT4, octamer-binding transcription factor 4; PAD, peripheral arterial occlusive disease; PBS, poly(1,4-butylene succinate); PCL, polycaprolactone; PCL/PDO, poly-ε-caprolactone/polydioxanone; PCR, polymerase chain reaction; PDGF, platelet-derived growth factor; PDMS, poly(dimethyl-siloxane); PEGDA, poly(ethylene glycol) diacrylate; PET, poly(ethylene terephthalate); PGA, poly(glycolic acid); PLA, poly(lactic acid); PLCL, poly(L-lactide-*co*-caprolactone); PLGA. poly(lactide-*co*-glycolide); PS, polystyrene; PU, polyurethane; PVA, poly(vinyl alcohol); REDV, Arg-Glu-Asp-Val (arginine-glutamic acid-aspartic acid-valine); RNA, ribonucleic acid; RUNX2, runt-related transcription factor 2; SD, standard deviation; SHR, spontaneously hypertensive rats; *SMTN*, smoothelin gene; SOX2, (sex determining region Y)-box 2; SPF, specific pathogen-free; sr-RNA, synthetic self-replicating ribonucleic acid; SRY, sex-determining region Y; SSEA4, stage-specific embryonic antigen-4; TEBV, totally engineered blood vessel; TEVG, tissue-engineered vascular grafts; TGF-β1, transforming growth factor-beta1; TNFs, tumor necrosis factors; TPSLEQRTVYAK, Thr-Pro-Ser-Leu-Glu-Gln-Arg-Thr-Val-Tyr-Ala-Lys (threonine-proline-serine-leucine-glutamic acid-glutamine-arginine-threonine-valine-tyrosine-alanine-lysine); TPU, thermoplastic polyurethane; TPUU, thermoplastic poly(urethane urea); UPI, epsin-mimetic endothelium-targeting chimeric peptide (containing an ubiquitin-interacting motif, a plasma membrane targeting sequence from the Lyn kinase H4 domain, and a tumor homing sequence iRGD); VE-cadherin, vascular endothelial cadherin; VEGF, vascular endothelial growth factor; VICs, valve interstitial cells; VSMCs, vascular smooth muscle cells; WHO, World Health Organization; WJSCs, Wharton's jelly stem cells.

References

1. Gupta S, Khanal S, Bhavnani N, Mathias A, Lallo J, Kiriakou A, Ferrell J, Raman P. Sex-specific differences in atherosclerosis, thrombospondin-1, and smooth muscle cell differentiation in metabolic syndrome versus non-metabolic syndrome mice. Front Cardiovasc Med 2022;9:1020006. https://doi.org/10.3389/fcvm.2022.1020006

2. World Health Organization. Cardiovascular diseases (CVDs). June 11, 2021. https://www.who.int/news-room/fact-sheets/detail/cardiovascular-diseases-(cvds) (accessed December 10, 2023).
3. OECD, European Observatory on Health Systems and Policies. Czechia: Country Health Profile 2021. OECD. 2021; https://health.ec.europa.eu/system/files/2021-12/2021_chp_cs_english.pdf (accessed December 10, 2023)
4. Robert J. Sex differences in vascular endothelial cells. Atherosclerosis 2023;384:117278. https://doi.org/10.1016/j.atherosclerosis.2023.117278
5. Bacakova L, Travnickova M, Filova E, Matějka R, Stepanovska J, Musilkova J, Zarubova J, Molitor M. The role of vascular smooth muscle cells in the physiology and pathophysiology of blood vessels. In: Muscle Cell and Tissue - Current Status of Research Field. K Sakuma (ed), IntechOpen. London, United Kingdom, 2018, pp 229-256. https://doi.org/10.5772/intechopen.77115
6. Loukotová J, Bacáková L, Zicha J, Kunes J. The influence of angiotensin II on sex-dependent proliferation of aortic VSMC isolated from SHR. Physiol Res 1998;47:501-505.
7. Ely DL, Falvo J, Dunphy G, Caplea A, Salisbury R, Turner M. The spontaneously hypertensive rat Y chromosome produces an early testosterone rise in normotensive rats. J Hypertens 1994;12:769-774. https://doi.org/10.1097/00004872-199407000-00007
8. Ely D, Caplea A, Dunphy G, Daneshvar H, Turner M, Milsted A, Takiyyuddin M. Spontaneously hypertensive rat Y chromosome increases indexes of sympathetic nervous system activity. Hypertension 1997;29:613-618. https://doi.org/10.1161/01.HYP.29.2.613
9. Ueda K, Lu Q, Baur W, Aronovitz MJ, Karas RH. Rapid estrogen receptor signaling mediates estrogen-induced inhibition of vascular smooth muscle cell proliferation. Arterioscler Thromb Vasc Biol 2013;33:1837-1843. https://doi.org/10.1161/ATVBAHA.112.300752
10. Hogg ME, Vavra AK, Banerjee MN, Martinez J, Jiang Q, Keefer LK, Chambon P, Kibbe MR. The role of estrogen receptor α and β in regulating vascular smooth muscle cell proliferation is based on sex. J Surg Res 2012;173:e1-e10. https://doi.org/10.1016/j.jss.2011.09.021
11. Sivritas D, Becher MU, Ebrahimian T, Arfa O, Rapp S, Bohner A, Mueller CF, Umemura T, Wassmann S, Nickenig G, Wassmann K. Antiproliferative effect of estrogen in vascular smooth muscle cells is mediated by Kruppel-like factor-4 and manganese superoxide dismutase. Basic Res Cardiol 2011;106:563-575. https://doi.org/10.1007/s00395-011-0174-z
12. Benditt EP, Benditt JM. Evidence for a monoclonal origin of human atherosclerotic plaques. Proc Natl Acad Sci USA 1973;70:1753-1756. https://doi.org/10.1073/pnas.70.6.1753
13. Pearson TA, Kramer EC, Solez K, Heptinstall RH. The human atherosclerotic plaque. Am J Pathol 1977;86:657-664.
14. Benditt EP, Barrett T, McDougall JK. Viruses in the etiology of atherosclerosis. Proc Natl Acad Sci USA 1983;80:6386-6389. https://doi.org/10.1073/pnas.80.20.6386
15. Bacakova L, Mares V. Cell kinetics of aortic smooth muscle cells in long-term cultures prepared from rats raised under conventional and spf conditions. Physiol Res 1995;44:389-398.
16. Schwartz CJ, Valente AJ, Sprague EA, Kelley JL, Suenram CA, Rozek MM. Atherosclerosis as an inflammatory process: The roles of the monocyte-macrophage a. Ann N Y Acad Sci 1985;454:115-120. https://doi.org/10.1111/j.1749-6632.1985.tb11849.x
17. Takahashi K, Takeya M, Sakashita N. Multifunctional roles of macrophages in the development and progression of atherosclerosis in humans and experimental animals. Med Electron Microsc 2002;35:179-203. https://doi.org/10.1007/s007950200023
18. Mensah EA, Daneshtalab N, Tabrizchi R. Differential biomechanics in resistance arteries of male compared with female Dahl hypertensive rats. J Hypertens 2022;40:596-605. https://doi.org/10.1097/HJH.0000000000003053
19. Sakkers TR, Mokry M, Civelek M, Erdmann J, Pasterkamp G, Diez Benavente E, den Ruijter HM. Sex differences in the genetic and molecular mechanisms of coronary artery disease. Atherosclerosis 2023;384:117279. https://doi.org/10.1016/j.atherosclerosis.2023.117279

20. Hartman RJG, Owsiany K, Ma L, Koplev S, Hao K, Slenders L, Civelek M, Mokry M, Kovacic JC, Pasterkamp G, Owens G, Björkegren JLM, den Ruijter HM. Sex-stratified gene regulatory networks reveal female key driver genes of atherosclerosis involved in smooth muscle cell phenotype switching. Circulation 2021;143:713-726. https://doi.org/10.1161/CIRCULATIONAHA.120.051231
21. Vogt BJ, Peters DK, Anseth KS, Aguado BA. Inflammatory serum factors from aortic valve stenosis patients modulate sex differences in valvular myofibroblast activation and osteoblast-like differentiation. Biomater Sci 2022;10:6341-6353. https://doi.org/10.1039/D2BM00844K, https://doi.org/10.1039/D2BM90082C
22. Chlupáč J, Filová E, Bačáková L. Blood vessel replacement: 50 years of development and tissue engineering paradigms in vascular surgery. Physiol Res 2009;S119-S140. https://doi.org/10.33549/physiolres.931918
23. Chlupac J, Matejka R, Konarik M, Novotny R, Simunkova Z, Mrazova I, Fabian O, Zapletal M, Pulda Z, Lipensky JF, Stepanovska J, Hanzalek K, Broz A, Novak T, Lodererova A, Voska L, Adla T, Fronek J, Rozkot M, Forostyak S, Kneppo P, Bacakova L, Pirk J. Vascular remodeling of clinically used patches and decellularized pericardial matrices recellularized with autologous or allogeneic cells in a porcine carotid artery model. Int J Mol Sci 2022;23:3310. https://doi.org/10.3390/ijms23063310
24. Zilla P, Deutsch M, Bezuidenhout D, Davies NH, Pennel T. Progressive reinvention or destination lost? Half a century of cardiovascular tissue engineering. Front Cardiovasc Med 2020;7:159. https://doi.org/10.3389/fcvm.2020.00159
25. Voorhees AB, Jaretzki A, Blakemore AH. The use of tubes constructed from vinyon "n" cloth in bridging arterial defects a preliminary report: Ann Surg 1952;135:332-336. https://doi.org/10.1097/00000658-195203000-00006
26. Blakemore AH, Voorhers AB. The use of tubes constructed from vinyon "N" cloth in bridging arterial defects-experimental and clinical: Ann Surg 1954;140:324-334. https://doi.org/10.1097/00000658-195409000-00008
27. Gaudino M, Bakaeen FG, Benedetto U, Di Franco A, Fremes S, Glineur D, Girardi LN, Grau J, Puskas JD, Ruel M, Tam DY, Taggart DP, Antoniades C, Patrono C, Schwann TA, Tatoulis J, Tranbaugh RF. Arterial grafts for coronary bypass: a critical review after the publication of art and radial. Circulation 2019;140:1273-1284. https://doi.org/10.1161/CIRCULATIONAHA.119.041096
28. Ghandakly EC, Tipton AE, Bakaeen FG. Pathophysiology and management of saphenous vein graft disease. Expert Rev Cardiovasc 2023;21:565-572. https://doi.org/10.1080/14779072.2023.2233420
29. Kim Y, Jung JH, Hwang D, Yun W-S, Huh S, Kim H-K. Below-knee prosthetic bypass is a viable option for limb salvage in patients with extensive femoropopliteal occlusive disease. Vasc Specialist Int 2023;39:16. https://doi.org/10.5758/vsi.230028
30. Bram R, Almadidy Z, Souter J, Roskova I, Charbel FT. Vertebral artery to middle cerebral artery bypass for flow augmentation. Oper Neurosurg 2023; https://doi.org/10.1227/ons.0000000000000942
31. Kakisis JD, Liapis CD, Breuer C, Sumpio BE. Artificial blood vessel: the holy grail of peripheral vascular surgery. J Vasc Surg 2005;41:349-354. https://doi.org/10.1016/j.jvs.2004.12.026
32. Eghbalzadeh K, Guschlbauer M, Weber C, Wacker MT, Reinhardt S, Djordjevic I, Sabashnikov A, Maul A, Sterner-Kock A, Wahlers TCW, Scherner M, Wippermann J. Experimental studies for small diameter grafts in an in vivo sheep model-techniques and pitfalls. Thorac Cardiovasc Surg 2021;69:649-659. https://doi.org/10.1055/s-0039-1687887
33. Olausson M, Kuna VK, Travnikova G, Bäckdahl H, Patil PB, Saalman R, Borg H, Jeppsson A, Sumitran-Holgersson S. In vivo application of tissue-engineered veins using autologous peripheral whole blood: a proof of concept study. EBioMedicine 2014;1:72-79. https://doi.org/10.1016/j.ebiom.2014.09.001
34. Fronek J, Chlupac J. Transplantation surgery department at IKEM hospital, Prague, Czech Republic: increasing volume and improving outcomes through innovative clinical strategies and technical approaches. Transplantation 2023;107:2285-2289. https://doi.org/10.1097/TP.0000000000004633
35. Chen S, Wang J, Jia F, Shen Z, Zhang W, Wang Y, Ren K, Fu G, Ji J. Bioinspired NO release coating enhances endothelial cells and inhibits smooth muscle cells. J Mater Chem B 2022;10:2454-2462. https://doi.org/10.1039/D1TB01828K
36. Filova E, Parizek M, Olsovska J, Kamenik Z, Brynda E, Riedel T, Vandrovcova M, Lisa V, Machova L, Skalsky I, Szarszoi O, Suchy T, Bacakova L. Perivascular sirolimus-delivery system. Int J Pharm Sci 2011;404:94-101. https://doi.org/10.1016/j.ijpharm.2010.11.005

37. Skalský I, Filová E, Szárszoi O, Pařízek M, Lytvynets A, Malušková J, Lodererová A, Brynda E, Lisá V, Burdíková Z, Čapek M, Pirk J, Bačáková L. A periadventitial sirolimus-releasing mesh decreased intimal hyperplasia in a rabbit model. Physiol Res 2011;60:585-588. https://doi.org/10.33549/physiolres.932106
38. Skalský I, Szárszoi O, Filová E, Pařízek M, Lytvynets A, Malušková J, Lodererová A, Brynda E, Lisá V, Burdíková Z, Čapek M, Pirk J, Bačáková L. A perivascular system releasing sirolimus prevented intimal hyperplasia in a rabbit model in a medium-term study. Int J Pharm Sci 2012;427:311-319. https://doi.org/10.1016/j.ijpharm.2012.02.023
39. Weinberg CB, Bell E. A blood vessel model constructed from collagen and cultured vascular cells. Science 1986;231:397-400. https://doi.org/10.1126/science.2934816
40. Herring M, Gardner A, Glover J. Seeding human arterial prostheses with mechanically derived endothelium. J Vasc Surg 1984;1:279-289. https://doi.org/10.1016/0741-5214(84)90059-4, https://doi.org/10.1067/mva.1984.avs0010279
41. Shin'oka T, Imai Y, Ikada Y. Transplantation of a tissue-engineered pulmonary artery. N Engl J Med 2001;344:532-533. https://doi.org/10.1056/NEJM200102153440717
42. L'Heureux N, McAllister TN, de la Fuente LM. Tissue-engineered blood vessel for adult arterial revascularization. N Engl J Med 2007;357:1451-1453. https://doi.org/10.1056/NEJMc071536
43. Wystrychowski W, McAllister TN, Zagalski K, Dusserre N, Cierpka L, L'Heureux N. First human use of an allogeneic tissue-engineered vascular graft for hemodialysis access. J Vasc Surg 2014;60:1353-1357. https://doi.org/10.1016/j.jvs.2013.08.018
44. Kato N, Yamagishi M, Kanda K, Miyazaki T, Maeda Y, Yamanami M, Watanabe T, Yaku H. First successful clinical application of the in vivo tissue-engineered autologous vascular graft. Ann Thorac Surg 2016;102:1387-1390. https://doi.org/10.1016/j.athoracsur.2016.06.095
45. Gutowski P, Gage SM, Guziewicz M, Ilzecki M, Kazimierczak A, Kirkton RD, Niklason LE, Pilgrim A, Prichard HL, Przywara S, Samad R, Tente B, Turek J, Witkiewicz W, Zapotoczny N, Zubilewicz T, Lawson JH. Arterial reconstruction with human bioengineered acellular blood vessels in patients with peripheral arterial disease. J Vasc Surg 2020;72:1247-1258. https://doi.org/10.1016/j.jvs.2019.11.056
46. Gutowski P, Guziewicz M, Ilzecki M, Kazimierczak A, Lawson JH, Prichard HL, Przywara S, Samad R, Tente W, Turek J, Witkiewicz W, Zapotoczny N, Zubilewicz T, Niklason LE. Six-year outcomes of a phase II study of human-tissue engineered blood vessels for peripheral arterial bypass. JVS-Vascular Science 2023;4:100092. https://doi.org/10.1016/j.jvssci.2022.11.001
47. Laube HR, Duwe J, Rutsch W, Konertz W. Clinical experience with autologous endothelial cell-seeded polytetrafluoroethylene coronary artery bypass grafts. J Thorac Cardiovasc Surg 2000;120:134-141. https://doi.org/10.1067/mtc.2000.106327
48. Lamm P, Juchem G, Milz S, Schuffenhauer M, Reichart B. Autologous endothelialized vein allograft: a solution in the search for small-caliber grafts in coronary artery bypass graft operations. Circulation 2001;104:I108-I114. https://doi.org/10.1161/hc37t1.094527
49. Deutsch M, Eberl T, Fischlein T, Meinhart J, Minar E, Puschmann R, Schmid P, Zilla P. In vitro endothelialization of ePTFE vascular prostheses in clinical use: preliminary results]. Vasa Suppl 1990;30:219-220.
50. Zilla P, Deutsch M, Meinhart J, Puschmann R, Eberl T, Minar E, Dudczak R, Lugmaier H, Schmidt P, Noszian I, Fischlein T. Clinical in vitro endothelialization of femoropopliteal bypass grafts: An actuarial follow-up over three years. J Vasc Surg 1994;19:540-548. https://doi.org/10.1016/S0741-5214(94)70083-4
51. Meinhart J, Deutsch M, Zilla P. Eight years of clinical endothelial cell transplantation. Closing the gap between prosthetic grafts and vein grafts. ASAIO J 1997;43:M515-521. https://doi.org/10.1097/00002480-199709000-00034
52. Deutsch M, Meinhart J, Zilla P, Howanietz N, Gorlitzer M, Froeschl A, Stuempflen A, Bezuidenhout D, Grabenwoeger M. Long-term experience in autologous in vitro endothelialization of infrainguinal ePTFE grafts. J Vasc Surg 2009;49:352-362. https://doi.org/10.1016/j.jvs.2008.08.101

53. Shin'oka T, Matsumura G, Hibino N, Naito Y, Watanabe M, Konuma T, Sakamoto T, Nagatsu M, Kurosawa H. Midterm clinical result of tissue-engineered vascular autografts seeded with autologous bone marrow cells. J Thorac Cardiovasc Surg 2005;129:1330-1338. https://doi.org/10.1016/j.jtcvs.2004.12.047
54. Hibino N, McGillicuddy E, Matsumura G, Ichihara Y, Naito Y, Breuer C, Shinoka T. Late-term results of tissue-engineered vascular grafts in humans. J Thorac Cardiovasc Sur 2010;139:431-436.e1-2. https://doi.org/10.1016/j.jtcvs.2009.09.057
55. Sugiura T, Matsumura G, Miyamoto S, Miyachi H, Breuer CK, Shinoka T. Tissue-engineered vascular grafts in children with congenital heart disease: Intermediate term follow-up. J Thorac Cardiovasc Surg 2018;30:175-179. https://doi.org/10.1053/j.semtcvs.2018.02.002
56. Bockeria LA, Svanidze O, Kim A, Shatalov K, Makarenko V, Cox M, Carrel T. Total cavopulmonary connection with a new bioabsorbable vascular graft: First clinical experience. J Thorac Cardiovasc Surg 2017;153:1542-1550. https://doi.org/10.1016/j.jtcvs.2016.11.071
57. Bockeria L, Carrel T, Lemaire A, Makarenko V, Kim A, Shatalov K, Cox M, Svanidze O. Total cavopulmonary connection with a new restorative vascular graft: results at 2 years. J Thorac Dis 2020;12:4168-4173. https://doi.org/10.21037/jtd-19-739
58. Teebken, Puschmann, Rohde, Burgwitz, Winkler, Pichlmaier, Weidemann, Haverich. Human iliac vein replacement with a tissue-engineered graft. Vasa 2009;38:60-65. https://doi.org/10.1024/0301-1526.38.1.60
59. Olausson M, Patil PB, Kuna VK, Chougule P, Hernandez N, Methe K, Kullberg-Lindh C, Borg H, Ejnell H, Sumitran-Holgersson S. Transplantation of an allogeneic vein bioengineered with autologous stem cells: a proof-of-concept study. The Lancet 2012;380:230-237. https://doi.org/10.1016/S0140-6736(12)60633-3
60. McAllister TN, Maruszewski M, Garrido SA, Wystrychowski W, Dusserre N, Marini A, Zagalski K, Fiorillo A, Avila H, Manglano X, Antonelli J, Kocher A, Zembala M, Cierpka L, de la Fuente LM, L'Heureux N. Effectiveness of haemodialysis access with an autologous tissue-engineered vascular graft: a multicentre cohort study. The Lancet 2009;373:1440-1446. https://doi.org/10.1016/S0140-6736(09)60248-8
61. Peck M, Dusserre N, McAllister TN, L'Heureux N. Tissue engineering by self-assembly. Materials Today 2011;14:218-224. https://doi.org/10.1016/S1369-7021(11)70117-1
62. Lawson JH, Glickman MH, Ilzecki M, Jakimowicz T, Jaroszynski A, Peden EK, Pilgrim AJ, Prichard HL, Guziewicz M, Przywara S, Szmidt J, Turek J, Witkiewicz W, Zapotoczny N, Zubilewicz T, Niklason LE. Bioengineered human acellular vessels for dialysis access in patients with end-stage renal disease: two phase 2 single-arm trials. The Lancet 2016;387:2026-2034. https://doi.org/10.1016/S0140-6736(16)00557-2
63. Kirkton RD, Santiago-Maysonet M, Lawson JH, Tente WE, Dahl SLM, Niklason LE, Prichard HL. Bioengineered human acellular vessels recellularize and evolve into living blood vessels after human implantation. Sci Transl Med 2019;11:eaau6934. https://doi.org/10.1126/scitranslmed.aau6934
64. Jakimowicz T, Przywara S, Turek J, Pilgrim A, Macech M, Zapotoczny N, Zubilewicz T, Lawson JH, Niklason LE. Five year outcomes in patients with end stage renal disease who received a bioengineered human acellular vessel for dialysis access. EJVES Vascular Forum 2022;54:58-63. https://doi.org/10.1016/j.ejvsvf.2022.01.003
65. Nakayama Y, Kaneko Y, Okumura N, Tatsumi E. Long-term follow up of first-in-human study in bypass of stenosis av shunt by an autologous in-body-tissue-engineered (biotube) vascular graft. Eur Heart J 2018;39. https://doi.org/10.1093/eurheartj/ehy565.P2664
66. Nakayama Y, Kaneko Y, Okumura N, Terazawa T. Initial 3-year results of first human use of an in-body tissue-engineered autologous "Biotube" vascular graft for hemodialysis. J Vasc Access 2020;21:110-115. https://doi.org/10.1177/1129729819852550
67. Higashita R, Miyazaki M, Oi M, Ishikawa N. First-in-human results of an in-body tissue architecture-induced tissue-engineered vascular graft "Biotube" for application in distal bypass for chronic limb-threatening ischemia. J Vasc Surg Cases 2022;8:488-493. https://doi.org/10.1016/j.jvscit.2022.07.007
68. Carrabba M, Madeddu P. Current strategies for the manufacture of small size tissue engineering vascular grafts. Front Bioeng Biotechnol 2018;6:41. https://doi.org/10.3389/fbioe.2018.00041
69. Boccafoschi F, Botta M, Fusaro L, Copes F, Ramella M, Cannas M. Decellularized biological matrices: an interesting approach for cardiovascular tissue repair and regeneration. J Tissue Eng Regen Med 2017;11:1648-1657. https://doi.org/10.1002/term.2103

70. Bergmeister H, Podesser BK. Preclinical in vivo assessment of tissue engineered vascular grafts and selection of appropriate animal models. In: Tissue-Engineered Vascular Grafts. BH Walpoth, H Bergmeister, GL Bowlin, D Kong, JI Rotmans, P Zilla (eds), Springer International Publishing. Cham, 2020, pp 63-93. https://doi.org/10.1007/978-3-030-05336-9_5
71. Yang Y, Lei D, Zou H, Huang S, Yang Q, Li S, Qing F-L, Ye X, You Z, Zhao Q. Hybrid electrospun rapamycin-loaded small-diameter decellularized vascular grafts effectively inhibit intimal hyperplasia. Acta Biomater 2019;97:321-332. https://doi.org/10.1016/j.actbio.2019.06.037
72. Shi J, Teng Y, Li D, He J, Midgley AC, Guo X, Wang X, Yang X, Wang S, Feng Y, Lv Q, Hou S. Biomimetic tri-layered small-diameter vascular grafts with decellularized extracellular matrix promoting vascular regeneration and inhibiting thrombosis with the salidroside. Materials Today Bio 2023;21:100709. https://doi.org/10.1016/j.mtbio.2023.100709
73. Cai Z, Tan Z, Tian R, Chen X, Miao P, Yao C, Wang C, Yu Z, Gu Y. Acellular vascular scaffolds preloaded with heparin and hepatocyte growth factor for small-diameter vascular grafts might inhibit intimal hyperplasia. Cell Transplant 2022;31:096368972211345. https://doi.org/10.1177/09636897221134541
74. Xie X, Wu Q, Liu Y, Chen C, Chen Z, Xie C, Song M, Jiang Z, Qi X, Liu S, Tang Z, Wu Z. Vascular endothelial growth factor attenuates neointimal hyperplasia of decellularized small-diameter vascular grafts by modulating the local inflammatory response. Front Bioeng Biotechnol 2022;10:1066266. https://doi.org/10.3389/fbioe.2022.1066266
75. Gou K, Hu J-J, Baek S. Mechanical characterization of human umbilical arteries by thick-walled models: Enhanced vascular compliance by removing an abluminal lining. J Mech Behav Biomed Mater 2023;142:105811. https://doi.org/10.1016/j.jmbbm.2023.105811
76. Wong V, Gada S, Singh M, Merna N. The development of small-caliber vascular grafts using human umbilical artery: an evaluation of methods. Tissue Eng Part C Methods 2023;29:1-10. https://doi.org/10.1089/ten.tec.2022.0144
77. Tardalkar KR, Marsale TB, Bhamare NC, Kshersagar JR, Patil JK, Adnaik A, Joshi MG. Heparin coated decellularized xenogeneic small diameter vascular conduit for vascular repair with early luminal reendothelialization. Cell Tissue Bank 2023;24:449-469. https://doi.org/10.1007/s10561-022-10046-0
78. Falkner F, Mayer SA, Thomas B, Zimmermann SO, Walter S, Heimel P, Thiele W, Sleeman JP, Bigdeli AK, Kiss H, Podesser BK, Kneser U, Bergmeister H, Schneider KH. Acellular human placenta small-diameter vessels as a favorable source of super-microsurgical vascular replacements: a proof of concept. Bioengineering 2023;10:337. https://doi.org/10.3390/bioengineering10030337
79. Wang B, Wang X, Kenneth A, Drena A, Pacheco A, Kalvin L, Ibrahim E-S, Rossi PJ, Thatcher K, Lincoln J. Developing small-diameter vascular grafts with human amniotic membrane: long-term evaluation of transplantation outcomes in a small animal model. Biofabrication 2023;15:025004. https://doi.org/10.1088/1758-5090/acb1da
80. Gorbenko N, Rinaldi G, Sanchez A, Merna N. Small-caliber vascular grafts engineered from decellularized leaves and cross-linked gelatin. Tissue Eng Part A 2023;29:397-409. https://doi.org/10.1089/ten.tea.2022.0223
81. Wang H, Xiao Y, Fang Z, Zhang Y, Yang L, Zhao C, Meng Z, Liu Y, Li C, Han Q, Feng Z. Fabrication and performance evaluation of PLCL-hCOLIII small-diameter vascular grafts crosslinked with procyanidins. Int J Biol Macromol 2023;251:126293. https://doi.org/10.1016/j.ijbiomac.2023.126293
82. Filová E, Staňková L, Eckhardt A, Svobodová J, Musílková J, Pala J, Hadraba D, Brynda E, Koňařík M, Pirk J, Bačáková L. Modification of human pericardium by chemical crosslinking. Physiol Res 2020;69:49-59. https://doi.org/10.33549/physiolres.934335
83. Guo J, Huang J, Lei S, Wan D, Liang B, Yan H, Liu Y, Feng Y, Yang S, He J, Kong D, Shi J, Wang S. Construction of rapid extracellular matrix-deposited small-diameter vascular grafts induced by hypoxia in a bioreactor. ACS Biomater Sci Eng 2023;9:844-855. https://doi.org/10.1021/acsbiomaterials.2c00809
84. Huyan Y, Chang Y, Song J. Application of homograft valved conduit in cardiac surgery. Front Cardiovasc Med 2021;8:740871. https://doi.org/10.3389/fcvm.2021.740871

85. Sievers H-H, Stierle U, Schmidtke C, Bechtel M. Decellularized pulmonary homograft (SynerGraft) for reconstruction of the right ventricular outflow tract: first clinical experience. Zeitschrift für Kardiologie 2003;92:53-59. https://doi.org/10.1007/s00392-003-0883-x
86. Filova E, Steinerova M, Travnickova M, Knitlova J, Musilkova J, Eckhardt A, Hadraba D, Matejka R, Prazak S, Stepanovska J, Kucerova J, Riedel T, Brynda E, Lodererova A, Honsova E, Pirk J, Konarik M, Bacakova L. Accelerated in vitro recellularization of decellularized porcine pericardium for cardiovascular grafts. Biomed Mater 2021;16:025024. https://doi.org/10.1088/1748-605X/abbdbd
87. Straka F, Schornik D, Masin J, Filova E, Mirejovsky T, Burdikova Z, Svindrych Z, Chlup H, Horny L, Vesely J, Pirk J, Bacakova L. A new approach to heart valve tissue engineering based on modifying autologous human pericardium by 3D cellular mechanotransduction. J Biomater Tissue Eng 2017;7:527-543. https://doi.org/10.1166/jbt.2017.1598
88. Straka F, Schornik D, Masin J, Filova E, Mirejovsky T, Burdikova Z, Svindrych Z, Chlup H, Horny L, Daniel M, Machac J, Skibová J, Pirk J, Bacakova L. A human pericardium biopolymeric scaffold for autologous heart valve tissue engineering: cellular and extracellular matrix structure and biomechanical properties in comparison with a normal aortic heart valve. J Biomat Sci-Polym E 2018;29:599-634. https://doi.org/10.1080/09205063.2018.1429732
89. Bacakova L, Zarubova J, Travnickova M, Musilkova J, Pajorova J, Slepicka P, Kasalkova NS, Svorcik V, Kolska Z, Motarjemi H, Molitor M. Stem cells: their source, potency and use in regenerative therapies with focus on adipose-derived stem cells - a review. Biotechnol Adv 2018;36:1111-1126. https://doi.org/10.1016/j.biotechadv.2018.03.011
90. Garzon I, Chato-Astrain J, Campos F, Fernandez-Valades R, Sanchez-Montesinos I, Campos A, Alaminos M, D'Souza RN, Martin-Piedra MA. Expanded differentiation capability of human Wharton's jelly stem cells toward pluripotency: a systematic review. Tissue Eng Part B Rev 2020;26:301-312. https://doi.org/10.1089/ten.teb.2019.0257
91. Matějka R, Koňařík M, Štěpanovská J, Lipenský J, Chlupáč J, Turek D, Pražák Š, Brož A, Šimůnková Z, Mrázová I, Forostyak S, Kneppo P, Rosina J, Bačáková L, Pirk J. Bioreactor processed stromal cell seeding and cultivation on decellularized pericardium patches for cardiovascular use. Appl Sci 2020;10:5473. https://doi.org/10.3390/app10165473
92. Bacakova L, Travnickova M, Filova E, Matejka R, Stepanovska J, Musilkova J, Zarubova J, Molitor M. Vascular smooth muscle cells (VSMCs) in blood vessel tissue engineering: the use of differentiated cells or stem cells as VSMC precursors. In: *Muscle Cell and Tissue - Current Status of Research Field.* K Sakuma (ed), IntechOpen. 2018. https://doi.org/10.5772/intechopen.77108
93. MedMedia. Relatus Med. Erster Bypass mit gezüchteten Zellen von Wiener Ärzten implantiert. October 25, 2020. https://www.medmedia.at/relatus-med/erster-bypass-mit-gezuechteten-zellen-von-wiener-aerzten-implantiert/ (accessed April 19, 2024).
94. Bordenave L, Fernandez P, Rémy-Zolghadri M, Villars S, Daculsi R, Midy D. In vitro endothelialized ePTFE prostheses: clinical update 20 years after the first realization. Clin Hemorheol Microcirc 2005;33:227-234.
95. Rademacher A, Paulitschke M, Meyer R, Hetzer R. Endothelialization of PTFE vascular grafts under flow induces significant cell changes. Int J Artif Organs 2001;24:235-242. https://doi.org/10.1177/039139880102400412
96. Alaminos M, Pérez-Köhler B, Garzón I, García-Honduvilla N, Romero B, Campos A, Buján J. Transdifferentiation potentiality of human wharton's jelly stem cells towards vascular endothelial cells. J Cell Physiol 2010;223:640-647. https://doi.org/10.1002/jcp.22062
97. Boonkaew B, Suwanpitak S, Pattanapanyasat K, Sermsathanasawadi N, Wattanapanitch M. Efficient generation of endothelial cells from induced pluripotent stem cells derived from a patient with peripheral arterial disease. Cell Tissue Res 2022;388:89-104. https://doi.org/10.1007/s00441-022-03576-2
98. Fan X, Cyganek L, Nitschke K, Uhlig S, Nuhn P, Bieback K, Duerschmied D, El-Battrawy I, Zhou X, Akin I. Functional characterization of human induced pluripotent stem cell-derived endothelial cells. Int J Mol Sci 2022;23:8507. https://doi.org/10.3390/ijms23158507
99. Takahashi K, Yamanaka S. Induction of pluripotent stem cells from mouse embryonic and adult fibroblast cultures by defined factors. Cell 2006;126:663-676. https://doi.org/10.1016/j.cell.2006.07.024

100. Takahashi K, Tanabe K, Ohnuki M, Narita M, Ichisaka T, Tomoda K, Yamanaka S. Induction of pluripotent stem cells from adult human fibroblasts by defined factors. Cell 2007;131:861-872. https://doi.org/10.1016/j.cell.2007.11.019
101. Yu J, Vodyanik MA, Smuga-Otto K, Antosiewicz-Bourget J, Frane JL, Tian S, Nie J, Jonsdottir GA, Ruotti V, Stewart R, Slukvin II, Thomson JA. Induced pluripotent stem cell lines derived from human somatic cells. Science 2007;318:1917-1920. https://doi.org/10.1126/science.1151526
102. Steinle H, Weber M, Behring A, Mau-Holzmann U, von Ohle C, Popov A-F, Schlensak C, Wendel HP, Avci-Adali M. Reprogramming of urine-derived renal epithelial cells into ipscs using srrna and consecutive differentiation into beating cardiomyocytes. Mol. Ther. Nucleic Acids 2019;17:907-921. https://doi.org/10.1016/j.omtn.2019.07.016
103. Weber M, Fech A, Jäger L, Steinle H, Bühler L, Perl RM, Martirosian P, Mehling R, Sonanini D, Aicher WK, Nikolaou K, Schlensak C, Enderle MD, Wendel HP, Linzenbold W, Avci-Adali M. Hydrojet-based delivery of footprint-free iPSC-derived cardiomyocytes into porcine myocardium. Sci Rep 2020;10:16787. https://doi.org/10.1038/s41598-020-73693-x
104. Weber J, Weber M, Feile A, Schlensak C, Avci-Adali M. Development of an in vitro blood vessel model using autologous endothelial cells generated from footprint-free hipscs to analyze interactions of the endothelium with blood cell components and vascular implants. Cells 2023;12:1217. https://doi.org/10.3390/cells12091217
105. Zhang M, Fukushima Y, Nozaki K, Nakanishi H, Deng J, Wakabayashi N, Itaka K. Enhancement of bone regeneration by coadministration of angiogenic and osteogenic factors using messenger RNA. Inflamm Regener 2023;43:32. https://doi.org/10.1186/s41232-023-00285-3
106. Tremblay P-L, Hudon V, Berthod F, Germain L, Auger FA. Inosculation of tissue-engineered capillaries with the host's vasculature in a reconstructed skin transplanted on mice. Am J Transplant 2005;5:1002-1010. https://doi.org/10.1111/j.1600-6143.2005.00790.x
107. Phua QH, Han HA, Soh B-S. Translational stem cell therapy: vascularized skin grafts in skin repair and regeneration. J Transl Med 2021;19:83. https://doi.org/10.1186/s12967-021-02752-2
108. Florey HW, Greer SJ, Kiser J, Poole JC, Telander R, Werthessen NT. The development of the pseudointima lining fabric grafts of the aorta. Br J Exp Pathol 1962;43:655-660.
109. Hirschi KK, Rohovsky SA, D'Amore PA. Cell-cell interactions in vessel assembly: a model for the fundamentals of vascular remodelling. Transpl Immunol 1997;5:177-178. https://doi.org/10.1016/S0966-3274(97)80034-2
110. Filova E, Supova M, Eckhardt A, Vrbacky M, Blanquer A, Travnickova M, Knitlova J, Suchy T, Ryglova S, Braun M, Burdikova Z, Schätz M, Jencova V, Lisnenko M, Behalek L, Prochazkova R, Sedlacek R, Kubasova K, Bacakova L. Adipose-derived stem cells in reinforced collagen gel: a comparison between two approaches to differentiation towards smooth muscle cells. Int J Mol Sci 2023;24:5692. https://doi.org/10.3390/ijms24065692
111. Li S, Zhao F, Tang Y, Zhang Y, Rong H, Liu L, Gao R, Liu X, Huangfu Y, Bai Y, Feng Z, Guo Z, Dong A, Wang W, Kong D, Huang P. Bioinspired, anticoagulative, 19 f mri-visualizable bilayer hydrogel tubes as high patency small-diameter vascular grafts. Small 2023;19:2302621. https://doi.org/10.1002/smll.202302621
112. Moura D, Pereira AT, Ferreira HP, Barrias CC, Magalhães FD, Bergmeister H, Gonçalves IC. Poly(2-hydroxyethyl methacrylate) hydrogels containing graphene-based materials for blood-contacting applications: From soft inert to strong degradable material. Acta Biomater 2023;164:253-268. https://doi.org/10.1016/j.actbio.2023.04.031
113. Fallon ME, Le HH, Bates NM, Yao Y, Yim EKF, Hinds MT, Anderson DEJ. Hemocompatibility of micropatterned biomaterial surfaces is dependent on topographical feature size. Front Physiol 2022;13:983187. https://doi.org/10.3389/fphys.2022.983187
114. Yao Y, Zaw AM, Anderson DEJ, Jeong Y, Kunihiro J, Hinds MT, Yim EKF. Fucoidan and topography modification improved in situ endothelialization on acellular synthetic vascular grafts. Bioact Mater 2023;22:535-550. https://doi.org/10.1016/j.bioactmat.2022.10.011
115. Jin Q, Yu C, Xu L, Zhang G, Ju J, Hou R. Combined light-cured and sacrificial hydrogels for fabrication of small-diameter bionic vessels by 3D bioprinting. Technol Health Care 2023;31:1203-1213. https://doi.org/10.3233/THC-220393

116. Tu C, Zhang Y, Xiao Y, Xing Y, Jiao Y, Geng X, Zhang A, Ye L, Gu Y, Feng Z. Hydrogel-complexed small-diameter vascular graft loaded with tissue-specific vascular extracellular matrix components used for tissue engineering. Biomater Adv 2022;142:213138. https://doi.org/10.1016/j.bioadv.2022.213138
117. Yang GH, Kang D, An S, Ryu JY, Lee K, Kim JS, Song M-Y, Kim Y-S, Kwon S-M, Jung W-K, Jeong W, Jeon H. Advances in the development of tubular structures using extrusion-based 3D cell-printing technology for vascular tissue regenerative applications. Biomater Res 2022;26:73. https://doi.org/10.1186/s40824-022-00321-2
118. Stepanovska J, Supova M, Hanzalek K, Broz A, Matejka R. Collagen bioinks for bioprinting: a systematic review of hydrogel properties, bioprinting parameters, protocols, and bioprinted structure characteristics. Biomedicines 2021;9:1137. https://doi.org/10.3390/biomedicines9091137
119. Xu H, Liu Z, Wei Y, Hu Y, Zhao L, Wang L, Liang Z, Lian X, Chen W, Wang J, Yu Z, Ma X, Huang D. Complexation-induced resolution enhancement pleiotropic small diameter vascular constructs with superior antibacterial and angiogenesis properties. Adv Healthcare Materials 2023;12:2301809. https://doi.org/10.1002/adhm.202301809
120. Alasvand N, Behnamghader A, Milan PB, Simorgh S, Mobasheri A, Mozafari M. Tissue-engineered small-diameter vascular grafts containing novel copper-doped bioactive glass biomaterials to promote angiogenic activity and endothelial regeneration. Materials Today Bio 2023;20:100647. https://doi.org/10.1016/j.mtbio.2023.100647
121. Fukunishi T, Best CA, Sugiura T, Opfermann J, Ong CS, Shinoka T, Breuer CK, Krieger A, Johnson J, Hibino N. Preclinical study of patient-specific cell-free nanofiber tissue-engineered vascular grafts using 3-dimensional printing in a sheep model. J Thorac Cardiovasc Surg 2017;153:924-932. https://doi.org/10.1016/j.jtcvs.2016.10.066
122. Atari M, Saroukhani A, Manshaei M, Bateni P, Zargar Kharazi A, Vatankhah E, Haghjooy Javanmard S. Preclinical in vivo assessment of a cell-free multi-layered scaffold prepared by 3D printing and electrospinning for small-diameter blood vessel tissue engineering in a canine model. Biomater Sci 2023;11:6871-6880. https://doi.org/10.1039/D3BM00642E
123. Hu Q, Shen Z, Zhang H, Liu S, Feng R, Feng J, Ramalingam M. Designed and fabrication of triple-layered vascular scaffold with microchannels. J Biomat Sci-Polym E 2021;32:714-734. https://doi.org/10.1080/09205063.2020.1864083
124. Huang Z, Zhang Y, Liu R, Li Y, Rafique M, Midgley AC, Wan Y, Yan H, Si J, Wang T, Chen C, Wang P, Shafiq M, Li J, Zhao L, Kong D, Wang K. Cobalt loaded electrospun poly(ε-caprolactone) grafts promote antibacterial activity and vascular regeneration in a diabetic rat model. Biomaterials 2022;291:121901. https://doi.org/10.1016/j.biomaterials.2022.121901
125. Yan H, Cheng Q, Si J, Wang S, Wan Y, Kong X, Wang T, Zheng W, Rafique M, Li X, He J, Midgley AC, Zhu Y, Wang K, Kong D. Functionalization of in vivo tissue-engineered living biotubes enhance patency and endothelization without the requirement of systemic anticoagulant administration. Bioact Mater 2023;26:292-305. https://doi.org/10.1016/j.bioactmat.2023.03.003
126. Miceli GC, Palumbo FS, Bonomo FP, Zingales M, Licciardi M. Polybutylene succinate processing and evaluation as a micro fibrous graft for tissue engineering applications. Polymers 2022;14:4486. https://doi.org/10.3390/polym14214486
127. Yi B, Zhou B, Song Z, Yu L, Wang W, Liu W. Step-wise CAG@PLys@PDA-Cu^{2+} modification on micropatterned nanofibers for programmed endothelial healing. Bioact Mater 2023;25:657-676. https://doi.org/10.1016/j.bioactmat.2022.07.010
128. Rosalia M, Grisoli P, Dorati R, Chiesa E, Pisani S, Bruni G, Genta I, Conti B. Influence of electrospun fibre secondary morphology on antibiotic release kinetic and its impact on antimicrobic efficacy. Int J Mol Sci 2023;24:12108. https://doi.org/10.3390/ijms241512108
129. Obiweluozor FO, Kayumov M, Kwak Y, Cho H-J, Park C-H, Park J, Jeong Y-J, Lee D-W, Kim D-W, Jeong I-S. Rapid remodeling observed at mid-term in-vivo study of a smart reinforced acellular vascular graft implanted on a rat model. J Biol Eng 2023;17:1. https://doi.org/10.1186/s13036-022-00313-9

130. Zizhou R, Khoshmanesh K, Wang X, Houshyar S. Fabrication of nanocomposites with high elasticity and strength for the load-bearing layer of small-diameter vascular grafts. ACS Appl Mater Interfaces 2023;15:35411-35421. https://doi.org/10.1021/acsami.3c02397
131. Łopianiak I, Rzempołuch W, Civelek M, Cicha I, Ciach T, Butruk-Raszeja BA. Multilayered blow-spun vascular prostheses with luminal surfaces in Nano/Micro range: the influence on endothelial cell and platelet adhesion. J Biol Eng 2023;17:20. https://doi.org/10.1186/s13036-023-00337-9
132. Rohringer S, Grasl C, Ehrmann K, Hager P, Hahn C, Specht SJ, Walter I, Schneider KH, Zopf LM, Baudis S, Liska R, Schima H, Podesser BK, Bergmeister H. Biodegradable, self-reinforcing vascular grafts for in situ tissue engineering approaches. Adv Healthcare Materials 2023;12:2300520. https://doi.org/10.1002/adhm.202300520
133. Jia W, Liu L, Li M, Zhou Y, Zhou H, Weng H, Gu G, Xiao M, Chen Z. Construction of enzyme-laden vascular scaffolds based on hyaluronic acid oligosaccharides-modified collagen nanofibers for antithrombosis and in-situ endothelialization of tissue-engineered blood vessels. Acta Biomater 2022;153:287-298. https://doi.org/10.1016/j.actbio.2022.09.041
134. Lu X, Zou H, Liao X, Xiong Y, Hu X, Cao J, Pan J, Li C, Zheng Y. Construction of PCL-collagen@PCL@PCL-gelatin three-layer small diameter artificial vascular grafts by electrospinning. Biomed Mater 2023;18:015008. https://doi.org/10.1088/1748-605X/aca269
135. Wang Z, Mithieux SM, Vindin H, Wang Y, Zhang M, Liu L, Zbinden J, Blum KM, Yi T, Matsuzaki Y, Oveissi F, Akdemir R, Lockley KM, Zhang L, Ma K, Guan J, Waterhouse A, Pham NTH, Hawkett BS, Shinoka T, Breuer CK, Weiss AS. Rapid regeneration of a neoartery with elastic lamellae. Advanced Materials 2022;34:2205614. https://doi.org/10.1002/adma.202270323, https://doi.org/10.1002/adma.202205614
136. Wang Z, Zhang M, Liu L, Mithieux SM, Weiss AS. Polyglycerol sebacate-based elastomeric materials for arterial regeneration. J Biomedical Materials Res 2023;jbm.a.37583. https://doi.org/10.1002/jbm.a.37583
137. Sultana T, Fahad MAA, Park M, Kwon SH, Lee B-T. Physicochemical, in vitro and in vivo evaluation of VEGF loaded PCL-mpeg and PDGF loaded PCL-chitosan dual layered vascular grafts. J Biomed Mater Res B Appl Biomater 2024;112:e35325. https://doi.org/10.1002/jbm.b.35325
138. Settembrini A, Buongiovanni G, Settembrini P, Alessandrino A, Freddi G, Vettor G, Martelli E. In-vivo evaluation of silk fibroin small-diameter vascular grafts: state of art of preclinical studies and animal models. Front Surg 2023;10:1090565. https://doi.org/10.3389/fsurg.2023.1090565
139. Zhou S-Y, Li L, Xie E, Li M-X, Cao J-H, Yang X-B, Wu D-Y. Small-diameter PCL/PU vascular graft modified with heparin-aspirin compound for preventing the occurrence of acute thrombosis. Int J Biol Macromol 2023;249:126058. https://doi.org/10.1016/j.ijbiomac.2023.126058
140. Alkazemi H, Huang T, Mail M, Lokmic-Tomkins Z, Heath DE, O'Connor AJ. Spontaneous orthogonal alignment of smooth muscle cells and endothelial cells captures native blood vessel morphology in tissue-engineered vascular grafts. ACS Appl Mater Interfaces 2023;15:34631-34641. https://doi.org/10.1021/acsami.3c08511
141. Li G, Yang T, Liu Y, Su H, Liu W, Fang D, Jin L, Jin F, Xu T, Duan C. The proteins derived from platelet-rich plasma improve the endothelialization and vascularization of small diameter vascular grafts. Int J Biol Macromol 2023;225:574-587. https://doi.org/10.1016/j.ijbiomac.2022.11.116
142. Tang Y, Yin L, Gao S, Long X, Du Z, Zhou Y, Zhao S, Cao Y, Pan S. A small-diameter vascular graft immobilized peptides for capturing endothelial colony-forming cells. Front Bioeng Biotechnol 2023;11:1154986. https://doi.org/10.3389/fbioe.2023.1154986
143. Su H, Liu W, Li X, Li G, Guo S, Liu C, Yang T, Ou C, Liu J, Li Y, Wei C, Huang Q, Xu T, Duan C. Cellular energy supply for promoting vascular remodeling of small-diameter vascular grafts: a preliminary study of a new strategy for vascular graft development. Biomater Sci 2023;11:3197-3213. https://doi.org/10.1039/D2BM01338J
144. Changizi S, Sameti M, Bazemore GL, Chen H, Bashur CA. Epsin mimetic upi peptide delivery strategies to improve endothelization of vascular grafts. Macromol Biosci 2023;23:2300073. https://doi.org/10.1002/mabi.202300073
145. Kabirian F, Baatsen P, Smet M, Shavandi A, Mela P, Heying R. Carbon nanotubes as a nitric oxide nano-reservoir improved the controlled release profile in 3D printed biodegradable vascular grafts. Sci Rep 2023;13:4662. https://doi.org/10.1038/s41598-023-31619-3

146. Cheng C, Li H, Liu J, Wu L, Fang Z, Xu G. Mcp-1-loaded poly(L -lactide- co -caprolactone) fibrous films modulate macrophage polarization toward an anti-inflammatory phenotype and improve angiogenesis. ACS Biomater Sci Eng 2023;9:4356-4367. https://doi.org/10.1021/acsbiomaterials.3c00476
147. Zhang C, Cha R, Wang C, Chen X, Li Z, Xie Q, Jia L, Sun Y, Hu Z, Zhang L, Zhou F, Zhang Y, Jiang X. Red blood cell membrane-functionalized Nanofibrous tubes for small-diameter vascular grafts. Biomaterials 2023;297:122124. https://doi.org/10.1016/j.biomaterials.2023.122124
148. Li S, Yang L, Zhao Z, Wang J, Lv H, Yang X. Fabrication of mechanical skeleton of small-diameter vascular grafts via rolling on water surface. Biomed Mater 2023;18:035002. https://doi.org/10.1088/1748-605X/acb89a
149. Natsume K, Nakamura J, Sato K, Ohtsuki C, Sugawara-Narutaki A. Biological properties of self-assembled nanofibers of elastin-like block polypeptides for tissue-engineered vascular grafts: platelet inhibition, endothelial cell activation and smooth muscle cell maintenance. Regen Biomater 2023;10:rbac111. https://doi.org/10.1093/rb/rbac111
150. Xu W, Yao M, He M, Chen S, Lu Q. Precise preparation of a multilayer tubular cell sheet with well-aligned cells in different layers to simulate native arteries. ACS Appl Mater Interfaces 2023;15:19966-19975. https://doi.org/10.1021/acsami.3c00471
151. Ding K, Yu X, Wang D, Wang X, Li Q. Small diameter expanded polytetrafluoroethylene vascular graft with differentiated inner and outer biomacromolecules for collaborative endothelialization, anti-thrombogenicity and anti-inflammation. Colloids Surf B Biointerfaces 2023;229:113449. https://doi.org/10.1016/j.colsurfb.2023.113449
152. Zhang Q, Duncan S, Szulc DA, De Mestral C, Kutryk MJ. Development of a universal, oriented antibody immobilization method to functionalize vascular prostheses for enhanced endothelialization for potential clinical application. J Biol Eng 2023;17:37. https://doi.org/10.1186/s13036-023-00356-6
153. Miao C, Wang L, Shang Y, Du M, Yang J, Yuan J. Tannic acid-assisted immobilization of copper(ii), carboxybetaine, and argatroban on poly(ethylene terephthalate) mats for synergistic improvement of blood compatibility and endothelialization. Langmuir 2022;38:15683-15693. https://doi.org/10.1021/acs.langmuir.2c02508
154. Špaček M, Chlup H, Mitáš P, Veselý J, Lambert L, Mlček M, Krajíček M, Lindner J, Grus T. Three-layer collagen-based vascular graft designed for low-flow peripheral vascular reconstructions. J Appl Biomed 2019;17:52-52. https://doi.org/10.32725/jab.2019.002
155. Grus T, Lambert L, Mlcek M, Chlup H, Honsova E, Spacek M, Burgetova A, Lindner J. In vivo evaluation of short-term performance of new three-layer collagen-based vascular graft designed for low-flow peripheral vascular reconstructions. Biomed Res Int 2018;2018:1-7. https://doi.org/10.1155/2018/3519596
156. Lambert L, Novakova M, Lukac P, Cechova D, Sukenikova L, Hrdy J, Mlcek M, Chlup H, Suchy T, Grus T. Evaluation of the immunogenicity of a vascular graft covered with collagen derived from the european carp (*cyprinus carpio*) and bovine collagen. Biomed Res Int 2019;2019:1-8. https://doi.org/10.1155/2019/5301405
157. Mitas P, Grus T, Lambert L, Mlcek M, Chlup H, Honsova E, Dohnalova M, Suchy T, Burgetova A, Lindner J, Spacek M. The influence of purification of carp collagen used in a novel composite graft with sandwich construction of the wall on its biological properties and graft patency rates. Physiol Res 2019;68:603-610. https://doi.org/10.33549/physiolres.934117
158. Grus T, Chlup H, Mlček M, Beran M. Kompozitní cévní náhrada a způsob její výroby (Composite vascular replacement and the method of its production). Czech patent, Industrial Property Office of the Czech Republic, Registration Number: CZ308556B6. Application number: CZ2017427A, Registennred: 26.7.2017, Granted: 19.10.2020.
159. Chlupáč J, Filová E, Riedel T, Houska M, Brynda E, Remy-Zolghadri M, Bareille R, Fernandez P, Daculsi R, Bourget C, Bordenave L, Bačáková L. Attachment of human endothelial cells to polyester vascular grafts: pre-coating with adhesive protein assemblies and resistance to short-term shear stress. Physiol Res 2014;63:167-177. https://doi.org/10.33549/physiolres.932577
160. Blum KM, Roby LC, Zbinden JC, Chang Y-C, Mirhaidari GJM, Reinhardt JW, Yi T, Barker JC, Breuer CK. Sex and Tamoxifen confound murine experimental studies in cardiovascular tissue engineering. Sci Rep 2021;11:8037. https://doi.org/10.1038/s41598-021-87006-3

161. Li Y, Wen Y, Green M, Cabral EK, Wani P, Zhang F, Wei Y, Baer TM, Chen B. Cell sex affects extracellular matrix protein expression and proliferation of smooth muscle progenitor cells derived from human pluripotent stem cells. Stem Cell Res Ther 2017;8:156. https://doi.org/10.1186/s13287-017-0606-2
162. Randolph LN, Bao X, Oddo M, Lian XL. Sex-dependent VEGF expression underlies variations in human pluripotent stem cell to endothelial progenitor differentiation. Sci Rep 2019;9:16696. https://doi.org/10.1038/s41598-019-53054-z
163. Gammill H S, Lin C, Hubel CA. Endothelial progenitor cells and preeclampsia. Front Biosci 2007;12:2383. https://doi.org/10.2741/2240

Physiol. Res. 73 (Suppl. 1): S365-S376, 2024 *https://doi.org/10.33549/physiolres.935260*

REVIEW

Hemodynamic Mechanisms Initiating Salt-Sensitive Hypertension in Rat Model of Primary Aldosteronism

Michal PRAVENEC[1], Petr MLEJNEK[1], Miroslava ŠIMÁKOVÁ[1], Jan ŠILHAVÝ[1]

[1]Laboratory of Genetics of Model Diseases, Institute of Physiology, Czech Academy of Sciences, Prague, Czech Republic

Received October 17, 2023
Accepted December 14, 2023

Summary

Few studies have investigated the hemodynamic mechanism whereby primary hyperaldosteronism causes hypertension. The traditional view holds that hyperaldosteronism initiates hypertension by amplifying salt-dependent increases in cardiac output (CO) by promoting increases in sodium retention and blood volume. Systemic vascular resistance (SVR) is said to increase only as a secondary consequence of the increased CO and blood pressure. Recently, we investigated the primary hemodynamic mechanism whereby hyperaldosteronism promotes salt sensitivity and initiation of salt-dependent hypertension. In unilaterally nephrectomized male Sprague-Dawley rats given infusions of aldosterone or vehicle, we found that aldosterone promoted salt sensitivity and initiation of salt-dependent hypertension by amplifying salt-induced increases in SVR while decreasing CO. In addition, we validated mathematical models of human integrative physiology, derived from Guyton's classic 1972 model - Quantitative Cardiovascular Physiology-2005 and HumMod-3.0.4. Neither model accurately predicted the usual changes in sodium balance, CO, and SVR that normally occur in response to clinically realistic increases in salt intake. These results demonstrate significant limitations with the hypotheses inherent in the Guyton models. Together these findings challenge the traditional view of the hemodynamic mechanisms that cause salt-sensitive hypertension in primary aldosteronism.

Key words

Aldosterone • Blood pressure • Salt • Sodium • Rat

Corresponding author

M. Pravenec, Institute of Physiology, Czech Academy of Sciences, Vídeňská 1083, 14200 Prague, Czech Republic. E-mail: michal.pravenec@fgu.cas.cz

Introduction

NaCl-dependent hypertension is a clinical disorder of major public health significance and is a leading cause of cardiovascular death and disability worldwide [1,2]. In most cases, the etiology of NaCl-dependent hypertension is unknown. However, it has been estimated that a significant percentage of hypertensive individuals have a NaCl-dependent form of hypertension caused by mineralocorticoid excess when primary aldosteronism is the most common secondary form of hypertension [3-5]. In addition, it has become increasingly recognized that mineralocorticoid excess or increased sensitivity to mineralocorticoids may frequently contribute to salt-sensitive forms of hypertension that are resistant to treatment with multiple antihypertensive drugs [3,6]. In this review, we describe current knowledge about hemodynamic abnormality through which mineralocorticoids enable increases in salt intake to almost always initiate hypertension and what are the mechanisms that mediate that hemodynamic abnormality.

The main controversy on the hemodynamic initiation of mineralocorticoid-NaCl dependent hypertension

The hemodynamic factors that ultimately determine mean arterial pressure (MAP) are cardiac output (CO) and systemic vascular resistance (SVR). The main controversy of mechanisms initiating hypertension is whether mineralocorticoids enable increases in salt intake to initiate hypertension by causing

a mineralocorticoid-dependent abnormality in the level of CO (as held by the "CO theory"), or in SVR (as held by the "SVR theory"), or both. Some investigators have contended that an abnormally high level of CO is responsible [7-9], others have reported that an abnormally high level of SVR is responsible [10-12], and others have reported that either an abnormal level of CO or SVR or both are responsible [13,14]. Here we summarize the main competing theories on the initiation of mineralocorticoid-NaCl hypertension, discuss why this controversy on mechanisms has persisted, and explain how the current research resolves this controversy.

The cardiac output (CO) theory for initiation of mineralocorticoid-NaCl hypertension

The prevailing theory of mineralocorticoid-NaCl hypertension holds that mineralocorticoids enable increases in salt intake to hemodynamically initiate hypertension by initially causing an abnormally high level of cardiac output (CO) as a consequence of their ability to cause abnormally high levels of salt retention and blood volume [7,15-17]. This CO theory (also known as Guyton's "volume loading" theory) is diagrammed in Fig. 1 and explicitly holds that systemic vascular resistance (SVR) is normal during initiation of the hypertension and becomes abnormal later, after the initial increases in BP and CO have occurred. As shown in the left panel of Fig. 1, the CO theory holds that in normal individuals, administration of a high salt diet does not initiate hypertension because it is believed that normal individuals rapidly excrete a salt load and therefore, have little or no initial increases in sodium retention and CO in response to salt loading. According to the Guyton and Hall Textbook of Medical Physiology: "raising salt intake in the absence of impaired kidney function or excessive formation of anti-natriuretic hormones usually does not increase arterial pressure much because the kidneys rapidly eliminate the excess salt and blood volume is hardly altered" [18]. It should be noted that the Guyton and Hall textbook provides no data or references supporting the contention that normal subjects excrete a salt load so rapidly that they have little or no increases in salt retention and blood volume. It should also be noted that there is no evidence that normal subjects excrete a salt load more rapidly than subjects with mineralocorticoid excess given the same salt load. The salt-induced increases in CO that initiate the increased BP are transient and the pressure-dependent and/or flow-dependent autoregulation in peripheral tissues causes a fall in CO back towards normal and an increase in SVR above normal that sustains the hypertension (Fig. 1, right panel).

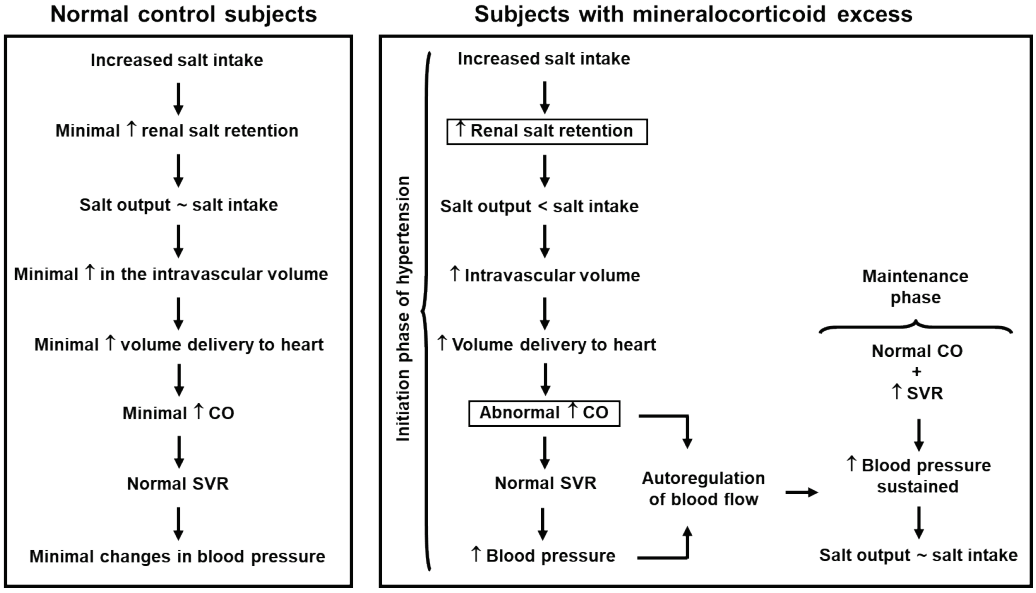

Fig. 1. The CO (Guyton's volume-loading) theory of the pathogenesis of NaCl-induced hypertension. Left panel. The mechanism held to mediate a normal, i.e., nonpressor, response to increases in salt intake (common pathway for salt resistance). Right panel. The mechanism held to mediate an abnormal, i.e., pressor, response to increases in salt intake (mechanism of salt sensitivity). According to the theory, an abnormal increase in the amount of renal salt reabsorption/retention is usually an early, critical abnormality that enables increased salt intake to initiate hypertension by increasing CO (boxes). Modified from [19].

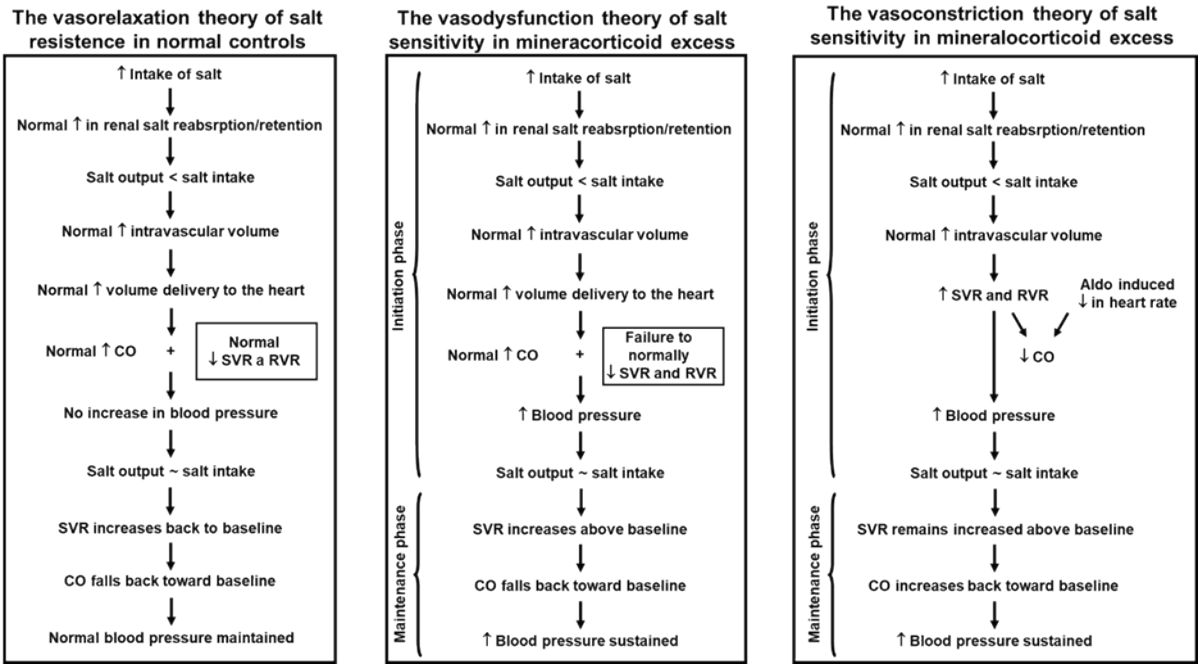

Fig. 2. The SVR theory of the pathogenesis of NaCl-induced hypertension. Left panel. Usual pathway yielding a normal (nonpressor) response to NaCl loading (mechanism of salt resistance, the vasorelaxation theory of salt resistance). This pathway depicts the initial sodium balance and hemodynamic responses to increases in salt intake usually observed in salt-resistant normotensive control subjects. Middle panel. Usual pathway yielding an abnormal (pressor) response to NaCl loading (mechanism of salt sensitivity, the vasodysfunction theory of salt sensitivity). Right panel. The vasoconstriction theory of salt sensitivity characterized by increased SVR and decreased CO. Reduced CO may be secondary to increased SVR and reduced heart rate.

The systemic vascular resistance (SVR) theory: The vasorelaxation theory of salt resistance, the vasodysfunction theory of salt sensitivity, and the vasoconstriction theory of salt sensitivity

- ***The vasorelaxation theory of salt resistance.*** In contrast to the CO theory, the SVR theory holds that during initiation of a high salt diet, the levels of systemic and renal vascular resistance (RVR) in response to salt loading, are abnormal, i.e., greater than those which occur during initiation of salt loading in normal controls, whereas the increases in sodium balance and CO are not abnormal, i.e., not greater than the increases in sodium balance and CO which occur during initiation of salt loading in normal controls. As shown in the left panel of Fig. 2 and contrary to popular belief, this theory holds that in normal controls, salt loading initially induces substantial increases in CO. However, BP does not increase because normal controls vasodilate and reduce SVR, thereby offsetting the pressor effects otherwise expected with NaCl-induced increases in CO.
- ***The vasodysfunction theory of salt sensitivity.*** The theory holds that in subjects with mineralocorticoid excess, salt loading induces similar increases in CO as in controls, i.e., increases in CO that are not greater than those induced by salt loading in controls, however, the subjects with mineralocorticoid excess fail to normally vasodilate and reduce vascular resistance like normal controls [20] (Fig. 2, middle panel).
- ***Vasoconstriction theory of salt sensitivity.*** It has been reported that in some cases of salt-induced hypertension with mineralocorticoid excess, increases in blood pressure are initiated by increases in vascular resistance in the absence of increases in CO or even with decreases in CO [11,21]. The induction of salt-dependent hypertension in these cases is better explained by a vasoconstriction theory of salt sensitivity (Fig. 2, right panel).

Why hasn't this controversy on hemodynamic initiation of mineralocorticoid hypertension been resolved?

There are three key reasons why previous studies have not resolved this controversy:

1. Surprisingly, all previous studies lacked necessary normal controls. None of the previous studies of this issue compared the changes in CO and SVR that occur during the initiation of salt loading in mineralocorticoid-treated subjects to those that occur during initiation of salt loading in normal controls not treated with mineralocorticoids [7-12,14]. Without the necessary normal controls, the previous studies could not determine whether the salt retention induced by giving a high salt diet and mineralocorticoids together, causes the initial CO or SVR responses to be abnormal or normal, i.e. different from the initial CO or SVR responses to salt retention induced by giving a high salt diet to normal controls alone (i.e., without mineralocorticoids). Without the use of adequate normal controls, previous investigators studying mineralocorticoid-NaCl hypertension [7-12,14] failed to recognize that the normal hemodynamic response to initiation of salt loading in control subjects not given mineralocorticoids involves substantial increases in salt retention, stroke volume, and CO together with substantial decreases in SVR that offset potential pressor effects of the increases in CO [22-25].

2. A mistaken assumption. Guyton and colleagues appear to have mistakenly assumed that normal subjects excrete a salt load very quickly and therefore, do not undergo substantial increases in salt retention, blood volume, and CO in response to substantial increases in salt intake [26-29]. In fact, it has never been demonstrated that normotensive salt-resistant subjects excrete a salt load faster than salt-sensitive subjects, with or without mineralocorticoid excess. In normal salt-resistant animals and humans, salt loading (increasing salt intake) induces substantial increases in salt retention, blood volume, stroke volume and cardiac output, similar to those induced by salt loading in salt-sensitive subjects [22-25]. The reason that salt does not increase BP in normal subjects is because normal subjects robustly vasodilate and reduce SVR in response to salt loading, not because normal subjects excrete a salt load faster than salt-sensitive subjects. The published data show that salt-sensitive subjects do not initially retain more of a salt load than true normal controls, i.e. salt-resistant subjects with normal blood pressure [22,24,25,30,31].

Because previous studies of mineralocorticoid hypertension were mainly correlational studies and lacked adequate normal controls (i.e., normal subjects studied during the initiation of salt retention induced by salt loading without mineralocorticoids), they were not capable of determining which of the observed hemodynamic changes (or lack thereof) were necessary or sufficient for initiation of the mineralocorticoid-NaCl hypertension. Interestingly, investigators who performed an intervention study found that preventing increases in CO with a beta adrenergic blocker did not prevent initiation of mineralocorticoid-NaCl hypertension. This indicated that an abnormally high level of CO was not necessary for initiation of the hypertension, and that an abnormality in SVR was involved in initiation of the hypertension [10,32]. However, these studies were largely ignored or dismissed based on questions raised about small sample sizes, experimental designs, and CO measurement methods [9,33].

3. Previous studies used inadequate hemodynamic monitoring techniques. Inconsistency in the hemodynamic findings reported by different investigators could be due to the questionable approaches that were used to monitor the hemodynamic variables. In previous studies, suboptimal techniques were used to monitor CO, SVR, and BP and the variables were not continuously measured beat to beat, 24 hours/day throughout the experiments. Two groups [7,12] indicated that they continuously sampled the hemodynamic variables for at least 20 hours per day yet, in fact, the sampling was intermittent and the sampling time in those studies actually totaled no more than 4 hours per day; these two studies gave conflicting results [7,12]. Furthermore, neither group examined changes in CO and SVR induced by salt loading in normal controls not given mineralocorticoids. Other studies were even less reliable because they did not even monitor CO and SVR daily and were not capable of detecting early events occurring during initiation of the salt retention and hypertension [8,9].

Testing computer models predicting human responses to a high salt diet

Guyton and colleagues pioneered the use of large-scale computer models to investigate potential physiologic abnormalities involved in the initiation and maintenance of salt-induced hypertension [34,35]. The original Guyton model was revised and expanded by Guyton and colleagues over decades. The most evolved derivative of the 1972 Guyton model is a large, multi-scale model called “HumMod” that includes a Windows-based graphical user interface [36].

In reviewing the literature on the 1972 Guyton model and the most evolved derivatives of the Guyton model, we could not find validation studies testing the capacity of the models to accurately predict sodium balance, cardiac output, and vascular resistance responses of normal subjects to increases in dietary salt within the real life range of salt intake in humans. Accurate quantitative characterization of the physiologic responses to salt loading in normal control subjects is a prerequisite for accurately determining which physiologic responses to salt loading are abnormal in salt sensitive subjects.

The lack of published validation studies of the historical Guyton model, or of its contemporary derivatives, HumMod and QCP models with respect to predicting normal sodium balance and hemodynamic responses to salt loading is surprising and prompted our recent investigation [37,38]. For validation testing, the predictions of the computer models were plotted against the human experimental data [25]. A model was considered to fail validation testing when the salt-induced change predicted by the model fell outside the 95 % confidence limits of the mean of the salt-induced changes observed in human studies. As can be seen in Fig. 3A, both model simulations vastly underestimated the cumulative amount of sodium that is usually retained in response to switching from a very low NaCl intake to a high salt intake in normal subjects (normotensive salt-resistant subjects). As can be seen in Fig. 3B, both computer models accurately predicted that in normal subjects, switching from a very low-salt diet to a high salt diet for 5 to 7 days causes minimal increases in blood pressure above baseline. On the other hand, contemporary computer models fail to accurately predict cardiac output (Fig. 3C) and systemic vascular resistance (Fig. 3D) responses to short-term salt loading in normal humans.

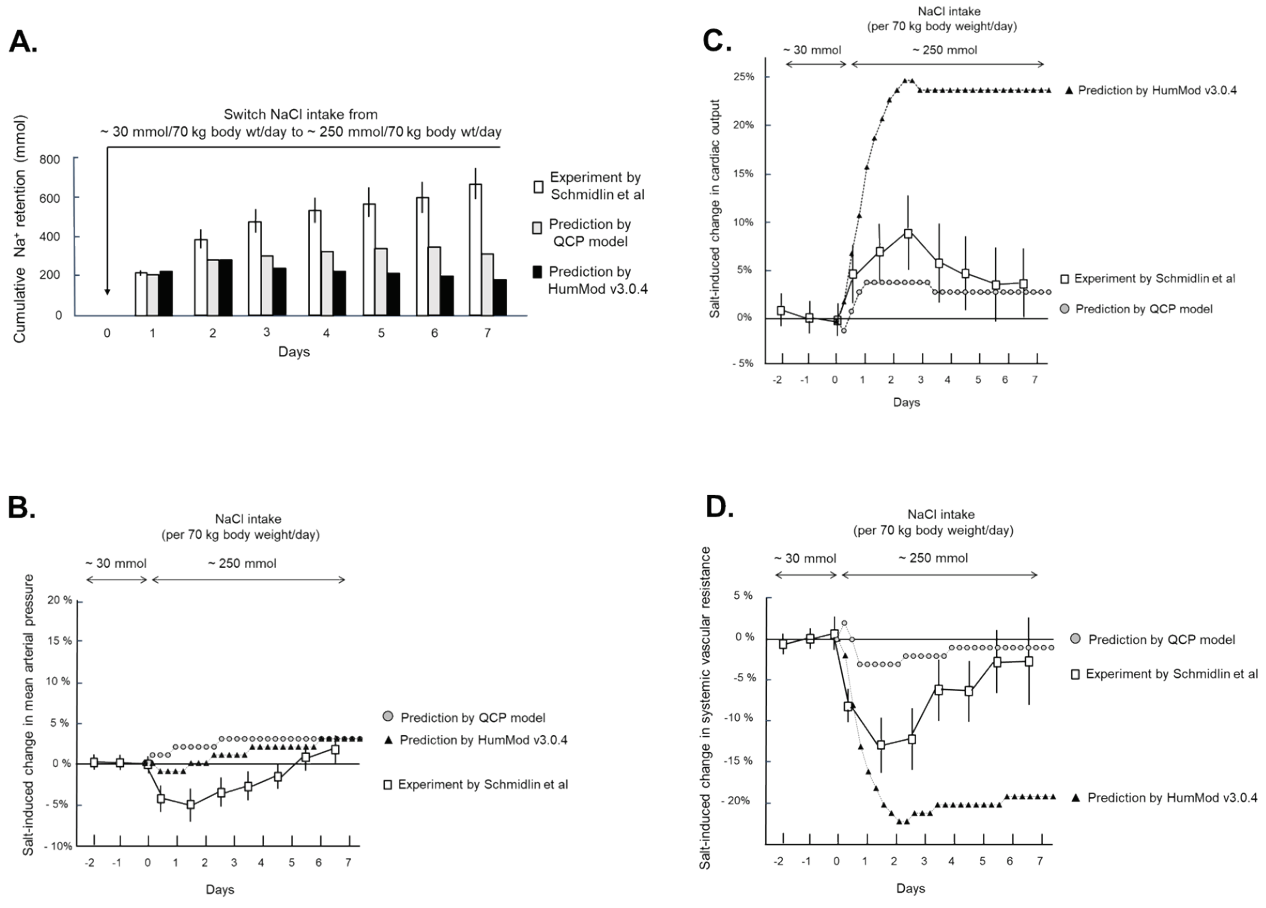

Fig. 3. Experimental and predicted short-term changes in cumulative sodium retention (**A**), mean arterial pressure (**B**), cardiac output (**C**), and systemic vascular resistance (**D**) induced by switching from a very low-salt diet to a high-salt diet. This figure shows percentage changes induced by switching NaCl intake from ≈30 mmol NaCl per 70 kg body weight per day to ≈250 mmol per 70 kg body weight per day according to the studies of Schmidlin *et al.* [25] in normotensive salt-resistant humans and according to the predictions of HumMod 3.0.4 and Quantitative Cardiovascular Physiology (QCP)-2005. Results of human studies are presented as means and 95 % CIs. Modified from [36].

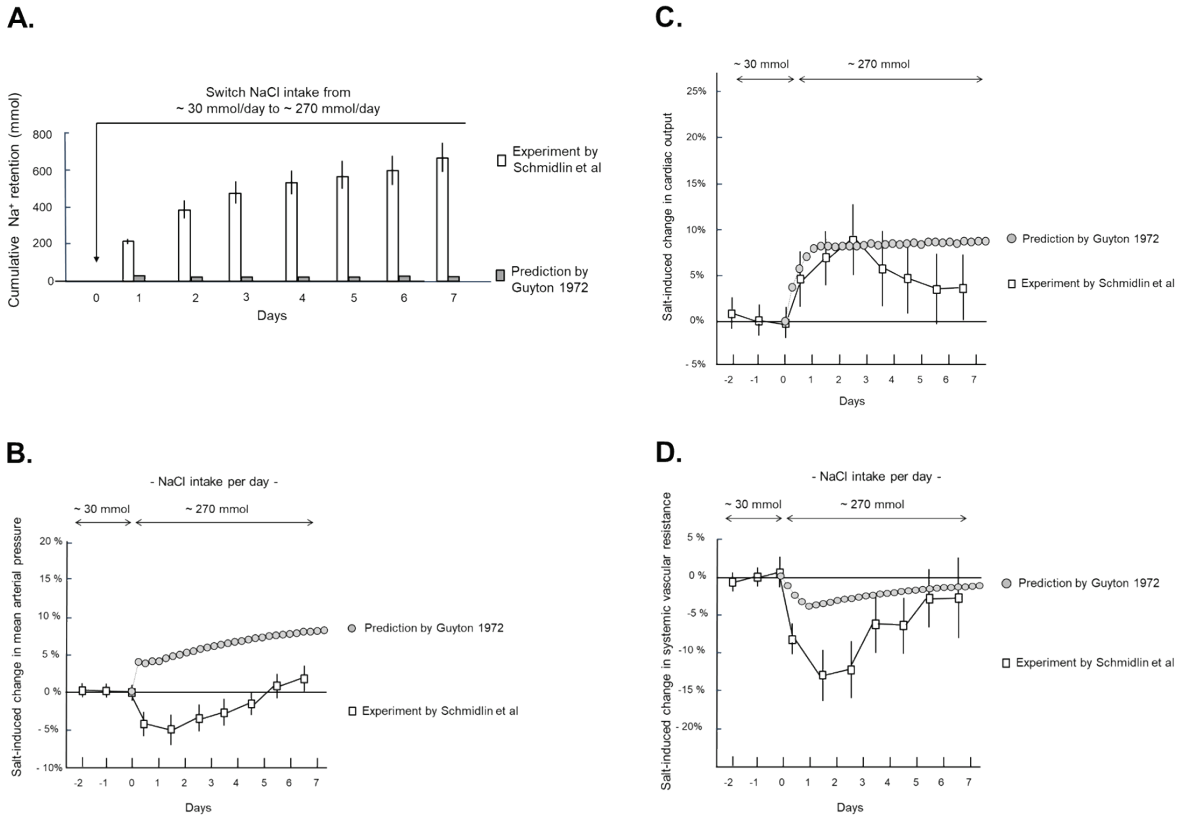

Fig. 4. Comparison of predictions from the 1972 Guyton model to the results from human studies [25]. This figure shows the percentage changes in cumulative sodium retention (**A**), mean arterial pressure (**B**), cardiac output (**C**), and systemic vascular resistance (**D**) predicted to occur in response to switching from a very low NaCl intake of 30 mmol/day to a high NaCl intake of 270 mmol/day for 7 days. Modified from [37].

However, both models appropriately reflect the general trends in these variables that normally occur in response to physiologic salt loading. Specifically, both models show that in normal subjects, non-extreme salt loading induces relatively little or no increase in blood pressure because normal subjects usually undergo robust vasodilation and reduce systemic vascular resistance sufficiently to offset the potential pressor effects of substantial salt-induced increases in cardiac output. These observations are consistent with the results of salt loading studies in normal salt-resistant humans and in animals [20,25]. These observations are also consistent with the vasodysfunction theory of salt sensitivity [19,20] which holds that in response to salt loading, normal subjects undergo substantial decreases in systemic vascular resistance that offset potential pressor effects of salt-induced increases in cardiac output whereas salt-sensitive subjects do not.

We also performed validation testing of the original 1972 Guyton model against the human experimental data [34]. As can be seen in Fig. 4A, Guyton model underestimated the cumulative amount of sodium that is usually retained in response to a high salt intake in normal subjects. In addition, the original 1972 Guyton model clearly overestimates the extent to which arterial pressure increases in response to salt loading in normal humans (Fig. 4B). Thus, the default subject with normal renal function simulated by the 1972 Guyton model is not normal and is salt sensitive according to criteria recommended for identifying salt sensitivity by the expert panel of the American Heart Association, and by other scientists with experience investigating salt sensitivity in humans [39]. The greater salt sensitivity in the 1972 Guyton model is not initiated by greater levels of sodium retention and cardiac output, but rather by greater levels of systemic vascular resistance due to a failure to vasodilate after salt loading (Fig. 4D).

It can be concluded that the results of testing computer models demonstrate significant limitations with the hypotheses inherent in Guyton models regarding the usual regulation of sodium balance, cardiac output and vascular resistance in response to increased salt intake in normal salt-resistant humans. Accurate understanding of the normal responses to salt loading is a prerequisite for accurately establishing abnormal responses to salt loading. Accordingly, the present results raise concerns

about the interpretation of studies of salt sensitivity with the various Guyton models.

Experimental testing hemodynamic mechanisms initiating salt-sensitive increases in blood pressure in a rat model of primary aldosteronism

In recent studies in a widely used rat model of primary aldosteronism, we directly tested the hemodynamic mechanism whereby hyperaldosteronism enhances salt sensitivity and initiation of salt-induced hypertension [21]. We continuously monitored mean arterial pressure (MAP), cardiac output (CO), and systemic vascular resistance (SVR), 24-hrs/day, 7 days/week using implanted arterial pressure probes and Doppler ultrasonic flow probes in unrestrained, unilaterally nephrectomized, male Sprague-Dawley rats receiving constant infusions of aldosterone or vehicle on low-salt diet and during transition to high-salt diet. We found that in aldosterone-treated animals, CO decreased during initiation of salt-induced increases in blood pressure and remained below control during the high-salt period. Thus, in hyperaldosteronism, initiation of salt-dependent hypertension was caused by primary increases in SVR, with reductions in CO.

Figure 5 shows the absolute values for 24-hr average MAP, CO, and SVR on the last 7 days of the low-salt diet (0.26 % NaCl) and on each day of the high-salt diet (4 % NaCl). In vehicle treated controls, switching from the low-salt to the high-salt diet initiated modest increases in MAP by increasing SVR while simultaneously decreasing CO. In aldosterone-treated rats compared with control rats, switching from a low-salt diet to a high-salt diet caused greater increases in MAP and SVR while simultaneously decreasing CO. Mean CO did not increase at any time during initiation of salt-induced increases in blood pressure in either the control rats or rats infused with aldosterone (Fig. 5). The results show that aldosterone enhances salt sensitivity and augments salt-induced hypertension by amplifying salt-dependent increases in SVR. Salt-dependent hypertension is initiated during decreases in CO, not increases in CO. CO decreased presumably as a consequence of increases in SVR, decreases in heart rate, and potentially increases in afterload.

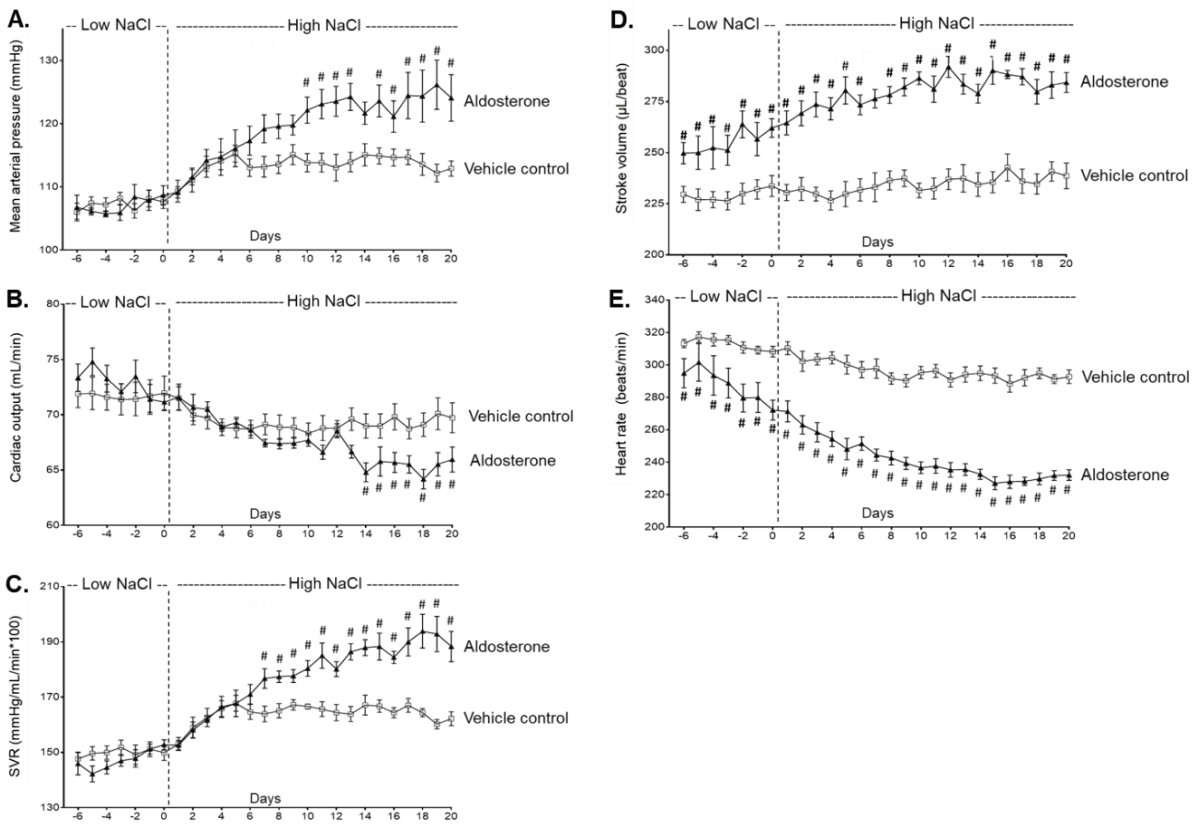

Fig. 5. Daily 24-hour averages (mean±SEM) of mean arterial pressure (MAP) (**A**), cardiac output (CO) (**B**), systemic vascular resistance (SVR) (**C**), stroke volume (**D**), and heart rate (**E**) during administration of a low-NaCl diet (0.26 % NaCl) and a high-NaCl diet (4 % NaCl) in control rats infused with vehicle and in rats infused with aldosterone. Modified from [21].

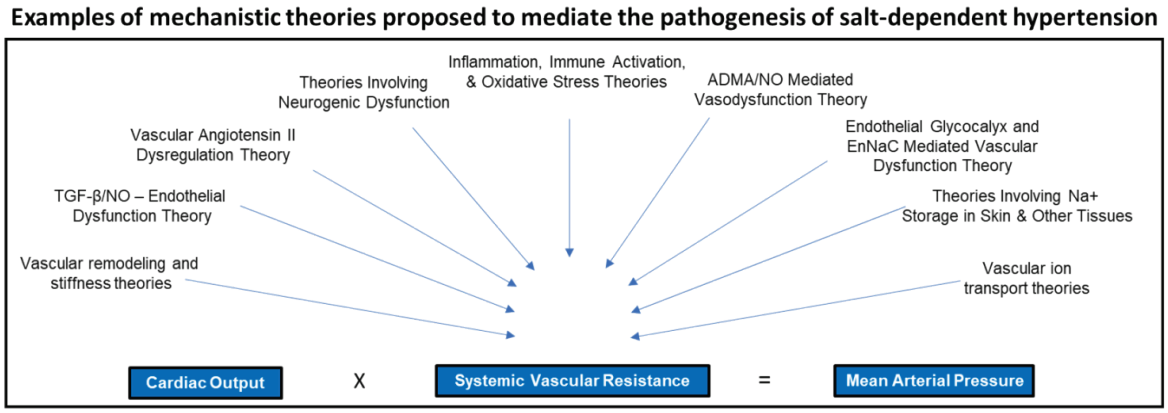

Fig. 6. Examples of mechanistic theories proposed to mediate the pathogenesis of salt-dependent hypertension. Some of these mechanistic theories might explain how the combination of excess aldosterone and salt promotes the increases in systemic vascular resistance that hemodynamically initiate salt-dependent hypertension in primary aldosteronism. ADMA indicates asymmetrical dimethylarginine; EnNaC, endothelial sodium channel; and TGF-β, transforming growth factor beta. Modified from [47].

The above described studies call into question the traditional theory of Guyton, Hall, and others [7, 16, 29,40-44] that in hyperaldosteronism, the salt-dependent hypertension is initiated by "a primary increase in cardiac output followed by a secondary vasoconstriction" [7]. Our findings demonstrate that in hyperaldosteronism, increases in CO are not necessary for initiation of the salt-dependent hypertension. In hyperaldosteronism, primary increases in SVR can drive increases in blood pressure and decreases in CO during initiation of salt-dependent hypertension. Although it is widely accepted that hyperaldosteronism can promote increases in sodium balance and fluid retention, it should not be assumed that the increases in sodium balance and fluid retention translate to increases in CO.

During administration of the low-salt diet and throughout administration of the high-salt diet, stroke volume was greater, and heart rate lower in the aldosterone-treated group than in the control group (Fig. 5). In the aldosterone-treated group, stroke volume trended upwards and heart rate trended downwards during administration of the low-salt diet and during transition to the high-salt diet. In vehicle-treated controls, stroke volume trended slightly upwards and heart rate trended slightly downwards during transition from the low-salt diet to the high-salt diet (Fig. 5).

It should be noted that a significant reduction in heart rate and increases in stroke volume occurred in aldosterone-treated rats even on the low-salt diet, that is, before initiation of salt-induced elevations in blood pressure. The heart rate changes are consistent with studies showing that aldosterone binds to GPERs (G-protein–coupled estrogen receptors) and decreases heart rate by activating GPER in cardiac vagal neurons of nucleus ambiguous [45]. Other investigators using continuous telemetry recordings have shown similar reductions in heart rate during initiation of hypertension induced by deoxycorticosterone (DOC) and salt [46].

A variety of mechanistic theories have been proposed to account for the pathogenesis of salt-dependent hypertension [21]. Figure 6 shows some examples of mechanistic theories that may explain how the combination of excess aldosterone and salt promotes increases in SVR that hemodynamically initiate hypertension.

Mechanism-based strategies to prevent salt sensitivity and salt-induced hypertension

Understanding of the responsible hemodynamic mechanisms will enable the design of new approaches to prevent salt-sensitive hypertension. According to the vasodysfunction theory, the induction of salt-induced hypertension involves the combination of normal salt-induced increases in sodium balance and cardiac output together with subnormal vasodilation and abnormal levels of vascular resistance (Fig. 2, middle panel). In such cases, initiation of salt-induced hypertension could be prevented by either (1) reducing the normal increases in sodium balance and cardiac output induced by increases in salt intake (i.e. reducing salt consumption) or, (2) preventing the abnormal vascular resistance responses to increases in salt intake (i.e. preventing vasodysfunction).

(Ad 1) Food salt reduction programs to decrease the risk for salt-induced increases in blood pressure and

cardiovascular events are based on the assumption that reducing the salt concentration of processed foods will substantially reduce mean salt intake in the general population. However, contrary to expectations, reducing the sodium density of nearly all foods consumed in England by 21 % had little or no effect on salt intake in the general population [47,48]. One way to effectively reduce sodium consumption is to use salt substitutes that are often prepared by mixing potassium chloride with sodium chloride. It is reported that most individuals cannot distinguish between regular salt and salt substitutes containing no more than 30 % potassium chloride. In March 2023, the United States Food and Drug Administration (FDA) announced plan to permit potassium-containing salt substitutes (75 % NaCl, 25 % KCl) in food manufacturing [49,50].

(Ad 2) We suggest that interventions to prevent salt-induced hypertension primarily focus on preventing the abnormal physiologic mechanisms that appear to commonly mediate salt sensitivity, i.e., preventing the abnormal vascular resistance responses to salt loading that are usually required for initiation of salt-induced increases in blood pressure. It is for instance possible to promote salt resistance by non-pharmacologic manipulation of nitric oxide (NO) activity by fortifying salty foods with nitrate-rich vegetable extracts. Recently, we have found that tiny amounts of inorganic nitrate in the form of sodium nitrate or beetroot juice can protect against initiation of salt-induced increases in blood pressure [51] (Morris *et al.* 2019). In the most widely used animal model of spontaneous salt sensitivity, the Dahl salt-sensitive rat, we found that providing a molar ratio of added nitrate in the form of beetroot juice to added salt of <1:100 conferred substantial protection against salt-induced increases in blood pressure [51].

Conclusions

The above described results provide evidence for the role of vasoconstriction theory in the pathogenesis of salt-dependent hypertension in hyperaldosteronism. Aldosterone promotes salt sensitivity and initiation of salt-dependent hypertension by amplifying salt-induced increases in SVR while decreasing CO. Increases in CO are not required for initiation or maintenance of hypertension. These findings challenge the traditional Guyton's volume-loading theory of the hemodynamic mechanisms that cause salt sensitive hypertension in primary aldosteronism.

Potassium-enriched salt substitutes and fortification of salty foods with nitrate-rich vegetable extracts are examples of mechanism-based methods for preventing salt-induced hypertension that do not depend on restricting salt intake to levels recommended by various regulatory authorities.

Conflict of Interest

There is no conflict of interest.

Acknowledgements

MP was supported by the grant LUAUS23095 within the INTER-EXCELLENCE program of the Ministry of Education, Youth, and Sports of the Czech Republic and by a program from the National Institute for Research of Metabolic and Cardiovascular Diseases (Program EXCELES, ID Project No. LX22NPO5104) funded by the European Union – Next Generation EU.

References

1. Ezzati M, Riboli E: Behavioral and dietary risk factors for noncommunicable diseases. N Engl J Med. 2013;369:954-964. https://doi.org/10.1056/NEJMra1203528
2. Kotchen TA, Cowley AW, Jr., Frohlich ED. Salt in health and disease a delicate balance. N Engl J Med. 2013;368:1229-1237. https://doi.org/10.1056/NEJMra1212606
3. Calhoun DA. Hyperaldosteronism as a common cause of resistant hypertension. Annu Rev Med. 2013;4:233-247. https://doi.org/10.1146/annurev-med-042711-135929
4. Stowasser M, Gordon RD. The renaissance of primary aldosteronism: what has it taught us? Heart Lung Circ. 2013;22:412-420. https://doi.org/10.1016/j.hlc.2013.01.006
5. Funder JW. Primary aldosteronism and salt. Pflugers Arch. 2015;467:587-594. https://doi.org/10.1007/s00424-014-1658-0
6. Egan BM, Li J. Role of aldosterone blockade in resistant hypertension. Semin Nephrol. 2014;34:273-284. https://doi.org/10.1016/j.semnephrol.2014.04.004

7. Montani JP, Mizelle HL, Adair TH, Guyton AC. Regulation of cardiac output during aldosterone-induced hypertension. J Hypertens Suppl. 1989;7:S206-207. https://doi.org/10.1097/00004872-198900076-00099
8. Distler A, Philipp T, Luth B, Wucherer G. Studies on the mechanism of mineralocorticoid-induced blood pressure increase in man. Clin Sci. 1979; 57:303s-305s. https://doi.org/10.1042/cs057303s
9. Schalekamp MA, Wenting GJ, Man In 'T Veld AJ. Pathogenesis of mineralocorticoid hypertension. Clin Endocrinol Metab. 1981;10:397-417. https://doi.org/10.1016/S0300-595X(81)80005-9
10. Conway J, Hatton R. Development of deoxycorticosterone acetate hypertension in the dog. Circ Res. 1978;43suppl 1:I-82-I6.
11. Obst M, Gross V, Luft FC. Systemic hemodynamics in non-anesthetized L-NAME- and DOCA-salt-treated mice. J Hypertens. 2004;22:1889-1894. https://doi.org/10.1097/00004872-200410000-00010, https://doi.org/10.1097/00004872-200406002-01038
12. May CN. Differential regional haemodynamic changes during mineralocorticoid hypertension. J Hypertens. 2006;24:1137-1146. https://doi.org/10.1097/01.hjh.0000226204.57818.46
13. Gomez-Sanchez EP. Mineralocorticoid receptors in the brain and cardiovascular regulation: minority rule? Trends Endocrinol Metab. 1990;22:179-187. https://doi.org/10.1016/j.tem.2011.02.001
14. Miller AWH, Bohr DF, Schork AM, Terris JM. Hemodynamic responses to DOCA in young pigs. Hypertension. 1979;1:591-597. https://doi.org/10.1161/01.HYP.1.6.591
15. Guyton AC, Hall JE, Coleman TG, Manning RD, Norman RA, Jr. The Dominant Role of the Kidneys in Long-Term Arterial Pressure Regulation in Normal and Hypertensive States. In: Laragh JH, Brenner BM, editors. Hypertension: Pathophysiology, Diagnosis, and Management. 2 ed. New York: Raven Press, Ltd.; 1995. p. 1311-26.
16. Lifton RP, Gharavi AG, Geller DS: Molecular mechanisms of human hypertension. Cell. 2001;104:545-556. https://doi.org/10.1016/S0092-8674(01)00241-0
17. Kawarazaki W, Fujita T. Aberrant Rac1-mineralocorticoid receptor pathways in salt-sensitive hypertension. Clin Exp Pharmacol Physiol. 2013;40:929-936. https://doi.org/10.1111/1440-1681.12177
18. Hall JE. Guyton and Hall Textbook of Medical Physiology. 12th ed. Philadelphia: Saunders Elsevier; 2012.
19. Morris RC Jr, Schmidlin O, Sebastian A, Tanaka M, Kurtz TW. Vasodysfunction that involves renal vasodysfunction, not abnormally increased renal retention of sodium, accounts for the initiation of salt-induced hypertension. Circulation. 2016;133:881-893. https://doi.org/10.1161/CIRCULATIONAHA.115.017923
20. Kurtz TW, Dicarlo SE, Pravenec M, Schmidlin O, Tanaka M, Morris RC Jr. An alternative hypothesis to the widely held view that renal excretion of sodium accounts for resistance to salt-induced hypertension. Kidney Int. 2016; 90:965-973. https://doi.org/10.1016/j.kint.2016.05.032
21. Kurtz TW, Morris RC Jr, Pravenec M, Lujan HL, Dicarlo SE: Hypertension in primary aldosteronism is initiated by salt-induced increases in vascular resistance with reductions in cardiac output. Hypertension. 2023;80:1077-1091. https://doi.org/10.1161/HYPERTENSIONAHA.123.20953
22. Greene AS, Yu ZY, Roman RJ, Cowley AW, Jr. Role of blood volume expansion in Dahl rat model of hypertension. Am J Physiol. 1990;258:H508-H514. https://doi.org/10.1152/ajpheart.1990.258.2.H508
23. Krieger Je, Liard Jf, Cowley AW, Jr. Hemodynamics, fluid volume, and hormonal responses to chronic high-salt intake in dogs. Am J Physiol. 1990;259(6 Pt 2):H1629-1636. https://doi.org/10.1152/ajpheart.1990.259.6.H1629
24. Schmidlin O, Sebastian AF, Morris RC, Jr. What initiates the pressor effect of salt in salt-sensitive humans? Observations in normotensive blacks. Hypertension. 2007;49:1032-1039. https://doi.org/10.1161/HYPERTENSIONAHA.106.084640
25. Schmidlin O, Forman A, Leone A, Sebastian A, Morris RC, Jr. Salt sensitivity in blacks: evidence that the initial pressor effect of NaCl involves inhibition of vasodilatation by asymmetrical dimethylarginine. Hypertension. 2011;58:380-385. https://doi.org/10.1161/HYPERTENSIONAHA.111.170175
26. Guyton AC, Coleman TG, Young DB, Lohmeier TE, Declue JW. Salt balance and long-term blood pressure control. Ann Rev Med. 1980;31:15-27. https://doi.org/10.1146/annurev.me.31.020180.000311
27. Guyton AC. Long-term arterial pressure control: an analysis from animal experiments and computer and graphic models. Am J Physiol. 1990;259(5 Pt 2):R865-877. https://doi.org/10.1152/ajpregu.1990.259.5.R865

28. Hall JE. Dominant Role of the Kidney in Long-Term Regulation of Arterial Pressure and in Hypertension: The Integrated System for Pressure Control. In: Guyton AC, Hall JE, editors. Guyton and Hall Textbook of Medical Physiology. 12 ed. Philadelphia: Saunders Elsevier; 2011.
29. Hall JE, Granger JP, Do Carmo JM, Da Silva AA, Dubinion J, George E, Hamza S, Speed J, Hall ME. Hypertension: physiology and pathophysiology. Compr Physiol. 2012;2:2393-2442. https://doi.org/10.1002/cphy.c110058
30. Ishii M, Atarashi K, Ikeda T, Hirata Y, Igari T, Uehara Y, Takagi M, Matsuoka H, Takeda T, Murao S. Role of the aldosterone system in the salt-sensitivity of patients with benign essential hypertension. Jpn Heart J. 1983;24:79-89. https://doi.org/10.1536/ihj.24.79
31. Wedler B, Brier M, Wiersbitzky M, Gruska S, Wolf E, Kallwellis R, Aronoff GR, Luft FC. Sodium kinetics in salt-sensitive and salt-resistant normotensive and hypertensive subjects. J Hypertens. 1992;10:663-669. https://doi.org/10.1097/00004872-199207000-00010
32. Bravo EL, Tarazi RC, Dustan HP. Multifactorial analysis of chronic hypertension induced by electrolyte-active steroids in trained, unanesthetized dogs. Circ Res. 1977;40(5 Suppl 1):I140-I145.
33. Cowley AW. The concept of autoregulation of total blood flow and its role in hypertension. Am J Med. 1980;68:906-916. https://doi.org/10.1016/0002-9343(80)90225-9
34. Guyton AC, Coleman TG, Granger HJ. Circulation: overall regulation. Annu Rev Physiol. 1972;34:13-46 https://doi.org/10.1146/annurev.ph.34.030172.000305
35. Guyton AC, Montani JP, Hall JE, Manning RD Jr. Computer models for designing hypertension experiments and studying concepts. Am J Med Sci. 1988;295:320-326. https://doi.org/10.1097/00000441-198804000-00018
36. Hester RL, Brown AJ, Husband L, Iliescu R, Pruett D, Summers R, Coleman TG. HumMod: A modeling environment for the simulation of integrative human physiology. Front Physiol. 2011;2:12. https://doi.org/10.3389/fphys.2011.00012
37. Kurtz TW, Dicarlo SE, Pravenec M, Ježek F, Šilar J, Kofránek J, Morris RC Jr. Testing computer models predicting human responses to a high-salt diet. Hypertension. 2018;72:1407-1416. https://doi.org/10.1161/HYPERTENSIONAHA.118.11552
38. Beard DA: Assessing the validity and utility of the Guyton model of arterial blood pressure control. Hypertension. 2018;72:1272-1273. https://doi.org/10.1161/HYPERTENSIONAHA.118.11998
39. Kurtz TW, Dicarlo SE, Pravenec M, Morris RC Jr. The American Heart Association Scientific Statement on Salt Sensitivity of Blood Pressure: Prompting consideration of alternative conceptual frameworks for the pathogenesis of salt sensitivity? J Hypertens. 2017; 25:2214-2225. https://doi.org/10.1097/HJH.0000000000001458
40. Coleman TG, Manning RD, Jr., Norman RA, Jr., Granger HJ, Guyton AC. The role of salt in experimental and human hypertension. Am J Med Sci. 1972;264:103-110. https://doi.org/10.1097/00000441-197208000-00002
41. Clore J, Schoolwerth A, Watlington CO. When is cortisol a mineralocorticoid? Kidney Int. 1992;42:1297-1308. https://doi.org/10.1038/ki.1992.421
42. Scholl Ui, Lifton R. Inherited disorders of renal salt homeostasis: Insights from molecular genetics studies. Alpern RJ, Moe OW, Caplan M, eds. In: Seldin and Giebisch's The Kidney. Elsevier; 2013: 1213-1240. https://doi.org/10.1016/B978-0-12-381462-3.00036-7
43. Hall JE: Guyton and Hall Textbook of Medical Physiology. Elsevier; 2015.
44. Hall JE: Guyton and Hall Textbook of Medical Physiology. Elsevier; 2021.
45. Brailoiu GC, Benamar K, Arterburn JB, Gao E, Rabinowitz JE, Koch WJ, Brailoiu E. Aldosterone increases cardiac vagal tone via G protein-coupled oestrogen receptor activation. J Physiol. 2013;591:4223-4235. https://doi.org/10.1113/jphysiol.2013.257204
46. Jacob F, Clark LA, Guzman PA, Osborn JW. Role of renal nerves in development of hypertension in DOCA-salt model in rats: a telemetric approach. Am J Physiol Heart Circ Physiol. 2005;289:H1519-H1529. https://doi.org/10.1152/ajpheart.00206.2005
47. Kurtz TW, Pravenec M, Dicarlo SE. Mechanism-based strategies to prevent salt sensitivity and salt-induced hypertension. Clin Sci (Lond). 2022;136:599-620. https://doi.org/10.1042/CS20210566
48. Kurtz TW, Pravenec M, Dicarlo SE. Strategies are needed to prevent salt-induced hypertension that do not depend on reducing salt intake. Am J Hypertens. 2020;33:116-118. https://doi.org/10.1093/ajh/hpz173

49. Little R, Ellison DH. Modifying dietary sodium and potassium intake: An end to the salt wars?: Salt series. Hypertension. 2023. Online ahead of print. https://doi.org/10.1161/HYPERTENSIONAHA.123.19487
50. FDA To Propose to Permit Salt Substitutes to Reduce Sodium in Standardized Foods (https://www.fda.gov/food/cfsan-constituent-updates/fda-propose-permit-salt-substitutes-reduce-sodium-standardized-foods)
51. Morris RC Jr, Pravenec M, Šilhavý J, Dicarlo SE, Kurtz TW. Small amounts of inorganic nitrate or beetroot provide substantial protection from salt-induced increases in blood pressure. Hypertension. 2019;73:1042-1048. https://doi.org/10.1161/HYPERTENSIONAHA.118.12234

Physiol. Res. 73 (Suppl. 1): S377-S387, 2024 *https://doi.org/10.33549/physiolres.935364*

REVIEW

Gliflozins in the Treatment of Non-diabetic Experimental Cardiovascular Diseases

Ivana VANĚČKOVÁ[1], Josef ZICHA[1]

[1]Laboratory of Experimental Hypertension, Institute of Physiology of the Czech Academy of Sciences, Prague, Czech Republic

Received March 4, 2024
Accepted March 21, 2024

Summary

A new class of antidiabetic drugs - gliflozins (inhibitors of sodium glucose cotransporter-2; SGLT-2i) stimulate glucose and sodium excretion, thereby contributing to improved glycemic control, weight loss and blood pressure reduction in diabetic patients. Large clinical trials in patients with type 2 diabetes treated with empagliflozin, canagliflozin or dapagliflozin have demonstrated their excellent efficacy in improving many cardiovascular outcomes, including the reduction of death from cardiovascular diseases, non-fatal myocardial infarction or stroke, and hospitalization for heart failure. Moreover, the beneficial effects of SGLT-2i were also demonstrated in the decrease in proteinuria, which leads to a lower risk of progression to end-stage renal disease and thus a delay in initiation of the renal replacement therapy. Unexpectedly, their cardioprotective and renoprotective effects have been demonstrated not only in patients with diabetes but also in those without diabetes. Recently, much effort has been focused on patients with heart failure (either with reduced or preserved ejection fraction) or liver disease. Experimental studies have highlighted pleiotropic effects of SGLT-2 inhibitors beyond their natriuretic and glycosuric effects, including reduction of fibrosis, inflammation, reactive oxygen species, and others. Our results in experimental non-diabetic models of hypertension, chronic kidney disease and heart failure are partially consistent with these findings. This raises the question of whether the same mechanisms are at work in diabetic and non-diabetic conditions, and which mechanisms are responsible for the beneficial effects of gliflozins under non-diabetic conditions. Are these effects cardio-renal, metabolic, or others? This review will focus on the effects of gliflozins under different pathophysiological conditions, namely in hypertension, chronic kidney disease, and heart failure, which have been evaluated in non-diabetic rat models of these diseases.

Key words

SGLT-2 inhibitor • Hypertension • Chronic kidney disease • Heart failure • Liver disease • Rat

Corresponding author

Ivana Vaněčková, Laboratory of Experimental Hypertension, Institute of Physiology of the Czech Academy of Sciences, Videnska 1083, CZ-14200, Prague 4, Czech Republic. E-mail: ivana.vaneckova@fgu.cas.cz

Introduction

A new class of antidiabetic drugs - gliflozins (inhibitors of sodium glucose cotransporter-2; SGLT-2) enhance glucose and sodium excretion, thereby contributing to improved glycemic control, weight loss and blood pressure reduction in diabetic patients. Their history dates back to the first half of the 19th century, when the first naturally occurring non-selective SGLT inhibitor, phlorizin, was exctracted from apple bark tree [1]. It induced not only glycosuria by acting on the renal SGLT-2 transporter, but also diarrhoea by inhibiting the intestinal SGLT-1 transporter. More than 15 years years ago, a first synthetic analog of phlorizin, dapagliflozin, was tested in the treatment of diabetic patients [2], followed shortly by empagliflozin and canagliflozin, all with high selectivity for SGLT-2 transporter [3,4]. The mechanism by which glucose is returned to the blood from the ultrafiltrate is a two-step process [5]. The first step is the reabsorption of glucose together with sodium from the glomerular filtrate against the concentration gradient *via* the sodium-glucose cotransporter-2 located in the S1 segment of the proximal tubule of kidney. The energy required for this process is generated by Na^+/K^+ ATPase. In the second step, glucose is transported back into circulation by GLUT-2 transporter accross the basolateral membrane of proximal tubule. Under the

physiological conditions, 90 % of the filtered glucose is reabsorbed in this part of the kidney. Inhibition of SGLT-2 transporter results in a substantial loss of glucose to the urine [6]. Diabetes is associated with glomerular hyperfiltration due to the disturbances in tubulo-glomerular feedback (TGF) mechanism. Importantly, SGLT-2 inhibitors are able to modulate TGF by increasing sodium delivery to the macula densa, ultimately leading to afferent arteriolar constriction [7]. Although the effects of gliflozins were originally restricted to the kidney and heart, the pleiotrophic effects of gliflozins have now been demonstrated in many other organs, such as the liver, pancreas or adipose tissue [8,9].

The beneficial cardiovascular effects of gliflozins were first demonstrated in diabetic patients with established cardiovascular disease (CVD) in EMPA-REG OUTCOME [3] trial with empagliflozin, which resulted in impressive improvement in many cardiovascular outcomes, including reductions of death from cardiovascular diseases, non-fatal myocardial infarction or stroke. Importantly, there was a significant reduction in hospitalization for heart failure. Two other clinical trials with canagliflozin (CANVAS) [4] or dapagliflozin (DECLARE-TIMI) [10] confirmed that these benefits are not unique to empagliflozin, but are class effects of all SGLT-2 inhibitors. Moreover, the CREDENCE trial [11] demonstrated significant reduction in proteinuria, which led to a lower risk of progression to end-stage renal disease and thus to a delay in the initiation of renal replacement therapy. Later, the benefits of gliflozin therapy were demonstrated not only in patients with diabetes but also in those without diabetes. The DAPA-CKD trial [12] and the EMPA-KIDNEY [13,14] were the trials, that showed renoprotection after canagliflozin or empagliflozin treatment in patients with chronic kidney disease with or without diabetes. In addition, patients with heart failure (HF) also benefited significantly from SGLT-2 inhibition, with the DAPA-HF trial [14] enrolling HF patients treated with dapagliflozin. Subsequently, trials in selected populations of HF patients with reduced ejection fraction (EMPEROR-REDUCED) [14] and preserved ejection fraction (EMPEROR-PRESERVED) [15] demonstrated not only cardiovascular but also renal benefits of empagliflozin treatment. Together, these clinical trials enrolled approximately one hundred thousands of patients with various diagnoses and demonstrated improvements of cardiovascular and renal parameters. The question is whether the same mechanisms are at work in diabetic and non-diabetic conditions, and which mechanisms are responsible for these beneficial effects of gliflozins [16]. Are these effects rather cardio-renal, metabolic, or others? This review will focus on the effects of gliflozins under different pathophysiological conditions, namely hypertension, chronic kidney disease and heart failure, as evaluated in non-diabetic rat models of these diseases.

Experimental models of hypertension

Ren-2 transgenic rats

The Ren-2 transgenic rat (TGR) is a model of angiotensin II-dependent hypertension resulting from the insertion of the mouse Ren-2 gene into the genome of normotensive Hannover-Sprague Dawley rats [17]. This hypertension develops early in life in heterozygous animals, but they survive well throughout life. The 8-week treatment with empagliflozin in adult 6-month-old heterozygous TGR resulted in the reduction

Table 1. Empagliflozin effects in three non-diabetic hypertensive models

	TGR	HHTG	SHR-CRP
Body weight	↓	↓	↓ (young)
Fat mass	↓	↓	↓ (adult)
Hyperphagia	↑	↑	NA
Proteinuria	↔	NA	↓ (young)
Liver function	↑	↑	↑ (adult)
Cardiac function	↔	↔	↑ (adult)
Inflammation	↓	↓ (liver)	↓ (young) kidneys
Oxidative stress	↓ (kidneys)	↓ (liver)	↓ (young) kidneys
Blood pressure	↓	↔	↔

TGR – Ren-2 transgenic rats, HHTG – hereditary hypertriglyceridemic rats, SHR-CRP – Spontaneously hypertensive rats expressing human C-reactive protein

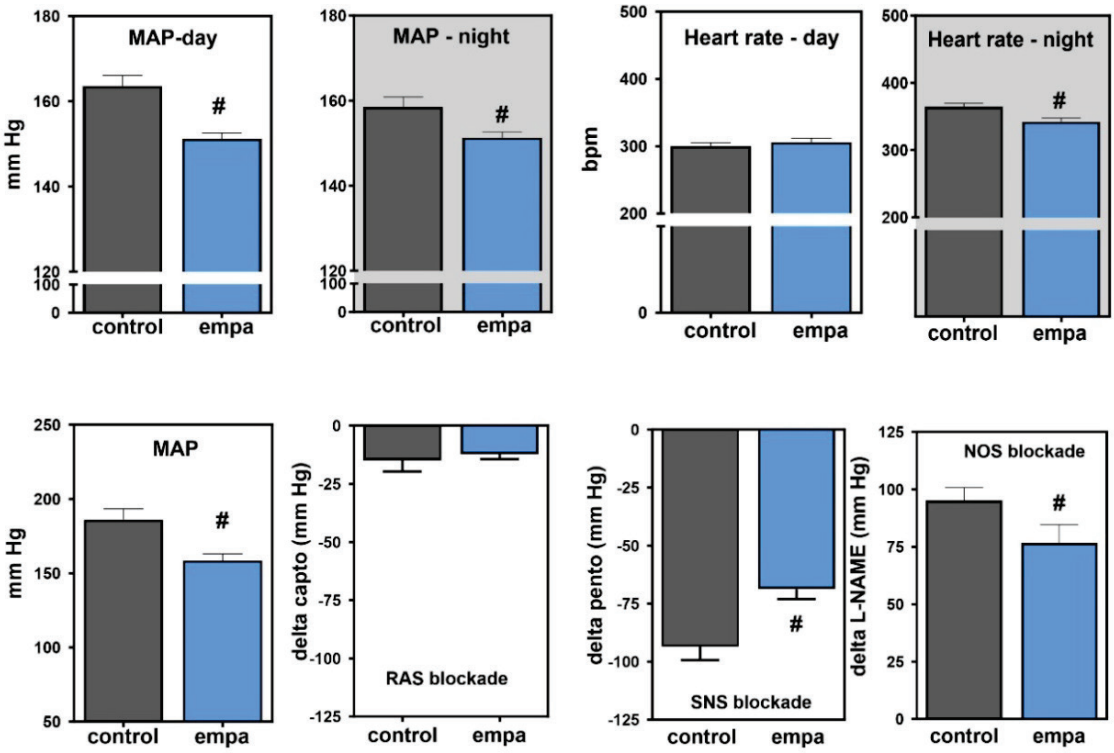

Fig. 1. Ren-2 transgenic rats. The effect of empagliflozin treatment on day and night blood pressure and heart rate measured by radiotelemetry (upper panel), and on mean arterial pressure (MAP) and its changes induced by sympathetic nervous system (SNS) blockade, renin-angiotensin system (RAS) blockade, and nitric oxide synthase (NOS) blockade in conscious rats of control and empagliflozin-treated Ren-2 transgenic rats (empa) (lower panel). # $p<0.05$ vs. control untreated group. Data are means ± SEM.

of their body weight and the size of fat depots despite their higher food consumption (Table 1) [18]. Moreover, telemetric blood pressure recording demonstrated a significant reduction of both daytime and nighttime blood pressure, which was associated with a decrease of heart rate during the active (dark) part of the day (Fig.1 upper panels). Our results showed that this BP decrease was mainly due to the attenuation of sympathetic vaso-constriction, with no effect of angiotensin II-dependent vasoconstriction (Fig.1 lower panels).

Unexpectedly, we did not find any effects of empagliflozin on renal function (with the exception of decreased plasma urea) or cardiac function. Regarding the metabolic effects of empagliflozin, there were significant reductions in plasma insulin and non-esterified fatty acid levels, as well as liver and myocardial triglyceride content. Importantly, empagliflozin exerted anti-inflammatory and antioxidant effects (reduction of plasma leptin, TNF-α and reduced/oxidized glutathione ratio in kidneys).

Hereditary hypertriglyceridemic rat

Hereditary hypertriglyceridemic rats (HHTG) are a non-obese prediabetic rat model [19] with several signs of metabolic syndrome, namely hyper-triglyceridemia and impaired glucose tolerance, represented by elevated non-fasting glucose and impaired oral glucose tolerance. Our study in adult 6-month-old HHTG [20] demonstrated that empagliflozin treatment not only improved glucose tolerance, as manifested by reduced fasting and non-fasting glucose, but also increased insulin sensitivity in skeletal muscles. Moreover, ectopic triglycerides and lipotoxic diacylglycerols in the liver were reduced after empagliflozin treatment. This was associated with decreased expression of lipogenic enzymes (Fasn and Scd1) and the lipogenic transcription factor Srebf1 in the liver. We also demonstrated changes in gene expression of the cytochrome P450 family involved in lipid metabolism. The decrease in hepatokines FGF21 and fetuin-A, as well as the attenuation of oxidative stress and increased antioxidant enzyme activity (superoxide dismutase and glutathione peroxidase) contributed to the beneficial hepato-protective effects of empagliflozin in this particular model. Similar to TGR rats, empagliflozin reduced body weight and fat mass in HHTG rats, independent of their hyperphagia. In contrast to TGR, telemetric BP monitoring did not detect any effect of SGLT-2 inhibition on blood pressure or heart rate (Fig. 2 upper panel) or on the major vasoactive systems contributing to BP maintenance (Fig. 2. lower panel). Similarly, we did not observe any effect on cardiac parameters evaluated by echocardiography.

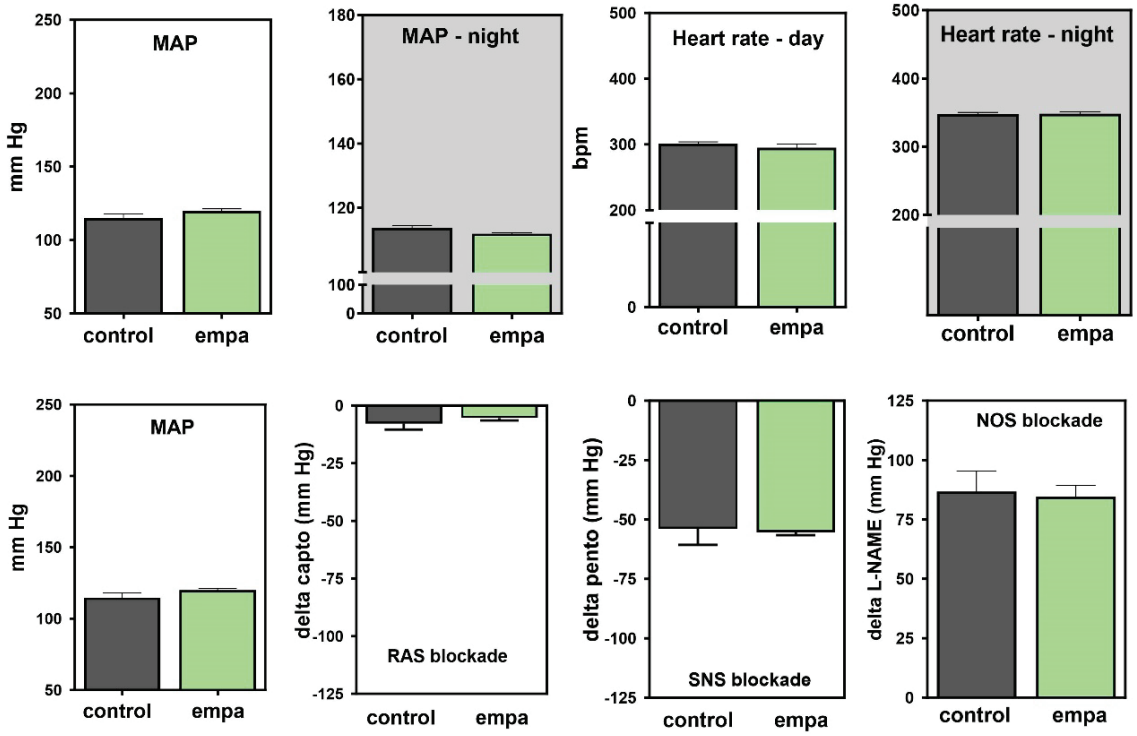

Fig. 2. Hereditary hypertriglyceridemic rats. The effect of empagliflozin treatment on day and night blood pressure and heart rate measured by radiotelemetry (upper panel), and on mean arterial pressure (MAP) and its changes induced by sympathetic nervous system (SNS) blockade, renin-angiotensin system (RAS) blockade, and nitric oxide synthase (NOS) blockade in conscious rats of control and empagliflozin-treated (empa) hereditary hypertriglyceridemic rats. Data are means ± SEM.

Spontaneously hypertensive rats expressing human C-reactive protein

Spontaneously hypertensive rats expressing human C-reactive protein (SHR-CRP) are a non-diabetic model of metabolic syndrome with severe hypertension, systemic inflammation, metabolic and hemodynamic disturbances, and target organ injury [21]. We analyzed the effect of empagliflozin treatment in both young (3-month-old) and adult (12-month-old) rats [22]. The beneficial effects of empagliflozin included not only reductions in body weight and fat mass, but also reduced ectopic fat accumulation in the liver and kidneys, the former being associated with decreased inflammation. Reduction of albuminuria was observed only in young SHR-CRP and was accompanied by attenuated oxidative stress. In contrast to adult TGR and HHTG rats, empagliflozin improved cardiac function in adult SHR-CRP by preventing the time-dependent increase in diastolic left ventricle wall thickness (both anterior and posterior) assesed by echocardiography (Fig. 3). In conclusion, empagliflozin exerted renoprotective effects in young SHR-CRP, which could be attributed to reduced renal lipid deposition and attenuation of renal oxidative stress and inflammation. In contrast to young SHR-CRP rats, the beneficial effects of empagliflozin in adult rats were related to cardiac and hepatic function.

Experimental models of chronic kidney disease

In our study [23], we evaluated renal function in relation to hypertension-induced end-organ damage in three models of chronic kidney disease with different pathophysiological background – Fawn-hooded hypertensive rats (FHH), in which hypertension, proteinuria, and focal glomerulosclerosis develop at a young age [24], and in two models of experimentally induced kidney damage – uninephrectomized rats on high salt intake (UNX+ HS) or rats with a stenosis of renal artery – two-kidney, one-clip (2K1C) Goldblatt hypertension [25].

Unexpectedly, we were unable to demonstrate renoprotective effects of empagliflozin treatment in any of these three models of chronic kidney disease [23]. Instead, a trend toward increased proteinuria was detected in all three groups following empagliflozin treatment, which was significant in FHH rats. Compared to the untreated group, the percentage increase in proteinuria during the eight weeks of empagliflozin treatment was 281 vs 201 % in FHH, 247 vs. 227 % in UNX+HS, and 219 vs. 153 % in 2K1C model. Consistent with this,

plasma MCP-1 levels were not improved by treatment. Moreover, the kidneys of all three models were substantially heavier than those of untreated rats (Table 2). Our tail-cuff blood pressure measurement did not show a blood pressure lowering effect of empagliflozin in the treated CKD groups (Fig. 4). The typical effects of SGLT-2 inhibition, namely reduction in body weight and fat mass, were detected only in FHH rats, with no effect in UNX+HS or 2K1C models (Table 2).

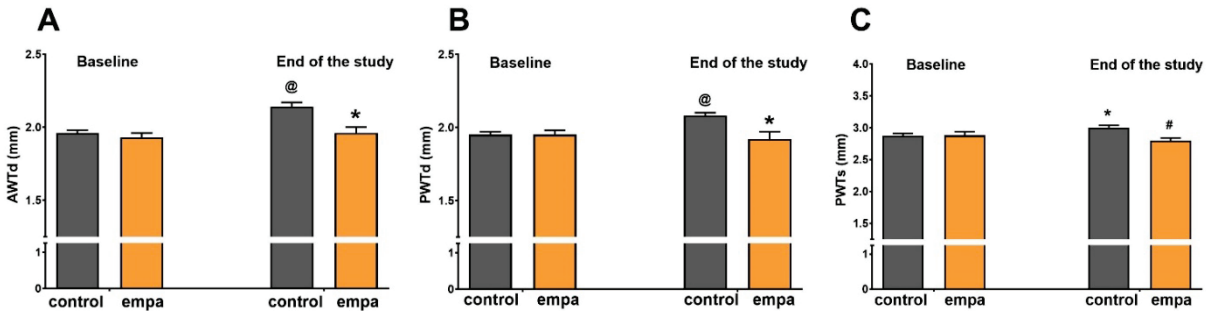

Fig. 3. Spontaneously hypertensive rats expressing human CRP. Anterior (**A**) and posterior (**B**) diastolic left ventricle wall thickness, systolic left ventricle wall thickness (**C**) at the beginning (baseline) and at the end of the experiment evaluated by echocardiography in adult control and empagliflozin-treated (empa) spontaneously hypertensive rats expressing human C-reactive protein. # p<0.05 vs. control untreated group, @ p<0.05 vs. respective baseline value. Data are means ± SEM.

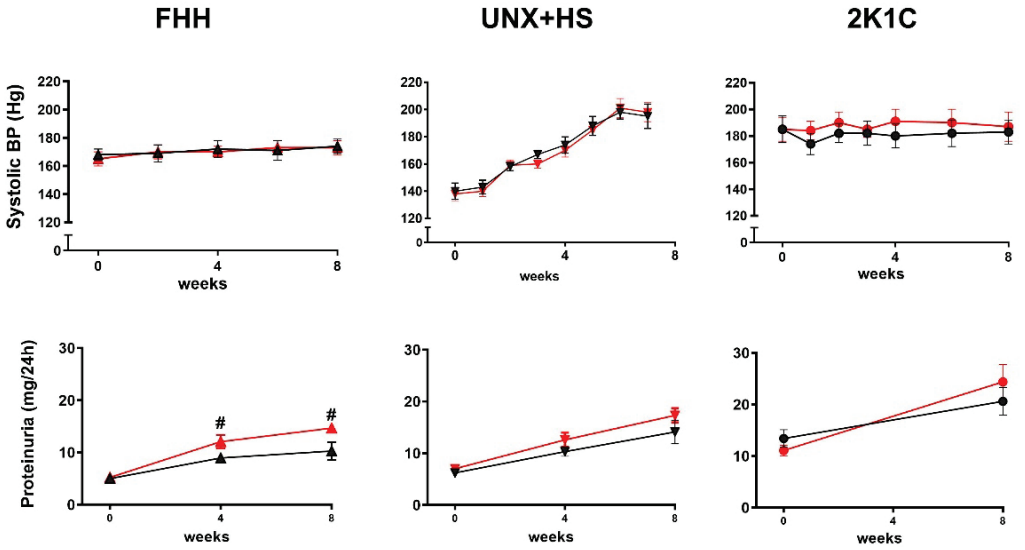

Fig. 4. The effect of empagliflozin treatment on systolic blood pressure measured by tail-cuff plethysmography (upper panel) and on proteinuria (lower panel) in control (black) and empagliflozin-treated (red) Fawn-hooded rats (FHH), uninephrectomized rats fed high-salt diet (UNX+HS) and in two-kidney one-clip (2K1C) Goldblatt hypertension. # p<0.05 vs. control untreated group. Data are means ± SEM.

Table 2. Empagliflozin effects in three non-diabetic models of chronic kidney disease

	FHH	UNX+HS	2K1C
Body weight	↓	↔	↔
Fat mass	↓	↔	↔
Relative kidney weight	↑	↑	↑
Proteinuria	↑	↔	↔
Oxidative stress	↔	↔	↔
Blood pressure	↔	↔	↔

Heart failure

Spontaneously hypertensive rats fed a high-fat diet

In this study [26], we used adult (6-month-old) male spontaneously hypertensive rats (SHR) fed a high-fat diet (60 % fat) for 4 months to induce heart failure. Since aging in SHR is naturally associated with progression to heart failure with preserved ejection fraction, relatively old animals were used in the study. In addition to cardiac dysfunction (both systolic and diastolic) observed in 50 % of the untreated animals, high-fat diet feeding induced mild liver steatosis, increased liver triglycerides and cholesterol levels, and worsened glucose tolerance in this diet-induced obesity model. Empagliflozin administered during the last two months of high-fat diet reduced body weight gain and improved glucose tolerance. In addition, hepato-protective effects included reduced ectopic lipid accumulation, lipoperoxidation, and inflammation. Importantly, this was associated with a reduction of pro-inflammatory HETEs while increasing anti-inflammatory EETs levels in the liver. While empagliflozin had no beneficial effect on kidney function, it significantly improved cardiac function (systolic, diastolic and pumping) without affecting blood pressure (Fig. 5 and Table 3).

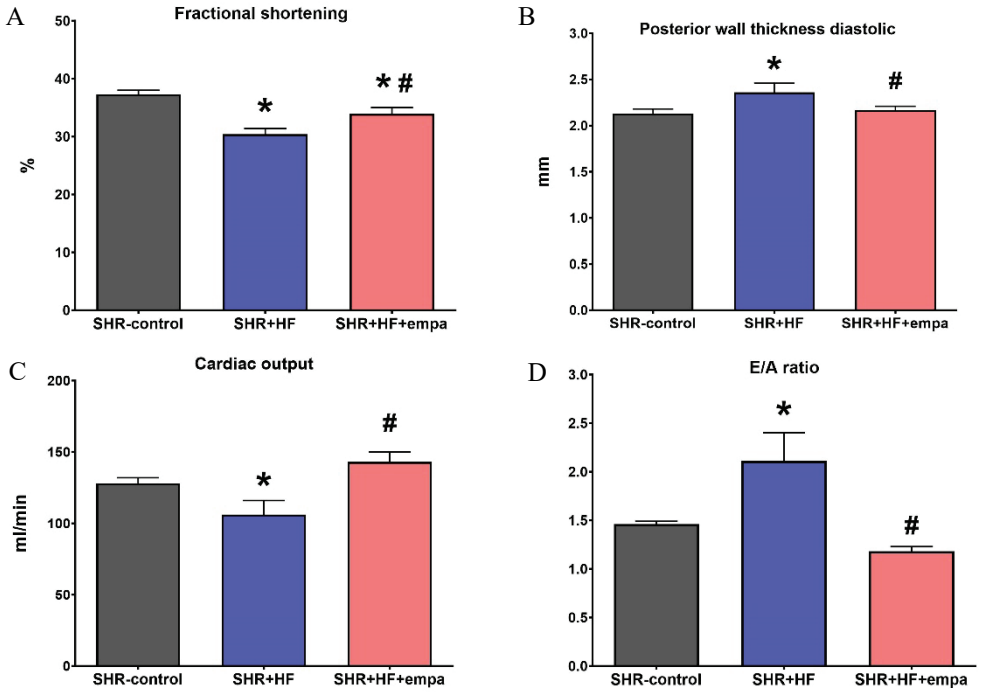

Fig. 5. Spontaneously hypertensive rats on high fat diet. The effect of empagliflozin treatment on fractional shortening (**A**), diastolic posterior wall thickness (**B**) cardiac output (**C**) and E/A ratio (**D**) in control spontaneously hypertensive rats (SHR), SHR fed a high-fat (SHR+HF) diet and empagliflozin-treated SHR-HF (SHR+HF+empa). * $p<0.05$ vs. control group fed a low-fat diet, # $p<0.05$ vs. untreated high-fat group. Data are means ± SEM.

Table 3. Empagliflozin effects in heart failure model

	SHR+HF
Body weight	↓
Fat mass	↔
Proteinuria	↔
Liver function	↑
Cardiac function	↑
Inflammation	↓
Oxidative stress	↓ (liver)
Blood pressure	↔

Discussion

Recently, several reviews on the effects of SGLT-2 inhibitors in non-diabetic animal models have been published [8,27-29] highlighting the main effects of gliflozins found in these studies. We would like to compare our results with these data and critically analyze the reasons for discrepancies between our and other studies.

Regarding the reduction of body mass and fat mass, our studies in hypertensive models are consistent

with most other experimental studies [30], although even an increase in body weight has been demonstrated in Dahl salt hypertensive rats after dapagliflozin treatment [31]. We also observed hyperphagia in TGR and HHTG rats, especially at the beginning of empagliflozin treatment. The increased food consumption is often associated with SGLT-2 inhibition and is probably due to the profound glucose excretion resulting in caloric loss. Interestingly, using a bioimpedance method, it has been shown that the weight loss during empagliflozin treatment contributes to the reduction of visceral and subcutaneous adipose tissue without affecting the lean body weight [32]. Moreover, our study in HHTG rats [20] demonstrated reduced hepatic lipid accumulation accompanied by decreased gene expression of the lipogenic enzymes Scd1, Fasn and lipogenic transcription factor Srebf1, which may also contribute to the reduction of lipid depots and body weight. On the other hand, in chronic kidney disease models, the effect on body weight and fat mass reduction was seen only in Fawn-hooded rats but not in uninephrectomized or 2K1C rats. This is in contrast to other experimental studies of CKD that have reported substantial reductions in body weight [33-35]. In SHR fed a high-fat diet, a model of heart and liver failure, body weight gains were reduced but there was no effect on fat mass. Whether these ambivalent responses are due to the fact that non-diabetic animals are less responsive to SGLT-2 inhibition than diabetic or pre-diabetic animals is debatable. The possible influence of different routes of application (food, drinking water, gavage), dose and type of SGLT-2 inhibitors cannot be excluded. Another explanation for different results could be the rat strain used.

Inconsistent results were also obtained regarding the effects of gliflozin treatment on cardiovascular function. We observed a moderate reduction in BP (15 mm Hg) and a significant reduction of nocturnal heart rate (22 bpm) after empagliflozin treatment in TGR [18], whereas there was no effect on BP level in HHTG rats [20], with BP measured telemetry in both experiments. The BP-lowering effect of empagliflozin in TGR was due to the reduced sympathetic vasoconstriction. On the other hand, tail-cuff BP monitoring demonstrated no gliflozin effect either in our three CKD models [23] or in SHR on high-fat diet [26]. Interestingly, we did not find an effect of empagliflozin treatment on cardiac function measured by echocardiography in TGR [18] and HHTG rats [20], but there was partial improvement of cardiac function in adult SHR-CRP [22]. Importantly, in SHR empagliflozin prevented the progression of high-fat diet-induced cardiac dysfunction (both systolic, diastolic and pumping) and restored cardiac parameters to the levels found in control SHR rats fed a low-fat diet [26]. Substantial (30 mm Hg) BP reductions were reported in 5/6 NX Sprague Dawley rats after both empagliflozin [33] and dapagliflozin [36] and in 5/6 NX Wistar rats on high-salt diet [37]. In contrast, Zhang *et al.* [34] found no BP effect in 5/6NX Sprague Dawley rats treated with dapagliflozin whereas a moderate BP reduction was reported in UNX Wistar rats treated with luseogliflozin [38]. We cannot provide a clear explanation for these discrepant results because the opposite results were obtained in the same strain and with the same type of gliflozin. However, the duration of the study, the age of animals, and last but not least, the dose of SGLT-2 inhibitor must be taken into account. In any case, one of the possible explanations for the antihypertensive effects of gliflozins could be the improvement of renal function and morphology due to reduced fibrosis [30,35,39], attenuated inflammation [33,40] or reduced oxidative stress [18,22], phenomena often reported in experimental studies following SGLT-2 inhibitors. The reduced fibrosis, inflammation and oxidative stress have also reported in several models of heart failure induced by myocardial infarction [41-44]. These effects probably precede the changes in proteinuria, as they have been described in many studies, whereas the functional improvement of renal function, such as improvement of creatinine clearance, proteinuria, or blood urea nitrogen, has been less frequently reported [35,45,46]. Perhaps these effects would have been more pronounced if treatment had been extended to months. In fact, the clinical trials with gliflozins, which usually lasted several years, generally showed nephroprotective effects in both diabetic and non-diabetic patients [4,13,47-49]. There is one short-term study supporting this hypothesis, which also failed to show the antiproteinuric effects in patients with focal segmental glomerulosclerosis after short (eight-week) dapagliflozin treatment [36].

It is generally accepted that the metabolic effects of SGLT-2 inhibition play an important role in mediating the beneficial effects of gliflozins. These effects have also been demonstrated in our experimental non-diabetic models [18,20]. We believe that a higher degree of metabolic dysfunction in the experimental model is associated with the higher efficacy of gliflozin treatment. Consistent with this, we have demonstrated significant metabolic effects in the prediabetic model, in hereditary

hypertriglyceridemic rats, and in TGR rats, in which we have observed important signs of metabolic syndrome, such as increased body and adipose tissue weight, together with increased plasma insulin and leptin levels. In HHTG rats [20], we found that empagliflozin modulated the expression of genes related to lipid synthesis (Fasn, Scd1) and fatty acid metabolism (Pparγ), as well as the transcription factor Nrf2 in the liver. The latter alteration may not only contribute to the reduction of oxidative stress, but also to the regulation of lipid metabolism by inhibiting lipogenesis. Recently, we have analyzed the relationship between metabolic effects and cardiac function in the spontaneously hypertensive rats feed a high-fat diet (a model of heart and liver failure) [26]. We hypothetize that cardioprotective effects – especially those affecting the systolic function – are secondary to hepatoprotective effects induced by SGLT-2 inhibition. Using correlation analysis, we demonstrated that ejection fraction and fractional shortening correlated with several metabolic parameters (ectopic lipid accumulation, lipoperoxidation, oxidative stress, 14,15-EETs and 20-HETEs). As many of these metabolic parameters were related to liver function, we suggest its direct or indirect influence on cardiac function. Whether the same is true in the opposite way remains to be determined in future studies.

In conclusion, SGLT-2 inhibitors have great potential in the treatment of both diabetic and non-diabetic patients due to their pleiotropic effects that go far beyond their hypoglycemic effects. However, it is clear from the previous paragraphs that there are still many issues that need to be addressed before their general acceptance in clinical practice.

Conflict of Interest

There is no conflict of interest.

Acknowledgements

This study was supported by institutional support from the Institute of Physiology, Czech Academy of Sciences, the grant Nr. RVO 67985823 and by the project National Institute for Research of Metabolic and Cardiovascular Diseases (Programme EXCELES, ID Project No. LX22NPO5104) – Funded by the European Union – Next Generation EU.

References

1. de Konnick LG, Annalen der Pharmacie, Über das Phloridzin (Phlorrhizin). Heidelberg, 1835;15:75-77.
2. Komoroski B, Vachharajani N, Feng Y, Li L, Kornhauser D, Pfister M. Dapagliflozin, a novel, selective SGLT2 inhibitor, improved glycemic control over 2 weeks in patients with type 2 diabetes mellitus. Clin Pharmacol Ther 2009;85:513-519. https://doi.org/10.1038/clpt.2008.250
3. Zinman B, Wanner C, Lachin JM, Fitchett D, Bluhmki E, Hantel S, Mattheus M, Devins T, Johansen OE, Woerle HJ, Broedl UC, Inzucchi SE. Empagliflozin, Cardiovascular Outcomes, and Mortality in Type 2 Diabetes. N Engl J Med 2015;373:2117-2128. https://doi.org/10.1056/NEJMoa1504720
4. Perkovic V, de Zeeuw D, Mahaffey KW, Fulcher G, Erondu N, Shaw W, Barrett TD, Weidner-Wells M, Deng H, Matthews DR, Neal B. Canagliflozin and renal outcomes in type 2 diabetes: results from the CANVAS Program randomised clinical trials. Lancet Diabetes Endocrinol 2018;6:691-704. https://doi.org/10.1016/S2213-8587(18)30141-4
5. Brown E, Rajeev SP, Cuthbertson DJ, Wilding JPH. A review of the mechanism of action, metabolic profile and haemodynamic effects of sodium-glucose co-transporter-2 inhibitors. Diabetes Obes Metab 2019;21 Suppl 2:9-18. https://doi.org/10.1111/dom.13650
6. Wright EM, Loo DD, Hirayama BA. Biology of human sodium glucose transporters. Physiol Rev 2011;91:733-794. https://doi.org/10.1152/physrev.00055.2009
7. Cherney DZ, Perkins BA, Soleymanlou N, Maione M, Lai V, Lee A, Fagan NM, Woerle HJ, Johansen OE, Broedl UC, von Eynatten M. Renal hemodynamic effect of sodium-glucose cotransporter 2 inhibition in patients with type 1 diabetes mellitus. Circulation 2014;129:587-597. https://doi.org/10.1161/CIRCULATIONAHA.113.005081
8. Androutsakos T, Nasiri-Ansari N, Bakasis AD, Kyrou I, Efstathopoulos E, Randeva HS, Kassi E. SGLT-2 Inhibitors in NAFLD: Expanding their role beyond diabetes and cardioprotection. Int J Mol Sci 2022;23:3107. https://doi.org/10.3390/ijms23063107

9. Pereira MJ, Eriksson JW. Emerging Role of SGLT-2 Inhibitors for the treatment of obesity. Drugs 2019;79:219-230. https://doi.org/10.1007/s40265-019-1057-0
10. Wiviott SD, Raz I, Bonaca MP, Mosenzon O, Kato ET, Cahn A, Silverman MG, Zelniker TA, Kuder JF, Murphy SA, Bhatt DL, Leiter LA, McGuire DK, Wilding JPH, Ruff CT, Gause-Nilsson IAM, Fredriksson M, Johansson PA, Langkilde AM, Sabatine MS. Dapagliflozin and cardiovascular outcomes in type 2 Diabetes. N Engl J Med 2019;380:347-357. https://doi.org/10.1056/NEJMoa1812389
11. Cannon CP, Perkovic V, Agarwal R, Baldassarre J, Bakris G, Charytan DM, de Zeeuw D, Edwards R, Greene T, Heerspink HJL, Jardine MJ, Levin A, Li JW, Neal B, Pollock C, Wheeler DC, Zhang H, Zinman B, Mahaffey KW. Evaluating the effects of canagliflozin on cardiovascular and renal events in patients with type 2 diabetes mellitus and chronic kidney disease according to baseline HbA1c, including those with HbA1c <7%: Results from the CREDENCE Trial. Circulation 2020;141:407-410. https://doi.org/10.1161/CIRCULATIONAHA.119.044359
12. Wheeler DC, Stefansson BV, Batiushin M, Bilchenko O, Cherney DZI, Chertow GM, Douthat W, Dwyer JP, Escudero E, Pecoits-Filho R, Furuland H, Górriz JL, Greene T, Haller H, Hou FF, Kang SW, Isidto R, Khullar D, Mark PB, McMurray JJV, Kashihara N, Nowicki M, Persson F, Correa-Rotter R, Rossing P, Toto RD, Umanath K, Van Bui P, Wittmann I, Lindberg M, Sjöström CD, Langkilde AM, Heerspink HJL. The dapagliflozin and prevention of adverse outcomes in chronic kidney disease (DAPA-CKD) trial: baseline characteristics. Nephrol Dial Transplant 2020;35:1700-1711. https://doi.org/10.1093/ndt/gfaa234
13. Herrington WG, Staplin N, Wanner C, Green JB, Hauske SJ, Emberson JR, Preiss D, Judge P, Mayne KJ, Ng SYA, Sammons E, Zhu D, Hill M, Stevens W, Wallendszus K, Brenner S, Cheung AK, Liu ZH, Li J, Hooi LS, Liu W, Kadowaki T, Nangaku M, Levin A, Cherney D, Maggioni AP, Pontremoli R, Deo R, Goto S, Rossello X, Tuttle KR, Steubl D, Petrini M, Massey D, Eilbracht J, Brueckmann M, Landray MJ, Baigent C, Haynes R. Empagliflozin in Patients with Chronic Kidney Disease. N Engl J Med 2023;388:117-127. https://doi.org/10.1056/NEJMoa2204233
14. Zannad F, Ferreira JP, Pocock SJ, Anker SD, Butler J, Filippatos G, Brueckmann M, Ofstad AP, Pfarr E, Jamal W, Packer M. SGLT2 inhibitors in patients with heart failure with reduced ejection fraction: a meta-analysis of the EMPEROR-Reduced and DAPA-HF trials. Lancet 2020;396:819-829. https://doi.org/10.1016/S0140-6736(20)31824-9
15. Anker SD, Butler J, Filippatos G, Ferreira JP, Bocchi E, Böhm M, Brunner-La Rocca HP, Choi DJ, Chopra V, Chuquiure-Valenzuela E, Giannetti N, Gomez-Mesa JE, Janssens S, Januzzi JL, Gonzalez-Juanatey JR, Merkely B, Nicholls SJ, Perrone SV, Piña IL, Ponikowski P, Senni M, Sim D, Spinar J, Squire I, Taddei S, Tsutsui H, Verma S, Vinereanu D, Zhang J, Carson P, Lam CSP, Marx N, Zeller C, Sattar N, Jamal W, Schnaidt S, Schnee JM, Brueckmann M, Pocock SJ, Zannad F, Packer M. Empagliflozin in heart failure with a preserved ejection fraction. N Engl J Med 2021;385:1451-1461. https://doi.org/10.1056/NEJMoa2107038
16. Rajasekeran H, Cherney DZ, Lovshin JA. Do effects of sodium-glucose cotransporter-2 inhibitors in patients with diabetes give insight into potential use in non-diabetic kidney disease? Curr Opin Nephrol Hypertens 2017;26:358-367. https://doi.org/10.1097/MNH.0000000000000343
17. Mullins JJ, Peters J, Ganten D. Fulminant hypertension in transgenic rats harbouring the mouse Ren-2 gene. Nature 1990;344:541-544. https://doi.org/10.1038/344541a0
18. Hojná S, Rauchová H, Malínská H, Marková I, Hüttl M, Papoušek F, Behuliak M, Miklánková D, Vaňourková Z, Neckář J, Kadlecová M, Kujal P, Zicha J, Vaněčková I. Antihypertensive and metabolic effects of empagliflozin in Ren-2 transgenic rats, an experimental non-diabetic model of hypertension. Biomed Pharmacother 2021;144:112246. https://doi.org/10.1016/j.biopha.2021.112246
19. Vrána A, Kazdová L. The hereditary hypertriglyceridemic nonobese rat: an experimental model of human hypertriglyceridemia. Transplant Proc 1990;22:2579.
20. Hüttl M, Markova I, Miklankova D, Zapletalova I, Poruba M, Haluzik M, Vaněčkova I, Malinska H. In a prediabetic model, empagliflozin improves hepatic lipid metabolism independently of obesity and before onset of hyperglycemia. Int J Mol Sci 2021;22:11513. https://doi.org/10.3390/ijms222111513
21. Pravenec M, Kajiya T, Zídek V, Landa V, Mlejnek P, Simáková M, Silhavý J, Malínská H, Oliyarnyk O, Kazdová L, Fan J, Wang J, Kurtz TW. Effects of human C-reactive protein on pathogenesis of features of the metabolic syndrome. Hypertension 2011;57:731-737. https://doi.org/10.1161/HYPERTENSIONAHA.110.164350

22. Malínská H, Hüttl M, Marková I, Miklánková D, Hojná S, Papoušek F, Šilhavý J, Mlejnek P, Zicha J, Hrdlička J, Pravenec M, Vaněčková I. Beneficial effects of Empagliflozin are mediated by reduced renal inflammation and oxidative stress in spontaneously hypertensive rats expressing human C-reactive protein. Biomedicines 2022;10:2066. https://doi.org/10.3390/biomedicines10092066
23. Hojná S, Kotsaridou Z, Vaňourková Z, Rauchová H, Behuliak M, Kujal P, Kadlecová M, Zicha J, Vaněčková I. Empagliflozin is not renoprotective in non-diabetic rat models of chronic kidney disease. Biomedicines 2022;10:2509. https://doi.org/10.3390/biomedicines10102509
24. Provoost AP. Spontaneous glomerulosclerosis: insights from the fawn-hooded rat. Kidney Int Suppl 1994;45:S2-5.
25. Drábková N, Hojná S, Zicha J, Vaněčková I. Contribution of selected vasoactive systems to blood pressure regulation in two models of chronic kidney disease. Physiol Res 2020;69:405-414. https://doi.org/10.33549/physiolres.934392
26. Hojná S MH, Hüttl M, Vaňourková Z, Marková Z, Miklánková D, Hrdlička J, Papoušek F, Neckář J, Kujal P, Behuliak M, Rauchová H, Kadlecová M, Sedmera D, Neffeová K, Zábrodská E, Olejníčková V, Zicha J, Vaněčková I. Hepatoprotective and cardioprotective effects of empagliflozin in spontaneously hypertensive rats fed a high-fat diet. Biomed Pharmacother 2024;174:116520. https://doi.org/10.1016/j.biopha.2024.116520
27. Castoldi G CR, Barzaghi F, Meani M, Zatti M, Perseghin G, Di Gioia CRT, Zerbini G. Sodium glucose cotransporter-2 inhibitors in non-diabetic kidney disease: evidence in experimental models. Pharmaceuticals 2024;17:362. https://doi.org/10.3390/ph17030362
28. Abdelrahman AM, Awad AS, Abdel-Rahman EM. Sodium-Glucose Co-Transporter 2 Inhibitors: Mechanism of action and efficacy in non-diabetic kidney disease from bench to bed-side. J Clin Med. 2024;13(4):956. https://doi.org/10.3390/jcm13040956
29. Panico C, Bonora B, Camera A, Chilelli NC, Prato GD, Favacchio G, Grancini V, Resi V, Rondinelli M, Zarra E, Pintaudi B. Pathophysiological basis of the cardiological benefits of SGLT-2 inhibitors: a narrative review. Cardiovasc Diabetol 2023;22:164. https://doi.org/10.1186/s12933-023-01855-y
30. Castoldi G, Carletti R, Barzaghi F, Meani M, Zatti G, Perseghin G, Di Gioia CRT, Zerbini G. Sodium glucose cotransporter-2 inhibitors in non-diabetic kidney disease: evidence in experimental models. Pharmaceuticals (Basel). 2024;17(3):362. https://doi.org/10.3390/ph17030362
31. Urbanek K, Cappetta D, Bellocchio G, Coppola MA, Imbrici P, Telesca M, Donniacuo M, Riemma MA, Mele E, Cianflone E, Naviglio S, Conte E, Camerino GM, Mele M, Bucci M, Castaldo G, De Luca A, Rossi F, Berrino L, Liantonio A, De Angelis A. Dapagliflozin protects the kidney in a non-diabetic model of cardiorenal syndrome. Pharmacol Res 2023;188:106659. https://doi.org/10.1016/j.phrs.2023.106659
32. Schork A, Saynisch J, Vosseler A, Jaghutriz BA, Heyne N, Peter A, Häring HU, Stefan N, Fritsche A, Artunc F. Effect of SGLT2 inhibitors on body composition, fluid status and renin-angiotensin-aldosterone system in type 2 diabetes: a prospective study using bioimpedance spectroscopy. Cardiovasc Diabetol 2019;18:46. https://doi.org/10.1186/s12933-019-0852-y
33. Kim S, Jo CH, Kim GH. Effects of empagliflozin on nondiabetic salt-sensitive hypertension in uninephrectomized rats. Hypertens Res 2019;42:1905-1915. https://doi.org/10.1038/s41440-019-0326-3
34. Zhang Y, Thai K, Kepecs DM, Gilbert RE. Sodium-glucose linked cotransporter-2 inhibition does not attenuate disease progression in the rat remnant kidney model of chronic kidney disease. PLoS One 2016;11:e0144640. https://doi.org/10.1371/journal.pone.0144640
35. Ali BH, Al Salam S, Al Suleimani Y, Al Za'abi M, Abdelrahman AM, Ashique M, Manoj P, Adham SA, Hartmann C, Schupp N, Nemmar A. Effects of the SGLT-2 Inhibitor canagliflozin on adenine-induced chronic kidney disease in rats. Cell Physiol Biochem 2019;52:27-39. https://doi.org/10.33594/000000003
36. Rajasekeran H, Reich HN, Hladunewich MA, Cattran D, Lovshin JA, Lytvyn Y, Bjornstad P, Lai V, Tse J, Cham L, Majumder S, Bowskill BB, Kabir MG, Advani SL, Gibson IW, Sood MM, Advani A, Cherney DZI. Dapagliflozin in focal segmental glomerulosclerosis: a combined human-rodent pilot study. Am J Physiol Renal Physiol 2018;314:F412-F422. https://doi.org/10.1152/ajprenal.00445.2017

37. Zeng S, Delic D, Chu C, Xiong Y, Luo T, Chen X, Gaballa MMS, Xue Y, Chen X, Cao Y, Hasan AA, Stadermann K, Frankenreiter S, Yin L, Krämer BK, Klein T, Hocher B. Antifibrotic effects of low dose SGLT2 inhibition with empagliflozin in comparison to Ang II receptor blockade with telmisartan in 5/6 nephrectomised rats on high salt diet. Biomed Pharmacother 2022;146:112606. https://doi.org/10.1016/j.biopha.2021.112606
38. Wan N, Fujisawa Y, Kobara H, Masaki T, Nakano D, Rahman A, Nishiyama A. Effects of an SGLT2 inhibitor on the salt sensitivity of blood pressure and sympathetic nerve activity in a nondiabetic rat model of chronic kidney disease. Hypertens Res 2020;43:492-499. https://doi.org/10.1038/s41440-020-0410-8
39. Kravtsova O, Levchenko V, Klemens CA, Rieg T, Liu R, Staruschenko A. Effect of SGLT2 inhibition on salt-induced hypertension in female Dahl SS rats. Sci Rep 2023;13:19231. https://doi.org/10.1038/s41598-023-46016-z
40. Reyes-Pardo H, Bautista R, Vargas-Robles H, Rios A, Sánchez D, Escalante B. Role of sodium/glucose cotransporter inhibition on a rat model of angiotensin II-dependent kidney damage. BMC Nephrol 2019;20:292. https://doi.org/10.1186/s12882-019-1490-z
41. Yurista SR, Silljé HHW, Oberdorf-Maass SU, Schouten EM, Pavez Giani MG, Hillebrands JL, van Goor H, van Veldhuisen DJ, de Boer RA, Westenbrink BD. Sodium-glucose co-transporter 2 inhibition with empagliflozin improves cardiac function in non-diabetic rats with left ventricular dysfunction after myocardial infarction. Eur J Heart Fail 2019;21:862-873. https://doi.org/10.1002/ejhf.1473
42. Kolijn D, Pabel S, Tian Y, Lódi M, Herwig M, Carrizzo A, Zhazykbayeva S, Kovács Á, Fülöp G, Falcão-Pires I, Reusch PH, Linthout SV, Papp Z, van Heerebeek L, Vecchione C, Maier LS, Ciccarelli M, Tschöpe C, Mügge A, Bagi Z, Sossalla S, Hamdani N. Empagliflozin improves endothelial and cardiomyocyte function in human heart failure with preserved ejection fraction via reduced pro-inflammatory-oxidative pathways and protein kinase Gα oxidation. Cardiovasc Res 2021;117:495-507. https://doi.org/10.1093/cvr/cvaa123
43. Daud E, Ertracht O, Bandel N, Moady G, Shehadeh M, Reuveni T, Atar S. The impact of empagliflozin on cardiac physiology and fibrosis early after myocardial infarction in non-diabetic rats. Cardiovasc Diabetol 2021;20:132. https://doi.org/10.1186/s12933-021-01322-6
44. Lee HC, Shiou YL, Jhuo SJ, Chang CY, Liu PL, Jhuang WJ, Dai ZK, Chen WY, Chen YF, Lee AS. The sodium-glucose co-transporter 2 inhibitor empagliflozin attenuates cardiac fibrosis and improves ventricular hemodynamics in hypertensive heart failure rats. Cardiovasc Diabetol 2019;18:45. https://doi.org/10.1186/s12933-019-0849-6
45. Lu YP, Wu HW, Zhu T, Li XT, Zuo J, Hasan AA, Reichetzeder C, Delic D, Yard B, Klein T, Krämer BK, Zhang ZY, Wang XH, Yin LH, Dai Y, Zheng ZH, Hocher B. Empagliflozin reduces kidney fibrosis and improves kidney function by alternative macrophage activation in rats with 5/6-nephrectomy. Biomed Pharmacother 2022;156:113947. https://doi.org/10.1016/j.biopha.2022.113947
46. Jaikumkao K, Pongchaidecha A, Chueakula N, Thongnak LO, Wanchai K, Chatsudthipong V, Chattipakorn N, Lungkaphin A. Dapagliflozin, a sodium-glucose co-transporter-2 inhibitor, slows the progression of renal complications through the suppression of renal inflammation, endoplasmic reticulum stress and apoptosis in prediabetic rats. Diabetes Obes Metab 2018;20:2617-2626. https://doi.org/10.1111/dom.13441
47. Neal B, Perkovic V, de Zeeuw D, Mahaffey KW, Fulcher G, Ways K, Desai M, Shaw W, Capuano G, Alba M, Jiang J, Vercruysse F, Meininger G, Matthews D. Efficacy and safety of canagliflozin, an inhibitor of sodium-glucose cotransporter 2, when used in conjunction with insulin therapy in patients with type 2 diabetes. Diabetes Care 2015;38:403-411. https://doi.org/10.2337/dc14-1237
48. Cherney DZI, Dekkers CCJ, Barbour SJ, Cattran D, Abdul Gafor AH, Greasley PJ, Laverman GD, Lim SK, Di Tanna GL, Reich HN, Vervloet MG, Wong MG, Gansevoort RT, Heerspink HJL. Effects of the SGLT2 inhibitor dapagliflozin on proteinuria in non-diabetic patients with chronic kidney disease (DIAMOND): a randomised, double-blind, crossover trial. Lancet Diabetes Endocrinol 2020;8:582-593. https://doi.org/10.1016/S2213-8587(20)30162-5
49. Heerspink HJL, Stefánsson BV, Correa-Rotter R, Chertow GM, Greene T, Hou FF, Mann JFE, McMurray JJV, Lindberg M, Rossing P, Sjöström CD, Toto RD, Langkilde AM, Wheeler DC. Dapagliflozin in patients with chronic kidney disease. N Engl J Med 2020;383:1436-1446. https://doi.org/10.1056/NEJMoa2024816

Physiol. Res. 73 (Suppl. 1): S389-S400, 2024 *https://doi.org/10.33549/physiolres.935270*

REVIEW

Muscarinic Receptors in Cardioprotection and Vascular Tone Regulation

Eva DOLEJŠÍ[1], Alena JANOUŠKOVÁ[1], Jan JAKUBÍK[1]

[1]Laboratory of Neurochemistry, Institute of Physiology, Czech Academy of Sciences, Prague, Czech Republic

Received October 31, 2023
Accepted February 8, 2024

Summary

Muscarinic acetylcholine receptors are metabotropic G-protein coupled receptors. Muscarinic receptors in the cardiovascular system play a central role in its regulation. Particularly M_2 receptors slow down the heart rate by reducing the impulse conductivity through the atrioventricular node. In general, activation of muscarinic receptors has sedative effects on the cardiovascular system, including vasodilation, negative chronotropic and inotropic effects on the heart, and cardioprotective effects, including antifibrillatory effects. First, we review the signaling of individual subtypes of muscarinic receptors and their involvement in the physiology and pathology of the cardiovascular system. Then we review age and disease-related changes in signaling via muscarinic receptors in the cardiovascular system. Finally, we review molecular mechanisms involved in cardioprotection mediated by muscarinic receptors leading to negative chronotropic and inotropic and antifibrillatory effects on heart and vasodilation, like activation of acetylcholine-gated inward-rectifier K^+-currents and endothelium-dependent and -independent vasodilation. We relate this knowledge with well-established cardioprotective treatments by vagal stimulation and muscarinic agonists. It is well known that estrogen exerts cardioprotective effects against atherosclerosis and ischemia-reperfusion injury. Recently, some sex hormones and neurosteroids have been shown to allosterically modulate muscarinic receptors. Thus, we outline possible treatment by steroid-based positive allosteric modulators of acetylcholine as a novel pharmacotherapeutic tactic.

Key words

Muscarinic receptors • Muscarinic agonists • Allosteric modulation • Cardiovascular system • Cardioprotection • Steroids

Corresponding author

Jan Jakubík, Institute of Physiology of the Czech Academy of Sciences, Vídeňská 1083, 142 00 Prague Czech Republic. Email: jan.jakubik@fgu.cas.cz

Introduction

Muscarinic acetylcholine receptors are membrane proteins that belong to the super-family of G-protein coupled receptors (GPCRs) that transmit their signals into the cell through heterotrimeric G-proteins. Five different subtypes referred to as M_1–M_5 exist in mammals. Individual subtypes differ in second-messenger signaling depending on coupling with individual G-proteins.

The M_1, M_3 and M_5 receptors are excitatory subtypes preferentially activating the $G_{q/11}$ class of G-proteins [1]. The activation of α-subunits of these G-proteins leads to activation of phospholipase C (PLC). PLC, in turn, produces the second messengers, diacylglycerol and 1,4,5-inositol trisphosphate (IP_3), which activate protein kinase C (PKC) and mobilize intracellular calcium stores, respectively. PKC phosphorylates several target proteins. The Ca^{2+} influx causes a variety of cascades of intracellular activity. The M_2 and M_4 receptors are inhibitory preferentially coupling with the $G_{i/o}$ class of G-proteins. Activated $G_{i/o}$ α-subunits inhibit adenylyl cyclase (AC) leading to a reduction in the production of cAMP. Although the preferential coupling, their specificity is not absolute. Importantly, βγ-dimers released upon activation of $G_{i/o}$ G-proteins activate the inward rectifying potassium channel and inhibit calcium channels in the heart, leading to decrease in excitatory potential [2, 3].

Muscarinic receptors mediate a wide range of physiological functions in the central nervous system (CNS) and the effects of the parasympathetic nervous

system in the periphery. All regions of the mammalian heart are innervated by parasympathetic (vagal) nerves, although the supraventricular tissues are more densely innervated than the ventricles. Heart rate is largely controlled by the internal pacemaker activity. In the absence of any external stimuli, sinoatrial pacing maintains the human heart rate in the range of 60-100 beats per minute [4]. Increased vagal tone diminishes heart rate and inotropy by modulation of potassium and calcium currents in the sinoatrial node [5]. Vagal tone balances increased inotropy and heart rate mediated by G_s-coupled β_2- and β_1-adrenergic receptors activated by adrenaline released from sympathetic neurons upon a load or systemic noradrenaline upon stress. The increased activity of the sympathetic nervous system leads to increased force of muscular contractions that in turn increases the stroke volume as well as peripheral vasoconstriction leading to high blood pressure that in the long term may lead to heart failure [6].

Non-neuronal acetylcholine (ACh) activity was also reported [7]. For example, muscarinic receptors have been localized at the endothelial cells of blood vessels as well as other tissues that lack cholinergic innervation including myocytes [8]. Many pieces of evidence also suggest the role of non-neuronal ACh in the modulation of the cardiovascular system [9].

Muscarinic receptors in the cardiovascular system in health

Effects of ACh in the cardiovascular system depend on the cell type and subtype of muscarinic receptors. In the heart muscarinic receptors mediate a decrease in inotropy and chronotropy and modulate parameters of ionic currents [10,11]. Based on ligand binding and cloning studies, the M_2 subtype is considered the predominant muscarinic receptor in the mammalian heart [12,13] as well as vasculature [14]. Later studies revealed expressions of other muscarinic subtypes with variable distribution throughout heart regions [15].

M_2 receptors

It was demonstrated that M_2 mRNA represents more than 90 % of total muscarinic mRNAs in rat atria and in either ventricle. The concentration of M_2 mRNA in the atria is more than twice as high as in the ventricles [15]. Pharmacologic evidence indicates that functional responses of atrial and ventricular cardiomyocytes to ACh are primarily associated with the activation of M_2 receptors [16]. Stimulation of M_2 receptors influences cardiac ion channels function *via* modulation of different cellular pathways. However, some cardiac effects of muscarinic receptor stimulation remain enigmatic.

In supraventricular (sinoatrial, atrial, and atrioventricular) myocytes, M_2 receptors positively modulate inwardly rectifying potassium channels *via* a membrane-delimited mechanism involving direct activation by the βγ-subunits released from the $G_{i/o}$ inhibitory G proteins (Fig. 1), resulting in hyperpolarization, thus slowing the heart rate by reducing the impulse conductivity through the atrioventricular node [16]. ACh also inhibits AC *via* M_2 receptors and $G_{i/o}$ α-subunits, resulting in a decrease in the production of cAMP.

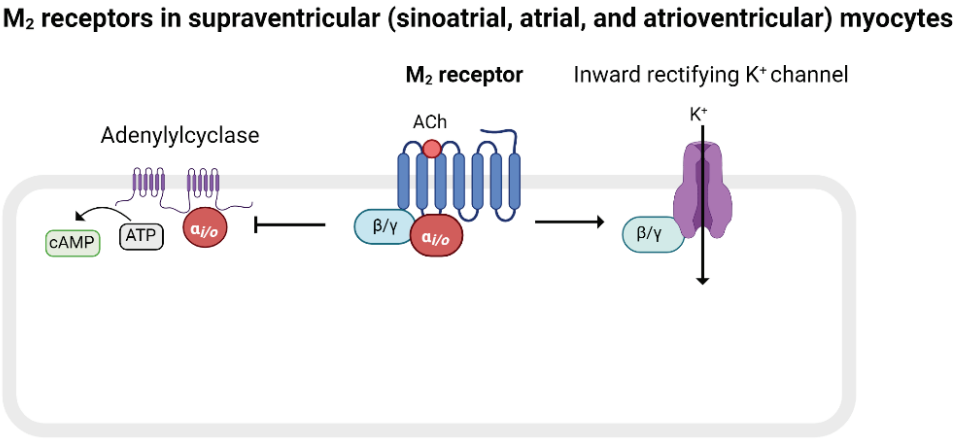

Fig. 1. M_2 receptor signaling in supraventricular myocytes. In supraventricular myocytes, M_2 receptors positively modulate inwardly rectifying potassium channels by the βγ-subunits released from the $G_{i/o}$ inhibitory G proteins resulting in hyperpolarization. Created with BioRender.com.

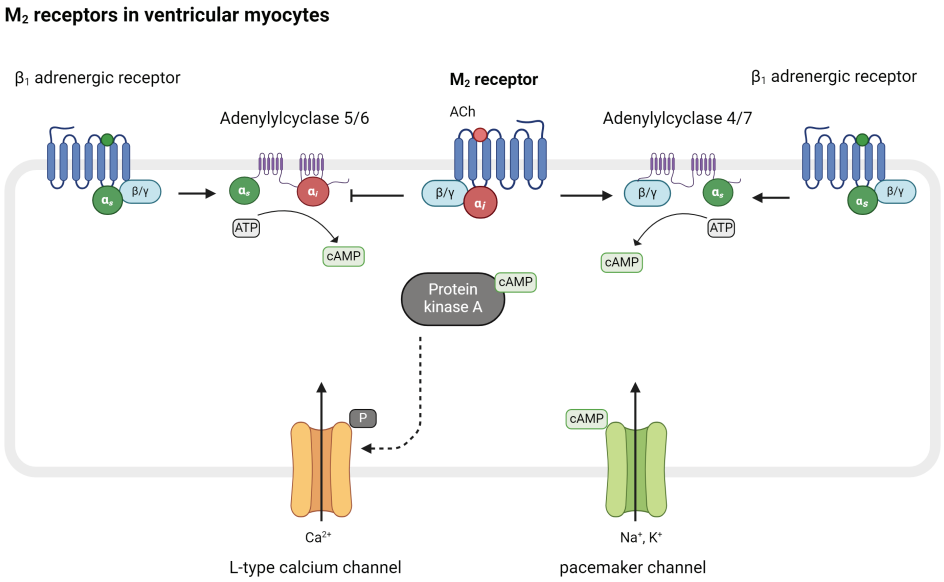

Fig. 2. M_2 receptor signaling in ventricular myocytes. In ventricular myocytes, M_2 receptors modulate the cAMP-dependent response to β-adrenergic receptor activation modulating activity of L-type Ca^{2+} and Na^+/K^+ pacemaker channels. Created with BioRender.com.

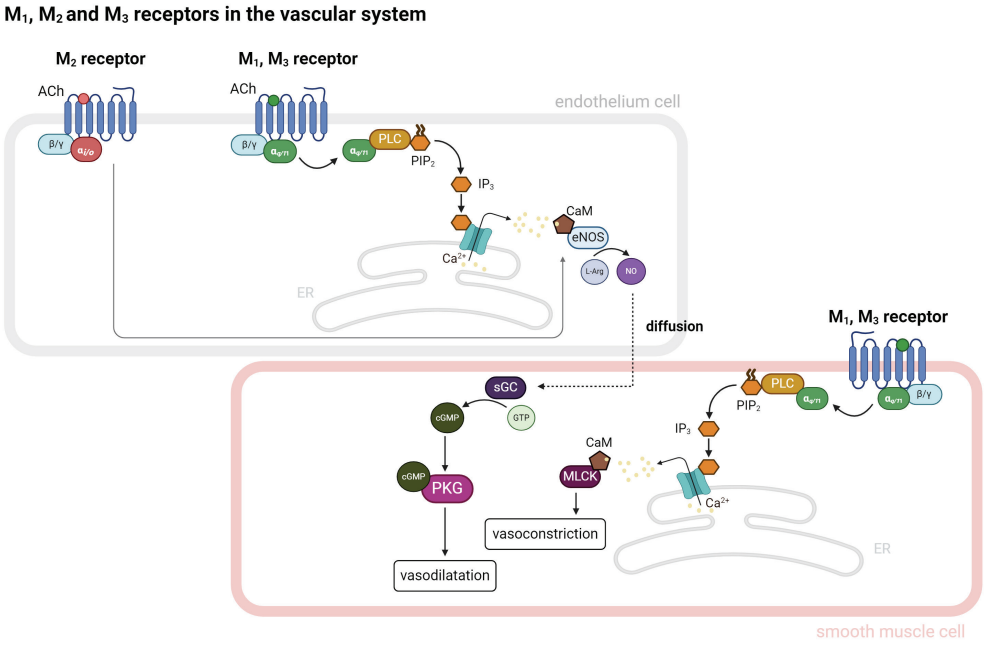

Fig. 3. Signaling of M_1, M_2 and M_3 receptors in the vascular system. In the vascular system, M_1, M_2 and M_3 receptors mediate vasodilation by release of NO from endotelium and cGMP-dependent removal of cytosolic calcium in smooth muscle cells, inhibiting the contractile apparatus and promoting vasodilation. Created with BioRender.com.

In ventricular myocytes stimulation of the M_2 receptor has been shown to modulate the cAMP-dependent response to β-adrenergic receptor activation (Fig. 2) [17]. Responses to activation of M_2 receptors are only observed in the presence of agonists that stimulate cAMP production. The activation of M_2 receptors inhibits AC5/6 *via* the $G_{i/o}$ α-subunits and stimulates AC4/7 *via* the βγ- subunits released from inhibitory $G_{i/o}$ G-proteins. Changes in cAMP affect targets of protein kinase A (PKA)-dependent phosphorylation such as L-type calcium channels. Altering L-type calcium channel activity plays an important role in the regulation of cardiac myocyte contractility. Changes in cAMP also directly regulate pacemaker channels, which are permeable to both Na^+ and K^+ [16]. Moreover, it was demonstrated that presynaptic M_2 receptors inhibit the release of sympathetic noradrenaline in mouse atria, effectively cross-regulating sympathetic tone [18].

In the vascular system, the muscarinic M_2 receptors are located specifically in the endothelium of the coronary vasculature from where they mediate endothelium-dependent vasodilation (Fig. 3) [19]. That is enacted through the release of NO from endothelium cells [20]. NO diffuses into the smooth muscle cell where it activates soluble guanylyl cyclase which converts GTP to cGMP. Cyclic GMP then activates cGMP-dependent protein kinase G, which results in the removal of cytosolic calcium, inhibiting the contractile apparatus and promoting vasodilation [21].

M_1 receptors

M_1 Muscarinic receptors are predominantly expressed in the CNS where they are involved in learning and memory [1]. However, the M_1 receptor has also been localized in numerous peripheral regions, including the cardiovascular system [22]. In the heart, the M_1 receptor is found in the cardiomyocytes of the human atria and ventricles [17,23]. The ACh gating of the inward-rectifier K+ channel is the main electrophysiological effector of vagal nerve stimulation in the atrium and contributes to atrial action potential duration shortening [24]. Although $G_{i/o}$ protein-coupled M_2 receptors are considered the predominant mediators of this process, it was shown that $G_{q/11}$-coupled M_1 receptors also participate in it (Fig. 4) [23].

Several experiments indicate that higher concentrations of muscarinic agonists than those needed for negative inotropy can induce opposite effects, including positive chronotropy and inotropy and prolonged duration of action potentials [11]. It was demonstrated using guinea pigs' ventricular cardiomyocytes that the M_1 receptors stimulate PLC and enhance the amplitude of the L-type calcium current, which may lead to a positive ionotropic effect, increase in heart rate and contractile force [25]. This effect was small and is elicited only by high concentrations of carbachol. The capability of the M_1 receptor to reverse depressed atrial contractility was demonstrated in the human myocardium [26]. It has been speculated that M_1 receptors in the human heart counterbalance the effects of M_2 receptors and might act as a limiting mechanism to prevent excessive suppression of cardiac activity [11].

The M_1 receptors have been reported to be distributed in the vasculature including arterial and venous smooth muscles and endothelium [27,28]. Overall, while stimulation of endothelial M_1 receptors leads to vasodilation, stimulation of M_1 receptors in smooth muscles leads to vasoconstriction. Many studies demonstrated that the M_1 receptors partially mediate ACh-induced vasodilation, which is dependent on the presence of an intact endothelium and the production of NO [14]. Moreover, it was demonstrated that M_1 may cause the endothelium-independent vasodilatation in rat mesenteric arteries that can be caused by the activation of M_1 receptors located on calcitonin gene-related peptide (CGRP)-containing neurons. The CGRP released from these neurons then acts at postsynaptic CGRP receptors on vascular smooth muscles causing the endothelium-independent vasodilation [28].

Although the principal effect of ACh in most vascular beds is endothelium-dependent vasodilatation, ACh can also produce direct vascular smooth muscle contraction. The M_1 receptors have been associated with vasoconstriction in several studies. For example, a study in guinea pig carotid arteries reported the M_1-mediated norepinephrine release, promoting constriction of the vascular tissue [29]. The dilation-constriction balance is influenced by vascular tone. In dilated arteries, the constrictor effect predominates. At high vascular tone, the vasodilatory response dominates [14].

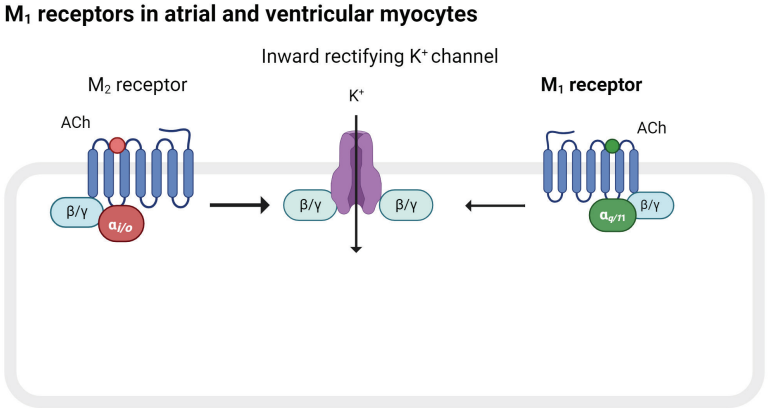

Fig. 4. Signaling of M_1 receptors in the heart. In the cardiomyocytes of the human heart M_1 receptors positively modulate inward-rectifier K^+ channel contributing to shortening of duration of atrial action potential duration. Created with BioRender.com

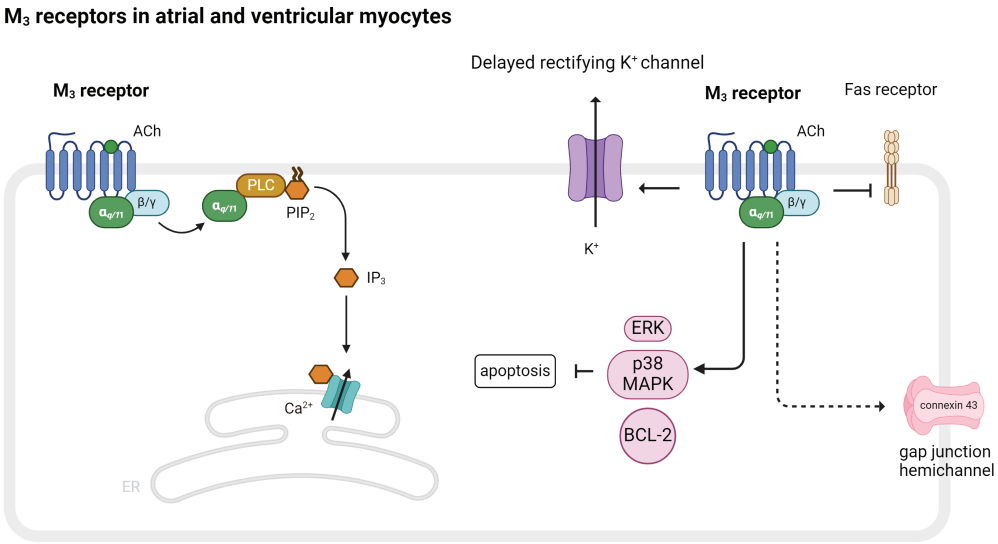

Fig. 5. Signaling of M_3 receptors in the heart. Through stimulation of intracellular phosphoinositide hydrolysis, M_3 receptors improve cardiac contraction. By the activation of a delayed rectifying K^+ current, M_3 receptors facilitate cardiac repolarization and exert negative chronotropic effects. Created with BioRender.com

M_3 receptors

The presence of muscarinic subtype M_3 was confirmed in both human atrial and ventricular tissues with 10-fold higher expression in ventricles [14]. Muscarinic M_3 receptors play an important role in the regulation and maintenance of cardiac function. M_3 receptors regulate intracellular phosphoinositide hydrolysis to improve cardiac contraction (Fig. 5). Through the activation of a delayed rectifying K^+ current M_3 receptors participate in cardiac repolarization and negative chronotropic actions. By activation of several antiapoptotic signaling molecules such as BCL-2 and ERKs, M_3 receptors enhance endogenous antioxidant capacity and reduce the apoptotic mediators (Fas and p38 MAPK) and Ca^{2+} overload resulting in cytoprotection [30,31]. Furthermore, M_3 receptors regulate the cell-to-cell communication *via* interaction with gap-junctional channel connexin 43. It was proposed that this interaction may be useful in coordinating the repolarization rates of the cardiomyocytes [32].

Muscarinic M_3 receptors are distributed throughout the vascular system in both endothelial cells and smooth muscle cells. Similarly to M_1 receptors, endothelial M_3 receptors mediate vasodilation and M_3 receptors in smooth muscles vasoconstriction. In several vascular beds, M_3 receptors have been shown to induce endothelium-dependent vasodilation, a process that, at least in part, is dependent on the release of NO [16]. It was suggested that in rat mesenteric arteries M_3 receptors mediate also endothelium-independent vasodilation [33]. Also in cats, activation of M_3 receptors in arteries with an intact endothelium leads to vasodilation, whereas activation of smooth muscles in the absence of endothelium induces vasoconstriction [34]. Furthermore, the experiments in bovine cerebral arteries reported M_3 receptor-mediated presynaptic inhibition of Ach and norepinephrine release, suggesting M_3 receptors regulate both vasoconstriction and vasodilation [35].

M_4 and M_5 receptors

Muscarinic receptors M_4 and M_5 appear to mediate the physiological function of ACh mainly in the central nervous system [1]. However, their presence was confirmed also in the cardiovascular system. Quantification of mRNA reported less than 1 % of the M_4 subtype and less than 5 % M_5 subtype of total muscarinic RNAs in the atria and ventricles [15]. Receptors that mediate muscarinic agonist-induced inhibition of high-voltage-activated Ca^{2+} channels in rat intracardiac neurons were identified as M_4 subtypes [36]. Although the function of $G_{i/o}$-coupled M_4 receptors overlaps with that of M_2 receptors, the role of M_4 facilitated bradycardia was not confirmed using M_4 knockout mice [37]. Some role for M_4 receptors in the control of K^+ channels was reported in canine atrial tissue [38].

RT-PCR experiments showed that M_5 receptor mRNA is present in several vascular tissues [39]. It was demonstrated that M_5 receptors mediate ACh-induced vasodilation in small cerebral blood vessels. A study on

M_5 KO mice demonstrated that outside of the cerebral vessels, M_5 does not appear to play a significant role in vasodilation [40].

Muscarinic receptors in the cardiovascular system in aging and disease

After heart failure, an increased sympathetic tone may help to preserve cardiac function initially, it may also contribute to cardiac remodeling. Hyperactivity of the sympathetic nervous system is coupled with decreased activation of the parasympathetic nervous system observed early after induction of cardiac remodeling [41]. In patients with chronic myocardial infarction, muscarinic receptors are upregulated in remote non-damaged ventricular regions, indicating compensatory mechanisms to cardiac remodeling, while the receptor density remains within normal values in myocardial regions containing damaged tissue [42]. The expression of M_2 receptors is also elevated as a response to chronic pain leading to atrial fibrillation [43]. The density of muscarinic receptors as well as parasympathetic activity drop with age, thus, their cardioprotective as well as pharmacotherapeutic potentials decline [44,45]. The non-neuronal cholinergic system is also found in human cardiomyocytes, which express choline acetyltransferase and the vesicular acetylcholine transporter, enzymes necessary for ACh synthesis and release. Experiments on transgenic mice suggest that a compensatory increase in cardiomyocyte acetylcholine levels may help offset cardiac remodeling in heart failure [46].

Muscarinic receptors in cardioprotection

The activation of muscarinic receptors has primarily calming effects on the cardiovascular system, including negative chronotropic and inotropic effects on heart and vasodilation, suggesting that vagal stimulation or muscarinic agonists and positive allosteric modulators may have cardioprotective properties.

Indeed, vagal stimulation performed intermittently antagonized the sympathetic system and reduced the infarct size [47]. Activation of efferent parasympathetic nerves is involved in remote ischemic preconditioning that was lost after sectioning of the vagus nerves and after administration of atropine [48]. During ischemia-reperfusion injury, both continuous vagus nerve stimulation and intermittent vagus nerve stimulation provide significant cardioprotective effects. These beneficial effects were abolished by muscarinic blockade, suggesting the importance of muscarinic receptor modulation during vagus nerve stimulation. The protective effects of vagus nerve stimulation could be due to its protection of mitochondrial function during ischemia-reperfusion [49]. Thus, vagal stimulation may be an intervention used for treating cardiovascular diseases.

The beneficial effects of muscarinic agonists were observed very early. Cholinergic agonists and cyclic GMP can prevent ventricular fibrillation in susceptible animals independently of heart rate changes [50]. Furthermore, the muscarinic agonist oxotremorine reduced the incidence of malignant arrhythmias resulting from transient ischemia and sympathetic hyperactivity. The extent of this protection was comparable to the administration of β_2-adrenergic antagonist propranolol in this same animal model. The effect appears to be only partially dependent on the reduction in heart rate because it was observed even after the correction of heart rate by atrial pacing [51]. The antifibrillatory effects obtained without the marked reduction in myocardial contractility during acute ischemia, including administration of β-blockers in individuals with myocardial infarctions, are of special interest. Muscarinic agonists may therefore represent a new approach to the prevention of sudden cardiac death.

The data on cardioprotective effects of muscarinic agonists are overwhelming and provide detailed mechanistic views. Ischemia induces the production of the cytokine tumour necrosis factor-α (TNF-α) and reactive oxygen species (ROS) in a time-dependent manner. ACh is capable of inhibiting ischemia-induced TNF-α production, ROS generation, and cell death through the M_2 receptor and mitogen-activated protein kinases (MAPKs) [52]. The activation of M_2 receptors in *ex vivo* rat hearts leads to an increase in the activity of ERK1/2 and PI3K/Akt kinases that inhibit endoplasmic reticulum-induced stress leading to cell apoptosis that in turn contributes to a reduction in infarct size and attenuation of myocardial injury [53]. Moreover, ACh induced cytoprotective mitophagy by enhancing PINK1/Parkin translocation to mitochondria in an M_2 receptor-dependent manner in H9c2 cardio-myocytes [54].

Basal and acetylcholine-gated inward-rectifier K^+-currents ($I_{K,ACh}$), which play a significant role in atrial repolarization are upregulated in chronic atrial

fibrillation. Not only M_2 receptors are involved in the cardioprotective effects of muscarinic agonists mediated by $I_{K,ACh}$. In human atrial cardiomyocytes, $G_{q/11}$ proteins activated by M_1-receptors act as donors of βγ-dimers that activate $I_{K,ACh}$. Their relative contribution to $I_{K,ACh}$ activation is increased in chronic atrial fibrillation patients [23].

M_3 receptors play a substantial role also in cardioprotection, including regulation of heart rate and cardiac repolarization, modulation of inotropic effects, cytoprotection against ischaemic injuries of the myocardium, regulation of cell-to-cell communication, and generation and maintenance of atrial fibrillation. Signal transduction mechanisms underlying these functions involve activation of an $I_{K,ACh}$ participating in cardiac repolarization, negative chronotropic actions, and anti-arrhythmic as well as pro-arrhythmic actions, interaction with gap-junctional channel connexin 43 to maintain cell-cell communication and excitation propagation, regulation of intracellular phosphoinositide hydrolysis to improve cardiac contraction and haemodynamic function, activation of anti-apoptotic signaling molecules, enhancing endogenous antioxidant capacity, and diminishing intracellular Ca^{2+} overload, all of which contribute to protection of the heart against ischemic injuries [31].

Specifically, the overexpression of M_3 receptors reduced the incidence of arrhythmias and mortality after myocardial infarction and reperfusion by protecting the myocardium from ischemia in mice. This effect was mediated by increasing the $I_{K,ACh}$ currents by downregulation of expression of microRNA-1 (a single-stranded 22 nucleotides long noncoding RNA) that causes arrhythmia [55]. Also, the upregulation of M_3 receptors during myocardial hypertrophy could alleviate the hypertrophic response induced by angiotensin II by the mechanism involving the inhibition of MAPK signaling through the downregulation of the AT_1-angiotensin receptor [56]. Activation of M_3 receptors overall improves cardiac function and reduces ischemic myocardial injuries by multiple signaling pathways leading to cytoprotection [57], inhibits cardiac fibroblast proliferation and collagen secretion by TGF-β1/Smad and p38MAPK pathways [58], and exerts protective effects against ischemia-induced arrhythmias in the rat by a reduction of intracellular Ca^{2+} overload *via* downregulation of L-type Ca^{2+} channels [59]. Activation of M_3 receptors 24 hours before an ischemic insult induced delayed preconditioning in rats, preserving phosphorylated connexin 43, which might contribute to the anti-arrhythmic effect, and reduce the infarct size induced by infarction-reperfusion by up-regulation of cyclooxygenase-2 [60].

The alternative to vagal stimulation and muscarinic agonists in cardioprotection may be positive allosteric modulation of acetylcholine binding and/or functional response. Such compounds increase the cardioprotective effects of endogenous acetylcholine, primarily sympathetic tone but also non-neuronal acetylcholine. Among the major advantages of allosteric modulators are the conservation of the time-space pattern of signaling and defiance of overdose. Positive allosteric modulators of acetylcholine at M_2 receptor as well as other subtypes were identified [61–63]. A recent study has shown that phosphorylation of cardiac ryanodine receptor 2 by protein kinase G, contributing to the cardioprotective effects of cholinergic stimulation, may be enhanced by the allosteric modulator LY2119620 [64].

The sex hormone estrogen has received increased attention for its ability to exert cardioprotective effects against atherosclerosis, but it has become clear that estrogen also exerts a direct protective effect against ischemia-reperfusion injury on the myocardium [65]. Estrogen cardioprotective effects are due to rapid nongenomic actions. Estrogen binds to membrane estrogen receptors (mERs). The mERs are a group of receptors activating various signaling pathways including tyrosine kinases and protein kinases PI3K, Akt, MAPK, Src, PKA and PKC, and phospholipase C increasing the concentration of intracellular calcium [66]. Several steroid compounds positively affected heart function, exerting positive inotropic activity *via* Na^+,K^+ ATPase [67] or L-type Ca^{2+} channels [68]. In the search for novel steroid derivatives with biological activity on heart failure, two steroid derivates acting *via* M_2 receptors were synthesized [69]. Current research indicates that the fast non-genomic effects of steroids mediated by muscarinic receptors are due to their allosteric modulation of muscarinic receptors [70,71]. Thus, steroid-based positive allosteric modulators of muscarinic receptors, primarily the M_2 subtype, represent a novel class of cardioprotective compounds. However, this concept has been only little explored so far.

Conclusions

The cardinal role of muscarinic receptors in cardioprotection is well established. Along with that,

muscarinic agonists and vagal stimulation are considered as viable cardioprotective treatments. In contrast, positive allosteric modulation of muscarinic receptors as an alternative or supplementary therapeutic approach is very little researched up to now, deserving attention and exploration.

Conflict of Interest

There is no conflict of interest.

Acknowledgements

This research was supported by the project National Institute for Neurology Research (Programme EXCELES, ID Project No. LX22NPO5107) - Funded by the European Union – Next Generation EU; Supported by the project National Institute for Research of Metabolic and Cardiovascular Diseases (Programme EXCELES, LX22NPO5104) - funded by the European Union - Next Generation EU; and supported by the Institutional support of Czech Academy of Sciences RVO:67985823.

Abbreviations

Ach, acetylcholine; AC, adenylyl cyclase; CNS, central nervous system; $I_{K,Ach}$, acetylcholine-gated inward-rectifier K^+-currents; IP_3, 1,4,5-inosito trisphosphate; MAPK, mitogen-activated protein kinase; PKA, protein kinase A; PKC, protein kinase C; PLC, phospholipase C; ROS, reactive oxygen species

References

1. Eglen RM. Overview of muscarinic receptor subtypes. In: Fryer AD, Arthur Christopoulos, Nathanson NM (eds) Handb Exp Pharmacol. Springer, Berlin Heidelberg, Gemany, pp 3-28. https://doi.org/10.1007/978-3-642-23274-9_1
2. Logothetis DE, Kurachi Y, Galper J, Neer EJ, Clapham DE. The beta gamma subunits of GTP-binding proteins activate the muscarinic K+ channel in heart. Nature 1987;325:321-326. https://doi.org/10.1038/325321a0
3. Ikeda SR. Voltage-dependent modulation of N-type calcium channels by G-protein beta gamma subunits. Nature 1996; 380:255-258. https://doi.org/10.1038/380255a0
4. Nunan D, Sandercock GRH, Brodie DA. A quantitative systematic review of normal values for short-term heart rate variability in healthy adults. Pacing Clin Electrophysiol 2010; 33:1407-1417. https://doi.org/10.1111/j.1540-8159.2010.02841.x
5. Howland RH. Vagus Nerve Stimulation. Curr Behav Neurosci Rep 2014; 1:64-73. https://doi.org/10.1007/s40473-014-0010-5
6. Triposkiadis F, Karayannis G, Giamouzis G, Skoularigis J, Louridas G, Butler J. The sympathetic nervous system in heart failure physiology, pathophysiology, and clinical implications. J Am Coll Cardiol 2009; 54:1747-762. https://doi.org/10.1016/j.jacc.2009.05.015
7. Wessler I, Kirkpatrick CJ, Racké K. Non-neuronal acetylcholine, a locally acting molecule, widely distributed in biological systems: expression and function in humans. Pharmacol Ther 1998; 77:59-79. https://doi.org/10.1016/S0163-7258(97)00085-5
8. Elhusseiny A, Cohen Z, Olivier A, Stanimirović DB, Hamel E. Functional acetylcholine muscarinic receptor subtypes in human brain microcirculation: identification and cellular localization. J Cereb Blood Flow Metab 1999; 19:794-802. https://doi.org/10.1097/00004647-199907000-00010
9. Kakinuma Y. Future perspectives of a cardiac non-neuronal acetylcholine system targeting cardiovascular diseases as an adjunctive tool for metabolic intervention. Int Immunopharmacol 2015; 29:185-188. https://doi.org/10.1016/j.intimp.2015.05.029
10. Hartzell HC. Regulation of cardiac ion channels by catecholamines, acetylcholine and second messenger systems. Prog Biophys Mol Biol 1988; 52:165-247. https://doi.org/10.1016/0079-6107(88)90014-4
11. Pappano AJ, Mubagwa K. Muscarinic agonist-induced actions on potassium and calcium channels in atrial myocytes: differential desensitization. Eur Heart J 1991; 12 Suppl F:70-75. https://doi.org/10.1093/eurheartj/12.suppl_F.70
12. Peralta EG, Ashkenazi A, Winslow JW, Smith DH, Ramachandran J, Capon DJ. Distinct primary structures, ligand-binding properties and tissue-specific expression of four human muscarinic acetylcholine receptors. EMBO J 1987; 6:3923-3929. https://doi.org/10.1002/j.1460-2075.1987.tb02733.x

13. Caulfield MP. Muscarinic receptors--characterization, coupling and function. Pharmacol Ther 1993; 58:319-79. https://doi.org/10.1016/0163-7258(93)90027-B
14. Saternos HC, Almarghalani DA, Gibson HM, Meqdad MA, Antypas RB, Lingireddy A, et al. Distribution and function of the muscarinic receptor subtypes in the cardiovascular system. Physiol Genomics 2018; 50:1-9. https://doi.org/10.1152/physiolgenomics.00062.2017
15. Krejčí A, Tuček S. Quantitation of mRNAs for M 1 to M 5 Subtypes of Muscarinic Receptors in Rat Heart and Brain Cortex. Mol Pharmacol 2002; 61:1267-1272. https://doi.org/10.1124/mol.61.6.1267
16. Harvey RD. Muscarinic receptor agonists and antagonists: effects on cardiovascular function. Handb Exp Pharmacol 2012; 299-316. https://doi.org/10.1007/978-3-642-23274-9_13
17. Brodde OE, Michel MC. Adrenergic and muscarinic receptors in the human heart. Pharmacol Rev 1999; 51:651-690.
18. Trendelenburg A-U, Gomeza J, Klebroff W, Zhou H, Wess J Heterogeneity of presynaptic muscarinic receptors mediating inhibition of sympathetic transmitter release: a study with M2- and M4-receptor-deficient mice. Br J Pharmacol 2003; 138:469-480. https://doi.org/10.1038/sj.bjp.0705053.
19. Vanhoutte PM, Cohen RA. Effects of acetylcholine on the coronary artery. Fed Proc 1984; 43:2878-2880.
20. Lefroy DC, Crake T, Uren NG, Davies GJ, Maseri A. Effect of inhibition of nitric oxide synthesis on epicardial coronary artery caliber and coronary blood flow in humans. Circulation 1993; 88:43-54. https://doi.org/10.1161/01.CIR.88.1.43
21. Palmer RM, Ferrige AG, Moncada S. Nitric oxide release accounts for the biological activity of endothelium-derived relaxing factor. Nature 1987; 327:524-526. https://doi.org/10.1038/327524a0
22. Myslivecek J, Klein M, Novakova M, Ricny J. The detection of the non-M2 muscarinic receptor subtype in the rat heart atria and ventricles. Naunyn Schmiedebergs Arch Pharmacol 2008; 378:103-116. https://doi.org/10.1007/s00210-008-0285-8
23. Heijman J, Kirchner D, Kunze F, Chrétien EM, Michel-Reher MB, Voigt N, et al. Muscarinic type-1 receptors contribute to IK,ACh in human atrial cardiomyocytes and are upregulated in patients with chronic atrial fibrillation. Int J Cardiol 2018; 255:61-68. https://doi.org/10.1016/j.ijcard.2017.12.050
24. Kovoor P, Wickman K, Maguire CT, Pu W, Gehrmann J, Berul CI, et al. Evaluation of the role of I(KACh) in atrial fibrillation using a mouse knockout model. J Am Coll Cardiol 2001; 37:2136-43. https://doi.org/10.1016/S0735-1097(01)01304-3
25. Gallo MP, Alloatti G, Eva C, Oberto A, Levi RC. M1 muscarinic receptors increase calcium current and phosphoinositide turnover in guinea-pig ventricular cardiocytes. J Physiol 1993; 471:41-60. https://doi.org/10.1113/jphysiol.1993.sp019890
26. Du XY, Schoemaker RG, Bos E, Saxena PR. Characterization of the positive and negative inotropic effects of acetylcholine in the human myocardium. Eur J Pharmacol 1995; 284:119-127. https://doi.org/10.1016/0014-2999(95)00384-W
27. Walch L, Gascard JP, Dulmet E, Brink C, Norel X. Evidence for a M(1) muscarinic receptor on the endothelium of human pulmonary veins. Br J Pharmacol 2000; 130:73-78. https://doi.org/10.1038/sj.bjp.0703301
28. Tangsucharit P, Takatori S, Zamami Y, Goda M, Pakdeechote P, Kawasaki H, et al. Muscarinic acetylcholine receptor M1 and M3 subtypes mediate acetylcholine-induced endothelium-independent vasodilatation in rat mesenteric arteries. J Pharmacol Sci 2016; 130:24-32. https://doi.org/10.1016/j.jphs.2015.12.005
29. Casado MA, Marín J, Salaices M. Evidence for M1 muscarinic cholinoceptors mediating facilitation of noradrenaline release in guinea-pig carotid artery. Naunyn Schmiedebergs Arch Pharmacol 1992; 346:391-394. https://doi.org/10.1007/BF00171079
30. Yang B, Lin H, Xu C, Liu Y, Wang H, Han H, et al. Choline produces cytoprotective effects against ischemic myocardial injuries: evidence for the role of cardiac m3 subtype muscarinic acetylcholine receptors. Cell Physiol Biochem 2005; 16:163-174. https://doi.org/10.1159/000089842
31. Wang H, Lu Y, Wang Z. Function of cardiac M3 receptors. Auton Autacoid Pharmacol 2007; 27:1-11. https://doi.org/10.1111/j.1474-8673.2006.00381.x

32. Yue P, Zhang Y, Du Z, Xiao J, Pan Z, Wang N, et al. Ischemia impairs the association between connexin 43 and M3 subtype of acetylcholine muscarinic receptor (M3-mAChR) in ventricular myocytes. Cell Physiol Biochem 2006; 17:129-136. https://doi.org/10.1159/000092074
33. From the American Association of Neurological Surgeons (AANS), American Society of Neuroradiology (ASNR), Cardiovascular and Interventional Radiology Society of Europe (CIRSE), Canadian Interventional Radiology Association (CIRA), Congress of Neurological and WSO (WSO), Sacks D, Baxter B, Campbell BC V, Carpenter JS, Cognard C, et al Multisociety Consensus Quality Improvement Revised Consensus Statement for Endovascular Therapy of Acute Ischemic Stroke. Int J Stroke 2018; 13:612-632. https://doi.org/10.1177/1747493018778713
34. Dauphin F, Hamel E. Muscarinic receptor subtype mediating vasodilation feline middle cerebral artery exhibits M3 pharmacology. Eur J Pharmacol 1990; 178:203-213. https://doi.org/10.1016/0014-2999(90)90476-M
35. Ferrer M, Galván R, Marín J, Balfagón G. Presynaptic muscarinic receptor subtypes involved in the inhibition of acetylcholine and noradrenaline release in bovine cerebral arteries. Naunyn Schmiedebergs Arch Pharmacol 1992; 345:619-626. https://doi.org/10.1007/BF00164574
36. Cuevas J, Adams DJ. M4 muscarinic receptor activation modulates calcium channel currents in rat intracardiac neurons. J Neurophysiol 1997; 78:1903-12. https://doi.org/10.1152/jn.1997.78.4.1903
37. Stengel PW, Gomeza J, Wess J, Cohen ML. M(2) and M(4) receptor knockout mice: muscarinic receptor function in cardiac and smooth muscle in vitro. J Pharmacol Exp Ther 2000; 292:877-885.
38. Yeh Y-H, Qi X, Shiroshita-Takeshita A, Liu J, Maguy A, Chartier D, et al. Atrial tachycardia induces remodelling of muscarinic receptors and their coupled potassium currents in canine left atrial and pulmonary vein cardiomyocytes. Br J Pharmacol 2007; 152:1021-1032. https://doi.org/10.1038/sj.bjp.0707376
39. Phillips JK, Vidovic M, Hill CE. Variation in mRNA expression of alpha-adrenergic, neurokinin and muscarinic receptors amongst four arteries of the rat. J Auton Nerv Syst 1997; 62:85-93. https://doi.org/10.1016/S0165-1838(96)00114-2
40. Yamada M, Lamping KG, Duttaroy A, Zhang W, Cui Y, Bymaster FP, et al. Cholinergic dilation of cerebral blood vessels is abolished in M(5) muscarinic acetylcholine receptor knockout mice. Proc Natl Acad Sci U S A 2001; 98:14096-14101. https://doi.org/10.1073/pnas.251542998
41. Binkley PF, Nunziata E, Haas GJ, Nelson SD, Cody RJ. Parasympathetic withdrawal is an integral component of autonomic imbalance in congestive heart failure: demonstration in human subjects and verification in a paced canine model of ventricular failure. J Am Coll Cardiol 1991; 18:464-472. https://doi.org/10.1016/0735-1097(91)90602-6
42. Mazzadi AN, Pineau J, Costes N, Le Bars D, Bonnefoi F, Croisille P, et al. Muscarinic receptor upregulation in patients with myocardial infarction: a new paradigm. Circ Cardiovasc Imaging 2009; 2:365-72. https://doi.org/10.1161/CIRCIMAGING.108.822106
43. Gong C, Ding Y, Liang F, Wu S, Tang X, Ding H, et al. Muscarinic receptor regulation of chronic pain-induced atrial fibrillation. Front Cardiovasc Med 2022; 9:934906. https://doi.org/10.3389/fcvm.2022.934906
44. Brodde OE, Konschak U, Becker K, Rüter F, Poller U, Jakubetz J, et al. Cardiac muscarinic receptors decrease with age. In vitro and in vivo studies. J Clin Invest 1998; 101:471-478. https://doi.org/10.1172/JCI1113
45. Dhein S, van Koppen CJ, Brodde OE. Muscarinic receptors in the mammalian heart. Pharmacol Res 2001; 44:161-82. https://doi.org/10.1006/phrs.2001.0835
46. Roy A, Dakroub M, Tezini GCS V, Liu Y, Guatimosim S, Feng Q, et al. Cardiac acetylcholine inhibits ventricular remodeling and dysfunction under pathologic conditions. FASEB J 2016; 30:688-701. https://doi.org/10.1096/fj.15-277046
47. Buchholz B, Donato M, Perez V, Deutsch ACR, Höcht C, Del Mauro JS, et al. Changes in the loading conditions induced by vagal stimulation modify the myocardial infarct size through sympathetic-parasympathetic interactions. Pflugers Arch 2015; 467:1509-1522. https://doi.org/10.1007/s00424-014-1591-2
48. Donato M, Buchholz B, Rodríguez M, Pérez V, Inserte J, García-Dorado D, et al. Role of the parasympathetic nervous system in cardioprotection by remote hindlimb ischaemic preconditioning. Exp Physiol 2013; 98:425-434. https://doi.org/10.1113/expphysiol.2012.066217

49. Shinlapawittayatorn K, Chinda K, Palee S, Surinkaew S, Thunsiri K, Weerateerangkul P, et al. Low-amplitude, left vagus nerve stimulation significantly attenuates ventricular dysfunction and infarct size through prevention of mitochondrial dysfunction during acute ischemia-reperfusion injury. Heart Rhythm 2013; 10:1700-7. https://doi.org/10.1016/j.hrthm.2013.08.009
50. Billman GE. Effect of carbachol and cyclic GMP on susceptibility to ventricular fibrillation. FASEB J 1990; 4:1668-1673. https://doi.org/10.1096/fasebj.4.6.2156744
51. De Ferrari GM, Vanoli E, Curcuruto P, Tommasini G, Schwartz PJ. Prevention of life-threatening arrhythmias by pharmacologic stimulation of the muscarinic receptors with oxotremorine. Am Heart J 1992; 124:883-890. https://doi.org/10.1016/0002-8703(92)90968-2
52. Li D-L, Liu J-J, Liu B-H, Hu H, Sun L, Miao Y, et al. Acetylcholine inhibits hypoxia-induced tumor necrosis factor-α production via regulation of MAPKs phosphorylation in cardiomyocytes. J Cell Physiol 2011; 226:1052-1059. https://doi.org/10.1002/jcp.22424
53. Liao F, Zheng Y, Cai J, Fan J, Wang J, Yang J, et al. Catestatin attenuates endoplasmic reticulum induced cell apoptosis by activation type 2 muscarinic acetylcholine receptor in cardiac ischemia/reperfusion. Sci Rep 2015; 5:16590. https://doi.org/10.1038/srep16590
54. Sun L, Zhao M, Yang Y, Xue R-Q, Yu X-J, Liu J-K, et al. Acetylcholine Attenuates Hypoxia/Reoxygenation Injury by Inducing Mitophagy Through PINK1/Parkin Signal Pathway in H9c2 Cells. J Cell Physiol 2016; 231:1171-1181. https://doi.org/10.1002/jcp.25215
55. Liu Y, Sun L, Pan Z, Bai Y, Wang N, Zhao J, et al. Overexpression of M_3 muscarinic receptor is a novel strategy for preventing sudden cardiac death in transgenic mice. Mol Med 2011; 17:1179-1187. https://doi.org/10.2119/molmed.2011.00093
56. Liu Y, Wang S, Wang C, Song H, Han H, Hang P, et al. Upregulation of M_3 muscarinic receptor inhibits cardiac hypertrophy induced by angiotensin II. J Transl Med 2013; 11:209. https://doi.org/10.1186/1479-5876-11-209
57. Yang B, Lin H, Xu C, Liu Y, Wang H, Han H, et al Choline produces cytoprotective effects against ischemic myocardial injuries: evidence for the role of cardiac m3 subtype muscarinic acetylcholine receptors. Cell Physiol Biochem 2005; 16:163-174. https://doi.org/10.1159/000089842
58. Zhao L, Chen T, Hang P, Li W, Guo J, Pan Y, et al. Choline attenuates cardiac fibrosis by inhibiting p38MAPK signaling possibly by acting on M3 muscarinic acetylcholine receptor. Front Pharmacol 2019; 10:1386. https://doi.org/10.3389/fphar.2019.01386
59. Wang S, Han H-M, Jiang Y-N, Wang C, Song H-X, Pan Z-Y, et al. Activation of cardiac M3 muscarinic acetylcholine receptors has cardioprotective effects against ischaemia-induced arrhythmias. Clin Exp Pharmacol Physiol 2012; 39:343-349. https://doi.org/10.1111/j.1440-1681.2012.05672.x
60. Zhao J, Su Y, Zhang Y, Pan Z, Yang L, Chen X, et al. Activation of cardiac muscarinic M3 receptors induces delayed cardioprotection by preserving phosphorylated connexin43 and up-regulating cyclooxygenase-2 expression. Br J Pharmacol 2010; 159:1217-1225. https://doi.org/10.1111/j.1476-5381.2009.00606.x
61. Jakubík J, Bacáková L, El-Fakahany EsamE, Tucek S. Positive cooperativity of acetylcholine and other agonists with allosteric ligands on muscarinic acetylcholine receptors. Mol Pharmacol 1997; 52:172-179. https://doi.org/10.1124/mol.52.1.172
62. Croy CH, Schober DA, Xiao H, Quets A, Christopoulos A, Felder CC. Characterization of the novel positive allosteric modulator, LY2119620, at the muscarinic M(2) and M(4) receptors. Mol Pharmacol 2014; 86:106-115. https://doi.org/10.1124/mol.114.091751
63. Jakubik J, El-Fakahany EE. Current advances in allosteric modulation of muscarinic receptors. Biomolecules 2020; 10:325. https://doi.org/10.3390/biom10020325
64. Baine S, Thomas J, Bonilla I, Ivanova M, Belevych A, Li J, et al. Muscarinic-dependent phosphorylation of the cardiac ryanodine receptor by protein kinase G is mediated by PI3K-AKT-nNOS signaling. J Biol Chem 2020; 295:11720-11728. https://doi.org/10.1074/jbc.RA120.014054
65. Moolman JA. Unravelling the cardioprotective mechanism of action of estrogens. Cardiovasc Res 2006; 69:777-80. https://doi.org/10.1016/j.cardiores.2006.01.001
66. Manavathi B, Kumar R. Steering estrogen signals from the plasma membrane to the nucleus: two sides of the coin. J Cell Physiol 2006; 207:594-604. https://doi.org/10.1002/jcp.20551

67. De Munari S, Cerri A, Gobbini M, Almirante N, Banfi L, Carzana G, et al. Structure-based design and synthesis of novel potent Na+,K+ -ATPase inhibitors derived from a 5alpha,14alpha-androstane scaffold as positive inotropic compounds. J Med Chem 2003; 46:3644-54. https://doi.org/10.1021/jm030830y
68. Pignier C, Keller M, Vié B, Vacher B, Santelli M, Niggli E, et al. A novel steroid-like compound F90927 exerting positive-inotropic effects in cardiac muscle. Br J Pharmacol 2006; 147:772-82. https://doi.org/10.1038/sj.bjp.0706673
69. Lauro F-V, Maria L-R, Tomas L-G, Francisco DC, Rolando G-M, Marcela R-N, et al. Design and synthesis of two new steroid derivatives with biological activity on heart failure via the M2-muscarinic receptor activation. Steroids 2020; 158:108620. https://doi.org/10.1016/j.steroids.2020.108620
70. Dolejší E, Szánti-Pintér E, Chetverikov N, Nelic D, Randáková A, Doležal V, et al Neurosteroids and steroid hormones are allosteric modulators of muscarinic receptors. Neuropharmacology 2021; 199:108798. https://doi.org/10.1016/j.neuropharm.2021.108798
71. Dolejší E, Chetverikov N, Szánti-Pintér E, Nelic D, Randáková A, Doležal V, et al Neuroactive steroids, WIN-compounds and cholesterol share a common binding site on muscarinic acetylcholine receptors. Biochem Pharmacol 2021; 192:114699. https://doi.org/10.1016/j.bcp.2021.114699

Physiol. Res. 73 (Suppl. 1): S401-S412, 2024 *https://doi.org/10.33549/physiolres.935306*

REVIEW

Look for the Scaffold: Multifaceted Regulation of Enzyme Activity by 14-3-3 Proteins

Veronika OBSILOVA[1], Tomas OBSIL[1,2]

[1]Laboratory of Structural Biology of Signaling Proteins, Institute of Physiology of the Czech Academy of Sciences, Division BIOCEV, Vestec, Czech Republic, [2]Department of Physical and Macromolecular Chemistry, Faculty of Science, Charles University, Prague, Czech Republic

Received December 19, 2023
Accepted January 31, 2024

Summary

Enzyme activity is regulated by several mechanisms, including phosphorylation. Phosphorylation is a key signal transduction process in all eukaryotic cells and is thus crucial for virtually all cellular processes. In addition to its direct effect on protein structure, phosphorylation also affects protein-protein interactions, such as binding to scaffolding 14-3-3 proteins, which selectively recognize phosphorylated motifs. These interactions then modulate the catalytic activity, cellular localisation and interactions of phosphorylated enzymes through different mechanisms. The aim of this mini-review is to highlight several examples of 14-3-3 protein-dependent mechanisms of enzyme regulation previously studied in our laboratory over the past decade. More specifically, we address here the regulation of the human enzymes ubiquitin ligase Nedd4-2, procaspase-2, calcium-calmodulin dependent kinases CaMKK1/2, and death-associated protein kinase 2 (DAPK2) and yeast neutral trehalase Nth1.

Key words

14-3-3 protein • Scaffold • Enzyme • Kinase • Procaspase-2 • Nedd4-2 • CaMKK2 • DAPK2

Corresponding authors

V. Obsilova and T. Obsil, Institute of Physiology of the Czech Academy of Sciences, Laboratory of Structural Biology of Signaling Proteins, Division BIOCEV, Prumyslova 595, 252 50 Vestec, Czech Republic. E-mail: veronika.obsilova@fgu.cas.cz or obsil@natur.cuni.cz

Introduction

Scaffold proteins are major regulators of many signalling pathways, playing a key role in cell biology. These proteins form platforms that facilitate the assembly of protein complexes, re-localisation of signalling molecules, and coordination of positive or negative feedback signals and ensure the correct course of signalling pathways. The first scaffold protein discovered was the yeast MAPK scaffold Ste5, which helps to link multiple protein kinases in the MAP kinase cascade in *S. cerevisiae* [1]. Binding of the scaffold molecule to the target protein is often facilitated by various stimuli, one of which is phosphorylation, the most prevalent post-translational modification in eukaryotes [2]. Protein phosphorylation occurs mostly on the side chains of serine, threonine and tyrosine residues, and the introduction of a negatively charged phosphate group then directly affects the structure of the protein and/or mediates new interactions, often through scaffold domains or proteins that specifically recognize phosphorylated motifs. Such proteins/domains include, among others, 14-3-3 proteins, WW, Polo-box, WD-40, leucine-rich repeats, BRCT and FHA domains [3].

14-3-3 proteins were discovered through studies on the phosphorylation-dependent regulation of tryptophan hydroxylase and Raf kinase [4-9]. 14-3-3 proteins are a family of highly evolutionarily conserved 30 kDa acidic proteins abundantly expressed in all eukaryotes, often in multiple isoforms, which form homo- and heterodimers [10-13]. In humans,

seven 14-3-3 protein isoforms denoted by the Greek letters (β, γ, ε, ζ, η, σ and τ) were identified. Numerous structural studies have shown that the 14-3-3 dimer adopts a rigid cup-shaped structure capable of accommodating two phosphorylated segments of the target protein(s) [8,14-17]. 14-3-3 binding motifs are often found in disordered regions of target proteins and bordering structured domains. Moreover, the affinity of the interaction between 14-3-3s and a particular phosphorylated motif appears to be strictly influenced by the sequence surrounding the phosphoresidue [18-20].

Three canonical 14-3-3 binding motifs have been described thus far: R[S/Φ][+](pS/pT)XP (mode I), RX[S/Φ][+](pS/pT)XP (mode II) and (pS/pT)X_{1-2}-COOH (mode III), where Φ means any hydrophobic amino acid and X means any amino acid [8,17,21]. However, the motifs of many well-characterised 14-3-3 binding partners deviate significantly from these canonical motifs. In fact, 14-3-3 proteins have also been shown to recognize unphosphorylated or glycosylated motifs (reviewed in [13]). Recently, 14-3-3 protein have also been shown to target viral proteins, such as N protein from SARS-CoV-2, as demonstrated by crystal structure and SAXS-based analysis [22-24]. This, together with the involvement of 14-3-3 proteins in the regulation of a number of other pathophysiological processes, suggests that 14-3-3 proteins are a promising drug target.

Thanks to advances in structural studies of 14-3-3 protein complexes, we now have a much better understanding of how these scaffolds regulate their binding partners. The mechanisms of these regulations can be divided into three basic modes: (1) direct conformational change of the target protein; (2) partial masking of the surface of the target protein; and (3) scaffolding facilitating the interaction between two proteins, as previously reviewed in [11-13,25-28]. In some cases, the regulatory mechanism is based on a combination of different modes. This mini-review focuses on mechanisms of 14-3-3-medited regulation of several enzymes recently studied in our research groups: (i) the yeast neutral trehalase Nth1; (ii) the ubiquitin ligase Nedd4-2; (iii) procaspase-2; (iv) death-associated protein kinase 2 (DAPK2); and (v) calcium-calmodulin dependent kinases (CaMKK).

14-3-3 protein complexes are often highly conformationally flexible and heterogeneous. For this reason, we use hybrid approaches to study these complexes, combining several structural biology methods such as protein crystallography, NMR, small-angle X-ray scattering (SAXS), chemical crosslinking and H/D exchange. While Nth1 activation and Nedd4-2 modulation exemplify mode 1 (direct structural change), caspase-2 activation inhibition is an example of mode 2 (masking of surfaces important for the localisation and activation of the enzyme). The protein kinases CaMKK and DAPK2 are inhibited similarly, with 14-3-3 proteins masking their key regulatory phosphorylation sites, the calmodulin binding site and the access to the catalytic center. In addition, 14-3-3 proteins further contribute to DAPK2 inhibition by stabilizing its dimerization, i.e., *via* regulatory mode 3.

Allosteric activation of yeast neutral trehalase Nth1

The main function of the neutral trehalase 1 (Nth1) from *Saccharomyces cerevisiae* is the hydrolysis of trehalose (α-D-glucopyranosyl-(1-1)-α-D-glucopyranoside) into two glucose molecules, which helps the yeast survive adverse conditions such as heat shock, starvation or oxidative stress [29-32]. Nth1 has two structured domains: a calcium-binding domain containing an EF-hand-like motif and a catalytic trehalase domain, which is responsible for the enzymatic activity. In addition, the unique N-terminal extension of Nth1, present only in the yeast trehalases, contains five serine residues whose phosphorylation by cAMP-dependent protein kinase (PKA) or by cyclin-dependent kinase 1 (Cdk1) generates 14-3-3 binding motifs [33-36]. The catalytic activity of Nth1 is entirely controlled by phosphorylation-dependent 14-3-3 (in yeast Bmh1/2) protein binding, with Ca^{2+} binding playing a modulatory role [34-39]. This regulatory mechanism has been shown to be common to yeast neutral trehalases from both budding yeast, such as *Saccharomyces cerevisiae* [35,40] or *Kluyveromyces lactis* [41] and fission yeast, such as *Schizosaccharomyces pombe* [37] or *Candida albicans* [42].

Nth1 is phosphorylated during the transition from the G1 to the S phase of the cell cycle through interplay between PKA and Cdk, which determines the ratio of different Nth1 phospho-isoforms (Fig. 1A) [43-46]. PKA phosphorylates Ser60 and Ser83, both of which are docking sites for 14-3-3 proteins [36]. However, PKA also phosphorylates residues Ser20 and Ser21, which also participate in Nth1 activation as they may represent a binding site for phosphatase PP2A, whose binding is reduced in the phospho-state (pSer20/pSer21). Under nutrient-rich conditions, when

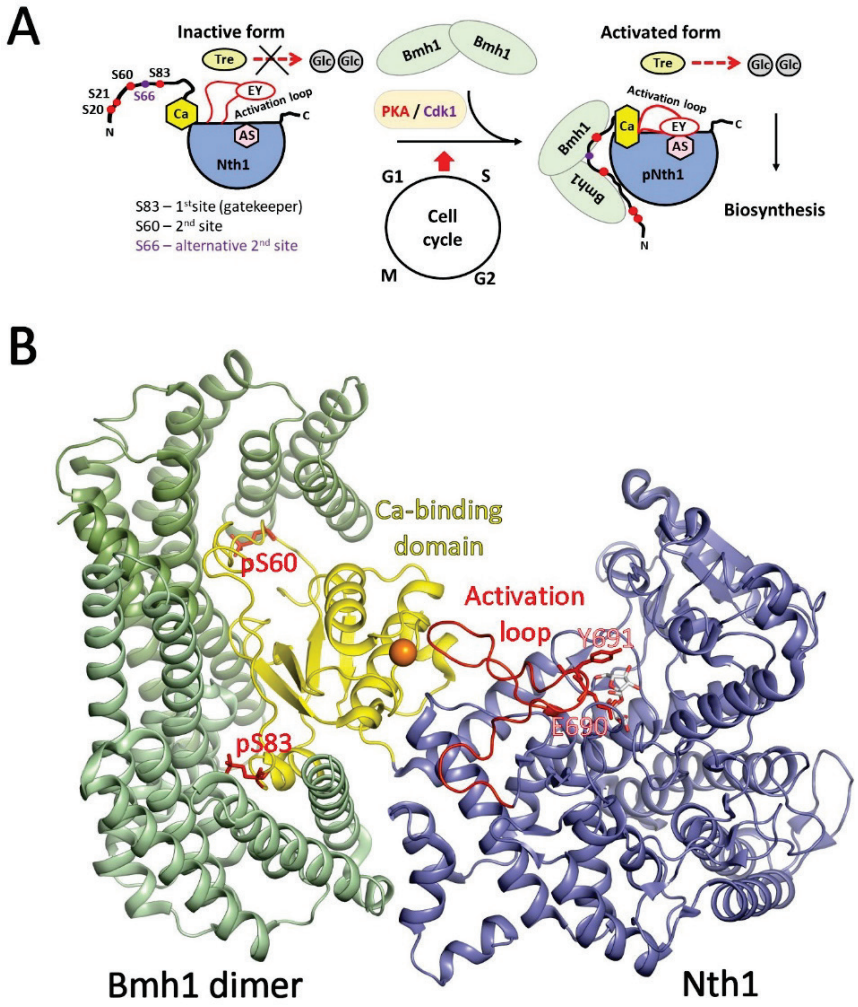

Fig. 1. Allosteric regulation of Nth1 by 14-3-3 protein. (**A**) Schematic model of 14-3-3-dependent regulation of Nth1. The inactive form of Nth1 is unable to hydrolyze trehalose to glucose. The N-terminal segment of Nth1 contains five phosphorylation sites, of which four are recognized by PKA and the other by Cdk1. The Ser83-containing motif serves as a gatekeeper, the dominant site for 14-3-3 protein binding, while the Ser60-containing motif functions as a secondary site [36,38,40]. An alternative secondary site is the Ser66-containing motif phosphorylated by Cdk1. The Ser20 and Ser21 sites are part of the binding site for the phosphatase, but this interaction is suppressed by phosphorylation [44]. Phosphorylated Nth1 is recognized by the yeast 14-3-3 protein during the G1 to S cell cycle transition [43]. 14-3-3 protein binding induces a conformational change in both the calcium and catalytic domains, creating a loop with all the residues necessary for catalysis. The active form of Nth1 then begins to metabolize trehalose to glucose. (**B**) Crystal structure of the Bmh1:Nth1 complex (PDB: 5N6N) [40]. The protomers of the Bmh1 homodimer are shown in two shades of green. The N-terminal extension and the calcium-binding domain are shown in yellow, and the catalytic domain is highlighted in blue. The phosphorylated Ser60 and Ser83, the regulatory loop and its two residues crucial for catalysis (Glu690 and Tyr691) are shown in red. The calcium ion is shown in orange. The figure was prepared with PyMOL (https://pymol.org/2/).

PKA has high activity, all four PKA sites Ser20, Ser21, Ser60 and Ser83 are phosphorylated. However, during slow growth, Ser60 is not efficiently phosphorylated by PKA, but Cdk phosphorylates a nearby Ser66 under these conditions, allowing its use as an alternative binding site for the 14-3-3 protein [44]. Thus, 14-3-3 protein binding to Nth1 is likely mediated by pSer60+pSer83 or pSer66+pSer83 phospho-motif pairs through the joint action of PKA and Cdk.

The molecular mechanism of 14-3-3 protein-mediated Nth1 activation was elucidated by solving the crystal structure of the complex of Nth1 phosphorylated at Ser60 and Ser83 with the yeast 14-3-3 protein Bmh1 [40]. This structure revealed that the Bmh1 dimer binds both phosphorylated motifs of the N-terminal segment of Nth1 and acts as an allosteric modulator by allowing the calcium-binding domain to interact with the catalytic domain. The interaction of these domains then stabilizes the conformation of the flexible loop (Fig. 1B, shown in red), which contains residues crucial for catalysis. In the absence of Bmh, the N-terminal segment of Nth1, including the calcium-binding domain, is flexible and does not interact with the catalytic domain. As a result, the loop containing the catalytic residues is disordered, so these residues are absent from the active center of the enzyme. Furthermore, Ca^{2+} binding to the site at the interface between the calcium-binding and catalytic domains further stabilizes interactions between these domains, thus explaining the potentiating effect of Ca^{2+} binding on Nth1 activity. This mechanism is consistent with our previous results from hydrogen-deuterium exchange coupled to mass spectrometry (HDX-MS), which have suggested that both Nth1 domains, especially the Ca-binding domain, undergo a significant conformational change upon 14-3-3 and/or Ca^{2+} protein binding [38,47].

Structural modulation of human ubiquitin ligase Nedd4-2

The main function of Neural precursor cell expressed developmentally downregulated 4 (Nedd4) E3 ligases is to tag proteins for ubiquitination as the final step in the ubiquitination cascade [48,49]. The Nedd4-2 ubiquitin ligase belongs to the Nedd4 family, whose members have a similar domain structure consisting of three distinct domains, namely the N-terminal C2 domain, which is responsible for membrane binding, two to four WW domains, responsible for binding to proline-rich sequence (PY motif) of protein substrates, and the catalytical HECT domain [50]. Nedd4-2 activity must be tightly regulated due to its pivotal role in animal physiology as this E3 ligase targets numerous membrane proteins [51,52]. We and others have shown that Nedd4-2 is regulated through phosphorylation and 14-3-3 protein binding, with three 14-3-3 binding motifs that contain Ser342, Ser367 and Ser448 and border the WW2 domain (Fig. 2A) [53-56].

Detailed biophysical analysis of the interaction between Nedd4-2 and 14-3-3η using analytical ultracentrifugation and protein crystallography confirmed the need for bidentate Nedd4-2 binding to the 14-3-3 protein dimer [56]. The highest binding affinity was observed in Nedd4-2 phosphorylated at Ser342 and Ser448. These sites are phosphorylated by SGK or PKA, and the motif containing pSer448 is the dominant site, also known as the gatekeeper. As shown by structural characterization of the Nedd4-$2_{335-455}$ and its complex with 14-3-3η using small angle X-ray scattering (SAXS) and chemical cross-linking, in the absence of 14-3-3η, the WW2 and WW3 domains interact with the HECT domain. Conversely, the WW3 domain is sequestered into the central channel of the 14-3-3η dimer in the complex [56]. In the complex, the WW3 and WW4 domains are sterically blocked and less mobile, whereas the catalytic site in the C-lobe of the HECT domain is more exposed and mobile, key findings that were revealed in a subsequent study based on time-resolved fluorescence measurements with 1,5-IAEDANS-labeled variants of Nedd4-2 [57]. Complex formation had little effect on the mobility of the WW2 domain and no effect on the WW1 domain, whose mobility remains unchanged.

In conclusion, 14-3-3 protein binding induces a structural rearrangement of Nedd4-2 by affecting interactions between its structured domains. As such, 14-3-3 proteins regulate the dynamic processes of membrane protein ubiquitination depending on the accessibility of individual WW domains of Nedd4-2. In addition, our data provided a solid platform for subsequent studies aimed at targeting the Nedd4-2:14-3-3 complex for potential therapeutic purposes, e.g., for the treatment of Nedd4-2-related diseases such as Parkinson's and renal disease, hypertension, and other conditions [58,59].

14-3-3 inhibits procaspase-2 activation by masking its dimerization surface

Procaspase-2 (proC2) functions as an initiator caspase, linking cellular metabolism to apoptosis [60,61]. But while most studies associated proC2 with tumor suppression, proC2 can also promote cancer by triggering neuroblastoma development [62]. Structurally, proC2 consists of three domains, namely the N-terminal caspase activation and recruitment domain (CARD) and large (p19) and small (p12) subunits [63]. In turn, proC2 activation requires dimerization and autocatalytic processing to form the p19:p12 mature active caspase-2 dimer [64].

The increase in NADPH levels generated by the pentose phosphate pathway leads to proC2 phosphorylation at Ser139 (human caspase-2 numbering) by calcium/calmodulin-dependent kinase II. This phosphorylation prevents the interaction between proC2 and the death domain-containing protein CRADD and enables protein 14-3-3 binding [65,66], thereby blocking both caspase-2 activation and apoptosis. Moreover, caspase-2 is also the most conserved and the only caspase known to be regulated by 14-3-3 protein [67].

As shown by various biochemical and biophysical studies, the interaction of human proC2 with 14-3-3 proteins is controlled by pSer139- and pSer164-containing motifs located in the linker between the CARD and p19 domains [68]. Both motifs are required for proC2 to establish stable interactions with 14-3-3 proteins, and pSer139 is the dominant site. An important aspect of caspase-2 activation is its localization. As the only caspase that is mainly located in the nucleus and Golgi complex, caspase-2 is activated both in the nucleus and in the cytoplasm [69-72]. Interestingly, the nuclear localisation signal (NLS) of caspase-2 is located between the two 14-3-3 binding motifs, suggesting that 14-3-3 protein binding could mask this signal sequence. Indeed, structural analysis of the proC2:14-3-3 complex using a combination of fluorescence spectroscopy, SAXS, NMR, chemical crosslinking, H/D exchange

coupled to MS and X-ray crystallography has revealed that 14-3-3 protein binding masks two important regions of proC2, NLS and the surface of the p12 domain around Cys436, which is involved in caspase-2 dimerization during its activation (Fig. 2B) [73,74]. Thus, our results indicate that 14-3-3 proteins play a dual role in regulating caspase-2 activation as they (i) block its activation by masking its dimerization surface and (ii) influence its cellular localisation by blocking its NLS.

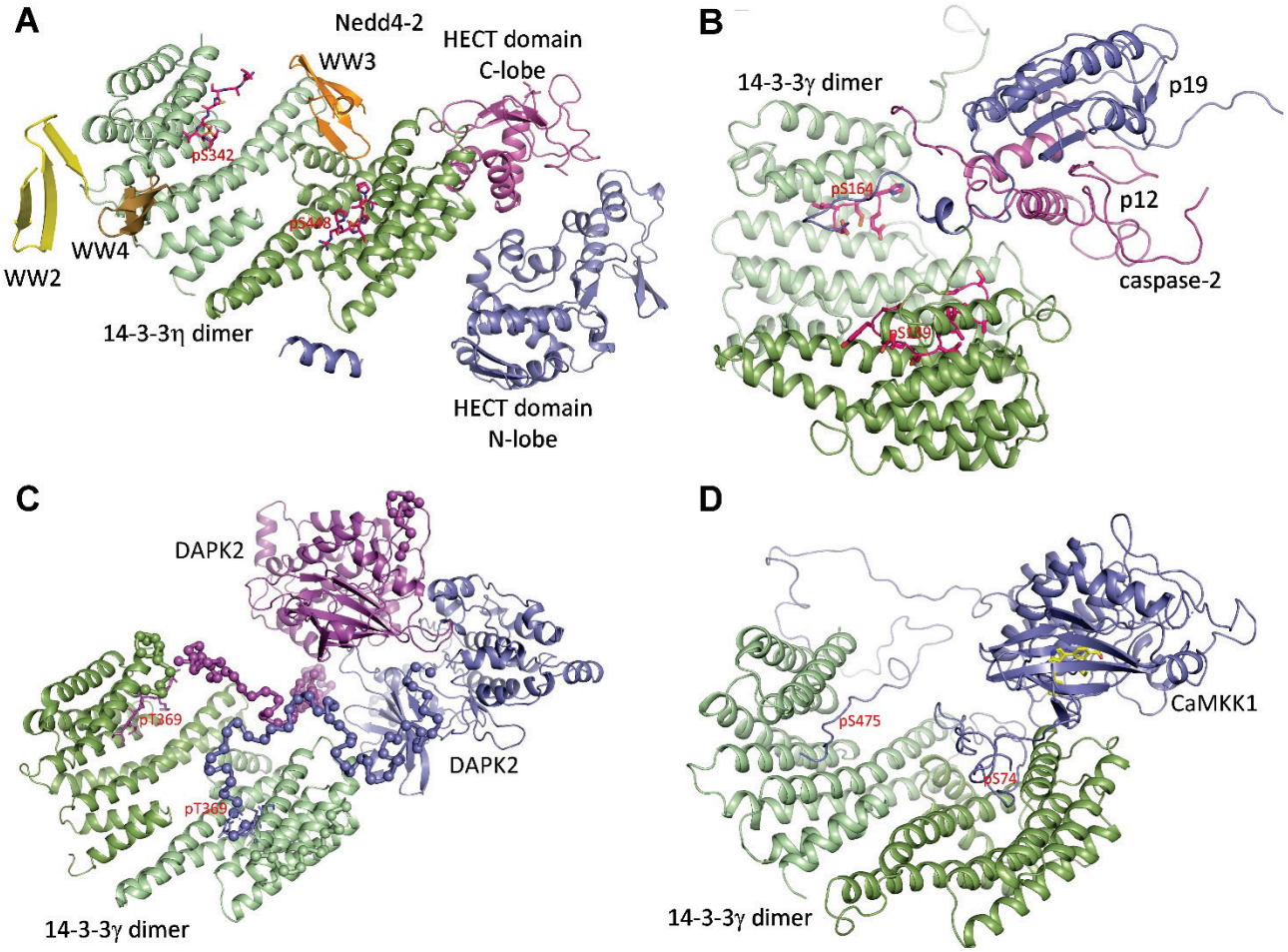

Fig. 2. Ribbon representation of SAXS-based structural models of select 14-3-3 protein complexes. The protomers of the 14-3-3γ and 14-3-3η homodimer are shown in two shades of green in all panels. (**A**) The best-scoring CORAL model of the Nedd4-2:14-3-3η complex constructed using crystal structures of HECT domain (PDB ID: 5HPK) [96], solution structures of WW1-3 domains (PDB ID: 1WR3, 1WR4, 1WR7) and 14-3-3γ with bound Nedd4-2 phosphopeptides pSer342 and pSer448 (PDB ID 6ZBT, 6ZC9)[56]. WW2-4 are shown in yellow, orange and sand, the N- and C-lobes of the HECT domain are shown in blue and magenta, respectively. (**B**) The best-scoring AllosMod-FoXS model of the procaspase-2:14-3-3γ complex [73] constructed using the crystal structure of caspase-2 (PDB ID: 3R7S) [97] and the 14-3-3γ with bound caspase-2 peptide phosphorylated on Ser139 and Ser164 (PDB ID 6SAD) [74]. p19 and p12 domains of procaspase-2 are shown in blue and magenta, respectively. (**C**) The best-scoring CORAL model of the DAPK2:14-3-3γ complex constructed using crystal structures of autoinhibited DAPK2 (PDB ID: 2A2A) [80,81] and 14-3-3γ with bound C-terminal DAPK2 phophopeptidepeptide pThr369 (PDB ID: 7A6R) [83]. The unstructured segments missing in the crystal structures were modelled as dummy residue chains, shown as spheres. Two protomers of DAPK2 dimer are shown in blue and magenta. (**D**) The best-scoring AllosMod-FoXS model of the pCaMKK1:14-3-3γ complex constructed using crystal structures of the kinase domain of CaMKK1 (PDB ID: 6CD6) and 14-3-3γ with bound CaMKK2 phosphopeptides (PDB ID: 6FEL and 6EWW) [94,95]. The position of the active site is indicated by the position of inhibitor in the crystal structure of CaMKK1 (yellow sticks). The figure was prepared with PyMOL (https://pymol.org/2/).

Mechanism of 14-3-3-mediated inhibition of human death-associated protein kinase 2 (DAPK2)

The main function of death-associated protein kinases (DAPK) is to control various cellular processes, including membrane blebbing, apoptosis, and autophagy [75,76]. This family of Ca^{2+}/calmodulin (CaM) dependent Ser/Thr protein kinases includes five members that differ in their cellular localization and interactome [77].

DAPK2 is the smallest member and consist of an N-terminal kinase domain, followed by an autoinhibitory region (AID) and a Ca^{2+}/CaM domain (CBD) [78,79]. DAPK2 activity is controlled by autoinhibition, autophosphorylation, dimerization and interaction with 14-3-3 proteins *via* the unique C-terminal tail containing a C-terminal (mode III) 14-3-3 binding motif around Thr369 [80,81].

DAPK2 activation requires a protomeric form of the enzyme either capable of binding Ca^{2+}/CaM or with AID phosphorylated at Ser299 to prevent AID-induced autoinhibition from blocking the catalytic site [78,82]. Our structural analysis of the DAPK2:14-3-3γ complex suggested that 14-3-3 inhibits DAPK2 by directly interacting with the AID and CBD segments of DAPK2 and by stabilising DAPK2 dimerization, which obstructs access to the active site (Fig. 2C) [80,83]. As a result, complex formation destabilises the interaction between DAPK2 and Ca^{2+}/CaM and protects the DAPK2 inhibitory autophosphorylation site Ser318 located in CBD from dephosphorylation, further preventing Ca^{2+}/CaM binding.

We have also shown that the interaction between 14-3-3γ and the C-terminal 14-3-3 binding motif of DAPK2 can be stabilized by the diterpene glycoside phytotoxin fusicoccin A (FC-A). FC-A fills a gap in the interface between the 14-3-3 ligand binding groove and the 14-3-3 binding motif of the client protein [84]. Thus, our findings provide mechanistic insights into 14-3-3-mediated DAPK2 inhibition and highlight the potential of the DAPK2:14-3-3 complex as a target for anti-inflammatory therapies.

Differential regulation of Ca^{2+}/CaM-dependent protein kinase kinases 1 and 2 by 14-3-3 proteins

CaMKK1 and CaMKK2 play a key role in many physiological and pathological processes in the cell by phosphorylating and activating downstream protein kinases CaMKI, CaMKIV and protein kinase B, thereby triggering the phosphorylation of their downstream targets [85-87]. Both CaMKKs share a common domain structure consisting of a kinase domain, a regulatory region with an autoinhibitory segment (AID) and a binding region for the calcium/calmodulin complex (CBD) [88]. Both CaMKKs are partly inhibited by PKA-mediated phosphorylation at multiple sites bordering the kinase domain [89]. In addition, phosphorylation by PKA creates two motifs for 14-3-3 protein binding to phosphorylated CaMKKs [90-92]. The high-affinity 14-3-3 binding motif is located at the C-terminus containing Ser475 and Ser511 in CaMKK1 and CaMKK2, respectively [92,93]. The second motif, which binds to 14-3-3 proteins with lower affinity and further stabilises complex formation, is located at the N-terminus and contains Ser74 and Ser100 in CaMKK1 and CaMKK2, respectively.

Previous studies have suggested that 14-3-3 binding protects the inhibitory phosphorylation site located in the CBD of both CaMKKs from dephosphorylation, thereby maintaining CaMKKs in a partly inhibited state mediated by PKA [90,92,94]. However, complex formation differently affects the remaining catalytic activity of phosphorylated CaMKKs. While the activity of phosphorylated CaMKK1 is significantly reduced by 14-3-3 binding, the activity of phosphorylated CaMKK2 remains almost unchanged after complex formation [90-92,94], as explained in our recent structural characterization of CaMKK1:14-3-3 and CaMKK2:14-3-3 complexes by SAXS, H/D exchange coupled to MS, and fluorescence spectroscopy [95]. This study revealed that complex formation inhibits Ca^{2+}/CaM binding and affects the structure of kinase domains and autoinhibitory segments of both CaMKKs, but the CaMKK1:14-3-3γ complex has a more compact and rigid structure in which the active site of the kinase domain interacts with the last two C-terminal helices of the 14-3-3γ protein (Fig. 2D). This conformation explains the 14-3-3-mediated inhibition of CaMKK1. In contrast, in the CaMKK2:14-3-3 complex, the kinase domain interacts with 14-3-3γ differently, and the complex has a looser structure, resulting in negligible inhibition of CaMKK2 catalytic activity. Thus, Ca^{2+}/CaM binding inhibition and the interaction of the CaMKK1 active site with the C-terminal segment of the 14-3-3γ protein provide the structural basis for 14-3-3-mediated CaMKK1 inhibition.

We have also shown that the interaction between the N-terminal 14-3-3 binding motif of CaMKKs and 14-3-3 proteins can be stabilised by FC-A and other fusicoccanes [93]. Moreover, this study also demonstrated that fusicoccanes stabilise the complex between phosphorylated full-length CaMKK2 and 14-3-3γ and slows down CaMKK2 dephosphorylation, thus keeping it in its phosphorylation-mediated inhibited state. Therefore, targeting the 14-3-3 ligand binding groove by small-molecule compounds may offer

an alternative strategy to suppress CaMKK2 activity.

Conclusions

Studies focusing on 14-3-3-mediated regulation of the five different enzymes mentioned in this review, namely Nth1, Nedd4-2, caspase-2, DAPK2 and CaMKK1/2, show the variability of these protein-protein interactions. The common denominator of these complexes is their involvement in key signalling processes in the cell, such as apoptosis, ubiquitination, cell cycle regulation, cell stress response, or metabolic regulation. 14-3-3 proteins bind to unstructured regions of these multi-domain enzymes, and interactions responsible for the actual regulation of the activity of the bound enzymes often occur far from the phosphorylated motifs within the structured domains. Structural studies also demonstrate that targeting protein-protein interactions in these complexes may enable us to develop new strategies for modulating these physiologically important enzymes.

Conflict of Interest

There is no conflict of interest.

Acknowledgements

Research on 14-3-3 proteins is funded in our laboratory by the Czech Science Foundation (Grant No. 23-04686S) and the Czech Academy of Sciences (RVO: 67985823 of the Institute of Physiology). We thank Dr. Carlos H. V. Melo for editing the article.

References

1. Choi KY, Satterberg B, Lyons DM, Elion EA. Ste5 tethers multiple protein kinases in the MAP kinase cascade required for mating in S. cerevisiae. Cell 1994;78:499-512. https://doi.org/10.1016/0092-8674(94)90427-8
2. Rubin CS, Rosen OM. Protein phosphorylation. Annu Rev Biochem 1975;44:831-887. https://doi.org/10.1146/annurev.bi.44.070175.004151
3. Reinhardt HC, Yaffe MB. Phospho-Ser/Thr-binding domains: navigating the cell cycle and DNA damage response. Nat Rev Mol Cell Biol 2013;14:563-580. https://doi.org/10.1038/nrm3640
4. Furukawa Y, Ikuta N, Omata S, Yamauchi T, Isobe T, Ichimura T. Demonstration of the phosphorylation-dependent interaction of tryptophan hydroxylase with the 14-3-3 protein. Biochem Biophys Res Commun 1993;194:144-149. https://doi.org/10.1006/bbrc.1993.1796
5. Fantl WJ, Muslin AJ, Kikuchi A, Martin JA, MacNicol AM, Gross RW, Williams LT. Activation of Raf-1 by 14-3-3 proteins. Nature 1994;371:612-614. https://doi.org/10.1038/371612a0
6. Freed E, Symons M, Macdonald SG, McCormick F, Ruggieri R. Binding of 14-3-3 proteins to the protein kinase Raf and effects on its activation. Science 1994;265:1713-1716. https://doi.org/10.1126/science.8085158
7. Fu H, Xia K, Pallas DC, Cui C, Conroy K, Narsimhan RP, Mamon H, Collier RJ, Roberts TM. Interaction of the protein kinase Raf-1 with 14-3-3 proteins. Science 1994;266:126-129. https://doi.org/10.1126/science.7939632
8. Yaffe MB, Rittinger K, Volinia S, Caron PR, Aitken A, Leffers H, Gamblin SJ, Smerdon SJ, Cantley LC. The structural basis for 14-3-3:phosphopeptide binding specificity. Cell 1997;91:961-971. https://doi.org/10.1016/S0092-8674(00)80487-0
9. Yaffe MB, Elia AE. Phosphoserine/threonine-binding domains. Curr Opin Cell Biol 2001;13:131-138. https://doi.org/10.1016/S0955-0674(00)00189-7
10 Aitken A. 14-3-3 proteins: a historic overview. Semin Cancer Biol 2006;16:162-172. https://doi.org/10.1016/j.semcancer.2006.03.005
11. Obsil T, Obsilova V. Structural basis of 14-3-3 protein functions. Semin Cell Dev Biol 2011;22:663-672. https://doi.org/10.1016/j.semcdb.2011.09.001
12. Sluchanko NN. Association of Multiple Phosphorylated Proteins with the 14-3-3 Regulatory Hubs: Problems and Perspectives. J Mol Biol 2018;430:20-26. https://doi.org/10.1016/j.jmb.2017.11.010
13. Obsilova V, Obsil T. Structural insights into the functional roles of 14-3-3 proteins. Front Mol Biosci 2022;9:1016071. https://doi.org/10.3389/fmolb.2022.1016071
14. Liu D, Bienkowska J, Petosa C, Collier RJ, Fu H, Liddington R. Crystal structure of the zeta isoform of the 14-3-3 protein. Nature 1995;376:191-194. https://doi.org/10.1038/376191a0

15. Xiao B, Smerdon SJ, Jones DH, Dodson GG, Soneji Y, Aitken A, Gamblin SJ. Structure of a 14-3-3 protein and implications for coordination of multiple signalling pathways. Nature 1995;376:188-191. https://doi.org/10.1038/376188a0
16. Yang X, Lee WH, Sobott F, Papagrigoriou E, Robinson CV, Grossmann JG, Sundstrom M, Doyle DA, Elkins JM. Structural basis for protein-protein interactions in the 14-3-3 protein family. Proc Natl Acad Sci U S A 2006;103:17237-17242. https://doi.org/10.1073/pnas.0605779103
17. Rittinger K, Budman J, Xu J, Volinia S, Cantley LC, Smerdon SJ, Gamblin SJ, Yaffe MB. Structural analysis of 14-3-3 phosphopeptide complexes identifies a dual role for the nuclear export signal of 14-3-3 in ligand binding. Mol Cell 1999;4:153-166. https://doi.org/10.1016/S1097-2765(00)80363-9
18. Bustos DM, Iglesias AA. Intrinsic disorder is a key characteristic in partners that bind 14-3-3 proteins. Proteins 2006;63:35-42. https://doi.org/10.1002/prot.20888
19. Sluchanko NN, Bustos DM. Intrinsic disorder associated with 14-3-3 proteins and their partners. Prog Mol Biol Transl Sci 2019;166:19-61. https://doi.org/10.1016/bs.pmbts.2019.03.007
20. Tinti M, Johnson C, Toth R, Ferrier DE, Mackintosh C. Evolution of signal multiplexing by 14-3-3-binding 2R-ohnologue protein families in the vertebrates. Open Biol 2012;2:120103. https://doi.org/10.1098/rsob.120103
21. Ganguly S, Weller JL, Ho A, Chemineau P, Malpaux B, Klein DC. Melatonin synthesis: 14-3-3-dependent activation and inhibition of arylalkylamine N-acetyltransferase mediated by phosphoserine-205. Proc Natl Acad Sci U S A 2005;102:1222-1227. https://doi.org/10.1073/pnas.0406871102
22. Eisenreichova A, Boura E. Structural basis for SARS-CoV-2 nucleocapsid (N) protein recognition by 14-3-3 proteins. J Struct Biol 2022;214:107879. https://doi.org/10.1016/j.jsb.2022.107879
23. Tugaeva KV, Hawkins D, Smith JLR, Bayfield OW, Ker DS, Sysoev AA, Klychnikov OI, Antson AA, Sluchanko NN. The Mechanism of SARS-CoV-2 Nucleocapsid Protein Recognition by the Human 14-3-3 Proteins. J Mol Biol 2021;433:166875. https://doi.org/10.1016/j.jmb.2021.166875
24. Tugaeva KV, Sysoev AA, Kapitonova AA, Smith JLR, Zhu P, Cooley RB, Antson AA, Sluchanko NN. Human 14-3-3 Proteins Site-selectively Bind the Mutational Hotspot Region of SARS-CoV-2 Nucleoprotein Modulating its Phosphoregulation. J Mol Biol 2023;435:167891. https://doi.org/10.1016/j.jmb.2022.167891
25. Fu H, Subramanian RR, Masters SC. 14-3-3 proteins: structure, function, and regulation. Annu Rev Pharmacol Toxicol 2000;40:617-647. https://doi.org/10.1146/annurev.pharmtox.40.1.617
26. Tzivion G, Avruch J. 14-3-3 proteins: active cofactors in cellular regulation by serine/threonine phosphorylation. J Biol Chem 2002;277:3061-3064. https://doi.org/10.1074/jbc.R100059200
27. Bridges D, Moorhead GB. 14-3-3 proteins: a number of functions for a numbered protein. Sci STKE 2004;2004:re10. https://doi.org/10.1126/stke.2422004re10
28. Sluchanko NN. Reading the phosphorylation code: binding of the 14-3-3 protein to multivalent client phosphoproteins. Biochem J 2020;477:1219-1225. https://doi.org/10.1042/BCJ20200084
29. Kopp M, Muller H, Holzer H. Molecular analysis of the neutral trehalase gene from Saccharomyces cerevisiae. J Biol Chem 1993;268:4766-4774. https://doi.org/10.1016/S0021-9258(18)53463-3
30. Kopp M, Nwaka S, Holzer H. Corrected sequence of the yeast neutral trehalase-encoding gene (NTH1): biological implications. Gene 1994;150:403-404. https://doi.org/10.1016/0378-1119(94)90462-6
31. Nwaka S, Holzer H. Molecular biology of trehalose and the trehalases in the yeast Saccharomyces cerevisiae. Prog Nucleic Acid Res Mol Biol 1998;58:197-237. https://doi.org/10.1016/S0079-6603(08)60037-9
32. Wera S, De Schrijver E, Geyskens I, Nwaka S, Thevelein JM. Opposite roles of trehalase activity in heat-shock recovery and heat-shock survival in Saccharomyces cerevisiae. Biochem J 1999;343(Pt 3):621-626. https://doi.org/10.1042/bj3430621
33. Uno I, Matsumoto K, Adachi K, Ishikawa T. Genetic and biochemical evidence that trehalase is a substrate of cAMP-dependent protein kinase in yeast. J Biol Chem 1983;258:10867-10872. https://doi.org/10.1016/S0021-9258(17)44356-0
34. Ortiz CH, Maia JC, Tenan MN, Braz-Padrao GR, Mattoon JR, Panek AD. Regulation of yeast trehalase by a monocyclic, cyclic AMP-dependent phosphorylation-dephosphorylation cascade system. J Bacteriol 1983;153:644-651. https://doi.org/10.1128/jb.153.2.644-651.1983

35. Panni S, Landgraf C, Volkmer-Engert R, Cesareni G, Castagnoli L. Role of 14-3-3 proteins in the regulation of neutral trehalase in the yeast Saccharomyces cerevisiae. FEMS Yeast Res 2008;8:53-63. https://doi.org/10.1111/j.1567-1364.2007.00312.x
36. Veisova D, Macakova E, Rezabkova L, Sulc M, Vacha P, Sychrova H, Obsil T, Obsilova V. Role of individual phosphorylation sites for the 14-3-3-protein-dependent activation of yeast neutral trehalase Nth1. Biochem J 2012;443:663-670. https://doi.org/10.1042/BJ20111615
37. Franco A, Soto T, Vicente-Soler J, Paredes V, Madrid M, Gacto M, Cansado J. A role for calcium in the regulation of neutral trehalase activity in the fission yeast Schizosaccharomyces pombe. Biochem J 2003;376:209-217. https://doi.org/10.1042/bj20030825
38. Kopecka M, Kosek D, Kukacka Z, Rezabkova L, Man P, Novak P, Obsil T, Obsilova V. Role of the EF-hand-like motif in the 14-3-3 protein-mediated activation of yeast neutral trehalase Nth1. J Biol Chem 2014;289:13948-13961. https://doi.org/10.1074/jbc.M113.544551
39. Schepers W, Van Zeebroeck G, Pinkse M, Verhaert P, Thevelein JM. In Vivo Phosphorylation of SER21 and SER83 during Nutrient-induced Activation of the Yeast PKA Target Trehalase. J Biol Chem 2012;287:44130-44142. https://doi.org/10.1074/jbc.M112.421503
40. Alblova M, Smidova A, Docekal V, Vesely J, Herman P, Obsilova V, Obsil T. Molecular basis of the 14-3-3 protein-dependent activation of yeast neutral trehalase Nth1. Proc Natl Acad Sci U S A 2017;114:E9811-E9820. https://doi.org/10.1073/pnas.1714491114
41. Amaral FC, Van Dijck P, Nicoli JR, Thevelein JM. Molecular cloning of the neutral trehalase gene from Kluyveromyces lactis and the distinction between neutral and acid trehalases. Arch Microbiol 1997;167:202-208. https://doi.org/10.1007/s002030050436
42. Eck R, Bergmann C, Ziegelbauer K, Schonfeld W, Kunkel W. A neutral trehalase gene from Candida albicans: molecular cloning, characterization and disruption. Microbiology 1997;143(Pt 12):3747-3756. https://doi.org/10.1099/00221287-143-12-3747
43. Ewald JC, Kuehne A, Zamboni N, Skotheim JM. The Yeast Cyclin-Dependent Kinase Routes Carbon Fluxes to Fuel Cell Cycle Progression. Molecular Cell 2016;62:532-545. https://doi.org/10.1016/j.molcel.2016.02.017
44. Dengler L, Ord M, Schwab LM, Loog M, Ewald JC. Regulation of trehalase activity by multi-site phosphorylation and 14-3-3 interaction. Sci Rep 2021;11:962. https://doi.org/10.1038/s41598-020-80357-3
45. Zhang L, Winkler S, Schlottmann FP, Kohlbacher O, Elias JE, Skotheim JM, Ewald JC. Multiple Layers of Phospho-Regulation Coordinate Metabolism and the Cell Cycle in Budding Yeast. Front Cell Dev Biol 2019;7:338. https://doi.org/10.3389/fcell.2019.00338
46. Zhao G, Chen Y, Carey L, Futcher B. Cyclin-Dependent Kinase Co-Ordinates Carbohydrate Metabolism and Cell Cycle in S. cerevisiae. Molecular Cell 2016;62:546-557. https://doi.org/10.1016/j.molcel.2016.04.026
47. Macakova E, Kopecka M, Kukacka Z, Veisova D, Novak P, Man P, Obsil T, Obsilova V. Structural basis of the 14-3-3 protein-dependent activation of yeast neutral trehalase Nth1. Biochim Biophys Acta 2013;1830:4491-4499. https://doi.org/10.1016/j.bbagen.2013.05.025
48. Kumar S, Tomooka Y, Noda M. Identification of a set of genes with developmentally down-regulated expression in the mouse brain. Biochem Biophys Res Commun 1992;185:1155-1161. https://doi.org/10.1016/0006-291X(92)91747-E
49. Kumar S, Harvey KF, Kinoshita M, Copeland NG, Noda M, Jenkins NA. cDNA cloning, expression analysis, and mapping of the mouse Nedd4 gene. Genomics 1997;40:435-443. https://doi.org/10.1006/geno.1996.4582
50. Andre B, Springael JY. WWP, a new amino acid motif present in single or multiple copies in various proteins including dystrophin and the SH3-binding Yes-associated protein YAP65. Biochem Biophys Res Commun 1994;205:1201-1205. https://doi.org/10.1006/bbrc.1994.2793
51. Goel P, Manning JA, Kumar S. NEDD4-2 (NEDD4L): the ubiquitin ligase for multiple membrane proteins. Gene 2015;557:1-10. https://doi.org/10.1016/j.gene.2014.11.051
52. Harvey KF, Kumar S. Nedd4-like proteins: an emerging family of ubiquitin-protein ligases implicated in diverse cellular functions. Trends Cell Biol 1999;9:166-169. https://doi.org/10.1016/S0962-8924(99)01541-X

53. Bhalla V, Daidie D, Li H, Pao AC, LaGrange LP, Wang J, Vandewalle A, ET AL. Serum- and glucocorticoid-regulated kinase 1 regulates ubiquitin ligase neural precursor cell-expressed, developmentally down-regulated protein 4-2 by inducing interaction with 14-3-3. Mol Endocrinol 2005;19:3073-3084. https://doi.org/10.1210/me.2005-0193
54. Nagaki K, Yamamura H, Shimada S, Saito T, Hisanaga S, Taoka M, Isobe T, Ichimura T. 14-3-3 Mediates phosphorylation-dependent inhibition of the interaction between the ubiquitin E3 ligase Nedd4-2 and epithelial Na+ channels. Biochemistry 2006;45:6733-6740. https://doi.org/10.1021/bi052640q
55. Chandran S, Li H, Dong W, Krasinska K, Adams C, Alexandrova L, Chien A, Hallows KR, Bhalla V. Neural precursor cell-expressed developmentally down-regulated protein 4-2 (Nedd4-2) regulation by 14-3-3 protein binding at canonical serum and glucocorticoid kinase 1 (SGK1) phosphorylation sites. J Biol Chem 2011;286:37830-37840. https://doi.org/10.1074/jbc.M111.293233
56. Pohl P, Joshi R, Petrvalska O, Obsil T, Obsilova V. 14-3-3-protein regulates Nedd4-2 by modulating interactions between HECT and WW domains. Commun Biol 2021;4:899. https://doi.org/10.1038/s42003-021-02419-0
57. Joshi R, Pohl P, Strachotova D, Herman P, Obsil T, Obsilova V. Nedd4-2 binding to 14-3-3 modulates the accessibility of its catalytic site and WW domains. Biophys J 2022;121:1299-1311. https://doi.org/10.1016/j.bpj.2022.02.025
58. Huang X, Dixit VM. Drugging the undruggables: exploring the ubiquitin system for drug development. Cell Res 2016;26:484-498. https://doi.org/10.1038/cr.2016.31
59. Stevers LM, Sijbesma E, Botta M, MacKintosh C, Obsil T, Landrieu I, Cau Y, ET AL. Modulators of 14-3-3 Protein-Protein Interactions. J Med Chem 2018;61:3755-3778. https://doi.org/10.1021/acs.jmedchem.7b00574
60. Pop C, Salvesen GS. Human caspases: activation, specificity, and regulation. J Biol Chem 2009;284:21777-21781. https://doi.org/10.1074/jbc.R800084200
61. Krumschnabel G, Manzl C, Villunger A. Caspase-2: killer, savior and safeguard--emerging versatile roles for an ill-defined caspase. Oncogene 2009;28:3093-3096. https://doi.org/10.1038/onc.2009.173
62. Dorstyn L, Puccini J, Nikolic A, Shalini S, Wilson CH, Norris MD, Haber M, Kumar S. An unexpected role for caspase-2 in neuroblastoma. Cell Death Dis 2014;5:e1383. https://doi.org/10.1038/cddis.2014.342
63. Duan H, Dixit VM. RAIDD is a new 'death' adaptor molecule. Nature 1997;385:86-89. https://doi.org/10.1038/385086a0
64. Tinel A, Tschopp J. The PIDDosome, a protein complex implicated in activation of caspase-2 in response to genotoxic stress. Science 2004;304:843-846. https://doi.org/10.1126/science.1095432
65. Nutt LK, Margolis SS, Jensen M, Herman CE, Dunphy WG, Rathmell JC, Kornbluth S. Metabolic regulation of oocyte cell death through the CaMKII-mediated phosphorylation of caspase-2. Cell 2005;123:89-103. https://doi.org/10.1016/j.cell.2005.07.032
66. Nutt LK, Buchakjian MR, Gan E, Darbandi R, Yoon SY, Wu JQ, Miyamoto YJ, ET AL. Metabolic control of oocyte apoptosis mediated by 14-3-3zeta-regulated dephosphorylation of caspase-2. Dev Cell 2009;16:856-866. https://doi.org/10.1016/j.devcel.2009.04.005
67. Miles MA, Kitevska-Ilioski T, Hawkins CJ. Old and Novel Functions of Caspase-2. Int Rev Cell Mol Biol 2017;332:155-212. https://doi.org/10.1016/bs.ircmb.2016.12.002
68. Kalabova D, Smidova A, Petrvalska O, Alblova M, Kosek D, Man P, Obsil T, Obsilova V. Human procaspase-2 phosphorylation at both S139 and S164 is required for 14-3-3 binding. Biochem Biophys Res Commun 2017;493:940-945. https://doi.org/10.1016/j.bbrc.2017.09.116
69. Mancini M, Machamer CE, Roy S, Nicholson DW, Thornberry NA, Casciola-Rosen LA, Rosen A. Caspase-2 is localized at the Golgi complex and cleaves golgin-160 during apoptosis. J Cell Biol 2000;149:603-612. https://doi.org/10.1083/jcb.149.3.603
70. Colussi PA, Harvey NL, Kumar S. Prodomain-dependent nuclear localization of the caspase-2 (Nedd2) precursor. A novel function for a caspase prodomain. J Biol Chem 1998;273:24535-24542. https://doi.org/10.1074/jbc.273.38.24535
71. Baliga BC, Colussi PA, Read SH, Dias MM, Jans DA, Kumar S. Role of prodomain in importin-mediated nuclear localization and activation of caspase-2. J Biol Chem 2003;278:4899-4905. https://doi.org/10.1074/jbc.M211512200
72. Ando K, Parsons MJ, Shah RB, Charendoff CI, Paris SL, Liu PH, Fassio SR, ET AL. NPM1 directs PIDDosome-dependent caspase-2 activation in the nucleolus. J Cell Biol 2017;216:1795-1810. https://doi.org/10.1083/jcb.201608095

73. Smidova A, Alblova M, Kalabova D, Psenakova K, Rosulek M, Herman P, Obsil T, Obsilova V. 14-3-3 protein masks the nuclear localization sequence of caspase-2. FEBS J 2018;285:4196-4213. https://doi.org/10.1111/febs.14670
74. Kalabova D, Filandr F, Alblova M, Petrvalska O, Horvath M, Man P, Obsil T, Obsilova V. 14-3-3 protein binding blocks the dimerization interface of caspase-2. FEBS J 2020;287:3494-3510. https://doi.org/10.1111/febs.15215
75. Bialik S, Kimchi A. The death-associated protein kinases: structure, function, and beyond. Annu Rev Biochem 2006;75:189-210. https://doi.org/10.1146/annurev.biochem.75.103004.142615
76. Farag AK, Roh EJ. Death-associated protein kinase (DAPK) family modulators: Current and future therapeutic outcomes. Med Res Rev 2019;39:349-385. https://doi.org/10.1002/med.21518
77. Shiloh R, Bialik S, Kimchi A. The DAPK family: a structure-function analysis. Apoptosis 2014;19:286-297. https://doi.org/10.1007/s10495-013-0924-5
78. Kawai T, Nomura F, Hoshino K, Copeland NG, Gilbert DJ, Jenkins NA, Akira S. Death-associated protein kinase 2 is a new calcium/calmodulin-dependent protein kinase that signals apoptosis through its catalytic activity. Oncogene 1999;18:3471-3480. https://doi.org/10.1038/sj.onc.1202701
79. Ber Y, Shiloh R, Gilad Y, Degani N, Bialik S, Kimchi A. DAPK2 is a novel regulator of mTORC1 activity and autophagy. Cell Death Differ 2015;22:465-475. https://doi.org/10.1038/cdd.2014.177
80. Patel AK, Yadav RP, Majava V, Kursula I, Kursula P. Structure of the dimeric autoinhibited conformation of DAPK2, a pro-apoptotic protein kinase. J Mol Biol 2011;409:369-383. https://doi.org/10.1016/j.jmb.2011.03.065
81. Simon B, Huart AS, Temmerman K, Vahokoski J, Mertens HD, Komadina D, Hoffmann JE, Yumerefendi H, Svergun DI, Kursula P, Schultz C, McCarthy AA, Hart DJ, Wilmanns M. Death-Associated Protein Kinase Activity Is Regulated by Coupled Calcium/Calmodulin Binding to Two Distinct Sites. Structure 2016;24:851-861. https://doi.org/10.1016/j.str.2016.03.020
82. Shiloh R, Gilad Y, Ber Y, Eisenstein M, Aweida D, Bialik S, Cohen S, Kimchi A. Non-canonical activation of DAPK2 by AMPK constitutes a new pathway linking metabolic stress to autophagy. Nat Commun 2018;9:1759. https://doi.org/10.1038/s41467-018-03907-4
83. Horvath M, Petrvalska O, Herman P, Obsilova V, Obsil T. 14-3-3 proteins inactivate DAPK2 by promoting its dimerization and protecting key regulatory phosphosites. Commun Biol 2021;4:986. https://doi.org/10.1038/s42003-021-02518-y
84. Wurtele M, Jelich-Ottmann C, Wittinghofer A, Oecking C. Structural view of a fungal toxin acting on a 14-3-3 regulatory complex. EMBO J 2003;22:987-994. https://doi.org/10.1093/emboj/cdg104
85. Gocher AM, Azabdaftari G, Euscher LM, Dai S, Karacosta LG, Franke TF, Edelman AM. Akt activation by Ca(2+)/calmodulin-dependent protein kinase kinase 2 (CaMKK2) in ovarian cancer cells. J Biol Chem 2017;292:14188-14204. https://doi.org/10.1074/jbc.M117.778464
86. Mizuno K, Ris L, Sanchez-Capelo A, Godaux E, Giese KP. Ca2+/calmodulin kinase kinase alpha is dispensable for brain development but is required for distinct memories in male, though not in female, mice. Mol Cell Biol 2006;26:9094-9104. https://doi.org/10.1128/MCB.01221-06
87. Yano S, Tokumitsu H, Soderling TR. Calcium promotes cell survival through CaM-K kinase activation of the protein-kinase-B pathway. Nature 1998;396:584-587. https://doi.org/10.1038/25147
88. Tokumitsu H, Wayman GA, Muramatsu M, Soderling TR. Calcium/calmodulin-dependent protein kinase kinase: identification of regulatory domains. Biochemistry 1997;36:12823-12827. https://doi.org/10.1021/bi971348i
89. Tokumitsu H, Sakagami H. Molecular Mechanisms Underlying Ca(2+)/Calmodulin-Dependent Protein Kinase Kinase Signal Transduction. Int J Mol Sci 2022;23:11025. https://doi.org/10.3390/ijms231911025
90. Davare MA, Saneyoshi T, Guire ES, Nygaard SC, Soderling TR. Inhibition of calcium/calmodulin-dependent protein kinase kinase by protein 14-3-3. J Biol Chem 2004;279:52191-52199. https://doi.org/10.1074/jbc.M409873200
91. Ichimura T, Taoka M, Hozumi Y, Goto K, Tokumitsu H. 14-3-3 Proteins directly regulate Ca(2+)/calmodulin-dependent protein kinase kinase alpha through phosphorylation-dependent multisite binding. FEBS Lett 2008;582:661-665. https://doi.org/10.1016/j.febslet.2008.01.037
92. Langendorf CG, O'Brien MT, Ngoei KRW, McAloon LM, Dhagat U, Hoque A, Ling NXY, Dite TA, Galic S, Loh K, Parker MW, Oakhill JS, Kemp BE, Scott JW. CaMKK2 is inactivated by cAMP-PKA signaling and 14-3-3 adaptor proteins. J Biol Chem 2020;295:16239-16250. https://doi.org/10.1074/jbc.RA120.013756

93. Lentini Santo D, Petrvalska O, Obsilova V, Ottmann C, Obsil T. Stabilization of Protein-Protein Interactions between CaMKK2 and 14-3-3 by Fusicoccins. ACS Chem Biol 2020;15:3060-3071. https://doi.org/10.1021/acschembio.0c00821
94. Psenakova K, Petrvalska O, Kylarova S, Lentini Santo D, Kalabova D, Herman P, Obsilova V, Obsil T. 14-3-3 protein directly interacts with the kinase domain of calcium/calmodulin-dependent protein kinase kinase (CaMKK2). Biochim Biophys Acta 2018;1862:1612-1625. https://doi.org/10.1016/j.bbagen.2018.04.006
95. Petrvalska O, Honzejkova K, Koupilova N, Herman P, Obsilova V, Obsil T. 14-3-3 protein inhibits CaMKK1 by blocking the kinase active site with its last two C-terminal helices. Protein Sci 2023;32:e4805. https://doi.org/10.1002/pro.4805
96. Zhang W, Wu KP, Sartori MA, Kamadurai HB, Ordureau A, Jiang C, Mercredi PY, Murchie R, Hu J, Persaud A, Mukherjee M, Li N, Doye A, Walker JR, Sheng Y, Hao Z, Li Y, Brown KR, Lemichez E, Chen J, Tong Y, Harper JW, Moffat J, Rotin D, Schulman BA, Sidhu SS. System-Wide Modulation of HECT E3 Ligases with Selective Ubiquitin Variant Probes. Mol Cell 2016;62:121-136. https://doi.org/10.1016/j.molcel.2016.02.005
97. Tang Y, Wells JA, Arkin MR. Structural and enzymatic insights into caspase-2 protein substrate recognition and catalysis. J Biol Chem 2011;286:34147-34154. https://doi.org/10.1074/jbc.M111.247627

Physiol. Res. 73 (Suppl. 1): S413-S434, 2024 *https://doi.org/10.33549/physiolres.935346*

REVIEW

Disease-Associated Variants in *GRIN1*, *GRIN2A* and *GRIN2B* genes: Insights into NMDA Receptor Structure, Function, and Pathophysiology

Miloslav KORINEK[1], Miriam CANDELAS SERRA[1], Fatma Elzahraa S. ABDEL RAHMAN[1,3], Mark DOBROVOLSKI[1,4], Viktor KUCHTIAK[1,3], Vera ABRAMOVA[1,4], Klevinda FILI[1,4], Eni TOMOVIC[1,3], Barbora HRCKA KRAUSOVA[1], Jan KRUSEK[1], Jiri CERNY[1], Ladislav VYKLICKY[1], Ales BALIK[1,2], Tereza SMEJKALOVA[1]

[1]Institute of Physiology of the Czech Academy of Sciences, Prague, Czech Republic, [2]Institute of Physiology of the Czech Academy of Sciences, Division BIOCEV, Vestec, Czech Republic, [3]Faculty of Science, Charles University, Prague, Czech Republic, [4]Third Faculty of Medicine, Charles University, Prague, Czech Republic

Received February 29, 2024
Accepted March 19, 2024

Summary

N-methyl-D-aspartate receptors (NMDARs) are a subtype of ionotropic glutamate receptors critical for synaptic transmission and plasticity, and for the development of neural circuits. Rare or *de-novo* variants in *GRIN* genes encoding NMDAR subunits have been associated with neurodevelopmental disorders characterized by intellectual disability, developmental delay, autism, schizophrenia, or epilepsy. In recent years, some disease-associated variants in *GRIN* genes have been characterized using recombinant receptors expressed in non-neuronal cells, and a few variants have also been studied in neuronal preparations or animal models. Here we review the current literature on the functional evaluation of human disease-associated variants in *GRIN1*, *GRIN2A* and *GRIN2B* genes at all levels of analysis. Focusing on the impact of different patient variants at the level of receptor function, we discuss effects on receptor agonist and co-agonist affinity, channel open probability, and receptor cell surface expression. We consider how such receptor-level functional information may be used to classify variants as gain-of-function or loss-of-function, and discuss the limitations of this classification at the synaptic, cellular, or system level. Together this work by many laboratories worldwide yields valuable insights into NMDAR structure and function, and represents significant progress in the effort to understand and treat *GRIN* disorders.

Keywords

NMDA receptor • *GRIN* genes • Genetic variants • Electrophysiology • Synapse • Animal models

Corresponding authors

Ales Balik, Department of Cellular Neurophysiology, Institute of Physiology of the Czech Academy of Sciences, Division BIOCEV, Prumyslova 595, 252 50 Vestec, Czech Republic. E-mail: ales.balik@fgu.cas.cz; Tereza Smejkalova, Department of Cellular Neurophysiology, Institute of Physiology of the Czech Academy of Sciences, Videnska 1083, 142 00 Prague 4, Czech Republic. E-mail: tereza.smejkalova@fgu.cas.cz

Introduction

N-methyl-D-aspartate receptors (NMDARs), encoded by *GRIN* genes, are ionotropic glutamate receptors present at virtually all excitatory synapses in the central nervous system. Classical NMDARs have a characteristic biophysical signature, with a requirement for the binding of two agonists (glutamate and glycine/ D-serine), strong block by Mg^{2+} at resting membrane potentials, high Ca^{2+} permeability, and relatively slow activation and deactivation kinetics [1]. These properties enable NMDARs to serve as coincidence detectors of presynaptic glutamate release and postsynaptic depolarization that removes the Mg^{2+} block. The resulting NMDAR-mediated Ca^{2+} influx is a key signal regulating activity-dependent changes in synaptic strength [2] that underlie the development of neural circuits and their

ability to process and store information [1]. Given this physiological role, dysfunction of NMDAR signaling is considered to be a significant factor in the etiology of diverse neurological disorders. In recent years, rare or *de-novo* variants of *GRIN* genes have been identified in patients with neurodevelopmental syndromes characterized by intellectual disability, developmental delay, with features of autism, schizophrenia, or epilepsy [3], sometimes collectively referred to as *GRIN* disorders.

There are seven NMDAR genes, *GRIN1*, *GRIN2A-D* and *GRIN3A-B*, encoding GluN1, GluN2A-D and GluN3A-B subunits, respectively. NMDARs are assembled as heterotetramers of two obligatory GluN1 subunits and two GluN2 and/or GluN3 subunits [1]. Aside from the GluN1 subunit, GluN2A and GluN2B are the most abundant subunits in principal neurons in the forebrain [4], with the GluN2B expression beginning early during embryonic development, followed by the expression of GluN2A postnatally; the expression of both GluN2A and GluN2B persists until and throughout adulthood [1]. NMDAR complexes can be diheteromeric (i.e., containing two GluN1 and two identical GluN2 subunits) or triheteromeric (containing two GluN1 and two different GluN2 subunits). Receptors containing different combinations of GluN2 subunits have different functional and pharmacological properties [5] and likely play different physiological roles [6]. It has been suggested that the majority of NMDARs in the adult forebrain are GluN1/GluN2A/GluN2B triheteromers [7,8] (but see [9]), whose structure and function has been explored in recent years, thanks to new methods for selectively expressing or isolating triheteromeric receptor complexes [5,10,11].

NMDAR subunits have a modular design: each subunit contains an extracellular amino-terminal domain (ATD), an agonist-binding domain (ABD), a trans-membrane domain (TMD), and a cytoplasmic carboxy-terminal domain (CTD), interconnected by polypeptide linkers [1]. Recent structural studies of NMDAR complexes in different conformational states [12] or exploring receptor conformational dynamics [13,14,15] have greatly improved our understanding of NMDARs at the molecular level. NMDAR gating is a coordinated process involving agonist-induced structural rearrangements of the core gating machinery formed by the ABDs and the TMDs of all four subunits. The gating mechanism is regulated by voltage-dependent channel block by Mg^{2+}, and by endogenous allosteric modulation by H^{+}, Zn^{2+}, Ca^{2+}, and several classes of naturally present small molecules [16]. All domains participate in endogenous allosteric modulation. The role of the ATDs in mediating the effects of H^{+} and Zn^{2+} is particularly well described [17]. Our own recent work has contributed to the characterization of NMDAR modulation by endogenous neurosteroids [18,19,20, 21,22] and membrane cholesterol [23,24], that interact primarily with the TMDs. Ca^{2+}-dependent NMDAR modulation involves membrane-proximal regions of the CTDs [25,26,21]. While the intrinsically disordered CTDs resist structural characterization, they are known to contain residues that can undergo post-translational modification, and binding sites for intracellular signaling and scaffolding proteins. The CTDs thus play an important role in regulating NMDAR trafficking, signaling, and even gating [27]. Disease-associated *GRIN* gene variants are found in all receptor domains, and the variant pathogenic effects may be related to any aspect of receptor function, including the gating process, as well as changes in receptor allosteric modulation, post-translational modification, protein-protein interactions or trafficking.

Either excessive or insufficient NMDAR function is associated with neurological or neuro-psychiatric disorders, suggesting a narrow physiological window of NMDAR activity [4]. Consistent with this, *GRIN* genes have low frequencies of variation in the healthy population [28,29,3,1]. In recent years, many *GRIN* gene variants have been identified through high-throughput sequencing in patients with neurological and neuropsychiatric symptoms [28,30,3]. To date, over 700 disease-associated *GRIN* gene variants absent in the healthy population (https://gnomad.broadinstitute.org) have been described, distributed among the different NMDAR subunits, but predominantly found in GluN2A (311 variants, 43 %), GluN2B (258 variants, 35 %) and GluN1 (91 variants, 13 %) [1]. Several different databases collect information about disease-associated *GRIN* gene variants (https://www.ncbi.nlm.nih.gov/clinvar; https://webapp2.pharm.emory.edu/cferv; https://www.grin-database.de/gen_table; https://alf06.uab.es/grindb/home). Most frequent are missense variants in exon regions that result in a single amino acid substitution in the protein sequence. Some patients carry nonsense or frameshift variants that introduce a premature stop codon. Variants in 5′ or 3′ untranslated regions, introns, or splice sites, or large-scale chromosomal rearrangements have also been reported [31]. In an overwhelming majority of cases the

variants arise *de novo* and the variant is present in only one allele of the affected gene [3].

To understand how different variants may lead to disease, many groups have embarked on functional characterization of individual patient-derived *GRIN* gene variants. Here we review the published reports of the functional evaluation of disease-associated variants in *GRIN1*, *GRIN2A*, and *GRIN2B* genes. Most of the reports so far have examined recombinant receptors composed of GluN subunits heterologously expressed in non-neuronal cell types, such as *Xenopus* oocytes or HEK293 cells. Typically, these studies use well-established patch-clamp electrophysiology and immunofluorescence microscopy methods, allowing some comparison across studies and research groups. We have focused on four parameters most commonly used to assess NMDAR function: receptor affinity for glutamate, receptor affinity for glycine, channel open probability (P_o), and receptor cell surface expression. Based on such parameters, pathogenic variants can be classified as loss-of-function (LoF) or gain-of-function (GoF), and therefore as candidates for therapeutic positive or negative pharmacological modulation, respectively. We discuss whether and how the variant position within the subunit amino acid sequence may predict its receptor-level functional consequence(s) [32] and its LoF or GoF classification.

Individual variant pathogenicity at the receptor level, however, may not accurately predict its functional effects at the synaptic, cellular, or system level. Relatively fewer reports include functional data from *in-vitro* neuronal preparations and only a handful of *in-vivo* studies in animal models exist to date. We briefly summarize this work and argue for the need to include these more physiologically relevant experimental models in future studies of the etiology of *GRIN* disorders.

Functional characterization of *GRIN* gene variants in non-neuronal systems

Our literature search found 74 studies [32a] of recombinant receptors heterologously expressed in non-neuronal systems (Tables 1, 2, 3) together reporting functional data for 45 disease-associated GluN1 variants, 72 GluN2A variants, and 70 GluN2B variants (49 %, 23 %, and 27 % of disease-associated GluN1, GluN2A, and GluN2B variants reported in [1], respectively). This represents a substantial body of work that is beginning to yield insights not only into the mechanisms of pathogenicity of different *GRIN* gene variants, but also into NMDAR structure and function more generally.

Importantly, patients are typically heterozygous for their *GRIN* gene variant, so any individual patient's NMDARs may be functionally heterogeneous: some may be composed entirely of unaffected subunits and some may include one or two subunits containing the potentially pathogenic variant combined with unaffected subunits of various types. It is therefore necessary to study not only diheteromeric receptors containing two variant subunits, but also triheteromeric receptors containing only one potentially pathogenic variant subunit. Typically, the function of triheteromeric receptors containing one variant subunit was found to be intermediate between the function of wild-type receptors and diheteromeric receptors containing two variant subunits [33,34,35,36,37,38]. For some variants, triheteromeric receptors show a functional deficit comparable to diheteromeric receptors (e.g., GluN2A-D731N [39]; GluN2A-N616K [40]). While studies of triheteromeric receptors are essential, here we focus on results obtained for diheteromeric receptors (Tables 1, 2, 3, Figs 1, 2, 3, 4), because these data represent the majority of the available information.

It is useful when studies directly compare effects of different variants, ideally with multiple functional parameters assessed in the same system [34,41,42,40,43,44,45]. These data often illustrate that individual variants can affect multiple functional parameters, sometimes in contradictory directions, complicating simple variant classification as LoF or GoF [43,44,45]. Some studies have proposed ways to integrate information about multiple functional parameters into one readout, for example by estimating how a variant would affect synaptic charge transfer or Ca^{2+} influx, to evaluate the overall impact of the variant on physiologically relevant NMDAR signaling [34,44,46].

Though imperfect, variant classification as LoF or GoF has prompted pharmacological investigations with the goal of identifying suitable NMDAR modulators that could correct the functional change associated with different disease-associated variants. Most generally, negative allosteric modulators show promise in treating certain GoF variants [47,48], while positive modulators may compensate for the effects of LoF variants [49,50]. Ultimately, pharmacological intervention should be more sophisticated and specifically target the functional parameters altered by the variant. Importantly, individual variants can show reduced or enhanced sensitivity to different modulators [51,42,52,53,50,48], further

emphasizing the need to tailor therapy to the specific variant present. While we do not discuss rescue pharmacology of disease-associated *GRIN* gene variants any further in this review, the relevant references are included. Several clinical case studies illustrate the benefit of pharmacological treatment for some carriers of pathogenic *GRIN* gene variants [54,28,55,56,57,58], and it is results like these that motivate the continued effort to characterize the functional impact of different *GRIN* gene variants in order to design appropriate therapy.

Glutamate and glycine affinity

The ABD of the GluN1 subunit binds the NMDAR co-agonist glycine or D-serine, while the ABDs of GluN2 subunits bind the agonist glutamate. NMDAR affinity for glutamate depends on the types of GluN2 subunits present in the receptor complex, with GluN2A associated with a lower glutamate affinity than GluN2B [1]. Receptor affinity for glutamate influences the rate of receptor deactivation following a brief synaptic-like glutamate transient [59], such that a lower-affinity receptor–glutamate interaction (typical for GluN2A-containing receptors) results in faster kinetics of receptor deactivation, while a higher-affinity interaction (characteristic for GluN2B-containing receptors) leads to slower deactivation. Receptor deactivation kinetics in turn influence the charge transfer and the Ca^{2+} influx through synaptically activated NMDARs, with consequences for downstream signalling [1]. In addition, the quality control of the nascent receptor complexes in the endoplasmic reticulum (ER) is based, in part, on glutamate and glycine affinity, and receptors with very low agonist and/or co-agonist affinity fail to reach the cell

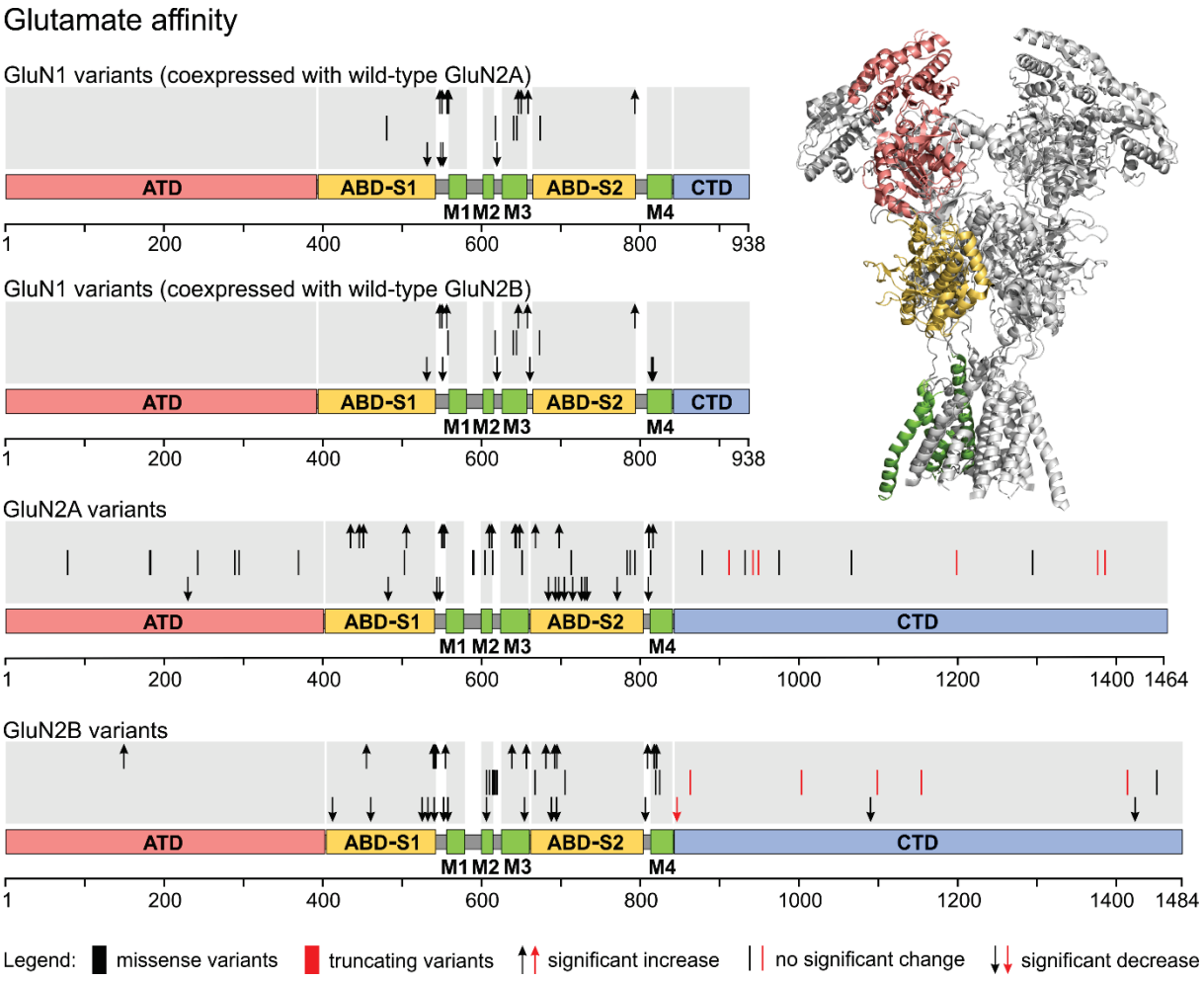

Fig. 1. Effects of disease-associated *GRIN* gene variants on glutamate affinity. Relationship between the amino acid positions of individual variants (scale shown below the schematic of the domain structure of each subunit) and the observed effect on glutamate affinity (increase, decrease, no change), as determined for diheteromeric recombinant receptors in non-neuronal cells. ATD, amino-terminal domain; ABD-S1 and ABD-S2, agonist-binding domain segments S1 and S2; M1–M4, transmembrane domain (TMD) helices; CTD, carboxy-terminal domain. Inset shows human GluN1/GluN2A diheteromeric complex (PDB: 7EU7) with GluN1 ATD, ABD, and TMD highlighted in colors corresponding to the schematic of the domain structure; the CTD is not included in this receptor structure.

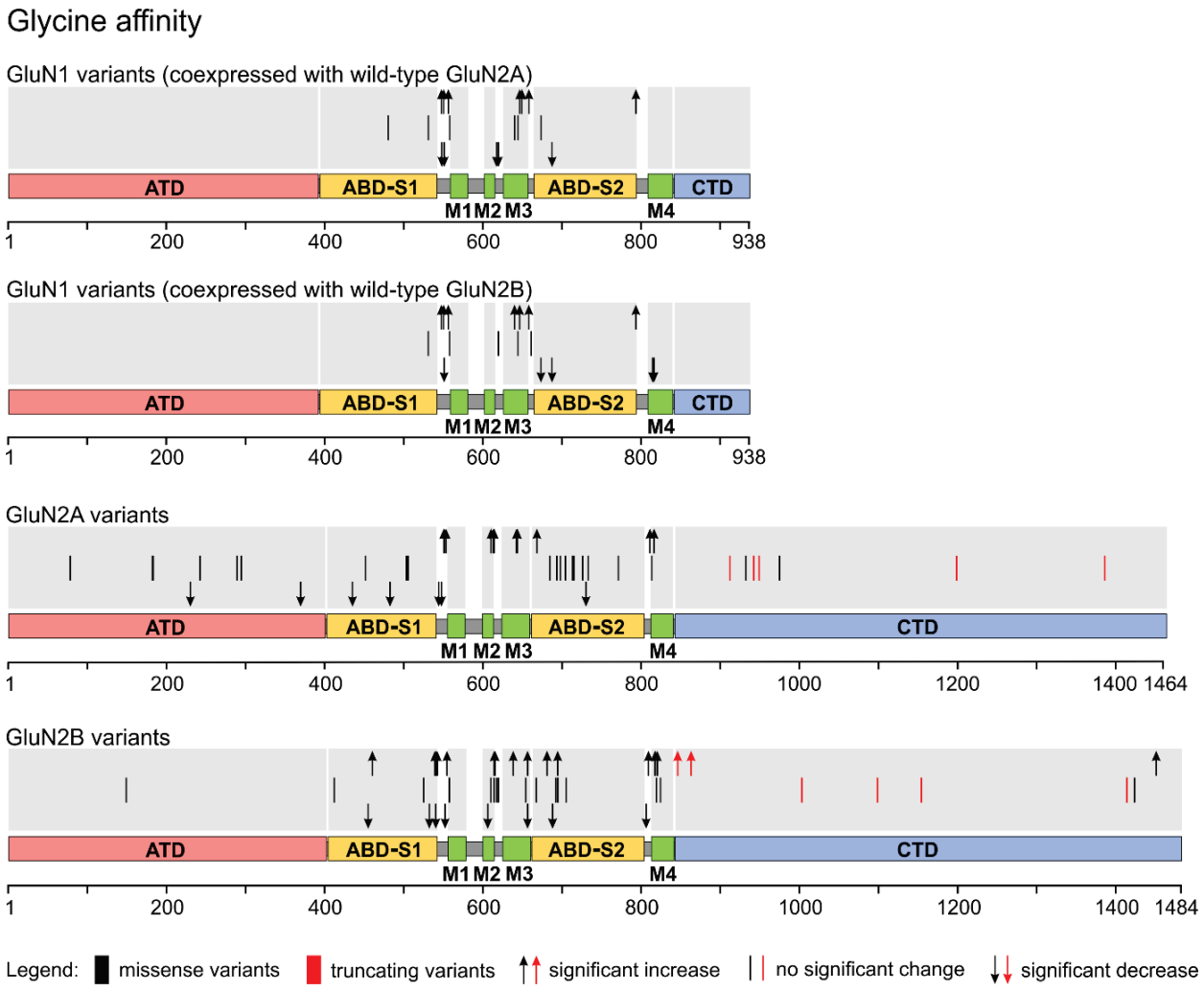

Fig. 2. Effects of disease-associated *GRIN* gene variants on glycine affinity. Relationship between the amino acid positions of individual variants (scale shown below the schematic of the domain structure of each subunit) and the observed effect on glycine affinity (increase, decrease, no change), as determined for diheteromeric recombinant receptors in non-neuronal cells. Abbreviations as in Figure 1.

surface [60]. Glutamate and glycine affinity thus represent key functional parameters influencing NMDAR signalling. In whole-cell patch-clamp measurements of agonist-evoked currents, a change in the receptor affinity for glutamate or glycine is quantified as a change in the concentration of glutamate or glycine that evokes a half-maximal current response (EC_{50}), with a higher affinity associated with a lower EC_{50} value and *vice versa*.

For disease-associated variants for which agonist/co-agonist affinity was reported we summarize the consensus regarding the observed changes (increase, decrease, or no change), or indicate if different studies reached different conclusions (Tables 1,2,3). We plot the qualitative change in glutamate or glycine affinity as a function of the amino acid position of the variant (Figs. 1,2). Missense variants causing significant changes in glutamate or glycine affinity tend to be localized in the ABDs, ABD-TMD linkers, and in the TMDs [34,41,42,61,32]. Variants in the ATDs and the CTDs are considerably understudied, but those that have been evaluated tend to leave the agonist/co-agonist affinity intact, with some exceptions [62,63]. It is difficult to predict the direction of the change based on the location of the variant in the subunit amino acid sequence. This could be related to the nature of the amino acid substitution in the variant, as illustrated by two different disease-associated variants affecting serine S541 in GluN2B: a substitution of this serine by glycine (S541G) results in a significant increase of both glutamate and glycine affinities but a substitution of the same serine by arginine (S541R) results in a significant decrease of glutamate and glycine affinities [45]. Cases where the same residue is altered by more than one disease-associated variant (Tables 1, 2, 3) need further study.

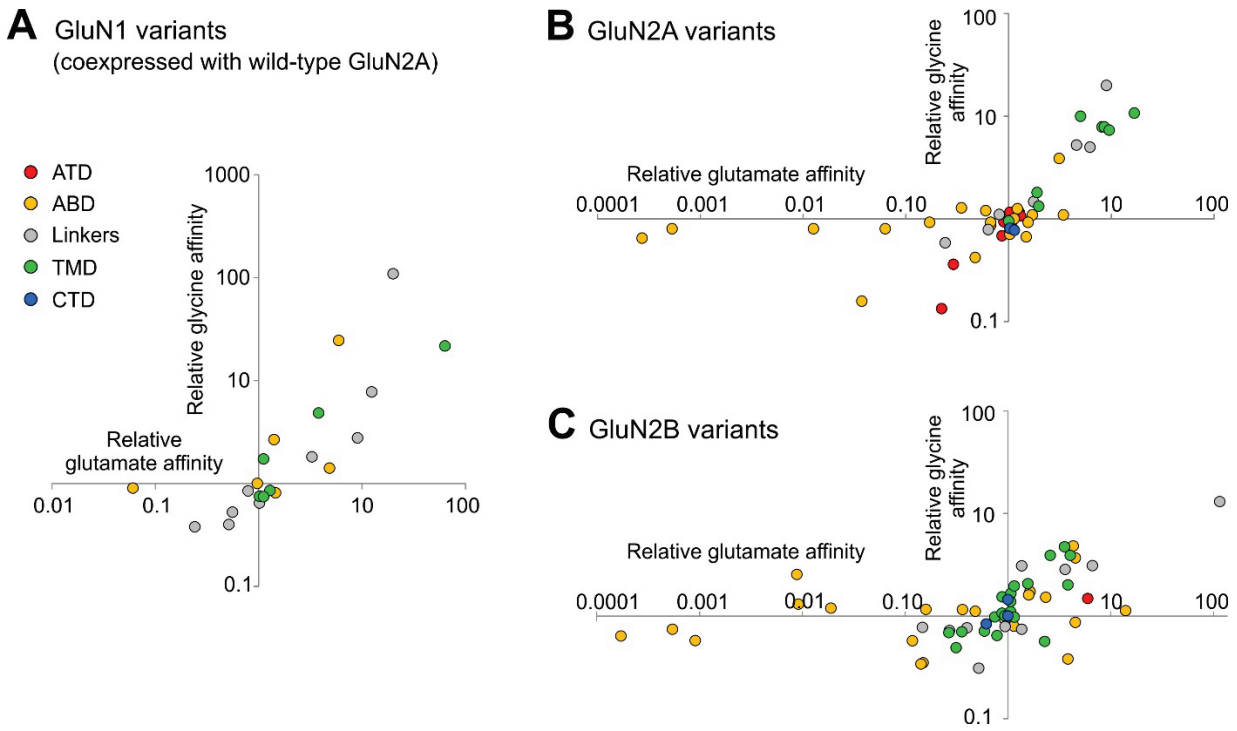

Fig. 3. Relationship between disease-associated missense *GRIN* gene variant effects on glutamate and glycine affinity. Glutamate vs. glycine affinity for individual missense *GRIN* gene variants relative to wild-type as determined for diheteromeric recombinant receptors in non-neuronal cells. The position of each variant within the domain structure of the subunit is indicated by color.

Interestingly, it is very common that variants in GluN1 change not only the affinity for glycine that binds to the GluN1 ABD, but also the affinity for glutamate that binds to the ABDs of the unaffected GluN2 subunits. Similarly, GluN2 variants are often associated with a change in the affinity not only for glutamate but also for glycine. This observation may be related to the fact that glutamate and glycine binding sites in the NMDAR complex are allosterically coupled [64,1]. Indeed, Figure 3 shows that the changes in glutamate and glycine affinity observed for individual variants are correlated. Several variants show a very large (>10-fold) change in glutamate affinity, with variants associated with the strongest decrease in glutamate affinity located in the GluN2A or GluN2B ABDs. For glycine, >10-fold increase in affinity can be seen for several variants but none show >10-fold decrease in affinity. The transient concentration of glutamate released into the synaptic cleft is supersaturating for the glutamate binding sites at the GluN2 subunits [65,1], thus even a substantial decrease in glutamate affinity may be relatively well tolerated. On the other hand, the binding sites for glycine/D-serine at the GluN1 subunits are likely not saturated by ambient co-agonist concentrations [66,67], so a substantial decrease in glycine affinity may be too damaging.

Channel open probability

Upon agonist/co-agonist binding, the channel may undergo the transition from the closed to the open state. Based on kinetic models of NMDAR activation [59,68], channel open probability (P_o) can be expressed in terms of the rate constants of transitions to and from the open state. The P_o is influenced by the combination of GluN2 subunits in the NMDAR complex, with GluN2A associated with a higher P_o than GluN2B [1]. In single-channel experiments the P_o typically refers to the proportion of the total recording time that the channel spends in the open state under conditions of steady-state activation by saturating agonist/co-agonist concentrations [38]. In whole-cell patch-clamp experiments, the P_o can be estimated from the time course of receptor inhibition by an open-channel blocker MK-801 [42], or from the degree of potentiation induced in receptors containing GluN1-A652C (or GluN2A-A650C) by a cysteine-modifying reagent MTSEA that locks receptors in the open state [34,40].

NMDAR P_o has been evaluated for only a small proportion of disease-associated variants (Fig. 4). Given that channel gating fundamentally involves the TMDs, the P_o is particularly influenced by missense variants in the ABD-TMD linkers [34,45] and the TMD helices

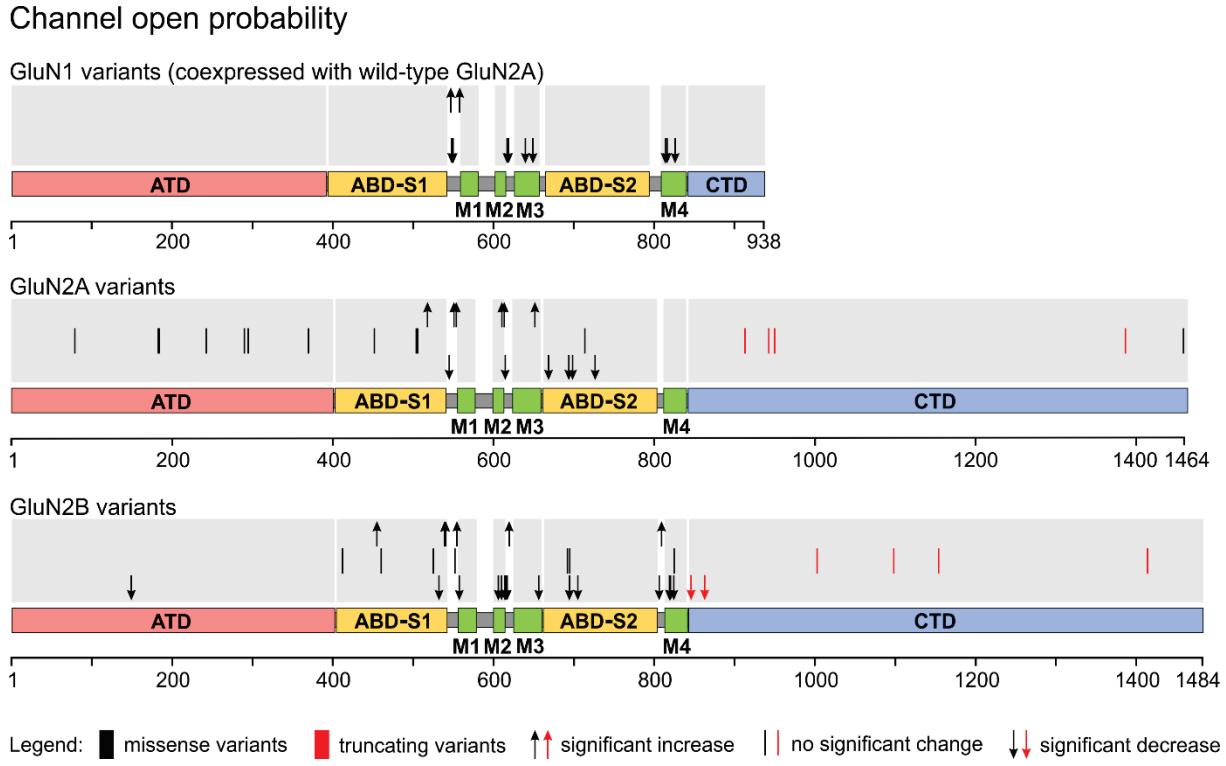

Fig. 4. Effects of disease-associated *GRIN* gene variants on NMDAR P_o. Relationship between the amino acid positions of individual variants and the observed qualitative effect on NMDAR P_o (increase, decrease, no change), as determined for diheteromeric recombinant receptors in non-neuronal cells. Abbreviations as in Figure 1.

[42,38,40]. Membrane regions determine additional aspects of NMDAR channel function, such as Ca^{2+} permeability and Mg^{2+} block, so disease-associated variants located in the TMDs often have a complex receptor-level functional phenotype [38,40,69,48]. Similar to the analysis of agonist/co-agonist affinities, missense variants in the ATDs or the CTDs generally do not change the P_o, but additional variants in these domains should be tested.

Receptor cell surface expression

The assembly of NMDAR complexes and their delivery to the cell surface is a key prerequisite for proper receptor signalling, therefore receptor surface expression is an essential parameter influencing the functional outcome associated with individual disease-associated variants. Heterotetrameric NMDAR complex is assembled in the ER [60], with the ATDs, ABDs, and TMDs all participating in proper protein folding and subunit assembly. In addition, several different polypeptide motifs promoting ER retention or ER export have been described, most located in the CTDs of GluN1 or GluN2A/GluN2B subunits [70]. In neurons, the abundance of NMDAR complexes in the postsynaptic membrane is regulated by the interplay between receptor internalization driven by endocytic signal sequences in the CTDs and receptor anchoring in the synapse *via* interactions between the CTDs and synaptic scaffolding proteins [27]. To analyze receptor surface expression, most studies have used the endogenous trafficking system of stable cell lines (HEK293T or COS-7). A commonly used approach is to express variant or wild-type GluN subunit with a tag fused to its extracellular end. Surface and intracellular expression of the studied subunit can then be assessed by sequential immunofluorescent labeling performed under non-permeabilizing and permeabilizing conditions, respectively [41,42,43,53,71]. Some studies have used surface protein biotinylation assays [37,72], or expressed β-lactamase fused to the ATD of the studied GluN subunit and performed a colorimetric measurement of β-lactamase activity on the surface of transfected cells [34,40,45].

Disease-associated missense variants in the ABDs and the TMDs in all subunits can influence receptor surface expression (Fig. 5). Interestingly, while many ABD or TMD variants decrease receptor surface expression [34,37,41,42,53], only a few have been found to have the opposite effect [42,73,71,45]. This suggests

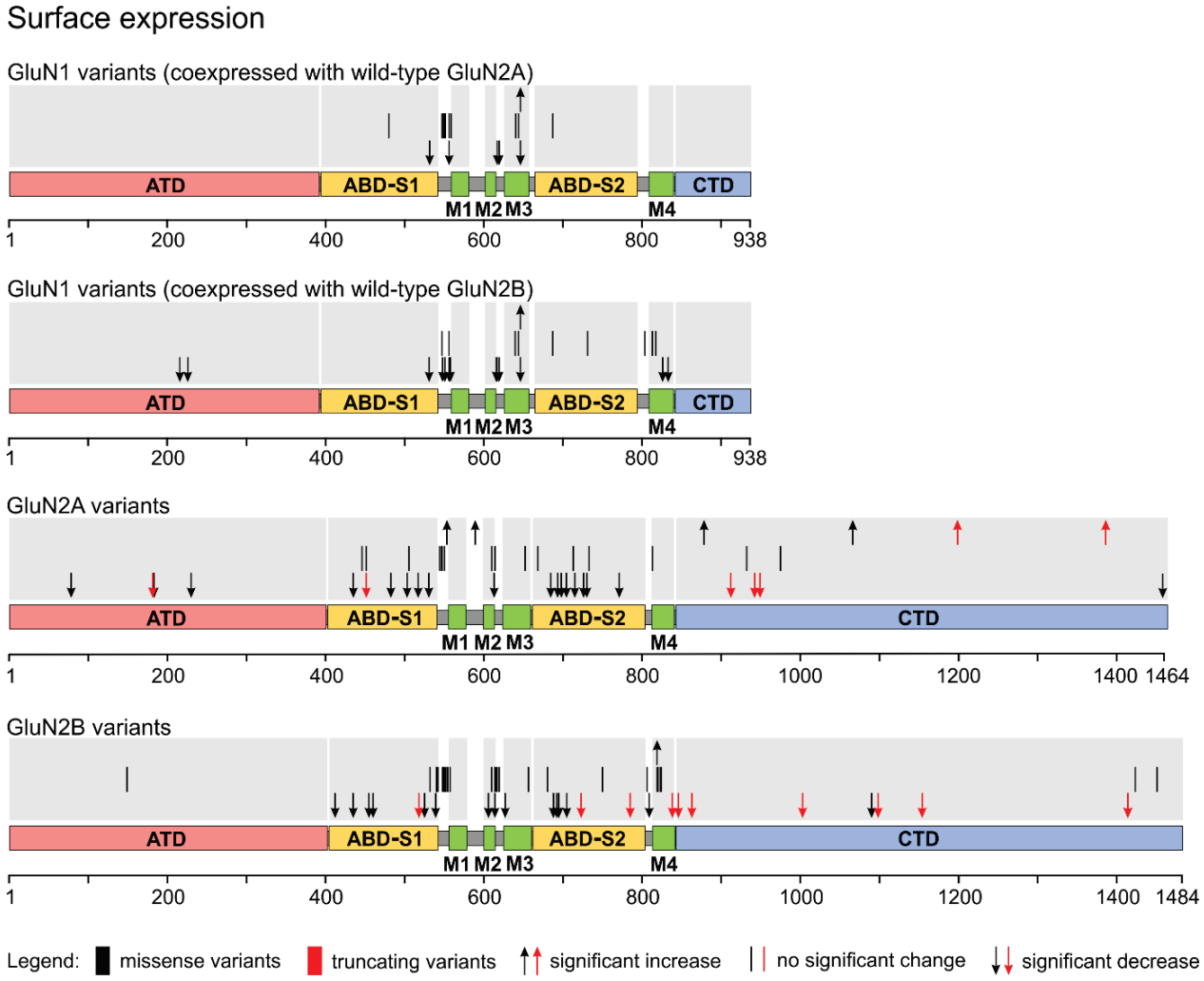

Fig. 5. Effects of disease-associated *GRIN* gene variants on receptor surface expression. Relationship between the amino acid positions of individual variants and the observed effect (increase, decrease, no change) on the variant-containing subunit surface expression, as determined for recombinant receptors in non-neuronal cells. Abbreviations as in Figure 1.

that the nascent receptor quality control is very strict, and any conformational changes that may affect tetramer stability or impair agonist binding or receptor gating prevent receptor trafficking to the cell surface. In contrast to the agonist/co-agonist affinity and the P_o that tend to be relatively unaffected by missense variants in the ATDs and CTDs, receptor surface expression is sensitive to variants in these domains, possibly because disease-associated variants may impair receptor assembly regulated by the ATDs, or disrupt the trafficking and sorting signal sequences present in the CTDs [43,73,74]. Non-neuronal cell lines used for surface expression analyses express only some scaffolding proteins, but biochemical assays can be used to show that certain disease-associated variants in the GluN2A or GluN2B CTDs disrupt the binding of the affected subunits to synaptic scaffolding proteins such as PSD-95 [62,75,63], predicting a deficit in synaptic targeting of these variant-containing subunits.

Disease-associated *GRIN* gene variants resulting in protein truncation

Some disease-associated *GRIN* gene variants introduce a premature stop codon predicted to create a truncated protein. Protein-truncating variants (PTVs) account for 20-25 % of disease-associated *GRIN* gene variants and they tend to be associated with a less severe clinical presentation [29,76,1]. Interestingly, GluN1 PTVs in the heterozygous condition are non-pathogenic [76]. Some authors consider PTVs to be null variants [29], assuming that the variant-containing mRNA is degraded by nonsense-mediated decay, producing simple haploinsufficiency. However, it is likely that mRNA surveillance mechanisms may activate compensatory changes in the expression of the unaffected allele or other

functionally related genes [77]. Further, nonsense-mediated decay is less efficient in neurons, particularly early in development, leaving open the possibility that truncated proteins may be expressed to some extent [78].

Nevertheless, GluN1, GluN2A, or GluN2B subunits truncated in any domain other than the CTD are virtually absent from the cell surface [79,76] (Fig. 5); such PTVs can thus be considered functionally null. In contrast, for PTVs affecting the CTD, the truncated protein is expressed and can be analyzed functionally [22] (Figs. 1, 2, 4). All CTD truncating variants studied so far lead to altered subunit surface expression, but for the most part they do not affect the receptor functionally [22]. Only the variants causing the most extensive CTD truncation (e.g., GluN2B-R847X and GluN2B-I864SfsX20) show some effects on agonist/co-agonist affinity, receptor desensitization, and the P_o [22]. While more work is needed, data so far suggest that, compared to missense variants, *GRIN* gene PTVs in any domain other than the CTD form a more homogeneous group leading to haploinsufficiency, with relatively milder symptoms in carriers. These findings may open new possibilities for non-pharmacological (genetic) therapy for patients with more damaging *GRIN* variants that could possibly be silenced by a newly introduced premature stop codon in the aberrant *GRIN* allele.

Functional characterization of *GRIN* gene variants in neurons *in vitro*

Much useful functional information about disease-associated *GRIN* gene variants has been gained from studies in non-neuronal heterologous expression systems, but there are aspects of NMDAR function that are influenced by conditions specific to neurons. NMDARs operate in a highly specialized subcellular compartment – the synapse – where they interact with a specific microenvironment characterized by distinct membrane composition and a dense network of scaffolding and signaling proteins. Neuronal NMDARs assemble as various combinations of different subunits, and the effects of disease-associated variants should be characterized in this context. To study a disease-associated variant in neurons it is necessary to work out a strategy for expressing the variant-containing subunit in the presence or absence of native subunits expressed endogenously [80]. This is a challenge and an opportunity: with appropriate experimental design studies in neurons can elucidate effects of disease-associated variants under more physiological and clinically relevant conditions.

To study NMDARs with a defined subunit composition in neurons, one group focused on the obligatory GluN1 subunit, using shRNA knockdown of native GluN1 combined with the expression of variant-containing GluN1 subunits [61,53,71]. This strategy, assuming efficient knockdown, results in receptors containing two copies of the variant-containing GluN1 subunit, similar to non-neuronal heterologous expression of diheteromeric receptors. Indeed, in these studies, experiments in neurons largely confirmed effects of GluN1 variants observed in non-neuronal models.

It is more complicated to characterize effects of disease-associated GluN2 subunit variants, because the different GluN2 subunit types may partially substitute for each other. Since NMDARs in principal neurons in the cortex and hippocampus predominantly contain GluN2A and/or GluN2B subunits [4], Cre-Lox recombination in excitatory neurons prepared from *Grin2a*$^{fl/fl}$/*Grin2b*$^{fl/fl}$ mice effectively eliminates the majority of native GluN2 subunit expression [6]. In a series of elegant molecular replacement experiments, GluN2A or GluN2B subunits containing specific disease-associated variants were introduced together with Cre-recombinase in neurons from *Grin2a*$^{fl/fl}$/*Grin2b*$^{fl/fl}$ mice [62,81,82]. In the simplest case, native GluN2A and GluN2B are both eliminated and replaced only with wild-type or variant GluN2A [81] or only with wild-type or variant GluN2B [62,82]. The results of such experiments tend to confirm the LoF or GoF phenotypes of the variants, similar to results observed in non-neuronal systems. Most revealing, however, are experiments in *Grin2a*$^{fl/fl}$ mice where native GluN2A is replaced with variant-containing GluN2A, while the native GluN2B expression is left intact [81], or experiments in *Grin2b*$^{fl/fl}$ mice where native GluN2B is replaced with variant-containing GluN2B, while the native GluN2A expression is intact [82]. In the first case, surprisingly, the outcome of expressing either LoF or GoF GluN2A variants is similar, with excitatory postsynaptic currents (EPSCs) characterized by slower deactivation kinetics. This reflects either the GoF of the GluN2A variant or, in case of the LoF GluN2A variants, the increased relative contribution of native GluN2B subunits to synaptic NMDAR currents [81]. In the second case, the expression of either LoF or GoF GluN2B variants in the presence of native GluN2A results in EPSCs with faster deactivation kinetics, in part because the GoF phenotype of certain GluN2B variants is lost in

triheteromeric receptors containing the GluN2B variant together with wild-type GluN2A [82]. These results suggest that for some variants the functional phenotype at the receptor level may not accurately predict the functional phenotype at the synaptic level, underscoring the need for more work in neuronal preparations.

Many studies have expressed variant subunits in neurons on the background of endogenous expression of native subunits. This approach is technically relatively simple and can address cell surface or synaptic expression of subunits harboring disease-associated variants in the presence of neuronal trafficking and scaffolding machinery. Several studies have expressed tagged variant-containing subunits in neurons and used immunofluorescence microscopy to evaluate the levels of dendritic surface expression of the different variants [34,62,79,75,76,61,53,71,22]. Synaptic localization of variant subunits can be examined more specifically, for example by quantifying colocalization between the tagged subunit and endogenous PSD-95 [22]. A few reports include surface expression data for the same variants in a non-neuronal system and in neurons, in some cases finding comparable results [79,61,53,71], and in other cases finding qualitative or quantitative differences between variant subunit trafficking in neurons and in non-neuronal systems [34,76,22].

Functionally, expressing a disease-associated variant subunit in neurons on the background of endogenous expression of native subunits may approximate the situation in patients heterozygous for the variant, if the method used does not result in significant overexpression of the introduced subunit [51,79]. Such experiments tend to show that in the presence of native wild-type subunits, the functional consequences of the variant are more subtle than in non-neuronal heterologous expression systems, with wild-type subunits partially mitigating the effects of the pathogenic variant [51]. Studies of this type can also begin to address possible indirect effects of changes in NMDAR signaling due to disease-associated variants on synapse structure and function and the development of neural networks [79,75,63].

Functional characterization of *GRIN* gene variants in animal models

Methods used to introduce subunits containing disease-associated variants to neurons in culture or in acute slices only achieve transient expression of the target subunit in a subset of cells in the preparation. As a result, these experiments can only describe relatively acute and cell-autonomous effects of disease-associated variants [80]. However, in patients, the *GRIN* gene variant is permanently present in all cells, and patient symptoms may be related to circuit-level effects of the variant, possibly influenced by compensatory changes of gene expression, synapse structure or function, or circuit connectivity. Transgenic animal models can be used to reveal how changes in NMDAR signaling due to the widespread and chronic presence of the pathogenic *GRIN* gene variant may affect the nervous system function and development.

Mouse strains with targeted disruption of *Grin1* [83], *Grin2a* [84], or *Grin2b* [85] may serve as models of null variants in the corresponding human *GRIN* genes, with heterozygous animals representing the condition of patients. Mouse strains with truncated *Grin2a* or *Grin2b* gene leading to the expression of GluN2A or GluN2B subunits lacking the CTDs have also been created [86]. While homozygous animals of these strains have been characterized, data about heterozygous animals are limited. Heterozygous $Grin1^{-/+}$ mice are healthy and their neurons have normal NMDAR responses [83], consistent with the finding that truncating human *GRIN1* variants in the heterozygous condition are not pathogenic [76]. Recently, some studies have examined selected parameters in heterozygous $Grin2a^{-/+}$ mice [87,88,89] and $Grin2b^{-/+}$ mice [90], generally observing a milder phenotype in heterozygous compared to homozygous animals. Still, much more work is needed to understand the effects of *GRIN2A* or *GRIN2B* haploinsufficiency at the cellular, circuit, and system level. Additional useful data may emerge from using a zebrafish (*Danio rerio*) model to study the developmental roles of different NMDAR subunits [91,92].

Very few transgenic mouse models of specific patient-derived *GRIN* gene variants have been created to date. In 2010, a large-scale mutagenesis project at RIKEN generated a mouse strain expressing GluN1-R844C [93], a variant subsequently identified in two patients with severe intellectual disability, motor disorder, and seizures [94]. At the receptor level this variant has no apparent functional phenotype and in heterozygous mice it is associated with hyperactivity and increased novelty-seeking behavior [93].

Three mouse strains expressing patient-derived GluN2A variants, all associated with intellectual disability and epilepsy, have been described. The variant

GluN2A-S644G [95] increases glutamate and glycine affinity and prolongs NMDAR EPSC deactivation, and in heterozygous animals it is associated with abnormal network activity, hyperactive behaviors, and mixed effects on seizure susceptibility [95]. The variant GluN2A-K879R increases subunit surface expression [74], and in heterozygous animals it is associated with increased NMDAR EPSC amplitude but faster deactivation, altered levels of surface expression of NMDAR and AMPAR subunits, synaptic plasticity deficits, and impaired cognitive function [74]. The variant GluN2A-V685G reduces NMDAR glutamate affinity and surface expression [34], and reduces NMDAR EPSC amplitude, yet this LoF variant increases seizure susceptibility in heterozygous mice, possibly due to circuit-level effects on excitation/inhibition balance [96].

To our knowledge, two mouse models of disease-associated GluN2B variants, both found in patients with intellectual disability and autism, have been created to date. The variant GluN2B-C456Y [90] strongly reduces receptor surface expression [34] and in heterozygous animals it is associated with smaller and faster NMDAR EPSCs, mild deficits in long-term synaptic depression, and hypoactivity and reduced anxiety [90]. The variant GluN2B-L825V reduces receptor P_o [42] (but see [38]), and in heterozygous animals it leads to NMDAR EPSCs with faster deactivation, hypoactivity in the open field, impaired sensorimotor gating, and cognitive inflexibility [97].

Together, these examples illustrate how difficult it is to extrapolate the receptor-level functional phenotype of a given variant to its circuit-level or system-level effects that ultimately underlie symptoms in carriers. Many more disease-associated *GRIN* gene variants need to be studied in animal models and their impact should be examined thoroughly, not only in the canonical circuits (hippocampus, cortex), but in multiple brain regions, over the course of development, and in both sexes. A better understanding of how different *GRIN* gene variants lead to neurological and neuropsychiatric disease is a prerequisite for finding effective therapies for *GRIN* disorders.

Conclusions

Here we present a comprehensive review of the literature on the functional evaluation of human disease-associated variants in *GRIN1, GRIN2A* and *GRIN2B* genes. Most information so far comes from studies of receptor-level effects of *GRIN* gene variants in non-neuronal systems. These studies establish that variants in the core gating region comprised of the ABDs, the TMDs, and the ABD-TMD linkers frequently lead to profound changes of receptor function manifested as changes in agonist/co-agonist affinity, channel open probability, and/or receptor surface expression. Variants in the ATDs and the CTDs can significantly affect receptor surface expression, but have been relatively overlooked so far. An individual variant often influences multiple functional parameters, which may complicate variant classification as LoF or GoF, and the receptor-level functional impact may not accurately predict the consequences observed at the synaptic, cellular, or circuit level in neuronal preparations or animal models. Taking advantage of the more physiological experimental models in the future should lead to further advances in the understanding of the role of NMDAR signaling in healthy nervous system function, and in the etiology of *GRIN* disorders.

Conflict of Interest

There is no conflict of interest.

Acknowledgements

This work was supported by the Czech Science Foundation: 23-04922S; the Ministry of Education, Youth and Sports of the Czech Republic: Program LT—INTER-EXCELLENCE LTAUSA19122; the Charles University Grant Agency: 410122 and 318323; institutional support RVO: 67985823.

Abbreviations

ATD, amino-terminal domain; ABD-S1 and ABD-S2, agonist-binding domain segments S1 and S2; CTD, carboxy-terminal domain; del, deletion; dup, duplication; ins, insertion; fs, frame shift; M1–M4, transmembrane domain (TMD) helices; Ter, termination codon.

Table 1. Functional characterization of disease-associated variants in *GRIN1*/GluN1.

DNA	Protein	Coexpressed with GluN2A				Coexpressed with GluN2B			Functional characterization references	
		P_o	Glu[1]	Gly[2]	Surface Expression	Glu[1]	Gly[2]	Surface Expression	Non-neuronal cells	Neurons
c.649C>T	R217W					↓			[94], [43]	
c.679G>C	D227H							↓	[43]	
c.803G>A	W247Ter							↓	[76]	
c.977del	P305RfsTer21							↓	[76]	
c.1378A>G	I460V*		⇄	⇄	⇄				[98]	[98]
c.1567C>T	R523C								[99]	
c.1595C>A	P532H		↓	⇄	↓	↓	⇄	↓	[100]	
c.1643G>A	R548Q	↑	↑	↑	⇄	↑	↑	⇄	[45]	
c.1705C>T	R548W				⇄				[43]	
c.1645A>C	S549R	↓	↓	↓	⇄			↓	[94], [45]	
c.1652T>C	L551P	↓	↑	↑	⇄	↑	↑		[45]	
c.1656C>G	D552E		↓	↓	⇄	↓	↓	↓	[94], [37], [46]	
c.1666C>T	Q556Ter							↓	[94], [76]	
c.1670C>T	P557L				⇄			↓	[73]	
c.1670C>G	P557R		↑	↑	↓	↑	↑	⇄	[94], [37]	
c.1676A>G	Q559R	↑	↑	⇄	⇄	⇄	⇄	↓	[45]	
c.1679_1681dup	S560insS				⇄			↓	[94], [45], [101]	
c.1851C>A	S617C							↓	[43]	
c.1852G>C	G618R	↓	⇄	↓	↓	⇄		↓	[94]	
c.1854_1859dup	I619_G620dup							↓	[43]	
c.1858G>C	G620R	↓	↓	↓	⇄/↓	↓	⇄	⇄/↓	[94], [102], [40], [43]	
c.1923G>A	M641I	↓	⇄	⇄	↓	⇄	↑	⇄	[94], [56], [46], [53], [57]	[53]
c.1921A>G	M641V							⇄	[43]	
c.1933G>T	A645S*		⇄	⇄/↑	⇄	⇄	⇄	⇄	[94], [53], [98]	[53], [98]
c.1939T>C	Y647H*		↑	↑	↓				[98]	[98]
c.1940A>C	Y647S				↓			↓	[94], [53]	[53]
c.1940A>G	Y647C		↑	↑	↑	↑	↑	↑	[103]	
c.1950C>G	N650K	↓	↑	↑					[94], [71]	[71]
c.1975C>T	R659W		↑	↑		↑	↑		[103]	
c.1984G>A	E662K					↓	⇄		[94], [101]	
c.2021A>T	N674I		⇄	⇄		⇄	↓		[103]	
c.2063C>A	S688Y			↓	⇄		↓		[61]	[61]
c.2196T>G	D732E							⇄	[43]	
c.2365G>A	D789N								[103]	
c.2381G>A	R794Q		↑	↑		↑	↑		[103]	
c.2414C>T	P805L							⇄	[43]	
c.2413C>T	P805S							⇄	[43]	
c.2441C>A	A814D							⇄	[43]	
c.2443G>A	G815R	↓				↓	↓		[94], [38], [46]	
c.2444G>T	G815V	↓							[94], [38]	
c.2449T>C	F817L	↓				↓	↓		[94], [38]	
c.2515A>G	M818V							⇄	[43]	
c.2479G>A	G827R	↓						↓	[94], [38], [43]	
c.2500G>C	E834Q							↓	[43]	
c.2530C>T	R844C								[94]	[93]

[1]Affinity for glutamate [2]Affinity for glycine ↑ = increase compared to WT ↓ = decrease compared to WT ⇄ = no change compared to WT

Color denotes the domain: red = ATD; yellow = ABD; grey = linkers; green = TMD; blue = CTD

Abbreviations: del, deletion; dup, duplication; ins, insertion; fs, frame shift; Ter, termination codon. All variants refer to the sequence of GluN1-1a. *Variants GluN1-I460V, GluN1-A645S, and GluN1-Y647H were studied in GluN1-3b [96] where they correspond to I481V, A666S, and Y668H, respectively. In this and all other Tables, when the literature provides multiple measurements of the same parameter for the same variant, we consider this parameter to be significantly increased (decreased) if most studies report a significantly increased (decreased) value. Where no clear consensus exists, different reported outcomes are indicated.

Table 2. Functional characterization of disease-associated variants in *GRIN2A*/GluN2A.

DNA	Protein	P_o	Glu[1]	Gly[2]	Surface Expression	Functional characterization references	
						Non-neuronal cells	Neurons
c.172G>T	E58Ter					[104]	
c.236C>G	P79R	⇄	⇄	⇄	↓	[41], [35]	[35]
c.544del	E182NfsTer22				↓	[76]	
c.547T>A	F183I	⇄	⇄	⇄		[35]	
c.551T>G	I184S	⇄	⇄	⇄	↓	[35], [105]	
c.692G>A	C231Y		↓	↓	↓	[41], [35]	
c.728C>T	A243V	⇄	⇄	⇄		[35], [46]	
c.869C>T	A290V	⇄	⇄	⇄		[35]	
c.883G>A	G295S	⇄	⇄	⇄		[35]	
c.1108C>T	R370W	⇄	⇄	↓		[35]	[35]
c.1306T>C	C436R		↑	↓	↓	[41], [35], [34], [49]	[81], [82]
c.1341T>A	N447K		↑		⇄	[107]	
c.1354G>A	V452M	⇄	↑	⇄	⇄	[34]	
c.1354insT	V452CfsTer11				↓	[76]	
c.1447G>A	G483R		↓	↓	↓	[41], [34], [49], [108]	
c.1510C>T	R504W	⇄	⇄	⇄	↓	[34]	
c.1517T>C	V506A	⇄	↑	⇄	⇄	[34]	
c.1553G>A	R518H	↑			↓	[105], [34], [106]	[81]
c.1592C>T	T531M				↓	[34], [109]	[81]
c.1634C>T	S545L	↓	↓	↓	⇄	[45]	
c.1639_1641del	S547del				⇄	[45]	
c.1642G>A	A548T		↓	↓	⇄	[37], [49]	
c.1651G>A	E551K	↑	↑	↑	⇄	[47], [45]	
c.1655C>G	P552R		↑	↑	⇄	[47], [37], [110]	[37]
c.1661G>C	S554T	↑	↑	↑	↑	[45]	
c.1757G>A	R586K					[111]	[111]
c.1770A>C	K590N		⇄		↑	[73]	
c.1771G>A	G591R		⇄			[104]	
c.1815A>G	I605M		⇄			[104]	
c.1832T>A	L611Q	↑	↑	↑	⇄	[40], [48]	
c.1841A>G	N614S	↑	↑	↑	↓	[40], [48], [46]	
c.1845C>A	N615K	↓	⇄	↑	⇄	[112], [54], [40], [69], [113], [48], [114]	[69]
c.1844A>G	N615S*						[115]
c.1923G>A	M641I					[56]	
c.1928C>A	A643D		↑	↑		[116], [49]	
c.1930A>G	S644G		↑	↑		[47], [95]	[95]
c.1945C>G	L649V		↑			[47]	
c.1954T>G	F652V	↑	⇄			[110], [106]	
c.1959G>A	M653I					[104]	
c.2007G>T	K669N	↓	↑	↑	⇄	[34]	[81]
c.2054T>C	V685G		↓	⇄	↓	[34], [49]	
c.2081T>C	I694T	↓	↓	⇄	↓	[34]	
c.2093A>G	Y698C		↓			[104]	
c.2095C>T	P699S	⇄/↓	↑	⇄	↓	[34], [49], [108]	
c.2100C>G	Y700Ter					[104]	
c.2113A>G	M705V		↓	⇄	↓	[41], [34], [49], [46]	
c.2140G>A	E714K	⇄	⇄	⇄	⇄	[41], [34]	
c.2146G>A	A716T		↓	⇄	↓	[105], [34], [49], [108]	
c.2179G>A	A727T	↓	↓	⇄	↓	[34], [49], [108], [104]	
c.2191G>A	D731N		↓	↓	↓	[41], [39], [34], [49]	
c.2200G>C	V734L		↓	⇄	⇄	[34], [49], [108]	
c.2314A>G	K772E		↓	⇄	↓	[34], [49]	
c.2351G>C	G784A		⇄			[104]	
c.2364G>A	M788I		⇄			[104]	
c.2380C>A	L794M		⇄			[104]	
c.2427C>A	S809R					[104]	
c.2432A>C	Q811P		↓			[104]	
c.2434C>A	L812M		↑	↑		[47], [54], [33], [104]	
c.2441T>C	I814T		⇄	⇄	⇄	[41], [38], [46]	
c.2449A>G	M817V		↑	↑		[38], [47], [36]	
c.2636A>G	K879R		⇄		↑	[74], [73]	[74]
c.2738C>A	S913Ter	⇄	⇄	⇄	↓	[22]	[22]
c.2797G>A	D933N		⇄	⇄	⇄	[41]	
c.2829C>G	Y943Ter	⇄	⇄	⇄	↓	[22]	[22]
c.2848C>T	Q950Ter	⇄	⇄	⇄	↓	[22]	[22]
c.2927A>G	N976S		⇄	⇄	⇄	[41]	
c.3199C>T	R1067W		⇄		↑	[73]	
c.3596del	P1199RfsTer32		⇄			[117]	[117]
c.3884T>C	I1295T		⇄			[104]	
c.4128del	L1377fs		⇄			[104]	
c.4161C>G	Y1387Ter	⇄	⇄	⇄	↑	[22]	[22]
c.4375A>G	S1459G	⇄			↓	[75], [118]	[75], [118]

[1]Affinity for glutamate [2]Affinity for glycine ↑ = increase compared to WT ↓ = decrease compared to WT ⇄ = no change compared to WT

Color denotes the domain: red = ATD; yellow = ABD; grey = linkers; green = TMD; blue = CTD

Abbreviations as in Table 1. *The variant GluN2A-N615S has not been found in humans, but it is closely related to the patient variant GluN2A-N615K and has been characterized in a transgenic mouse model [112].

Table 3. Functional characterization of disease-associated variants in *GRIN2B*/GluN2B.

DNA	Protein	P_o	Glu[1]	Gly[2]	Surface Expression	Functional characterization references	
						Non-neuronal cells	Neurons
c.448A>G	I150V	↓	↑	⇄	⇄	[44]	
c.1238A>G	E413G	⇄	↓	⇄	↓	[119], [50], [49], [108], [120], [34]	[34], [121]
c.1306T>C	C436R				↓	[49], [34]	[82]
c.1367G>A	C456Y	↑	↑	↓	↓	[49], [108], [34]	[82], [90]
c.1382G>T	C461F	⇄	↓	↑	↓	[49], [51], [34]	[51], [34], [82]
c.1555C>T	R519Ter				↓	[76]	[76]
c.1576T>C	S526P	⇄	↓	⇄	↓	[44]	
c.1598G>A	G533D	↑	↑	↑	↓	[44]	
c.1619G>A	R540H	↓	↓	↓	⇄	[50], [30], [122], [34], [51], [82]	[82]
c.1623C>G	S541R		↓	↓	⇄	[28], [49], [45]	
c.1621A>G	S541G	↑	↑	↑	⇄	[45]	
c.1627G>C	G543R		↑	↑	⇄	[47], [45]	
c.1646C>T	A549V				⇄	[45]	
c.1649T>C	F550S				⇄	[45]	
c.1652T>C	L551S				⇄	[45]	
c.1658C>T	P553L		↓			[37], [42], [51]	[51]
c.1657C>A	P553T	⇄	↓	↓	⇄	[45], [55]	[55]
c.1664G>A	S555N	↑	↑	↑	⇄	[45]	
c.1664G>T	S555I				⇄	[45]	
c.1672G>A	V558I	↓	↓	⇄	⇄	[50], [28], [42]	
c.1821G>T	W607C	↓	↓	↓	↓	[50], [40], [48], [42]	
c.1820G>C	W607S	↓	⇄	↓	↓	[44]	
c.1832G>T	G611V	↓	⇄	⇄	⇄	[40], [28], [48]	
c.1844A>T	N615I	↓	⇄	⇄	⇄	[50], [30], [40], [122], [48], [42], [51], [114]	[51]
c.1845C>G	N615K	↓	⇄	↑	↓	[40], [48]	
c.1848C>G	N616K	↓	⇄	↑	⇄	[40], [48]	
c.1853T>G	V618G	↓	⇄	⇄	⇄	[50], [94], [40], [122], [48], [42], [51], [114]	[51]
c.1858G>A	V620M	↑	⇄	⇄	⇄	[40], [48]	
c.1883C>T	S628F				↓	[50], [42]	
c.1906G>C	A636P					[50]	
c.1916C>T	A639V		↑	↑		[47]	
c.1963A>T	I655F		↓	⇄		[28]	
c.1970A>G	E657G		↑	↓	⇄	[50], [42]	
c.1971G>C	E657D	↓	↑	↑	⇄	[44]	
c.2002G>A	D668N		⇄	⇄		[50]	
c.2044C>T	R682C		↑	↑	⇄	[50], [34], [112]	
c.2045G>A	R682H		↑	↑	⇄	[44]	
c.2065G>T	G689C		↓	↓	↓	[52]	[52]
c.2065G>A	G689S		↓	↓	↓	[44], [52]	[52]
c.2079A>T	R693S	⇄	↑	⇄	↓	[44]	
c.2084T>G	I695S	↓	↓	↑	↓	[44]	
c.2084T>C	I695T	↓	↓	⇄	↓	[44]	
c.2087G>A	R696H	⇄	↑	⇄	↓	[34], [82]	[82]
c.2116A>G	M706V	↓	⇄	⇄	↓	[44], [28], [108]	
c.2172-2A>G	G724Ter				↓	[79]	[79], [123]
c.2252T>C	I751T				⇄	[58]	
c.2355del	D786MfsTer23				↓	[76]	[76]
c.2419G>A	E807K	↓	↓	↓	⇄	[50], [44]	
c.2430C>A	S810R		↑	↑		[28]	
c.2429G>A	S810N	↑	↑	↑	↓	[44]	
c.2443G>A	G815R					[38]	
c.2453T>C	M818T		↑	↑		[47], [28]	
c.2455G>A	A819T		↑	↑		[47], [28]	
c.2459G>C	G820A	↓	⇄	⇄	⇄	[38], [50], [28], [42]	
c.2459G>A	G820E	↓			↑	[38], [58], [42]	
c.2461G>T	V821F	↓	↑	↑	⇄	[44]	
c.2471T>G	M824R				⇄	[42]	
c.2473T>G	L825V	⇄/↓	⇄	⇄	⇄	[38], [50], [28], [42], [51]	
c.2477G>A	G826E	⇄				[38]	
c.2515G>T	E839Ter				↓	[76]	[76]
c.2539C>T, c.2539-2540CG>TA	R847Ter	↓	↓	↑	↓	[76], [22]	[76], [22]
c.2589del	I864SfsTer20	↓	⇄	↑	↓	[22]	[22]
c.3012C>G	Y1004Ter	⇄	⇄	⇄	↓	[22]	[22]
c.3272A>C	K1091T		↓		↓	[63]	[63]
c.3295del	R1099AfsTer51	⇄	⇄	⇄	↓	[22]	[22]
c.3465C>ACATCTA	Y1155Ter	⇄	⇄	⇄	↓	[22]	[22]
c.4244C>T	S1415L		⇄	⇄	↓	[62]	[62]
c.4244del	S1415Ter	⇄	⇄	⇄	↓	[22]	[22]
c.4270C>T	L1424F		↓	⇄	⇄	[62]	[62]
c.4355C>T	S1452F		⇄	↑	⇄	[62]	[62]

[1]Affinity for glutamate [2]Affinity for glycine ↑ = increase compared to WT ↓ = decrease compared to WT ⇄ = no change compared to WT

Color denotes the domain: red = ATD; yellow = ABD; grey = linkers; green = TMD; blue = CTD

Abbreviations as in Table 1.

References

1. Hansen KB, Wollmuth LP, Bowie D, Furukawa H, Menniti FS, Sobolevsky AI, Swanson GT, et al. Structure, function, and pharmacology of glutamate receptor ion channels. Pharmacol Rev 2021; 73:1469-658. https://doi.org/10.1124/pharmrev.120.000131
2. Korte M, Schmitz D. Cellular and system biology of memory: Timing, molecules, and beyond. Physiol Rev 2016; 96:647-93. https://doi.org/10.1152/physrev.00010.2015
3. Benke TA, Park K, Krey I, Camp CR, Song R, Ramsey AJ, Yuan H, et al. Clinical and therapeutic significance of genetic variation in the GRIN gene family encoding NMDARs. Neuropharmacology 2021; 199:108805. https://doi.org/10.1016/j.neuropharm.2021.108805
4. Hanson JE, Yuan H, Perszyk RE, Banke TG, Xing H, Tsai MC, Menniti FS, et al. Therapeutic potential of N-methyl-D-aspartate receptor modulators in psychiatry. Neuropsychopharmacology 2024; 49:51-66. https://doi.org/10.1038/s41386-023-01614-3
5. Hansen KB, Ogden KK, Yuan H, Traynelis SF. Distinct functional and pharmacological properties of triheteromeric GluN1/GluN2A/GluN2B NMDA receptors. Neuron 2014; 81:1084-96. https://doi.org/10.1016/j.neuron.2014.01.035
6. Gray JA, Shi Y, Usui H, During MJ, Sakimura K, Nicoll RA. Distinct modes of AMPA receptor suppression at developing synapses by GluN2A and GluN2B: Single-Cell NMDA receptor subunit deletion *in vivo*. Neuron 2011; 71:1085-101. https://doi.org/10.1016/j.neuron.2011.08.007
7. Rauner C, Köhr G. Triheteromeric NR1/NR2A/NR2B receptors constitute the major N-methyl-D-aspartate receptor population in adult hippocampal synapses. J Biol Chem 2011; 286:7558-66. https://doi.org/10.1074/jbc.M110.182600
8. Tovar KR, McGinley MJ, Westbrook GL. Triheteromeric NMDA receptors at hippocampal synapses. J Neurosci 2013; 33:9150-60. https://doi.org/10.1523/JNEUROSCI.0829-13.2013
9. Kellermayer B, Ferreira JS, Dupuis J, Levet F, Grillo-Bosch D, Bard L, Linarès-Loyez J, et al. Differential nanoscale topography and functional role of GluN2-NMDA receptor subtypes at glutamatergic synapses. Neuron 2018; 100:106-119.e7. https://doi.org/10.1016/j.neuron.2018.09.012
10. Stroebel D, Carvalho S, Grand T, Zhu S, Paoletti P. Controlling NMDA receptor subunit composition using ectopic retention signals. J Neurosci 2014; 34:16630-6. https://doi.org/10.1523/JNEUROSCI.2736-14.2014
11. Lü W, Du J, Goehring A, Gouaux E. Cryo-EM structures of the triheteromeric NMDA receptor and its allosteric modulation. Science 2017; 355. https://doi.org/10.1126/science.aal3729
12. Zhou C, Tajima N. Structural insights into NMDA receptor pharmacology. Biochem Soc Trans 2023; 51:1713-31. https://doi.org/10.1042/BST20230122
13. Cerny J, Bozikova P, Balik A, Marques SM, Vyklicky L. NMDA Receptor opening and closing-transitions of a molecular machine revealed by molecular dynamics. Biomolecules 2019; 9. https://doi.org/10.3390/biom9100546
14. Durham RJ, Paudyal N, Carrillo E, Bhatia NK, Maclean DM, Berka V, Dolino DM, et al. Conformational spread and dynamics in allostery of NMDA receptors. Proc Natl Acad Sci U S A 2020; 117:3839-47. https://doi.org/10.1073/pnas.1910950117
15. Vyklicky V, Stanley C, Habrian C, Isacoff EY. Conformational rearrangement of the NMDA receptor amino-terminal domain during activation and allosteric modulation. Nat Commun 2021; 12. https://doi.org/10.1038/s41467-021-23024-z
16. Mony L, Paoletti P. Mechanisms of NMDA receptor regulation. Curr Opin Neurobiol 2023; 83:102815. https://doi.org/10.1016/j.conb.2023.102815
17. Jalali-Yazdi F, Chowdhury S, Yoshioka C, Gouaux E. Mechanisms for zinc and proton inhibition of the GluN1/GluN2A NMDA receptor. Cell 2018; 175:1520-1532.e15. https://doi.org/10.1016/j.cell.2018.10.043
18. Vyklicky V, Krausova B, Cerny J, Balik A, Zapotocky M, Novotny M, Lichnerova K, et al. Block of NMDA receptor channels by endogenous neurosteroids: Implications for the agonist induced conformational states of the channel vestibule. Sci Rep 2015; 5:1-15. https://doi.org/10.1038/srep10935

19. Vyklicky V, Smejkalova T, Krausova B, Balik A, Korinek M, Borovska J, Horak M, et al. Preferential inhibition of tonically over phasically activated nmda receptors by pregnane derivatives. J Neurosci 2016; 36:2161-75. https://doi.org/10.1523/JNEUROSCI.3181-15.2016
20. Krausova BH, Kysilov B, Cerny J, Vyklicky V, Smejkalova T, Ladislav M, Balik A, et al. Site of action of brain neurosteroid pregnenolone sulfate at the N-methyl-D-aspartate receptor. J Neurosci 2020; 40:5922-36. https://doi.org/10.1523/JNEUROSCI.3010-19.2020
21. Hubalkova P, Ladislav M, Vyklicky V, Smejkalova T, Krausova BH, Kysilov B, Krusek J, et al. Palmitoylation controls nmda receptor function and steroid sensitivity. J Neurosci 2021; 41:2119-34. https://doi.org/10.1523/JNEUROSCI.2654-20.2021
22. Kysilov B, Kuchtiak V, Hrcka Krausova B, Balik A, Korinek M, Fili K, Dobrovolski M, et al. Disease-associated nonsense and frame-shift variants resulting in the truncation of the GluN2A or GluN2B C-terminal domain decrease NMDAR surface expression and reduce potentiating effects of neurosteroids. Cell Mol Life Sci 2024; 81:36. https://doi.org/10.1007/s00018-023-05062-6
23. Korinek M, Vyklicky V, Borovska J, Lichnerova K, Kaniakova M, Krausova B, et al. Cholesterol modulates open probability and desensitization of NMDA receptors. J Physiol 2015; 593:2279-93. https://doi.org/10.1113/jphysiol.2014.288209
24. Korinek M, Gonzalez-Gonzalez IM, Smejkalova T, Hajdukovic D, Skrenkova K, Krusek J, Horak M, et al. Cholesterol modulates presynaptic and postsynaptic properties of excitatory synaptic transmission. Sci Rep 2020; 10:1-18. https://doi.org/10.1038/s41598-020-69454-5
25. Iacobucci GJ, Popescu GK. Ca2+-Dependent Inactivation of GluN2A and GluN2B NMDA Receptors Occurs by a Common Kinetic Mechanism. Biophys J 2020; 118:798. https://doi.org/10.1016/j.bpj.2019.07.057
26. Bhatia NK, Carrillo E, Durham RJ, Berka V, Jayaraman V. Allosteric Changes in the NMDA Receptor Associated with Calcium-Dependent Inactivation. Biophys J 2020; 119:2349. https://doi.org/10.1016/j.bpj.2020.08.045
27. Warnet XL, Bakke Krog H, Sevillano-Quispe OG, Poulsen H, Kjaergaard M. The C-terminal domains of the NMDA receptor: How intrinsically disordered tails affect signalling, plasticity and disease. Eur J Neurosci 2021; 54:6713-39. https://doi.org/10.1111/ejn.14842
28. Platzer K, Yuan H, Schütz H, Winschel A, Chen W, Hu C, Kusumoto H, et al. GRIN2B encephalopathy: Novel findings on phenotype, variant clustering, functional consequences and treatment aspects. J Med Genet 2017; 54:460-70. https://doi.org/10.1136/jmedgenet-2016-104509
29. Strehlow V, Heyne HO, Vlaskamp DRM, Marwick KFM, Rudolf G, De Bellescize J, Biskup S, et al. GRIN2A - related disorders: Genotype and functional consequence predict phenotype. Brain 2019; 142:80-92. https://doi.org/10.1093/brain/awy304
30. Lemke JR, Hendrickx R, Geider K, Laube B, Schwake M, Harvey RJ, James V, et al. GRIN2B mutations in west syndrome and intellectual disability with focal epilepsy. Ann Neurol 2014; 75:147-54. https://doi.org/10.1002/ana.24073
31. Hirschfeldova K, Cerny J, Bozikova P, Kuchtiak V, Rausch T, Benes V, Spaniel F, et al. Evidence for the association between the intronic haplotypes of ionotropic glutamate receptors and first-episode schizophrenia. J Pers Med 2021; 11. https://doi.org/10.3390/jpm11121250
32. Amin JB, Moody GR, Wollmuth LP. From bedside-to-bench: What disease-associated variants are teaching us about the NMDA receptor. J Physiol 2021; 599:397-416. https://doi.org/10.1113/JP278705
32a. Xu Y, Song R, Perszyk RE, Chen W, Kim S, Park KL, Allen JP, et al. De novo GRIN variants in M3 helix associated with neurological disorders control channel gating of NMDA receptor. Cell Mol Life Sci 2024; 81(1):153. (Added in proof). https://doi.org/10.1007/s00018-023-05069-z
33. Yuan H, Hansen KB, Zhang J, Mark Pierson T, Markello TC, Fajardo KVF, Holloman CM, et al. Functional analysis of a de novo GRIN2A missense mutation associated with early-onset epileptic encephalopathy. Nat Commun 2014;5. https://doi.org/10.1038/ncomms4251
34. Swanger SA, Chen W, Wells G, Burger PB, Tankovic A, Bhattacharya S, Strong KL, et al. Mechanistic insight into nmda receptor dysregulation by rare variants in the GluN2A and GluN2B agonist binding domains. Am J Hum Genet 2016; 99:1261. https://doi.org/10.1016/j.ajhg.2016.10.002

35. Serraz B, Grand T, Paoletti P. Altered zinc sensitivity of NMDA receptors harboring clinically-relevant mutations. Neuropharmacology 2016; 109:196-204. https://doi.org/10.1016/j.neuropharm.2016.06.008
36. Chen W, Tankovic A, Burger PB, Kusumoto H, Traynelis SF, Yuan H. Functional evaluation of a de novo GRIN2A mutation identified in a patient with profound global developmental delay and refractory epilepsy. Mol Pharmacol 2017; 91:317-30. https://doi.org/10.1124/mol.116.106781
37. Ogden KK, Chen W, Swanger SA, McDaniel MJ, Fan LZ, Hu C, Tankovic A, et al. Molecular Mechanism of Disease-Associated Mutations in the Pre-M1 Helix of NMDA Receptors and Potential Rescue Pharmacology. PLoS Genetics 2017; 13: 1-35. https://doi.org/10.1371/journal.pgen.1006536
38. Amin JB, Leng X, Gochman A, Zhou HX, Wollmuth LP. A conserved glycine harboring disease-associated mutations permits NMDA receptor slow deactivation and high Ca^{2+} permeability. Nat Commun 2018; 9. https://doi.org/10.1038/s41467-018-06145-w
39. Gao K, Tankovic A, Zhang Y, Kusumoto H, Zhang J, Chen W, Xiangwei W, et al. A de novo loss-of-function GRIN2A mutation associated with childhood focal epilepsy and acquired epileptic aphasia. PLoS One 2017; 12:1-20. https://doi.org/10.1371/journal.pone.0170818
40. Li J, Zhang J, Tang W, Mizu RK, Kusumoto H, XiangWei W, Xu Y, et al. De novo GRIN variants in NMDA receptor M2 channel pore-forming loop are associated with neurological diseases. Hum Mutat 2019; 40:2393-413. https://doi.org/10.1002/humu.23895
41. Addis L, Virdee JK, Vidler LR, Collier DA, Pal DK, Ursu D. Epilepsy-associated GRIN2A mutations reduce NMDA receptor trafficking and agonist potency-molecular profiling and functional rescue. Sci Rep 2017;7:1-14. https://doi.org/10.1038/s41598-017-00115-w
42. Vyklicky V, Krausova B, Cerny J, Ladislav M, Smejkalova T, Kysilov B, Korinek M, et al. Surface expression, function, and pharmacology of disease-associated mutations in the membrane domain of the human GluN2B subunit. Front Mol Neurosci 2018;11:1-20. https://doi.org/10.3389/fnmol.2018.00110
43. Santos-gómez A, Miguez-cabello F, Juliá-palacios N, García-navas D, Soto-insuga V, García-peñas JJ, Fuentes P, et al. Paradigmatic de novo grin1 variants recapitulate pathophysiological mechanisms underlying grin1-related disorder clinical spectrum. Int J Mol Sci 2021; 22:1-19. https://doi.org/10.3390/ijms222312656
44. Myers SJ, Yuan H, Perszyk RE, Zhang J, Kim S, Nocilla KA, Allen JP, et al. Classification of missense variants in the N-methyl-d-aspartate receptor GRIN gene family as gain- or loss-of-function. Hum Mol Genet 2023; 32:2857-71. https://doi.org/10.1093/hmg/ddad104
45. Xie L, McDaniel MJ, Perszyk RE, Kim S, Cappuccio G, Shapiro KA, Muñoz-Cabello B, et al. Functional effects of disease-associated variants reveal that the S1-M1 linker of the NMDA receptor critically controls channel opening. Cell Mol Life Sci 2023; 80:1-19. https://doi.org/10.1007/s00018-023-04705-y
46. Moody G, Musco A, Bennett J, Wollmuth LP. An integrated approach to evaluate the functional effects of disease-associated NMDA receptor variants. Neuropharmacology 2023; 240:109703. https://doi.org/10.1016/j.neuropharm.2023.109703
47. Han W, Yuan H, Allen JP, Kim S, Shaulsky GH, Perszyk RE, Traynelis SF, et al. Opportunities for Precision Treatment of GRIN2A and GRIN2B Gain-of-Function Variants in Triheteromeric N-Methyl-D-Aspartate Receptors. J Pharmacol Exp Ther 2022; 381:54-66. https://doi.org/10.1124/jpet.121.001000
48. Song R, Zhang J, Perszyk RE, Camp CR, Tang W, Kannan V, Li J, et al. Differential responses of disease-related GRIN variants located in pore-forming M2 domain of N-methyl-D-aspartate receptor to FDA-approved inhibitors. J Neurochem 2023: 1-14. https://doi.org/10.1111/jnc.15942
49. Tang W, Liu D, Traynelis SF, Yuan H. Positive allosteric modulators that target NMDA receptors rectify loss-of-function GRIN variants associated with neurological and neuropsychiatric disorders. Neuropharmacology 2020; 177:108247. https://doi.org/10.1016/j.neuropharm.2020.108247
50. Kysilov B, Hrcka Krausova B, Vyklicky V, Smejkalova T, Korinek M, Horak M, Chodounska H, et al. Pregnane-based steroids are novel positive NMDA receptor modulators that may compensate for the effect of loss-of-function disease-associated GRIN mutations. Br J Pharmacol 2022; 179:3970-90. https://doi.org/10.1111/bph.15841

51. Fedele L, Newcombe J, Topf M, Gibb A, Harvey RJ, Smart TG. Disease-associated missense mutations in GluN2B subunit alter NMDA receptor ligand binding and ion channel properties. Nat Commun 2018; 9. https://doi.org/10.1038/s41467-018-02927-4
52. Kellner S, Abbasi A, Carmi I, Heinrich R, Garin-Shkolnik T, Hershkovitz T, Giladi M, et al. Two de novo GluN2B mutations affect multiple NMDAR-functions and instigate severe pediatric encephalopathy. Elife. 2021; 10. https://doi.org/10.7554/eLife.67555
53. Kolcheva M, Kortus S, Krausova BH, Barackova P, Misiachna A, Danacikova S, Kaniakova M, et al. Specific pathogenic mutations in the M3 domain of the GluN1 subunit regulate the surface delivery and pharmacological sensitivity of NMDA receptors. Neuropharmacology 2021; 189:108528. https://doi.org/10.1016/j.neuropharm.2021.108528
54. Pierson TM, Yuan H, Marsh ED, Fuentes-Fajardo K, Adams DR, Markello T, Golas G, et al. GRIN2A mutation and early-onset epileptic encephalopathy: personalized therapy with memantine. Ann Clin Transl Neurol 2014; 1:190-8. https://doi.org/10.1002/acn3.39
55. Soto D, Olivella M, Grau C, Armstrong J, Alcon C, Gasull X, Santos-Gómez A, et al. L-Serine dietary supplementation is associated with clinical improvement of loss-of-function GRIN2B-related pediatric encephalopathy. Sci Signal 2019; 12:1-16. https://doi.org/10.1126/scisignal.aaw0936
56. Xu Y, Song R, Chen W, Strong K, Shrey D, Gedela S, Traynelis SF, et al. Recurrent seizure-related GRIN1 variant: Molecular mechanism and targeted therapy. Ann Clin Transl Neurol 2021;8:1480-94. https://doi.org/10.1002/acn3.51406
57. Lewis SA, Shetty S, Gamble S, Heim J, Zhao N, Stitt G, Pankratz M, et al. Intrathecal magnesium delivery for Mg^{++}-insensitive NMDA receptor activity due to GRIN1 mutation. Orphanet J Rare Dis 2023; 18:1-5. https://doi.org/10.1186/s13023-023-02756-9
58. den Hollander B, Veenvliet ARJ, Rothuizen-Lindenschot M, van Essen P, Peters G, Santos-Gómez A, Olivella M, et al. Evidence for effect of L-serine, a novel therapy for GRIN2B-related neurodevelopmental disorder. Mol Genet Metab 2023; 138. https://doi.org/10.1016/j.ymgme.2023.107523
59. Lester RAJ, Jahr CE. NMDA channel behavior depends on agonist affinity. J Neurosci 1992; 12:635-43. https://doi.org/10.1523/JNEUROSCI.12-02-00635.1992
60. Benske TM, Mu TW, Wang YJ. Protein quality control of N-methyl-D-aspartate receptors. Front Cell Neurosci 2022; 16:1-25. https://doi.org/10.3389/fncel.2022.907560
61. Skrenkova K, Song J man, Kortus S, Kolcheva M, Netolicky J, Hemelikova K, Kaniakova M, et al. The pathogenic S688Y mutation in the ligand-binding domain of the GluN1 subunit regulates the properties of NMDA receptors. Sci Rep 2020; 10:1-15. https://doi.org/10.1038/s41598-020-75646-w
62. Liu S, Zhou L, Yuan H, Vieira M, Sanz-Clemente A, Badger JD, Lu W, et al. A rare variant identified within the GluN2B C-terminus in a patient with autism affects NMDA receptor surface expression and spine density. J Neurosci 2017; 37:4093-102. https://doi.org/10.1523/JNEUROSCI.0827-16.2017
63. Wang X, Mei D, Gou L, Zhao S, Gao C, Guo J, Luo S, et al. Functional evaluation of a novel GRIN2B missense variant associated with epilepsy and intellectual disability. Neuroscience 2023; 526:107-20. https://doi.org/10.1016/j.neuroscience.2023.06.018
64. Mayer ML, Vyklicky L, Clements J. Regulation of NMDA receptor desensitization in mouse hippocampal neurons by glycine. Nat 1989; 338:425-7. https://doi.org/10.1038/338425a0
65. Clements JD, Lester RAJ, Tong G, Jahr CE, Westbrook GL. The time course of glutamate in the synaptic cleft. Science 1992; 258:1498-501. https://doi.org/10.1126/science.1359647
66. Bergeron R, Meyer TM, Coyle JT, Greene RW. Modulation of N-methyl-D-aspartate receptor function by glycine transport. Proc Natl Acad Sci U S A 1998; 95:15730-4. https://doi.org/10.1073/pnas.95.26.15730
67. Stroebel D, Mony L, Paoletti P. Glycine agonism in ionotropic glutamate receptors. Neuropharmacology 2021; 193:108631. https://doi.org/10.1016/j.neuropharm.2021.108631
68. Jahr CE. High probability opening of NMDA receptor channels by L-glutamate. Science 1992; 255:470-2. https://doi.org/10.1126/science.1346477

69. Marwick KFM, Hansen KB, Skehel PA, Hardingham GE, Wyllie DJA. Functional assessment of triheteromeric NMDA receptors containing a human variant associated with epilepsy. J Physiol 2019; 597:1691-704. https://doi.org/10.1113/JP277292
70. Lau CG, Zukin RS. NMDA receptor trafficking in synaptic plasticity and neuropsychiatric disorders. Nat Rev Neurosci 2007; 8:413-26. https://doi.org/10.1038/nrn2153
71. Kolcheva M, Ladislav M, Netolicky J, Kortus S, Rehakova K, Krausova BH, Hemelikova K, et al. The pathogenic N650K variant in the GluN1 subunit regulates the trafficking, conductance, and pharmacological properties of NMDA receptors. Neuropharmacology 2023; 222:109297. https://doi.org/10.1016/j.neuropharm.2022.109297
72. Wang CC, Held RG, Chang SC, Yang L, Delpire E, Ghosh A, Hall B, et al. A critical role for gluN2B-containing NMDA receptors in cortical development and function. Neuron 2011; 72:789-805. https://doi.org/10.1016/j.neuron.2011.09.023
73. Liu XR, Xu XX, Lin SM, Fan CY, Ye TT, Tang B, Shi YW, et al. GRIN2A Variants Associated With Idiopathic Generalized Epilepsies. Front Mol Neurosci 2021; 14:1-15. https://doi.org/10.3389/fnmol.2021.720984
74. Li QQ, Chen J, Hu P, Jia M, Sun JH, Feng HY, Qiao FC, et al. Enhancing GluN2A-type NMDA receptors impairs long-term synaptic plasticity and learning and memory. Mol Psychiatry 2022; 27:3468-78. https://doi.org/10.1038/s41380-022-01579-7
75. Mota Vieira M, Nguyen TA, Wu K, Badger JD, Collins BM, Anggono V, Lu W, et al. An Epilepsy-Associated GRIN2A Rare Variant Disrupts CaMKIIα Phosphorylation of GluN2A and NMDA Receptor Trafficking. Cell Rep 2020; 32:108104. https://doi.org/10.1016/j.celrep.2020.108104
76. Santos-Gómez A, Miguez-Cabello F, Garciá-Recio A, Locubiche-Serra S, Garciá-Diáz R, Soto-Insuga V, Guerrero-López R, et al. Disease-associated GRIN protein truncating variants trigger NMDA receptor loss-of-function. Hum Mol Genet 2020; 29:3859-71. https://doi.org/10.1093/hmg/ddaa220
77. El-Brolosy MA, Kontarakis Z, Rossi A, Kuenne C, Günther S, Fukuda N, Kikhi K, et al. Genetic compensation triggered by mutant mRNA degradation Europe PMC Funders Group. Nature 2019; 568:193-7. https://doi.org/10.1038/s41586-019-1064-z
78. Lee PJ, Yang S, Sun Y, Guo JU. Regulation of nonsense-mediated mRNA decay in neural development and disease. J Mol Cell Biol 2021; 13:269-81. https://doi.org/10.1093/jmcb/mjab022
79. Sceniak MP, Fedder KN, Wang Q, Droubi S, Babcock K, Patwardhan S, Wright-Zornes J, et al. An autism-associated mutation in GluN2B prevents NMDA receptor trafficking and interferes with dendrite growth. J Cell Sci 2019; 132:1-14. https://doi.org/10.1242/jcs.232892
80. Sabo SL, Lahr JM, Offer M, Weekes ALA, Sceniak MP. GRIN2B-related neurodevelopmental disorder: current understanding of pathophysiological mechanisms. Front Synaptic Neurosci 2023; 14:1-17. https://doi.org/10.3389/fnsyn.2022.1090865
81. Elmasri M, Hunter DW, Winchester G, Bates EE, Aziz W, Van Der Does DM, Karachaliou E, et al. Common synaptic phenotypes arising from diverse mutations in the human NMDA receptor subunit GluN2A. Commun Biol 2022; 5:1-17. https://doi.org/10.1038/s42003-022-03115-3
82. Elmasri M, Lotti JS, Aziz W, Steele OG, Karachaliou E, Sakimura K, Hansen KB, et al. Synaptic Dysfunction by Mutations in GRIN2B: Influence of Triheteromeric NMDA Receptors on Gain-Of-Function and Loss-Of-Function Mutant Classification. Brain Sci 2022;12. https://doi.org/10.3390/brainsci12060789
83. Forrest D, Yuzaki M, Soares HD, Ng L, Luk DC, Sheng M, Stewart CL, et al. Targeted disruption of NMDA receptor 1 gene abolishes NMDA response and results in neonatal death. Neuron 1994; 13:325-38. https://doi.org/10.1016/0896-6273(94)90350-6
84. Sakimura K, Kutsuwada T, Ito I, Manabe T, Takayama C, Kushiya E, Yagi T, et al. Reduced hippocampal LTP and spatial learning in mice lacking NMDA receptor ε1 subunit. Nat 1995; 373:151-5. https://doi.org/10.1038/373151a0
85. Kutsuwada T, Sakimura K, Manabe T, Takayama C, Katakura N, Kushiya E, Natsume R, et al. Impairment of Suckling Response, Trigeminal Neuronal Pattern Formation, and Hippocampal LTD in NMDA Receptor ε2 Subunit Mutant Mice. Neuron 1996; 16:333-44. https://doi.org/10.1016/S0896-6273(00)80051-3

86. Sprengel R, Suchanek B, Amico C, Brusa R, Burnashev N, Rozov A, Hvalby O, et al. Importance of the Intracellular Domain of NR2 Subunits for NMDA Receptor Function In Vivo. Cell 1998; 92:279-89. https://doi.org/10.1016/S0092-8674(00)80921-6
87. Herzog LE, Wang L, Yu E, Choi S, Farsi Z, Song BJ, Pan JQ, et al. Mouse mutants in schizophrenia risk genes GRIN2A and AKAP11 show EEG abnormalities in common with schizophrenia patients. Transl Psychiatry 2023; 13. https://doi.org/10.1038/s41398-023-02393-7
88. Camp CR, Vlachos A, Klöckner C, Krey I, Banke TG, Shariatzadeh N, Ruggiero SM, et al. Loss of Grin2a causes a transient delay in the electrophysiological maturation of hippocampal parvalbumin interneurons. Commun Biol 2023; 6. https://doi.org/10.1038/s42003-023-05298-9
89. Farsi Z, Nicolella A, Simmons SK, Aryal S, Shepard N, Brenner K, Lin S, et al. Brain-region-specific changes in neurons and glia and dysregulation of dopamine signaling in Grin2a mutant mice. Neuron 2023; 111:3378-3396.e9. https://doi.org/10.1016/j.neuron.2023.08.004
90. Shin W, Kim K, Serraz B, Cho YS, Kim D, Kang M, Lee EJ, et al. Early correction of synaptic long-term depression improves abnormal anxiety-like behavior in adult GluN2B-C456Y-mutant mice. PLoS Biol 2020;18:1-28. https://doi.org/10.1371/journal.pbio.3000717
91. Zoodsma JD, Keegan EJ, Moody GR, Bhandiwad AA, Napoli AJ, Burgess HA, Wollmuth LP, et al. Disruption of grin2B, an ASD-associated gene, produces social deficits in zebrafish. Mol Autism 2022;13:1-17. https://doi.org/10.1186/s13229-022-00516-3
92. Zoodsma JD, Chan K, Bhandiwad AA, Golann DR, Liu G, Syed SA, Napoli AJ, et al. A Model to Study NMDA Receptors in Early Nervous System Development. J Neurosci 2020; 40:3631-45. https://doi.org/10.1523/JNEUROSCI.3025-19.2020
93. Furuse T, Wada Y, Hattori K, Yamada I, Kushida T, Shibukawa Y, Masuya H, et al. Phenotypic characterization of a new Grin1 mutant mouse generated by ENU mutagenesis. Eur J Neurosci 2010; 31:1281-91. https://doi.org/10.1111/j.1460-9568.2010.07164.x
94. Lemke JR, Geider K, Helbig KL, Heyne HO, Schütz H, Hentschel J, Courage C, et al. Delineating the GRIN1 phenotypic spectrum: A distinct genetic NMDA receptor encephalopathy. Neurology 2016; 86:2171-8. https://doi.org/10.1212/WNL.0000000000002740
95. Amador A, Bostick CD, Olson H, Peters J, Camp CR, Krizay D, Chen W, et al. Modelling and treating GRIN2A developmental and epileptic encephalopathy in mice. Brain 2020; 143:2039. https://doi.org/10.1093/brain/awaa147
96. Zhao T, Zhong R, Zhang X, Li G, Zhou C, Fang S, Ding Y, et al. Efavirenz restored NMDA receptor dysfunction and inhibited epileptic seizures in GluN2A/Grin2a mutant mice. Front Neurosci 2023; 17. https://doi.org/10.3389/fnins.2023.1086462
97. Candelas Serra M, Kuchtiak V, Kubik-Zahorodna A, Kysilov B, Fili K, Abramova V, Dobrovolski M, et al. Characterization of mice carrying a neurodevelopmental disease-associated GluN2B(L825V) variant. J Neurosci (accepted). https://doi.org/10.1523/JNEUROSCI.2291-23.2024
98. Ragnarsson L, Zhang Z, Das SS, Tran P, Andersson Å, des Portes V, Desmettre Altuzarra C, et al. GRIN1 variants associated with neurodevelopmental disorders reveal channel gating pathomechanisms. Epilepsia 2023; 1:0-3. https://doi.org/10.1111/epi.17776
99. Kalbaugh TL, VanDongen HMA, VanDongen AMJ. Ligand-binding residues integrate affinity and efficacy in the NMDA receptor. Mol Pharmacol 2004;66:209-19. https://doi.org/10.1124/mol.66.2.209
100. Zhang J, Tang W, Bhatia NK, Xu Y, Paudyal N, Liu D, Kim S, et al. A *de novo* GRIN1 variant associated with myoclonus and developmental delay: from molecular mechanism to rescue pharmacology. Front Genet 2021; 12:1-16. https://doi.org/10.3389/fgene.2021.694312
101. Hamdan FF, Gauthier J, Araki Y, Lin DT, Yoshizawa Y, Higashi K, Park AR, et al. Excess of de novo deleterious mutations in genes associated with glutamatergic systems in nonsyndromic intellectual disability. Am J Hum Genet 2011; 88:306-16. https://doi.org/10.1016/j.ajhg.2011.02.001, https://doi.org/10.1016/j.ajhg.2011.03.011

102. Chen W, Shieh C, Swanger SA, Tankovic A, Au M, McGuire M, Tagliati M, et al. GRIN1 mutation associated with intellectual disability alters NMDA receptor trafficking and function. J Hum Genet 2017; 62:589-97. https://doi.org/10.1038/jhg.2017.19
103. Fry AE, Fawcett KA, Zelnik N, Yuan H, Thompson BAN, Shemer-Meiri L, Cushion TD, et al. De novo mutations in GRIN1 cause extensive bilateral polymicrogyria. Brain 2018; 141:698-712. https://doi.org/10.1093/brain/awx358
104. Shepard N, Baez-Nieto D, Iqbal S, Kurganov E, Budnik N, Campbell AJ, Pan JQ, et al. Differential functional consequences of GRIN2A mutations associated with schizophrenia and neurodevelopmental disorders. Sci Rep 2024; 14:2798. https://doi.org/10.1038/s41598-024-53102-3
105. Sibarov DA, Bruneau N, Antonov SM, Szepetowski P, Burnashev N, Giniatullin R. Functional properties of human NMDA receptors associated with epilepsy-related mutations of GluN2A subunit. Front Cell Neurosci 2017; 11:1-10. https://doi.org/10.3389/fncel.2017.00155
106. Lesca G, Rudolf G, Bruneau N, Lozovaya N, Labalme A, Boutry-Kryza N, Salmi M, et al. GRIN2A mutations in acquired epileptic aphasia and related childhood focal epilepsies and encephalopathies with speech and language dysfunction. Nat Genet 2013; 45:1061-6. https://doi.org/10.1038/ng.2726
107. Xu XX, Liu XR, Fan CY, Lai JX, Shi YW, Yang W, Su T, et al. Functional Investigation of a GRIN2A Variant Associated with Rolandic Epilepsy. Neurosci Bull 2018; 34:237-46. https://doi.org/10.1007/s12264-017-0182-6
108. Tang W, Beckley JT, Zhang J, Song R, Xu Y, Kim S, Quirk MC, et al. Novel neuroactive steroids as positive allosteric modulators of NMDA receptors: mechanism, site of action, and rescue pharmacology on GRIN variants associated with neurological conditions. Cell Mol Life Sci 2023; 80. https://doi.org/10.1007/s00018-022-04667-7
109. Carvill GL, Regan BM, Yendle SC, O'Roak BJ, Lozovaya N, Bruneau N, Burnashev N, et al. GRIN2A mutations cause epilepsy-aphasia spectrum disorders. Nat Genet 2013; 45:1073-6. https://doi.org/10.1038/ng.2727
110. Iacobucci GJ, Liu B, Wen H, Sincox B, Zheng W, Popescu GK. Complex functional phenotypes of NMDA receptor disease variants. Mol Psychiatry 2022; 27:5113-23. https://doi.org/10.1038/s41380-022-01774-6
111. Marwick KFM, Parker P, Skehel P, Hardingham G, Wyllie DJA. Functional assessment of the NMDA receptor variant GluN2AR586K. Wellcome Open Res 2017; 2:1-16. https://doi.org/10.12688/wellcomeopenres.10985.1, https://doi.org/10.12688/wellcomeopenres.10985.2
112. Endele S, Rosenberger G, Geider K, Popp B, Tamer C, Stefanova I, Milh M, et al. Mutations in GRIN2A and GRIN2B encoding regulatory subunits of NMDA receptors cause variable neurodevelopmental phenotypes. Nat Genet 2010; 42:1021-6. https://doi.org/10.1038/ng.677
113. Marwick KFM, Skehel PA, Hardingham GE, Wyllie DJA. The human NMDA receptor GluN2AN615K variant influences channel blocker potency. Pharmacol Res Perspect 2019; 7:1-7. https://doi.org/10.1002/prp2.495
114. Chen X, Keramidas A, Harvey RJ, Lynch JW. Effects of GluN2A and GluN2B gain-of-function epilepsy mutations on synaptic currents mediated by diheteromeric and triheteromeric NMDA receptors. Neurobiol Dis 2020; 140:104850. https://doi.org/10.1016/j.nbd.2020.104850
115. Bertocchi I, Eltokhi A, Rozov A, Chi VN, Jensen V, Bus T, Pawlak V, et al. Voltage-independent GluN2A-type NMDA receptor Ca2+ signaling promotes audiogenic seizures, attentional and cognitive deficits in mice. Commun Biol 2021; 4:1-21. https://doi.org/10.1038/s42003-021-01717-x, https://doi.org/10.1038/s42003-020-01538-4
116. Fernández-Marmiesse A, Kusumoto H, Rekarte S, Roca I, Zhang J, Myers SJ, Traynelis SF, et al. A novel missense mutation in GRIN2A causes a non-epileptic neurodevelopmental disorder. Mov Disord 2018;33:992. https://doi.org/10.1002/mds.27315
117. Vieira MM, Peng S, Won S, Hong E, Inati SK, Thurm A, Thiam AH, et al. A Frameshift Variant of GluN2A Identified in an Epilepsy Patient Results in NMDA Receptor Mistargeting. J Neurosci 2024; 44:JN-RM-0557-23. https://doi.org/10.1523/JNEUROSCI.0557-23.2023
118. Yong XLH, Zhang L, Yang L, Chen X, Tan JZA, Yu X, Chandra M, et al. Regulation of NMDA receptor trafficking and gating by activity-dependent CaMKIIα phosphorylation of the GluN2A subunit. Cell Rep 2021;36:109338. https://doi.org/10.1016/j.celrep.2021.109338

119. Adams DR, Yuan H, Holyoak T, Arajs KH, Hakimi P, Markello TC, Wolfe LA, et al. Three rare diseases in one Sib pair: RAI1, PCK1, GRIN2B mutations associated with Smith-Magenis Syndrome, cytosolic PEPCK deficiency and NMDA receptor glutamate insensitivity. Mol Genet Metab 2014; 113:161-70. https://doi.org/10.1016/j.ymgme.2014.04.001
120. Wells G, Yuan H, McDaniel MJ, Kusumoto H, Snyder JP, Liotta DC, Traynelis SF, et al. The GluN2B-Glu413Gly NMDA receptor variant arising from a de novo GRIN2B mutation promotes ligand-unbinding and domain opening. Proteins Struct Funct Bioinforma 2018; 86:1265-76. https://doi.org/10.1002/prot.25595
121. Bell S, Maussion G, Jefri M, Peng H, Theroux JF, Silveira H, Soubannier V, et al. Disruption of GRIN2B Impairs Differentiation in Human Neurons. Stem Cell Reports 2018;11:183-96. https://doi.org/10.1016/j.stemcr.2018.05.018
122. Mullier B, Wolff C, Sands ZA, Ghisdal P, Muglia P, Kaminski RM, André VM, et al. GRIN2B gain of function mutations are sensitive to radiprodil, a negative allosteric modulator of GluN2B-containing NMDA receptors. Neuropharmacology 2017; 123:322-31. https://doi.org/10.1016/j.neuropharm.2017.05.017
123. Bahry JA, Fedder-Semmes KN, Sceniak MP, Sabo SL. An Autism-Associated de novo Mutation in GluN2B Destabilizes Growing Dendrites by Promoting Retraction and Pruning. Front Cell Neurosci 2021; 15:1-11. https://doi.org/10.3389/fncel.2021.692232

REVIEW

Anandamide-Mediated Modulation of Nociceptive Transmission at the Spinal Cord Level

Diana SPICAROVA[1], Jiri PALECEK[1]

[1]Laboratory of Pain Research, Institute of Physiology of the Czech Academy of Sciences, Prague, Czech Republic

Received April 2, 2024
Accepted June 10, 2024

Summary

Three decades ago, the first endocannabinoid, anandamide (AEA), was identified, and its analgesic effect was recognized in humans and preclinical models. However, clinical trial failures pointed out the complexity of the AEA-induced analgesia. The first synapses in the superficial laminae of the spinal cord dorsal horn represent an important modulatory site in nociceptive transmission and subsequent pain perception. The glutamatergic synaptic transmission at these synapses is strongly modulated by two primary AEA-activated receptors, cannabinoid receptor 1 (CB_1) and transient receptor potential vanilloid 1 (TRPV1), both highly expressed on the presynaptic side formed by the endings of primary nociceptive neurons. Activation of these receptors can have predominantly inhibitory (CB_1) and excitatory (TRPV1) effects that are further modulated under pathological conditions. In addition, dual AEA-mediated signaling and action may occur in primary sensory neurons and dorsal horn synapses. AEA application causes balanced inhibition and excitation of primary afferent synaptic input on superficial dorsal horn neurons in normal conditions, whereas peripheral inflammation promotes AEA-mediated inhibition. This review focuses mainly on the modulation of synaptic transmission at the spinal cord level and signaling in primary nociceptive neurons by AEA *via* CB_1 and TRPV1 receptors. Furthermore, the spinal analgesic effect in preclinical studies and clinical aspects of AEA-mediated analgesia are considered.

Key words

Anandamide • CB_1 • TRPV1 • NAPE • Spinal cord • Synaptic transmission

Corresponding author

D. Spicarova, Laboratory of Pain Research, Institute of Physiology CAS, Videnska 1083, 142 00 Praha 4, Czech Republic. E-mail: Diana.Spicarova@fgu.cas.cz

Introduction

Pain modulation and analgesic effects of the endocannabinoid anandamide (AEA, *N*-arachidonoyl-ethanolamine) were recognized in humans and intensively studied in experimental rodent models [1-7]. However, the underlying mechanisms of AEA anti-nociceptive action still need to be understood better due to the complexity of the AEA metabolism, trafficking and storage, the whole endocannabinoid system balance, and AEA dual effects on sensory processing and signaling [8-10]. The scientific effort to understand and modulate AEA-mediated signaling at the spinal cord level has substantial implications for the development of new possible therapeutic strategies for pain relief.

Anandamide as a part of the endocannabinoid system and endocannabinoidome

The endocannabinoid system consists of classical cannabinoid CB_1 and CB_2 receptors, endo-cannabinoids – AEA and 2-arachidonoylglycerol (2-AG), and their synthesizing and degradation enzymes [11]. It exerts homeostatic function and controls a wide range of various physiological roles like emotional processing, learning and memory, sleep, appetite, cardiovascular functions, reproduction, temperature control, immune

response, inflammation and pain. The essential role of the endocannabinoid system in CNS is neuromodulation, affecting synaptic plasticity, as well as nociceptive synaptic transmission [12]. Imbalance or malfunction of endocannabinoid system is involved in nervous system disorders such as anxiety, depression, schizophrenia, multiple sclerosis, neurodegeneration, stroke, epilepsy, addiction, and pathological pain states [13-15].

Lately, a new concept of endocannabinoidome has been established (Fig. 1). The endocannabinoidome extends the boundaries of the endocannabinoid system to include endocannabinoid-like lipid mediators that are biochemically related to the endocannabinoids. These lipids include a family of *N*-acylethanolamines (NAEs), including *N*-palmitoylethanolamine (PEA), *N*-oleoylethanolamine (OEA), *N*-linoleoylethanolamine (LEA), *N*-docosahexaenoylethanolamine (DHEA), a family of 2-acylglycerols (2-oleoyl glycerol, 2-OG; 2-linoleoyl glycerol, 2-LG), *N*-acyl neurotransmitters (*N*-acyl dopamines, *N*-acyl serotonins) or also lipoamino acids (*N*-acyl taurines, *N*-acyl glycines). The endocannabinoidome further encompasses enzymes for the mentioned bioactive lipids syntheses and degradation, and their receptors, among others, orphan G-protein coupled receptors (GPR55, GPR110, GPR18 or GPR119), one of the key nociceptive receptors – transient receptor potential vanilloid 1 (TRPV1) or nuclear peroxisome proliferator-activated receptors PPARα and PPARγ [1]. Changes in AEA metabolism/level within the wider endocannabinoidome may alter metabolic pathways of other lipid mediators and modulate alternative signaling with an impact on physiological functions. The endocannabinoidome exerts a more comprehensive impact on health and body homeostasis and thus should also be considered in clinical studies related to AEA.

AEA is an arachidonic acid derivative, *N*-arachidonoylethanolamine, a naturally occurring compound within the body belonging to the larger family of NAEs. It was the first endocannabinoid identified from the porcine brain and was later isolated and measured in humans and rats [16,17]. The word Ananda means bliss and happiness in Sanskrit, which fits well with current research that describes AEA-mediated signaling through the CB_1 receptor to produce analgesic, anxiolytic, and antidepressant effects [7,18-20].

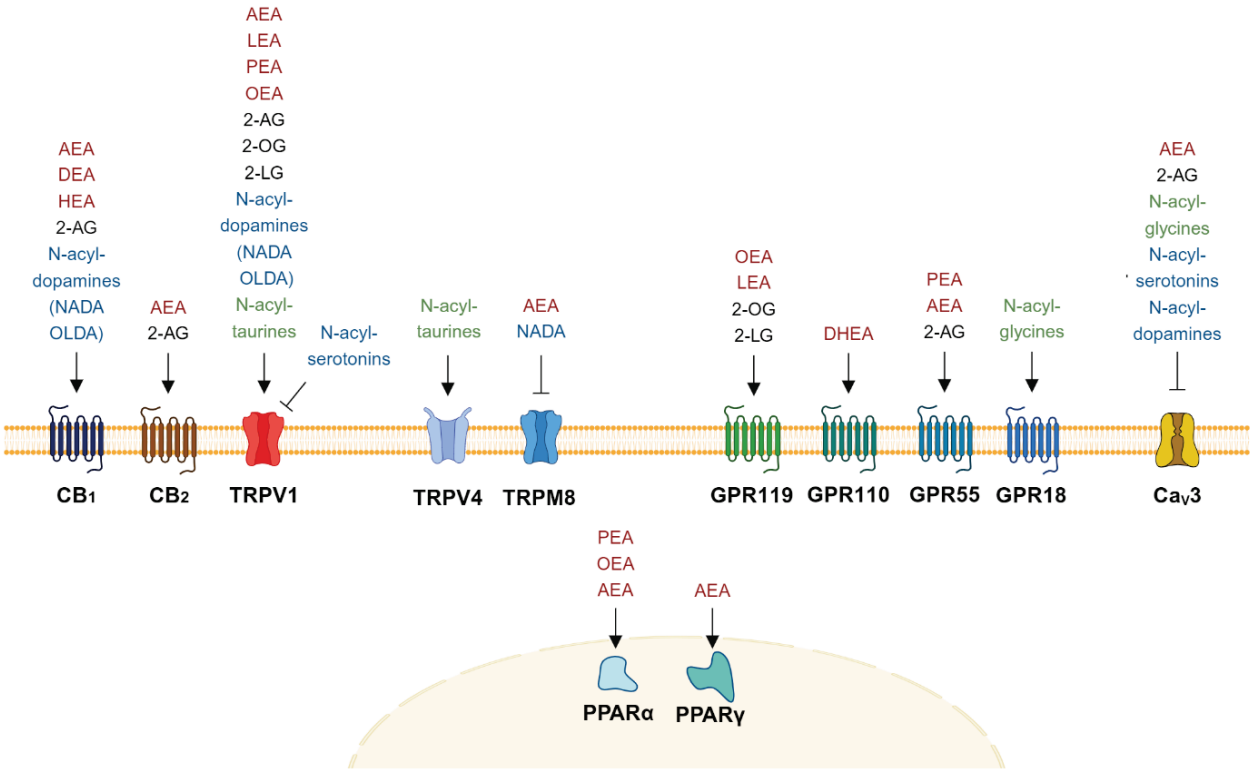

Fig. 1. Endocannabinoidome receptors and mediators. Groups of endocannabinoid-like lipid mediators are distinguished in colors: *N*-acylethanolamines in red, 2-acylglycerols in black, *N*-acyl neurotransmitters in blue, and lipoamino acids in green. Abbreviations: 2-AG, 2-arachidonoylglycerol; AEA, *N*-arachidonoylethanolamine (anandamide); DEA, *N*-docosatetraenoylethanolamine; DHEA, *N*-docosahexaenoylethanolamine; HEA, *N*-homo-γ-linolenylethanolamine; LEA, *N*-linoleoylethanolamine; NADA, *N*-arachidonoyldopamine; OEA, *N*-oleoylethanolamine; OLDA, *N*-oleoyldopamine; PEA, *N*-palmitoylethanolamine. The image was created with BioRender.com.

AEA was initially identified to bind preferentially to the CB_1 receptor and with lower affinity to the CB_2 receptor [16]. Later, the activation of nonselective cation channel TRPV1 by AEA was recognized, while its efficacy at human TRPV1 was reported to be higher than that at rat TRPV1 [21,22]. Thus, AEA acts as an endocannabinoid and endovanilloid; the CB_1 and TRPV1 being the main AEA activated receptors. Other molecular targets affected by AEA were also recognized – including nuclear receptors PPARγ and PPARα, voltage-gated T-type calcium channels (Ca_V3) and sodium channels [23-27]. AEA activation of both CB_1 and TRPV1 receptors at the first nociceptive synapse in the spinal cord dorsal horn plays an important role in pain modulation. The action of AEA at this synapse is complex, as the effect of presynaptic CB_1 receptor activation on neurotransmitter release is inhibitory, and the main impact of TRPV1 activation is excitatory.

Anandamide metabolism

Under neuronal stimulation, AEA is produced in and released from neurons in a Ca^{2+}-dependent manner [28]. Furthermore, the Ca^{2+}-independent formation of AEA was later demonstrated after PKC and PAK activation in primary sensory neurons, also named dorsal root ganglion (DRG) neurons [29]. Redundant biosynthetic pathways of AEA were characterized; phospholipase A2 group IV E (PLA2G4E, cPLA2ε) was identified as Ca^{2+}-dependent N-acyltransferase (Ca-NAT), which catalyzes the formation of AEA precursor *N*-acylphosphatidylethanolamine (NAPE) from phosphatidylethanolamine (PE) and phosphatidylcholine (PC), with a transfer of the acyl group of PC to the amine of PE [30]. In brain lysate, Ca-NAT activity preferably generates N-arachidonoyl-containing (p)NAPEs with polyunsaturated acyl groups at the sn-2 position [1,31]. On the other hand, Ca^{2+}-independent N-acyltransferases (NATs) termed phospholipase A and acyltransferase (PLAAT) can also generate NAPE [32,33]. The main enzyme converting NAPE to AEA is *N*-acylphosphatidylethanolamine phospholipase D (NAPE-PLD), which catalyzes the AEA syntheses in a Ca^{2+}-sensitive manner [34]. But, AEA may also be synthesized from NAPE by other Ca^{2+}-insensitive enzymes [35].

In the CNS, the enzyme fatty acid amino hydrolase (FAAH) primarily degrades AEA to arachidonic acid and ethanolamine. It is important to note that it accepts multiple fatty acid amides as a substrate, including palmitoyl- and oleoyl-ethanolamide [36]. In addition to the hydrolytic pathway, AEA undergoes oxygenation by cyclooxygenase 2 (COX-2), 5-, 12-, 15-lipoxygenase (LOX) and cytochrome P450 monooxygenases to create prostaglandin-ethanolamides, hydroxyl-eicosatetraenoyl-ethanolamides (HETE-EAs) and epoxy-eicosatrienoyl-ethanolamide see for reviews [1,8].

Interaction between CB_1 receptor and TRPV1 channel signaling in DRG neurons

In nociceptive DRG neurons, an opposite role for CB_1 and TRPV1 receptor activation was suggested, while AEA may activate both and trigger complex effects. AEA acts as a low-efficacy TRPV1 agonist. The efficacy of AEA may be affected by the number of TRPV1 channels in the plasmatic membrane, their phosphorylation, AEA metabolism, efflux or uptake, trafficking, storage, and the critical role also plays the concomitant CB_1 receptor activation [8,37-41]. The AEA-mediated effects may differ based on the expression of the target receptors. Neurons expressing only CB_1 receptors or only TRPV1 channels may exert the opposite AEA-induced effects. In neonatal rat cultured neurons, the AEA-mediated inhibitory or excitatory effect was reported in size-segregated DRG populations of neurons. In supporting experiments, Ca^{2+} transients were evoked by KCl-induced depolarization and AEA application inhibited or potentiated these Ca^{2+} transients [42]. The CB_1 activation-mediated inhibitory effect on depolarization-induced Ca^{2+} transients was also shown in primary culture of adult DRG neurons, which additionally rarely responded to capsaicin [43]. The dual effect of AEA application on synaptic input from primary nociceptive fibers was demonstrated at the first nociceptive synapses formed by these nociceptive DRG endings in acute spinal cord slices [10].

However, CB_1 and TRPV1 receptors exhibit high co-expression within the DRG neurons [44-46], suggesting complex AEA-mediated regulation based on CB_1/TRPV1 crosstalk in these neurons. In transfected cells over-expressing both receptors, a dual effect of CB_1 activation on capsaicin evoked, TRPV1-mediated Ca^{2+} response was described. Activation of the CB_1 receptor inhibited or enhanced capsaicin-induced responses depending on the signaling pathways activated. Inhibition of TRPV1 channel responses was mediated by negative regulation of the cAMP signaling *via* CB_1 receptor activation. The opposite

effect, potentiation of TRPV1 channel responses, was mediated *via* phosphatidylinositol 3-kinase (PI3K) and phospholipase C (PLC) pathways stimulated by CB_1 receptor activation [47]. Meanwhile, the activation of diverse intracellular signaling cascades, such as PI3K, PLC-PKC or PKA are known to sensitize the TRPV1 channel to the agonist [38,41,48-53]. Further, it was shown that the constitutive activity of the CB_1 receptor maintains the TRPV1 channel in a sensitized state [54]. The effect of AEA thus depends on the activation/regulation of CB_1 and TRPV1 receptors and the concomitant CB_1-mediated regulation of specific intracellular signaling with an impact on the TRPV1 sensitization. The order in which individual receptors are activated could also play a role [47,54]. A later study suggested that CB_1-supported TRPV1 sensitization and the induction of TRPV1 responsiveness to AEA in DRG neurons may be underlined by the spatial proximity of both receptors [55].

On the other hand, reduction of TRPV1 sensitization after CB_1 receptor activation was also shown in experiments where AEA in subthreshold concentration for TRPV1 activation facilitated heat-induced Ca^{2+} transients that were further enhanced by CB_1 receptor inhibition. The Ca^{2+} transients induced by AEA in the concentration to activate TRPV1 were reduced by simultaneous CB_1 receptor activation by CB_1 agonist HU210 [56]. Capsaicin evoked TRPV1-mediated cationic influx was attenuated by CB_1 receptor activation, which in addition also reduced the number of capsaicin-responsive cells in these experiments [40,57]. Remarkably, experiments in spinal cord slices showed that AEA induced a concentration-dependent release of neuropeptide, calcitonin gene-related peptide (CGRP) and substance P (SP), *via* TRPV1 channel activation on central terminals of DRG neurons [58]. This TRPV1-mediated pronociceptive process of neuropeptide release in the dorsal horn was reduced by CB_1 activation [59]. Thus, AEA activation of CB_1 receptors on central terminals of DRG neurons may concomitantly affect the sensitization/activation of TRPV1 channels, and the final AEA effect could be concentration and receptors proximity dependent. In addition, the increase in intracellular Ca^{2+} concentration in DRG neurons stimulates the formation of endogenous AEA. Newly synthesized AEA was shown to mediate TRPV1-dependent Ca^{2+} influx subsequently. Thus, AEA was proposed to act as an intracellular messenger, amplifying intracellular concentration of Ca^{2+} *via* TRPV1 channels [39].

A fatty acid binding protein 5 (FABP5) is an intracellular carrier for AEA transport to FAAH-mediated hydrolyses. A conditional knockout strategy was used to selectively ablate FABP5 in the TRPV1 channel expressing DRG neurons. This genetic approach elevated AEA, PEA, and OEA levels in DRGs, while 2-AG levels remained unchanged. Elevated AEA levels in nociceptive DRGs after FABP5 deletion attenuated nerve growth factor-mediated TRPV1 sensitization *via* CB_1 receptor activation, and the emergence of antinociceptive effects mediated by CB_1 was thus revealed [60].

CB_1 and TRPV1 receptors modulation of transmitter release in spinal cord dorsal horn

The first synapses of the pain pathway are localized in the spinal cord dorsal horn, particularly in the superficial laminae. Nociceptive signaling from the periphery is transmitted from DRG neurons, to dorsal horn neurons, which convey signaling to higher brain areas. AEA acts on the CB_1 and TRPV1 receptors expressed at presynaptic endings of primary afferents and modulate neurotransmitter release. Activation of presynaptic CB_1 receptors decreases glutamate release by a well-established mechanism of trimeric $G_{i/o}$-protein cascade stimulation, inhibiting adenylyl cyclase, decreasing calcium conductance by inhibition of high-voltage activated N- and P/Q-type Ca^{2+} channels, and increasing the potassium conductance *via* stimulation of inwardly rectifying and A-type outward potassium channels (Fig. 2) [61,62]. In comparison, CB_1 receptor coupling to G_s-protein, stimulating adenylyl cyclase, was unmasked when the $G_{i/o}$-protein cascade was inhibited [63]. Whereas the isoform of adenylyl cyclase expressed in cells may be crucial in the CB_1 receptor activation-induced dual effect on adenylyl cyclase [64].

TRPV1 activation-mediated responses are characterized by two phenomena – desensitization and tachyphylaxis. During TRPV1 stimulation, the channel activity is Ca^{2+}-dependently reduced, and TRPV1 thus undergoes rapid desensitization. Tachyphylaxis occurs during repetitive agonist stimulation while the TRPV1-mediated responses are diminished. TRPV1 channel activation at presynaptic ending allows Ca^{2+} influx through the opened pore, increasing Ca^{2+} concentration in the cytosol and dramatically enhancing spontaneous glutmate release [65-67]. Potent TRPV1 agonist capsaicin application elicited action potentials in superficial dorsal horn neurons, but evoked glutamate release induced by electrical stimulation of the dorsal root was prevented [65,66]. Thus, the facilitation of spontaneous glutamate

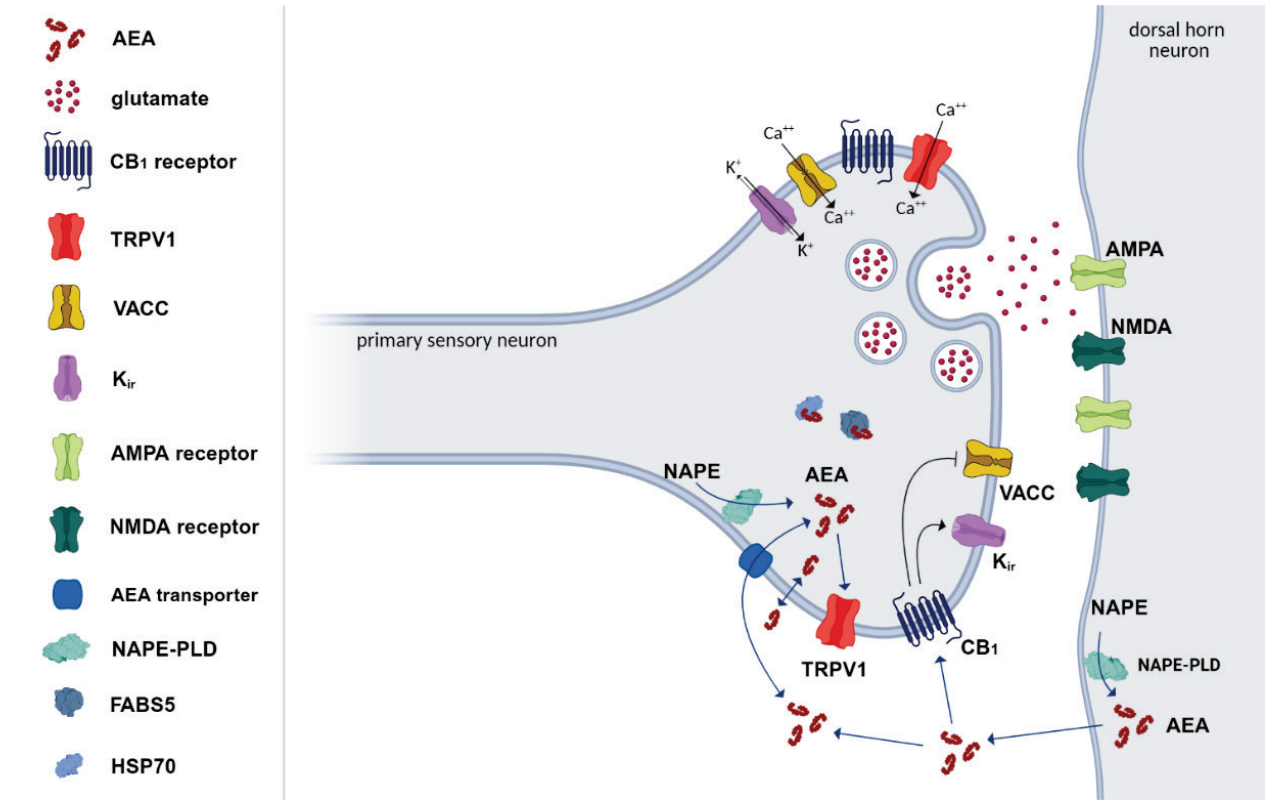

Fig. 2. Simplified illustration of AEA action at the first nociceptive synapse formed by the central terminal of the primary sensory neuron and the secondary spinal cord dorsal horn neuron. Autocrine and retrograde signaling of AEA is suggested, whereas AEA is synthesized in addition to other enzymes by Ca^{2+}-dependent NAPE-PLD in both primary and secondary nociceptive neurons. (The contribution of glial cells to AEA signaling is not depicted). Translocation of the lipid molecule of AEA across the plasma membrane by diffusion and a membrane transporter was proposed. Intracellular carriers, including the fatty acid binding protein 5 (FABP5) and the heat shock protein 70 (HSP70), may facilitate the intracellular transport of AEA, for example, towards the FAAH for degradation. Two primary AEA-activated receptors are abundantly expressed on the presynaptic side, where they regulate glutamate release. At lower concentrations, the CB_1 receptor is suggested to be activated, while at higher concentrations, both the CB_1 and TRPV1 receptors are activated. In addition, AEA could directly inhibit low-voltage-activated calcium channels (Ca_V3) to modulate the excitability of neuron. The reduction in transmitter release after CB_1 receptor activation is attributed to the inhibition of high-voltage-activated calcium channels (VACC) and the activation of inwardly rectifying potassium channels (K_{ir}). The image was created with BioRender.com.

release by capsaicin was sufficient to transmit nociceptive information further along the pain pathway by activating second-order neurons even when the action potential-evoked glutamate release from primary afferent endings was blocked. Furthermore, *in vivo* electrophysiological experiments demonstrated that spinal administration of TRPV1 antagonist capsazepine reduced nociceptive fibers (Aδ- and C-) stimulation-evoked responses of dorsal horn neurons [68]. It is suggested that endogenous AEA primarily activates CB_1 receptors under normal conditions, and its concentration is insufficient for TRPV1 channel stimulation on the central endings of DRG neurons.

Modulation of synaptic transmission at first nociceptive synapses by anandamide

In the superficial spinal cord dorsal horn, the patch-clamp recording of the dorsal root electrical stimulation-evoked excitatory postsynaptic currents (eEPSCs) from lamina II neurons revealed inhibition of the eEPSC amplitude by AEA application. Meanwhile, AEA attenuated evoked excitatory transmission more effectively during Aδ-fiber than C-fiber stimulation. A similar decrease of eEPSC amplitude was demonstrated after the CB_1 receptor agonist WIN55,212-2 application [69,70]. The effects of AEA on spontaneous synaptic transmission were reported inconsistently, from no detected change in the frequency of miniature EPSC (mEPSC) [70] to a concentration-dependent effect of AEA [71]. In the latter experiments, mEPSCs were recorded, and the low AEA concentration-induced inhibition of frequency was suggested to be mediated *via* CB_1 receptors activation, and the higher AEA concentration-induced excitatory effect *via* TRPV1 channels [71].

A recent study evaluated AEA modulation by recording mEPSC from neurons in lamina I and $II_{(outer)}$ in

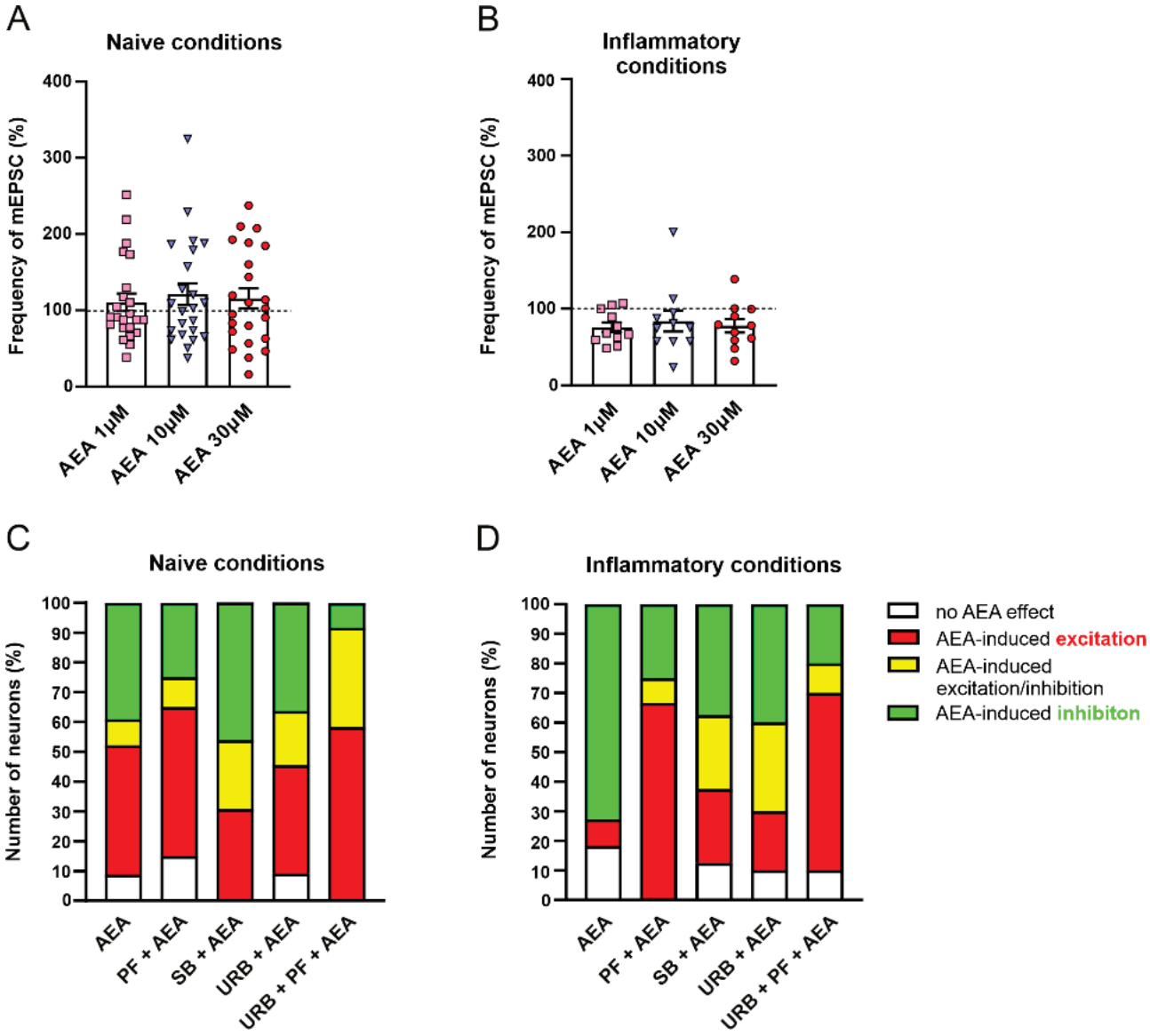

Fig. 3. Peripheral inflammation enhanced the inhibitory effect of AEA application on dorsal horn neurons mEPSC frequency in spinal cord slices. (**A, B**) Normalized frequency of mEPSC during acute AEA application (1 μM, 10 μM, and 30 μM, 4 min each concentration) in control conditions (A) and 24 h after induction of peripheral inflammation (B) by subcutaneous carrageenan injection. Statistical analysis showed a significant difference between control and inflammatory conditions in each AEA concentration tested (1 μM AEA, $p<0.05$; 10 μM AEA, $p<0.05$; 30 μM AEA, $p<0.05$). (**C**) Application of AEA induced decrease or increase of mEPSC frequency in a comparable number of superficial dorsal horn neurons in control conditions. The number of neurons with mEPSC frequency inhibition by AEA application was reduced after inhibition of the CB_1 receptor (PF514273 application) and especially after CB_1 and FAAH co-inhibition (PF514273/URB597 co-application) used as a pretreatment. (**D**) After peripheral inflammation, most neurons received synaptic input inhibited by the AEA application (73 %). Pretreatment with PF514273 and PF514273/URB597 reduced the inhibitory and enhanced the excitatory AEA-induced effect. Abbreviations: PF (PF514273, CB_1 receptor antagonist), SB (SB366791, TRPV1 antagonist), URB (URB597, FAAH inhibitor). The figure was adapted from Pontearso *et al.* [10].

acute slices [10]. The results suggested that applied AEA had a dual effect on mEPSC frequency with similar size populations of recorded neurons showing inhibition and excitation. This balanced AEA effect on mEPSC frequency was changed following peripheral inflammation when AEA-induced decrease of neurotransmitter release from primary afferent fibers (mEPSC frequency) was dominant (Fig. 3). The excitatory effect of AEA application was evident only when CB_1 receptors and FAAH were inhibited [10]. Notably, these described effects of exogenous AEA application contrast with those observed following the application of its precursor 20:4-NAPE, which increased levels of endo-genous AEA and consistently inhibited both action potential-dependent and -independent excitatory synaptic transmission, as evidenced by the recording of eEPSC, sEPSC, and mEPSC [9,72]. In these experiments, AEA was synthesized in spinal cord slices from 20:4-NAPE primarily by NAPE-PLD (Fig. 4) [72]. The 20:4-NAPE

mediated inhibition was also present after peripheral inflammation while the underlying mechanisms were altered. In naïve animals, the 20:4-NAPE effect was mediated by CB_1 receptors, but after inflammation, the TRPV1 channel-mediated mechanism was also involved [9,72]. The physiological mechanism of AEA syntheses by available catabolic enzymes, together with their cellular distribution and level of enzymatic activity, regulate AEA concentration locally and may have a crucial role in the AEA-induced modulation of nociception [9]. The local production of AEA from its precursor could thus be advantageous for analgesic purposes in clinical settings.

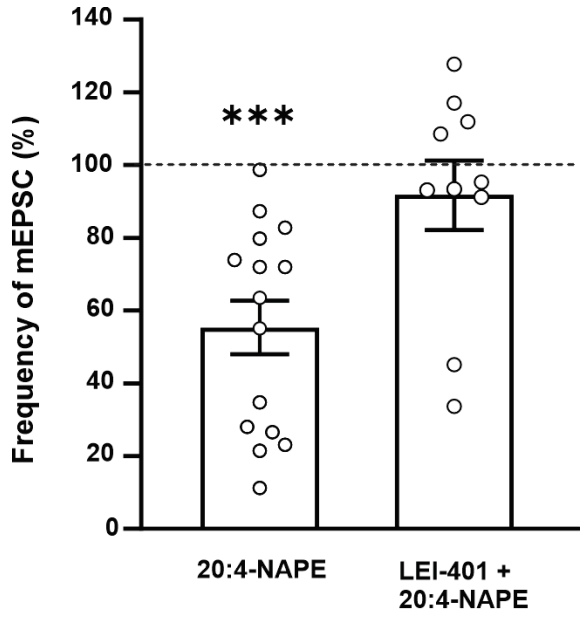

Fig. 4. Application of the AEA precursor 20:4-NAPE decreased excitatory synaptic transmission at the first nociceptive synapses *via* NAPE-PLD activation. Application of 20:4-NAPE (20 μM, 4 min) decreased the frequency of mEPSC (n = 15, *** p<0.001) recorded from superficial dorsal horn neurons in acute spinal cord slices. Incubation of slices with the NAPE-PLD inhibitor LEI-401 (1 μM, 2 h) prevented the effect of acutely applied 20:4-NAPE (20 μM, 4 min) on mEPSC frequency. The figure was adapted from Spicarova *et al.* [72].

Well-known endocannabinoid retrograde signaling described at synapses in the brain was also recognized in the spinal cord dorsal horn. Activation of spinal metabotropic glutamate receptor 5 ($mGluR_5$) stimulated endocannabinoid-mediated stress-induced analgesia by retrograde signaling *via* diacylglycerol lipase – 2-arachidonoylglycerol – CB_1 receptor pathway [73]. In other experiments different conditioning stimulation protocols known to induce endocannabinoid production and CB_1 receptor-dependent synaptic plasticity in other brain areas [74,75] were employed in spinal cord slices. Low-frequency stimulation of primary afferent fibers combined with depolarization of postsynaptic neuron led to profound long-term depression mediated by CB_1 receptors [76]. These results indicated that CB_1 receptors activation in primary afferent fibers could prevent long-term potentiation underlying hypersensitive states.

Various populations of excitatory and inhibitory spinal interneurons form neuronal circuits in the dorsal horn and modulate the nociceptive signaling from the periphery. This signaling is also affected by descending modulation from higher brain areas. Many studies aimed at spinal nociception are performed in spinal cord slices. This preparation decreases the degree of complexity of spinal nociceptive signaling by eliminating functional descending pathways. Despite the expression on central terminals of primary sensory neurons, CB_1 receptors are also expressed in dorsal horn interneurons [44,73,77-79]. Their activation may decrease the inhibitory neurotransmitter release, leading to increased excitability of nociceptive dorsal horn neurons. Thus, an unexpected role of endocannabinoids acting on inhibitory interneurons as mediators of heterosynaptic pain sensitization was revealed in the dorsal horn [77].

Analgesia mediated by spinal anandamide

Treatment with cannabinoids induces analgesia by acting at the peripheral, spinal, and supraspinal levels [2,4,18,80,81]. Intrathecal (i.t.) administration of the CB_1 receptor antagonist, SR141716A, induced thermal hyperalgesia and facilitated responses of dorsal horn neurons evoked by transcutaneous electrical stimulation. These experiments suggested tonic activation of spinal CB_1 receptors modulating nociceptive threshold [82,83]. In comparison, i.t. administration as well as topical application of CB_1 receptor agonist WIN55,212-2 produced analgesia. When ineffective i.t. doses of WIN55,212-2 were used with topical tail immersion in the WIN55,212-2 solution, an antinociceptive effect was markedly potentiated. Thus, antinociceptive synergy occurred in both peripheral and spinal application sites [84]. Spinal administration of AEA had inconsistent effects on neuronal responses evoked by transcutaneous electrical stimulation of nociceptive primary afferent fibers in control animals. In contrast, under inflammatory conditions, AEA reduced these responses *via* CB_1 receptor activation [85]. Intrathecal application of WIN55,212-2 *via* activation of CB_1 receptors attenuated

mechanical hypersensitivity associated with peripheral inflammation induced by complete Freud's adjuvant (CFA) injection and also present after peripheral neuropathy caused by partial ligation of the sciatic nerve [86,87]. Increased AEA level in the spinal cord was reported in neuropathic pain model with chronic constriction injury (CCI) of the sciatic nerve [88]. Intrathecal AEA administration blocked carrageenan-induced thermal hyperalgesia [89] and CCI-induced mechanical allodynia *via* both CB_1 and TRPV1 receptor-dependent mechanisms [90]. Suppression of spinal AEA degradation by FAAH inhibition led to the TRPV1-mediated analgesic effect in neuropathic rats while supporting experiments indicated the lipoxygenase-mediated remodeling of AEA metabolism [91].

Clinical aspects of anandamide-mediated analgesia

Ongoing research focuses on the use of exo- and endo-cannabinoids to treat pain. Exocannabinoids, naturally occurring phytocannabinoids from the cannabis plant, and synthetic cannabinoids differentiate from endocannabinoids synthesized within the body in chemical structure and pharmacological properties upon activation of the classical cannabinoid receptors CB_1 and CB_2, reflecting their different origins. The beneficial effect of Sativex (Nabiximols), a cannabis-based pharmaceutical product containing Δ^9-tetrahydro-cannabinol (Δ^9-THC) and cannabidiol (CBD) approved for pain and spasticity treatment in patients with multiple sclerosis in 2005 in Canada, was confirmed in patients with peripheral neuropathic pain in further clinical trials [92,93]. The approval of Sativex encouraged further studies of new analgesics targeting the endocannabinoid system, modulating AEA levels and related signaling.

Clinical trials looking for AEA analgesic properties in pathological pain states and neurological disorders were supported by positive preclinical results [91,94,95]. However, the failure of these clinical trials testifies to the complexity of the AEA-induced effect, including the regulation of a wide range of physiological processes, which could underlie severe side effects. It also demonstrates the difficulty of the translation of promising results from animal models to clinical settings in humans. Several inhibitors of the AEA degradation enzyme FAAH entered clinical trials also with a focus on pain relief. These FAAH inhibitors elevated plasma AEA levels and were well tolerated [96]. However, clinical trials targeted at pain relief failed to produce analgesia in patients with osteoarthritic pain manifestation [97]. Clinical interest in this area waned when phase I of clinical trials testing BIA 10-2474 was terminated for tragic fatality in the group of volunteers receiving the highest dose [98]. Activity-based protein profiling revealed off-target BIA 10-2474 activities that may have contributed to the induced neurotoxicity [99]. However, the adverse effects of BIA 10-2474 remain unexplained [100]. The great hope of clinicians was to test peripherally restricted cannabinoid agonists based on preclinical research clearly showing the analgesic effects of peripheral cannabinoid receptor activation [2,3,81]. However, clinical trials using AZD1940 and AZD1704 have failed to produce any analgesic effect [101,102]. It is unclear if an optimal activation of CB_1 receptors to produce analgesia was achieved or if peripheral CB_1 receptor stimulation failed to inhibit nociceptive signaling [103]. A better understanding of the underlying mechanisms of AEA-induced effects and the differences between rodents and humans is essential to advance preclinical and translational research.

Conflict of Interest

There is no conflict of interest.

Acknowledgements

This work was supported by project LX22NPO5104 - funded by the European Union Next Generation EU and Institutional support RVO67985823.

References

1. Mock ED, Gagestein B, van der Stelt M. Anandamide and other N-acylethanolamines: A class of signaling lipids with therapeutic opportunities. Prog Lipid Res 2023;89:101194. https://doi.org/10.1016/j.plipres.2022.101194
2. Clapper JR, Moreno-Sanz G, Russo R, Guijarro A, Vacondio F, Duranti A, Tontini A, ET AL. Anandamide suppresses pain initiation through a peripheral endocannabinoid mechanism. Nat Neurosci 2010;13:1265-1270. https://doi.org/10.1038/nn.2632
3. Calignano A, La Rana G, Giuffrida A, Piomelli D. Control of pain initiation by endogenous cannabinoids. Nature 1998;394:277-281. https://doi.org/10.1038/28393

4. Police A, Shankar VK, Pandey P, Rangappa S, Doerksen RJ, Narasimha Murthy S. Novel topical anandamide formulation for alleviating peripheral neuropathic pain. Int J Pharm 2023;641:123085. https://doi.org/10.1016/j.ijpharm.2023.123085
5. Habib AM, Okorokov AL, Hill MN, Bras JT, Lee MC, Li S, Gossage SJ, ET AL. Microdeletion in a FAAH pseudogene identified in a patient with high anandamide concentrations and pain insensitivity. Br J Anaesth 2019;123:e249-e253. https://doi.org/10.1016/j.bja.2019.02.019
6. Mikaeili H, Habib AM, Yeung CW, Santana-Varela S, Luiz AP, Panteleeva K, Zuberi S, ET AL. Molecular basis of FAAH-OUT-associated human pain insensitivity. Brain 2023;146:3851-3865. https://doi.org/10.1093/brain/awad098
7. Fride E, Mechoulam R. Pharmacological activity of the cannabinoid receptor agonist, anandamide, a brain constituent. Eur J Pharmacol 1993;231:313-314. https://doi.org/10.1016/0014-2999(93)90468-W
8. Maccarrone M. Metabolism of the Endocannabinoid Anandamide: Open Questions after 25 Years. Front Mol Neurosci 2017;10:166. https://doi.org/10.3389/fnmol.2017.00166
9. Nerandzic V, Mrozkova P, Adamek P, Spicarova D, Nagy I, Palecek J. Peripheral inflammation affects modulation of nociceptive synaptic transmission in the spinal cord induced by N-arachidonoylphosphatidylethanolamine. Br J Pharmacol 2018;175:2322-2336. https://doi.org/10.1111/bph.13849
10. Pontearso M, Slepicka J, Bhattacharyya A, Spicarova D, Palecek J. Dual effect of anandamide on spinal nociceptive transmission in control and inflammatory conditions. Biomed Pharmacother 2024;173:116369. https://doi.org/10.1016/j.biopha.2024.116369
11. Howlett AC, Barth F, Bonner TI, Cabral G, Casellas P, Devane WA, Felder CC, ET AL International Union of Pharmacology. XXVII. Classification of cannabinoid receptors. Pharmacol Rev 2002;54:161-202. https://doi.org/10.1124/pr.54.2.161
12. Lu HC, Mackie K. An Introduction to the Endogenous Cannabinoid System. Biol Psychiatry 2016;79:516-525. https://doi.org/10.1016/j.biopsych.2015.07.028
13. Di Marzo V. The endocannabinoidome as a substrate for noneuphoric phytocannabinoid action and gut microbiome dysfunction in neuropsychiatric disorders. Dialogues Clin Neurosci 2020;22:259-269. https://doi.org/10.31887/DCNS.2020.22.3/vdimarzo
14. Cristino L, Bisogno T, Di Marzo V. Cannabinoids and the expanded endocannabinoid system in neurological disorders. Nat Rev Neurol 2020;16:9-29. https://doi.org/10.1038/s41582-019-0284-z
15. Donvito G, Nass SR, Wilkerson JL, Curry ZA, Schurman LD, Kinsey SG, Lichtman AH. The Endogenous Cannabinoid System: A Budding Source of Targets for Treating Inflammatory and Neuropathic Pain. Neuropsychopharmacology 2018;43:52-79. https://doi.org/10.1038/npp.2017.204
16. Devane WA, Hanus L, Breuer A, Pertwee RG, Stevenson LA, Griffin G, Gibson D, ET AL. Isolation and structure of a brain constituent that binds to the cannabinoid receptor. Science 1992;258:1946-1949. https://doi.org/10.1126/science.1470919
17. Felder CC, Nielsen A, Briley EM, Palkovits M, Priller J, Axelrod J, Nguyen DN, ET AL. Isolation and measurement of the endogenous cannabinoid receptor agonist, anandamide, in brain and peripheral tissues of human and rat. FEBS Lett 1996;393:231-235. https://doi.org/10.1016/0014-5793(96)00891-5
18. Hohmann AG, Suplita RL, Bolton NM, Neely MH, Fegley D, Mangieri R, Krey JF, ET AL. An endocannabinoid mechanism for stress-induced analgesia. Nature 2005;435:1108-1112. https://doi.org/10.1038/nature03658
19. Gobbi G, Bambico FR, Mangieri R, Bortolato M, Campolongo P, Solinas M, Cassano T, ET AL. Antidepressant-like activity and modulation of brain monoaminergic transmission by blockade of anandamide hydrolysis. Proc Natl Acad Sci U S A 2005;102:18620-18625. https://doi.org/10.1073/pnas.0509591102
20. Kathuria S, Gaetani S, Fegley D, Valino F, Duranti A, Tontini A, Mor M, ET AL. Modulation of anxiety through blockade of anandamide hydrolysis. Nat Med 2003;9:76-81. https://doi.org/10.1038/nm803
21. Zygmunt PM, Petersson J, Andersson DA, Chuang H, Sorgard M, Di Marzo V, Julius D, Hogestatt ED. Vanilloid receptors on sensory nerves mediate the vasodilator action of anandamide. Nature 1999;400:452-457. https://doi.org/10.1038/22761
22. Smart D, Gunthorpe MJ, Jerman JC, Nasir S, Gray J, Muir AI, Chambers JK, ET AL. The endogenous lipid anandamide is a full agonist at the human vanilloid receptor (hVR1). Br J Pharmacol 2000;129:227-230. https://doi.org/10.1038/sj.bjp.0703050

23. Chemin J, Nargeot J, Lory P. Chemical determinants involved in anandamide-induced inhibition of T-type calcium channels. J Biol Chem 2007;282:2314-2323. https://doi.org/10.1074/jbc.M610033200
24. Kim HI, Kim TH, Shin YK, Lee CS, Park M, Song JH. Anandamide suppression of Na+ currents in rat dorsal root ganglion neurons. Brain Res 2005;1062:39-47. https://doi.org/10.1016/j.brainres.2005.09.004
25. O'Sullivan SE. Cannabinoids go nuclear: evidence for activation of peroxisome proliferator-activated receptors. Br J Pharmacol 2007;152:576-582. https://doi.org/10.1038/sj.bjp.0707423
26. Okura D, Horishita T, Ueno S, Yanagihara N, Sudo Y, Uezono Y, Sata T. The endocannabinoid anandamide inhibits voltage-gated sodium channels Nav1.2, Nav1.6, Nav1.7, and Nav1.8 in Xenopus oocytes. Anesth Analg 2014;118:554-562. https://doi.org/10.1213/ANE.0000000000000070
27. Sun Y, Alexander SP, Garle MJ, Gibson CL, Hewitt K, Murphy SP, Kendall DA, Bennett AJ. Cannabinoid activation of PPAR alpha; a novel neuroprotective mechanism. Br J Pharmacol 2007;152:734-743. https://doi.org/10.1038/sj.bjp.0707478
28. Di Marzo V, Fontana A, Cadas H, Schinelli S, Cimino G, Schwartz JC, Piomelli D. Formation and inactivation of endogenous cannabinoid anandamide in central neurons. Nature 1994;372:686-691. https://doi.org/10.1038/372686a0
29. Vellani V, Petrosino S, De Petrocellis L, Valenti M, Prandini M, Magherini PC, McNaughton PA, Di Marzo V. Functional lipidomics. Calcium-independent activation of endocannabinoid/endovanilloid lipid signalling in sensory neurons by protein kinases C and A and thrombin. Neuropharmacology 2008;55:1274-1279. https://doi.org/10.1016/j.neuropharm.2008.01.010
30. Ogura Y, Parsons WH, Kamat SS, Cravatt BF. A calcium-dependent acyltransferase that produces N-acyl phosphatidylethanolamines. Nat Chem Biol 2016;12:669-671. https://doi.org/10.1038/nchembio.2127
31. Astarita G, Ahmed F, Piomelli D. Identification of biosynthetic precursors for the endocannabinoid anandamide in the rat brain. J Lipid Res 2008;49:48-57. https://doi.org/10.1194/jlr.M700354-JLR200
32. Jin XH, Okamoto Y, Morishita J, Tsuboi K, Tonai T, Ueda N. Discovery and characterization of a Ca2+-independent phosphatidylethanolamine N-acyltransferase generating the anandamide precursor and its congeners. J Biol Chem 2007;282:3614-3623. https://doi.org/10.1074/jbc.M606369200
33. Tsuboi K, Uyama T, Okamoto Y, Ueda N. Endocannabinoids and related N-acylethanolamines: biological activities and metabolism. Inflamm Regen 2018;38:28. https://doi.org/10.1186/s41232-018-0086-5
34. Okamoto Y, Morishita J, Tsuboi K, Tonai T, Ueda N. Molecular characterization of a phospholipase D generating anandamide and its congeners. J Biol Chem 2004;279:5298-5305. https://doi.org/10.1074/jbc.M306642200
35. Varga A, Jenes A, Marczylo TH, Sousa-Valente J, Chen J, Austin J, Selvarajah S, ET AL. Anandamide produced by Ca(2+)-insensitive enzymes induces excitation in primary sensory neurons. Pflugers Arch 2014;466:1421-1435. https://doi.org/10.1007/s00424-013-1360-7
36. Cravatt BF, Giang DK, Mayfield SP, Boger DL, Lerner RA, Gilula NB. Molecular characterization of an enzyme that degrades neuromodulatory fatty-acid amides. Nature 1996;384:83-87. https://doi.org/10.1038/384083a0
37. Ross RA. Anandamide and vanilloid TRPV1 receptors. Br J Pharmacol 2003;140:790-801. https://doi.org/10.1038/sj.bjp.0705467
38. Spicarova D, Palecek J. The role of the TRPV1 endogenous agonist N-Oleoyldopamine in modulation of nociceptive signaling at the spinal cord level. J Neurophysiol 2009;102:234-243. https://doi.org/10.1152/jn.00024.2009
39. van der Stelt M, Trevisani M, Vellani V, De Petrocellis L, Schiano Moriello A, Campi B, McNaughton P, ET AL. Anandamide acts as an intracellular messenger amplifying Ca2+ influx via TRPV1 channels. EMBO J 2005;24:3026-3037. https://doi.org/10.1038/sj.emboj.7600784
40. Goncalves Dos Santos G, Li R, Ng MPE, Lemes JBP, Vieira WF, Nagy I, Tambeli CH, Parada CA. CB1 receptor-dependent desensitisation of TRPV1 channels contributes to the analgesic effect of dipyrone in sensitised primary sensory neurons. Br J Pharmacol 2020;177:4615-4626. https://doi.org/10.1111/bph.15170
41. Bhave G, Hu HJ, Glauner KS, Zhu W, Wang H, Brasier DJ, Oxford GS, Gereau RW 4th. Protein kinase C phosphorylation sensitizes but does not activate the capsaicin receptor transient receptor potential vanilloid 1 (TRPV1). Proc Natl Acad Sci U S A 2003;100:12480-12485. https://doi.org/10.1073/pnas.2032100100
42. Evans RM, Scott RH, Ross RA. Multiple actions of anandamide on neonatal rat cultured sensory neurones. Br J Pharmacol 2004;141:1223-1233. https://doi.org/10.1038/sj.bjp.0705723

43. Khasabova IA, Simone DA, Seybold VS. Cannabinoids attenuate depolarization-dependent Ca2+ influx in intermediate-size primary afferent neurons of adult rats. Neuroscience 2002;115:613-625. https://doi.org/10.1016/S0306-4522(02)00449-9
44. Farquhar-Smith WP, Egertova M, Bradbury EJ, McMahon SB, Rice AS, Elphick MR. Cannabinoid CB(1) receptor expression in rat spinal cord. Mol Cell Neurosci 2000;15:510-521. https://doi.org/10.1006/mcne.2000.0844
45. Ahluwalia J, Urban L, Capogna M, Bevan S, Nagy I. Cannabinoid 1 receptors are expressed in nociceptive primary sensory neurons. Neuroscience 2000;100:685-688. https://doi.org/10.1016/S0306-4522(00)00389-4
46. Binzen U, Greffrath W, Hennessy S, Bausen M, Saaler-Reinhardt S, Treede RD. Co-expression of the voltage-gated potassium channel Kv1.4 with transient receptor potential channels (TRPV1 and TRPV2) and the cannabinoid receptor CB1 in rat dorsal root ganglion neurons. Neuroscience 2006;142:527-539. https://doi.org/10.1016/j.neuroscience.2006.06.020
47. Hermann H, De Petrocellis L, Bisogno T, Schiano Moriello A, Lutz B, Di Marzo V. Dual effect of cannabinoid CB1 receptor stimulation on a vanilloid VR1 receptor-mediated response. Cell Mol Life Sci 2003;60:607-616. https://doi.org/10.1007/s000180300052
48. Koh DS, Stratiievska A, Jana S, Otto SC, Swanson TM, Nhim A, Carlson S, ET AL. OptoPI3K, genetic code expansion, and click chemistry reveal mechanisms underlying reciprocal regulation between TRPV1 and PI3K. bioRxiv: the preprint server for biology 2023. https://doi.org/10.7554/eLife.91012.1
49. Li T, Wang G, Hui VCC, Saad D, de Sousa Valente J, La Montanara P, Nagy I. TRPV1 feed-forward sensitisation depends on COX2 upregulation in primary sensory neurons. Sci Rep 2021;11:3514. https://doi.org/10.1038/s41598-021-82829-6
50. Spicarova D, Nerandzic V, Palecek J. Update on the role of spinal cord TRPV1 receptors in pain modulation. Physiol Res 2014;63(Suppl 1):S225-S236. https://doi.org/10.33549/physiolres.932713
51. Joseph J, Qu L, Wang S, Kim M, Bennett D, Ro J, Caterina MJ, Chung MK. Phosphorylation of TRPV1 S801 Contributes to Modality-Specific Hyperalgesia in Mice. J Neurosci 2019;39:9954-9966. https://doi.org/10.1523/JNEUROSCI.1064-19.2019
52. Adamek P, Heles M, Palecek J. Mechanical allodynia and enhanced responses to capsaicin are mediated by PI3K in a paclitaxel model of peripheral neuropathy. Neuropharmacology 2019;146:163-174. https://doi.org/10.1016/j.neuropharm.2018.11.027
53. Koivisto AP, Belvisi MG, Gaudet R, Szallasi A. Advances in TRP channel drug discovery: from target validation to clinical studies. Nat Rev Drug Discov 2022;21:41-59. https://doi.org/10.1038/s41573-021-00268-4
54. Fioravanti B, De Felice M, Stucky CL, Medler KA, Luo MC, Gardell LR, Ibrahim M, ET AL. Constitutive activity at the cannabinoid CB1 receptor is required for behavioral response to noxious chemical stimulation of TRPV1: antinociceptive actions of CB1 inverse agonists. J Neurosci 2008;28:11593-11602. https://doi.org/10.1523/JNEUROSCI.3322-08.2008
55. Chen J, Varga A, Selvarajah S, Jenes A, Dienes B, Sousa-Valente J, Kulik A, ET AL. Spatial Distribution of the Cannabinoid Type 1 and Capsaicin Receptors May Contribute to the Complexity of Their Crosstalk. Sci Rep 2016;6:33307. https://doi.org/10.1038/srep33307
56. Fischbach T, Greffrath W, Nawrath H, Treede RD. Effects of anandamide and noxious heat on intracellular calcium concentration in nociceptive drg neurons of rats. J Neurophysiol 2007;98:929-938. https://doi.org/10.1152/jn.01096.2006
57. Mahmud A, Santha P, Paule CC, Nagy I. Cannabinoid 1 receptor activation inhibits transient receptor potential vanilloid type 1 receptor-mediated cationic influx into rat cultured primary sensory neurons. Neuroscience 2009;162:1202-1211. https://doi.org/10.1016/j.neuroscience.2009.05.024
58. Tognetto M, Amadesi S, Harrison S, Creminon C, Trevisani M, Carreras M, Matera M, ET AL. Anandamide excites central terminals of dorsal root ganglion neurons via vanilloid receptor-1 activation. J Neurosci 2001;21:1104-1109. https://doi.org/10.1523/JNEUROSCI.21-04-01104.2001
59. Lever IJ, Malcangio M. CB(1) receptor antagonist SR141716A increases capsaicin-evoked release of Substance P from the adult mouse spinal cord. Br J Pharmacol 2002;135:21-24. https://doi.org/10.1038/sj.bjp.0704506

60. Bogdan DM, Studholme K, DiBua A, Gordon C, Kanjiya MP, Yu M, Puopolo M, Kaczocha M. FABP5 deletion in nociceptors augments endocannabinoid signaling and suppresses TRPV1 sensitization and inflammatory pain. Sci Rep 2022;12:9241. https://doi.org/10.1038/s41598-022-13284-0
61. Mackie K, Lai Y, Westenbroek R, Mitchell R. Cannabinoids activate an inwardly rectifying potassium conductance and inhibit Q-type calcium currents in AtT20 cells transfected with rat brain cannabinoid receptor. J Neurosci 1995;15:6552-6561. https://doi.org/10.1523/JNEUROSCI.15-10-06552.1995
62. Mackie K. Mechanisms of CB1 receptor signaling: endocannabinoid modulation of synaptic strength. Int J Obes (Lond) 2006;30(Suppl 1):S19-S23. https://doi.org/10.1038/sj.ijo.0803273
63. Felder CC, Joyce KE, Briley EM, Glass M, Mackie KP, Fahey KJ, Cullinan GJ, ET AL. LY320135, a novel cannabinoid CB1 receptor antagonist, unmasks coupling of the CB1 receptor to stimulation of cAMP accumulation. J Pharmacol Exp Ther 1998;284:291-297.
64. Rhee MH, Bayewitch M, Avidor-Reiss T, Levy R, Vogel Z. Cannabinoid receptor activation differentially regulates the various adenylyl cyclase isozymes. J Neurochem 1998;71:1525-1534. https://doi.org/10.1046/j.1471-4159.1998.71041525.x
65. Baccei ML, Bardoni R, Fitzgerald M. Development of nociceptive synaptic inputs to the neonatal rat dorsal horn: glutamate release by capsaicin and menthol. J Physiol 2003;549:231-242. https://doi.org/10.1113/jphysiol.2003.040451
66. Yang K, Kumamoto E, Furue H, Li YQ, Yoshimura M. Action of capsaicin on dorsal root-evoked synaptic transmission to substantia gelatinosa neurons in adult rat spinal cord slices. Brain Res 1999;830:268-273. https://doi.org/10.1016/S0006-8993(99)01408-0
67. Caterina MJ, Schumacher MA, Tominaga M, Rosen TA, Levine JD, Julius D. The capsaicin receptor: a heat-activated ion channel in the pain pathway. Nature 1997;389:816-824. https://doi.org/10.1038/39807
68. Kelly S, Chapman V. Spinal administration of capsazepine inhibits noxious evoked responses of dorsal horn neurons in non-inflamed and carrageenan inflamed rats. Brain Res 2002;935:103-108. https://doi.org/10.1016/S0006-8993(02)02552-0
69. Morisset V, Urban L. Cannabinoid-induced presynaptic inhibition of glutamatergic EPSCs in substantia gelatinosa neurons of the rat spinal cord. J Neurophysiol 2001;86:40-48. https://doi.org/10.1152/jn.2001.86.1.40
70. Luo C, Kumamoto E, Furue H, Chen J, Yoshimura M. Anandamide inhibits excitatory transmission to rat substantia gelatinosa neurones in a manner different from that of capsaicin. Neurosci Lett 2002;321:17-20. https://doi.org/10.1016/S0304-3940(01)02471-5
71. Morisset V, Ahluwalia J, Nagy I, Urban L. Possible mechanisms of cannabinoid-induced antinociception in the spinal cord. Eur J Pharmacol 2001;429:93-100. https://doi.org/10.1016/S0014-2999(01)01309-7
72. Spicarova D, Nerandzic V, Muzik D, Pontearso M, Bhattacharyya A, Nagy I, Palecek J. Inhibition of synaptic transmission by anandamide precursor 20:4-NAPE is mediated by TRPV1 receptors under inflammatory conditions. Front Mol Neurosci 2023;16:1188503. https://doi.org/10.3389/fnmol.2023.1188503
73. Nyilas R, Gregg LC, Mackie K, Watanabe M, Zimmer A, Hohmann AG, Katona I. Molecular architecture of endocannabinoid signaling at nociceptive synapses mediating analgesia. Eur Neurosci 2009;29:1964-1978. https://doi.org/10.1111/j.1460-9568.2009.06751.x
74. Wilson RI, Nicoll RA. Endogenous cannabinoids mediate retrograde signalling at hippocampal synapses. Nature 2001;410:588-592. https://doi.org/10.1038/35069076
75. Kreitzer AC, Regehr WG. Retrograde inhibition of presynaptic calcium influx by endogenous cannabinoids at excitatory synapses onto Purkinje cells. Neuron 2001;29:717-727. https://doi.org/10.1016/S0896-6273(01)00246-X
76. Kato A, Punnakkal P, Pernia-Andrade AJ, von Schoultz C, Sharopov S, Nyilas R, Katona I, Zeilhofer HU. Endocannabinoid-dependent plasticity at spinal nociceptor synapses. J Physiol 2012;590:4717-4733. https://doi.org/10.1113/jphysiol.2012.234229
77. Pernia-Andrade AJ, Kato A, Witschi R, Nyilas R, Katona I, Freund TF, Watanabe M, ET AL. Spinal endocannabinoids and CB1 receptors mediate C-fiber-induced heterosynaptic pain sensitization. Science 2009;325:760-764. https://doi.org/10.1126/science.1171870
78. Veress G, Meszar Z, Muszil D, Avelino A, Matesz K, Mackie K, Nagy I. Characterisation of cannabinoid 1 receptor expression in the perikarya, and peripheral and spinal processes of primary sensory neurons. Brain Struct Funct 2013;218:733-750. https://doi.org/10.1007/s00429-012-0425-2

79. Hegyi Z, Kis G, Hollo K, Ledent C, Antal M. Neuronal and glial localization of the cannabinoid-1 receptor in the superficial spinal dorsal horn of the rodent spinal cord. Eur J Neurosci 2009;30:251-262. https://doi.org/10.1111/j.1460-9568.2009.06816.x
80. Woodhams SG, Sagar DR, Burston JJ, Chapman V. The role of the endocannabinoid system in pain. Handb Exp Pharmacol 2015;227:119-143. https://doi.org/10.1007/978-3-662-46450-2_7
81. Agarwal N, Pacher P, Tegeder I, Amaya F, Constantin CE, Brenner GJ, Rubino T, ET AL. Cannabinoids mediate analgesia largely via peripheral type 1 cannabinoid receptors in nociceptors. Nat Neurosci 2007;10:870-879. https://doi.org/10.1038/nn1916
82. Richardson JD, Aanonsen L, Hargreaves KM. SR 141716A, a cannabinoid receptor antagonist, produces hyperalgesia in untreated mice. Eur J Pharmacol 1997;319:R3-4. https://doi.org/10.1016/S0014-2999(96)00952-1
83. Chapman V. The cannabinoid CB1 receptor antagonist, SR141716A, selectively facilitates nociceptive responses of dorsal horn neurones in the rat. Br J Pharmacol 1999;127:1765-1767. https://doi.org/10.1038/sj.bjp.0702758
84. Dogrul A, Gul H, Akar A, Yildiz O, Bilgin F, Guzeldemir E. Topical cannabinoid antinociception: synergy with spinal sites. Pain 2003;105:11-16. https://doi.org/10.1016/S0304-3959(03)00068-X
85. Harris J, Drew LJ, Chapman V. Spinal anandamide inhibits nociceptive transmission via cannabinoid receptor activation in vivo. Neuroreport 2000;11:2817-2819. https://doi.org/10.1097/00001756-200008210-00041
86. Martin WJ, Loo CM, Basbaum AI. Spinal cannabinoids are anti-allodynic in rats with persistent inflammation. Pain 1999;82:199-205. https://doi.org/10.1016/S0304-3959(99)00045-7
87. Fox A, Kesingland A, Gentry C, McNair K, Patel S, Urban L, James I. The role of central and peripheral Cannabinoid1 receptors in the antihyperalgesic activity of cannabinoids in a model of neuropathic pain. Pain 2001;92:91-100. https://doi.org/10.1016/S0304-3959(00)00474-7
88. Petrosino S, Palazzo E, de Novellis V, Bisogno T, Rossi F, Maione S, Di Marzo V. Changes in spinal and supraspinal endocannabinoid levels in neuropathic rats. Neuropharmacology 2007;52:415-422. https://doi.org/10.1016/j.neuropharm.2006.08.011
89. Richardson JD, Aanonsen L, Hargreaves KM. Antihyperalgesic effects of spinal cannabinoids. Eur J Pharmacol 1998;345:145-153. https://doi.org/10.1016/S0014-2999(97)01621-X
90. Starowicz K, Makuch W, Osikowicz M, Piscitelli F, Petrosino S, Di Marzo V, Przewlocka B. Spinal anandamide produces analgesia in neuropathic rats: possible CB(1)- and TRPV1-mediated mechanisms. Neuropharmacology 2012;62:1746-1755. https://doi.org/10.1016/j.neuropharm.2011.11.021
91. Starowicz K, Makuch W, Korostynski M, Malek N, Slezak M, Zychowska M, Petrosino S, ET AL. Full inhibition of spinal FAAH leads to TRPV1-mediated analgesic effects in neuropathic rats and possible lipoxygenase-mediated remodeling of anandamide metabolism. PLoS One 2013;8:e60040. https://doi.org/10.1371/journal.pone.0060040
92. Serpell M, Ratcliffe S, Hovorka J, Schofield M, Taylor L, Lauder H, Ehler E. A double-blind, randomized, placebo-controlled, parallel group study of THC/CBD spray in peripheral neuropathic pain treatment. Eur J Pain 2014;18:999-1012. https://doi.org/10.1002/j.1532-2149.2013.00445.x
93. Perras C. Sativex for the management of multiple sclerosis symptoms. Issues Emerg Health Technol 2005:(72):1-4.
94. Cravatt BF, Demarest K, Patricelli MP, Bracey MH, Giang DK, Martin BR, Lichtman AH. Supersensitivity to anandamide and enhanced endogenous cannabinoid signaling in mice lacking fatty acid amide hydrolase. Proc Natl Acad Sci U S A 2001;98:9371-9376. https://doi.org/10.1073/pnas.161191698
95. Jhaveri MD, Richardson D, Kendall DA, Barrett DA, Chapman V. Analgesic effects of fatty acid amide hydrolase inhibition in a rat model of neuropathic pain. J Neurosci 2006;26:13318-13327. https://doi.org/10.1523/JNEUROSCI.3326-06.2006
96. Di Marzo V. New approaches and challenges to targeting the endocannabinoid system. Nat Rev Drug Discov 2018;17:623-639. https://doi.org/10.1038/nrd.2018.115
97. Huggins JP, Smart TS, Langman S, Taylor L, Young T. An efficient randomised, placebo-controlled clinical trial with the irreversible fatty acid amide hydrolase-1 inhibitor PF-04457845, which modulates endocannabinoids but fails to induce effective analgesia in patients with pain due to osteoarthritis of the knee. Pain 2012;153:1837-1846. https://doi.org/10.1016/j.pain.2012.04.020
98. Mallet C, Dubray C, Duale C. FAAH inhibitors in the limelight, but regrettably. Int J Clin Pharmacol Ther 2016;54:498-501. https://doi.org/10.5414/CP202687

99. van Esbroeck ACM, Janssen APA, Cognetta AB 3rd, Ogasawara D, Shpak G, van der Kroeg M, Kantae V, ET AL. Activity-based protein profiling reveals off-target proteins of the FAAH inhibitor BIA 10-2474. Science 2017;356:1084-1087. https://doi.org/10.1126/science.aaf7497
100. Rocha JF, Santos A, Gama H, Moser P, Falcao A, Pressman P, Wallace Hayes A, Soares-da-Silva P. Safety, Tolerability, and Pharmacokinetics of FAAH Inhibitor BIA 10-2474: A Double-Blind, Randomized, Placebo-Controlled Study in Healthy Volunteers. Clin Pharmacol Ther 2022;111:391-403. https://doi.org/10.1002/cpt.2290
101. Kalliomaki J, Annas P, Huizar K, Clarke C, Zettergren A, Karlsten R, Segerdahl M. Evaluation of the analgesic efficacy and psychoactive effects of AZD1940, a novel peripherally acting cannabinoid agonist, in human capsaicin-induced pain and hyperalgesia. Clin Exp Pharmacol Physiol 2013;40:212-218. https://doi.org/10.1111/1440-1681.12051
102. Pacher P, Kunos G. Modulating the endocannabinoid system in human health and disease--successes and failures. FEBS J 2013;280:1918-1943. https://doi.org/10.1111/febs.12260
103. Milligan AL, Szabo-Pardi TA, Burton MD. Cannabinoid Receptor Type 1 and Its Role as an Analgesic: An Opioid Alternative? J Dual Diagn 2020;16:106-119. https://doi.org/10.1080/15504263.2019.1668100

Physiol. Res. 73 (Suppl. 1): S449-S470, 2024 *https://doi.org/10.33549/physiolres.935401*

REVIEW

Chemogenetic Tools and their Use in Studies of Neuropsychiatric Disorders

Markéta NEŘOLDOVÁ[1], Aleš STUCHLÍK[1]

[1]Laboratory of Neurophysiology of Memory, Institute of Physiology of the Czech Academy of Sciences, Prague, Czech Republic

Received May 11, 2024
Accepted June 25, 2024

Summary

Chemogenetics is a newly developed set of tools that allow for selective manipulation of cell activity. They consist of a receptor mutated irresponsive to endogenous ligands and a synthetic ligand that does not interact with the wild-type receptors. Many different types of these receptors and their respective ligands for inhibiting or excitating neuronal subpopulations were designed in the past few decades. It has been mainly the G-protein coupled receptors (GPCRs) selectively responding to clozapine-*N*-oxide (CNO), namely Designer Receptors Exclusively Activated by Designer Drugs (DREADDs), that have been employed in research. Chemogenetics offers great possibilities since the activity of the receptors is reversible, inducible on demand by the ligand, and non-invasive. Also, specific groups or types of neurons can be selectively manipulated thanks to the delivery by viral vectors. The effect of the chemogenetic receptors on neurons lasts longer, and even chronic activation can be achieved. That can be useful for behavioral testing. The great advantage of chemogenetic tools is especially apparent in research on brain diseases since they can manipulate whole neuronal circuits and connections between different brain areas. Many psychiatric or other brain diseases revolve around the dysfunction of specific brain networks. Therefore, chemogenetics presents a powerful tool for investigating the underlying mechanisms causing the disease and revealing the link between the circuit dysfunction and the behavioral or cognitive symptoms observed in patients. It could also contribute to the development of more effective treatments.

Key words

Chemogenetics • DREADDs • PSAMs • Neuropsychiatric disorders

Corresponding author

A. Stuchlík, Laboratory of Neurophysiology of Memory, Institute of Physiology of the Czech Academy of Sciences, Prague, Czech Republic. E-mail: ales.stuchlik@fgu.cas.cz

Introduction

In neuroscience, especially brain research, the need for selective modulation of separate brain areas or neuronal subpopulations has become increasingly pressing. Especially in the case of brain diseases, understanding the brain's circuitry is crucial for finding the underlying causes and possible targets for medication. It has been shown that the dysfunction of specific networks or connections between different brain areas leads to the impairments and behavioral changes caused by the disease. It can be seen in Alzheimer's disease as the hyperactivity of the hippocampus preceding neurodegeneration [1], the hypofunction of the prefrontal cortex in schizophrenia [2], or the impairments in attention-deficit/hyperactivity disorder (ADHD) [3]. However, studying these circuits, their activity, and how they influence one another with the current methods is not always optimal. For example, lesions do not allow for investigation of different areas' interplay and functional connectivity [4]. Optogenetics is a very invasive method, only targeting a small spot for a short time [5]. That is why chemogenetics could lead to significant advances in this field.

How we got to chemogenetics

This paper is a part of the issue of the Physiological Research, which commemorates the 70th anniversary of the Institute of Physiology of the Czech Academy of Sciences. The Laboratory of Neurophysiology of Memory at this Institute has made significant advancements in the study of memory mechanisms, progressing from traditional techniques to the utilization of chemogenetics. This shift reflects a broader trend in neuroscience toward integrating molecular, cellular, and systemic approaches to understanding cognitive functions.

Initially, the department focused on traditional neurophysiological and behavioral studies. These included examining the hippocampus [6-8] and its roles in spatial navigation and memory, a classic model for studying the neurobiological mechanisms underlying learning, decision-making, and other higher cognitive processes. Over time, the department's research expanded to include various aspects of spatial orientation in laboratory rodents, the role of brain structures and neurotransmitter systems in spatial behavior [9-12], and the study of cognitive deficits associated with modeled neuropsychiatric diseases [13].

The transition to chemogenetics was a natural progression of the department's evolving research interests and capabilities. Chemogenetics offers a more precise way to manipulate and study specific neuronal populations and their functions. This method allows for the control of neuronal activity using engineered receptors and specific, pharmacologically inert ligands. By adopting this technique, the laboratory can investigate the neural basis of behavior with greater specificity and detail, contributing significantly to both fundamental knowledge and applied outcomes in neuroscience.

Through these developments, the department has advanced our understanding of memory and cognitive processes and made significant contributions to the study of neurodegenerative and neuropsychiatric disorders. The adoption of chemogenetics by the Laboratory of Neurophysiology of Memory exemplifies the ongoing evolution in neuroscience research, where cutting-edge techniques are increasingly employed to unravel the complexities of the brain and behavior.

What is chemogenetics

Chemogenetics is a field interconnecting biology and chemistry that seeks to engineer proteins (especially GPCRs) to show an altered interaction with endogenous and synthetic ligands for more precise and rapid control of cellular activity. These synthesized proteins retain all their functions except their ligand specificity, so they selectively respond only to specific small molecules, usually artificially synthesized [14,15]. These engineered proteins can then be used to investigate physiological mechanisms (on the level of cells, organs, or whole organisms and their behavior) or potentially for therapy. The creation of chemogenetic tools permitted the control of a specific type of GPCR (in a particular subpopulation of cells) by a single specific ligand. These tools allow for a more targeted control by eliminating the activation of other molecular targets. They also help identify the signalling pathways affected and the subsequent consequences for better analysis of cell functions [16,17]. Neuroscientists use these predominantly to non-invasively control cell signalling in freely moving animals (mainly rats and mice) to distinguish between such cells' normal and pathological function and their effects on certain behaviors [18].

The most commonly used chemogenetic tools are Receptors Activated Solely by Synthetic Ligands (RASSLs) [19] and DREADDs [20]. New tools have also emerged, like the engineered Ligand-Gated Ion Channels (eLGIC) [21].

RASSLs were first generated by modifying the extracellular loop of the G-protein coupled human κ-opioid receptor so it would not bind the endogenous protein ligands (like dynorphin). Because these receptors have a different binding site for the small molecules and the protein ligands, they remained capable of being activated by small synthetic molecules chosen for the experiment after the mutation. The limitations of this approach are the residual affinity of these small synthetic molecules for the wild-type receptors, which is primarily an issue for experiments *in vivo* [14], and the high constitutive activity of RASSLs [22].

DREADD technology is the one overcoming these shortcomings. These chemogenetic tools have low constitutive activity and suppressed affinity for any endogenous ligands, binding only biologically inert synthetic ligands. The muscarinic receptors are the GPCRs most often used for DREADDs, with the synthetic ligand being clozapine *N*-oxide, which is

biologically almost inert. They are usually created using a novel directed molecular evolution method [17].

Lastly, the eLGICs permit control of the ion conductance of neurons *via* a ligand-binding domain of a particular ion channel mutated into a Pharmacologically Selective Actuator Module (PSAM). PSAM responds only to a specific Pharmacologically Selective Effector Molecule (PSEM), which can activate or silence these neurons [21]. One of the first studies on LGICs used an invertebrate chloride channel activated by ivermectin to function as a neuron-silencing tool [23]. Later on, the effectiveness of this tool was improved by mutating a human α1 glycine receptor to respond to ivermectin because this receptor showed increased cell expression and better sensitivity [24].

The principles and mechanisms

Due to chemogenetics being a relatively new tool, this chapter goes over the different ways of generating the modified receptors, how they are delivered to the site of interest, and methods for activating them. Generally speaking, chemogenetics is based on orthogonal chemical genetics, where a particular protein is changed (mainly in its binding domain) to respond only to a specific molecule. This small molecule is artificially synthesized and usually silent in interactions with endogenous receptors [16,25]. Except for RASSLs, these small molecules can interact with wild-type receptors, making this tool unsuited for *in vivo* systems where their activity could interfere with that of the RASSLs [14].

Furthermore, the specific protein is mutated, so it would be activated by the orthogonal ligand (one that does not interact with the endogenous system) and retain all the other protein functions. It is usually also engineered not to accept the endogenous ligands, only the orthogonal ones, making it an orthogonal protein [26]. The directed molecular evolution approach usually executes this mutation and selection process in DREADDs (and eLGICs). This approach creates a library of mutants by random mutagenesis *via* error-prone polymerase chain reaction (PCR). These mutants are afterward screened for high affinity for the designer ligand while showing low to no affinity for the endogenous ligand. The selection is achieved by making the GPCR activity in the yeast population crucial for survival and placing them on a selective medium with the synthesized ligand. Like this, only the yeast cells with GPCRs activated by the synthetic ligand will survive and be used for the experiments [17].

On the other hand, RASSLs are created by rational design. This approach consists of modeling and evaluating a chosen protein's structure to mutate it by site-specific mutagenesis. The rational design method is faster and more directed, but structural data is needed compared to the directed molecular evolution approach [27].

The application of chemogenetics requires gene transfer, facilitated mainly by viral vectors (more precisely, retroviruses). Adeno-associated viruses (AAV) are the most commonly used as they do not produce high immune response cytotoxicity. Therefore, their expression lasts longer, making them practical and safer for studying behavior [28]. Also, different serotypes of recombinant AAV allow for targeted gene transfer into specific tissues or organs. Some of these serotypes even permit labeling neuronal populations that are harder to reach *via* retrograde transport [28]. Moreover, AAV (more precisely recombinant rAAV) can be altered through direct evolution to increase their efficiency of retrograde transport and expression, for example, by changing capsid variants. Such alterations can be helpful in research and clinical gene therapy [30].

Other types of vectors can also be used for gene transfer in chemogenetics. Lentiviruses (based on HIV) were shown to have more efficient transduction, meaning that the vector spreads into more cells [31]. Some types of herpes simplex virus (HSV) move retrogradely and allow studying even the regions of the brain that are harder to reach [32]. HSV is also useful for their larger capacity since they can carry longer gene sequences or multiple transgenes [33].

The choice of the promoter is also crucial as it enables the targeting of specific cell types based on the nuanced expression levels of certain genes [34,35]. To further specify the location of the transcript, transgenic mice expressing the enzyme Cre-recombinase in a specific cell type are used. In that case, the DREADD coding gene is inverted. It can be transcribed only in the cells with Cre-recombinase because it can excise the gene based on loxP sites (in the case of a double-floxed inverted open reading frame), making it available for transcription [36].

DREADDs can be effectively used for circuit-specific interrogation, particularly useful for studying brain diseases (schematically shown in Fig. 1). First, the designer receptors are applied to the area by injecting the virus vector, then activated on demand by a specific ligand. This targeting and activation of a particular neuronal circuitry can be accomplished in multiple ways.

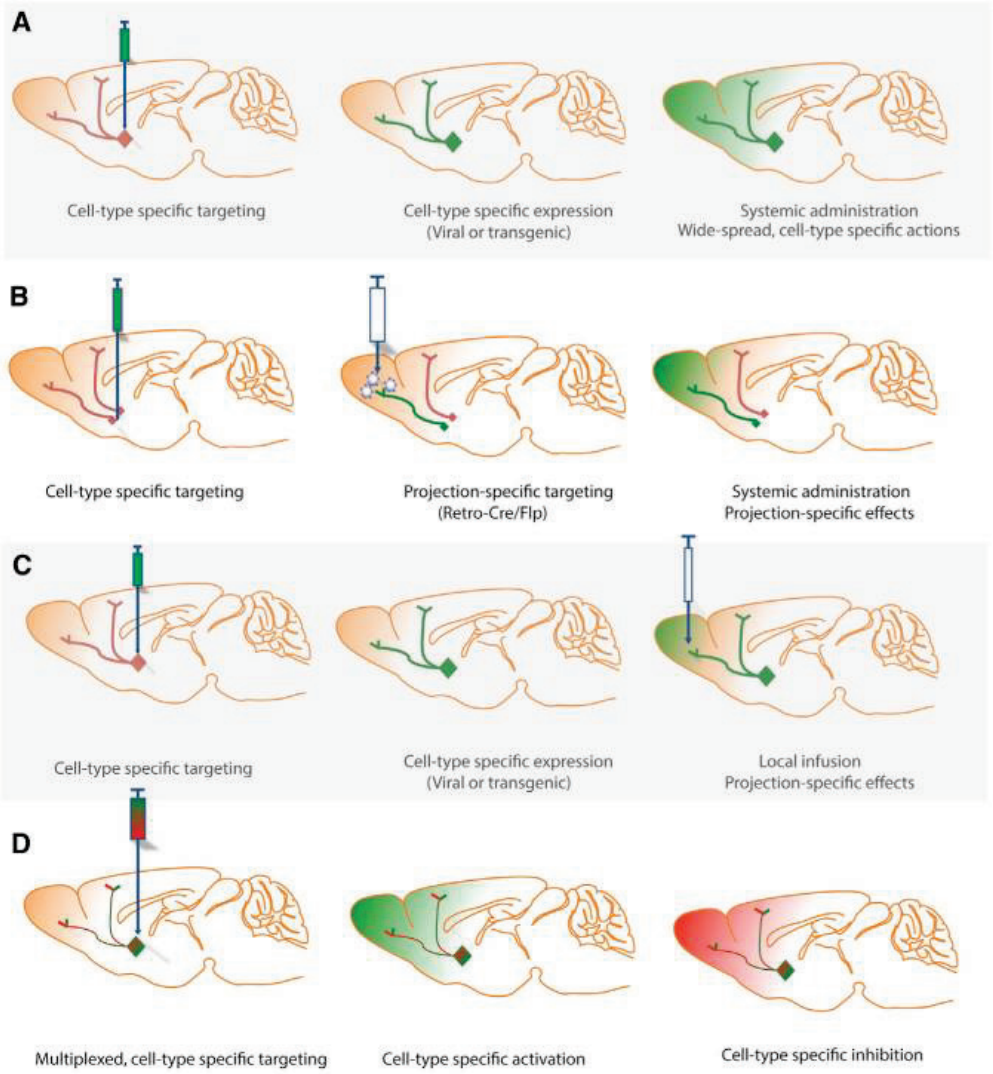

Fig 1. Schematic representation of different approaches to DREADD expression and activation in the brain. (**A**) Expression of DREADDs in a specific cell type by viral vectors or transgenically (*via* an externally inducible transgene promoter) and their subsequent activation by systemic administration of the appropriate ligand. (**B**) Injection of cell-type-specific viral vector and then of the Cre-recombinase carrying viral vector transported retrogradely from the neuron's projection site to activate the transcription of the sequence from the first virus. The expressed DREADD is then activated by systemic administration of the ligand. (**C**) Cell-type-specific expression of DREADDs as in (A) but with the selective activation of chosen projections by local (intracranial) ligand injection. (**D**) Expression of different DREADDs in specific cell types for multiplexed control of their activity (source: from [38], copyright purchased).

It can be done by targeting a specific cell type thanks to a corresponding promoter and then selectively activating the subpopulation by local intracranial administration of the ligand. Usually, it is CNO microinjected through the intracranial cannula(s) into a particular brain subregion of interest. Like this, DREADDs can be activated solely in this region, such as the dorsal dentate gyrus terminals of the entorhinal cortex. The issue with this method is its invasiveness as the cannulas are surgically implanted, going through the skull into the brain region [37]. Another possibility for modulating the activity of specific brain circuits is the dual viral-vector methodology. For example, Cre-dependent DREADD is injected into a region with cell bodies of the studied neurons. The retrograde vector with Cre-recombinase is injected into the area where the studied neurons are projecting. Therefore, the expression of DREADDs will be limited only to the neurons projecting from the first region to the second one injected. Afterward, the expressed DREADDs can be activated by systematically injecting the drug, which is not invasive and allows for easier manipulation [32].

As was already partially discussed, there are different ways of designer drug administration. The administration choice depends on the chemogenetic receptor type and the experimental design. It can be

delivered systemically, intracranially, or orally. Also, there are multiple different ligands from which to choose (this will be discussed in greater detail further). Nonetheless, CNO is the most commonly utilized ligand for DREADDs (the prevalent chemogenetic tool used) [39]. Systemic drug injection is advantageous due to its easy manipulation and non-invasiveness while keeping an effective and rapid control of targeted neurons (within 10 minutes after systemic CNO application, the response is activated, with a peak after 20 minutes) [40]. However, the dose of the synthetic ligand can have varying effects based on the receptor used, the type of brain region, and the behavior targeted [41]. Intracranial administration permits selective control of specific brain regions or even the subpopulations of neurons and their specific projections. However, as suggested, its invasiveness reduces the method's applicability [42]. Last, oral administration is usually used for chronic activation of the chemogenetic receptor. It is added to food or water, freely available to the tested animals, and is less stressful than injections. Still, the presence of CNO in water could aggravate its taste, leading to higher water consumption when removed, which could interfere with the study results [43].

G-protein coupled receptors

Since the most prevalently used chemogenetic tools are DREADDs (and RASSLs) based on GPCRs, it is necessary to discuss their mode of function, why they are an effective tool for cell activity modulation, and some shortcomings. GPCRs are seven-transmembrane receptors forming complexes with G-proteins or β-Arrestins. These two compete for the receptor as the complex with β-Arrestins blocks the binding of G-proteins on the receptor, desensitizing it and impeding the G-protein coupled signaling pathways [44]. Therefore, the activated receptor can bind only to one of the two at a time, creating agonist-induced selectivity. Atop the desensitization effect, β-Arrestins can also lead to the internalization of the GPCR and, therefore, cause issues concerning the dosing of the ligand in experiments using GPCR-based chemogenetics [45]. Furthermore, the type of ligand, receptor type, and cellular context can bias the receptor toward one signaling pathway over others, also called functional selectivity [46].

Even though various ligands activate G-protein coupled receptors, they can also signal without them, with higher or lower probability based on the receptor type, called constitutive activity. That is especially crucial to account for when using chemogenetics. If the expression of the receptor in the target cell is high, it can generate a phenotype even in the absence of a ligand due to its constitutive activity. Even though DREADDs generally have low constitutive activity, it is essential to consider this factor [22].

The signaling pathways GPCRs activate are numerous, and their effects can be more far-reaching than just silencing or enhancing neuronal activity. Unfortunately, it is not always sure whether the silencing or enhancing of neuronal firing happens through a canonical or non-canonical pathway and how the different receptor isoforms may influence the signaling pathways. However, it may be important information since the isoforms can lead to additional changes in cell activity [47]. Furthermore, some have separate extracellular binding sites for endogenous protein and small molecule ligands such as CNO. Therefore, the binding site for an endogenous ligand can be altered to be dysfunctional while keeping a high affinity for the small molecule and the original mode of function of the receptor [17].

All the above and the fact that GPCRs are one of the most prevalent receptors in cells, therefore playing a part in many cell functions, make them an excellent tool for use in various scenarios. It permits studying a whole range of cellular activities and behaviors. So even, despite some caveats, they have undeniable advantages for use as chemogenetics.

Types of chemogenetic tools

Chemogenetics is a superordinate term for multiple tools (as outlined in previous chapters) based on engineering proteins to alter their ligand specificity for rapid and precise control of cell signaling *in vivo*. Therefore, specifying these different types and how they function would be appropriate (schematically shown in Fig. 2).

Kinases

Kinases were among the first genetically modified proteins to work as chemogenetic tools. They were generated by creating a functionally silent mutation in the ATP [16] or GTP [48] binding sites, respectively, and then an already existing corresponding kinase (or GTPase) inhibitor was synthesized to attach to the altered site. Thanks to this approach, the effect of its inhibition on the cell could be observed. Furthermore, the specific signaling pathway it engages in and the role

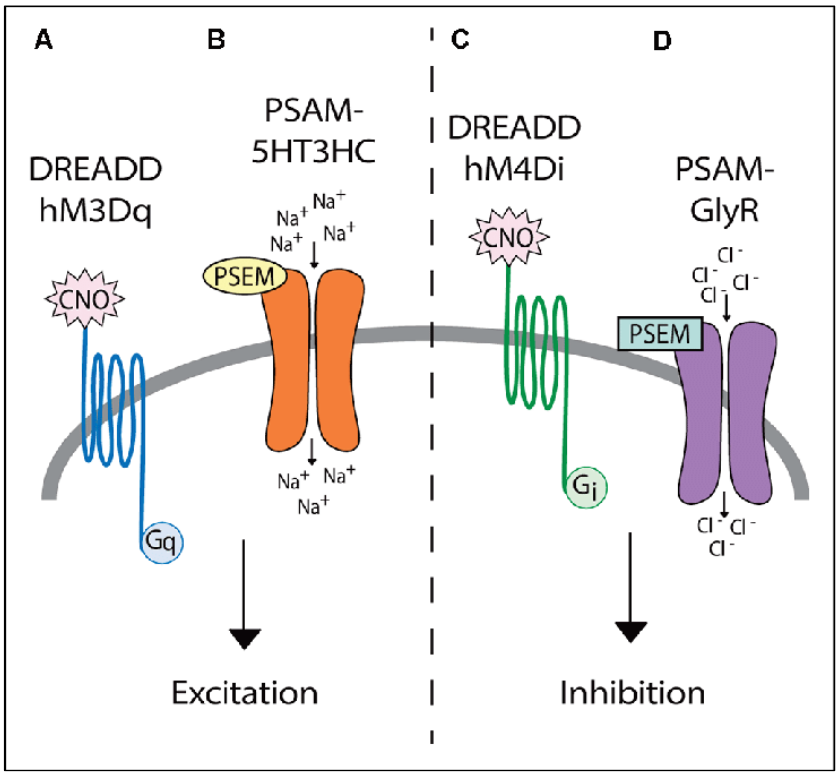

Fig. 2. Schematic representation of four different types of chemogenetic tools. On the left, (**A**) DREADD hM3Dq and (**B**) PSAM-5HT3HC act through depolarization of the neuronal membrane to produce excitation. On the right, (**C**) DREADD hM4Di and (**D**) PSAM-GlyR hyperpolarize the membrane to induce inhibition. The DREADDs activate the respective G-protein coupled signaling cascades after CNO binds. The PSAMs, on the other hand, are activated by PSEMs and directly open ion channels, causing the appropriate effect by selective ion influx (sodium for excitation and chloride for inhibition) [55].

of the kinase in the cell could be reconstructed. This approach is essential for treating diseases since it can uncover the signaling cascade and specific targets for drugs in therapy. For example, the research on the v-Src and Fyn kinases, which play a significant role in oncogenesis, focused on uncovering their signaling pathways. These kinases were mutated in their binding site (point mutation of Ile338 to Gly) to only respond to a synthetically altered inhibitor, ATP-analogue, called compound 3g [49]. A similar study was conducted only with a different ATP-analogue for the v-Src kinase [50]. The paper on ephrine B-type (EphB) tyrosine kinase, which plays a significant role in brain development, employed a similar approach. A targeted mutation of Ile amino acid residue to Gly permitted the activation of such kinases by a synthetic molecule (like PP1) inert with the wild-type kinase. This study revealed the importance of EphB tyrosine kinase signaling in many areas of neuronal development [51].

Enzymes

Another class of proteins grouped under the chemogenetic tools is enzymes. Here, the studies focus on developing artificial enzymes that mimic the naturally occurring enzymatic processes to study their natural function or, for example, to improve their efficiency. A protein scaffold and a catalytic group can be linked to create a new enzyme. On top of that, a change in the position of functional groups in the binding site can play a significant role in ligand selectivity, affecting the efficiency of the enzymatic reaction. This use of chemogenetically modified enzymes in research was demonstrated in a study on the myosin isoenzyme. Its binding site was changed to selectively bind an ATP-analogue that does not activate other isoenzymes to determine the enzyme's specific function [25], introducing Lys residues into the active site of artificial transaminase was conducted to improve its selectivity for the substrate. The improved selectivity led to an increase in the kinetic rate of the reaction.

G-protein coupled receptors: RASSLs and DREADDs

To date, the chemogenetic technology based on GPCRs is the most popular tool in many areas of science, especially in behavioral studies. These tools include the RASSL and DREADDs. Similar attempts as with the kinases have been introduced for GPCRs. Furthermore, GPCRs are also often targets of pharmacological remedies; therefore, studying their affinity and selectivity for ligands is crucial. It was first explored on the β-adrenergic receptor by embedding a point mutation of Asp113 in the binding site to change the receptor's specificity for a ligand, creating the first GPCR-based chemogenetic tool [53].

The RASSLs were created to study the downstream effects of G-protein-coupled receptors because it is hard to separate the function of one from the other due to their abundance in the organism. The RASSLs were first based on the κ-opioid receptor coupled with the G_i protein. Coward *et al*. [14] created chimeric receptors with parts from μ and δ opioid receptors. This resulted in decreased affinity for the peptide ligands but retained it for the small molecules, as these have different binding sites on the receptor. Like this, it is possible to study and control the activity of GPCRs and their physiological effects selectively by small molecule drugs.

Nonetheless, these small molecules can still activate wild-type receptors, so DREADDs were developed for use *in vivo*. They are also based on the GPCRs but are created so only a synthetic naturally inert ligand activates them, eliminating the simultaneous activation of wild-type GPCRs. DREADDs are now the most used chemogenetic tools with various types of receptors and ligands (more specified in the Synthetic receptors and ligands chapter). A particular one is the κ-opioid DREADD (KORD), which is based on the human κ-opioid receptor and is used to inhibit neuronal activity. It is different since it responds to Salvinorin B instead of CNO, unlike the other DREADDs (human muscarinic receptor-based). Thanks to that, it deals with the issues arising from the back-metabolization of CNO to clozapine [54]. It allows for multiplexed control of cell activity [20].

Ligand-gated ion channels

The last category of chemogenetic technologies, based on ion channels, is eLGIC, sometimes called PSAM. They rapidly control ion conductance on the cell membrane and, therefore, neuron activity. Again, that makes them valuable in studying the effects of these ions on the molecular level and their far-reaching consequences on behavior. A chimeric LGIC has a mutated ligand-binding domain called PSAM, which can interact only with pharmacologically selective effector molecules (PSEMs). These are small molecules that do not bind to the native receptor. Like this, effective neuron-activating or -inhibiting systems can be created, depending on the ion channels chosen and altered. Their advantage is using multiple eLGICs within one cell population or with different tools like optogenetics [21].

Recent advances in ligand-gated ion channel (LGIC) research have introduced the eLGIC type, a novel system based on acetylcholine receptors called BARNI (Biologically Advanced Receptor for Novel Interactions). This innovative type of LGIC is noteworthy due to its activation through a clinically approved ligand, which underscores its potential for simplified clinical translation and application. The ability of BARNI to be activated by an existing, clinically approved compound significantly reduces the regulatory and developmental hurdles typically associated with new therapeutic interventions, making it an attractive candidate for rapid integration into clinical practice [56].

The BARNI system leverages acetylcholine receptors' structural and functional properties, which play critical roles in various physiological processes, including muscle activation and cognitive function [57]. The BARNI system circumvents the often lengthy and costly process of novel ligand development and approval by utilizing a clinically approved ligand. This strategy aligns with recent trends in drug repurposing, where existing drugs are adapted for new therapeutic applications, thus speeding up the transition from bench to bedside [58].

Moreover, the clinical applicability of the BARNI system is further enhanced by its potential to be used in a range of therapeutic contexts. For instance, acetylcholine receptor modulation has been implicated in treating neurological disorders such as Alzheimer's disease and myasthenia gravis [59]. The eLGIC type's ability to precisely target these receptors could lead to more effective therapies with fewer side effects than traditional treatments [60]. Furthermore, using a clinically approved ligand means that safety profiles are already well-established, thereby reducing the risk of adverse effects in patients [56].

Synthetic receptors and ligands

Receptors

Over the years of using chemogenetic tools in science, many receptors and ligands have been created to suit the needs of the experimental design or improve the required characteristics of chemogenetic tools, like selectivity or off-target activity.

As seen in Table 1, multiple classes of proteins are used in chemogenetics: kinases, enzymes, channels, and GPCRs, which are the most explored and widely applied. From GPCRs, the most employed receptors are those based on the human muscarinic receptor, which has given rise to DREADD technology. Due to that, this chapter will be focused mainly on the DREADDs. Multiple types of DREADDs have been engineered and

Table 1. Table illustrating the different types of chemogenetic tools used.

Name	Protein(s)	Ligand	Reference
Representative kinases			
Allele-specific kinase inhibitors	v-I388G	Compound 3g	[50]
Analogue-sensitive kinases	v-Src (I338G, v-Src-as1), c-Fyn (T339G, c-Fyn-as1), c-Abl (T315A, c-Abl-as2), CAMK IIα (F89G, CAMK IIα-as1) and CDK2 (F80G, CDK2-as1)	K252a and PPI analogs	[49]
Rapamycin-insensitive TOR complex	TORC2 V2227L	BEZ235	[26]
ATP-binding pocket mutations in EphB1/2/3	*Ephb*1^{T697G}, *Ephb*2^{T699A}, and *Ephb*3^{T706}	PP1 analogs	[51]
ATP-binding pocket mutations of TrkA/B/C	*TrkA*^{F592A}, *TrkB*^{F616A}, and *TrkC*^{F617A}	1NMPP1 and 1NaPP1	[61]
Representative enzymes			
Metalloenzymes	Achiral biotinylated rhodium diphosphine complexes		[62]
Engineered transaminases	Chemically conjugating a pyridoxamine moiety within the large cavity of intestinal fatty acid binding protein	Enhanced activity	[52]
Representative GPCRs			
Allele-specific GPCRs	β2-adrenergic receptor, D113S	1-(3′,4′-dihydroxy phenyl)-3-methyl-L-butanone (L-185,870)	[53]
RASSL-G_i	κ-opioid chimeric receptor	Spiradoline	[14]
Engineered GPCRs	5-HT2A serotonin receptor F340→L340	Ketanserin analogues	[63]
G_i-DREADD	M2- and M4 mutant muscarinic receptors	Clozapine-N-Oxide	[17]
G_q-DREADD	M1, M3, and M5- mutant muscarinic receptors	Clozapine-N-Oxide	[17]
G_s-DREADD	Chimeric M3-frog Adrenergic receptor	Clozapine-N-Oxide	[64]
Arrestin-DREADD	M3Dq R165L	Clozapine-N-Oxide	[65]
Axonally-targeted silencing	hM4D-neurexin variant	Clozapine-N-Oxide	[66]
KORD	κ-opioid receptor D138N mutant	Salvinorin B	[20]
Representative channels			
GluCl	Insect Glutmate chloride channel; Y182F mutation	Ivermectin	[67]
TrpV1	TrpV1 in TrpV1 knock-out mice	capsaicin	[68]
PSAM	Chimeric channels PSAMQ79G,L141S PSAM-GlyR fusions	PSEM9S PSEM89S; PSSEM22S	[21]

The kinases as the first chemogenetics developed at the top, including the allele-specific inhibitors, analogue-sensitive kinases, the rapamycin-insensitive target of rapamycin (TOR) complex, ATP-binding pocket mutations in ephrin B-type receptor (EphB) 1/2/3 and ATP-binding pocket mutations of tropomyosin receptor kinase (Trk) A/B/C. Each subtype of kinases has examples of proteins used as chemogenetic tools (like Ca^{2+}/calmodulin-dependent protein kinase II (CAMKII) or cyclin-dependent kinase 2, the target of rapamycin complex 2 (TORC2), EphB2 or TrkA) and their respective ligands. Then, the groups of enzymes are modified to classify as chemogenetics: metalloenzymes and engineered transaminases and their effect, such as enhanced activity. The third group is the largest, containing the GPCRs used as chemogenetics with allele-specific and engineered GPCRs, RASSLs, and DREADDs, again with the specific receptors (like the muscarinic, adrenergic, serotonin, or opioid receptors) and their ligands, which have been used in research. The last group includes the channels: glutamate Cl^- channel (GluCl), transient receptor potential vanilloid 1 (TrpV1) channel, and PSAM like the PSAM-Glycine receptor (GlyR) fusion.

coupled with different G proteins and, therefore, various signaling pathways, G_q, $G_{i,}$ or G_s, as specified further.

For DREADDs based on G_q signaling, human M1, M3, and M5 muscarinic receptors are mutated to obtain selective activation by CNO. The human muscarinic M3 DREADD (hM3Dq) is most prevalent from these. Their activation leads to phosphatidylinositol hydrolysis, which stimulates the release of intracellular Ca^{2+}, resulting in increased neuronal firing [17,69]. Because the release of Ca^{2+} ions plays an essential role in many cell types, it has been used more widely. For example, in the research of glial cells [40] or pancreatic β cells, where the activation of pathways, including insulin receptor substrate 2 (IRS2), by these DREADDs was crucial [70].

G_i-coupled DREADDs are used for neuronal silencing, with the human muscarinic M4 DREADD (hM4Di) being a popular inhibitor for experiments. This DREADD derived from the human M4 muscarinic receptor activates the G-protein coupled inwardly rectifying potassium channel (GIRK) pathway by Gβ/γ, which subsequently leads to hyperpolarization of the neuron, therefore silencing the neuron's firing [17]. Furthermore, relatively recently, a new inhibitory DREADD called KORD was created. It exploits a mutated version of the κ-opioid receptor, which answers to the binding of Salvinorin B instead of CNO. Due to the activation by different ligands, KORD, and muscarinic-based receptors can allow for more diverse, bi-directional (when G_q-based DREADDs are used) control when expressed in the same neuronal population [20].

Last, concerning the types of DREADDs, G_s-coupled ones have been developed and used *in vivo* to study medium spiny neurons [71] or β-cells in the pancreas [64]. These are based on the human M3 muscarinic receptor and signal either by $G\alpha_s$ or the closely related subunit $G\alpha_{olf}$. The activation of these G-proteins results in increased cyclic adenosine monophosphate (cAMP) concentration. This activation of neurons expressing the corresponding DREADD manifests as certain associated behaviors. In the case of striatopallidal medium spiny neuron activation, it decreases the locomotion of tested rats [71].

For PSAMs, many different receptors have been engineered for silencing and enhancing neuronal firing. The α7-5HT3 channels have been developed as the activators, while eLGICs based on the glycine and γ-Aminobutyric acid (GABA) receptors act as inhibitors [21].

Ligands

Regarding the types of ligands, the choice depends on the specific chemogenetic tool, but since DREADDs are the most explored ones, this paragraph will focus on ligands used for DREADD activation. CNO is the most popular and first paired with DREADDs because it has a high affinity for human muscarinic receptors. Also, it is biologically inert in the presence of only the wild-type receptors [17]. Unfortunately, this was later found to be only partially true since CNO does exhibit some off-target activity and is also back-metabolized in the brain to clozapine and *N*-desmethyl clozapine (NDMC) in both rats and mice [39]. And these molecules are not biologically inert [72]. Gomez *et al.* [73] suggested that it might be the back-metabolized clozapine that crosses the blood-brain barrier and possibly activates the DREADDs instead of CNO (which has low permeability of the blood-brain barrier) since it also shows a great affinity for DREADDs.

On the other hand, [74] showed that the CNO crosses the blood-brain barrier (BBB) to an extent and could be more readily available to bind to the DREADDs instead of clozapine which binds unspecifically in the brain tissue. Moreover, it was shown that CNO, even in the micromolar doses, causes off-target effects on many endogenous receptors (dopaminergic, serotonergic, muscarinic, or even adrenergic), which again hinders its suitability for use as a DREADD ligand. Nonetheless, there has not been agreement on whether these off-target effects cause some behavioral changes or not. A study using the five-choice-serial-reaction task did not observe any [74], while another one reported changes in amphetamine-induced locomotion and startle response following even low doses of CNO [54].

One possible alternative to CNO use is low doses of clozapine, which do not seem to cause behavioral effects, instead of high concentrations of CNO (needed for it to cross the BBB). This approach could eliminate the back-conversion that is highly variable between species or even sexes and can confound the experimental results. However, uncertainty about the off-target effects of clozapine remains [74]. Another ligand that could substitute CNO is compound 21 (C21). It does not back-metabolize to clozapine, and it readily crosses the BBB. Unfortunately, it exhibits off-target competitive inhibition of many endogenous GPCRs. However, no behavioral consequences of this effect have been reported [74].

Moreover, in low doses (of 0.5 mg/kg), the off-target effects can be eliminated while keeping sufficient activation of the DREADD. Nonetheless, the optimal dose may differ between males and females, complicating the experimental design [75]. The next ligand used for DREADDs is salvinorin B. It is a derivate of salvinorin A, a specific ligand of the κ-opioid receptor, mutated not to activate the endogenous receptor or other receptors (like the muscarinic ones). It is successfully used as the KORD activator, resulting in significant behavioral changes by silencing specific neuronal populations [20]. Last, perlapine could serve as another valuable ligand to substitute CNO in activating hM3Dq, but no other types of DREADDs as it does not have a strong enough affinity for those. Its affinity for the hM3Dq is even higher than that of CNO [76].

Unfortunately, not many of these ligands can potentially be used as therapeutics. CNO is back-metabolized to clozapine with off-target effects, and perlapine does not have an affinity high enough for hM4Dq (the DREADDs most prospective for the treatment of brain diseases like schizophrenia). The only ligands with possible applications are C21 [77] or an already approved drug for schizophrenia, olanzapine, which was newly discovered to have an affinity for hM4Dq receptors and, therefore, could be used as a therapeutic ligand in humans. Unfortunately, in the doses needed for this activation, it binds to the native dopamine D2 receptors and causes side effects of treatment [78].

Deschloroclozapine is a potent, selective, and metabolically stable agonist used in chemogenetics to activate designer receptors exclusively activated by designer drugs (DREADDs). This compound is particularly valuable due to its high affinity and efficacy in binding to the engineered G protein-coupled receptors (GPCRs) without interacting with endogenous receptors, thus minimizing off-target effects [79]. In experimental settings, deschloroclozapine can selectively modulate neuronal activity, enabling precise control over specific neural circuits [38]. This facilitates the study of complex brain functions and behaviors and the investigation of disease mechanisms and potential therapeutic interventions in neurological and psychiatric disorders [73]. Its usage represents a significant advancement in chemogenetic methodologies, providing a powerful tool for dissecting cellular and molecular functions *in vivo* with high specificity and temporal precision.

Selected brain diseases studied using chemogenetics

Since DREADDs are the most used chemogenetic tools, this work will mainly focus on the application of DREADDs in the research of brain diseases, with the occasional mention of other chemogenetic technologies. It will focus on the neuronal circuit's dysfunctions since chemogenetics are most apt to regulate these as they can be expressed in larger areas of the brain or the downstream projections of specific neuronal populations and for more extended periods.

Alzheimer's disease

Chemogenetics has been used in the research to determine the underlying causes of AD impairments and possible early diagnosis or treatment targets (schematically shown in Fig. 3). Rodriguez *et al.* [80] showed that when the entorhinal cortex activity was reduced, the accumulation of Aβ plaques and tau neurofibrils decreased, too. They used the hM4Di and its synthetic ligand CNO to produce chronic attenuation of neuronal activity for six weeks in human amyloid protein precursor (hAPP)/Aβ overproducing 16-month-old transgenic mice. They detected mainly diffuse, small-sized plaques affected by the change in firing activity, pointing to its effect on new plaque accumulation but not clearance. Furthermore, it impacted the phosphorylated tau protein aggregation in neurons downstream from the entorhinal cortex in the hippocampus. Still, the effects were not distinct compared to the Aβ plaques accumulation.

A similar study by Peng and Grutzendler [81] further supports these findings. They used the hM3Dq for neuronal activation and hM4Di for neuronal inhibition to evaluate their effects on Aβ plaques. CNO was administered daily for 30 or 60 days. They also found that the attenuation of neuronal activity reduced the accumu-

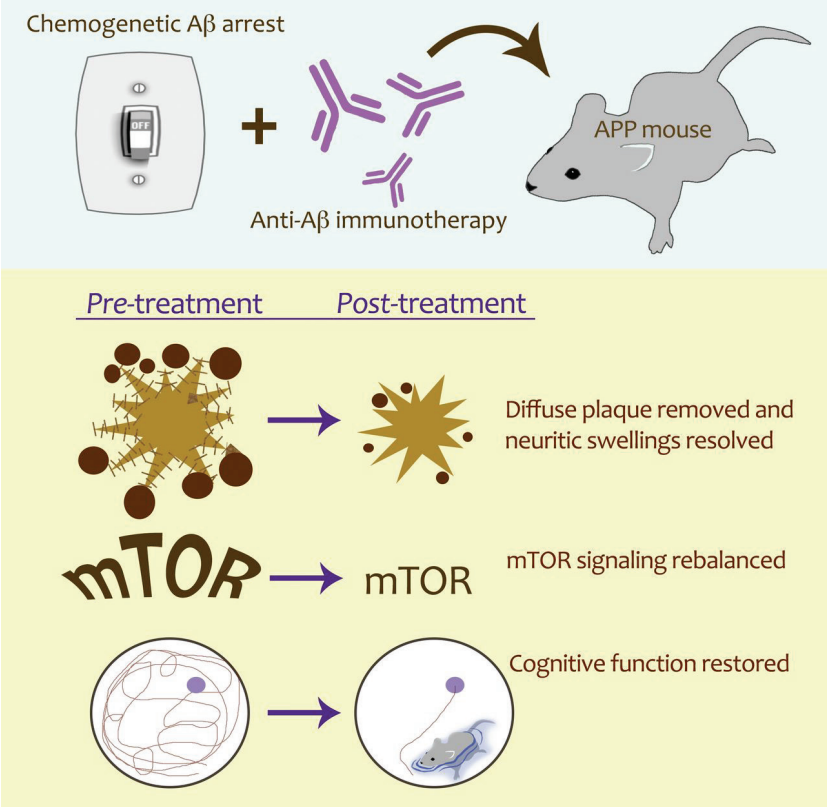

Fig. 3. This picture illustrates the possibility of improving cognitive impairments in an AD mouse model by employing chemogenetic and immunotherapeutic approaches to reduce Aβ plaque accumulation and restore normal mammalian TOR signaling (adapted from [83]).

lation of Aβ plaques and the diameter of the halo of oligomeric Aβ (which plays a vital role in axonal dystrophy) in the controlled neurons of cortical layer V. The exact mode of action leading to the decreased deposition of Aβ plaques was not found. The examination of thalamic nuclei, which receive the projections from DREADD-controlled neurons, showed that the neuronal activity could influence the production and axonal or somatodendritic release of Aβ plaques, leading to its accumulation and the subsequent neuronal dystrophy instead of changes in transcription or translation of APP or associated proteins. This could eventually lead to discovering potential treatment targets to reduce β-amyloid deposition and pathological neuronal dystrophy.

Another study focused on the locus coeruleus, an important noradrenergic region that plays a role in spatial memory and is impaired in AD. Here, the aggregation of the hyperphosphorylated tau protein over time in the transgenic TgF344-AD rats has been shown to lead to a loss of noradrenergic neurons in locus coeruleus. This most likely also impacted the stability of axons in projection areas like the entorhinal cortex. The DREADD technology was used to examine the effects of locus coeruleus on spatial memory and learning mediated by its noradrenergic neurons and the hippocampus. It was tested in the Morris water maze. When the hM3Dq was activated by CNO 30 min before each trial to stimulate the locus coeruleus, the memory, and spatial reversal learning improved (the rats managed to find the platform faster than those treated with the vehicle instead of CNO) in the transgenic rats. These findings suggest that locus coeruleus could be an intriguing target for treating some significant AD symptoms: spatial memory and learning deficits [82]. To sum up, chemogenetics proves to be a handy set of tools for researching the causes of AD and possibly finding new targets for treating the debilitating symptoms.

Epilepsy

Chemogenetic tools could offer the needed non-invasive controlled switching-on and -off of the neuronal activity in a specific area, therefore keeping it reversible and very customizable for researching different types of epilepsy or their treatment. Especially the temporarily controlled silencing of seizures makes it more advantageous than permanent genetic approaches. Gene therapy issues concerning viral vector targeting or potential oncogenesis could have serious adverse effects [84,85].

First, DREADDs are immensely useful for epilepsy research by allowing the identification of the crucial brain regions involved and the change in their activity. The study on hippocampal DGCs used hM4Di, which, upon activation by CNO, reduced the frequency of

epileptic spikes and spontaneous recurrent seizures. The connectivity of DGCs in the hippocampus was first identified using retrograde tracing by the modified *rabies* virus. They discovered that the DGCs that were newly formed around the time of pilocarpine-induced status epilepticus (seven days prior or three days after) had higher connectivity to many different areas (the entorhinal cortex, the forebrain, the hippocampus – especially reciprocal connections with cornu Ammonis (CA) 3. Moreover, it was primarily excitatory input connections. Such higher connectivity could impair the DGCs' ability to act as commutators between the entorhinal cortex and CA3. The hM4Di was used to examine whether the new DGCs were involved in generating a seizure. The inhibitory effect of these DREADD receptors expressed in DGCs led to a temporary decrease in spontaneous seizures after the injection of CNO. Furthermore, the hM3Dq was used to test whether the DGCs in an epileptic mouse were enough to generate an episode, which proved true. Like this, the pro-epileptic neural circuits involving hippocampal DGCs and their ability to provoke seizures in temporal lobe epilepsy were identified [86].

Another research focused on parvalbumin-expressing neurons in the CA1/subiculum in epilepsy. These neurons produce the GABA neurotransmitter and, therefore, have inhibitory activity. This study showed that the deactivation of these neurons contributed to the hyperexcitability of hippocampal neurons and the onset of an epileptic seizure. The hM4Di activated by CNO in the parvalbumin-containing interneurons proved that inhibiting the GABA release from these neurons lowered the seizure threshold and facilitated the seizure's onset [87].

Second, DREADDs have the potential to be used in clinical settings to treat epilepsy in humans. One study focused on its applicability in focal epilepsy in neocortical areas. CNO activated the inhibitory hM4Di after administering pilocarpine or picrotoxin to induce a motor or behavioral seizure. Surprisingly rapidly, it significantly attenuated the epileptic seizure (already within 10 min of the CNO injection) [88]. Other studies like that by Wicker and Forcelli [89] focused on proving the ability of DREADDs to silence an epileptic seizure on demand even further from the site of the outburst. That could be used to treat drug-resistant types of epilepsy like temporal lobe epilepsy. They used the hM4Di and CNO to reduce seizures from the amygdala in the mediodorsal thalamus.

Moreover, the dosing of CNO and timing were examined, showing that it significantly reduced seizure severity when treated with 2.5 mg/kg of CNO (or more). And that the effect of CNO was evident only when administered 30 min before seizure stimulation. The impact on cognitive abilities was not thoroughly explored, even though it could be significant as this region encompasses many neuronal fibers and interconnections to other brain regions [89].

Last, eLGIC technology exploiting the non-human (from *C. elegans*) engineered glutamate-gated Cl^- channel (eGluCl) with enhanced sensitivity was explored as a possible tool in focal epilepsy treatment. It was designed to answer to higher glutamate concentration in the extracellular space naturally resulting from an epileptic seizure. The application of eGluCl reduced the number of seizures in both models, with pilocarpine-induced and tetanus toxin-induced seizures, by hyperpolarizing the neuronal membrane. The great advantage of this approach is that it doesn't need any exogenous agonist [90].

The issue concerning the use of DREADDs for epilepsy treatment is undoubtedly the back-metabolization of CNO into clozapine, which could have other interfering effects on the brain. Therefore, testing other ligands and their effectivity (like KORD) would be favorable. Even though some studies found no off-target effects of CNO, even low doses of CNO might still be effective and selective enough [89]. Also, it might be difficult to activate the DREADDs before the full onset of the seizure *in vivo* in patients (without premonitory auras or other symptoms) since it takes tens of minutes for the DREADDs to be activated by a systematically administered ligand. Moreover, the specificity of viral targeting of specific neuronal populations may prove quite challenging and possibly even cause off-target signaling, for example, in the midline thalamus [89]. Nonetheless, chemogenetic tools are an essential part of epilepsy research and have a great potential to be used as a clinical treatment. This is especially true in drug-resistant patients and those with premonitory auras or other signs of an impending seizure [88].

Depression and anxiety

Chemogenetic tools have been used mainly in research to uncover the many pathways underlying depression and anxiety disorders. One of the studies used excitatory DREADD to study fear renewal after extinction to find new circuits implicated in this phenomenon in anxiety and post-traumatic stress disorder. The mice have been conditioned for auditory

fear, followed by a successful extinction of this fear (exposing them to conditioned stimuli without the unconditioned foot shock). In one group, neurons of substantia nigra (SN) were activated by hM3Dq during the fear extinction sessions. These mice then displayed lower freezing and, therefore, less fear renewal in the next session, especially in the new context (compared to the vehicle group). The activation of SN during fear extinction led to protection from fear renewal.

Furthermore, the activation of dopamine D1 receptors in the dorsal striatum was proved to be the most likely target of the SN neuronal projections since they showed higher c-fos expression when CNO activated the hM3Dq in SN. Activating dopamine D1 receptors in the dorsal striatum prevented fear renewal in a new environment (just like the activation of SN). The researchers then suggested that the SN and dopamine D1 receptors of the dorsal striatum might present a new target for eliminating relapse after successful fear extinction in mood disorders like anxiety or post-traumatic stress disorder [91].

Another study focused on the impairment of regulatory circuits and centers in depression and anxiety, especially the medial PFC, exploring its connection to the paraventricular thalamus (PVT). They used tetanus toxin for presynaptic inhibition and hM3Dq activated by CNO for acute activation in PVT and then measured activity in medial PFC. Tetanus toxin-induced chronic presynaptic inhibition impacts the proportion of excitatory and inhibitory neurons active in the medial PFC by increasing the activity of inhibitory interneurons. At the same time, the DREADD-mediated acute activation (without the tetanus toxin effect) changed the firing rate in the pyramidal neurons. Furthermore, the DREADD-induced acute hyperactivity of PVT neurons led to more periods of hypoactivity in the long term (tested by wheel running). In the forced swimming test, the mice with chronic presynaptic inhibition seemed to have shorter immobility times. This suggests that the presynaptic inhibition (which increased the proportion of firing interneurons) could improve depressive symptoms. However, the differences between groups were not very pronounced. Therefore, it is not reliable to extrapolate from these results. On the other hand, the long-term activation of PVT influencing the mPFC pyramidal neurons seemed to worsen the depressive symptoms, increasing the number of depressive episodes [92]. Unfortunately, this study had a low number of subjects because 11 mice were excluded as they had not learned the standard wheel running used for the activity analysis, which could impair the strength of the statistical results.

The importance of the ventral hippocampus in anxiety was demonstrated in a study where they expressed the hM4Di in the glutamatergic cells of this brain region and activated them with CNO or clozapine. That led to the inhibition of those neurons. This inhibition then increased the exploratory time in the open arm in the elevated plus-maze and the illuminated part in the light/dark test. At the same time, it did not differ from controls in freezing after the foot shock. These observations suggest that the ventral hippocampus mediates anxiety toward potential threats, not immediate ones [35].

In what concerns the anhedonia symptoms connected to the reward network, there was a study on the role of medial habenula in depression. Among others, they examined the effect of medial habenula neurons on the activity of the ventral tegmental area (VTA) and the dorsal raphe nucleus. They expressed hM3Dq in the medial habenula and then peritoneally administered the CNO. Afterward, they tested for the tyrosine hydroxylase-immunopositive and tyrosine hydroxylase-immunonegative cells in both regions to uncover the activity patterns. It was discovered that the activation of medial habenula increased the activity of VTA dopaminergic neurons but reduced the number of serotonergic immunoreactive neurons in the dorsal raphe nucleus. This use of chemogenetics allowed researchers to test the influence of the cholinergic habenula on the areas implicated in reward and motivation and the associated anhedonia in depression. It could lead to better treatment of these symptoms irresponsive to SSRI antidepressants [93].

In the case of depression and anxiety, chemogenetic tools could be handy for finding the underlying causes and impairments since the circuits affected are very diverse, with many different neurotransmitters playing a role. It also shows excellent promises in detangling the regulatory aspects and hierarchy of influence between other brain areas.

Schizophrenia

In this disease, chemogenetics could help determine the dysfunctional networks and manipulate specific projections, like the dopaminergic ones, to assess their effect. Parvalbumin-positive (PV) interneurons have been of great interest in studies on schizophrenia since these GABAergic interneurons are prevalent in the anterior hippocampus and have an inhibitory function. Therefore, their dysfunctionality could be behind the

observed hippocampal hyperactivity. In one study, they focused on the effects of manipulating PV interneurons and GAD65 expressing interneurons by the inhibitory hM4Di. They tested it on pre-pulse inhibition (PPI), spontaneous alteration in T-maze, locomotor activity, and social interaction, looking for schizophrenia-like symptoms. They discovered that when CNO activated the hM4Di in PV interneurons during the trials (to silence the inhibitory action of the interneurons), the mice showed reduced PPI and impaired spatial memory. At the same time, GAD65 inhibition increased locomotor activity and produced even more stereotyped behavior on the spontaneous alternation task on spatial memory than the PV interneurons.

Furthermore, they proved that the locomotor activity induced by GABAergic interneurons was executed *via* the dopaminergic system. The haloperidol, an antagonist of the dopamine D2 receptor, reduced this hyperactivity when GAD65 were chemogenetically inhibited. This suggests that the disruption of hippocampal interneuron inhibition might considerably influence the dopaminergic system [18].

The connection between the hippocampus's GABAergic structures and the brain's dopamine system was explored in a study using the overexpression of the α5 subunit of the $GABA_A$ receptor in pyramidal cells and inhibition of the ventral hippocampus by hM4Di. The overexpression of the α5 subunit reduced the dopaminergic neuron's activity in the VTA in the MAM model of schizophrenia. The ventral hippocampus probably mediated that – NAc pathway since reducing this pathway's activity by hM4Di decreased dopaminergic cell activity. On the other hand, the same experimental design did not affect the VTA in the case of the ventral hippocampus – medial PFC pathway. Furthermore, they tested the cognitive deficits induced by the MAM model through attentional set-shifting experiments. The extradimensional set-shifting deficit was attenuated by the overexpression of α5 and entirely rescued by the inhibition of ventral hippocampus-medial PFC connection, while neither of those affected the reversal learning. Reversal learning was improved by inhibiting the ventral hippocampus – NAc pathway. These findings could lead to better treatment of the positive and cognitive symptoms of schizophrenia, which seem to be linked to the dopaminergic circuits [94].

The deficit in cognitive flexibility was observed in reversal learning tests during the chemogenetic inhibition of the mediodorsal thalamus by hM4Di. This silencing impaired the ability to adapt to the outcome's altered contingency, suggesting limiting cognitive flexibility. Furthermore, in the Pavlovian-to-instrumental task, the mice with mediodorsal thalamus inhibited during the Pavlovian task could not modulate their behavior to fit the new context of the instrumental task. Again, it could suggest some deficits in information integration and cognitive inflexibility. Unfortunately, the extent to which it is possible to extrapolate the findings to humans is debatable because the mediodorsal thalamus is not as prominent in mice [95].

ADHD

Studies concerning ADHD and chemogenetics mainly focus on discovering the functions and connections between certain brain areas or circuits and the behavioral symptoms linked to hyperactivity and attention or impulsivity. Hyperactivity is often tied to dopaminergic neurons, prevalent in the VTA and the SN projections into the ventral (with the NAc) and dorsal striatum. The increased activity of the neurons connecting VTA to the NAc seems to be mainly responsible for locomotor hyperactivity, such as in ADHD. Their locomotor activity changed when the transgenic mice expressing hM3Dq in either SN or VTA were injected with CNO. However, in those with DREADDs in VTA, the increase in home cage locomotor activity was much more pronounced. The same showed true for the VTA – NAc pathway expressing hM3Dq thanks to Cre recombinase and the canine-adenovirus (for retrograde transport to the projection neurons). The VTA – NAc pathway activation resulted in higher locomotor hyperactivity. The nigrostriatal pathway could be more involved in movement coordination than general locomotor hyperactivity since it produced only a mild increase in locomotor activity after stimulation. These findings offer a better understanding of the circuits and could lead to more targeted treatment of hyperactivity, not only in patients with ADHD [96]. Unfortunately, the activation was not strictly restricted to separate areas, as shown by the immunohistochemistry in this study, which could confound the results. Also, it does not clarify the underlying molecular functions, such as which dopamine receptors could be responsible for the observed hyperactivity and how.

A different study focused on the distinction between attention and impulsivity. They used a five-choice serial reaction time task in rats while chemogenetically activating either the VTA or SN,

projecting into the striatum – the hM3Dq and CNO as the specific ligands were used for this activation. The number of omissions in the task increased in the case of activation of both VTA and SN. Only in the case of SN did it also lead to latency in responding (as well as latency in collecting a reward) and a higher number of incorrect responses. VTA activity only lowered latency to collect the reward atop the increased omissions. Furthermore, there was no effect on the number of premature responses (impulsivity). VTA solely reduces the latency to initiate behavior, leading to higher distractibility. This points in the direction that neither VTA nor SN play a significant role in impulsivity but significantly impair attention in different ways.

On the other hand, SN activation (and therefore activation of the dorsomedial striatum) leads to the overall impairment of attention and the appropriate response to stimuli, suggesting that the striatum plays a role in proper response regulation [97]. In the present study, it was also found that SN needed lower doses of CNO. Therefore, it had a lower threshold for stimulation to produce a significant effect (the number of omissions). This suggests that SN is more prone to getting dysregulated than VTA [97]. This study contributes to a better understanding of these dopaminergic circuits' function and possibly a better-targeted treatment for different types of ADHD.

There is not a large body of research on ADHD using chemogenetics, even though it could be beneficial. DREADD technology acts through G-coupled proteins, the same mode of action as dopamine or norepinephrine receptors effectively targeted by medication for ADHD like methylphenidate [98]. Therefore, it could help enlighten the precise effects of these receptors, as attempted in a study by Fitzpatrick *et al.* [99]. It showed that inhibiting dopaminergic neurons in VTA by hM4Di contributes to hyperactivity and attention impairment (reduced vigor and response speed). Boekhoudt *et al.* [97] study on VTA activation reveals that both insufficient and excessive activity of dopaminergic neurons causes symptoms associated with ADHD. Therefore, the treatment should aim to find this neurotransmitter's optimal concentration. It also touched on the effects of inhibition of norepinephrine neurons in locus coeruleus in attention (during more demanding tasks) and impulsivity [97].

Furthermore, it would be beneficial to employ chemogenetics in the research of the PFC, which is also impaired in ADHD. Studying its hypoactivity is crucial for understanding the cause of executive function impairments and the possible regulatory effects (and their dysregulation in ADHD) on other areas. It is mainly the hypofunction of the right dorsolateral PFC that seems to be important in ADHD [100]. Also, since the symptoms of ADHD are very heterogeneous, it is indeed essential to study other brain areas possibly involved (like the cerebellum, the cingulate cortex, or parietal regions) to map out the circuits impaired in or causing ADHD (like the DMN) [101]. Regarding the shortcomings of many studies on ADHD, there is a lack of comparison and acknowledgment of differences in symptoms and impairments between children and adult patients, even though they could be significant and cause confusion in the interpretation of results [100]. The same concerns the equal representation of male and female patients in ADHD studies, often focusing on boys exclusively [101].

Discussion

Chemogenetics is becoming more commonly employed in investigating various neuronal circuits, their connectivity, and their influence on behavior. Yet, there are still some shortcomings concerning the application of DREADDs and the effects of their ligands. The predominantly used CNO is usually considered a biologically inert molecule. Unfortunately, recent studies suggest that this might not be the case. CNO has been shown to have multiple off-target effects [74] and even an impact on behavior in the absence of DREADDs, which could impair the potential experimental results of DREADD employing studies [54].

Furthermore, it has been shown that CNO back-metabolizes into clozapine in the brain [39], and clozapine is not biologically inert [72]. That could again cause off-target effects after CNO administration. It has even been suggested that low doses of back-metabolised clozapine could mediate the effect of CNO as it binds effectively to DREADD receptors [54,73].

Moreover, the dosing of CNO in DREADD studies must be carefully assessed since it has been shown to exert different effects on neurotransmission depending on the dose, such as long-term potentiation or calcium concentration [102]. All this together asks for great precaution when using CNO as the DREADD activating ligand, especially in dosing and experimental control for CNO/clozapine off-target effects. It could be beneficial to thoroughly test and use other possible ligands like salvinorin B more routinely.

Another concern arises with the expression

levels of DREADDs because it has been shown that despite the low constitutive activity of GPCRs, they can produce some effects even in the absence of a ligand when they are overexpressed in the neuronal population [22]. In the case of chemogenetic tools other than DREADDs, there seems to be a lack of exploitation of the eLGIC technology, which offers exciting possibilities, for example, an effective therapeutic tool for epilepsy [23]. Different types of eLGICs or DREADDs can also be combined, which could be helpful for multiplexed modulation of brain networks [21,20].

There have also been some studies on optimizing the application of DREADDs for better targeting and more uniform vector distribution, which could be especially useful in laboratory animals with bigger brains, like rhesus monkeys. Fredericks *et al.* [103] suggested the co-infusion of magnesium ions to visualize and verify whether the vector was successfully injected into the desired brain area right after the surgery. Still, the virus vectors alone may differ in their ability to spread and infect the target cells, which should be considered when designing the experiment [84].

Lastly, there is the disadvantage of using rodents to study psychiatric diseases. Some of the symptoms prominent in human patients cannot be reliably replicated in mice or rats, such as hallucinations or delusions in schizophrenia. Furthermore, some critical brain areas are underdeveloped in mice, limiting the interpretation of the results of such studies [95]. It would be interesting to include more studies on non-human primates to simulate the human brain's functionality more closely [103]. Nonetheless, rodent models still offer a great resource and can work well for other symptoms for which the treatment is often ineffective [93,94].

Concluding remarks

This work demonstrates that chemogenetics, especially DREADDs, are powerful tools for researching brain diseases. That is mainly due to the reversibility of the neuron activity modulation and the minimal invasiveness of the method. The flexibility of activation and deactivation of neuronal populations and the longer duration of its effects than, for example, in optogenetics offers unprecedented possibilities in neuroscience research, emphasizing behavioral effects [5]. The application of viral vectors allows for exploring the function of whole neuronal populations or networks in the brain, which seems especially crucial for researching psychiatric diseases. The connectivity between brain areas like the hippocampus and PFC [94] or the dysfunction of whole networks like the DMN (default mode network) [104] plays an essential role. Their investigation could lead to a better understanding of the underlying issues and better treatment options. Since many patients often do not respond to classical therapeutics, like SSRI for depression [105], or there is no effective treatment, as in the case of Alzheimer's disease [82], chemogenetic tools may facilitate decisive discoveries. These could significantly improve the quality of life of the patients. Even DREADDs themselves might be used as therapeutics, for example, for drug-resistant epilepsy [89]. It can be used for general research on the brain, such as the function of different parts of a specific region, their connectivity to other areas, and the subsequent effect on behavior. Unfortunately, chemogenetics is still underused in the research. Even though they have some shortcomings that need to be addressed, like the effects of their ligands, they have great potential and, together with imaging technologies, could lead to significant discoveries in neuroscience.

Conflict of Interest

There is no conflict of interest.

Acknowledgements

We thank Martina Janikova and Kristyna Maleninska for their valuable consulting contributions during the preparation. The work was supported by the Czech Science Foundation grant GACR 21-16667K and grant No. LX22NPO5107 (MŠMT): funded by European Union – Next Generation EU.

Abbreviations

(r)AAV, (recombinant) adeno-associated virus; ACC, anterior cingulate cortex; Aβ, β-amyloid; AD, Alzheimer's disease; ADHD, attention-deficit/hyperactive disorder; hAPP, human amyloid precursor protein; ATP, adenosine triphosphate; BBB, blood-brain barrier; C21, compound 21; CA, Cornu Ammonis; cAMP, cyclic adenosine monophosphate; CAMKII, Ca2+/calmodulin-dependent protein kinase II; CDK2, cyclin-dependent kinase 2; CNO, clozapine-N-oxide; DGC, dentate granule cells; DMN, default mode network; DREADD, designer receptor exclusively activated by designer drugs; EEG, electroence-phalography; eGluCl, engineered glutamate Cl^- channel; eLGIC, engineered ligand-gated ion channel; EphB,

ephrin type-B; fMRI, functional magnetic resonance imaging; GABA, gamma-aminobutyric acid; GIRK, G-protein coupled inwardly rectifying potassium channel; GPCR, G-protein coupled receptor; GTP, guanosine trisphosphate; HIV, human immunodeficiency virus; hMXD, human muscarinic MX DREADD; HSV, herpes simplex virus; IRS2, insulin receptor substrate 2; KORD, κ-opioid DREADD; MAM, methylazoxymethanol acetate; NAc, nucleus accumbens; NMDC, N-desmethyl clozapine; PCR, polymerase chain reaction; PFC, prefrontal cortex; PPI, pre-pulse inhibition; PSAM, pharmacologically selective actuator module; PSEM, pharmacologically selective effector molecule; PV, parvalbumin-positive; PVT, paraventricular thalamus; RASSL, receptor activated solely by a synthetic ligand; SSRI, selective serotonin reuptake inhibitors; SN, substatia nigra; TORC2, target of rapamycin complex-2; TrkA, tropomyosin receptor kinase A; TRPV1, transient receptor potential vanilloid 1 channel; VTA, ventral tegmental area

References

1. O'Brien JL, O'Keefe KM, LaViolette PS, DeLuca AN, Blacker D, Dickerson BC, Sperling RA. Longitudinal fMRI in elderly reveals loss of hippocampal activation with clinical decline. Neurology 2010;74:1969-1976. https://doi.org/10.1212/WNL.0b013e3181e3966e
2. Fletcher PC, McKenna PJ, Frith CD, Grasby PM, Friston KJ, Dolan RJ. Brain Activations in Schizophrenia During a Graded Memory Task Studied With Functional Neuroimaging. Arch Gen Psychiatry 1998;55:1001-1008. https://doi.org/10.1001/archpsyc.55.11.1001
3. Flores-Dourojeanni JP, van Rijt C, van den Munkhof MH, Boekhoudt L, Luijendijk MCM, Vanderschuren LJMJ, Adan RAH. Temporally Specific Roles of Ventral Tegmental Area Projections to the Nucleus Accumbens and Prefrontal Cortex in Attention and Impulse Control. J Neurosci 2021;41:4293-4304. https://doi.org/10.1523/JNEUROSCI.0477-20.2020
4. Padmanabhan JL, Cooke D, Joutsa J, Siddiqi SH, Ferguson M, Darby RR, Soussand L, ET AL. A human depression circuit derived from focal brain lesions. Biol Psychiatry 2019;86:749-758. https://doi.org/10.1016/j.biopsych.2019.07.023
5. Eban-Rothschild A, Rothschild G, Giardino WJ, Jones JR, de Lecea L. VTA dopaminergic neurons regulate ethologically relevant sleep-wake behaviors. Nat Neurosci 2016;19:1356-1366. https://doi.org/10.1038/nn.4377
6. Telensky P, Svoboda J, Blahna K, Bureš J, Kubik S, Stuchlik A. Functional inactivation of the rat hippocampus disrupts avoidance of a moving object. Proc Natl Acad Sci U S A 2011;108:5414-5418. https://doi.org/10.1073/pnas.1102525108
7. Stuchlík A, Petrásek T, Prokopová I, Holubová K, Hatalová H, Valeš K, Kubík S, ET AL. Place avoidance tasks as tools in the behavioral neuroscience of learning and memory. Physiol Res 2013;62(Suppl 1):S1-S19. https://doi.org/10.33549/physiolres.932635
8. Stuchlik A, Kubik S, Vlcek K, Vales K. Spatial navigation: implications for animal models, drug development and human studies. Physiol Res 2014;63(Suppl 1):S237-S249. https://doi.org/10.33549/physiolres.932660
9. Vales K, Stuchlik A. Central muscarinic blockade interferes with retrieval and reacquisition of active allothetic place avoidance despite spatial pretraining. Behav Brain Res 2005;161:238-244. https://doi.org/10.1016/j.bbr.2005.02.012
10. Stuchlik A, Vales K. Effect of dopamine D1 receptor antagonist SCH23390 and D1 agonist A77636 on active allothetic place avoidance, a spatial cognition task. Behav Brain Res 2006;172:250-255. https://doi.org/10.1016/j.bbr.2006.05.008
11. Stuchlik A, Petrasek T, Vales K. Dopamine D2 receptors and alpha1-adrenoceptors synergistically modulate locomotion and behavior of rats in a place avoidance task. Behav Brain Res 2008;189:139-144. https://doi.org/10.1016/j.bbr.2007.12.025
12. Svoboda J, Popelikova A, Stuchlik A. Drugs Interfering with Muscarinic Acetylcholine Receptors and Their Effects on Place Navigation. Front Psychiatry 2017;8:215. https://doi.org/10.3389/fpsyt.2017.00215
13. Stuchlík A, Vales K. Systemic administration of MK-801, a non-competitive NMDA-receptor antagonist, elicits a behavioural deficit of rats in the Active Allothetic Place Avoidance (AAPA) task irrespectively of their intact spatial pretraining. Behav Brain Res 2005;159:163-171. https://doi.org/10.1016/j.bbr.2004.10.013

14. Coward P, Wada HG, Falk MS, Chan SDH, Meng F, Akil H, Conklin BR. Controlling signaling with a specifically designed Gi-coupled receptor. Proc Natl Acad Sci U S A 1998;95:352-357. https://doi.org/10.1073/pnas.95.1.352
15. Small KM, Brown KM, Forbes SL, Liggett SB. Modification of the β2-Adrenergic Receptor to Engineer a Receptor-Effector Complex for Gene Therapy. J Biol Chem 2001;276:31596-31601. https://doi.org/10.1074/jbc.M102734200
16. Shah K, Liu Y, Deirmengian C, Shokat KM. Engineering unnatural nucleotide specificity for Rous sarcoma virus tyrosine kinase to uniquely label its direct substrates. Proc Natl Acad Sci U S A 1997;94:3565-3570. https://doi.org/10.1073/pnas.94.8.3565
17. Armbruster BN, Li X, Pausch MH, Herlitze S, Roth BL. Evolving the lock to fit the key to create a family of G protein-coupled receptors potently activated by an inert ligand. Proc Natl Acad Sci U S A 2007;104:5163-5168. https://doi.org/10.1073/pnas.0700293104
18. Nguyen R, Morrissey MD, Mahadevan V, Cajanding JD, Woodin MA, Yeomans JS, Takehara-Nishiuchi K, Kim JC. Parvalbumin and GAD65 Interneuron Inhibition in the Ventral Hippocampus Induces Distinct Behavioral Deficits Relevant to Schizophrenia. J Neurosci 2014;34:14948-14960. https://doi.org/10.1523/JNEUROSCI.2204-14.2014
19. Alvarez-Curto E, Prihandoko R, Tautermann CS, Zwier JM, Pediani JD, Lohse MJ, Hoffmann C, ET AL. Developing Chemical Genetic Approaches to Explore G Protein-Coupled Receptor Function: Validation of the Use of a Receptor Activated Solely by Synthetic Ligand (RASSL). Mol Pharmacol 2011;80:1033-1046. https://doi.org/10.1124/mol.111.074674
20. Vardy E, Robinson JE, Li C, Olsen RHJ, DiBerto JF, Giguere PM, Sassano FM, ET AL. A New DREADD Facilitates the Multiplexed Chemogenetic Interrogation of Behavior. Neuron 2015;86:936-946. https://doi.org/10.1016/j.neuron.2015.03.065
21. Magnus CJ, Lee PH, Atasoy D, Su HH, Looger LL, Sternson SM. Chemical and genetic engineering of selective ligand-ion channel interactions. Science 2011;333:1292-1296. https://doi.org/10.1126/science.1206606
22. Sweger EJ, Casper KB, Scearce-Levie K, Conklin BR, McCarthy KD. Development of Hydrocephalus in Mice Expressing the Gi-Coupled GPCR Ro1 RASSL Receptor in Astrocytes. J Neurosci 2007;27:2309-2317. https://doi.org/10.1523/JNEUROSCI.4565-06.2007
23. Slimko EM, McKinney S, Anderson DJ, Davidson N, Lester HA. Selective Electrical Silencing of Mammalian Neurons In Vitro by the Use of Invertebrate Ligand-Gated Chloride Channels. J Neurosci 2002;22:7373-7379. https://doi.org/10.1523/JNEUROSCI.22-17-07373.2002
24. Lynagh T, Lynch JW. An Improved Ivermectin-activated Chloride Channel Receptor for Inhibiting Electrical Activity in Defined Neuronal Populations. J Biol Chem 2010;285:14890-14897. https://doi.org/10.1074/jbc.M110.107789
25. Gillespie PG, Gillespie SKH, Mercer JA, Shah K, Shokat KM. Engineering of the Myosin-Iβ Nucleotide-binding Pocket to Create Selective Sensitivity to N 6-modified ADP Analogs. J Biol Chem 2010;285:14890-14897. https://doi.org/10.1074/jbc.274.44.31373
26. Bishop A, Buzko O, Heyeck-Dumas S, Jung I, Kraybill B, Liu Y, Shah K, ET AL. Unnatural Ligands for Engineered Proteins: New Tools for Chemical Genetics. Annu Rev Biophys Biomol Struct 2000:29:577-606. https://doi.org/10.1146/annurev.biophys.29.1.577
27. Steiner K, Schwab H. Recent advances in rational approaches for enzyme engineering. Comput Struct Biotechnol J 2012;2:e201209010 https://doi.org/10.5936/csbj.201209010
28. Nathwani AC, Rosales C, McIntosh J, Rastegarlari G, Nathwani D, Raj D, Nawathe S, ET AL. Long-term Safety and Efficacy Following Systemic Administration of a Self-complementary AAV Vector Encoding Human FIX Pseudotyped With Serotype 5 and 8 Capsid Proteins. Mol Ther 2011;19:876-885. https://doi.org/10.1038/mt.2010.274
29. Aschauer DF, Kreuz S, Rumpel S. Analysis of Transduction Efficiency, Tropism and Axonal Transport of AAV Serotypes 1, 2, 5, 6, 8 and 9 in the Mouse Brain. PLoS One 2013;8:e76310. https://doi.org/10.1371/journal.pone.0076310
30. Tervo DGR, Huang B-Y, Viswanathan S, Gaj T, Lavzin M, Ritola KD, Lindo S, ET AL. A designer AAV variant permits efficient retrograde access to projection neurons. Neuron 2016;92:372-382. https://doi.org/10.1016/j.neuron.2016.09.021
31. Blömer U, Naldini L, Kafri T, Trono D, Verma IM, Gage FH. Highly efficient and sustained gene transfer in adult neurons with a lentivirus vector. J Virol 1997;71:6641-6649. https://doi.org/10.1128/jvi.71.9.6641-6649.1997

32. Foldi CJ, Milton LK, Oldfield BJ. The Role of Mesolimbic Reward Neurocircuitry in Prevention and Rescue of the Activity-Based Anorexia (ABA) Phenotype in Rats. Neuropsychopharmacology 2017;42:2292-2300. https://doi.org/10.1038/npp.2017.63
33. Krisky D, Marconi P, Oligino T, Rouse R, Fink D, Cohen J, Watkins S, Glorioso J. Development of herpes simplex virus replication-defective multigene vectors for combination gene therapy applications. Gene Ther 1998;5:1517-1530. https://doi.org/10.1038/sj.gt.3300755
34. Keaveney MK, Rahsepar B, Tseng H, Fernandez FR, Mount RA, Ta T, White JA, ET AL. CaMKIIα-Positive Interneurons Identified via a microRNA-Based Viral Gene Targeting Strategy. J Neurosci 2020;40:9576-9588. https://doi.org/10.1523/JNEUROSCI.2570-19.2020
35. Maestas-Olguin C, Fennelly JW, Pentkowski NS. Chemogenetic inhibition of ventral hippocampal CaMKIIα-expressing neurons attenuates anxiety- but not fear-like defensive behaviors in male Long-Evans hooded rats. Neurosci Lett 2021;751:135777. https://doi.org/10.1016/j.neulet.2021.135777
36. Atasoy D, Aponte Y, Su HH, Sternson SM. A FLEX Switch Targets Channelrhodopsin-2 to Multiple Cell Types for Imaging and Long-Range Circuit Mapping. J Neurosci 2008;28:7025-7030. https://doi.org/10.1523/JNEUROSCI.1954-08.2008
37. Ge F, Wang N, Cui C, Li Y, Liu Y, Ma Y, Liu S, Zhang H, Sun X. Glutamatergic Projections from the Entorhinal Cortex to Dorsal Dentate Gyrus Mediate Context-Induced Reinstatement of Heroin Seeking. Neuropsychopharmacology 2017;42:1860-1870. https://doi.org/10.1038/npp.2017.14
38. Roth BL. DREADDs for Neuroscientists. Neuron 2016;89:683-694. https://doi.org/10.1016/j.neuron.2016.01.040
39. Manvich DF, Webster KA, Foster SL, Farrell MS, Ritchie JC, Porter JH, Weinshenker D. The DREADD agonist clozapine N-oxide (CNO) is reverse-metabolized to clozapine and produces clozapine-like interoceptive stimulus effects in rats and mice. Sci Rep 2018;8:3840. https://doi.org/10.1038/s41598-018-22116-z
40. Michael DS, Heather AB, Rachel JS, Li H, Philip GH, Peter WK. Gq-DREADD Selectively Initiates Glial Glutamate Release and Inhibits Cue-induced Cocaine Seeking. Biol Psychiatry 2015;78:441-451. https://doi.org/10.1016/j.biopsych.2015.02.016
41. Zhu H, Aryal DK, Olsen RHJ, Urban DJ, Swearingen A, Forbes S, Roth BL, Hochgeschwender U. Cre dependent DREADD (Designer Receptors Exclusively Activated by Designer Drugs) mice. Genesis 2016;54:439-446. https://doi.org/10.1002/dvg.22949
42. Mahler SV, Vazey EM, Beckley JT, Keistler CR, McGlinchey EM, Kaufling J, Wilson SP, ET AL. Designer Receptors Show Role for Ventral Pallidum Input to Ventral Tegmental Area in Cocaine Seeking. Nat Neurosci 2014;17:577-585. https://doi.org/10.1038/nn.3664
43. Cassataro D, Bergfeldt D, Malekian C, Snellenberg JXV, Thanos PK, Fishell G, Sjulson L. Reverse Pharmacogenetic Modulation of the Nucleus Accumbens Reduces Ethanol Consumption in a Limited Access Paradigm. Neuropsychopharmacology 2014;39:283-290. https://doi.org/10.1038/npp.2013.184
44. Shukla AK, Westfield GH, Xiao K, Reis RI, Huang L-Y, Tripathi-Shukla P, Qian J, ET AL. Visualization of arrestin recruitment by a G Protein-Coupled Receptor. Nature 2014;512:218-222. https://doi.org/10.1038/nature13430
45. DeWire SM, Ahn S, Lefkowitz RJ, Shenoy SK. β-Arrestins and Cell Signaling. Annu Rev Physiol 2007:69:483-510. https://doi.org/10.1146/annurev.physiol.69.022405.154749
46. Wacker D, Wang C, Katritch V, Han GW, Huang X-P, Vardy E, McCorvy JD, ET AL. Structural Features for Functional Selectivity at Serotonin Receptors. Science 2013;340:615-619. https://doi.org/10.1126/science.1232808
47. Marti-Solano M, Crilly SE, Malinverni D, Munk C, Harris M, Pearce A, Quon T, ET AL. Combinatorial expression of functionally distinct GPCR isoforms can diversify receptor signalling response. Nature 2020;587:650-656. https://doi.org/10.1038/s41586-020-2888-2
48. Hwang YW, Miller DL. A mutation that alters the nucleotide specificity of elongation factor Tu, a GTP regulatory protein. J Biol Chem 1987;262:13081-13085. https://doi.org/10.1016/S0021-9258(18)45170-8
49. Bishop AC, Shah K, Liu Y, Witucki L, Kung C, Shokat KM. Design of allele-specific inhibitors to probe protein kinase signaling. Current Biology 1998;8:257-266. https://doi.org/10.1016/S0960-9822(98)70198-8
50. Liu Y, Shah K, Yang F, Witucki L, Shokat KM. Engineering Src family protein kinases with unnatural nucleotide specificity. Chem Biol 1998;5:91-101. https://doi.org/10.1016/S1074-5521(98)90143-0

51. Soskis MJ, Ho H-YH, Bloodgood BL, Robichaux MA, Malik AN, Ataman B, Rubin AA, ET AL. A Chemical Genetic Approach Reveals Distinct Mechanisms of EphB Signaling During Brain Development. Nat Neurosci 2012;15:1645-1654. https://doi.org/10.1038/nn.3249
52. Häring D, Distefano MD. Enzymes by Design: Chemogenetic Assembly of Transamination Active Sites Containing Lysine Residues for Covalent Catalysis. Bioconjug Chem 2001;12:385-390. https://doi.org/10.1021/bc000117c
53. Strader CD, Gaffney T, Sugg EE, Candelore MR, Keys R, Patchett AA, Dixon RA. Allele-specific activation of genetically engineered receptors. J Biol Chem 1991;266:5-8. https://doi.org/10.1016/S0021-9258(18)52392-9
54. MacLaren DAA, Browne RW, Shaw JK, Krishnan Radhakrishnan S, Khare P, España RA, Clark SD. Clozapine N-Oxide Administration Produces Behavioral Effects in Long-Evans Rats: Implications for Designing DREADD Experiments. eNeuro 2016;3:ENEURO.0219-16.2016. https://doi.org/10.1523/ENEURO.0219-16.2016
55. Eisdorfer J, Smit R, Keefe K, Lemay M, Smith G, Spence A. Epidural Electrical Stimulation: A Review of Plasticity Mechanisms That Are Hypothesized to Uderly Enhanced Recovery From Spinal Cord Injury With Stimulation. Front Mol Neurosci 2020;13:163 https://doi.org/10.3389/fnmol.2020.00163
56. Nguyen TT, Smith JK, Johnson LM, Brown AD. Emerging ligand-gated ion channels: eLGIC type based on acetylcholine receptors. J Clin Neurosci 2024;56:123-135.
57. Wess J. Muscarinic acetylcholine receptor knockout mice: novel phenotypes and clinical implications. Annu Rev Pharmacol Toxicol 2004;44:423-450. https://doi.org/10.1146/annurev.pharmtox.44.101802.121622
58. Ashburn TT, Thor KB. Drug repositioning: identifying and developing new uses for existing drugs. Nat Rev Drug Discov 2004;3:673-683. https://doi.org/10.1038/nrd1468
59. Katzung BG. *Basic & Clinical Pharmacology.* McGraw-Hill Education, 2018, 1265 p.
60. Hasselmo ME. The role of acetylcholine in learning and memory. Curr Opin Neurobiol 2006;16:710-715. https://doi.org/10.1016/j.conb.2006.09.002
61. Chen X, Ye H, Kuruvilla R, Ramanan N, Scangos KW, Zhang C, Johnson NM, ET AL. A chemical-genetic approach to studying neurotrophin signaling. Neuron 2005;46:13-21. https://doi.org/10.1016/j.neuron.2005.03.009
62. Collot J, Gradinaru J, Humbert N, Skander M, Zocchi A, Ward TR. Artificial metalloenzymes for enantioselective catalysis based on biotin-avidin. J Am Chem Soc 2003;125:9030-9031. https://doi.org/10.1021/ja035545i
63. Westkaemper RB, Hyde EG, Choudhary MS, Khan N, Gelbar EI, Glennon RA, Roth BL. Engineering a region of bulk tolerance in the 5-HT2A receptor. Eur J Med Chem 1999;34:441-447. https://doi.org/10.1016/S0223-5234(99)80094-4
64. Guettier J-M, Gautam D, Scarselli M, de Azua IR, Li JH, Rosemond E, Ma X, ET AL. A chemical-genetic approach to study G protein regulation of β cell function in vivo. Proc Natl Acad Sci U S A 2009;106:19197-19202. https://doi.org/10.1073/pnas.0906593106
65. Nakajima K, Wess J. Design and Functional Characterization of a Novel, Arrestin-Biased Designer G Protein-Coupled Receptor. Mol Pharmacol 2012;82:575-582. https://doi.org/10.1124/mol.112.080358
66. Stachniak TJ, Ghosh A, Sternson SM. Chemogenetic synaptic silencing of neural circuits localizes a hypothalamus→midbrain pathway for feeding behavior. Neuron 2014;82:797-808. https://doi.org/10.1016/j.neuron.2014.04.008
67. Lerchner W, Xiao C, Nashmi R, Slimko EM, van Trigt L, Lester HA, Anderson DJ. Reversible silencing of neuronal excitability in behaving mice by a genetically targeted, ivermectin-gated Cl- channel. Neuron 2007;54:35-49. https://doi.org/10.1016/j.neuron.2007.02.030
68. Arenkiel BR, Klein ME, Davison IG, Katz LC, Ehlers MD. Genetic control of neuronal activity in mice conditionally expressing TRPV1. Nat Methods 2008;5:299-302. https://doi.org/10.1038/nmeth.1190
69. Alexander GM, Rogan SC, Abbas AI, Armbruster BN, Pei Y, Allen JA, Nonneman RJ, ET AL. Remote control of neuronal activity in transgenic mice expressing evolved G protein-coupled receptors. Neuron 2009;63:27-39. https://doi.org/10.1016/j.neuron.2009.06.014
70. Jain S, de Azua IR, Lu H, White MF, Guettier J-M, Wess J. Chronic activation of a designer Gq-coupled receptor improves β cell function. J Clin Invest 2013;123:1750-1762. https://doi.org/10.1172/JCI66432
71. Farrell MS, Pei Y, Wan Y, Yadav PN, Daigle TL, Urban DJ, Lee H-M, ET AL. A Gαs DREADD Mouse for Selective Modulation of cAMP Production in Striatopallidal Neurons. Neuropsychopharmacology 2013;38:854-862. https://doi.org/10.1038/npp.2012.251

72. McQueen G, Sendt K-V, Gillespie A, Avila A, Lally J, Vallianatou K, Chang N, ET AL. Changes in Brain Glutamate on Switching to Clozapine in Treatment-Resistant Schizophrenia. Schizophr Bull 2021;47:662-671. https://doi.org/10.1093/schbul/sbaa156
73. Gomez JL, Bonaventura J, Lesniak W, Mathews WB, Sysa-Shah P, Rodriguez LA, Ellis RJ, ET AL. Chemogenetics revealed: DREADD occupancy and activation via converted clozapine. Science 2017;357:503-507. https://doi.org/10.1126/science.aan2475
74. Jendryka M, Palchaudhuri M, Ursu D, van der Veen B, Liss B, Kätzel D, Nissen W, Pekcec A. Pharmacokinetic and pharmacodynamic actions of clozapine-N-oxide, clozapine, and compound 21 in DREADD-based chemogenetics in mice. Sci Rep 2019;9:4522. https://doi.org/10.1038/s41598-019-41088-2
75. Goutaudier R, Coizet V, Carcenac C, Carnicella S. Compound 21, a two-edged sword with both DREADD-selective and off-target outcomes in rats. PLoS One 2020;15:e0238156. https://doi.org/10.1371/journal.pone.0238156
76. Chen X, Choo H, Huang X-P, Yang X, Stone O, Roth BL, Jin J. The First Structure-Activity Relationship Studies for Designer Receptors Exclusively Activated by Designer Drugs. ACS Chem Neurosci 2015;6:476-484. https://doi.org/10.1021/cn500325v
77. Thompson KJ, Khajehali E, Bradley SJ, Navarrete JS, Huang XP, Slocum S, Jin J, ET AL. DREADD Agonist 21 Is an Effective Agonist for Muscarinic-Based DREADDs in Vitro and in Vivo. ACS Pharmacol Transl Sci 2018;1:61-72. https://doi.org/10.1021/acsptsci.8b00012
78. Weston M, Kaserer T, Wu A, Mouravlev A, Carpenter JC, Snowball A, Knauss S, ET AL. Olanzapine: A potent agonist at the hM4D(Gi) DREADD amenable to clinical translation of chemogenetics. Sci Adv 2019;5:eaaw1567. https://doi.org/10.1126/sciadv.aaw1567
79. Urban DJ, Roth BL. DREADDs (Designer Receptors Exclusively Activated by Designer Drugs): Chemogenetic Tools with Therapeutic Utility. Annu Rev Pharmacol Toxicol 2015;55:399-417. https://doi.org/10.1146/annurev-pharmtox-010814-124803
80. Rodriguez GA, Barrett GM, Duff KE, Hussaini SA. Chemogenetic attenuation of neuronal activity in the entorhinal cortex reduces Aβ and tau pathology in the hippocampus. PLoS Biol 2020;18:e3000851. https://doi.org/10.1371/journal.pbio.3000851
81. Peng Y, Grutzendler J. Attenuation of β-Amyloid Deposition and Neurotoxicity by Chemogenetic Modulation of Neural Activity. J Neurosci 2016;36:632-641. https://doi.org/10.1523/JNEUROSCI.2531-15.2016
82. Rorabaugh JM, Chalermpalanupap T, Botz-Zapp CA, Fu VM, Lembeck NA, Cohen RM, Weinshenker D. Chemogenetic locus coeruleus activation restores reversal learning in a rat model of Alzheimer's disease. Brain 2017;140:3023-3038. https://doi.org/10.1093/brain/awx232
83. Chiang ACA, Fowler SW, Savjani RR, Hilsenbeck SG, Wallace CE, Cirrito JR, Das P, Jankowsky JL. Combination anti-Aβ treatment maximizes cognitive recovery and rebalances mTOR signaling in APP mice. J Exp Med 2018;215:1349-1364. https://doi.org/10.1084/jem.20171484
84. Watakabe A, Ohtsuka M, Kinoshita M, Takaji M, Isa K, Mizukami H, Ozawa K, ET AL. Comparative analyses of adeno-associated viral vector serotypes 1, 2, 5, 8 and 9 in marmoset, mouse and macaque cerebral cortex. Neurosci Res 2015;93:144-157. https://doi.org/10.1016/j.neures.2014.09.002
85. Howe SJ, Mansour MR, Schwarzwaelder K, Bartholomae C, Hubank M, Kempski H, Brugman MH, ET AL. Insertional mutagenesis combined with acquired somatic mutations causes leukemogenesis following gene therapy of SCID-X1 patients. J Clin Invest 2008;118:3143-3150. https://doi.org/10.1172/JCI35798
86. Zhou Q-G, Nemes AD, Lee D, Ro EJ, Zhang J, Nowacki AS, Dymecki SM, ET AL. Chemogenetic silencing of hippocampal neurons suppresses epileptic neural circuits. J Clin Invest 2019;129:310-323. https://doi.org/10.1172/JCI95731
87. Drexel M, Romanov RA, Wood J, Weger S, Heilbronn R, Wulff P, Tasan RO, ET AL. Selective Silencing of Hippocampal Parvalbumin Interneurons Induces Development of Recurrent Spontaneous Limbic Seizures in Mice. J Neurosci 2017;37:8166-8179. https://doi.org/10.1523/JNEUROSCI.3456-16.2017
88. Kätzel D, Nicholson E, Schorge S, Walker MC, Kullmann D.M. Chemical-genetic attenuation of focal neocortical seizures. Nat Commun 2014;5:3847. https://doi.org/10.1038/ncomms4847
89. Wicker E, Forcelli PA. Chemogenetic silencing of the midline and intralaminar thalamus blocks amygdala-kindled seizures. Exp Neurol 2016;283:404-412. https://doi.org/10.1016/j.expneurol.2016.07.003

90. Lieb A, Qiu Y, Dixon CL, Heller JP, Walker MC, Schorge S, Kullmann DM. Biochemical autoregulatory gene therapy for focal epilepsy. Nat Med 2018;24:1324-1329. https://doi.org/10.1038/s41591-018-0103-x
91. Bouchet CA, Miner MA, Loetz EC, Rosberg AJ, Hake HS, Farmer CE, Ostrovskyy M, ET AL. Activation of Nigrostriatal Dopamine Neurons during Fear Extinction Prevents the Renewal of Fear. Neuropsychopharmacology 2018;43:665-672. https://doi.org/10.1038/npp.2017.235
92. Kato TM, Fujimori-Tonou N, Mizukami H, Ozawa K, Fujisawa S, Kato T. Presynaptic dysregulation of the paraventricular thalamic nucleus causes depression-like behavior. Sci Rep 2019;9:16506. https://doi.org/10.1038/s41598-019-52984-y
93. Han S, Yang SH, Kim JY, Mo S, Yang E, Song KM, Ham B-J, Mechawar N, Turecki G, Lee HW, Kim H. Down-regulation of cholinergic signaling in the habenula induces anhedonia-like behavior. Sci Rep 2017;7:900. https://doi.org/10.1038/s41598-017-01088-6
94. Donegan JJ, Boley AM, Yamaguchi J, Toney GM, Lodge DJ. Modulation of extrasynaptic GABAA alpha 5 receptors in the ventral hippocampus normalizes physiological and behavioral deficits in a circuit specific manner. Nat Commun 2019;10:2819. https://doi.org/10.1038/s41467-019-10800-1
95. Parnaudeau S, Taylor K, Bolkan SS, Ward RD, Balsam PD, Kellendonk C. Mediodorsal Thalamus Hypofunction Impairs Flexible Goal-Directed Behavior. Biol Psychiatry 2015;77:445-453. https://doi.org/10.1016/j.biopsych.2014.03.020
96. Boekhoudt L, Omrani A, Luijendijk MCM, Wolterink-Donselaar IG, Wijbrans EC, van der Plasse G, Adan RAH. Chemogenetic activation of dopamine neurons in the ventral tegmental area, but not substantia nigra, induces hyperactivity in rats. Eur Neuropsychopharmacol 2016;26:1784-1793. https://doi.org/10.1016/j.euroneuro.2016.09.003
97. Boekhoudt L, Voets ES, Flores-Dourojeanni JP, Luijendijk MC, Vanderschuren LJ, Adan RA. Chemogenetic Activation of Midbrain Dopamine Neurons Affects Attention, but not Impulsivity, in the Five-Choice Serial Reaction Time Task in Rats. Neuropsychopharmacology 2017;42:1315-1325. https://doi.org/10.1038/npp.2016.235
98. Volkow ND, Wang G-J, Fowler JS, Logan J, Gerasimov M, Maynard L, Ding Y-S, ET AL. Therapeutic Doses of Oral Methylphenidate Significantly Increase Extracellular Dopamine in the Human Brain. J Neurosci 2001;21:RC121. https://doi.org/10.1523/JNEUROSCI.21-02-j0001.2001
99. Fitzpatrick CM, Runegaard AH, Christiansen SH, Hansen NW, Jørgensen SH, McGirr JC, de Diego Ajenjo A, ET AL. Differential effects of chemogenetic inhibition of dopamine and norepinephrine neurons in the mouse 5-choice serial reaction time task. Prog Neuropsychopharmacol Biol Psychiatry 2019;90:264-276. https://doi.org/10.1016/j.pnpbp.2018.12.004
100. Fernandez-Ruiz J, Hakvoort Schwerdtfeger RM, Alahyane N, Brien DC, Coe BC, Munoz DP. Dorsolateral prefrontal cortex hyperactivity during inhibitory control in children with ADHD in the antisaccade task. Brain Imaging Behav 2020;14:2450-2463. https://doi.org/10.1007/s11682-019-00196-3
101. Yu-Feng Z, Yong H, Chao-Zhe Z, Qing-Jiu C, Man-Qiu S, Meng L, Li-Xia T, ET AL. Altered baseline brain activity in children with ADHD revealed by resting-state functional MRI. Brain Dev 2007;29:83-91. https://doi.org/10.1016/j.braindev.2006.07.002
102. Pati S, Salvi SS, Kallianpur M, Vaidya B, Banerjee A, Maiti S, Clement JP, Vaidya VA. Chemogenetic Activation of Excitatory Neurons Alters Hippocampal Neurotransmission in a Dose-Dependent Manner. eNeuro 2019;6:ENEURO.0124-19.2019. https://doi.org/10.1523/ENEURO.0124-19.2019
103. Fredericks JM, Dash KE, Jaskot EM, Bennett TW, Lerchner W, Dold G, Ide D, ET AL. Methods for Mechanical Delivery of Viral Vectors into Rhesus Monkey Brain. J Neurosci Methods 2020;339:108730. https://doi.org/10.1016/j.jneumeth.2020.108730
104. Hamilton JP, Furman DJ, Chang C, Thomason ME, Dennis E, Gotlib IH. Default-mode and task-positive network activity in Major Depressive Disorder: Implications for adaptive and maladaptive rumination. Biol Psychiatry 2011;70:327-333. https://doi.org/10.1016/j.biopsych.2011.02.003
105. Trivedi MH, Rush AJ, Wisniewski SR, Nierenberg AA, Warden D, Ritz L, Norquist G, ET AL. Evaluation of Outcomes With Citalopram for Depression Using Measurement-Based Care in STAR*D: Implications for Clinical Practice. Am J Psychiatry 2006;163:28-40. https://doi.org/10.1176/appi.ajp.163.1.28

Physiol. Res. 73 (Suppl. 1): S471-S476, 2024 *https://doi.org/10.33549/physiolres.935292*

REVIEW

Mathematical Models of Diffusion in Physiology

Jiří JANÁČEK[1]

[1]Laboratory of Biomathematics, Institute of Physiology of the Czech Academy of Sciences, Praha 4, Czech Republic

Received November 30, 2023
Accepted January 2, 2024

Summary

Diffusion is a mass transport phenomenon caused by chaotic thermal movements of molecules. Studying the transport in specific domain is simplified by using evolutionary differential equations for local concentration of the molecules instead of complete information on molecular paths [1]. Compounds in a fluid mixture tend to smooth out its spatial concentration inhomogeneities by diffusion. Rate of the transport is proportional to the concentration gradient and coefficient of diffusion of the compound in ordinary diffusion. The evolving concentration profile $c(x,t)$ is then solution of evolutionary partial differential equation

$$\frac{\partial c}{\partial t} = D\Delta c$$

where D is diffusion coefficient and Δ is Laplacian operator. Domain of the equation may be a region in space, plane or line, a manifold, such as surface embedded in space, or a graph. The Laplacian operates on smooth functions defined on given domain. We can use models of diffusion for such diverse tasks as: a) design of method for precise measurement of receptors mobility in plasmatic membrane by confocal microscopy [2], b) evaluation of complex geometry of trabeculae in developing heart [3] to show that the conduction pathway within the embryonic ventricle is determined by geometry of the trabeculae.

Key words

Diffusion • Mathematical modeling • FRAP • Plasma membrane • Trabeculation

Corresponding author

J. Janáček, Laboratory of Biomathematics, Institute of Physiology CAS, Vídeňská 1083, 14200 Praha 4, Czech Republic. E-mail: Jiri.Janacek@fgu.cas.cz

Introduction

Energy of thermal molecular movements is distributed into various modes according to configuration and environment of the molecules. Besides rotational and vibrational modes there are thermal molecular translations, chaotic motions causing the phenomenon of diffusion. The speed of the ordinary diffusion is fully characterized by diffusion coefficient (D) [1]. Ordinary diffusion takes place in homogeneous environment and the diffusion in structured or compartmentalized environment is usually anomalous. Anomalies in diffusion can be utilized for studying the underlying structure, for example, mean square displacement (MSD) of a particle, which is linear function of time in ordinary diffusion ($MSD(t) = D\,t$), can serve this purpose.

Specific methods of optical microscopy study molecular translations on scales ranging from single molecule up to the size of field of view.

Single fluorescently labelled molecule can be tracked in real time by superresolution microscope Minflux [4]. This method provides real path of the molecule, hence all parameters of the movements can be calculated, but very special equipment is needed and it tracks only one target at a time.

Fluorescence fluctuation techniques follow fluctuation of local concentration of the molecules. Fluorescence correlation spectroscopy (FCS) calculates diffusion coefficient D from time correlations of fluorescence in static focal volume [5]. Methods based on spatiotemporal correlations of fluorescence (ImCS) [6] provide information on anomalies in diffusion in MSD function. Those techniques require very low

concentration of fluorophores (i.e. dim fluorescence), units to tens molecules per focal volume, to obtain fluctuating fluorescence signals.

Methods operating in coarsest spatial scale calculate the diffusion coefficient D (or apparent D if the diffusion is in fact anomalous) from time evolution of the molecules concentration profile. Widely used is fluorescence recovery after photobleaching (FRAP) [5,7]. We analyzed dynamics of receptors on plasmatic membranes by FRAP on periphery of cell. We developed customized model of bleaching and diffusion in vertical plane in order to evaluate properly the FRAP experiment using microscopic objective with high numerical aperture [2].

Mathematical model of the evolving concentration profile is partial differential equation (PDE) of diffusion on a given domain. The diffusion coefficient D is calculated by fitting model FRAP curve to the measured one.

Properties of the Laplacian operator reflect form (i.e. dimension, shape and size) of the equation domain. Regular domains in Euclidean spaces [8,9] and fractal domains [10] were characterized by asymptotic properties of the operator eigenvalues.

We studied geometry of trabeculation in developing mouse embryonic heart using solutions of diffusion equation on graph obtained by skeletonization of the trabeculae. The directionality of the trabeculae was calculated from directionality of the equation solutions. [3]. The connectivity of the trabecular graph was characterized by fracton dimension estimated from asymptotics of the Laplacian operator eigenvalues.

Equations of diffusion

The Laplacian operator in one dimension (along line) is

$$\Delta c = \frac{\partial^2 c}{\partial x^2}$$

hence, the simplest (one-dimensional) equation of diffusion along line is

$$\frac{\partial c}{\partial t} = D\frac{\partial^2 c}{\partial x^2}$$

The equation has special solutions, so called Green functions, centered in point y

$$\frac{1}{2\sqrt{\pi Dt}} e^{-\frac{(x-y)^2}{4Dt}}$$

and we obtain diffusion profile $c(x,t)$ evolving from arbitrary initial profile $c(x,0)$ by integration

$$\frac{1}{2\sqrt{\pi Dt}} \int_{-\infty}^{\infty} e^{-\frac{(x-y)^2}{4Dt}} c(x,0)dy$$

For example, the profile evolving from $c(x,0)$, concentration equal to zero in interval from $-l/2$ to $l/2$ and equal to one elsewhere (Fig. 1a), can be expressed explicitly by formula

$$c(x,t) = 1 - \frac{1}{2}\left(Erf\frac{\left(\frac{l}{2} - x\right)}{2\sqrt{Dt}} + Erf\frac{\left(\frac{l}{2} + x\right)}{2\sqrt{Dt}} \right)$$

[11], where $Erfy = \int_0^y e^{-z^2}\, dz$ is error function.

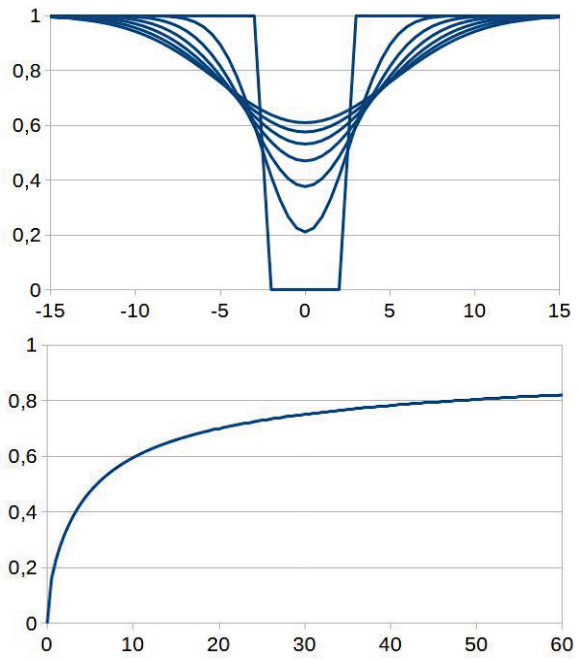

Fig. 1. (**a**) Concentration profile evolving in time, D=1. l=5. Time step 2 s. (**b**) Integral of the profile from -2,5 to 2,5 as function of time.

Diffusion of fluorescent receptors on vertical plasmatic membrane

Mobility of fluorescent molecules is studied by microscopic technique called fluorescence recovery after photobleaching (FRAP). Region of interest (ROI) in the target object is irreversibly bleached and then we record the light recovered by flow of fluorescent molecules into ROI.

FRAP along a tubule, e.g. neurite can be evaluated by fitting one-dimensional model curve to the recorded data

$$F(t) = F_0 + (F_\infty - F_0)F(Dt)$$

where F_0 is the postbleach value of F and F_∞ is the limit at infinity and F is calculated from the ordinary diffusion model (with D=1) as the amount of matter transported into the interval from $-l/2$ to $l/2$ up to time t by the integral of the concentration profile over the interval

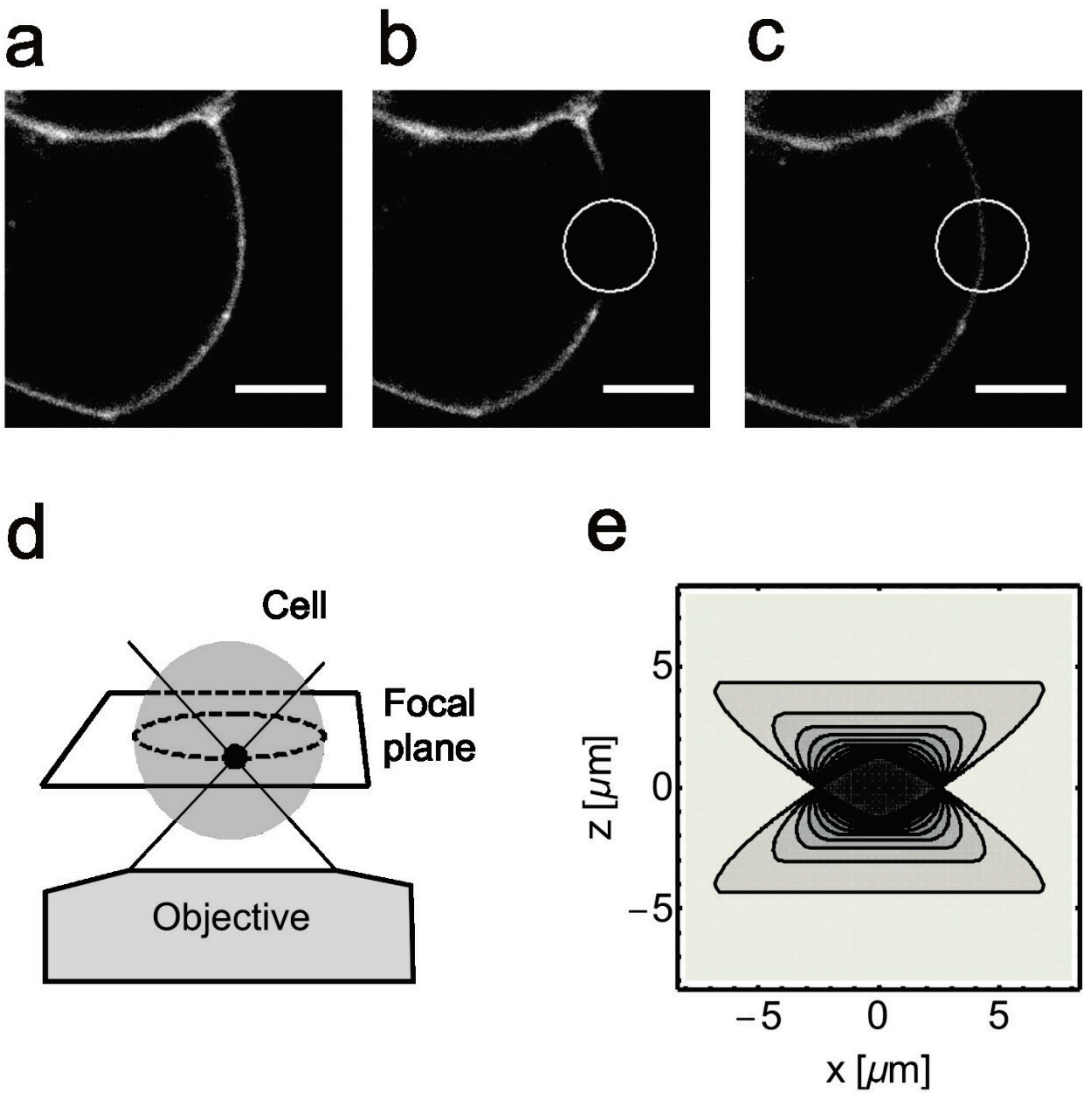

Fig. 2. FRAP measurement of plasma membrane protein mobility using „equatorial set-up". (**a-c**) Confocal images of the HEK293 cell expressing δ-OR-eYFP in the course of FRAP experiment: the optical section of the cell before the bleach (**a**), shortly after the bleach (**b**) and after the recovery of fluorescence signal in the bleached region of interest (ROI) (**c**). The white circle in b and c represents ROI used for recording the fluorescence recovery curve. Scale bars represent 5 μm. (**d**) Scheme of confocal imaging of plasma membrane region within the equatorial plane of the cell. (**e**) Axial profile of photobleaching irradiance calculated for horizontal circular ROI with diameter of 5 μm and water immersion objective with numerical aperture (NA) 1,2.

(Fig. 1b), which can be expressed in closed form as

$$F(t) = 1 - \frac{2\sqrt{t}}{l\sqrt{\pi}}\left(e^{-\frac{l^2}{4t}} - 1\right) - Erf\,\frac{l}{2\sqrt{t}}$$

See 7.2 in [12] for integral of *Erf*.

Mobility of molecules constrained to plasmatic membrane may be assessed by FRAP. The signal from plasmatic membrane with ROI on the periphery of the cell (Fig. 2a,b,c) obtained by confocal microscope equipped with objective with high numerical aperture cannot be analyzed neither by the above 1 dimensional model nor by other models found in FRAP literature [13], because the cone of light from high NA objective has obtuse apical angle and the bleached region on the horizontal plane approximating the plasma membrane (Fig. 2d) has hour-glass shape [14]. Analysis of FRAP of fluorescently labelled opioid receptors thus required development of new specific model [2]. We started with analytical expression for irradiance $I(x, z)$ applied in the bleaching in circular ROI (Fig. 2e) where horizontal coordinate x and axial coordinate z have origin in the center of ROI (see Appendix and [2] for details).

Concentration of fluorophore $c(x, z, t)$ in vertical x, z-plane obeys the diffusion equation:

$$\frac{\partial c}{\partial t} = D\left(\frac{\partial^2 c}{\partial x^2} + \frac{\partial^2 c}{\partial z^2}\right)$$

where D is the diffusion coefficient.

The initial, normalized concentration of fluorophore is calculated from 3D irradiation intensity

$I(x,z)$ (defined in Appendix) by formula:

$$c(x,z,0) = e^{-\alpha T\, I(x,z)}$$

where α is rate constant and T is duration of the bleaching pulse. Let $D = 1$.

$$c(x,z,t) = \frac{1}{4\pi t}\int_{-\infty}^{\infty}\int_{-\infty}^{\infty} e^{-\frac{(x-\xi)^2+(z-\zeta)^2}{4t}} c(x,z,0)d\xi\, d\zeta$$

Let $K = \alpha T\, I$ [7], the model FRAP recovery curve F_K is then obtained by integration of the fluorophore concentration over the linear segment,

$$F_K(t) = \frac{1}{2R}\int_{-R}^{R} c(x,0,t)dx$$

which is equal to:

$$F_K(t) = \frac{1}{8R\sqrt{\pi t}}\int_{-\infty}^{\infty} e^{-\frac{z^2}{t}} J_K(z,t)dz$$

where

$$J_K(z,t) = \int_{-\infty}^{\infty}\left(Erf\frac{R-x}{2\sqrt{t}} + Erf\frac{R+x}{2\sqrt{t}}\right)e^{-\alpha T I(x,z)}dx$$

The double integral in equation for F_K (t) is evaluated for using a numerical procedure in program *Mathematica (Wolfram)*. The example of F_K (t) curves is depicted in Figure 3a.

Experimental FRAP curve, such as that at Figure 3b, is fitted by function

$$F(t) = F_\infty F_K(Dt)$$

where F_∞ is the limit at infinity.

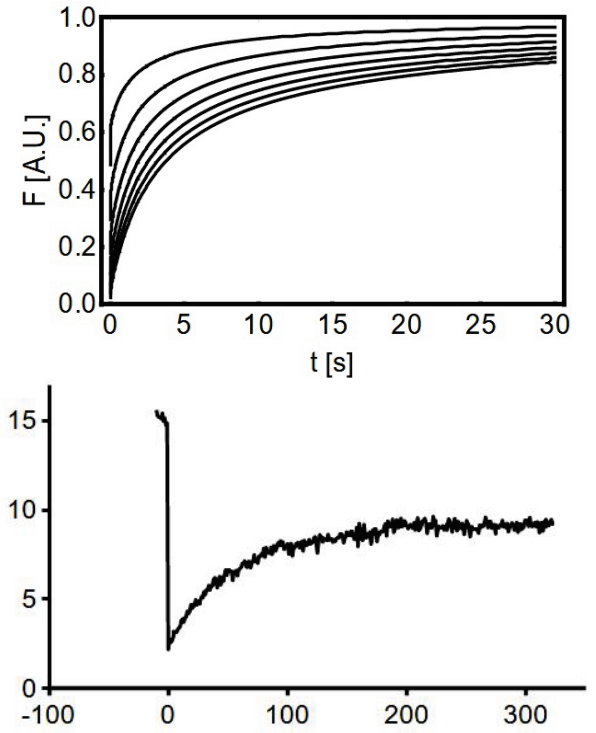

Fig. 3. (**a**) Simulated fluorescence recovery (FRAP) curves for various values of bleaching intensity K=0,5 to 3,5, numerical aperture NA=1,2, refractive index n=1,33 and diffusion coefficient D=1. (**b**) an example of real FRAP signal from plasmatic membrane on the periphery of cell.

Directionality of trabeculae in embryonic heart

Trabeculae in embryonic heart of Nkx-2.5:GFP mice were visualized in 3D using confocal microscope with 10× dry objective [3].

The binary image obtained by segmentation of the original image was skeletonized obtaining the graph (Fig. 4a) representing the trabeculae.

Local anisotropy of the trabecular structure is characterized by directionality of heat conduction, or equivalently by directionality of Brownian motion. For this purpose we use the graph $G = (V, E)$ with edges weighted by s- "conductance" (equal to reciprocal distance)

$$s(v_i, v_j) = \|v_i - v_j\|^{-1}$$

as the model of the trabecular structure.

The graph Laplacian Δ is I × I matrix with elements

$$\Delta_{ii} = -\sum_{(v_i,v_j)\in E} r(v_i, v_j)$$

$$\Delta_{ij} = r(v_i, v_j) \text{ if } i \neq j \text{ for } (v_i, v_j) \in E$$

$$\text{and } \Delta_{ij} = 0 \text{ for } (v_i, v_j) \notin E$$

The Laplacian is employed in formulation of the diffusion equation on the graph:

$$\frac{\partial c}{\partial t}(v,t) = \Delta c(v,t),\ \ v \in V, t \geq 0.$$

λ_n- eigenvalues and φ_n- orthonormal eigenvectors of the graph Laplacian Δ are related by equations

$$\Delta\varphi_n = \lambda_n\varphi_n, n = 1 \ldots I$$

so that $e^{\lambda_n t}\varphi_n(v)$ are generators of solutions of the diffusion equation.

The Green functions of the diffusion equation are defined using the eigenvectors and eigendomains as:

$$K(x,y,t) = \sum_{n=1}^{I} \varphi_n(x)\varphi_n(y)e^{\lambda_n t}$$

Second moments of the Green function in each point $y \in V$ can be calculated as:

$$T_{lk}(y,t) = \sum_{x\in V}\sum_{n=1}^{I} \varphi_n(y)\varphi_n(x)e^{\lambda_n t}(x_l - y_l)(x_k - y_k)$$

$$l, k = 1,2,3$$

Eigenvalues were calculated by DSBEVX routine in LAPACK library [15].

Eigenvectors were calculated by inverse iterations:

$$(\Delta - \lambda I)\varphi = b_m$$

$$b_{m+1} = \pm\frac{\varphi}{\|\varphi\|}$$

using LU decomposition from Numerical Recipes [16]. The tensor of the heat kernel second moments $T(y,t)$ was calculated, the values were interpolated and

visualized (Fig. 4b) in Amira 6.5 (FEI) using the module Tensor View.

Eigenvalues λ_n were distributed as $n^{\frac{2}{d}}$, where d correspond to (fractal) dimension growing from value 2.1 at ED10 to 2.5 at ED14.

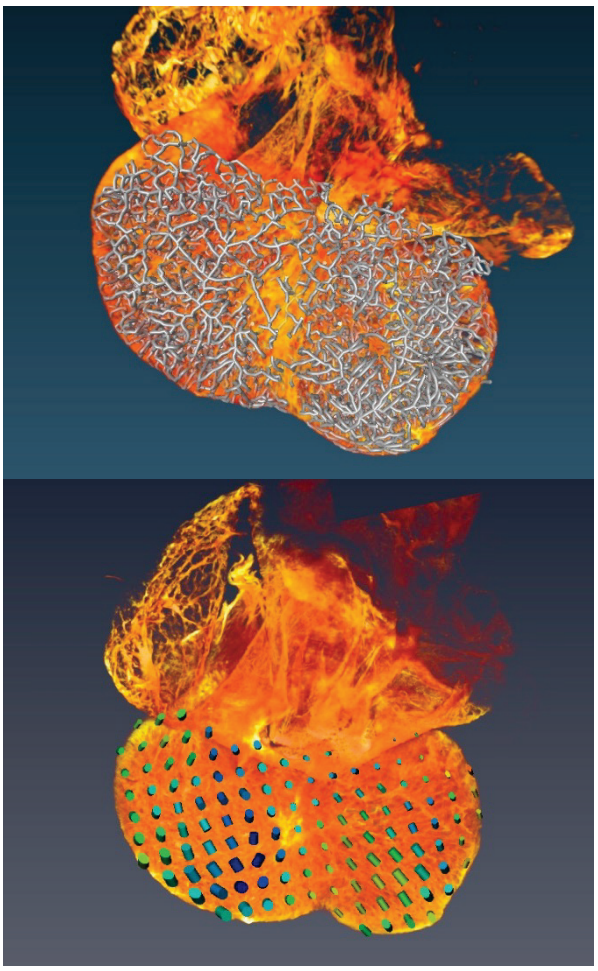

Fig. 4. (**a**) Graph of skeletonized trabeculae in mouse embryonic heart. (**b**) directionality tensor of diffusion on the graph.

Discussion and Conclusions

We demonstrated custom made FRAP model for evaluation of receptor mobility measured on periphery of cell by microscope with high numerical aperture. Using precise model is necessary, because 1D model, that is used for evaluation of this experiment with objective with low numerical aperture, would overestimate the value of diffusion coefficient by factor of two.

The history of the study of asymptotics of Laplacian operator eigenvalue in relation to its domain is long and interesting. First results were obtained in theoretical studies on radiation of the dark body [8] and they were completed by results on vibrational modes of solid bodies [9] and of fractals [10]. Trabeculae in embryonic heart have complicated structure of open foam that is difficult to characterize by conventional geometrical parameters. Dimension calculated from asymptotics of Laplacian eigenvalues somehow characterizes local connectivity of the structure, that is slightly lower than that of regular 3D grid. Fractal characterization of heart trabeculae were used also by others [17] and it can be applied in future to characterization of other complicated biological structures and network like objects.

Conflict of Interest

There is no conflict of interest.

References

1. Einstein A. Über die von der molekularkinetischen Theorie der Wärme geforderte Bewegung von in ruhenden Flüssigkeiten suspendierten Teilchen. Ann Phys 1905;17:549-560. https://doi.org/10.1002/andp.19053220806
2. Janáček J, Brejchová J, Svoboda P. Determination of delta-opioid receptor molecules mobility in living cells plasma membrane by novel method of FRAP analysis. Biochim Biophys Acta Biomembr 2019;1861:1346-1354. https://doi.org/10.1016/j.bbamem.2019.04.012
3. Olejníčková V, Šaňková B, Sedmera D, Janáček J: Trabecular architecture determines impulse propagation through the early embryonic mouse heart. Front Physiol 2019;9:1876. https://doi.org/10.3389/fphys.2018.01876
4. Balzarotti F, Eilers Y, Gwosch KC, Gynnå AH, Westphal V, Stefani FD, Elf J, Hell SW. Nanometer resolution imaging and tracking of fluorescent molecules with minimal photon fluxes. Science 2017;355:606-612. https://doi.org/10.1126/science.aak9913
5. Koppel DE, Axelrod D, Schlessinger J, Elson E, Webb WW, Dynamics of fluorescence marker concentration as a probe of mobility. Biophys J 1976;16:1315-1329. https://doi.org/10.1016/S0006-3495(76)85776-1

6. Planes N, Vanderheyden PPML, Gratton E, Caballero-George C. Image mean square displacement to study the lateral mobility of Angiotensin II type 1 and Endothelin 1 type A receptors on living cells. Microsc Res Tech 2020;83:381-392. https://doi.org/10.1002/jemt.23425
7. Axelrod D, Koppel DE, Schlessinger J, Elson E, Webb WW. Mobility measurements by analysis of fluorescence photobleaching recovery kinetics. Biophys J 1976;16:1055-1069. https://doi.org/10.1016/S0006-3495(76)85755-4
8. Weyl H. Das asymptotische Verteilungsgesetzt der Eigenverte linearer partieller Differentialgleichungen (mit einer Anwendung auf die Theorie der Hohlraumstrahlung). Math Ann 1912;71:441-479. https://doi.org/10.1007/BF01456804
9. Kac M. Can one hear the shape of a drum? Am Math Month 1966;73.4/2:1-23. https://doi.org/10.1080/00029890.1966.11970915
10. Alexander S, Orbach R. Density of states on fractals: fractons. J Phys Lett 1982;43:625-631. https://doi.org/10.1051/jphyslet:019820043017062500
11. Crank J. The Mathematics of Diffusion, Clarendon Press, 1956.
12. Abramowitz M, Stegun I. Handbook of Mathematical Functions with Formulas, Graphs, and Mathematical Tables. United States Department of Commerce, National Bureau of Standards, 1964.
13. Loren N, Hagman J, Jonasson JK, Deschout H, Bernin D, Cella-Zanacchi F, Diaspro A, McNally JG, Ameloot M, Smisdom N, Nyden M, Hermansson AM, Rudemo M, Braeckmans K, Fluorescence recovery after photo-bleaching in material and life sciences: putting theory into practice. Q Rev Biophys 2015;48:323-387. https://doi.org/10.1017/S0033583515000013
14. Mazza D, Cella F, Vicidomini G, Krol S, Diaspro A. Role of three-dimensional bleach distribution in confocal and two-photon fluorescence recovery after photobleaching experiments. Appl Opt 2007;46:7401-7411. https://doi.org/10.1364/AO.46.007401
15. Anderson E, Bai Z, Bischof C, Blackford S, Demmel J, Dongarra J, Du Croz J, Greenbaum A, Hammarling S, McKenney A, Sorensen D. LAPACK Users' Guide. Third ed. Philadelphia, Society for Industrial and Applied Mathematics; 1999. https://doi.org/10.1137/1.9780898719604
16. Press WH, Teukolsky SA, Vetterling WT, Flannery BP. Numerical recipes in C : the art of scientific computing, Second ed. Cambridge, New York, Cambridge University Press, 1992.
17. Meyer HV, Dawes TJW, Serrani M, Bai W, Tokarczuk P, Cai J, de Marvao A, Henry A, Lumbers RT, Gierten J, Thumberger T, Wittbrodt J, Ware JS, Rueckert D, Matthews PM, Prasad SK, Costantino ML, Cook SA, Birney E, O'Regan DP. Genetic and functional insights into the fractal structure of the heart. Nature 2020;584:589-594. https://doi.org/10.1038/s41586-020-2635-8

Appendix

Let n be refractive index of the immersion media, let β be half angle of the objective light cone satisfying the relation $NA = n \sin\beta$ for numerical aperture NA of the objective and let region of interest (ROI) be a circle with radius R, then $I(r, z)$, where horizontal coordinate $r>0$ and axial coordinate z have origin in the center of ROI, can be calculated using formula for the area of intersection of two circles with radii R and $|z|\tan\beta$ and distance between the two centers r.

$$I(r,z) = I \quad \text{for } 0 < r < R - |z|\tan\beta,$$
$$I(r,z) = 0 \quad \text{for } r > R + |z|\tan\beta, \text{ and}$$
$$I(r,z) = \frac{I}{\pi(|z|\tan\beta)^2}\left(\phi(R,|z|\tan\beta,r) + \phi(|z|\tan\beta,R,r)\right) \text{ for } |r-R| < |z|\tan\beta.$$

where φ is function

$$\phi(\rho_1,\rho_2,d) = \rho_2^2\left(\arccos\frac{d^2+\rho_2^2-\rho_1^2}{2d\rho_2} - \frac{d^2+\rho_2^2-\rho_1^2}{2d\rho_2}\sqrt{1-\left(\frac{d^2+\rho_2^2-\rho_1^2}{2d\rho_2}\right)^2}\right),$$

representing the area of the circular segment cut off from the circle with radius ρ_2 by a chord of another circle with radius ρ_1 where d is the distance of circles centers. The expression for φ follows from the law of cosines.

Finally, $I(x,z) = I(|x|,z)$ for negative x.

Metabolomics and Lipidomics for Studying Metabolic Syndrome: Insights into Cardiovascular Diseases, Type 1 & 2 Diabetes, and Metabolic Dysfunction-Associated Steatotic Liver Disease

Stanislava RAKUSANOVA[1], Tomas CAJKA[1]

[1]Institute of Physiology of the Czech Academy of Sciences, Prague, Czech Republic

Supplementary Materials

Table S1. Metabolomics and lipidomics cohort studies focused on cardiovascular disease

Table S2. Metabolomics and lipidomics cohort studies focused on type 1 and type 2 diabetes

Table S3. Metabolomics and lipidomics cohort studies focused on metabolic dysfunction-associated steatotic liver disease

Table S1. Metabolomics and lipidomics cohort studies focused on cardiovascular disease

Subjects (n)	Cohort	Matrix	Platforms	Reported metabolites (n)	Markers	Outcomes	Ref.
Discovery cohort: n = 4,824 (27.8% female) Replication cohort: n = 1,716 (56.3% female)	Participants with 15.8 years follow-up	Serum	NMR	41	Isoleucine Leucine Phenylalanine Glycerol Cholesterol Total lipid concentrations, Glycerides and other Phospholipids, Fatty acids, Fatty acids ratios — see the original paper.	• Association with adherence to dietary recommendations provided by the Alternative Healthy Eating Index	[1]
European cohort: n = 352 USA cohort: n = 1,777	European participants (100% Caucasian) with either abdominal aortic aneurysm or sub-aneurysmal aortic dilations, and healthy non-aneurysm subjects US participants (96% Caucasian) with abdominal aortic diameter of 3.0 cm or greater, and subjects with history of dilated aorta with measurements of abdominal aortic diameter less than 3 cm or no prior aortic aneurysm, and no MI, stroke or death over the following 3 years	Plasma	LC-MS/MS	3	Choline Trimethylamine *N*-oxide Trimethylamine	• Association of elevated TMAO with increased abdominal aortic aneurysm incidence	[2]
Low-risk cohort: n = 620 Borderline-risk cohort: n = 110 Intermediate-risk cohort: n = 225 Highrisk cohort: n = 147 (53.3% female)	Participants with LDL levels less than 190 mg/dl and no pre-existing coronary artery disease or myocardial infarction	Plasma	LC-MS/MS	50	Alanine Arginine Aspartic acid CAR 4:0-DC CAR 8:1 CAR 16:0-OH Citrulline Glutamic acid Glutamine Glycine Histidine Phenylalanine Threonine Tryptophan	• Association with the 10-year ASCVD risk score • Identification of metabolic pathways associated with the development of 10-year ASCVD events	[3]
EPIC-Potsdam Study cohort: Common reference subcohort: n = 1262 T2D subcohort: n = 1886 (775 incident cases) CVD subcohort: n = 1671 (551 incident cases) **DIVAS study cohort:** CVD risk subcohort: n = 113 (on 3 different isoenergic diets)	General population Patients with estimated moderate CVD risk	Plasma	DMS-MS/MS	282	CE 20:3 DG 16:0 DG 18:0 FA 15:0 FA 20:4 LPC 18:2 MG 15:0 MG 20:4 PC 20:3 PE 20:3 TG 16:0 TG 18:0 TG 18:2 TG 18:3 TG 22:1	• Association with cardiometabolic disease risk and T2D risk • Dietary fat intervention as a potential tool for primary disease prevention	[4]

Subjects (n)	Cohort	Matrix	Platforms	Reported metabolites (n)	Markers	Outcomes	Ref.
Discovery cohort: n = 1,162 (36.3% female) Validation cohorts: n = 2,331 (US, 33.2% female), n = 832 (European, 29.9% female)	Stable participants undergoing elective diagnostic cardiac evaluation	Plasma	LC-MS/MS	5	N^1-Methyl-2-pyridone-5-carboxamide N^1-Methyl-4-pyridone-3-carboxamide Phenylacetylglutamine Trimethylamine *N*-oxide Trimethyllysine	• Association of terminal breakdown products of excess niacin with residual CVD risk	[5]
Phase I: Discovery cohort: n = 3,613 Validation cohorts: n = 121,733 **Phase II:** n = 118,120	UK Biobank participants have undergone a wide range of physical measures, provided information on their lifestyle and medical history (follow-up)	Plasma	NMR	111	Multiple markers – see the original paper.	• Association with a healthy lifestyle • Association of healthy lifestyle-associated metabolites with coronary artery disease (CAD)	[6]
Discovery cohort: n = 1,028 Validation cohort: n = 1,670	Discovery cohort: Participants free of coronary heart disease (10 years follow-up)	Plasma	LC-MS/MS	32	LPC 18:1 LPC 18:2 MG 18:2 SM d28:1	• Association of MG 18:2 with coronary heart disease • Association of LPCs with body mass index, C-reactive protein and with less evidence of subclinical CVD	[7]
Discovery cohort: n = 1,833 (57% female) Validation cohorts: n = 1,522 Low walnut intake subcohort: n = 691 High walnut intake subcohort: n = 467	Participants at high cardiovascular risk	Plasma	LC-MS	385	4-Hydroxy-3-methylacetophenone Cyclohexylamine Guanine Isocitric acid *N*-Acetylaspartic acid Piperine Serine Sorbitol Succinic acid Bilirubin Biliverdin CAR 10:2 LPC 14:0 LPC 16:1 MG 22:1 PC 36:4 PE 36:5 PS 40:6 TG 54:6	• Association of walnut consumption with a lower risk of incident T2D and CVD in a Mediterranean population at high cardiovascular risk	[8]
Study cohort: n = 1,057	Participants with symptomatic coronary artery disease	Blood-platelets	LC-MS/MS	767	CAR 10:0 CAR 14:0 CAR 14:1 CAR 16:0 CAR 16:1 FA 18:1 FA 18:2 FA 18:2;2O LPE 18:1|LPE 0:0/18:1 LPE 18:1|LPE 18:1/0:0 LPE 18:2|LPE 0:0/18:2 LPE 18:2|LPE 18:2/0:0 LPE 20:1|LPE 20:1/0:0 LPE 20:3|LPE 0:0/20:3 LPE 20:3|LPE 20:3/0:0 LPE 20:4 LPE 20:5 LPE 22:4|LPE 0:0/22:4 LPE 22:4|LPE 22:4/0:0 LPE 22:5	• Association of adverse cardiovascular events with alterations in the platelet lipidome	[9]

Subjects (n)	Cohort	Matrix	Platforms	Reported metabolites (n)	Markers	Outcomes	Ref.
					LPE 22:6 LPS 18:1|LPS 0:0/18:1 PC 34:2;O PE 34:3|PE 16:1_18:2;O PI 36:4|PI 16:0_20:4 PI 38:5|PI 18:1_20:4 TG 48:1|TG 14:0_16:0_18:1 TG 48:2|TG 16:0_14:1_18:1		
Study cohort: n = 1,021 (48.3% female)	Participants with T2D and were followed up for CVD over the subsequent 10 years	Serum	NMR	228	3-Hydroxybutyric acid Acetic acid Creatinine Glycine Lactic acid Leucine Phenylalanine	• Association with 10-year cardiovascular risk in people with type 2 diabetes • Metabolite-based risk score created	[10]
Malmo Diet and Cancer-Cardiovascular cohort: n = 4,067	General population followed up to 23 years and stratified into risk groups	Plasma	DI-MS/MS	184	*Sum of lipid subclasses:* Ceramide Cholesteryl ester Cholesterol Diacylglycerol Ether-phosphatidylcholine Ether-phosphatidylethanolamine Lysophosphatidylcholine Lysophosphatidylethanolamine Phosphatidylcholine Phosphatidylethanolamine Phosphatidylinositol	• Possible identification of lipidomic risk before disease incidence (CVD and T2D)	[11]
Discovery cohort 1: n = 99 Discovery cohort 2: n = 1,162 Validation cohort: n = 2,140	Sequential stable subjects without evidence of acute coronary syndrome undergoing elective diagnostic coronary angiography for evaluation of CAD with longitudinal (3–5 years) follow-up	Plasma	HILIC-MS/MS LC-MS/MS		Trimethyllysine Trimethylamine *N*-oxide	• Association with CVD risks	[12]
Study cohort: n = 2,278 (50% female)	Participants were followed up for CVD incident (almost 10 years)	Plasma	LC-MS/MS	790 (37)	Dimethylglycine *N*-Acetylmethionine (top findings)	• Association with CVD risks	[13]
Study cohort: n = 5,072	Participants with diabetes	Plasma	NMR	44	3-Hydroxybutyric acid Acetic acid Acetoacetatic acid Acetone Alanine Citric acid Creatinine Glucose Glutamine Glycine Histidine Isoleucine Lactic acid Leucine Phenylalanine Pyruvic acid Tyrosine Valine	• Association of multiple healthy lifestyle factors with improved circulating metabolites from different pathways	[14]

Subjects (n)	Cohort	Matrix	Platforms	Reported metabolites (n)	Markers	Outcomes	Ref.
Discovery cohort: n = 1,833 (57.6% female) Validation subcohort: n = 1,522	Participants at high risk of CVD (1-year follow-up)	Plasma	LC-MS/MS	382	1-Methylguanine γ-Aminobutyric acid (GABA) Aminoisobutyric acid Asparagine Cortisol Creatine Cytosine Glycodeoxycholic acid Hippuric acid Homoarginine Hypoxanthine Lactic acid Lysine N^1-Acetylspermidine *N*-Acetylaspartic acid *N*-Acetylornithine *N*-Carbamoyl-β-alanine Piperine Pyroglutamic acid Sorbitol Sucrose Trimethylbenzene CAR 7:0 CAR 18:2 CAR 18:0 DG 34:3 DG 36:0 LPC 16:1 MG 22:1 PC 34:3 PC 36:4 PC 38:4 PE 32:0 PE 38:6 PE 40:7 SM d34:2|SM d18:1/16:1 TG 50:3 TG 50:4 TG 55:2 TG 56:2	• Association of legume consumption with T2D incidence, but not with CVD incidence risk	[15]
Study cohort: n_1 = 5,991; n_2 = 3,779 (38.9% female)	Participants with an 8-year follow-up	Plasma	LC-MS/MS	342	CE 24:0 LPI 18:2 PC 38:5 PC O-34:2 PC O-36:1 PC P-40:6 PE 38:6 PI 38:3 SM d42:1	• Association with future cardiovascular events and cardiovascular death	[16]
Discovery cohort: n = 1,162 Validation cohort: n = 4,000	Sequential stable subjects undergoing elective diagnostic cardiac evaluation with longitudinal (3 years) follow-up	Plasma	HILIC-MS LC-MS/MS	5 (top-ranked)	Phenylacetylglutamine	• Association with cardiovascular disease and death in humans	[17]

Subjects (n)	Cohort	Matrix	Platforms	Reported metabolites (n)	Markers	Outcomes	Ref.
Discovery cohort: n = 1,149 Validation cohort: n = 3,954	Participants with preserved kidney function undergoing elective diagnostic cardiac evaluation with longitudinal follow-up (5 years)	Plasma	GC-MS LC-MS/MS	N/A	*p*-Cresol sulfate Indoxyl sulfate	• Association with CVD risk and overall mortality	[18]
Study cohort: n = 2,627	Participants were invited to attend a health examination for additional tests and collection of 8–12 h fasting blood samples (mean 12.9 years follow-up)	Plasma	HILIC-MS LC-MS/MS	79	Hex2Cer d34:2|Hex2Cer d18:2/16:0 HexCer d36:1|HexCer d18:1/18:0 HexCer d34:1|HexCer d18:1/16:0 HexCer d42:2|HexCer d18:2/24:0 SM d34:1|SM d18:1/16:0 SM d36:1|SM d18:1/18:0 SM d36:2|SM d18:2/18:0 SM d42:1|SM d18:1/24:0	• Association with higher CVD risk	[19]
Study cohort: n_1=50; n_2=4,007	Healthy participants before and after the suppression of intestinal microbiota with oral broad-spectrum antibiotics underwent phosphatidylcholine challenge (ingestion of two hard-boiled eggs and deuterium [d_9]-labeled phosphatidylcholine) Participants undergoing elective diagnostic cardiac catheterization with no history of acute coronary syndrome	Plasma	LC-MS/MS	3	Betaine Choline Trimethylamine *N*-oxide	• Association among intestinal microbiota-dependent metabolism of dietary phosphatidylcholine, TMAO levels, and adverse CVD events	[20]
Discovery cohort: n = 3,867 Validation cohort: n = 3,569	Participants were free of known CVD at baseline	Serum	NMR	N/A	1,5-Anhydrosorbitol 1-Methylhistidine 3-Hydroxybutyric acid 5-Oxoproline Acetaminophen + glucuronide Alanine Aspartic acid Citratic acid Glucose Glutamatic acid Glutamine Glycerol Glycine Histidine Lactic acid Lysine Mannose Methionine myo-Inositol Dimethylglycine Phenylalanine Glyceryl groups of lipids Lipids (CH2-CO) Lipids (CH2-CH2-C=, CH2-CH2-CO) Lipids (CH2-CH2-CH=CH) Lipids (CH3-CH2-R, (CH2)n) Lipids (CH3-CH2-R, CH3-CH2-C=)	• Association with atherosclerosis and incident CVD	[21]
Discovery cohort: n = 50 Validation cohort: n = 25	Stable patients undergoing elective cardiac evaluation who subsequently experienced a heart attack, stroke or death over the ensuing three-year period vs. age- and gender-matched subjects who did not	Plasma	LC-MS/MS	18	Betaine Choline Trimethylamine *N*-oxide	• Identification of markers as predictors of CVD risk • Discovery of a relationship between gut-flora-dependent metabolism of dietary	[22]

Subjects (n)	Cohort	Matrix	Platforms	Reported metabolites (n)	Markers	Outcomes	Ref.
						phosphatidylcholine and CVD pathogenesis	
Discovery cohort: n = 1,157 Validation cohorts: n_1 = 2,149; n_2 = 833	Stable subjects undergoing cardiac risk assessment Healthy volunteers (n = 8)	Plasma	GC-MS LC-MS/MS	N/A	Creatinine Erythritol Xylitol	• Association with major adverse cardiovascular event	[23]
Discovery cohort: n = 1,157 Validation cohort: n = 2,149	Stable subjects undergoing elective diagnostic cardiac evaluations Healthy volunteers (n = 10)	Plasma	GC-MS LC-MS/MS	N/A	Creatinine Erythritol Xylitol	• Association with major adverse cardiovascular event	[24]
Discovery cohort: n = 7,256 Validation cohorts: n_1 = 2,622; n_2 = 3,563	Participants were followed up for CVD incident (15 years)	Serum	NMR	68	3-Hydroxybutyric acid Acetic acid Acetoacetatic acid Alanine Citratic acid Glucose Glutamine Glycerol Glycine Histidine Isoleucine Lactic acid Leucine Phenylalanine Pyruvic acid Tyrosine Valine Docosahexaenoic acid (FA 22:6) Linoleic acid (FA 18:2) Monounsaturated FA Omega-3 FA Omega-6 FA Polyunsaturated FA Saturated FA	• Association with incident CVD	[25]
Study cohort: n = 4,007	Participants undergoing elective diagnostic cardiac catheterization with no history of an acute coronary syndrome	Plasma	LC-MS/MS	18	Choline Trimethylamine Trimethylamine *N*-oxide	• Discovery of increased levels of TMAO as a predictor of incident risk for thrombotic events • Association between specific dietary nutrients, gut microbes, platelet function, and thrombosis risk	[26]

Table S2. Metabolomics and lipidomics cohort studies focused on type 1 and type 2 diabetes

Subjects (n)	Cohort	Matrix	Platforms	Reported metabolites (n)	Markers	Outcomes	Ref.
Study cohort: n = 170 (48% female)	Children with high genetic risk for T1D	Plasma	GC-MS LC-MS/MS	91	γ-Aminobutyric acid (GABA) Glycine Tagatose Arabitol myo-Inositol Adipic acid Cer d38:1 Cer d39:1 LPC 18:3 LPC 20:3 LPC 20:5 SM d41:2	• Utilization of multi-omics data for the modeling of complex, multifactorial diseases, like T1D	[27]
Study cohort: n = 152 (47.4% female)	Children with T1D (n=76) and healthy control children (n=76)	Cord blood serum	LC-MS/MS	106	PC 32:1 PC 36:4 PC 38:4 PC 38:5 PC 38:5 PC 38:6 PC 40:4 PC 40:5 PC 40:5 PC 40:7 PC 40:8 PC sum PE 38:4 PE 38:4 PE 40:4	• Cord-blood metabolic patterns may be a valuable measure of type 1 diabetes risk	[28]
Study cohort: n = 101 (37.6% female)	Children who progressed to T1D (PT1D; n = 30), children who developed at least one islet autoantibody but did not progress to T1D during the follow-up (P1Ab; n = 33), and their age-matched controls (CTR; n = 38)	Cord blood plasma	LC-MS/MS	232 lipid species	CE 18:2 TG 46:2 TG 46:2 TG 48:1 TG 51:3	• Identification of lipids that can be predictive of the risk of progression to T1D • Comparison of lipidomic profiles of all subcohorts	[29]
Study cohort: n = 120	Children progressed to T1D; children developed at least a single islet autoantibody but did not progress to T1D during the follow-up; matched controls	Plasma	LC-MS/MS	45	CE 20:5 PC 33:0 TG 54:4|TG 18:2_18:1_18:1 TG 56:5	• Children who progress to T1D in the follow-up tend to have a distinct and persistently dysregulated lipid profile as compared to those who later progress to islet autoimmunity but not to T1D	[30]
Study cohort: n = 120	Progressors to T1D (n = 40); children tested positive for at least one antibody in a minimum of two consecutive samples but did not progress to clinical T1D during the follow-up (n = 40); control children remained islet autoantibody-negative during the follow-up (n = 40)	Plasma	GC-MS	94	2-Ketoisocaproic acid 3,4-Dihydroxybutanoic acid Aspartic acid Bisphenol A Glutamic acid Glycerol-2-phosphate Levoglucosan Malic acid Methionine Pyruvic acid	• Association of unique metabolomic profile with T1D	[31]
Study cohort: n = 2,124	Children with high genetic risk for T1D	Plasma	GC-MS LC-MS/MS	357	5-Methoxytryptamine Alanine Glutamic acid Isoleucine Leucine	• Studying autoantibodies and metabolomic markers, which are associated with the risk of progression to T1D	[32]

Subjects (n)	Cohort	Matrix	Platforms	Reported metabolites (n)	Markers	Outcomes	Ref.
					Methionine Proline Valine Vitamin E α-Ketoglutaric acid		
Study cohort: n = 166	T1D patients (n = 85) and healthy controls (n = 81). All patients had a stable dose of insulin usage for more than 3 months (dose change <10%)	Serum Urine	LC-MS/MS	54 (serum) 45 (urine)	4-(2-Aminophenyl)-2,4-dioxobutanoic acid 4-Pyridoxic acid 5-Hydroxytryptophan 5-Methoxyindole-3-acetic acid Hypoxanthine Thromboxane B3	• Identification of altered metabolic profiles in T1D individuals with different time in range (TIR)	[33]
Study cohort: n = 286	Infants later developed T1D (n=33); infants developed different numbers of islet autoantibodies during the follow-up (n=110); controls matched for sex, HLA-DQB1 genotype, city of birth, and period of birth (n=143)	Cord blood serum	LC-MS/MS	137	PC 32:0|PC 16:0_16:0 PC 32:1|PC 16:0_16:1 PC 34:1|PC 16:0_18:1 PC 34:3|PC 16:0_18:3 PC 36:1|PC 18:0_18:1 PC 38:3|PC 18:0_20:3 SM d34:1|SM d18:1/16:0 SM d36:1|SM d18:1/18:0 SM d38:0|SM d18:0/20:0 SM d38:1|SM d18:1/20:0 SM d42:1|SM d18:0/24:1 SM d42:2|SM d18:1/24:1 SM d42:2|SM d18:0/24:2 SM d42:3|SM d18:2/24:1	• Association with high risk for progression to T1D	[34]
Study cohort: n = 343	Children, who later developed type 1 diabetes (n=166), and random control children in the Norwegian Mother, Father, and Child cohort (n=177)	Cord blood plasma	LC-MS/MS	27	Aminoadipic acid Indoxyl sulfate Tryptophan	• Association with T1D	[35]
Study cohort: n = 655	Children with high genetic risk for T1D	Plasma	GC-MS	139	Ascorbic acid Piperidone	• Association with progression to T1D	[36]
Study cohort: n = 141	Children with T1D (n=76) and gender- and age-matched healthy controls (n=65)	Serum	GC-MS	70	1,5-Anhydroglucitol Adenine Fructose Glycerol-α-phosphate Inosine Levoglucosan Pyruvic acid Uridine Xylulose	• Association with T1D and with the duration of the disease	[37]
Study cohort: n = 11,896	Participants from four prospective population-based cohorts in Finland (follow-up for 7.8–15 years)	Serum	NMR	229	3-Hydroxybutyric acid Acetatic acid Acetoacetatic acid Citratic acid Creatinine Glutamine Glycerol Glycine Histidine Isoleucine Lactic acid Leucine Phenylalanine Pyruvic acid	• Association with risk of developing diabetes • Association with deterioration in post-load glucose and insulin resistance than with future fasting hyperglycemia	[38]

Subjects (n)	Cohort	Matrix	Platforms	Reported metabolites (n)	Markers	Outcomes	Ref.
					Tyrosine Valine		
Study cohort: n = 1,016	General population	Plasma	NMR	49	3-Hydroxybutyric acid Acetatic acid Alanine Citratic acid Creatine Creatine phosphate Creatinine Cysteine Glutamine CH2CH2CO- CH2N- Isobutyratic acid Isopropanol Leucine *N*-Acetylglutamine *O*-Phosphoethanolamine Phenylpropionic acid Proline Pyruvic acid	• Strong inverse association of healthy lifestyle with incident T2D	[39]
Study cohort: n = 1,138	Participants from four prospective population-based cohorts	Plasma	LC-MS/MS	70	2-Methylbutyroylcarnitine Cortisol Deoxycholic acid Tyrosine γ-Glutamyl-leucine Barogenin CerPE 38:2 LPC 20:2 MG 18:2 PC 42:7 SM d33:1 SM d34:2 SM d36:3|SM d18:2/18:1	• Association with incident T2D	[40]
Study cohorts: n_1 = 1,261; n_2 = 2,580	Clinically healthy participants (follow-up for 3 years)	Plasma	LC-MS/MS	N/A	2-Hydroxybutyric acid LPC 18:2	• Association with insulin resistance and glucose intolerance	[41]
Study cohort: n = 2,282 Incident T2D cohort: n = 800	General population	Serum	FI-MS	163	Glycine Hexose Phenylalanine LPC 18:2 PC O-34:3 PC O-40:6 PC O-42:5 PC O-44:4 PC O-44:5 PC O-32:1 PC 36:1 PC 38:3 PC 40:5 SM d34:2|SM d18:1/16:1	• Association with increased or decreased risk of T2D	[42]
Study cohort: n_1 = 1,813; n_2 = 451	1,813 participants without any signs of T2D 451 participants with newly diagnosed T2D	Serum	FI-MS LC-MS/MS	134	Alanine/glycine	• Association of analine/glycine ration with T2D	[43]

Subjects (n)	Cohort	Matrix	Platforms	Reported metabolites (n)	Markers	Outcomes	Ref.
Study cohort: n = 5844 (90% female)	Female and male nurses	Plasma	LC-MS/MS	186	1-Methylnicotinamide 1-Methylguanosine Aminoisobutyric acid Caffeine CAR 2:0 CAR 5:0 CAR 5:0-DC Cortisone Dimethylglycine Guanidoacetic acid N^2,N^2-Dimethylguanosine N^4-Acetylcytidine *N*-Acetylspermidine *N*-Acetyltryptophan *N*-Carbamoyl-β-alanine Piperine Ribothymidine Tryptophan Biliverdin Cer d34:1|Cer d18:1/16:0 LPE 18:2 PC 34:2 PC P-34:4 PC P-38:4 PE 36:4 PE P-36:2 SM d38:1|SM d18:1/20:0	• Association between inflammatory and insulinemic dietary patterns, plasma inflammatory/insulin biomarkers, plasma metabolomics and risk of type 2 diabetes.	[44]
Study cohort: n = 2240	T2D participants, prediabetes participants, and normal glucose tolerance participants	Serum	FI-MS LC-MS/MS	123	Glycine CAR 16:0 LPC 18:2 PC O-36:0	• Association with incident T2D	[45]
Study cohort: n = 4,442 (61% female)	Participants without diabetes at baseline	Plasma	LC-MS/MS	6	Betaine Carnitine Choline Crotonobetaine γ-Butyrobetaine Trimethylamine *N*-oxide	• Association with incident T2D	[46]
Study cohort: n = 1571	Healthy participants (follow-up for 14 years)	Plasma	NMR LC-MS	24	1,5-Anhydroglucitol 2-Hydroxybutyric acid 2-Oxoglutaric acid Glycerol Glycine betaine Isoleucine Lactic acid Methionine Pyruvic acid Tyrosine PC 34:2;O TG 48:0 TG 48:1 TG 50:5	• Increase of the long-term prediction performance in combination with classical measurements	[47]

Subjects (n)	Cohort	Matrix	Platforms	Reported metabolites (n)	Markers	Outcomes	Ref.
Discovery cohort: n = 3,821 Validation cohort: n = 14,651	Participants with normal glucose regulation	Serum	LC-MS/MS	667 (discovery cohort) 250 (validation cohort)	CE 14:0 LPI 16:1 PC 34:3 PE 38:4|PE 18:0_20:4 TG 48:1 (16:0) TG 48:1 (16:1) TG 48:2 (16:0) TG 48:2 (16:1) TG 48:2 (18:1) TG 48:3 (16:1) TG 50:0 (18:0) TG 50:1 (16:0) TG 50:1 (16:1) TG 50:1 (18:0) TG 50:2 (16:0) TG 50:2 (16:1) TG 50:2 (16:2) TG 50:2 (18:1) TG 50:3 (16:0) TG 50:3 (16:1) TG 50:3 (16:2) TG 51:0 (17:0) TG 51:2 (17:0) TG 51:3 (17:1) TG 53:2 (19:0) TG 53:3 (16:0) TG 54:3 (16:0) TG 54:3 (16:0) TG 54:4 (16:0) TG 54:4 (16:1) TG 54:5 (16:0) TG 54:5 (16:1) TG 54:6 (20:4) TG 54:7 (20:4) TG 54:7 (22:6) TG 55:6 (19:3) TG 56:5(18:1) TG 56:5(22:4) TG 56:6(22:5)	• Association of biomarkers and lipid pathway dysregulation with T2D onset	[48]
Study cohort: n = 2,204 (100% female)	Participants with T2D or impaired fasting glucose + normoglycemic control participants	Plasma Urine	LC-MS/MS GC-MS	447	2-Hydroxybutyric acid 1,5-Anhydroglucitol Arabinose Citrulline Dimethylarginine Erythritol Fructose Glucose Isoleucine Lactic acid Leucine Malic acid Mannose *N*-Acetylglycine Octanoylcarnitine Proline	• Association with incident T2D and IFG	[49]

Subjects (n)	Cohort	Matrix	Platforms	Reported metabolites (n)	Markers	Outcomes	Ref.
					Uric acid Valine 10-Heptadecenoic acid (FA 17:1n7) 15-Methylpalmitic acid (FA iso-17:0) 3-Methyl-2-oxobutanoic acid 3-Methyl-2-oxovaleric acid 4-Methyl-2-oxopentanoic acid 5-Dodecenoic acid (FA 12:1n7) Adrenic acid (FA 22:4n6) Arachidonic acid (FA 20:4n6) Cholesterol Heptanoic acid (FA 7:0) Myristic acid (FA 14:0) Myristoleic acid (FA 14:1n5) Palmitoleic acid (FA 16:1n7) SM d34:1|SM d18:1/16:0 Pelargonic acid (FA 9:0) Pentadecanoic acid (FA 15:0)		
Study cohort: n = 1,150	Participants with normal fasting glucose (follow-up for 20 years)	Plasma	LC-MS/MS	N/A	5-Hydroxyindoleacetic acid Glucose Glycine Isocitric acid Phenylalanine Taurine 2-Aminodipic acid 3-Methyladipic acid CE 20:3 DG 36:1 LPC 18:1 LPC 18:2 PC 36:4 SM d42:1|SM d18:1/24:0 TG 48:0 TG 48:1 TG 52:1 TG 54:8 TG 58:11	• Association with improved prediction of T2D beyond conventional risk factors	[50]
Discovery cohort: n = 543 Validation cohort: n = 1,044	Non-diabetic participants (follow-up)	Serum	LC-MS/MS GC-MS	568	2-Hydroxybutyric acid Bilirubin Glucose Glutamic acid Glutamine Histidine Isoleucine Mannose Trehalose Valine α-Tocopherol	• Association with positive or negative impact on progression to T2D	[51]
Study cohort: n = 1,248	Participants with 6.5 years follow-up	Plasma	DMS-MS/MS GC-MS	N/A	*Lipid classes containing species with FA 15:0 and FA 17:0:* CE 15:0 CE 17:0 DG 15:0 FA 15:0	• Association with incident T2D	[52]

Subjects (n)	Cohort	Matrix	Platforms	Reported metabolites (n)	Markers	Outcomes	Ref.
					FA 17:0 LPC 15:0 LPC 17:0 LPE 17:0 MG 15:0 MG 17:0 PC 15:0 PC 17:0 PE 17:0 PL-OCFA (phospholipid species containing odd-chain fatty acids) TG 15:0 TG 17:0		
Study cohorts: n_1 = 1,039; n_2 = 520	Participants with mean follow-ups: 4.61 and 7.57 years	Plasma	LC-MS/MS	166	CE 16:1 LPC 15:0 LPC 18:2 PC 33:3 PC 35:3 PC 40:7 PC 43:6 PC 44:1 SM d34:2 SM d41:2 TG 46:1 (12:0) TG 48:1 (16:0) TG 48:2 (14:0) TG 49:7 (16:0) TG 50:1 (16:0) TG 50:2 (16:0) TG 50:3 (18:1) TG 51:7 (16:0) TG 52:5 (18:2) TG 52:6 (18:2) TG 54:3 (18:0) TG 54:4 (18:2) TG 54:5 (18:2) TG 54:6 (18:2) TG 54:7 (18:3) TG 56:5 (20:4)	• Association with incident T2D	[53]
Study cohort: n = 2,939	Participants without diabetes prevalence	Serum	LC-MS/MS	245	3-(4-Hydroxyphenyl)lactic acid Asparagine Erythritol Isoleucine Leucine Trehalose Valine	• Association with incident T2D (protective biomarker of diabetes risk)	[54]

Subjects (n)	Cohort	Matrix	Platforms	Reported metabolites (n)	Markers	Outcomes	Ref.
Study cohort: n = 2,103	Participants with a 6-year follow-up	Plasma	LC-MS/MS	34	Carnitine 3-Dehydroxycarnitine 3-Dehydrocarnitine CAR 2:0 CAR 3:0 CAR 3:0-DC CAR 4:0 CAR 5:0 CAR 5:0-OH CAR 5:1 CAR 6:0 CAR 6:0-OH CAR 6:0-DC CAR 7:0-DC CAR 8:0 CAR 8:1 CAR 10:0 CAR 10:0-DC CAR 12:0 CAR 12:0-OH CAR 12:1 CAR 12:0-DC CAR 14:0 CAR 14:0-OH CAR 14:1-OH CAR 16:0 CAR 16:1 CAR 16:2 CAR 18:0 CAR 18:0-OH CAR 18:1 CAR 18:2 CAR 20:0 CAR 20:4	• Association with improved predictive ability for type 2 diabetes beyond conventional risk factors	[55]
Study cohort: n = 3,234	Participants were assigned to 1) intensive lifestyle, 2) metformin, or 3) placebo (all followed up for 3.2 years)	Plasma	HILIC-MS/MS	84	Betaine Methionine sulfoxide Serine	• Association with incident T2D	[56]

Table S3. Metabolomics and lipidomics cohort studies focused on metabolic dysfunction-associated steatotic liver disease

Subjects (n)	Cohort	Matrix	Platforms	Reported metabolites (n)	Markers	Outcomes	Ref.
Study cohort: n = 121,032	Participants with a mean 12.6-year follow-up	Plasma	NMR	170	3-Hydroxybutyric acid Acetic acid Acetoacetatic acid Acetone Alanine Citric acid Creatinine Glucose Glutamine Glycine Histidine Isoleucine Lactic acid Leucine Phenylalanine Pyruvic acid Tyrosine Valine Docosahexaenoic acid (FA 22:6) Linoleic acid (FA 18:2) Omega-3 FA Omega-6 FA	• Positive and negative association with MASLD	[57]
Study cohort: n = 10,809	Participants with and without MASLD	Plasma	NMR	123	Tyrosine	• Association with MASLD	[58]
Study cohort: n = 3,048	Participants have been followed up since birth, including questionnaires and clinical assessments starting from age 7 years	Plasma	NMR	154	3-Hydroxybutyric acid Acetic acid Acetoacetatic acid Alanine Creatinine Glutamine Histidine Isoleucine Leucine Phenylalanine Tyrosine Valine	• Association with incident MASLD	[59]
Study cohort: n = 928 (67% female)	Participants with and without MASLD	Plasma	CE-MS	94	4-Methyl-2-oxopentanoic acid Alanine Glutamic acid Isoleucine Leucine Proline Tryptophan Tyrosine Valine Glycerophosphorylcholine	• Association with both MASLD and cardio-ankle vascular index (CAVI)	[60]
Study cohort: n = 1,479 Study subcohort: n = 447 (known age)	Participants were not treated for cancer or infectious disease or had undergone surgery in the previous year, and they had no history of cancer or an infectious disease.	Serum	LC-MS/MS	N/A	Oleic acid-hydroxy oleic acid (OAHOA) Sphingosine Uric acid	• Association with MASLD	[61]
Study cohort: n = 997 (53% female)	Participants free of prevalent myocardial infarction or congestive heart failure at the first examination cycle	Plasma	HILIC-MS/MS	179	Anandamide	• Association with MASLD severity, the presence of nonalcoholic steatohepatitis, and fibrosis	[62]

Subjects (n)	Cohort	Matrix	Platforms	Reported metabolites (n)	Markers	Outcomes	Ref.
Study cohort: n = 559	Participants with and without MASLD	Plasma	LC-MS/MS	11	Dihydrothymine Serine Tryptophan LPC 18:1 LPE 20:0	• Screening tool for MASLD	[63]
Study cohort: n = 1,154 (50% female) Control cohort: n = 350	Participants with biopsy-proven MASLD and participants from the general population with similar gender and age to the cohort of patients with MASLD	Serum	LC-MS NMR	105	PC 32:0|PC 16:0_16:0 PC 32:2|PC 14:0_18:2 PC 34:2|PC 16:0_18:2 PC 36:1|PC 18:0_18:1 PC 36:3 PC 36:6|PC 18:3_18:3 PC 37:5 PC 38:2|PC 20:0_18:2 PC 38:3|PC 18:0_20:3 SM d32:1 SM d39:1 TG 48:3	• Identification of three MASLD subgroups, independent of histological disease severity	[64]
Study cohort: n = 627	Histologically characterized participants. Participants include the full spectrum of disease, from histologically normal liver tissue through NAFL to NASH-F4 (cirrhosis)	Serum	LC-MS/MS GC-MS/MS	211	*Markers of fibrosis 0–1 vs. 2–4:* 2-Hydroxybutyric acid 3-Hydroxybutyric acid LPC O-16:0 LPC P-16:0 LPC 18:2 LPC 20:4 Oleic acid PC 32:0|PC 16:0/16:0 PC 32:1 PC 37:4 PC O-34:2 PC O-34:3 PE 16:0/18:1 PE 34:2 PE 38:6 SM d42:1|SM d18:1/24:0 SM d36:0 SM d41:1 TG 56:4 TG 58:6	• Identification of a key metabolic 'watershed' in the progression of liver damage, separating severe disease from mild	[65]
Discovery cohort: n = 1,546 Internal validation cohort: n = 377 Prospective validation cohort: n = 749	Participants with and without MASLD (4 years follow-up	Feces	LC-MS/MS	198	Taurocholic acid	• Positive association with both a higher microbiome risk score and MASLD risk	[66]

References

1. Akbaraly T, Würtz P, Singh-Manoux A, Shipley MJ, Haapakoski R, Lehto M, Desrumaux C, Kähönen M, Lehtimäki T, Mikkilä V, ET AL. Association of circulating metabolites with healthy diet and risk of cardiovascular disease: analysis of two cohort studies. Sci Rep 2018;8:8620. https://doi.org/10.1038/s41598-018-26441-1

2. Benson TW, Conrad KA, Li XS, Wang Z, Helsley RN, Schugar RC, Coughlin TM, Wadding-Lee C, Fleifil S, Russell HM, ET AL. Gut microbiota–derived trimethylamine N-oxide contributes to abdominal aortic aneurysm through inflammatory and apoptotic mechanisms. Circulation 2023;147:1079-1096. https://doi.org/10.1161/CIRCULATIONAHA.122.060573

3. Dehghanbanadaki H, Dodangeh S, Parhizkar Roudsari P, Hosseinkhani S, Khashayar P, Noorchenarboo M, Rezaei N, Dilmaghani-Marand A, Yoosefi M, Arjmand B, ET AL. Metabolomics profile and 10-year atherosclerotic cardiovascular disease (ASCVD) risk score. Front Cardiovasc Med 2023;10:https://doi.org/10.3389/fcvm.2023.1161761

4. Eichelmann F, Sellem L, Wittenbecher C, Jäger S, Kuxhaus O, Prada M, Cuadrat R, Jackson KG, Lovegrove JA, Schulze MB. Deep lipidomics in human plasma: Cardiometabolic disease risk and effect of dietary fat modulation. Circulation 2022;146:21-35. https://doi.org/10.1161/circulationaha.121.056805

5. Ferrell M, Wang Z, Anderson JT, Li XS, Witkowski M, DiDonato JA, Hilser JR, Hartiala JA, Haghikia A, Cajka T, ET AL. A terminal metabolite of niacin promotes vascular inflammation and contributes to cardiovascular disease risk. Nat Med 2024;30:424-434. https://doi.org/10.1038/s41591-023-02793-8

6. Fu Z, Liu Q, Liang J, Weng Z, Li W, Xu J, Zhang X, Xu C, Gu A. Association between NMR metabolomic signatures of healthy lifestyle and incident coronary artery disease. Eur J Prev Cardiol 2022;30:243-253. https://doi.org/10.1093/eurjpc/zwac252

7. Ganna A, Salihovic S, Sundström J, Broeckling CD, Hedman ÅK, Magnusson PKE, Pedersen NL, Larsson A, Siegbahn A, Zilmer M, ET AL. Large-scale metabolomic profiling identifies novel biomarkers for incident coronary heart disease. PLOS Genet 2014;10:e1004801. https://doi.org/10.1371/journal.pgen.1004801

8. Guasch-Ferré M, Hernández-Alonso P, Drouin-Chartier JP, Ruiz-Canela M, Razquin C, Toledo E, Li J, Dennis C, Wittenbecher C, Corella D, ET AL. Walnut consumption, plasma metabolomics, and risk of type 2 diabetes and cardiovascular disease. J Nutr 2021;151:303-311. https://doi.org/10.1093/jn/nxaa374

9. Harm T, Dittrich K, Brun A, Fu X, Frey M, Petersen Uribe A, Schwarz F-J, Rohlfing A-K, Castor T, Geisler T, ET AL. Large-scale lipidomics profiling reveals characteristic lipid signatures associated with an increased cardiovascular risk. Clin Res Cardiol 2023;112:1664-1678. https://doi.org/10.1007/s00392-023-02260-x

10. Huang Z, Klaric L, Krasauskaite J, Khalid W, Strachan MWJ, Wilson JF, Price JF. Combining serum metabolomic profiles with traditional risk factors improves 10-year cardiovascular risk prediction in people with type 2 diabetes. Eur J Prev Cardiol 2023;30:1255-1262. https://doi.org/10.1093/eurjpc/zwad160

11. Lauber C, Gerl MJ, Klose C, Ottosson F, Melander O, Simons K. Lipidomic risk scores are independent of polygenic risk scores and can predict incidence of diabetes and cardiovascular disease in a large population cohort. PLOS Biol 2022;20:e3001561. https://doi.org/10.1371/journal.pbio.3001561

12. Li XS, Wang Z, Cajka T, Buffa JA, Nemet I, Hurd AG, Gu X, Skye SM, Roberts AB, Wu Y, ET AL. Untargeted metabolomics identifies trimethyllysine, a TMAO-producing nutrient precursor, as a predictor of incident cardiovascular disease risk. JCI Insight 2018;3:https://doi.org/10.1172/jci.insight.99096

13. Lind L, Fall T, Ärnlöv J, Elmståhl S, Sundström J. Large-scale metabolomics and the incidence of cardiovascular disease. J Am Heart Assoc 2023;12:e026885. https://doi.org/10.1161/JAHA.122.026885

14. Lu Q, Chen J, Li R, Wang Y, Tu Z, Geng T, Liu L, Pan A, Liu G. Healthy lifestyle, plasma metabolites, and risk of cardiovascular disease among individuals with diabetes. Atherosclerosis 2023;367:48-55. https://doi.org/10.1016/j.atherosclerosis.2022.12.008

15. Margara-Escudero HJ, Paz-Graniel I, García-Gavilán J, Ruiz-Canela M, Sun Q, Clish CB, Toledo E, Corella D, Estruch R, Ros E, ET AL. Plasma metabolite profile of legume consumption and future risk of type 2 diabetes and cardiovascular disease. Cardiovasc Diabetol 2024;23:38. https://doi.org/10.1186/s12933-023-02111-z

16. Mundra PA, Barlow CK, Nestel PJ, Barnes EH, Kirby A, Thompson P, Sullivan DR, Alshehry ZH, Mellett NA, Huynh K, ET AL. Large-scale plasma lipidomic profiling identifies lipids that predict cardiovascular events in secondary prevention. JCI Insight 2018;3:https://doi.org/10.1172/jci.insight.121326

17. Nemet I, Saha PP, Gupta N, Zhu W, Romano KA, Skye SM, Cajka T, Mohan ML, Li L, Wu Y, ET AL. A cardiovascular disease-linked gut microbial metabolite acts via adrenergic receptors. Cell 2020;180:862-877.e22. https://doi.org/10.1016/j.cell.2020.02.016

18. Nemet I, Funabashi M, Li XS, Dwidar M, Sangwan N, Skye SM, Romano KA, Cajka T, Needham BD, Mazmanian SK, ET AL. Microbe-derived uremic solutes enhance thrombosis potential in the host. mBio 2023;14:e0133123. https://doi.org/10.1128/mbio.01331-23

19. Seah JYH, Chew WS, Torta F, Khoo CM, Wenk MR, Herr DR, Choi H, Tai ES, van Dam RM. Plasma sphingolipids and risk of cardiovascular diseases: a large-scale lipidomic analysis. Metabolomics 2020;16:89. https://doi.org/10.1007/s11306-020-01709-8

20. Tang WHW, Wang Z, Levison BS, Koeth RA, Britt EB, Fu X, Wu Y, Hazen SL. Intestinal microbial metabolism of phosphatidylcholine and cardiovascular risk. N Engl J Med 2013;368:1575-1584. https://doi.org/10.1056/NEJMoa1109400

21. Tzoulaki I, Castagné R, Boulangé CL, Karaman I, Chekmeneva E, Evangelou E, Ebbels TMD, Kaluarachchi MR, Chadeau-Hyam M, Mosen D, ET AL. Serum metabolic signatures of coronary and carotid atherosclerosis and subsequent cardiovascular disease. Eur Heart J 2019;40:2883-2896. https://doi.org/10.1093/eurheartj/ehz235

22. Wang Z, Klipfell E, Bennett BJ, Koeth R, Levison BS, DuGar B, Feldstein AE, Britt EB, Fu X, Chung Y-M, ET AL. Gut flora metabolism of phosphatidylcholine promotes cardiovascular disease. Nature 2011;472:57-63. https://doi.org/10.1038/nature09922

23. Witkowski M, Nemet I, Alamri H, Wilcox J, Gupta N, Nimer N, Haghikia A, Li XS, Wu Y, Saha PP, ET AL. The artificial sweetener erythritol and cardiovascular event risk. Nat Med 2023;29:710-718. https://doi.org/10.1038/s41591-023-02223-9

24. Witkowski M, Nemet I, Li XS, Wilcox J, Ferrell M, Alamri H, Gupta N, Wang Z, Tang WHW, Hazen SL. Xylitol is prothrombotic and associated with cardiovascular risk. Eur Heart J 2024;https://doi.org/10.1093/eurheartj/ehae244

25. Würtz P, Havulinna AS, Soininen P, Tynkkynen T, Prieto-Merino D, Tillin T, Ghorbani A, Artati A, Wang Q, Tiainen M, ET AL. Metabolite profiling and cardiovascular event risk: A prospective study of 3 population-based cohorts. Circulation 2015;131:774-85. https://doi.org/10.1161/circulationaha.114.013116

26. Zhu W, Gregory JC, Org E, Buffa JA, Gupta N, Wang Z, Li L, Fu X, Wu Y, Mehrabian M, ET AL. Gut microbial metabolite TMAO enhances platelet hyperreactivity and thrombosis risk. Cell 2016;165:111-124. https://doi.org/10.1016/j.cell.2016.02.011

27. Balzano-Nogueira L, Ramirez R, Zamkovaya T, Dailey J, Ardissone AN, Chamala S, Serrano-Quílez J, Rubio T, Haller MJ, Concannon P, ET AL. Integrative analyses of TEDDY Omics data reveal lipid metabolism abnormalities, increased intracellular ROS and heightened inflammation prior to autoimmunity for type 1 diabetes. Genome Biol 2021;22:39. https://doi.org/10.1186/s13059-021-02262-w

28. La Torre D, Seppänen-Laakso T, Larsson HE, Hyötyläinen T, Ivarsson SA, Lernmark Å, Orešič M, Group atDS. Decreased cord-blood phospholipids in young age–at–onset type 1 diabetes. Diabetes 2013;62:3951-3956. https://doi.org/10.2337/db13-0215

29. Lamichhane S, Ahonen L, Sparholt Dyrlund T, Dickens AM, Siljander H, Hyöty H, Ilonen J, Toppari J, Veijola R, Hyötyläinen T, ET AL. Cord-blood lipidome in progression to islet autoimmunity and type 1 diabetes. Biomolecules 2019;9:33. https://doi.org/10.3390/biom9010033

30. Lamichhane S, Ahonen L, Dyrlund TS, Kemppainen E, Siljander H, Hyöty H, Ilonen J, Toppari J, Veijola R, Hyötyläinen T, ET AL. Dynamics of plasma lipidome in progression to islet autoimmunity and type 1 diabetes – Type 1 diabetes prediction and prevention study (DIPP). Sci Rep 2018;8:10635. https://doi.org/10.1038/s41598-018-28907-8

31. Lamichhane S, Kemppainen E, Trošt K, Siljander H, Hyöty H, Ilonen J, Toppari J, Veijola R, Hyötyläinen T, Knip M, ET AL. Circulating metabolites in progression to islet autoimmunity and type 1 diabetes. Diabetologia 2019;62:2287-2297. https://doi.org/10.1007/s00125-019-04980-0

32. Li Q, Parikh H, Butterworth MD, Lernmark Å, Hagopian W, Rewers M, She J-X, Toppari J, Ziegler A-G, Akolkar B, ET AL. Longitudinal metabolome-wide signals prior to the appearance of a first islet autoantibody in children participating in the TEDDY study. Diabetes 2020;69:465-476. https://doi.org/10.2337/db19-0756

33. Ma L, Liu J, Deng M, Zhou L, Zhang Q, Xiao X. Metabolomics analysis of serum and urine in type 1 diabetes patients with different time in range derived from continuous glucose monitoring. Diabetol Metab Syndr 2024;16:21. https://doi.org/10.1186/s13098-024-01257-4

34. Oresic M, Gopalacharyulu P, Mykkänen J, Lietzen N, Mäkinen M, Nygren H, Simell S, Simell V, Hyöty H, Veijola R, ET AL. Cord serum lipidome in prediction of islet autoimmunity and type 1 diabetes. Diabetes 2013;62:3268-74. https://doi.org/10.2337%2Fdb13-0159

35. Tapia G, Suvitaival T, Ahonen L, Lund-Blix NA, Njølstad PR, Joner G, Skrivarhaug T, Legido-Quigley C, Størdal K, Stene LC. Prediction of type 1 diabetes at birth: Cord blood metabolites vs genetic risk score in the Norwegian Mother, Father, and Child cohort. J Clin Endocrinol Metab 2021;106:e4062-e4071. https://doi.org/10.1210/clinem/dgab400

36. Webb-Robertson B-JM, Nakayasu ES, Frohnert BI, Bramer LM, Akers SM, Norris JM, Vehik K, Ziegler A-G, Metz TO, Rich SS, ET AL. Integration of infant metabolite, genetic, and islet autoimmunity signatures to predict type 1 diabetes by age 6 years. J Clin Endocrinol Metab 2022;107:2329-2338. 10.1210/clinem/dgac225

37. Zhang J, Wu W, Huang K, Dong G, Chen X, Xu C, Ni Y, Fu J. Untargeted metabolomics reveals gender- and age- independent metabolic changes of type 1 diabetes in Chinese children. Front Endocrinol 2022;13:1-11. https://doi.org/10.3389/fendo.2022.1037289

38. Ahola-Olli AV, Mustelin L, Kalimeri M, Kettunen J, Jokelainen J, Auvinen J, Puukka K, Havulinna AS, Lehtimäki T, Kähönen M, ET AL. Circulating metabolites and the risk of type 2 diabetes: a prospective study of 11,896 young adults from four Finnish cohorts. Diabetologia 2019;62:2298-2309. https://doi.org/10.1007/s00125-019-05001-w

39. Delgado-Velandia M, Gonzalez-Marrachelli V, Domingo-Relloso A, Galvez-Fernandez M, Grau-Perez M, Olmedo P, Galan I, Rodriguez-Artalejo F, Amigo N, Briongos-Figuero L, ET AL. Healthy lifestyle, metabolomics and incident type 2 diabetes in a population-based cohort from Spain. Int J Behav Nutr Phys Act 2022;19:8. https://doi.org/10.1186/s12966-021-01219-3

40. Fall T, Salihovic S, Brandmaier S, Nowak C, Ganna A, Gustafsson S, Broeckling CD, Prenni JE, Kastenmüller G, Peters A, ET AL. Non-targeted metabolomics combined with genetic analyses identifies bile acid synthesis and phospholipid metabolism as being associated with incident type 2 diabetes. Diabetologia 2016;59:2114-2124. https://doi.org/10.1007/s00125-016-4041-1

41. Ferrannini E, Natali A, Camastra S, Nannipieri M, Mari A, Adam KP, Milburn MV, Kastenmüller G, Adamski J, Tuomi T, ET AL. Early metabolic markers of the development of dysglycemia and type 2 diabetes and their physiological significance. Diabetes 2013;62:1730-7. https://doi.org/10.2337/db12-0707

42. Floegel A, Stefan N, Yu Z, Mühlenbruch K, Drogan D, Joost HG, Fritsche A, Häring HU, Hrabě de Angelis M, Peters A, ET AL. Identification of serum metabolites associated with risk of type 2 diabetes using a targeted metabolomic approach. Diabetes 2013;62:639-48. https://doi.org/10.2337/db12-0495

43. Lee KS, Lee YH, Lee SG. Alanine to glycine ratio is a novel predictive biomarker for type 2 diabetes mellitus. Diabetes Obes Metab 2024;26:980-988. https://doi.org/10.1111/dom.15395

44. Lee DH, Jin Q, Shi N, Wang F, Bever AM, Liang L, Hu FB, Song M, Zeleznik OA, Zhang X, ET AL. The metabolic potential of inflammatory and insulinaemic dietary patterns and risk of type 2 diabetes. Diabetologia 2024;67:88-101. https://doi.org/10.1007/s00125-023-06021-3

45. Lee H-S, Xu T, Lee Y, Kim N-H, Kim Y-J, Kim J-M, Cho SY, Kim K-Y, Nam M, Adamski J, ET AL. Identification of putative biomarkers for type 2 diabetes using metabolomics in the Korea Association REsource (KARE) cohort. Metabolomics 2016;12:178. https://doi.org/10.1007/s11306-016-1103-9

46. Lemaitre RN, Jensen PN, Wang Z, Fretts AM, McKnight B, Nemet I, Biggs ML, Sotoodehnia N, de Oliveira Otto MC, Psaty BM, ET AL. Association of Trimethylamine N-Oxide and Related Metabolites in Plasma and Incident Type 2 Diabetes: The Cardiovascular Health Study. JAMA Netw Open 2021;4:e2122844-e2122844. https://doi.org/10.1001/jamanetworkopen.2021.22844

47. Liu J, Semiz S, van der Lee SJ, van der Spek A, Verhoeven A, van Klinken JB, Sijbrands E, Harms AC, Hankemeier T, van Dijk KW, ET AL. Metabolomics based markers predict type 2 diabetes in a 14-year follow-up study. Metabolomics 2017;13:104. https://doi.org/10.1007/s11306-017-1239-2

48. Lu J, Lam SM, Wan Q, Shi L, Huo Y, Chen L, Tang X, Li B, Wu X, Peng K, ET AL. High-coverage targeted lipidomics reveals novel serum lipid predictors and lipid pathway dysregulation antecedent to type 2 diabetes onset in normoglycemic chinese adults. Diabetes Care 2019;42:2117-2126. https://doi.org/10.2337/dc19-0100

49. Menni C, Fauman E, Erte I, Perry JR, Kastenmüller G, Shin SY, Petersen AK, Hyde C, Psatha M, Ward KJ, ET AL. Biomarkers for type 2 diabetes and impaired fasting glucose using a nontargeted metabolomics approach. Diabetes 2013;62:4270-6. https://doi.org/10.2337/db13-0570

50. Merino J, Leong A, Liu C-T, Porneala B, Walford GA, von Grotthuss M, Wang TJ, Flannick J, Dupuis J, Levy D, ET AL. Metabolomics insights into early type 2 diabetes pathogenesis and detection in individuals with normal fasting glucose. Diabetologia 2018;61:1315-1324. https://doi.org/10.1007/s00125-018-4599-x

51. Peddinti G, Cobb J, Yengo L, Froguel P, Kravić J, Balkau B, Tuomi T, Aittokallio T, Groop L. Early metabolic markers identify potential targets for the prevention of type 2 diabetes. Diabetologia 2017;60:1740-1750. https://doi.org/10.1007/s00125-017-4325-0

52. Prada M, Wittenbecher C, Eichelmann F, Wernitz A, Drouin-Chartier J-P, Schulze MB. Association of the odd-chain fatty acid content in lipid groups with type 2 diabetes risk: A targeted analysis of lipidomics data in the EPIC-Potsdam cohort. Clin Nutr 2021;40:4988-4999. https://doi.org/10.1016/j.clnu.2021.06.006

53. Qiu G, Wang H, Yan Q, Ma H, Niu R, Lei Y, Xiao Y, Zhou L, Yang H, Xu C, ET AL. A lipid signature with perturbed triacylglycerol co-regulation, identified from targeted lipidomics, predicts risk for type 2 diabetes and mediates the risk from adiposity in two prospective cohorts of chinese adults. Clin Chem 2022;68:1094-1107. https://doi.org/10.1093/clinchem/hvac090

54. Rebholz CM, Yu B, Zheng Z, Chang P, Tin A, Köttgen A, Wagenknecht LE, Coresh J, Boerwinkle E, Selvin E. Serum metabolomic profile of incident diabetes. Diabetologia 2018;61:1046-1054. https://doi.org/10.1007/s00125-018-4573-7

55. Sun L, Liang L, Gao X, Zhang H, Yao P, Hu Y, Ma Y, Wang F, Jin Q, Li H, ET AL. Early prediction of developing type 2 diabetes by plasma acylcarnitines: A population-based study. Diabetes Care 2016;39:1563-1570. https://doi.org/10.2337/dc16-0232

56. Walford GA, Ma Y, Clish C, Florez JC, Wang TJ, Gerszten RE. Metabolite profiles of diabetes incidence and intervention response in the diabetes prevention program. Diabetes 2016;65:1424-33. https://doi.org/10.2337/db15-1063

57. Gagnon E, Manikpurage HD, Mitchell PL, Girard A, Gobeil É, Bourgault J, Bégin F, Marette A, Thériault S, Arsenault BJ. Large-scale metabolomic profiling and incident non-alcoholic fatty liver disease. iScience 2023;26:107127. https://doi.org/10.1016/j.isci.2023.107127

58. Gobeil É, Maltais-Payette I, Taba N, Brière F, Ghodsian N, Abner E, Bourgault J, Gagnon E, Manikpurage HD, Couture C, ET AL. Mendelian randomization analysis identifies blood tyrosine levels as a biomarker of non-alcoholic fatty liver disease. Metabolites 2022;12:440. https://doi.org/10.3390/metabo12050440

59. Hartley A, Santos Ferreira DL, Anderson EL, Lawlor DA. Metabolic profiling of adolescent non-alcoholic fatty liver disease [version 2; peer review: 2 approved]. Wellcome Open Res 2019;3:166. https://doi.org/10.12688/wellcomeopenres.14974.2

60. Hirata A, Harada S, Iida M, Kurihara A, Fukai K, Kuwabara K, Kato S, Matsumoto M, Sata M, Miyagawa N, ET AL. Association of Nonalcoholic Fatty Liver Disease with Arterial Stiffness and its Metabolomic Profiling in Japanese Community-Dwellers. J Atheroscler Thromb 2024;31:1-17. http://doi.org/10.5551/jat.64616

61. Hu X-Y, Li Y, Li L-Q, Zheng Y, Lv J-H, Huang S-C, Zhang W, Liu L, Zhao L, Liu Z, ET AL. Risk factors and biomarkers of non-alcoholic fatty liver disease: an observational cross-sectional population survey. BMJ Open 2018;8:e019974. http://dx.doi.org/10.1136/bmjopen-2017-019974

62. Kimberly WT, O'Sullivan JF, Nath AK, Keyes M, Shi X, Larson MG, Yang Q, Long MT, Vasan R, Peterson RT, ET AL. Metabolite profiling identifies anandamide as a biomarker of nonalcoholic steatohepatitis. JCI Insight 2017;2:https://doi.org/10.1172/jci.insight.92989

63. Khusial R, Cioffi C, Caltharp S, Krasinskas A, Alazraki A, Knight-Scott J, Cleeton R, Castillo-Leon E, Jones D, Pierpont B, ET AL. Development of a plasma screening panel for pediatric nonalcoholic fatty liver disease using metabolomics. Hepatol Commun 2019;3:https://doi.org/10.1002/hep4.1417

64. Martínez-Arranz I, Bruzzone C, Noureddin M, Gil-Redondo R, Mincholé I, Bizkarguenaga M, Arretxe E, Iruarrizaga-Lejarreta M, Fernández-Ramos D, Lopitz-Otsoa F, ET AL. Metabolic subtypes of patients with NAFLD exhibit distinctive cardiovascular risk profiles. Hepatology 2022;76:1121-1134. https://doi.org/10.1002/hep.32427

65. McGlinchey AJ, Govaere O, Geng D, Ratziu V, Allison M, Bousier J, Petta S, de Oliviera C, Bugianesi E, Schattenberg JM, ET AL. Metabolic signatures across the full spectrum of non-alcoholic fatty liver disease. JHEP Rep 2022;4:100477. https://doi.org/10.1016/j.jhepr.2022.100477

66. Zeng F, Su X, Liang X, Liao M, Zhong H, Xu J, Gou W, Zhang X, Shen L, Zheng J-S, ET AL. Gut microbiome features and metabolites in non-alcoholic fatty liver disease among community-dwelling middle-aged and older adults. BMC Med 2024;22:104. https://doi.org/10.1186/s12916-024-03317-y

Straight even-chain fatty acids

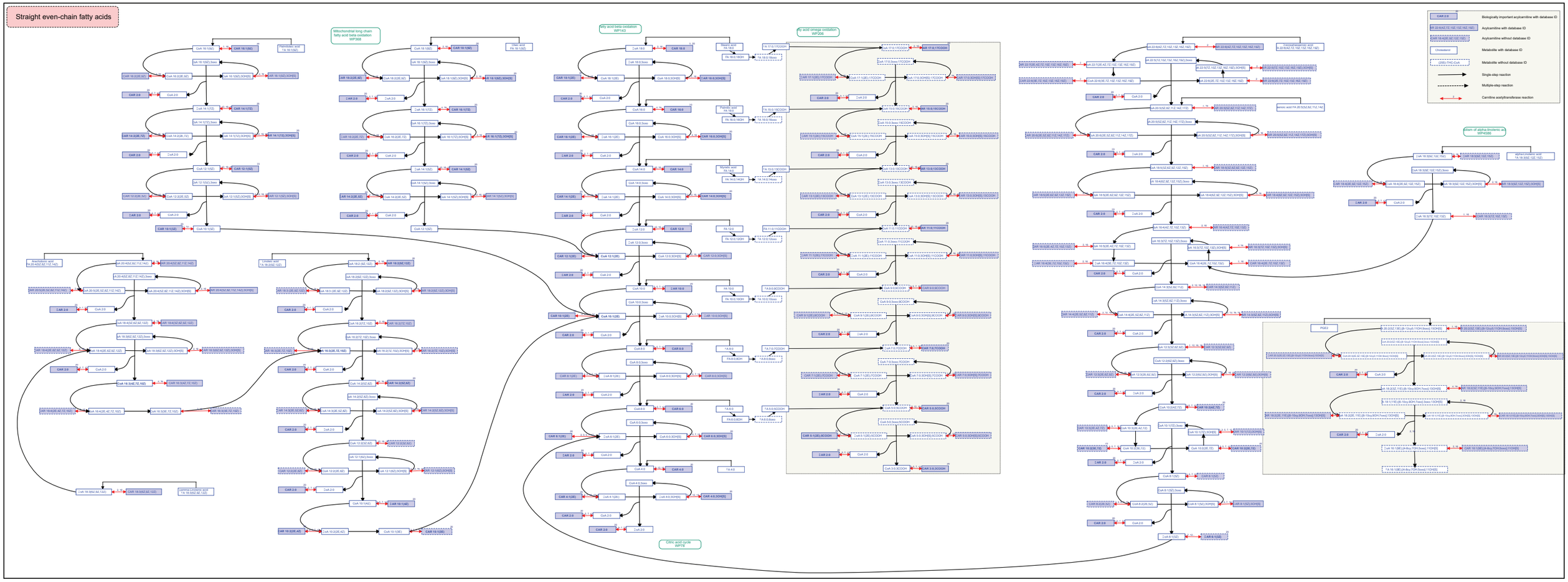

Branched chain lipids

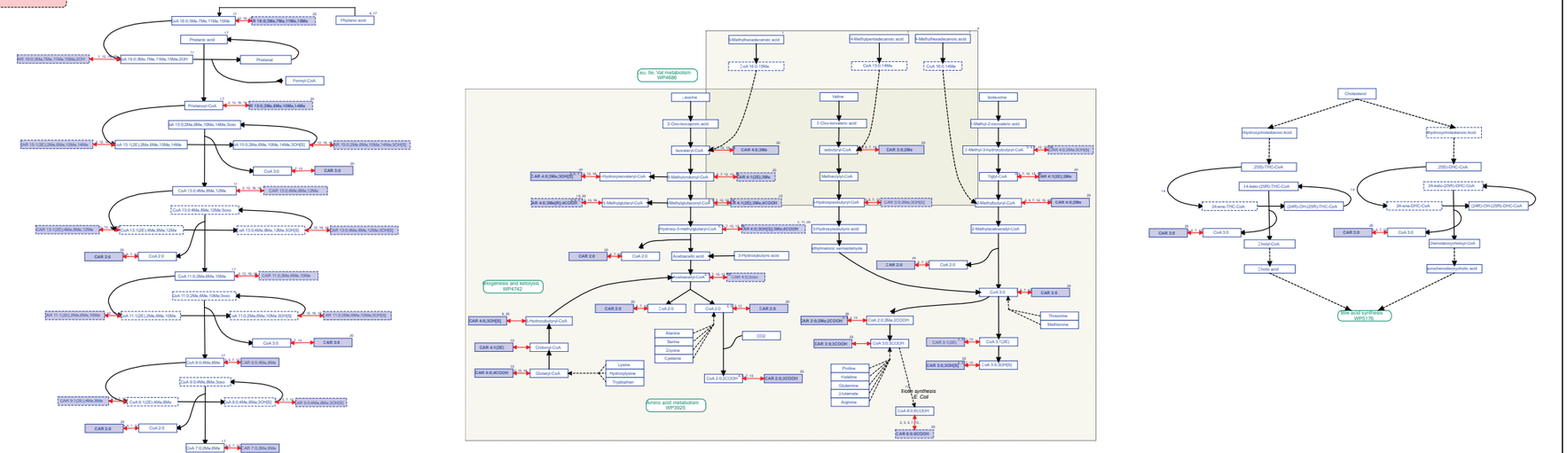

Straight odd-chain fatty acids